



UNIVERSITAT_{DE}
BARCELONA

From the design to the *in vivo* evaluation of novel soluble epoxide hydrolase inhibitors

Sandra Codony Gisbert



Aquesta tesi doctoral està subjecta a la llicència **Reconeixement- NoComercial – SenseObraDerivada 4.0. Espanya de Creative Commons.**

Esta tesis doctoral está sujeta a la licencia **Reconocimiento - NoComercial – SinObraDerivada 4.0. España de Creative Commons.**

This doctoral thesis is licensed under the **Creative Commons Attribution-NonCommercial-NoDerivs 4.0. Spain License.**



UNIVERSITAT DE BARCELONA
FACULTAT DE FARMÀCIA I CIÈNCIES DE L'ALIMENTACIÓ
LABORATORI DE QUÍMICA FARMACÈUTICA
DEPARTAMENT DE FARMACOLOGIA, TOXICOLOGIA I QUÍMICA TERAPÈUTICA

**FROM THE DESIGN TO THE *IN VIVO* EVALUATION OF NOVEL
SOLUBLE EPOXIDE HYDROLASE INHIBITORS**

SANDRA CODONY GISBERT

2020

UNIVERSITAT DE BARCELONA
FACULTAT DE FARMÀCIA I CIÈNCIES DE L'ALIMENTACIÓ
PROGRAMA DE DOCTORAT DE QUÍMICA ORGÀNICA

**FROM THE DESIGN TO THE *IN VIVO* EVALUATION OF
NOVEL SOLUBLE EPOXIDE HYDROLASE INHIBITORS**

Memòria presentada per Sandra Codony Gisbert per optar al títol de
Doctora per la Universitat de Barcelona

Director i tutor:

Codirectora:

Doctoranda:

Dr. Santiago Vázquez Cruz

Dra. Carmen Escolano Mirón

Sandra Codony Gisbert

Barcelona, 2020

“The most certain way to succeed is always
to try just one more time”

Thomas A. Edison

El treball experimental recollit en aquesta memoria s'ha realitzat en el Laboratori de Química Farmacèutica de la Facultat de Farmàcia i Ciències de l'Alimentació de la Universitat de Barcelona, sota la direcció del Dr. Santiago Vázquez Cruz i la Dra. Carmen Escolano Mirón.

Aquest treball ha estat finançat pel *Ministerio de Economía y Competitividad* (projectes SAF2017-82771-R i SAF2015-64146-R), per la Generalitat de Catalunya (2017-SGR-00106), per la *Fundació "La Caixa"* (programa "CaixaImpulse 2015"), per *Spain EIT Health* (programa "Proof of concept 2016") i per la *Fundació Bosch i Gimpera* (programa F21).

La realització de la present Tesis Doctoral ha estat possible gràcies a la concessió d'una beca APIF (Ajut de Personal Investigador en Formació) durant els anys 2017-2020, otorgada per la Universitat de Barcelona. A més, la realització de l'estada predoctoral al *The Institute of Cancer Research* a Sutton (Regne Unit) va ser finançada gràcies a l'ajut per a estades pre-doctorals a l'estranger de la Fundació Pedro i Pons i d'un ajut en el marc del "Programa de formació per a professorat i personal investigador amb contractació temporal" de la Universitat de Barcelona.

Agraïments

M'agradaria dedicar unes paraules a totes les persones que m'heu acompanyat durant la realització d'aquesta tesi doctoral, per l'ajuda, el suport i la paciència que tots vosaltres heu tingut amb mi... gràcies de tot cor!

En primer lloc, i com no podia ser d'altra manera, voldria donar les gràcies al meu director de tesi. Muchas gracias Santi por dejarme formar parte de tu grupo de investigación desde hace ya 7 años y por haberme contagiado tu pasión por la química médica y la investigación en general. Gracias por enseñarme tanto, por todos los consejos siempre acertados, las charlas infinitas en tu despacho, tu apoyo en los momentos de estrés máximo y tu paciencia cada vez que me merecía un... "¡Como el primer día!" Pero, sobre todo, querría agradecerte la confianza que has depositado en mí, por hacerme crecer cada día tanto personal como profesionalmente y por ser mucho más que un jefe.

També m'agradaria agrair als altres professors de la Unitat de Química Farmacèutica, els que han fet que anar a treballar cada dia sigui com formar part d'una gran família. Gracias a Carmen, por avalarme con la beca y por mantener el orden y la disciplina en el laboratorio; a Diego, por ser tan cercano y estar siempre disponible para cualquier duda, charla o pizza day :) y a Rodolfo, por tanta sabiduría e implementar los tan necesarios Group Meetings.

No podia faltar el meu agraïment a tota la gent que facilita la feina dia rere dia a la facultat. A la Maite, per tots els tràmits burocràtics; i a la Laura, per haver fet que el laboratori funcioni molt millor! Gràcies també al Javier, l'Armando, el Josep Galdón i l'Ana Linares.

Aquesta tesi doctoral no hagués tingut sentit sense la contribució científica de tots els grups de recerca que han col·laborat en el projecte d'investigació. Així doncs, voldria donar les gràcies al grup del Professor Bruce D. Hammock i al Dr. Cristophe Morisseau de la Universitat de California Davis; al grup de "Drug Screening Platform" de la Universitat de Santiago de Compostela, en especial a la Prof. Mabel Loza, y als Drs. José M. Santamaría i José Brea; als Drs. Julen Oyarzábal i Antonio Pineda-Luceda, del CIMA de Navarra; a la Dra. Belén Pérez, de la UAB; a les Drs. Concepción Pérez i Maribel Rodríguez-Franco, de l'Institut de Química Mèdica, del CSIC de Madrid; als Drs. Sílvia Osuna i Ferran Feixas i a la Carla Calvó-Tusell de la Universitat de Girona; als Drs. Rubén

Corpas i Coral Sanfeliu, de l'Institut d'Investigacions Biomèdiques de Barcelona; i als Drs. Enrique J. Cobos i José M. Entrena, de la Universitat de Granada. Tampoc puc deixar d'agrair als farmacòlegs més propers dels que he après tant i m'han fet veure la farmacologia des d'un altre punt de vista: els Drs. Manel Vázquez i Javier Pizarro, i els Drs. Mercé Pallás i Christian Griñán del Departament de Farmacologia de la nostra Facultat.

Voldria també mostrar un profund agraïment a les meves cuquis, sense les quals la realització d'aquesta tesi doctoral no hagués estat el mateix. En primer lloc a l'Eugènia, per tants i tants moments compartits, per ser-hi SEMPRE quan se't necessita, pel teu suport incondicional i per saber convertir els moments durs en somriures gegants...has sigut un pilar indispensable. A Andreea, mi rubia favorita! Gracias por acompañarme en este viaje universitario durante ya 10 años... esta aventura la empezamos juntas y, como no podía ser de otra manera, la acabaremos de la mano. Gracias por tu alegría contagiosa, por ser alguien en quien poder confiar ciegamente y por todas las charlas y consejos en el despachito. Evidentment a la Katia, per convertir-te en poc temps en molt més que una amiga.. pels cafès, per resoldre els meus dubtes de química, pels.. "vols riure..?" i per tantes coses viscudes juntes... A Dundee, Alacant o Barcelona, sé que sempre podré comptar amb tu pel que sigui. I finalment, però no menys important, a la Bea, per saber escoltar com ningú i donar els consells més apropiats, per la teva disposició a ajudar constantment ja sigui al laboratori o fora, i per ser una de les millors persones que conec. Tot i no ser una cuqui com a tal, no puc deixar d'agrair a l'Oscar, per estar sempre disponible per fer un biquini, per les nits inacabables, pels consells químics i per tenir sempre un somriure contagiós a la cara.

Gràcies també a tots els companys del laboratori per tants moments compartits. Al Sergio, Andrea, Marina, Ouldouz, Elsa, Juan... per les cerveses del divendres, per estar sempre allà per resoldre qualsevol dubte i per fer que anar al laboratori cada dia sigui com anar a retrobar-se amb els amics més que anar a treballar. Noemí i Cristian, molta sort pels que comenceu ara!

També agrair a les "viejas glorias"! Ane, Ornella, Irene, Sònia, Matías, Elena... Especialment a la Marta, per ensenyar-me des de zero aquell estiu de 2013 i transmetre'm la passió per la investigació, fet pel qual no he deixat el laboratori des de llavors; i a la Rosana, por ser mi referente y aprender tanto de tí, de tu organización y de tu forma de trabajar. Gràcies també al Javi i al David, per amenitzar els dies al laboratori i mantenir un ambient "festiu", per les sortides nocturnes i per la vostre

alegria infinita. I al Carles, per aparèixer sempre pel laboratori amb alguna història per explicar, pels consells científics i per aportar tant al projecte.

No vull deixar de banda tota la gent que ha anat passant pel laboratori, ja sigui com a treballs dirigits, treballs fi de grau, màsters o Erasmus. Estic segura que he après alguna cosa de cadascun de vosaltres i heu propiciat un molt bon ambient al laboratori. Gràcies!! Agrair també als meus mindus: Arnau, Maria, Natàlia... per les vostres ganes de treballar i per haver-me ajudat a aprendre a ensenyar, que tampoc és fàcil.

També vull agrair a la gent del "Institute of Cancer Research", lloc on vaig fer una estada de tres mesos. First, at Dr. Swen Hoelder for hosting me in your research group and giving me the opportunity to work in both chemical and biological laboratories, getting deeply involved in the project. Thanks a lot to Rosemary and Catherine, for your patience and advice in the lab and for being always so nice with me. To all the "ICR Young Team", especially to Jan, for all the great conversations and for encouraging me to go bouldering; and to Edgar, for being the best spanish-team in table football. Harshnira, Alice, Ben, Françoise, Agi, Mahad, Barbara, Iona, Suzanne, Charlie...thanks for all the moments we shared. Gràcies també a totes les persones que em van fer sentir una mica més a prop de casa: Aitor, Albert L., Pol, Belén... i, sobretot, a l'Albert, per ser el millor guia de Londres (i Barcelona ;)) que es pot tenir.

Gràcies també als amics de sempre, per interessar-vos i preguntar sense malícia "Com va la tesi?" "Quan presentes?" "Encara no has acabat"? etc, per la vostra comprensió i per haver-me fet costat durant tot aquest temps.

A la meva família, un dels millors tresors que tinc... sense ells res d'això no hauria estat possible. Gràcies per ajudar-me i recolzar-me sempre, incondicionalment. Sabeu millor que ningú que aquest camí no ha estat sempre fàcil, no heu deixat que dubtés mai de mi i m'heu donat totes les forces que he necessitat per arribar fins aquí... mai podré deixar d'agrar-vos per tant. Als papes, per ensenyar-me que s'ha de lluitar per aconseguir els somnis i que aquests s'han de perseguir, per escoltar-me, donar-me consell i recolzar-me sempre amb les meves decisions. Al Jordi i al David, per tota la paciència que heu tingut, per ajudar-me sobretot en la fase final de la tesi i per totes les sessions de psicologia tant necessàries per mi. I a la Laura, per la paciència durant les meves explicacions inacabables i per tenir sempre paraules d'ànim a punt. GRÀCIES.

Summary

Epoxieicosatrienoic acids (EETs) are endogenous chemical mediators derived from arachidonic acid that show anti-inflammatory, antihypertensive, analgesic, angiogenic and antiatherosclerotic effects. Soluble epoxide hydrolase (sEH) converts EETs to their corresponding dihydroxyeicosatrienoic acids, whereby the biological effects of EETs are diminished, eliminated, or altered. Therefore, it has been proposed that inhibition of sEH may have therapeutic effects in various inflammatory and pain-related diseases. A number of very potent sEH inhibitors (sEHIs) have been developed, several of them featuring an adamantane moiety that may account for the low solubility and poor pharmacokinetic profile that have hampered their progress into clinics. In this context, the present thesis has been focused on the design and synthesis of novel sEHIs replacing the adamantane moiety by adamantane-like scaffolds in order to improve their drug-like properties. First, the introduction of an oxygen atom in the adamantane nucleus of known sEHIs provided a new family of 2-oxadamantane-based inhibitors endowed with nanomolar potency and improved aqueous solubility and permeability. A screening cascade was conducted in order to biologically characterize the new inhibitors and to select a candidate for subsequent *in vivo* studies, which revealed that the candidate reduced inflammatory and endoplasmic reticulum stress markers and diminished the pancreatic damage in a murine model of cerulein-induced acute pancreatitis (AP). Second, the exploration of the size of the lipophilic unit of sEHIs showed that the active center of sEH is flexible and can accommodate both larger and smaller polycycles than adamantane, and that the replacement of the adamantane moiety by larger polycyclic rings led to more potent compounds than the replacement by smaller ones. Taking into account these results, the last step was the development of a new family of sEHIs bearing the benzohomoadamantane scaffold, which features in its structure the synthetically versatile homoadamantane unit fused with an aromatic ring. This new family encompasses compounds endowed with excellent inhibitory activities in human, murine and rat sEH, improved water solubility and good microsomal stability. Further *in vitro* profiling and pharmacokinetic studies allowed us to select different candidates for the *in vivo* efficacy studies. One of them significantly reduced pancreatic damage and improved the health status of the animals after the induction of AP by cerulein. On the other hand, the compound optimized for the treatment of neuropathic pain fully abolished the capsaicin-induced allodynia in mice, outperforming other sEHI tested. Overall, a plethora of very potent sEHIs endowed with improved DMPK properties that present efficacy in several *in vivo* murine models have been developed in the present Thesis.

Abbreviation list

AA	Arachidonic acid
AD	Alzheimer's disease
AP	Acute Pancreatitis
AEPU	<i>N</i> -adamantyl- <i>N'</i> -[5-(2-(2-ethoxyethoxy)ethoxy)pentyl]urea
AP	Acute pancreatitis
AUDA	12-(3-(1-adamant-1-yl)ureido)dodecanoic acid
BBB	Blood-brain barrier
cAMP	Cyclic adenosine monophosphate
CDU	<i>N</i> -cyclohexyl- <i>N'</i> -dodecylurea
CNS	Central Nervous System
COPD	Chronic obstructive pulmonary disease
COXs	Cyclooxygenases
COXIBs	COX-2-selective inhibitors
CUDA	12-(3-cyclohexylureido)dodecanoic acid
CYP	Cytochromes
DCU	<i>N,N'</i> -dicyclohexylurea
DAST	Diethylaminosulfur trifluoride
DCM	Dichloromethane
DiHETrEs	Dihydroxyeicosatrienoic acids
DiHFAs	Dihydroxy-fatty acids
DNA	Deoxyribonucleic acid
DMF	Dimethylformamide
DMPK	Drug metabolism and pharmacokinetics
DMSO	Dimethylsulfoxide
EDCI	<i>N</i> -Ethyl- <i>N'</i> -(3-dimethylaminopropyl)carbodiimide
EETs	Epoxyeicosatrienoic acids
EH	Epoxide hydrolases
EpFAs	Epoxy-fatty acids

ER	Endoplasmic reticulum
FAs	Fatty acids
FDA	Food and Drug Administration
GABA	γ -aminobutyric acid
GPCRs	G-Protein coupled receptors
GSK	GlaxoSmithKline
HDL	High-density lipoprotein
hERG	Human ether-a-go-go-related gene
HETEs	Hydroxyeicosatetraenoic acids
HOBt	Hydroxybenzotriazole
IL	Interleukin
iNOS	Inducible nitric oxide synthase
IKK	I κ B kinase
kDa	Kilodalton
KO	Knock out
LTA4	Leukotriene A4
LHS	Left-hand side
LipE	Lipophilic ligand efficiency
LOXs	Lipoxygenases
LTs	Leukotrienes
mEH	Microsomal epoxide hydrolase
MetS	Metabolic syndrome
MTD	Maximum tolerated dose
NADP	Nicotinamide adenine dinucleotide phosphate
NP	Neuropathic Pain
NF- κ B	Nuclear factor κ B
NO	Nitric Oxide
NMDA	<i>N</i> -methyl-D-aspartic acid
NSAIDs	Non-steroidal anti-inflammatory drugs
Papp	Apparent permeability coefficient

PBMC	Peripheral Blood Mononuclear Cells
PBS	Phosphate-buffered saline
PD	Pharmacodynamic
PGIs	Prostacyclins
PGE ₂	Prostaglandin E2
PGs	Prostaglandins
PK	Pharmacokinetic
PLA2	Phospholipase A2
PPARs	Peroxisome proliferator-activated receptors
PUFA	Polyunsaturated fatty acids
RAF-1	Raf-1 Proto-Oncogene, Serine/Threonine Kinase
RHS	Right-hand side
SAR	Structure-activity relationship
sEH	Soluble epoxide hydrolase
sEHIs	Soluble epoxide hydrolase inhibitors
STZ	Streptozotocin
<i>t</i> -AUCB	<i>Trans</i> -4-[4-(3-adamantan-1-yl-ureido)cyclohexyloxy]benzoic acid
THLE-2	Transformed Human Liver Epithelial-2 cell line
TPPU	1-(1-Propionylpiperidin-4-yl)-3-[4-(trifluoromethoxy)phenyl]urea
<i>t</i> -TUCB	<i>Trans</i> -4-[4-[3-(4-trifluoromethoxyphenyl)-ureido]cyclohexyloxy]benzoic acid
TNF- α	Tumor necrosis factor α
TXs	Thromboxanes
UCD	University of California Davis
VCAM-1	Vascular cell adhesion molecule-1
VEGF	Vascular endothelial growth factor
11 β -HSD1	11beta-hydroxysteroid dehydrogenase type 1

Index

1.	INTRODUCTION	21
1.1.	<i>Arachidonic acid cascade</i>	<i>23</i>
1.2.	<i>Epoxyeicosatrienoic acids (EETs)</i>	<i>24</i>
1.3.	<i>Soluble epoxide hydrolase</i>	<i>26</i>
	Epoxide Hydrolases.....	26
	sEH: structure and function	27
	sEH: tissue and subcellular distribution.....	30
1.3.1.		
1.3.2.	1.4. sEH as a potential therapeutic target.....	30
1.3.3.		
	Inflammation	31
	Vasodilatation and Cardiovascular Diseases.....	32
1.4.1.		
1.4.2.	Pain.....	34
1.4.3.	Diabetes and Metabolic Syndrome	36
1.4.4.	Pulmonary Diseases.....	38
1.4.5.	Central Nervous System (CNS) Disorders	39
1.4.6.	Other potential indications for sEHs.....	40
1.4.7.		
	1.5. Design of sEHIs	40
1.5.1.		
1.5.2.	Early inhibitors.....	41
1.5.3.	Discovery of the pharmacophore	41
1.5.4.	Adamantane-based inhibitors	44
1.5.5.	Improved adamantane-based sEHIs	46
1.5.6.	Non adamantane-based sEHs.....	48
1.5.7.	sEHs in clinical trials.....	51
1.5.8.	Marketed drugs with sEH inhibition activity.....	53
1.6.1.	Potential side effects of sEHs.....	54
1.6.2.		
	1.6. Previous work in our research group.....	55
	Polycyclic scaffolds	55
	sEH inhibition.....	57
4.1.1.	2. OBJECTIVES	61
4.1.2.		
4.1.3.	3. RESULTS AND DISCUSSION	67
4.1.4.		
4.1.5.	CHAPTER 1 2-OXAADAMANTANE-BASED sEHIs	69
	Introduction.....	71
	Discussion	73
	Journal article	81
	Supporting information	103
	Patent Application	139

	CHAPTER 2 EXPLORING THE SIZE OF THE LIPOPHILIC UNIT OF sEHs	183
	Introduction	185
	Discussion	187
	Journal Article	195
	Supplementary material	205
	CHAPTER 3 BENZOHOMOADAMANTANE-BASED sEHs (I)	229
4.2.1	Introduction	231
4.2.2	Discussion	232
4.2.3	Draft Manuscript	247
4.2.4	Supporting Information	305
4.3.1	CHAPTER 4 BENZOHOMOADAMANTANE-BASED sEHs (II)	327
4.3.2	Introduction	329
4.3.3	Discussion	330
4.3.4	Draft Manuscript	341
4.4.1	Supplementary material	405
4.4.2	CHAPTER 5 BENZOHOMOADAMANTANE-BASED sEHs (III)	441
4.4.3	Introduction	443
4.4.4	Discussion and results	444
4.5.1	Experimental section	450
4.5.2	Patent application	461
	4. CONCLUSIONS	541
	4.1. 2-Oxadadamantane-based sEHs	543
	4.2. Exploring the size of the lipophilic unit of sEHs	544
	4.3. Benzohomoadamantane-based sEHs (I)	544
	4.4. Benzohomoadamantane-based sEHs (II and III)	545
	5. PERSPECTIVES	547
5.1.1	5.1. 3-Alkyl 2-oxadamantane derivatives	549
5.1.2	5.2. New benzohomoadamantane-based sEHs	550
5.2.1	New amides as sEHs	551
5.2.2	Further exploration of the aromatic ring	552
5.2.3	Further exploration of the RHS	553
5.2.3.1	Bicyclic compounds:	553
5.2.3.2	Spirocycles:	554
5.2.3.3	3,3-disubstituted ureas:	555
5.2.3.4	Aromatic derivatives:	556
	Results Dissemination	559

1. INTRODUCTION

1.1. Arachidonic acid cascade

Arachidonic acid (AA) is an essential ω -6, 20-carbon polyunsaturated fatty acid that is abundant in the phospholipids of cellular membrane. In response to a stimulus such as growth factors, hormones or cytokines, phospholipase A2 (PLA2) promotes its cleavage from the membrane being released to the cytosol, where it is involved in numerous cell signaling and regulation pathways and making it available for its oxidation by the enzymes of the AA cascade.^{1,2} Released AA can be metabolized to different classes of chemical mediators called eicosanoids via three pathways: cyclooxygenases (COXs), lipoxygenases (LOXs) and cytochromes (CYP) (Figure 1). The COX pathway includes COX-1 and COX-2 that catalyze the production of prostaglandin H2 which, in turn, is transformed to other prostaglandins (PGs), prostacyclins (PGIs) and thromboxanes (TXs), endowed with pro-inflammatory properties. In contrast, leukotrienes (LTs) are generated by the 5-LOX pathway which plays a significant part in the cause of asthma, arthritis, allergy and inflammation.³ Both pathways have been extensively studied and pharmaceutically targeted. Of note, COXs are very popular targets for the treatment of inflammatory diseases. Non-steroidal anti-inflammatory drugs (NSAIDs), that block the COX-1 and COX-2 enzymes, and coxibs, that selectively block COX-2, lead to a decrease in pro-inflammatory metabolites.⁴ On the other hand, zileuton, clinically used for asthma, is the only FDA approved 5-LOX inhibitor.^{5,6}

Most research has been focused on the cyclooxygenase and lipoxygenase pathways, but increasing attention is being paid to the third branch of the AA cascade, the CYP450. The CYP pathway produces two types of eicosanoid products, the epoxyeicosatrienoic acids (EETs), formed by CYP epoxygenases, and the hydroxyeicosatetraenoic acids (HETEs), formed by CYP oxidases.⁷ The oxygenase pathway converts AA via CYP4A to HETEs such as 20-HETE, exhibiting pro-inflammatory and vasoconstrictor properties. In contrast, the epoxygenase pathway catalyses the formation of four regioisomers of EETs (5,6-, 8,9-, 11,12- and 14,15-EETs) via the subfamilies CYP2C and CYP2J. EETs are

¹ Harizi, H.; Corcuff, J. B.; Gualde, N. *Trends Mol. Med.* **2008**, *14*, 461-469.

² Hanna, V. S.; Hafez, E. A. A. *J. Adv. Res.* **2018**, *11*, 23-32.

³ Funk, C. D. *Science* **2001**, *294*, 1871-1875.

⁴ Meirer, K.; Steinhilber, D.; Proschak, E. *Basic Clin. Pharmacol. Toxicol.* **2014**, *114*, 83-91.

⁵ Rubin, P.; Mollison, K. W. *Prostaglandins Other Lipid Med.* **2007**, *83*, 188-197.

⁶ Sinha, S.; Doble, M.; Manju, S. L. *Bioorg. Med. Chem* **2019**, *27*, 3745-3759

⁷ Spector, A. A.; Norris, A. W. *Am. J. Physiol. Cell Physiol.* **2007**, *292*, C996-C1012.

endowed with potent antiinflammatory and antihypertensive properties and have been reported to produce beneficial effects in disease models related to cardiovascular diseases, diabetes, inflammatory pain and other indications.⁸

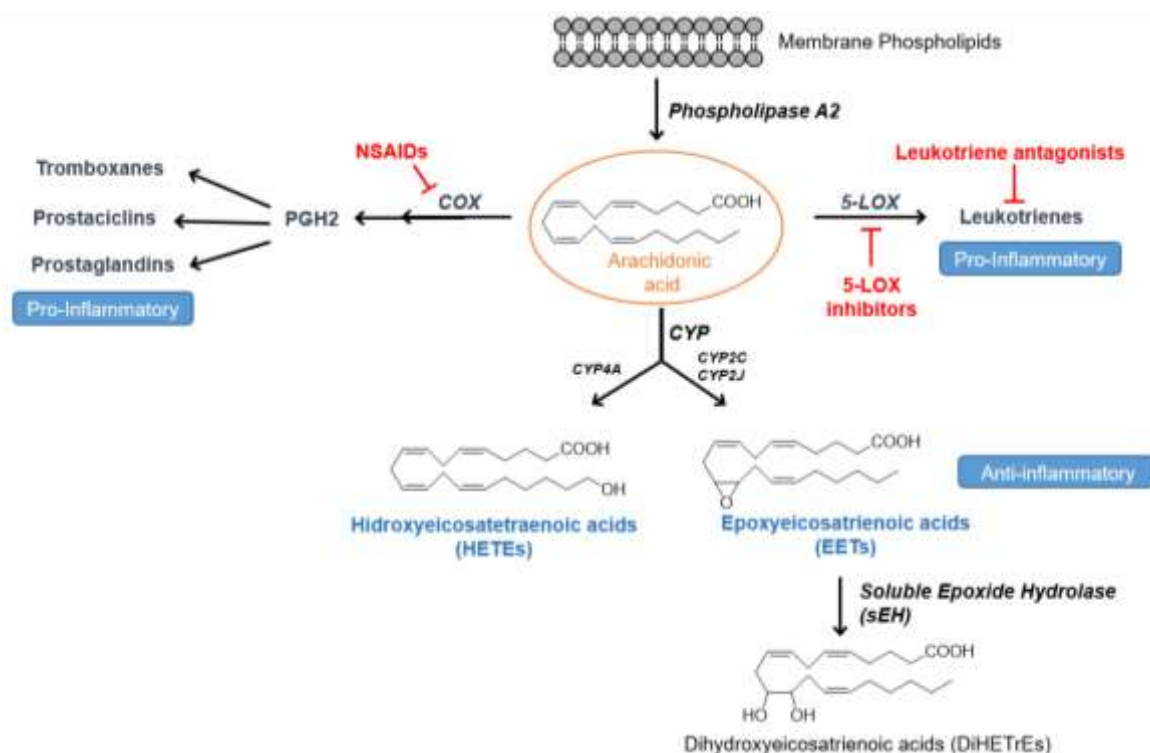


Figure 1. Arachidonic acid cascade. Three metabolic pathways of AA: the COX, LOX and CYP450 enzymatic routes, resulting in the production of several chemical mediators involved in inflammatory processes. Inhibitors of COX are used for the treatment of pain and inflammation. Leukotriene antagonists and 5-LOX inhibitors are indicated in asthmatic and allergic states.

1.2. Epoxyeicosatrienoic acids (EETs)

EETs are chemical mediators that move biological processes toward a homeostatic or status quo condition. Storage, metabolism and excretion of EETs are all processes highly interlinked to maintain tissue homeostasis. Once formed, EETs undergo hydrolysis by soluble epoxide hydrolase (sEH) to the corresponding dihydroxyeicosatrienoic acids (DiHETrEs) that present less activity than the EETs and, therefore, hydrolysis by sEH is considered a quenching process.⁸

⁸ Kaspera, R.; Totah, R. A. *Expert Opin. Drug Metab. Toxicol.* **2009**, *5*, 757-771.

Although the EETs receptor or receptors still remain unknown, they have been suggested to act through specific G-Protein coupled receptors (GPCRs) to intracellular signaling cascades, however none of which have been identified to date. These lipidic mediators present autocrine and paracrine functions due to binding to the GPCRs, activating ion channels and several intracellular signal transduction pathways. Their potent anti-inflammatory property is produced by inhibiting the activity of I κ B kinase (IKK) and tumor necrosis factor α (TNF- α), thus decreasing the activation of cytokine-induced NF- κ B and its subsequent transcriptional activity and, consequently, diminishing the inflammatory process.⁴ Moreover, EETs activate different subfamilies of nuclear peroxisome proliferator-activated receptors (PPARs), decreasing the expression of inducible COX-2.

Apart from the anti-inflammatory property, EETs exhibit other beneficial effects on biological systems, such as analgesic, anti-hypertensive, anti-platelet aggregation, fibrinolytic, pro-angiogenic and anti-apoptotic effects.^{9,10}

Consequently, since the discovery of the biological role of EETs and their metabolism, the inhibition of sEH has emerged as a promising therapeutic strategy for the treatment of several conditions. Considering the interesting properties of the EETs and their inactivation when transformed to DiHETrEs, the study of sEH has gained importance in recent years, especially regarding the design of sEH inhibitors (sEHIs) that increase the concentration of the EETs and, consequently, maintaining their anti-inflammatory, vasodilator and/or analgesic effect. In this context, it is noteworthy that there have been described different alternative metabolic routes that ensure the regulation of EETs concentration in plasma and tissues.¹¹ For this reason, the complete inhibition of sEH may only lead to a moderate increase of EET levels, limiting the target-related side effects with the administration of potent sEHIs.

⁹ El-Sherbeni, A. A.; El-Kadi, A. O. S. *Arch. Toxicol.* **2014**, *88*, 2013-2032.

¹⁰ Dufлот, T.; Roche, C.; Lamoureux, F.; Guerrot, D.; Bellien, J. *Expert Opin. Drug Discov.* **2014**, *9*, 229-243.

¹¹ Imig, J. D. *Physiol. Rev.* **2012**, *92*, 101-130.

1.3. Soluble epoxide hydrolase

Epoxide Hydrolases

Epoxide hydrolases (EH) represent a group of enzymes that convert various types of epoxides to vicinal diols by the addition of a water molecule. There are several EH in mammals which are named according their subcellular location, including soluble epoxide hydrolase (sEH), microsomal epoxide hydrolase (mEH), cholesterol epoxide hydrolase, which hydrates the 5,6-oxide of cholesterol and other 5-epoxy steroids, and leukotriene A4 hydrolase and hepoxilin A3 hydrolase.¹² However, the most studied EHs have been the sEH and mEH, which clearly differ in specificity towards certain substrates. While the mEH activity is focused on the metabolism of xenobiotic epoxides and degrades preferentially epoxides on cyclic systems, the sEH produce the hydrolysis of endogenous epoxy-fatty acids, such as the oxidation of linoleic acid, linolenic acid or the EETs.¹³ Thus, the main metabolic pathway of EETs is the soluble epoxide hydrolase (sEH, EPHX2, EC 3.3.2.3), which transform EETs to their corresponding DiHETrEs whereby the biological effects of EETs are diminished, eliminated or altered (Figure 2).¹³

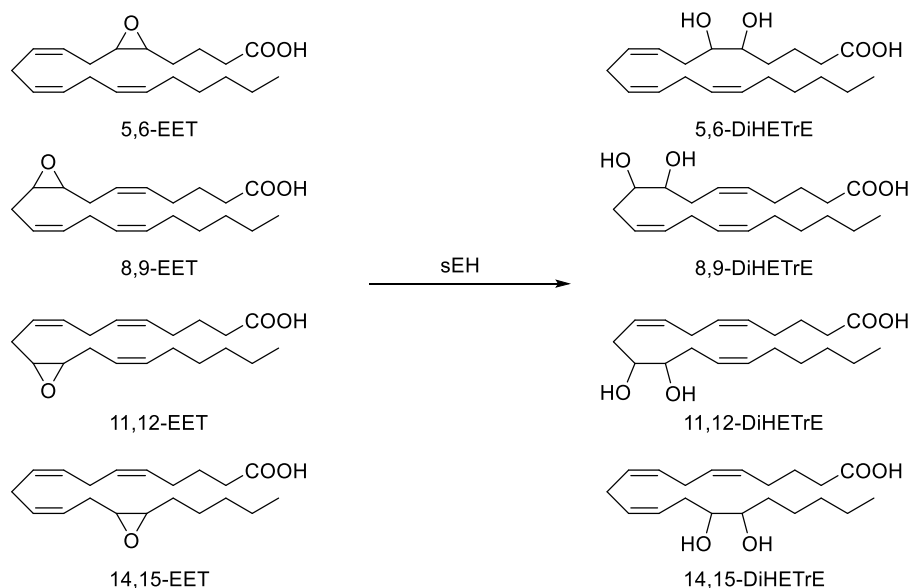


Figure 2. Transformation of active EETs to inactive DiHETrEs by the sEH enzyme.

¹² Newman, J.W.; Morisseau, C.; Hammock, B. D. *Prog. Lipid Res.* **2005**, *44*, 1-51.

¹³ Morisseau, C.; Hammock, B. D. *Annu. Rev. Pharmacol. Toxicol.* **2005**, *45*, 311-333.

sEH: structure and function

The human sEH is encoded by the *EPHX2* gene, composed of 19 exons and located in the short branch of chromosome 8, that encode for 555 amino acid residues. This enzyme belongs to the α/β -hydrolase fold family of proteins and is a homodimer composed of two monomeric subunits of 62 kDa arranged in anti-parallel fashion and separated by a short proline-rich linker (Figure 3).^{14,15,16}

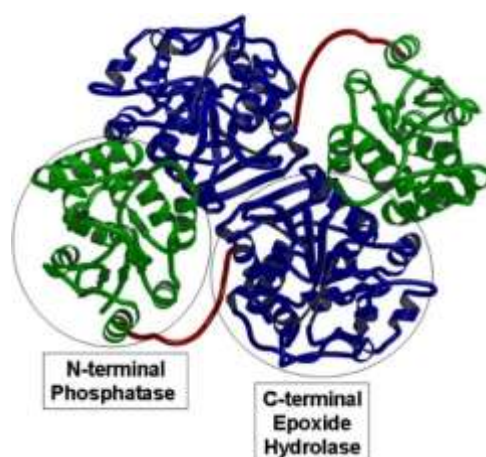


Figure 3. Structure of the human sEH dimer. The *N*-terminal domains are in green, the *C*-terminal domains are in blue, and the proline-rich linker segment (Ile-219-Asp-234) is in red. PDB 1S80.¹⁷ Figure taken from reference 14.

This enzyme, localized in the cytosol and in peroxisomes, has two distinct activities in two separate structural domains of each monomer.¹⁷ The *N*-terminal domain exhibits a phosphatase activity that hydrolyzes lipid phosphatases, while the *C*-terminal domain presents the epoxide hydrolase activity that converts epoxides to their corresponding diols.¹⁸

In contrast to the well-understood function of the *C*-terminal hydrolase domain, the role of the *N*-terminal phosphatase domain remains unclear.¹⁹ *In vitro*, the phosphatase

¹⁴ Harris, T. R.; Hammock, B. D. *Gene* **2013**, 526, 61-74.

¹⁵ Gomez, G. A.; Morisseau, C.; Hammock, B. D.; Christianson, D. W. *Biochemistry* **2004**, 43, 4716-4723.

¹⁶ Arand, M.; Cronin, A.; Oesch, F.; Mowbray, S. L.; Jones, T. A. *Drug Metab. Rev.* **2003**, 35, 365-383.

¹⁷ Gorman, J.; Shapiro, L. *Acta Crystallogr. Sect. D* **2004**, 60, 1600-1605.

¹⁸ Morisseau, C.; Sahdeo, S.; Cortopassi, G.; Hammock, B. D. *Anal. Biochem.* **2013**, 434, 105-111.

¹⁹ Kramer, J. S.; Woltersdorf, S.; Dufлот, T.; Hiesinger, K.; Lillich, F. F.; Knöll, F.; Wittman, S. K.; Klinger, F.-M.; Brunst, S.; Chaikuad, A.; Morisseau, C.; Hammock, B. D.; Buccellati, C.; Sala, A.; Rovati, G. E.; Leuillier,

activity of the *N*-terminal domain is able to hydrolyze diverse lipid phosphates, including farnesyl pyrophosphate, sphingosine-1-phosphate, and lysophosphatidic acid.²⁰ Although the mechanism of lipid phosphate hydrolysis is well-investigated,²¹ neither its endogenous substrate nor its physiological and possibly pathophysiological role have yet been identified.

In contrast, the function of the *C*-terminal domain is well-known and it provides the EH activity. The catalytic mechanism of the sEH has been elucidated in the last few years in order to define the key residues involved in the hydrolysis of the epoxides. All the EH are characterized by a catalytic triad that includes a nucleophilic aspartic acid and a histidine-aspartic pair and have a two-step mechanism involving the formation of a covalent intermediate. Computational studies and X-ray crystallographic data revealed that sEH has an “L shaped” hydrophobic pocket, whose branches measure 10 and 15 Å, respectively, and with the catalytic triad placed between them (Figure 4).²² Despite being mainly hydrophobic, each branch of the pocket features residues that are involved in specific interactions, such as hydrogen bonds, Van der Waals and π -stacking interactions. In addition, the branches are open to the solvent.

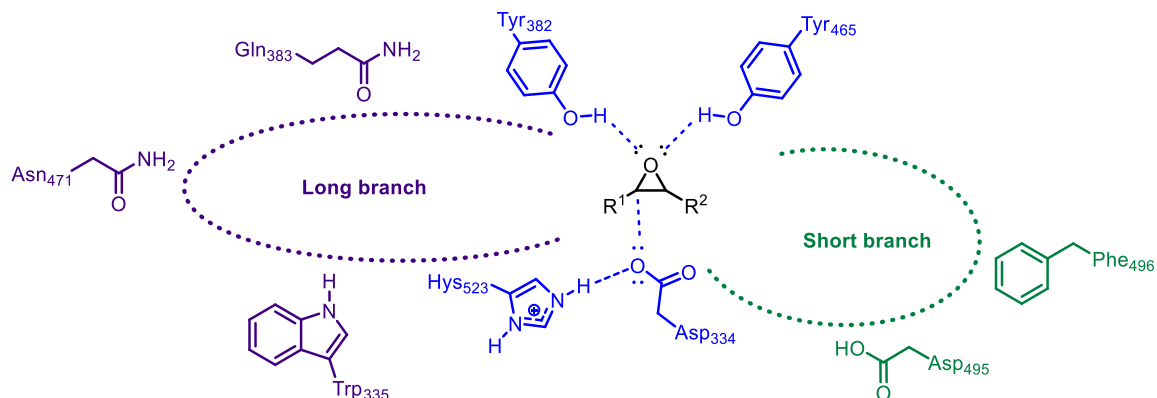


Figure 4. Schematic representation of the catalytic pocket of the sEH. Catalytic center (blue), long branch (purple) and short branch (green).

M.; Fraineau, S.; Rondeaux, J.; Hernandez-Olmos, V.; Heering, J.; Merk, D.; Pogoryelov, D.; Steinhilber, D.; Knapp, S.; Beillen, J.; Proschak, E. *J. Med. Chem.* **2019**, *62*, 8443-8460.

²⁰ Morisseau, C.; Schebb, N. H.; Dong, H.; Ulu, A.; Aronov, P. A.; Hammock, B. D. *Biochem. Biophys. Res. Commun.* **2012**, *419*, 796-800.

²¹ De Vivo, M.; Ensing, B.; Dal Peraro, M.; Gomez, G. A.; Christianson, D. W.; Klein, M. L. *J. Am. Chem. Soc.* **2007**, *129*, 387-394.

²² Amano, Y.; Yamaguchi, T.; Tanabe, E. *Bioorg. Med. Chem.* **2014**, *22*, 2427-2434.

The catalytic center is placed in the corner of the “L-shaped” tunnel and consists of two tyrosine residues (Tyr 382 and Tyr 465) that polarizes the epoxide by acting as hydrogen bond donors to activate the epoxide ring opening by the backside attack via an S_N2 -type reaction of the nucleophilic carboxylate of an aspartic acid residue (Asp334), oriented and activated by a histidine residue (His523), to form a hydroxyl alkyl-enzyme intermediate. Then, after different proton shifts, the intermediate is rapidly attacked by a water molecule releasing a diol product and the original enzyme (Figure 5).^{14,15,23,24,25}

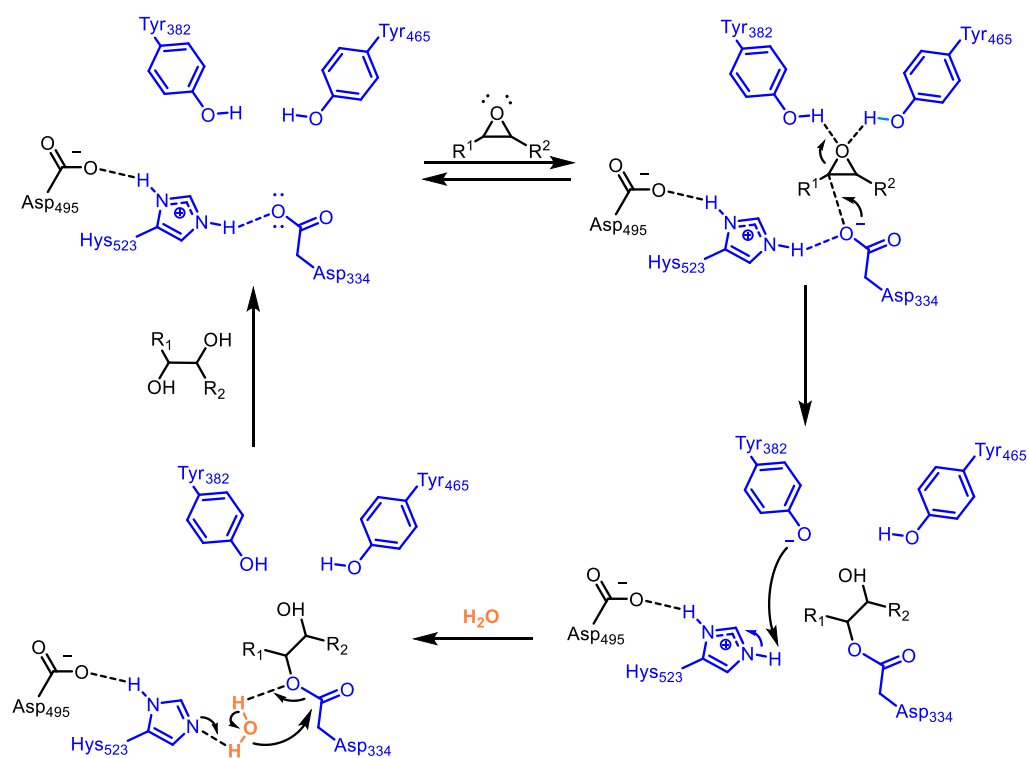


Figure 5. Putative catalytic mechanism of human sEH. The catalytic center (blue) promotes the hydrolysis of the epoxide of EET (black) to the corresponding DiHETrE using a water molecule (orange). In the last step of the cycle, the triad is reformed in order to hydrolyse another EET. Adapted from reference 13.

²³ Borhan, B.; Jones, A. D.; Pinot, F.; Grant, D. F.; Kurth, M. J.; Hammock, B. D. *J. Biol. Chem.* **1995**, *270*, 26923-26930.

²⁴ Arand, M.; Wagner, H.; Oesch, F. *J. Biol. Chem.* **1996**, *271*, 4223-4229.

²⁵ Schitt, B.; Bruice, T. C. *J. Am. Chem. Soc.* **2002**, *124*, 14558-14570.

sEH: tissue and subcellular distribution

Human sEH presents a widespread distribution pattern in several tissues and organs.²⁶ The specific activity of sEH is highest in the liver, followed by the kidney, lung, heart and brain. Moreover, sEH activity has also been observed in spleen, adrenals, intestine, urinary bladder, vascular endothelium and smooth muscle, placenta, skin, mammary gland, testicles and leucocytes.^{12,27}

Regarding the subcellular location, the sEH was historically referred to as the cytosolic EH based on the primary isolation of characteristic activity in cytosolic cellular fractions. Indeed, approximately 60% of the total sEH activity was isolated in the cytosol. However, the sEH has also been shown to localize in peroxisomes, being isolated in the light mitochondrial fraction.¹²

1.4. sEH as a potential therapeutic target

The beneficial properties of EETs and the regulation of their levels by the action of the sEH enzyme has gained interest in the last decades due to the huge therapeutical potential derived from the inhibition of the sEH. Indeed, the efficacy of sEHIs for the treatment of different diseases have been demonstrated in several animal models (Figure 6). The beneficial properties of EETs and the advantages from inhibiting sEH in several conditions will be discussed below.



Figure 6. Potential applications for sEHIs.

²⁶ Enayetallah, A. E.; French, R. A.; Thibodeau, M. S.; Grant, D. F. *J. Histochem. Cytochem.* **2004**, *52*, 447-454.

²⁷ Gill, S. S.; Hammock, B. D. *Biochem. Pharmacol.* **1980**, *29*, 389-395.

Inflammation

Inflammation is a complex, highly orchestrated process that has a domino-like effect on the initiation and development of a wide range of systemic illnesses.²⁸ In recent years, several *in vivo* and *in vitro* studies have provided support for the concept that EETs exhibit a broad spectrum of anti-inflammatory activity against acute and chronic inflammation.^{7,11,29,30}

EETs have been reported to play an important role in regulating inflammation³¹ following three main mechanisms: inhibition of the activation of nuclear factor κ B (NF- κ B) induced by TNF- α , activation of subfamilies of nuclear PPARs and down-regulating COX-2 transcription, resulting in lower production of pro-inflammatory prostaglandin E2 (PGE₂).^{32,33,34,35} Additionally, 11,12-EET blocks the nuclear translocation of the NF- κ B, by inhibiting the IKK, increases vascular cell adhesion molecule-1 (VCAM-1) expression in endothelial cells and decreases interleukin-1 β -induced fever, all of them known as pro-inflammatory mediators.²⁸ Moreover, EETs have been reported to activate GPCR, fact that increases the cyclic adenosine monophosphate (cAMP) levels. Given that the agents that elevate cAMP also inhibit the NF- κ B transcription, they are known to be anti-inflammatory agents (Figure 7).⁷

²⁸ Shahabi, P.; Siest, G.; Visvikis-siest, S. *Drug Metab. Rev.* **2014**, *46*, 33-56.

²⁹ Campbell, W. B.; Fleming, I. *Pflugers Arch.-Eur. J. Physiol.* **2010**, *459*, 881-895.

³⁰ Deng, Y.; Theken, K. N.; Lee, C. R. *J. Mol. Cell Cardiol.* **2010**, *48*, 331-341.

³¹ Node, K.; Huo, Y.; Ruan, X.; Yang, B.; Spiecker, M.; Ley, K.; Zeldin, D. C.; Liao, J. K. *Science* **1999**, *285*, 1276-1279.

³² Imig, J.; Hammock, B. *Nat. Rev. Drug Discov.* **2009**, *8*, 794-805.

³³ Morisseau, C. *Biochimie* **2013**, *95*, 91-95.

³⁴ Liu, Y.; Zhang, Y.; Schmelzer, K.; Lee, T.S.; Fang, X.; Zhu, Y.; Spector, A. A.; Gill, S.; Morisseau, C.; Hammock, B. D.; Shyy, J. Y.-J. *Proc. Natl. Acad. Sci. U. S. A.* **2005**, *102*, 16747-16752.

³⁵ Morisseau, C.; Hammock, B. D. *Annu. Rev. Pharmacol. Toxicol.* **2013**, *53*, 37-58.

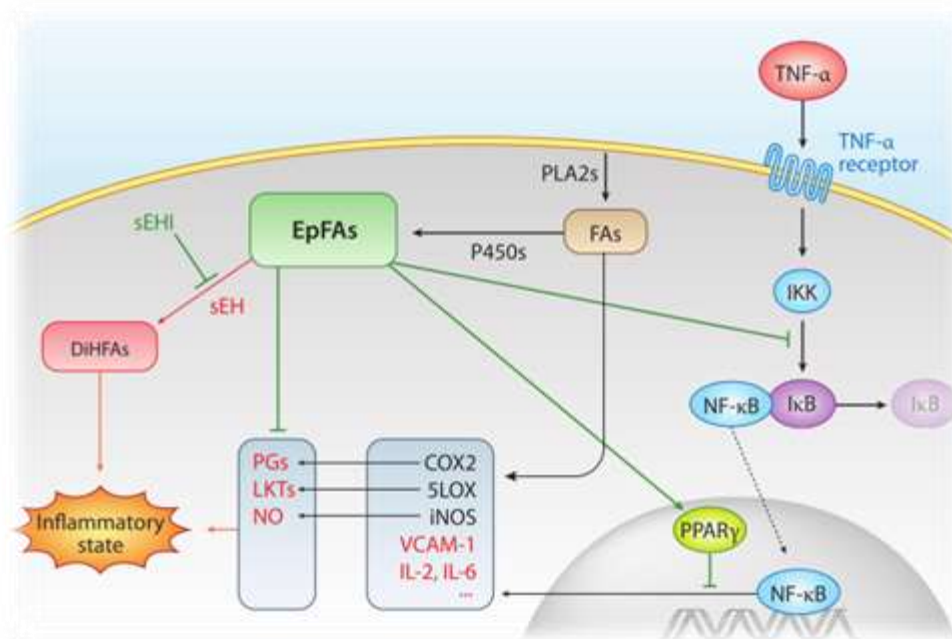


Figure 7. Effect of sEHIs by increasing epoxy-fatty acids (EpFAs) levels and blocking inflammation process through several mechanisms. PLA2: phospholipase A2. FAs: fatty acids. DiHFAs: dihydroxy-fatty acids. IKK: I κ B kinase. iNOS: inducible nitric oxide synthase. VCAM-1: vascular cell adhesion molecule 1. IL: interleukin. NO: nitric oxide. Figure taken from reference 35.

1.4.2.

Vasodilatation and Cardiovascular Diseases

Another therapeutic area of interest for sEHIs is cardiovascular diseases, especially due to the potent vasodilatory effects that present EETs. There are a number of mechanisms by which EETs can potentially affect blood pressure including direct effects on vascular tone in small resistance arteries and ascending dilation as well as action in the kidney through enhanced natriuresis.^{35,36}

All regioisomeric EETs are vasodilators, with 11,12-EET and 14,15-EET presenting the most important vasodilator activity. These two regioisomeric EETs are generated by endothelial cells and dilate blood vessels by activating large-conductance Ca^{2+} -activated K^+ channels on vascular smooth muscle cells, resulting in K^+ efflux from the smooth muscle cell and subsequent membrane hyperpolarization leading to a dilation of the vessels (Figure 8).^{32,37}

³⁶ Imig, J. D. *Am. J. Physiol. Regul. Integr. Comp. Physiol.* **2004**, *287*, R35.

³⁷ Ellinsworth, D. C.; Earley, S.; Murphy, T. V.; Sandow, S. L. *Pflugers Arch.* **2014**, *466*, 389-405.

This vasodilator effect of EETs has been confirmed by several studies using different sEHIs in various animal models of hypertension, resulting in an increase of the EET levels and the reduction of blood pressure.^{38,39}

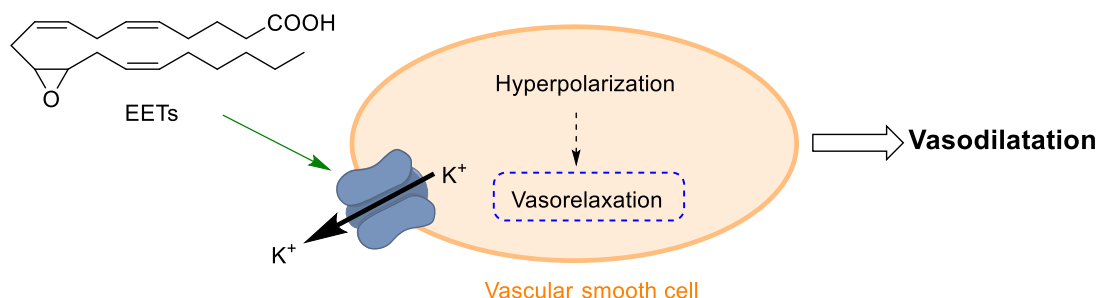


Figure 8: Mechanism of action for EETs on vascular tone, remarking the final relaxation of the muscle cell and subsequent dilation of blood vessels.

Apart from the vasodilatory activity of EET, the inhibition of sEH presents other benefits in cardiovascular diseases. Given that atherosclerosis is considered to be an inflammatory disease and is frequently associated with hypertension, it has been demonstrated that the inhibition of sEH in a mammalian model of atherosclerosis by an orally sEHI attenuates the atherosclerotic lesion formation.⁴⁰ Moreover, the inhibition of sEH in mice effectively decreases plasma LDL-C levels and effectively raises circulating high-density lipoprotein (HDL) and decreases the size of atherosclerotic plaque, inducing regression of atherosclerosis.⁴¹

Finally, it has been shown that sEHs have cardiovascular-protective effects in cerebral ischaemia, cardiac ischaemia, cardiac hypertrophy and arrhythmia,^{42,43,44,45}

³⁸ Loch, D.; Hoey, A.; Morisseau, C.; Hammock, B. O.; Brown, L. *Cell Biochem. Biophys.* **2007**, *47*, 87-98.

³⁹ Imig, J. D.; Zhao, X.; Zaharis, C. Z.; Olearczyk, J. J.; Pollock, D. M.; Newman, J. W.; Kim, I.-H.; Watanabe, T.; Hammock, B. D. *Hypertension* **2005**, *46*, 975-981.

⁴⁰ Ulu, A.; Davis, B. B.; Tsai, H.-J.; Kim, I.-H.; Morisseau, C.; Inceoglu, B.; Fiehn, O.; Hammock, B. D.; Weiss, R. H. *J. Cardiovasc. Pharmacol.* **2008**, *52*, 314-323.

⁴¹ Shen, L.; Peng, H.; Peng, R.; Fan, Q.; Zhao, S.; Xu, D.; Morisseau, C.; Chiamvimonvat, N.; Hammock, B. D. *Atherosclerosis* **2015**, *239*, 557-565.

⁴² Shrestha, A.; Krishnamurthy, P. T.; Thomas, P.; Hammock, B. D.; Hwang, S. H. *J. Pharm. Pharmacol.* **2014**, *66*, 1251-1258.

⁴³ Xu, D.; Davis, B. B.; Wang, Z.; Zhao, S.; Wasti, B.; Liu, Z.; Li, N.; Morisseau, C.; Chiamvimonvat, N.; Hammock, B. D. *Int. J. Cardiol.* **2013**, *167*, 1298-1304.

⁴⁴ Zhang, W.; Otsuka, T.; Sugo, N.; Ardeshiri, A.; Alhadid, Y. K.; Iliff, J. J.; DeBarber, A. E.; Koop, D. R.; Alkayed, N. J. *Stroke* **2008**, *39*, 2073-2078.

⁴⁵ Xu, D.; Li, N.; He, Y.; Timofeyev, V.; Lu, L.; Tsai, H.; Kim, I.; Tuteja, D.; Mateo, R. K. P.; Singapuri, A.; Davis, B. B.; Low, R.; Hammock, B. D.; Chiamvimonvat, N. *Proc. Natl. Acad. Sci. U. S. A.* **2006**, *103*, 18733-18738.

among others, suggesting that these agents have broad potential for the treatment of many cardiovascular diseases and associated morbidity.^{46,47,48}

Pain

Given the effectiveness in reducing inflammation in some rodent models,^{7,11,29,30,49} it was thought the sEHs to also reduce inflammatory pain. Using both thermal and mechanical models of hyperalgesia and allodynia in pain states induced by lipopolysaccharide, TNF- α , and carrageenan, sEHs were shown to return the pain sensation to normal state in a dose dependent manner.⁵⁰ Interestingly, the sEHs synergize in reducing inflammatory pain with NSAIDs and COX-2-selective inhibitors (COXIBs), and they reduce the vascular side effects associated with the use of these drugs.⁵¹

A different type of pain is the neuropathic pain (NP), which is a component of many disease states, such as diabetes mellitus, and there is no current treatment to treat it efficiently. Taking into account the effectiveness in reducing inflammation and inflammatory pain in some rodent models, it was not surprising that the inhibition of sEH also reduce NP.^{50,52,53} Although NSAIDs such as diclofenac are widely used for NP, their behavior in controlled studies is erratic. In the streptozotocin (STZ)-induced Type 1 diabetes rat model, celecoxib did not present beneficial effects on diabetes-induced NP, and diclofenac slightly reduced pain. However, the sEHs synergized with these COX inhibitors to reduce pain perception.⁵¹ In fact, it has been shown that sEHs can be used effectively in combination with NSAIDs and COXIBs not only to treat inflammatory pain but possibly also neuropathic and other chronic pain conditions while reducing the cardiovascular side effects associated with the long-term use of these COX inhibitors.⁵⁴

⁴⁶ Spector, A. A., Fang, X., Snyder, G. D., Weintraub, N. L. *Prog. Lipid Res.* **2004**, *43*, 55–90.

⁴⁷ Imig, J. D. *Cardiovasc. Drug Rev.* **2006**, *24*, 169–188.

⁴⁸ Marino, J. P. Jr. *Curr. Top. Med. Chem.* **2009**, *9*, 452-463.

⁴⁹ Pillarisetti, S.; Khanna, I. *Inflamm. Allergy Drug Targets* **2012**, *11*, 143-158.

⁵⁰ Hammock, B. D.; Wagner, K.; Inceoglu, B. *Pain Manage.* **2011**, *1*, 383-386.

⁵¹ Liu, J.-Y.; Li, N.; Yang, J.; Li, N.; Qiu, H.; Ai, D.; Chiamvimonvat, N.; Zhu, Y.; Hammock, B. D. *Proc. Natl. Acad. Sci. U. S. A.* **2010**, *107*, 17017-17022.

⁵² Wagner, K.; Inceoglu, B.; Dong, H.; Yang, J.; Hwang, S. H.; Jones, P.; Morisseau, C.; Hammock, B. D. *Eur. J. Pharmacol.* **2013**, *700*, 93-101.

⁵³ Sing, K.; Lee, S.; Liu, J.; Wagner, K. M.; Pakhomova, S.; Dong, H.; Morisseau, C.; Fu, S. H.; Yang, J.; Wang, P.; Ulu, A.; Mate, C. A.; Nguyen, L. V.; Hwang, S. H.; Edin, M. L.; Mara, A. A.; Wul, H.; Newcomer, M. E.; Zeldin, D. C.; Hammock, B. D. *J. Med. Chem.* **2014**, *57*, 7016-7030.

⁵⁴ Schmelzer, K. R.; Inceoglu, B.; Kubala, L.; Kim, I.; Jinks, S. L.; Eiserich, J. P.; Hammock, B. D. *Proc. Natl. Acad. Sci. U. S. A.* **2006**, *103*, 13646-13651.

Indeed, the sEHs have proven to be more potent than the commonly used gabapentin for pain relief in diabetic NP.⁵⁴

The mechanism by which the sEH intervenes in the nociception process has been confirmed to imply opioid and GABAergic pathways, as well as PPARs.⁵⁵ On one hand, EETs activate both PPAR α and PPAR γ inhibiting inflammatory gene expression including cytokines, vascular adhesion molecules, exert antioxidant properties and inhibit NF κ B activity. Moreover, intrathecal administration of an agonist of PPAR γ rapidly attenuated mechanical and thermal hypersensitivity associated with nerve injury in a dose-dependent manner.⁵⁶ Therefore, the activation of PPARs by EETs can affect not only inflammation but also pain. On the other hand, the antinociception produced by 14,15-EET appear to require opioid receptor without having any direct binding or affinity to them. Thus it appears that 14,15-EET activates, by yet to be identified mechanism, β -endorphin and met-enkephalin, which subsequently act on μ - and δ -opioid receptors to produce antinociception (Figure 9).⁵⁵ Additionally, it has been shown that NP is largely regulated by endoplasmic reticulum (ER) stress and that sEHs modulate this parameter.^{57,58}

In fact, the current objective of the pharmaceutical company EicOsis is to establish sEH as a valid therapeutic strategy for NP. Indeed, its candidate EC5026 has been recently introduced in phase 1 clinical trials for the treatment of NP associated with diabetes and has been given “fast-track” status for its clinical development by the FDA.^{59,60}

⁵⁵ Pillarisetti, S.; Khanna, I. *Drug Discov. Today* **2015**, *20*, 1382-1390.

⁵⁶ Oliveira, A. C. P.; Bertollo, C. M.; Rocha, L. T. S.; Nascimento, E. B.; Costa, K. A.; Coelho, M. M. *Eur. J. Pharmacol.* **2007**, *561*,194–201.

⁵⁷ Bettaieb, A.; Nagata, N.; Aboubechara, D.; Chahed, S.; Morisseau, C.; Hammock, B. D.; Haj, F. G. *J. Biol. Chem.* **2013**, *288*, 14189-14199.

⁵⁸ Inceoglu, B.; Bettaieb, A.; Trindade da Silva, C. A.; Lee, K. S. S.; Haj, F. G.; Hammock, B. D. *Proc. Natl. Acad. Sci. U. S. A.* **2015**, *112*, 9082-9087.

⁵⁹ U.S. National Library of Medicine. Clinicaltrials.gov. (2019). Identifier NCT04228302.

⁶⁰ <https://www.eicosis.com> (assessed 21 April, 2020).

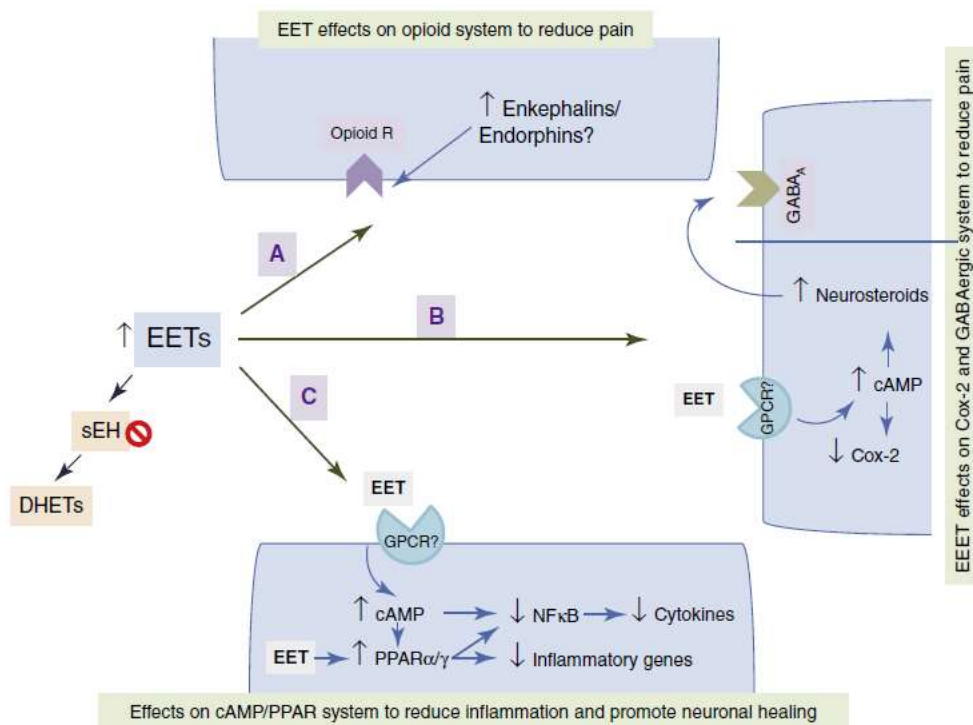


Figure 9. sEH inhibition can provide beneficial effects in NP through several pathways. EETs interact with GPCRs. **A:** 14,15 EET can induce, in neuronal cells, the endogenous opioid system (met-enkephalin and β -endorphin). Endogenous opioids can in turn act on opioid receptors to provide effective pain relief. **B:** In the presence of elevated cAMP, EETs can repress induction of COX-2 gene and induce StARD1 gene responsible for neurosteroids production, that are potent positive allosteric modulators of γ -aminobutyric acid A (GABA_A) receptor which play a crucial role in processing of peripheral nociceptive messages. **C:** EETs, through elevation of cAMP and/or activation of PPARs, can produce anti-inflammatory effects in neuronal and vascular endothelial cells. Figure taken from reference 55.

Diabetes and Metabolic Syndrome

Metabolic syndrome (MetS) is a multifactorial disease that consists of dyslipidemia, cardiovascular disease, type 2 diabetes mellitus, and obesity. MetS affects multiple organs and particularly their sensitivity to insulin. Indeed, insulin insensitivity is a characteristic feature of MetS and reflects the fact that higher concentrations of insulin are required to initiate insulin-dependent signaling events as well as the removal of glucose from the bloodstream. CYP-sEH pathway is intimately involved in regulating metabolic pathways and this pathway is altered in MetS and diabetes. Lipids regulate different metabolic processes, such as EETs, that play a significant role in the physiology and pathophysiology of the endocrine system in relation to glucose homeostasis.

In fact, EETs control the insulin release and the modulation of insulin sensitivity.⁶¹ In several different animal models of diabetes, increased expression of the sEH has been associated with increased ER stress in hepatic and adipose tissue. In contrast, poly unsaturated fatty acids (PUFA)-epoxides protect diverse tissues against diabetes and insulin resistance by reducing ER stress.⁶² It was observed that sEH KO (*Ephx2(-/-)*) mice presented a significant decrease in plasma glucose,⁶³ while prevented hyperglycaemia and increased insulin secretion in mice treated with STZ, a model of chemically induced diabetes.⁶⁴ Moreover, these findings were also confirmed with the pharmacological inhibition of sEH, that attenuated the hyperglycaemia induced in diabetic STZ-mice, improved glucose tolerance without affecting insulin tolerance and significantly reduced islet cell apoptosis, suggesting that the sEH inhibition provides significant protection against islet β -cell damage and improves glucose homeostasis in STZ-induced diabetes.⁶⁵

As mentioned before, EETs can activate PPAR- γ and, consequently, regulate adipogenesis and mediate the levels of different lipids contributing to metabolic homeostasis.^{66,67} Moreover, expression of sEH is increased in developing adipose tissue of obese mice, suggesting a role of sEH and EETs in lipid regulation and adipogenesis. Therefore, it has been shown that the inhibition of sEH has therapeutic potential in the control of diet-induced prediabetes and MetS. Indeed, the chronic administration of a potent sEHI in a chronic high-carbohydrate, high-fat feeding rats ameliorated the symptoms of MetS *in vivo* including glucose, insulin and lipid abnormalities, changes in pancreatic structure, increased cytosolic blood pressure and cardiovascular and liver structural and functional abnormalities. Moreover, the sEH inhibition also improved plasma liver enzymes and decreased steatosis compared to untreated animals.⁶⁸

⁶¹ Falck, J. R.; Manna, S.; Moltz, J.; Chacos, N.; Capdevila, J. *Biochem. Biophys. Res. Commun.* **1983**, *114*, 743-749.

⁶² Dos Santos, L. R. B.; Fleming, I. *Prostaglandins Other Lipid Mediat.* **2020**, *148*, 106407.

⁶³ Luria, A.; Bettaieb, A.; Xi, Y.; Shieh, G.-J.; Liu, H.-C.; Inoue, H.; Tsai, H.-J.; Imig, J. D.; Haj, F. G.; Hammock, B. D. *Proc. Natl. Acad. Sci. U. S. A.* **2011**, *108*, 9038-9043.

⁶⁴ Luo, P.; Chang, H.H.; Zhou, Y.; Zhang, S.; Hwang, S. H.; Morisseau, C.; Wang, C.-Y.; Inscho, E. W.; Hammock, B. D.; Wang, M.H. *J. Pharmacol. Exp. Ther.* **2010**, *334*, 430-438.

⁶⁵ Chen, L.; Fan, C.; Zhang, Y.; Bakri, M.; Dong, H.; Morisseau, C.; Maddipati, K. R.; Lui, P.; Wang, C.-Y.; Hammock, B. D.; Wang, M.-H. *Prostaglandins Other Lipid Mediat.* **2013**, *104-105*, 42-48.

⁶⁶ Iyer, A.; Fairlie, D. P.; Prins, J. B.; Hammock, B. D.; Brown, L. *Nat. Rev. Endocrinol.* **2010**, *6*, 71-82.

⁶⁷ De Taeye, B. M.; Morisseau, C.; Coyle, J.; Covington, J. W.; Luria, A.; Yang, J.; Murphy, S. B.; Friedman, D. B.; Hammock, B. B.; Vaughan, D. E. *Obesity* **2010**, *18*, 489-498.

⁶⁸ Iyer, A.; Kauter, K.; Alam, M. A.; Hwang, S. H.; Morisseau, C.; Hammock, B. D.; Brown, L. *Exp. Diabetes Res.* **2012**, *2012*, 14-16.

Finally, it has been shown that an increase in sEH expression may account for some of the organotypic changes usually linked with the development of insulin resistance. In this sense, one potential application for sEHs is the treatment of diabetic retinopathy, where sEH expression and activity is elevated.⁶⁹

Pulmonary Diseases

Whereas LOX inhibitors and other drugs are widely used to reduce acute lung inflammation, new drugs are needed for chronic lung inflammation.⁷⁰ In this sense, it was shown that epoxy fatty acids regulate pulmonary vascular tone and human lung inflammation.⁷¹ It was confirmed administering sEHs to a smoke-induced rat chronic obstructive pulmonary disease (COPD) model, which attenuate the inflammation associated with acute exposure to tobacco smoke.⁷² Moreover, the inhibition of sEH also improved lung function by reducing tobacco smoke-induced respiratory resistance and tissue damping.⁷³ Additionally, the administration of a sEHI alleviated bleomycin-induced inflammation and maintained the alveolar structure of the pulmonary tissues in a mouse model of pulmonary fibrosis.⁷⁴ These data suggest that sEH may be a potential therapeutic target for the treatment of COPD and other pulmonary disorders that present an inflammatory component, such as asthma and cystic fibrosis.

Indeed, the sEHI GSK2256294, developed by GlaxoSmithKline, is currently in clinical trials for the treatment of COPD in obese smokers. To date, it has been well-tolerated and demonstrated sustained inhibition of sEH activity.⁷⁵

⁶⁹ Hu, J.; Dziumbila, S.; Lin, J.; Bibli, S.-I.; Zukunftm S.; de Mos, J.; Awwad, K.; Frömel, T.; Jungmann, A.; Devraj, K.; Cheng, Z.; Wang, L.; Fauser, S.; Eberhart, C. G.; Sodhi, A.; Hammock, B. D.; Liebner, S.; Müller, O. J.; Glaubitz, C.; Hammes, H.-P.; Popp, R.; Fleming, I. *Nature*, **2017**, *552*, 248-252.

⁷⁰ Matera, M. G.; Calzetta, L.; Segreti, A.; Cazzola, M. *Expert Opin. Emerg. Drugs* **2012**, *17*, 61-82.

⁷¹ Morin, C.; Sirois, M.; Echave, V.; Albadine, R.; Rousseau, E. *Am. J. Respir. Cell Mol. Biol.* **2010**, *43*, 564–575.

⁷² Smith, K. R.; Pinkerton, K. E.; Watanabe, T.; Pedersen, T. L.; Ma, S. J.; Hammock, B. D. *Proc. Natl. Acad. Sci. U. S. A.* **2005**, *102*, 2186-2191.

⁷³ Wang, L.; Yang, J.; Guo, L.; Uyeminami, D.; Dong, H.; Hammock, B. D.; Pinkerton, K. E. *Am. J. Respir. Cell Mol. Biol.* **2012**, *46*, 614–22.

⁷⁴ Zhou, Y.; Sun, G. Y.; Liu, T.; Duan, J. X.; Zhou, H. F.; Lee, K. S.; Hammock, B. D.; Fang, X.; Jiang, J. X.; Guan, C. X. *Cell Tissue Res.* **2016**, *363*, 399-409.

⁷⁵ Lazaar, A. L.; Yang, L.; Boardley, R. L.; Goyal, N. S.; Robertson, J.; Baldwin, S. J.; Newby, D. E.; Wilkinson, I. B.; Tal-Singer, R.; Mayer, R. J.; Cheriyan, J. *Br. J. Clin. Pharmacol.* **2016**, *81*, 971-979.

Central Nervous System (CNS) Disorders

The study of the potential application of sEHs in neurodegenerative diseases has started recently. sEH is widely expressed in neurons, astrocytes and microvascular endothelial cells in the cortex, hippocampus and central nervous system vasculature, indicating that EETs are extensively metabolized in the CNS and exert a wide range of physiological effects, such as regulating neurohormone and neuropeptide release, promoting communication between neurons, and forming nerve-derived relaxing factors.⁷⁶ In fact, it has been described that EETs present neuroprotective effects by regulating neuronal excitability, increasing cerebral blood flow, inhibiting neuronal apoptosis, reducing neuroinflammation, promoting the recovery of neural function after a traumatic brain injury and reducing endoplasmic reticulum and oxidative stress.⁷⁷ Therefore, sEH has been shown to be a therapeutic target against a wide array of disease models with neuroinflammation as a common pathology and neuronal loss possibly through multiple anti-inflammatory and pro-survival signalling pathways.^{78,79} Indeed, several studies have related the inhibition of sEH with different CNS diseases such as neurodegenerative disorders,^{78,80,81} stroke,⁸² Parkinson,^{83,84,85} Alzheimer's disease (AD)^{86,87} or psychiatric diseases,^{83,88,89} among others.

⁷⁶ Nelson, J. W.; Young, J. M.; Borkar, R. N.; Woltjer, R. L.; Quinn, J. F.; Silbert, L. C.; Grafe, M. R.; Alkayed, N. J. *Prostaglandins Other Lipid Mediat.* **2014**, *113-115*, 30-37.

⁷⁷ Wang, L.; Luo, G.; Zhang, L.-F.; Geng, H.-X. *Prostaglandins Other Lipid Mediat.* **2018**, *138*, 9-14.

⁷⁸ Atone, J.; Wagner, K.; Hashimoto, K.; Hammock, B. D. *Prostaglandins Other Lipid Med.* **2020**, *147*, 106385.

⁷⁹ Zarriello, S. Tuazon, J. P.; Corey, S.; Schimmel, S.; Rajani, M.; Gorsky, A.; Incontri, D.; Hammock, B. D.; Borlongan, C. V. *Progress in Neurobiology* **2019**, *172*, 23–39

⁸⁰ Poli, G.; Corda, E.; Martino, P. A.; Dall'ara, P.; Bareggi, S. R.; Bondiolotti, G.; Iulini, B.; Mazza, M.; Casalone, C.; Hwang, S. H.; Hammock, B. D.; Inceoglu, B. *Life Sci.* **2013**, *21*, 1145-1150.

⁸¹ Wagner, K. M.; McReynolds, C. B.; Schmidt, W. K.; Hammock, B. D. *Pharmacol. Ther.* **2017**, *180*, 62-76.

⁸² Zhang, W.; Koerner, I. P.; Noppens, R.; Grafe, M.; Tsai, H. J.; Morisseau, C.; Luria, A.; Hammock, B. D.; Falck, J. R.; Alkayed, N. J. *J. Cereb. Blood Flow Metab.* **2007**, *27*, 1931-1940.

⁸³ Hashimoto, K. *Front. Pharmacol.* **2019**, *10*, 36.

⁸⁴ Qian, R.; Ma, M.; Yang, J.; Nonaka, R.; Yamaguchi, A.; Ishikawa, K.; Kobayashi, K.; Murayama, S.; Hwang, S. H.; Saiki, S.; Akamatsu, W.; Hattori, N.; Hammock, B. D.; Hashimoto, K. *Proc. Natl. Acad. Sci. U. S. A.* **2018**, *115*, E5815-E5823.

⁸⁵ Pallàs, M.; Vázquez, S.; Sanfeliu, C.; Galdeano, C.; Griñán-Ferré, C. *Biomolecules* **2020**, *10*, 703.

⁸⁶ Lee, H. T.; Lee, K. I.; Chen, C. H.; Lee, T.-S. *J. Neuroinflammation* **2019**, *16*, 267.

⁸⁷ Liang, Z.; Zhang, B.; Xu, M.; Morisseau, C.; Hwang, S. H.; Hammock, B. D.; Li, Q. *ACS Chem. Neurosci.* **2019**, *10*, 4018-4030.

⁸⁸ Ren, Q. *Front. Pharmacol.* **2019**, *10*, 420.

⁸⁹ Swardfager, W.; Hennebelle, M.; Yu, D.; Hammock, B. D.; Levitt, A. J.; Hashimoto, K.; Taha, A. Y. *Neurosci. Biobehav. Rev.* **2018**, *87*, 56-66.

Other potential indications for sEHs

The inhibition of sEH has been also considered for the treatment of other conditions. In brief, inhibitors of the sEH display a protective effect on renal damage induced by hypertension or inflammation.^{90,91} On the other hand, given the structural similarity of some sEHs with sorafenib, the only FDA-approved small molecule used for the treatment of advanced hepatocellular carcinoma, they have showed similar cytotoxicity than sorafenib in various human cancer cell lines.^{92,93,94}

1.5. Design of sEHs

Given the aforementioned enormous therapeutic potential of the regulation of EETs levels, the extensive knowledge about the mechanism of action of the sEH and the growing number of crystal structures of the enzyme that helped in the identification of a diversity of functional groups that can be considered for the ligand design, it seems reasonable that several academic groups and pharmaceutical companies have been interested on the discovery of potent sEHs for the development of therapeutic agents. Indeed, since the early 2000s, inhibitors of sEH have been under active development and major advances have been made in their potency and pharmacokinetic properties, allowing oral administration.

From an academic point of view, the research group of Prof. Bruce D. Hammock from the University of California Davis (UCD) has been the major contributor of sEHs.^{35,95,96,97} Some pharmaceutical companies have also entered the arena of the discovery of potent sEHs, such as Boehringer Ingelheim, Merck, Astellas Pharma, Hoffman La Roche, Sumitomo, Pfizer and AstraZeneca. Although all of them have published several

⁹⁰ Zhao, X.; Yamamoto, T.; Newman, J. W.; Kim, I.H.; Watanabe, T.; Hammock, B. D.; Stewart, J.; Pollock, J. S.; Pollock, D. M.; Imig, J. D. *J. Am. Soc. Nephrol.* **2004**, *15*, 1244-1253.

⁹¹ Olearczyk, J. J.; Quigley, J. E.; Mitchell, B. C.; Yamamoto, T.; Kim, I.-H.; Newman, J. W.; Luria, A.; Hammock, B. D.; Imig, J. D. *Clin. Sci.* **2009**, *116*, 61-70.

⁹² Lui, J.-Y.; Park, S.-H.; Morisseau, C.; Hwang, S. H.; Hammock, B. D.; Weiss, R. H. *Mol. Cancer Ther.* **2009**, *8*, 2193-2203.

⁹³ Wecksler, A. T.; Hwang, S. H.; Wettersten, H. I.; Gilda, J. E.; Patton, A.; Leon, L. J.; Carraway, K. L.; Gomes, A. V.; Baar, K.; Weiss, R. H.; Hammock, B. D. *Anticancer. Drugs* **2014**, *25*, 433-446.

⁹⁴ Wecksler, A. T.; Hwang, S. H.; Liu, J.Y.; Wettersten, H. I.; Morisseau, C.; Wu, J.; Weiss, R. H.; Hammock, B. D. *Cancer Chemother. Pharmacol.* **2015**, *75*, 161-171.

⁹⁵ Shen, H. C. *Expert Opin. Ther. Pat.* **2010**, *20*, 941-956.

⁹⁶ Kodani, S. D.; Hammock, B. D. *Drug Metab. Dispos.* **2015**, *43*, 788-802.

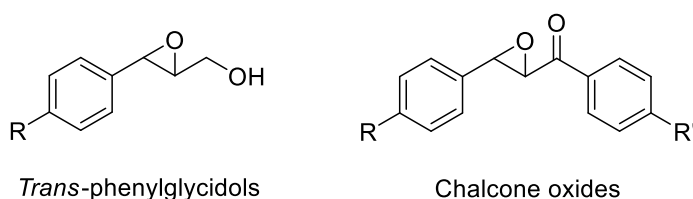
⁹⁷ Shen, H. C.; Hammock, B. D. *J. Med. Chem.* **2012**, *55*, 1789-1808.

articles and have applied for patent applications, it seems that nowadays only GSK is actively working on this field, having a candidate in several clinical trials.

The structural types of sEHs are extremely broad, which is consistent with the wide binding pocket of the enzyme. An historical review of the discovery of sEH follows below.

Early inhibitors

The first compounds to show inhibitory activity of sEH were *trans*-3-phenylglycidols and substituted chalcone oxides (Figure 10). The *trans*-3-phenylglycidols are enantioselective slow-binding inhibitors of sEH. Some examples showed potency in the low micromolar range, except the ones that do not feature the hydroxyl group that presented a clear decreased potency.⁹⁸ Substituted chalcone oxides are more potent inhibitors than the previous ones, mostly because their mechanism of action involves a stable covalent enzyme-inhibitor intermediate.⁹⁹ Unfortunately, these early inhibitors of the sEH were too unstable for their effective use in *in vitro* and *in vivo* assays, because they were rapidly inactivated by glutathione transferases.^{96,97,100}



1.5.2.

Figure 10. Early inhibitors of the sEH.

Discovery of the pharmacophore

Since the early 2000s, several pharmacophores have emerged demonstrating that functional groups such as ureas, carbamates, amides, thioureas and, in a less extent, thioesters, carbonates and esters fit well into the active site of the sEH. Therefore, in recent years, there has been a significant and rapid development of compounds

⁹⁸ Dietze, E. C.; Kuwano, E.; Casas, J.; Hammock, B. D. *Biochem. Pharmacol.* **1991**, *42*, 1163-1175.

⁹⁹ Morisseau, C.; Du, G.; Newman, J. W.; Hammock, B. D. *Arch. Biochem. Biophys.* **1998**, *356*, 214-228.

¹⁰⁰ Mullin, C. A.; Hammock, B. D. *Arch. Biochem. Biophys.* **1982**, *216*, 423-439.

featuring mainly a urea or amide group as reversible sEHIs.^{101,102,103,104} The design of these compounds was based on the knowledge of the catalytic mechanism of the enzyme. Indeed, urea is the most used group as a central pharmacophore for the design of sEHIs, as it mimics the endogenous epoxide substrate by binding to the key residues of the catalytic center. Thus, the oxygen atom of the carbonyl of the urea presents hydrogen bond interactions with both tyrosines, Tyr382 and Tyr465, mimicking the oxygen atom of the endogenous epoxide. On the other hand, the NH groups of the urea act as hydrogen bond donors to the aspartic acid residue Asp334. For this reason, these inhibitors are known as transition state competitive inhibitors (Figure 11).¹⁰⁵

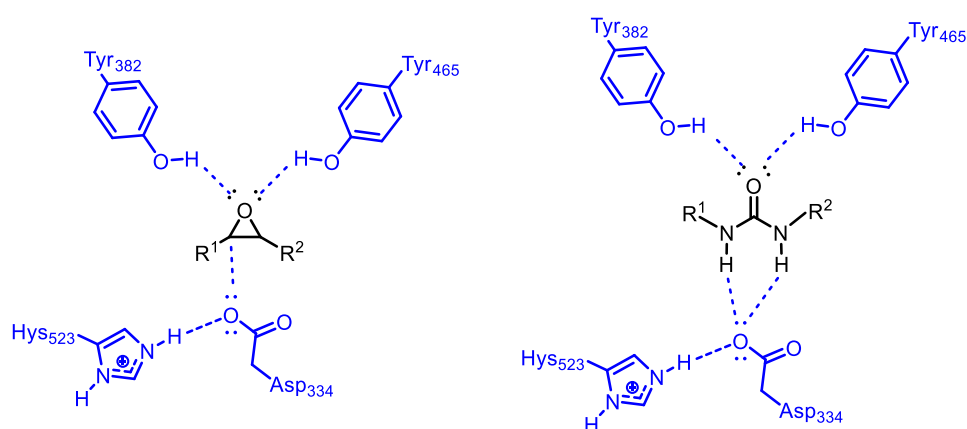


Figure 11. Schematic representation of the hydrogen bond interactions of the endogenous epoxide and the urea group with the active site of the sEH. Adapted from reference 105.

Urea derivatives are a subclass of selective and stable sEHIs with improved bioavailability compared with chalcone oxides and *trans*-3-phenylglycidols. Ureas are potent inhibitors of both the rodent and human sEH with IC₅₀ in the low nanomolar or even subnanomolar range.

¹⁰¹ Morisseau, C.; Goodrow, M. H.; Dowdy, D.; Zheng, J.; Greene, J. F.; Sanborn, J. R.; Hammock, B. D. *Proc. Natl. Acad. Sci. U. S. A.* **1999**, *96*, 8849-8854.

¹⁰² Nakagawa, Y.; Wheelock, C. E.; Morisseau, C.; Goodrow, M. H.; Hammock, G.; Hammock, B. D. *Bioorg. Med. Chem.* **2000**, *8*, 2663-2675.

¹⁰³ McElroy, N. R.; Jurs, P. C.; Morisseau, C.; Hammock, B. D. *J. Med. Chem.* **2003**, *46*, 1066-1080.

¹⁰⁴ Anandan, S. K.; Do, Z. N.; Webb, H. K.; Patel, D. V.; Gless, R. D. *Bioorg. Med. Chem. Lett.* **2009**, *19*, 1066-1070.

¹⁰⁵ Gomez, G. A.; Morisseau, C.; Hammock, B. D.; Christianson, D. W. *Protein Sci.* **2006**, *15*, 58-64.

The first lead was a common reaction side product in organic chemistry, *N,N'*-dicyclohexylurea (DCU), displaying good inhibitory activity against the human enzyme.¹⁰¹ Indeed, DCU was the first urea used *in vivo* to demonstrate potential beneficial cardiovascular actions of the sEHIs, lowering blood pressure in hypertensive rats, although it did not have the physical properties necessary for pharmaceutical formulation.¹⁰⁶ Then, one cyclohexyl group was substituted by an alkyl chain to obtain *N*-cyclohexyl-*N'*-dodecylurea (CDU), that presented *in vivo* efficacy protecting the kidney in a rat model of angiotensine-dependent hypertension.⁹⁰ Unfortunately, the use of this drug was also limited due to its rapid metabolisation in hepatic microsomes, leading to a more water-soluble carboxylic derivative.¹⁰⁷ Then, to increase water solubility and allow oral administration, a carboxylic acid was added at the end of the hydrocarbon chain to form the 12-(3-cyclohexylureido)dodecanoic acid (CUDA).

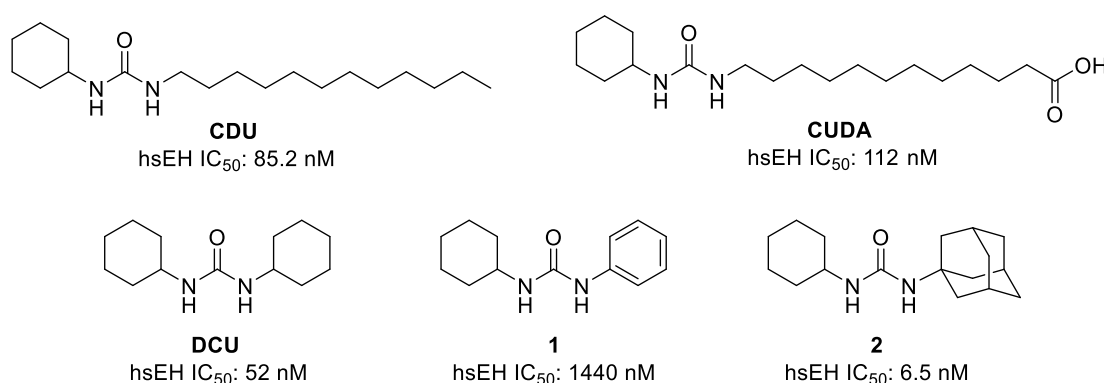


Figure 12. First series of cyclohexyl-based potent sEHIs with limited stability and water solubility.

In fact, different carbocyclic substituents were introduced, such as phenyl, cyclooctyl and adamantyl groups, among others, leading to potent inhibitors (Figure 12). Regrettably, these dialkylureas presented high melting points and limited water solubility.¹⁰⁸

¹⁰⁶ Yu, Z.; Xu, F.; Huse, L. M.; Morisseau, C.; Draper, A. J.; Newman, J. W.; Parker, C.; Graham, L.; Engler, M. M.; Hammock, B. D.; Zeldin, D. C.; Kroetz, D. L. *Circ. Res.* **2000**, *87*, 992-998.

¹⁰⁷ Watanabe, T.; Morisseau, C.; Newman, J. W.; Hammock, B. D. *Drug Metab. Dispos.* **2003**, *31*, 846-853.

¹⁰⁸ Morisseau, C.; Goodrow, M. H.; Newman, J. W.; Wheelock, C. E.; Dowdy, D. L.; Hammock, B. D. *Biochem. Pharmacol.* **2002**, *63*, 1599-1608.

Adamantane-based inhibitors

From this first series of compounds, the adamantane moiety presented the highest inhibition activity against the human sEH. Taking into account the characteristics of the binding site of sEH and the overall high hydrophobicity of the tunnel, the introduction of an adamantane ring proved to be a successful strategy for the space-filling of the cavity.^{1,5,3.} Incorporation of functional polar groups, such as carboxylic acid, into the alkyl chain of adamantyl-based ureas resulted in compounds that were weak structural mimics of EETs with improved physical properties.^{108,109} In this sense, a substitution of the cyclohexyl of CUDA by an adamantyl group led to 12-(3-(1-adamantyl)ureido)dodecanoic acid (AUDA), that exhibited excellent inhibition of murine and human sEH and enhanced water solubility.¹⁰⁸ AUDA emerged as an improved sEHI and has been extensively used as a tool molecule to validate efficacy in models of hypertension, cardio-protection and inflammation.^{39,43,109,110} Moreover, addition of polar ethylene glycol linkers in the alkyl chain afforded new compounds with similar properties as AUDA, such as N-adamantyl-*N'*-[5-(2-(2-ethoxyethoxy)ethoxy)pentyl]urea (AEPU) (Figure 13).

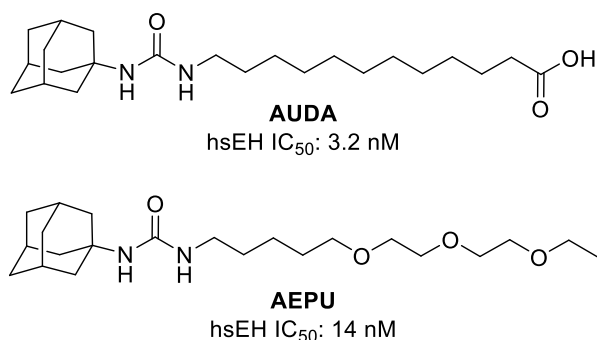


Figure 13. Improved sEH featuring an adamantane moiety with enhanced water solubility but presenting rapid metabolism.

¹⁰⁹ Dorrance, A. M.; Rupp, N.; Pollock, D. M.; Newman, J. W.; Hammock, B. D.; Imig, J. D. *J. Cardio. Pharm.* **2005**, *46*, 842-848.

¹¹⁰ Gross, G. J.; Nithipatikom, K. *Curr. Opin. Investig. Drugs* **2009**, *10*, 253-258.

These compounds further improved water solubility and lowered melting points than DCU and CDU, but they were still rapidly metabolised through β -oxidation because of the alkyl chain.^{111,112} In order to improve physical properties, particularly solubility and stability of these disubstituted ureas, extensive SAR studies were carried out to introduce new polar pharmacophores. Importantly, with the aim to eliminate the possibility of β -oxidation, the alkyl chain was replaced by a conformationally restricted molecule in the right-hand side (RHS) of the molecule, such as a heterocycle or a phenyl ring.^{113,114} The group of Prof. B. D. Hammock designated a general structure for the design of new sEHs, with the urea or amide moiety as the primary pharmacophore that interacts with the catalytic triad of sEH. At least one free NH is needed, since hydrogen bond-stabilized salt bridges are formed between this group and residues of the C-terminal domain of sEH.¹¹⁵ This fact supports the hypothesis that ureas and their derivatives mimic features that are present in transient intermediates or transition states that occur during the epoxide ring opening of the EETs by sEH. Then, a secondary pharmacophore was designed with polar functional groups such as carbonyl, ester, ether, sulfonamide, or amide being ~ 7 Å away from the urea carbonyl, in order to improve aqueous solubility and PK (pharmacokinetic) properties without reducing potency. Moreover, a polar tertiary pharmacophore such as an ester, ether, acid, or amine that is 13 atoms or ~ 17 Å away from the urea carbonyl was also identified. The linker that connects the primary and the secondary pharmacophores, or the secondary and the tertiary pharmacophores, can be either a conformationally flexible alkyl or restricted cyclic structures such as aryl, cycloalkyl, or azacycloalkyl group (Figure 14).^{97,116} Interestingly, it was discovered that when the linker is constituted by conformationally restricted cyclic groups, the oral bioavailability is higher than with flexible alkyl chains. Apart from improving metabolic stability of the compounds, the incorporation of the secondary and tertiary pharmacophores enhanced the water solubility and lowered the melting points.

¹¹¹ Hwang, S. H.; Tsai, H.; Liu, J.; Morisseau, C.; Hammock, B. D. *J. Med. Chem.* **2007**, *50*, 3825-3840.

¹¹² Liu, J.-Y.; Tsai, H.-J.; Morisseau, C.; Lango, J.; Hwang, S. H.; Watanabe, T.; Kim, I.-H.; Hammock, B. D. *Biochem. Pharmacol.* **2015**, *98*, 718-731.

¹¹³ Jones, P. D.; Tsai, H. J.; Do, Z. N.; Morisseau, C.; Hammock, B. D. *Bioorg. Med. Chem. Lett.* **2006**, *16*, 5212-5216.

¹¹⁴ Rose, T. E.; Morisseau, C.; Liu, J.-Y.; Inceoglu, B.; Jones, P. D.; Sanborn, J. R.; Hammock, B. D. *J. Med. Chem.* **2010**, *53*, 7067-7075.

¹¹⁵ Ingraham, R.H.; Gless, R. D.; Lo, H. Y. *Curr. Med. Chem.* **2011**, *18*, 587-603.

¹¹⁶ Kim, I. H.; Heitzler, F. R.; Morisseau, C.; Nishi, K.; Tsai, H. J.; Hammock, B. D. *J. Med. Chem.* **2005**, *48*, 3621-3629.

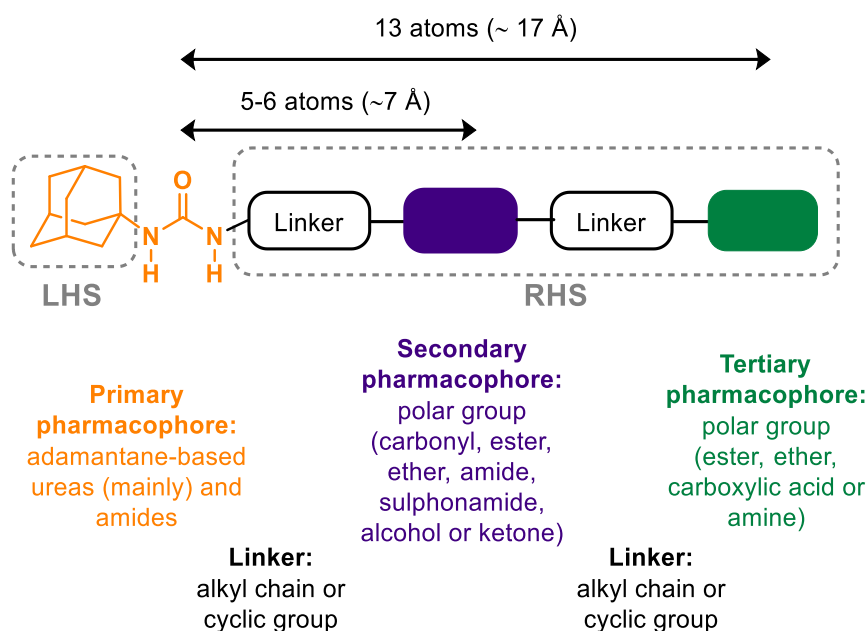


Figure 14. Representation of general structure for the design of improved adamantane-based inhibitors. RHS: Right-hand side. LHS: Left-hand side. Figure adapted from reference 97.

1.5.4. Improved adamantane-based sEHIs

In order to eliminate the possibility of β -oxidation, the alkyl chain was replaced by a conformational restricted group. The linker between the primary and secondary pharmacophores was defined as a saturated ring, such as piperidine or cyclohexane (*trans*-4-[4-(3-adamantan-1-yl-ureido)cyclohexyloxy]benzoic acid, *t*-AUCB), or an aromatic ring, as in the case of the salicylate **3** (Figure 15).

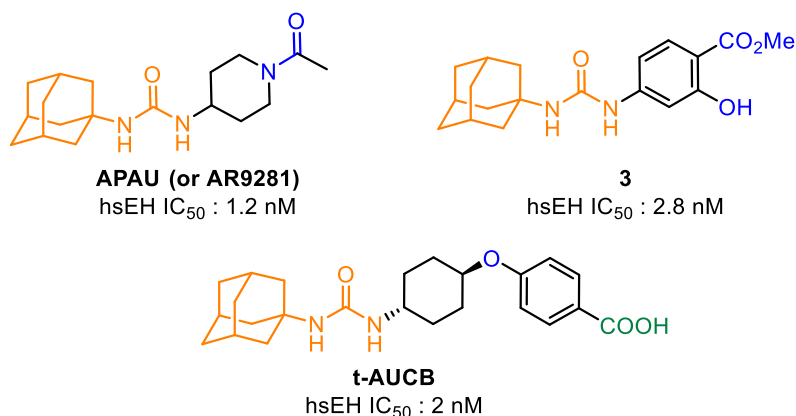


Figure 15. Structures of some potent sEHIs featuring a conformationally restricted RHS, with improved microsomal stability against β -oxidation. Primary pharmacophore coloured in orange, linkers in black, secondary pharmacophore in blue and tertiary pharmacophore in green.

In the case of the salicylate urea-based sEH **3**, where the linker is a phenyl group, the compound exhibited good potency and excellent stability, which was further reflected by its superior oral drug exposure compared with AUDA.¹¹⁷ Another compound designed following the general structure described by Prof. Hammock was *t*-AUCB (Figure 16), an orally bioavailable sEH with excellent inhibitory potency against the sEH from a variety of species, and stable against the human microsomes.¹¹¹

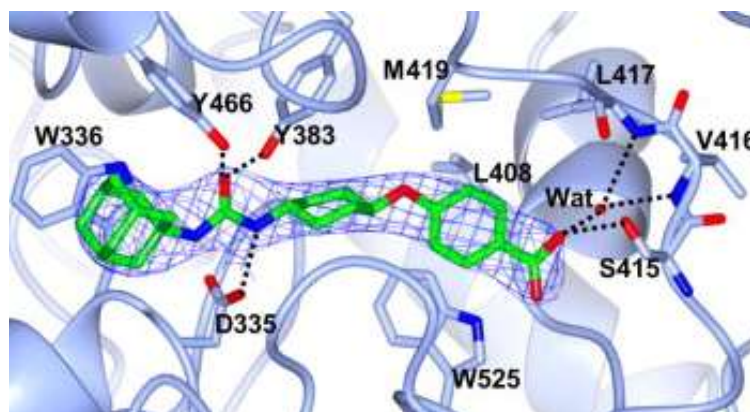


Figure 16. Crystal structure of *t*-AUCB (green) bound to sEH (PDB ID code 3WKE). Figure taken from reference 22.

Importantly, a piperidine moiety was identified as a promising linker between the primary and secondary pharmacophores, resulting in highly potent analogues such as APAU,¹¹³ that presented promising results in several *in vitro* and *in vivo* efficacy studies^{118,119,120,121, 122, 123} and was the first sEH inhibitor to reach clinical trials.

¹¹⁷ Kasagami, T.; Kim, I. H.; Tsai, H.-J.; Nishi, K.; Hammock, B. D.; Morisseau, C. *Bioorg. Med. Chem. Lett.* **2009**, *19*, 1784–1789.

¹¹⁸ Anandan, S.-K.; Webb, H. K.; Chen, D.; Wang, Y.-X.; Aavula, B. R.; Cases, S.; Cheng, Y.; Do, Z. N.; Mehra, U.; Tran, V.; Vincelette, J.; Waszczuk, J.; White, K.; Wong, K. R.; Zhang, L.-N.; Jones, P. D.; Hammock, B. D.; Patel, D. V.; Whitcomb, R.; MacIntyre, D. E.; Sabry, J.; Gless, R. *Bioorg. Med. Chem. Lett.* **2011**, *21*, 983, 988.

¹¹⁹ Guglielmino, K.; Kaleena, Harris, T. R.; Vu, V.; Dong, H.; Dutrow, G.; Evans, J. E.; Graham, J.; Cummings, B. P.; Havel, P. J.; Chiamvimonvat, N.; Despa, S.; Hammock, B. D.; Despa, F. *Am. J. Physiol. Heart Circ. Physiol.* **2012**, *303*, H853-H862.

¹²⁰ Lakkapa, N.; Krishnamurty, P. T.; M. D., P.; Hammock, B. D.; Hwang, S. H. *Neurotoxicology*, **2019**, *70*, 135-145.

¹²¹ Zhang, L.-N.; Vincelette, J.; Chen, D.; Gless, R. D.; Anandan, S.-K.; Rubanyi, G. M.; Webb, H. K.; MacIntyre, D. E.; Wang, Y.-X. *Eur. J. Pharmacol.* **2011**, *654*, 68-74.

¹²² Imig, J. D.; Carpenter, M. A.; Shaw, S. *Pharmaceuticals*, **2009**, *2*, 217-227.

¹²³ Do Carmo, J. M.; da Silva, A. A.; Morgan, J.; Wang, Y.-X.; Munusamy, S.; Hall, J. E. *Nutr. Metab. Cardiovasc. Dis.* **2012**, *22*, 598-604.

Non adamantane-based sEHs

Although the adamantane-based inhibitors are endowed with excellent inhibitory potencies, it has been shown that the adamantane moiety does not possess the optimal drug-like properties. First, the high lipophilicity of the adamantane moiety permits this group to fit very well in the hydrophobic pocket of the sEH, but compromises negatively the water solubility of the molecule. This is an important parameter as poorly soluble compounds not only create problems for *in vitro* and *in vivo* assays in drug discovery, but also place a significant burden on drug development.¹²⁴ Second, the adamantane nucleus is prone to rapid metabolism *in vivo* giving rise to a variety of less active or even inactive hydroxylated derivatives. This results in low drug concentrations in blood and short *in vivo* half-life.¹¹² Finally, the important lipophilicity of the adamantane moiety results in an increased probability of binding to multiple targets, leading to possible side effects and/or toxicity.

Given the aforementioned issues of the adamantane nucleus, the left-hand side of the compounds was modified replacing the adamantyl moiety either by a phenyl ring or by other polycyclic rings, resulting in several analogues with subnanomolar IC₅₀ against sEH.¹¹⁴ Moreover, some pharmaceutical companies have also entered in the field of the discovery of potent sEHs without featuring the adamantane moiety, mainly in the context of the treatment of hypertension (Figures 17 and 18).^{125,126,127,128,129,130,131} The properties of the most relevant examples are discussed below.

¹²⁴ Di, L.; Fish, P. V.; Mano, T. *Drug Discov. Today* **2012**, *17*, 486-495.

¹²⁵ Takai, K.; Nakajima, T.; Takanashi, Y.; Sone, T.; Nariai, T.; Chiyo, N.; Nakatani, S.; Ishikawa, C.; Yamaguchi, N.; Fujita, K.; Yamada, K. *Bioorg. Med. Chem.* **2014**, *22*, 1548-1557.

¹²⁶ Taylor, S. J.; Soleymanzadeh, F.; Eldrup, A. B.; Farrow, N. A.; Muegge, I.; Kukulka, A.; Kabcenell, A. K.; De Lombaert, S. *Bioorg. Med. Chem. Lett.* **2009**, *19*, 5864-5868.

¹²⁷ Eldrup, A. B.; Soleymanzadeh, F.; Farrow, N. A.; Kukulka, A.; De Lombaert, S. *Bioorg. Med. Chem. Lett.* **2010**, *20*, 571-575.

¹²⁸ Kato, Y.; Fuchi, N.; Nishimura, Y.; Watanabe, Q.; Yagi, M.; Nakadera, Y.; Higashi, E.; Yamada, M.; Aoki, T.; Kigoshi, H. *Bioorg. Med. Chem. Lett.* **2014**, *24*, 565-570.

¹²⁹ Shen, H. C.; Ding, F.-X.; Wang, S.; Deng, Q.; Zhang, X.; Chen, Y.; Zhou, G.; Xu, S.; Chen, H.; Tong, X.; Tong, V.; Mitra, K.; Kumar, S.; Tsai, C.; Stevenson, A. S.; Pai, L.-Y.; Alonso-Galicia, M.; Chen, X.; Soisson, S. M.; Roy, S.; Zhang, B.; Tata, J. R.; Berger, J. P.; Colletti, S. L. *J. Med. Chem. Lett.* **2009**, *52*, 5009-5012.

¹³⁰ Xing, L.; McDonald, J. J.; Kolodziej, S. A.; Kurumbail, R. G.; Williams, J. M.; Warren, C. J.; O'Neal, J. M.; Skepner, J. E.; Roberds, S. L. *J. Med. Chem.* **2011**, *54*, 1211-1222.

¹³¹ Eldrup, A. B.; Soleymanzadeh, F.; Taylor, S. J.; Muegge, I.; Farrow, N. A.; Joseph, D.; McKellop, K.; Man, C. C.; Kukulka, A.; De Lombaert, S. *J. Med. Chem.* **2009**, *52*, 5880-5895.

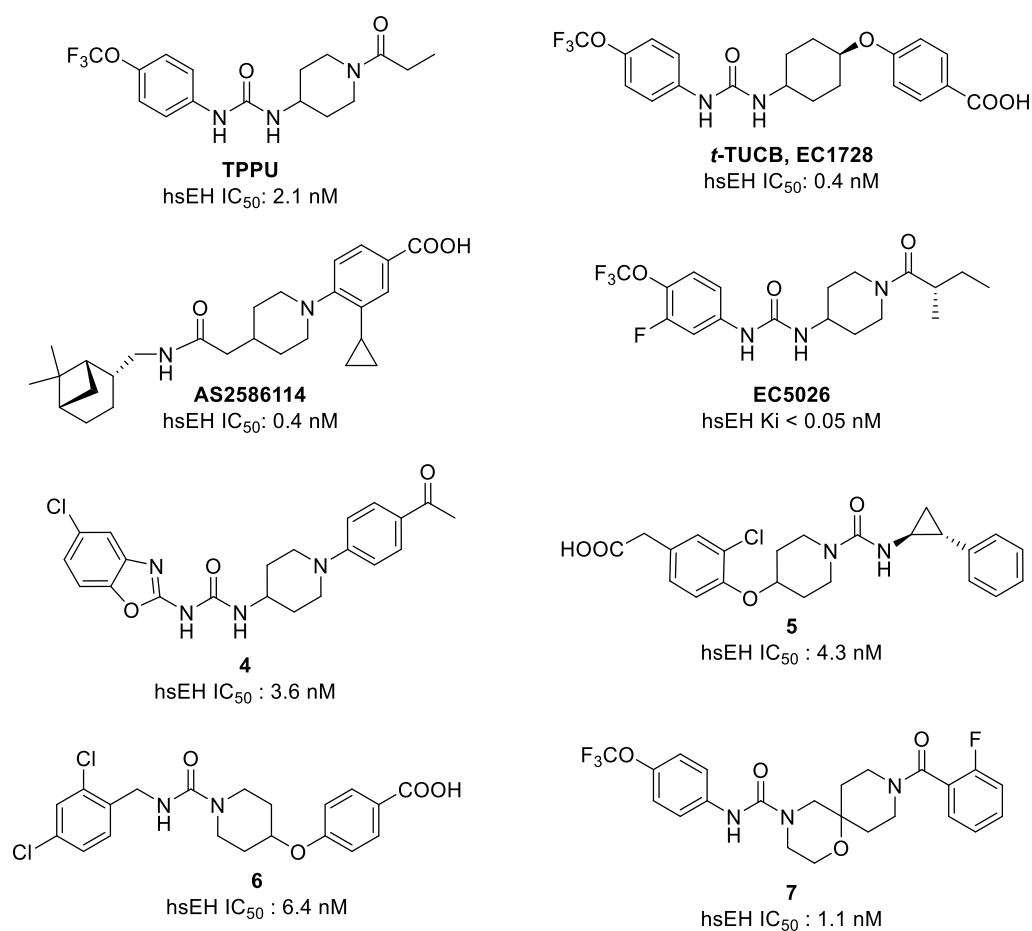


Figure 17. Structure and potency of some of the most relevant sEHIs featuring a phenyl ring or alternative hydrophobic polycyclic rings in the LHS of the molecule.

TPPU was developed by the group of Prof. Hammock at UCD. It is an analogue of the clinical candidate APAU (AR9281), in which the adamantane moiety has been replaced by a substituted phenyl ring. TPPU maintains the excellent inhibitory activity of previous ureas, improving solubility and pharmacokinetic properties compared to APAU.¹¹⁴

TPPU is commercially available and is the most widely used sEHI in both *in vitro* and *in vivo* assays to demonstrate the efficacy of sEHI in several disease models, including dogs and primates,^{114,132,133,134,135,136} and moderately penetrates the blood-brain barrier (BBB).¹³⁷ Moreover, apart from inhibiting the sEH, it is a potent inhibitor of p38 kinase, also involved in inflammatory processes.⁸⁷

t-TUCB (EC1728) was also developed by Prof. Hammock's group.¹¹¹ This potent sEHI has been successfully tested in several animal models^{42,138,139} and, importantly, in the treatment of laminitis suffered by horses.¹⁴⁰ Due to the promising results on treating this inflammation that progress to the inability to walk, the company EicOsis, a *spin-off* from the UCD, is developing this product for veterinary use.¹⁴¹

AS2586114, an amide developed by Astellas Pharma, is a very potent human, murine, and rat sEHI, with very good solubility, excellent pharmacokinetic properties, and able to cross the BBB. Although it does not feature an adamantane moiety, it incorporates another bicyclic hydrocarbon in the left-hand side of the molecule. There are several publications with this inhibitor proving its efficacy in different CNS-related disorders.^{142,143}

¹³² Tsai, H.-J.; Hwang, S. H.; Morisseau, C.; Yang, J.; Jones, P. D.; Kasagami, T.; Kim, I.-H.; Hammock, B. D. *Eur. J. Pharm. Sci.* **2010**, *40*, 222-238.

¹³³ Ulu, A.; Appt, S.; Morisseau, C.; Hwang, S. H.; Jones, P.; Rose, T.; Dong, H.; Lango, J.; Yang, J.; Tsai, H.; Miyabe, C.; Fortenbach, C.; Adams, M.; Hammock, B. D. *Br. J. Pharmacol.* **2012**, *165*, 1401-1412.

¹³⁴ Liu, J.-Y.; Lin, Y.-P.; Qiu, H.; Morisseau, C.; Rose, T. E.; Hwang, S. H.; Chiamvimonvat, N.; Hammock, B. D. *Eur. J. Pharm. Sci.* **2013**, *48*, 619-627.

¹³⁵ Guo, Y.; Luo, F.; Zhang, X.; Chen, J.; Shen, L.; Zhu, Y.; Xu, D. *J. Cell. Mol. Med.* **2018**, *22*, 1489-1500.

¹³⁶ Harris, T. R.; Bettaieb, A.; Kodani, S.; Dong, H.; Myers, R.; Chiamvimonvat, N.; Haj, F. G.; Hammock, B. D. *Toxicol. Appl. Pharm.* **2015**, *286*, 102-111.

¹³⁷ Ostermann, A. I.; Herbers, J.; Willenberg, I.; Chen, R.; Hwang, S. H.; Greite, R.; Morisseau, C.; Gueler, F.; Hammock, B. D.; Schebb, N. H. *Prostaglandins Other Lipid Med.* **2015**, *121*, 131-137.

¹³⁸ Zhang, C.-H.; Zheng, L.; Gui, L.; Lin, J.-Y.; Zhu, Y.-M.; Deng, W.-S.; Luo, M. *Clin. Res. Hepatol. Gas.* **2018**, *42*, 118-125.

¹³⁹ Guedes, A. G. P.; Aristizabal, F.; Sole, A.; Adedeji, A.; Brosnan, R.; Knych, H.; Yang, J.; Hwang, S.-H.; Morisseau, C.; Hammock, B. D. *J. Vet. Pharmacol. Ther.* **2018**, *41*, 230-238.

¹⁴⁰ Guedes, A.G. P.; Morisseau, C.; Sole, A.; Soares, J. H. N.; Ulu, A.; Dong, H.; Hammock, B. D. *Vet. Anaesth. Analg.* **2013**, *40*, 440-448.

¹⁴¹ <https://www.eicosis.com/our-approach/animal-health/> (Accessed April 21, 2020).

¹⁴² Ma, M.; Ren, Q.; Fujita, Y.; Ishima, T.; Zhang, J.C.; Hashimoto, K. *Pharmacol. Biochem. Behav.* **2013**, *110*, 98-103.

¹⁴³ Taguchi, N.; Nakayama, S.; Tanaka, M. *Neurosci. Res.* **2016**, *111*, 56-63.

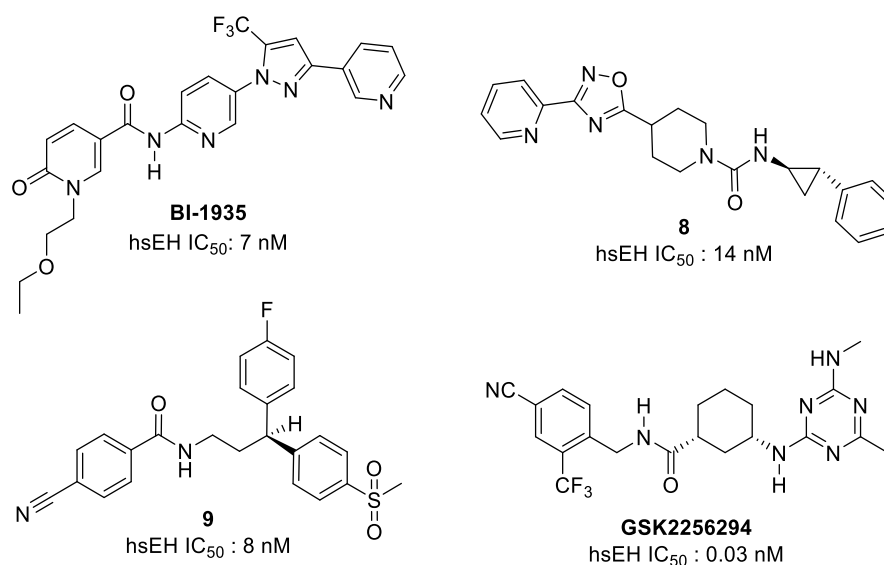


Figure 18. Structure and potency of non-adamantane based sEHIs unrelated with TPPU or *t*-TUCB.

BI-1935, is another amide, developed by Boehringer Ingelheim, with low nanomolar potency in the human and rat sEH, and endowed with excellent pharmacokinetics properties. It showed a dose dependent effect on mean arterial pressure blood pressure in Dahl salt sensitive rats. It is freely offered by Boehringer Ingelheim through its open discovery program “opnMe”.¹⁴⁴

1.5.6.

sEHIs in clinical trials

To date, three sEHIs have reached clinical trials for different indications: APAU, GSK2256294 and EC5026. Unfortunately, none of them had got into the market yet.

APAU, also known as **AR9281**, was the first sEHI that entered clinical trials for the treatment of mild to moderate hypertension in patients with type 2 diabetes. It was discovered by the group of Prof. Hammock, at the UCD, and developed by the *spin-off* Arete Therapeutics. This potent compound is orally available but presented poor water solubility and variable pharmacokinetic profile, apart from extensive metabolism. It showed a high level of safety but failed in phase II because it did not show efficacy in

¹⁴⁴ <https://opnme.com/molecules/seh-bi-1935> (Accessed April 21, 2020).

early-stage hypertension and impaired glucose tolerance.¹⁴⁵ This failure was attributed to poor PK properties and variable effects of the inhibitor *in vivo*.¹⁴⁶

The second inhibitor to reach clinical trials was the amide **GSK2256294**, developed by GlaxoSmithKline (GSK) using a DNA-encoded chemical library. Indeed, it is the first molecule discovery from this technology to enter human clinical testing.¹⁴⁷ This compound present excellent sEH inhibitory potency in the subnanomolar range, very good pharmacokinetic profile^{148,149} and is not able to cross the BBB. GSK started the safety phase I in 2013 and demonstrated that it was well-tolerated and showed sustained *in vivo* inhibition of sEH enzyme activity.⁷⁶ Initially, this compound was evaluated for the treatment of COPD in obese smokers,^{150,151} but, recently, GSK started a phase II clinical trial to verify its efficacy in the treatment of subarachnoid hemorrhage.¹⁵² Moreover, GSK is also recruiting patients for another phase II with its candidate to evaluate its effect on insulin sensitivity.¹⁵³ Importantly, both studies are still active. On the other hand, GSK has recently published the effects of the topical administration of **GSK2256294** in a preclinical mouse model of diabetic wound healing,¹⁵⁴ and the effects of oral administration in preclinical models of ulcerative colitis

¹⁴⁵ Chen, D.; Whitcomb, R.; MacIntyre, E.; Tran, V.; Do, Z. N.; Sabry, J.; Patel, D. V.; Anandan, S. K.; Gless, R.; Webb, H. K. *J. Clin. Pharmacol.* **2012**, *52*, 319-328.

¹⁴⁶ Evaluation of Soluble Epoxide Hydrolase (sEH) Inhibitor in Patients With Mild to Moderate Hypertension and Impaired Glucose Tolerance. U.S. National Library of Medicine. Clinicaltrials.gov Identifier NCT00847899.

¹⁴⁷ Belyanskaya, S. L.; Ding, Y.; Callahan, J. F.; Lazaar, A. L.; Israel, D. I. *ChemBioChem*, **2017**, *18*, 837-842.

¹⁴⁸ Thalji, R. K.; McAtee, J. J.; Belyanskaya, S.; Brandt, M.; Brown, G. D.; Costell, M. H.; Ding, Y.; Dodson, J. W.; Eisennagel, S. H.; Fries, R. E.; Gross, J. W.; Harpel, M. R.; Holt, D. A.; Israel, D. I.; Jolivet, L. J.; Krosky, D.; Li, H.; Lu, Q.; Mandichak, T.; Roethke, T.; Schnackenberg, C. G.; Schwartz, B.; Shewchuk, L. M.; Xie, W.; Behm, D. J.; Douglas, S. A.; Shaw, A. L.; Marino Jr, J. P. *Bioorg. Med. Chem. Lett.* **2013**, *23*, 3584-3588.

¹⁴⁹ Podolin, P. L.; Bolognese, B. J.; Foley, J. F.; Long III, E.; Peck, B.; Umbrecht, S.; Zhang, X.; Zhu, P.; Schwartz, B.; Xie, W.; Quinn, C.; Qi, H.; Sweitzer, S.; Chen, S.; Galop, M.; Ding, Y.; Belyanskaya, S. L.; Israel, D. I.; Morgan, B. A.; Behm, D. J.; Marino Jr, J. P.; Kurali, E.; Barnette, M. S.; Mayer, R. J.; Booth-Genthe, C. L.; Callahan, J. F. *Proc. Natl. Acad. Sci. U. S. A. Prostaglandins Other Lipid Mediators* **2013**, *104*, 25-31.

¹⁵⁰ Yang, L.; Cheriyan, J.; Lazaar, A.; Maki-Petaja K.; Wilkinson, I. *J. Am. College Card.* **2016**, *67*, 2308.

¹⁵¹ Yang, L.; Cheriyan, J.; Gutterman, D. D.; Mayer, R. J.; Ament, Z.; Griffin, J. L.; Lazaar, A. L.; Newby, D. E.; Tal-Singer, R.; Wilkinson, I. B. *Chest* **2017**, *151*, 555-563.

¹⁵² Subarachnoid Hemorrhage and Soluble Epoxide Hydrolase Inhibition Trial (SUSHI). U.S. National Library of Medicine. Clinicaltrials.gov Identifier NCT03318783.

¹⁵³ Soluble epoxide hydrolase inhibition and insulin resistance. U.S. National Library of Medicine. Clinicaltrials.gov Identifier NCT03486223.

¹⁵⁴ Reisdorf, W. C.; Rajpal, N.; Gehman, A. J.; Jain, P.; Burgert, M. E.; Sonti, S.; Agarwal, P.; Rajpal, D. K. *BioRxiv* Mar. 8, 2019. <http://dx.doi.org/10.1101/571984> (accessed 25 March, 2020).

and Crohn's disease, suggesting that the inhibition of the sEH is a promising therapeutic strategy for the treatment of inflammatory bowel disease.¹⁵⁵

Finally, **EC5026**, developed by EicOsis, a new *spin-off* from the UCD, also led by Prof. Bruce D. Hammock. This potent compound is inspired by TPPU, adding a fluorine atom in the benzene ring in order to increase the water solubility.¹⁵⁶ Phase I clinical trials started in December 2019¹⁵⁷ and the goal of the company is to evaluate its efficacy in diabetic neuropathic pain and in the treatment of chemotherapy-induced neuropathic pain.¹⁵⁸

Marketed drugs with sEH inhibition activity

1.5.7. It is also interesting that some marketed drugs present effects on sEH. Even they were not designed against this enzyme, they have inhibitory activity of sEH and, even more interesting, it seems beneficial for their effect.

This is the case of the anticancer drug sorafenib (Figure 19), which is a multikinase inhibitor that targets RAF-1 and VEGF receptor kinase.¹⁵⁹ Structurally, it contains a suitable pharmacophore for inhibiting sEH, and it has been shown that it presents inhibitory activity in both *in vitro* and *in vivo* assays.^{92,160} Interestingly, the off-target effect of sorafenib on sEH is beneficial to reduce some of the side effects that are associated with this class of drugs when they are administered at high doses.¹⁴⁹

¹⁵⁵ Reisdorf, W. C.; Xie, Q.; Zeng, X.; Xie, W.; Rajpal, N.; Hoang, B.; Burgert, M. E.; Kumar, V.; Hurle, M. R.; Rajpal, D. K.; O'Donnell, S.; MacDonald, T. T.; Vossenkämper, A.; Wang, L.; Reilly, M.; Votta, B. J.; Sánchez, Y.; Agarwal, P. *PLoS One* **2019**, *14*, e0215033.

¹⁵⁶ Hammock, B. D.; Lee, K. S. S.; Inceoglu, A. B. (Eicosis). WO 2015/148954 A1. March 27, 2014.

¹⁵⁷ Safety, Tolerability, and Pharmacokinetics of Oral EC5026 in Health Human Subjects. (2019) U.S. National Library of Medicine. Clinicaltrials.gov Identifier NCT04228302.

¹⁵⁸ <http://www.eicosis.com/news.html> (accessed March 25, 2020).

¹⁵⁹ Wilhelm, S.; Carter, C.; Lynch, M.; Lowinger, T.; Dumas, J.; Smith, R.; Schwartz, B.; Simatov, R.; Kelley, S. *Drug Discovery*, **2006**, *5*, 835-844.

¹⁶⁰ Liu, J.-Y.; Park, S.-H.; Morisseau, C.; Hwang, S. H.; Hammock, B. D.; Weiss, R. H. *Mol. Cancer Ther.* **2009**, *8*, 2193–2203.

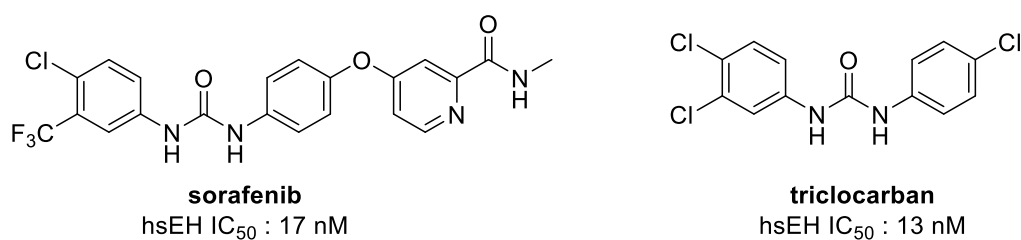


Figure 19. Structure and sEH inhibitory potency of the marketed drugs sorafenib and triclocarban.

Another case is triclocarban (Figure 19), an antimicrobial agent that has been widely used for over 40 years in personal care products, for instance soaps or disinfectants.¹⁶¹ This substance presented sEH inhibition both *in vitro*¹⁰¹ and in a murine model, leading to anti-inflammatory *in vivo* effects.¹⁶² Despite this, it has been demonstrate that exposure to triclocarban by environmental contamination to produce systemic inhibition of the sEH and lead to significant alterations in the immune system is unlikely. Nevertheless, the regular use of personal care products with triclocarban as an antimicrobial might result in downstream biological effects, which are anticipated to be greater near the site of application and could be either beneficial (dental and dermal inflammation, as well as other inflammatory diseases) or unwanted.^{92,162} Indeed, triclocarban was banned by the FDA in 2016.¹⁶³

1.5.8.

Potential side effects of sEHIs

During phase I clinical trials with AR9281 it was not observed any adverse reaction, even when it was administrated at high doses, up to 2 grams every day for seven consecutive days.¹⁴⁵ Despite this observation, it is worth mentioning that sEHIs might cause side effects, that can be either related to their mechanism of action or related to other effects produced by the compounds themselves. The higher potency and best pharmacokinetic profile of the compounds, the less possibility to produce adverse reactions, obtaining a good therapeutic index for that product. Importantly, a search for *off-target* effects needs to be systematically considered. Some important potential *off-targets* of sEHIs are CYP enzymes, the microsomal EH, kinases and hERG and other ion

¹⁶¹ Schebb, N. H.; Inceoglu, B.; Ahn, K. C.; Morisseau, C.; Gee, S. J.; Hammock, B. D. *Environ. Sci. Technol.* **2011**, *45*, 3109–3115.

¹⁶² Liu, J. Y.; Qiu, H.; Morisseau, C.; Hwang, S. H.; Tsai, H. J.; Ulu, A.; Chiamvimonvat, N.; Hammock, B. D. *Toxicol. Appl. Pharmacol.* **2011**, *255*, 200–206.

¹⁶³ <https://cen.acs.org/articles/94/web/2016/09/FDA-bans-triclosan-triclocarban-consumer.html> (accessed June 25, 2020)

channels. To date, no significant *off-target* actions by sEHs of different chemical structures have been reported.^{97,115} As mentioned before, even with total inhibition or knockout of sEH, it is difficult to obtain large increase in plasma levels of EETs, because other metabolic pathways regulates EETs concentrations, thus limiting the mechanism-related side effects.^{11,97} Nevertheless, some effects of epoxy-fatty acids suggest caution. For instance, EETs present an angiogenic effect, particularly in the presence of vascular endothelial growth factor, that is attractive in wound healing or the treatment of some developmental abnormalities, but it can produce a dangerous effect by enhancing growth and metastasis of some tumours.¹⁶⁴ Moreover, sEHs stabilize blood clotting time.¹⁶⁵ For this reason, sEHI could interact with agents such as rofecoxib, which decrease clotting time, or aspirin, which increase clotting time.¹⁶⁶ Many people take aspirin or other drugs to increase clotting time, for this reason, overcoming this side effect could be seen as crucial. These data also suggest that the benefits and risks of EET mimics and sEHs should be balanced and that patient populations be selected carefully.

1.6. Previous work in our research group

1.6.1. Polycyclic scaffolds

In the past years, the research group of Dr. Santiago Vázquez has been focused on the synthesis of bioactive compounds derived from adamantane-like polycyclic moieties and their application to different biological targets. Thus, ring-expanded, ring-contracted, oxa-derivatives and related compounds have been synthesized by the group and their biological effects have been evaluated by several pharmacologists on different targets of therapeutic interest (Figure 20).

¹⁶⁴ Fleming, I. *Cancer Metastasis Rev.* **2011**, *30*, 541-555.

¹⁶⁵ Sudhakar, V.; Shaw, S.; Imig, J. D. *Curr. Med. Chem.* **2010**, *17*, 1181-90.

¹⁶⁶ Marnett, L.J. *Annu. Rev. Pharmacol. Toxicol.* **2009**, *49*, 265-90.

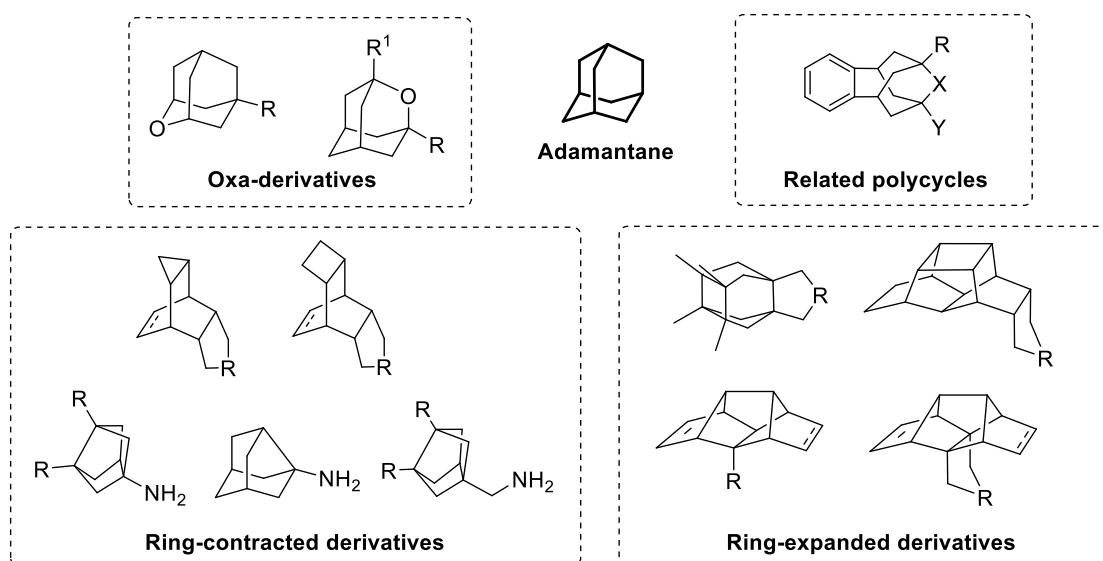


Figure 20. Some of the polycyclic scaffolds synthesized and used by the group of Dr. Santiago Vázquez for the design of bioactive compounds.

The potential therapeutic effects of many of these polycycles as adamantane surrogates have been determined on several targets, such as the M2 channel of the influenza A virus,^{167,168,169,170,171} or the human NMDA channel.^{172,173,174,175,176,177}

¹⁶⁷ Duque, M. D.; Ma, C.; Torres, E.; Wang, J.; Naesens, L.; Juárez-Jiménez, J.; Camps, P.; Luque, F. J.; DeGrado, W. F.; Lamb, R. A.; Pinto, L. H.; Vázquez, S. *J. Med. Chem.* **2011**, *54*, 2646-2657.

¹⁶⁸ Rey-Carrizo, M.; Torres, E.; Ma, C.; Barniol-Xicota, M.; Wang, J.; Wu, Y.; Naesens, L.; Degrado, W. F.; Lamb, R. A.; Pinto, L. H.; Vázquez, S. *J. Med. Chem.* **2013**, *56*, 9265-9274.

¹⁶⁹ Torres, E.; Leiva, R.; Gazzarrini, S.; Rey-Carrizo, M.; Frigolé-Vivas, M.; Moroni, A.; Naesens, L.; Vázquez, S. *ACS Med. Chem. Lett.* **2014**, *5*, 831-836.

¹⁷⁰ Rey-Carrizo, M.; Barniol-Xicota, M.; Ma, C.; Frigolé-Vivas, M.; Torres, E.; Naesens, L.; Llabrés, S.; Juárez-Jiménez, J.; Luque, F. J.; Degrado, W. F.; Lamb, R. A.; Pinto, L. H.; Vázquez, S. *J. Med. Chem.* **2014**, *57*, 5738-5747.

¹⁷¹ Rey-Carrizo, M.; Gazzarrini, S.; Llabrés, S.; Frigolé-Vivas, M.; Juárez-Jiménez, J.; Font-Bardia, M.; Naesens, L.; Moroni, A.; Luque, F. J.; Vázquez, S.; Santiago, V. *Eur. J. Med. Chem.* **2015**, *96*, 318-329.

¹⁷² Camps, P.; Duque, M. D.; Vázquez, S.; Naesens, L.; De Clercq, E.; Sureda, F. X.; López-Querol, M.; Camins, A.; Pallàs, M.; Prathalingam, S. R.; Kelly, J. M.; Romero, V.; Ivorra, D.; Cortés, D. *Bioorg. Med. Chem.* **2008**, *16*, 9925-9936.

¹⁷³ Duque, M. D.; Camps, P.; Profire, L.; Montaner, S.; Vázquez, S.; Sureda, F. X.; Mallol, J.; López-Querol, M.; Naesens, L.; De Clercq, E.; Prathalingam, S. R.; Kelly, J. M. *Bioorg. Med. Chem.* **2009**, *17*, 3198-3206.

¹⁷⁴ Duque, M. D.; Camps, P.; Torres, E.; Valverde, E.; Sureda, F. X.; López-Querol, M.; Camins, A.; Prathalingam, S. R.; Kelly, J. M.; Vázquez, S. *Bioorg. Med. Chem.* **2010**, *18*, 46-57.

¹⁷⁵ Torres, E.; Duque, M. D.; López-Querol, M.; Taylor, M. C.; Naesens, L.; Ma, C.; Pinto, L. H.; Sureda, F. X.; Kelly, J. M.; Vázquez, S. *Bioorg. Med. Chem.* **2012**, *20*, 942-948.

¹⁷⁶ Valverde, E.; Sureda, F. X.; Vázquez, S. *Bioorg. Med. Chem.* **2014**, *22*, 2678-2683.

¹⁷⁷ Leiva, R.; Phillips, M. B.; Turcu, A. L.; Gratacòs-Batlle, E.; León-García, L.; Sureda, F. X.; Soto, D.; Johnson, J. W.; Vázquez, S. *ACS Chem. Neurosci.* **2018**, *9*, 2722-2730.

More recently, we have explored these polycyclic scaffolds in other targets, such as the human P2X7 channel¹⁷⁸ and the 11 β -HSD1 enzyme.^{179,180}

Importantly, the investigations of the group related to the inhibition of the M2 channel of the influenza virus, showed, through a combination of synthesis, antiviral tests and computational modeling, that adamantane moiety is not always the best polycycle to occupy a lipophilic space on a biological target.

sEH inhibition

Despite the efforts made from academic and industrial research groups in the development of new drug candidates, only a few sEHs have entered into clinical trials, and any have reached the market yet, as mentioned previously. This fact demonstrates that the drug discovery process of sEHs is complex and very challenging. Some of the main development limitations are the inappropriate physicochemical properties of the compounds, especially high lipophilicity, low water solubility and metabolic liability. Considering that the adamantane nucleus does not possess the optimum properties for the development of urea-based sEHs because of its lipophilicity, solubility and stability, the group of Dr. Santiago Vázquez hypothesized that the replacement of the adamantane moiety of known sEHs by other polycyclic structures may afford compounds with improved PK and PD (pharmacodynamic) profiles by changing their physicochemical properties while maintaining a good binding affinity for the target.

Therefore, in the context of Dr. Elena Valverde's Thesis, it was started a new project related to the discovery of novel sEHs featuring adamantane-like scaffolds as hydrophobic moieties. In order to evaluate the effect of the new scaffolds in the inhibitory potency of sEH, they were placed as the LHS of the urea group and a selected unit from the literature was chosen as the RHS. Particularly, the 2,3,4-trifluorophenyl group was selected due to its facile synthesis and high inhibitory activity against sEH (Figure 21).¹⁸¹

¹⁷⁸ Barniol-Xicota, M.; Kwak, S.-H.; Lee, S.-D.; Caseley, E.; Valverde, E.; Jiang, L.-H.; Kim, Y.-C.; Vázquez, S. *Bioorg. Med. Chem. Lett.* **2017**, *27*, 759-763.

¹⁷⁹ Leiva, R.; Seira, C.; McBride, A.; Binnie, M.; Luque, F. J.; Bidon-Chanal, A.; Webster, S. P.; Vázquez, S. *Bioorg. Med. Chem. Lett.* **2015**, *25*, 4250-4253.

¹⁸⁰ Valverde, E.; Seira, C.; McBride, A.; Binnie, M.; Luque, F. J.; Webster, S. P.; Bidon-Chanal, A.; Vázquez, S. *Bioorg. Med. Chem.* **2015**, *23*, 7607-7617.

¹⁸¹ Brown, J. R.; North, E. J.; Hurdle, J. G.; Morisseau, C.; Scarborough, J. S.; Sun, D.; Korduláková, J.; Scherman, M. S.; Jones, V.; Grzegorzewicz, A.; Crew, R. M.; Jackson, M.; McNeil, M. R.; Lee, R. E. *Bioorg. Med. Chem.* **2011**, *19*, 5585-5595.

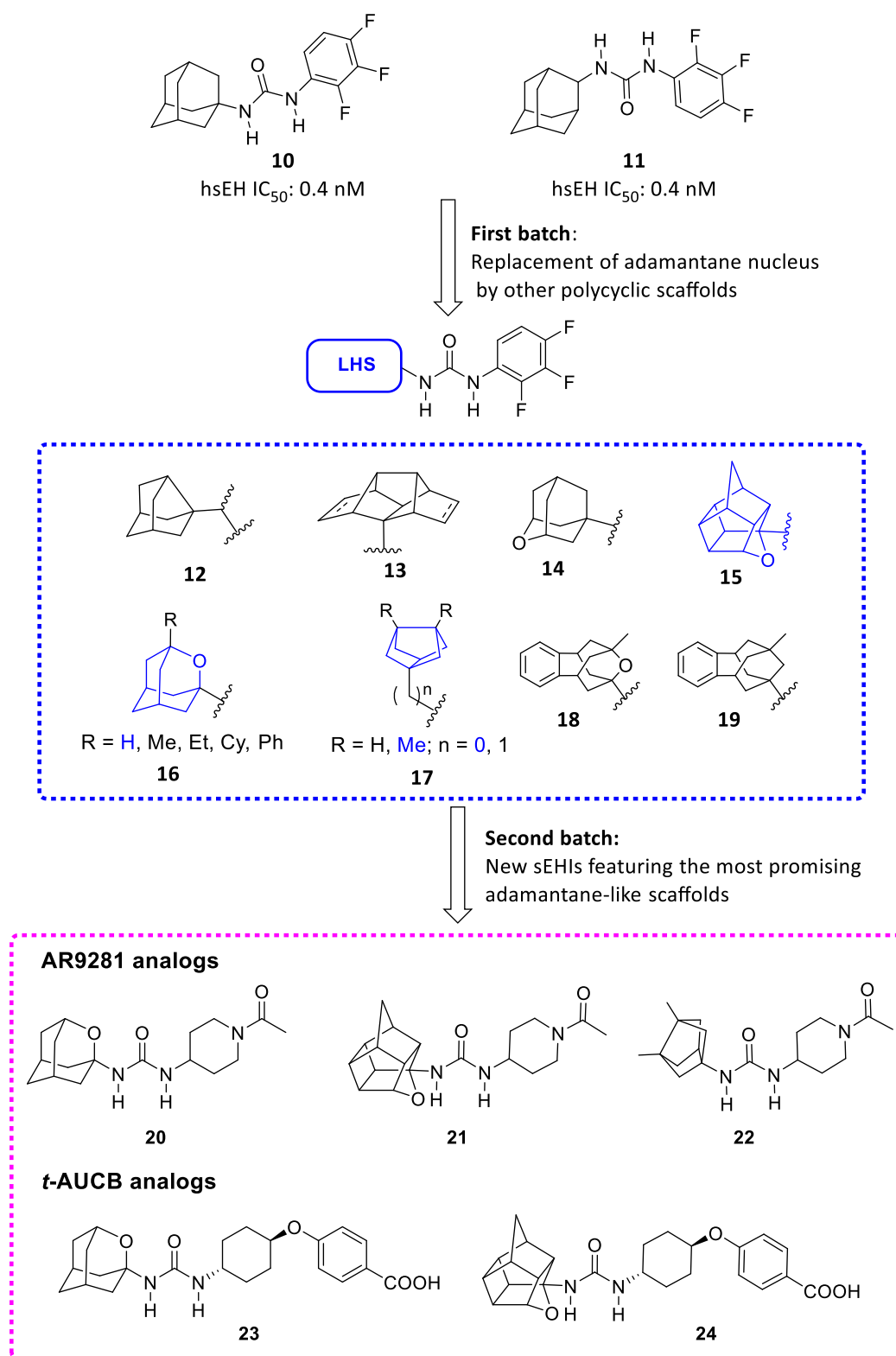


Figure 21. First batch of new sEHIs featuring adamantane-like scaffolds, with the most promising ones highlighted in blue; and second batch of new sEHIs analogs of AR9281 and *t*-AUCB, featuring the most promising adamantane-like scaffolds.

Satisfyingly, all the new adamantyl-like ureas were potent sEHs, with IC_{50} in the low nanomolar range, between 4 and 40 nM. Moreover, in order to confirm the ability of the new scaffolds to replace the adamantane in sEHs, a second batch of compounds was synthesized with the more promising scaffolds (highlighted in blue in Figure 21), adding in the RHS the substituents of the potent sEHs APAU and *t*-AUCB. The selection of the polycycles was made in accordance to sEH inhibitory activity, solubility values and lipophilic ligand efficiency (LipE) calculation, which is an estimate of the specificity of a molecule in binding to the target relative to lipophilicity.

The compounds of the second batch showed IC_{50} values between 10 and 50 nM, slightly less potent than the adamantyl standards *t*-AUCB and APAU. But, importantly, they presented improved solubility values, especially by those scaffolds bearing an oxygen atom in their structure.

In order to better understand the improved drug-like properties by replacing the adamantane nucleus by an oxa-polycyclic scaffold, it was measured the inhibition activity of the human sEH, experimental solubility, melting point and permeability of the 2-oxadamantanes **20**, **23** and **16**, analogs of AR9281, *t*-AUCB and **10**, respectively (Table 1). Gratifyingly, in the three series it was observed that the compounds featuring the 2-oxadamantane nucleus presented lower melting points, improved water solubility and higher membrane permeability through Caco-2 cells. Notwithstanding, the introduction of the oxygen atom in the adamantane scaffold slightly reduced the potency.

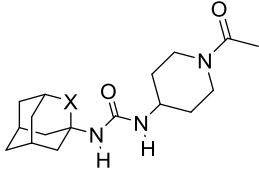
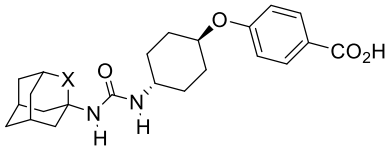
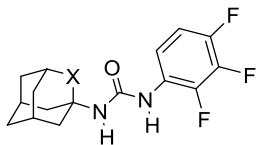
Compounds	X	h sEH IC ₅₀ (nM) ^[a]	Solubility (μM) ^[b]	Melting Point (°C)	Permeability (Caco-2)		ER ^[c]
					Papp (nm/s) A→B	Papp (nm/s) B→A	
	CH ₂	8.0	24	202-204 ¹⁸²	2.2	141.2	64.5
20	O	29.9	59	172-173	22.4	94.5	4.3
	CH ₂	0.5	25	250-255 ¹¹¹	1.9	210.3	111
23	O	9.0	>100	255-257	1.4	75.5	55.4
	CH ₂	7.7	16	216-219	6.7	4.6	0.69
16	O	21.3	27	196-198	168	151	0.9

Table 1. Human sEH IC₅₀ and solubility, melting point and permeability values for known adamantane inhibitors AR9281, *t*-AUCB and **11**, and their oxygen analogs **20**, **23** and **16**. ^aIC₅₀ values are the average of three replicates. The fluorescent assay as performed here has a standard error between 10 and 20%, suggesting that differences of two-fold or greater are significant. Because of the limitations of the assay, it is difficult to distinguish among potencies <0.5 nM. ^bSolubility in a 1% DMSO/99% PBS buffer solution. ^cThe efflux ratio was calculated as ER = (Papp B → A)/(Papp A → B).

¹⁸² Gless, R. D. (Arete Therapeutics). WO 2008/094862 A1, January 29, 2007.

2. OBJECTIVES

Despite the promising results obtained to date with several sEHs, it is still a major challenge to develop new compounds with optimal solubility, better pharmacokinetic profiles while maintaining the excellent potency of the already developed compounds.

Considering that the adamantane-based derivatives present low solubility values and rapid metabolism, which represent two clear drawbacks for their further development, the research group of Dr. Santiago Vázquez started a new line of research focused on the design, synthesis and evaluation of new sEHs with the aim of obtaining compounds with better solubility values and optimized physicochemical properties. Therefore, in the context of Dr. Elena Valverde's Thesis it was found that the replacement of the adamantane nucleus of known sEHs by other polycyclic scaffolds, especially those that present an oxygen atom in their structure such as the 2-oxadamantane moiety, lead to slightly less potent compounds but with improved solubility values, lower melting points and higher membrane permeability than their adamantane-based counterparts.

Taking into account all this information, four main objectives were proposed for the present Thesis:

1. Given that designing bioactive compounds is a multifactorial process and, in view of the significant increase in aqueous solubility and permeability and the decrease of the melting point of the compounds bearing the 2-oxadamantane nucleus, it was considered to further explore this moiety as a scaffold for designing new sEHs. Thus, the first goal was the synthesis of further 2-oxadamantane-based sEHs, analogs of AR9281, in order to explore their potency and drug metabolism and pharmacokinetics (DMPK) properties such as solubility, metabolic stability, permeability and cytotoxicity. A screening cascade would allow us to select a suitable candidate in order to perform an *in vivo* proof of concept study in a murine model of acute pancreatitis (AP) (Figure 22). These results are disclosed in the **Chapter 1** of this Thesis.

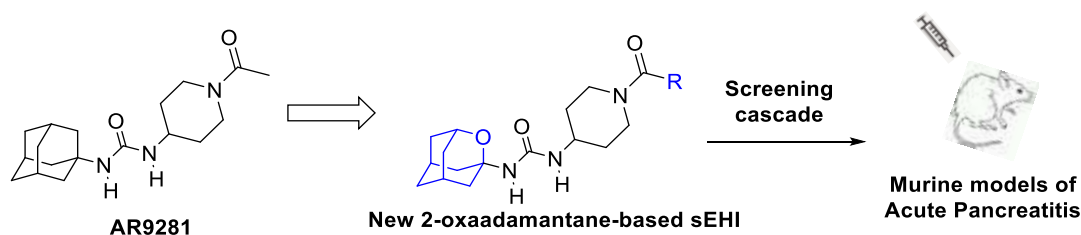


Figure 22. Replacement of adamantane nucleus of AR9281 by the 2-oxaadamantane moiety to select a candidate for the *in vivo* assays.

- To explore the optimal size of the lipophilic unit of the sEHIs, synthesizing analogs of AR9281, *t*-AUCB and **11** where the adamantane nucleus is replaced by other polycyclic units of larger or smaller volume. The main purpose was to assess if alterations in the size of the lipophilic unit attached to the urea significantly impact its potency against the human sEH as well as influencing solubility, permeability and metabolic stability. In the context of Dr. Elena Valverde's Thesis, several sEHIs with ring-contracted analogs of adamantane were synthesized. In the present thesis, ring-contracted analogs such as noradamantane and larger analogs such as diamantane were envisaged as scaffolds for the synthesis of new sEHIs (Figure 23). These results are disclosed in **Chapter 2**.

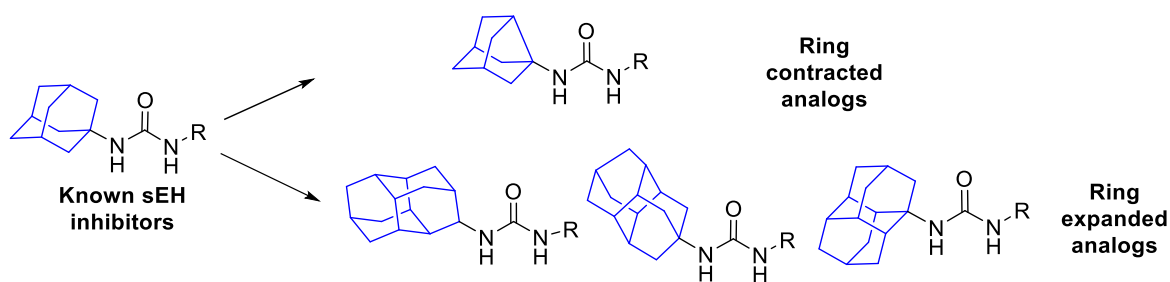


Figure 23. Replacement of the adamantane nucleus by smaller or larger units.

- Considering the improved properties of the replacement of the adamantane nucleus of AR9281 or *t*-AUCB by the phenyl ring of TPPU and EC5026, we considered the synthesis of new inhibitors bearing the very versatile benzohomoadamantane scaffold as the hydrophobic moiety of sEHIs. This polycyclic, readily accessible system, features in its structure the synthetically versatile homoadamantane unit fused with an aromatic ring. Thus, this

underexplored scaffold merges the phenyl ring of TPPU and EC5026 with the polycyclic core of AR9281 and *t*-AUCB. A screening cascade would allow us to select two candidates for *in vivo* efficacy studies in a murine model of acute pancreatitis and in a predictive model of neuropathic pain (Figure 24). These results are disclosed in **Chapters 3 and 4**, respectively.

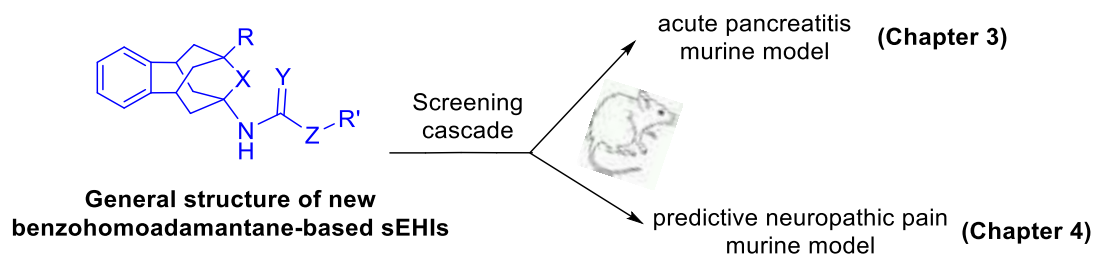


Figure 24. Replacement of adamantane nucleus or phenyl ring of known sEHIs by the benzohomoadamantane moiety.

4. Taking into account the previous work made in Chapters 3 and 4 around the benzohomoadamantane moiety as a suitable scaffold for the design and synthesis of sEHIs, we wanted to further explore this polycyclic nucleus. Thus, the hydrogen atoms of the aromatic ring were then substituted by several electron donating and electron withdrawing groups in order to obtain new benzohomoadamantane-based ureas as sEHIs (Figure 25). The results are disclosed in **Chapter 5**.

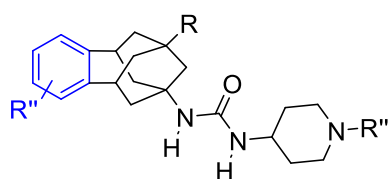


Figure 25. Exploration of the substituents of the aromatic ring of the benzohomoadamantane scaffold for the synthesis of new sEHIs

3. RESULTS AND DISCUSSION

CHAPTER 1

2-OXAADAMANTANE-BASED

sEHIs

Introduction

Despite of the efforts made to obtain sEHIs with excellent potency, the pronounced lipophilicity of the adamantane group of the known sEHIs compromises negatively the overall water solubility of the molecules, an important physicochemical parameter in the early stages of drug discovery,^{124,183} thus limiting the discovery of new drug-like sEHIs. In order to fix that problem, we hypothesized that the introduction of an oxygen atom in several polycyclic scaffolds should increase the solubility and may impact in the overall drug-like properties of the known adamantane-based sEHIs without seriously compromising the inhibitory potency. Given the background of the group in the synthesis of polycyclic compounds and the synthetic accessibility of several oxapolycyclic amines,^{173,184,185,186} in the context of Elena Valverde's Thesis, it was replaced the adamantane nucleus of the known potent sEHIs **10** and **11** by selected polycyclic scaffolds bearing an oxygen atom, furnishing the compounds **25**, **26** and **16**, presenting IC₅₀ values against the human sEH in the same range of potency, around 30 nM (Figure 26).

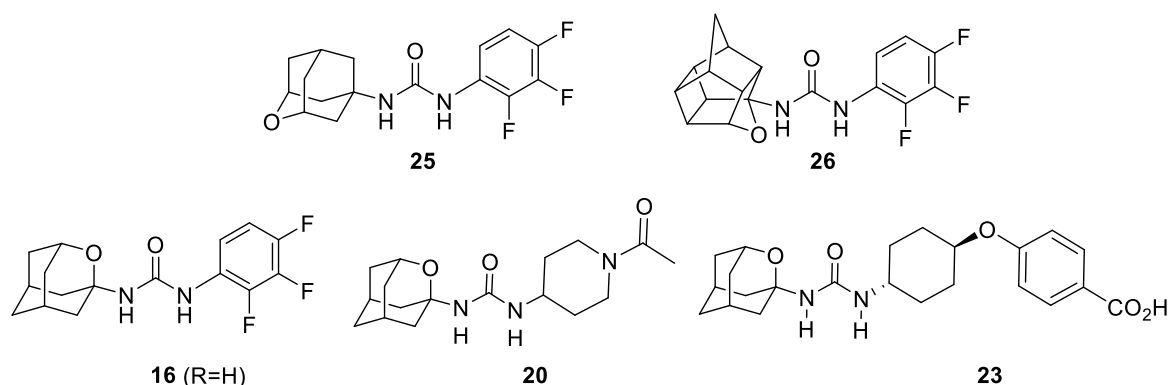


Figure 26. Some of the oxapolycyclic-based sEHIs designed in the context of Dr. Elena Valverde's Thesis.

¹⁸³ Bhattachar, S. N.; Deschenes, L. A.; Wesley, J. A. *Drug Discov. Today*. **2006**, 11, 1012-1018.

¹⁸⁴ Gagneux, A. R.; Meier, R. *Tetrahedron Lett.* **1969**, 10, 1365-1368.

¹⁸⁵ Onajole, O. K.; Coovadia, Y.; Kruger, H. G.; Maguire, G. E. M.; Pillay, M.; Govender, T. *Eur. J. Med. Chem.* **2012**, 54, 1-9.

¹⁸⁶ Leiva, R.; Gazzarrini, S.; Esplugas, R.; Moroni, A.; Naesens, L.; Sureda, F. X.; Vázquez, S. *Tetrahedron Lett.* **2015**, 56, 1272-1275.

Taking into account that the 2-oxaadmantane-1-amine was synthetically much more accessible than its isomer 2-oxaadmantane-5-amine and the chiral nature of the polycyclic core of compound **16**, the synthesis of the oxa-analogs of AR9281 and *t*-AUCB was subsequently performed only with the 2-oxaadmantane-1-amine, obtaining compounds **20** and **23**.

Interestingly, although less potent than their adamantane analogs, the novel 2-oxaadmantane-derived ureas were nanomolar inhibitors of the human enzyme. Gratifyingly the 2-oxaadmantane derivatives presented lower melting points, higher solubility values and increased membrane permeability.

In view of the enhanced properties of the 2-oxaadmantane sEHIs **16**, **20** and **23**, it was envisaged the synthesis of two families of analogs of **16** with general structure **I** (undertaken in the context of Eugènia Pujol's experimental postgraduate Master) and analogs of **20** with general structure **II**, synthesized in the context of the present PhD Thesis (Figure 27).

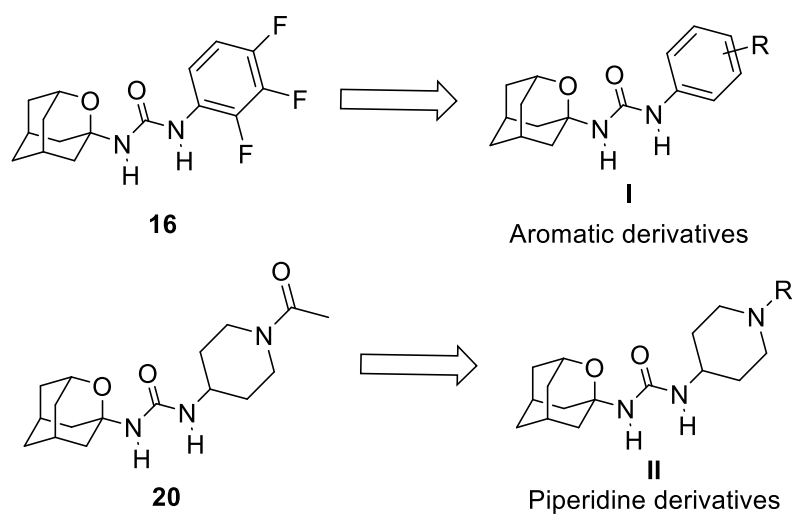
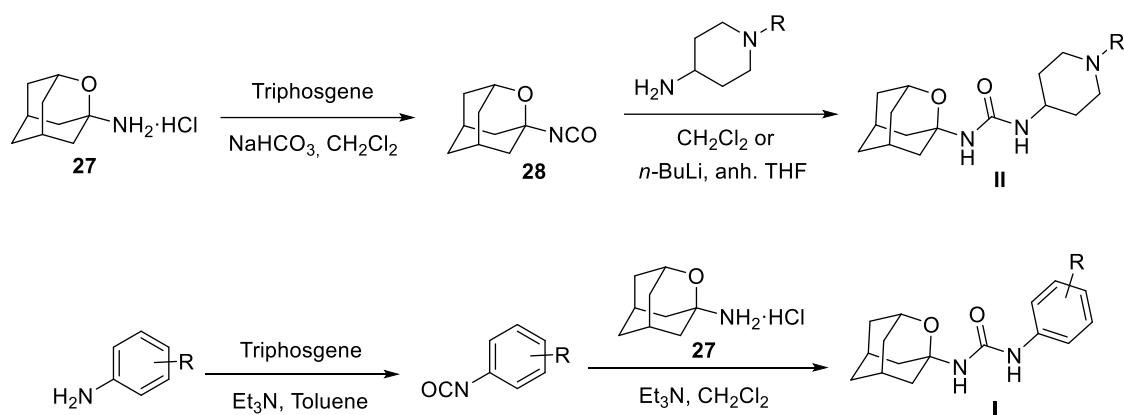


Figure 27. General structures **I** and **II** of the compounds prepared in this project, analogs of compounds **16** and **20**, respectively.

After exploring the potency of the new analogs as inhibitors of the human and murine sEH, their cytotoxicity and DMPK properties were evaluated for selecting a candidate to perform an *in vivo* proof of concept study in two murine models of AP.

Discussion

The compounds presented in this Thesis followed two different synthetic strategies. The first route involved the synthesis of isocyanate **28** from amine **27**, followed by its reaction with the amines containing the RHS of the ureas, either directly or, for the less nucleophilic amines, after deprotonation with a strong base such as *n*-butyllithium. The second pathway involved the reaction of amine **27** in the presence of triethylamine with the isocyanate derived from the different anilines containing the RHS of the urea (Scheme 1).

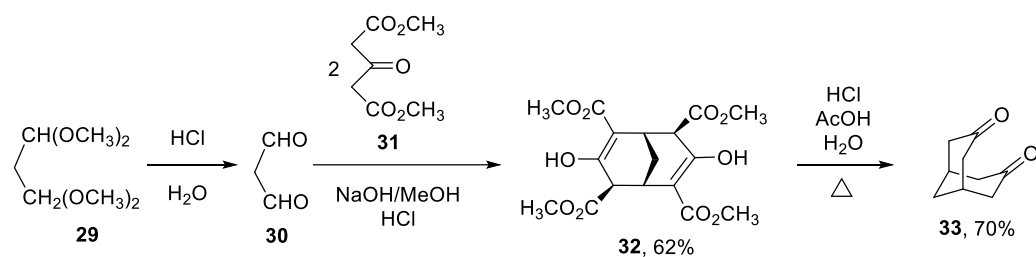
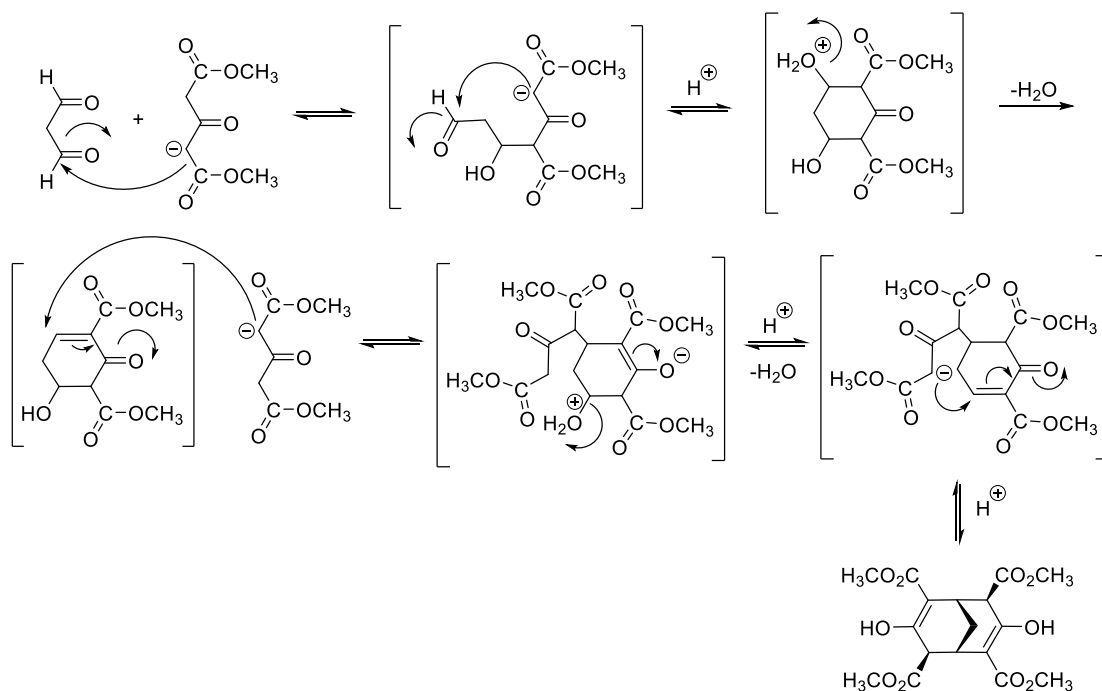


Scheme 1. General synthetic procedures for the preparation of 2-oxadamant-1-yl ureas.

For the first approach, it was necessary the preparation of the key isocyanate **28**, starting from 2-oxadamantane-1-amine, **27**, in turn available from ketone **33**.^{187,188} The synthesis of **33** started with a Weiss reaction, which implies the condensation of malondialdehyde, **30**, prepared *in situ* from tetramethoxypropane, **29**, with two equivalents of dimethyl 1,3-acetonedicarboxylate, **31**, in basic media. Interestingly, this reaction consists in two aldol condensations, two dehydrations and two Michael reactions, that affords the tetraester **32**. Then, hydrolysis and decarboxylation of the tetraester furnish the symmetric diketone **33** (Scheme 2).

¹⁸⁷ Stetter, H.; Tacke, P. *Chem. Ber.* **1963**, *96*, 694.

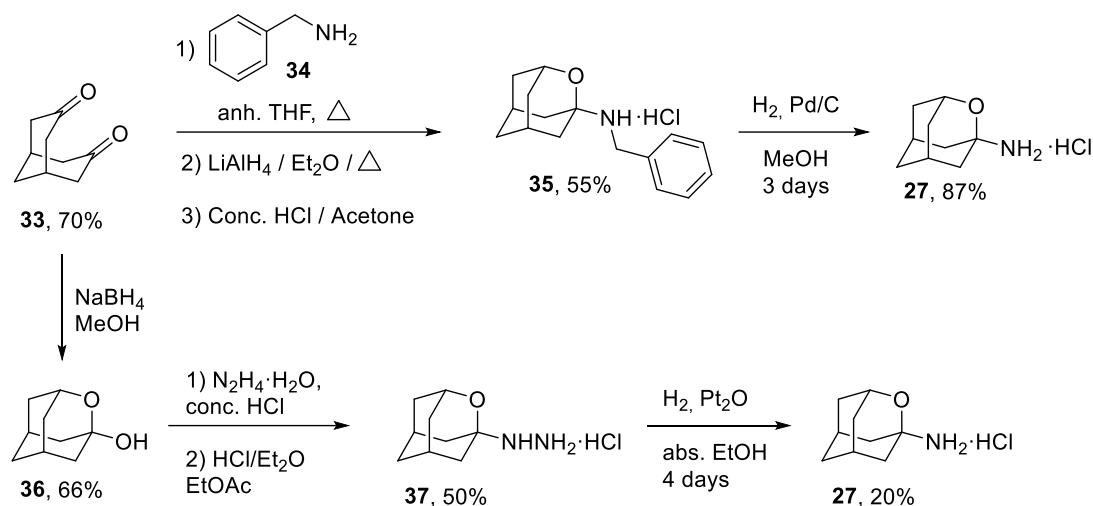
¹⁸⁸ Bertz, S. H.J. *Org. Chem.* **1985**, *50*, 3585.

**Mechanism of the Weiss reaction:****Scheme 2.** Synthesis of ketone **33** and simplified mechanism of the Weiss reaction.

Once the diketone **33** was obtained, two different procedures were followed for the synthesis of 2-oxadamantane-1-amine **27**. The first procedure was described by Gagneux and Meier and involves the reductive amination of diketone **33**.¹⁸⁴ Thus, the reaction of **33** with benzylamine **34**, followed by reduction with LiAlH_4 led to the amine **35** in 55% overall yield. Finally, the hydrogenolysis of the benzyl group of **35** furnished the desired amine **27**.

Alternatively, the reaction of diketone **33** with sodium borohydride led to the alcohol **36**, as reported previously by the team of Prof. Pelayo Camps and Prof. Diego

Muñoz-Torrero.^{189,190} The subsequent reaction with aqueous hydrazine furnished the hydrazine **37**, which was subjected to a catalytic hydrogenation to afford the desired amine **27** (Scheme 3).



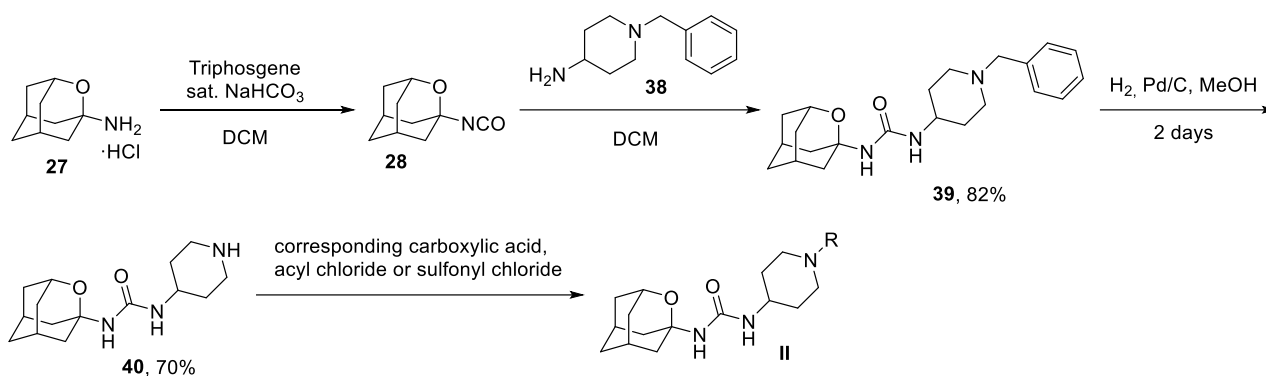
Scheme 3. Two synthetic procedures followed to obtain the 2-oxadamantane-1-amine, **27**.

The present Thesis has been mainly focused on the synthesis and evaluation of the analogs of compound **20**, bearing a piperidine moiety in the RHS of the urea and the 2-oxadamantane-1-yl as a polycyclic scaffold in the LHS.

For the preparation of this family of compounds, a straightforward synthesis was followed in order to obtain the different piperidine-substituted compounds. Starting from 2-oxadamantane-1-amine, **27**, in the presence of triphosgene and an aqueous solution of NaHCO_3 , led to the isocyanate **28**. Then, it was treated with 1-benzylpiperidine-4-amine, **38**, furnishing the urea **39**, which was subjected to a debenzilation by catalytic hydrogenation to obtain urea **40**. This compound was used as a starting point for the synthesis of several analogs of **20** by the reaction of **40** with either the corresponding carboxylic acids in the presence of coupling agents such as HOBt and EDCI·HCl in ethyl acetate, or with the corresponding acyl chlorides or sulfonyl chlorides in the presence of a base such as triethylamine in dichloromethane as a solvent (Scheme 4).

¹⁸⁹ Camps, P.; El Achab, R.; Font-Bardia, M.; Görbig, D. M.; Morral, J.; Muñoz-Torrero, D.; Solans, X.; Simon, M. *Tetrahedron*, **1996**, *52*, 5867-5880.

¹⁹⁰ Camps, P.; El Achab, R.; Görbig, D.M.; Morral, J.; Muñoz-Torrero, D.; Badia, A.; Baños, J. E.; Vivas, N. M.; Barril, X.; Orozco, M.; Luque, F. J. *J. Med. Chem.* **1999**, *42*, 3227-3242.



Scheme 4. Synthetic pathway for the synthesis of several analogs of **20**.

Alternatively, in those cases where the substituted aminopiperidines were commercially available, isocyanate **28** was directly reacted with them to obtain the final products. Overall, eleven new ureas were synthesized (Figure 28). Of note, compound **50** was synthesized as an analog of **16**.

Once all the analogs of **16** and **20** were synthesized, a screening cascade was performed in order to select the best candidate for the *in vivo* studies in a murine model of acute pancreatitis. As a first step for the biological characterization of the novel ureas, their potency as human and murine sEHIs was tested by Dr. Christophe Morisseau, from the group of Prof. Bruce D. Hammock at the UCD.

In line with the activities of compounds **16** and **20**, the new 2-oxadamantane-based ureas presented IC₅₀ in the nanomolar range although, for the examples where comparison was available, they were less potent than their adamantane analogs. This fact was computationally rationalized by molecular dynamics simulations performed by the group of Prof. Silvia Osuna, at the University of Girona. This computational study suggested that the introduction of an oxygen atom into the adamantane scaffold restricts its orientation within the hydrophobic pocket and weakens hydrogen bonds between the carbonyl group of 2-oxadamantane-based inhibitors and the Asp335 residue of the enzyme.

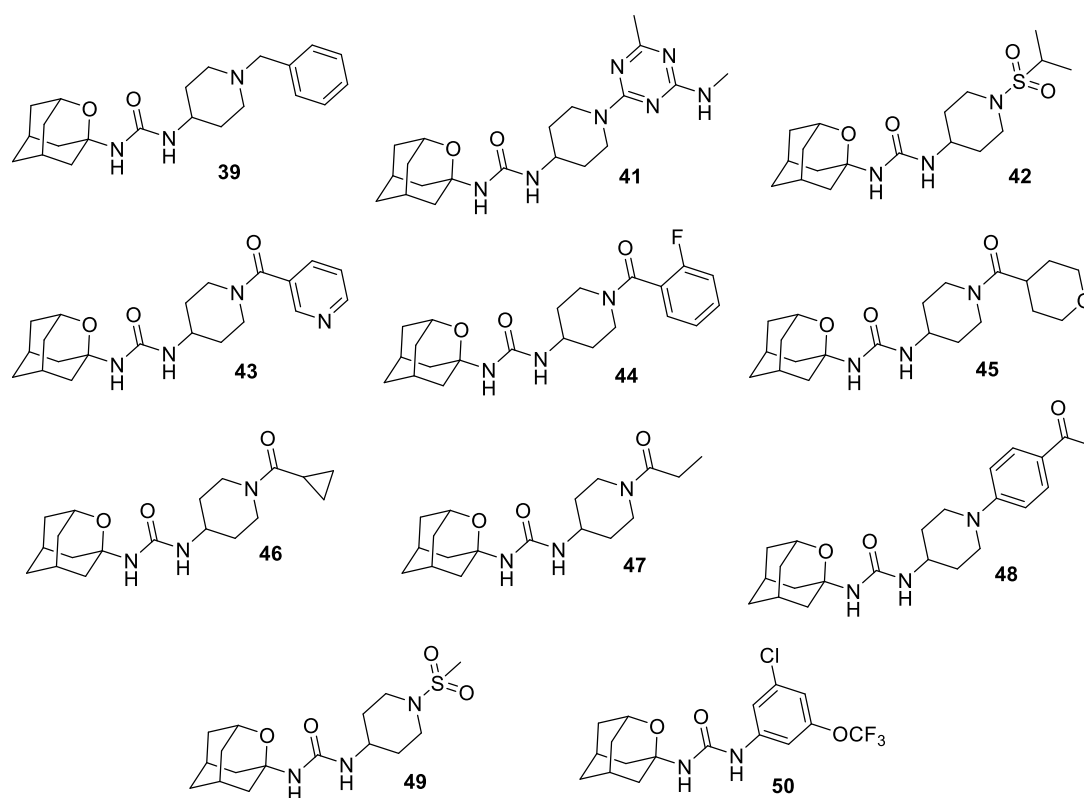


Figure 28. Structure of the 2-oxadamantyl-based ureas synthesized in the present Thesis.

Considering both the human and murine sEH inhibitory activity, four piperidine-substituted 2-oxadamant-1-yl ureas, **20**, **42**, **44** and **48**, were selected for being moved forward in the screening cascade. Thus, these four inhibitors were characterized in terms of cytotoxicity in 2 different cell lines [Transformed Human Liver Epithelial-2 cell line (THLE-2) and Peripheral Blood Mononuclear Cells (PBMC)], performed by the group of Dr Julen Oyarzabal and Dr Antonio Pineda-Lucena of the Center for Applied Medical Research of Navarra (Spain); solubility, microsomal stability (human, mouse and rat species), human ether-a-go-go-related gene (hERG) inhibition and cytochromes P450 (CYP) inhibition, experiments performed by the group of Prof. M. Isabel Loza and Prof. José M. Brea of the Drug Screening Platform/Biofarma Research Group of the University of Santiago de Compostela (Spain); and predicted brain permeability (PAMPA-BBB), experiment performed by Prof. Belén Pérez of the Autonomous University of Barcelona (Spain). Finally, an *in vitro* study of efficacy was performed by Dr. Javier Pizarro, from the group of Prof. Manuel Vázquez-Carrera of the University of Barcelona. These studies allowed us to select the best candidate to perform the *in vivo* studies. The selected compound was the sulfonamide **42**, whose properties are collected in table 2.

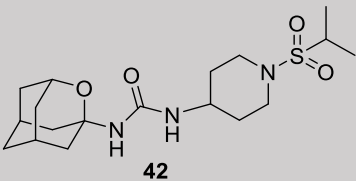
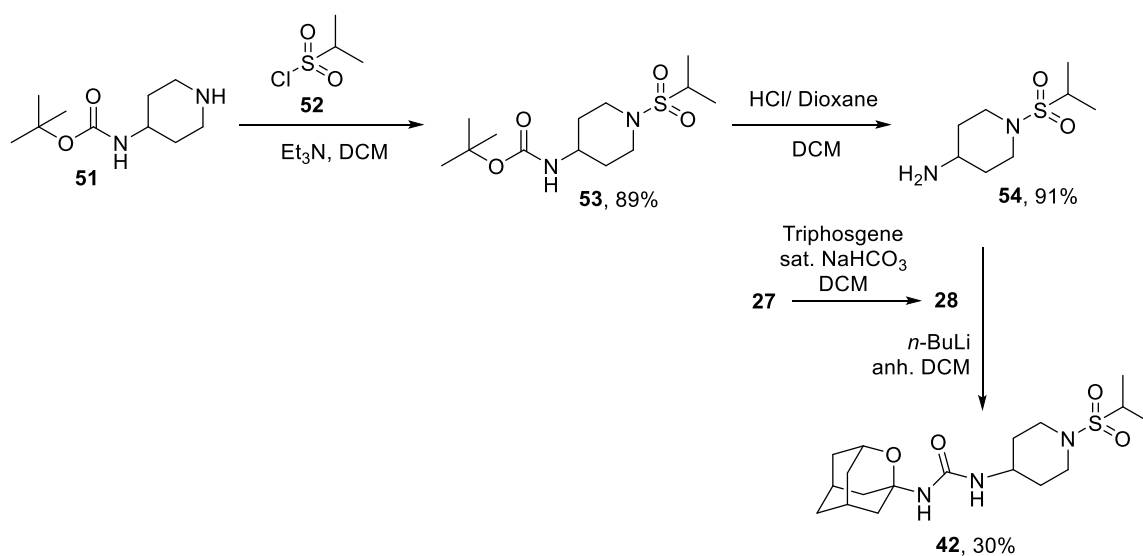
Compound	
sEH IC ₅₀ (nM)	Human: 197 Mice: 79 Rat: 2
PAMPA-BBB	CNS-
Solubility in 1% DMSO:99% PBS buffer (μM)	34
Liver microsomal stability (% parent at 60 min)	Human: 73 Rat: 64 Mice: 64
Selectivity over CYP2C19 (% inh. at 10 μM)	1 ± 1
Cytotoxicity – LC ₅₀ (μM)	THLE cells: >100 PBMC cells: >20
<i>In vitro</i> proof of concept efficacy study in AR42J pancreatic rat cells	Reduction of inflammatory and ER stress markers

Table 2. Biological profiling of the selected compound **42**.

At this point, it was crucial the synthesis of compound **42** in a larger scale in order to obtain enough compound to perform the *in vivo* assays: maximum tolerated dose (MTD) study, two pharmacokinetic studies and two *in vivo* efficacy studies in murine models of acute pancreatitis. Taking this into account, the synthetic pathway of **42** was modified in order to obtain a more convergent synthesis with better conversion in each step of the route. Thus, the commercially available Boc-protected aminopiperidine **51** was coupled with the sulfonyl chloride **52**. Removal of the Boc group in acidic media led to the sulfonamide **54** in excellent yield. Finally, **54** was reacted with the isocyanate **28** in the presence of *n*-butyllithium to afford the desired compound **42** in medium yield (Scheme 5).



Scheme 5. Optimized synthetic pathway for the obtention of the selected compound **42**.

A pharmacokinetic study allowed us to select the intraperitoneal route for the administration of **42** in the following *in vivo* studies, and the MTD study showed that the selected compound was well tolerated up to 80 mg/kg. Of note, both studies were performed by the company Draconis Pharma.

Finally, in the efficacy *in vivo* studies, C57BL/6J mice were treated with the selected sEH inhibitor before (prevention) and after (treatment) the induction of AP by cerulein, following protocols already published by Bettaieb *et al.*¹⁹¹ Gratifyingly, in both the pre-induction and post-induction studies, the administration of 30 mg/kg of **42** diminished the overexpression of inflammatory and ER stress markers induced by cerulein and reduced pancreatic damage. These results suggest that sEHIs may be of clinical interest for treating AP. Due to the promising biological activity of **42**, further optimization of new sEH inhibitors for the treatment of AP, an unmet medical need, was explored in the present Thesis.

All the compounds disclosed in this Chapter as well as the 2-oxadamantane-based sEHIs synthesized in the context of Eugènia Pujol's experimental postgraduate Master have been protected by a patent application.¹⁹²

¹⁹¹ Bettaieb, A.; Chahed, S.; Bachaalany, S.; Griffey, S.; Hammock, B. D.; Haj, F. G. *Mol. Pharmacol.* **2015**, *88*, 281-290.

¹⁹² Vázquez Cruz, S.; Valverde Murillo, E.; Leiva Martínez, R.; Vázquez Carrera, M.; Codony Gisbert S. (Universitat de Barcelona). WO 2017/017048 A1, July 28, 2015.

Moreover, the aforementioned results have been submitted for publication to the *Journal of Medicinal Chemistry*.¹⁹³ The current draft of this manuscript is included.

Of note, while this Thesis was in progress, our group, in collaboration with those of Prof. Mercè Pallàs (UB), Carles Galdeano (UB) and Bruce D. Hammock (UCD), reported an *in vivo* study with the oxa-derivative **23** in two murine models of neurodegeneration and AD,¹⁹⁴ where we have firmly established sEH as a promising target for the treatment of AD.

¹⁹³ Codony, S.; Pujol, E.; Pizarro, J.; Feixas, F.; Valverde, E.; Loza, M. I.; Brea, J. M.; Saez, E.; Oyarzabal, J.; Pineda-Lucena, A.; Pérez, B.; Pérez, C.; Rodríguez-Franco, M. I.; Leiva, R.; Osuna, S.; Morisseau, C.; Hammock, B. D.; Vázquez-Carrera, M.; Vázquez, S. *J. Med. Chem.* (submitted 20th February, **2020**).

¹⁹⁴ Griñán-Ferré, C.; Codony, S.; Pujol, E.; Yang, J.; Leiva, R.; Escolano, C.; Puigoriol-Illamola, D.; Companys-Aleman, J.; Corpas, R.; Sanfeliu, C.; Loza, M. I.; Brea, J.; Morisseau, C.; Hammock, B. D.; Vázquez, S.; Pallàs, M.; Galdeano, C. *Neurotherapeutics*, **2020**, <https://doi.org/10.1007/s13311-020-00854-1>.

2-Oxaadamant-1-yl Ureas as Soluble Epoxide Hydrolase Inhibitors: *In Vivo* Evaluation in a Murine Model of Acute Pancreatitis

Sandra Codony, Eugènia Pujol, Javier Pizarro, Ferran Feixas, Elena Valverde, M. Isabel Loza, José M. Brea, Elena Saez, Julen Oyarzabal, Antonio Pineda-Lucena, Belén Pérez, Concepción Pérez, María Isabel Rodríguez-Franco, Rosana Leiva, Silvia Osuna, Christophe Morisseau, Bruce D. Hammock, Manuel Vázquez-Carrera, and Santiago Vázquez*

Cite This: <https://dx.doi.org/10.1021/acs.jmedchem.0c00310>

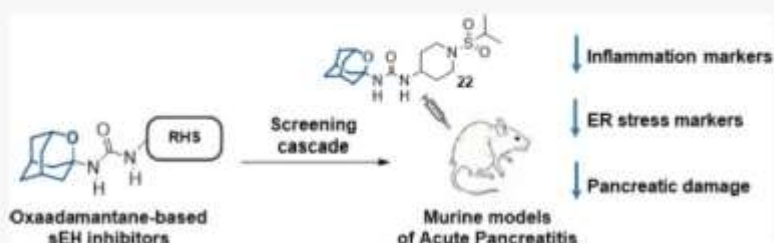
Read Online

ACCESS |

Metrics & More

Article Recommendations

Supporting Information



ABSTRACT: *In vivo* pharmacological inhibition of soluble epoxide hydrolase (sEH) reduces inflammatory diseases, including acute pancreatitis (AP). Adamantyl ureas are very potent sEH inhibitors, but the lipophilicity and metabolism of the adamantane group compromise their overall usefulness. Herein, we report that the replacement of a methylene unit of the adamantane group by an oxygen atom increases the solubility, permeability, and stability of three series of urea-based sEH inhibitors. Most of these oxa-analogues are nanomolar inhibitors of both the human and murine sEH. Molecular dynamics simulations rationalize the molecular basis for their activity and suggest that the presence of the oxygen atom on the adamantane scaffold results in active site rearrangements to establish a weak hydrogen bond. The 2-oxaadamantane **22**, which has a good solubility, microsomal stability, and selectivity for sEH, was selected for further *in vitro* and *in vivo* studies in models of cerulein-induced AP. Both in prophylactic and treatment studies, **22** diminished the overexpression of inflammatory and endoplasmic reticulum stress markers induced by cerulein and reduced the pancreatic damage.

INTRODUCTION

Arachidonic acid (AA) is a polyunsaturated fatty acid that is released from membrane phospholipids of activated cells by the action of phospholipase A₂ stimulation. AA can be converted into different metabolites, which can either enhance inflammation or help in its resolution. The cyclooxygenases (COXs) and the lipoxygenases (LOXs) convert AA to proinflammatory and nociceptive prostaglandins and leukotrienes, respectively.¹ Both pathways have been pharmaceutically targeted.² In contrast, a third metabolic route, the cytochrome P450 pathway, has been scarcely explored. Cytochrome enzymes can convert AA to epoxyeicosatrienoic acids (EETs), which are endowed with potent anti-inflammatory properties.^{3–5} However, soluble epoxide hydrolase (sEH, EPHX2, EC 3.3.2.3) rapidly hydrolyzes EETs to their corresponding dihydroxyeicosatrienoic acids (DiHETrEs), which show altered biological activity.^{6,7} *In vivo* pharmacological inhibition of sEH has been previously shown to stabilize the concentration of EETs, reducing inflammation and pain, suggesting that sEH is a potential target for the treatment of various diseases.^{8,9}

Structural studies revealed that sEH has an L-shaped hydrophobic pocket with the catalytic residues at the corner.^{10,11} Ureas, amides, and carbamates were shown to bind strongly to the catalytic residues of sEH. Taking into account the characteristics of the active site and the overall high hydrophobicity of the pocket, the introduction of lipophilic groups on both sides of the central urea has proven a successful strategy for the space-filling of the cavity and increasing van der Waals interactions, leading to several potent sEH inhibitors.¹² Indeed, a vast number of potent sEH inhibitors incorporate an adamantane moiety, including AR9281, the first sEH inhibitor to enter clinical trials (Figure 1).^{13–15}

Received: February 20, 2020

Published: August 6, 2020

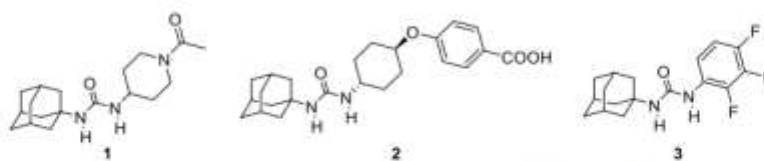
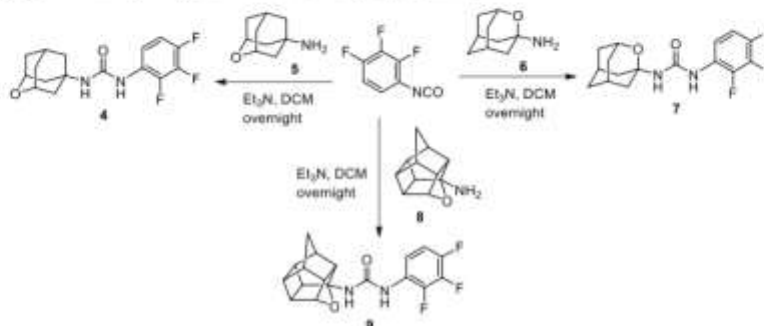
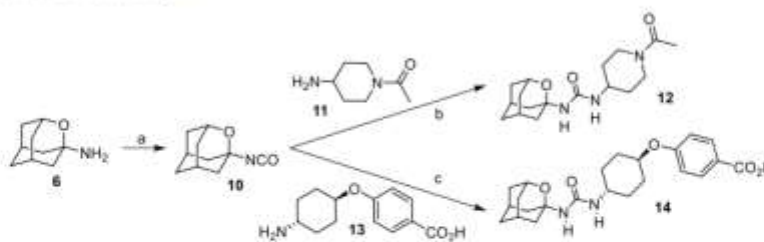


Figure 1. Adamantane-based sEH inhibitors **1** (AR9281, APAU, UC1153), **2** (*t*-AUCB),¹⁶ and **3**.¹⁷

Scheme 1. Synthesis of 2,3,4-Trifluorophenyl-Derived Ureas, **4**, **7**, and **9**

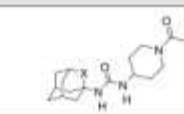
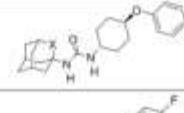
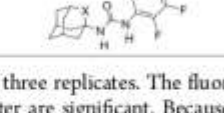
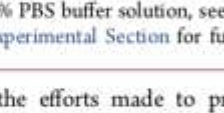
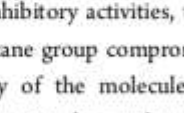
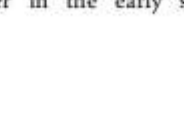


Scheme 2. Synthesis of Ureas **12** and **14**¹⁷



^aReagents and conditions: (a) Triphosgene, sat. NaHCO₃, DCM, 30 min; (b) **11**, DCM, overnight, 52% overall yield; (c) **13**, DCM, overnight, 24% overall yield. See the Experimental Section and Supporting Information for further details.

Table 1. Human sEH IC₅₀ and Solubility, Melting Point, and Permeability Values for Known Adamantane Inhibitors AR9281, *t*-AUCB, and **3**, and Their Oxygen Analogues **12**, **14**, and **7**

Compounds	X	h sEH IC ₅₀ (nM) ^a	Solubility (μM) ^b	Melting Point (°C)	Permeability (Caco-2) Papp (nm/s) A→B B→A	ER ^c
 1 , AR9281 (UC1153)	CH ₂	8.0	24	202–204 ^d	2.2 141.2 64.5	
 12	O	29.9	59	172–173	22.4 94.5 4.3	
 2 , <i>t</i> -AUCB	CH ₂	0.5	25	250–255 ^e	1.9 210.3 111	
 14	O	9.0	>100	255–257	1.4 75.5 55.4	
 3	CH ₂	7.7	16	216–219	6.7 4.6 0.69	
 7	O	21.3	27	196–198	168 151 0.9	

^aIC₅₀ values are the average of three replicates. The fluorescent assay as performed here has a standard error between 10 and 20%, suggesting that differences of two-fold or greater are significant. Because of the limitations of the assay, it is difficult to distinguish among potencies <0.5 nM.²⁵

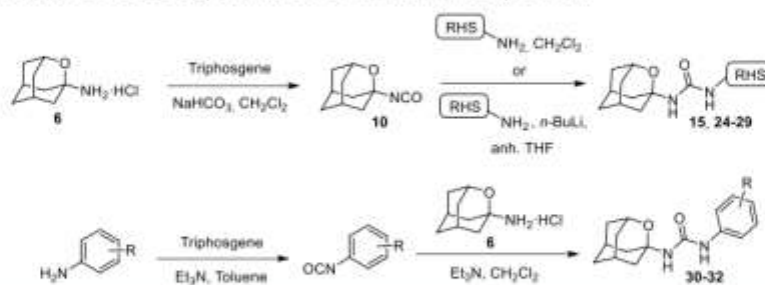
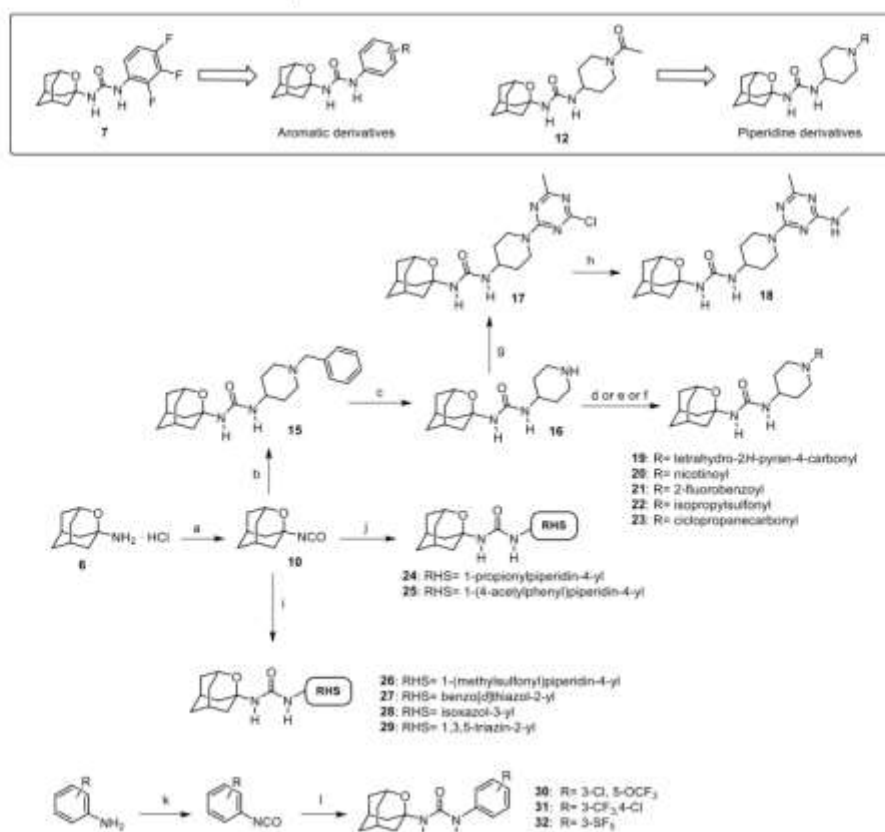
^bSolubility in a 1% DMSO/99% PBS buffer solution, see the Experimental Section for details. ^cThe efflux ratio was calculated as ER = (Papp B → A)/(Papp A → B). See the Experimental Section for further details. ^dTaken from ref 27. ^eTaken from ref 16.

However, regardless of the efforts made to procure drug candidates with excellent inhibitory activities, the pronounced lipophilicity of the adamantane group compromises negatively the overall water solubility of the molecule, an important physicochemical parameter in the early stages of drug

discovery,^{18,19} thus limiting the discovery of new drug-like sEH inhibitors.

To solve this problem, we hypothesized that the introduction of an oxygen atom should increase the solubility and may impact the overall drug-like properties of the known adamantane-based sEH inhibitors without seriously compro-

Scheme 3. Synthetic Procedures for the Preparation of 2-Oxaadamant-1-yl Ureas

Scheme 4. Synthesis of New 2-Oxaadamant-1-yl Ureas^{af}

^aReagents and conditions: (a) triphosgene, sat. NaHCO₃, DCM, 30 min; (b) 1-benzylpiperidin-4-amine, DCM, overnight; (c) H₂, Pd/C, MeOH, conc. HCl, 5 days. (d) Corresponding carboxylic acid, HOBt, EDCI-HCl, Et₃N, EtOAc, 24 h; (e) corresponding sulfonyl chloride, Et₃N, DCM, overnight; (f) corresponding acyl chloride, Et₃N, DCM, overnight; (g) 2,4-dichloro-6-methyl-1,3,5-triazine, DIPEA, DCM, 30 min; (h) methylamine hydrochloride, DIPEA, DCM, 40 °C, 40 min; (i) corresponding amine, *n*-BuLi, anh. THF, overnight; (j) corresponding amine, DCM, overnight; (k) triphosgene, Et₃N, toluene, 70 °C, 2 h; (l) 6-HCl, Et₃N, DCM, overnight. See the Experimental Section and Supporting Information for further details.

missing the inhibitory potency. Taking into account the availability of several oxapolycyclic amines,^{20–23} herein we have replaced the adamantane nucleus of known sEH inhibitors by selected polycyclic scaffolds bearing an oxygen atom. Encouragingly, previous research conducted around adamantane surrogates showed that the 2-oxaadamant-1-yl substituent is a suitable replacement moiety for the clinically approved antiviral drug amantadine.²⁴

RESULTS AND DISCUSSION

Chemistry. To test our hypothesis, the adamantane core present in inhibitor 3 was initially replaced by three known

oxapolycyclic amines, 5, 6, and 8.^{20–23} The reaction of commercially available 2,3,4-trifluorophenylisocyanate with 5, 6, and 8 gave ureas 4, 7, and 9, respectively, in 83, 94, and 94% yield (Scheme 1).

The three ureas were tested as human sEH inhibitors using a previously reported fluorescent-based assay.²⁵ The three compounds displayed IC₅₀ values in the same range of potency (47.4, 21.3, and 31.3 nM for 4, 7, and 9, respectively), although less potent than 3 (IC₅₀ = 7.7 nM).

Taking into account that (i) the 2-oxaadamantane-1-amine, 6, was synthetically much more accessible than its isomer 2-oxaadamantane-5-amine, 5, and (ii) the chiral nature of amine

8, the synthesis of the oxa-analogues of AR9281 and *t*-AUCB was subsequently performed only with amine 6.

For the synthesis of urea 12, amine 6 was treated with triphosgene to yield isocyanate 10, which was then reacted with the commercially available 1-acetyl-4-aminopiperidine, 11. Similarly, the reaction of 10 with 4-((*trans*-4-aminocyclohexyl)oxy)benzoic acid, 13, prepared as previously reported,²⁶ furnished urea 14 (Scheme 2).

Interestingly, although less potent than their hydrocarbon counterparts, the novel oxaadamantane-derived ureas were nanomolar inhibitors of the human sEH (see Table 1). Often, a high melting point is indicative for bad physical properties such as low solubility in water and organic solvents. The adamantane-derived inhibitors have limited solubility in water and high melting points (Table 1), which likely affect their *in vivo* efficacy and certainly make formulation difficult. Gratifyingly, in AR9281 and the compound 3 series, the oxaadamantane derivatives exhibited lower melting points than their adamantane counterparts, while *t*-AUCB and 14 presented approximately the same value (Table 1). Remarkably, as expected, the compounds featuring the 2-oxaadamantane moiety exhibited higher solubility values, in the three series, than the ones presenting the adamantane scaffold (compare AR9281 vs 12, *t*-AUCB vs 14, and 3 vs 7 in Table 1). Pleasingly, in addition to the expected improvement in the solubility, the membrane permeability improved for the three series. Thus, in the AR9281 (1 and 12) and *t*-AUCB (2 and 14) series, a decrease in the efflux ratio was observed when the methylene unit was replaced by an oxygen atom. On the other hand, in the trifluorophenyl analogues, the efflux ratio was already low, but the substitution led to an increase in both AB and BA permeability (see Table 1).

Certainly, the introduction of the oxygen atom in the adamantane scaffold reduced the potency. Notwithstanding, designing bioactive compounds is a multifactorial process; therefore, in view of the significant increase in aqueous solubility and permeability and the decrease of the melting point arising from the replacement of a methylene unit of the adamantane by an oxygen atom, the synthesis of two families of analogues of 7 and 12 was undertaken using diverse right-hand side (RHS) fragments selected from previous series of known sEH inhibitors.^{15,17,28–32} After exploring their potency as sEH inhibitors, their cytotoxicity and DMPK properties were assessed for selecting a candidate to perform an *in vivo* proof-of-concept study in a murine model of acute pancreatitis (AP), for which an sEH inhibitor showed effectiveness at reducing symptoms.^{33,34} Of note, an *in vivo* study of the third oxa-derivative, 14, has been disclosed recently elsewhere.³⁵

Two different synthetic procedures were followed to obtain the derivatives of 7 and 12 (Schemes 3 and 4). The first route involved the synthesis of isocyanate 10 from amine 6, followed by its reaction with the amines containing the RHS of the ureas, either directly (compounds 15, 24, and 25), or, for the less nucleophilic amines, after deprotonation with a strong base such as *n*-butyllithium (compounds 26–29). The second pathway involved the reaction of amine 6 in the presence of triethylamine with the isocyanate derived from the different anilines containing the RHS of the urea (compounds 30–32).

The reaction of isocyanate 10 with commercially available 1-benzylpiperidin-4-amine furnished urea 15, which, upon debenzilation by catalytic hydrogenation in methanol, led to 16. The reaction of piperidine 16 with commercially available 2,4-dichloro-6-methyl-1,3,5-triazine furnished urea 17, which

upon reaction with methylamine led to urea 18. Of note, the triazine unit is a feature of several sEH inhibitors disclosed by GSK, including its clinical candidate GSK2256294.^{31,32} The reaction of 16 with a series of acyl chlorides, sulfonyl chlorides, or carboxylic acids provided the desired ureas 19–23 in moderate to good yields.

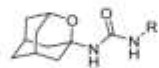
Compound 24 was directly obtained from 10 and the commercially available 1-(4-aminopiperidin-1-yl)propan-1-one. Similarly, the reaction of 10 with 1-(4-(4-aminopiperidin-1-yl)phenyl)ethan-1-one, prepared as reported in the literature,³⁶ furnished urea 25. When the amines were not nucleophilic enough to attack isocyanate 10, the presence of a strong base such as *n*-butyllithium was necessary in order to deprotonate the amine. The subsequent reaction of the anion with 10 led to ureas 26–29 in low to moderate yields (Scheme 4).

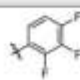
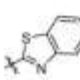
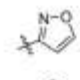
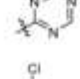
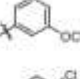
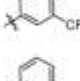

Finally, a different synthetic strategy was undertaken for the synthesis of the phenyl derivatives 30–32, which involved the treatment of 6 with the corresponding arylisocyanates in the presence of triethylamine. In turn, the intermediate isocyanates were either commercially available or synthesized from the reaction of the corresponding anilines with triphosgene, in the presence of triethylamine in hot toluene (Scheme 4).

sEH Inhibition and Structure–Activity Relationships.

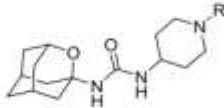
As a first step for the biological characterization of the novel ureas, their potency as human and murine sEH inhibitors was tested (Tables 2 and 3). In line with the good activity of 7,


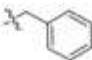
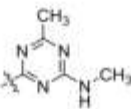
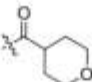
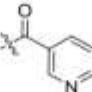
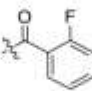
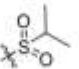
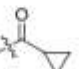
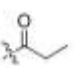
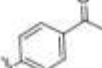
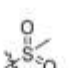
Table 2. Human (hsEH) and Murine (msEH) sEH IC₅₀ of the Aromatic and Heteroaromatic Series of 2-Oxaadamant-1-yl Ureas



Compound	R	IC ₅₀ (nM) ^a	
		hsEH	msEH
7		21.3	553
27		782	14721
28		911	3853
29		1448	>100,000
30		52.6	1857
31		19.7	344
32		35.9	723

^aReported IC₅₀ values are the average of three replicates. The fluorescent assay as performed here has a standard error between 10 and 20%, suggesting that differences of twofold or greater are significant. Because of the limitations of the assay, it is difficult to distinguish among potencies <0.5 nM.²³

Table 3. Human (hsEH) and Murine (msEH) sEH IC₅₀ of the Piperidine Series of 2-Oxaadamant-1-yl Ureas


Compound	R	IC ₅₀ (nM) ^a	
		hsEH	msEH
12		29.9	92.3
15		1093	n.d. ^b
18		496	365
19		491	512
20		159	291
21		46	75.9
22		197	79.1
23		213	130
24		356	234
25		82.5	107
26		247	174

^aReported IC₅₀ values are the average of three replicates. The fluorescent assay as performed here has a standard error between 10 and 20%, suggesting that differences of twofold or greater are significant. Because of the limitations of the assay, it is difficult to distinguish among potencies <0.5 nM.²⁵ ^bn.d.: not determined.

compounds 30–32 were potent inhibitors of the human sEH, while the compounds featuring a heteroaromatic ring attached to the urea group, 27–29, were poor inhibitors of the human enzyme (IC₅₀ > 500 nM). However, regardless of the presence of an aromatic or heteroaromatic ring as the RHS of the urea, all compounds were very poor inhibitors of the murine enzyme. For this reason, this set of derivatives was not further evaluated.

Table 3 collects the structures and the IC₅₀ values of 10 analogues of 12. As previously seen with the analogues of 7, the introduction of the triazine group, 18, yielded a poor inhibitor of the human sEH. However, the introduction of an aryl derivative, 25, resulted in a two-digit nanomolar inhibitor. In the adamantane series of AR9281 derivatives, the replacement of the methyl group of the acetyl unit in the piperidine by a broad range of alkyl and aryl substituents did not significantly impact the activity.¹⁵ By way of contrast, within our series of 2-oxaadmantane derivatives, subtle variations in the N-substituent of the piperidine led to significant changes. Increasing the size of the alkyl group from the methyl of 12 to propyl (24), cyclopropyl (23), and tetrahydropyranyl (19) resulted in a 10–15-fold reduction of the potency. Also, while the introduction of a 2-fluorophenyl group (21) furnished a good sEH inhibitor, the 3-pyridyl unit, as in 20, caused a 3-fold drop in inhibitory activity. While the replacement of the acetyl group in AR9281 by a benzyl unit did not affect the inhibitory activity,¹⁵ the same change in the 2-oxaadmantane series (12 vs 15) led to an important reduction (almost 40-fold) of the potency (Table 3). Finally, the substitution of the acetyl group of 12 for two alkylsulfonamide groups, as in 22 and 26, yielded a six- and eightfold reduction of the activity, respectively.

Furthermore, all the compounds were also evaluated as murine sEH inhibitors (Table 3). Although there were a few minor inconsistencies, in general, the most potent compounds in the human sEH were also the most potent inhibitors of the murine sEH. Considering both the human and murine sEH inhibitory activity, compounds 12, 21, 22, and 25 were selected for further studies.

In Silico Study: Molecular Basis of 2-Oxaadamant-1-yl Ureas as sEH Inhibitors. To elucidate the conformational and molecular basis of the inhibitory mechanism of 2-oxaadmant-1-yl ureas and, in particular, the molecular impact of the replacement of a methylene unit by an oxygen atom on the activity, molecular dynamics (MD) simulations of sEH were carried out in the presence of two selected compounds (22 and 26). The ability of sEH to recognize and properly bind both small and bulky inhibitors (as the ones depicted in Tables 1–3) will depend on the grade of plasticity of its active site. Indeed, some epoxide hydrolases present rich conformational dynamics of key structural elements surrounding the active site, which play a crucial role for recognizing bulky epoxide substrates and inhibitors of different sizes.³⁷ To explore the conformational dynamics of sEH, and how compounds 22 and 26 are accommodated in the active site, three replicates of 250 ns of MD simulations were performed for four different systems: (a) in the *apo* state; (b) in the presence of compound 26 (IC₅₀ = 247.2 nM) bound in the active site; (c) with the inhibitor AR9273 (the hydrocarbon counterpart of 26, IC₅₀ = 1.9 nM,¹³ PDB ID: SALZ³⁸) bound; and (d) with compound 22 (IC₅₀ = 197.1 nM) present in the active site (see Figure 2). The changes on the active site volume along the MD simulations were monitored using the computational tool POCKET VOLUME MEASURER (POVME)³⁹ to capture the conformational plasticity of the sEH active site. In the *apo* state, the volume fluctuates between 70 and 500 Å³, providing an average value of 253 ± 62 Å³ (see Figure 2b). The high fluctuation of the active site volume in the *apo* state already suggests that inhibitors of different sizes can fit in the binding pocket. The visual analysis of the shape of the pocket clearly shows the presence of two hydrophobic pockets separated by

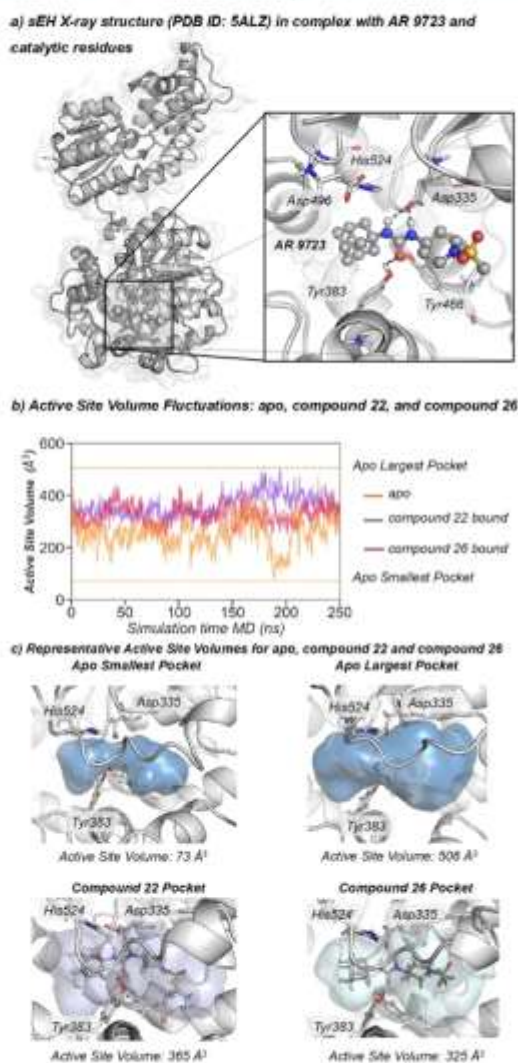


Figure 2. (a) Representation of sEH structure (PDB: 5ALZ), active site catalytic residues (nucleophilic Asp335, Tyr383, Tyr466, and the histidine–aspartic acid pair His524–Asp496). (b) Plot of the fluctuations of the active site volume for the *apo* state (orange line, $253 \pm 62 \text{ \AA}^3$), compound 22 bound (purple line, $361 \pm 43 \text{ \AA}^3$), and compound 26 bound (red line, $324 \pm 41 \text{ \AA}^3$) along a representative 250 ns MD simulation trajectory. (c) Representative sEH structures with the active site volume obtained from MD simulations of *apo*, 22, and 26.

catalytic Asp335 and Tyr383 residues (L-shaped hydrophobic pocket, see Figure 2c). The first hydrophobic pocket is located below the catalytic His524, which is known to accommodate the adamantane moiety, according to X-ray data (see Figure 2 and PDB ID: 5ALZ). The other pocket is located on the right-hand site of Asp335 and Tyr383 residues and encompasses also the hydrophobic entrance tunnel. The size of both pockets significantly changes along the MD simulations, the “adamantane” pocket being the smallest most of the simulation time. When either compound 22 or 26 is bound in the active site, the average volume is 361 ± 43 and $324 \pm 41 \text{ \AA}^3$, respectively, in line with the bulkier isopropylsulfonyl group of 22. As shown in Figure 2b, both inhibitors restrain the flexibility of the active site in comparison with the significant fluctuations observed in the *apo* state. MD simulations show

that sEH presents a pocket with significant conformational plasticity and its breathing capability can be key to recognize and bind inhibitors of different sizes.⁴⁰ Compounds 22 and 26 are both capable of restricting the inner flexibility of sEH active site residues, keeping the active site blocked. The large active site volumes sampled indicate that there is room for further functionalization of both the oxadamantyl moiety and the RHS of the urea.

To gain a deeper insight into the molecular basis of the inhibitory mechanism of 2-oxadamantyl derivatives, we monitored key interactions between the three inhibitors (AR9273, 26, and 22) and relevant active site residues along the 250 ns MD simulations of sEH (see Figure 3). The three selected distances correspond to the one between the carboxylic group of the catalytic Asp335 and one of the NH groups of the inhibitor, and the distances between the carbonyl group of the urea inhibitors and the OH group of either Tyr383 or Tyr466 residues (Figure 3a). MD simulations show that the three hydrogen bonds remain significantly stable along the whole simulation time for the hydrocarbon-based AR9273 ($d(C_{\text{Asp335}}-\text{NH}_{\text{AR 9273}}) = 2.55 \pm 0.17 \text{ \AA}$, $d(\text{OH}_{\text{Tyr383}}-\text{O}_{\text{AR 9273}}) = 1.76 \pm 0.17 \text{ \AA}$, and $d(\text{OH}_{\text{Tyr466}}-\text{O}_{\text{AR 9273}}) = 2.21 \pm 0.83 \text{ \AA}$). In the case of oxadamantane-based 22 and 26 compounds, the hydrogen bonds are less stable than for AR9273 and fluctuate along the simulation time, indicating a lower affinity toward the active site of sEH ($d(C_{\text{Asp335}}-\text{NH}_{26}) = 2.66 \pm 0.19 \text{ \AA}$, $d(\text{OH}_{\text{Tyr383}}-\text{O}_{26}) = 2.01 \pm 0.83 \text{ \AA}$, $d(\text{OH}_{\text{Tyr466}}-\text{O}_{26}) = 2.67 \pm 0.81 \text{ \AA}$ for 26 and $d(C_{\text{Asp335}}-\text{NH}_{22}) = 2.74 \pm 0.40 \text{ \AA}$, $d(\text{OH}_{\text{Tyr383}}-\text{O}_{22}) = 2.50 \pm 1.54 \text{ \AA}$, $d(\text{OH}_{\text{Tyr466}}-\text{O}_{22}) = 2.06 \pm 0.71 \text{ \AA}$ for 22).

The simulations indicate that the adamantane group of AR9273 freely rotates inside the hydrophobic pocket, establishing weak interactions with the surrounding Tyr383, Leu408, Met419, Val498, His524, and Trp525. This situation totally changes with the introduction of an oxygen atom into the adamantane scaffold, which restricts the rotation of the adamantane moiety inside the hydrophobic pocket, introducing an entropic penalty that is partially compensated by more persistent interactions with surrounding residues (see the detailed analysis of noncovalent interactions in Figure S1). This restricted flexibility induces a dipole moment in the pocket that reshapes the interactions between catalytic residues (see Figure 3b). Interestingly, the oxadamantane group rapidly orients to establish an interaction between the oxo group and both a water molecule and the positively charged His524 residue (see Figures 3b and S1). The orientation toward the water molecule occupying the active site occurs in both 22 and 26 simulations. To unravel in more detail the network of interactions established when the oxygen group is present in the adamantane scaffold, we represented the noncovalent interactions (NCI) between compound 22 and active site residues computed with NCIPLOT (see Figure S1).⁴¹ The NCI analysis reveals a hydrogen bond interaction between the water molecule and the oxo group, and a wide ion dipole interaction surface between the oxygen and the protonated His524. Additionally, several hydrophobic interactions between the adamantane group and residues Phe267, Tyr383, Leu408, Leu417, Met419, and Trp525 are observed (see Figure S1). However, in the presence of AR9273, the water molecule establishes a network of hydrogen bonds with His524 and Glu269 that keeps Asp335 interacting with the NH groups of the inhibitor. In 22 and 26, this water molecule preferentially interacts with the oxadamantane moiety rather

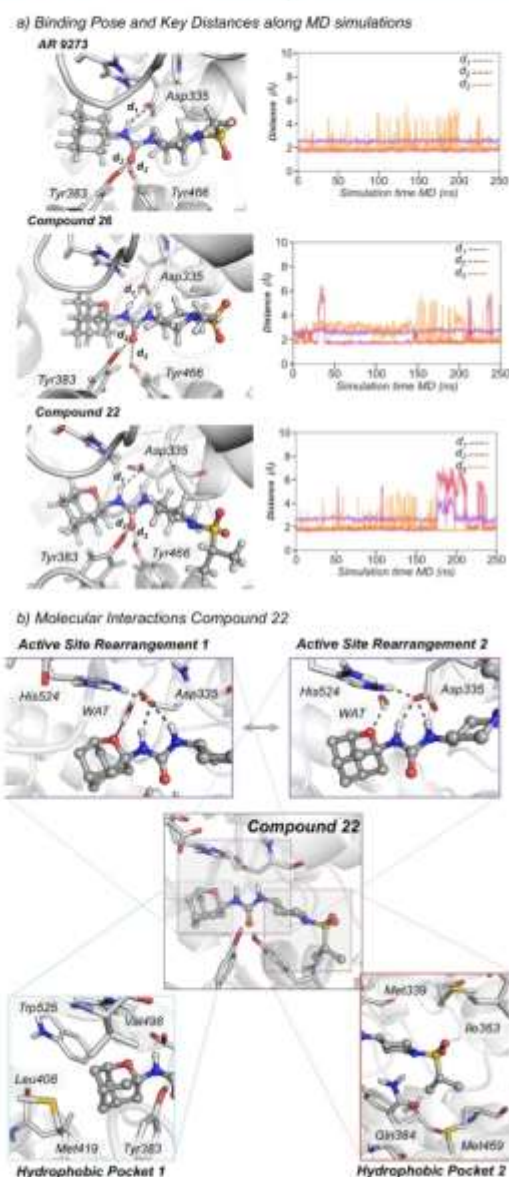


Figure 3. (a) Representative structures of AR9273, 22, and 26 bound in the active site of sEH obtained from MD simulations. Plot of the distance between the carboxylic group of the catalytic Asp335 and the amide groups of the inhibitor (purple line, $d_1(C\gamma_{Asp335}-NH_{INH})$) and the distances between the carbonyl group of the urea inhibitors and the OH group of either Tyr383 (red line, $d_2(OH_{Tyr383}-O_{INH})$) or Tyr466 residues (orange line, $d_3(OH_{Tyr466}-O_{INH})$) along the MD simulations of AR 9273 ($d_1(C\gamma_{Asp335}-NH_{AR\ 9273}) = 2.55 \pm 0.17$ Å, $d_2(OH_{Tyr383}-O_{AR\ 9273}) = 1.76 \pm 0.17$ Å, and $d_3(OH_{Tyr466}-O_{AR\ 9273}) = 2.21 \pm 0.83$ Å), 22 ($d_1(C\gamma_{Asp335}-NH_{26}) = 2.66 \pm 0.19$ Å, $d_2(OH_{Tyr383}-O_{26}) = 2.01 \pm 0.83$ Å, $d_3(OH_{Tyr466}-O_{26}) = 2.67 \pm 0.81$ Å), and 26 ($d_1(C\gamma_{Asp335}-NH_{22}) = 2.74 \pm 0.40$ Å, $d_2(OH_{Tyr383}-O_{22}) = 2.50 \pm 1.54$ Å, $d_3(OH_{Tyr466}-O_{22}) = 2.06 \pm 0.71$ Å). (b) Key molecular interactions between 22 and active site residues.

than with His524, which establishes a hydrogen bond with Asp335 that has undergone a reorientation of its side chain (see active site rearrangements in Figure 3b). This destabilizes the interactions between Asp335 and the carbonyl group of the inhibitor, lowering the affinity of 22 and 26 for the sEH active site. To estimate the binding affinities, we computed the

relative binding free energy using the thermodynamic integration (TI) method between compound 22 and its adamantane counterpart containing a methylene unit instead of an oxygen (22-CH₂). Both ligands present a similar affinity toward the sEH active site, being the relative binding free energy of compound 22-CH₂ with respect to compound 22 around -0.8 kcal/mol. These observations are in line with the obtained IC₅₀ values that indicate slightly higher affinity for adamantane derivatives. Therefore, the introduction of an oxygen atom into the adamantane scaffold introduces a network of interactions that altogether restrict its orientation within the hydrophobic pocket, having an impact on the affinity of oxadamantane inhibitors for sEH.

Finally, we assessed the *in silico* lipophilicity of compounds 22 and 22-CH₂ by computing the log *P* from the solvation free energy differences using the M06-2X functional with Solvation Model based on Density (SMD) implicit solvation and the def2-SVP basis set.⁴² The computed log *P* of compound 22 is 0.77 while that of 22-CH₂ is 2.44. In line with the above reported experimental solubilities, these results predict a significant decrease in lipophilicity when the oxygen atom is introduced in the adamantane scaffold of compound 22.

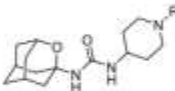
Biological Profiling of the Selected sEH Inhibitors.

The four more potent inhibitors were characterized in terms of cytotoxicity in two different cell lines [Transformed Human Liver Epithelial-2 cell line (THLE-2) and Peripheral Blood Mononuclear Cells (PBMCs)], solubility, microsomal stability (human, mouse, and rat species), hERG (human ether-a-go-go-related gene) inhibition, cytochromes P450 (CYP) inhibition, and predicted brain permeability, in order to select the best candidate to perform an *in vivo* study in a murine model of AP. None of the tested compounds appeared to be cytotoxic for the THLE-2 at the highest concentration tested (100 μM). Additionally, compounds 12, 21, and 22 were not cytotoxic in the PBMC at the highest concentration tested (20 μM) (Table 4).

Taking into account that AP is a peripherally restricted inflammatory disease, we wanted to prioritize compounds showing negative BBB permeation in order to avoid potential side effects resulting from central inhibition of sEH. The selected compounds were further tested for predicted brain permeation in the widely used *in vitro* parallel artificial membrane permeability assay-blood-brain barrier (PAMPA-BBB) model.⁴³ With the sole exception of 25, all the compounds have predicted limited BBB penetration (Table 4).

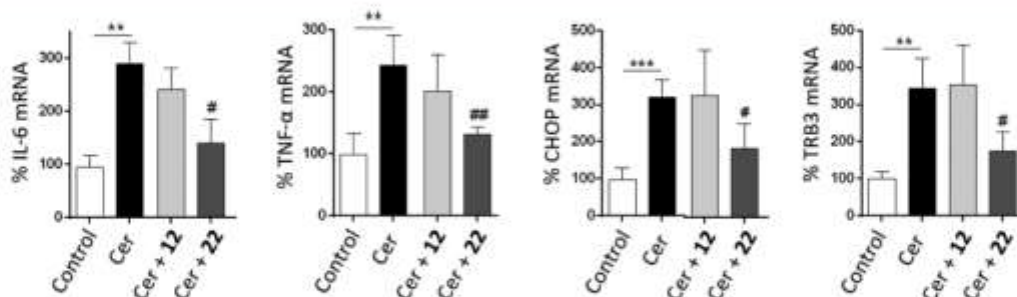
Next, the solubility was experimentally determined in a 1% DMSO/99% PBS buffer solution. In the adamantane series, when the methyl group of the amide of AR9281 was replaced by bigger substituents, the potency was retained or even increased, but the solubility dramatically dropped.¹⁵ Pleasantly, all the oxadamantanes presented good to excellent solubilities (see Table 4), greater than that of the adamantane-based inhibitors 1–3, as expected.

The microsomal stability of 12, 21, 22, and 25 was evaluated in human, mice, and rat liver microsomes, which are widely used to determine the likely degree of primary metabolic clearance in the liver. Although compound 21 displayed unsatisfactory stabilities in the three species and 25 presented poor stability in human microsomes, compounds 12 and 22 showed good microsomal stabilities in the three species (see Table 4). Furthermore, the study of cytochrome P450 (CYP) inhibition was performed in order to examine the inhibitory potency of 12 and 22, the compounds with better overall

Table 4. Cytotoxicity (in THLE-2 and PBMC Lines), PAMPA-BBB, Solubility, and Microsomal Stability Values of Selected Compounds


Compound	R	Cytotoxicity LC ₅₀ (μM)		PAMPA- BBB	Solubility ^(a) (μM)	Microsomal stability ^(b)		
		PBMC	THLE-2			Human	Mouse	Rat
12		>20	>100	CNS-	59	88.8	80.5	85.1
21		>20	>100	CNS-	>100	30.2	39.5	19.3
22		>20	>100	CNS-	34	72.7	63.9	63.9
25		ND	>100	CNS-	81.5	40	73	84

^aSolubility in a 1% DMSO/99% PBS buffer solution. ^bPercentage of remaining compound after 60 min of incubation with human, mice, and rat microsomes in the presence of NADPH at 37 °C. Metabolism of testosterone was used as a positive control. See the Experimental Section for details.

**Figure 4.** Results of the *in vitro* study of cerulein-induced AP in AR42J pancreatic rat cells. *IL-6*, *TNF α* , *CHOP*, and *TRB3* mRNA levels are presented as the mean \pm SEM ($n = 5$ per group). ** $p < 0.01$, *** $p < 0.001$ vs control. # $p < 0.05$, ## $p < 0.01$ vs Cer.

microsomal stabilities, against human recombinant cytochrome P450 enzymes, mainly CYP1A2, CYP2C9, CYP2C19, CYP2D6, and CYP3A4, through a fluorescence-detection method. These assays were of great interest not only for the detection of possible drug–drug interactions but also in terms of selectivity as EETs are formed by cytochrome P450 isoforms, especially CYP2C19, followed by CYP1A2 and CYP2J2 to a lesser extent. Satisfactorily, the tested compounds showed very low potency (higher than 10 μ M), inhibiting the different cytochromes tested (see Table S2 in the Supporting Information). This potency is much lower (more than 100-fold) than the potency observed either in human or in murine sEH. Inhibition of the hERG channel is an important toxicology screen because of its known association with cardiotoxicity. Inhibitors 12 and 22 showed minimal inhibition on hERG at 10 μ M (see Table S2 in the Supporting Information). Therefore, the selected inhibitors are considered not to present a risk with CYP or hERG inhibition. Finally, three representative inhibitors were tested for selectivity against *h*COX-2 and *h*LOX-5, two enzymes involved in the AA cascade. Neither the *N*-acyl piperidines 21 and 24 nor the *N*-sulfonyl piperidine 22 displayed significant inhibition of these enzymes (see Table S3 in the Supporting Information).

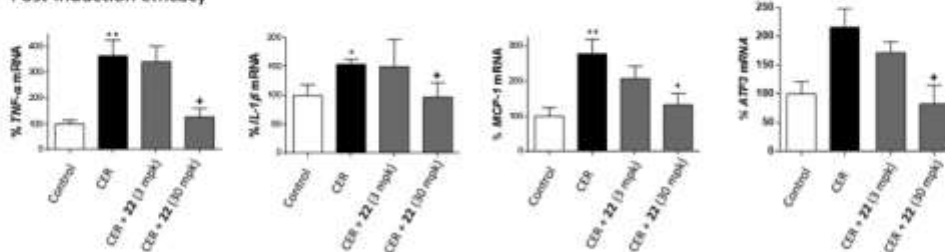
In Vitro Proof of Concept: AP. AP is a serious and life-threatening inflammatory disease and one of the most common gastrointestinal disorders worldwide without specific therapies available.^{44–46} Recently, it was shown that the EPHX2 whole-body knockout (KO) mice exhibit attenuated cerulein- and arginine-induced AP³³ and that pharmacological inhibition of sEH can modulate the severity of AP before and after induction of disease because of the potent anti-inflammatory properties of the EETs and the reduction of the endoplasmic reticulum (ER) stress.³⁴

In order to select a candidate for *in vivo* studies and verify the positive effect of the new sEH inhibitors on AP, we performed an *in vitro* proof of concept in the AR42J pancreatic acinar rat cell line that expresses sEH,⁴⁷ a well-established model for evaluating the potential therapeutic activity of compounds for AP.^{48,49} Given that this is a rat-derived cell line and the inhibitory activity of 12 and 22 was previously evaluated for the human and murine enzymes (see above), we first confirmed that the selected inhibitors presented potency in the rat enzyme. Both compounds inhibited the rat sEH, compound 22 being slightly more potent than 12 (IC₅₀ of 1.9 and 3.3 nM, respectively).

Table 5. Pharmacokinetic Parameters in Mouse for ip and iv Administration Routes of Compound 22 at 1 mg/kg

route	$T_{1/2}$ (h)	T_{max} (h)	C_{max} (ng/mL)	C_v (ng/mL)	AUC_{last} (h-ng/mL)	$AUC_{inf-obs}$ (h-ng/mL)	V_z (L/kg)	Cl (L/h/kg)
ip	3.02	0.16	117.33		34.67	35.20	124.02	28.41
iv	2.80	0.16	108.33	236.23	59.1	59.63	67.73	16.77

Post-induction efficacy



Pre-induction efficacy

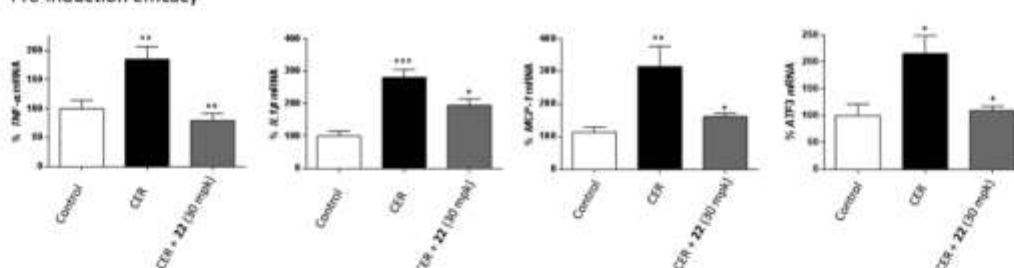


Figure 5. Results of the *in vivo* studies of cerulein-induced AP in the post- and preinduction models. *TNF- α* , *IL-1 β* , *MCP-1*, and *ATF3* mRNA levels are presented as the mean \pm SEM ($n = 5$ per group). * $p < 0.05$, ** $p < 0.01$, *** $p < 0.001$ vs control. * $p < 0.05$, ** $p < 0.01$ vs cerulein (CER).

For the *in vitro* study of efficacy, AR42J cells were treated with cerulein (Cer), a well-known inducer of AP, and with the selected compounds, following an established procedure.⁴⁹ Inflammatory (IL-6 and *TNF- α*) and ER stress (CHOP and TRB3) markers were measured (Figure 4). As expected, cells treated with cerulein (10 nM) showed an increase in the expression of inflammatory and ER stress markers, while coincubation of the cells with cerulein and the sEH inhibitors 12 and 22 (60 μ M) caused a significant reduction in the mRNA levels of these markers. Notably, compound 22 completely abolished the increase in the expression of IL-6, CHOP, and TRB3 and strongly attenuated the increment in *TNF- α* caused by cerulein exposure. Consequently, compound 22 was chosen for the *in vivo* efficacy studies in two mice models of AP. Overall, 22 has low nanomolar inhibition of the murine sEH, does not exhibit cytotoxicity, does not inhibit cytochrome P450s or hERG, has good microsomal stability, predicted poor brain penetration, and has a reasonable solubility value.

Pharmacokinetic Study of 22. To determine its pharmacokinetic profile in mouse, compound 22 was administered either by intravenous (iv) or intraperitoneal (ip) routes at a single dose of 1 mg/kg (see Figure S2 and Tables S4 and S5 in the Supporting Information). Pharmacokinetic parameters are shown in Table 5. For both administration routes, T_{max} and C_{max} values were similar. Good exposures of compound 22 were obtained, indicating bioavailability of 59%. High volumes of distribution and clearance were obtained with both administration routes, indicating that while 22 is well distributed across all tissues, it is eliminated quite fast. Considering the results obtained, 22 was administered ip in the subsequent *in vivo* studies.

Maximum Tolerated Dose Study of 22. In order to determine the potential acute toxicological effect, compound 22 was ip daily administered to mice at variable doses (5, 10, 20, and 80 mg/kg) for 5 consecutive days. No toxic effects were observed based on body weight along the treatment as well as the absence of apparent behavior problems and petechiae, indicating that compound 22 is well tolerated.

In Vivo Efficacy Study. To determine the effects of the administration of compound 22 on AP, C57BL/6J mice were treated with this sEH inhibitor before (prevention) and after (treatment) the induction of AP by cerulein, following already published protocols (see Figure S3 in the Supporting Information and the Experimental Section).³⁴ The post-induction efficacy study was performed in order to simulate a treatment study. In this protocol, cerulein was administered several times before the administration of compound 22.

Results of the postinduction efficacy study are shown in Figure 5. In line with previous reports,³⁴ mice treated with cerulein presented a significant increase in the mRNA abundance of inflammatory (*TNF- α* , *IL-1 β* , and *MCP-1*) and ER stress (*ATF3*) markers. Although the administration of compound 22 at 3 mg/kg did not cause a significant reduction of inflammatory and ER stress markers, administration of 30 mg/kg produced a significant reduction in the four markers studied compared to mice treated only with cerulein.

Considering that the dosage of 30 mg/kg was the one that presented significant effects on the postinduction model, the preinduction efficacy study was performed only at 30 mg/kg. Results (Figure 5) indicate that administration of 22 significantly reduced an increase of inflammatory (*TNF- α* , *IL-1 β* , and *MCP-1*) and ER stress (*ATF3*) markers produced by cerulein administration. Interestingly, AP is the most

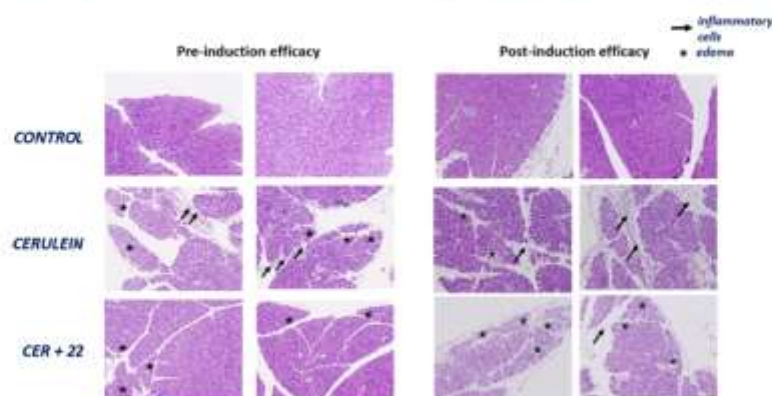


Figure 6. Representative H&E-stained sections of the pancreas from the preinduction (left) and postinduction (right) efficacy studies. CER: cerulein. Arrows indicate the presence of inflammatory cells and asterisks the presence of edema.

common complication of the endoscopic retrograde cholangiopancreatography (ERCP), a well-established technique for the treatment of pathological conditions of the biliary tract and pancreas. ERCP-related AP occurs in up to 9% of ERCPs in unselected prospective studies. The severity of post-ERCP pancreatitis can range from mild disease with full recovery to critical illness with necrotizing pancreatitis, multiorgan failure, prolonged hospitalization, and even death.⁵⁰ The efficacy of preinduction compound **22** on AP suggests that such treatment might be of interest to patients before the ERCP procedure, in order to diminish the probabilities of suffering of AP as a complication of this classic procedure.

Histopathology. Additionally, the severity of cerulein-induced pancreatitis in control and sEH inhibitor-treated mice was determined by histologic analyses. Pathologic changes were studied on H&E-stained pancreas sections from control, cerulein-treated, and cerulein- and **22**-treated mice in both the preinduction and postinduction AP models. As anticipated, the administration of cerulein caused a significant increase in edema and inflammation. In contrast, mice treated with compound **22** after or before the induction of AP exhibited a significant decrease in cerulein-induced edema and inflammation (Figure 6).

CONCLUSIONS

Several sEH inhibitors feature an adamantane moiety in their structure; however, its lipophilicity negatively compromises the solubility and PK properties of these compounds. In this work, a new family of sEH inhibitors bearing a 2-oxadamantane moiety in order to improve those characteristics were synthesized. Most of the compounds were nanomolar inhibitors of the human and murine sEH, although somehow less potent than their adamantane counterparts. Molecular modeling suggests that the introduction of the oxygen atom into the adamantane scaffold restricts its orientation within the hydrophobic pocket and weakens hydrogen bonds between the inhibitor and the enzyme. Biological profiling (solubility, cytotoxicity, metabolic stability, predicted BBB penetration, CYP450s and hERG inhibition) allowed us to select compound **22** for *in vivo* studies in a murine model of cerulein-induced AP. In both preinduction and postinduction studies, **22** diminished the overexpression of inflammatory and ER stress markers induced by cerulein and reduced pancreatic damage. Because of the promising biological activity of **22**,

further optimization of new sEH inhibitors for the treatment of AP, an unmet medical need, is underway.

Finally, the adamantane unit is a typically used polycyclic scaffold in many drug discovery programs.^{51,52} It is already present in nine clinically approved drugs and in many clinical candidates. Nonetheless, the use of its oxapolycyclic analogues has largely been neglected in drug discovery. This work may pave the way for the evaluation of less lipophilic scaffolds in several other targets, currently being explored with adamantanes.

EXPERIMENTAL SECTION

Chemical Synthesis. General Methods. Commercially available reagents and solvents were used without further purification unless stated otherwise. Preparative normal phase chromatography was performed on a CombiFlash Rf 150 (Teledyne Isco) with prepacked RediSep Rf silica gel cartridges. Thin-layer chromatography was performed with aluminum-backed sheets with silica gel 60 F254 (Merck, ref 1.05554), and spots were visualized with UV light and 1% aqueous solution of KMnO_4 . Melting points were determined in open capillary tubes with an MFB 595010M Gallenkamp; 400 MHz ^1H and 100.6 MHz ^{13}C NMR spectra were recorded on a Varian Mercury 400 or on a Bruker 400 Avance III spectrometer; 500 MHz ^1H NMR spectra were recorded on a Varian Inova 500 spectrometer. The chemical shifts are reported in ppm (δ scale) relative to internal tetramethylsilane, and coupling constants are reported in Hertz (Hz). Assignments given for the NMR spectra of selected new compounds have been carried out on the basis of DEPT, COSY $^1\text{H}/^1\text{H}$ (standard procedures), and COSY $^1\text{H}/^{13}\text{C}$ (gHSQC and gHMBC sequences) experiments. IR spectra were run on a PerkinElmer Spectrum RX I, a PerkinElmer Spectrum TWO, or a Nicolet Avatar 320 FT-IR spectrophotometer. Absorption values are expressed as wave-numbers (cm^{-1}); only significant absorption bands are given. High-resolution mass spectrometry (HRMS) analyses were performed with an LC/MSD TOF Agilent Technologies spectrometer. The elemental analyses were carried out in a Flash 1112 series thermofinnigan elemental microanalyzer (AS) to determine C, H, N, and S. The structure of all new compounds was confirmed by elemental analysis and/or accurate mass measurement, IR, ^1H NMR, and ^{13}C NMR. The analytical samples of all the new compounds, which were subjected to pharmacological evaluation, possessed purity $\geq 95\%$ as evidenced by their elemental analyses or their HPLC/MS. HPLC/MS were determined with a HPLC Agilent 1260 Infinity II LC/MSD coupled to a photodiode array and mass spectrometer. The sample (5 μL) 0.5 mg/mL in methanol/acetonitrile was injected using a Agilent Poroshell 120 EC-C18, 2.7 μm , 50 mm \times 4.6 mm column at 40 $^\circ\text{C}$. The mobile phase was a mixture of A = water with 0.05% formic acid and B = acetonitrile with 0.05% formic acid, with the method described as follows: flow 0.6 mL/min, 5% B–95% A 3 min, 100% B 4

min, 95% B–5% A 1 min. Purity is given as % of absorbance at 210 or 254 nm.

1-(2-Oxaadamant-5-yl)-3-(2,3,4-trifluorophenyl)urea, 4. In a round-bottom flask equipped with a stir bar under the nitrogen atmosphere, 1.2 equiv of 2-oxaadamantyl-1-amine hydrochloride was added to anh. DCM (~110 mM). To this suspension, 1.0 equiv of 2,3,4-trifluorophenylisocyanate followed by 7 equiv of triethylamine was added. The reaction mixture was stirred at room temperature overnight. Then, the solvent was removed under vacuum and the resulting crude was purified by column chromatography (SiO₂, hexane/EtOAc mixtures). Evaporation under vacuum of the appropriate fractions gave urea **4** (24 mg, 83% yield) as a white solid. Mp 211–213 °C. IR (ATR) ν : 3344, 2937, 2856, 2478, 2362, 1681, 1621, 1556, 1504, 1473, 1434, 1402, 1361, 1320, 1288, 1236, 1183, 1146, 1107, 1076, 1035, 1020, 1005, 992, 948, 921, 890, 810, 793, 775, 761, 724, 686, 656, 636 cm⁻¹. ¹H NMR (400 MHz, CD₃OD): δ 1.66 [dm, J = 12.8 Hz, 2 H, 8(10)-H_a], 1.98 [dm, J = 12.4 Hz, 2 H, 8(10)-H_b], 2.06 [d, J = 12 Hz, 2 H, 4(9)-H_a], 2.14–2.21 [complex signal, 4 H, 4(9)-H_b, 6-H₂], 2.25 (m, 1 H, 7-H), 4.17 [broad s, 2 H, 1(3)-H], 7.01 (m, 1 H, 5'-H), 7.68 (m, 1 H, 6'-H). ¹³C NMR (100.6 MHz, CD₃OD): δ 28.8 (CH, C7), 36.0 [CH₂, C8(10)], 41.2 [CH₂, C6], 41.8 [CH₂, C4(9)], 50.6 (C, C5), 70.9 [CH, C1(3)], 112.2 (CH, dd, ²J_{C-F} = 17.8 Hz, ³J_{C-F} = 3.7 Hz, C5'), 116.8 (CH, C6'), 126.8 (C, d, ²J_{C-F} = 6.5 Hz, Ar-C1'), 141.0 (C, d, ¹J_{C-F} = 247 Hz, Ar-C3'), 143.5 (C, d, ¹J_{C-F} ~ 245 Hz, Ar-C4'), 147.5 (C, d, ¹J_{C-F} = 242 Hz, Ar-C2'), 156.2 (C, CO). MS (DIP), m/z (%): significant ions: 173 [(C₇H₂F₃NO)⁺, 4], 149 (100), 148 (62), 147 (16), 137 [(C₉H₁₁O)⁺, 8], 93 (49). HRMS: calcd for [C₁₆H₁₇F₃N₂O₂ - H]⁺, 325.1169; found, 325.1173.

1-(2-Oxaadamant-1-yl)-3-(2,3,4-trifluorophenyl)urea, 7. In a round-bottom flask equipped with a stir bar under the nitrogen atmosphere, 1.2 equiv of 2-oxaadamantyl-1-amine hydrochloride was added to anh. DCM (~110 mM). To this suspension, 1.0 equiv of 2,3,4-trifluorophenylisocyanate followed by 7 equiv of triethylamine was added. The reaction mixture was stirred at room temperature overnight. Then, the solvent was removed under vacuum. Purification by column chromatography (SiO₂, hexane/EtOAc mixtures) of the crude and evaporation under vacuum of the appropriate fractions gave urea **7** (163 mg, 94% yield) as a white solid. mp 196–198 °C. IR (ATR) ν : 3300–2800 (3293, 3232, 3127, 2933, 2857), 1702, 1640, 1621, 1563, 1509, 1489, 1471, 1446, 1373, 1349, 1340, 1317, 1294, 1257, 1239, 1227, 1200, 1165, 1117, 1099, 1080, 1020, 996, 976, 963, 932, 912, 884, 840, 805, 788, 757, 683, 653 cm⁻¹. ¹H NMR (500 MHz, CD₃OD): δ 1.68 [dm, J = 12.5 Hz, 2 H, 4(10)-H_a], 1.89 [complex signal, 4 H, 6-H₂, 8(9)-H_a], 2.00 [dm, J = 12.5 Hz, 2 H, 4(10)-H_b], 2.26 [broad signal, 2 H, 5(7)-H], 2.32 [d, J = 12.5 Hz, 8(9)-H_b], 4.23 [broad s, 1 H, 3-H], 7.03 (m, 1 H, 5'-H), 7.75 (m, 1 H, 6'-H). ¹³C NMR (125.7 MHz, CD₃OD): δ 29.6 [CH, C5(7)], 35.6 [CH₂, C4(10)], 35.8 (CH₂, C6), 40.9 [CH₂, C8(9)], 72.5 (CH, C3), 82.2 (C, C1), 112.3 (CH, dd, ²J_{C-F} = 18 Hz, ³J_{C-F} = 4 Hz, C5'), 116.8 (CH, C6'), 126.5 (C, d, ²J_{C-F} = 8.8 Hz, Ar-C1'), 141.0 (C, dt, ¹J_{C-F} = 246 Hz, ²J_{C-F} = 15 Hz, Ar-C3'), 143.8 (C, dd, ¹J_{C-F} = 244 Hz, ²J_{C-F} = 11 Hz, Ar-C4'), 147.6 (C, dd, ¹J_{C-F} = 244 Hz, ²J_{C-F} = 9 Hz, Ar-C2'), 156.0 (C, CO). HRMS: calcd for [C₁₆H₁₇F₃N₂O₂ + H]⁺, 327.1315; found, 327.1319.

1-(4-Oxahexacyclo[5.4.1.0^{2,6}.0^{3,10}.0^{5,9}.0^{8,11}]dodecan-3-yl)-3-(2,3,4-trifluorophenyl)urea, 9. In a round-bottom flask equipped with a stir bar under the nitrogen atmosphere, 1.2 equiv of 2-oxaadamantyl-1-amine hydrochloride was added to anh. DCM (~110 mM). To this suspension, 1.0 equiv of 2,3,4-trifluorophenyl isocyanate followed by 7 equiv of triethylamine was added. The reaction mixture was stirred at room temperature overnight. Then, the solvent was removed under vacuum. Purification by column chromatography (SiO₂, hexane/EtOAc mixtures) of the crude and evaporation under vacuum of the appropriate fractions gave urea **9** (374 mg, 94% yield) as a white solid. Mp 152–154 °C. IR (ATR) ν : 3329, 3192, 3118, 2975, 1701, 1641, 1621, 1559, 1509, 1470, 1342, 1321, 1287, 1253, 1205, 1183, 1166, 1127, 1071, 1020, 996, 951, 933, 911, 867, 839, 798, 757, 708, 688, 655, 635, 593 cm⁻¹. ¹H NMR (400 MHz, CDCl₃): δ 1.60 (dt, J = 10.8 Hz, J' = 1.6 Hz, 1 H, 12-H_a), 1.95

(dt, J = 10.8 Hz, J' = 1.6 Hz, 1 H, 12-H_b), 2.50 (broad t, J = 5.2 Hz, 1 H, 7-H), 2.57 (t, J = 4.8 Hz, 1 H, 1-H), 2.66 (m, 8 H, 2-H), 2.75–2.84 (complex signal, 3 H, 2-H, 10-H, 11-H), 2.88–3.01 (complex signal, 2 H, 6-H, 9-H), 4.83 (t, J = 5.2 Hz, 1 H, 5-H), 5.94 (broad s, 1 H, 1-NH), 6.90 (m, 1 H, 5'-H), 7.82 (m, 1 H, 6'-H), 8.06 (broad s, 1 H, 3-NH). ¹³C NMR (100.6 MHz, CDCl₃): δ 41.4 (CH, C8), 41.6 (CH, C11), 43.2 (CH, C1), 43.5 (CH₂, C12), 44.6 (CH, C9), 44.9 (CH, C7), 46.3 (CH, C10), 54.8 (CH, C6), 57.0 (CH, C2), 84.1 (CH, C5), 103.1 (C, C3), 111.3 (CH, dd, ²J_{C-F} = 17.7 Hz, ³J_{C-F} = 3.9 Hz, C5'), 115.2 (CH, m, C6'), 124.5 (C, dd, ²J_{C-F} = 8 Hz, ³J_{C-F} = 3.5 Hz, C1'), 139.8 (C, ddd, ¹J_{C-F} = 252 Hz, ²J_{C-F} = 16.4 Hz, ³J_{C-F} = 13.7 Hz, C3'), 142.3 (C, ddd, ¹J_{C-F} = 251 Hz, ²J_{C-F} = 11.7 Hz, ³J_{C-F} = 3.2 Hz, C4'), 146.6 (C, ddd, ¹J_{C-F} = 245.8 Hz, ²J_{C-F} = 10 Hz, ³J_{C-F} = 2.7 Hz, C2'), 154.7 (C, CO). MS (DIP), m/z (%): significant ions: 348 (M⁺, 18), 173 [(C₇H₂F₃NO)⁺, 17], 159 [(C₁₁H₁₁O)⁺, 35], 147(100), 146(13), 131(24), 91(15). HRMS: calcd for [C₁₈H₁₅F₃N₂O₂ + H]⁺, 349.1158; found, 349.1160.

2-Oxaadamant-1-yl isocyanate, 10. Triphosgene (940 mg, 3.16 mmol) was added in a single portion to a solution of 2-oxaadamantyl-1-amine hydrochloride (1.20 g, 6.32 mmol) in DCM (42 mL) and saturated aqueous NaHCO₃ solution (17 mL). The resulting biphasic mixture was stirred at room temperature for 30 min. Thereafter, the two phases were separated and the organic layer was washed with brine, dried over anh. Na₂SO₄, and filtered. Evaporation under vacuum below 30 °C provided isocyanate **10** as a yellow gum, which was used in the next step without further purification.

1-(1-Acetylpiperidin-4-yl)-3-(oxaadamant-1-yl)urea, 12. Under anhydrous conditions, a solution of isocyanate **10** (323 mg, 1.80 mmol) in anh. DCM (20 mL) was added to a solution of 1-acetyl-4-aminopiperidine (308 mg, 2.16 mmol) in anh. DCM (10 mL), followed by triethylamine (0.50 mL, 3.61 mmol). The reaction mixture was stirred at room temperature overnight. The solution was then concentrated under vacuum to give an orange gum (720 mg). Purification by column chromatography (SiO₂, DCM/methanol mixtures) gave urea **12** (300 mg, 52% yield) as a white solid. The analytical sample was obtained by washing with pentane. Mp 172–173 °C. IR (ATR) ν : 3322, 2920, 2850, 2188, 2153, 2000, 1637, 1549, 1428, 1369, 1313, 1264, 1234, 1192, 1139, 1090, 1046, 995, 959, 879, 816, 773, 731 cm⁻¹. ¹H NMR (400 MHz, CDCl₃): δ 1.28–1.41 (complex signal, 2 H, 3-H_{ax} and 5-H_{ax}), 1.58–1.96 (complex signal, 9 H, 8'-H_{ax}, 9'-H_{ax}, 4'-H_{ax}, 10'-H_{ax}, 6'-H_{ax}, and 3-H_{eq} or 5-H_{eq}), 1.98–2.22 (complex signal, 6 H, COCH₃, 8'-H_{eq}, 9'-H_{eq}, and 5-H_{eq} or 3-H_{eq}), 2.27 [broad s, 2 H, 5'(7')-H], 2.86 (dt, J = 11.2 Hz, J' = 2.8 Hz, 1 H, 6-H_{ax} or 2-H_{ax}), 3.18 (dt, J = 10.8 Hz, J' = 2.8 Hz, 1 H, 2-H_{ax} or 6-H_{ax}), 3.70 (dm, J = 14 Hz, 1 H, 2-H_{eq} or 6-H_{eq}), 3.87 (m, 1 H, 4-H), 4.27 (broad s, 1 H, 3'-H), 4.35 (broad d, J = 14.0 Hz, 1 H, 6-H_{eq} or 2-H_{eq}), 4.75 (s, 1 H, 3-NH), 6.06 (d, J = 8 Hz, 1-NH). ¹³C NMR (100.6 MHz, CDCl₃): δ 21.4 (CH₃, CH₃CO), 27.9 [CH, C5'(7')], 32.1 (CH₂, C3 or C5), 33.2 (CH₂, C5 or C3), 34.6 [broad CH₂, C4', C6' and C10'], 40.0 (CH₂, C8' or C9'), 40.2 (CH₂, C9' or C8'), 40.4 (CH₂, C2 or C6), 45.1 (CH₂, C6 or C2), 46.5 (CH, C4), 71.0 (CH, C3'), 80.6 (C, C1'), 156.7 (C, CO), 168.9 (C, CH₃CO). MS (DIP), m/z (%): significant ions: 321 (M⁺, 34), 197 (32), 179 [(C₁₀H₁₃NO₂)⁺, 34], 154 (100), 153 (18), 137 [(C₉H₁₃O)⁺, 33], 136 (32), 126 (15), 125 (51), 122 (21), 111 (17), 96 (41), 95 (18), 94 (45), 84 (19), 83 (37), 82 (54), 79 (22), 67(20), 57 (23), 56 (32), 55 (15). HRMS: calcd for [C₁₇H₂₃N₃O₃ + H]⁺, 322.2125; found, 322.2124.

trans-4-[4-(3-Oxaadamant-1-yl-ureido)-cyclohexyloxy]benzoic Acid, 14. A solution of 2-oxaadamant-1-yl isocyanate (400 mg, 2.23 mmol) in anh. DCM (25 mL) was added to a solution of *t*-4-[(4-aminocyclohexyl)oxy]benzoic acid²⁶ (728 mg, 2.68 mmol) in anh. DCM (12 mL), followed by triethylamine (1.24 mL, 8.94 mmol) under nitrogen. The reaction mixture was stirred at room temperature overnight. Water (50 mL) was then added, and the phases were separated. The organic layer was extracted with further water (2 × 50 mL) and the pH of the combined aqueous phases was adjusted to pH ~2 with 5 N HCl solution, prior to extraction with DCM (3 × 50 mL). The combined organic layers were dried over anh. Na₂SO₄, filtered, and concentrated under vacuum, yielding urea **14** (220 mg,

24% yield) as a white solid. The analytical sample was obtained by crystallization from methanol/diethyl ether. mp 255–275 °C. IR (ATR) ν : 3364, 3267, 3198, 3061, 2922, 2559, 2348, 2187, 2068, 2011, 1977, 1672, 1601, 1552, 1443, 1369, 1347, 1320, 1231, 1196, 1172, 1110, 1091, 1049, 1027, 989, 959, 863, 828, 774, 698, 640 cm^{-1} . ^1H NMR (400 MHz, CD_3OD): δ 1.37 [m, 2 H, 3'(5')- H_{ax}], 1.55 [m, 2 H, 2'(6')- H_{ax}], 1.65 [dm, $J = 12.4$ Hz, 2 H, 4'(10')- H_{ax}], 1.78 [dm, $J = 11.6$ Hz, 2 H, 8'(9')- H_{ax}], 1.86 [complex signal, 2 H, 6'- H_2], 1.94 [m, 2 H, 4'(10')- H_{e}], 2.01 [m, 2 H, 3'(5')- H_{eq}], 2.10 [m, 2 H, 2'(6')- H_{eq}], 2.22 [broad s, 2 H, 5'(7')-H], 2.28 [dm, $J = 15.5$ Hz, 2 H, 8'(9')- H_{e}], 3.57 (m, 1 H, 4'-H), 4.18 (broad s, 1 H, 3'-H), 4.40 (m, 1 H, 1'-H), 6.92 [d, $J = 8.8$ Hz, 2 H, 3(S)-H], 7.93 [d, $J = 8.8$ Hz, 2 H, 2(6)-H]. ^{13}C NMR (100.6 MHz, CD_3OD): δ 29.6 [CH, C5'(7')], 31.0 [CH₂, C2'(6')], 31.4 [CH₂, C3'(5')], 35.7 [CH₂, C4'(10')], 35.9 (CH₂, C6'), 41.0 [CH₂, C8'(9')], 48.6 (CH, C4'), 72.3 (CH, C3'), 75.8 (CH, C1'), 81.9 (C, C1'), 115.9 [CH, C3(S)], 126.8 (C, C1), 132.6 [CH, C2(4)], 159.0 (C, CO), 162.4 (C, C4 and CO₂H). MS (DIP), m/z (%): significant ions: 414 (M⁺, 0.2), 179 [(C₁₀H₁₃NO₂)⁺, 27], 138 [(C₇H₁₄O)⁺, (C₇H₃O₂)⁺, 100], 122 (29), 121 (39), 111 (21), 108 (10), 98 (99), 96 (30), 94 (45), 82 (18), 81 (97), 79 (41), 67 (19), 65 (15), 56 (42), 55 (16). HRMS: calcd for [C₂₃H₃₀N₂O₅ + H]⁺, 415.2227; found, 415.2230.

1-(2-Oxaadamant-1-yl)-3-(1-benzylpiperidin-4-yl)urea, 15. To a solution of 2-oxaadamant-1-yl isocyanate (1.25 g, 6.97 mmol) in DCM (10 mL) was added 1-benzylpiperidin-4-amine (1.60 g, 8.37 mmol). The reaction mixture was stirred at room temperature overnight. The solvents were evaporated under vacuum to give a yellow gum (3.06 g). Column chromatography (DCM/methanol mixtures) gave urea 15 as a yellowish solid (2.54 g, 82% yield). mp 153–154 °C. IR (ATR): 694, 745, 768, 989, 110, 1194, 1225, 1319, 1372, 1441, 1484, 1540, 1664, 1918, 1959, 2918 cm^{-1} . ^1H NMR (400 MHz, CDCl_3): δ 1.50 [dq, $J = 3.6$ Hz, $J' = 10.4$ Hz, 2 H, 3(S)- H_{ax}], 1.59–1.70 [complex signal, 4 H, 8'(9')- H_{ax} , 4'(10')- H_{ax}], 1.75–1.87 [complex signal, 2 H, 6'- H_2], 1.86–1.97 [complex signal, 4 H, 3(S)- H_{ax} , 4'(10')- H_{e}], 2.13–2.22 [complex signal, 4 H, 2(6)- H_{ax} , 8'(9')- H_{e}], 2.26 [broad s, 2 H, 5'(7')-H], 2.74 [d, $J = 11.2$ Hz, 2 H, 2(6)- H_{e}], 3.49 [s, 2 H, 7-H₂], 3.71 (m, 1 H, 4-H), 4.24 (t, $J = 4$ Hz, 1 H, 3'-H), 4.65 (s, 1 H, 1'-NH), 6.04 (d, $J = 8.4$ Hz, 1 H, 4-NH), 7.24 (m, 1 H, 11-H), 7.28–7.32 [complex signal, 4 H, 9-H, 10-H, 12-H and 13-H]. ^{13}C NMR (100.5 MHz, CDCl_3): δ 27.9 [CH, C5'(7')], 32.6 [CH₂, C3(S)], 34.6 [(CH₂, C4'(10'))], 34.7 (CH₂, C6'), 40.1 [(CH₂, C8'(9'))], 46.2 (CH, C4), 52.1 [CH₂, C2(6)], 63.2 (CH₂, C7), 70.9 (CH, C3'), 80.6 (C, C1'), 126.9 (CH, C11), 128.2 [CH, C10(12) or C9(13)], 129.2 [CH, C9(13) or C10(12)], 138.2 (C, C8), 156.7 (C, CO). HRMS: calcd for [C₂₂H₃₁N₃O₂ + H]⁺, 370.2489; found, 370.2488.

1-(2-Oxaadamant-1-yl)-3-(piperidin-4-yl)urea, 16. To a solution of 1-(2-oxaadamant-1-yl)-3-(1-benzylpiperidin-4-yl)urea (2.40 g, 6.50 mmol) in methanol (20 mL), palladium on carbon 10% wt. (300 mg) and HCl 37% (1 mL) were added. The reaction mixture was hydrogenated for 5 days. The palladium on carbon was filtered, and the solvent was evaporated under vacuum. The crude was dissolved in DCM and washed with 2 N NaOH solution (2 × 30 mL). The organic phase was dried over anhydrous Na₂SO₄ and filtered. Evaporation under vacuum of the organics gave urea 16 as a white solid (1.28 g, 70% yield). The product was used in the next step without further purification. The analytical sample was obtained by crystallization from hot DCM (825 mg). Mp 164–165 °C. ^1H NMR (400 MHz, CDCl_3): δ 1.37 [m, 2 H, 3(S)- H_{ax}], 1.60–1.73 [complex signal, 6 H, 4'(10')- H_{ax} , 8'(9')- H_{ax}], 1.77–1.88 (m, 2 H, 6'- H_2), 1.90–2.01 [complex signal, 4 H, 4'(10')- H_{e} , 3(S)- H_{e}], 2.19 [dm, $J = 12$ Hz, 2 H, 8'(9')- H_{e}], 2.28 [broad s, 2 H, 5'(7')-H], 2.71 [ddd, 2 H, $J = 13$ Hz, $J' = 11.8$ Hz, $J'' = 2.8$ Hz, 2(6)- H_{e}], 3.04 [dt, 2 H, $J = 13$ Hz, $J' = 4$ Hz, 2(6)- H_{ax}], 3.77 (m, 1 H, 4-H), 4.29 (broad s, 1 H, 3'-H), 4.56 (s, 1 H, 1'-NH), 6.06 (d, $J = 8.0$ Hz, 4-NH). HRMS: calcd for [C₁₅H₂₂N₃O₂ + H]⁺, 280.2020; found, 280.2022.

1-(2-Oxaadamant-1-yl)-3-(1-(4-chloro-6-methyl-1,3,5-triazin-2-yl)piperidin-4-yl)urea, 17. To a solution of 2,4-dichloro-6-methyl-1,3,5-triazine (130 mg, 0.78 mmol) in DCM (4 mL) were added 1-(2-oxaadamant-1-yl)-3-(piperidin-4-yl)urea (220 mg, 0.78 mmol) and

DIPEA (305 mg, 2.36 mmol). The reaction mixture was stirred at room temperature for 30 min. Column chromatography (DCM/methanol mixtures) gave urea 17 as a white solid (54 mg, 9% yield). mp 196–197 °C. IR (ATR) ν : 708, 762, 845, 907, 964, 992, 1075, 1116, 1168, 1194, 1219, 1243, 1271, 1315, 1364, 1444, 1485, 1527, 1578, 1671, 1953, 1974, 1994, 2180, 2335, 2852, 2914 cm^{-1} . ^1H NMR (400 MHz, CDCl_3): δ 1.38–1.47 [complex signal, 2 H, 3(S)- H_{ax}], 1.60–1.71 [complex signal, 4 H, 6'- H_2 and 8'(9')- H_{ax}], 1.76–1.87 [m, 2 H, 4'(10')- H_{ax}], 1.87–1.95 [m, 2 H, 4'(10')- H_{e}], 2.02–2.21 [complex signal, 4 H, 3(S)- H_{e} and 8'(9')- H_{e}], 2.27 [s, 2 H, 5'(7')-H], 2.39 (s, 3 H, CH₃), 3.16–3.24 [m, 2 H, 2(6)- H_{e}], 3.69 (m, 1 H, 4-H), 4.26 (broad s, 1 H, 3'-H), 4.55 (d, $J = 13.6$ Hz, 1 H, 2- H_{e} or 6- H_{e}), 4.63 (d, $J = 13.6$ Hz, 1 H, 6- H_{e} or 2- H_{e}), 4.68 (s, 1 H, 1'-NH), 6.10 (d, $J = 7.6$ Hz, 1H, 1-NH). ^{13}C NMR (100.5 MHz, CDCl_3): δ 25.4 (CH₃), 27.9 [CH, C5'(7')], 32.36 (CH₂, C3 or C5), 32.39 (CH₂, C5 or C3), 34.63 [CH₂, C4'(10')], 34.64 (CH₂, C6'), 40.1 (CH₂, C8' or C9'), 40.2 (CH₂, C9' or C8'), 42.4 (CH₂, C2 or C6), 42.5 (CH₂, C6 or C2), 46.6 (CH, C4), 71.0 (CH, C3'), 80.7 (C, C1'), 156.7 (C, CO), 164.1 (C, C8), 170.2 (C, C7), 177.3 (C, C9). HRMS: calcd for [C₁₉H₂₇ClN₆O₂ + H]⁺, 407.1957; found, 407.1952.

1-(2-Oxaadamant-1-yl)-3-(1-(4-methyl-6-(methylamino)-1,3,5-triazin-2-yl)piperidin-4-yl)urea, 18. Methylamine hydrochloride (160 mg, 2.36 mmol) and DIPEA (407 mg, 3.15 mmol) were added to the solution of 1-(2-oxaadamant-1-yl)-3-(1-(4-chloro-6-methyl-1,3,5-triazin-2-yl)piperidin-4-yl)urea in DCM (5 mL) obtained in the previous step. The reaction mixture was stirred at 40 °C for 4 h. The solvent was evaporated under vacuum to give a yellow gum (830 mg). Column chromatography (DCM/methanol mixtures) gave urea 18 as a gray solid (27 mg, 8% yield). Mp 203–204 °C. IR (ATR) ν : 653, 803, 880, 993, 1085, 1118, 1189, 1235, 1317, 1366, 1442, 1532, 1644, 1943, 2143, 2337, 2843, 2920 cm^{-1} . ^1H NMR (400 MHz, CDCl_3): δ 1.35–1.44 [complex signal, 2 H, 3(S)- H_{ax}], 1.61 (d, $J = 12.0$ Hz, 2 H, 6'- H_2), 1.69 [d, $J = 12.4$, 2 H, 8'(9')- H_{ax}], 1.77–1.86 [complex signal, 2 H, 4'(10')- H_{ax}], 1.91 (d, $J = 10.4$ Hz, 2 H, 4'(10')- H_{e}), 1.99–2.04 [complex signal, 2 H, 3(S)- H_{e}], 2.17 [d, $J = 12.0$ Hz, 2 H, 8'(9')- H_{e}], 2.24–2.27 [complex signal, 5 H, 5'(7')-H and CCH₃], 2.93 (d, $J = 4.8$ Hz, 3 H, NCH₃), 3.15 (t, $J = 12.0$ Hz, 2 H, 2(6)- H_{e}), 3.93 (m, 1 H, 4-H), 4.25 (t, $J = 4.4$ Hz, 1 H, 3'-H), 4.56 [broad s, 2 H, 2(6)- H_{ax}], 4.73 (s, 1 H, 1'-NH), 6.09 (d, $J = 7.6$ Hz, 1 H, 1-NH). ^{13}C NMR (100.5 MHz, CDCl_3): δ 25.2 (CH₃, C10), 27.5 (CH₃, C11), 27.9 [CH, C5'(7')], 32.5 (CH₂, C3(S)), 34.63 [CH₂, C4'(10')], 34.66 (CH₂, C6'), 40.1 [CH₂, C9'(8')], 41.7 [CH₂, C2(6)], 46.8 (CH, C4), 70.9 (CH, C3'), 80.6 (C, C1'), 156.7 (C, CO), 164.3 (C, C8), 173.9 (C, C7), 177.3 (C, C9). HRMS: calcd for [C₂₀H₃₃N₇O₂ + H]⁺, 402.2612; found, 402.2608.

1-(2-Oxaadamant-1-yl)-3-(1-(tetrahydro-2H-pyran-4-carbonyl)piperidin-4-yl)urea, 19. To a solution of 1-(2-oxaadamant-1-yl)-3-(piperidin-4-yl)urea (150 mg, 0.53 mmol) in EtOAc (10 mL), tetrahydro-2H-pyran-4-carboxylic acid (70 mg, 0.53 mmol), HOBt (109 mg, 0.80 mmol), EDCI-HCl (125 mg, 0.80 mmol), and triethylamine (0.15 mL, 1.07 mmol) were added. The reaction mixture was stirred at room temperature for 24 h. To the resulting suspension was added water (15 mL), and the two phases were separated. The organic phase was washed with saturated aqueous NaHCO₃ solution (15 mL) and brine (15 mL). The combined aqueous phases were extracted with DCM (3 × 30 mL). The combined organic phases were dried over anhydrous Na₂SO₄ and filtered. Evaporation under vacuum of the organics gave urea 19 as colorless crystals (190 mg, 90% yield). Mp 150–152 °C. IR (ATR) ν : 641, 770, 878, 990, 1085, 1121, 1194, 1240, 1318, 1367, 1442, 1550, 1633, 2010, 2067, 2341, 2919 cm^{-1} . ^1H NMR (400 MHz, CDCl_3): δ 1.30–1.39 [complex signal, 2 H, 6- H_{ax} , 2- H_{ax}], 1.55–1.71 [complex signal, 6 H, 4'(10')- H_{ax} , 8'- H_{ax} , 9'- H_{ax} , 9- H_{ax} , 13- H_{ax}], 1.75–2.00 [complex signal, 7 H, 6'- H_2 , 2- H_{e} or 6- H_{e} , 4'(10')- H_{e} , 9- H_{e} , 13- H_{e}], 2.10 (t, $J = 13.2$ Hz, 2 H, 2- H_{e} or 6- H_{e} , 8'- H_{e} or 9'- H_{e}), 2.22 (d, $J = 12.0$ Hz, 1 H, 9'- H_{e} or 8'- H_{e}), 2.27 [broad s, 2 H, 5'(7')-H], 2.72 (tt, $J = 11.2$ Hz, $J' = 3.6$ Hz, 1 H, 8-H), 2.86 (t, $J = 11.2$ Hz, 1 H, 3-H, or 5-H), 3.18 (t, $J = 11.2$ Hz, 1 H, 5-H, or 3-H), 3.43 [td, $J = 12.0$ Hz, $J' = 2$ Hz, 2 H, 10(12)- H_{e}], 3.80 (d, $J = 14.0$ Hz, 1 H, 5- H_{e} or 3- H_{e}), 3.88 (m, 1 H, 4-H), 4.00 [d, $J = 11.2$ Hz, 2 H, 10(12)- H_{ax}], 4.27 (t, $J = 3.6$ Hz, 1 H, 3'-

H), 4.38 (dm, $J = 13.6$ Hz, 1 H, 3-H_b or 5-H_b), 4.75 (s, 1 H, 1'-NH), 6.07 (d, $J = 8.0$ Hz, 1 H, 4-NH). ¹³C NMR (100.5 MHz, CDCl₃): δ 27.9 [CH, C5'(7')], 29.08 (CH₂, C9 or C13), 29.14 (CH₂, C13 or C9), 32.2 (CH₂, C2 or C6), 33.6 (CH₂, C6 or C2), 34.59 (CH₂, C6'), 34.61 [CH₂, C4'(10')], 37.6 (CH, C8), 40.0 (CH₂, C8' or C9'), 40.2 (CH₂, C9' or C8'), 40.7 (CH₂, C3 or C5), 44.0 (CH₂, C5 or C3), 46.7 (CH, C4), 67.2 [CH₂, C10(12)], 71.0 (CH, C3'), 80.7 (C, C1'), 156.7 (C, CO), 172.7 (COR). HRMS: calcd for [C₂₁H₃₃N₃O₄ + H]⁺, 392.2544; found, 392.2553.

1-(2-Oxaadamant-1-yl)-3-(1-nicotinoylpiperidin-4-yl)urea, 20. To a solution of 1-(2-oxaadamant-1-yl)-3-(piperidin-4-yl)urea (150 mg, 0.53 mmol) in EtOAc (10 mL), nicotinic acid (66 mg, 0.53 mmol), HOBT (109 mg, 0.805 mmol), EDCI-HCl (125 mg, 0.80 mmol), and triethylamine (0.15 mL, 1.07 mmol) were added. The reaction mixture was stirred at room temperature for 24 h. Water (15 mL) was added to the resulting suspension, and the two phases were separated. The organic phase was washed with saturated aqueous NaHCO₃ solution (15 mL) and brine (15 mL). The combined aqueous phases were basified with 1N NaOH solution (30 mL) and extracted with DCM (3 × 30 mL). The combined organic phases were dried over anhydrous Na₂SO₄ and filtered. Evaporation under vacuum of the organics gave a white solid (140 mg). Column chromatography (DCM/methanol mixtures) gave pure urea **20** as a white solid (63 mg, 32% yield). mp 187–188 °C. IR (ATR) ν: 618, 711, 736, 767, 824, 990, 1114, 1132, 1194, 1219, 1245, 1269, 1318, 1367, 1436, 1483, 1537, 1622, 1666, 2051, 2144, 2217, 2919 cm⁻¹. ¹H NMR (400 MHz, CDCl₃): δ 1.37 (m, 1 H, 5-H_a or 3-H_a), 1.51 (m, 1 H, 3-H_a or 5-H_a), 1.60–1.72 [complex signal, 4 H, 8'(9')-H_a and 6'-H_a], 1.82 [m, 2 H, 4'(10')-H_a], 1.92 (d, $J = 12.4$ Hz, 2 H, 3-H_b and 5-H_b), 1.97–2.09 [complex signal, 2 H, 4'(10')-H_b], 2.15 [broad s, 2 H, 8'(9')-H_b], 2.27 [broad s, 2 H, 5'(7')-H], 3.02–3.28 [complex signal, 2 H, 2(6)-H_a], 3.57–3.75 [complex signal, 1 H, 2-H_b or 6-H_b], 3.93 (m, 1 H, 4-H), 4.29 (t, $J = 4.4$ Hz, 1 H, 3'-H), 4.50 (m, 1 H, 6-H_b or 2-H_b), 4.80 (s, 1 H, 1'-NH), 6.12 (d, $J = 7.6$ Hz, 1 H, 4-NH), 7.31–7.40 (dd, $J = 8.0$ Hz, $J' = 4.4$ Hz, 1 H, 10-H), 7.74 (d, $J = 8.0$ Hz, 1 H, 9-H), 8.66 (complex signal, 2 H, 11-H, 13-H). ¹³C NMR (100.5 MHz, CDCl₃): δ 27.9 [CH, C5'(7')], 32.2 (CH₂, C3 or C5), 33.3 (CH₂, C5 or C3), 34.60 (CH₂, C6'), 34.63 [CH₂, C4'(10')], 40.1 (CH₂, C8'(9')), 41.3 (CH₂, C2 or C6), 46.6 (CH, C4 and CH₂, C6 or C2), 71.0 (CH, C3'), 80.7 (C, C1'), 123.5 (C, C10), 131.7 (C, C8), 134.8 (C, C9), 147.7 (C, C11 or C13), 150.7 (C, C13 or C11), 156.7 (C, CO), 167.7 (C, COR). HRMS: calcd for [C₂₁H₂₉N₄O₃ + H]⁺, 385.2234; found, 385.2238.

1-(2-Oxaadamant-1-yl)-3-(1-(2-fluorobenzoyl)piperidin-4-yl)urea, 21. To a solution of 1-(2-oxaadamant-1-yl)-3-(piperidin-4-yl)urea (120 mg, 0.43 mmol) in EtOAc (10 mL), 2-fluorobenzoic acid (61 mg, 0.43 mmol), HOBT (87 mg, 0.64 mmol), EDCI-HCl (100 mg, 0.64 mmol), and triethylamine (0.12 mL, 0.86 mmol) were added. The reaction mixture was stirred at room temperature for 24 h. Water (15 mL) and DCM (20 mL) were added to the resulting suspension, and the two phases were separated. The organic phase was washed with saturated aqueous NaHCO₃ solution (15 mL), brine (15 mL), dried over anhydrous Na₂SO₄, and filtered. Evaporation under vacuum of the organics gave urea **21** as a white solid (131 mg, 77% yield). The analytical sample was obtained as a white solid (111 mg) by crystallization from hot EtOAc. mp 193–194 °C. IR (ATR) ν: 630, 785, 925, 987, 1010, 1093, 1121, 1191, 1243, 1318, 1372, 1447, 1462, 1491, 1555, 1615, 1684, 1974, 2351, 2925, 3338 cm⁻¹. ¹H NMR (400 MHz, CDCl₃): δ 1.38 (broad s, 1 H, 5-H_a or 3-H_a), 1.45–1.54 (m, 1 H, 3-H_a or 5-H_a), 1.61–1.71 (complex signal, 4 H, 6'-H_a, 8'-H_a, 9'-H_a), 1.82 [m, 2 H, 4'(10')-H_a], 1.90–1.99 [complex signal, 3 H, 5-H_b or 3-H_b, 4'(10')-H_b], 2.06 (m, 1 H, 3-H_b or 5-H_b), 2.13 (m, 1 H, 9-H_b or 8-H_b), 2.20 (dq, $J = 12.4$ Hz, $J' = 2.0$ Hz, 1 H, 8'-H_b or 9'-H_b), 2.27 [s, 2 H, 5'(7')-H], 3.06–3.19 (complex signal, 2 H, 2-H_a, 6-H_a), 3.5 (d, $J = 13.6$ Hz, 1 H, 2-H_b or 6-H_b), 3.92 (m, 1 H, 4-H), 4.29 (s, 1 H, 3'-H), 4.53 (dm, $J = 13.6$ Hz, 1 H, 6-H_b or 2-H_b), 4.74 (s, 1 H, 1'-NH), 6.09 (d, $J = 7.6$ Hz, 1 H, 4-NH), 7.08 (m, 1 H, 10-H), 7.19 (td, $J = 7.6$ Hz, $J' = 1.2$ Hz, 1 H, 13-H), 7.34–7.41 (complex signal, 2 H, 11-H, 12-H). ¹³C NMR (100.5 MHz, CDCl₃): δ 27.95 (CH, C5' or C7'), 27.97 (CH, C7' or C5'), 32.2 (CH₂, C3 or

C5), 33.1 (CH₂, C5 or C3), 34.7 [CH₂, C6' and C4'(10')], 40.1 (CH₂, C8' or C9'), 40.2 (CH₂, C9' or C8'), 40.8 (CH₂, C6 or C2), 45.9 (CH₂, C2 or C6), 46.6 (CH, C4), 71.0 (CH, C3'), 80.7 (C, C1'), 115.7 (CH, d, $J_{C-F} = 21.4$ Hz, C10), 124.2 (C, d, $J_{C-F} = 17.9$ Hz, C8), 124.7 (CH, d, $J_{C-F} = 3.5$ Hz, C13), 129.0 (CH, d, $J_{C-F} = 3.8$ Hz, C11), 131.2 (CH, d, $J_{C-F} = 7.9$ Hz, C12), 156.7 (C, CO), 158.1 (C, d, $J_{C-F} = 247.3$ Hz, C9), 165.2 (C, COR). HRMS: calcd for [C₂₁H₂₈FN₃O₃ + H]⁺, 402.2187; found, 402.2187.

1-(2-Oxaadamant-1-yl)-3-(1-(isopropylsulfonyl)piperidin-4-yl)urea, 22. To a solution of 1-(2-oxaadamant-1-yl)-3-(piperidin-4-yl)urea (250 mg, 0.895 mmol) in DCM (10 mL), triethylamine (0.15 mL, 1.07 mmol) was added. The mixture was cooled down in an ice bath (0 °C), and propane-2-sulfonyl chloride (127 mg, 0.89 mmol) was added dropwise. The reaction mixture was stirred at room temperature overnight and quenched by the addition of HCl solution (37% (2 mL)). The organic phase was collected, and the aqueous layer was extracted with EtOAc (4 × 30 mL). The combined organic phases were dried over anhydrous Na₂SO₄ and filtered. Evaporation of the organics gave an oil that was then dissolved in DCM (20 mL) and washed with 2 N NaOH solution (3 × 20 mL). The organic phase was dried over anhydrous Na₂SO₄ and filtered. Evaporation under vacuum of the organics gave **22** as a white solid (88 mg, 26% yield). The analytical sample was obtained by crystallization from hot DCM as a white solid (60 mg). mp 190–191 °C. IR (ATR) ν: 618, 729, 842, 884, 935, 961, 1010, 1041, 1093, 1116, 1132, 1196, 1243, 1269, 1292, 1320, 1374, 1444, 1547, 1635, 2930, 3333 cm⁻¹. ¹H NMR (400 MHz, CDCl₃): δ 1.32 [d, $J = 6.8$ Hz, 6 H, 8(9)-H], 1.50 [dq, $J = 4.0$ Hz, $J' = 11.2$ Hz, 2 H, 3(5)-H_a], 1.63 [d, $J = 12.0$ Hz, 2 H, 4'(10')-H_a], 1.69 [d, $J = 12.4$ Hz, 2 H, 8'(9')-H_a], 1.82 (complex signal, 2 H, 6'-H_a), 1.92 [d, $J = 12.0$ Hz, 2 H, 4'(10')-H_b], 2.0 [broad d, $J = 13.2$ Hz, 2 H, 3(5)-H_b], 2.16 [d, $J = 11.2$ Hz, 2 H, 8'(9')-H_b], 2.27 [broad s, 2 H, 5'(7')-H], 3.01 [ddd, $J = 2.4$ Hz, $J' = J'' = 13.6$ Hz, 2 H, 2(6)-H_a], 3.17 (sept, 1 H, 7-H), 3.75 [dm, $J = 13.2$ Hz, 2 H, 2(6)-H_b], 3.81 (m, 1 H, 4-H), 4.28 (t, $J = 4.4$ Hz, 1 H, 3'-H), 4.74 (s, 1 H, 1'-NH), 6.08 (d, $J = 8.0$ Hz, 1 H, 4-NH). ¹³C NMR (100.5 MHz, CDCl₃): δ 16.7 [CH₃, C8(9)], 27.9 [CH, C5'(7')], 33.1 [CH₂, C3(5)], 34.61 [CH₂, C4'(10')], 34.63 (CH₂, C6'), 40.1 [CH₂, C8'(9')], 45.4 [CH₂, C2(6)], 46.3 (CH, C4), 53.4 (CH, C7), 71.0 (CH, C3'), 80.6 (C, C1'), 156.7 (C, CO). HRMS: calcd for [C₁₈H₃₁N₃O₄S + H]⁺, 386.2108; found, 386.2113.

1-(2-Oxaadamant-1-yl)-3-(1-(cyclopropanecarbonyl)piperidin-4-yl)urea, 23. To a solution of 1-(2-oxaadamant-1-yl)-3-(piperidin-4-yl)urea (300 mg, 1.07 mmol) in DCM (10 mL), cyclopropanecarbonyl chloride (112 mg, 1.07 mmol) and triethylamine (0.18 mL, 1.29 mmol) were added. The reaction mixture was stirred at room temperature overnight and quenched by the addition of aqueous HCl (37% solution (3 mL)). The organic phase was collected, and the aqueous phase was extracted with EtOAc (4 × 10 mL). The combined organic phases were washed with NaOH 2N (2 × 30 mL), dried over anhydrous Na₂SO₄, and filtered. Evaporation under vacuum of the organics gave urea **23** as a yellow oil (382 mg, 48% yield). The analytical sample was obtained as a white solid (180 mg) by crystallization from hot EtOAc. mp 197–198 °C. IR (ATR) ν: 612, 729, 816, 876, 922, 961, 992, 1085, 1132, 1191, 1219, 1266, 1310, 1369, 1447, 1555, 1604, 1640, 2925, 3307 cm⁻¹. ¹H NMR (400 MHz, CDCl₃): δ 0.73 [m, 2 H, 9(10)-H_a], 0.95 [m, 2 H, 9(10)-H_b], 1.32–1.46 (complex signal, 2 H, 3-H_a, 5-H_a), 1.60–1.71 (complex signal, 4 H, 6'-H_a, 8'-H_a, 9'-H_a), 1.74 (m, 1 H, 8-H), 1.79–1.97 [complex signal, 5 H, 3-H_b or 5-H_b and 4'(10')-H_a], 2.05–2.21 (complex signal, 3 H, 5-H_b or 3-H_b and 9'-H_b, 8'-H_b), 2.27 [broad s, 2 H, 5'(7')-H], 2.90 (t, $J = 12.4$ Hz, 1 H, 6-H_a or 2-H_a), 3.27 (t, $J = 11.6$ Hz, 1 H, 2-H_a or 6-H_a), 3.90 (m, 1 H, 4-H), 4.07 (m, 1 H, 2-H_b or 6-H_b), 4.27 (t, $J = 4.4$ Hz, 1 H, 3'-H), 4.35 (m, 1 H, 6-H_b or 2-H_b), 4.80 (broad s, 1 H, 1'-NH), 6.08 (d, $J = 8.0$ Hz, 1 H, 4-NH). ¹³C NMR (100.5 MHz, CDCl₃): δ 7.3 [CH₂, C9(10)], 10.9 (CH, C8), 27.9 [CH, C5'(7')], 32.2 (CH₂, C3 or C5), 33.4 (CH₂, C5 or C3), 34.6 [CH₂, C6' and C4'(10')], 40.0 (CH₂, C9' or C8'), 40.2 (CH₂, C8' or C9'), 41.2 (CH₂, C6 or C2), 44.3 (CH₂, C2 or C6), 46.8 (CH, C4), 71.0 (CH, C3'), 80.7 (C, C1'), 156.8 (C, CO), 171.9 (C, COR). HRMS: calcd for [C₁₉H₂₉N₃O₃ + H]⁺, 348.2282; found, 348.2289.

1-(2-Oxaadamantan-1-yl)-3-(1-propionylpiperidin-4-yl)urea, 24. To a solution of 2-oxaadamant-1-yl isocyanate (2.11 mmol) in DCM (5 mL) was added 1-(4-aminopiperidin-1-yl)propan-1-one (330 mg, 2.11 mmol). The reaction mixture was stirred at room temperature overnight. The solvent was evaporated under vacuum to give a yellow gum (823 mg). Column chromatography (DCM/methanol mixtures) gave urea 24 as a white solid (280 mg, 40% yield). mp 165–166 °C. The analytical sample was obtained by crystallization from hot EtOAc. IR (ATR) ν : 887, 930, 965, 995, 1011, 1092, 1119, 1137, 1195, 1218, 1247, 1267, 1321, 1375, 1444, 1556, 1620, 1647, 2332, 2367, 2852, 2927, 3336 cm^{-1} . $^1\text{H NMR}$ (400 MHz, CDCl_3): δ 1.13 (t, $J = 7.6$ Hz, 3 H, CH_3), 1.28–1.40 (complex signal, 2 H, 3- H_a , 5- H_a), 1.60–1.70 [complex signal, 4 H, 9'- H_b , 8'- H_b , 4'(10')- H_b], 1.75–1.87 (m, 2 H, 6'- H_2), 1.87–1.97 [complex signal, 3 H, 4'(10')- H_b , 3- H_b , or 5- H_b], 2.04 (dm, $J = 12.8$ Hz, 1 H, 5- H_b or 3- H_b), 2.09–2.22 (complex signal, 2 H, 9'- H_b , 8'- H_b), 2.27 [broad s, 2 H, 5'(7')-H], 2.33 (q, $J = 7.6$ Hz, 2 H, CH_2CH_3), 2.87 (m, 1 H, 6- H_a or 2- H_a), 3.15 (m, 1 H, 2- H_a or 6- H_a), 3.74 (dm, $J = 13.6$ Hz, 1 H, 2- H_b or 6- H_b), 3.87 (m, 1 H, 4-H), 4.26 (t, $J = 4.0$ Hz, 1 H, 3'-H), 4.37 (dm, $J = 13.6$ Hz, 1 H, 6- H_b or 2- H_b), 4.72 (s, 1 H, 1'-NH), 6.06 (d, $J = 8.0$ Hz, 1 H, 4-NH). $^{13}\text{C NMR}$ (100.5 MHz, CDCl_3): δ 9.5 (CH_3 , CH_2CH_3), 26.5 (CH_2 , CH_2CH_3), 27.9 [CH , $\text{CS}'(7')$], 32.2 (CH_2 , C3 or C5), 33.3 (CH_2 , C5 or C3), 34.6 [CH_2 , C6', C4'(10')], 40.0 (CH_2 , C9' or C8'), 40.2 (CH_2 , C8' or C9'), 40.5 (CH_2 , C6 or C2), 44.1 (CH_2 , C2 or C6), 46.6 (CH, C4), 71.0 (CH, C3'), 80.6 (C, C1'), 156.7 (C, CO), 172.2 (C, CO). HRMS: calcd for $[\text{C}_{15}\text{H}_{29}\text{N}_3\text{O}_3 + \text{H}]^+$, 336.2282; found, 336.2274.

1-(1-(4-Acetylphenyl)piperidin-4-yl)-3-(2-oxaadamant-1-yl)urea, 25. To a solution of 2-oxaadamant-1-yl isocyanate (188 mg, 1.05 mmol) in DCM (5 mL), 1-(4-(4-aminopiperidin-1-yl)phenyl)ethan-1-one³⁶ (230 mg, 1.05 mmol) and triethylamine (0.15 mL, 1.05 mmol) were added. The reaction mixture was stirred at room temperature overnight. The solvents were evaporated under vacuum to give an orange solid (410 mg). Column chromatography (DCM/methanol mixtures) gave urea 25 as a white solid (183 mg, 45% yield). mp 190–191 °C. IR (ATR) ν : 674, 723, 770, 819, 866, 915, 953, 974, 995, 1111, 1134, 1194, 1222, 1279, 1315, 1330, 1475, 1537, 1597, 1653, 1992, 2160, 2341, 2930 cm^{-1} . $^1\text{H NMR}$ (400 MHz, CDCl_3): δ 1.53 [dq, $J = 4.0$ Hz, $J' = 12.8$ Hz, 2 H, 3(5)- H_a], 1.59–1.64 (complex signal, 2 H, 6'- H_2), 1.69 [dm, $J = 12.0$ Hz, 2 H, 9'(8')- H_b], 1.77–1.94 [complex signal, 4 H, 4'(10')- H_b], 2.06 [dm, $J = 12.8$ Hz, 2 H, 3(5)- H_b], 2.17 [dm, $J = 12.4$ Hz, 2 H, 9'(8')- H_b], 2.27 [broad s, 2 H, 5'(7')-H], 2.50 (s, 3 H, COCH_3), 3.08 [ddd, $J = 2.6$ Hz, $J' = 11.2$ Hz, $J'' = 13.6$ Hz, 2 H, 2(6)- H_a], 3.78 [dt, $J = 13.6$ Hz, $J' = 4.0$ Hz, 2 H, 2(6)- H_b], 3.92 (m, 1 H, 4-H), 4.26 [broad s, 1 H, 3'-H], 4.74 (s, 1 H, 1'-NH), 6.07 (d, $J = 7.6$ Hz, 1 H, 4-NH), 6.86 [d, $J = 9.2$ Hz, 2 H, 9(11)-H], 7.85 [d, $J = 9.2$ Hz, 2 H, 8(12)-H]. $^{13}\text{C NMR}$ (100.5 MHz, CDCl_3): δ 26.0 (CH_3 , C13), 27.9 [CH , $\text{CS}'(7')$], 32.0 [CH_2 , C3(5)], 34.6 (CH_2 , C6' and C4'(10')), 40.1 (CH_2 , C9'(8')), 46.57 (CH, C4), 46.59 [CH_2 , C2(6)], 71.0 (CH, C3'), 80.6 (C, C1'), 113.4 [CH, C9(11)], 127.1 (C, C10), 130.5 [CH, C8(12)], 153.7 (C, C7), 156.7 (C, CO), 196.3 (C, COCH_3). HRMS: calcd for $[\text{C}_{23}\text{H}_{31}\text{N}_3\text{O}_3 + \text{H}]^+$, 398.2438; found, 398.2448.

1-(2-Oxaadamantan-1-yl)-3-(1-(methylsulfonyl)piperidin-4-yl)urea, 26. To a solution of 1-amino-2-oxaadamantane hydrochloride (265 mg, 1.4 mmol) in DCM (6 mL) and saturated aqueous NaHCO_3 solution (6 mL) was added triphosgene (153 mg, 0.52 mmol). The biphasic mixture was stirred at room temperature for 30 min, the two phases were separated, and then the organic layer was washed with brine (5 mL), dried over anhydrous Na_2SO_4 , filtered, and evaporated under vacuum to obtain 1–2 mL of a solution of isocyanate in DCM. 1-(Methylsulfonyl)piperidin-4-amine was suspended in anhydrous THF (10 mL) under the argon atmosphere, and the mixture was cooled down to -78 °C. Then, *n*-butyllithium (2.5 M in hexanes, 0.73 mL, 1.82 mmol) was added dropwise for 20 min. Meanwhile, the isocyanate from the previous step was dissolved in anhydrous THF and cooled down to 0 °C. The deprotonated amine was then tempered to 0 °C, and the solution of isocyanate in THF was added. The mixture was stirred at room temperature overnight. The reaction was quenched by the addition of methanol (5 mL), and the

solvent was evaporated to obtain a yellow gum (707 mg). Column chromatography (DCM/methanol mixtures) gave urea 26 as a white solid (47 mg, 10% yield). mp 213–214 °C. IR (NaCl disk) ν : 629, 667, 729, 772, 824, 849, 885, 929, 954, 960, 968, 993, 1012, 1042, 1052, 1095, 1118, 1142, 1159, 1203, 1246, 1272, 1293, 1334, 1355, 1376, 1446, 1466, 1562, 1637, 2850, 2922, 3323 cm^{-1} . $^1\text{H NMR}$ (400 MHz, CDCl_3): δ 1.54 [m, 2 H, 3(5)- H_a], 1.63 [d, $J = 12.4$ Hz, 2 H, 4'(10')- H_b], 1.70 [d, $J = 12.0$ Hz, 2 H, 9'(8')- H_b], 1.81 (m, 2 H, 6'- H_2), 1.91 [dm, $J = 11.2$ Hz, 2 H, 4'(10')- H_b], 2.06 [ddm, $J = 12.8$ Hz, $J' = 3.6$ Hz, 2 H, 3(5)- H_b], 2.15 [d, $J = 11.6$ Hz, 2 H, 9'(8')- H_b], 2.27 [broad s, $J = 3.2$ Hz, 2 H, 5'(7')-H], 2.77 (s, 3 H, 7-H), 2.82 [ddd, $J = J' = 12.0$ Hz, $J'' = 2.8$ Hz, 2 H, 2(6)- H_a], 3.70 [dm, $J = 12.0$ Hz, 2 H, 2(6)- H_b], 3.77 (m, 1 H, 4-H), 4.27 (t, $J = 4.4$ Hz, 1 H, 3'-H), 4.82 (s, 1 H, 1'-NH), 6.06 (d, $J = 8.0$ Hz, 1 H, 4-NH). $^{13}\text{C NMR}$ (100.5 MHz, CDCl_3): δ 27.9 [CH , $\text{CS}'(7')$], 32.2 (CH_2 , C3(5)), 34.6 [CH_2 , C4'(10') and C6'], 34.9 (CH_2 , C7), 40.1 (CH_2 , C9'(8')), 45.0 [CH_2 , C2(6)], 46.1 (CH, C4), 71.0 (CH, C3'), 80.7 (C, C1'), 156.7 (C, CO). HRMS: calcd for $[\text{C}_{16}\text{H}_{27}\text{N}_3\text{O}_3 + \text{H}]^+$, 358.1795; found, 358.1803.

1-(2-Oxaadamantan-1-yl)-3-(benzo[d]thiazol-2-yl)urea, 27. 2-Amino-1,3-benzothiazole (114 mg, 0.76 mmol) was dissolved in anhydrous THF (7 mL) under argon and cooled to -78 °C on dry ice in an acetone bath. Then, *n*-butyllithium (2.5 M in hexanes, 0.31 mL, 0.76 mmol) was added dropwise for 20 min. Afterward, the reaction mixture was removed from dry ice in an acetone bath and tempered to 0 °C in an ice bath. Meanwhile, 2-oxaadamant-1-yl isocyanate (150 mg, 0.84 mmol) was dissolved in anhydrous THF (4 mL) under argon and was continuously added to the reaction mixture. The mixture was stirred at room temperature overnight. Methanol (3 mL) was added to quench any unreacted *n*-butyllithium. The precipitate formed was filtered and washed with ice-cold THF to afford urea 27 as a white solid (151 mg, 42% overall yield). mp 240 °C (dec). IR (ATR) ν : 731, 757, 788, 822, 866, 884, 920, 964, 995, 1046, 1093, 1119, 1191, 1248, 1274, 1323, 1341, 1377, 1452, 1514, 1537, 1597, 1718, 1904, 1992, 2036, 2134, 2201, 2852, 2894, 2930, 3064, 3255, 3322 cm^{-1} . $^1\text{H NMR}$ (400 MHz, DMSO): δ 1.57 [dm, $J = 12.0$ Hz, 2 H, 4'(10')- H_b], 1.73–1.98 [complex signal, 6 H, 4'(10')- H_b , 6'- H_2 , 8'(9')- H_b], 2.18 [m, 2 H, 5'(7')-H], 2.23 [dm, $J = 12.4$ Hz, 2 H, 8'(9')- H_b], 4.11 (m, 1 H, 3'-H), 7.16 (ddd, $J = 8.0$ Hz, $J' = 8.0$ Hz, $J'' = 1.2$ Hz, 1 H, 5-H or 6-H), 7.27 (ddd, $J = 8.0$ Hz, $J' = 7.2$ Hz, $J'' = 1.2$ Hz, 1 H, 6-H or 5-H), 7.58 (dm, $J = 7.6$ Hz, 1 H, 7-H), 7.79–7.86 (complex signal, 2 H, 4-H, 1'-NH or 2-NH). $^{13}\text{C NMR}$ (100.5 MHz, DMSO): δ 27.7 [CH , $\text{CS}'(7')$], 34.46 [CH_2 , C4'(10')], 34.48 (CH2, C6'), 39.5 [CH_2 , C8'(9')], 69.3 (CH, C3'), 80.5 (C, C1'), 118.7 (CH, C7), 120.9 (CH, C4), 121.3 [(CH, C5 or C6), (C, C7a)], 125.1 (CH, C6 or C5), 131.2 [(C, C2), (C, C3)], 149.4 (C, CO). HRMS: calcd for $[\text{C}_{17}\text{H}_{19}\text{N}_3\text{O}_2\text{S} + \text{H}]^+$, 330.1271; found, 330.1272.

1-(2-Oxaadamantan-1-yl)-3-(isoxazol-3-yl)urea, 28. 3-Aminoisoxazole (103 mg, 1.22 mmol) was dissolved in anhydrous THF (13 mL) under argon and cooled to -78 °C on dry ice in an acetone bath. Then, *n*-butyllithium (2.5 M in hexanes, 0.50 mL, 1.22 mmol) was added dropwise for 20 min. Afterward, the reaction mixture was removed from dry ice in an acetone bath and tempered to 0 °C in an ice bath. Meanwhile, 2-oxaadamant-1-yl isocyanate (258 mg, 1.34 mmol) was dissolved in anhydrous THF (6 mL) under argon and was continuously added to the reaction mixture. The mixture was stirred at room temperature overnight. Methanol (4.5 mL) was added to quench any unreacted *n*-butyllithium. The organic solvents were evaporated under vacuum to give an orange gum (371 mg). Column chromatography (hexane/EtOAc mixtures) gave urea 28 as a white solid (90 mg, 22% overall yield). mp 193 °C. IR (ATR) ν : 768, 788, 824, 888, 929, 959, 965, 987, 1014, 1050, 1075, 1093, 1116, 1196, 1260, 1288, 1324, 1377, 1395, 1444, 1475, 1566, 1598, 1672, 1685, 1920, 2005, 2051, 2158, 2215, 2323, 2369, 2851, 2923, 3082, 3179, 3287 cm^{-1} . $^1\text{H NMR}$ (400 MHz, CDCl_3): δ 1.64 [dm, $J = 11.8$ Hz, 2 H, 4'(10')- H_b], 1.77–1.96 [complex signal, 4 H, 6'- H_2 , 8'(9')- H_b], 2.03 [dm, $J = 11.8$ Hz, 2 H, 4'(10')- H_b], 2.25 [dm, $J = 12.4$ Hz, 2 H, 8'(9')- H_b], 2.30 [m, 2 H, 5'(7')-H], 4.34 (m, 1 H, 3'-H), 6.11 [broad s, 1'-NH], 6.75 (s, 1 H, 4-H), 8.19 (d, $J = 1.6$ Hz, 1 H, 5-H), 8.95 [broad s, 1 H, 3-NH]. $^{13}\text{C NMR}$ (100.5 MHz, CDCl_3): δ 28.0 [CH,

C5'(7')), 34.55 [CH₂, C4'(10')], 34.58 (CH₂, C6'), 40.2 [CH₂, C8'(9')], 71.2 (CH, C3'), 81.2 (C, C1'), 98.7 (CH, C4), 153.6 (C, C3), 158.2 [(C, CO), (CH, C5)]. HRMS: calcd for [C₁₃H₁₇N₃O₃ + H]⁺, 264.1343; found, 264.1345.

1-(2-Oxaadamantan-1-yl)-3-(1,3,5-triazin-2-yl)urea, 29. 2-Amino-1,3,5-triazine (245 mg, 2.55 mmol) was dissolved in anh. THF (20 mL) under argon and cooled to -78 °C on dry ice in an acetone bath. Then, *n*-butyllithium (2.5 M in hexanes, 1.05 mL, 2.55 mmol) was added dropwise for 20 min. Afterward, the reaction mixture was removed from dry ice in an acetone bath and tempered to 0 °C in an ice bath. Meanwhile, 2-oxaadamant-1-yl isocyanate (539 mg, 2.80 mmol) was dissolved in anh. THF (8 mL) under argon and was continuously added to the reaction mixture. The mixture was stirred at room temperature overnight. Methanol (9 mL) was added to quench any unreacted *n*-butyllithium. A white precipitate formed among the orange solution was filtered and washed with ice-cold THF to afford urea **29** as a white solid (340 mg, 35% overall yield). mp 157–158 °C. IR (ATR) ν : 700, 783, 824, 887, 965, 997, 1080, 1117, 1186, 1194, 1270, 1320, 1343, 1372, 1395, 1402, 1480, 1482, 1502, 1590, 1625, 1700, 2000, 2055, 2170, 2260, 2345, 2546, 2847, 2922, 3233, 3383, 3498 cm⁻¹. ¹H NMR (400 MHz, DMSO): δ 1.54 [dm, *J* = 12.0 Hz, 2 H, 4'(10')-H_a], 1.66–1.98 [complex signal, 6 H, 4'(10')-H_b, 6'-H₂, 8'(9')-H₂], 2.15 [m, 2 H, 5'(7')-H], 2.26 [dm, *J* = 12.0 Hz, 2 H, 8'(9')-H_b], 4.05 (m, 1 H, 3'-H), 7.31 (broad s, 1 H, 2-NH), 8.34 (s, 2 H, 4-H, 6-H). ¹³C NMR (100.5 MHz, DMSO): δ 27.7 [CH, C5'(7')], 34.60 [CH₂, C4'(10')], 34.63 (CH₂, C6'), 39.6 (CH₂, C8'(9')), 69.1 (CH, C3'), 80.1 (C, C1'), 164.7 (C, CO), 165.2 [(CH, C4, C6), (C, C2)]. HRMS: calcd for [C₁₃H₁₇N₃O₂ + H]⁺, 276.1455; found, 276.1454.

1-(2-Oxaadamantan-1-yl)-3-(3-chloro-5-(trifluoromethoxy)phenyl)urea, 30. A solution of 3-chloro-5-(trifluoromethoxy)aniline (200 mg, 0.94 mmol) in toluene (3 mL) was treated with triphosgene (140 mg, 0.47 mmol). Immediately, triethylamine (0.13 mL, 0.94 mmol) was added, and the reaction mixture was stirred at 70 °C for 2 h. Afterward, pentane (0.5 mL) was added and a white precipitate was formed. The mixture was filtered, and pentane was evaporated under vacuum at room temperature to give the isocyanate in toluene solution that was used in the next step without further purification. To a solution of 3-(trifluoromethoxy)-5-chlorophenylisocyanate from the previous step were added DCM (5 mL), 2-oxaadamantan-1-amine hydrochloride (161 mg, 0.85 mmol), and triethylamine (0.24 mL, 1.71 mmol). The suspension was stirred at room temperature overnight. The mixture was evaporated under vacuum to give a residue that was then dissolved in DCM (20 mL) and washed with 2N HCl solution. The organic phase was dried over anh. Na₂SO₄ and filtered. Evaporation under vacuum of the organics gave urea **30** (284 mg, 89% overall yield) as an orange solid. The analytical sample was obtained as a white solid (100 mg) by crystallization from hot DCM. mp 177–178 °C. IR (ATR) ν : 672, 747, 935, 964, 995, 1093, 1116, 1152, 1191, 1212, 1248, 1416, 1465, 1550, 1599, 1664, 2930, 3302 cm⁻¹. ¹H NMR (400 MHz, CDCl₃): δ 1.70 [dm, *J* = 12.4 Hz, 2 H, 4'(10')-H_a], 1.76–1.94 [complex signal, 4 H, 6'-H₂, 8'(9')-H₂], 2.01 [dm, *J* = 12.4 Hz, 2 H, 4'(10')-H_b], 2.18 [dm, *J* = 12.4 Hz, 2 H, 8'(9')-H_b], 2.32 [m, 2 H, 5'(7')-H], 4.41 (m, 1 H, 3'-H), 5.36 (broad s, 1 H, 1'-NH), 6.87 (m, 1 H, 4-H), 7.29–7.35 (complex signal, 2 H, 2-H, 6-H), 8.47 (broad s, 1 H, 1-NH). ¹³C NMR (100.5 MHz, CDCl₃): δ 27.9 [CH, C5'(7')], 34.4 (CH₂, C6'), 34.7 [CH₂, C4'(10')], 40.5 [CH₂, C8'(9')], 71.5 (C, C3'), 81.2 (C, C1'), 110.0 (CH, C6), 115.1 (CH, C4), 117.2 (CH, C2), 120.3 (q, *J* = 258.3 Hz, C, CF₃), 135.1 (C, C3), 141.0 (C, C1), 149.8 (m, C, C5), 154.6 (C, CO). HRMS: calcd for [C₁₇H₁₈ClF₃N₂O₃ + H]⁺, 391.1031; found, 391.1038.

1-(2-Oxaadamantan-1-yl)-3-(4-chloro-3-(trifluoromethyl)phenyl)urea, 31. To a solution of the commercial 4-chloro-3-(trifluoromethyl)phenyl isocyanate (191 mg, 0.84 mmol) in DCM were added 2-oxaadamantan-1-amine hydrochloride (145 mg, 0.76 mmol) and triethylamine (0.21 mL, 1.52 mmol). The reaction mixture was stirred at room temperature overnight. The mixture was evaporated under vacuum to give a solid that was then dissolved in EtOAc (20 mL) and washed with 2 N HCl solution (10 mL). The

organic phase was dried over anh. Na₂SO₄ and filtered. Evaporation under vacuum of the organics gave urea **31** as a white solid (238 mg, 83% yield). The analytical sample was obtained by crystallization from hot EtOAc (127 mg). mp 196 °C. IR (ATR) ν : 661, 721, 765, 785, 824, 835, 881, 930, 961, 987, 1028, 1093, 1114, 1134, 1170, 1191, 1209, 1253, 1289, 1297, 1323, 1374, 1416, 1485, 1550, 1586, 1607, 1671, 2118, 2144, 2217, 2351, 2847, 2925, 3054, 3100, 3235, 3286 cm⁻¹. ¹H NMR (400 MHz, CDCl₃): δ 1.69 [dm, *J* = 12.6 Hz, 2 H, 4'(10')-H_a], 1.77–1.93 [complex signal, 4 H, 6'-H₂, 8'(9')-H₂], 2.01 [dm, *J* = 12.6 Hz, 2 H, 4'(10')-H_b], 2.19 [m, *J* = 12.0 Hz, 2 H, 8'(9')-H_b], 2.32 [m, 2 H, 5'(7')-H], 4.41 (m, 1 H, 3'-H), 5.42 (broad s, 1H, 1'-NH), 7.37 (d, *J* = 8.6 Hz, 1 H, 5-H), 7.56 (dd, *J* = 8.6 Hz, *J'* = 2.6 Hz, 6-H), 7.71 (d, 1 H, *J* = 2.6 Hz, 2-H), 8.4 (broad s, 1 H, 1-NH). ¹³C NMR (100.5 MHz, CDCl₃): δ 27.9 [CH, C5'(7')], 34.4 (CH₂, C6'), 34.7 [CH₂, C4'(10')], 40.4 [CH₂, C8'(9')], 71.4 (CH, C3'), 81.2 (C, C1'), 118.2 (q, ¹*J*_{C-F} = 6.0 Hz, CH, C2), 122.7 (q, ¹*J*_{C-F} = 273 Hz, C, CF₃), 123.2 (CH, C6), 125.1 (C, C4), 128.5 (q, ²*J*_{C-F} = 31.3 Hz, C, C3), 131.8 (CH, C5), 137.7 (C, C1), 154.8 (C, CO). HRMS: calcd for [C₁₇H₁₈ClF₃N₂O₂ + H]⁺, 375.1082; found, 375.1090.

1-(2-Oxaadamantan-1-yl)-3-(3-(pentafluoro- λ^6 -sulfanyl)phenyl)urea, 32. A solution of 3-(pentafluoro- λ^6 -sulfanyl)aniline (185 mg, 0.84 mmol) in toluene (3.6 mL) was treated with triphosgene (125 mg, 0.42 mmol). Immediately, triethylamine (0.12 mL, 0.84 mmol) was added, and the reaction mixture was stirred at 70 °C for 2 h. Afterward, pentane (0.5 mL) was added and a white precipitate was formed. The mixture was filtered, and pentane was evaporated under vacuum at room temperature to give the isocyanate in toluene solution that was used in the next step without further purification. To a solution of the 3-(pentafluoro- λ^6 -sulfanyl)phenyl isocyanate from the previous step were added DCM (5 mL), 2-oxaadamantan-1-amine hydrochloride (145 mg, 0.76 mmol), and triethylamine (0.21 mL, 1.52 mmol). The suspension was stirred at room temperature overnight. The mixture was evaporated under vacuum to give a solid that was then dissolved in DCM (20 mL) and washed with aqueous 2N HCl solution. The organic phase was dried over anh. Na₂SO₄ and filtered. Evaporation under vacuum of the organics gave urea **32** (237 mg, 71% overall yield) as a pale yellow solid. The analytical sample was obtained by crystallization from hot EtOAc as a white solid (75 mg). mp 203 °C. IR (ATR) ν : 649, 685, 734, 785, 824, 835, 863, 946, 959, 990, 1093, 1114, 1199, 1250, 1256, 1292, 1318, 1369, 1431, 1478, 1537, 1591, 1671, 1966, 2041, 2930, 3080, 3224, 3286 cm⁻¹. ¹H NMR (400 MHz, CDCl₃): δ 1.69 [dm, *J* = 11.8 Hz, 2 H, 4'(10')-H_a], 1.78–1.94 [complex signal, 4 H, 6'-H₂, 8'(9')-H₂], 2.01 [dm, *J* = 11.8 Hz, 2 H, 4'(10')-H_b], 2.21 [m, *J* = 12.4 Hz, 2 H, 8'(9')-H_b], 2.32 [m, 2 H, 5'(7')-H], 4.42 (m, 1 H, 3'-H), 5.43 (broad s, 1H, 1'-NH), 7.35 (d, *J* = 8.2 Hz, 1 H, 6-H), 7.39 (dq, *J* = 8.2 Hz, *J'* = 1.2 Hz, 1 H, 5-H), 7.52 (d, *J* = 8.2 Hz, 1 H, 4-H), 7.86 (t, *J* = 2.0 Hz, 1 H, 2-H), 8.50 (broad s, 1 H, 1-NH). ¹³C NMR (100.5 MHz, CDCl₃): δ 27.9 [CH, C5'(7')], 34.5 (CH₂, C6'), 34.7 [CH₂, C4'(10')], 40.4 [CH₂, C8'(9')], 71.4 (CH, C3'), 81.2 (C, C1'), 116.9 (m, CH, C2), 120.1 (m, CH, C4), 122.3 (CH, C6), 128.9 (CH, C5), 139.2 (C, C1), 154.3 (C, C3), 154.9 (C, CO). HRMS: calcd for [C₁₆H₁₉F₅N₂O₂S + H]⁺, 399.1160; found, 399.1172.

Determination of IC₅₀ sEH Inhibitors in Human, Murine, and Rat Purified sEH. IC₅₀ is the concentration of a compound that reduces the sEH activity by 50%. The IC₅₀ values reported herein were determined using a fluorescent-based assay (CMNPC as the substrate).⁵³ The fluorescent assay was used with purified recombinant human, mouse, or rat sEH proteins. The enzymes were incubated at 30 °C with the inhibitors ([I]_{final} = 0.4–100,000 nM) for 5 min in 100 mM sodium phosphate buffer (200 μ L, pH 7.4) containing 0.1 mg/mL of BSA and 1% of DMSO. The substrate (CMNPC) was then added ([S]_{final} = 5 μ M). Activity was assessed by measuring the appearance of the fluorescent 6-methoxynaphthaldehyde product (λ_{ex} = 330 nm, λ_{em} = 465 nm) every 30 s for 10 min at 30 °C on a SpectraMax M2 (molecular devices). Results were obtained by regression analysis from a linear region of the curve.

In Silico Study. MD Simulations Details. The parameters for AR9273, **22**, and **26**, for the MD simulations were generated within

the ANTECHAMBER module of AMBER 18⁵⁴ using the general AMBER force field (GAFF),⁵⁵ with partial charges set to fit the electrostatic potential generated at the HF/6-31G(d) level by the RESP model.⁵⁶ The charges were calculated according to the Merz-Singh-Kollman scheme^{57,58} using Gaussian 09.⁵⁹

MD simulations of sEH were carried out using PDB 5ALZ (crystallized with AR9273)³⁸ as a reference. For the MD simulations in the *apo* state, the AR9273 was removed from the active site. The oxadamantyl derivatives corresponding to compounds **22** and **26** were manually prepared using the AR9273 structure as the starting point. From these coordinates, conventional MD simulations were used to explore the conformational plasticity of sEH in the *apo* state and in the presence of AR9273, **22**, and **26** bound in the active site. Amino acid protonation states were predicted using the H++ server (<http://biophysics.cs.vt.edu/H++>). The MD simulations have been carried out with the following protonation of histidine residues: HIE146, HIE239, HIP251, HID265, HIP334, HIE420, HIES06, HIE513, HIE518, and HIP524.

Each system was immersed in a pre-equilibrated truncated octahedral box of water molecules with an internal offset distance of 10 Å. All systems were neutralized with explicit counterions (Na⁺ or Cl⁻). A two-stage geometry optimization approach was performed. First, a short minimization of the positions of water molecules with positional restraints on the solute by a harmonic potential with a force constant of 500 kcal mol⁻¹ Å⁻² was done. The second stage was an unrestrained minimization of all the atoms in the simulation cell. Then, the systems were gently heated in six 50 ps steps, increasing the temperature by 50 K each step (0–300 K) under constant-volume, periodic-boundary conditions and the particle-mesh Ewald approach⁶⁰ to introduce long-range electrostatic effects. For these steps, a 10 Å cutoff was applied to Lennard-Jones and electrostatic interactions. Bonds involving hydrogen were constrained with the SHAKE algorithm.⁶¹ Harmonic restraints of 10 kcal mol⁻¹ were applied to the solute, and the Langevin equilibration scheme was used to control and equalize the temperature.⁶² The time step was kept at 2 fs during the heating stages, allowing potential inhomogeneities to self-adjust. Each system was then equilibrated for 2 ns with a 2 fs time step at a constant pressure of 1 atm. Finally, conventional MD trajectories at constant volume and temperature (300 K) were collected. In total, three replicas of 250 ns MD simulations for sEH in the *apo* state and in the presence of AR9273, **22**, and **26** were run, gathering a total of 3 μs of MD simulation time. The relative binding free energy was calculated for compounds **22** and **22-CH₂** using the TI method.⁶³ The NPT ensemble was used for equilibrating the system and the production runs for the TI calculations using a time step of 1 fs and the same simulation protocols as described above. The schedule of lambda windows chosen consists of 11 λ values: 0.0, 0.1, 0.2, 0.3, 0.4, 0.5, 0.6, 0.7, 0.8, 0.9, 1.0. The initial equilibrations of 4 ns were performed using a λ of 0.5 and this configuration was used as the starting point for neighboring lambda windows. The TI runs were run for 4 ns and frames were collected every 0.5 ps for postanalysis and relative binding free energy calculations.

The octanol/water partition coefficient, log *P*, of compound **22** and **22-CH₂** was calculated from the solvation free energy differences using the M06-2X functional⁶⁴ with SMD implicit solvation⁶⁵ and the def2-SVP basis set⁶⁶ as described by Guan et al.⁴² Solvated geometry optimizations were performed using M06-2X/def2-SVP and SMD using water and 1-octanol as solvents. To calculate the log *P*, the free energies obtained at 298.15 K using octanol and water as solvents were employed to compute the standard free energy associated with the transfer of the solute from the water to octanol phases as

$$\log P = \frac{\Delta G_{\text{solvation(water)}} - \Delta G_{\text{solvation(octanol)}}}{2.303RT} \quad (1)$$

Solubility. The stock solutions (10⁻² M) of assayed compounds were diluted to decreased molarity, from 300 to 0.1 μM, in 384 well transparent plate (Greiner 781801) with 1% DMSO/99% PBS buffer. Then, they were incubated at 37 °C and the light scattering was measured after 2 h in a NEPHELOstar Plus (BMG LABTECH). The

results were adjusted to a segmented regression to obtain the maximum concentration in which compounds are soluble.

Permeability. The Caco-2 cells were cultured to confluency, trypsinized, and seeded onto a 96-filter transwell insert (Corning) at a density of ~10,000 cells/well in DMEM cell culture medium supplemented with 10% foetal bovine serum, 2 mM L-glutamine, and 1% penicillin/streptomycin. Confluent Caco-2 cells were subcultured at passages 58–62 and grown in a humidified atmosphere of 5% CO₂ at 37 °C. Following an overnight attachment period (24 h after seeding), the cell medium was replaced with fresh medium in both the apical and basolateral compartments every other day. The cell monolayers were used for transport studies 21 days post seeding. The monolayer integrity was checked by measuring the transepithelial electrical resistance (TEER) obtaining values ≥500 Ω/cm². On the day of the study, after the TEER measurement, the medium was removed and the cells were washed twice with prewarmed (37 °C) Hank's Balanced Salt Solution (HBSS) buffer to remove traces of the medium. Stock solutions were made in dimethyl sulfoxide (DMSO) and further diluted in HBSS (final DMSO concentration 1%). Each compound and reference compounds (Colchicine, E3S) were all tested at a final concentration of 10 μM. For A → B directional transport, the donor working solution was added to the apical (A) compartment and the transport media as receiver working solution was added to the basolateral (B) compartment. For B → A directional transport, the donor working was added to the basolateral (B) compartment and transport media as the receiver working solution was added to the apical (A) compartment. The cells were incubated at 37 °C for 2 h with gentle stirring.

At the end of the incubation, samples were taken from both donor and receiver compartments and transferred into 384-well plates and analyzed by UPLC-MS/MS. The detection was performed using an ACQUITY UPLC/Xevo TQD System. After the assay, Lucifer yellow was used to further validate the cell monolayer integrity, cells were incubated with LY 10 μM in HBSS for 1 h at 37 °C, obtaining permeability (Papp) values for LY of ≤10 nm/s, confirming the well-established Caco-2 monolayer.

Cytotoxicity in PBMCs Cells + 1.5% PHA. Cytotoxic effects of assayed compounds were tested using peripheral blood mononuclear cells isolated following the regular density gradient centrifugation procedure with Ficol. Cells were plated in 96-well black microplates at 270,000 cells/well density with RPMI medium [containing 10% FBS, 1% NEAA, 1% P/S, and 1.5% PHA (phytohaemagglutinin)]. The tested compounds were solubilized in 100% DMSO in a concentration curve way and then diluted with cell culture medium containing 2% DMSO. The final concentrations of the test compounds (0.2% DMSO) ranged from 0 to 20 μM in a final volume of 150 μL. Microplates were maintained at 37 °C (5% CO₂, 95% humidity) for 3 days. Following this 72 h exposure to test compounds, cell viability in each well was determined by measuring the concentration of cellular adenosine triphosphate (ATP) using the ATP1Step Kit as described by the manufacturer (Perkin-Elmer). In a typical procedure, 80 μL of cell reagent was added to all wells of each test plate followed by incubation for 10 min at room temperature on an orbital shaker. ATP concentration was determined by reading chemical luminescence using the Envision plate reader (PerkinElmer). The percentage of viable cells relative to the non-drug-treated controls was determined for each well and LC₅₀ values were calculated as concentrations projected to kill 50% of the cells following a 72 h exposure.

Cytotoxicity in THLE-2 Cells. Cytotoxic effects of assayed compounds were tested using the immortalized human liver cell line THLE-2 (ATCC CRL-2706). Cells were cultured in BEGM medium (Clonetics #CC-4175) containing all the supplements kit except additional EGF and G418. Medium was completed by adding 0.7 μg/mL phosphoethanolamine, 0.5 ng/mL epidermal growth factor, antibiotics (penicillin and streptomycin), and 10% fetal bovine serum (FBS). Cells were plated in 96-well black microplates at 10,000 cells/well density and were incubated at 37 °C (5% CO₂, 95% humidity) for 24 h to allow the cells to adhere and form a monolayer. Test compounds were solubilized in 100% DMSO in a concentration

curve way and then diluted with cell culture medium containing 10% DMSO. The final concentrations of the test compounds (1% DMSO) ranged from 0 to 100 μM in a final volume of 200 μL . Microplates were maintained at 37 °C (5% CO_2 , 95% humidity) for 3 days. Following this 72 h exposure to test compounds, cell viability in each well was determined by measuring the concentration of cellular ATP using the ATP1Step Kit as described by the manufacturer (Perkin-Elmer). In a typical procedure, 50 μL of cell reagent was added to all wells of each test plate followed by incubation for 10 min at room temperature on an orbital shaker. ATP concentration was determined by reading chemical luminescence using the Envision plate reader (PerkinElmer). The percentage of viable cells relative to the non-drug-treated controls was determined for each well and LC_{50} values were calculated as concentrations projected to kill 50% of the cells following a 72 h exposure.

Parallel Artificial Membrane Permeation Assays–Blood–Brain Barrier. To evaluate the brain penetration of the different compounds, a parallel artificial membrane permeation assay for blood–brain barrier was used, following the method described by Di et al.⁴³ The *in vitro* permeability (P_e) of 14 commercial drugs through lipid extract of porcine brain membrane together with the test compounds was determined. Commercial drugs and assayed compounds were tested using a mixture of PBS/EtOH (70:30). Assay validation was made by comparing the experimental permeability with the reported values of the commercial drugs by bibliography and lineal correlation between experimental and reported permeability of the 14 commercial drugs using the parallel artificial membrane permeation assay was evaluated ($y = 1.5219x - 0.9129$; $R^2 = 0.9387$). From this equation and taking into account the limits established by Di et al.⁴³ for BBB permeation, we established the ranges of permeability as compounds of high BBB permeation (CNS+): P_e ($10^{-6} \text{ cm s}^{-1}$) > 5.149; compounds of low BBB permeation (CNS-): P_e ($10^{-6} \text{ cm s}^{-1}$) < 2.131; and compounds of uncertain BBB permeation (CNS+/-): $5.149 > P_e$ ($10^{-6} \text{ cm s}^{-1}$) > 2.131.

Cytochrome P450 Inhibition Assay. The objective of this study was to screen the inhibition potential of the compounds using recombinant human cytochrome P450 enzymes CYP3A4 (BFC and DBF substrates) and probe substrates with fluorescent detection. Incubations were conducted in a 200 μL volume in 96-well microtiter plates (COSTAR 3915). The addition of the mixture buffer-cofactor (KH_2PO_4 , buffer, 1.3 mM NADP, 3.3 mM MgCl_2 , 0.4 U/mL glucose-6-phosphate dehydrogenase), control supersomes, the standard inhibitor Ketoconazole (Sigma K1003), and previously diluted compounds to plates was carried out by a liquid handling station (Zephyr Caliper). The plate was then preincubated at 37 °C for 5 min in 100 μL volume, and reaction was initiated by the addition of prewarmed enzyme/substrate (E/S) mix. The E/S mix contained buffer (KH_2PO_4), enzyme (CYP), substrate 7-benzoyloxytrifluoromethyl coumarin (7-BFC), and Dibenzylfluorescein (DBF) in a reaction volume of 200 μL . Reactions were terminated after various times depending on the substrate by addition of STOP solution (ACN/TrisHCl 0.5 M 80:20 (BFC) or 2 N NaOH for CYP3A4 (DBF)). Fluorescence per well was measured using a fluorescence plate reader (Tecan M1000 pro) and percentage of inhibition was calculated.

Microsomal Stability. The human microsomes employed were purchased from Tebu-Xenotech. The compound was incubated at 37 °C with the microsomes in a 50 mM phosphate buffer (pH = 7.4) containing 3 mM MgCl_2 , 1 mM NADP, 10 mM glucose-6-phosphate, and 1 U/mL glucose-6-phosphate-dehydrogenase. Samples (75 μL) were taken from each well at 0, 10, 20, 40, and 60 min and transferred to a plate containing 75 μL of acetonitrile, and 30 μL of 0.5% formic acid in water was added for improving the chromatographic conditions. The plate was centrifuged (46,000g, 30 min) and supernatants were taken and analyzed in a UPLC-MS/MS (Xevo-TQD, Waters) by employing a BEH C18 column and an isocratic gradient of 0.1% formic acid in H_2O : 0.1% formic acid acetonitrile (60:40). The metabolic stability of the compounds was calculated

from the logarithm of the remaining compounds at each of the time points studied.

Inhibition of Human Lipoxygenase-5 (hLOX-5). AA and 2',7'-dichlorodihydrofluorescein diacetate (H_2DCFDA) were obtained from Sigma. Human recombinant LOX-5 was purchased from Cayman Chemical. For the determination of hLOX-5 activity, the method described by Pufahl et al. was followed.⁶⁷ The assay solution consisted of 50 mM Tris (pH 7.5), 2 mM EDTA, 2 mM CaCl_2 , 3 μM AA, 10 μM ATP, 10 μM H_2DCFDA , and 100 mU/well hLOX-5. For the enzyme inhibition studies the compounds to be tested were added to the assay solution prior to AA and ATP and were preincubated for a period of 10 min at room temperature, after which AA and ATP were added. The enzymatic reaction was carried out for 20 min and terminated by the addition of 40 μL of acetonitrile. The fluorescence measurement, 485 nm excitation and 520 nm emission, was performed on a FLUOstar OPTIMA (BMG LABTECH, Offenburg, Germany). The IC_{50} is defined as the concentration of compound that inhibits enzymatic activity by 50% over the untreated enzyme control.

In Vitro Proof of Concept. Rat pancreatic AR42J acinar cells were purchased from ATCC and cultured in RPMI-1680 (Gibco) supplemented with 10% fetal bovine serum, 2 mM glutamine, 100 $\mu\text{g}/\text{mL}$ streptomycin, and 100 units/ml penicillin at 37 °C in a humidified atmosphere containing 5% CO_2 . The medium was changed every 48 h. AR42J cells plated into a six-well plate and incubated for 24–48 h (one or the other) were pretreated with sEH inhibitors for 1 h and, later, treated with sEH inhibitors plus cerulein 10 nM (treated group) for 8 h. The same volume of saline serum (0.9% NaCl) was added to the control cultures (control group).

Pharmacokinetic Study. Mice used in this study were Hsd/ICR (CD-1) (females, 6–7 weeks old supplied by ENVIGO). The animals were housed under sterile conditions at a constant temperature of 20–22 °C and relative humidity (45–65%) under daily cycles of light/darkness (12 h). Manipulation was performed in laminar flow hood and sterilized water and food were available ad libitum. The procedure involving experimental animals was approved by the "Ethical Committee of Animal Experimentation" of the animal facility plate at Science Park of Barcelona (Platform of Applied Research in Animal Laboratory). Once approved by the Institutional ethical committee, this procedure was additionally approved by the ethical committee of the Catalonian authorities according to the Catalonian and Spanish regulatory laws and guidelines governing experimental animal care. Along with the procedures for using experimental animals, we also established a continuous supervision and control of the animals to monitor their degree of suffering and if needed to sacrifice them according to the defined end point criteria described by the United Kingdom Coordinating Committee of Cancer Research (UKCCCR), by the Canadian Council on Animal Care (1998), by the Institute for Laboratory Research Journal (2000), by the Conference 22–25 November 1998 Zeist (The Netherlands), and by the Guidelines for the welfare and use of animals in cancer research (2010). The euthanasia method applied was by CO_2 saturated atmosphere. Formulations were prepared the day of the study. The vehicle was saline solution + 5% DMSO. Twenty-one mice were administered iv with a single dose of 1 mg/kg of compound 22. The volume of administration was 5 mL/kg. The 21 mice were administered ip with a single dose of 1 mg/kg of compound 22. The volume of administration was 10 mL/kg. Animals were weighed before each administration to adjust the required volume. Compound 22 was administered by ip or iv and animals were killed under a CO_2 -saturated atmosphere to obtain blood samples. Blood samples were collected at different times post administration: 0 h, 10', 30', 1 h, 2 h, 4 h, 6 h, and 24 h. Samples were taken by cardiac puncture at different times post administration (three animals per time). Blood was collected on recipients containing 5 μL of EDTA 0.5 M. Blood was centrifuged at 5000 rpm for 10 min. Each plasma sample (100 μL) (BK, calibration standards and study samples) was mixed with 300 μL of methanol and 60 μL of ISTD in a Sirocco plate. The plate was centrifuged at 2000 rpm for 10 min. After that, the sample were dried at 40 °C under N_2 streaming and reconstituted with 110 μL of

MeOH/H₂O 0.1% HCOOH 1:1. Concentrations of compound 22 were analyzed by UPLC-MS.

Maximum Tolerated Dose Study. Mice used in this study were Hsd/ICR (CD-1) females, 6–7 weeks old supplied by ENVIGO. Animals were housed under sterile conditions at a constant temperature of 20–22 °C and relative humidity (45–65%) under daily cycles of light/darkness (12 h). Manipulation was performed in laminar flow hood and sterilized water and food were available ad libitum. The procedure involving experimental animals was approved by the “Ethical Committee of Animal Experimentation” of the animal facility plate at Science Park of Barcelona (Platform of Applied Research in Animal Laboratory). Once approved by the Institutional ethical committee, this procedure was additionally approved by the ethical committee of the Catalonian authorities according to the Catalonian and Spanish regulatory laws and guidelines governing experimental animal care. Along with the procedures for using experimental animals, we also establish a continuous supervision and control of the animals to monitor their degree of suffering and if needed to sacrifice them according to the defined end point criteria described by the United Kingdom Coordinating Committee of Cancer Research (UKCCCR), by the Canadian Council on Animal Care (1998), by the Institute for Laboratory Research Journal (2000), by the Conference 22–25 November 1998 Zeist (The Netherlands), and by the Guidelines for the welfare and use of animals in cancer research (2010). The euthanasia method applied was by CO₂-saturated atmosphere. Animal weight was monitored daily. The criteria for end point before the end of the assay was that the mean of weight loss from any group reaches 15% or more; also, any individual mouse with a loss of 20% should be sacrificed. Body weight was monitored daily previous to administration. The body weight loss was calculated according to the formula ((weight – weight start)/weight start) × 100. Compound 22 was administered by ip for 5 consecutive days and, after that, animals’ weight was monitored for 5 days more. Then, animals were killed under a CO₂-saturated atmosphere to obtain samples. Five groups were performed taking into account the administered dose. G1: Control vehicle, 5 days (*n* = 6). G2: Compound 22 at 80 mg/kg, 5 days (*n* = 6). G3: Compound 22 at 20 mg/kg, 5 days (*n* = 6). G4: Compound 22 at 10 mg/kg, 5 days (*n* = 6). G5: Compound at 5 mg/kg, 5 days (*n* = 6).

In Vivo Efficacy Study. Compound 22 was administered before (pre) and after (post) induction of AP with cerulein (50 µg/kg body weight, 12 times at 1 h intervals) in 8- to 10-week-old male mice (C57BL/6J), as previously described.³⁴ In the postinduction studies, 22 (3 and 30 mg/kg) was administered in one injection 24 h after induction of AP. In the preinduction studies, sEH inhibitors were administered at the same dose for 5 consecutive days 2 times/day before induction of AP. Animals were sacrificed 24 h after the end of the treatment and blood and tissues were collected and flash-frozen at –80 °C. The mice were treated in accordance with the European Community Council Directive 86/609/EEC and the procedures established by the *Departament d’Agricultura, Ramaderia i Pesca of the Generalitat de Catalunya*.

Histologic Analyses. A portion of the pancreas was fixed in 4% paraformaldehyde and sections were stained with H&E to observe the morphologic changes. Histologic analysis was performed as previously described.³⁴

RNA Preparation and Quantitative RT-PCR. RNA was extracted from AR42J cells and pancreatic tissue using Trisure reagent (Trisure Bio-38032, Bio-Rad) according to the manufacturer’s recommended protocol. Normally, 1 µg of total RNA was reverse-transcribed into cDNA and the relative levels of specific mRNAs were assessed by real-time PCR with a MiniOpticon Real-Time PCR system (Bio-Rad). The primer sequences used are shown in the Supporting Information.

■ ASSOCIATED CONTENT

● Supporting Information

The Supporting Information is available free of charge at <https://pubs.acs.org/doi/10.1021/acs.jmedchem.0c00310>.

¹H and ¹³C NMR spectra and elemental analysis data of the new compounds, inhibition of hLOX-5 and hCOX-2 and pharmacokinetic data of compound 22 (PDF)

Molecular formula string and data (CSV)

■ AUTHOR INFORMATION

Corresponding Author

Santiago Vázquez – *Laboratori de Química Farmacèutica (Unitat Associada al CSIC), Departament de Farmacologia, Toxicologia i Química Terapèutica, Facultat de Farmàcia i Ciències de l’Alimentació, and Institute of Biomedicine (IBUB), Universitat de Barcelona, 08028 Barcelona, Spain;*
● orcid.org/0000-0002-9296-6026; Phone: +34 934024533; Email: svazquez@ub.edu

Authors

Sandra Codony – *Laboratori de Química Farmacèutica (Unitat Associada al CSIC), Departament de Farmacologia, Toxicologia i Química Terapèutica, Facultat de Farmàcia i Ciències de l’Alimentació, and Institute of Biomedicine (IBUB), Universitat de Barcelona, 08028 Barcelona, Spain*

Eugènia Pujol – *Laboratori de Química Farmacèutica (Unitat Associada al CSIC), Departament de Farmacologia, Toxicologia i Química Terapèutica, Facultat de Farmàcia i Ciències de l’Alimentació, and Institute of Biomedicine (IBUB), Universitat de Barcelona, 08028 Barcelona, Spain*

Javier Pizarro – *Pharmacology, Departament de Farmacologia, Toxicologia i Química Terapèutica, Facultat de Farmàcia i Ciències de l’Alimentació, and Institute of Biomedicine (IBUB), Universitat de Barcelona, 08028 Barcelona, Spain; Spanish Biomedical Research Center in Diabetes and Associated Metabolic Diseases (CIBERDEM)-Instituto de Salud Carlos III, 28029 Madrid, Spain; Pediatric Research Institute-Hospital Sant Joan de Déu, 08950 Esplugues de Llobregat, Spain*

Ferran Feixas – *CompBioLab Group, Departament de Química and Institut de Química Computacional i Catàlisi (IQCC), Universitat de Girona, 17003 Girona, Spain*

Elena Valverde – *Laboratori de Química Farmacèutica (Unitat Associada al CSIC), Departament de Farmacologia, Toxicologia i Química Terapèutica, Facultat de Farmàcia i Ciències de l’Alimentació, and Institute of Biomedicine (IBUB), Universitat de Barcelona, 08028 Barcelona, Spain*

M. Isabel Loza – *Drug Screening Platform/Biofarma Research Group, CIMUS Research Center, University of Santiago de Compostela (USC), 15782 Santiago de Compostela, Spain*

José M. Brea – *Drug Screening Platform/Biofarma Research Group, CIMUS Research Center, University of Santiago de Compostela (USC), 15782 Santiago de Compostela, Spain*

Elena Saez – *Small Molecule Discovery Platform, Molecular Therapeutics Program, Center for Applied Medical Research (CIMA), University of Navarra, 31008 Pamplona, Spain*

Julen Oyarzabal – *Small Molecule Discovery Platform, Molecular Therapeutics Program, Center for Applied Medical Research (CIMA), University of Navarra, 31008 Pamplona, Spain;* ● orcid.org/0000-0003-1941-7255

Antonio Pineda-Lucena – *Small Molecule Discovery Platform, Molecular Therapeutics Program, Center for Applied Medical Research (CIMA), University of Navarra, 31008 Pamplona, Spain*

Belén Pérez – *Department of Pharmacology, Therapeutics and Toxicology, Institute of Neurosciences, Autonomous University of Barcelona, 08193 Barcelona, Spain*

Concepción Pérez – Institute of Medicinal Chemistry, Spanish National Research Council (CSIC), 28006 Madrid, Spain

María Isabel Rodríguez-Franco – Institute of Medicinal Chemistry, Spanish National Research Council (CSIC), 28006 Madrid, Spain; orcid.org/0000-0002-6500-792X

Rosana Leiva – Laboratori de Química Farmacèutica (Unitat Associada al CSIC), Universitat de Barcelona, 08028 Barcelona, Spain

Sílvia Osuna – CompBioLab Group, Departament de Química and Institut de Química Computacional i Catàlisi (IQCC), Universitat de Girona, 17003 Girona, Spain; Institució Catalana de Recerca i Estudis Avançats (ICREA), 08010 Barcelona, Spain; orcid.org/0000-0003-3657-6469

Christophe Morisseau – Department of Entomology and Nematology and Comprehensive Cancer Center, University of California, Davis, Davis, California 95616, United States

Bruce D. Hammock – Department of Entomology and Nematology and Comprehensive Cancer Center, University of California, Davis, Davis, California 95616, United States; orcid.org/0000-0003-1408-8317

Manuel Vázquez-Carrera – Pharmacology, Departament de Farmacologia, Toxicologia i Química Terapèutica, Facultat de Farmàcia i Ciències de l'Alimentació, and Institute of Biomedicine (IBUB), Universitat de Barcelona, 08028 Barcelona, Spain; Spanish Biomedical Research Center in Diabetes and Associated Metabolic Diseases (CIBERDEM)-Instituto de Salud Carlos III, 28029 Madrid, Spain; Pediatric Research Institute-Hospital Sant Joan de Déu, 08950 Esplugues de Llobregat, Spain

Complete contact information is available at:
<https://pubs.acs.org/10.1021/acs.jmedchem.0c00310>

Author Contributions

S.C., E.P., and E.V. synthesized and chemically characterized the compounds. J.P. and M.V.-C. designed and carried out the AR42J cell line and the *in vivo* experiments. C.M. and B.D.H. performed the determination of the IC₅₀ in human, murine, and rat sEH. F.F. and S.O. performed MD calculations. M.L.L. and J.M.B. carried out DMPK studies. E.S., J.O., and A.P.-L. performed cytotoxicity studies. B.P. carried out the PAMPA studies. C.P. and M.I.R.-F. performed the hLOX-5 studies. S.C., E.P., J.P., R.L., C.M., B.D.H., M.V.-C., and S.V. analyzed the data. R.L. and S.V. conceived the idea. S.C. and S.V. wrote the manuscript with feedback from all the authors. All authors have given approval to the final version of the manuscript.

Notes

The authors declare the following competing financial interest(s): S.C., E.V., R.L., M.V.-C. and S.V. are inventors of the Universitat de Barcelona patent application on sEH inhibitors WO2017/017048. C.M. and B.D.H. are inventors of the University of California patents on sEH inhibitors licensed to EicOsis. None of the other authors has any disclosures to declare.

ACKNOWLEDGMENTS

This work was funded by the Spanish Ministerio de Economía, Industria y Competitividad (grants SAF2017-82771-R to S.V., SAF2015-64146-R, and RTI2018-093999-B-I00 to M.V.-C., RTI2018-093955-B-C21 to M.I.R.-F., PGC2018-102192-B-I00 to S.O. and RTI2018-101032-J-I00 to F.F.), the CaixaImpulse 2015 Programme, the Spain EIT Health (Proof of concept 2016), the European Regional Development Fund (ERDF),

the Xunta de Galicia (GRC2014/011 and ED431C2018-21), the Fundació Bosch i Gimpera, Universitat de Barcelona (F21 grant), the Generalitat de Catalunya (2017 SGR 106, 2017 SGR 124 and 2017 SGR 1707), the Fundació Fuentes Dutor, the European Research Council (ERC-2015- StG-679001-NetMoDEzyme to S.O.), and the European Community (MSCA-IF-2014-EF-661160-MetAcemby to F.F.). S.C. and E.P. acknowledge PhD fellowships from the Universitat de Barcelona (APIF grants). E.V. and R.L. thank the Institute of Biomedicine of the University of Barcelona (IBUB) and the Spanish Ministerio de Educación, Cultura y Deporte (FPU grant), respectively, for PhD grants. Partial support was provided by NIH-NIEHS River Award R35 ES03443, NIH-NIEHS Superfund Program P42 ES004699, NINDS R01 DK107767, and NIDDK R01 DK103616. The content is solely the responsibility of the authors and does not necessarily represent the official views of the National Institutes of Health. We thank Daniel Closa (IIBB-CSIC, Barcelona, Spain) for advice regarding the histological analyses.

ABBREVIATIONS USED

AP, acute pancreatitis; ATF3, activating transcription factor 3; ATR, attenuated total reflectance; BEGM, bronchial epithelial growth medium; BEH, ethylene bridged hybrid; BFC, benzyloxytrifluoromethylcoumarin; CER, cerulein; CHOP, C/EBP homologous protein; DBF, dibenzylfluorescein; DiHETrE, dihydroxyeicosatrienoic acids; DIPEA, diisopropylethyl amine; E/S, enzyme/substrate; EDCI-HCl, 1-ethyl-3-(3-dimethylaminopropyl)carbodiimide hydrochloride; EETs, epoxyeicosatrienoic acids; ER, endoplasmic reticulum; ERCP, endoscopic retrograde cholangiopancreatography; EtOAc, ethyl acetate; FBS, fetal bovine serum; Fs, femtosecond; G418, geneticin; H&E, hematoxylin and eosin; HOBt, hydroxybenzotriazole; hSEH, human soluble epoxide hydrolase; IL, interleukin; KO, knockout; LC₅₀, concentration of the compound that is lethal for 50% of the exposed population; LOX, lipoxygenases; MCP-1, monocyte chemoattractant protein 1; mSEH, murine-soluble epoxide hydrolase; NCI, noncovalent interactions; ND, not done; NEAA, nonessential amino acid; P/S, penicillin/streptomycin solution; PBMC, peripheral blood mononuclear cell; Pe, permeability; PHA, phytohaemagglutinin; PHOME, (3-phenyl-oxiranyl)-acetic acid cyano-(6-methoxy-naphthalen-2-yl)-methyl ester; PMSF, phenylmethylsulfonyl fluoride; RHS, right-hand side; RPMI, Roswell Park Memorial Institute; sEH, soluble epoxide hydrolase; SMD, solvation model based on density; THLE-2, transformed human liver epithelial-2 cell line; TI, thermodynamic integration; TRB3, tribbles homolog 3

REFERENCES

- (1) The Role of Bioactive Lipids in Cancer, Inflammation and Related Diseases. In *Advances in Experimental Medicine and Biology*; Honn, K. V., Zeldin, D. C., Eds.; Springer: Cham, 2019; Vol. 1161.
- (2) Meirer, K.; Steinhilber, D.; Proschak, E. Inhibitors of the arachidonic acid cascade: interfering with multiple pathways. *Basic Clin. Pharmacol. Toxicol.* **2014**, *114*, 83–91.
- (3) Kaspera, R.; Totah, R. A. Epoxyeicosatrienoic Crmation, metabolism and potential role in tissue physiology and pathophysiology. *Expert Opin. Drug Metab. Toxicol.* **2009**, *5*, 757–771.
- (4) Fleming, I. Cytochrome P450-dependent eicosanoid production and crosstalk. *Curr. Opin. Lipidol.* **2011**, *22*, 403–409.
- (5) Capdevila, J. H.; Falck, J. R. The arachidonic acid monooxygenase: from biochemical curiosity to physiological/pathophysiological significance. *J. Lipid Res.* **2018**, *59*, 2047–2062.

- (6) Morisseau, C.; Hammock, B. D. Impact of soluble epoxide hydrolase and epoxyeicosanoids on human health. *Annu. Rev. Pharmacol. Toxicol.* **2013**, *53*, 37–58.
- (7) Harris, T. R.; Hammock, B. D. Soluble epoxide hydrolase: gene structure, expression and deletion. *Gene* **2013**, *526*, 61–74.
- (8) Pillarisetti, S.; Khanna, I. A multimodal disease modifying approach to treat neuropathic pain - inhibition of soluble epoxide hydrolase (sEH). *Drug Discov. Today* **2015**, *20*, 1382–1390.
- (9) Wagner, K. M.; McReynolds, C. B.; Schmidt, W. K.; Hammock, B. D. Soluble epoxide hydrolase as a therapeutic target for pain, inflammatory and neurodegenerative diseases. *Pharmacol. Ther.* **2017**, *180*, 62–76.
- (10) Borhan, B.; Jones, A. D.; Pinot, F.; Grant, D. F.; Kurth, M. J.; Hammock, B. D. Mechanism of soluble epoxide hydrolase. *J. Biol. Chem.* **1995**, *270*, 26923–26930.
- (11) Gómez, G. A.; Morisseau, C.; Hammock, B. D.; Christianson, D. W. Structure of human epoxide hydrolase reveals mechanistic inferences on bifunctional catalysis in epoxide and phosphate ester hydrolysis. *Biochemistry* **2004**, *43*, 4716–4723.
- (12) Shen, H. C.; Hammock, B. D. Discovery of inhibitors of soluble epoxide hydrolase: a target with multiple potential therapeutic indications. *J. Med. Chem.* **2012**, *55*, 1789–1808.
- (13) Anandan, S.-K.; Webb, H. K.; Chen, D.; Wang, Y.-X.; Aavula, B. R.; Cases, S.; Cheng, Y.; Do, Z. N.; Mehra, U.; Tran, V.; Vincelette, J.; Waszczuk, J.; White, K.; Wong, K. R.; Zhang, L.-N.; Jones, P. D.; Hammock, B. D.; Patel, D. V.; Whitcomb, R.; MacIntyre, D. E.; Sabry, J.; Gless, R. 1-(1-Acetyl-piperidin-4-yl)-3-adamantan-1-yl-urea (AR9281) as a potent, selective, and orally available soluble epoxide hydrolase inhibitor with efficacy in rodent models of hypertension and dysglycemia. *Bioorg. Med. Chem. Lett.* **2011**, *21*, 983–988.
- (14) Chen, D.; Whitcomb, R.; MacIntyre, E.; Tran, V.; Do, Z. N.; Patel, D. V.; Anandan, S. K.; Gless, R.; Webb, H. K.; Webb, H. K. Pharmacokinetics and pharmacodynamics of AR9281, an inhibitor of soluble epoxide hydrolase, in single- and multiple-dose studies in healthy human subjects. *J. Clin. Pharmacol.* **2012**, *52*, 319–328.
- (15) Jones, P. D.; Tsai, H.-J.; Do, Z. N.; Morisseau, C.; Hammock, B. D. Synthesis and SAR of conformationally restricted inhibitors of soluble epoxide hydrolase. *Bioorg. Med. Chem. Lett.* **2006**, *16*, 5212–5216.
- (16) Hwang, S. H.; Tsai, H.-J.; Liu, J.-Y.; Morisseau, C.; Hammock, B. D. Orally bioavailable potent soluble epoxide hydrolase inhibitors. *J. Med. Chem.* **2007**, *50*, 3825–3840.
- (17) Brown, J. R.; North, E. J.; Hurdle, J. G.; Morisseau, C.; Scarborough, J. S.; Sun, D.; Korduláková, J.; Scherman, M. S.; Jones, V.; Grzegorzewicz, A.; Crew, R. M.; Jackson, M.; McNeil, M. R.; Lee, R. E. The structure-activity relationship of urea derivatives as anti-tuberculosis agents. *Bioorg. Med. Chem.* **2011**, *19*, 5585–5595.
- (18) Bhattachar, S. N.; Deschenes, L. A.; Wesley, J. A. Solubility: it's not just for physical chemists. *Drug Discovery Today* **2006**, *11*, 1012–1018.
- (19) Di, L.; Fish, P. V.; Mano, T. Bridging solubility between drug discovery and development. *Drug Discovery Today* **2012**, *17*, 486–495.
- (20) Gagneux, A. R.; Meier, R. 1-Substituted 2-heteroadamantanes. *Tetrahedron Lett.* **1969**, *10*, 1365–1368.
- (21) Duque, M. D.; Camps, P.; Profire, L.; Montaner, S.; Vázquez, S.; Sureda, F. X.; Mallol, J.; López-Querol, M.; Naesens, L.; Clercq, E. D.; Radhika Prathalingam, S.; Kelly, J. M. Synthesis and pharmacological evaluation of (2-oxaadamantan-1-yl)amines. *Bioorg. Med. Chem.* **2009**, *17*, 3198–3206.
- (22) Onajole, O. K.; Coovadia, Y.; Kruger, H. G.; Maguire, G. E. M.; Pillay, M.; Govender, T. Novel polycyclic 'cage'-1,2-diamines as potential anti-tuberculosis agents. *Eur. J. Med. Chem.* **2012**, *54*, 1–9.
- (23) Leiva, R.; Gazzarrini, S.; Esplugas, R.; Moroni, A.; Naesens, L.; Sureda, F. X.; Vázquez, S. Ritter reaction-mediated syntheses of 2-oxaadamantan-5-amine, a novel amantadine analog. *Tetrahedron Lett.* **2015**, *56*, 1272–1275.
- (24) Duque, M. D.; Ma, C.; Torres, E.; Wang, J.; Naesens, L.; Juárez-Jiménez, J.; Camps, P.; Luque, F. J.; DeGrado, W. F.; Lamb, R. A.; Pinto, L. H.; Vázquez, S. Exploring the size limit of templates for inhibitors of the M2 ion channel of influenza A virus. *J. Med. Chem.* **2011**, *54*, 2646–2657.
- (25) Jones, P. D.; Wolf, N. M.; Morisseau, C.; Whetstone, P.; Hock, B.; Hammock, B. D. Fluorescent substrates for soluble epoxide hydrolase and application to inhibition studies. *Anal. Biochem.* **2005**, *343*, 66–75.
- (26) Hammock, B. D.; Hwang, S. H.; Weckler, A. T.; Morisseau, C. Sorafenib derivatives as soluble epoxide hydrolase inhibitors. WO 2012112570 A1, Aug 23, 2012.
- (27) Gless, R. D. Processes for the preparation of piperidinyl-substituted urea compounds. U.S. Patent 0,207,908 A1, Aug 28, 2008.
- (28) Rose, T. E.; Morisseau, C.; Liu, J.-Y.; Inceoglu, B.; Jones, P. D.; Sanborn, J. R.; Hammock, B. D. 1-Aryl-3-(1-acylpiperidin-4-yl)urea inhibitors of human and murine soluble epoxide hydrolase: structure-activity relationships, pharmacokinetics, and reduction of inflammatory pain. *J. Med. Chem.* **2010**, *53*, 7067–7075.
- (29) Lee, K. S. S.; Liu, J.-Y.; Wagner, K. M.; Pakhomova, S.; Dong, H.; Morisseau, C.; Fu, S. H.; Yang, J.; Wang, P.; Ulu, A.; Mate, C. A.; Nguyen, L. V.; Hwang, S. H.; Edin, M. L.; Mara, A. A.; Wulff, H.; Newcomer, M. E.; Zeldin, D. C.; Hammock, B. D. Optimized inhibitors of soluble epoxide hydrolase improve in vitro target residence time and in vivo efficacy. *J. Med. Chem.* **2014**, *57*, 7016–7030.
- (30) North, E. J.; Scherman, M. S.; Bruhn, D. F.; Scarborough, J. S.; Maddox, M. M.; Jones, V.; Grzegorzewicz, A.; Yang, L.; Hess, T.; Morisseau, C.; Jackson, M.; McNeil, M. R.; Lee, R. E. Design, synthesis and anti-tuberculosis activity of 1-adamantyl-3-heteroaryl ureas with improved in vitro pharmacokinetic properties. *Bioorg. Med. Chem.* **2013**, *21*, 2587–2599.
- (31) Thalji, R. K.; McAtee, J. J.; Belyanskaya, S.; Brandt, M.; Brown, G. D.; Costell, M. H.; Ding, Y.; Dodson, J. W.; Eisennagel, S. H.; Fries, R. E.; Gross, J. W.; Harpel, M. R.; Holt, D. A.; Israel, D. I.; Jolivet, L. J.; Krosky, D.; Li, H.; Lu, Q.; Mandichak, T.; Roethke, T.; Schnackenberg, C. G.; Schwartz, B.; Shewchuk, L. M.; Xie, W.; Behm, D. J.; Douglas, S. A.; Shaw, A. L.; Marino, J. P., Jr. Discovery of 1-(1,3,5-triazin-2-yl)piperidine-4-carboxamides as inhibitors of soluble epoxide hydrolase. *Bioorg. Med. Chem. Lett.* **2013**, *23*, 3584–3588.
- (32) Lazaar, A. L.; Yang, L.; Boardley, R. L.; Goyal, N. S.; Robertson, J.; Baldwin, S. J.; Newby, D. E.; Wilkinson, I. B.; Tal-Singer, R.; Mayer, R. J.; Cheriyan, J. Pharmacokinetics, pharmacodynamics and adverse event profile of GSK2256294, a novel soluble epoxide hydrolase inhibitor. *Br. J. Clin. Pharmacol.* **2016**, *81*, 971–979.
- (33) Bettaieb, A.; Chahed, S.; Tabet, G.; Yang, J.; Morisseau, C.; Griffey, S.; Hammock, B. D.; Haj, F. G. Effects of soluble epoxide hydrolase deficiency on acute pancreatitis in mice. *PLoS One* **2014**, *9*, No. e113019.
- (34) Bettaieb, A.; Chahed, S.; Bachaalany, S.; Griffey, S.; Hammock, B. D.; Haj, F. G. Soluble epoxide hydrolase pharmacological inhibition ameliorates experimental acute pancreatitis in mice. *Mol. Pharmacol.* **2015**, *88*, 281–290.
- (35) Griñán-Ferré, C.; Codony, S.; Pujol, E.; Yang, J.; Leiva, R.; Escolano, C.; Puigoriol-Illamola, D.; Companys-Alemany, J.; Corpas, R.; Sanfeliu, C.; Pérez, B.; Loza, M. I.; Brea, J.; Morisseau, C.; Hammock, B. D.; Vázquez, S.; Pallàs, M.; Galdeano, C. Pharmacological inhibition of soluble epoxide hydrolase as a new therapy for Alzheimer's disease. *Neurotherapeutics*; Springer, 2020.
- (36) Xie, L.; Ochterski, J. W.; Gao, Y.; Han, B.; Caldwell, T. M.; Xu, Y.; Peterson, J. M.; Ge, P.; Ohliger, R. Dipiperazinyl ketones and related analogs. WO 20070106496 A2, Feb 8, 2007.
- (37) Serrano-Hervás, E.; Casadevall, G.; Garcia-Borrás, M.; Feixas, F.; Osuna, S. Epoxide hydrolase conformational heterogeneity for the resolution of bulky pharmacologically relevant epoxide substrates. *Chem.—Eur. J.* **2018**, *24*, 12254–12258.
- (38) Öster, L.; Tapani, S.; Xue, Y.; Käck, H. Successful generation of structural information for fragment-based drug discovery. *Drug Discovery Today* **2015**, *20*, 1104–1111.

- (39) Durrant, J. D.; Votapka, L.; Sørensen, J.; Amaro, R. E. POVME 2.0: An enhanced tool for determining pocket shape and volume characteristics. *J. Chem. Theory Comput.* **2014**, *10*, S047–S056.
- (40) Codony, S.; Valverde, E.; Leiva, R.; Brea, J.; Isabel Loza, M.; Morisseau, C.; Hammock, B. D.; Vázquez, S. Exploring the size of the lipophilic unit of the soluble epoxide hydrolase inhibitors. *Bioorg. Med. Chem.* **2019**, *27*, 115078.
- (41) Contreras-García, J.; Johnson, E. R.; Keinan, S.; Chaudret, R.; Piquemal, J.-P.; Beratan, D. N.; Yang, W. NCIPLOT: A Program for Plotting Noncovalent Interaction Regions. *J. Chem. Theory Comput.* **2011**, *7*, 625–632.
- (42) Guan, D.; Lui, R.; Matthews, S. LogP prediction performance with the SMD solvation model and the M06 density functional family for SAMPL6 blind prediction challenge molecules. *J. Comput.-Aided Mol. Des.* **2020**, *34*, 511–522.
- (43) Di, L.; Kerns, E. H.; Fan, K.; McConnell, O. J.; Carter, G. T. High throughput artificial membrane permeability assay for blood-brain barrier. *Eur. J. Med. Chem.* **2003**, *38*, 223–232.
- (44) Yadav, D.; Lowenfels, A. B. The epidemiology of pancreatitis and pancreatic cancer. *Gastroenterology* **2013**, *144*, 1252–1261.
- (45) Forsmark, C. E.; Swaroop Vege, S.; Wilcox, C. M. Acute pancreatitis. *N. Engl. J. Med.* **2016**, *375*, 1972–1981.
- (46) Krishna, S. G.; Kamboj, A. K.; Hart, P. A.; Hinton, A.; Conwell, D. L. The Changing Epidemiology of Acute Pancreatitis Hospitalizations. *Pancreas* **2017**, *46*, 482–488.
- (47) Weber, H.; Hühns, S.; Jonas, L.; Sparmann, G.; Bastian, M.; Schuff-Werner, P. Hydrogen peroxide-induced activation of defense mechanisms against oxidative stress in rat pancreatic acinar AR42J cells. *Free Radical Biol. Med.* **2007**, *42*, 830–841.
- (48) González, A.; Santofimia-Castaño, P.; Salido, G. M. Culture of pancreatic AR42J cell for use as a model for acinar cell function. *Pancreapedia: Exocrine pancreas Knowledge Base*. 2011, <https://www.pancreapedia.org/tools/methods/culture-of-pancreatic-ar42j-cell-for-use-as-model-for-acinar-cell-function> (accessed December 23, 2019).
- (49) Mareninova, O. A.; Orabi, A. I.; Husain, S. Z. Experimental acute pancreatitis: in vitro models. *Pancreapedia: Exocrine pancreas Knowledge Base*. 2015, <https://www.pancreapedia.org/reviews/experimental-acute-pancreatitis-in-vitro-models> (accessed December 23, 2019).
- (50) Afghani, E.; Pandol, S. J.; Shimosegawa, T.; Sutton, R.; Wu, B. U.; Vege, S. S.; Gorelick, F.; Hirota, M.; Windsor, J.; Lo, S. K.; Freeman, M. L.; Lerch, M. M.; Tsuji, Y.; Melmed, G. Y.; Wassef, W.; Mayerle, J. Acute Pancreatitis-Progress and Challenges. *Pancreas* **2015**, *44*, 1195–1210.
- (51) Liu, J.; Obando, D.; Liao, V.; Lifa, T.; Codd, R. The many faces of the adamantyl group in drug design. *Eur. J. Med. Chem.* **2011**, *46*, 1949–1963.
- (52) Wanka, L.; Iqbal, K.; Schreiner, P. R. The lipophilic bullet hits the targets: medicinal chemistry of adamantane derivatives. *Chem. Rev.* **2013**, *113*, 3516–3604.
- (53) Morisseau, C.; Hammock, B. D. Measurement of soluble epoxide hydrolase (sEH) activity. *Curr. Protoc. Toxicol.* **2007**, *33*, 4.23.1.
- (54) Case, D. A.; Ben-Shalom, I. Y.; Brozell, S. R.; Cerutti, D. S.; Cheatham, T. E. I.; Cruzeiro, V. W. D.; Darden, T. A.; Duke, R. E.; Ghoreishi, D.; Gilson, M. K.; Gohlke, H.; Goetz, A. W.; Greene, D.; Harris, R.; Homeyer, N.; Izadi, S.; Kovalenko, A.; Kurtzman, T.; Lee, T. S.; LeGrand, S.; Li, P.; Lin, C.; Liu, J.; Luchko, T.; Luo, R.; Mermelstein, D. J.; Merz, K. M.; Miao, Y.; Monard, G.; Nguyen, C.; Nguyen, H.; Omelyan, I.; Onufriev, A.; Pan, F.; Qi, R.; Roe, D. R.; Roitberg, A.; Sagui, C.; Schott-Verdugo, S.; Shen, J.; Simmerling, C. L.; Smith, J.; Salomon-Ferrer, R.; Swails, J.; Walker, R. C.; Wang, J.; Wei, H.; Wolf, R. M.; Wu, X.; Xiao, L.; York, D. M.; Kollman, P. A. *AMBER 2018*; University of California: San Francisco, CA, 2018.
- (55) Wang, J.; Wolf, R. M.; Caldwell, J. W.; Kollman, P. A.; Case, D. A. Development and testing of a general amber force field. *J. Comput. Chem.* **2004**, *25*, 1157–1174.
- (56) Bayly, C. I.; Cieplak, P.; Cornell, W.; Kollman, P. A. A well-behaved electrostatic potential based method using charge restraints for deriving atomic charges: the RESP model. *J. Phys. Chem.* **1993**, *97*, 10269–10280.
- (57) Besler, B. H.; Merz, K. M., Jr.; Kollman, P. A. Atomic charges derived from semiempirical methods. *J. Comput. Chem.* **1990**, *11*, 431–439.
- (58) Singh, U. C.; Kollman, P. A. An approach to computing electrostatic charges for molecules. *J. Comput. Chem.* **1984**, *5*, 129–145.
- (59) Frisch, M. J.; Trucks, G. W.; Schlegel, H. B.; Scuseria, G. E.; Robb, M. A.; Cheeseman, J. R.; Scalmani, G.; Barone, V.; Mennucci, B.; Petersson, G. A.; Nakatsuji, H.; Caricato, M.; Li, X.; Hratchian, H. P.; Izmaylov, A. F.; Bloino, J.; Zheng, G.; Sonnenberg, J. L.; Hada, M.; Ehara, M.; Toyota, K.; Fukuda, R.; Hasegawa, J.; Ishida, M.; Nakajima, T.; Honda, Y.; Kitao, O.; Nakai, H.; Vreven, T.; Montgomery, J. A., Jr.; Peralta, J. E.; Ogliaro, F.; Bearpark, M.; Heyd, J. J.; Brothers, E.; Kudin, K. N.; Staroverov, V. N.; Kobayashi, R.; Normand, J.; Raghavachari, K.; Rendell, A.; Burant, J. C.; Iyengar, S. S.; Tomasi, J.; Cossi, M.; Rega, N.; Millam, J. M.; Klene, M.; Knox, J. E.; Cross, J. B.; Bakken, V.; Adamo, C.; Jaramillo, J.; Gomperts, R.; Stratmann, R. E.; Yazyev, O.; Austin, A. J.; Cammi, R.; Pomelli, C.; Ochterski, J. W.; Martin, R. L.; Morokuma, K.; Zakrzewski, V. G.; Voth, G. A.; Salvador, P.; Dannenberg, J. J.; Dapprich, S.; Daniels, A. D.; Farkas, Ö.; Foresman, J. B.; Ortiz, J. V.; Cioslowski, J.; Fox, D. J. *Gaussian 09*, Revision A.02; Gaussian, Inc.: Pittsburgh, PA, 2009.
- (60) Sagui, C.; Darden, T. A. Molecular dynamics simulations of biomolecules: long-range electrostatic effects. *Annu. Rev. Biophys. Biomol. Struct.* **1999**, *28*, 155–179.
- (61) Ryckaert, J.-P.; Ciccotti, G.; Berendsen, H. J. C. Numerical integration of the cartesian equations of motion of a system with constraints: molecular dynamics of *n*-alkanes. *J. Comput. Phys.* **1977**, *23*, 327–341.
- (62) Wu, X.; Brooks, B. R. Self-guided Langevin dynamics simulation method. *Chem. Phys. Lett.* **2003**, *381*, 512–518.
- (63) Song, L. F.; Lee, T.-S.; Zhu, C.; York, D. M.; Merz, K. M., Jr. Using AMBER18 for relative free energy calculations. *J. Chem. Inf. Model.* **2019**, *59*, 3128–3135.
- (64) Zhao, Y.; Truhlar, D. G. The M06 suite of density functionals for main group thermochemistry, thermochemical kinetics, non-covalent interactions, excited states, and transition elements: two new functionals and systematic testing of four M06-class functionals and 12 other functionals. *Theor. Chem. Acc.* **2008**, *120*, 215–241.
- (65) Marenich, A. V.; Cramer, C. J.; Truhlar, D. G. Universal solvation model based on solute electron density and on a continuum model of the solvent defined by the bulk dielectric constant and atomic surface tensions. *J. Phys. Chem. B* **2009**, *113*, 6378–6396.
- (66) Weigend, F.; Ahlrichs, R. Balanced basis sets of split valence, triple zeta valence and quadruple zeta valence quality for H to Rn: design and assessment of accuracy. *Phys. Chem. Chem. Phys.* **2005**, *7*, 3297–3305.
- (67) Pufahl, R. A.; Kasten, T. P.; Hills, R.; Gierse, J. K.; Reitz, B. A.; Weinberg, R. A.; Masferrer, J. L. Development of a fluorescence-based enzyme assay of human 5-lipoxygenase. *Anal. Biochem.* **2007**, *364*, 204–212.

SUPPORTING INFORMATION FOR

2-Oxaadamant-1-yl ureas as soluble epoxide hydrolase

inhibitors: *in vivo* evaluation in a murine model

of acute pancreatitis

*Sandra Codony¹, Eugènia Pujol¹, Javier Pizarro^{2,3,4}, Ferran Feixas⁵, Elena Valverde^{1,2},
M. Isabel Loza⁶, José M. Brea⁶, Elena Saez⁷, Julen Oyarzabal⁷, Antonio Pineda-
Lucena⁷, Belén Pérez⁸, Concepción Pérez⁹, María Isabel Rodríguez-Franco⁹, Rosana
Leiva¹, Silvia Osuna^{5,10}, Christophe Morisseau¹¹, Bruce D. Hammock¹¹, Manuel
Vázquez-Carrera^{2,3,4}, Santiago Vázquez^{1*}*

¹Laboratori de Química Farmacèutica (Unitat Associada al CSIC), and ²Pharmacology, Departament de Farmacologia, Toxicologia i Química Terapèutica, Facultat de Farmàcia i Ciències de l'Alimentació, and Institute of Biomedicine (IBUB), Universitat de Barcelona, Av. Joan XXIII, 27-31, 08028 Barcelona, Spain.

³Spanish Biomedical Research Center in Diabetes and Associated Metabolic Diseases (CIBERDEM)-Instituto de Salud Carlos III, 28029 Madrid, Spain.

⁴Pediatric Research Institute-Hospital Sant Joan de Déu, 08950 Esplugues de Llobregat, Spain.

⁵CompBioLab Group, Departament de Química and Institut de Química Computacional i Catàlisi (IQCC), Universitat de Girona, C/ Maria Aurèlia Capmany 69, 17003 Girona, Spain.

⁶Drug Screening Platform/Biofarma Research Group, CIMUS Research Center. University of Santiago de Compostela (USC), 15782 Santiago de Compostela, Spain.

⁷Small Molecule Discovery Platform, Molecular Therapeutics Program, Center for Applied Medical Research (CIMA), University of Navarra, 31008 Pamplona, Spain.

⁸Department of Pharmacology, Therapeutics and Toxicology, Institute of Neurosciences, Autonomous University of Barcelona, 08193 Bellaterra, Barcelona, Spain.

⁹Institute of Medicinal Chemistry, Spanish National Research Council (CSIC), c/Juan de la Cierva 3, 28006 Madrid, Spain.

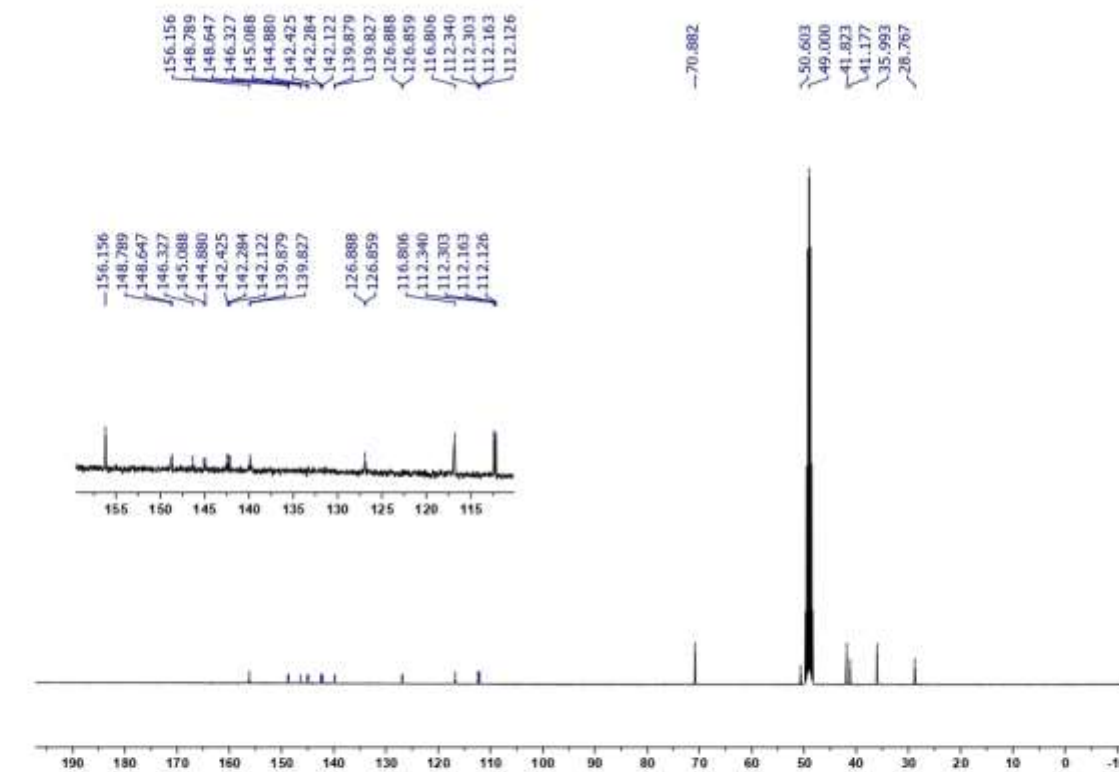
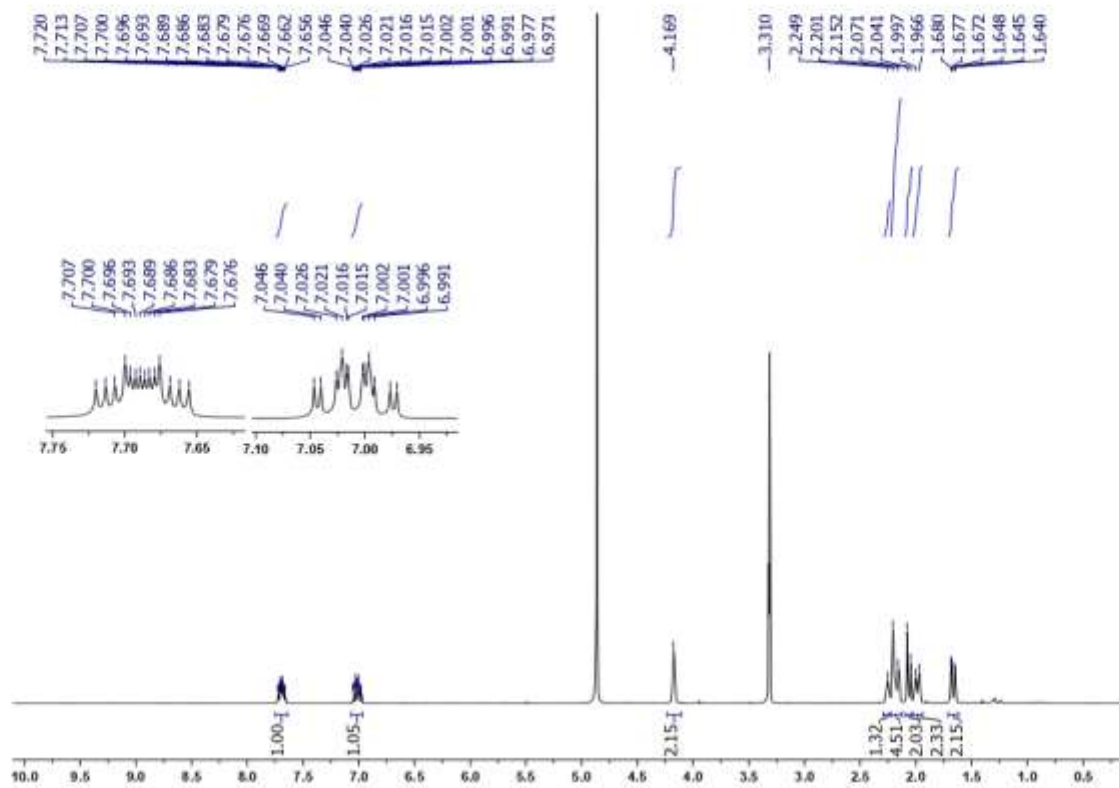
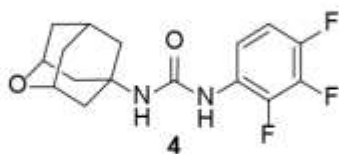
¹⁰Institució Catalana de Recerca i Estudis Avançats (ICREA), 08010 Barcelona, Spain.

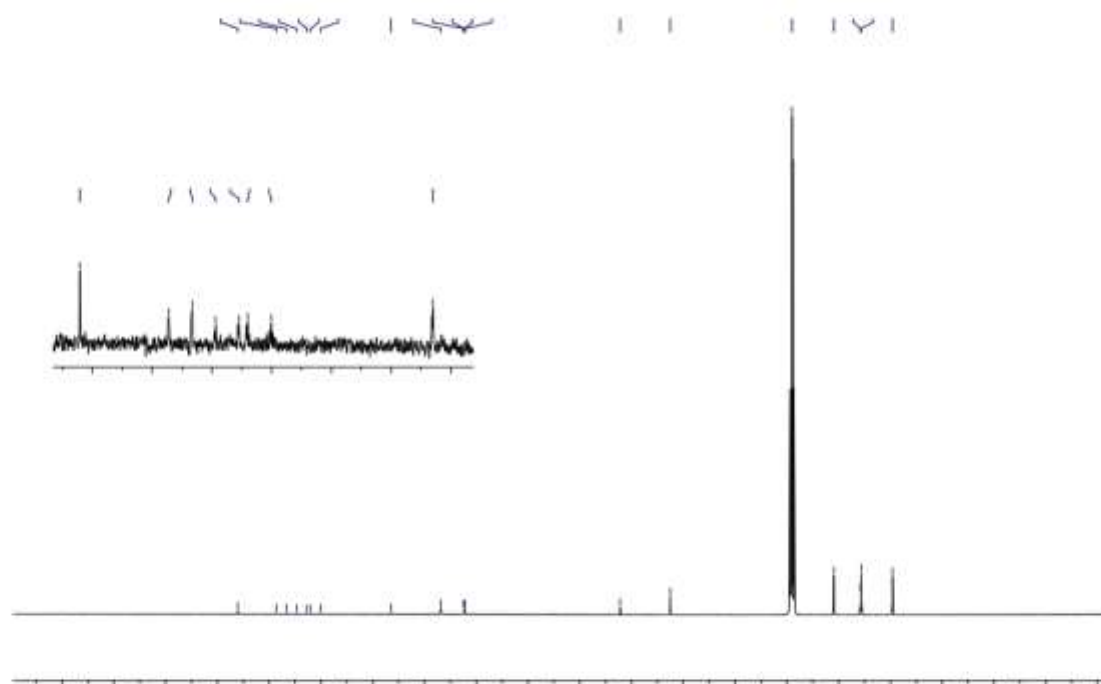
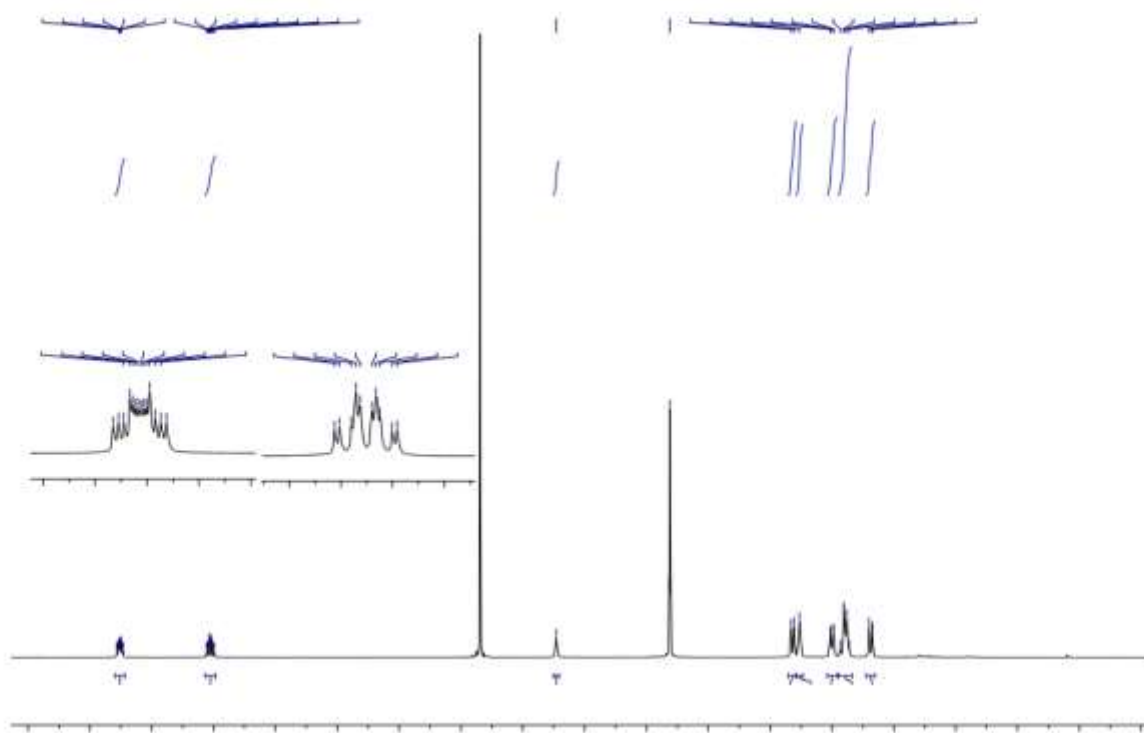
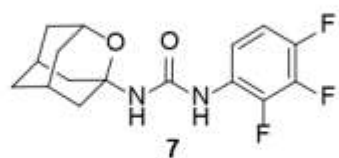
¹¹Department of Entomology and Nematology and Comprehensive Cancer Center, University of California, Davis, CA 95616, USA.

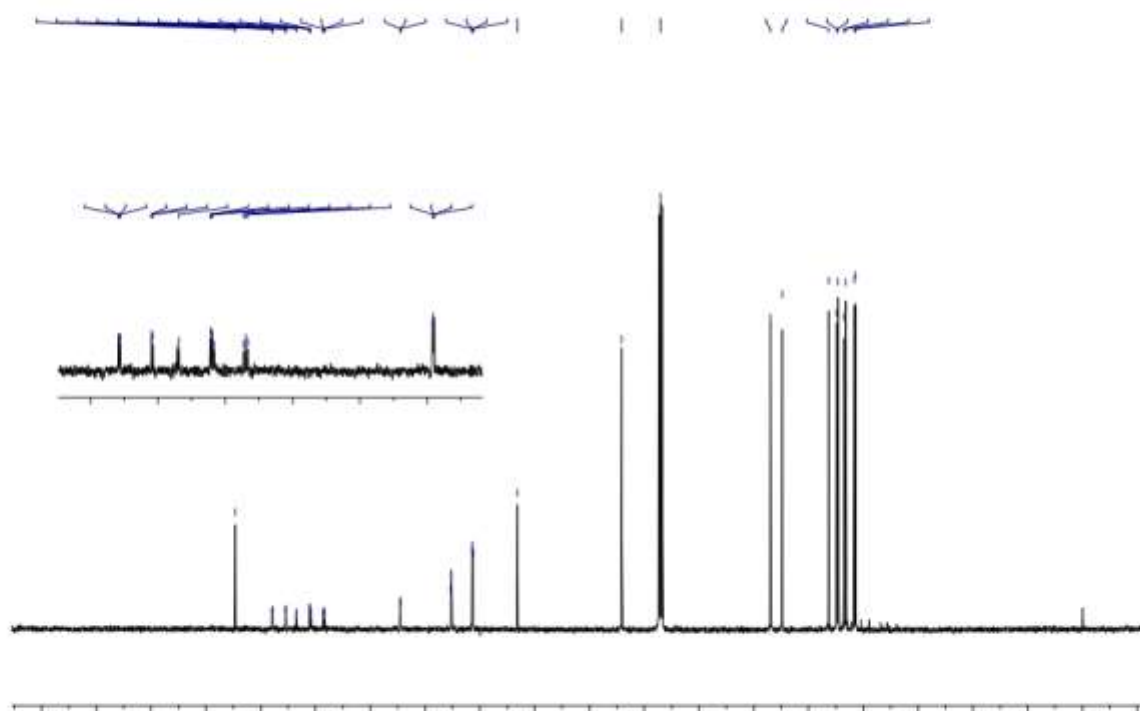
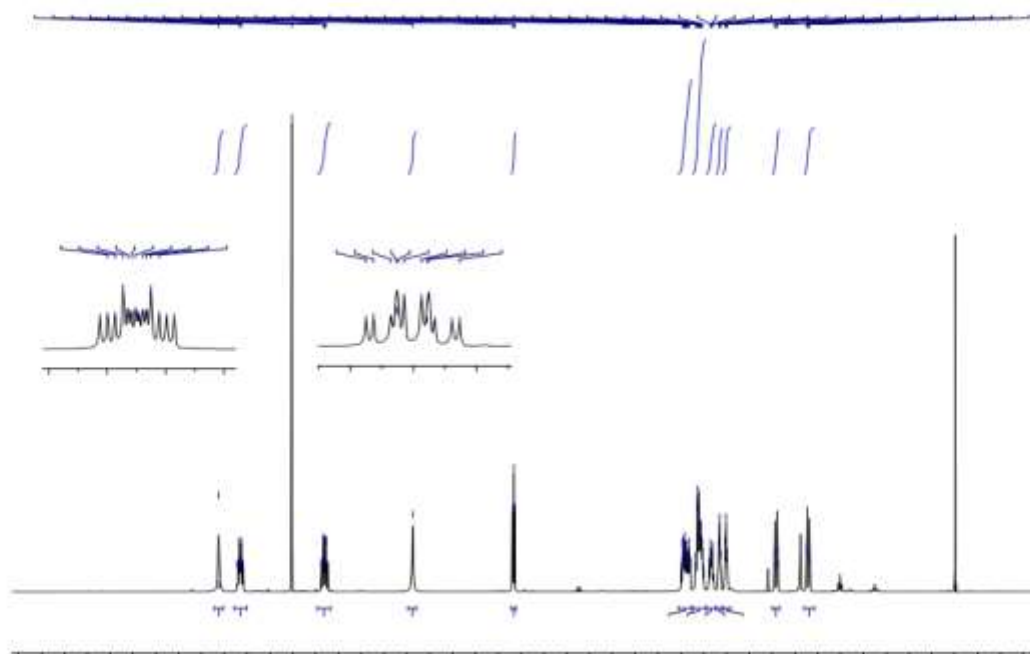
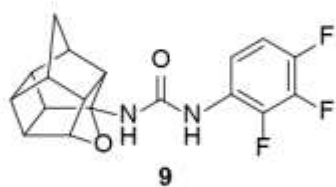
Table of contents

¹ H and ¹³ C NMR spectra of compound 4	Page S5
¹ H and ¹³ C NMR spectra of compound 7	Page S6
¹ H and ¹³ C NMR spectra of compound 9	Page S7
¹ H and ¹³ C NMR spectra of compound 12	Page S8
¹ H and ¹³ C NMR spectra of compound 14	Page S9
¹ H and ¹³ C NMR spectra of compound 15	Page S10
¹ H and ¹³ C NMR spectra of compound 17	Page S11
¹ H and ¹³ C NMR spectra of compound 18	Page S12
¹ H and ¹³ C NMR spectra of compound 19	Page S13
¹ H and ¹³ C NMR spectra of compound 20	Page S14
¹ H and ¹³ C NMR spectra of compound 21	Page S15
¹ H and ¹³ C NMR spectra of compound 22	Page S16
¹ H and ¹³ C NMR spectra of compound 23	Page S17
¹ H and ¹³ C NMR spectra of compound 24	Page S18
¹ H and ¹³ C NMR spectra of compound 25	Page S19
¹ H and ¹³ C NMR spectra of compound 26	Page S20
¹ H and ¹³ C NMR spectra of compound 27	Page S21
¹ H and ¹³ C NMR spectra of compound 28	Page S22
¹ H and ¹³ C NMR spectra of compound 29	Page S23
¹ H and ¹³ C NMR spectra of compound 30	Page S24
¹ H and ¹³ C NMR spectra of compound 31	Page S25
¹ H and ¹³ C NMR spectra of compound 32	Page S26
HPLC/Ms data of compound 15	Page S27
HPLC/Ms data of compound 27	Page S28
HPLC/Ms data of compound 29	Page S29
HPLC/Ms data of compound 32	Page S30
Table S1: Elemental analysis data.	Page S31
Table S2: Cytochromes and hERG inhibition.	Page S32
Table S3: <i>h</i> COX-2 and <i>h</i> LOX-5 inhibition.	Page S32

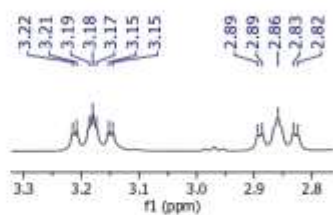
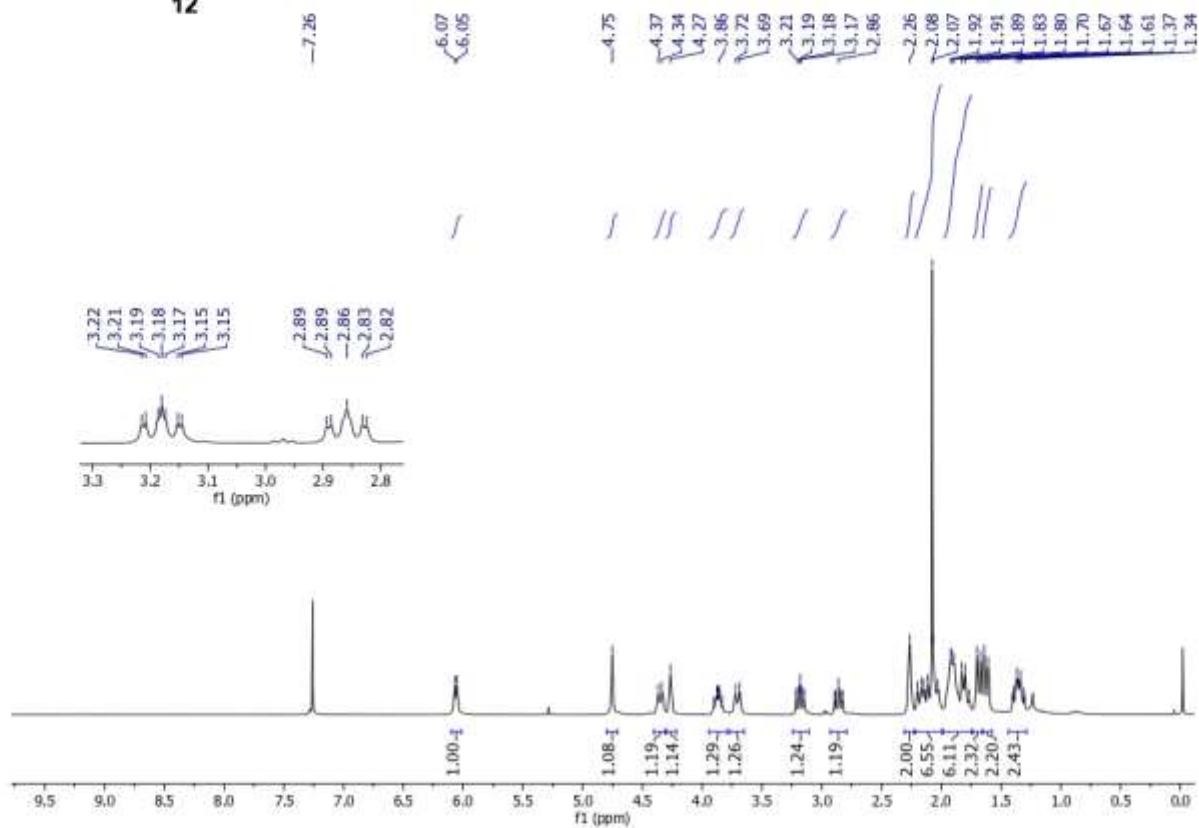
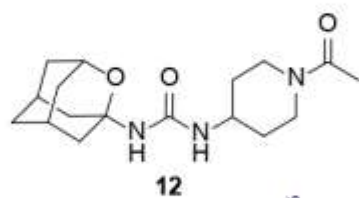
Table S4: Concentrations of 22 in mouse plasma iv administration.	Page S33
Table S5: Concentrations of 22 in mouse plasma ip administration.	Page S34
Figure S1: Representation of the noncovalent interactions at the active site of sEH in the presence of compound 22 .	Page S35
Figure S2: Concentration vs time for ip and iv administration of 22 .	Page S36
Figure S3: Experimental procedures of the <i>in vivo</i> efficacy studies.	Page S36







S7



168.85

156.69

80.64

77.00

70.98

46.54

45.12

40.37

40.20

40.02

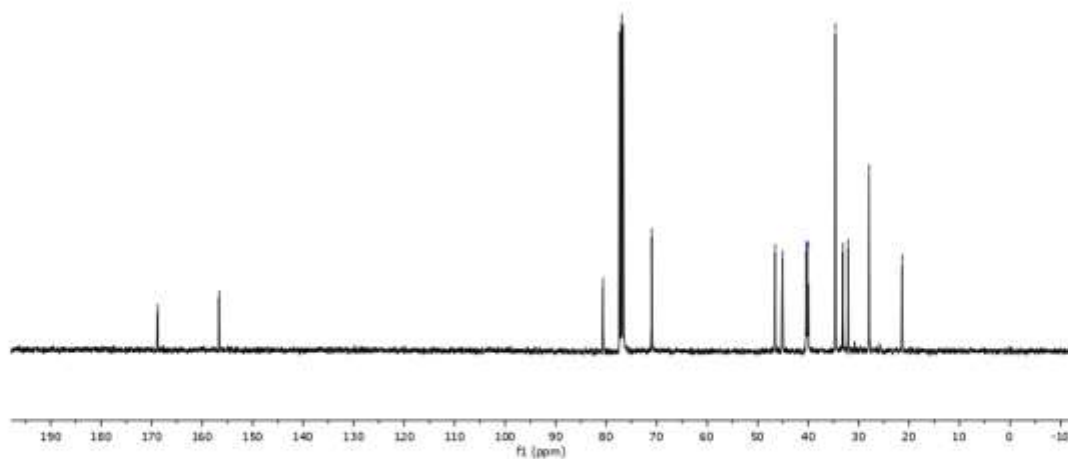
34.62

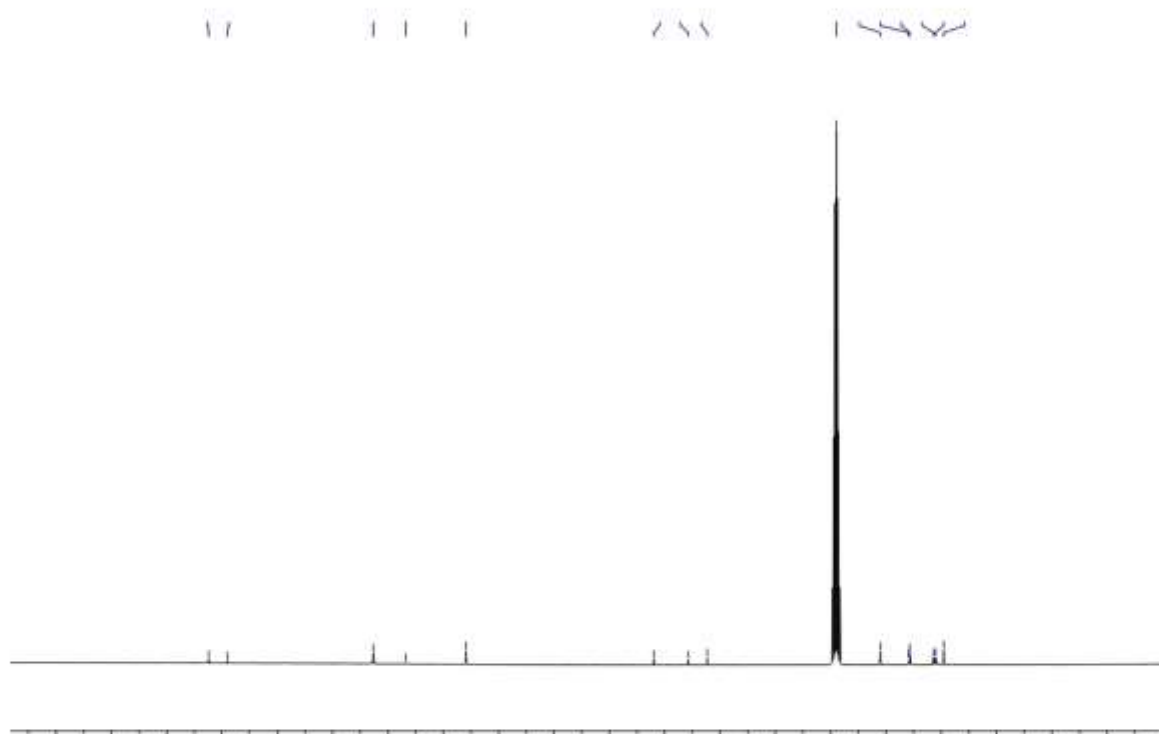
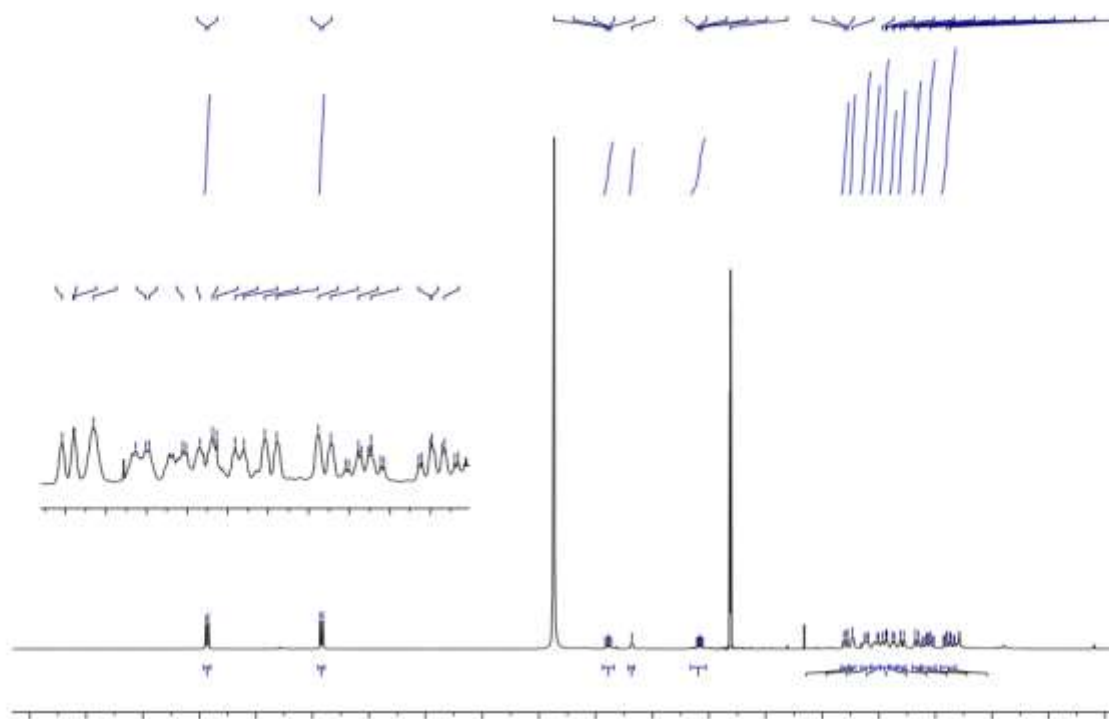
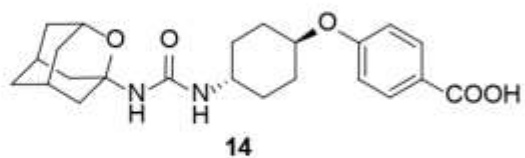
33.17

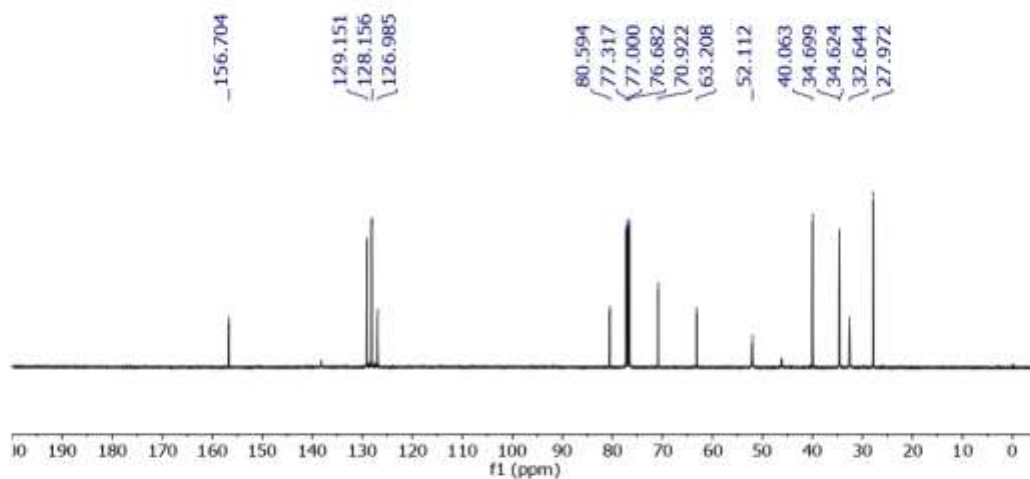
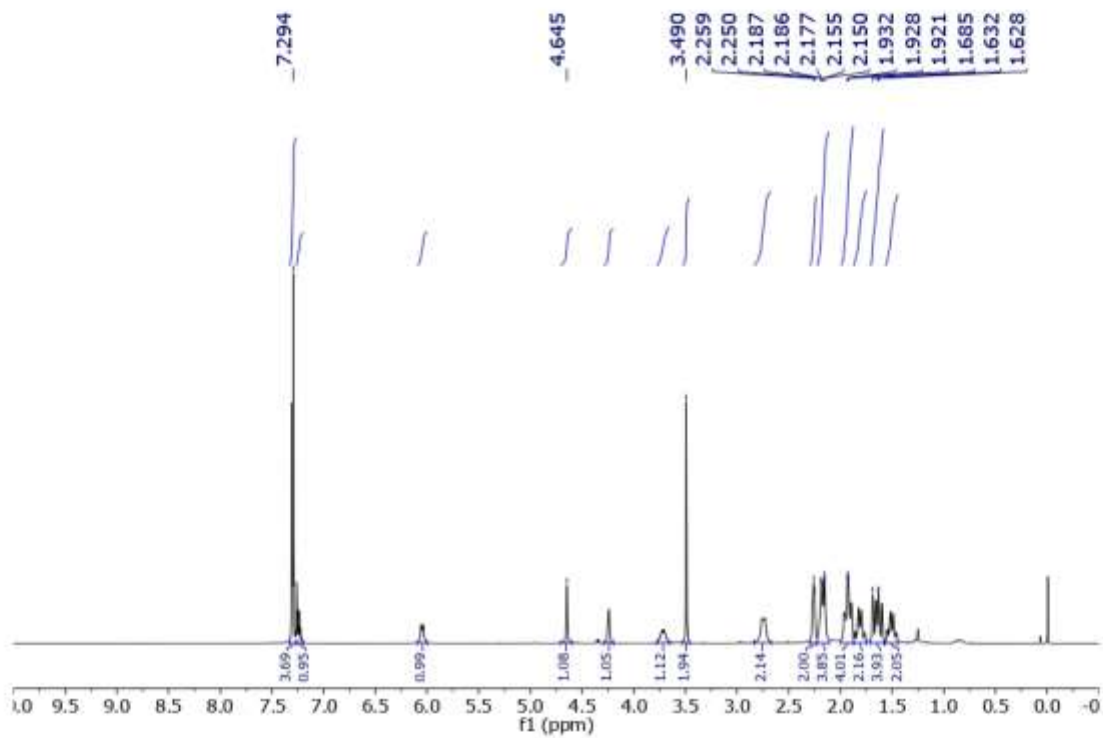
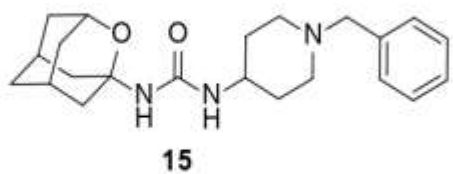
32.11

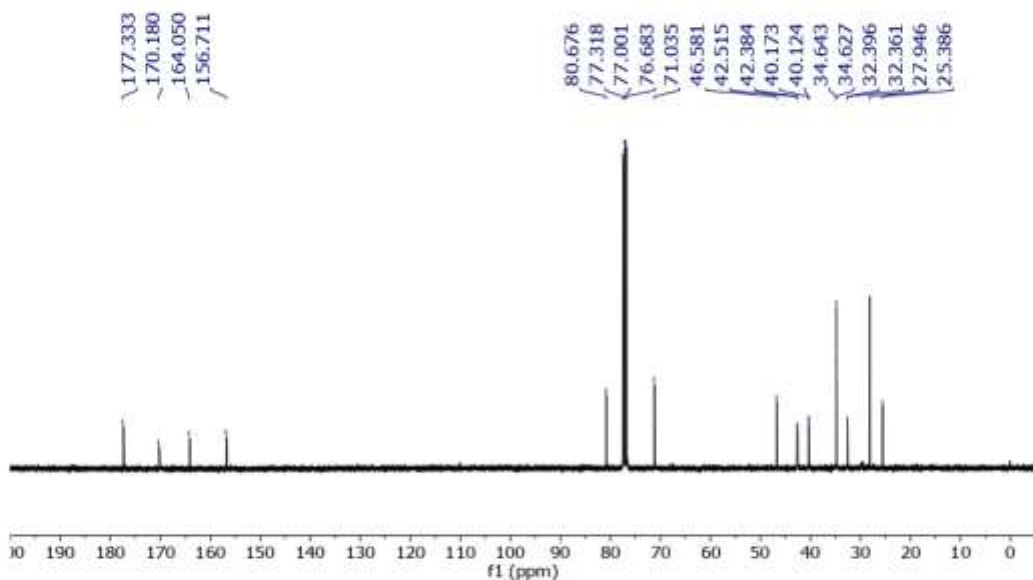
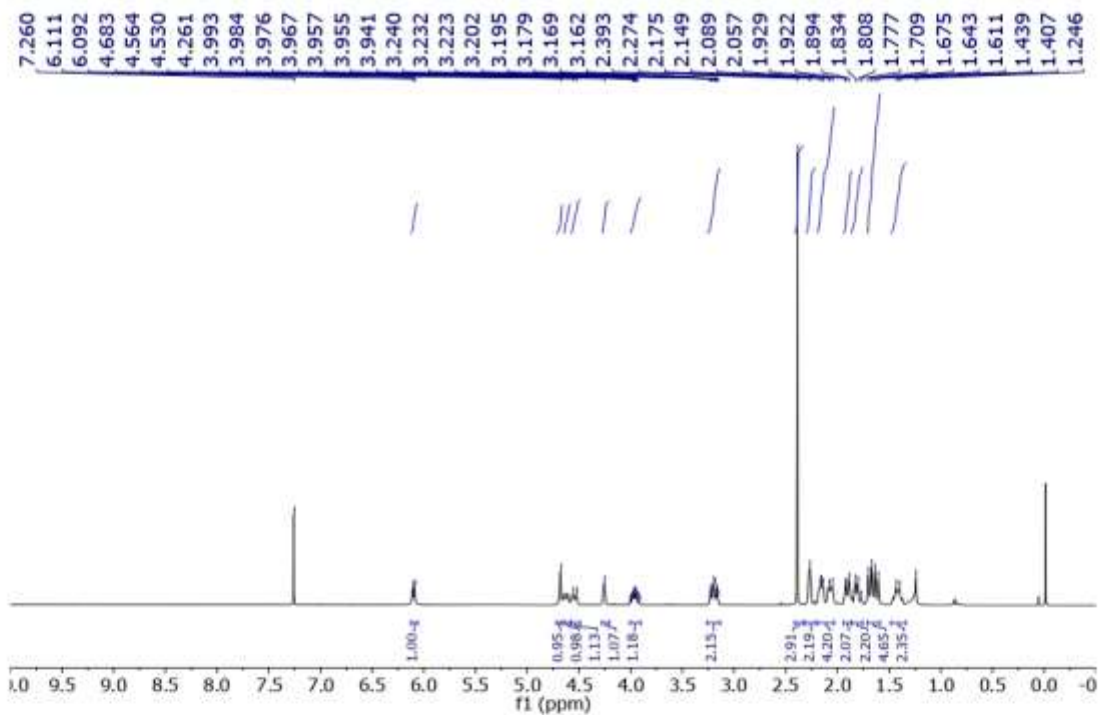
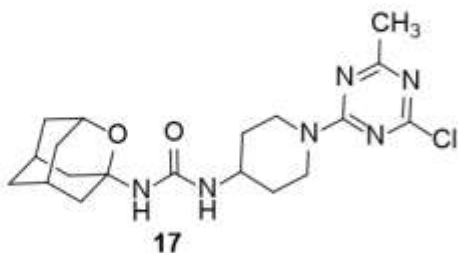
27.93

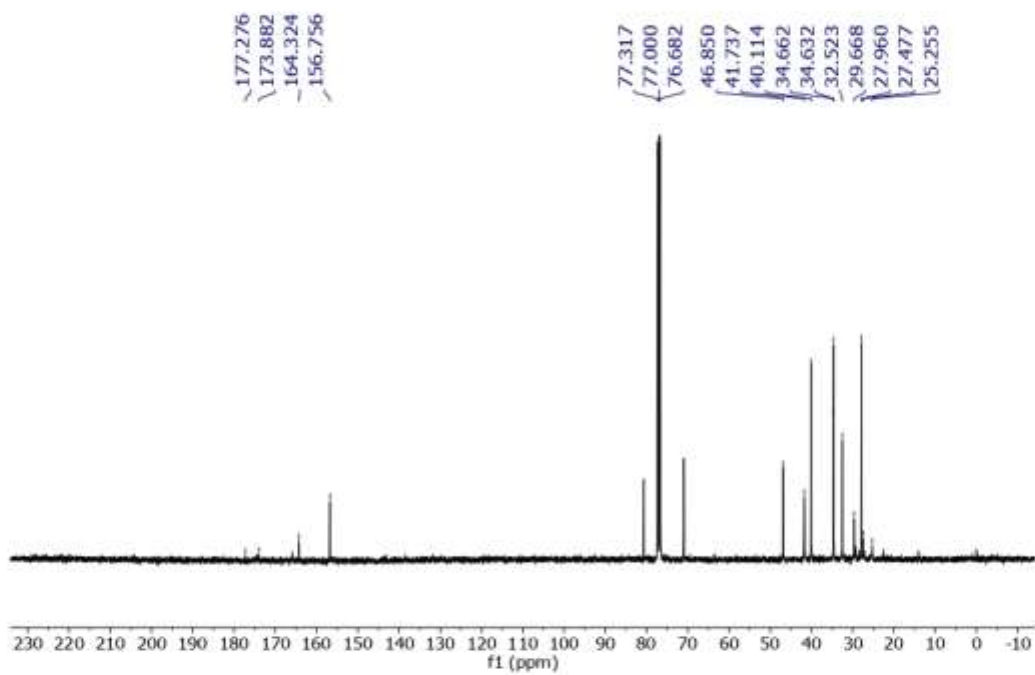
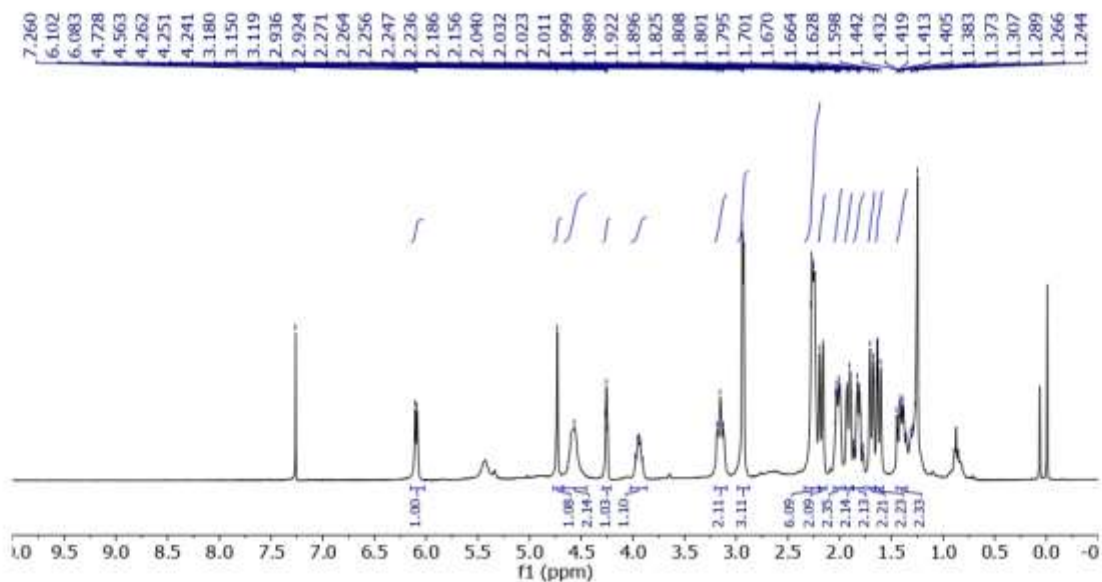
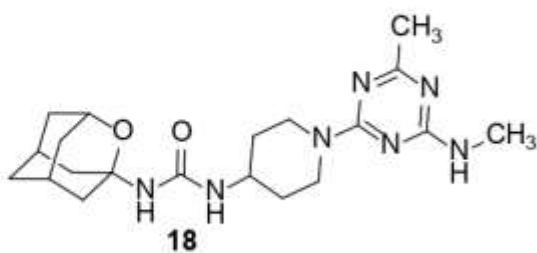
21.40

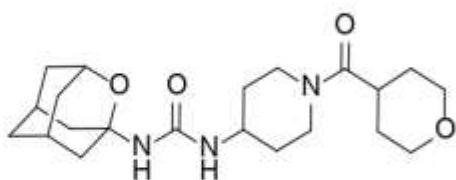




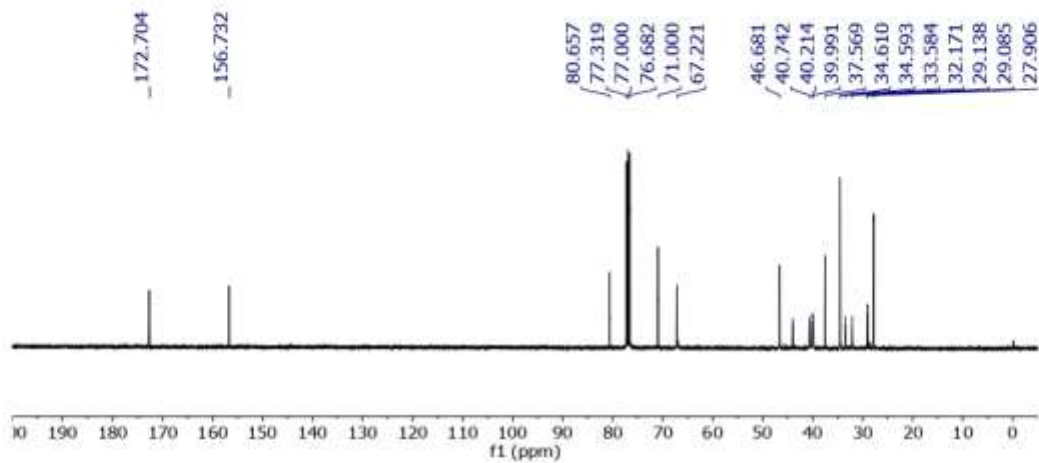
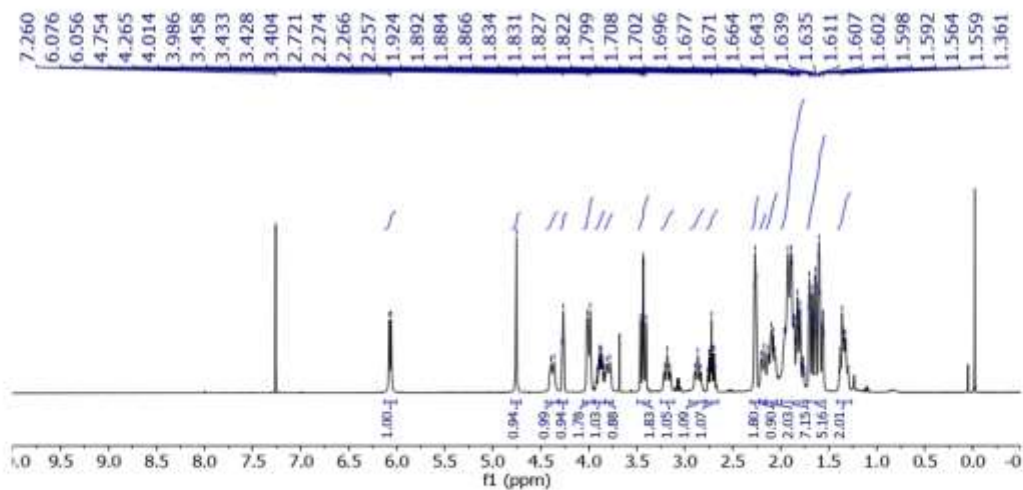


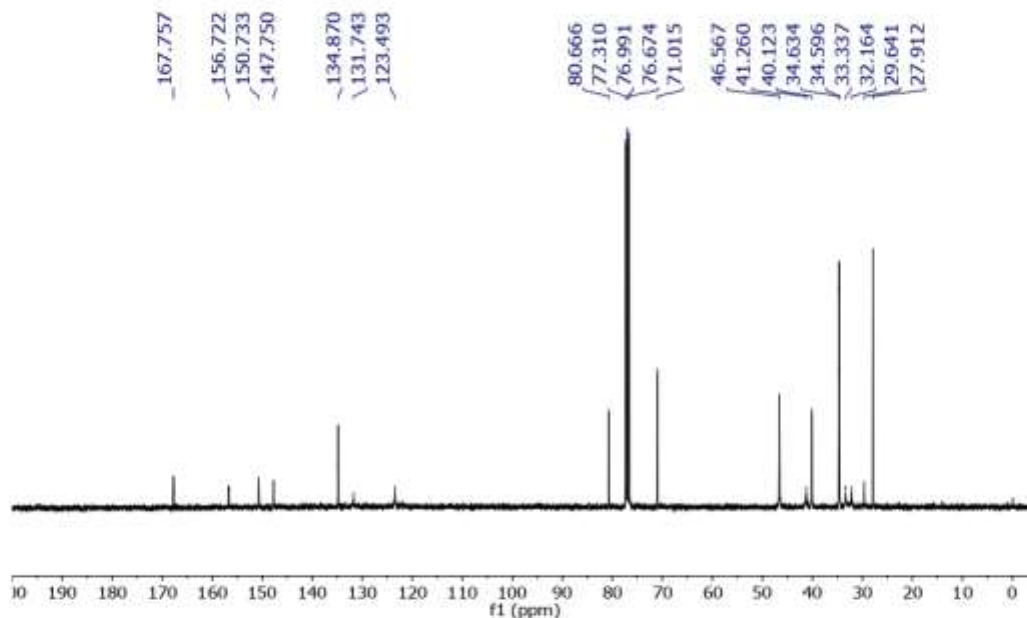
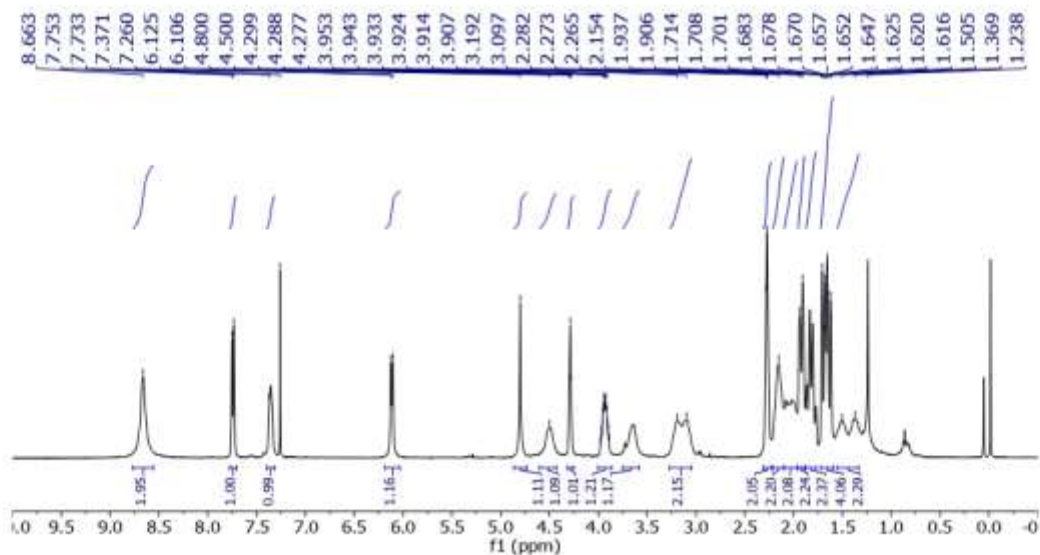
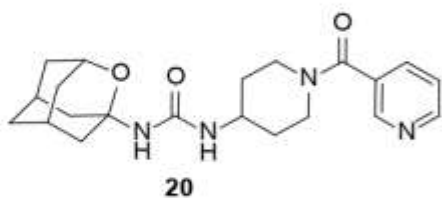


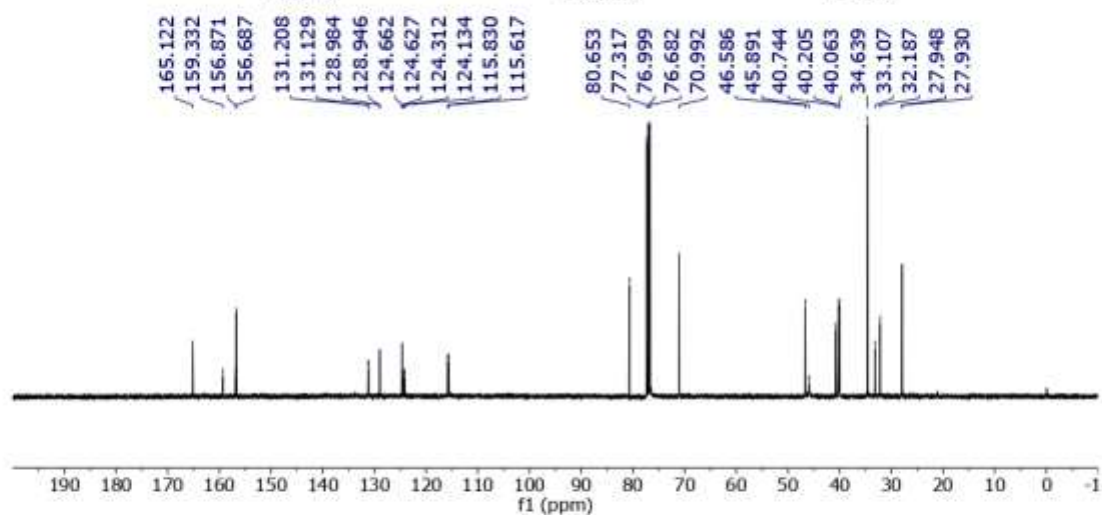
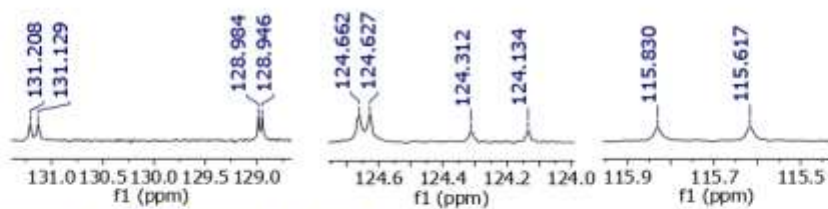
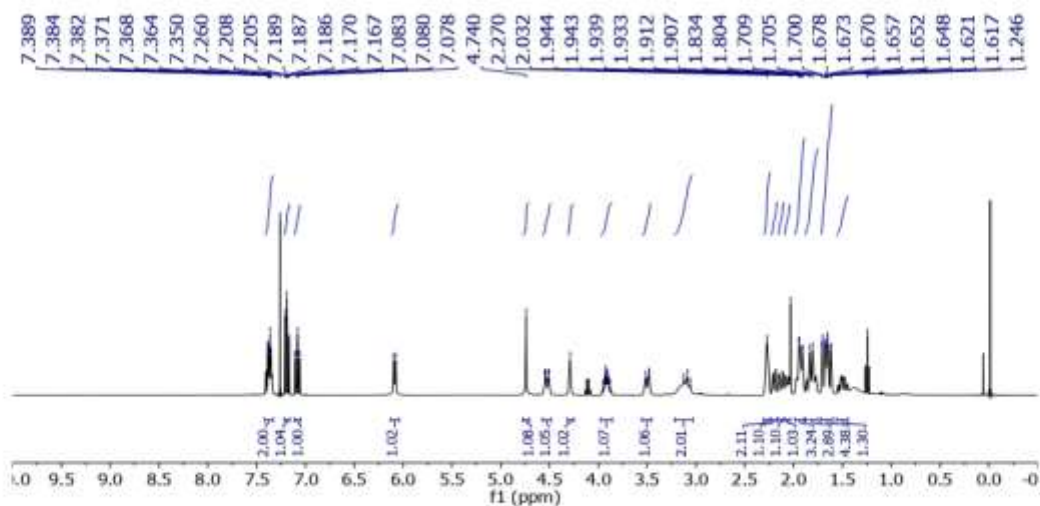
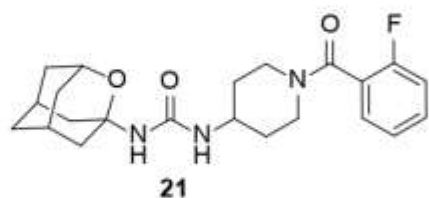


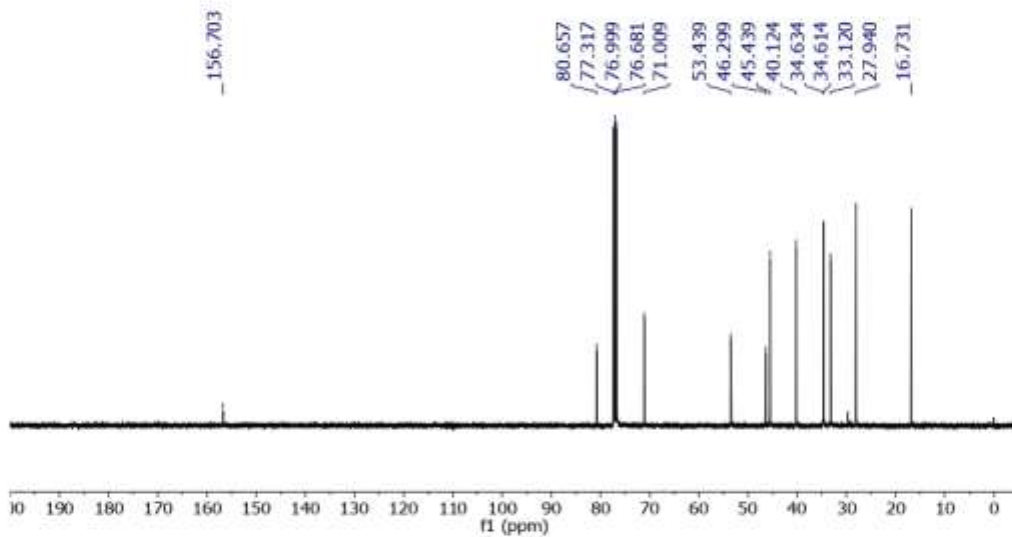
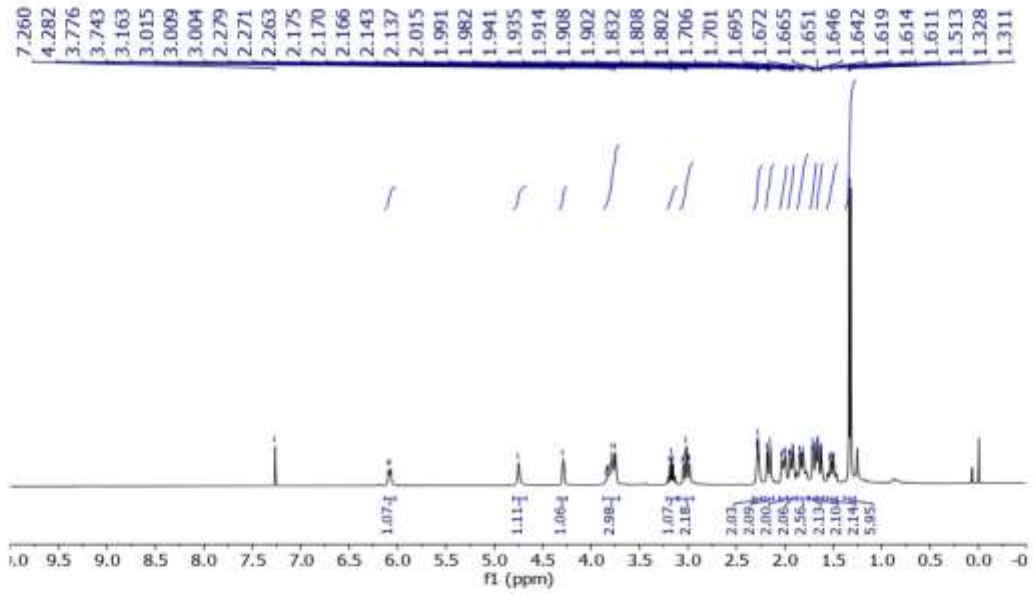
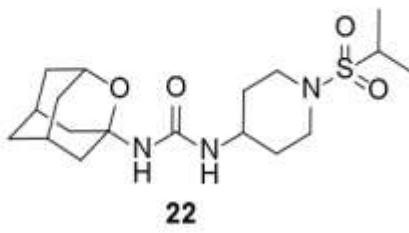


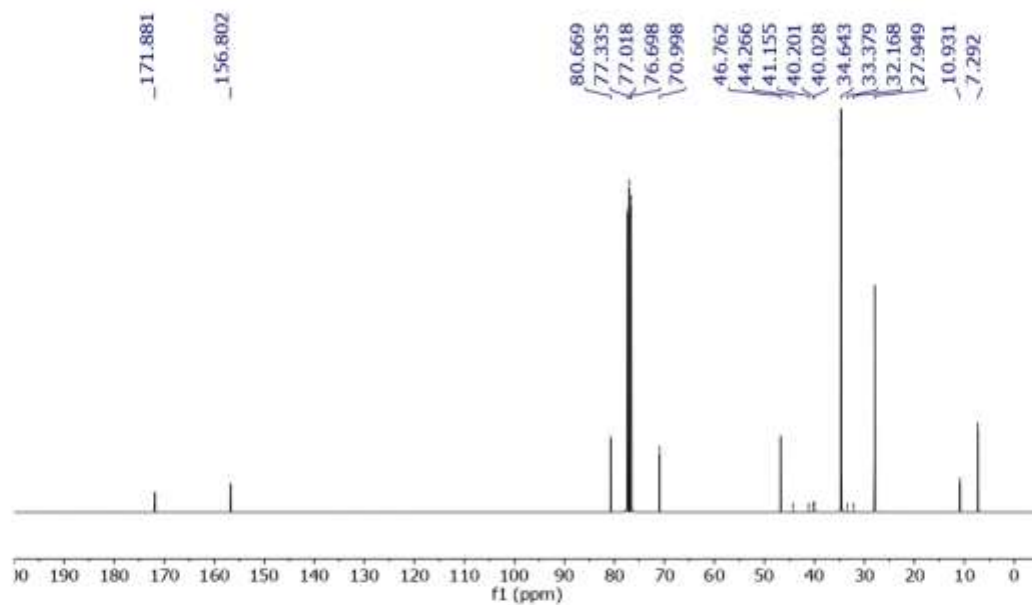
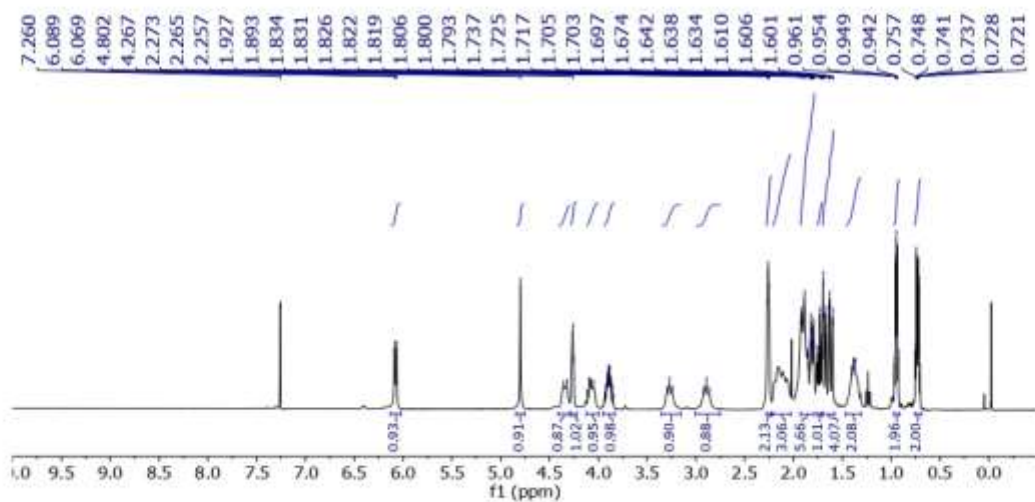
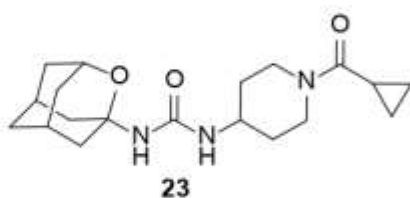
19

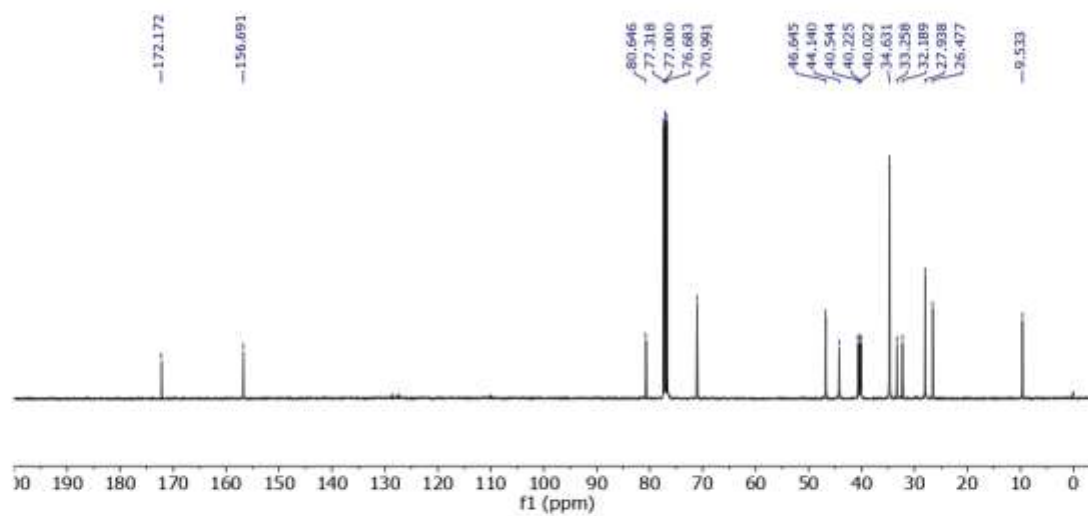
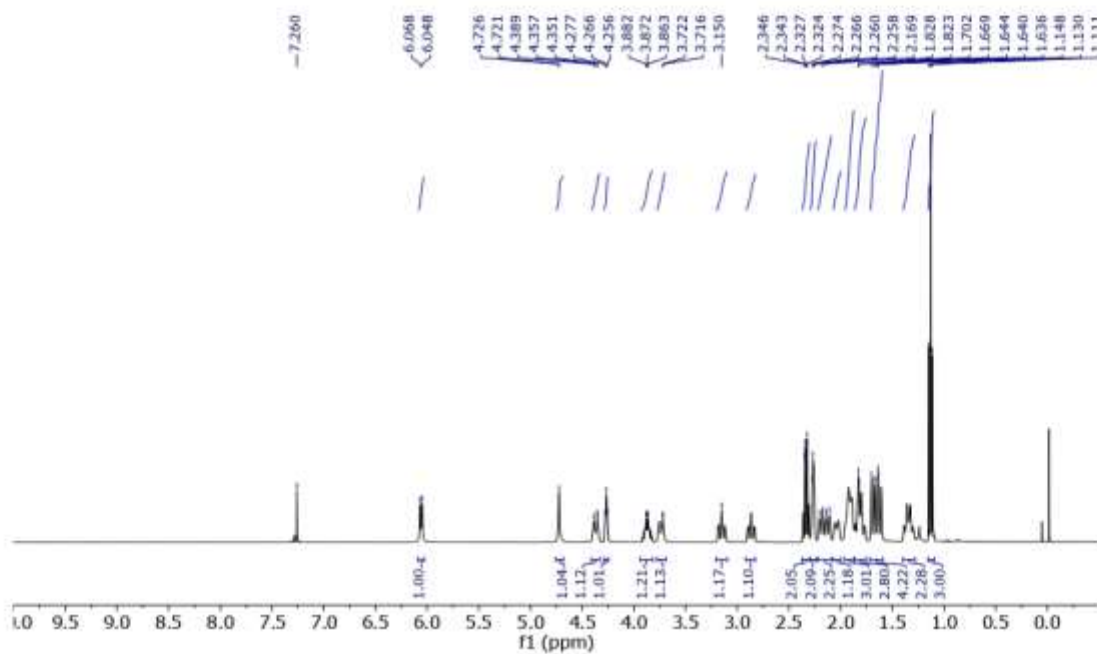
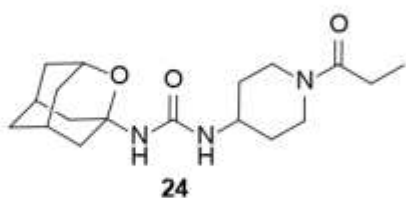


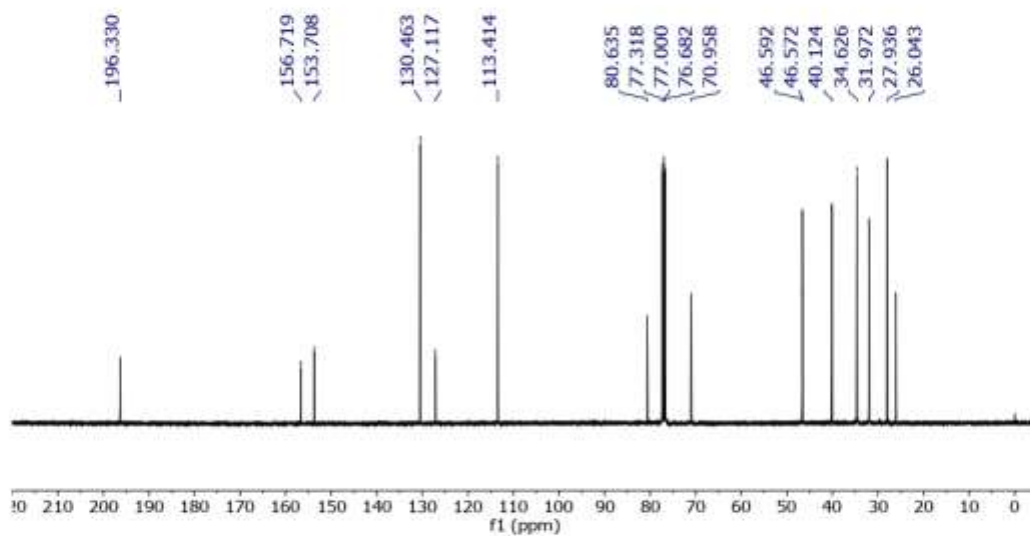
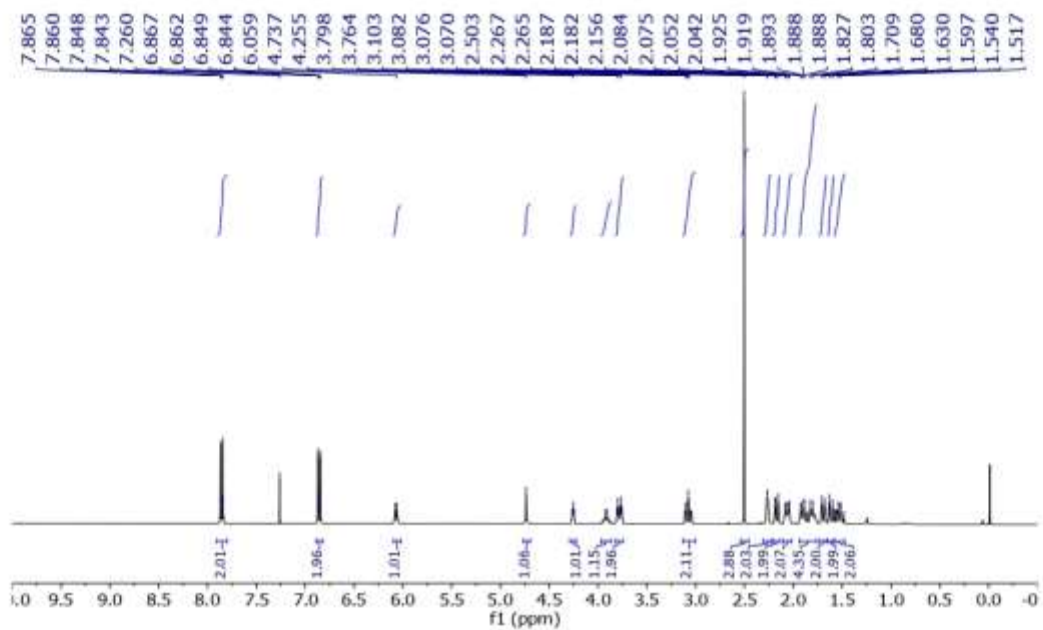
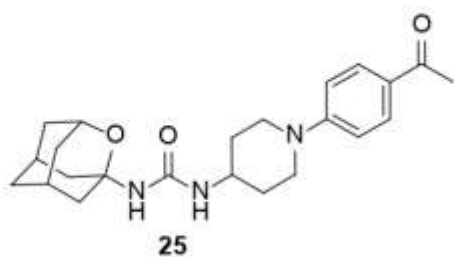




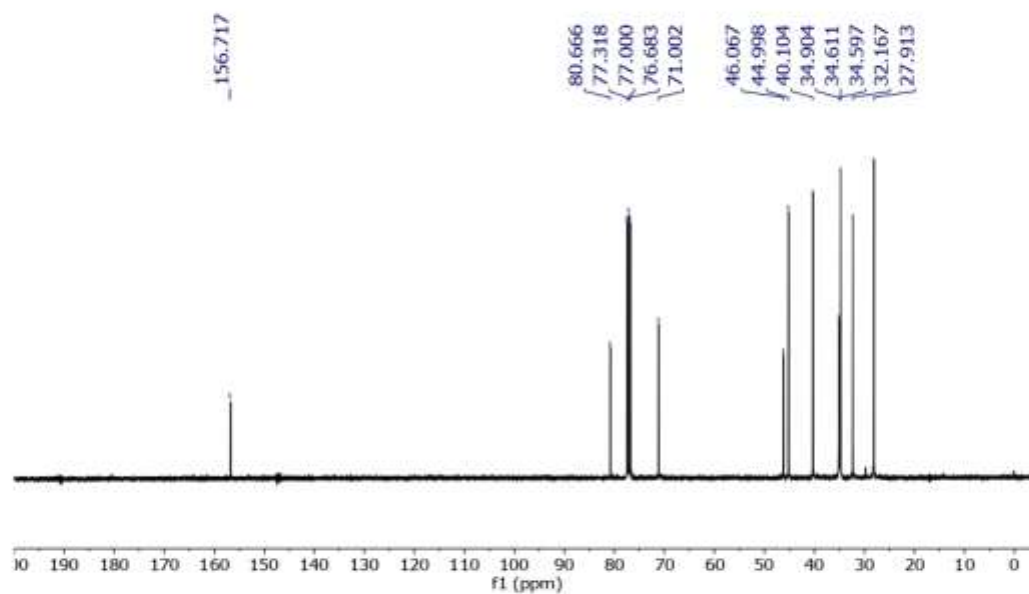
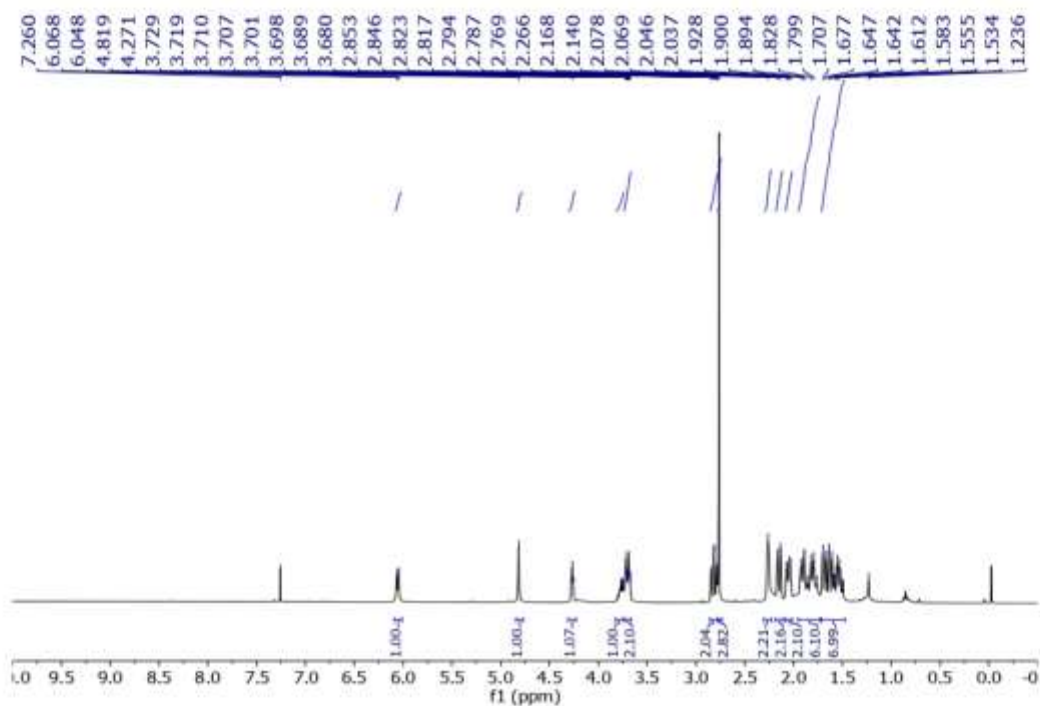
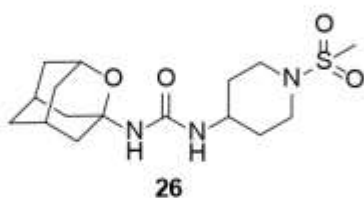


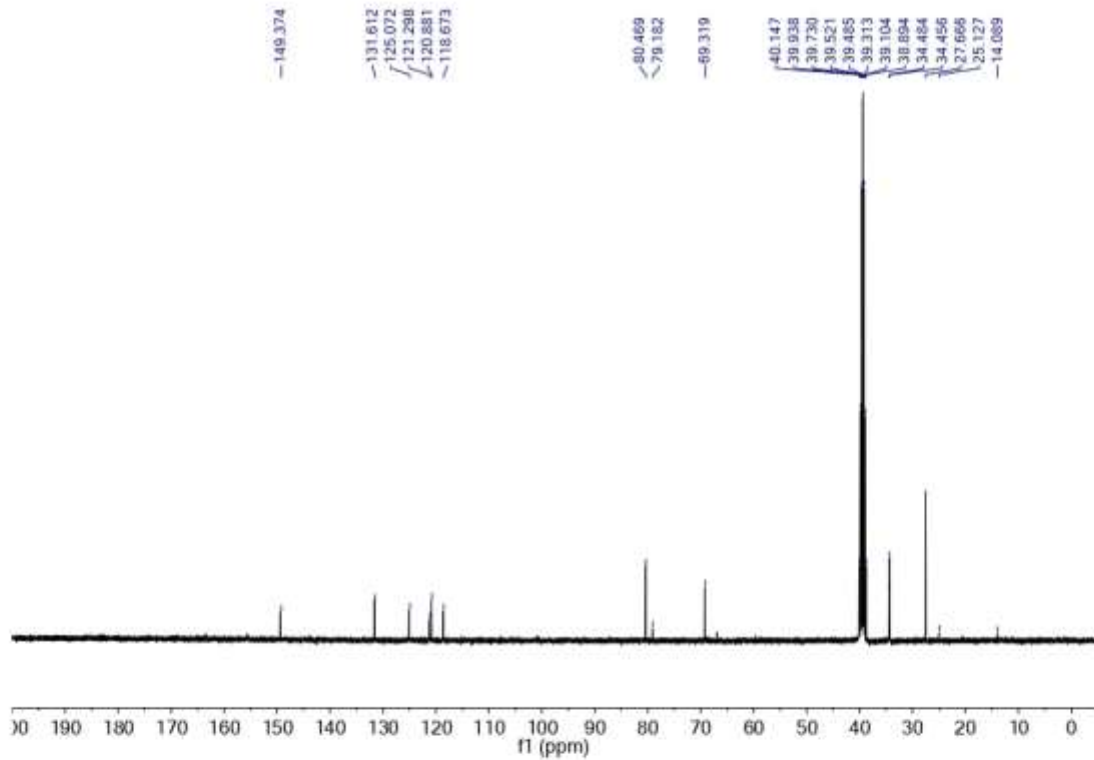
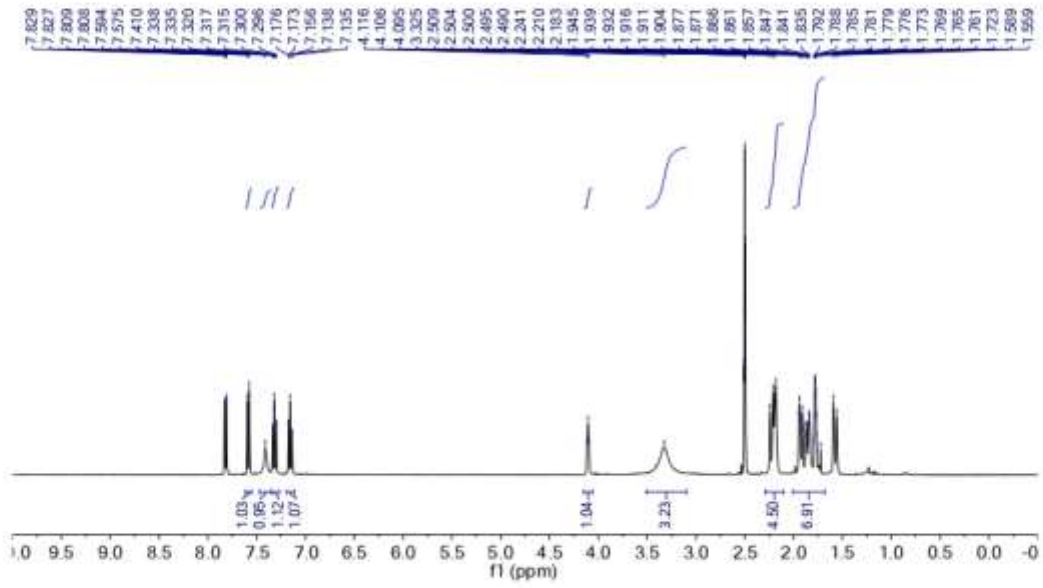
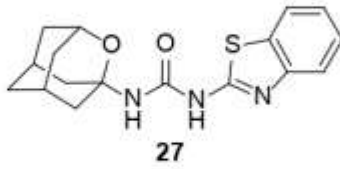


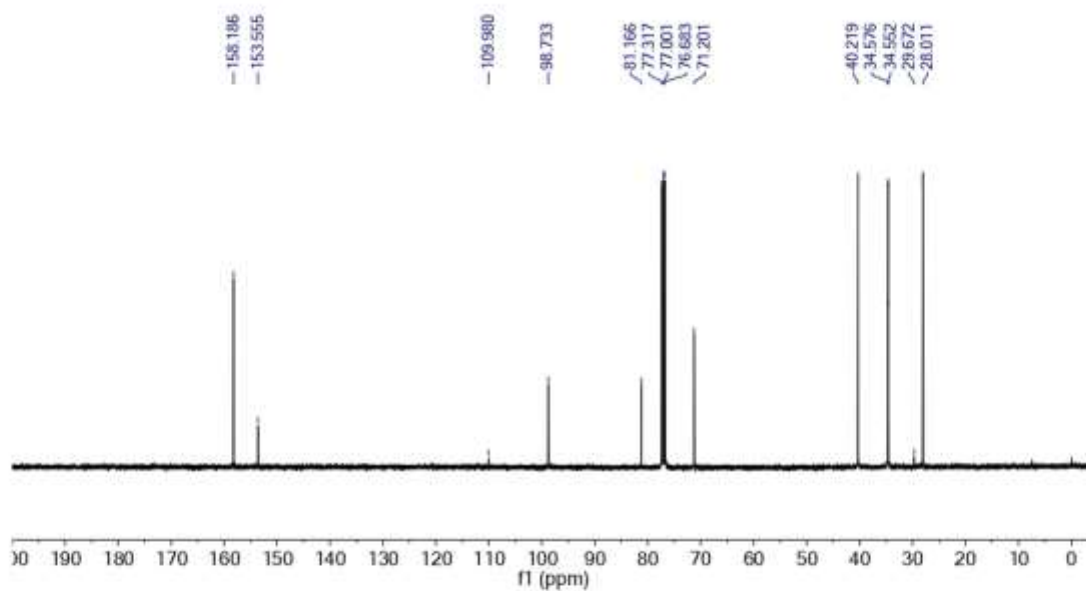
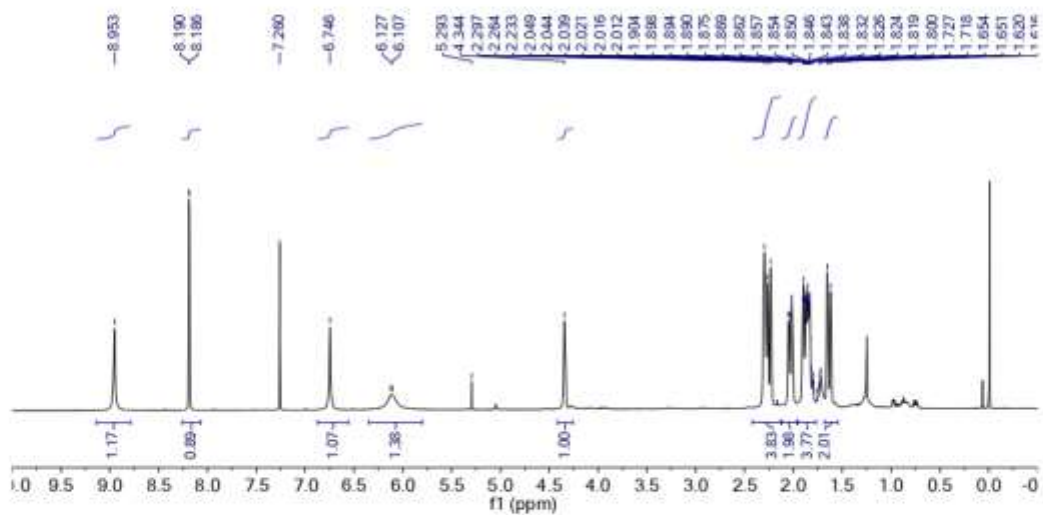
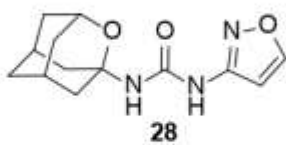


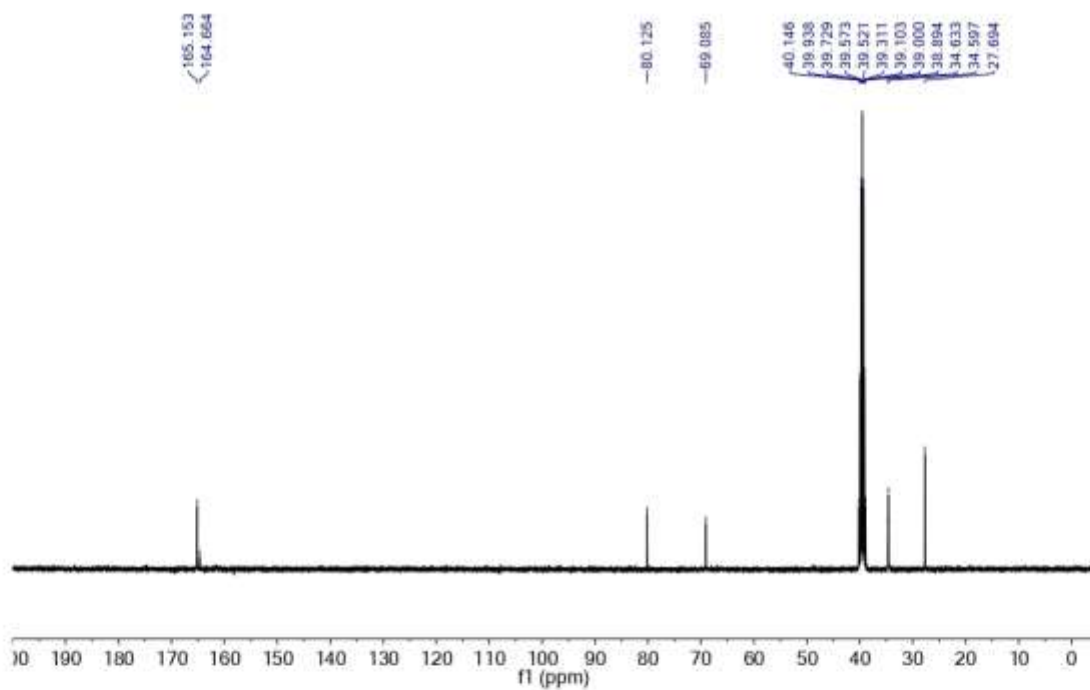
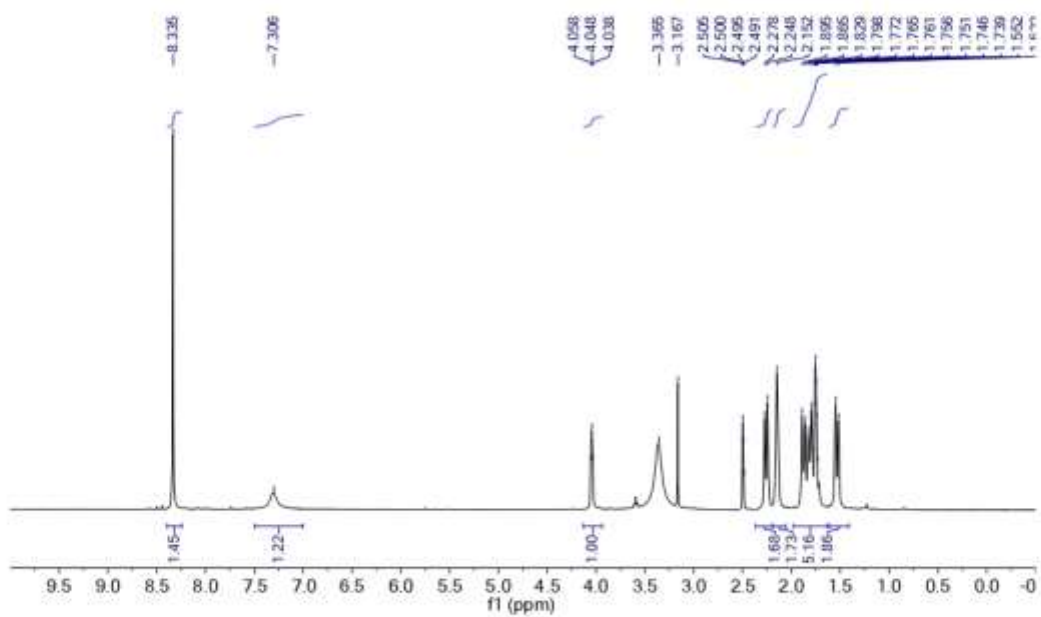
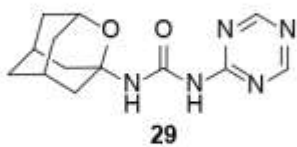


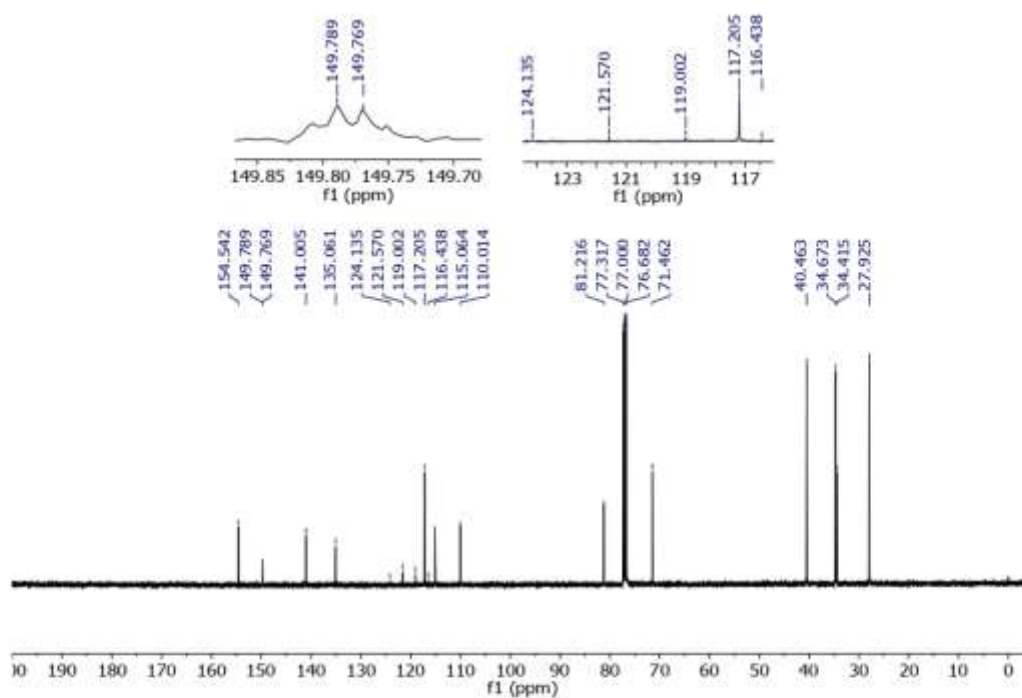
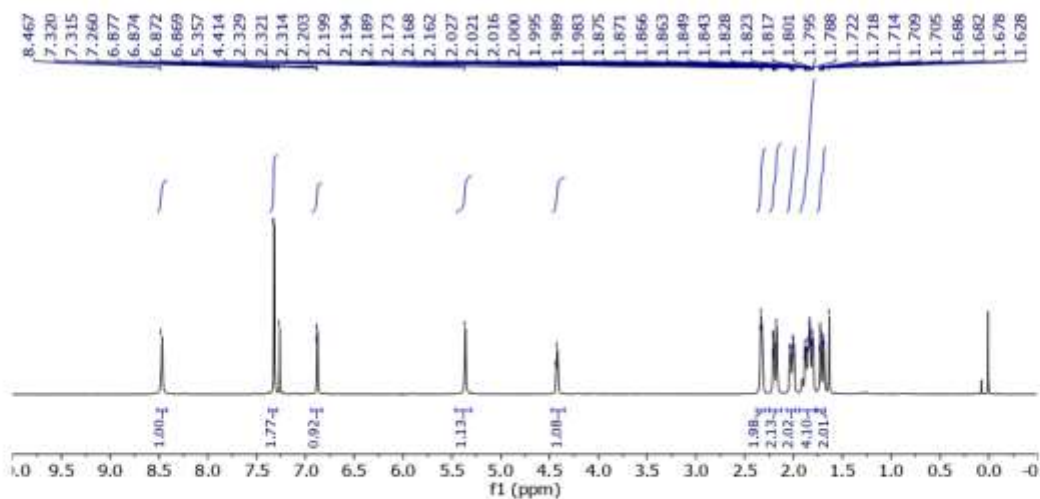
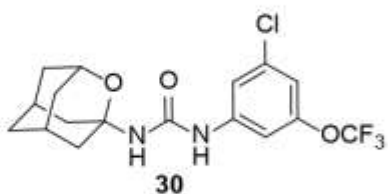
S19

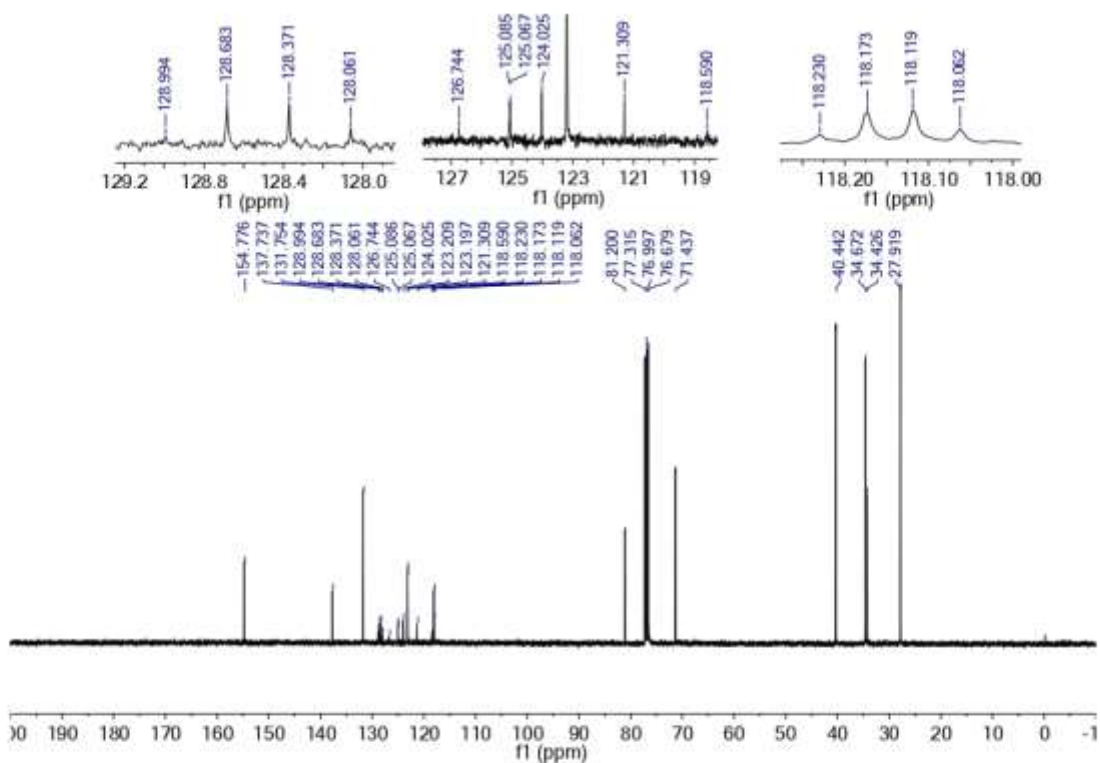
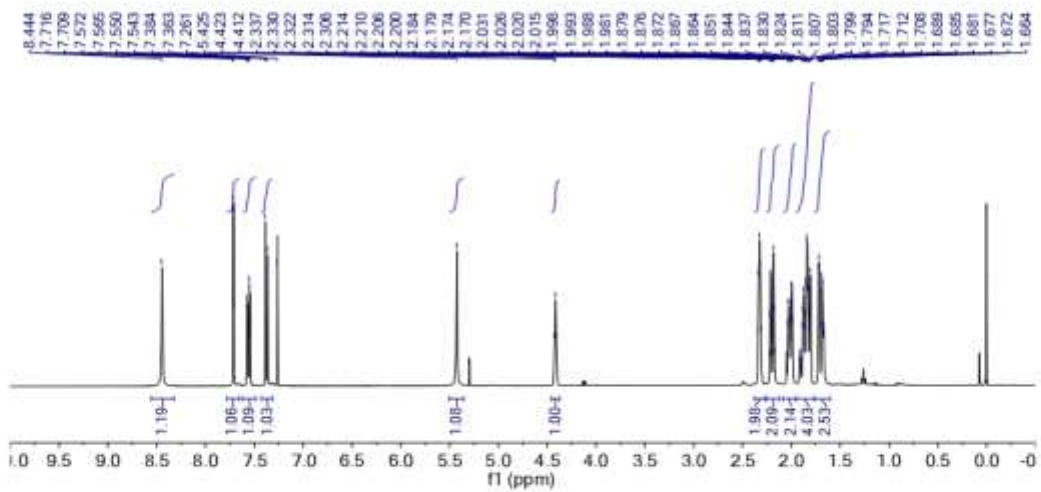
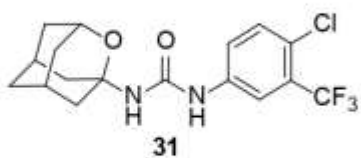


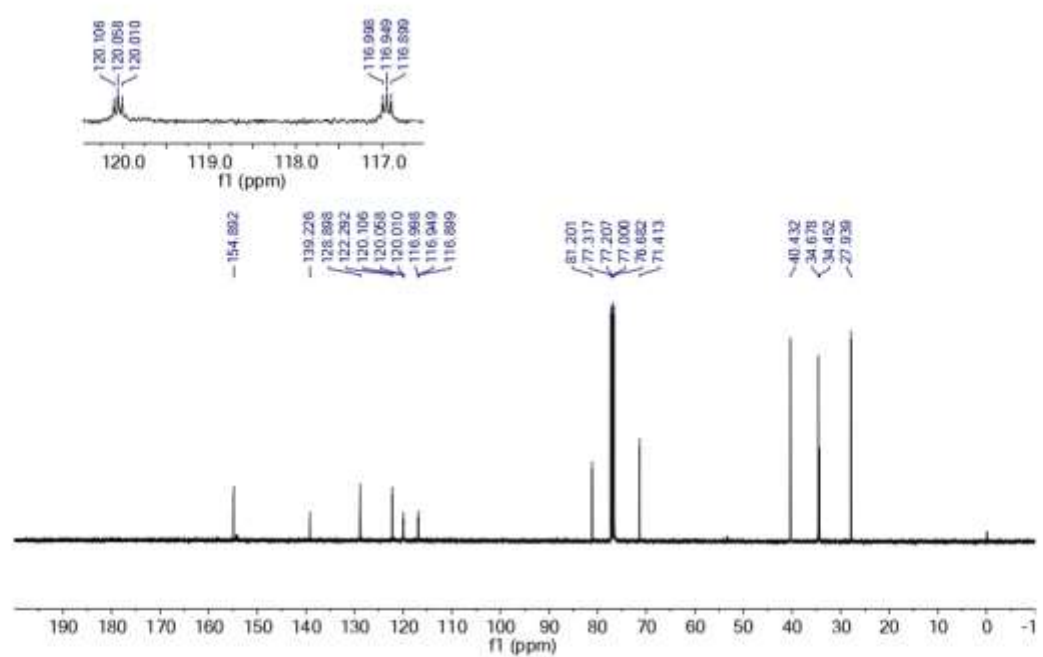
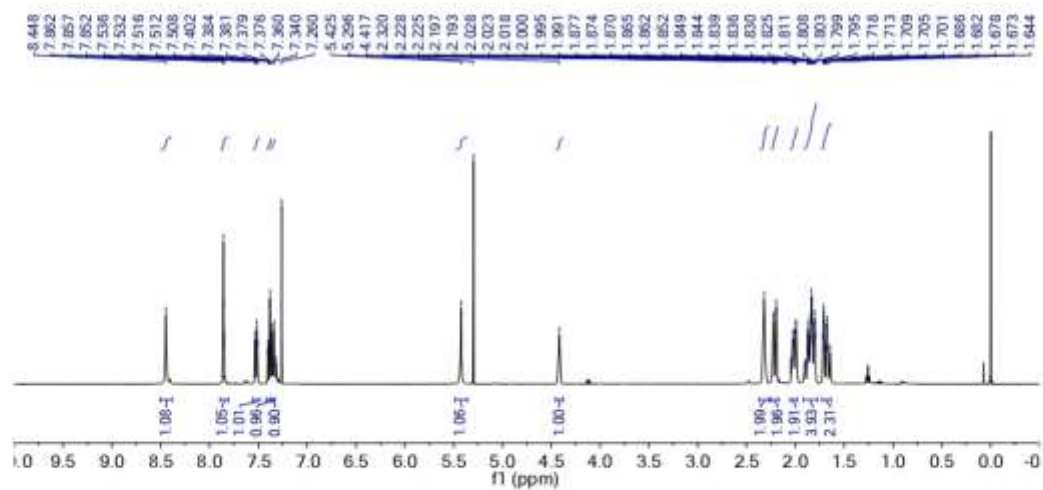
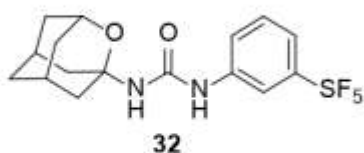




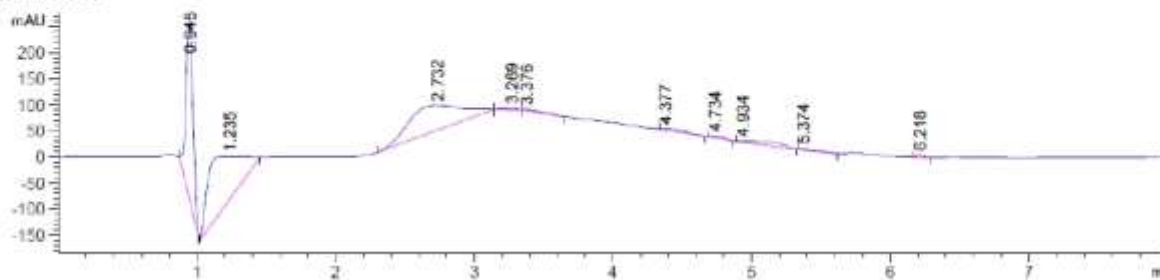




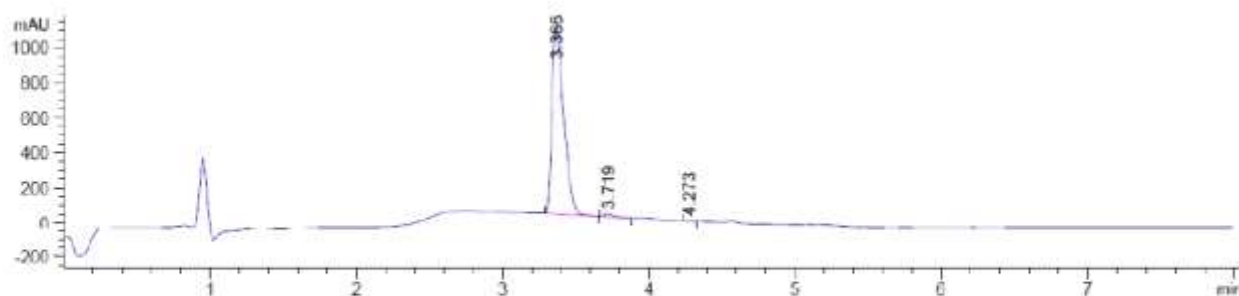




Blank test



Compound 15

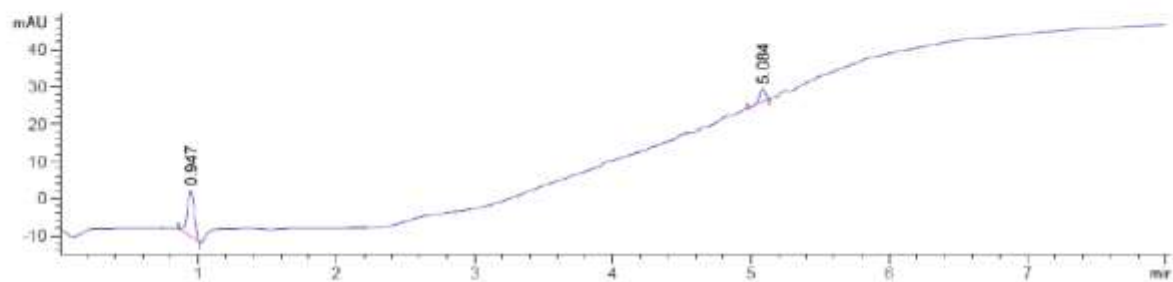


Signal 1: DAD1 A, Sig=210,4 Ref=360,100

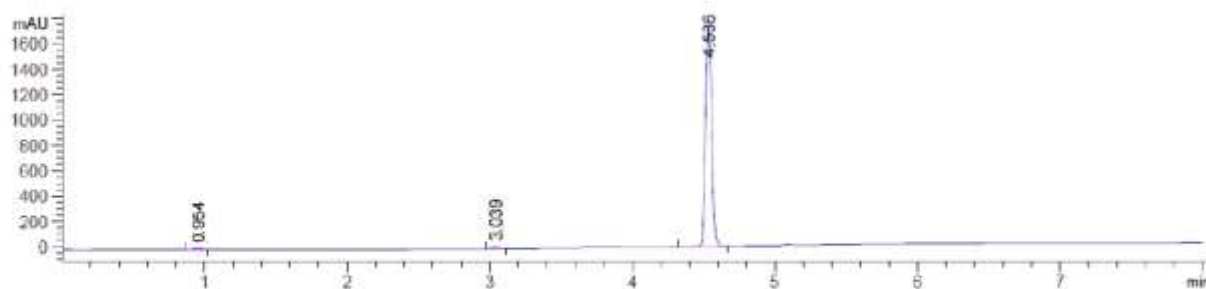
Peak #	RetTime [min]	Type	Width [min]	Area [mAU*s]	Height [mAU]	Area %
1	3.366	BB	0.0829	5963.42188	1071.34827	98.6912
2	3.719	BB	0.0618	71.82229	17.53464	1.1886
3	4.273	BB	0.0426	7.26377	2.76769	0.1202

Totals : 6042.50793 1091.65060

Blank test



Compound 27

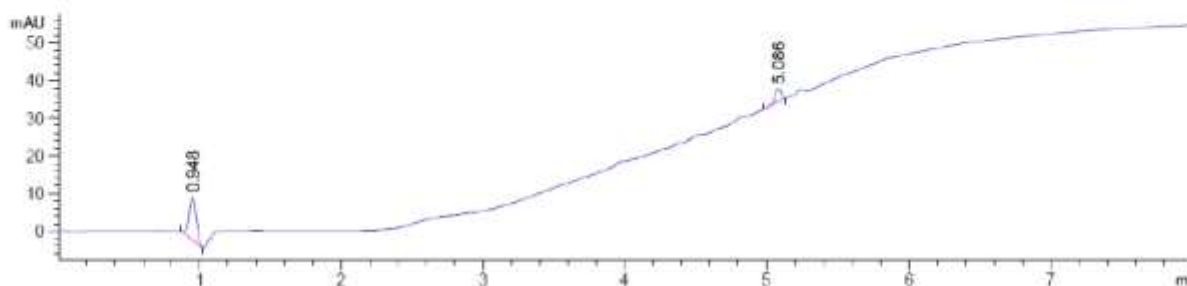


Signal 1: DAD1 A, Sig=245,4 Ref=360,100

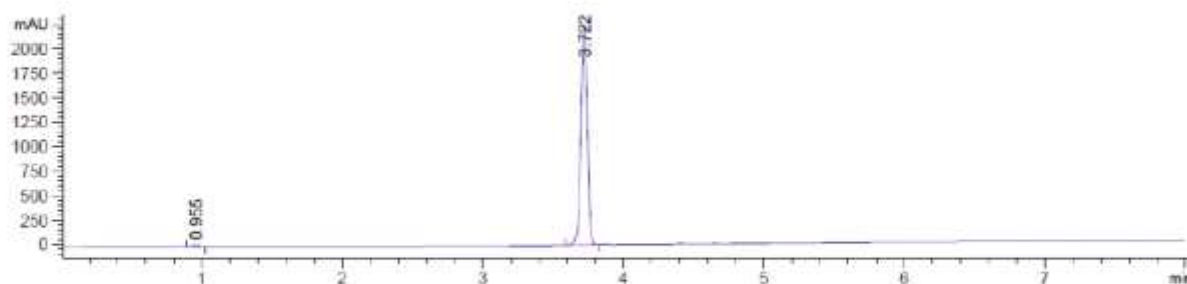
Peak #	RetTime [min]	Type	Width [min]	Area [mAU*s]	Height [mAU]	Area %
1	0.954	BB	0.0605	44.98075	11.80430	0.8516
2	3.039	BB	0.0472	61.01562	20.20074	1.1552
3	4.536	BB	0.0487	5175.71143	1738.31812	97.9931

Totals : 5281.70779 1770.32316

Blank test



Compound 29

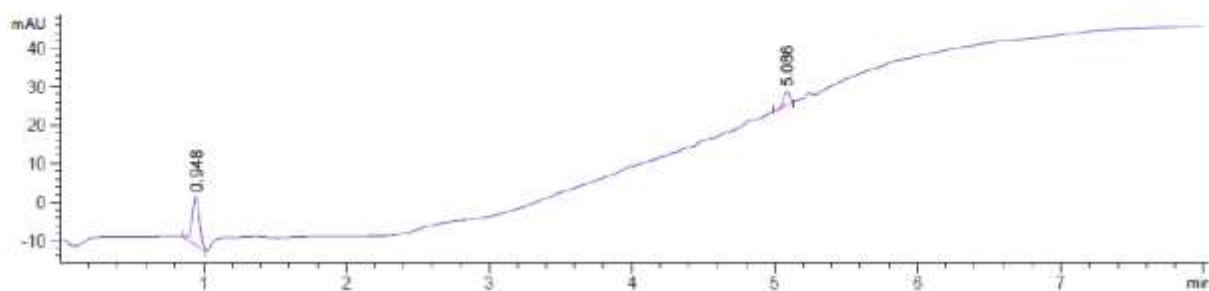


Signal 1: DAD1 A, Sig=245,4 Ref=360,100

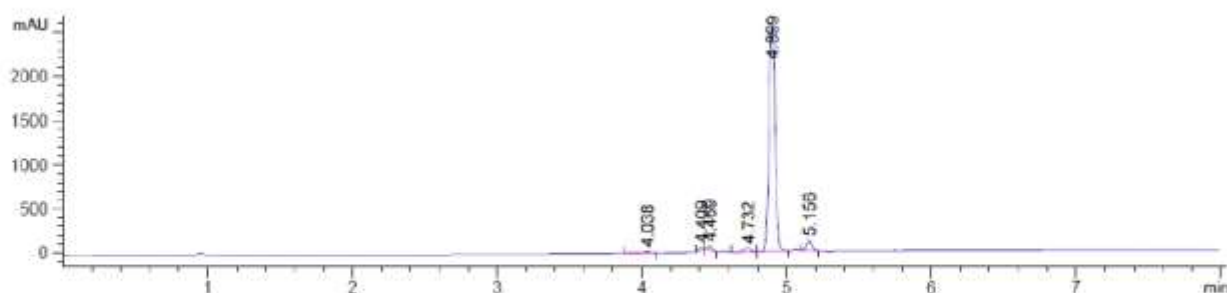
Peak #	RetTime [min]	Type	Width [min]	Area [mAU*s]	Height [mAU]	Area %
1	0.955	BB	0.0576	54.87747	15.40726	0.7659
2	3.722	BB	0.0488	7110.12598	2253.27002	99.2341

Totals : 7165.00344 2268.67728

Blank test



Compound 32



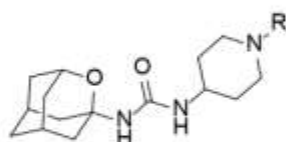
Signal 1: DAD1 A, Sig=245,4 Ref=360,100

Peak #	RetTime [min]	Type	Width [min]	Area [mAU*s]	Height [mAU]	Area %
1	4.038	BB	0.0495	54.91798	17.09327	0.6652
2	4.409	BB	0.0349	67.59186	31.65423	0.8187
3	4.469	BB	0.0404	115.69170	47.56844	1.4013
4	4.732	BB	0.0697	158.29762	38.69275	1.9173
5	4.899	BB	0.0465	7533.47803	2546.79443	91.2457
6	5.156	BB	0.0443	326.27591	117.92603	3.9519

Totals : 8256.25310 2799.72915

Compound	Molecular Formula	Calculated			Found		
		C	H	N	C	H	N
4	$C_{16}H_{17}F_3N_2O_2 \cdot 0.5H_2O$	57.31	5.41	8.35	57.46	5.70	8.22
7	$C_{16}H_{17}F_3N_2O_2$	58.89	5.25	8.58	59.00	5.60	8.57
9	$C_{18}H_{15}F_3N_2O_2$	62.07	4.34	8.04	62.04	4.43	7.98
12	$C_{17}H_{27}N_3O_3 \cdot 0.25H_2O$	62.65	8.50	12.89	62.64	8.61	12.74
14	$C_{23}H_{30}N_2O_5 \cdot 0.1H_2O$	66.36	7.31	6.73	66.13	7.32	6.64
17	$C_{19}H_{27}ClN_6O_2 \cdot 0.7C_3H_6O$	56.62	7.03	18.78	56.22	6.74	18.53
18	$C_{20}H_{31}N_7O_2 \cdot 0.2C_5H_{12} \cdot 1.1C_3H_6O$	60.83	8.40	20.43	61.01	8.15	20.30
19	$C_{21}H_{33}N_3O_4 \cdot 1H_2O$	61.59	8.61	10.26	62.20	8.55	10.38
20	$C_{21}H_{28}N_4O_3 \cdot 0.25C_6H_{14} \cdot 0.1CH_2Cl_2$	65.49	7.71	13.52	65.42	7.61	13.54
21	$C_{22}H_{28}FN_3O_3$	65.82	7.03	10.47	65.88	7.25	10.36
22	$C_{18}H_{31}N_3O_4S \cdot 0.5H_2O$	54.80	8.18	10.65	55.03	7.93	10.46
23	$C_{19}H_{29}N_3O_3 \cdot 1H_2O$	62.44	8.55	11.50	62.81	8.54	11.07
24	$C_{18}H_{29}N_3O_3 \cdot 0.6C_4H_8O_2$	63.10	8.77	10.82	62.94	8.96	10.97
25	$C_{23}H_{31}N_3O_3 \cdot 0.25H_2O$	68.72	7.90	10.45	68.96	7.78	10.21
26	$C_{16}H_{27}N_3O_4S \cdot 0.2C_5H_{12} \cdot 0.15C_3H_6O$	55.07	8.02	11.04	55.48	7.57	10.60
28	$C_{13}H_{17}N_3O_3$	59.30	6.51	15.96	59.46	6.70	14.31
30	$C_{17}H_{18}ClF_3N_2O_3$	52.25	4.64	7.17	52.05	4.80	7.02
31	$C_{17}H_{18}ClF_3N_2O_2$	54.48	4.84	7.47	54.57	4.84	7.64

Table S1: Elemental analysis data.



Compound	R	Cytochrome inhibition ^[a]						hERG inhibition ^[c]
		CYP 1A2	CYP 2C9	CYP 2C19	CYP 2D6	CYP 3A4 ^[b]		
						(BFC)	(DBF)	
12		6 ± 2	2 ± 2	3 ± 3	3 ± 1	20 ± 4	17 ± 1	2 ± 2
22		1 ± 1	1 ± 1	1 ± 1	1 ± 1	37 ± 3	2 ± 2	2 ± 2

Table S2. Inhibition (expressed as % of inhibition) of recombinant human cytochrome P450 enzymes and of hERG channel by selected inhibitors. ^aThe cytochrome inhibition was tested at 10 μM for compound **12** and at 1 μM for compound **22**. ^bFor the study of CYP3A4, two different substrates were used: benzyloxytrifluoromethylcoumarin (BFC) and dibenzylfluorescein (DBF). ^cThe hERG inhibition was tested at 10 μM. All the values represent the mean ± SD of three measurements (n = 3).

Compound	IC ₅₀ <i>h</i> LOX-5	<i>h</i> COX-2 (10 μM)
21	> 100 μM	11.4 %
22	> 100 μM	3.8 %
24	> 100 μM	13.6 %

Table S3: IC₅₀ in human LOX-5 (*h*LOX-5) and inhibition (expressed as % of inhibition) of human COX-2 (*h*COX-2) at 10 μM for compounds **21**, **22** and **24**. Inhibition of *h*COX-2 was performed at Eurofins (catalogue reference 4186).

Time	ID	Total Concentration (ng/mL)	Mean (ng/mL)	SD (ng/mL)
0 h	Mouse 1	0	0	0
	Mouse 2	0		
	Mouse 3	0		
0.16 h	Mouse 1	140	117.33	32.58
	Mouse 2	132		
	Mouse 3	80		
0.5 h	Mouse 1	5.61	5.85	0.22
	Mouse 2	6.05		
	Mouse 3	5.9		
1 h	Mouse 1	1.41	2.71	2.12
	Mouse 2	5.16		
	Mouse 3	1.56		
2 h	Mouse 1	0.4	0.30	0.09
	Mouse 2	0.23		
	Mouse 3	0.27		
4 h	Mouse 1	0.13	0.14	0.01
	Mouse 2	0.15		
	Mouse 3	0.14		
6 h	Mouse 1	0.23	0.12	0.12
	Mouse 2	0		
	Mouse 3	0.13		
24 h	Mouse 1	0	0.00	0.00
	Mouse 2	0		
	Mouse 3	0		

Table S4: Mean of concentrations of **22** in mouse plasma at different times after ip administration at 1 mg/kg.

Time	ID	Total Concentration (ng/mL)	Mean (ng/mL)	SD (ng/mL)
0 h	Mouse 1	0	0	0
	Mouse 2	0		
	Mouse 3	0		
0.16 h	Mouse 1	94.22	108.39	12.43
	Mouse 2	113.52		
	Mouse 3	117.44		
0.5 h	Mouse 1	37.55	20.75	14.69
	Mouse 2	10.30		
	Mouse 3	14.40		
1 h	Mouse 1	2.67	4.66	3.30
	Mouse 2	8.47		
	Mouse 3	2.83		
2 h	Mouse 1	0.18	0.35	0.19
	Mouse 2	0.31		
	Mouse 3	0.56		
4 h	Mouse 1	0.13	0.14	0.02
	Mouse 2	0.14		
	Mouse 3	0.16		
6 h	Mouse 1	0.13	0.13	0.00
	Mouse 2	0.13		
	Mouse 3	0.13		
24 h	Mouse 1	0.00	0.00	0.00
	Mouse 2	0.00		
	Mouse 3	0.00		

Table S5: Mean of concentrations of **22** in mouse plasma at different times after iv administration at 1 mg/kg.

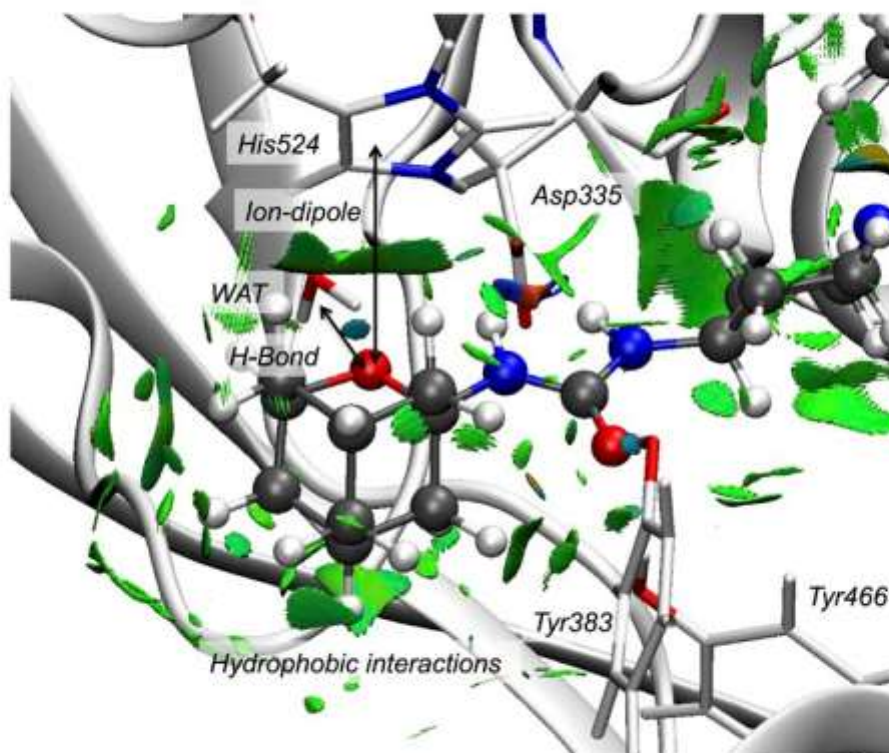


Figure S1. Representation of the noncovalent interactions (computed with NCIPLOT) at the active site of sEH in the presence of compound **22**. The weak interactions are shown as green surfaces, hydrogen-bonds are depicted in blue, and repulsive interactions in red. The interaction surfaces of the hydrogen-bond between the oxygen atom of compound **22** and the active site water molecule and the ion-dipole interaction between protonated His524 and the oxygen atom of compound **22** are highlighted. Additionally, several hydrophobic interactions between the adamantane group and residues Phe267, Tyr383, Leu408, Leu417, Met419, and Trp525 are observed.

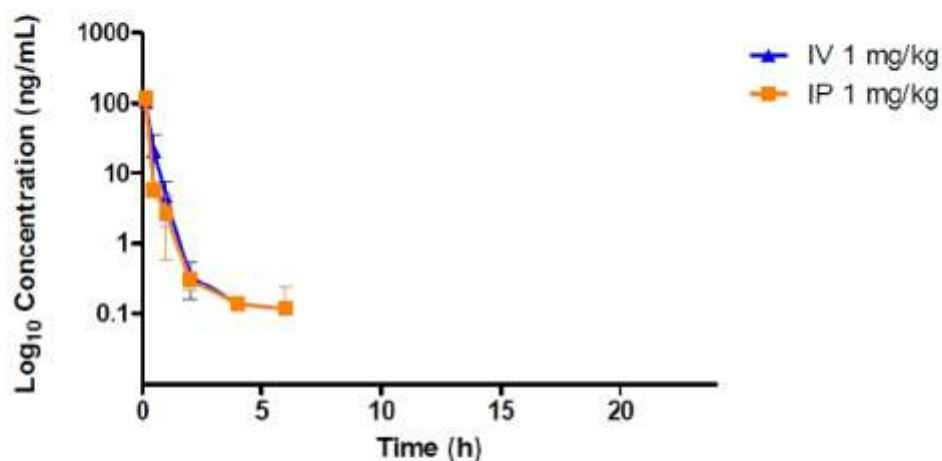


Figure S2: Concentration (scale log 10) vs time for ip and iv administration at 1 mg/kg of compound 22.

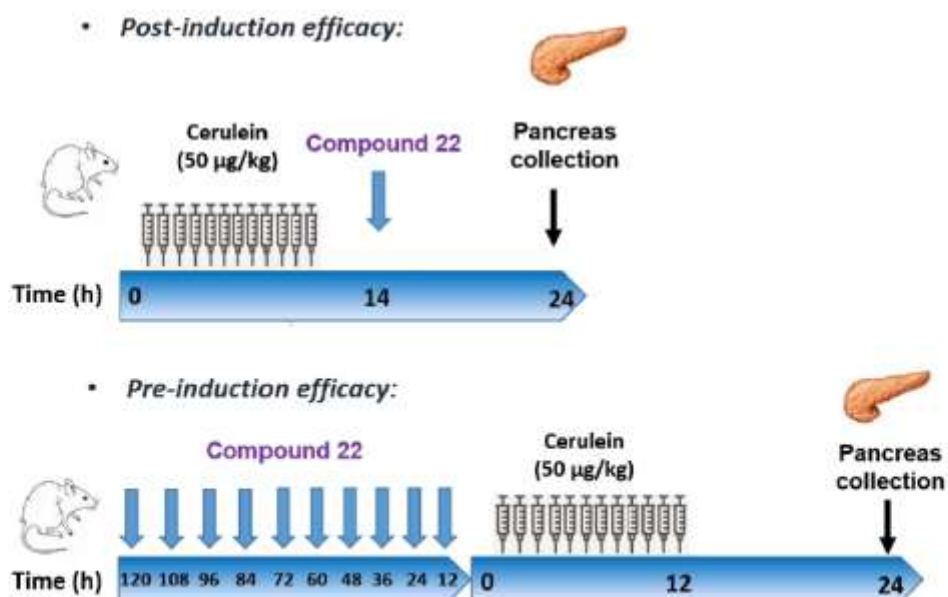


Figure S3: Experimental procedures of the two *in vivo* efficacy experiments of compound 22.

Patent Application

(12) INTERNATIONAL APPLICATION PUBLISHED UNDER THE PATENT COOPERATION TREATY (PCT)

(19) World Intellectual Property
Organization
International Bureau



(10) International Publication Number
WO 2017/017048 A1

(43) International Publication Date
2 February 2017 (02.02.2017)

- (51) International Patent Classification:
C07D 405/14 (2006.01) *C07D 417/12* (2006.01)
C07D 311/96 (2006.01) *A61K 31/352* (2006.01)
C07D 405/12 (2006.01) *A61K 31/453* (2006.01)
C07D 413/12 (2006.01) *A61P 9/12* (2006.01)
- (21) International Application Number:
PCT/EP2016/067620
- (22) International Filing Date:
25 July 2016 (25.07.2016)
- (25) Filing Language: English
- (26) Publication Language: English
- (30) Priority Data:
15178618.3 28 July 2015 (28.07.2015) EP
- (71) Applicant: UNIVERSITAT DE BARCELONA [ES/ES];
Centre de Patents de la UB, Baldíri Reixac 4 - Torre D,
08028 Barcelona (ES).
- (72) Inventors: VÁZQUEZ CRUZ, Santiago; Universitat de
Barcelona, Centre de Patents de la UB -, Baldíri Reixac 4 -
Torre D, 08028 Barcelona (ES). VALVERDE MUR-
ILLO, Elena; Abat Escarré 12, 43711 Banyeres del Pened-
ès (ES). LEIVA MARTÍNEZ, Rosana; Passatge Lluís
Pellicer 12, 1r 2a, 08036 Barcelona (ES). VÁZQUEZ
CARRERA, Manuel; Universitat de Barcelona, Centre de
Patents de la UB -, Baldíri Reixac 4 - Torre D, 08028 Bar-

celona (ES). CODONY GISBERT, Sandra; Sant Erme-
negild 20-22, 08006 Barcelona (ES).

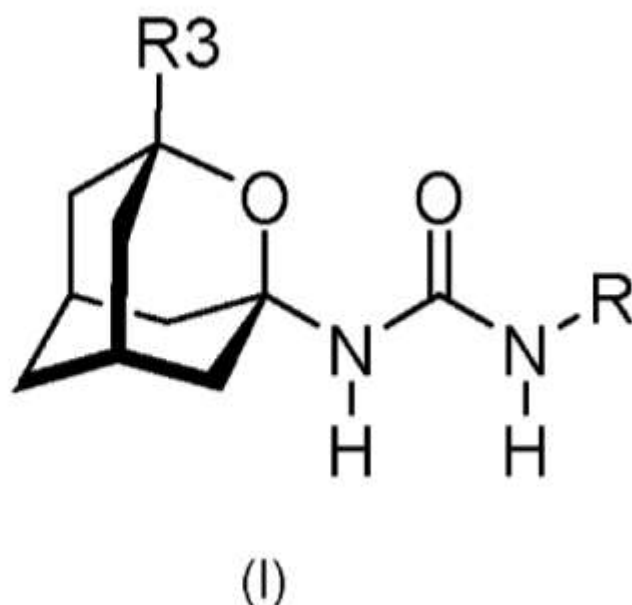
- (81) Designated States (unless otherwise indicated, for every
kind of national protection available): AE, AG, AL, AM,
AO, AT, AU, AZ, BA, BB, BG, BH, BN, BR, BW, BY,
BZ, CA, CH, CL, CN, CO, CR, CU, CZ, DE, DK, DM,
DO, DZ, EC, EE, EG, ES, FI, GB, GD, GE, GH, GM, GT,
HN, HR, HU, ID, IL, IN, IR, IS, JP, KE, KG, KN, KP, KR,
KZ, LA, LC, LK, LR, LS, LU, LY, MA, MD, ME, MG,
MK, MN, MW, MX, MY, MZ, NA, NG, NI, NO, NZ, OM,
PA, PE, PG, PH, PL, PT, QA, RO, RS, RU, RW, SA, SC,
SD, SE, SG, SK, SL, SM, ST, SV, SY, TH, TJ, TM, TN,
TR, TT, TZ, UA, UG, US, UZ, VC, VN, ZA, ZM, ZW.
- (84) Designated States (unless otherwise indicated, for every
kind of regional protection available): ARIPO (BW, GH,
GM, KE, LR, LS, MW, MZ, NA, RW, SD, SL, ST, SZ,
TZ, UG, ZM, ZW), Eurasian (AM, AZ, BY, KG, KZ, RU,
TJ, TM), European (AL, AT, BE, BG, CH, CY, CZ, DE,
DK, EE, ES, FI, FR, GB, GR, HR, HU, IE, IS, IT, LT, LU,
LV, MC, MK, MT, NL, NO, PL, PT, RO, RS, SE, SI, SK,
SM, TR), OAPI (BF, BJ, CF, CG, CI, CM, GA, GN, GQ,
GW, KM, ML, MR, NE, SN, TD, TG).

Declarations under Rule 4.17:

- as to applicant's entitlement to apply for and be granted a
patent (Rule 4.17(ii))

[Continued on next page]

(54) Title: ANALOGS OF ADAMANTYLUREAS AS SOLUBLE EPOXIDE HYDROLASE INHIBITORS



(57) Abstract: N-(2-oxadamantan-1-yl)ureas of formula I, where R³ is H, C₁-C₃ alkyl, cyclohexyl or phenyl; R is -[CH₂]_n -Y; n is 0-15; in -[CH₂]_n - 0-n/3 of the methylene groups are optionally replaced by non adjacent oxygen atoms; and Y is a 3- or 4-substituted phenyl, a 3- or 4-substituted cyclohexyl, a N-substituted piperidin-4-yl, a N-substituted piperidin-3-yl, a di- or tri-fluorosubstituted phenyl, 4-chloro-3-trifluoromethylphenyl, 3-chloro-4-trifluoromethylphenyl, 4-fluoro-3-trifluoromethylphenyl, or 3-fluoro-4-trifluoromethylphenyl; have epoxide hydrolase (sEH) inhibitory activities similar to those of their N-(adamantan-1-yl)urea analogs. Thus, compounds I are useful as API for the treatment of sEH mediated diseases. Besides, in general, compounds (I) have higher water solubilities and lower melting points, what make them more promising from the point of view of pharmacokinetics and formulation.

WO 2017/017048 A1

Published:

— with international search report (Art. 21(3))

Analogs of adamantylureas as soluble epoxide hydrolase inhibitors

The present invention relates to the field of pharmaceutical products for human and veterinary medicine, particularly to soluble epoxide hydrolase (sEH) inhibitors and their
5 therapeutic indications.

BACKGROUND ART

A total of more than 100 patent publications have described multiple classes of sEH
10 inhibitors, based on different chemical structures, such as amides, thioamides, ureas, thioureas, carbamates, acyl hydrazones and chalcone oxides (cf. e.g. H.C. Shen, "Soluble epoxide hydrolase inhibitors: a patent review", *Expert. Opin. Ther. Patents* 2010, vol. 20, pp. 941-956, a review with 149 references). sEH inhibition has been associated to various beneficial biological effects, that may be translated into therapeutic treatment for
15 hypertension, atherosclerosis, pulmonary diseases, kidney diseases, stroke, pain, neuropathic pain, inflammation, pancreatitis, immunological disorders, eye diseases, cancer, obesity, diabetes, metabolic syndrome, preeclampsia, anorexia nervosa, depression, erectile dysfunction, wound healing, NSAID-induced ulcers, emphysema, scrapie and Parkinson's disease (cf. e.g. H.C. Shen and B.D. Hammock, "Discovery of
20 inhibitors of soluble epoxide hydrolase: A target with multiple potential therapeutic indications", *J. Med. Chem.* 2012, vol. 55, pp. 1789-1808, a review with 117 references).

Despite the high inhibitory activity of many of the reported sEH inhibitory compounds, until now no sEH inhibitor has reached the market, what illustrates the difficulty of developing
25 sEH inhibitors as human active pharmaceutical ingredients (API). Some of the development limitations are: lack of selectivity, chemical and metabolic instability, and inappropriate physical properties, especially low water solubility. Therefore, there is a need for development of new sEH inhibitory compounds that, having an acceptable inhibitory activity, overcome some of these limitations.

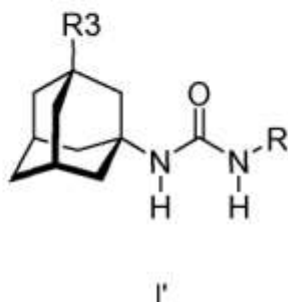
30

SUMMARY OF INVENTION

Inventors have found that by the simultaneous triple selection of: (i) urea as the core chemical functional group; (ii) the adamantan-1-yl group, optionally 3-substituted, as one
35 of the N-substituents of urea; and (iii) the replacement of the 2-methylene biradical of the adamantan-1-yl moiety by an oxygen atom, new sEH inhibitors are obtained that, compared with their adamantyl analogs, have similar activity, improved water solubility,

and lower melting points.

Many N-(adamantan-1-yl)ureas of general formula I' have been reported to be sEH inhibitors. Virtually all of them are unsubstituted in position 3 of the adamant-1-yl moiety, i.e. they have R₃ = H in their formula I'.



A vast majority of the specifically reported 3-unsubstituted N-(adamantan-1-yl)ureas with sEH inhibitor activity are disclosed in the following five patent documents, here referred to as Pat-Doc1 to Pat-Doc 5:

Pat-Doc 1: US 20050164951 A1; "Inhibitors for the soluble epoxide hydrolase"; University of California; 117 pp.; Chemical Abstracts Service Accession Number (CAS AN) = 2005:672863. This documents specifically discloses about 130 sEH inhibitors encompassed by formula I'.

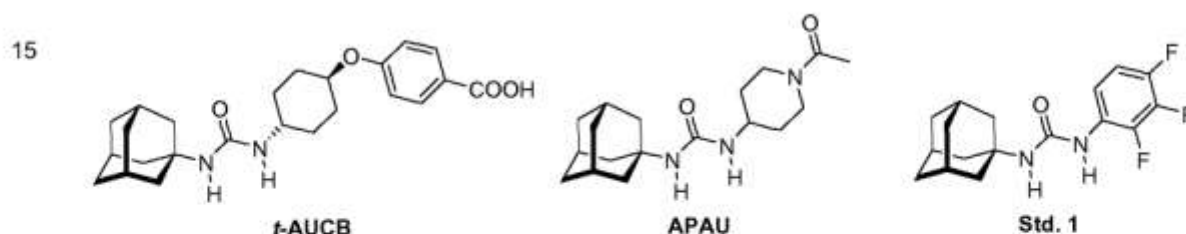
Pat-Doc 2: WO 2006045119 A2; "Improved inhibitors for the soluble epoxide hydrolase"; University of California; 179 pp.; CAS AN = 2006:386356. This document specifically discloses about 110 sEH inhibitors encompassed by formula I' which are not disclosed in Pat-Doc 1.

Pat-Doc 3: WO 2007106525 A1; "Piperidinyl, indolyl, pirinidyl, morpholinyl and benzimidazolyl urea derivatives as inhibitors of soluble epoxide hydrolase for the treatment of hypertension, inflammations and other diseases"; University of California & Arete Therapeutics; 116 pp.; CAS AN = 2007:1061416. This document specifically discloses 48 sEH inhibitors encompassed by formula I' which are not disclosed neither in Pat-Doc 1 nor in Pat-Doc 2.

Pat-Doc 4: WO 2008040000 A2; "Soluble epoxide hydrolase inhibitors"; Arete Therapeutics; 73 pp.; CAS AN = 2008:411908. This document specifically discloses 12 sEH inhibitors encompassed by formula I' which are not disclosed in any of the other Pat-Doc documents.

Pat-Doc 5: WO 2008051875 A2; "Soluble epoxide hydrolase inhibitors"; Arete Therapeutics; 58 pp.; CAS AN = 2008:529196. This document specifically discloses 6 sEH inhibitors encompassed by formula I' which are not disclosed in any of the other Pat-Doc documents.

Although hundreds of N-(adamantan-1-yl)ureas of the general formula I' with R3 = H have been specifically disclosed as sEH inhibitors, many of them in the aforementioned five Pat-Doc documents, only few are in pharmaceutical development. Among the latter the three below have been considered especially relevant by inventors, and inventors have synthesized and tested the analog N-(2-oxadamantan-1-yl)ureas of these three N-(adamantan-1-yl)ureas for illustrative comparative purposes.



An aspect of the present invention relates to the provision of compounds of formula I



or stereoisomers or pharmaceutically acceptable salts thereof, wherein:

30 R3 is a radical selected from the group consisting of H, C₁-C₃ alkyl, cyclohexyl and phenyl;

R is a radical $-\text{[CH}_2\text{]}_n\text{-Y}$, wherein n is an integer between 0 and 15, and in the $-\text{[CH}_2\text{]}_n\text{-}$ biradical an integer between 0 and n/3 of the methylene groups are optionally replaced by oxygen atoms in such a way that there are not two oxygen atoms which are adjacent;

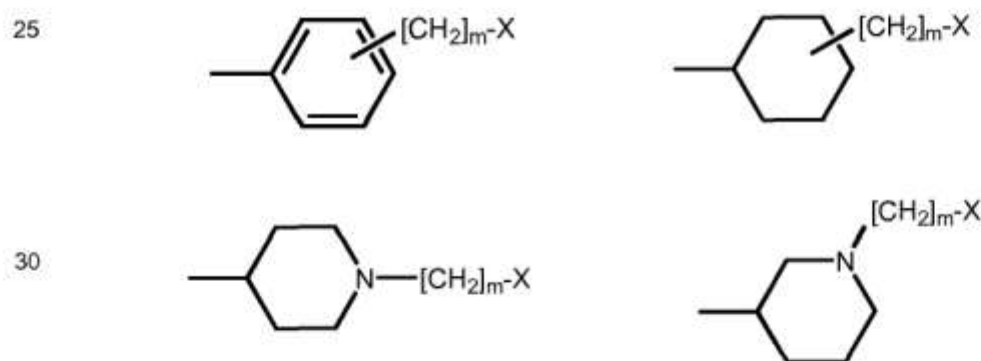
35 Y is a radical selected from the group consisting of: phenyl; a substituted phenyl; cyclohexyl; a substituted cyclohexyl; a piperidinyl; a substituted piperidinyl; a C- or N-

radical from a 5- or 6-membered aromatic heterocycle; and a C- or N-radical from a 5- or 6-membered aromatic heterocycle which is fused with a benzene ring; with the proviso that I is not 1-(2-oxadamantan-1-yl)-3-(3,4-dichlorophenyl)urea.

- 5 The compound 1-(2-oxadamantan-1-yl)-3-(3,4-dichlorophenyl)urea is not considered part of the present invention because its preparation was mentioned in patent US 3,539,626 (published in 1970, with priority of 1965), where some substituted ureas and thioureas are disclosed, saying that they have antibacterial activity (although no experimental data are provided). It is noteworthy that, of the more than twenty specific compounds which are prepared in this document, this is the only one having the 2-oxadamantan-1-yl moiety, all
10 the others having the adamantan-1-yl moiety.

In particular embodiments, Y is a radical selected from the group consisting of:

- 15 di- and tri-substituted phenyl radicals, wherein the two or three substituents, equal or different, are independently selected from the group consisting of F, Cl, SF₅, CF₃, OH, OCF₃, C₁-C₃ alkyl, and (C₁-C₃)-OCO;
- a C- or N-radical from a 5- or 6-membered aromatic heterocycle, having in the cycle one, two or three atoms of N, S or O;
- a C- or N-radical from a 5- or 6-membered aromatic heterocycle having in the cycle
20 one, two or three atoms of N, S or O, which is fused with a benzene ring; and radicals having one of the following four general formulas, wherein bonds crossing positions 3 and 4 of the phenyl and cyclohexyl rings mean substitution either in position 3 or in position 4 of the radical ring;



- wherein m is an integer between 0 and 15, and in the $-\text{[CH}_2\text{]}_m-$ biradical an integer
35 between 0 and $m/3$ methylene groups are optionally replaced by oxygen atoms in such a way that there are not two oxygen atoms which are adjacent;
X being a radical selected from the group consisting of:

H, F, Cl, SF₅, CF₃, OCF₃, OH, CN, COOH, C₁-C₃ alkyl, (C₁-C₃ alkyl)CO,
(C₁-C₃ alkyl)SO₂;

phenyl, phenoxy, benzoyl, mono-substituted phenyl, mono-substituted benzoyl and
mono-substituted phenoxy wherein the substituent is selected from the group
consisting of F, Cl, CHO, COCH₃, COOH, and H₂NSO₂;

(C₁-C₁₅ linear alkyl)O, (C₄-C₁₅ linear alkyl)CO, (C₁-C₁₅ linear alkyl)OCO,
(C₁-C₁₅ linear alkyl)NHCO, (C₁-C₁₅ linear alkyl)CONH, (C₄-C₁₅ linear alkyl)SO₂,
(C₁-C₁₅ linear alkyl)NHSO₂, (C₁-C₁₅ linear alkyl)SO₂NH;

(C₃-C₆ carbocyclyl)O, (C₃-C₆ carbocyclyl)CO, (C₃-C₆ carbocyclyl)OCO,
(C₃-C₆ carbocyclyl)NHCO, (C₃-C₆ carbocyclyl)CONH, (C₃-C₆ carbocyclyl)SO₂,
(C₃-C₆ carbocyclyl)NHSO₂, (C₃-C₆ carbocyclyl)SO₂NH;

(5/6-membered-N/O-heterocyclyl)O, (5/6-membered-N/O-heterocyclyl)CO,
(5/6-membered-N/O-heterocyclyl)OCO, (5/6-membered-N/O-
heterocyclyl)NHCO, (5/6-membered-N/O-heterocyclyl)CONH, (5/6-membered-
N/O-heterocyclyl)SO₂, (5/6-membered-N/O-heterocyclyl)NHSO₂, and
(5/6-membered-N/O-heterocyclyl)SO₂NH; wherein 5/6-membered-N/O-

heterocyclyl is a C- or N-radical from a 5- or 6-membered
heterocycle, the heterocycle being aromatic or non-aromatic, the
heterocycle having in the cycle one, two or three atoms of N, S or O;

and wherein the 5/6-membered-N/O-heterocyclyl radical is optionally
substituted by one or two substituents, equal or different, independently
selected from the group consisting of F, Cl, CF₃, C₁-C₃ alkyl, and (C₁-C₃
alkyl)NH.

In particular embodiments, Y is a radical selected from the group consisting of:
di- and a tri-fluorosubstituted phenyl radicals;

4-chloro-3-trifluoromethylphenyl;

3-chloro-4-trifluoromethylphenyl;

4-fluoro-3-trifluoromethylphenyl,

3-fluoro-4-trifluoromethylphenyl; and

radicals having the above-mentioned four formulas, with an X that is a radical selected
from the group consisting of: H, F, Cl, CF₃, OCF₃, OH, CN, COOH, (C₁-C₁₅ linear alkyl)O,
(C₁-C₁₅ linear alkyl)CO, (C₁-C₁₅ linear alkyl)OCO, phenyl, phenoxy, mono-substituted
phenyl and mono-substituted phenoxy, wherein the substituent is COOH, Cl or H₂NSO₂;

(C₁-C₁₅ linear alkyl)NHCO, (C₁-C₁₅ linear alkyl)CONH, (C₁-C₁₅ linear alkyl)SO₂, (C₁-C₁₅
linear alkyl)NHSO₂, (C₁-C₁₅ linear alkyl)SO₂NH; (5/6-membered-N/O-heterocyclyl)O, (5/6-
membered-N/O-heterocyclyl)CO, (5/6-membered-N/O-heterocyclyl)OCO, (5/6-membered-

N/O- heterocyclyl)-NHCO, (5/6-membered-N/O-heterocyclyl)CONH; (5/6-membered-N/O-heterocyclyl)SO₂, (5/6-membered-N/O-heterocyclyl)NHSO₂, and (5/6-membered-N/O-heterocyclyl)SO₂NH; wherein 5/6-membered-N/O-heterocyclyl now means a C-radical or a N-radical from any 5- or 6-membered heterocycle, the heterocycle being aromatic or non-aromatic, and the heterocycle having in the cycle either one N atom, or two N atoms, or simultaneously one N atom and one O atom.

In particular embodiments, compounds I have an integer n between 0 and 3, and consequently only one methylene group is optionally replaced by an oxygen atom. In another particular embodiment n is 0, and consequently R = Y.

In particular embodiments compounds I have an Y of the following formula.



In other particular embodiments compounds I have an Y of the following formula.



In other particular embodiments compounds I have an Y of the following formula.



More particular embodiments are those where Y have the three aforementioned general formula where integer m is between 0 and 3; and most particular those where m = 0.

30

In particular embodiments of the aforementioned compounds, X is a radical selected from the group consisting of: H, F, Cl, CF₃, OCF₃, OH, CN, COOH, (C₁-C₅ linear alkyl)O, (C₁-C₅ linear alkyl)CO, (C₁-C₅ linear alkyl)OCO, (C₁-C₅ linear alkyl)NHCO, (C₁-C₅ linear alkyl)CONH, (C₁-C₅ linear alkyl)SO₂, (C₁-C₅ linear alkyl)NHSO₂, (C₁-C₅ linear alkyl)SO₂NH, 2-pyridinyl, 3-pyridinyl, 4-pyridinyl, 4-morpholinyl, phenyl, phenoxy, a mono-substituted phenyl and a mono-substituted phenoxy, whose substitution in the two latter cases is done by a radical selected from the group consisting of COOH, Cl and

35

H₂NSO₂. Even more particular are the following specific compounds:

1-(2-oxadamantan-1-yl)-3-(1-acetylpiperidin-4-yl)urea; and
trans-1-(2-oxadamantan-1-yl)-3-[4-(4-carboxyphenoxy)cyclohexyl]urea.

- 5 Particular embodiments are also those compounds of formula I where Y is a trifluorosubstituted phenyl radical, 4-chloro-3-trifluoromethylphenyl, 3-chloro-4-trifluoromethylphenyl, 4-fluoro-3-trifluoromethylphenyl, or 3-fluoro-4-trifluoromethylphenyl.

Even more particular are the following specific compounds:

- 1-(2-oxadamantan-1-yl)-3-(2,3,4-trifluorophenyl)urea;
10 1-(3-methyl-2-oxadamantan-1-yl)-3-(2,3,4-trifluorophenyl)urea;
1-(3-ethyl-2-oxadamantan-1-yl)-3-(2,3,4-trifluorophenyl)urea;
1-(3-cyclohexyl-2-oxadamantan-1-yl)-3-(2,3,4-trifluorophenyl)urea;
1-(3-phenyl-2-oxadamantan-1-yl)-3-(2,3,4-trifluorophenyl)urea;

- 15 Other aspect of the present invention relates to pharmaceutical compositions comprising therapeutically effective amounts of compounds of formula I, or stereoisomers or pharmaceutically acceptable salts thereof, and adequate amounts of pharmaceutically acceptable excipients. Pharmacy in the context of the present invention relates both to human medicine and veterinary medicine.

- 20 From the results of the accompanying illustrative examples and by analogy with compounds of formula I' of prior art, inventors have concluded that compounds of formula I are sEH inhibitors. Thus, other aspect of the present invention relates to compounds of formula I, or stereoisomer or pharmaceutically acceptable salts thereof, for use in the
25 treatment of sEH mediated diseases. In particular embodiments the sEH mediated diseases are hypertension, atherosclerosis, pulmonary diseases, kidney diseases, stroke, pain, neuropathic pain, inflammation, pancreatitis, immunological disorders, eye diseases, cancer, obesity, diabetes, metabolic syndrome, preeclampsia, anorexia nervosa, depression, erectile dysfunction, wound healing, NSAID-induced ulcers, emphysema, scrapie and Parkinson's disease. In other words, the present invention is related to
30 methods of treatment of human patients suffering from a sEH mediated disease, by administration of pharmaceutical compositions comprising compounds of formula I and adequate amounts of pharmaceutically acceptable excipients. Methods for treatment of the aforementioned particular sEH mediated diseases are particular embodiments of the
35 present invention. And the aforementioned pharmaceutical compositions also forms part of the present invention.

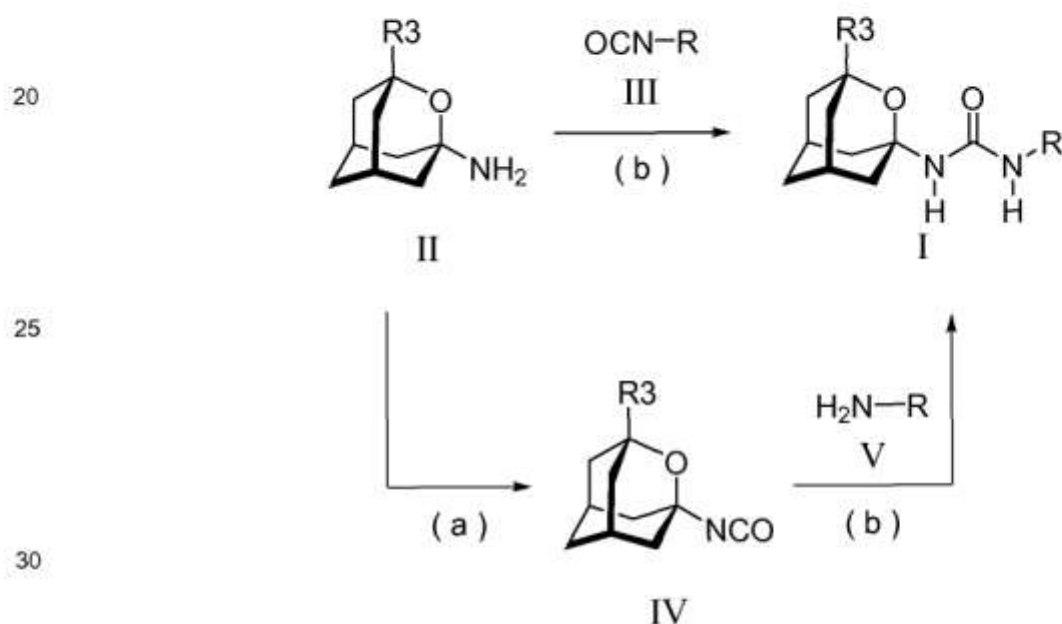
As compounds of formula I have never been disclosed for use in animal therapy, including human therapy, an aspect of the present invention relates to compounds of formula I, or stereoisomers or pharmaceutically acceptable salts thereof, for use as active pharmaceutical ingredients.

5

According to other aspect of the present invention, there are provided two alternative processes for the preparation of compounds of formula I from amines of formula II, as shown in the accompanying scheme.

10 According to the first alternative, amine of formula II, preferably in the form of a salt such as the hydrochloride, is reacted with isocyanate of formula OCN-R, in an inert solvent such as dichloromethane (DCM), and in the presence of a base such as triethylamine. According to the second alternative, in a first step (a) amine of formula II, preferably in the form of a salt, is converted into isocyanate of formula IV by reaction with an (NH₂→NCO)

15 converting reagent such as triphosgene, and in an inert solvent such as DCM. In a second step (b), amine of formula R-NH₂ is reacted with isocyanate of formula IV, a chemical transformation analogous to the one of the first alternative.



As a third alternative, not shown in the scheme, some compounds I with a given substituent R may be obtained from compounds I with a substituent R', R' being a precursor or a R-protected group. In the examples this is illustrated by the preparation of a compound I with R = piperidin-4-yl by palladium-catalyzed hydrogenation of a compound I with R' = benzylpiperidin-4-yl.

35

Amines of formula II are either commercially available or obtainable from known starting materials as disclosed in the art (cf. e.g. M.D. Duque et al., "Synthesis and pharmacological evaluation of (2-oxadamantan-1-yl)amines"; *Bioorg. Med. Chem.* 2009, vol. 17, pp. 3198-3206). Isocyanates of formula OCN-R and amines of formula R-NH₂ are either commercially available or obtainable as disclosed in the art, e.g. in the aformentioned documents Pat-Doc 1 and Pat-Doc 2.

IC₅₀ values of Table 1 illustrate that the N-(2-oxadamantan-1-yl)ureas of the present invention have an sEH inhibitory activity similar to their analog N-(adamantan-1-yl)ureas which are disclosed in the art as sEH inhibitors. In fact, compounds I_a to I_g have IC₅₀ values lower than 22 nM, which represents an acceptable activity for the target. Therefore, the introduction of an R3 radical in the 3 position of the 2-oxadamantyl moiety (illustrated by compounds I_b to I_e) does not involve a decrease in activity. It is noteworthy than compound I_a has an IC₅₀ value of 2.58 nM, which is significantly lower than the one of its parent adamantyl analog (7.74 nM, Std 1).

Experimental value of solubility (S) for compound I_a in Table 1 is higher than S for compound Std 1. In general, the N-(2-oxadamantan-1-yl)ureas of the present invention have water solubilities similar or higher than their analog N-(adamantan-1-yl)ureas which are disclosed in the art as sEH inhibitors, what is in accordance with their calculated values of logP, shown in same table as clogP. Results in Table 1 illustrate that compounds I_a to I_e have melting points substantially lower than their analog N-(adamantan-1-yl)ureas which are disclosed in the art as sEH inhibitors. Since it is known (cf. e.g. S.H. Hwang et al., "Orally bioavailable potent sEH inhibitors"; *J. Med. Chem.* 2007, vol. 50, pp. 3825-3840) that N-(adamantan-1-yl)ureas that are both poorly soluble in water and have a stable crystal structure as indicated by a high melting point are difficult to formulate, the physicochemical properties of the N-(2-oxadamantan-1-yl)ureas of the present invention are good both from the point of view of pharmacokinetics and formulation. This fact, together with their acceptable sEH inhibitory activities, makes the N-(2-oxadamantan-1-yl)ureas of the present invention promising API for the treatment of sEH mediated diseases.

The *in vitro* results of Example 24 and Table 2 show that compounds I_a and I_g behave in a manner similar to the compound used as comparative standard, in the reduction of endoplasmic reticulum (ER) stress induced by palmitate. Since it has been suggested that ER stress is involved in the appearance of insulin resistance, inflammation, neuropathic

pain, metabolic syndrome and related disorders, the facts that sEH inhibitors of formula I significantly reduce ER stress, that they are not cytotoxic, and that they can pass the cell membrane, also contribute to the conclusion that the N-(2-oxadamantan-1-yl)ureas of the present invention are promising API for the treatment of sEH mediated diseases.

5

According to Example 25, and the corresponding results in Table 3, inventors have found that selected compounds of the present invention present appropriate sEH inhibition activity values in pancreatic rat cells (AR42j), what makes them promising API for treatment of e.g. pancreatitis.

10

According to Example 26, and the corresponding results in Table 3, inventors have found that selected compounds of the present invention present relative low cytotoxicity values in human liver cells, what makes them promising for human treatment.

15

According to Example 27, and the corresponding results in Table 3, inventors have found that selected compounds of the present invention are likely able to cross the blood-brain barrier, what makes them promising for treating CNS diseases or disorders.

20

The epoxidation of arachidonic acid (AA) by selected cytochrome P450 epoxygenases generates epoxyeicosatrienoic acids (EETs). These EETs show anti-inflammatory, antihypertensive, analgesic, angiogenic, and antiatherosclerotic effects in rodents and humans. sEH converts EETs to their corresponding dihydroxyeicosatrienoic acids (DHETs), whereby the biological effects of EETs are diminished, eliminated, or altered. Among the P450 enzymes, it is known that CYP2C19 and CYP1A2 have the highest formation rate of EETs from AA (cf. A.A. El-Sherbeni et al. "Repurposing resveratrol and fluconazole to modulate human cytochrome P450-mediated arachidonic acid metabolites", *Molecular Pharmaceutics* 2016, vol. 13, pp. 1278-1288). For this reason, a highly desirable aspect of any new sEH inhibitor is selectivity in front of CYP2C19 and CYP1A2. Some selected compounds of the present invention (Ia, Ig, If, Io, Is, Iu, Iv, and Ix) were tested for their inhibition at 1 μ M of the human cytochrome P450 enzymes CYP1A2 and CYP2C19, and all displayed very weak inhibition ($\leq 6\%$).

25

30

Throughout the description and claims the word "comprise" and variations of the word, are not intended to exclude other technical features, additives, components, or steps.

35

Furthermore, the word "comprise" encompasses the case of "consisting of". Additional objects, advantages and features of the invention will become apparent to those skilled in the art upon examination of the description or may be learned by practice of the invention.

The following examples are provided by way of illustration, and they are not intended to be limiting of the present invention. Furthermore, the present invention covers all possible combinations of particular and preferred embodiments described herein.

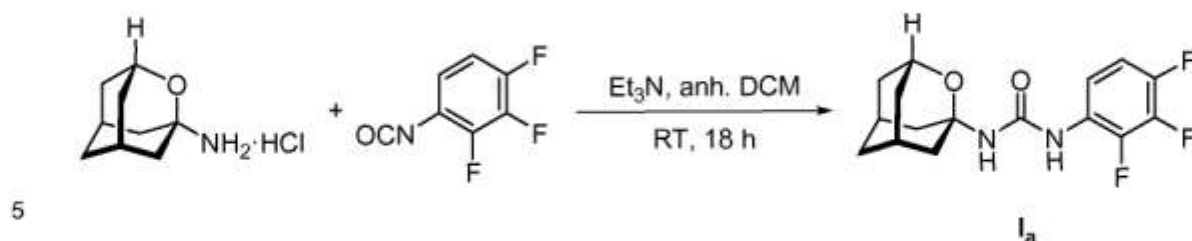
5 EXAMPLES

Analytical methods

- Melting points were determined in open capillary tubes with a MFB 595010 M Gallenkamp melting point apparatus.
- 10 - Infrared (IR) spectra, using the attenuated total reflectance (ATR) technique, were run on a Perkin-Elmer Spectrum RX I spectrophotometer. Absorption values are expressed as wavenumbers (cm^{-1}); only significant absorption bands are given.
- Gas Chromatography/Mass Spectrometry (GC/MS) analysis was carried out in an inert Agilent Technologies 5975 gas chromatograph equipped with an Agilent 122-5532 DB-
15 5MS 1b (30 m \times 0.25 mm) capillary column with a stationary phase of phenylmethylsilicon (5% diphenyl-95% dimethylpolysiloxane), using the following conditions: initial temperature of 50 °C (1 min), with a gradient of 10 °C/min up to 300 °C, and a temperature in the source of 250 °C, Solvent Delay (SD) of 4 min and a pressure of 7.35 psi. The direct insertion probe (DIP) technique was used. The electron impact (70 eV) or
20 chemical ionization (CH_4) techniques were used. Only significant ions are given: those with higher relative ratio, except for the ions with higher m/e values.
- Elemental analyses was carried out at the Microanalysis Service of the IIQAB (CSIC, Barcelona, Spain) with a Carlo Erba model 1106 analyzer.
- Column chromatography was performed on silica gel 60 Å C.C (35-70 mesh, SDS, ref
25 2000027). Thin-layer chromatography was performed with aluminum-backed sheets with silica gel 60 F254 (Sigma-Aldrich, ref 60805), and spots were visualized with UV light, 1% aqueous solution of KMnO_4 and/or iodine.
- Analytical grade solvents were used for crystallization, while pure for synthesis solvents were used in the reactions, extractions and column chromatography.
- 30 - The analytical samples of all of the new compounds which were subjected to pharmacological evaluation possess a purity $\geq 95\%$ as evidenced by their elemental analyses.

Example 1a: Preparation of 1-(2-oxadamantan-1-yl)-3-(2,3,4-trifluorophenyl)urea, I_a

35

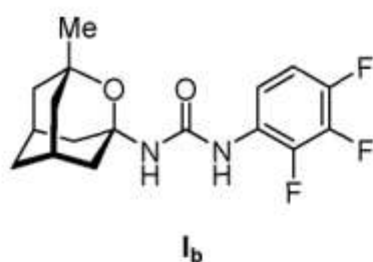


In a round-bottom flask equipped with a stir bar under nitrogen atmosphere 1.2 eq. of (2-oxaadaman-1-yl)amine hydrochloride was added to anhydrous dichloromethane (DCM) (~110 mM). To this suspension 1.0 eq. of 2,3,4-trifluorophenyl isocyanate followed by 7 eq. of triethylamine (TEA) was added. The reaction mixture was stirred at room temperature overnight. Then the solvent was removed under *vacuo* and the resulting crude was purified by column chromatography (SiO₂, Hexane/Ethylacetate mixture) of the crude and evaporation in *vacuo* of the appropriate fractions gave the urea **I_a** (163 mg, 94% yield) as a white solid, mp 196-198 °C. IR (ATR): 3300-2800 (3293, 3232, 3127, 2933, 2857), 1702, 1640, 1621, 1563, 1509, 1489, 1471, 1446, 1373, 1349, 1340, 1317, 1294, 1257, 1239, 1227, 1200, 1165, 1117, 1099, 1080, 1020, 996, 976, 963, 932, 912, 884, 840, 805, 788, 757, 683, 653 cm⁻¹. MS (DIP), *m/e* (%): 179 (11), 172 (18), 149 (97), 148 (100), 146 (36), 121 (12), 120 (10), 118 (13), 111 (11), 95 (17), 94 (26), 93 (11), 79 (20), 68 (18).

20 Anal. Calcd for C₁₆H₁₇F₃N₂O₂·0.05Pentane: C 59.15, H 5.37, F 17.28, N 8.49. Found: C 59.00, H 5.60, F 17.22, N 8.57.

Example 1b: Preparation of 1-(3-methyl-2-oxaadaman-1-yl)-3-(2,3,4-trifluorophenyl)urea, **I_b**

25



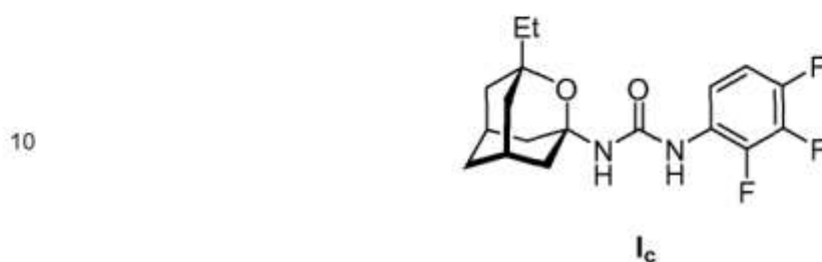
30

Using (3-methyl-2-oxaadaman-1-yl)amine in a process analogous to the one of Example 1a, the title compound was obtained in a 93% yield. Mp 195-197 °C. IR (ATR): 3300-2800 (3270, 3227, 3128, 2976, 2927, 2856), 1701, 1641, 1622, 1564, 1509, 1492, 1471, 1373, 1341, 1322, 1301, 1286, 1256, 1228, 1213, 1200, 1171, 1136, 1106, 1090, 1072, 1034, 1006, 991, 972, 959, 921, 899, 885, 804, 788, 755, 682, 670, 652 cm⁻¹. MS (DIP), *m/e*

35

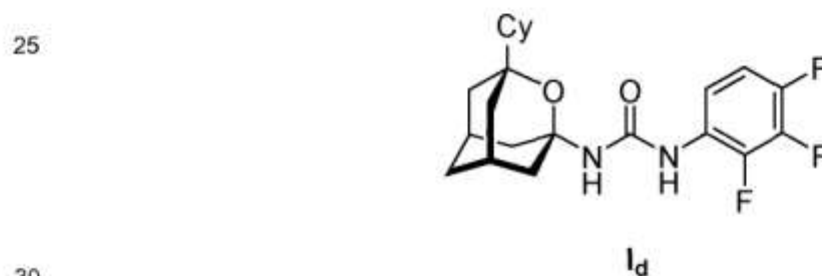
(%): 172 (13), 150 (14), 149 (100), 148 (80), 147 (25), 109 (10), 108 (14), 107 (11), 95 (10), 93 (25). Anal. Calcd for $C_{17}H_{19}F_3N_2O_2 \cdot 0.05H_2O$: C 59.84, H 5.64, F 16.70, N 8.21. Found: C 59.91, H 5.90, F 16.52, N 8.22.

5 **Example 1c: Preparation of 1-(3-ethyl-2-oxaadamantan-1-yl)-3-(2,3,4-trifluorophenyl)urea, 1c**



Using (3-ethyl-2-oxaadamantan-1-yl)amine in a process analogous to the one of Example
15 1a, the title compound was obtained in a 96% yield. Mp 165-166 °C. IR (ATR): 3300-2800 (3288, 3238, 3128, 2970, 2927, 2850), 1702, 1641, 1622, 1563, 1509, 1471, 1371, 1341, 1322, 1301, 1254, 1227, 1209, 1172, 1091, 1010, 996, 965, 939, 921, 896, 803, 788, 755, 669, 653 cm^{-1} . MS (DIP), *m/e* (%): 354 (M^+ , 5), 148 (14), 146 (100), 94 (10), 93 (10). Anal. Calcd for $C_{18}H_{21}F_3N_2O_2 \cdot 0.01EtOAc$: C 60.99, H 5.98, F 16.04, N 7.89. Found: C 60.97, H
20 6.06, F 16.23, N 7.84.

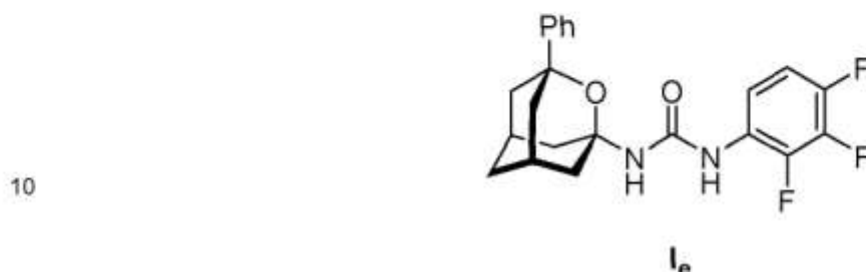
Example 1d: Preparation of 1-(3-cyclohexyl-2-oxaadamantan-1-yl)-3-(2,3,4-trifluorophenyl)urea, 1d



Using (3-cyclohexyl-2-oxaadamantan-1-yl)amine in a process analogous to the one of
Example 1a, the title compound was obtained in a 94% yield. Mp 193-195 °C. IR (ATR):
3300-2800 (3309, 3227, 3107, 2925, 2855), 1681, 1622, 1537, 1513, 1470, 1326, 1300,
35 1256, 1234, 1211, 1084, 1061, 1014, 994, 975, 892, 853, 825, 809, 763, 702, 678, 655
 cm^{-1} . MS (DIP), *m/e* (%): 408 (M^+ , 5), 178 (37), 176 (21), 172 (19), 152 (23), 148 (11), 147
(100), 135 (16), 120 (10), 110 (12), 95 (13), 94 (19), 93 (12), 83 (15), 81 (11), 67 (11), 55

(16). Anal. Calcd for $C_{22}H_{27}F_3N_2O_2 \cdot 0.60MeOH$: C 63.47, H 6.88, N 6.55. Found: C 63.44, H 7.17, N 6.63.

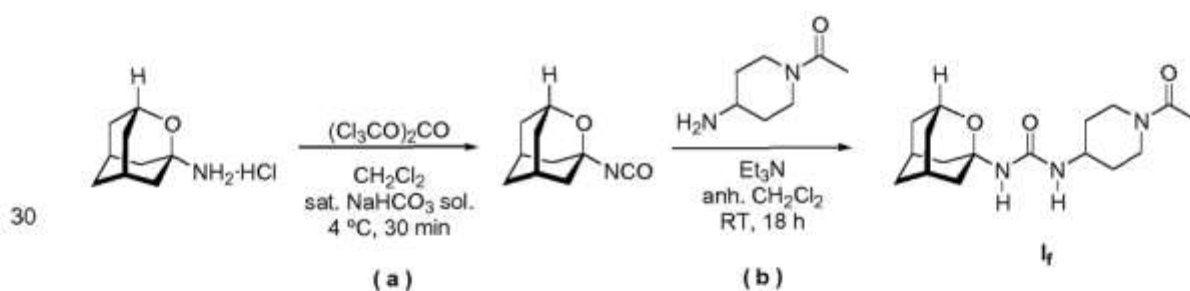
5 **Example 1e: Preparation of 1-(3-phenyl-2-oxaadmantan-1-yl)-3-(2,3,4-trifluorophenyl)urea, I_e**



Using (3-phenyl-2-oxaadmantan-1-yl)amine in a process analogous to the one of
 15 Example 1a, the title compound was obtained in a 70% yield. Mp 150-152 °C. IR (ATR): 3300-2800 (3312, 3238, 3118, 2922, 2856), 1697, 1621, 1555, 1514, 1470, 1324, 1262, 1235, 1208, 1179, 1094, 1079, 1017, 993, 976, 945, 897, 803, 751, 696, 669, 653 cm^{-1} . MS (DIP), m/e (%): 402 (M^+ , 13), 255 (19), 229 (13), 212 (14), 184 (15), 172 (25), 171 (15), 170 (14), 155 (22), 147 (100), 146 (11), 145 (15), 143 (10), 142 (27), 129 (16), 128 (10), 120 (16), 119 (10), 118 (26), 115 (10), 110 (17), 105 (26), 91 (17), 77 (23), 57 (12).
 20 Anal. Calcd for $C_{22}H_{21}F_3N_2O_3 \cdot 1.0H_2O$: C 62.85, H 5.51, N 6.66. Found: C 62.79, H 5.45, N 6.69.

25 **Example 2: Preparation of 1-(2-oxaadmantan-1-yl)-3-(1-acetylpiperidin-4-yl)urea, I_f**

25



35 **Step (a):** In a three-necked round-bottom flask equipped with a stir bar, low temperature thermometer and gas inlet, triphosgene (392 mg, 1.32 mmol) was added in a single portion to a solution of (2-oxaadmantan-1-yl)amine hydrochloride (500 mg, 2.63 mmol) in DCM (35 mL) and saturated aqueous $NaHCO_3$ solution (15 mL). The biphasic mixture was

stirred vigorously at 4 °C for 30 minutes. Afterwards, the phases were separated and the organic layer was washed with brine (20 mL), dried over anh. Na₂SO₄ and filtered. Evaporation under *vacuo* provided (2-oxaadamantan-1-yl)isocyanate (408 mg, 86% yield), that was used in next step without further purification. IR (ATR): 2235 (NCO band) cm⁻¹.

5

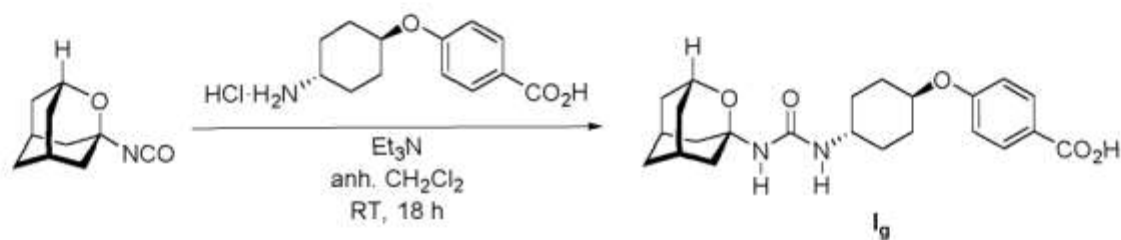
Step (b): Under anhydrous conditions, a solution of (2-oxaadamantan-1-yl)isocyanate (323 mg, 1.80 mmol) in anh. DCM (20 mL) was added to a solution of 1-acetyl-4-aminopiperidine (308 mg, 2.16 mmol) in anh. DCM (10 mL), followed by TEA (0.50 mL, 3.61 mmol). The reaction mixture was stirred at room temperature overnight. The solution

10 was then concentrated under *vacuo* to give an orange gum (720 mg). Purification by column chromatography (SiO₂, DCM/methanol mixture) gave the title compound I_f (300 mg, 52% yield) as a white solid. The analytical sample was obtained by washing with pentane, mp 172-173 °C. IR (ATR): 3322, 2920, 2850, 2153, 2000, 1637, 1549, 1428, 1369, 1313, 1264, 1234, 1192, 1139, 1090, 1046, 995, 959, 879, 816, 773, 731 cm⁻¹. MS (DIP), *m/e* (%): 321 (M⁺, 34), 197 (32), 179 (34), 169 (14), 155 (11), 154 (100), 153 (18), 143 (12), 138 (13), 137 (33), 136 (32), 127 (10), 126 (15), 125 (51), 124 (14), 122 (21), 111 (17), 110 (13), 99 (12), 96 (41), 95 (18), 94 (45), 93 (11), 85 (10), 84 (19), 83 (37), 82 (54), 81 (10), 79 (22), 70 (12), 69 (10), 68 (13), 67 (20), 57 (23), 56 (32), 55 (15). Anal. Calcd for C₁₇H₂₇N₃O₃·0.2H₂O: C 62.82, H 8.50, N 12.93. Found: C 62.70, H 8.59, N 12.74.

20

Example 3: Preparation of *trans*-1-(2-oxaadamantan-1-yl)-3-[4-(4-carboxyphenoxy)cyclohexyl]urea, I_g

25



30

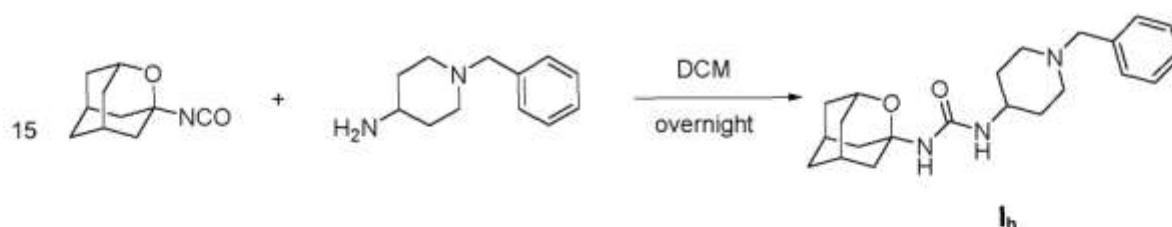
A solution of (2-oxaadamantan-1-yl)isocyanate (400 mg, 2.23 mmol) in anh. DCM (25 mL) was added to a solution of *trans*-4-(4-aminocyclohexyloxy)benzoic acid hydrochloride (728 mg, 2.68 mmol) in anh. DCM (12 mL), followed by TEA (1.24 mL, 8.94 mmol) under nitrogen. The reaction mixture was stirred at room temperature overnight. Water (50 mL)

35 was then added and the phases were separated. The organic layer was extracted with further water (2 x 50 mL) and the pH of the combined aqueous phases was adjusted to pH ~ 2 with 5N HCl solution, prior extraction with DCM (3 x 50 mL). The combined organic

layers were dried over anh. Na_2SO_4 , filtered and concentrated under *vacuo* yielding **I_g** (220 mg, 24% yield) as a white solid. The analytical sample was obtained by crystallization with methanol/diethyl ether, mp 255-275 °C. IR (ATR): 3364, 3267, 3198, 3061, 2922, 2559, 2348, 2187, 2068, 2011, 1977, 1672, 1601, 1552, 1443, 1369, 1347, 1320, 1231, 1196, 1172, 1110, 1091, 1049, 1027, 989, 959, 863, 828, 774, 698, 640 cm^{-1} . MS (DIP), *m/e* (%): 179 (27), 153 (13), 139 (11), 138 (100), 124 (11), 122 (29), 121 (39), 111 (21), 108 (10), 98 (99), 96 (30), 95 (14), 94 (45), 93 (13), 82 (18), 81 (97), 80 (12), 79 (41), 77 (11), 69 (13), 67 (19), 65 (15), 57 (11), 56 (42), 55 (16), 53 (12). Anal. Calcd for $\text{C}_{23}\text{H}_{30}\text{N}_2\text{O}_5 \cdot 0.1\text{H}_2\text{O}$: C 66.36, H 7.31, N 6.73. Found: C 66.13, H 7.32, N 6.64.

10

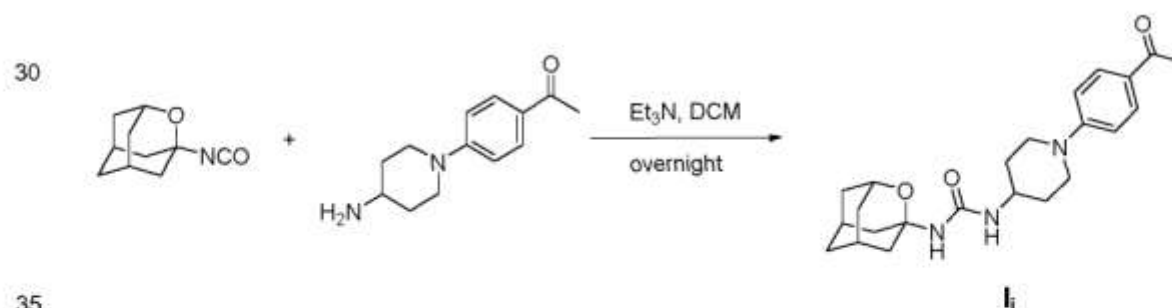
Example 4: Preparation of 1-(2-oxaadmant-1-yl)-3-(1-benzylpiperidin-4-yl)urea, **I_h**



To a solution of 2-oxaadmant-1-yl isocyanate (1.25 g, 6.97 mmol) in DCM (10 mL) was added 1-benzylpiperidin-4-amine (1.60 g, 8.37 mmol). The reaction mixture was stirred at room temperature overnight. The solvents were evaporated under vacuum to give a yellow gum (3.06 g). Column chromatography (dichloromethane/methanol mixtures) gave **I_h** as a yellowish solid (2.54 g, 82% yield). Mp 153-154 °C. IR (ATR): 694, 745, 768, 989, 110, 1194, 1225, 1319, 1372, 1441, 1484, 1540, 1664, 1918, 1959, 2918 cm^{-1} . Accurate mass calcd for $[\text{C}_{22}\text{H}_{31}\text{N}_3\text{O}_2+\text{H}]^+$: 370.2489 Found: 370.2488.

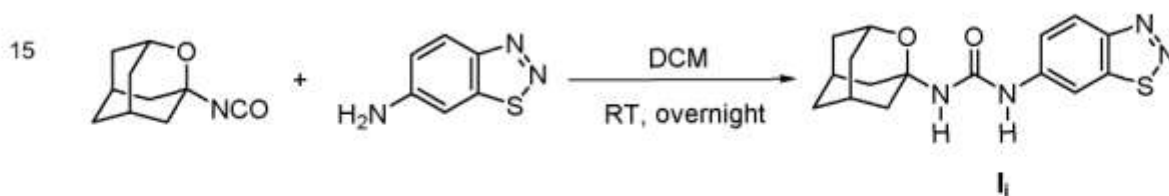
25

Example 5: Preparation of 1-(1-(4-acetylphenyl)piperidin-4-yl)-3-(2-oxaadmant-1-yl)urea, **I_i**



To a solution of 2-oxaadmantan-1-yl isocyanate (188 mg, 1.05 mmol) in DCM (5 ml), 1-(4-(4-aminopiperidin-1-yl)phenyl)ethan-1-one (230 mg, 1.05 mmol, prepared following the procedure reported in WO2007016496) and triethylamine (0.15 mL, 1.05 mmol) were added. The reaction mixture was stirred at room temperature overnight. The solvents were evaporated under vacuum to give an orange solid (410 mg). Column chromatography (Dichloromethane/Methanol mixtures) gave **I_i** as a white solid (183 mg, 45% yield), mp 190-191 °C. IR (ATR): 674, 723, 770, 819, 866, 915, 953, 974, 995, 1111, 1134, 1194, 1222, 1279, 1315, 1330, 1475, 1537, 1597, 1653, 1992, 2160, 2341, 2930 cm⁻¹. Anal. Calcd for C₂₃H₃₁N₃O₃ · 0.25 H₂O: C 68.72%, H 7.90%, N 10.45%. Found: C 68.66%, H 7.78%, N 10.21%.

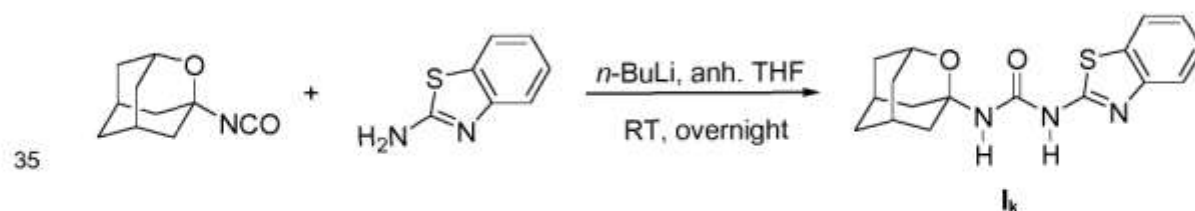
Example 6: Preparation of 1-(2-oxaadmantan-1-yl)-3-(benzo[d][1,2,3]thiadiazol-6-yl)urea, **I_j**



20 A solution of 2-oxaadmantan-1-yl isocyanate (150 mg, 0.84 mmol) in DCM was treated with benzo[d][1,2,3]thiadiazol-6-amine (115 mg, 0.76 mmol). The reaction mixture was stirred at room temperature overnight. The solvents were evaporated under vacuum to give a brownish orange solid (299 mg). **I_j** was obtained by crystallization from hot EtOAc as a pale orange solid (175 mg, 70% yield), mp 199 °C. IR (ATR): 760, 206, 818, 822, 880, 964, 999, 1062, 1088, 1132, 1179, 1194, 1246, 1288, 1320, 1350, 1372, 1405, 1453, 1471, 1537, 1572, 1661, 1681, 1928, 1940, 2069, 2129, 2188, 2263, 2421, 2471, 2560, 2848, 2918, 3111, 3121, 3260, 3338, 3533, 3642, 3776, 3880 cm⁻¹. Anal. Calcd for C₁₆H₁₈N₄O₂S · 0.1 C₄H₈O: C 58.07%, H 5.59%, N 16.52%, S 9.45%. Found: C 58.20%, H 5.46%, N 16.54%, S 9.19%.

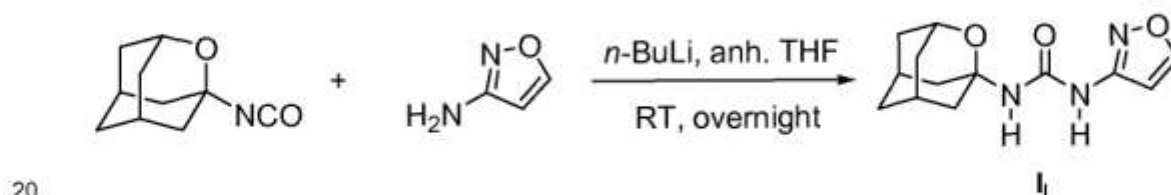
30

Example 7: Preparation of 1-(2-oxaadmantan-1-yl)-3-(benzo[d]thiazol-2-yl)urea, **I_k**



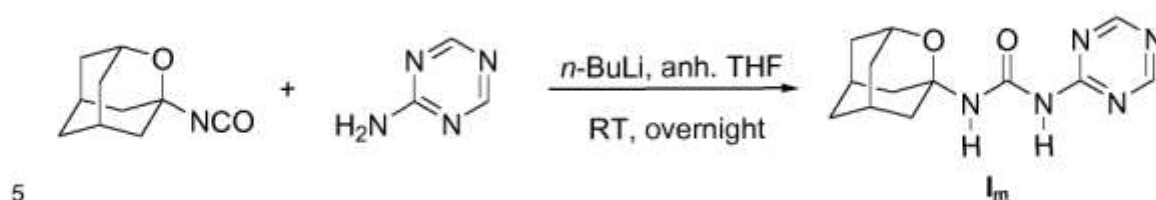
2-amino-1,3-benzothiazole (114 mg, 0.76 mmol) was dissolved in anh. THF (7 mL) under argon and cooled to -78 °C on a dry ice in acetone bath. Then, 2.5 M *n*-butyllithium in hexanes (0.31 mL, 0.76 mmol) was added dropwise during 20 minutes. Afterwards, the reaction mixture was removed from the dry ice in acetone bath and tempered to 0 °C with an ice bath. Meanwhile, 2-oxaadmant-1-yl isocyanate (150 mg, 0.84 mmol) was dissolved in anh. THF (4 mL) under argon and was continuously added to the reaction mixture. The mixture was stirred at room temperature overnight. Methanol (3 mL) was added to quench any unreacted *n*-butyllithium. The precipitate formed was filtered and washed with ice-cold THF to afford **1_k** as a white solid (151 mg, 42% yield), mp 240 °C (dec). IR (ATR): 731, 757, 788, 822, 866, 884, 920, 964, 995, 1046, 1093, 1119, 1191, 1248, 1274, 1323, 1341, 1377, 1452, 1514, 1537, 1597, 1718, 1904, 1992, 2036, 2134, 2201, 2852, 2894, 2930, 3064, 3255, 3322 cm⁻¹. Accurate mass calcd for [C₁₇H₁₉N₃O₂S+H]⁺: 330.1271 Found: 330.1272.

Example 8: Preparation of 1-(2-oxaadamantan-1-yl)-3-(isoxazol-3-yl)urea, 1_l



3-aminoisoxazole (103 mg, 1.22 mmol) was dissolved in anh. THF (13 mL) under argon and cooled to -78 °C on a dry ice in acetone bath. Then, 2.5 M *n*-butyllithium in hexanes (0.50 mL, 1.22 mmol) was added dropwise during 20 minutes. Afterwards, the reaction mixture was removed from the dry ice in acetone bath and tempered to 0 °C with an ice bath. Meanwhile, 2-oxaadmant-1-yl isocyanate (258 mg, 1.34 mmol) was dissolved in anh. THF (6 mL) under argon and was continuously added to the reaction mixture. The mixture was stirred at room temperature overnight. Methanol (4.5 mL) was added to quench any unreacted *n*-butyllithium. The organic solvents were evaporated under vacuum to give an orange gum (371 mg). Column chromatography (Hexane/Ethyl Acetate mixtures) gave **1_l** as a white solid (90 mg, 22% yield), mp 193 °C. IR (ATR): 768, 788, 824, 888, 929, 959, 965, 987, 1014, 1050, 1075, 1093, 1116, 1196, 1260, 1288, 1324, 1377, 1395, 1444, 1475, 1566, 1598, 1672, 1685, 1920, 2005, 2051, 2158, 2215, 2323, 2369, 2851, 2923, 3082, 3179, 3287 cm⁻¹. Anal. Calcd for C₁₃H₁₇N₃O₃: C 59.30%, H 6.51%, N 15.96%. Found: C 59.46%, H 6.70%, N 14.31%.

Example 9: Preparation of 1-(2-oxaadamantan-1-yl)-3-(1,3,5-triazin-2-yl)urea, 1_m



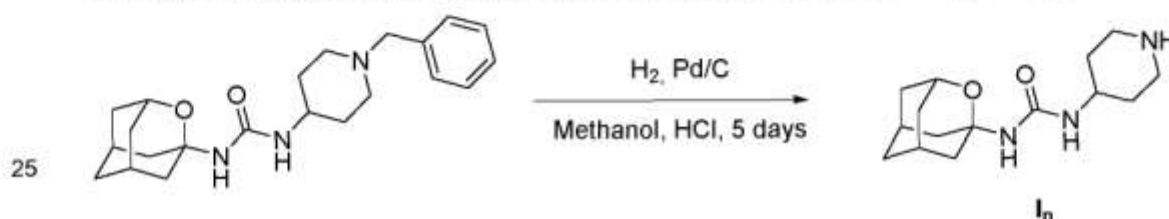
2-amino-1,3,5-triazine (245 mg, 2.55 mmol) was dissolved in anhydrous THF (20 mL) under argon and cooled to $-78\text{ }^{\circ}\text{C}$ on a dry ice in acetone bath. Then, 2.5 M *n*-butyllithium in hexanes (1.05 mL, 2.55 mmol) was added dropwise during 20 minutes. Afterwards, the reaction mixture was removed from the dry ice in acetone bath and tempered to $0\text{ }^{\circ}\text{C}$ with an ice bath. Meanwhile, 2-oxaadmant-1-yl isocyanate (539 mg, 2.80 mmol) was dissolved in anhydrous THF (8 mL) under argon and was continuously added to the reaction mixture. The mixture was stirred at room temperature overnight. Methanol (9 mL) was added to quench any unreacted *n*-butyllithium. A white precipitate formed among the orange solution was filtered and washed with ice-cold THF to afford **Im** as a white solid (340 mg, 35% yield), mp $157\text{--}158\text{ }^{\circ}\text{C}$. IR (ATR): $700, 783, 824, 887, 965, 997, 1080, 1117, 1186, 1194, 1270, 1320, 1343, 1372, 1395, 1402, 1480, 1482, 1502, 1590, 1625, 1700, 2000, 2055, 2170, 2260, 2345, 2546, 2847, 2922, 3233, 3383, 3498\text{ cm}^{-1}$. Accurate mass calcd for $[\text{C}_{13}\text{H}_{17}\text{N}_5\text{O}_2+\text{H}]^+$: 276.1455. Found: 276.1454.

10

15

20

Example 10: Preparation of 1-(2-oxaadmant-1-yl)-3-(piperidin-4-yl)urea, **In**

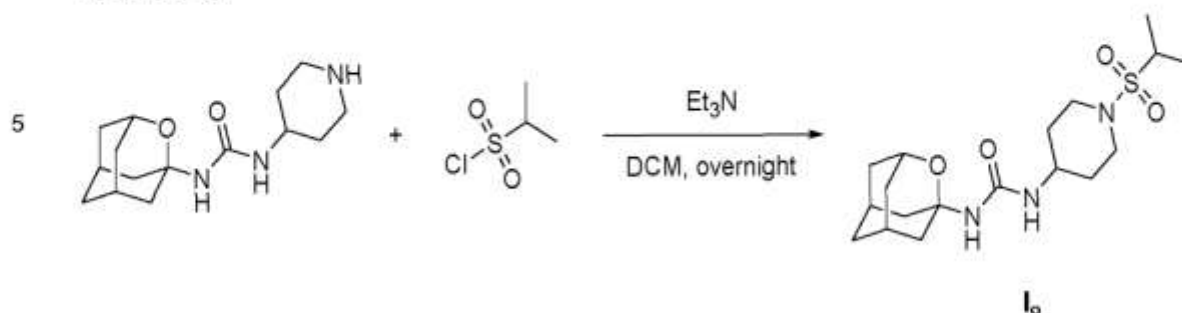


To a solution of 1-(2-oxaadmant-1-yl)-3-(1-benzylpiperidin-4-yl)urea (2.40 g, 6.50 mmol) in methanol (20 mL), Palladium on carbon 10% wt. (300 mg) and HCl 37% (1 mL) were added. The reaction mixture was hydrogenated for 5 days. The palladium on carbon was filtered and the solvent was evaporated under vacuum. The crude was dissolved in DCM and washed with 2N NaOH solution (2 x 30 mL). The organic phase was dried over anhydrous Na_2SO_4 and filtered. Evaporation under vacuum of the organics gave **In** as a white solid (1.28 g, 70% yield). The analytical sample was obtained by crystallization from hot DCM (825 mg), Accurate mass calcd. for $[\text{C}_{15}\text{H}_{25}\text{N}_3\text{O}_2+\text{H}]^+$: 280.2020. Found: 280.2022.

30

35

Example 11: Preparation of 1-(2-oxaadamant-1-yl)-3-(1-(isopropylsulfonyl)piperidin-4-yl)urea, I_o



10

To a solution of 1-(2-oxaadamant-1-yl)-3-(piperidin-4-yl)urea (250 mg, 0.895 mmol) in DCM (10 mL), triethylamine (0.15 mL, 1.07 mmol) was added. The mixture was cooled down with an ice bath (0°C) and propane-2-sulfonyl chloride (127 mg, 0.89 mmol) was added dropwise. The reaction mixture was stirred at room temperature overnight and quenched by the addition of HCl solution 37% (2 mL). The organic phase was collected and the aqueous layer was extracted with EtOAc (4 x 30 mL). The combined organic phases were dried over anhydrous Na₂SO₄ and filtered. Evaporation of the organics gave an oil that was then dissolved in DCM (20 mL) and washed with 2N NaOH solution (3 x 20 mL). The organic phase was dried over anhydrous Na₂SO₄ and filtered. Evaporation under vacuum of the

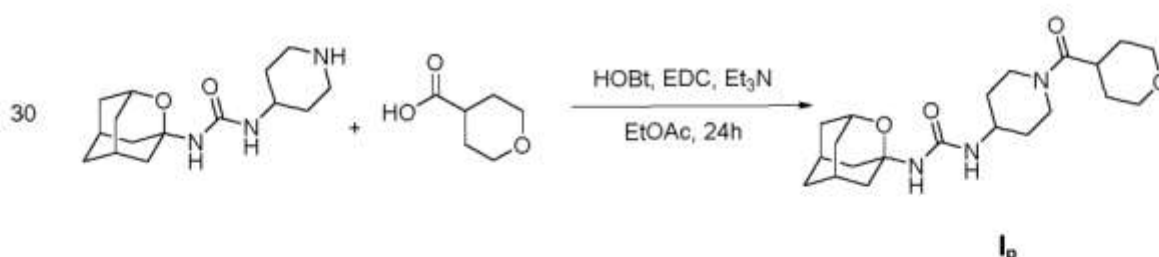
15

20

25

organics gave **I_o** as a white solid (88 mg, 26% yield). The analytical sample was obtained by crystallization from hot DCM as a white solid (60 mg), mp 190-191 °C. IR (ATR): 618, 729, 842, 884, 935, 961, 1010, 1041, 1093, 1116, 1132, 1196, 1243, 1269, 1292, 1320, 1374, 1444, 1547, 1635, 2930, 3333 cm⁻¹. Anal. Calcd for C₁₈H₃₁N₃O₄S · 0.3 CH₂Cl₂ · 0.2 C₆H₁₄: C 54.69%, H 8.01%, N 9.81%. Found: C 54.72%, H 7.91%, N 9.86%.

Example 12: Preparation of 1-(2-oxaadamant-1-yl)-3-(1-(tetrahydro-2H-pyran-4-carbonyl)piperidin-4-yl)urea, I_p

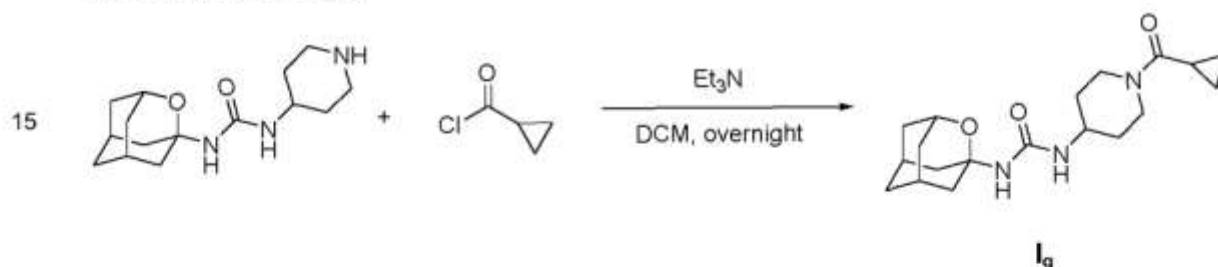


35 To a solution of 1-(2-oxaadamant-1-yl)-3-(piperidin-4-yl)urea (150 mg, 0.53 mmol) in EtOAc (10 mL), tetrahydro-2H-pyran-4-carboxylic acid (70 mg, 0.53 mmol), HOBt (109 mg, 0.80 mmol), EDC (125 mg, 0.80 mmol) and triethylamine (0.15 mL, 1.07 mmol) were

added. The reaction mixture was stirred at room temperature for 24 hours. To the resulting suspension was added water (15 mL) and the two phases were separated. The organic phase was washed with saturated aqueous NaHCO₃ solution (15 mL) and brine (15 mL). The combined aqueous phases were extracted with DCM (3 x 30 mL). The combined organic phases were dried over anh. Na₂SO₄ and filtered. Evaporation under vacuum of the organics gave **I_p** as colorless crystals (190 mg, 90% yield), mp 150-152 °C. IR (ATR): 641, 770, 878, 990, 1085, 1121, 1194, 1240, 1318, 1367, 1442, 1550, 1633, 2010, 2067, 2341, 2919 cm⁻¹. Anal. Calcd for C₂₁H₃₃N₃O₄ · 0.8 H₂O: C 62.14%, H 8.59%, N 10.35%. Found: C 62.20%, H 8.55%, N 10.38%.

10

Example 13: Preparation of 1-(2-oxadamant-1-yl)-3-(1-(cyclopropanecarbonyl)-piperidin-4-yl)urea, **I_q**

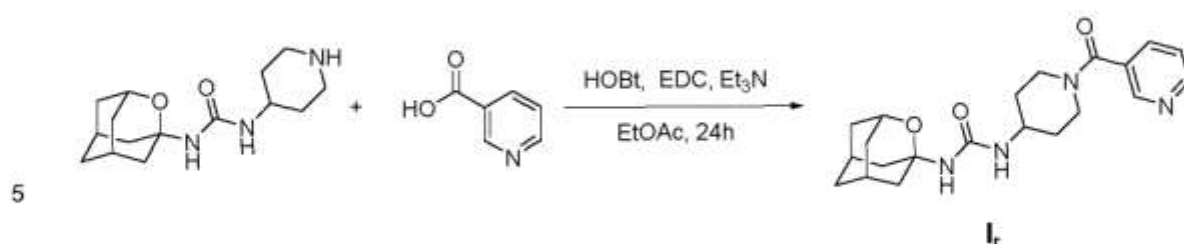


20 To a solution of 1-(2-oxadamant-1-yl)-3-(piperidin-4-yl)urea (300 mg, 1.07 mmol) in DCM (10 mL), cyclopropanecarbonyl chloride (112 mg, 1.07 mmol) and triethylamine (0.18 mL, 1.29 mmol) were added. The reaction mixture was stirred at room temperature overnight and quenched by the addition of aqueous HCl 37% solution (3 mL). The organic phase was collected and the aqueous phase was extracted with EtOAc (4 x 10 mL). The combined organic phases were washed with NaOH 2N (2 x 30 mL), dried over anh. Na₂SO₄ and filtered. Evaporation under vacuum of the organics gave **I_q** as a yellow oil (382 mg, 48% yield). The analytical sample was obtained as a white solid (180 mg) by crystallization from hot EtOAc. Mp 197-198 °C. IR (ATR): 612, 729, 816, 876, 922, 961, 992, 1085, 1132, 1191, 1219, 1266, 1310, 1369, 1447, 1555, 1604, 1640, 2925, 3307 cm⁻¹. Anal. Calcd for C₁₉H₂₅N₃O₃ · 0.9 H₂O: C 62.75%, H 8.54%, N 11.55%. Found: C 63.10%, H 8.57% N 11.15%.

30

Example 14: Preparation of 1-(2-oxadamant-1-yl)-3-(1-(nicotinoyl)piperidin-4-yl)urea **I_r**

35



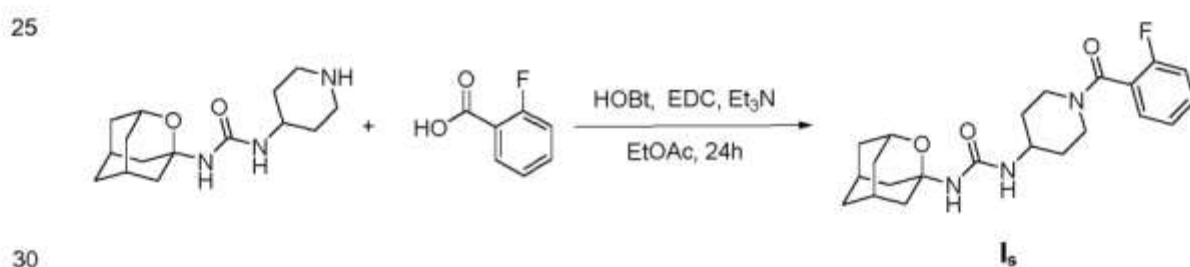
To a solution of 1-(2-oxadamant-1-yl)-3-(piperidin-4-yl)urea (150 mg, 0.53 mmol) in EtOAc (10 mL), nicotinic acid (66 mg, 0.53 mmol), HOBt (109 mg, 0.805 mmol), EDC (125 mg, 0.80 mmol) and triethylamine (0.15 mL, 1.07 mmol) were added. The reaction mixture was stirred at room temperature for 24 hours. Water (15 mL) was added to the resulting suspension and the two phases were separated. The organic phase was washed with saturated aqueous NaHCO₃ solution (15 mL) and brine (15 mL). The combined aqueous phases were basified with 1N NaOH solution (30 mL) and extracted with DCM (3 x 30 mL). The combined organic phases were dried over anhydrous Na₂SO₄ and filtered. Evaporation under vacuum of the organics gave a white solid (140 mg). Column chromatography (Dichloromethane/Methanol mixtures) gave pure **1_r** as a white solid (63 mg, 32% yield), mp 187-188 °C. IR (ATR): 618, 711, 736, 767, 824, 990, 1114, 1132, 1194, 1219, 1245, 1269, 1318, 1367, 1436, 1483, 1537, 1622, 1666, 2051, 2144, 2217, 2919 cm⁻¹. Accurate mass calcd for [C₂₁H₂₈N₄O₃+H]⁺: 385.2234. Found: 385.2238.

10

15

20

Example 15: Preparation of 1-(2-oxadamant-1-yl)-3-(1-(2-fluorobenzoyl)piperidin-4-yl)urea, **1_s**

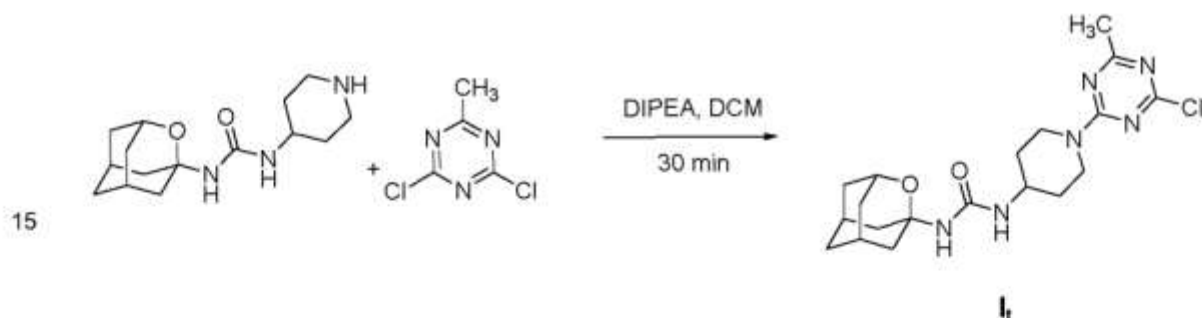


To a solution of 1-(2-oxadamant-1-yl)-3-(piperidin-4-yl)urea (120 mg, 0.43 mmol) in EtOAc (10 mL), 2-fluorobenzoic acid (61 mg, 0.43 mmol), HOBt (87 mg, 0.64 mmol), EDC (100 mg, 0.64 mmol) and triethylamine (0.12 mL, 0.86 mmol) were added. The reaction mixture was stirred at room temperature for 24 hours. Water (15 mL) and DCM (20 mL) were added to the resulting suspension and the two phases were separated. The organic phase was washed with saturated aqueous NaHCO₃ solution (15 mL), brine (15 mL),

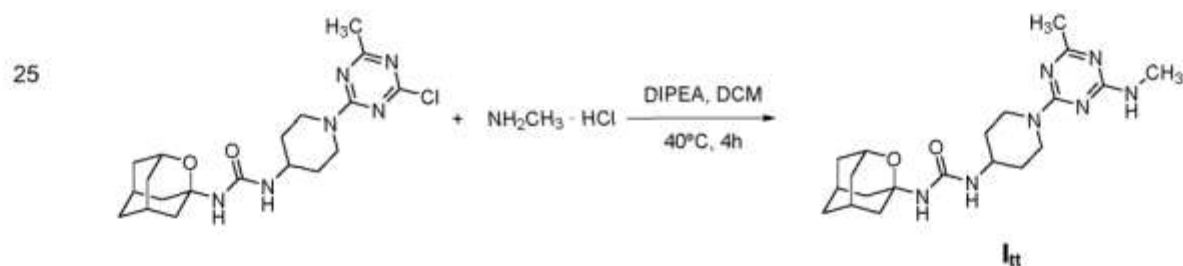
35

dried over anh. Na_2SO_4 and filtered. Evaporation under vacuum of the organics gave **I₃** as a white solid (131 mg, 77% yield). The analytical sample was obtained as a white solid (111 mg) by crystallization from hot EtOAc. Mp 193-194 °C. IR (ATR): 630, 785, 925, 987, 1010, 1093, 1121, 1191, 1243, 1318, 1372, 1447, 1462, 1491, 1555, 1615, 1684, 1974, 2351, 2925, 3338 cm^{-1} . Anal. Calcd for $\text{C}_{22}\text{H}_{28}\text{FN}_3\text{O}_3$: C 65.82%, H 7.03%, N 10.47%. Found: C 65.88%, H 7.25%, N 10.36%.

Example 16: Preparation of 1-(2-oxaadamant-1-yl)-3-(1-(4-chloro-6-methyl-1,3,5-triazin-2-yl)piperidin-4-yl)urea **I₃; and 1-(2-oxaadamant-1-yl)-3-(1-(4-methyl-6-(methylamino)-1,3,5-triazin-2-yl)piperidin-4-yl)urea, **I₄****



To a solution of 2,4-dichloro-6-methyl-1,3,5-triazine (130 mg, 0.78 mmol) in DCM (4 mL) were added 1-(2-oxaadamant-1-yl)-3-(piperidin-4-yl)urea (220 mg, 0.78 mmol) and DIPEA (305 mg, 2.36 mmol). The reaction mixture was stirred at room temperature for 30 minutes. The yellow solution was used in the next step without further purification.



30 Methylamine hydrochloride (160 mg, 2.36 mmol) and DIPEA (407 mg, 3.15 mmol) were added to the solution of 1-(2-oxaadamant-1-yl)-3-(1-(4-chloro-6-methyl-1,3,5-triazin-2-yl)piperidin-4-yl)urea in DCM obtained in the previous step. The reaction mixture was stirred at 40°C for 4 hours. The solvent was evaporated under vacuum to give a yellow gum (830 mg). Column chromatography (Dichloromethane/Methanol mixtures) gave **I₄** as a white solid (54 mg, 9% yield) and **I₃** as a grey solid (27 mg, 8% yield).

35

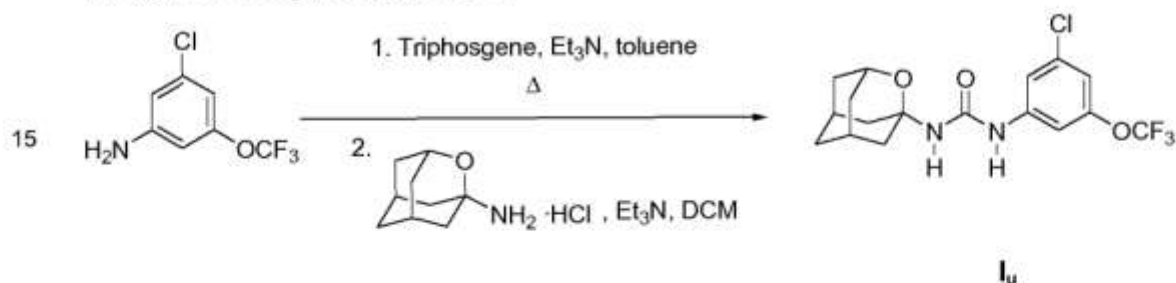
I_{tt} : Mp 203-204 °C. IR (ATR): 653, 803, 880, 993, 1085, 1118, 1189, 1235, 1317, 1366, 1442, 1532, 1644, 1943, 2143, 2337, 2843, 2920 cm^{-1} . Accurate mass calcd for $[\text{C}_{20}\text{H}_{31}\text{N}_7\text{O}_2+\text{H}]^+$: 402.2612. Found: 402.2608.

5

I_t : Mp 196-197 °C. IR (ATR): 708, 762, 845, 907, 964, 992, 1075, 1116, 1168, 1194, 1219, 1243, 1271, 1315, 1364, 1444, 1485, 1527, 1578, 1671, 1953, 1974, 1994, 2180, 2335, 2852, 2914 cm^{-1} . Accurate mass calcd for $[\text{C}_{19}\text{H}_{27}\text{ClN}_6\text{O}_2+\text{H}]^+$: 407.1957. Found: 407.1952.

10

Example 17: Preparation of 1-(2-oxadamant-1-yl)-3-(3-chloro-5-trifluoromethoxy)phenyl)urea, I_u



20 1. A solution of 3-chloro-5-(trifluoromethoxy)aniline (200 mg, 0.94 mmol) in toluene (3 mL) was treated with triphosgene (140 mg, 0.47 mmol). Immediately, triethylamine (0.13 mL, 0.94 mmol) was added and the reaction mixture was stirred at 70 °C for 2 hours. Afterwards, pentane (0.5 mL) was added and a white precipitate was formed. The mixture was filtered and pentane was evaporated under vacuum at room temperature to give the isocyanate in toluene solution that was used in the next step without further purification.

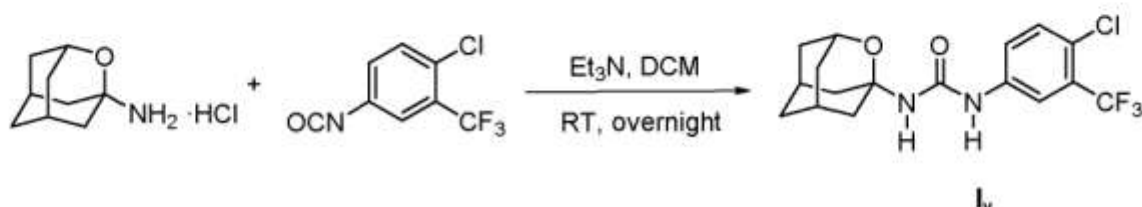
25

2. To a solution of 3-(trifluoromethoxy)-5-chlorophenyl isocyanate from the previous step were added DCM (5 mL), 2-oxadamantan-1-amine hydrochloride (161 mg, 0.85 mmol) and triethylamine (0.24 mL, 1.71 mmol). The suspension was stirred at room temperature overnight. The mixture was evaporated under vacuum to give a residue that was then dissolved in DCM (20 mL) and washed with 2N HCl solution. The organic phase was dried over anhydrous Na_2SO_4 and filtered. Evaporation under vacuum of the organics gave I_u (284 mg, 89% overall yield) as an orange solid. The analytical sample was obtained as a white solid (100 mg) by crystallization from hot DCM, mp 177-178 °C. IR (ATR): 672, 747, 935, 964, 995, 1093, 1116, 1152, 1191, 1212, 1248, 1416, 1465, 1550, 1599, 1664, 2930,

35

3302 cm^{-1} . Anal. Calcd for $\text{C}_{17}\text{H}_{18}\text{ClF}_3\text{N}_2\text{O}_3$: C 52.25%, H 4.64%, N 7.17%. Found: C 52.05%, H 4.8%, N 7.02%.

Example 18: Preparation of 1-(2-oxaadaman-1-yl)-3-(4-chloro-3-(trifluoromethyl)phenyl)urea, I_v

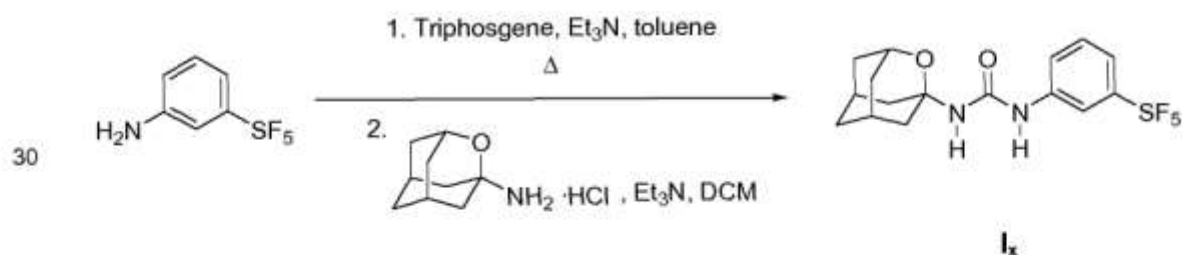


To a solution of the 4-chloro-3-(trifluoromethyl)phenyl isocyanate (191 mg, 0.84 mmol) in DCM were added 2-oxaadaman-1-amine hydrochloride (145 mg, 0.76 mmol) and triethylamine (0.21 mL, 1.52 mmol). The reaction mixture was stirred at room temperature overnight. The mixture was evaporated under vacuum to give a solid that was then dissolved in EtOAc (20 mL) and washed with 2N HCl solution (10 mL). The organic phase was dried over anhydrous Na_2SO_4 and filtered. Evaporation under vacuum of the organics gave I_v as a white solid (238 mg, 83% yield). The analytical sample was obtained by crystallization from hot EtOAc (127 mg), mp 196 °C. IR (ATR): 661, 721, 765, 785, 824, 835, 881, 930, 961, 987, 1028, 1093, 1114, 1134, 1170, 1191, 1209, 1253, 1289, 1297, 1323, 1374, 1416, 1485, 1550, 1586, 1607, 1671, 2118, 2144, 2217, 2351, 2847, 2925, 3054, 3100, 3235, 3286 cm^{-1} . Anal. Calcd for $\text{C}_{17}\text{H}_{18}\text{ClF}_3\text{N}_2\text{O}_2$: C 54.48%, H 4.84%, N 7.47%. Found: C 54.57%, H 4.84%, N 7.64%.

15

20

Example 19: Preparation of 1-(2-oxaadaman-1-yl)-3-(3-(pentafluoro- λ^6 -sulfanyl)phenyl)urea, I_x

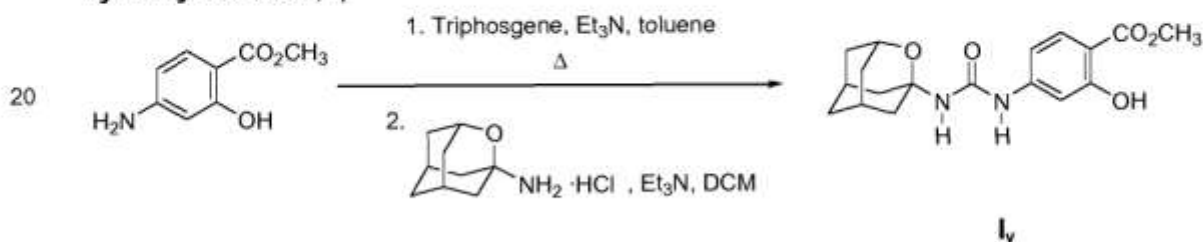


1. A solution of 3-(pentafluoro- λ^6 -sulfanyl)aniline (185 mg, 0.84 mmol) in toluene (3.6 mL) was treated with triphosgene (125 mg, 0.42 mmol). Immediately, triethylamine (0.12 mL, 0.84 mmol) was added and the reaction mixture was stirred at 70 °C for 2 hours.

Afterwards, pentane (0.5 mL) was added and a white precipitate was formed. The mixture was filtered and pentane was evaporated under vacuum at room temperature to give the isocyanate in toluene solution that was used in the next step without further purification.

- 5 2. To a solution of the 3-(pentafluoro- λ^6 -sulfanyl)phenyl isocyanate were added DCM (5 mL), 2-oxaadamantan-1-amine hydrochloride (145 mg, 0.76 mmol) and triethylamine (0.21 mL, 1.52 mmol). The suspension was stirred at room temperature overnight. The mixture was evaporated under vacuum to give a solid that was then dissolved in DCM (20 mL) and washed with aqueous 2N HCl solution. The organic phase was dried over anhydrous
- 10 Na_2SO_4 and filtered. Evaporation under vacuum of the organics gave **I_x** (237 mg, 71% overall yield) as a pale yellow solid. The analytical sample was obtained by crystallization from hot EtOAc as a white solid (75 mg), mp 203 °C. IR (ATR): 649, 685, 734, 785, 824, 835, 863, 946, 959, 990, 1093, 1114, 1199, 1250, 1256, 1292, 1318, 1369, 1431, 1478, 1537, 1591, 1671, 1966, 2041, 2930, 3080, 3224, 3286 cm^{-1} . Accurate mass calcd for
- 15 $[\text{C}_{16}\text{H}_{19}\text{F}_5\text{N}_2\text{O}_2\text{S}+\text{H}]^+$: 399.1160 Found: 399.1172.

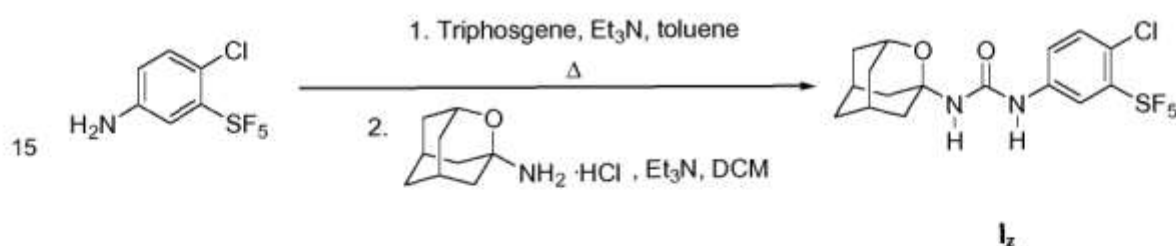
Example 20: Preparation of methyl 4-(3-(2-oxaadamantan-1-yl)ureido)-2-hydroxybenzoate, I_y



- 25 1. A solution of Methyl 4-amino-2-hydroxybenzoate (140 mg, 0.84 mmol) in toluene (3.6 mL) was treated with triphosgene (124 mg, 0.42 mmol). Immediately, triethylamine (0.12 mL, 0.84 mmol) was added and the reaction mixture was stirred at 70 °C for 2 hours. Afterwards, pentane (0.5 mL) was added and a white precipitate was formed. The mixture was filtered and pentane was evaporated under vacuum at room temperature to provide
- 30 the isocyanate in toluene solution that was used in the next step without further purification.
2. To a solution of the Methyl 2-hydroxy-4-isocyanatobenzoate were added DCM (5 mL), 2-oxaadamantan-1-amine hydrochloride (145 mg, 0.76 mmol) and triethylamine (0.21 mL,
- 35 1.52 mmol). The orange solution was stirred at room temperature overnight. The mixture was evaporated under vacuum to give a solid that was then dissolved in DCM (20 mL)

and washed with aqueous 2N HCl solution. The organic phase was dried over anhydrous Na_2SO_4 and filtered. Evaporation under vacuum of the organics gave 240 mg of a yellow solid. Column chromatography (dichloromethane/methanol mixtures) gave **I₁** as a beige solid (47 mg, 16% overall yield), mp 202 °C. IR (ATR): 700, 711, 760, 780, 827, 837, 868, 886, 928, 956, 992, 1008, 1033, 1095, 1106, 1157, 1194, 1222, 1219, 1253, 1294, 1315, 1333, 1346, 1369, 1405, 1439, 1540, 1599, 1628, 1671, 1976, 2082, 2211, 2273, 2366, 2852, 2925, 3116, 3245 cm^{-1} . Anal. Calcd for $\text{C}_{18}\text{H}_{22}\text{N}_2\text{O}_5 \cdot 0.5 \text{H}_2\text{O}$: C 60.83%, H 6.52%, N 7.88%. Found: C 60.87%, H 6.51%, N 7.58%.

Example 21: Preparation of 1-(2-oxaadamantan-1-yl)-3-(4-chloro-3-(pentafluoro- λ^6 -sulfanyl)phenyl)urea, **I₂**



1. A solution of 4-chloro-3-(pentafluoro- λ^6 -sulfanyl)aniline (340 mg, 1.34 mmol) in toluene (4 mL) was treated with triphosgene (199 mg, 0.67 mmol). Immediately, triethylamine (0.82 mL, 1.34 mmol) was added and the reaction mixture was stirred at 70 °C for 2 hours. Afterwards, pentane (1 mL) was added and a white precipitate formed. The mixture was filtered and pentane was evaporated under vacuum at room temperature to give the isocyanate in toluene solution that was used in the next step without further purification.

25

2. To a solution of the 4-chloro-3-(pentafluoro- λ^6 -sulfanyl)phenyl isocyanate were added DCM (5 mL), 2-oxaadamantan-1-amine hydrochloride (285 mg, 1.50 mmol) and triethylamine (0.38 mL, 2.74 mmol). The suspension was stirred at room temperature overnight. The mixture was evaporated under vacuum to give a solid that was then dissolved in DCM (40 mL) and washed with aqueous 2N HCl solution. The organic phase was dried over anhydrous Na_2SO_4 and filtered. Evaporation under vacuum of the organics gave 493 mg of a brown solid. Column chromatography (Hexane/Ethyl Acetate mixtures) gave **I₂** as a pale orange solid (116 mg, 20% overall yield), mp 217-218 °C. IR (ATR): 646, 672, 700, 742, 757, 783, 814, 827, 853, 899, 935, 964, 995, 1008, 1033, 1067, 1093, 1116, 1132, 1147, 1194, 1250, 1294, 1310, 1354, 1374, 1442, 1480, 1535, 1553, 1589, 1602, 1659, 1958, 1976, 2005, 2015, 2093, 2196, 2852, 2919, 3095, 3317 cm^{-1} . Accurate mass calcd for $[\text{C}_{16}\text{H}_{18}\text{ClF}_5\text{N}_2\text{O}_2\text{S}-\text{H}]$: 431.0625. Found: 431.0629.

35

Example 22: *In vitro* determination of sEH inhibition activity

The following fluorescent assay was used for determination of the sEH inhibition activity (IC_{50}), with the substrate and comparative control compounds ("standards") indicated below.

Substrate: 3-(Phenyl-oxiranyl)-acetic acid cyano-(6-methoxy-naphthalen-2-yl)-methyl ester (PHOME; from Cayman Chemical, item number 10009134; CAS 1028430-42-3); cf. N.M. Wolf et al., *Anal. Biochem.* 2006, vol. 355, pp. 71-80.

Standard 1 (Std 1): 1-(Adamantan-1-yl)-3-(2,3,4-trifluorophenyl)urea. **Standard 2 (Std 2):** 1-(Adamantan-2-yl)-3-(2,3,4-trifluorophenyl)urea (cf. E.J. North et al., *Bioorg. Med. Chem.* 2013, vol. 21, pp. 2587-2599).

Solutions:

- Assay buffer: Bis/Tris HCl 25 mM pH 7.0 containing 0.1 mg/mL of bovine serum albumin (BSA).

- PHOME at 200 μ M in DMSO.

- Solution of recombinant human sEH (Cayman Chemical, item number 10011669), diluted with assay buffer.

- Inhibitors dissolved in DMSO at appropriated concentrations.

Protocol: In a black 96-well plate (Greiner Bio-One, item number 655900), fill the background wells with 90 μ L and the positive control and inhibitor wells with 85 μ L of assay buffer. Add 5 μ L of DMSO to background and positive control wells, and then add 5 μ L of inhibitor solution in inhibitor wells. Add 5 μ L of the solution of hSEH to the positive control and inhibitor wells and mix several time. Prepare a 1/21 dilution of the solution of PHOME with assay buffer according to final volume required, and then add 105 μ L of each well. Shake carefully the plate for 10 seconds and incubate for 5 minutes at room temperature. Read the appearance of fluorescence with excitation wavelength: 337 nm, and emission wavelength: 460 nm (FLUOStar OPTIMA microplate reader, BMG). The intensity of fluorescence was used to analyze and calculate the IC_{50} values. Results were obtained by regression analysis from at least three data points in a linear region of the curve. IC_{50} values are average of minimum three independent replicates. Results are given as means \pm Standard Error (cf. Table 1).

Example 23: Determination of water solubility

The stock solutions (10^{-2} M) of the assayed compounds were diluted to decreased molarity, from 200 μ M to 1.02 nM, in 384 well transparent plate (Greiner 781101) with 5% DMSO : 95% PBS buffer. After, they were incubated at 37 °C and solubility S (Table 1)

was read after 2 and 4 h in a NEPHELOstar Plus (BMG LABTECH). Results were adjusted to a segmented regression to obtain the maximum concentration in which compounds are soluble.

- 5 **Table 1: sEH inhibition activity, clogP, solubility and melting points of selected compounds (I) compared with the selected standard**

Compound	IC ₅₀ (nM) ± SE	clogP	S (µg/L)	mp (°C)
Std 1	7.74 ± 0.06	4.04	66	216-219
la	2.58 ± 0.28	2.71	77	196-198
lb	21.3 ± 5.4	3.23	63	195-197
lc	8.1 ± 3.2	3.76	77	165-166
ld	17.5 ± 3.6	5.26	--	193-195
le	21.3 ± 4.3	4.27	--	150-152
lf	19.8 ± 6.2	-0.37	>100	172-173
lg	13.4 ± 4.0	3.70	>100	255-257
lo	--	1.06	>100	190-191
ls	--	1.66	>100	193-194
lu	--	4.57	45	177-178
lv	--	4.45	60	196
lx	--	3.65	>100	203

- 10 **Example 24: Amelioration of the endoplasmic reticulum (ER) stress, illustrated by the reduction of expression of genes involved**

Cell culture: Huh-7 cells were maintained in a humid atmosphere of 5% CO₂ at 37 °C in high glucose (25 mM) Dulbecco's modified Eagle's medium supplemented with 10% heat-inactivated fetal bovine serum, 1% of penicillin/streptomycin (10.000 units/mL of penicillin and 10.000 µg/mL of streptomycin) and 1% of amphotericin B (250 µg/mL).

- 15 **Cell treatment:** Huh-7 cells were serum-starved overnight prior treatment. Lipid-containing media were prepared by conjugation of palmitic acid with 2% fatty acid-free BSA, as previously described (cf. L. Salvado et al., "Oleate prevents saturated-fatty-acid-induced ER stress, inflammation, and insulin resistance in skeletal muscle cells through an AMPK-dependent mechanism", *Diabetologia* 2013, vol. 56, pp. 1372-1382). For RNA
20 extraction, cells were pre-treated with the inhibitors (final concentration 1 µM) for 1 hour before treatment with palmitate (final concentration 0.5 mM) and inhibitors (final

concentration 1 μ M). For each condition, at least 3 replicates were performed. Following 48 hours of incubation, RNA were extracted as described below.

Real-Time PCR: Total RNA in hepatocytes was harvested by TRIsure (Bioline) according to the manufacturer's instructions. The extracted RNA was dissolved in RNase-free water and concentrations of total RNA were quantified using a NanoDrop 2000c spectrophotometer (Thermo Scientific). First-stranded cDNA was synthesized from 0.5 μ g total RNA (Life Technologies). Primer Express Software (Applied Biosystems, Foster City, CA, USA) was used to design the primers examined with SYBR Green I (primers are described in X. Palomer et al., "PPAR β/δ attenuates palmitate-induced endoplasmic reticulum stress and induces autophagic markers in human cardiac cells", *Int. J. Cardiol.* 2014, vol. 174, pp. 110-118). The PCR reaction contained 10 ng of reverse-transcribed RNA, 2X IQ™ SYBRGreen Supermix (BioRad, Barcelona, Spain) and 900 nmol/L concentration of each primer. Optical primer amplification efficiency for each primer set was assessed and a dissociation protocol was carried out to assure a single PCR product. PCR assays were performed on a MiniOpticon™ Real-Time PCR system (BioRad). Thermal cycling conditions were as follows: activation of Taq DNA polymerase at 95 °C for 10 min, followed by 40 cycles of amplification at 95 °C for 15 sec and 60 °C for 1 min. The relative levels of specific mRNA were estimated from the value of the threshold cycle (Ct) of the real-time PCR adjusted by that of a housekeeping gene (GAPDH) through the formula $2^{\Delta\Delta C_t}$ ($\Delta C_t = \text{Gene of interest Ct} - \text{GAPDH Ct}$). Cf. Table 2, where CT: control, PAL: palmitate. ***, $P < 0.001$ vs control; #, $P < 0.05$ vs palmitate; ###, $P < 0.01$ vs palmitate; ####, $P < 0.001$ vs palmitate

Table 2. Levels of ATF3, CHOP and BiP mRNA after administration of selected compounds

Gene	CT	PAL	PAL + Std 2	PAL + Ia	PAL + Ig
ATF3	100.0 \pm 29.4	585.5 \pm 102.3 (***)	225.6 \pm 21.2 (###)	191.4 \pm 22.6 (###)	286.7 \pm 59.9 (###)
BiP	100.0 \pm 10.7	242.9 \pm 25.9 (***)	135.1 \pm 16.2 (###)	129.0 \pm 20.5 (###)	174.9 \pm 31.4 (#)
CHOP	100.0 \pm 12.2	224.5 \pm 9.8 (***)	141.8 \pm 23.7 (###)	129.9 \pm 37.6 (###)	147.6 \pm 15.9 (##)

Example 25: *In vitro* determination of sEH inhibition activity in AR42j cells

The following fluorescent cell-based assay was used for determination of the sEH inhibition activity (IC_{50}), with the Cellular KIT (Cell-Based Assay sEH inhibitor) (Cayman. Ref. 600090).

CBA-Buffer (10X): Cell-Based sEH Assay Buffer 60 mL (Item No. 600091).

CBA Digitonin Solution: 250 μ L (Item No. 600092).

CBA sEH Substrate: 100 μ L Epoxy-Fluor7 in DMSO (Item No. 600095).

CBA Standard: 100 μ L of 100 μ M CBA 6-methoxy-2-naphthalaldehyde (Item No. 600094).

CBA sEH Positive Control: 10 μ L of 1 mg/mL recombinant human sEH (Item No. 600093).

- 5 **CBA sEH inhibitor:** 50 μ L of 10 mM AUDA in DMSO (Item No. 600096).

Solutions preparation:

- Assay buffer 1x: add 10 mL of the CBA-Buffer (10X) to 90 mL of distilled water.

- Lysis Buffer: add 50 μ L of the CBA Digitonin Solution to 10 mL of Buffer Assay 1x.

- 10 - Substrate Solution: dilute 10 μ L of CBA sEH Substrate with 10 mL of Assay Buffer 1x.

- Standards: preparation of 7 concentrations of CBA 6-methoxy-2-naphthalaldehyde from 0 until 2 μ M with Assay Buffer 1x.

- sEH Positive Control: Prepare another stock A (1 μ g/ml: 1 μ L CBA sEH Positive Control + 1mL Assay Buffer 1x). From the already prepared stock A, prepare 250 μ L of sEH (10

- 15 ng/mL): 2.5 μ L sEH stock A + 250 μ L Assay Buffer 1x).

- sEH Inhibitor AUDA: dilute 10 μ L CBA sEH Inhibitor with 500 ml Assay Buffer 1x.

- Inhibitors dissolved in DMSO at appropriated concentrations.

- Protocol:** Seed cells in a 96-well plate at a density of (2×10^4) - (5×10^4) cells/well in 100 μ L
20 of culture medium with or without compounds to be tested. Incubation of the cells in a CO₂
incubator at 37 °C for 48 hours. Aspirate the culture medium and add 200 μ L of Assay
Buffer 1x to each well. Centrifuge the plate at 800 rpm for 5 minutes. Aspirate the
supernatant and add 100 μ L of Lysis Buffer to each well. Incubate with gentle shaking on
an orbital shaker for 30 minutes at room temperature. Centrifuge the plate at 3000 rpm for
25 20 minutes at 4 °C. Transfer 90 μ L of the supernatants to the 96-Well Solid Plate (black).
Add 10 μ L Assay Buffer 1x or 10 μ L of the AUDA solution to appropriate wells. For
positive control wells, add 100 μ L of the 10 ng/mL sEH Positive Control to two wells. Add
200 μ L of 6-methoxy-2-Naphthalaldehyde Standards to corresponding wells of the black
plate. Add 100 μ L of the sEH Substrate Solution to each well, except the standards.
30 Incubate the plate at 37 °C for 30 minutes. Read the appearance of fluorescence with
excitation wavelength: 337 nm, and emission wavelength of each well: 460 nm (Modulus
microplate 9300-002, Turner Biosystems). The intensity of fluorescence was used to
analyze and calculate inhibition percentages, shown in the Table as average of minimum
three independent replicates. Results are given as means \pm Standard Error (cf. Table 3).

35

Example 26: Determination of cytotoxicity in THLE-2 cells

Cytotoxic effects of assayed compounds were tested using the immortalized human liver cell line THLE-2 (ATCC CRL-2706). Cells were cultured in BEGM medium (Clonetics #CC-4175) containing all the supplements kit except additional EGF and G418. Medium was completed by adding 0.7 µg/mL phosphoethanolamine, 0.5 ng/mL epidermal growth factor, antibiotics (penicillin and streptomycin) and 10% fetal bovine serum (FBS).

Cells were plated in 96-well black microplates at 10,000 cells/well density and were incubated at 37 °C (5% CO₂, 95% humidity) for 24 h to allow the cells to adhere and form a monolayer. Test compounds were solubilized in 100% DMSO at a concentration curve way and then diluted with cell culture medium containing 10% DMSO. The final concentrations of the test compounds (1% DMSO) ranged from 0-100 µM in a final volume of 200 µL. Microplates were maintained at 37°C (5% CO₂, 95% humidity) during 3 days. Following this 72 h exposure to test compounds, cell viability in each well was determined by measuring the concentration of cellular adenosine triphosphate (ATP) using the ATP1Step Kit as described by the manufacturer (Perkin-Elmer). In a typical procedure, 50 µL of cell reagent is added to all wells of each test plate followed by incubation for 10 min at room temperature on an orbital shaker. ATP concentration was determined by reading chemical luminescence using the Envision plate reader (PerkinElmer). The percentage of viable cells relative to the non-drug treated controls was determined for each well and LC₅₀ values were calculated as concentrations projected to kill 50% of the cells following a 72 h exposure, an average of minimum two independent replicates. Results are given as means ± Standard Error (cf. Table 3).

Example 27: Parallel Artificial Membrane Permeation Assays- Blood-Brain Barrier

To evaluate the brain penetration of the different compounds, a parallel artificial membrane permeation assay for blood-brain barrier (PAMPA-BBB) was used, following the method described by L. Di et al., "High throughput artificial membrane permeability assay for blood-brain barrier", *Eur. J. Med. Chem.* 2003, vol. 38. pp. 223-232. The *in vitro* permeability (P_e) of the test compounds through lipid extract of porcine brain membrane was determined. Assayed compounds were tested using a mixture of PBS:EtOH (70:30). Assay validation was made by comparing the experimental permeability with the reported values of the commercial drugs by bibliography and lineal correlation between experimental and reported permeability of the fourteen commercial drugs using the parallel artificial membrane permeation assay was evaluated ($y = 1.537 x - 0.967$; $R^2 = 0.9382$). From this equation and taking into account the limits established by Di et al. for BBB permeation, the ranges of permeability were established, as follows. Compounds of

high BBB permeation (CNS+): $Pe (10^{-6} \text{ cm s}^{-1}) > 5.181$; compounds of low BBB permeation (CNS-): $Pe (10^{-6} \text{ cm s}^{-1}) < 2.107$; and compounds of uncertain BBB permeation (CNS+/-): $5.181 > Pe (10^{-6} \text{ cm s}^{-1}) > 2.107$. The permeability results from the assayed compounds are averages of three independent replicates and a predictive penetration in the CNS is also given. Qualitative results are shown in Table 3 (n.d. = not determined).

Table 3. sEH inhibition activity in cell culture, cytotoxicity, and CNS prediction

Compound	% Inhn. \pm SE (100 μM)	LC ₅₀ (μM)	CNS prediction
Std 1	56.6 \pm 11.0	n.d.	--
la	35.8 \pm 4.7	>100	CNS+
lb	n.d.	>100	CNS+
lc	n.d.	>100	CNS+
lg	58.3 \pm 3.2	>100	CNS+
lf	42.1 \pm 5.0	>100	n.d.
lo	40.89 \pm 1.99	>100	CNS-
ls	45.3 \pm 3.5	>100	CNS-
lv	51.6 \pm 6.6	45.8 \pm 3.8	CNS+

LIST OF REFERENCES

Non-patent literature cited in the description

- 5 H.C. Shen, *Expert. Opin. Ther. Patents* 2010, vol. 20, pp. 941-956.
H.C. Shen and B.D. Hammock, *J. Med. Chem.* 2012, vol. 55, pp. 1789-1808.
M.D. Duque et al., *Bioorg. Med. Chem.* 2009, vol. 17, pp. 3198-3206.
S.H. Hwang et al., *J. Med. Chem.* 2007, vol. 50, pp. 3825-3840.
A.A. El-Sherbeni et al., *Molecular Pharmaceutics* 2016, vol. 13, pp. 1278-1288.
- 10 N.M. Wolf et al., *Anal. Biochem.* 2006, vol. 355, pp. 71-80.
E.J. North et al., *Bioorg. Med. Chem.* 2013, vol. 21, pp. 2587-2599.
L. Salvado et al., *Diabetologia* 2013, vol. 56, pp. 1372-1382.
X. Palomer et al., *Int. J. Cardiol.* 2014, vol. 174, pp. 110-118.
L. Di et al., *Eur. J. Med. Chem.* 2003, vol. 38, pp. 223-232.

15

Patent documents cited in the description

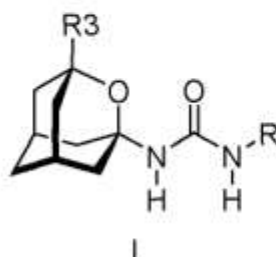
- US 20050164951 A1 (University of California)
WO 2006045119 A2 (University of California)
- 20 WO 2007106525 A1 (University of California & Arete Therapeutics)
WO 2008040000 A2 (Arete Therapeutics)
WO 2008051875 A2 (Arete Therapeutics)
US 3,539,626 A (Geigy Chemical Corporation)
WO 2007016496 (Neurogen Corporation)

25

CLAIMS

1. A compound of formula I

5



10

or a stereoisomer or a pharmaceutically acceptable salt thereof, wherein:

R3 is a radical selected from the group consisting of H, C₁-C₃ alkyl, cyclohexyl and phenyl;

15

R is a radical $-\text{[CH}_2\text{]}_n\text{-Y}$, wherein n is an integer between 0 and 15, and in the $-\text{[CH}_2\text{]}_n\text{-}$ biradical an integer between 0 and n/3 of the methylene groups are optionally replaced by oxygen atoms in such a way that there are not two oxygen atoms which are adjacent;

20

Y is a radical selected from the group consisting of: phenyl; a substituted phenyl; cyclohexyl; a substituted cyclohexyl; a piperidinyl; a substituted piperidinyl; a C- or N-radical from a 5- or 6-membered aromatic heterocycle; and a C- or N-radical from a 5- or 6-membered aromatic heterocycle fused with a benzene ring; with the proviso that I is not 1-(2-oxaadamantan-1-yl)-3-(3,4-dichlorophenyl)urea.

2. The compound according to claim 1, wherein Y is a radical selected from the group consisting of:

25

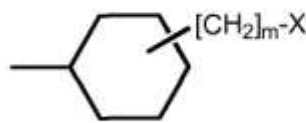
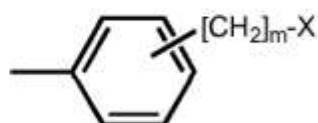
di- and tri-substituted phenyl radicals, wherein the two or three substituents, equal or different, are independently selected from the group consisting of F, Cl, SF₅, CF₃, OH, OCF₃, C₁-C₃ alkyl, and (C₁-C₃)-OCO;

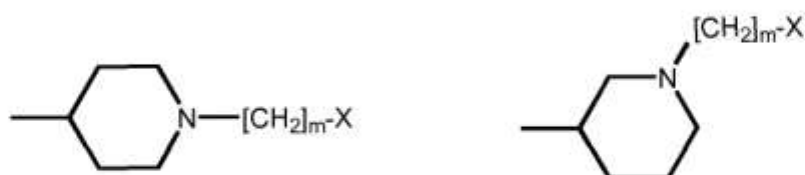
a C- or N-radical from a 5- or 6-membered aromatic heterocycle, having in the cycle one, two or three atoms of N, S or O;

30

a C- or N-radical from a 5- or 6-membered aromatic heterocycle having in the cycle one, two or three atoms of N, S or O, which is fused with a benzene ring; and radicals having one of the following four general formulas, wherein bonds crossing positions 3 and 4 of the phenyl and cyclohexyl rings mean substitution either in position 3 or in position 4 of the radical ring;

35





5

wherein m is an integer between 0 and 15, and in the $-[\text{CH}_2]_m$ - biradical an integer between 0 and $m/3$ methylene groups are optionally replaced by oxygen atoms in such a way that there are not two oxygen atoms which are adjacent; and X is a radical selected from the group consisting of:

10

H, F, Cl, SF_5 , CF_3 , OCF_3 , OH, CN, COOH, C_1 - C_3 alkyl, $(\text{C}_1$ - C_3 alkyl)CO, $(\text{C}_1$ - C_3 alkyl) SO_2 ;

phenyl, benzoyl, phenoxy, mono-substituted phenyl, mono-substituted benzoyl and mono-substituted phenoxy wherein the substituent is selected from the group consisting of F, Cl, CHO, COCH_3 , COOH, and H_2NSO_2 ;

15

$(\text{C}_1$ - C_{15} linear alkyl)O, $(\text{C}_4$ - C_{15} linear alkyl)CO, $(\text{C}_1$ - C_{15} linear alkyl)OCO, $(\text{C}_1$ - C_{15} linear alkyl)NHCO, $(\text{C}_1$ - C_{15} linear alkyl)CONH, $(\text{C}_4$ - C_{15} linear alkyl) SO_2 , $(\text{C}_1$ - C_{15} linear alkyl)NHSO₂, $(\text{C}_1$ - C_{15} linear alkyl) SO_2NH ;

20

$(\text{C}_3$ - C_6 carbocyclyl)O, $(\text{C}_3$ - C_6 carbocyclyl)CO, $(\text{C}_3$ - C_6 carbocyclyl)OCO, $(\text{C}_3$ - C_6 carbocyclyl)NHCO, $(\text{C}_3$ - C_6 carbocyclyl)CONH, $(\text{C}_3$ - C_6 carbocyclyl) SO_2 , $(\text{C}_3$ - C_6 carbocyclyl)NHSO₂, $(\text{C}_3$ - C_6 carbocyclyl) SO_2NH ;

25

$(5/6$ -membered-N/O-heterocyclyl)O, $(5/6$ -membered-N/O-heterocyclyl)CO, $(5/6$ -membered-N/O-heterocyclyl)OCO, $(5/6$ -membered-N/O-heterocyclyl)NHCO, $(5/6$ -membered-N/O-heterocyclyl)CONH, $(5/6$ -membered-N/O-heterocyclyl) SO_2 , $(5/6$ -membered-N/O-heterocyclyl)NHSO₂, and $(5/6$ -membered-N/O-heterocyclyl) SO_2NH ; wherein 5/6-membered-N/O-heterocyclyl is a C- or N-radical from a 5- or 6-membered heterocycle, the heterocycle being aromatic or non-aromatic, the heterocycle having in the cycle one, two or three atoms of N, S or O; wherein the 5/6-membered-N/O-heterocyclyl radical is optionally substituted by one or two substituents, equal or different, independently selected from the group consisting of F, Cl, CF_3 , C_1 - C_3 alkyl, and $(\text{C}_1$ - C_3 alkyl)NH.

30

3. The compound according to claim 2, wherein Y is a radical selected from the group consisting of:

35

di- and a tri-fluorosubstituted phenyl radicals;

4-chloro-3-trifluoromethylphenyl;

3-chloro-4-trifluoromethylphenyl;

4-fluoro-3-trifluoromethylphenyl;
 3-fluoro-4-trifluoromethylphenyl; and
 radicals having the four general formulas as defined in claim 2, wherein X is a radical
 selected from the group consisting of:

- 5 H, F, Cl, CF₃, OCF₃, OH, CN, COOH;
 phenyl, phenoxy, mono-substituted phenyl and mono-substituted phenoxy,
 wherein the substituent is COOH, Cl or H₂NSO₂ ;
 (C₁-C₁₅ linear alkyl)O, (C₁-C₁₅ linear alkyl)CO, (C₁-C₁₅ linear alkyl)OCO,
 (C₁-C₁₅ linear alkyl)NHCO, (C₁-C₁₅ linear alkyl)CONH, (C₁-C₁₅ linear alkyl)SO₂ ,
 10 (C₁-C₁₅ linear alkyl)NHSO₂ , (C₁-C₁₅ linear alkyl)SO₂NH;
 (5/6-membered-N/O-heterocyclyl)O, (5/6-membered-N/O-heterocyclyl)CO,
 (5/6-membered-N/O-heterocyclyl)OCO, (5/6-membered-N/O-heterocyclyl)-
 NHCO, (5/6-membered-N/O-heterocyclyl)CONH;
 (5/6-membered-N/O-heterocyclyl)SO₂, (5/6-membered-N/O-heterocyclyl)NHSO₂, and
 15 (5/6-membered-N/O-heterocyclyl)SO₂NH; wherein 5/6-membered-N/O-
 heterocyclyl is a C-radical or a N-radical from any 5- or 6-membered heterocycle,
 the heterocycle being aromatic or non-aromatic, and the heterocycle having in the
 cycle either one N atom, or two N atoms, or simultaneously one N atom and one O
 atom.

- 20 4. The compound according to any of the claims 1-3, wherein in radical R integer n is
 between 0 and 3, and consequently only one methylene group is optionally replaced by an
 oxygen atom.
- 25 5. The compound according to any of the claims 1-4, wherein in radical R integer n is 0,
 and consequently R = Y.

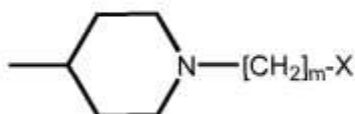
6. The compound according to any of the claims 2-5, wherein Y is a radical having the
 following formula:



7. The compound according to any of the claims 2-5, wherein Y is a radical having the
 following formula:



8. The compound according to any of the claims 2-5, wherein Y is a radical having the following formula:



5

9. The compound according to any of the claims 2-8, wherein integer m is between 0 and 3, and consequently only one methylene group is optionally replaced by an oxygen atom.

10. The compound according to any of the claims 2-9, wherein integer m is 0.

11. The compound according to any of the claims 2-10, wherein X is a radical selected from the group consisting of: H, F, Cl, CF_3 , OCF_3 , OH, CN, COOH, $(\text{C}_1\text{-C}_5 \text{ linear alkyl})\text{O}$, $(\text{C}_1\text{-C}_5 \text{ linear alkyl})\text{CO}$, $(\text{C}_1\text{-C}_5 \text{ linear alkyl})\text{OCO}$, $(\text{C}_1\text{-C}_5 \text{ linear alkyl})\text{NHCO}$, $(\text{C}_1\text{-C}_5 \text{ linear alkyl})\text{CONH}$, $(\text{C}_1\text{-C}_5 \text{ linear alkyl})\text{SO}_2$, $(\text{C}_1\text{-C}_5 \text{ linear alkyl})\text{NHSO}_2$, $(\text{C}_1\text{-C}_5 \text{ linear alkyl})\text{SO}_2\text{NH}$, 2-pyridinyl, 3-pyridinyl, 4-pyridinyl, 4-morpholinyl, phenyl, phenoxy, a mono-substituted phenyl and a mono-substituted phenoxy, whose substitution in the two latter cases is done by a radical selected from the group consisting of COOH, Cl and H_2NSO_2 .

20

12. The compound according to any of the claims 1-5, wherein Y is selected from the group consisting of:

- a tri-fluorosubstituted phenyl radical;
- 4-chloro-3-trifluoromethylphenyl;
- 3-chloro-4-trifluoromethylphenyl;
- 4-fluoro-3-trifluoromethylphenyl, and
- 3-fluoro-4-trifluoromethylphenyl.

25

13. The compound according to any of the claims 1-12, wherein R3 is H.

30

14. The compound according to any of the claims 1-3, which is selected from the group consisting of:

- 1-(2-oxadamantan-1-yl)-3-(2,3,4-trifluorophenyl)urea;
- 1-(3-methyl-2-oxadamantan-1-yl)-3-(2,3,4-trifluorophenyl)urea;
- 1-(3-ethyl-2-oxadamantan-1-yl)-3-(2,3,4-trifluorophenyl)urea;
- 1-(3-cyclohexyl-2-oxadamantan-1-yl)-3-(2,3,4-trifluorophenyl)urea;
- 1-(3-phenyl-2-oxadamantan-1-yl)-3-(2,3,4-trifluorophenyl)urea;

35

1-(2-oxadamantan-1-yl)-3-(1-acetylpiperidin-4-yl)urea; and
trans-1-(2-oxadamantan-1-yl)-3-[4-(4-carboxyphenoxy)cyclohexyl]urea.

15. A pharmaceutical composition comprising a therapeutically effective amount of a
5 compound as defined in any of the claims 1-14, or a stereoisomer or a pharmaceutically
acceptable salt thereof, and adequate amounts of pharmaceutically acceptable excipients.

16. A compound as defined in any of the claims 1-14, or a stereoisomer or a
pharmaceutically acceptable salt thereof, for use as an active pharmaceutical ingredient.

10

17. A compound as defined in any of the claims 1-14, or a stereoisomer or a
pharmaceutically acceptable salt thereof, for use in the treatment of a soluble epoxide
hydrolase mediated disease in an animal, including a human.

18. The compound for use according to claim 17, wherein the soluble epoxide hydrolase
15 mediated disease is selected from the group consisting of hypertension, atherosclerosis,
pulmonary diseases, kidney diseases, stroke, pain, neuropathic pain, inflammation,
pancreatitis, immunological disorders, eye diseases, cancer, obesity, diabetes, metabolic
syndrome, preeclampsia, anorexia nervosa, depression, erectile dysfunction, wound
20 healing, NSAID-induced ulcers, emphysema, scrapie and Parkinson's disease.

19. A method of treatment of an animal -including a human- suffering from a soluble
epoxide hydrolase mediated disease, comprising the administration of a therapeutically
effective amount of a compound as defined in any of the claims 1-14, or a stereoisomer or
25 a pharmaceutically acceptable salt thereof, together with adequate amounts of
pharmaceutically acceptable excipients.

20. The method according to claim 19, wherein the soluble epoxide hydrolase mediated
disease is selected from the group consisting of hypertension, atherosclerosis, pulmonary
30 diseases, kidney diseases, stroke, pain, neuropathic pain, inflammation, pancreatitis,
immunological disorders, eye diseases, cancer, obesity, diabetes, metabolic syndrome,
preeclampsia, anorexia nervosa, depression, erectile dysfunction, wound healing, NSAID-
induced ulcers, emphysema, scrapie and Parkinson's disease.

35

INTERNATIONAL SEARCH REPORT

International application No
PCT/EP2016/067620

A. CLASSIFICATION OF SUBJECT MATTER
 INV. C07D405/14 C07D311/96 C07D405/12 C07D413/12 C07D417/12
 A61K31/352 A61K31/453 A61P9/12

ADD.

According to International Patent Classification (IPC) or to both national classification and IPC

B. FIELDS SEARCHED

Minimum documentation searched (classification system followed by classification symbols)
 C07D A61K A61P

Documentation searched other than minimum documentation to the extent that such documents are included in the fields searched

Electronic data base consulted during the international search (name of data base and, where practicable, search terms used)

EPO-Internal, CHEM ABS Data, WPI Data

C. DOCUMENTS CONSIDERED TO BE RELEVANT

Category*	Citation of document, with indication, where appropriate, of the relevant passages	Relevant to claim No.
X	WO 2007/106525 A1 (UNIV CALIFORNIA [US]; ARETE THERAPEUTICS [US]; HAMMOCK BRUCE D [US]; J) 20 September 2007 (2007-09-20) cited in the application claim 1	1-20
A	HONG C SHEN: "Soluble epoxide hydrolase inhibitors: a patent review", EXPERT OPINION ON THERAPEUTIC PATENTS, vol. 20, no. 7, 1 July 2010 (2010-07-01), pages 941-956, XP055182103, ISSN: 1354-3776, DOI: 10.1517/13543776.2010.484804 cited in the application the whole document	1-20

Further documents are listed in the continuation of Box C.

See patent family annex.

* Special categories of cited documents :

A document defining the general state of the art which is not considered to be of particular relevance

E earlier application or patent but published on or after the international filing date

L document which may throw doubts on priority claim(s) or which is cited to establish the publication date of another citation or other special reason (as specified)

O document referring to an oral disclosure, use, exhibition or other means

P document published prior to the international filing date but later than the priority date claimed

T later document published after the international filing date or priority date and not in conflict with the application but cited to understand the principle or theory underlying the invention

X document of particular relevance; the claimed invention cannot be considered novel or cannot be considered to involve an inventive step when the document is taken alone

Y document of particular relevance; the claimed invention cannot be considered to involve an inventive step when the document is combined with one or more other such documents, such combination being obvious to a person skilled in the art

& document member of the same patent family

Date of the actual completion of the international search

2 September 2016

Date of mailing of the international search report

13/09/2016

Name and mailing address of the ISA/

European Patent Office, P.B. 5818 Patentlaan 2
 NL - 2280 HV Rijswijk
 Tel. (+31-70) 340-2040,
 Fax: (+31-70) 340-3016

Authorized officer

Wolf, Claudia

1

INTERNATIONAL SEARCH REPORT

International application No
PCT/EP2016/067620

C(Continuation). DOCUMENTS CONSIDERED TO BE RELEVANT

Category*	Citation of document, with indication, where appropriate, of the relevant passages	Relevant to claim No.
A	GB 1 125 559 A (GEIGY AG J R) 28 August 1968 (1968-08-28) example 3 basis for the proviso in the claims; -----	1-14

INTERNATIONAL SEARCH REPORT

Information on patent family members

International application No

PCT/EP2016/067620

Patent document cited in search report	Publication date	Patent family member(s)	Publication date
WO 2007106525	A1	20-09-2007	AR 059826 A1 30-04-2008
			AU 2007225170 A1 20-09-2007
			BR PI0708788 A2 14-06-2011
			CA 2646154 A1 20-09-2007
			CN 101405264 A 08-04-2009
			EA 200801969 A1 30-12-2008
			EP 2029539 A1 04-03-2009
			JP 5298005 B2 25-09-2013
			JP 2009530287 A 27-08-2009
			KR 20080109846 A 17-12-2008
			NZ 570657 A 24-02-2012
			TW 200808723 A 16-02-2008
			US 2007225283 A1 27-09-2007
			US 2013137726 A1 30-05-2013
			US 2013274476 A1 17-10-2013
			WO 2007106525 A1 20-09-2007
			ZA 200807266 B 25-11-2009

GB 1125559	A	28-08-1968	AT 267540 B 10-01-1969
			AT 267543 B 10-01-1969
			BE 689823 A 17-05-1967
			CH 456570 A 31-07-1968
			DE 1246722 B 10-08-1967
			ES 333486 A1 01-01-1968
			FR 6433 M 04-11-1968
			FR 1504098 A 01-12-1967
			GB 1125559 A 28-08-1968
			NL 6616214 A 19-05-1967
			NO 119270 B 27-04-1970
			SE 325024 B 22-06-1970

CHAPTER 2

**EXPLORING THE SIZE OF THE
LIPOPHILIC UNIT OF sEHIs**

Introduction

It has already been mentioned that crystallographic studies revealed that sEH has an active site with a catalytic triad at the corner of an L-shaped hydrophobic pocket. Taking this into account, lipophilic groups such as cyclohexyl or adamantyl are commonly present in potent sEHs in order to establish hydrophobic interactions with the lipophilic pocket of the enzyme. In fact, many sEHs (such as AR9281, *t*-AUCB and **10**, Figure 29) feature a common structure of Ad-NH-C(O)-NH-R, where Ad is adamant-1-yl and R is alkyl, aryl or heterocyclyl groups and have been evaluated in several *in vivo* models.^{195,196,197,198,199,200,201,202,203,204,205}

Although the adamantane moiety has been extensively used as a suitable polycyclic scaffold for the synthesis of potent sEHs, the poor metabolic stability of the adamantane nucleus could limit their use as a drug for treating patients.¹³² Despite this, alternative polycyclic hydrocarbons as lipophilic unit of sEHs have been little explored.

In this project, we have synthesized and pharmacologically evaluated a series of ring contracted and ring expanded analogs of three potent adamantane-based sEHs, AR9281, *t*-AUCB and **10**, in order to explore if alterations in the size of the lipophilic unit attached to the urea significantly impact its potency toward the human and murine sEH as well as influencing solubility, permeability and metabolic stability (Figure 29).

¹⁹⁵ Kim, I.-H.; Nishi, K.; Kasagami, T.; Morisseau, C.; Liu, J.-Y.; Tsai, H.-J.; Hammock, B. D. *Bioorg. Med. Chem. Lett.* **2012**, *22*, 5889-5892.

¹⁹⁶ Huang, S.-X.; Cao, B.; Morisseau, C.; Jin, Y.; Long, Y.-Q.; Hammock, B. D. *Med. Chem. Commun.* **2012**, *3*, 379-384.

¹⁹⁷ Kim, I.-H.; Lee, I.-H.; Nishiwaki, H.; Hammock, B. D.; Nishi, K. *Bioorg. Med. Chem.* **2014**, *22*, 1163-1175.

¹⁹⁸ Burmistrov, V.; Morisseau, C.; Lee, K. S. S.; Shihadih, D. S.; Harris, T. R.; Butov, G. M.; Hammock, B. D. *Bioorg. Med. Chem. Lett.* **2014**, *24*, 2193-2197.

¹⁹⁹ Burmistrov, V.; Morisseau, C.; Danilov, D.; Harris, T. R.; Dalinger, I.; Vatsadze, I.; Shkineva, T.; Butov, G. M.; Hammock, B. D. *Bioorg. Med. Chem. Lett.* **2015**, *25*, 5514-5519.

²⁰⁰ Kim, I.-H.; Park, Y.-K.; Nishiwaki, H.; Hammock, B. D.; Nishi, K. *Bioorg. Med. Chem.* **2015**, *23*, 7199-7210.

²⁰¹ Burmistrov, V. V.; Butov, G. M.; Karlov, D. S.; Palyulin, V. A.; Zefirov, N. S.; Morisseau, C.; Hammock, B. D. *Russ. J. Bioorg. Chem.* **2016**, *42*, 404-414.

²⁰² Burmistrov, V.; Morisseau, C.; Harris, T. R.; Butov, G. M.; Hammock, B. D. *Bioorg. Chem.* **2018**, *76*, 510-527.

²⁰³ Burmistrov, V.; Morisseau, C.; Pitushkin, D.; Karlov, D.; Fayullin, R. R.; Butov, G. M.; Hammock, B. D. *Bioorg. Med. Chem. Lett.* **2018**, *28*, 2302-2313.

²⁰⁴ Burmistrov, V. V.; Butov, G. M. *Russ. J. Org. Chem.* **2018**, *54*, 1307-1312.

²⁰⁵ D'yachenko, V. S.; Danilov, D. V.; Shkineva, T. K.; Vatsadze, I. A.; Burmistrov, V. V.; Butov, G. M. *Chem. Heterocycl. Compd.* **2019**, *55*, 129-134.

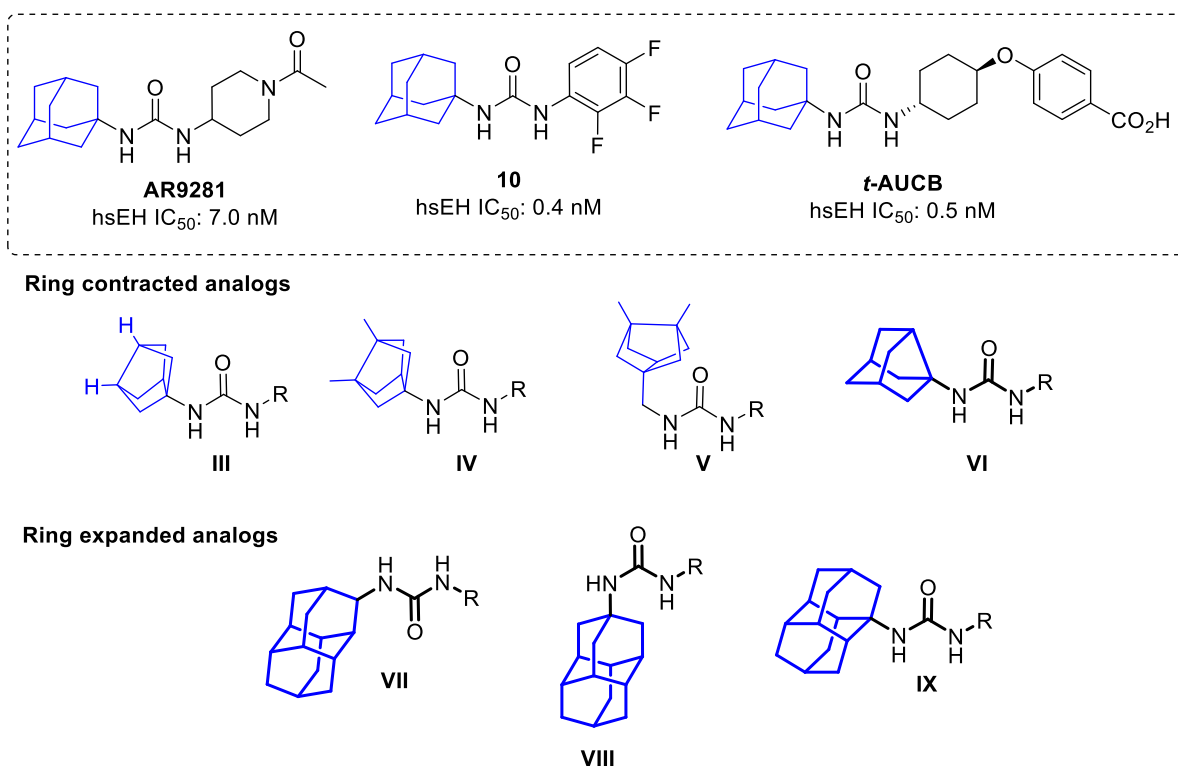


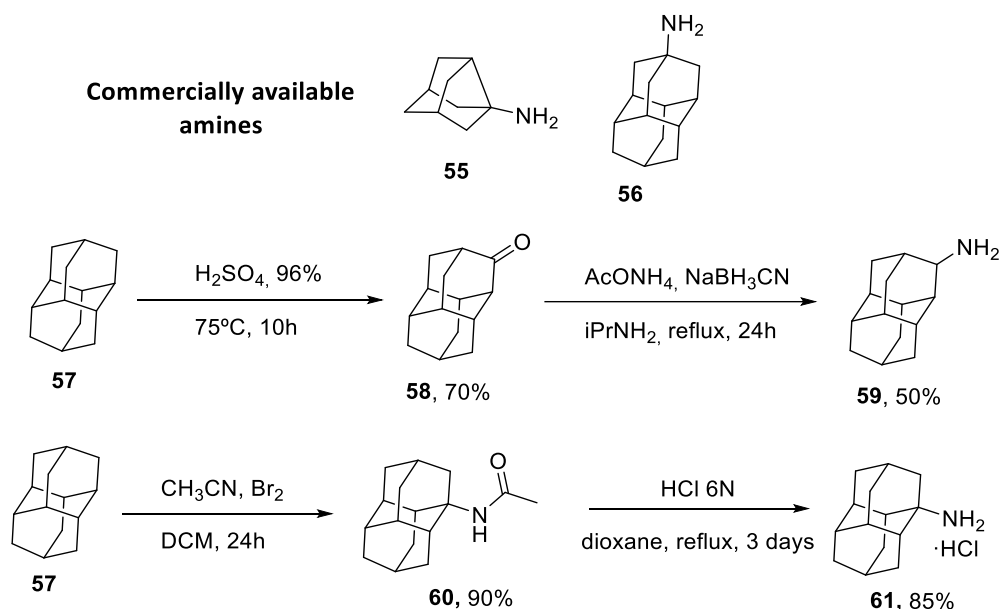
Figure 29. Known adamantyl-based sEHIs **AR9281**, **10** and **t-AUCB**, and their envisaged ring contracted and ring expanded. The ring-contracted analogs of general formula **III**, **IV** and **V** had been already synthesized in the context of Dr. Elena Valverde's Thesis, while the derivatives of general structures **VI**, **VII**, **VIII** and **IX** (highlighted in bold) were synthesized in the present Thesis.

Figure 29 collects all the ring-contracted and ring-expanded analogs of AR9281, **10** and **t-AUCB** envisaged to be synthesized and evaluated in this project. Of note, the bisnoradamantane-based ureas of general structure **III**, **IV** and **V** had been already synthesized and evaluated in the context of Dr. Elena Valverde's Thesis, presenting all of them IC₅₀ values in the low nanomolar range against the human sEH. Thus, in order to further explore the impact of the size of the polycyclic hydrocarbon as de lipophilic unit of sEHIs, in the present Thesis it was envisaged the synthesis of the ring contracted analogs featuring the noradamantane moiety of general formula **VI** and the ring expanded analogs derived from diamantane of general structures **VII**, **VIII** and **IX**.

Discussion

Ureas can be synthesized by the reaction of isocyanates with primary amines. Thus, for the synthesis of the new ring contracted and ring expanded analogs, it was necessary to obtain the corresponding polycyclic amines which, in the presence of triphosgene, lead to the desired isocyanates.

Fortunately, the ring contracted 3-noradamantanamine, **55**, and the diamantane-4-amine, **56**, are commercially available. In contrast, it was needed to synthesize the diamantane-3-amine, **59**, and diamantane-2-amine, **61**, starting from diamantane in both cases.

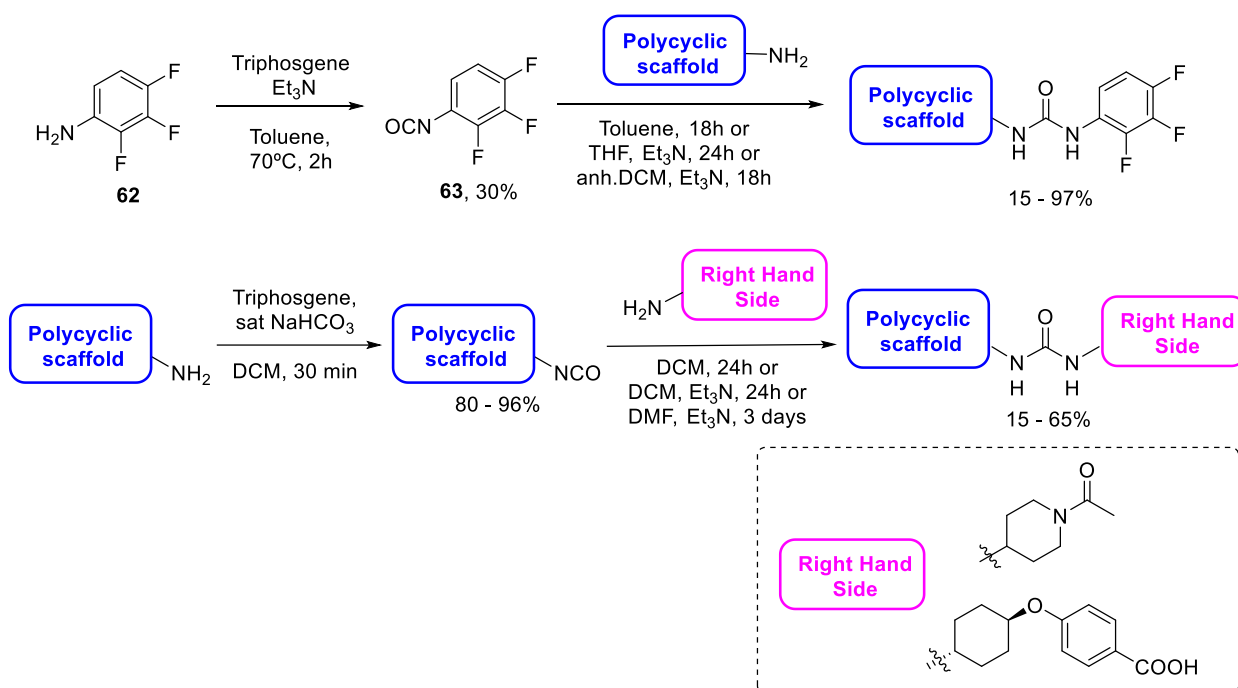


Scheme 6. Structures and synthesis of the polycyclic amines used for the obtention of the new ring contracted and ring expanded analogs.

The diamantanamine **59** was synthesized in two steps from commercially available diamantane, **57**. Oxidation of **57** with sulfuric acid followed by a reductive amination of ketone **58** by ammonium acetate and sodium cyanoborohydride led to the desired amine **59**. In contrast, the treatment of **57** with bromine and acetonitrile afforded the amide **60**, which was hydrolyzed in acidic media to obtain the diamantanamine **61** (Scheme 6).

Finally, the synthesis of the final ureas bearing the different polycycles was undertaken. The synthetic pathway revolved around the reaction of either the

isocyanate of the corresponding polycyclic amine with a suitable aliphatic amine or the reaction of 2,3,4-trifluorophenylisocyanate **63** with the corresponding polycyclic amine. The isocyanates were prepared from the corresponding polycyclic amines in the presence of triphosgene and sodium hydrogen carbonate, using dichloromethane as a solvent or, in the case of 2,3,4-trifluorophenylisocyanate **63**, it was obtained from the reaction of 2,3,4-trifluorophenylaniline **62** with triphosgene in the presence of triethylamine and toluene at 80 °C (Scheme 7).

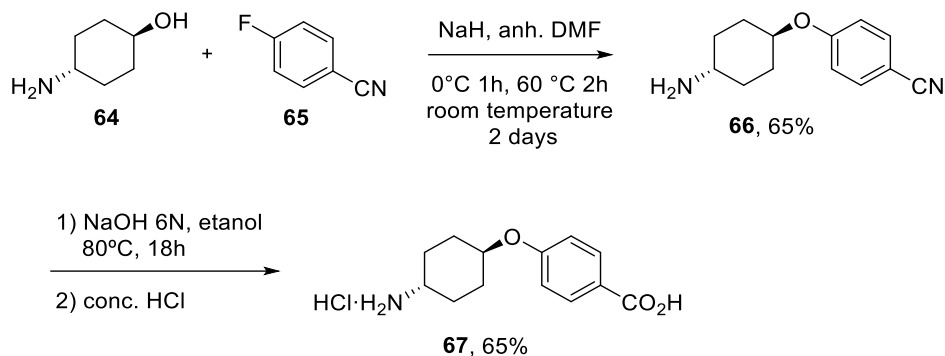


Scheme 7. General synthesis of the new ureas bearing ring contracted and ring expanded analogs of adamantane.

As mentioned, the new compounds were designed as analogs of the known sEHIS AR9281, **10** and *t*-AUCB. Thus, apart from the trifluoroaniline as the RHS of the inhibitors, for the obtention of analogs of **10**, 1-acetyl-4-aminopiperidine and *t*-4-[(4-aminocyclohexyl)oxy]benzoic acid were used for the synthesis of the analogs of AR9281 and *t*-AUCB, respectively. In contrast to the substituted aminopiperidine, the *t*-4-[(4-aminocyclohexyl)oxy]benzoic acid **67** was not commercially available. Thus, it was synthesized as previously reported by Hwang *et al.*²⁰⁶ The synthetic pathway consisted

²⁰⁶ Hwang, S. H.; Weckler, A. T.; Zhang, G.; Morisseau, C.; Nguyen, L. V.; Fu, S. H.; Hammock, B. D. *Bioorg. Med. Chem. Lett.* **2013**, *23*, 3732-3737.

in the nucleophilic aromatic substitution of 4-fluorobenzonitrile **65** by *trans*-aminocyclohexanol **64**, and consecutive hydrolysis of the nitrile **66** to the carboxylic acid **67** under basic conditions (Scheme 8).



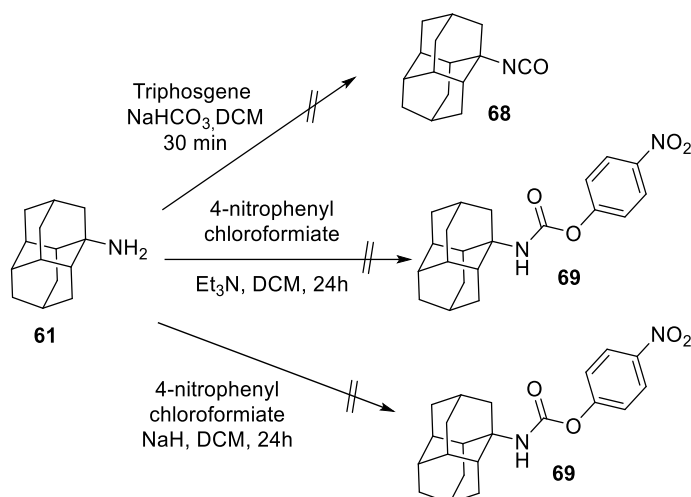
Scheme 8. Synthesis of the aminoacid **67**.

Unfortunately, all our attempts to synthesize ureas derived from diamantanamine **61** were unsuccessful. For the preparation of these ureas, we could not apply the synthetic approach used for the other ones. The reaction of **61** with triphosgene in the presence of sodium hydrogen carbonate and triphosgene did not afford the expected isocyanate **68**. Given this result, it was necessary the search of new methodologies for the synthesis of ureas. As an alternative to isocyanates, ureas can be synthesized through the formation of carbamate intermediates,^{207,208} that can be generated by the reaction of an amine with a chloroformate. Then, the carbamate can react with an amine to provide the desired urea. Regrettably, the reaction of **61** with the highly reactive 4-nitrophenyl chloroformate did not afford the carbamate **69**, even in the presence of a strong base such as sodium hydride (Scheme 9).

One hypothesis for the poor reactivity of amine **61** is the steric hindrance around the amino group resulting from 1-3-diaxial interactions with the surrounding hydrogen atoms, thus preventing the attack of the lone pair of electrons of the nitrogen group to triphosgene or the chloroformate.

²⁰⁷ Gallou, I.; Eriksson, M.; Zeng, X.; Senanayake, C.; Farina, V. J. *Org. Chem.* **2005**, *70*, 6960–6963.

²⁰⁸ Ghosh, A. K.; Brindisi, M. *J. Med. Chem.* **2020**, *63*, 2751–2788.



Scheme 9. Attempts to obtain isocyanate **68** and carbamate **69** from diamantanamine **61**.

In the end, several ring contracted and ring expanded analogs of **10**, *t*-AUCB and AR9281 were synthesized and evaluated (Figure 30). Compounds **10** and **11** were also obtained for comparative purposes.

First, the potency of the new compounds as human and murine sEHs was tested by Dr Christophe Morisseau from the group of Prof. Bruce D. Hammock at the UCD. As described in the article, results showed that the reduction of the polycyclic moiety from adamantane to bisnoradamantane led to a reduction of the potency. Interestingly, the inhibitory potency was restored by the introduction of two methyl groups in the bridgehead positions of the bisnoradamantane moiety, probably because the addition of the methyl groups compensates the reduction in size from the adamantane to the bisnoradamantane scaffold. Regarding the ring expanded analogs, diamantane ureas analogs of AR9281 and *t*-AUCB showed IC₅₀ values in the same range as that of their adamantane-based compounds. However, within the trifluorophenyl series analogs of **10**, the diamantane derivative was considerably less potent than its adamantane derivative, probably due to an opposite binding orientation in the hydrophobic pocket of the sEH, as previously observed for a different series of sEHs.¹⁰⁵

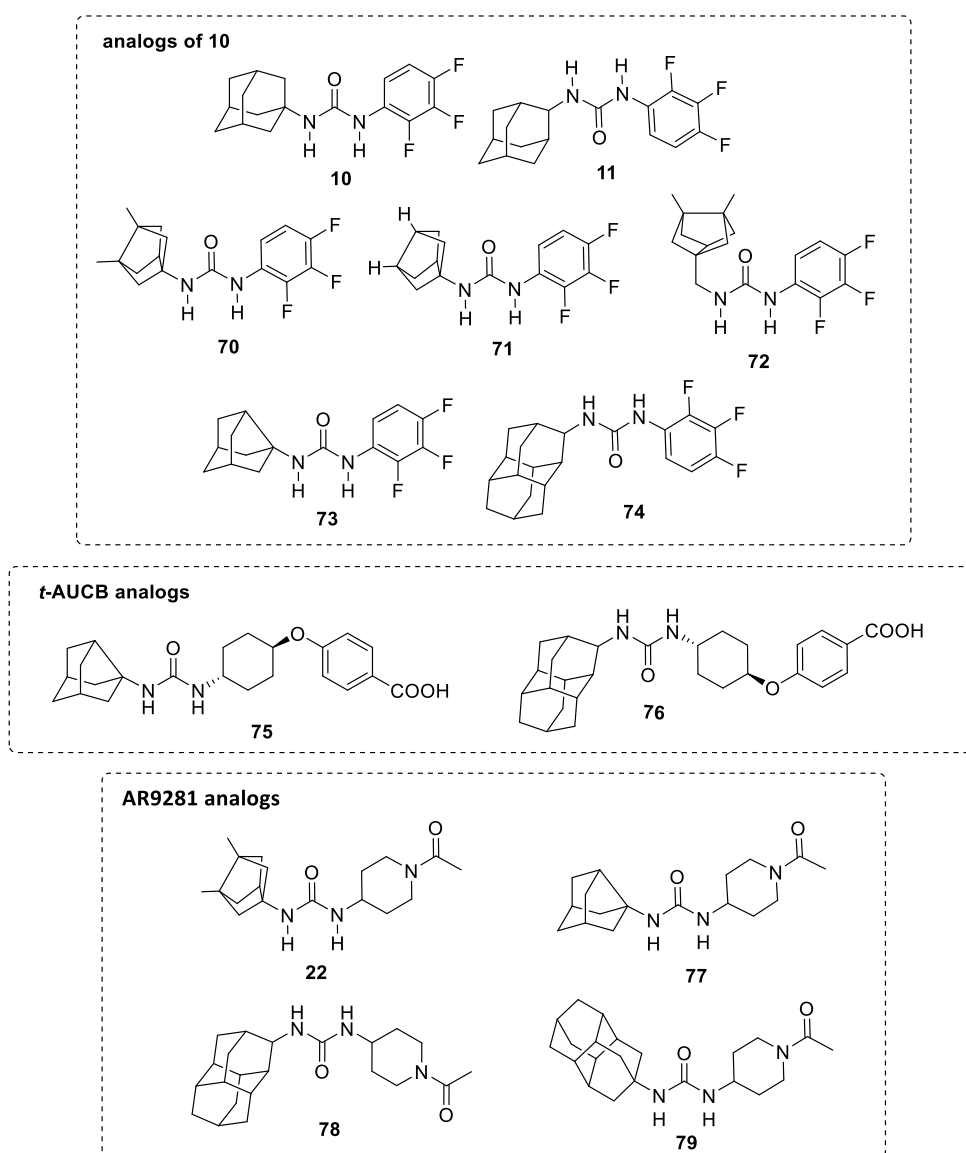


Figure 30. Ring contracted and ring expanded analogs of the adamantane-based sEHs AR9281, **10** and *t*-AUCB synthesized in this project.

Interestingly, we did not find significant differences between the inhibitory activities in human and murine species when we tested the inhibition of the murine sEH of AR9281 and three analogs (**22**, **77** and **78**), despite it has been considered that steric parameters have stronger effects on the potency of inhibitors against murine sEH rather than on the human enzyme.^{22,105,202,209}

²⁰⁹ Jones, P. D.; Wolf, N. M.; Morisseau, C.; Whetstone, P.; Hock, B.; Hammock, B.D. *Anal. Biochem.* **2005**, *343*, 66-75.

Next, microsomal stability, experimental solubility and permeability of the new ureas were determined by the group of Prof. M. Isabel Loza and Prof. José M. Brea of the Drug Screening Platform/Biofarma Research Group of the University of Santiago de Compostela (Spain).

The *in vitro* stability of some representative new ureas in human microsomes was assessed in order to examine the impact of the different hydrophobic units in their metabolic stabilities. Given that diamantane moiety features more tertiary carbon atoms than the adamantane ring, which are prone to be hydroxylated, it was anticipated the adamantane-based ureas to be more stable than their diamantane-based analogs. This hypothesis was confirmed by the experimental results that showed that diamantane derivatives were extremely labile compounds, with their adamantane counterparts being considerably more stable. Moreover, ring contracted analogs bearing the bisnoradamantane and the noradamantane units presented similar or slightly reduced microsomal stability than those bearing the adamantane moiety.

Additionally, experimental solubility of the new ureas was also determined. As expected, the diamantane derivatives were dramatically less soluble than their adamantane, noradamantane or bisnoradamantane counterparts. Of note, the acetylpiperidine serie presented the highest solubility values, with the two other series having similar solubility.

Finally, the permeability assays through Caco-2 cells showed that the size of the lipophilic unit of the sEHs seemed to be of little relevance regarding permeability. Concerning the right-hand side of the ureas, acetylpiperidine derivatives were endowed with the best permeability, while the trifluorophenyl compounds displayed much lower permeability. As expected, benzoic acid derivatives were the less permeable compounds.

With all this information, we conclude that the catalytic center of the sEH enzyme can accommodate polycycles of very different sizes, from the small bisnoradamantane moiety to the very large diamantane group. Interestingly, it seems that the replacement of the adamantane moiety by larger polycyclic rings led to more potent compounds than the replacement by smaller ones, particularly within the *t*-AUCB and AR9281 analogs.

These results were published in *Bioorganic Medicinal Chemistry* in 2019. This article is included in the following pages of this Thesis.²¹⁰

²¹⁰ Codony, S.; Valverde, E.; Leiva, R.; Brea, J.; Loza, M. I.; Morisseau, C.; Hammock, B. D.; Vázquez, S. *Bioorg. Med. Chem.* **2019**, *27*, 115078.



Contents lists available at ScienceDirect

Bioorganic & Medicinal Chemistry

journal homepage: www.elsevier.com/locate/bmc

Exploring the size of the lipophilic unit of the soluble epoxide hydrolase inhibitors

Sandra Codony^a, Elena Valverde^a, Rosana Leiva^a, José Brea^b, M. Isabel Loza^b, Christophe Morisseau^c, Bruce D. Hammock^c, Santiago Vázquez^{a,*}^a Laboratori de Química Farmacèutica (Unitat Associada al CSIC), Facultat de Farmàcia i Ciències de l'Alimentació, and Institute of Biomedicine (IBUB), Universitat de Barcelona, Av. Joan XXIII 27-31, Barcelona E-08028, Spain^b Biospharma Screening Platform, Biospharma Research Group, Centro de Investigación en Medicina Molecular y Enfermedades Crónicas (CIMUS), Universidad de Santiago de Compostela, Spain^c Department of Entomology and Nematology, and UCD Comprehensive Cancer Center, University of California, Davis, CA 95616, USA

ARTICLE INFO

Keywords:

Adamantane
Inhibitor
Isocyanate
Soluble epoxide hydrolase
Urea

ABSTRACT

Soluble epoxide hydrolase (sEH) inhibitors are potential drugs for several diseases. Adamantyl ureas are excellent sEH inhibitors but have limited metabolic stability. Herein, we report the effect of replacing the adamantane group by alternative polycyclic hydrocarbons on sEH inhibition, solubility, permeability and metabolic stability. Compounds bearing smaller or larger polycyclic hydrocarbons than adamantane yielded all good inhibition potency of the human sEH ($0.4 \leq IC_{50} \leq 21.7$ nM), indicating that sEH is able to accommodate inhibitors of very different size. Human liver microsomal stability of adamantane containing inhibitors is lower than that of their corresponding adamantane counterparts.

1. Introduction

Arachidonic acid (AA), a polyunsaturated fatty acid, plays important roles in cellular signaling as a second messenger and is also a precursor for a wide variety of lipid mediators that are involved in many physiological and pathophysiological processes. The first step in the biosynthesis of these mediators, known as eicosanoids or oxylipins, is an oxidation, which can be catalyzed by cyclooxygenases (COX), lipoxygenases (LOX), and cytochrome P450 enzymes.¹ Most research on AA derivatives has focused on prostaglandins, processed by COX, and leukotrienes, originated from LOX. Both types of metabolites are potent inflammatory mediators and, consequently, several pharmaceuticals have been produced to alleviate inflammatory conditions. These included non-selective COX-1 and COX-2 inhibitors (e.g., ibuprofen, indomethacin), selective COX-2 inhibitors (e.g., celecoxib, etoricoxib), and 5-LOX inhibitors (e.g., zileuton).²⁻⁴

Comparatively, the third pathway remains relatively unexplored. Cytochromes P450 enzymes transform AA to various biologically active compounds, including epoxyeicosatrienoic acids (EETs).^{5,6} EETs are reported to exhibit anti-inflammatory and anti-nociceptive properties and are involved in the regulation of blood pressure and cellular stress.⁷⁻¹¹ Soluble epoxide hydrolase (sEH, *EPHX2*, E.C. 3.3.2.3), a member of the α/β -hydrolase fold family of enzymes, catalyzes the

hydrolysis of EETs to the corresponding dihydroxyeicosatrienoic acids (DHETs), reducing the beneficial activities of EETs.¹²⁻¹⁵ The inhibition of sEH *in vivo* by potent, selective inhibitors results in an increase of the concentration of the EETs, reducing blood pressure and inflammatory and pain states, thereby suggesting that sEH inhibitors may serve as novel agents for treating hypertension, inflammatory diseases, pain and, more recently, neurodegenerative diseases.¹⁶⁻²¹

X-ray crystallographic studies revealed that sEH has an active site with a catalytic triad at the corner of an L-shaped hydrophobic pocket. The triad includes a nucleophilic aspartic acid, which attacks the epoxide carbon-highly polarized by hydrogen bonds with two tyrosine residues, and a histidine-aspartic acid pair, which activates the hydrolysis of the acyl-enzyme intermediate.²² Therefore, lipophilic groups such as cyclohexyl or adamantyl are commonly present in potent sEH inhibitors in order to establish hydrophobic interactions with the pocket. In fact, the first sEH inhibitor to enter in clinical trials was AR9281, an adamantyl urea (Fig. 1).²³ Specifically, hundreds of sEH inhibitors featuring a common structure of Ad-NH-C(O)-NH-R, where Ad is adamantan-1-yl and R is alkyl, aryl or heterocyclyl groups, have been synthesized and, subsequently, evaluated in several *in vivo* models (Fig. 1).²³⁻³⁵ However, the poor metabolic stability of some adamantane containing ureas could limit their usefulness to treat patients.³⁶ Notwithstanding the high potency generally associated to

* Corresponding author.

E-mail address: svazquez@ub.edu (S. Vázquez).<https://doi.org/10.1016/j.bmc.2019.115078>

Received 3 May 2019; Received in revised form 31 July 2019; Accepted 25 August 2019

Available online 26 August 2019

0968-0896/ © 2019 Elsevier Ltd. All rights reserved.

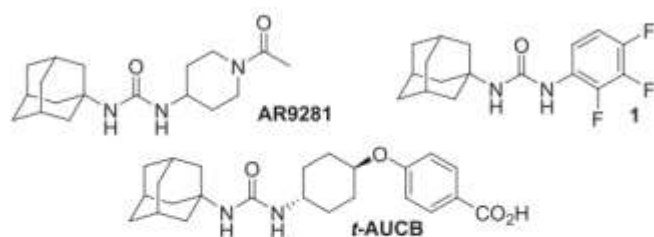


Fig. 1. Adamantyl-based sEH inhibitors.

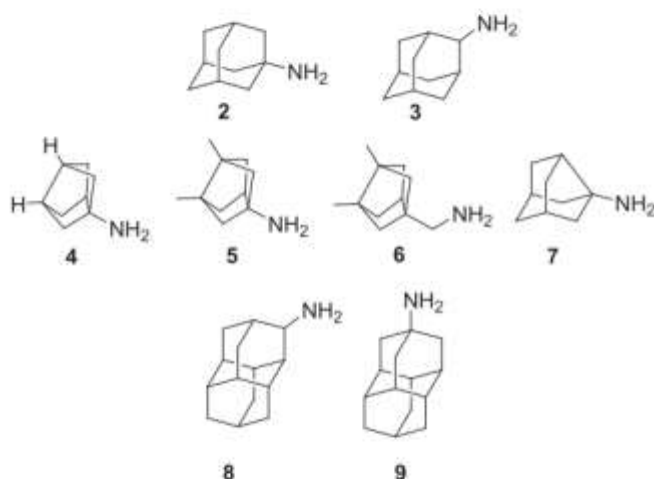


Fig. 2. Polycyclic amines used in this study.

adamantane-derived sEH inhibitors, alternative polycyclic hydrocarbons have been scarcely evaluated.

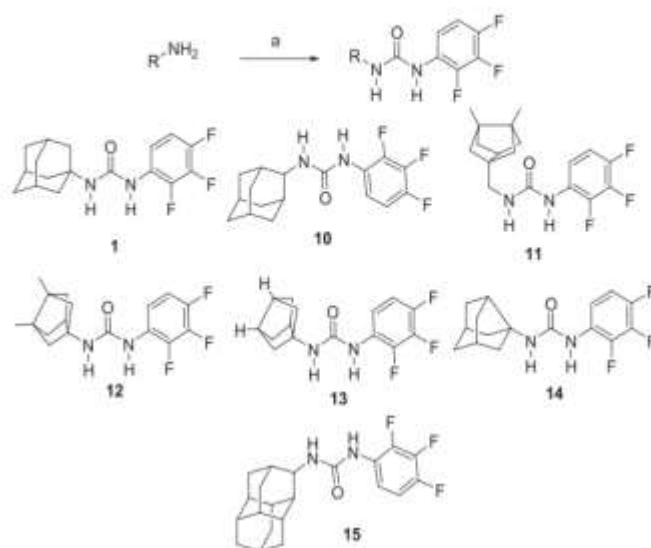
In this work, a series of ring-contracted and ring-expanded analogs of three potent adamantane sEH inhibitors, AR9281 ($IC_{50} = 7.0$ nM),²³ t-AUCB ($IC_{50} = 0.5$ nM),³⁷ and **1** ($IC_{50} = 0.4$ nM),³⁸ were synthesized and pharmacologically evaluated in order to test if alterations in the size of the lipophilic unit attached to the urea significantly impact its potency toward the human sEH (Figs. 1 and 2) as well as influencing solubility, permeability and metabolic stability.

2. Results and discussion

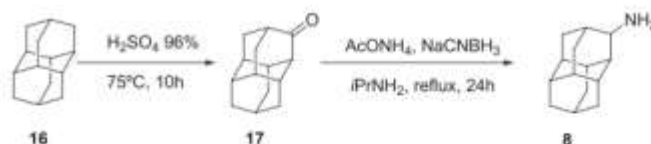
2.1. Chemistry

Adamantyl ureas are typically synthesized by the reaction of adamantyl isocyanates with a primary amine. Alternatively, the reaction of amantadine (1-adamantylamine) with an isocyanate also furnishes adamantyl ureas. Taking into account that 2,3,4-trifluorophenylisocyanate is a commercially available compound, for the preparation of the analogs of urea **1**, we reacted this isocyanate with four different amines, **4–7**, featuring smaller polycyclic rings than adamantane. Bisnoradamantane amines **4**, **5** and **6** were synthesized following reported procedures,^{39,40} while noramantadine **7** is commercially available. For comparative purposes, we also synthesized, using the same reaction, urea **1** and its isomer **10** (Scheme 1).

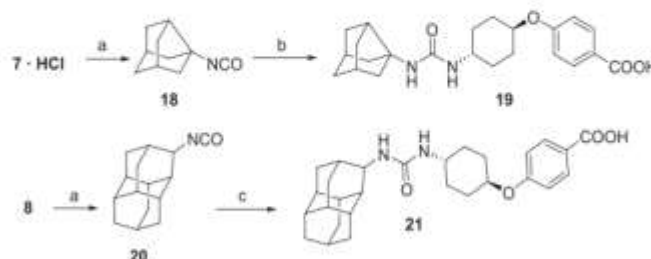
In order to obtain the ring-expanded analog **15**, we started from diamantanamine **8**, which was synthesized in two steps from commercially available diamantane, **16**. Oxidation of **16** with sulfuric acid followed by a reductive amination of ketone **17** by ammonium acetate and NaCNBH₃ led to amine **8** (Scheme 2). For the synthesis of the ring-contracted and ring-expanded analogs of t-AUCB and AR9281, we first prepared the required isocyanate by the reaction of the corresponding polycyclic amine with triphosgene. The reaction of these isocyanates with either t-4-[(4-aminocyclohexyl)oxy]benzoic acid (Scheme 3) or N-acetyl-4-aminopiperidine, **22** (Scheme 4), furnished the desired



Scheme 1. Synthesis of analogs containing a trifluorophenyl unit. Reagents and conditions: (a) 2,3,4-trifluorophenylisocyanate, Et₃N, anh. DCM, overnight.



Scheme 2. Synthesis of diamantanamine **8**.



Scheme 3. Synthesis of t-AUCB analogs. Reagents and conditions: (a) triphosgene, NaHCO₃, DCM, 30 min; (b) t-4-[(4-aminocyclohexyl)oxy]benzoic acid, Et₃N, DCM, 30 °C, overnight; (c) t-4-[(4-aminocyclohexyl)oxy]benzoic acid, Et₃N, DMF, 50 °C, 3 days.

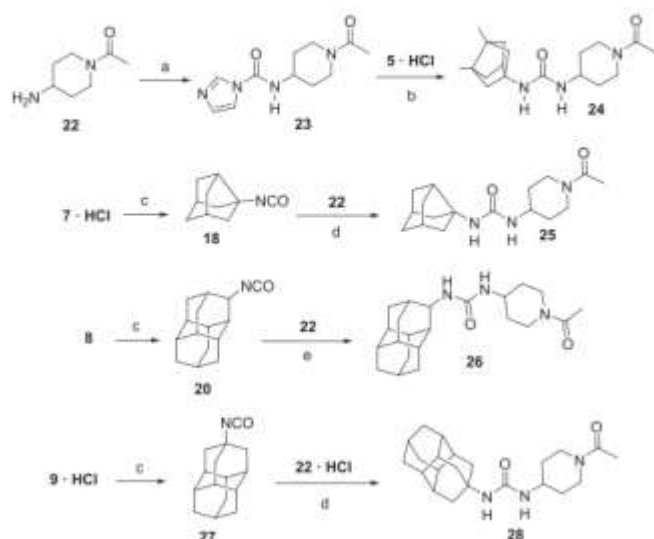
compounds. An alternative procedure was employed for the synthesis of urea **24**, involving the activation of **22** with 1,1'-carbonyldiimidazole (Scheme 4).

2.2. sEH inhibition and structure-activity relationships

The potency of the new compounds as human soluble epoxide hydrolase inhibitors was tested using a previously reported sensitive fluorescent-based assay (Table 1).⁴¹

Within the series of the 2,3,4-trifluorophenyl inhibitors, sequential ring contraction from adamantanes **1** or **10** to noradamantane **14** and to bisnoradamantane **13** resulted in a decrease of the inhibitory potency (compare entries **1** and **2** vs **5** and **6**, Table 1), likely because of the reduction of hydrophobic interactions between the ring-contracted moiety and the lipophilic pocket of the enzyme and the increase of desolvation energy to transfer the molecule from the solution state to the receptor cavity. This reduction in potency was also observed in the other two series of sEH inhibitors (compare entry **11** vs **13**, and entry **8** vs **9**, Table 1).

Nevertheless, the inhibitory potency was restored by the



Scheme 4. Synthesis of AR9281 analogs. Reagents and conditions: (a) 1,1'-carbonyldiimidazole, 1,2-dichloroethane, 50 °C, 21 h; (b) Et₃N, CHCl₃, 50 °C, 24 h; (c) triphosgene, Et₃N, DCM, 30 min; (d) DCM, Et₃N, overnight; (e) DCM, overnight.

Table 1
Inhibitory activities against the human and murine sEH.

Entry	Compound	IC ₅₀ (nM) human sEH ^a	IC ₅₀ (nM) murine sEH ^a
1	1	0.4	ND ^b
2	10	0.4	ND
3	11	0.4	ND
4	12	0.5	ND
5	13	3.2	ND
6	14	3.3	ND
7	15	8.0	ND
8	<i>t</i> -AUCB	0.5	ND
9	19	8.6	ND
10	21	0.5	ND
11	AR9281	8.0	3.0
12	24	6.5	3.3
13	25	21.7	ND
14	26	3.4	5.0
15	28	7.2	1.8

^a Reported IC₅₀ values are the average of three replicates. The fluorescent assay as performed here has a standard error between 10 and 20% suggesting that differences of two-fold or greater are significant. Because of the limitations of the assay it is difficult to distinguish among potencies < 0.5 nM.⁴¹

^b ND: not determined.

introduction of two methyl groups in the bridgehead positions of the bisnoradamantane moiety (compare entries 1 and 2 vs entries 3 and 4, and entry 11 vs entry 12, Table 1), probably because the addition of the methyl groups compensates the reduction in size from the adamantane to the bisnoradamantane scaffold. Furthermore, the results showed that the introduction of a methylene unit between the hydrophobic moiety and the urea does not affect the potency of the compounds (compare entry 3 vs 4, Table 1).

Taking into account that the reduction of the polycyclic moiety from adamantane to bisnoradamantane led, within the three series of inhibitors, to a reduction of the potency, we wondered if the opposite was true. That is, whether an increase in the size of the lipophilic unit of the inhibitor would lead to more potent compounds.

With the aim of exploring the ring-expanded analogs, the adamantane ring was replaced by the much larger diamantane moiety. Somehow surprisingly, considering the substantial increase in size and previous consideration of the adamantyl group as the marginal biggest group as the *N*-substituent for sEH inhibitors,⁴² diamantane ureas **26**

and **28** showed IC₅₀ values in the same range as that of AR9281 (compare entry 11 vs entries 14 and 15). Considering that **26** was slightly more potent than its isomer **28**, we synthesized two further analogs derived from diamantane **8**, i.e., the new ureas **15** and **21**, analogs of inhibitors **1** and *t*-AUCB, respectively. In line with the aforementioned results, diamantane derivative **21** showed to be as potent as *t*-AUCB (compare entry 8 vs 10, Table 1). However, within the trifluorophenyl series, the diamantane derivative **15** was considerably less potent than adamantane derivatives **1** or **10** (compare entries 1 and 2 vs 7, Table 1). The dissimilar behavior of **15** compared with **21** and **26** could be due to an opposite binding orientation of **15** compared to that of **21** and **26**, as observed previously for a different series of sEH inhibitors.⁴³

Typically, steric parameters have stronger effects on the potency of inhibitors against murine sEH rather than on the human sEH.^{32,41,43,44} For example, it has recently been reported that the progressive introduction of one, two or three methyl groups in the bridgehead positions of the adamantane unit of *t*-AUCB did not lead to significant changes in the IC₅₀ values against the human enzyme, while leading to a gradual increase in the IC₅₀ values against the murine enzyme.³² However, when we tested the inhibition of the murine sEH by AR9281 and three analogs (**24**, **26** and **28**), we did not find significant differences between their activities in human and murine species (Table 1).

2.3. Microsomal stability

It is known that the adamantane nucleus is prone to rapid metabolism *in vivo* giving rise to a variety of inactive hydroxylated derivatives. This results in low drug concentrations in blood and short *in vivo* half-life. Metabolism studies have shown that the bridgehead hydroxylation (tertiary carbon) is favored over the secondary carbon positions, producing water-soluble hydroxyadamantane derivatives in the liver, which are then easily excreted.⁴⁵ Additionally, metabolic studies showed that liver microsomes from phenobarbital-treated rats readily metabolize diamantane to mono-, di- and possibly tri-hydroxy derivatives.^{46,47} It is also known that several diamantanes are cytochromes P450 inhibitors.^{48,49}

Considering the aforementioned metabolism liability of the adamantane and diamantane scaffolds, we assessed the *in vitro* stability of some representative new ureas in human microsomes in order to examine the impact of the different hydrophobic units in their metabolic stabilities.

As anticipated, diamantane derivatives were extremely labile compounds, with their adamantane counterparts being considerably more stable (compare entries 1 vs 6, 7 vs 9, and 10 vs 13 and 14, Table 2). These results are in the line with what was expected, since diamantane moiety features more tertiary carbon atoms than the adamantane ring, which are prone to be hydroxylated.

Finally, the bisnoradamantane and the noradamantane units seem to have similar (compare entries 1 vs 3 and 4, and 1 vs 5 and 10 vs 12, Table 2) or somehow reduced (compare entries 7 vs 8 and 10 vs 11, Table 2) microsomal stability than adamantane.

2.4. Solubility and lipophilicity

In order to assess the impact of the polycyclic scaffold in the solubility of the inhibitors, we experimentally determined their solubility in a 1% DMSO: 99% PBS buffer solution.

As expected, within the trifluorophenylurea series, the solubility highly increases from diamantane **15** to adamantane **1** (18 and 57 μM, respectively, Table 2) and then, slightly further increases to the noradamantane **14** and to the bisnoradamantane **13** (65 and 82 μM, respectively, Table 2). In fact, the diamantane derivatives were dramatically less soluble than their adamantane, noradamantane or bisnoradamantane counterparts (compare entries 6 vs 1, 3, 4 and 5, entries 9 vs 7 and 8 and entries 13 and 14 vs 10 and 11, Table 2).

Table 2
Solubility and microsomal stability of the new compounds.

Entry	Compound	Microsomal stability ^a	Solubility (μM) ^b	Lipophilicity ^c
1	1	34.3%	57	4.1
2	10	19.4%	ND ^d	3.9
3	12	30.0%	66	4.1
4	13	41.9%	82	3.5
5	14	30.2%	65	3.8
6	15	0.0%	18	4.5
7	<i>t</i> -AUCB	93.5%	60	3.7
8	19	64.6%	76	3.4
9	21	14.6%	7	3.9
10	AR9281	80.1%	> 100	2.1
11	24	59.3%	> 100	2.2
12	25	88.7%	ND	1.8
13	26	0.0%	86	2.5
14	28	2.6%	85	2.6

^a Percentage of remaining compound after 60 min of incubation with human microsomes obtained from Tebu-Xenotech in the presence of NADP at 37 °C. Metabolism of testosterone was used as a positive control for metabolism (22.4% remaining compound).

^b Solubility in a 1% DMSO: 99% PBS buffer solution, see experimental section for details.

^c Lipophilicity refers to the consensus $\log P_{o/w}$ value calculated using the SwissADME program⁵⁰ for five predictive $\log P_{o/w}$ models (iLOGP, XLOGP3, WLOGP, MLOGP and SILICOIT).

^d ND: not determined.

Finally, considering the right-hand side of the inhibitors, the acetylpiperidine derivatives were the more soluble compounds, with the two other series having similar solubility.

Of note, the experimental solubility values showed a good correlation with the calculated lipophilicity values (see Table 2), the more soluble AR9281 analogs being the compounds with the lowest lipophilicity. As expected, for any given right-hand side unit, the diamantane derivatives showed always the higher lipophilicity.

2.5. Permeability

In order to evaluate the permeability of selected inhibitors, the Caco-2 cell permeability model was used in this study. Apparent permeability values (P_{app}) were determined from the amount permeated through the Caco-2 cell membranes at both apical-basolateral (A-B) and basolateral-apical (B-A) direction (Table 3).

Of note, the size of the lipophilic unit of the sEH inhibitors seems to be of little relevance regarding permeability, as evidenced through the comparison within the three series of inhibitors: the trifluorophenyl derivatives (compare entries 1 and 2 vs 3, Table 3), the benzoic acid derivatives (compare entries 4 vs 5, Table 3) and the acetylpiperidine derivatives (compare entries 6–8, Table 3). Regarding the right-hand side of the ureas, acetylpiperidine derivatives were endowed with the best permeability, while the trifluorophenyl compounds **1**, **10** and **15**

Table 3
Permeability in the Caco-2 cell line of selected sEH inhibitors.

Entry	Compound	P_{app} A \rightarrow B (nm/s)	P_{app} B \rightarrow A (nm/s)	ER ^a
1	1	11.8 \pm 1.3	1.8 \pm 0	0.2 \pm 0
2	10	2.3 \pm 0.1	7.3 \pm 0.3	3.2 \pm 0.2
3	15	16.2 \pm 2.4	5.4 \pm 0.1	0.3 \pm 0.1
4	<i>t</i> -AUCB	1.9 \pm 0.2	210.3 \pm 53.7	111 \pm 34.5
5	21	3.1 \pm 0.3	67.5 \pm 2.4	22.2 \pm 1.9
6	24	159.2 \pm 2.8	180.2 \pm 31.6	1.1 \pm 0.2
7	26	156.2 \pm 13.6	146.9 \pm 19.6	1.0 \pm 0.2
8	28	208.3 \pm 20.2	191.6 \pm 38.5	0.9 \pm 0.1

^a The efflux ratio was calculated as $ER = (P_{app} B \rightarrow A) / (P_{app} A \rightarrow B)$. See the experimental section for further details. Permeability of estrone-3-sulfate and colchicine were used as references.

displayed much lower permeability. As expected, benzoic acid derivatives *t*-AUCB and **21** were the less permeable compounds (Table 3).

3. Conclusions

Overall, it seems clear that the catalytic center of the sEH enzyme can accommodate polycycles of different sizes, ranging from the small bisnoradamantane moiety to the very large diamantane group. Notwithstanding this, it appears, particularly within the *t*-AUCB and AR9281 derivatives, that the replacement of the adamantane by larger polycyclic rings, such as the diamantanes, is better than the replacement by smaller ones.

Of note, although the present results highlight the interest of diamondoids as tools for investigating the size-limit of inhibitors,⁵¹ the low solubility and the high metabolic lability of these derivatives severely limits their potential use in medicinal chemistry.⁵²

4. Experimental section

4.1. Chemistry

4.1.1. General

Commercially available reagents and solvents were used without further purification unless stated otherwise. Preparative normal phase chromatography was performed on a CombiFlash Rf 150 (Teledyne Isco) with pre-packed RediSep Rf silica gel cartridges. Thin-layer chromatography was performed with aluminum-backed sheets with silica gel 60 F₂₅₄ (Merck, ref. 1.05554), and spots were visualized with UV light and 1% aqueous solution of KMnO₄. Melting points were determined in open capillary tubes with a MFB 595010M Gallenkamp. 400 MHz ¹H and 100.6 MHz ¹³C NMR spectra were recorded on a Varian Mercury 400 or on a Bruker 400 Avance III spectrometers. 500 MHz ¹H NMR spectra were recorded on a Varian Inova 500 spectrometer. The chemical shifts are reported in ppm (δ scale) relative to internal tetramethylsilane, and coupling constants are reported in Hertz (Hz). Assignments given for the NMR spectra of selected new compounds have been carried out on the basis of DEPT, COSY ¹H/¹H (standard procedures), and COSY ¹H/¹³C (gHSQC and gHMBC sequences) experiments. IR spectra were run on Perkin-Elmer Spectrum RX I, Perkin-Elmer Spectrum TWO or Nicolet Avatar 320 FT-IR spectrophotometers. Absorption values are expressed as wave-numbers (cm⁻¹); only significant absorption bands are given. High-resolution mass spectrometry (HRMS) analyses were performed with an LC/MSD TOF Agilent Technologies spectrometer. The elemental analyses were carried out in a Flash 1112 series Thermofinnigan elemental micro-analyzer (A5) to determine C, H, N and S. The structure of all new compounds was confirmed by elemental analysis and/or accurate mass measurement, IR, ¹H NMR and ¹³C NMR. The analytical samples of all the new compounds, which were subjected to pharmacological evaluation, possessed purity \geq 95% as evidenced by their elemental analyses.

4.1.2. Diamantan-3-one (17)

Diamantane, **16** (600 mg, 3.19 mmol), was suspended in conc. H₂SO₄ 96% (5 mL). The mixture was stirred at 75 °C for 10 h. The reaction mixture was cooled to room temperature and poured on ice. This aqueous solution was extracted with diethyl ether (3 \times 50 mL). The combined organic phases were dried over anh. Na₂SO₄ and filtered. Evaporation of the organics gave a white solid (494 mg). This residue was dissolved in DCM (20 mL). 25 g of neutrum alumina were added and the solvent was evaporated obtaining a white solid. Then, hexane (25 mL) was added, the suspension was stirred for 5 min and was filtered (\times 2). Diethyl ether (50 mL) was added, the suspension was stirred for 5 min and it was filtrated. Evaporation of the organics gave **17** as a white solid (440 mg, 69% yield). The spectroscopic data coincide with those described in the bibliography.^{53,54}

4.1.3. Diamantane-3-amine (8)

Diamantan-3-one, **17** (583 mg, 2.88 mmol) was dissolved in IPA (6 mL), followed by the addition of AcONH₄ (3.33 g, 43.22 mmol). The mixture was stirred at reflux for 1 h. Then, NaCNBH₃ (1.26 g, 20.17 mmol) was added. The reaction mixture was stirred at reflux for 24 h. The dark solution was cooled down to room temperature and 10 N NaOH was added until basic pH to quench the reaction. This mixture was extracted with DCM (3 × 50 mL) and the combined organic phases were dried over anhydrous Na₂SO₄ and filtered. Evaporation of the organics gave a white solid (580 mg) which was dissolved in EtOAc and extracted with 2 N HCl. The aqueous layer was basified with 5 N NaOH until basic pH and extracted with EtOAc. The combined organic phases were dried over anhydrous Na₂SO₄ and filtered. Evaporation of the organics *in vacuo* gave **8** as a white solid (390 mg, 66% yield). ¹H NMR (400 MHz, CDCl₃) δ: 1.50 (dt, *J* = 12.8 Hz, *J'* = 3.2 Hz, 1H), 1.61–1.83 (complex signal, 15H), 1.92–1.98 (complex signal, 2H), 2.91 (t, *J* = 2.8 Hz, 1H, 3-H). ¹³C NMR (100.6 MHz, CDCl₃) δ: 26.4 (CH), 31.1 (CH), 31.7 (CH₂), 32.4 (CH), 36.6 (CH), 37.0 (CH), 37.6, 37.7, 37.8, 38.83 and 38.0 (1 CH and 4 CH₂), 43.9 (CH), 56.4 (CH). HRMS-ESI⁺ *m/z* [M + H]⁺ calcd for [C₁₄H₂₁N + H]⁺: 204.1747, found: 204.1753.

4.1.4. General procedure for the synthesis of the ureas **1** and **10–15**

In a round-bottom flask equipped with a stir bar under nitrogen atmosphere the appropriate amine hydrochloride (1.2 mmol) was added to anhydrous DCM (~110 mM). To this suspension 2,3,4-trifluorophenyl isocyanate (1 mmol) followed by triethylamine (7 mmol) was added. The reaction mixture was stirred at room temperature overnight. Then the solvent was removed *in vacuo* and the resulting crude was purified by column chromatography.

4.1.5. 1-(1-Adamanty)-3-(2,3,4-trifluorophenyl)urea (**1**)

From adamantan-1-amine hydrochloride (**2-HCl**) (162 mg) and following the general procedure a crude was obtained. Column chromatography (SiO₂, Hexane/Ethyl Acetate mixture) followed by evaporation *in vacuo* of the appropriate fractions gave the urea **1** (280 mg, quantitative yield). The analytical sample was obtained by crystallization from methanol. The spectroscopic data coincide with those described in the bibliography.³⁷

4.1.6. 1-(2-Adamanty)-3-(2,3,4-trifluorophenyl)urea (**10**)

From adamantan-2-amine hydrochloride (**3-HCl**) (166 mg) and following the general procedure a crude was obtained. Column chromatography (SiO₂, Hexane/Ethyl Acetate mixture) followed by evaporation *in vacuo* of the appropriate fractions gave the urea **10** (270 mg, 94% yield). The analytical sample was obtained by crystallization from EtOAc/pentane. The spectroscopic data were identical to those previously published.³⁷

4.1.7. 1-[(3,7-Dimethyl(tricyclo[3.3.0.0^{3,7}]oct-1-yl)methyl)-3-(2,3,4-trifluorophenyl)urea (**11**)

From (3,7-dimethyltricyclo[3.3.0.0^{3,7}]octan-1-yl)methanamine hydrochloride (**6-HCl**) (50 mg) and following the general procedure a crude was obtained. Column chromatography (SiO₂, Hexane/Ethyl Acetate mixture) followed by concentration *in vacuo* of the appropriate fractions gave the urea **11** (82 mg, 98% yield) as a white solid, mp 133–134 °C. IR (ATR) ν: 3323, 2952, 2881, 1637, 1621, 1570, 1510, 1474, 1292, 1244, 1177, 1045, 1001, 985, 809, 794, 755, 682, 653 cm⁻¹. ¹H NMR (500 MHz, CD₃OD) δ: 1.17 (s, 6H, C3(7)-CH₃), 1.32–1.38 (complex signal, 4H, 4(6)-H_a and 2(8)-H_a), 1.42 (d, *J* = 7.5 Hz, 2H, 2(8)-H_b), 1.59 (dd, *J* = 8 Hz, *J'* = 3 Hz, 2H, 4(6)-H_b), 2.10 (t, *J* = 3 Hz, 1H, 5-H), 3.42 (s, 2H, CH₂-N), 7.01 (m, 1H, 5'-H), 7.75 (m, 1H, 6'-H). ¹³C NMR (125.7 MHz, CD₃OD) δ: 17.1 [CH₃, C3(7)-CH₃], 42.7 (CH, C5), 43.8 [CH₂, CH₂-N], 48.5 [C, C3(7)], 52.3 (C, C1), 54.9 [CH₂, C4(6)], 57.2 [CH₂, C2(8)], 112.3 (CH, dd, ²*J*_{C,F} = 17.7 Hz, ³*J*_{C,F} = 3.9 Hz, C5'), 116.7 (CH, C6'), 127.0 (C, d, ²*J*_{C,F} = 6 Hz, C1'), 141.5 (C, dt, ¹*J*_{C,F} = 247 Hz, ²*J*_{C,F} = 15 Hz, C3'), 143.6 (C, dd, ¹*J*_C

F = 246 Hz, ²*J*_{C,F} = 12 Hz, C4'), 147.5 (C, dd, ¹*J*_{C,F} = 243 Hz, ²*J*_{C,F} = 9 Hz, C2'), 157.8 (C, CO). MS (DIP), *m/z* (%); significant ions: 338 (M⁺, 1), 149 [(C₁₁H₁₇)⁺, 43], 148 (86), 147 [(C₆H₄F₃N)⁺, 42], 136 (19), 135 [(C₁₀H₁₅)⁺, 100], 119 (18), 107 (56), 106 (15), 105 (15), 93 (42), 91 (28), 79 (16), 77 (16). Elemental analysis: Calculated for C₁₈H₂₁F₃N₂O: C 63.89, H 6.26, N 8.28. Found: C 63.83, H 6.52, N 8.26.

4.1.8. 1-(3,7-Dimethyl(tricyclo[3.3.0.0^{3,7}]oct-1-yl)-3-(2,3,4-trifluorophenyl)urea (**12**)

From 3,7-dimethyltricyclo[3.3.0.0^{3,7}]octan-1-amine hydrochloride (**5-HCl**) (61 mg) and following the general procedure a crude was obtained. Column chromatography (SiO₂, Hexane/Ethyl Acetate mixture) followed by evaporation *in vacuo* of the appropriate fractions gave the urea **12** (50 mg, 47% yield) as a white solid, mp 174–175 °C. IR (ATR) ν: 3335, 2957, 2930, 2882, 2158, 2005, 1686, 1656, 1637, 1621, 1565, 1509, 1471, 1308, 1289, 1242, 1204, 1165, 1154, 1118, 1081, 1064, 1020, 1009, 964, 946, 816, 796, 719, 694, 678, 657 cm⁻¹. ¹H NMR (400 MHz, CDCl₃) δ: 1.15 [s, 6H, 3(7)-CH₃], 1.39 [dd, *J* = 8.4 Hz, *J'* = 3.6 Hz, 2H, 4(6)-H_a], 1.64 [dd, *J* = 7.6 Hz, *J'* = 3.6 Hz, 2H, 2(8)-H_a], 1.76 [dd, *J* = 8.4 Hz, *J'* = 3.0 Hz, 2H, 4(6)-H_b], 1.82 [d, *J* = 7.6 Hz, 2H, 2(8)-H_b], 2.38 (t, *J* = 3.0 Hz, 1H, 5-H), 5.47 (broad s, 1H, 1-NH), 6.75 (broad s, 1H, 3-NH), 6.89 (m, 1H, 5'-H), 7.80 (m, 1H, 6'-H). ¹³C NMR (100.6 MHz, CDCl₃) δ: 16.5 [CH₃, C3(7)-CH₃], 44.8 (CH, C5), 46.2 [C, C3(7)], 53.1 [CH₂, C4(6)], 57.5 [CH₂, C2(8)], 61.8 (C, C1), 111.4 (CH, dd, ²*J*_{C,F} = 17.7 Hz, ³*J*_{C,F} = 3.8 Hz, C5'), 115.0 (CH, t, ³*J*_{C,F} = 5 Hz, C6'), 124.8 (C, dd, ²*J*_{C,F} = 8 Hz, ³*J*_{C,F} = 3.4 Hz, C1'), 139.7 (C, ddd, ¹*J*_{C,F} = 249 Hz, ²*J*_{C,F} = 16.3 Hz, ³*J*_{C,F} = 13.7 Hz, C3'), 142.1 (C, ddd, ¹*J*_{C,F} = 244 Hz, ²*J*_{C,F} = 11.9 Hz, ³*J*_{C,F} = 3.2 Hz, C4'), 141.4 (C, ddd, ¹*J*_{C,F} = 245 Hz, ²*J*_{C,F} = 10 Hz, ³*J*_{C,F} = 2.8 Hz, C2'), 154.6 (C, CO). MS (EI), *m/z* (%); significant ions: 324 (M⁺, 8), 268 (15), 148 (44), 147 [(C₆H₄F₃N)⁺, 100], 146 (23), 136 (17), 134 (84), 122 (89), 121 (54), 120 (40), 119 (81), 110 (20), 109(51), 108 (50), 107 (28), 106 (16), 105 (21), 96 (17), 95 (70), 94 (54), 93 (52), 92 (18), 91 (44), 81 (17), 80 (18), 79 (37), 77 (33), 67 (24), 55 (16), 41 (23). Elemental analysis: Calculated for C₁₇H₁₉F₃N₂O: C 62.95, H 5.90, N 8.64. Found: C 63.12, H 6.17, N 8.48.

4.1.9. 1-(Tricyclo[3.3.0.0^{3,7}]oct-1-yl)-3-(2,3,4-trifluorophenyl)urea (**13**)

From tricyclo[3.3.0.0^{3,7}]octan-1-amine hydrochloride (**4-HCl**) (19 mg) and following the general procedure a crude was obtained. Column chromatography (SiO₂, Hexane/Ethyl Acetate mixture) followed by evaporation *in vacuo* of the appropriate fractions gave the urea **13** (24 mg, 66% yield) as a white solid, mp 185–186 °C. IR (ATR) ν: 3331, 3105, 2970, 2943, 2894, 2159, 1656, 1640, 1620, 1563, 1510, 1467, 1318, 1288, 1244, 1204, 1171, 1107, 1076, 1065, 1017, 979, 823, 800, 764, 723, 710, 690, 668, 645, 620 cm⁻¹. ¹H NMR (400 MHz, CDCl₃) δ: 1.51 [d, *J* = 8.8 Hz, 2H, 4(6)-Ha], 1.74 [complex signal, 6H, 4(6)-H_a, 2(8)-H₂], 2.34 [broad s, 2H, 3(7)-H], 2.42 (m, 1H, 5-H), 5.42 (broad s, 1H, 1-NH), 6.67 (broad s, 1H, 3-NH), 6.90 (m, 1H, 5'-H), 7.82 (m, 1H, 6'-H). ¹³C NMR (100.6 MHz, CDCl₃) δ: 32.8 [CH, C3(7)], 43.0 (CH, C5), 46.6 [CH₂, C4(6)], 51.1 [CH₂, C2(8)], 61.6 (C, C1), 111.4 (CH, dd, ²*J*_{C,F} = 17.7 Hz, ³*J*_{C,F} = 3.7 Hz, C5'), 115.1 (CH, t, ³*J*_{C,F} = 5.6 Hz, C6'), 124.8 (C, dd, ²*J*_{C,F} = 8 Hz, ³*J*_{C,F} = 3.5 Hz, C1'), 139.7 (C, dt, ¹*J*_{C,F} = 245 Hz, ²*J*_{C,F} = 15 Hz, C3'), 142.2 (C, dd, ¹*J*_{C,F} = 225 Hz, ²*J*_{C,F} = 12 Hz, C4'), 146.5 (C, dd, ¹*J*_{C,F} = 246 Hz, ²*J*_{C,F} = 10 Hz, Ar-C2'), 154.6 (C, CO). MS (DIP), *m/z* (%); significant ions: 296 (M⁺, 34), 268 (14), 267 (24), 254 (22), 147 [(C₆H₄F₃N)⁺, 77], 146 (23), 119 (14), 95 (29), 94 (100), 82 (29), 81 (62), 80(20), 79(18). Elemental analysis: Calculated for C₁₅H₁₅F₃N₂O: C 60.81, H 5.10, N 9.45. Found: C 60.87, H 5.34, N 9.19.

4.1.10. 1-(Tricyclo[3.3.1.0^{3,7}]non-3-yl)-3-(2,3,4-trifluorophenyl)urea (**14**)

From tricyclo[3.3.1.0^{3,7}]nonyl-3-amine hydrochloride (**7-HCl**) (100 mg) and following the general procedure, a yellow solid was obtained (191 mg). Column chromatography (Hexane/Ethyl Acetate

mixture) gave urea **14** as a white solid (52 mg, 57% yield), mp 192–193 °C. IR (ATR) ν : 661, 757, 798, 956, 1005, 1021, 1052, 1083, 1101, 1155, 1176, 1248, 1287, 1325, 1382, 1429, 1470, 1509, 1563, 1633, 1656, 2346, 2852, 2925, 3343 cm^{-1} . $^1\text{H NMR}$ (400 MHz, CDCl_3) δ : 1.54–1.69 [complex signal, 4H, 9- H_2 and 6(8)- H_{ax}], 1.92 [dd, $J = 10.0$ Hz, $J' = 2.8$ Hz, 2H, 2(4)- H_{ax}], 2.01–2.10 [complex signal, 4H, 6(8)- H_{eq} and 2(4)- H_{eq}], 2.25 [broad singlet, 2H, 1(5)-H], 2.40 [t, $J = 6.8$ Hz, $J' = 2.5$ Hz, 1(7)-H], 7.00 (m, 1H, 5'-H), 7.69 (m, 1H, 6'-H). $^{13}\text{C NMR}$ (100.6 MHz, CDCl_3) δ : 35.9 (CH_2 , C9), 38.8 (CH, C1 and C5), 44.3 (CH_2 , C6 and C6), 44.8 (CH, C7), 49.9 (CH_2 , C2 and C4), 65.3 (C, C3), 112.2 (CH, dd, $^2J_{C-F} = 18$ Hz, $^3J_{C-F} = 4$ Hz, C5'), 116.8 (CH, C6'), 126.9 (C, dd, $J = 3$ Hz, $J' = 8$ Hz, C1'), 139.9 (C, dt, $^1J_{C-F} = 247.4$, $^2J_{C-F} = 14$, C3'), 146–148 (complex signal, C4' and C2'), 156.8 (C, CO). Elemental analysis: Calcd for $\text{C}_{16}\text{H}_{17}\text{F}_3\text{N}_2\text{O} \cdot 0.25$ MeOH: C 61.31, H 5.70, N 8.80. Found: C 61.51, H 5.94, N 8.55.

4.1.11. 1-(Diamant-3-yl)-3-(2,3,4-trifluorophenyl)urea (**15**)

From diamantane-3-amine (**8**) (160 mg) and following the general procedure, a solid was obtained (291 mg). Column chromatography (Hexane/Dichloromethane mixture) gave the urea **15** (72 mg, 24% yield) as a white solid, mp 199–200 °C. IR (ATR) ν : 678, 806, 1002, 1025, 1088, 1210, 1249, 1289, 1467, 1513, 1564, 1623, 1671, 1862, 1933, 1997, 2107, 2198, 2357, 2413, 2903 cm^{-1} . $^1\text{H NMR}$ (400 MHz, CDCl_3) δ : 1.55–1.84 (complex signal, 17 diamantane-H), 3.87 (m, 1H, 3 diamantane-H), 5.57 (broad s, 1H, 1-NH), 6.90 (m, 1H, 5'-H), 7.09 (broad s, 1H, 3-NH), 7.74 (m, 1H, 6'-H). $^{13}\text{C NMR}$ (100.6 MHz, CDCl_3) δ : 26.1 (CH), 30.1 (CH), 32.3 (CH), 32.7 (CH_2), 36.3 (CH), 36.6 (CH), 37.2, 37.3, 37.35, 37.4 and 37.5 (1 CH and 4 CH_2), 37.7 (CH_2) 41.5 (CH, C4), 55.2 (CH, C3), 111.5 (CH, dd, $^2J_{C-F} = 18$ Hz, $^3J_{C-F} = 4$ Hz, C5'), 115.1 (CH, C6'), 125.0 (C, dd, $^2J_{C-F} = 8$ Hz, $^3J_{C-F} = 3$ Hz, C1'), 141.1 (C, dt, $^1J_{C-F} = 247$, $^2J_{C-F} = 16$, C3'), 146.5 (C, dm, $^1J_{C-F} = 246$ Hz, C4'), 146.9 (C, dm, $^1J_{C-F} = 248$ Hz, C2'), 154.6 (C, CO). Elemental analysis: Calcd for $\text{C}_{21}\text{H}_{23}\text{F}_3\text{N}_2\text{O} \cdot 0.25$ CH_2Cl_2 : C 64.18, H 5.96, N 7.04. Found: C 64.40, H 6.35, N 6.71.

4.1.12. Tricyclo[3.3.1.0^{3,7}]nonyl-3-isocyanate (**18**)

Tricyclo[3.3.1.0^{3,7}]nonyl-3-amine hydrochloride (**7-HCl**) (750 mg, 4.33 mmol) was suspended in DCM (52 mL) and aq. NaHCO_3 (22 mL) was added. Under argon atmosphere, the mixture was stirred and cooled to 4 °C on an ice bath. Immediately, trisphosgene (642 mg, 2.16 mmol) was added. The mixture was stirred at 4 °C for 30 min. The 2 phases were separated and the organic layer was washed with brine (2 \times 30 mL). The organic phase was dried over anhydrous Na_2SO_4 and filtered. Evaporation *in vacuo* of the organics gave **18** as a yellowish oil (360 mg, 51% yield) which was used in the next step without further purification.

4.1.13. 4-((Trans-4-(3-(tricyclo[3.3.1.0^{3,7}]non-3-yl)ureido)cyclohexyl)oxy)benzoic acid (**19**)

Under argon atmosphere, tricyclo[3.3.1.0^{3,7}]nonyl-3-isocyanate (**18**) (250 mg, 1.53 mmol) was dissolved in anhydrous DCM (16 mL). 4-((trans-4-aminocyclohexyl)oxy)benzoic acid⁵⁵ hydrochloride (497 mg, 1.83 mmol) and Et_3N (619 mg, 6.12 mmol) were added. The reaction mixture was stirred at 30 °C overnight. Water (60 mL) was added to the resulting mixture and two phases were separated. The aqueous phase was washed with DCM (2 \times 50 mL) and acidified until pH = 2 with 5 N HCl. This acid solution was extracted with DCM (5 \times 30 mL) and the organic layer was dried over anhydrous Na_2SO_4 , filtered and evaporated. The residue was dissolved in EtOAc, washed with 2 N HCl, dried over anhydrous Na_2SO_4 , filtered and evaporated. The organics were evaporated to afford a yellowish oil (70 mg, 12% yield). Urea **19** was obtained by crystallization from hot MeOH as white solid, mp 262–263 °C. IR (ATR) ν : 3377, 3334, 2926, 2862, 1683, 1628, 1605, 1556, 1508, 1456, 1421, 1382, 1326, 1304, 1248, 1163, 1129, 1119, 1096, 1008, 953, 902, 847, 775, 698, 636, 599 cm^{-1} . $^1\text{H NMR}$ (400 MHz, CD_3OD) δ : 1.36 (dq, $J = 3.2$ Hz, $J' = 13.2$ Hz, 2H, 3'(5')- H_{ax}), 1.51–1.66 [complex signal,

6H, 2'(6')- H_{ax} , 9"- H_2 and 6"(8")- H_{ax}], 1.86 [dd, $J = 10.0$ Hz, $J' = 2.8$ Hz, 2H, 2"(4")- H_{ax}], 1.98–2.05 [complex signal, 6H, 6"(8")- H_{eq} and 3'(5')- H_{eq} and 2"(4")- H_{eq}], 2.13 [dd, $J = 4$ Hz, $J' = 12.8$ Hz, 2H, 2'(6')- H_{eq}], 2.22 [broad s, 2H, 1'(5')-H], 2.34 (t, $J = 6.8$ Hz, 1H, 7"-H), 4.39 (m, 1H, 1'-H), 6.96 [d, $J = 9.2$ Hz, 2H, 3(5)-H], 7.93 [d, $J = 8.8$ Hz, 2H, 2(6)-H]. $^{13}\text{C NMR}$ (100.6 MHz, CD_3OD) δ : 29.1 [CH_2 , C2'(6')], 29.6 [CH_2 , C3'(5')], 33.9 (CH_2 , C9"), 36.7 [CH, C1'(5")], 42.3 [CH_2 , C6"(8")], 42.9 (CH, C7"), 46.8 (CH, C4'), 48.2 [CH_2 , C2"(4")], 63.3 (C, C3"), 74.0 (CH, C1'), 114.2 [CH, C3(5)], 121.2 (C, C1), 130.6 [CH, C2(6)], 157.9 (C, CO), 161.3 (C, C4), 166.5 (CO_2H). HRMS-ESI m/z [M-H]⁻ calcd for $[\text{C}_{23}\text{H}_{30}\text{N}_2\text{O}_4\text{-H}]^-$: 397.2133, found: 397.2147.

4.1.14. Diamantane-3-isocyanate (**20**)

Triphosgene (110 mg, 0.368 mmol) was added in a single portion to a solution diamantane-3-amine (**8**) (150 mg, 0.73 mmol) in DCM (10.5 mL) and saturated NaHCO_3 solution (4.5 mL). The resulting biphasic mixture was stirred at room temperature for 30 min. Then, the two phases were separated and the organic layer was washed with brine, dried over anhydrous Na_2SO_4 and filtered. Evaporation *in vacuo* provided the isocyanate **20** as a white solid (152 mg, 90% yield), which was used in the next step without further purification.

4.1.15. 4-((Trans-4-(3-(diamantane-3-yl)ureido)cyclohexyl)oxy)benzoic acid (**21**)

4-((Trans-4-aminocyclohexyl)oxy)benzoic acid hydrochloride⁵⁵ (196 mg, 0.720 mmol) is dissolved in DMF (5 mL) and diamantane-3-isocyanate (**20**) (150 mg, 0.65 mmol) was added followed by Et_3N (145 mg, 1.44 mmol). The reaction mixture was stirred at 50 °C for 3 days. The suspension was filtrated and the solvent was evaporated to obtain a brown solid (315 mg) which was dissolved in DCM and washed with 2 N HCl (2 \times 20 mL). The organic layer was dried over anhydrous Na_2SO_4 , filtered and evaporated. The resulting residue was crystallized from hot DCM affording the urea **21** (111 mg, 37% yield) as a white solid, mp 229–230 °C. IR (ATR) ν : 633, 695, 770, 845, 1031, 1052, 1088, 1163, 1243, 1312, 1504, 1568, 1599, 1710, 1956, 2020, 2237, 2346, 2496, 2868, 2904 cm^{-1} . $^1\text{H NMR}$ (400 MHz, CD_3OD) δ : 1.36 (dq, $J = 3.2$ Hz, $J' = 13.2$ Hz, 2H, 3'(5')- H_{ax}), 1.52–1.63 [complex signal, 3H, 2'(6')- H_{ax} and 1 diamantane-H], 1.67–1.91 (complex signal, 17 diamantane-H), 2.02 [dd, $J = 4.4$ Hz, $J' = 13.2$ Hz, 2H, 3'(5')- H_{eq}], 2.13 [dd, $J = 3.6$ Hz, $J' = 13.2$ Hz, 2H, 2'(6')- H_{eq}], 3.58 (m, 1H, 4-H'), 3.73 (t, $J = 2.8$ Hz, 1H, 3"-H), 4.39 (m, 1H, 1'-H), 6.95 [d, $J = 8.8$ Hz, 2H, 3(5)-H], 7.94 [d, $J = 8.8$ Hz, 2H, 2(6)-H]. $^{13}\text{C NMR}$ (100.6 MHz, CD_3OD) δ : 27.7 (CH), 31.1 [CH_2 , C2'(6')], 31.7 [CH_2 , C3'(5')], 31.8 (CH), 33.4 (CH), 33.6 (CH_2), 38.0 (CH), 38.2, 38.6, 38.74, 38.77, 38.93, 38.95, 39.0, 43.3 (CH), 48.9 (CH, C4'), 55.2 (CH, C3"), 76.0 (CH, C1'), 111.4 (C, C1), 116.1 [CH, C3(5)], 132.8 [CH, C2(6)], 159.9 (C, CO), 163.0 (C, C4), 170.3 (CO_2H). Elemental analysis: Calcd for $\text{C}_{28}\text{H}_{36}\text{N}_2\text{O}_4 \cdot 0.1$ CH_2Cl_2 : C 71.34, H 7.71, N 5.92. Found: C 71.36, H 7.85, N 5.70.

4.1.16. N-(1-Acetyl-piperidin-4-yl)-1H-imidazole-1-carboxamide (**23**)

N,N-carbonyldiimidazole (400 mg, 2.46 mmol) was suspended in anhydrous 1,2-dichloroethane (15 mL) under nitrogen. Then 1-acetyl-4-aminopiperidine (**22**) (250 mg, 1.76 mmol) was added and the reaction mixture was heated to 50 °C for 21 h. With an external ice bath, the mixture was cooled down for 30 min. The resulting solid was collected by filtration *in vacuo* and washed with 1,2-DCE (20 mL) affording **23** (312 mg, 75% yield) as a white solid, mp 191–193 °C. IR (ATR) ν : 3216, 3118, 3038, 2918, 2342, 2074, 1709, 1613, 1542, 1479, 1463, 1441, 1369, 1358, 1320, 1281, 1272, 1233, 1195, 1137, 1111, 1090, 1068, 1053, 1001, 984, 974, 916, 902, 859, 799, 748, 652 cm^{-1} . $^1\text{H NMR}$ (400 MHz, CDCl_3) δ : 1.37 (complex signal, 2H, 3- H_{ax} , 5- H_{ax}), 1.99 (dm, $J = 12.8$ Hz, $J' = 4$ Hz, 1H) and 2.21 (dm, $J = 12.8$ Hz, $J' = 4$ Hz, 1H) (3'- H_{eq} and 5'- H_{eq}), 2.09 (s, 3H, COCH_3), 2.69 (ddd, $J = 13$ Hz, $J' = 2.6$ Hz, 1H) and 3.21 (ddd, $J = 13$ Hz, $J' = 2.6$ Hz, 1H) (2'- H_{ax} and

6'-H_{ax}), 3.86 (dm, *J* = 13.6 Hz, 1H) and 4.67 (dm, *J* = 13.6 Hz, 1H) (2'-H_{eq} and 6'-H_{eq}), 4.10 (m, 1H, 4'-H), 7.06 (dd, *J* = 1.6 Hz, *J'* = 0.8 Hz, 1H, 4-H), 7.29 (broad d, *J* = 7.6 Hz, 1H, NH), 7.60 (dd, *J* = 1.6 Hz, *J'* = 1.2 Hz, 1H, 5-H), 8.29 (dd, *J* = 1.2 Hz, *J'* = 0.8 Hz, 1H, 2-H). ¹³C NMR (100.6 MHz, CDCl₃) δ: 21.5 (CH₃, COCH₃), 31.4 and 33.1 (CH₂, C3' and C5'), 40.9 and 45.6 (CH₂, C2' and C6'), 48.2 (CH, C4'), 116.2 (CH, C5), 130.3 (CH, C4), 136.2 (CH, C2), 148.5 (C, NHCNH), 169.2 (C, COCH₃). MS (DIP), *m/z* (%); significant ions: 169 (10), 168 (100), 153 (19), 126 (53), 125 (31), 85 (19), 84 (42), 83 (20), 82 (23), 81 (21), 68 (98), 57 (40), 56 (56), 55 (16). HRMS-ESI⁺ *m/z* [M+H]⁺ calcd for [C₁₁H₁₆N₄O₂+H]⁺: 237.1346, found: 237.1345.

4.1.17. 1-(1-Acetylpiperidin-4-yl)-3-(3,7-dimethyl(tricyclo[3.3.0.0^{3,7}]octa-1-yl)urea (24)

In a round bottom flask equipped with a condenser apparatus and magnetic stirrer a solution of 3,7-dimethyltricyclo[3.3.0.0^{3,7}]octan-1-amine hydrochloride (**5HCl**) (68 mg, 0.36 mmol) in chloroform (5 mL) was prepared, to which was added *N*-(1-acetylpiperidin-4-yl)-1*H*-imidazole-1-carboxamide (**23**) (172 mg, 0.73 mmol) followed by triethylamine (0.06 mL, 0.40 mmol). The solution was heated to 50 °C for 25 h, whereupon the reaction mixture was tempered to room temperature and evaporated *in vacuo* to dryness (384 mg). Purification by column chromatography (SiO₂, Dichloromethane/Methanol mixture) afforded **24** (90 mg, 77% yield) as a white solid, mp 165–167 °C. IR (ATR) ν: 3359, 3244, 2947, 2878, 2170, 2034, 1960, 1613, 1556, 1477, 1443, 1371, 1318, 1264, 1227, 1151, 1096, 1033, 978, 717, 639 cm⁻¹. ¹H NMR (400 MHz, CDCl₃) δ: 1.11 [s, 6H, 3'(7')-CH₃], 1.22 [complex signal, 2H, 2(6)-H_{ax}], 1.34 [dd, *J* = 8.2 Hz, *J'* = 3.4 Hz, 2H, 4'(6')-H_{ax}], 1.54 [dd, *J* = 7.4 Hz, *J'* = 3.4 Hz, 2H, 2'(8')-H_{ax}], 1.70 [dd, *J* = 8.2 Hz, *J'* = 2.6 Hz, 2H, 4'(6')-H_{ax}], 1.75 [d, *J* = 7.6 Hz, 2H, 2'(8')-H_{ax}], 1.90 and 2.03 (complex signal, 2H, 3-H_{ax} and 5-H_{ax}), 2.07 (s, 3H, COCH₃), 2.27 (t, *J* = 2.6 Hz, 1H, 5'-H), 2.75 (dt, *J* = 14.0 Hz, *J'* = 2.8 Hz, 1H, 2-H_{ax} or 6-H_{ax}), 3.14 (dt, *J* = 11.2 Hz, *J'* = 2.8 Hz, 2H, 6-H_{ax} or 2-H_{ax}), 3.73 (broad d, *J* = 13 Hz, 2H, 6-H_{eq} or 2-H_{eq}), 3.83 (m, 1H, 4-H), 4.42 (broad d, *J* = 13 Hz, 2H, 2-H_{eq} or 6-H_{eq}), 4.79 (d, *J* = 7.6 Hz, 1H, 1-NH), 5.18 (broad s, 1H, 3-NH). ¹³C NMR (100.6 MHz, CDCl₃) δ: 16.5 (CH₃, C3'(7')-CH₃), 21.4 (CH₃, COCH₃), 33.6 [CH₂, C3(5)], 40.6 (CH₂, C2), 44.7 (CH, C5'), 45.3 (CH₂, C6), 46.1 [C, C3'(7')], 46.9 (CH, C4), 53.2 [CH₂, C4'(6')], 57.6 [CH₂, C2'(8')], 61.7 (C, C1'), 157.4 (C, CO urea), 169.0 (C, COCH₃). MS (DIP), *m/z* (%); significant ions: 278 (10), 277 (58), 263 (20), 178 (10), 169 (25), 151 (18), 150 (22), 148 (25), 143 (100), 136 (26), 135 (43), 134 (31), 127 (16), 126 (23), 125 (17), 123 (11), 122 (86), 121 (29), 119 (25), 110 (22), 109 (86), 108 (48), 96 (18), 95 (62), 94 (29), 93 (16), 91 (15), 84 (31), 83 (16), 82 (33), 80 (11), 79 (12), 77 (11), 67 (11), 57 (13), 56 (25), 55 (17). Elemental analysis: Calculated for C₁₈H₂₉N₃O₂: C 67.68, H 9.15, N 13.15. Calculated for C₁₈H₂₉N₃O₂·1.0 H₂O: C 64.07, H 9.26, N 12.45. Found: C 64.00, H 9.31, N 12.40.

4.1.18. 1-(1-Acetylpiperidin-4-yl)-3-(tricyclo[3.3.1.0^{3,7}]non-3-yl)urea (25)

Under argon atmosphere, tricyclo[3.3.1.0^{3,7}]nonane-3-isocyanate (**18**) (360 mg, 2.20 mmol) was dissolved in anh. DCM (10 mL). 1-acetyl-4-aminopiperidine (375 mg, 2.64 mmol) and Et₃N (445 mg, 4.40 mmol) were added. The reaction mixture was stirred at room temperature overnight. The solvent was removed *in vacuo* and the residue was dissolved in EtOAc and washed with 2 N HCl. The organics were dried over anh. Na₂SO₄, filtered and evaporated *in vacuo* affording a white yellowish solid which was washed with acetone and EtOAc affording the urea **25** as a yellowish solid (240 mg, 36% yield), mp 164–165 °C. IR (ATR) ν: 638, 705, 783, 860, 904, 974, 992, 1059, 1139, 1230, 1269, 1318, 1361, 1429, 1555, 1620, 1659, 2351, 2919, 3328 cm⁻¹. ¹H NMR (400 MHz, CDCl₃) δ: 1.16–1.29 (complex signal, 2H, 4-H_{ax} and 5-H_{ax}), 1.47–1.61 [complex signal, 4H, 9'-H₂ and 6'(8')-H_{ax}], 1.80 [dd, *J* = 10.0 Hz, *J'* = 2.8 Hz, 2H, 2'(4')-H_{ax}], 1.84–2.01 [complex signal, 6H, 6'(8')-H_{eq}, 2'(4')-H_{eq}, 4-H_{eq} and 5-H_{eq}], 2.07 (s, 3H, 8-H), 2.23

[broad singlet, 2H, 1'(5')-H], 2.34 (t, *J* = 6.8 Hz, 1H, 7'-H), 2.74 (dt, *J* = 11.2 Hz, *J'* = 2.4 Hz, 1H, 2-H_{ax} or 6-H_{ax}), 3.13 (dt, *J* = 12 Hz, *J'* = 2.4 Hz, 1H, 6-H_{ax} or 2-H_{ax}), 3.71–3.85 (complex signal, 2H, 2-H_{eq} or 6-H_{eq} and 4-H), 4.43 (d, *J* = 13.6 Hz, 1H, 6-H_{eq} or 2-H_{eq}), 4.89 (d, *J* = 8.0 Hz, 1H, NH), 5.11 (s, 1H, NH). ¹³C NMR (100.6 MHz, CDCl₃) δ: 21.4 (CH₃, COCH₃), 32.5 (CH₂, C4 or C5), 33.7 (CH₂, C5 or C4), 34.8 (CH₂, C9'), 37.3 [CH, C1'(5')], 40.7 (CH₂, C2 or C6), 43.4 [CH₂, C6'(8')], 43.7 (CH, C7'), 45.4 (CH₂, C6 or C2), 46.7 (CH, C4), 49.30 and 49.32 (CH₂, C2' and C4'), 64.1 (C, C3'), 157.1 (CO, urea), 169.0 (CO, COCH₃). Elemental analysis: Calcd for C₁₇H₂₇N₃O₂·0.15C₅H₁₂: C 67.42, H 9.18, N 13.29. Found: C 66.38, H 9.00, N 13.05.

4.1.19. 1-(1-Acetylpiperidin-4-yl)-3-(diamant-3-yl)urea (26)

Diamantane-3-isocyanate (**20**) (155 mg, 0.67 mmol) was dissolved in DCM (3 mL) and 1-acetyl-4-aminopiperidine (115 mg, 0.811 mmol) dissolved in DCM (2 mL) was added. The mixture was stirred at room temperature overnight. Evaporation of the solvent gave a white solid (272 mg). Column chromatography (Dichloromethane/Methanol mixtures) gave the urea **26** (160 mg, 65% yield) as a white solid, mp 230–231 °C. IR (ATR) ν: 669, 727, 770, 808, 862, 917, 989, 1047, 1136, 1240, 1319, 1364, 1453, 1560, 1629, 1794, 1855, 1893, 1944, 1977, 2051, 2102, 2153, 2209, 2270, 2352, 2418, 2545, 2596, 2734, 2877, 3020, 3071, 3275, 3316, 3494, 3566, 3688 cm⁻¹. ¹H NMR (400 MHz, CD₃OD) δ: 1.32 [complex signal, 2H, 3(5)-H_{ax}], 1.66–1.82 (complex signal, 16H, diamantane-H), 1.85–1.98 (complex signal, 4H, 3-H_{eq}, 5-H_{eq}, 2 diamantane-H), 2.10 (s, 3H, COCH₃), 2.91 (dt, *J* = 11.2 Hz, *J'* = 2.8 Hz, 1H, 2-H_{ax} or 6-H_{ax}), 3.25 (dt, *J* = 11.2 Hz, *J'* = 3.2 Hz, 2H, 6-H_{ax} or 2-H_{ax}), 3.71–3.78 (complex signal, 2H, 4-H and 1'-H), 3.85 (dt, *J* = 14 Hz, *J'* = 2.4 Hz, 2H, 6-H_{eq} or 2-H_{eq}), 4.29 (dt, *J* = 13 Hz, *J'* = 2.8 Hz, 2H, 2-H_{eq} or 6-H_{eq}). ¹³C NMR (100.6 MHz, CD₃OD) δ: 21.2 (CH₃, COCH₃), 27.7 (CH), 31.8 (CH), 33.3 (CH₂, C3 or C5), 33.4 (CH₂), 33.6 (CH₂), 34.1 (CH₂, C5 or C3), 38.0, 38.1, 38.6, 38.7 (2 carbon), 38.91, 38.94 and 39.0 (3 CH₂ and 5 CH, diamantane signals), 41.6 (CH₂, C2 or C6), 43.3 (CH, C4'), 46.3 (CH₂, C6 or C2), 47.7 (CH, C4), 55.9 (CH, C3'), 159.7 (C, CO urea), 171.5 (C, COCH₃). HRMS-ESI⁺ *m/z* [M+H]⁺ calcd for [C₂₂H₃₃N₃O₂+H]⁺: 372.2646, found: 372.2644.

4.1.20. Diamantane-4-isocyanate (27)

Diamantane-4-amine hydrochloride (**9HCl**) (110 mg, 0.458 mmol) was suspended in DCM (2 mL) and aq. NaHCO₃ was added, followed by triphosgene (68 mg, 0.23 mmol). The biphasic mixture was stirred at room temperature for 30 min. The two phases were separated and the organic layer was washed with brine. The organics were dried over anh. Na₂SO₄, filtered and evaporated until 1 mL. The solution of isocyanate (**27**) in DCM was used in the next step without further purification.

4.1.21. 1-(1-Acetylpiperidin-4-yl)-3-(diamant-4-yl)urea (28)

To the solution of diamantane-4-isocyanate (**27**) (105 mg, 0.46 mmol) in DCM (1 mL) from the previous step is added 1-acetyl-4-aminopiperidine hydrochloride (**22HCl**) (98 mg, 0.55 mmol) and DCM (1 mL), followed by Et₃N. The mixture was stirred at room temperature overnight. DCM was added to the mixture and it was washed with 2 N HCl (30 mL). The organics were dried over anh. Na₂SO₄, filtered and evaporated to obtain a residue (48 mg). Column chromatography (Dichloromethane/Methanol mixture) gave the desired urea (**28**) (33 mg, 21% overall yield) as a beige solid, mp 195–196 °C. IR (ATR) ν: 3364, 2906, 2881, 2847, 1686, 1601, 1550, 1480, 1462, 1444, 1429, 1374, 1348, 1322, 1305, 1267, 1221, 1138, 1105, 1048, 1002, 986, 976, 918, 613, 597, 576 cm⁻¹. ¹H NMR (400 MHz, CDCl₃) δ: 1.19 (complex signal, 2H, 3-H_{ax} and 5-H_{ax}), 1.69–1.78 (complex signal, 10H, diamantane-H), 1.83–1.94 (complex signal, 11H, 3-H_{eq}, 5-H_{eq}, 9 diamantane-H), 2.08 (s, 3H, COCH₃), 2.73 (dt, *J* = 11.6 Hz, *J'* = 3.2 Hz, 1 H, 2-H_{ax} or 6-H_{ax}), 3.13 (dt, *J* = 11.6 Hz, *J'* = 3.2 Hz, 2H, 6-H_{ax} or 2-H_{ax}), 3.71–3.85 (complex signal, 2H, 4-H and 6-H_{eq} or 2-H_{eq}), 4.36 (broad s, NH, urea), 4.42–4.50 (complex signal, 2H, 2-H_{eq} or 6-H_{eq} and NH). ¹³C NMR (100.6 MHz, CDCl₃) δ: 21.4 (CH₃, COCH₃), 25.6 (CH,

C9), 32.4 (CH₂, C3 or C5), 33.6 (CH₂, C5 or C3), 36.6 (CH), 37.4 (CH₂), 38.7 (CH), 40.7 (CH₂, C2 or C6), 43.0 (CH₂), 45.4 (CH₂, C6 or C2), 46.9 (CH, C4), 49.8 (C, C4'), 156.6 (C, CO urea), 169.0 (C, COCH₃). HRMS-ESI⁺ *m/z* [M+H]⁺ calcd for [C₂₂H₃₃N₃O₂+H]⁺: 372.2646, found: 372.2657.

4.2. Solubility

A 10 mM stock solution of the compound was serially diluted in 100% DMSO and 1 μ L of this solution was added to a 384-well UV-transparent plate (Greiner) containing 99 μ L of PBS. The plate was incubated at 37 °C for 2 h and the light scattering was measured in a Nephelostar Plus reader (BMG LABTECH). The data was fitted to a segmented linear regression for measuring the compound solubility.

4.3. Microsomal stability

The human microsomes employed were purchased from Tebu-Xenotech. The compound was incubated at 37 °C with the microsomes in a 50 mM phosphate buffer (pH = 7.4) containing 3 mM MgCl₂, 1 mM NADP, 10 mM glucose-6-phosphate and 1 U/mL glucose-6-phosphate-dehydrogenase. Samples (75 μ L) were taken from each well at 0, 10, 20, 40 and 60 min and transferred to a plate containing 4 °C 75 μ L acetonitrile and 30 μ L of 0.5% formic acid in water were added for improving the chromatographic conditions. The plate was centrifuged (46,000g, 30 min) and supernatants were taken and analyzed in a UPLC-MS/MS (Xevo-TQD, Waters) by employing a BEH C18 column and an isocratic gradient of 0.1% formic acid in water: 0.1% formic acid acetonitrile (60:40). The metabolic stability of the compounds was calculated from the logarithm of the remaining compounds at each of the time points studied.

4.4. Permeability

The Caco-2 cells were cultured to confluency, trypsinized and seeded onto a filter transwell inserted at a density of ~10,000 cells/well in DMEM cell culture medium. Confluent Caco-2 cells were subcultured at passages 58–62 and grown in a humidified atmosphere of 5% CO₂ at 37 °C. Following an overnight attachment period (24 h after seeding), the cell medium was replaced with fresh medium in both the apical and basolateral compartments every other day. The cell monolayers were used for transport studies 21 days post seeding. The monolayer integrity was checked by measuring the transepithelial electrical resistance (TEER) obtaining values $\geq 500 \Omega/\text{cm}^2$. On the day of the study, after the TEER measurement, the medium was removed and the cells were washed twice with pre-warmed (37 °C) Hank's Balanced Salt Solution (HBSS) buffer to remove traces of medium. Stock solutions were made in dimethyl sulfoxide (DMSO), and further diluted in HBSS (final DMSO concentration 1%). Each compound and reference compounds (Colchicine, E3S) were all tested at a final concentration of 10 μ M. For A \rightarrow B directional transport, the donor working solution was added to the apical (A) compartment and the transport media as receiver working solution was added to the basolateral (B) compartment. For B \rightarrow A directional transport, the donor working was added to the basolateral (B) compartment and transport media as receiver working solution was added to the apical (A) compartment. The cells were incubated at 37 °C for 2 h with gentle stirring.

At the end of the incubation, samples were taken from both donor and receiver compartments and transferred into 384-well plates and analyzed by UPLC-MS/MS. The detection was performed using an ACQUITY UPLC/Xevo TQD System. After the assay, Lucifer yellow was used to further validate the cell monolayer integrity, cells were incubated with LY 10 μ M in HBSS for 1 h at 37 °C, obtaining permeability (Papp) values for LY of $\leq 10 \text{ nm}^2/\text{s}$ confirming the well-established Caco-2 monolayer.

Acknowledgments

This work was funded by the Spanish Ministerio de Economía, Industria y Competitividad (Grant SAF2017-82771-R to S.V.), the European Regional Development Fund (ERDF), the Xunta de Galicia (GRC2014/011 and ED431C2018-21) and the Generalitat de Catalunya (2017 SGR 106). S.C., E.V. and R.L. acknowledge PhD fellowships from the Universitat de Barcelona (APIF grant), the Institute of Biomedicine of the University of Barcelona (IBUB), and the Spanish Ministerio de Educacion, Cultura y Deporte (FPU grant), respectively. This work was supported in part by the NIEHS Grant R01 ES002710 (to B.D.H.) and NIEHS Superfund Research Program P42 ES004699.

Appendix A. Supplementary data

Supplementary data (¹H and ¹³C NMR spectra of the compounds) to this article can be found online at <https://doi.org/10.1016/j.bmc.2019.115078>.

References

- Meirer K, Steinhilber D, Proschak E. *Basic Clin Pharmacol Toxicol*. 2014;114:83–91.
- Chandrasekharan NV, Simmons DL. *Genome Biol*. 2004;5:241.
- Patrignani P, Patrono C. *Biochim Biophys Acta*. 1851;2015:422–432.
- Kuhn H, Banthiya S, van Leyen K. *Biochim Biophys Acta*. 2015;185:308–330.
- Zeldin DC. *J Biol Chem*. 2001;276:36059–126062.
- Christmas P. *Adv Pharmacol*. 2015;74:163–192.
- Imig JD. *Hypertension*. 2015;65:476–482.
- Yang L, Mäki-Petäjä K, Cheriyan J, McEniery C, Wilkinson IB. *Br J Clin Pharmacol*. 2015;80:28–44.
- Imig JD. *Adv Pharmacol*. 2016;77:105–141.
- Fan F, Roman RJ. *J Am Soc Nephrol*. 2017;28:2845–2855.
- Jamieson KI, Endo T, Darwesh AM, Samokhvalov V, Seubert JM. *Pharmacol Ther*. 2017;179:47–83.
- Arand M, Grant DF, Beetham JK, Friedberg F, Oesch F, Hammock BD. *FEBS Lett*. 1994;338:251–256.
- Oesch F. *Xenobiotica*. 1973;3:305–340.
- Harris TR, Hammock BD. *Gene*. 2013;526:61–74.
- Fleming I. *Pharmacol Rev*. 2014;66:1106–1140.
- Imig JD, Hammock BD. *Nat Rev Drug Discov*. 2009;8:794–805.
- Wang ZH, Davis BB, Jiang DQ, Zhao TT, Xu DY. *Curr Vasc Pharmacol*. 2013;11:105–111.
- Kodani SD, Hammock BD. *Drug Metab Dispos*. 2015;43:788–802.
- Pillarsetti S, Khanna I. *Drug Discov Today*. 2015;20:1382–1390.
- Wagner KM, McReynolds CB, Schmidt WK, Hammock BD. *Pharmacol Ther*. 2017;180:62–76.
- Zarruello S, Tuszon JP, Corey S, et al. *Prog Neurobiol*. 2019;172:23–39.
- Gómez GA, Morisseau C, Hammock BD, Christianson DW. *Biochemistry*. 2004;43:4716–4723.
- Jones PD, Tsai H-J, Do ZN, Morisseau C, Hammock BD. *Bioorg Med Chem Lett*. 2006;16:5212–5216.
- Shen HC, Hammock BD. *J Med Chem*. 2012;55:1789–1808.
- Kim I-H, Nishi K, Kasugami T, et al. *Bioorg Med Chem Lett*. 2012;22:5889–5892.
- Huang S-X, Cao B, Morisseau C, Jin Y, Long Y-Q, Hammock BD. *Med Chem Commun*. 2012;3:379–384.
- Kim I-H, Lee I-H, Nishiwaki H, Hammock BD, Nishi K. *Bioorg Med Chem*. 2014;22:1163–1175.
- Burmistrov V, Morisseau C, Lee KSS, et al. *Bioorg Med Chem Lett*. 2014;24:2193–2197.
- Burmistrov V, Morisseau C, Danilov D, et al. *Bioorg Med Chem Lett*. 2015;25:5514–5519.
- Kim I-H, Park Y-K, Nishiwaki H, Hammock BD, Nishi K. *Bioorg Med Chem*. 2015;23:7199–7210.
- Burmistrov VV, Butov GM, Karlov DS, et al. *Russ J Bioorg Chem*. 2016;42:404–414.
- Burmistrov V, Morisseau C, Harris TR, Butov GM, Hammock BD. *Bioorg Chem*. 2018;76:510–527.
- Burmistrov V, Morisseau C, Pitushkin D, et al. *Bioorg Med Chem Lett*. 2018;28:2302–2313.
- Burmistrov VV, Butov GM. *Russ J Org Chem*. 2018;54:1307–1312.
- D'yachenko VS, Danilov DV, Shkineva TK, Vatsadze IA, Burmistrov VV, Butov GM. *Chem Heterocycl Compd*. 2019;55:129–134.
- Tsai H-J, Hwang SH, Morisseau C, et al. *Eur J Pharm Sci*. 2010;40:222–238.
- Hwang SH, Tsai H-J, Liu J-Y, Morisseau C, Hammock BD. *J Med Chem*. 2007;50:3825.
- Brown JR, North EJ, Hurdle JG, et al. *Bioorg Med Chem*. 2011;19:5585–5595.
- Hoover JRE. US3496228; 1970.
- Camps P, Duque MD, Vázquez S, et al. *Bioorg Med Chem*. 2008;16:9925–9936.
- Jones PD, Wolf NM, Morisseau C, Whetstone P, Hock B, Hammock BD. *Anal Biochem*. 2005;343:66–75.
- Hwang SH, Morisseau C, Do Z, Hammock B. D. *Bioorg Med Chem Lett*.

- 2006;16:5773-5777.
43. Gómez GA, Morisseau C, Hammock BD, Christianson DW. *Protein Sci.* 2006;15:58-64.
 44. Amano Y, Yamaguchi T, Tanabe E. *Bioorg Med Chem.* 2014;22:2427-2434.
 45. Liu J-Y, Tsi H-J, Morisseau C, et al. *Biochem Pharmacol.* 2015;98:718-731.
 46. Hodek P, Jančík P, Anzenbacher P, Burkhard J, Janků J, Vodička L. *Xenobiotica.* 1988;18:1109-1118.
 47. Hodek P, Burkhard J, Janků J. *Gen Physiol Biophys.* 1995;14:225-239.
 48. Bořek-Dohalská L, Hodek P, Stiborová M. *Collect Czech Chem Commun.* 2000;65:122-132.
 49. Hodek P, Bořek-Dohalská L, Sopko B, et al. *J Enzyme Inhib Med Chem.* 2005;20:25-33.
 50. Daina A, Michielin O, Zoete V. *Sci Rep.* 2017;7:42717.
 51. Meggers E. *Angew Chem Int Ed.* 2011;50:2442-2448.
 52. Schwertléger H, Fokin AA, Schreiner PR. *Angew Chem Int Ed.* 2008;47:1022-1036.
 53. Courtney T, Johnston DE, McKervey MA, Rooney JJ. *J Chem Soc Perkin Trans.* 1972;1:2691-2696.
 54. Gund TM, Nomura M, Schleyer PVR. *J Org Chem.* 1974;39:2987-2994.
 55. Xier L, Ochterski JW, Gao Y, et al. WO 2007016496; 2007.

SUPPLEMENTARY MATERIAL FOR

Exploring the size of the lipophilic unit of the soluble epoxide hydrolase inhibitors

Sandra Codony^a, Elena Valverde^a, Rosana Leiva^a, José Brea^b, M. Isabel Loza^b, Christophe Morisseau^c, Bruce D. Hammock^c and Santiago Vázquez^{a,*}

^a*Laboratori de Química Farmacèutica (Unitat Associada al CSIC), Facultat de Farmàcia i Ciències de l'Alimentació, and Institute of Biomedicine (IBUB), Universitat de Barcelona, Av. Joan XXIII 27-31, 08028 Barcelona, Spain*

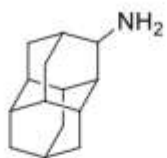
^b*Innopharma screening platform. Biofarma research group. Centro de Investigación en Medicina Molecular y Enfermedades Crónicas (CIMUS). Universidad de Santiago de Compostela. Spain.*

^c*Department of Entomology and Nematology, and UCD Comprehensive Cancer Center, University of California, Davis, CA 95616, USA.*

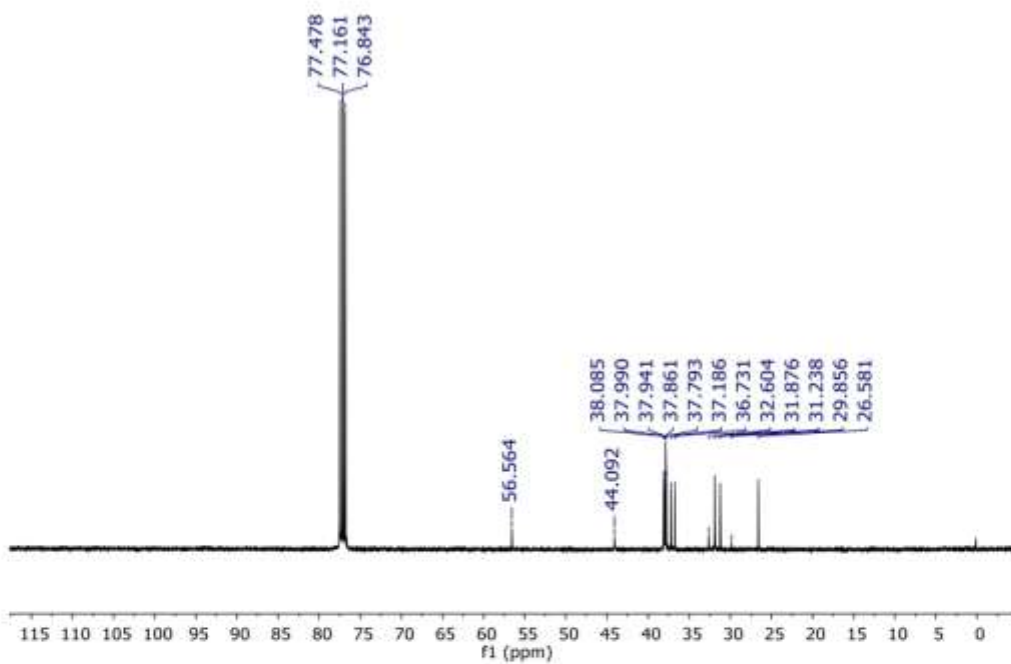
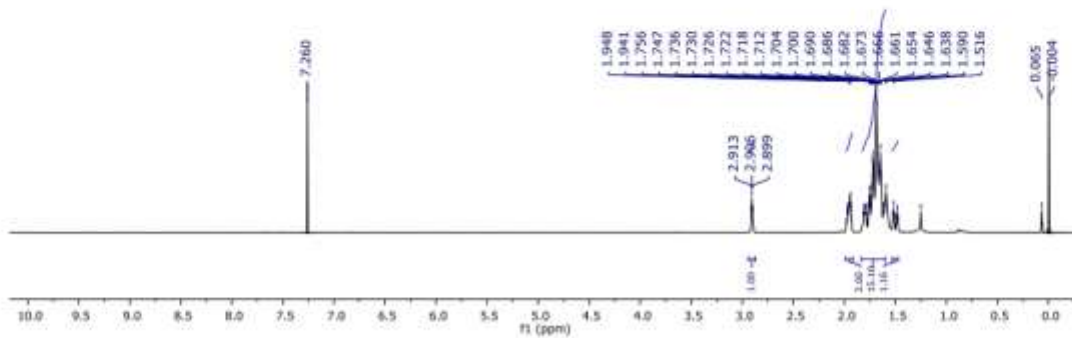
* Corresponding author. Tel.: +34-934024533; e-mail: svazquez@ub.edu

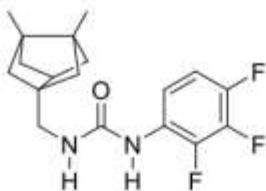
Table of contents

^1H and ^{13}C spectra of compound 8	Page S3
^1H and ^{13}C spectra of compound 11	Page S4
^1H and ^{13}C spectra of compound 12	Page S5
^1H and ^{13}C spectra of compound 13	Page S6
^1H and ^{13}C spectra of compound 14	Page S7
^1H and ^{13}C spectra of compound 15	Page S9
^1H and ^{13}C spectra of compound 19	Page S11
^1H and ^{13}C spectra of compound 21	Page S14
^1H and ^{13}C spectra of compound 24	Page S18
^1H and ^{13}C spectra of compound 25	Page S19
^1H and ^{13}C spectra of compound 26	Page S21
^1H and ^{13}C spectra of compound 28	Page S23

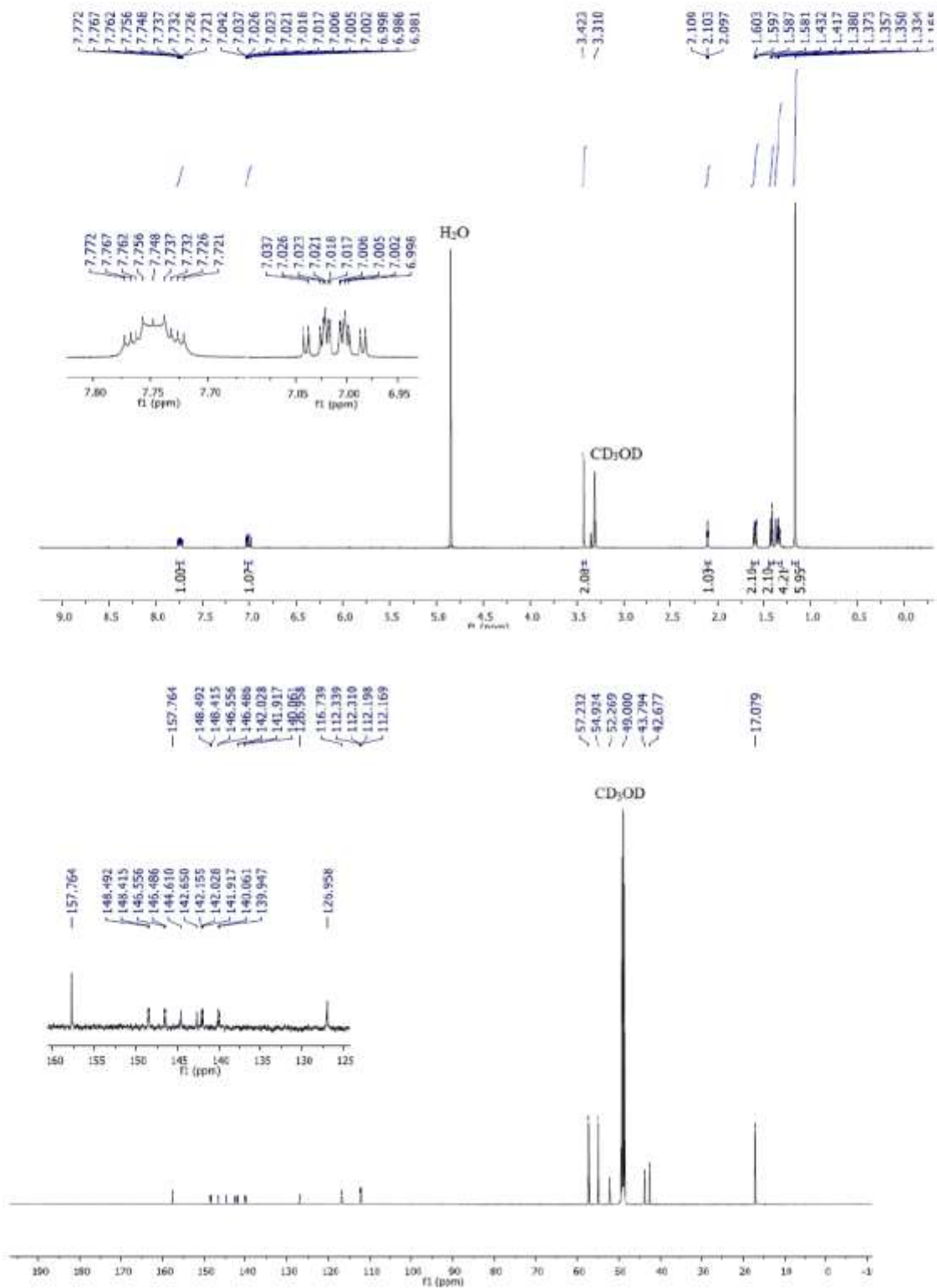


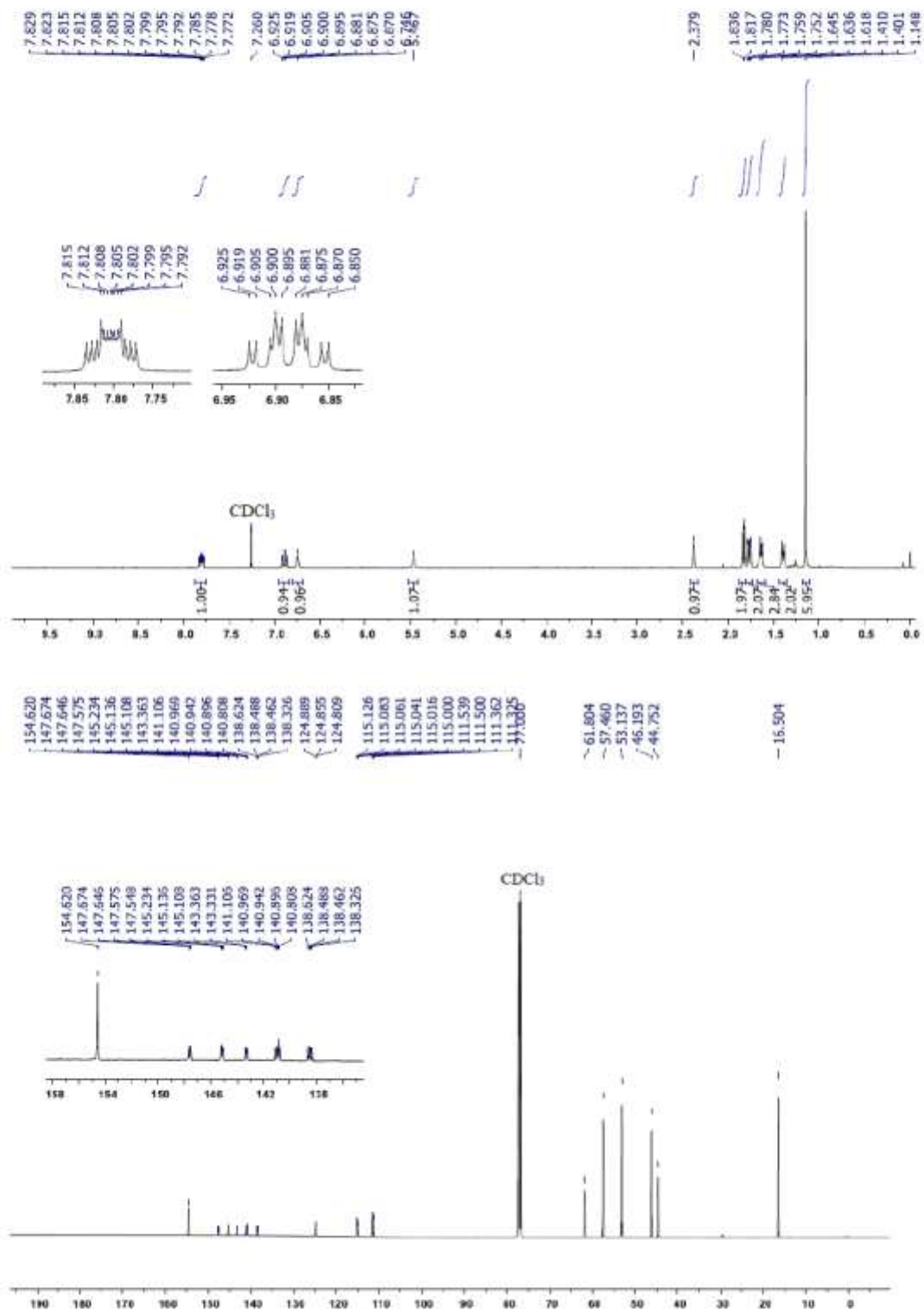
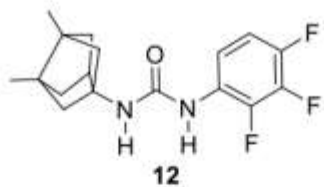
8

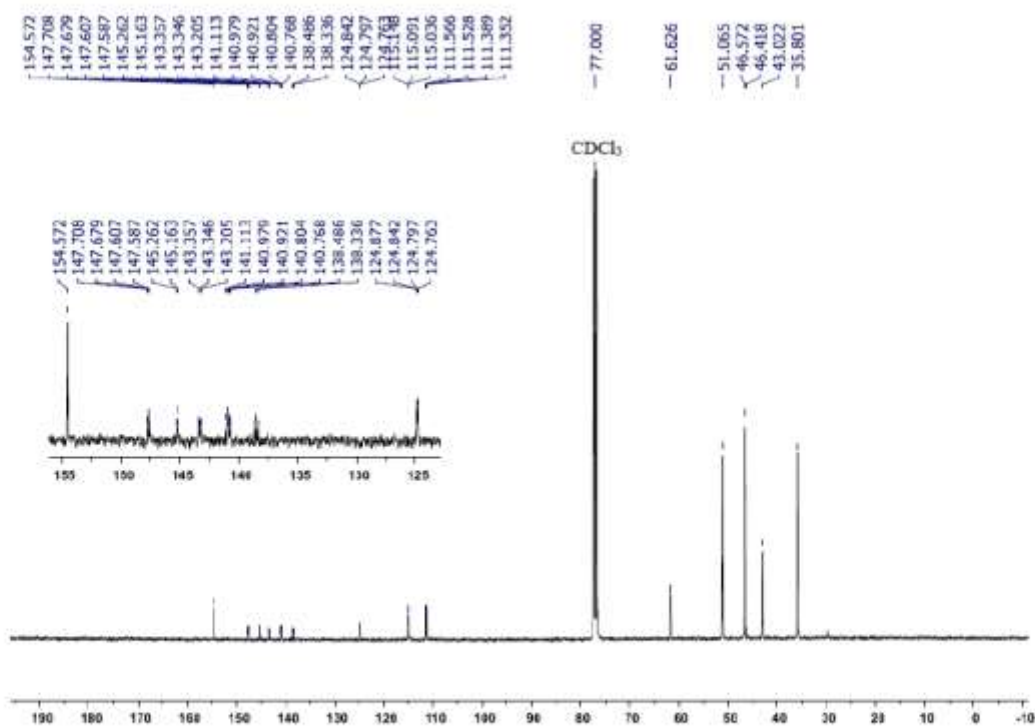
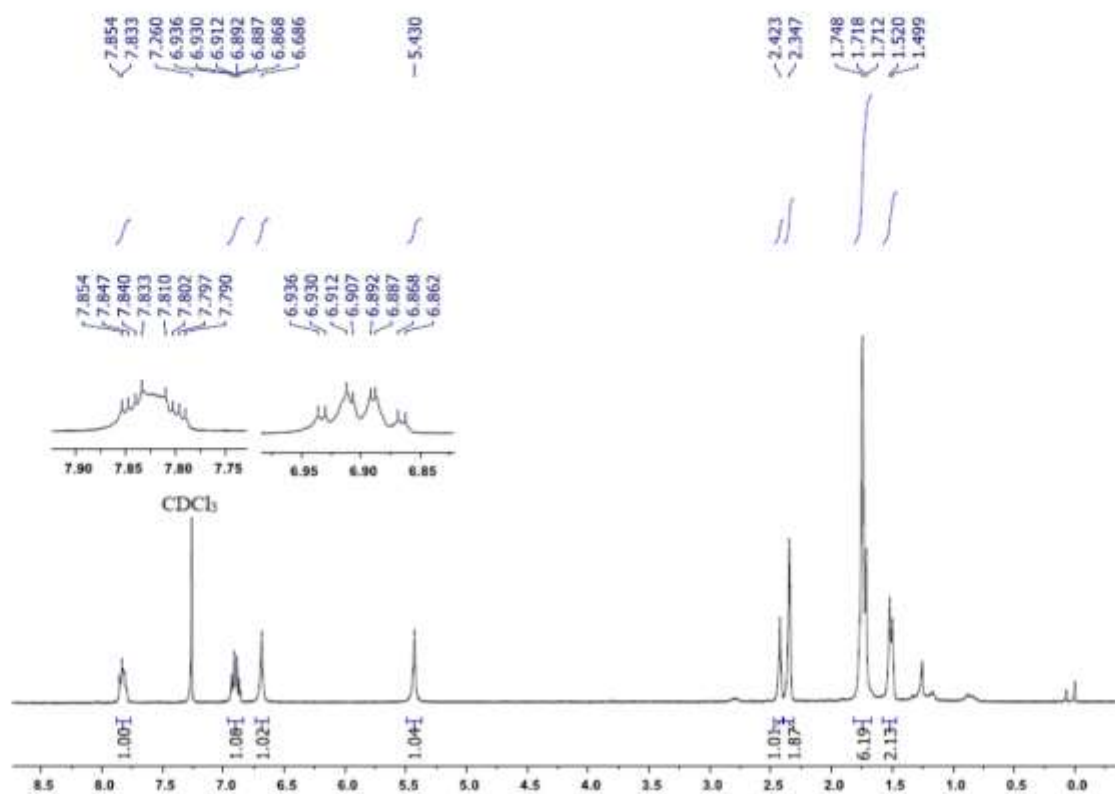
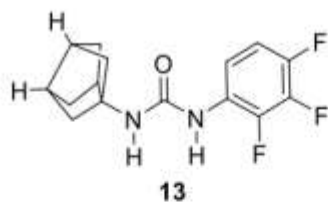


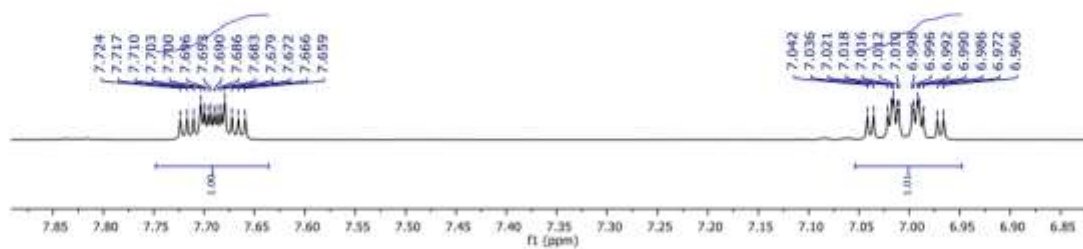
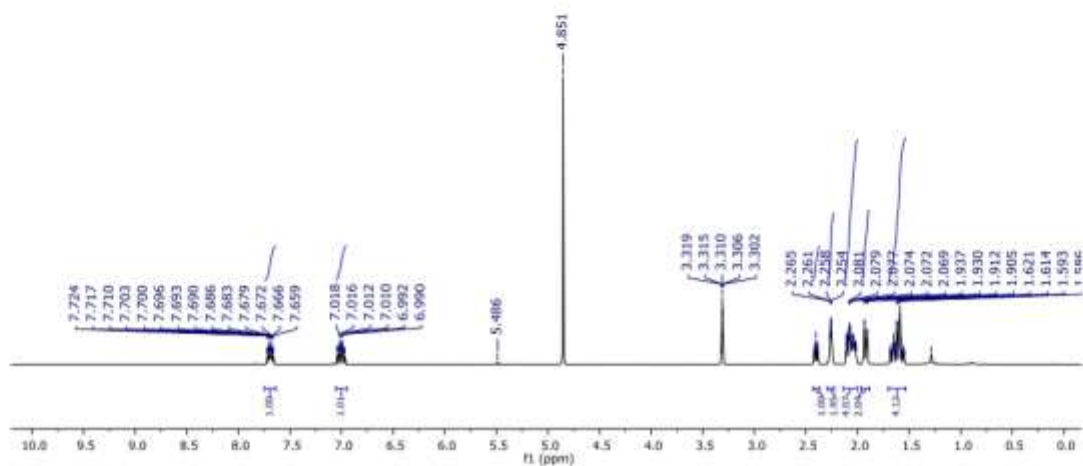
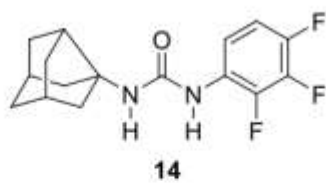


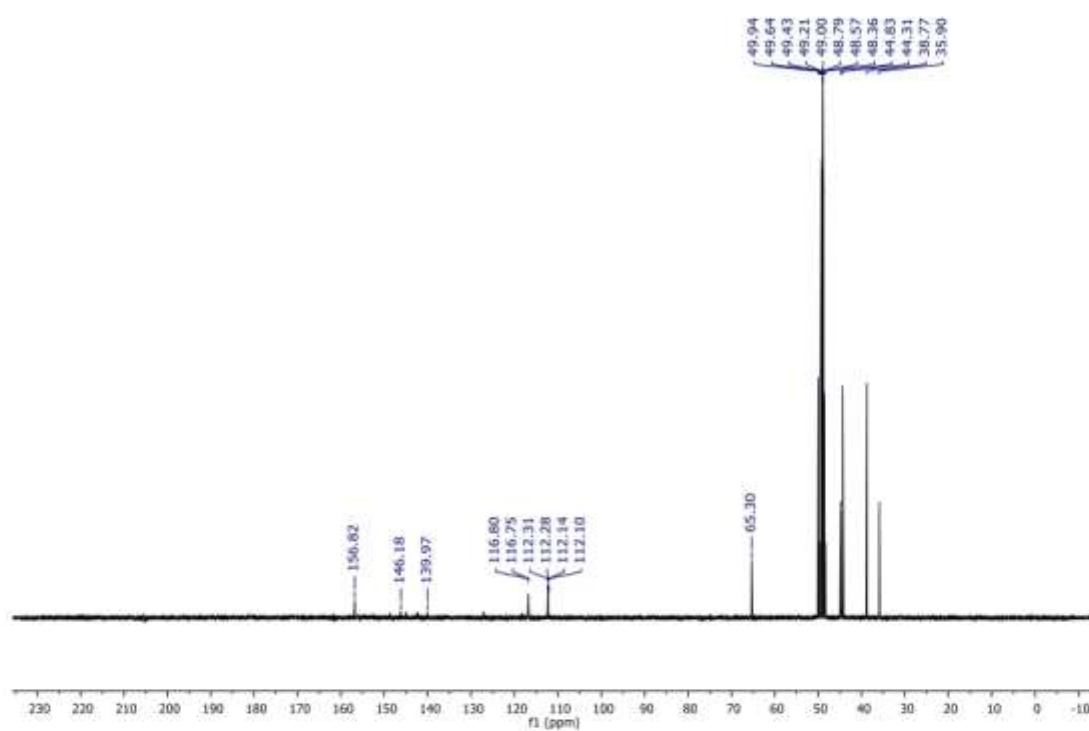
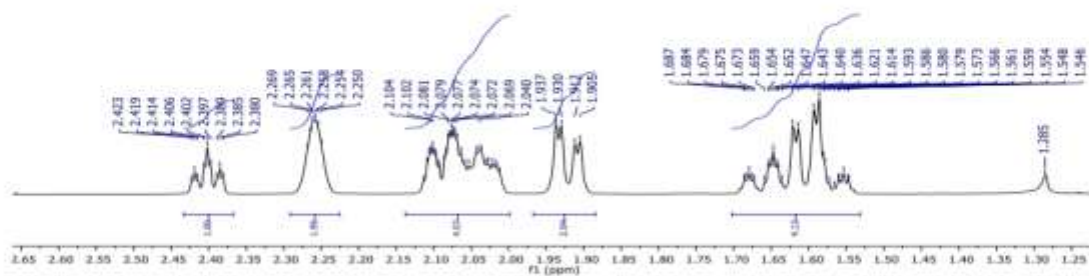
11

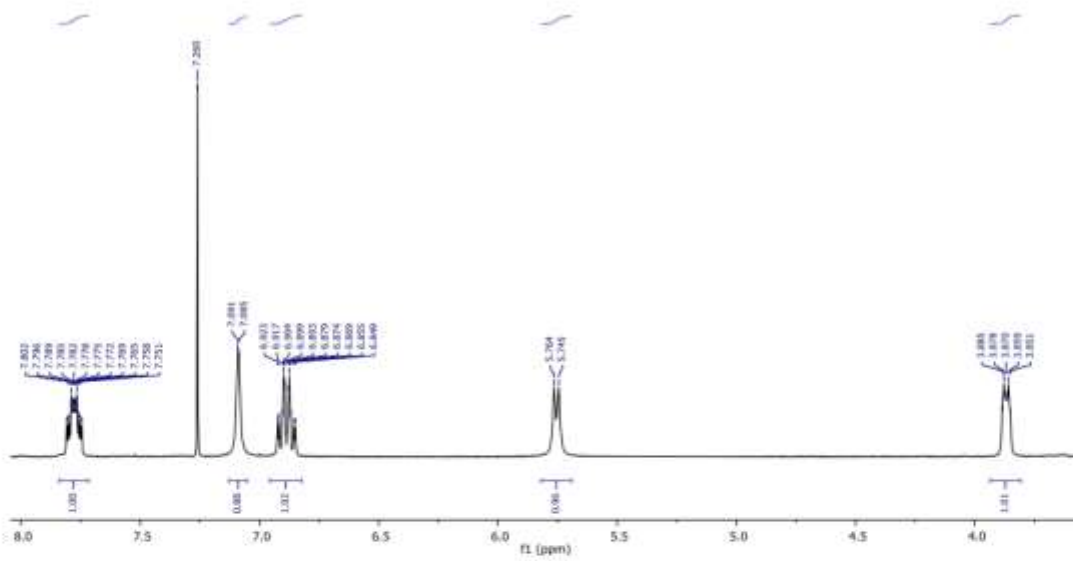
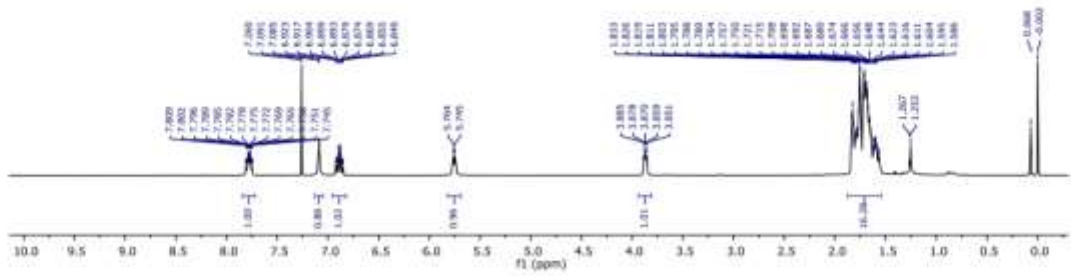
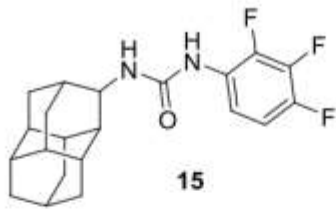


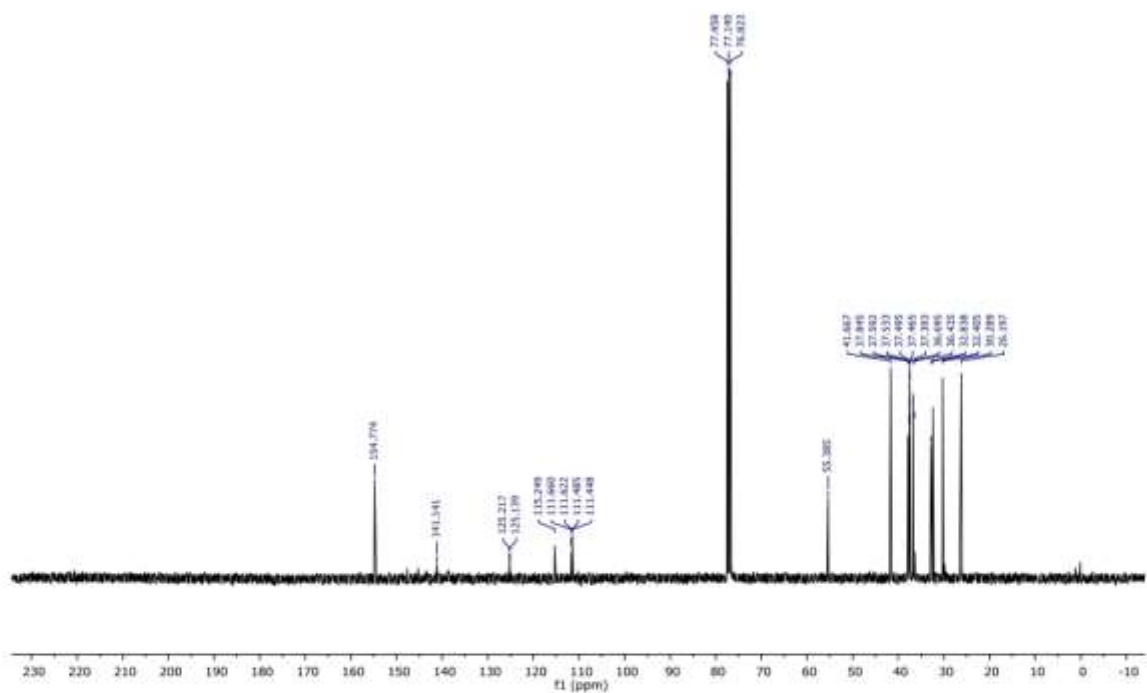
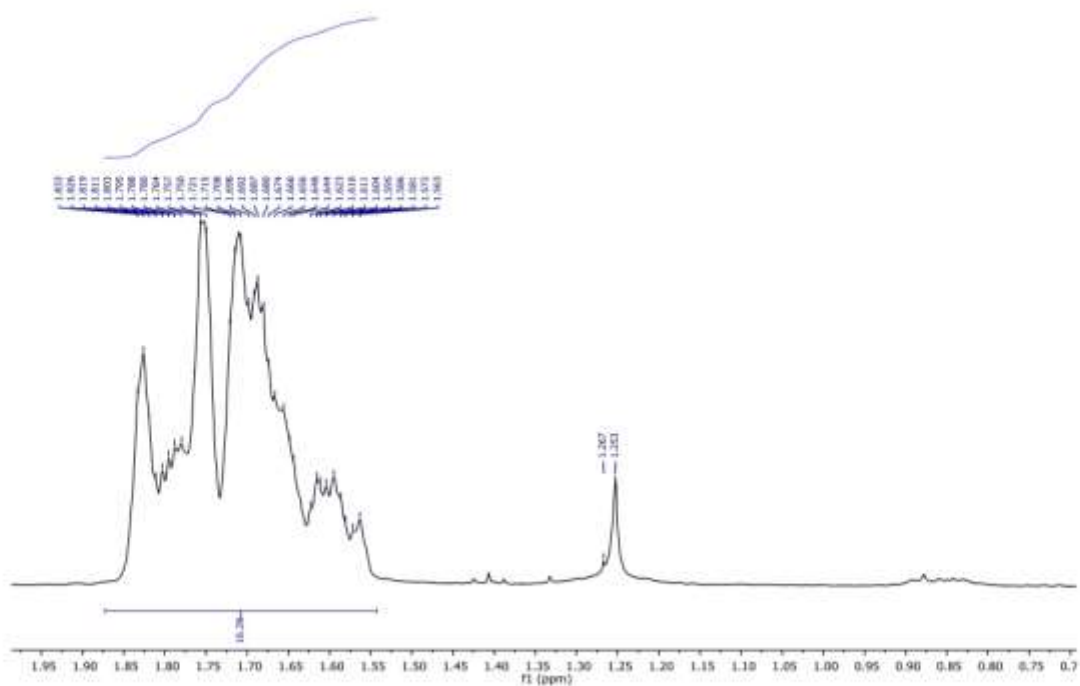


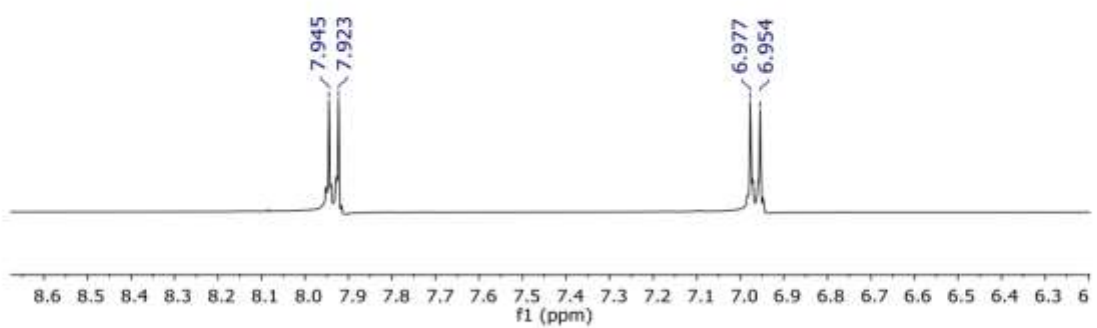
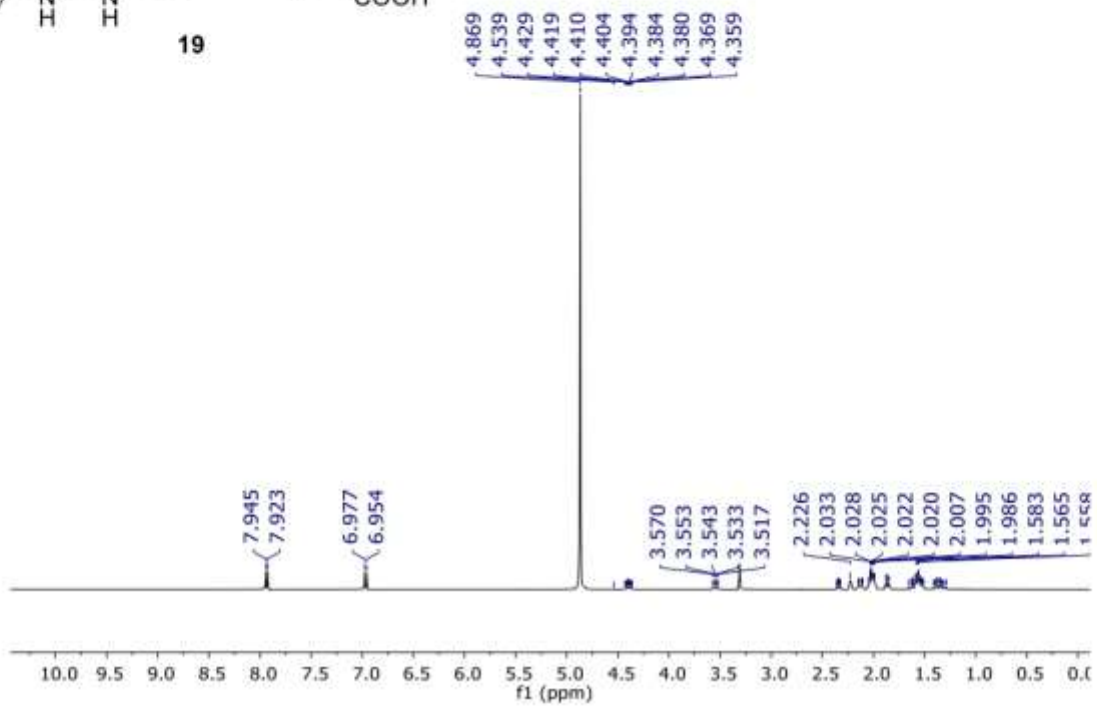
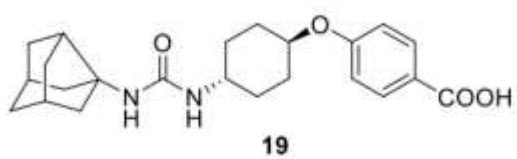


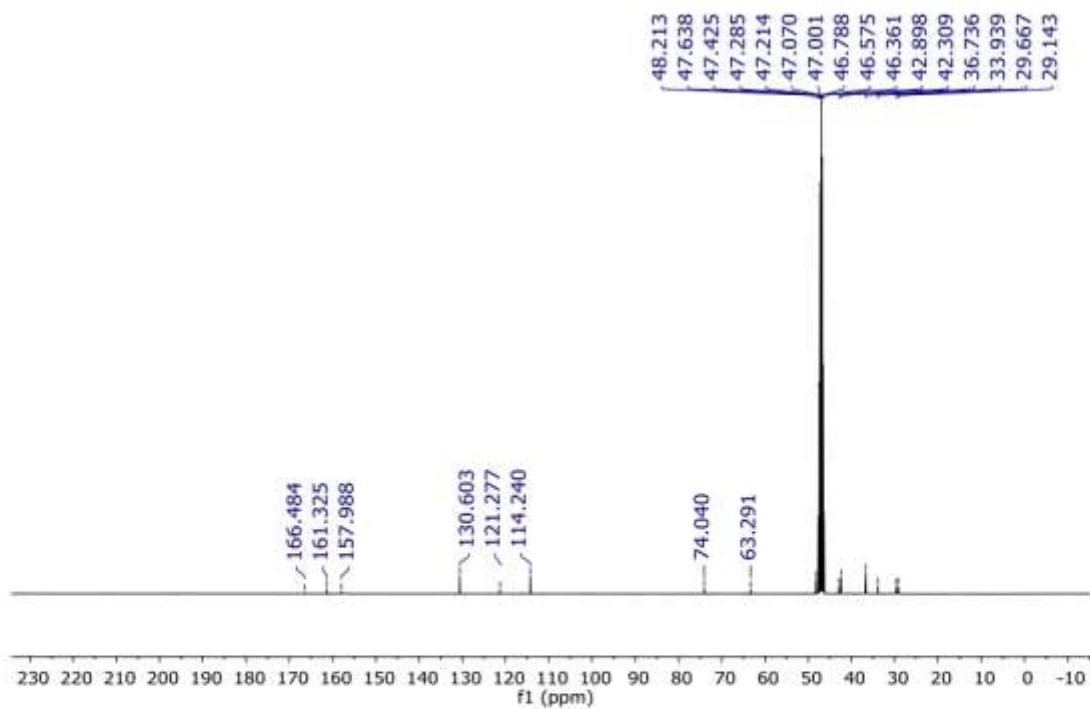
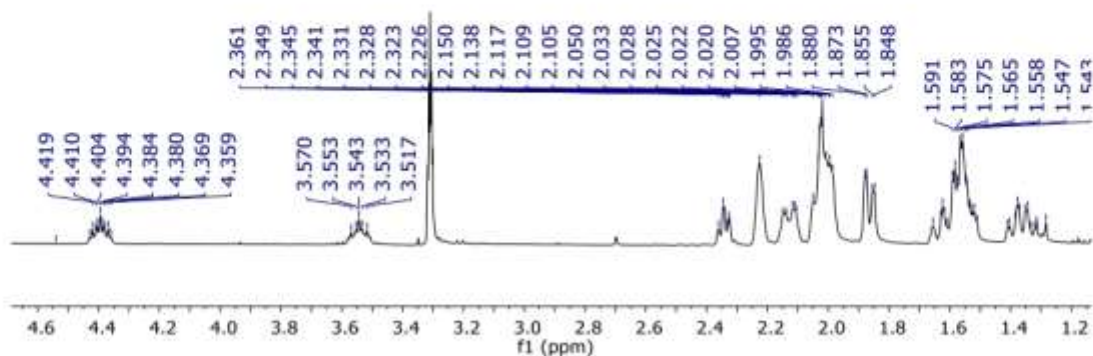


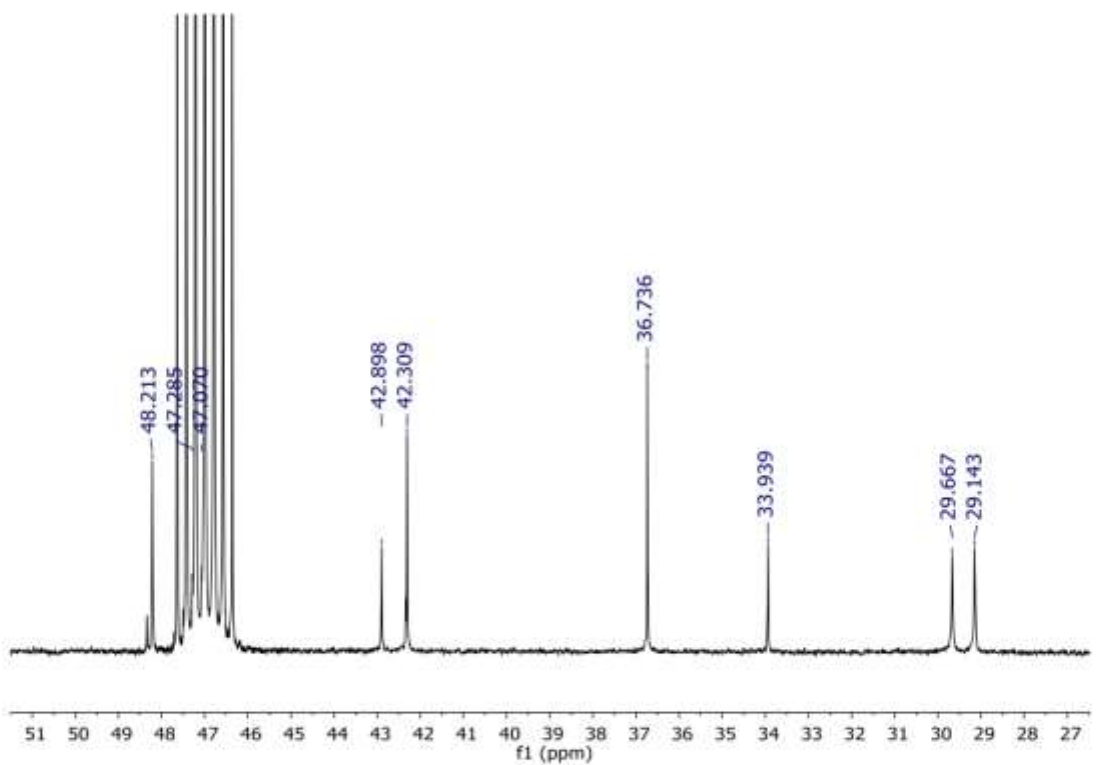
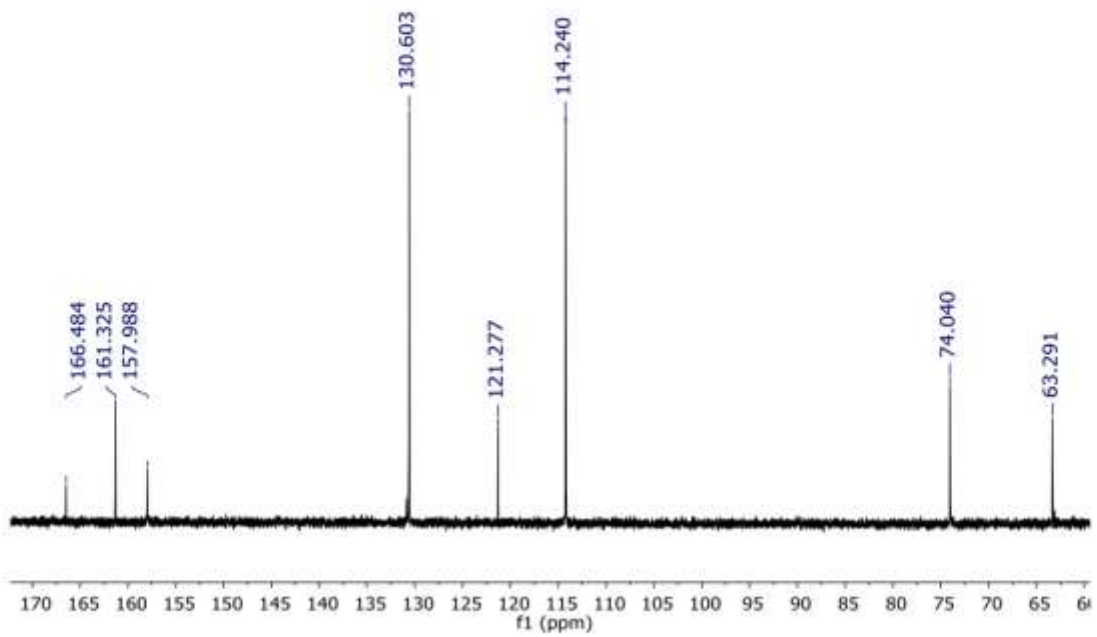


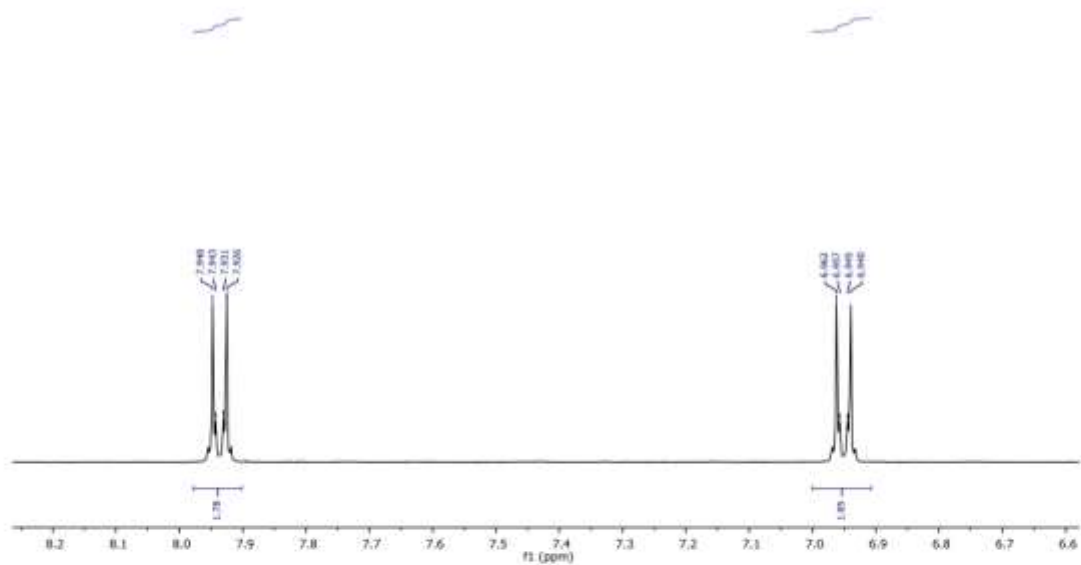
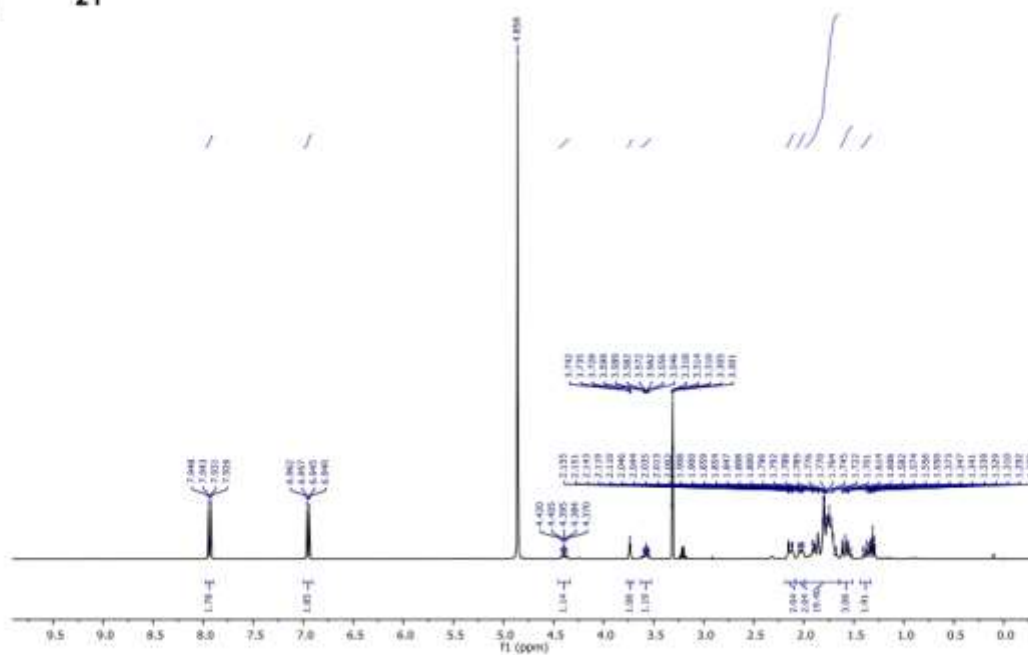
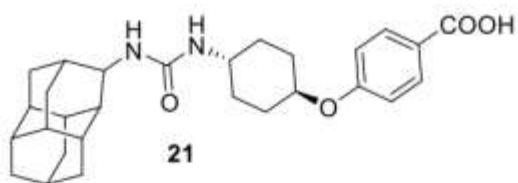


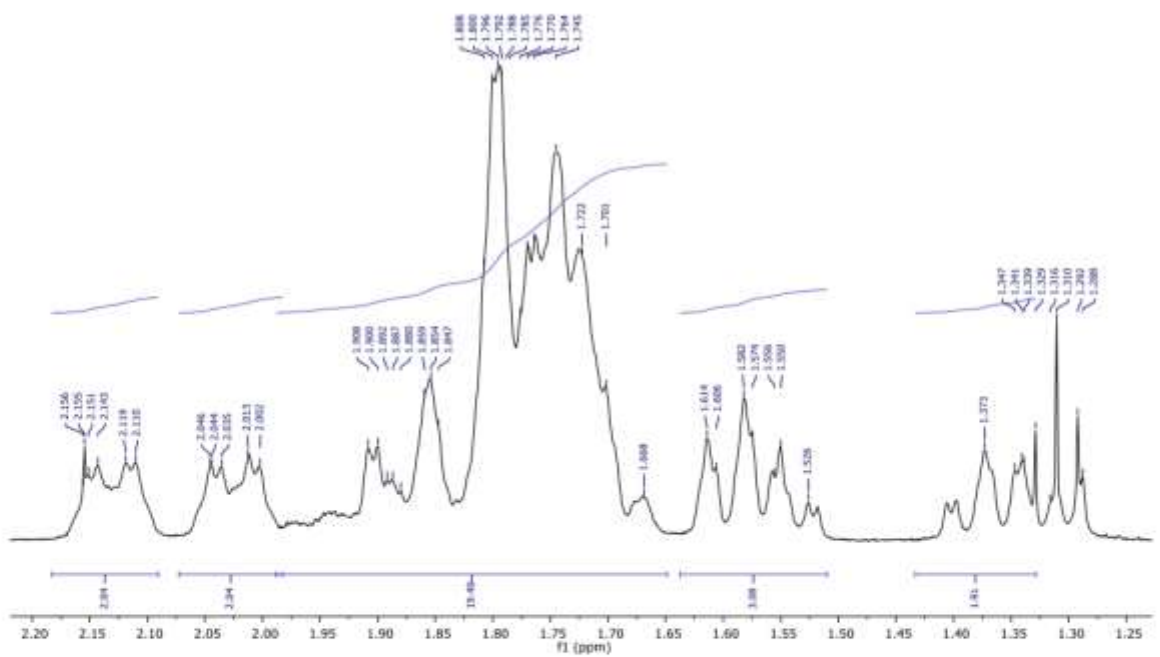
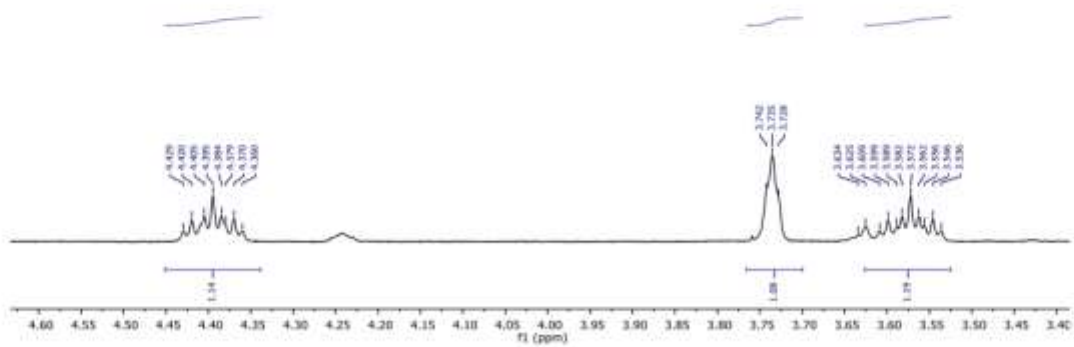


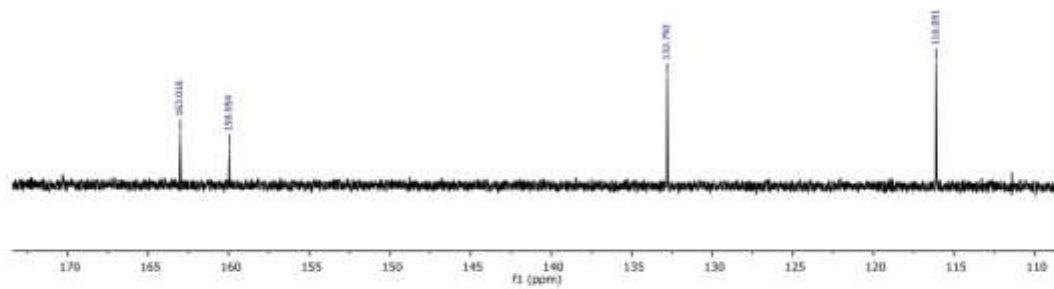
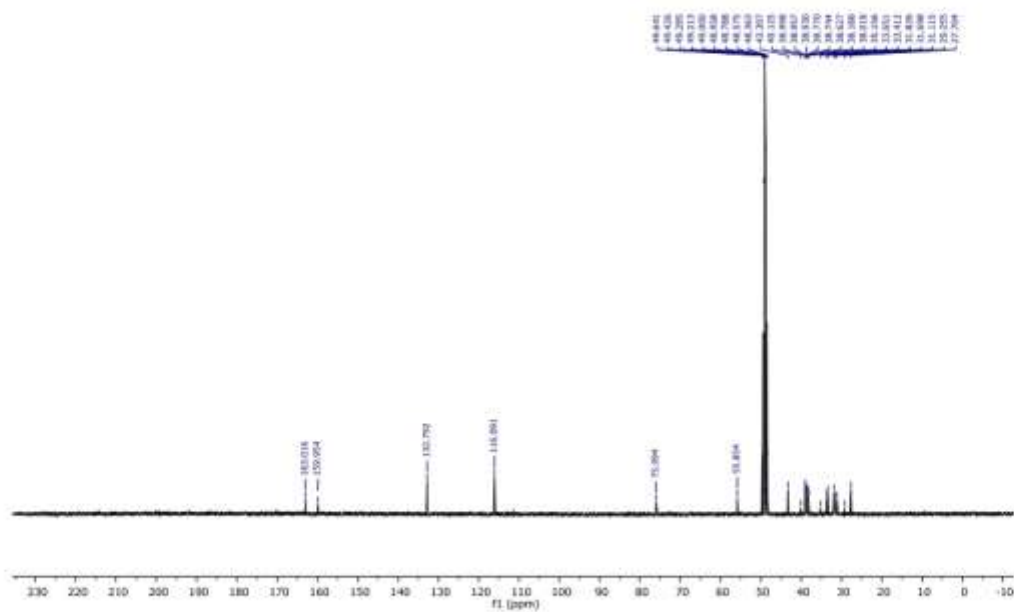


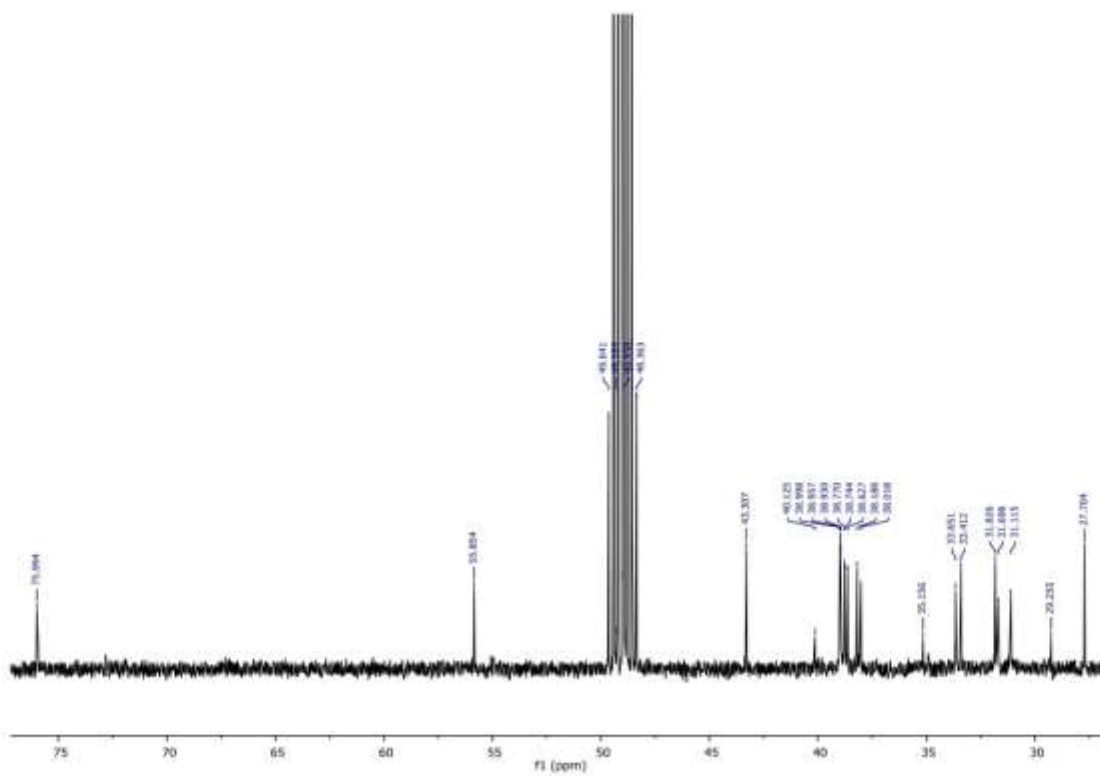


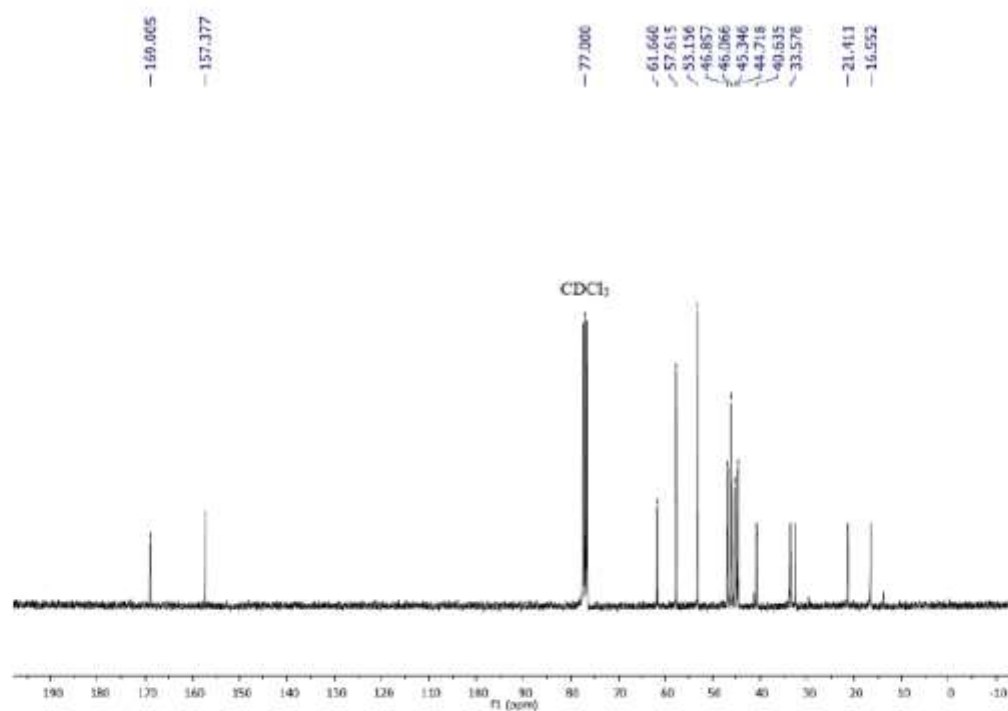
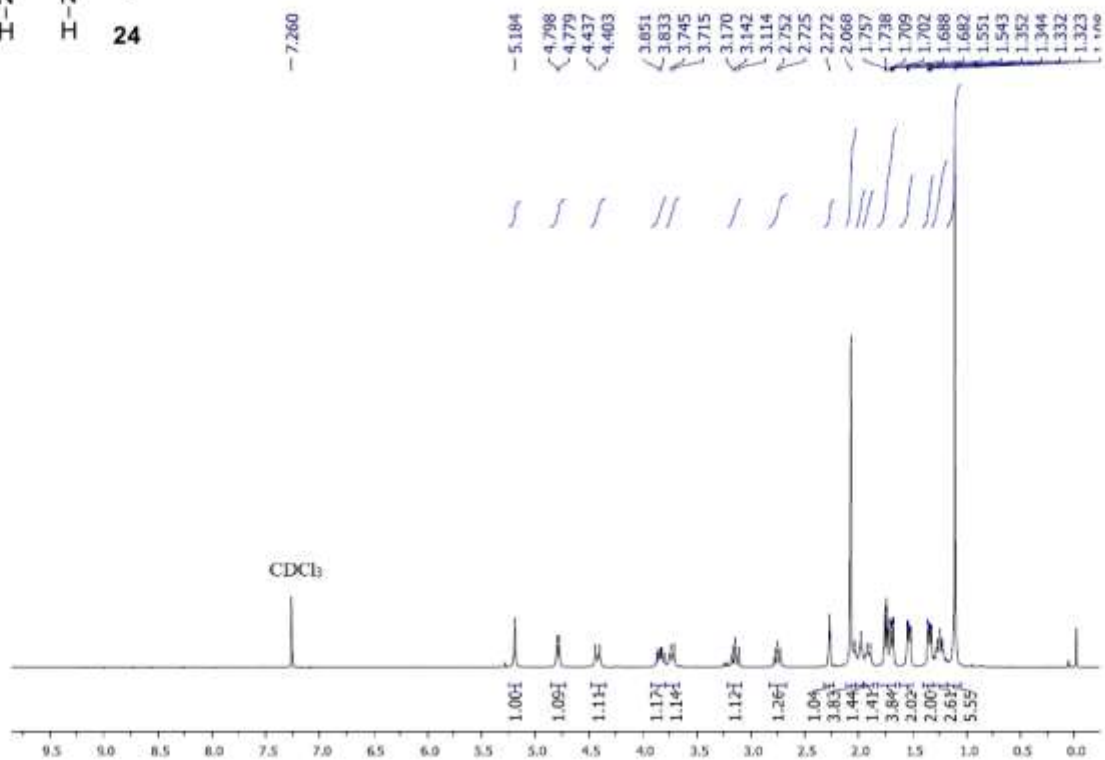
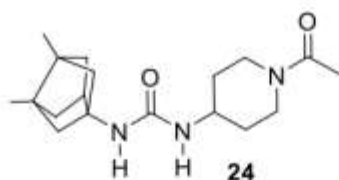


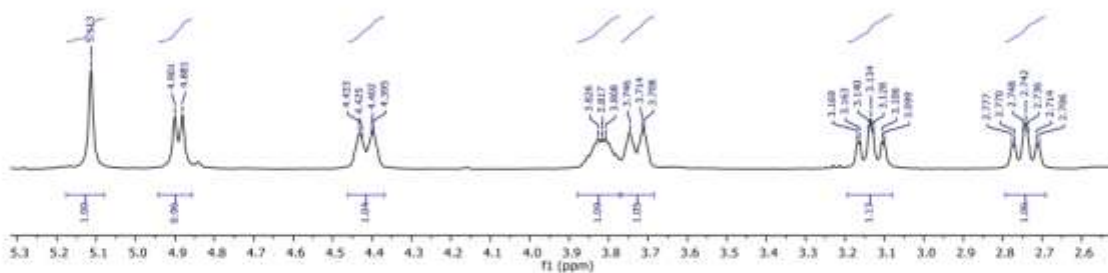
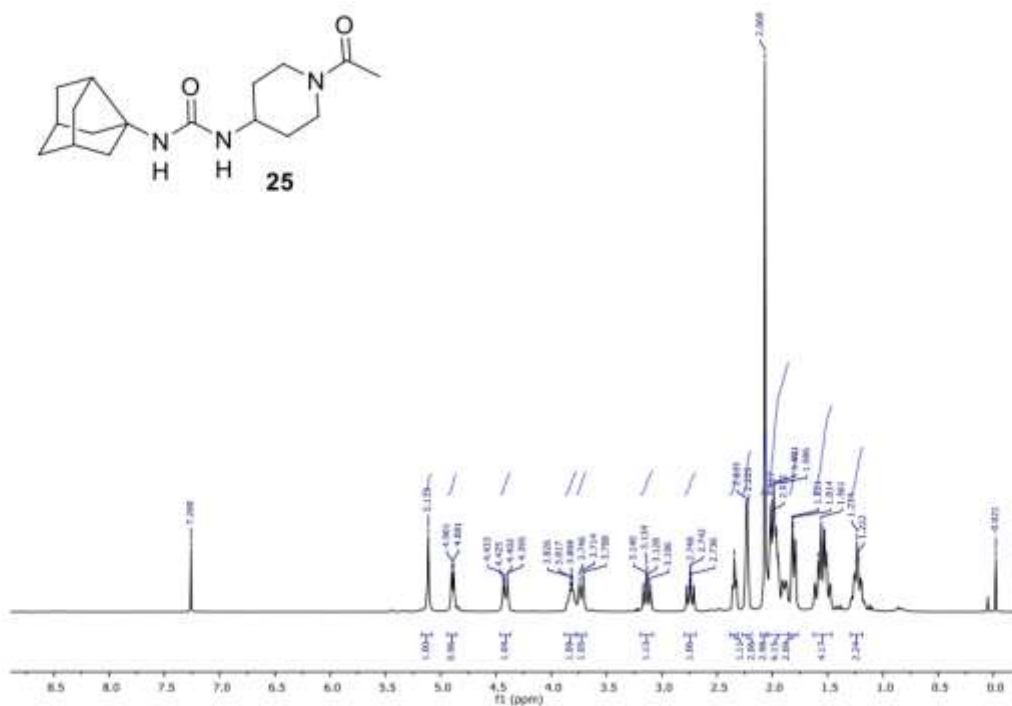
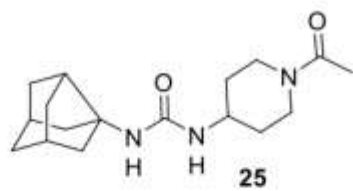


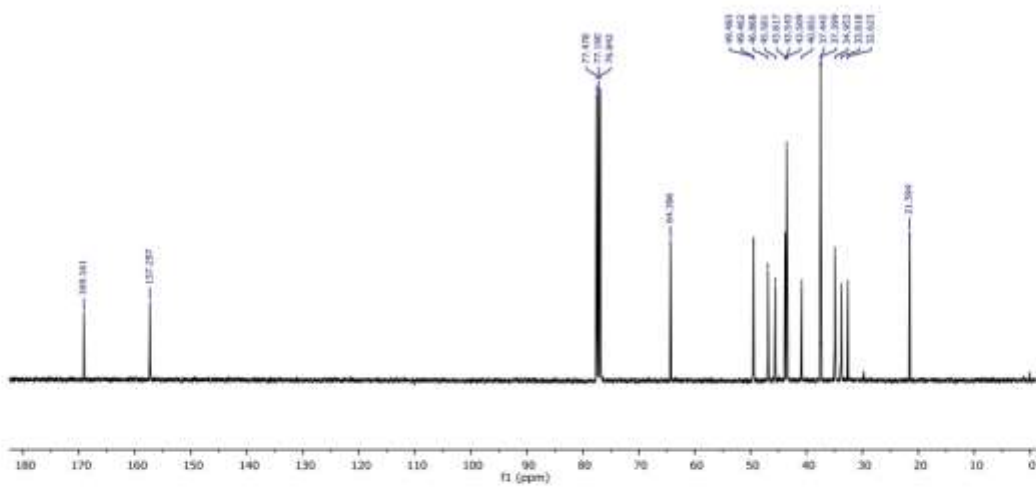
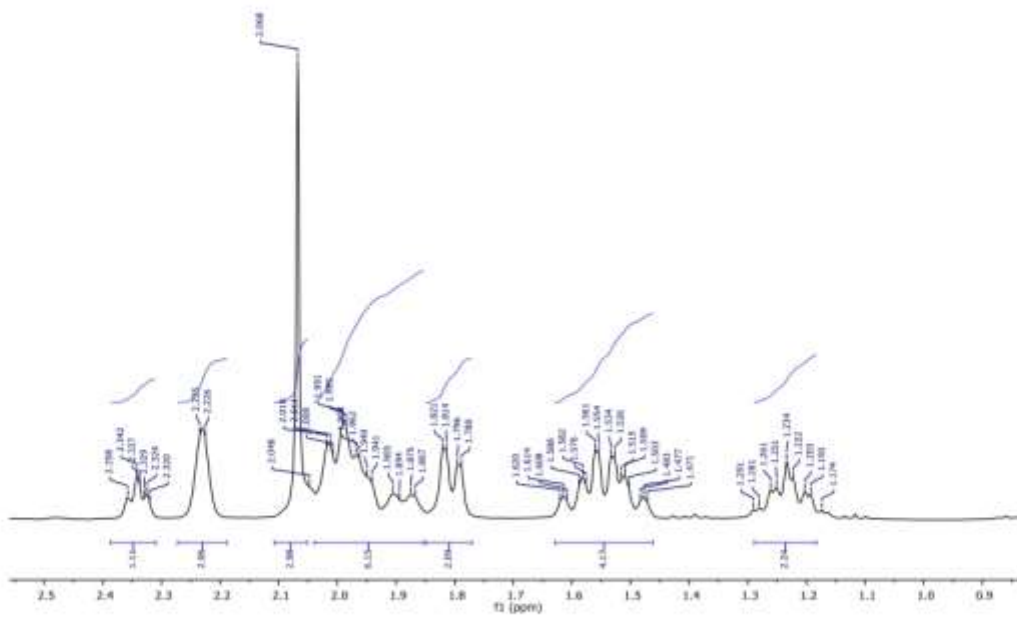


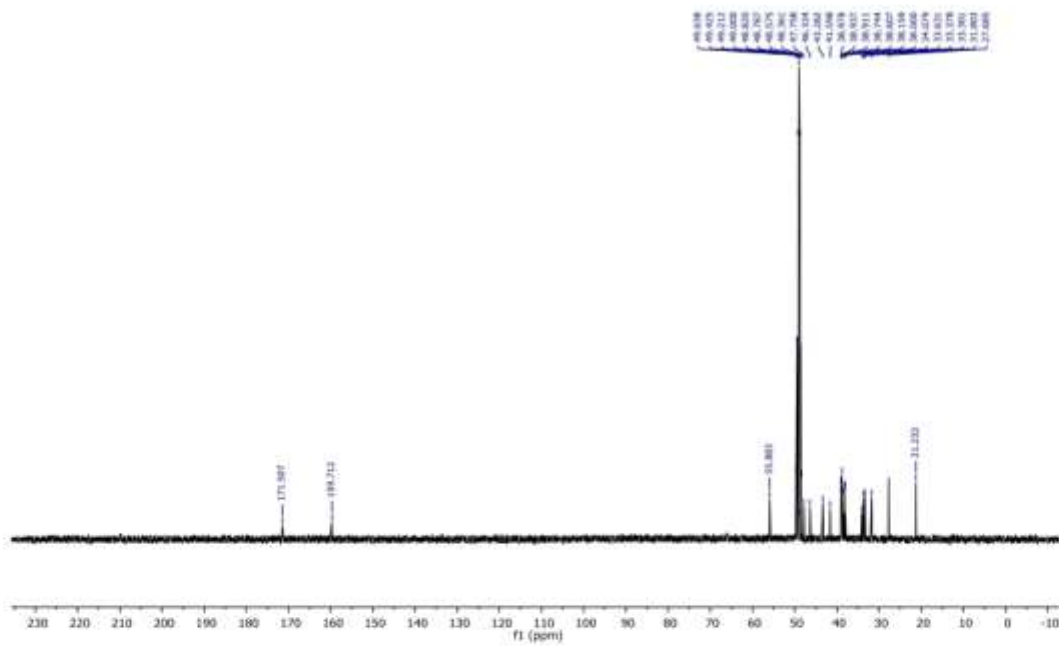
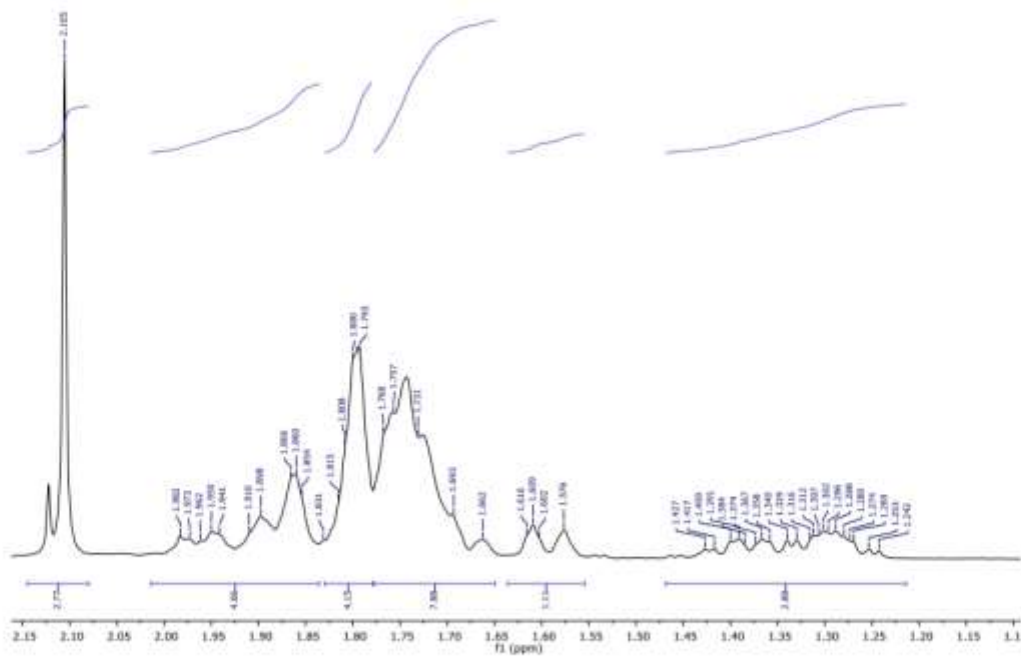


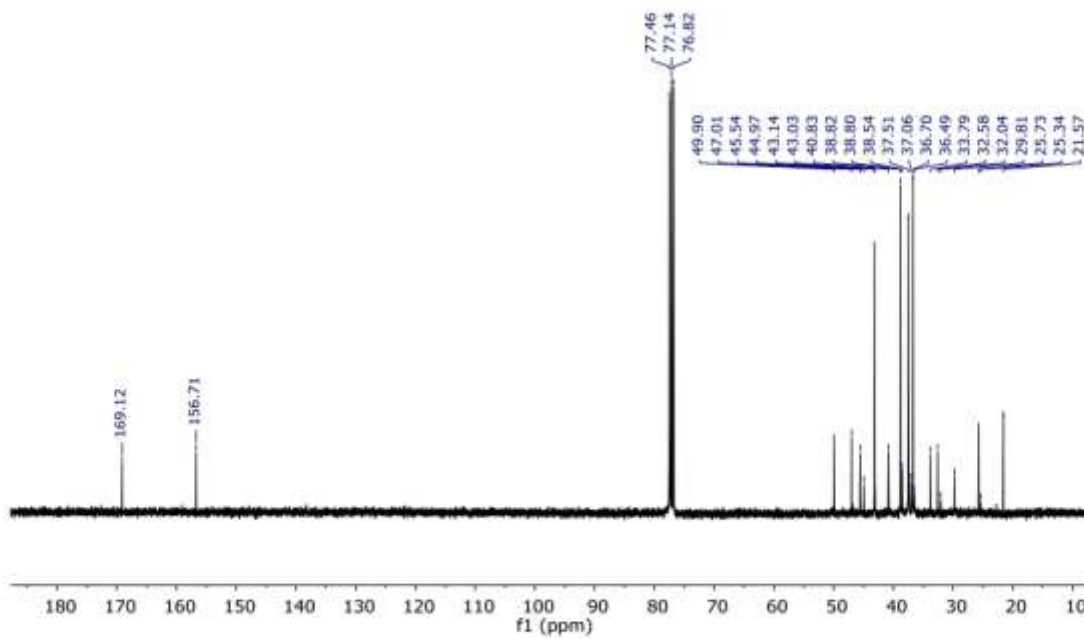
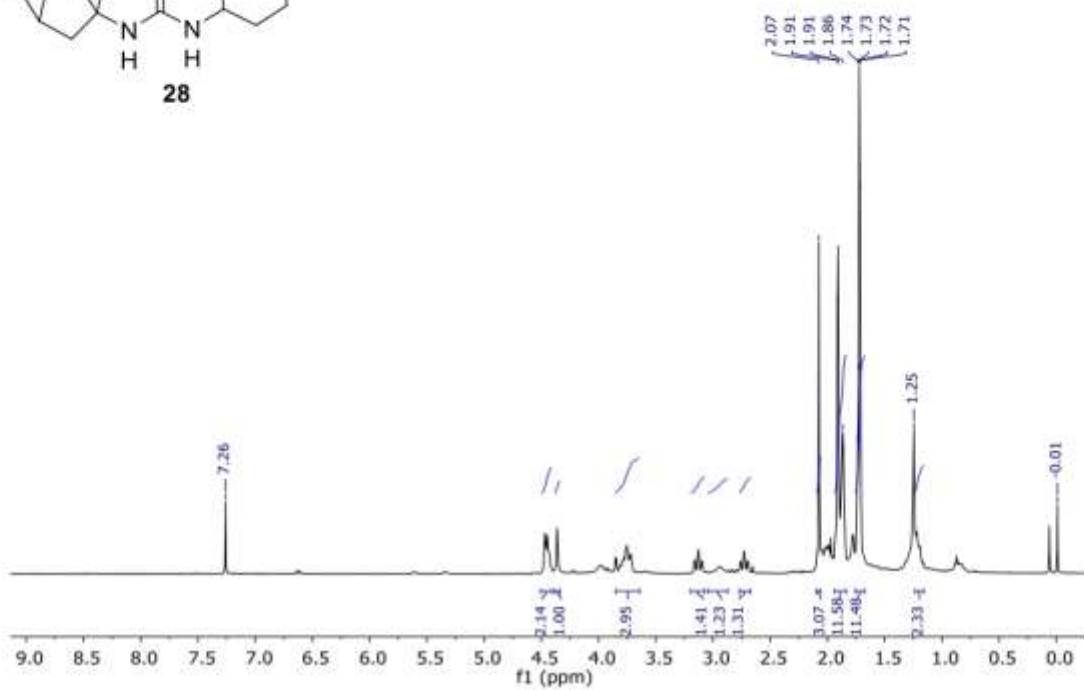
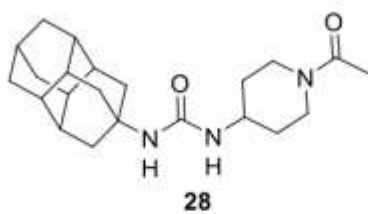












CHAPTER 3

BENZOHOMOADAMANTANE-BASED

sEHIs (I)

Introduction

Several of the very potent sEHs developed by both industry and academy present an adamantane moiety in their structure. Of note, the adamantane-based inhibitor AR9281^{3.3.1} was taken to clinical trials by Arete Therapeutics for the treatment of hypertension in diabetic patients. Although this compound showed a high level of safety even with the administration of 1.2 g/day, it failed in phase II in large part because of its poor pharmacokinetic properties, likely related with the adamantane moiety.¹⁴⁵ Taking this precedent, the group of Prof. Bruce D. Hammock developed a second family of sEHs presenting a phenyl ring as the hydrophobic moiety instead of the adamantane ring. Some of the compounds included in this new family are TPPU, used in several *in vitro* and *in vivo* studies,^{114,132,133,134,135,136} EC5026, currently in Phase 1 clinical trials for the treatment of neuropathic pain,⁶⁰ and *t*-TUCB (EC1728), an analog of the adamantane-based *t*-AUCB, which is being developed for veterinary uses by EicOsis (Figure 31).¹⁴¹ These three compounds are very potent inhibitors of human and murine sEH and have considerably better solubility and pharmacokinetic properties than AR9281.

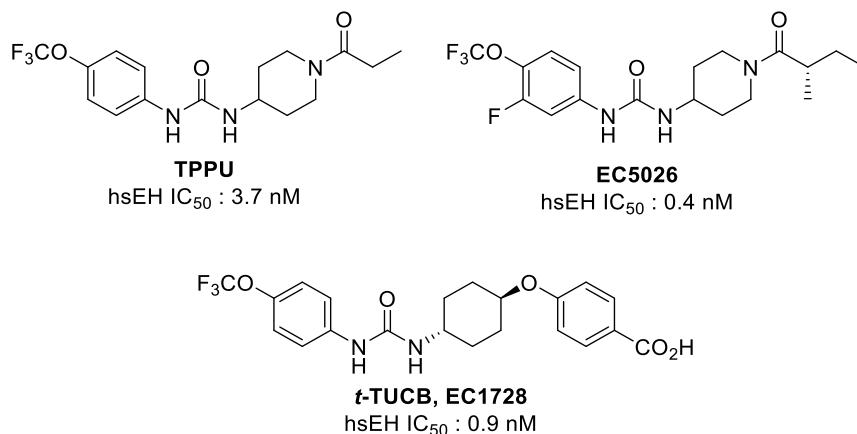


Figure 31. Structure and inhibitory activity of some non adamantane-based sEHs.

On the other hand, as shown in Chapter 2 of the present thesis, we found that the lipophilic pocket of the sEH enzyme can accommodate polycycles of very different size, and that the replacement of the adamantane moiety by larger polycyclic rings is better than the replacement by smaller ones.²¹⁰

Discussion

Taking into account that both adamantane and aromatic ring moieties (as in *t*-AUCB and *t*-TUCB, respectively) fit very well in the hydrophobic pocket of the sEH and that the replacement of adamantane by larger polycyclic rings (as in compound **76**) is a good strategy to obtain potent sEHIs, we designed a new family of sEHIs replacing the adamantyl or phenyl ring of the known sEHIs by the very versatile benzohomoadamantane scaffold as the hydrophobic moiety (Figure 32). This polycyclic, readily accessible, features in its structure the synthetically versatile homoadamantane unit fused with an aromatic ring, as shown in several previous work by our research group.^{174,175,176,211} We expected the new compounds to be potent and to achieve the optimum drug-like properties by modifying the substituents in the benzohomoadamantane scaffold and/or the RHS of the molecule.

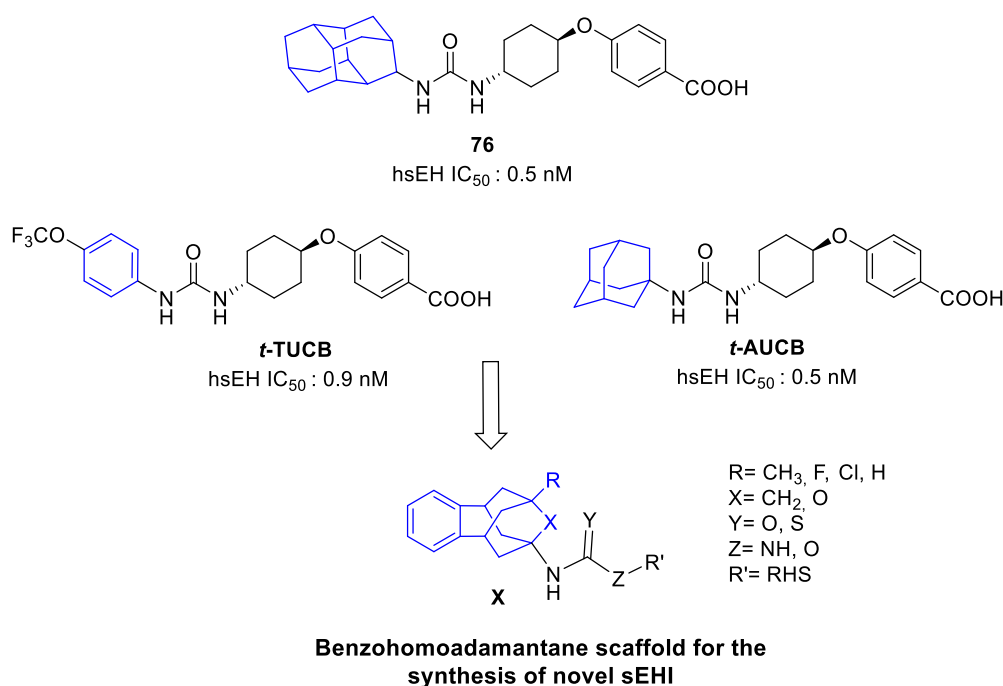


Figure 32. Design of new compounds featuring the benzohomoadamantane scaffold.

The R position of the benzohomoadamantane scaffold can be a methyl group or, alternatively, fluorine, chlorine or hydrogen atoms, among others. Moreover, the X position can be a methylene unit or an oxygen atom. Apart from these derivatizations in

²¹¹ Barniol-Xicota, M.; Escandell, A.; Valverde, E.; Julián, E.; Torrents, E.; Vázquez, S. *Bioorg. Med. Chem.* **2015**, *23*, 290-296.

the polycyclic ring, the new sEHIs can be linked to the RHS of the molecules using the urea, thiourea or carbamate linkers, depending on the nature of Y and Z substituents. Finally, the RHS position can be substituted by several radicals, thus further increasing the chemical diversity of this new family of compounds.

For the preparation of these new inhibitors, it was necessary to synthesize the appropriate polycyclic amines that were obtained following known procedures previously described by our group (Figure 33).^{174,175,176,211}

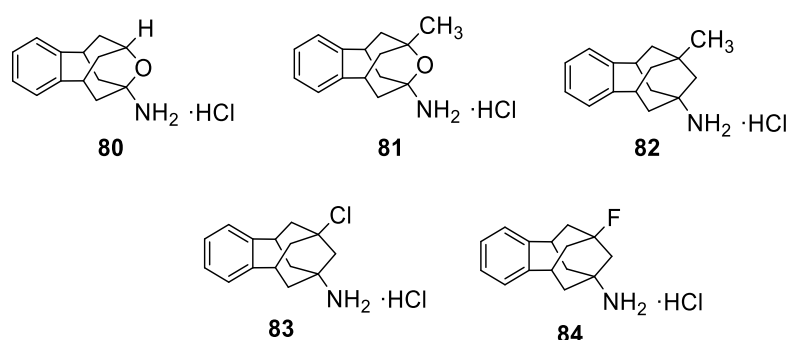
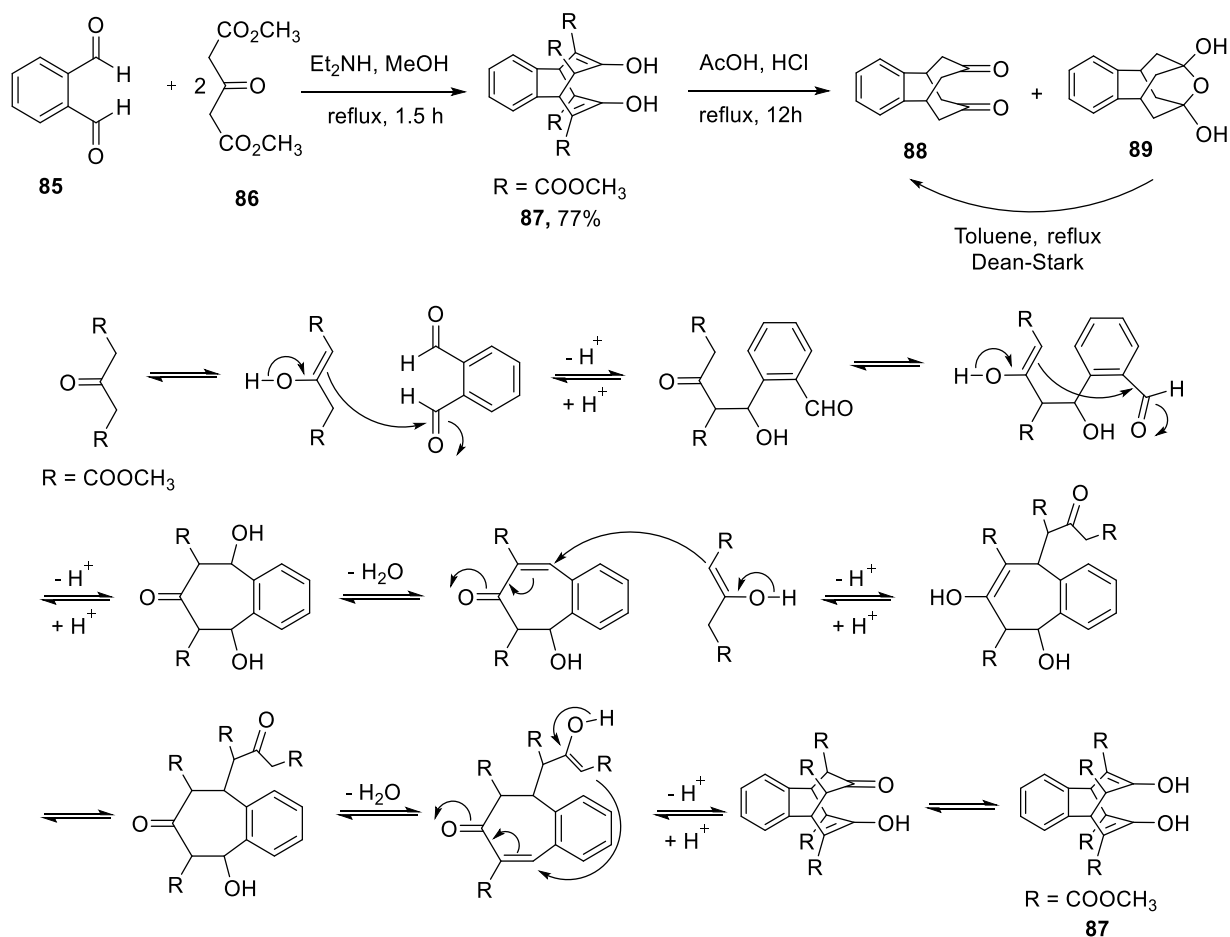


Figure 33. The benzohomoadamantane amines **80-84** used as starting materials for the obtention of the new compounds.

The first step for the synthesis of the desired polycyclic amines was the obtention of the known diketone **88**.²¹² Starting from the commercially available *o*-phthalaldehyde, **85**, and two equivalents of dimethyl-1,3-acetonedicarboxylate, **86** in the presence of diethylamine and methanol, a Weiss-Cook condensation took place affording tetraester intermediate **87**. Given the keto-enol tautomerism of **86**, the reaction started through a double aldol-type condensation and subsequent dehydration under basic catalysis. Then, the second equivalent of the **86** undertook a double Michael addition to the α,β -unsaturated ketone leading to the tetraester **87**.

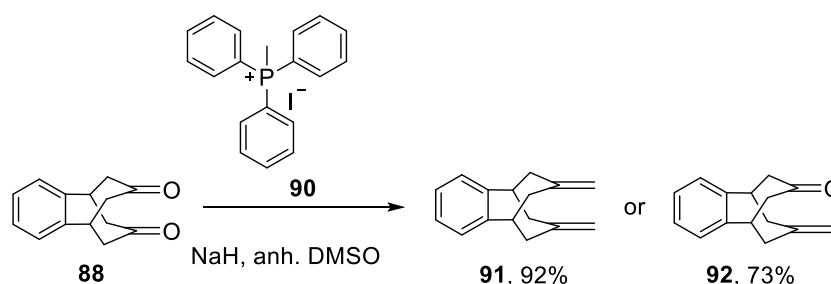
²¹² Föshlich, B.; Dukek, U.; Graessle, I.; Novotny, B.; Schupp, E.; Schwaiger, G.; Widmann, E. *Liebigs. Ann. Chem.* **1973**; *11*, 1839-1850.

Then, the tetraester **87** was subjected to hydrolysis in acidic media affording the corresponding acids, which decarboxylated *in situ* to give a mixture of diketone **88** and its hydrate, **89** (Scheme 10). In order to obtain the pure ketone, the mixture was dissolved in toluene and heated until reflux using a Dean-Stark apparatus to finally provide pure diketone **88**.



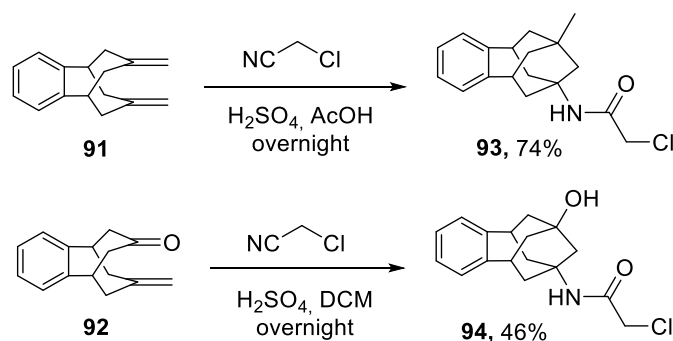
Scheme 10. Synthesis of diketone **88** from dialdehyde **85** and diester **86**.

The next step was a di-Wittig reaction of diketone **88** to form the diene **90** as a precursor for the obtention of the polycyclic amine **82**, or a mono-Wittig reaction of **88** to obtain the enone **91** as a precursor for the obtention of the polycyclic amines **83** and **84** (Scheme 11). Of note, amines **80** and **81** were also obtained from diketone **88** following a different synthetic procedure, which will be discussed later on.



Scheme 11. Conversion of diketone **88** to diene **91** or enone **92** through a controlled Wittig reaction.

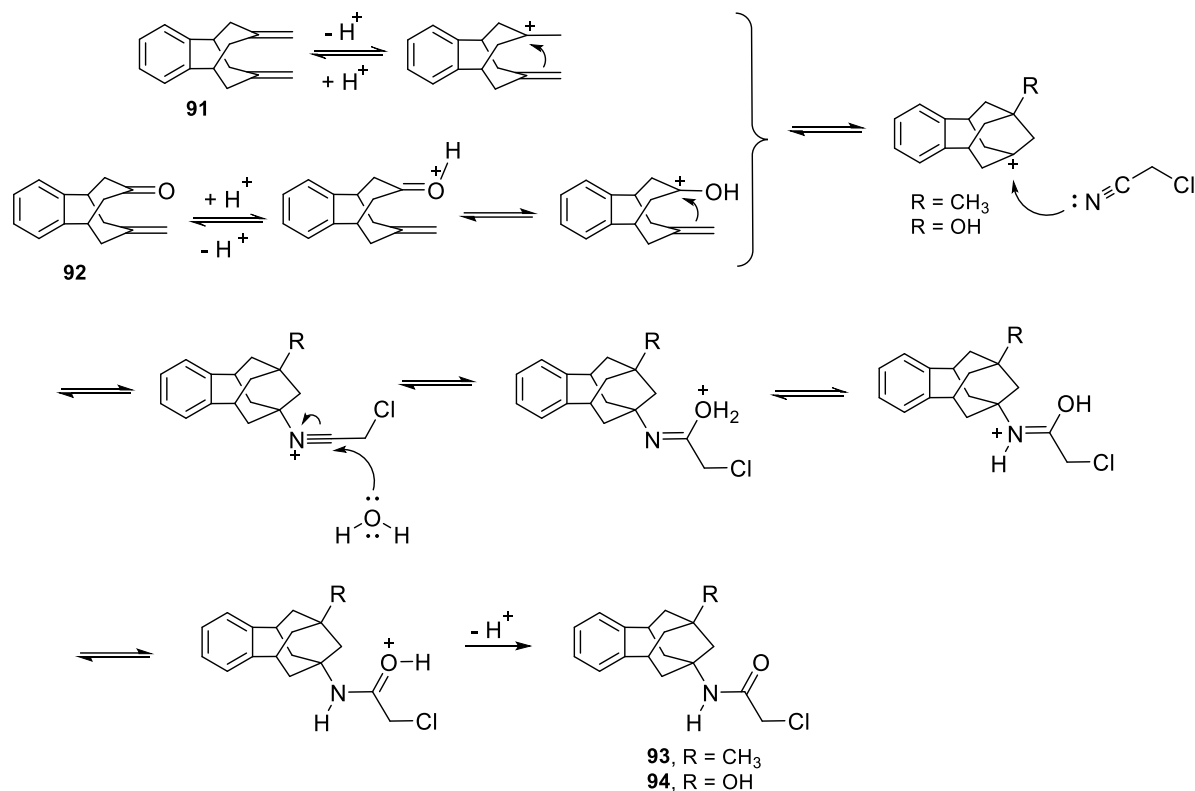
For these conversions it was required sodium hydride, anhydrous DMSO and methyltriphenylphosphonium iodide, **90**, prepared reacting triphenylphosphine and iodomethane for 5 hours using toluene as a solvent. The transformation of **88** to diene **91** or enone **92** was managed by controlling the equivalents of methyltriphenylphosphonium iodide. For the synthesis of **92**, the reaction took place using 1 eq. of diketone, 1.25 eq. of the phosphonium salt and 1.25 eq. of sodium hydride. In contrast, if the desired product was the diene **91**, it was necessary to use a larger excess of methyltriphenylphosphonium iodide (4.1 eq.) and sodium hydride (4.1 eq.). The synthesis continued with a Prins-Ritter transannular cyclization with chloroacetonitrile in the presence of acidic media in order to obtain the chloroacetamides **93** and **94** (Scheme 12).



Scheme 12. Preparation of chloroacetamides **93** and **94**.

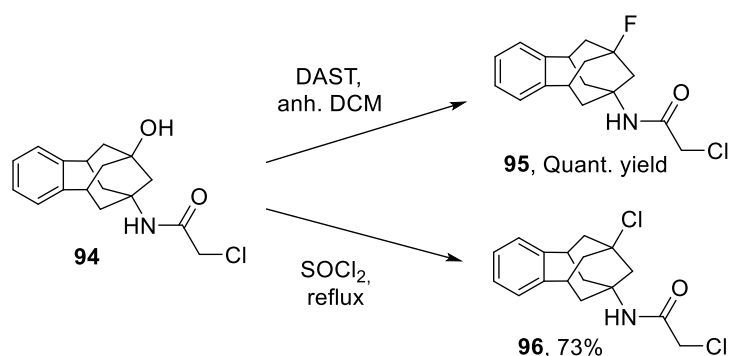
The reaction mechanism of the Prins-Ritter transannular cyclization that afforded the desired chloroacetamides is shown in Scheme 13. The first step of this reaction involves the protonation of either the double bond of the diene **91** or the carbonyl group of enone **92**. Then, in both cases, the π - electrons of the alkene attacked the formed cation to generate a tertiary carbenium ion. Next, the nitrogen atom of the nitrile group

attacked the carbocation to give a nitrilium ion intermediate, which was hydrolysed during the work up affording the desired chloroacetamides **93** and **94**.



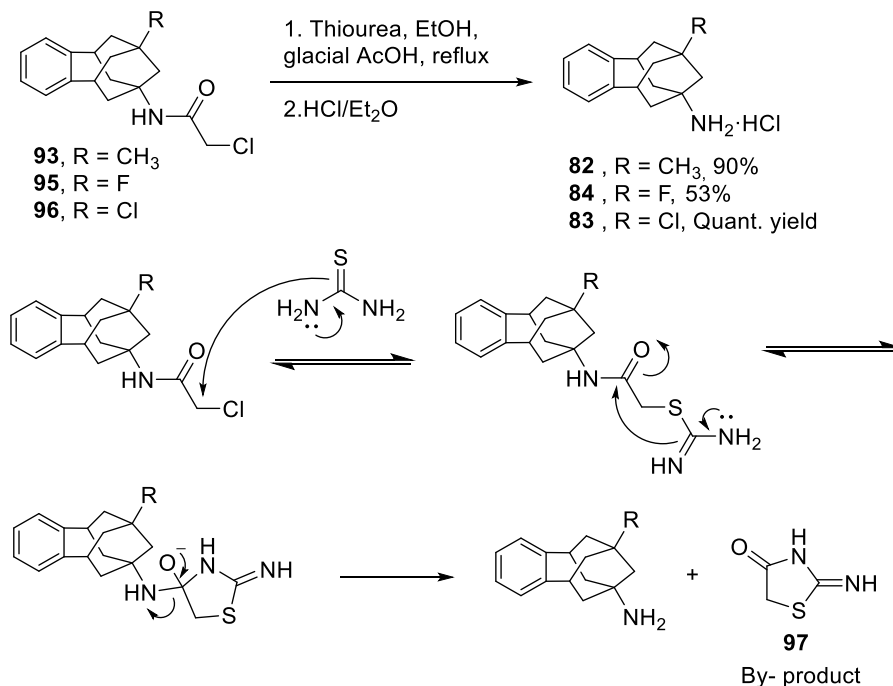
Scheme 13. Mechanism of the Prins-Ritter transannulation.

The next step in order to obtain the polycyclic amines **83** and **84** was the substitution of the hydroxyl group of **94** by a chlorine or fluorine atom, respectively. Thus, chloroacetamide **94** was treated either with the fluorinating agent (diethylamino)sulfur trifluoride (DAST) in dichloromethane to provide the fluorinated derivative **95**, or with thionyl chloride for one hour under reflux conditions affording the desired chloride, **96** (Scheme 14).



Scheme 14. Replacement of the hydroxyl group of **94** by fluorine or chlorine atoms.

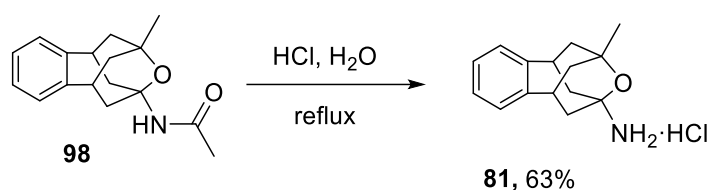
The final step for the obtention of the desired amines **82**, **83** and **84** was the hydrolysis of the amide group. Previous work of our research group determined that the aqueous hydrolysis of this type of amides gave either low yields in acid media or high yields but under extreme basic conditions, so the efficiency of the deprotection was improved using an alternative method. Thus, the final amines were prepared by removing the chloroacetamide group using thiourea and glacial acetic acid in absolute ethanol, providing the desired amines **82**, **83** and **84**. Once deprotected, amines were treated with an excess of hydrogen chloride in diethyl ether to obtain the corresponding hydrochlorides in medium to excellent yields (Scheme 15).



Scheme 15. Deprotection of chloroacetamides with thiourea and the mechanism of the reaction.

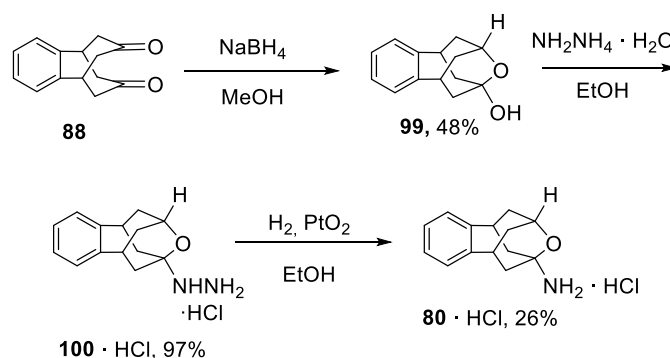
The mechanism of the deprotection started with a nucleophilic substitution of the chloride by the attack of the sulphur atom from the thiourea, followed by cyclization and the elimination of the amine provided the desired amines **82**, **83** and **84**. As aforementioned, amines **80** and **81** were synthesized following different synthetic procedures.

Amine **81** was prepared starting from the intermediate acetamide **98** previously synthesized by Dr. Elena Valverde, which was subjected to hydrolysis in acidic media to provide the desired amine (Scheme 16).



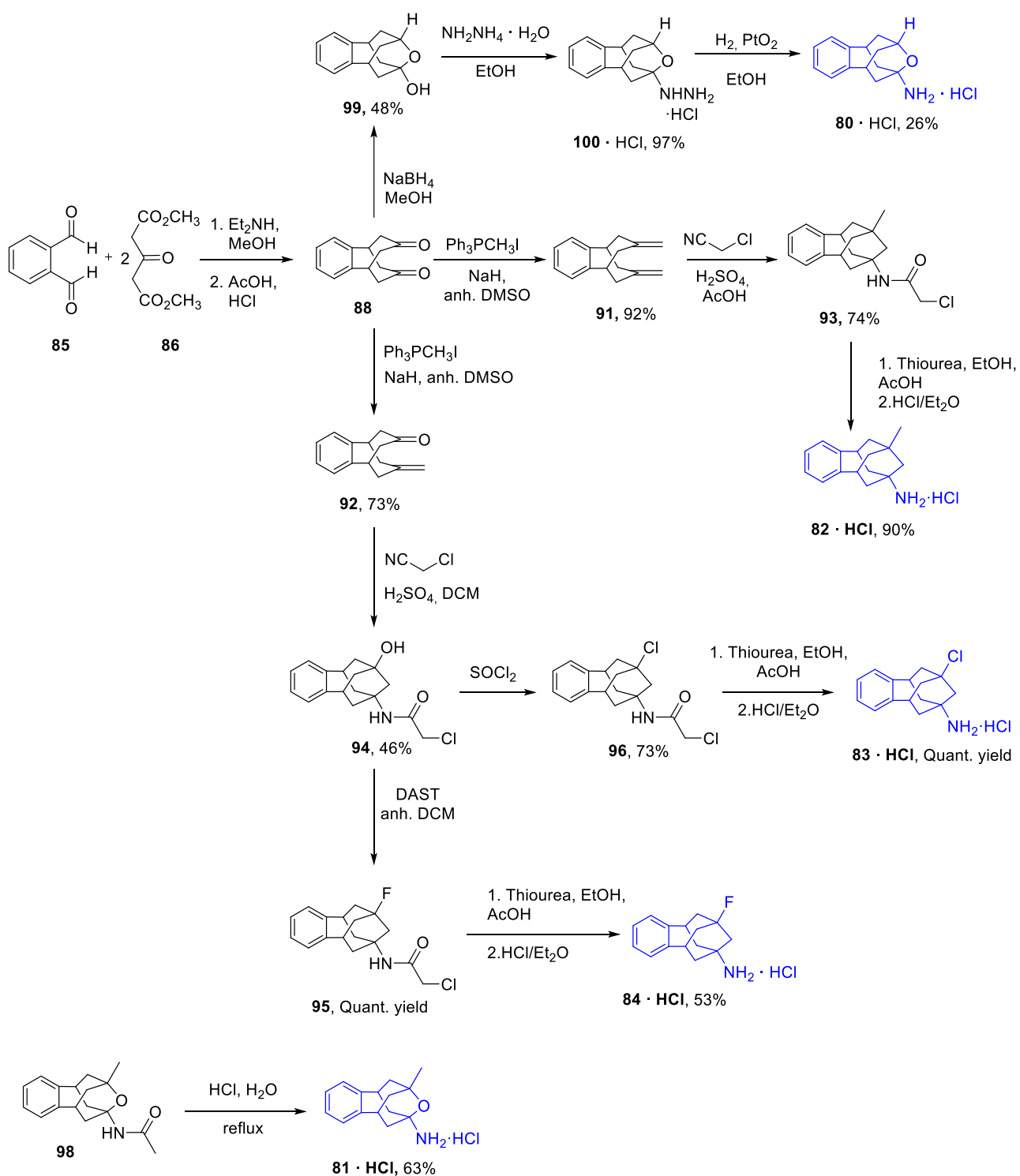
Scheme 16. Hydrolysis of the intermediate acetamide **98** in acidic conditions.

Finally, amine **80** was synthesized starting from ketone **88**, which was reduced by sodium borohydride to yield alcohol **99**. Then, **99** was treated with hydrazine in acidic media to provide hydrazine **100**, which was subjected to a catalytic hydrogenation at atmospheric pressure using platinum oxide as the catalyst affording the desired amine **80** (Scheme 17).



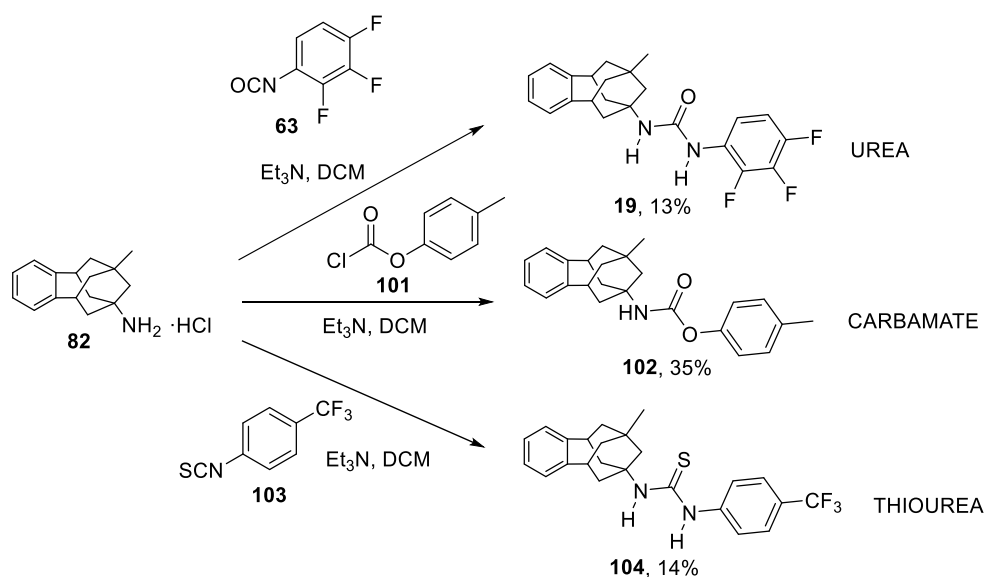
Scheme 17. Synthetic pathway for the obtention of amine **80**.

In summary, scheme 18 shows the whole synthetic pathway followed to obtain the required amines for the synthesis of the new sEHIs bearing the benzohomoadamantane scaffold.



Scheme 18. Synthetic routes for the obtention of the benzohomoadamantane amines synthesized in this work.

First, we wanted to see the impact of the main pharmacophore in the new family of benzohomoadamantane-based sEHIs. With this purpose, compounds presenting carbamate, thiourea and urea as the main pharmacophores were synthesized starting from the polycyclic amine **82** in order to explore their potency as sEHIs (Scheme 19). The reaction of amine **82** with the commercially available 2,3,4-trifluorophenyl isocyanate, **63**, *p*-tolyl chloroformate, **101**, and 4-(trifluoromethyl)phenyl isothiocyanate, **103**, furnished the desired urea **19**, carbamate **102** and thiourea **104**, respectively.



Scheme 19. Obtention of the new benzohomoadamantane-based urea **19**, carbamate **102** and thiourea **104**.

The potency of these compounds as sEHIs was evaluated by Dr Christophe Morisseau, from the group of Prof. Bruce D. Hammock at UCD. According to our expectations, urea **19** revealed as a very potent sEHI in the low nanomolar range, while carbamate **102** and thiourea **104** presented much lower potency. For this reason, carbamate and thiourea derivatives were discarded and the urea group was chosen as the main pharmacophore for the synthesis of further benzohomoadamantane-based inhibitors.

Having found that the benzohomoadamantane scaffold may successfully replace the adamantane group, the next step was the synthesis of three series of novel urea-based sEHIs related to the potent compound **10**, the clinical candidate AR9281, and *t*-AUCB (Figure 34).

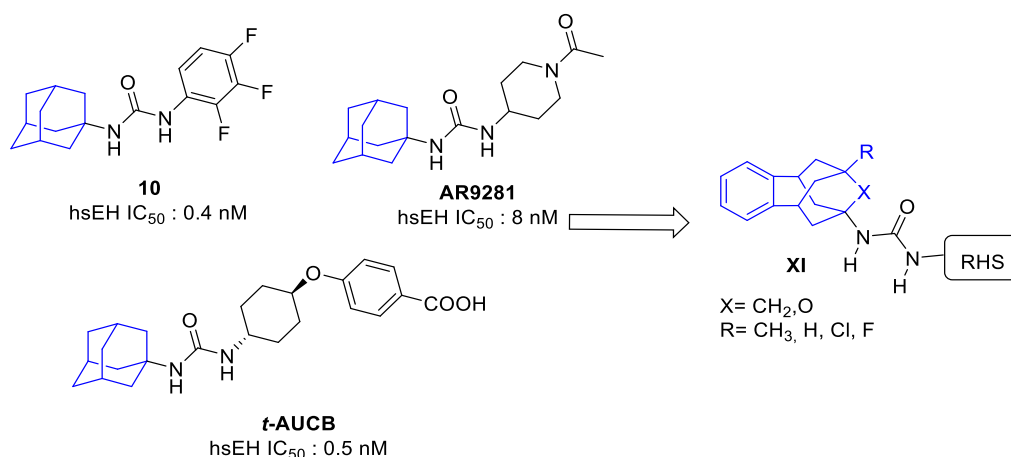
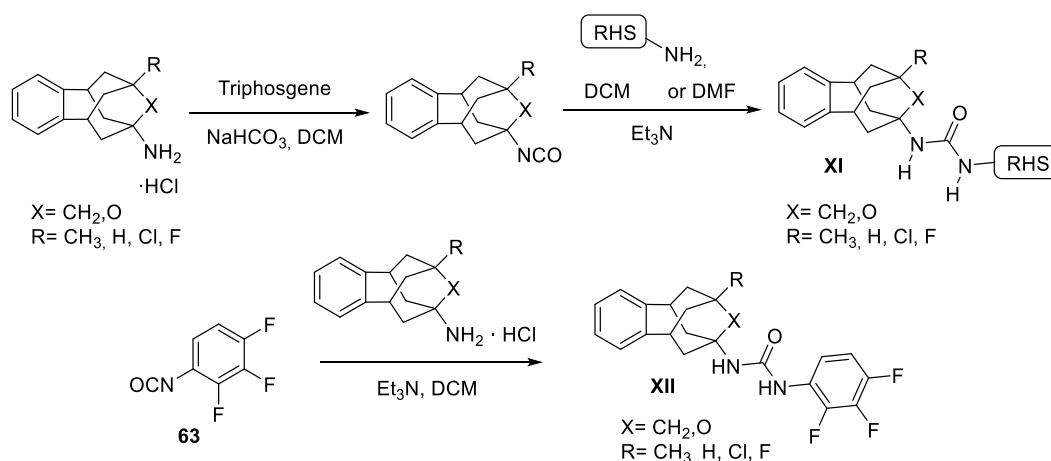


Figure 34. General structure **XI** of new ureas bearing the benzohomoadamantane moiety or its oxa-derivatives.

The synthesis was undertaken in a similar way as in the 2-oxaadamantane-based inhibitors disclosed in Chapter 1. In order to obtain **AR9281** and **t-AUCB** analogs, the isocyanate of the corresponding benzohomoadamantane amine was prepared by using triphosgene and sodium hydrogen carbonate. Then, the addition of the 1-acetyl-4-aminopiperidine in DCM or the 4-[(*trans*-4-aminocyclohexyl)oxy]benzoic in DMF provided the desired ureas. On the other hand, analogs of **10** were obtained by the direct reaction of the commercially available 2,3,4-trifluorophenyl isocyanate with the corresponding polycyclic amine in dichloromethane (Scheme 20).



Scheme 20. General synthetic pathways for the obtention of the new sEHIs.

The structures of all the benzohomoadamantane-based ureas synthesized in this work are shown in Figure 35. First, the potency of the new ureas as sEHIs was evaluated. As described in the following article, the comparison of the compounds presenting an

oxygen atom in their benzohomoadamantane scaffold with their analogs presenting a methylene unit showed that, in all cases, the compounds bearing an oxygen atom were less potent than their methylene counterparts. Of note, the substitution of the position R in the benzohomoadamantane scaffold from a methyl group to a hydrogen atom in the AR9281 analogs also produced an important drop of the inhibitory activities. Given the aforementioned results, the oxa-benzohomoadamantane scaffold was discarded due to its lack of potency and compounds bearing the benzohomoadamantane moiety were further evaluated.

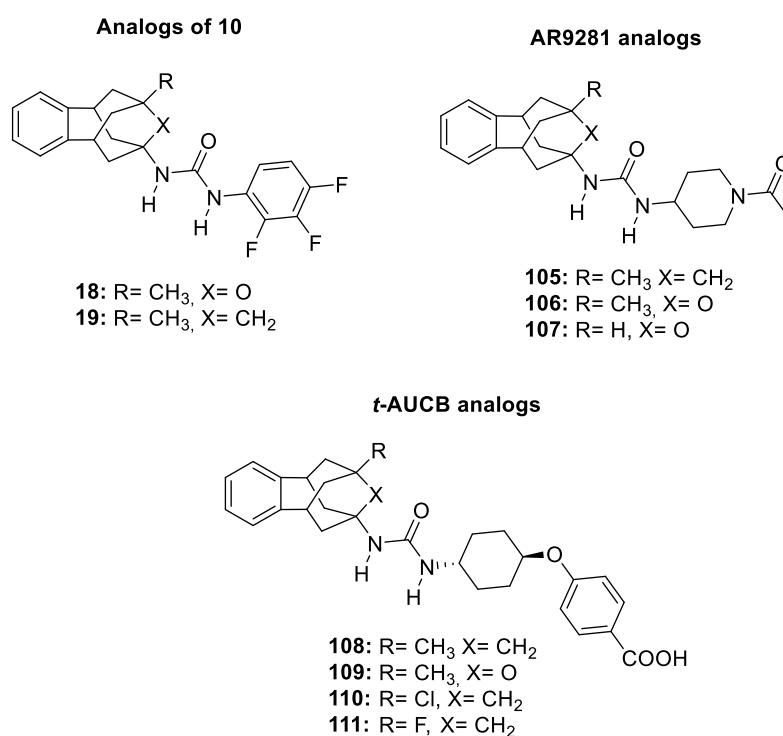


Figure 35. Structure of the new sEHIs bearing the benzohomoadamantane scaffold.

Next, we conducted a screening cascade consisting of experimental microsomal stability, solubility, permeability, cytochrome inhibition and hERG inhibition. All these assays were performed by the group of Prof. M. Isabel Loza and Prof. José M. Brea of the Drug Screening Platform/Biofarma Research Group of the University of Santiago de Compostela. Additionally, the cytotoxicity of the compounds in SH-SY5Y cells was evaluated by Drs Coral Sanfeliu and Rubén Corpas of the Institute of Biomedical Research of Barcelona (CSIC). Finally, we assessed, for a few selected compounds, the selectivity for two related targets: *h*LOX-5, measured by the group of Dr Maria I.

Rodríguez Franco, from the Institute of Medicinal Chemistry (CSIC, Madrid), and *h*COX-2, assessed by the company Eurofins.

As described in the article, the results showed that the acetylamino piperidine derivatives and the trifluorophenyl analogs bearing the benzohomoadamantane scaffold presented high metabolic liability. Hence, the *t*-AUCB series was selected and fully evaluated. Gratifyingly, the compounds did not present cytotoxicity in SH-SY5Y cells, cytochrome inhibition, *h*COX-s or *h*LOX-5 inhibition nor hERG inhibition. Therefore, the screening cascade allowed us to select compounds **108** and **110** for the *in vivo* studies, considering their biological profiling (Table 3). Both compounds presented excellent inhibitory activities against the human, murine and rat enzymes, acceptable microsomal stabilities, particularly in human microsomes, and better permeability through Caco-2 cells than *t*-AUCB.

Cpd	sEH IC ₅₀ (nM) ^a			Microsomal Stability ^b (h/m/r)	Solubility ^c (μM)	Permeability (Caco-2)		ER ^d	^e LD ₅₀ (μM)
	human	murine	rat			Papp (nm/s)	A→B		
<i>t</i> -AUCB	0.5	1.7	8.0 ^f	94/92/46	25	1.9	210.3	111	ND ^g
108	1	9.9	0.4	82/28/2	4	10	123.7	12.4	>100
110	0.4	0.4	0.4	89/29/52	13	21.5	46.6	2.1	>100
111	0.5	0.5	0.4	77/36/60	7	0.9	219.1	243.9	>100

Table 3. IC₅₀ in human, murine and rat sEH, microsomal stability, solubility and permeability values of the *t*-AUCB related compounds. ^aReported IC₅₀ values are the average of three replicates. The fluorescent assay as performed here has a standard error between 10 and 20% suggesting that differences of two-fold or greater are significant. Because of the limitations of the assay it is difficult to distinguish among potencies < 0.5 nM.²⁰⁹ ^bPercentage of remaining compound after 60 min of incubation with human, mice and rat microsomes obtained from Tebu-Xenotech in the presence of NADP at 37 °C. ^cSolubility in a 1% DMSO : 99% PBS buffer solution. See the experimental section of the accompanying article for further details. ^dThe efflux ratio was calculated as ER = (Papp B→A) / (Papp A→B). See the experimental section of the accompanying article for further details. ^esEH cytotoxicity tested by propidium iodide staining after 24h incubation in SH-SY5Y cells. See the experimental section of the accompanying article for further details. ^fTaken from reference 111. ^gND: Not determined.

Moreover, the CYP450 inhibition of **108** and **110** was evaluated using human recombinant cytochrome P450 enzymes. These assays were of great interest, mostly in terms of selectivity, as EETs are formed by several cytochrome P450 epoxygenase isoforms. Indeed, some ureas have been reported to inhibit cytochromes, such as SR 9186.^{213,214} Satisfactorily, the tested compounds did not significantly inhibit the evaluated cytochromes at the tested concentration of 10 μ M.

Before conducting the *in vivo* efficacy study, we performed PK studies with the two selected compounds. The results showed that compound **110** presented a better profile than **108**, considering its larger half-life, higher C_{max} and AUC and lowest clearance. Thus, **110** was selected for conducting the *in vivo* efficacy study in the well-known murine model of cerulein-induced AP.^{191,215,216}

The efficacy of the new sEH **110** was assessed by Draconis Pharma at 0.1 and 0.3 mg/kg in the cerulein-induced AP murine model using C57BL/6 male. The experimental procedure for the *in vivo* efficacy study was followed as described in already published protocols,¹⁹¹ administering intraperitoneally the selected compound after the induction of the AP by cerulein.

First, the health status of animals was analyzed by monitoring their body weight. Gratifyingly, treated animals with both doses (0.3 and 0.1 mg/kg) of **110** showed an increment in body weight after the last injection of cerulein, although only the group treated at 0.3 mg/Kg reached statistical significance. Of note, this increment was not observed in animals treated only with cerulein. In addition, we measured compound concentration in plasma and pancreatic tissue at 10 hours post-administration, confirming that the administration of both doses of 0.1 mg/Kg and 0.3 mg/Kg produced enough plasma levels of compound **110** to inhibit the sEH and that the selected compound was able to reach the pancreatic tissue with the dosage of 0.3 mg/Kg.

²¹³ Song, X.; Li, X.; Ruiz, C. H.; Yin, Y.; Feng, Y.; Kamenecka, T. M. *Bioorg. Med. Chem. Lett.* **2012**, *22*, 1611-1614.

²¹⁴ Li, X.; Song, X.; Kamenecka, T. M.; Cameron, M. D. *Drug Metab. Dispos.* **2012**, *40*, 1803-1809.

²¹⁵ Bettaieb, A.; Morisseau, C.; Hammock, B. D.; Haj, F. G. *Free Radic. Biol. Med.* **2014**, *75* Suppl 1, S32.

²¹⁶ Bettaieb, A.; Chahed, S.; Tabet, G.; Yang, J.; Morisseau, C.; Griffey, S.; Hammock, B. D.; Haj, F. G. *PLoS One* **2014**, *9*, e113019.

Finally, histologic analysis of pancreas showed that mice treated with **109** at both doses presented diminished cerulein-induced effects, being the group treated with 0.3 mg/kg the one that mostly reversed the pancreatic damage, edema and neutrophils infiltration.

These promising results revealed that, with a dosage of only 0.3 mg/kg, our candidate **110** showed effectiveness at reducing symptoms and pancreatic damaged in a mice model of cerulein-induced AP. Worth to mention, the dosage used in this study was 100 times lower than the one used with the 2-oxaadamantane-based inhibitor **42** disclosed in Chapter 1 and 10 times lower than the one employed in a related studied published using TPPU.¹⁹¹

The results of this work are disclosed in a draft article included in the following pages of this Thesis.

Noteworthy, the new sEHIs described herein bearing the benzohomoadamantane scaffold as well as the ones described in the next Chapters 4 and 5 of the present Thesis, have been protected by a patent application,²¹⁷ which is currently under exam. This document is attached at the end of the Chapter 5.

²¹⁷ Codony Gisbert, S.; Galdeano Cantador, C.; Leiva Martínez, R.; Larisa Turcu, A.; Valverde Murillo, E.; Vázquez Cruz, S. (Universitat de Barcelona). WO 2019/243414 A1, June 20, 2018.

From the design to the *in vivo* evaluation of
3.3.3
benzohomoadamantane-derived soluble
epoxide hydrolase inhibitors for the treatment
of acute pancreatitis

Sandra Codony¹, Carla Calvó-Tusell², Elena Valverde¹, Silvia Osuna^{2,3}, Christophe Morisseau⁴, M. Isabel Loza⁵, José Brea⁵, Concepción Pérez⁶, María Isabel Rodríguez-Franco⁶, Javier Pizarro-Delgado^{7,8,9}, Rubén Corpas^{10,11}, Christian Griñán-Ferré¹², Mercè Pallàs¹², Coral Sanfeliu^{10,11}, Manuel Vázquez-Carrera^{7,8,9}, Bruce D. Hammock⁴, Ferran Feixas², Santiago Vázquez^{1}*

¹Laboratori de Química Farmacèutica (Unitat Associada al CSIC), Departament de Farmacologia, Toxicologia i Química Terapèutica, Facultat de Farmàcia i Ciències de l'Alimentació, and Institute of Biomedicine (IBUB), Universitat de Barcelona, Av. Joan XXIII, 27-31, 08028 Barcelona, Spain.

²CompBioLab Group, Departament de Química and Institut de Química Computacional i Catàlisi (IQCC), Universitat de Girona, C/ Maria Aurèlia Capmany 69, 17003 Girona, Spain.

³Institució Catalana de Recerca i Estudis Avançats (ICREA), 08010 Barcelona, Spain.

⁴Department of Entomology and Nematology and Comprehensive Cancer Center, University of California, Davis, CA 95616, USA.

⁵Drug Screening Platform/Biofarma Research Group, CIMUS Research Center.

Departamento de Farmacología, Farmacia e Tecnología Farmacéutica. University of Santiago de Compostela (USC), 15782 Santiago de Compostela, Spain.

⁶Institute of Medicinal Chemistry, Spanish National Research Council (CSIC), C/Juan de la Cierva 3, 28006 Madrid, Spain.

⁷Pharmacology Section. Department of Pharmacology, Toxicology and Medicinal Chemistry, Faculty of Pharmacy and Food Sciences, University of Barcelona, and Institute of Biomedicine of the University of Barcelona (IBUB), Av. Joan XXIII, 27-31, 08028 Barcelona, Spain.

⁸Spanish Biomedical Research Center in Diabetes and Associated Metabolic Diseases (CIBERDEM)-Instituto de Salud Carlos III, 28029 Madrid, Spain.

⁹Pediatric Research Institute-Hospital Sant Joan de Déu, 08950 Esplugues de Llobregat, Spain.

¹⁰Institute of Biomedical Research of Barcelona (IIBB), CSIC and IDIBAPS, 08036 Barcelona, Spain.

¹¹CIBER Epidemiology and Public Health (CIBERESP)-Instituto de Salud Carlos III, 28029, Madrid, Spain.

¹²Pharmacology Section. Department of Pharmacology, Toxicology and Medicinal Chemistry, Faculty of Pharmacy and Food Sciences, and Institut de Neurociències, University of Barcelona, Av. Joan XXIII, 27-31, 08028 Barcelona, Spain.

* Corresponding author. Tel.: +34 934024533; *E-mail address*: svazquez@ub.edu (S. Vázquez).

KEYWORDS: acute pancreatitis, benzohomoadamantane, cerulein, inflammation, soluble epoxide hydrolase, urea.

ABSTRACT

The pharmacological inhibition of the soluble epoxide hydrolase (sEH) has been validated for the treatment of inflammatory and pain related diseases. Certainly, a number of very potent sEH inhibitors (sEHI) have been developed, several of them featuring adamantyl or phenyl moieties, such as the clinical candidates AR9281 or EC5026. Herein we report a new series of sEHI where these hydrophobic moieties have been replaced by the versatile benzohomoadamantane scaffold, that features a polycyclic unit fused with an aromatic ring. Most of these new sEHI are endowed with excellent inhibitory activities against the human and murine sEH. Molecular dynamics simulations revealed that the addition of an aromatic ring into the adamantane scaffold produced conformational rearrangements in the active site region and adjacent regions to stabilize the aromatic ring of the benzohomoadamantane core. A screening cascade (solubility, cytotoxicity, metabolic stability, CYP450s, *h*LOX-5, *h*COX-2 and hERG inhibition) allowed us to select a candidate for an *in vivo* efficacy study in a murine model of cerulein-induced acute pancreatitis. Of note, the administration of **22** produced an improvement of the health status of the animals and reduced pancreatic damage, showing that the benzohomoadamantane unit is a promising scaffold for the design of novel sEHI.

INTRODUCTION

Arachidonic acid, a polyunsaturated fatty acid, is metabolized by cyclooxygenases (COXs), lipoxygenases (LOXs), and cytochrome P450s (CYPs). The COX and LOX pathways mainly lead to the production of pro-inflammatory lipid mediators, such as prostaglandins and leukotrienes, and have been pharmaceutically targeted.¹ In contrast, the CYP pathway is involved in the production of pro- and anti-inflammatory lipid mediators. The CYP hydroxylases lead to 20-hydroxyeicosatetraenoic acid that present pro-inflammatory activity while the CYP epoxygenases produce epoxyeicosatrienoic acids (EETs), endowed with potent anti-inflammatory activity.² However, the EETs are rapidly metabolized by the soluble epoxide hydrolase enzyme (sEH, *EPHX2*, EC 3.3.2.3) into the corresponding dihydroxyeicosatrienoic acids, which present less biological activity.³⁻⁴ It is known that the pharmacological inhibition of sEH *in vivo* stabilizes the concentration of EETs, reducing inflammatory and pain states, suggesting sEH as a pharmacological target for the treatment of inflammatory diseases.⁵⁻⁶

X-ray crystallographic studies revealed that sEH has an L-shaped pocket with the active site at the corner. Although each branch of the pocket, of 10 and 15 Å of length, accepts a variety of functional groups, the entire pocket is essentially hydrophobic.⁷ Indeed, a number of very potent sEH inhibitors (sEHI) have been developed, several of them featuring lipophilic moieties such as adamantyl or phenyl groups (Figure 1).⁶ AR9281 was taken to phase II by Arete Therapeutics for the treatment of hypertension in diabetic patients, but failed largely because of its poor pharmacokinetic properties, likely related with its adamantane unit.⁸ Then, GSK2256294, developed for chronic obstructive pulmonary disease by GlaxoSmithKline, has entered to phase I clinical trial for obese smokers and other indications such as subarachnoidal hemorrhage or diabetic patients with insulin resistance.⁹ Taking the failure of AR9281 into account, EicOsis has recently

replaced the adamantane moiety of AR9281 by an aromatic ring for its drug candidate EC5026, currently in Phase 1 clinical trials for the treatment of neuropathic pain.¹⁰

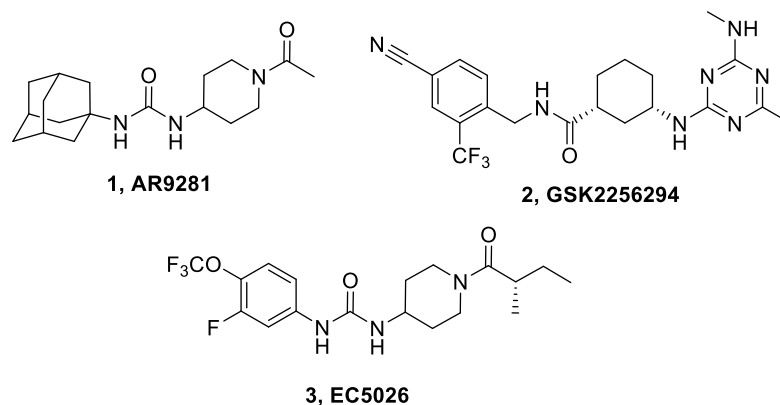


Figure 1. Structure of the three sEHI that have entered clinical trials.

We have recently found, using urea-based sEHI with lipophilic units of very different size, that the pocket of the sEH can accommodate polycycles of quite diverse volume, and that the replacement of the adamantane moiety by larger polycyclic rings, such as the diamantane moiety, may be better than the replacement by smaller ones. Indeed, urea **6**, a diamantane analog of the well-known sEHI **4**, *t*-AUCB, and **5**, *t*-TUCB, showed to be a subnanomolar inhibitor of the human sEH (hsEH) (Figure 2).¹¹

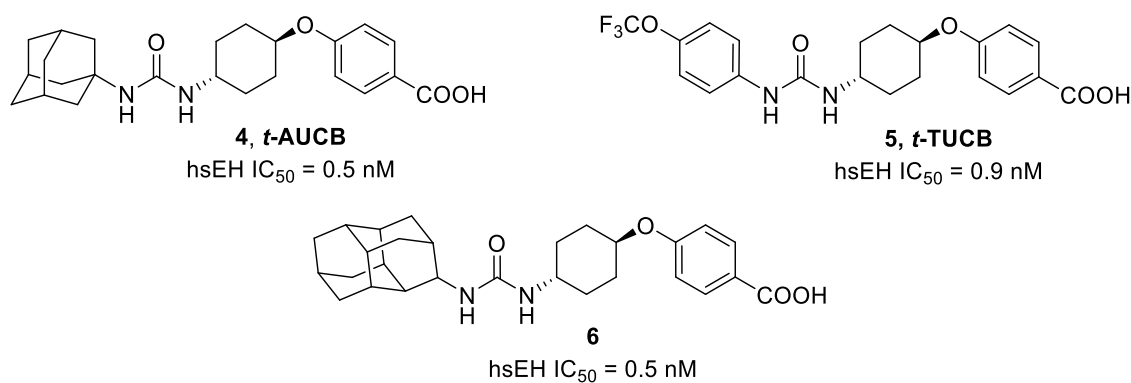


Figure 2. Structure and IC_{50} in hsEH of compounds **4-6**.

RESULTS AND DISCUSSION

Design and synthesis of new sEHI. Taking into account that both adamantane and aromatic ring moieties fit very well in the hydrophobic pocket of the sEH and that the replacement of adamantane by larger polycyclic rings seems to be a promising strategy to obtain more potent sEHI, herein we have designed and synthesized a novel series of sEHI bearing the very versatile benzohomoadamantane scaffold as the hydrophobic moiety. This polycyclic, readily accessible,^{12,13,14,15} system features a homoadamantane unit fused with an aromatic ring and permits several chemical derivatizations in its structure (Figure 3). We expected this new scaffold to lead to potent sEHI and to achieve the optimum drug-like properties by modifying the substituents in the benzohomoadamantane unit and/or the right-hand side (RHS) of the molecule.

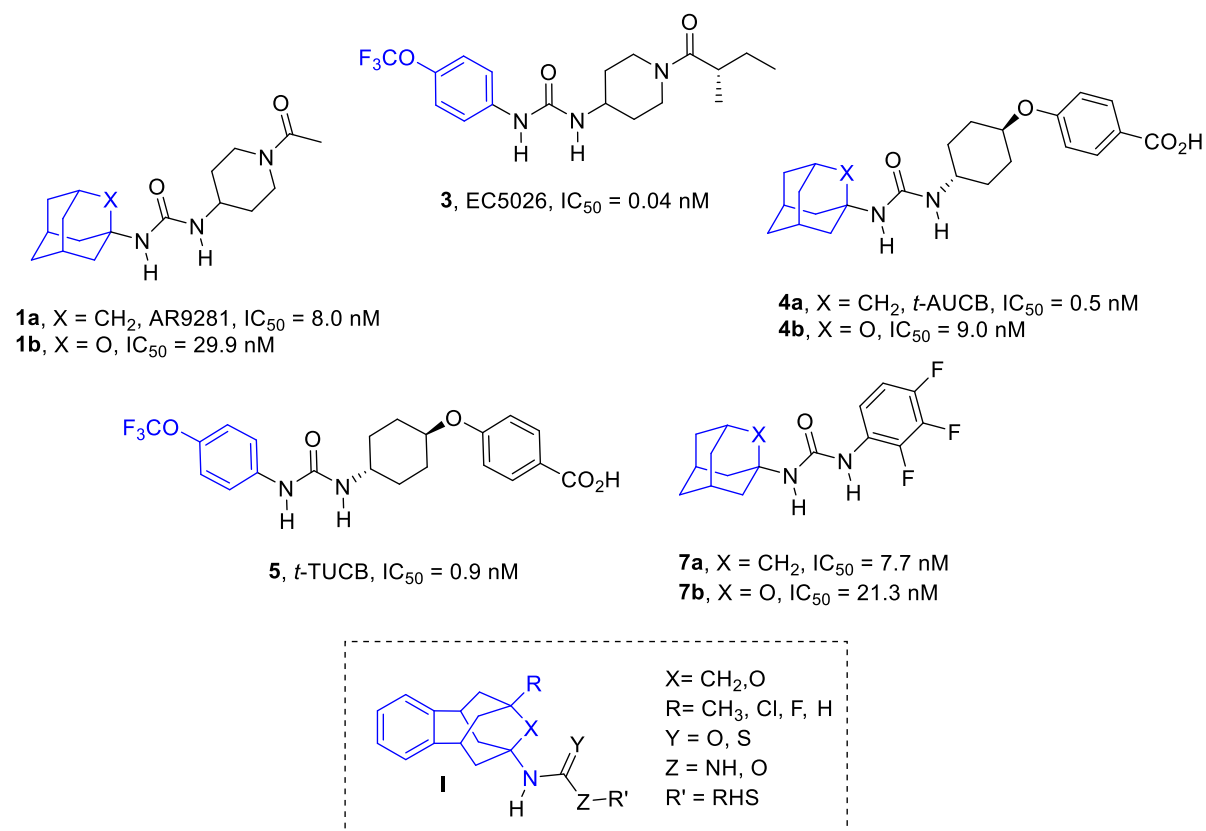


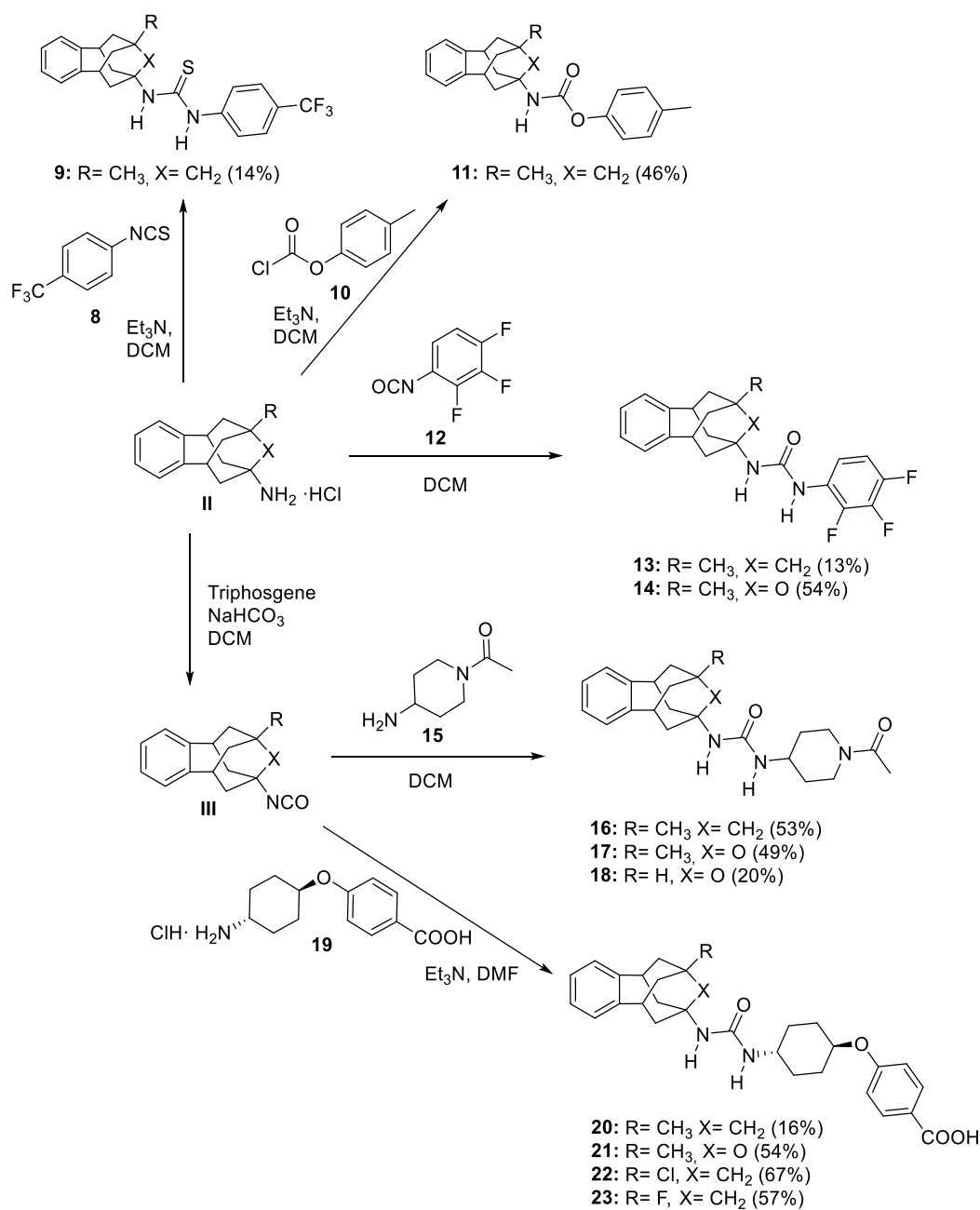
Figure 3. Known adamantyl- and phenyl-based sEHI **1a-b**, **3**, **4a-b**, **5** and **7a-b**, and general structure, **I**, of the new sEHI reported in this work. RHS = right-hand side (see below). IC₅₀ values refer to hSEH.

Thioureas, carbamates and, particularly, ureas, haven been reported as good pharmacophores for sEHI.⁶ For this reason, we first envisaged the synthesis of thiourea **9**, carbamate **11** and urea **13** in order to explore their relative potency as sEHI and to select the more suitable pharmacophore for the novel polycyclic scaffold (Scheme 1). The three compounds were easily synthesized in low to moderate yields from known 9-methyl-5,6,8,9,10,11-hexahydro-7*H*-5,9:7,11-dimethanobenzo[9]annulen-7-amine (**II**, R = CH₃, X = CH₂)¹² and 4-(trifluoromethyl)phenyl isothiocyanate, **8**, *p*-tolyl chloroformate, **10**, and 2,3,4-trifluorophenyl isocyanate, **12**, respectively (Scheme 1).

The inhibitory activities of the three compounds in human sEH were evaluated using a previously reported sensitive fluorescent-based assay (Table 1).¹⁶ While carbamate **11** was a very weak inhibitor (IC₅₀ = 12.7 μM) and thiourea **9** displayed only a moderate inhibition (IC₅₀ = 138 nM), urea **13** revealed as a very potent human sEHI (IC₅₀ = 1 nM) (Table 1). The superior potency of the urea is in agreement with previous results in other series of sEHI.^{17,18} For this reason, no further carbamates and thioureas derivatives were envisaged and the urea group was chosen as the main pharmacophore for the synthesis of further inhibitors.

Having found that this novel scaffold may successfully replace the adamantane and/or the phenyl group found in known sEHI, next we synthesized a series of benzohomoadamantane derivatives related with the potent sEHI AR9281, *t*-AUCB, *t*-TUCB, EC5026 and **7**, in order to explore their potency and DMPK properties. Of note, a very recent work has described that the replacement of a methylene unit of the

adamantane moiety by an oxygen atom lead to more soluble compounds while only slightly reducing the inhibitory activity against the sEH (e.g. **1b**, **4b** and **7b** in Figure 3).¹⁹ In this sense, an oxygen atom was introduced in the benzohomoadamantane scaffold in order to explore whether a similar trend was also followed within this new family of sEHI (Figure 3 and Scheme 1).



Scheme 1: Synthesis of new compounds **9**, **11**, **13-14**, **16-18** and **20-23**.

The synthesis of the new sEHI started from the suitably substituted benzohomoadamantane amines of general structure **II**.^{12,13,14,15} Thus, the synthesis of urea **14** involved the reaction of 5-methyl-1,5,6,7-tetrahydro-1,5:3,7-dimethanobenzo[*e*]oxonin-3(2*H*)-amine (**II**, R = CH₃, X = O) with 2,3,4-trifluorophenylisocyanate, **12**, in dichloromethane (Scheme 1). For the obtention of the piperidine derivatives, we first prepared the isocyanate of the corresponding polycyclic amine **II** by reaction with triphosgene and saturated aqueous solution of NaHCO₃. Once the desired isocyanate of general structure **III** was obtained, it was reacted with 1-acetyl-4-aminopiperidine **15** in dichloromethane to obtain ureas **16-18** in moderate overall yields (Scheme 1). Finally, the *t*-AUCB analogs **20-23** were obtained in low to moderate yields by the reaction, in the presence of triethylamine, of the corresponding isocyanate in DMF with 4-((*trans*-4-aminocyclohexyl)oxy)benzoic acid, **19**, prepared as previously reported (Scheme 1).²⁰

sEH inhibition and DMPK assays. The potency of the new compounds as inhibitors of the human sEH was tested using a previously reported sensitive fluorescent-based assay.¹⁶ Gratifyingly, the potency of the new benzohomoadamantane ureas was in the same range than that of their corresponding adamantane-based analogs (compare **13** vs **7**, **16** vs AR9281 and **20** vs *t*-AUCB) (Table 1). The comparison of the compounds presenting a methylene unit in the polycyclic scaffold with their analogs featuring an oxygen atom (**13** vs **14**, **16** vs **17** and **20** vs **21**, Scheme 1 and Table 1) showed that, in all cases, the compound bearing an oxygen atom was less potent than its methylene counterpart, results that are in line with those previously found within the adamantane series of sEHI.¹⁹ Interestingly, the AR9281 analogs **16** and **17** showed the largest difference (IC₅₀ values

of 3.1 nM vs 941 nM, respectively, Table 1). Also, the replacement of the methyl group of the position R of the polycyclic scaffold by a hydrogen atom in the AR9281 analogs produced a dramatic drop of the inhibitory activity (compare **17**, IC₅₀ = 941 nM vs **18**, IC₅₀ >10 μM in Table 1).

Cpd	h sEH ^a	
	IC ₅₀ (nM)	Microsomal Stability ^b (h / m / r)
9	138	ND ^c
11	>10000	ND
7	7.7	79 / 77 / 81
13	1.0	7 / 0.2 / ND
14	20	77 / 23 / 33
1, AR9281	8.0	72 / 100 / 87
16	3.1	1 / 0.5 / ND
17	941	ND
18	>10000	ND
4, t-AUCB	0.5	94 / 92 / 46
20	0.9	82 / 28 / 2
21	28	90 / 83 / ND

Table 1. Inhibition of human sEH and microsomal stability values of new benzohomoadamantane-based sEHI. ^aReported IC₅₀ values are the average of three replicates. The fluorescent assay as performed here has a standard error between 10 and 20% suggesting that differences of two-fold or greater are significant. Because of the limitations of the assay, it is difficult to distinguish among potencies < 0.5 nM.¹⁶ ^bPercentage of remaining compound after 60 min of incubation with human, mice and rat microsomes obtained from Tebu-Xenotech in the presence of NADP at 37 °C. ^cND: not determined.

Considering the metabolism liability of the adamantane and adamantane-related scaffolds,^{21,22} we evaluated the *in vitro* stability in human, mice and rat microsomes of the new ureas bearing the benzohomoadamantane moiety (Table 1). Within the trifluorophenyl series, the substitution of the adamantane nucleus by the

benzohomoadamantane scaffold showed an important decrease of the microsomal stability (compare **7** vs **13**, Table 1). By contrast, in the corresponding oxa-analog, **14**, the stability seemed to be restored in human, but not in mice neither in rat (compare **13** vs **14**, Table 1). Moreover, the analog of AR9281, **16**, presented very high metabolic liability in the three species, as there was found not more than 1% of the remaining compound after being incubated with microsomes for 60 minutes (compare AR9281 vs **16**, Table 1). Finally, within the *t*-AUCB series, the replacement of the adamantane moiety by the benzohomoadamantane scaffold led to similar stability in human microsomes, but to lower stability in mice and rat microsomes. Interestingly, in the oxa-analog **21** the stability was also maintained in mice microsomes (compare **20** and **21** vs *t*-AUCB, Table 1). Although it seems that the ureas presenting the oxa-benzohomoadamantane moiety were more stable in microsomes, taking into account that all these derivatives (**14**, **17**, **18** and **21**) were considerably less potent, this oxa-polycyclic scaffold was abandoned and only the ureas featuring the benzohomoadamantane core were further evaluated.

Overall, the *t*-AUCB family presented the most favorable properties in terms of potency and microsomal stability, and this series was selected for further optimization. As the adamantane nucleus contributes to the high lipophilicity of the known sEHI that compromises the solubility of these compounds, we next measured the solubility of the selected *t*-AUCB series in a 1% DMSO : 99% PBS buffer solution. As expected, the solubility decreases from the adamantane-based *t*-AUCB to the benzohomoadamantane analog **20** (Table 2) likely due to the increase from ten carbon atoms for the adamantane nucleus to sixteen for the new polycyclic scaffold. Taking this into account, we decided to explore novel substitutions in the R position of the benzohomoadamantane scaffold for improving solubility while maintaining or enhancing the potency and the microsomal stability of **20**. Thus, the methyl group of **20** was replaced by chlorine and fluorine atoms

leading to compounds **22** and **23**, respectively. The potency, microsomal stability, solubility and permeability of both compounds were assessed in order to explore their properties (Table 2).

Satisfactorily, the evaluation of the inhibition activity against the human sEH showed that both compounds **22** and **23** were slightly more potent than **20**, with IC₅₀ values in the same range than *t*-AUCB. Of note, **22** and **23** presented the same potency inhibiting the human, murine and rat enzymes, while *t*-AUCB was three- and twenty-fold less potent in the murine and the rat enzyme, respectively (Table 2).

Regarding metabolic stability, compounds **22** and **23** presented similar microsomal stabilities in human and mice than **20**, while were more stable in rat microsomes (Table 2). Furthermore, the experimental solubility values of these new halogenated compounds were determined. In line with a previous work with adamantane derivatives,²³ the solubility increases when the methyl group is replaced by a halogen atom (compare **20** vs **22** and **23**, Table 2), particularly for the chlorinated compound **22**.

The Caco-2 cell permeability model was used in order to evaluate the permeability of the compounds. Apparent permeability values (P_{app}) were determined from the amount permeated through the Caco-2 cell membranes at both apical-basolateral (A-B) and basolateral-apical (B-A) direction. Gratifyingly, compounds **20** and **22** presented higher permeability values than *t*-AUCB, being **22** the one that presented the best profile (Table 2).

Moreover, the cytotoxicity of **20**, **22** and **23** was evaluated in SH-SY5Y cells by propidium iodide staining, after 24 h of incubation. None of the compounds showed to be cytotoxic at the highest concentration tested (100 μM).

Cpd	sEH IC ₅₀ (nM) ^a			Microsomal Stability ^b (h / m / r)	Solubility ^c (μM)	Permeability (Caco-2)			LD ₅₀ ^e (μM)	IC ₅₀ <i>h</i> LOX-5 ^f (μM)	IC ₅₀ <i>h</i> COX-2 ^g (μM)
	human	murine	rat			Papp (nm/s) A→B	B→A	ER ^d			
4, <i>t</i>-AUCB	0.5	1.7	8.0 ^h	94 / 92 / 46	25	1.9	210.3	111	ND ⁱ	ND	ND
20	0.9	9.9	0.4	82 / 28 / 2	4	10	123.7	12.4	>100	>100	>10
22	0.4	0.4	0.4	89 / 29 / 52	13	21.5	46.6	2.1	>100	>100	>10
23	0.5	0.5	0.4	77 / 36 / 60	7	0.9	219.1	243.9	>100	>100	>10

Table 2. IC₅₀ in human and murine and rat sEH, microsomal stability, solubility and permeability values of the *t*-AUCB related compounds. ^aReported IC₅₀ values are the average of three replicates. The fluorescent assay as performed here has a standard error between 10 and 20% suggesting that differences of two-fold or greater are significant. Because of the limitations of the assay it is difficult to distinguish among potencies < 0.5 Nm.¹⁶ ^bPercentage of remaining compound after 60 min of incubation with human, mice and rat microsomes obtained from Tebu-Xenotech in the presence of NADP at 37 °C. ^cSolubility in a 1% DMSO : 99% PBS buffer solution, see experimental section for details. ^dThe efflux ratio was calculated as ER = (Papp B→A) / (Papp A→B). See the experimental section for further details. ^esEHI cytotoxicity tested by propidium iodide staining after 24h incubation in SH-SY5Y cells. See the experimental section for further details. ^fIC₅₀ in human LOX-5 (*h*LOX-5). See the experimental section for further details. ^gIC₅₀ in human COX-2 (*h*COX-2) performed by Eurofins (catalogue reference 4186). ^hTaken from reference 24. ⁱND: Not determined.

Finally, the three inhibitors **20**, **22** and **23** were tested for selectivity against *h*COX-2 and *h*LOX-5, two enzymes involved in the AA cascade. Neither **20** nor the halogenated analogs **22** and **23** significantly inhibited these enzymes (see Table 2).

Next, considering the best permeability of **20** and **22**, both compounds were selected for CYPs and hERG inhibition assays. Cytochromes P450 (CYP) inhibition was evaluated using human recombinant cytochrome P450 enzymes CYP1A2, CYP2C9, CYP2C19, CYP2D6 and CYP3A4, through a fluorescence-detection method. These assays were of great interest, not only for the detection of possible drug-drug interactions, but also in terms of selectivity, as EETs are formed by several cytochrome P450 epoxygenase

isoforms, particularly CYP2C19. Satisfactorily, the tested compounds did not significantly inhibit the evaluated cytochromes. We considered acceptable IC₅₀ values around 2 μM in the CYP2C19 taking into account that both compounds presented 2000-fold more potency inhibiting the sEH.

Cpd	Cytochrome inhibition ^a						hERG channel
	CYP	CYP	CYP	CYP	CYP 3A4 ^b		inhibition (% at 10 μM)
	1A2	2C9	2C19	2D6	(BFC)	(DBF)	
20	1 ± 2	17 ± 3	1.9 μM	1 ± 1	2 ± 2	14 ± 1	4
22	14 ± 4	31 ± 3	2.2 μM	11 ± 3	1 ± 2	52 ± 4	44

Table 3. Inhibition (expressed as % of inhibition at 10 μM or IC₅₀) of recombinant human cytochromes P450 enzymes and inhibition of the hERG channel (expressed as % of inhibition at 10 μM). ^aThe cytochrome inhibition was tested at 10 μM. IC₅₀ was calculated for those compounds that presented >50% of inhibition. ^bFor the study of CYP3A4, two different substrates were used: benzyloxytrifluoromethylcoumarin (BFC) and dibenzylfluorescein (DBF).

Regarding the hERG inhibition assay, both compounds inhibited the channel only 4% and 44% at 10 μM, respectively (Table 3). Overall, both compounds presented high potency inhibiting human, murine and rat enzymes, and did not significantly inhibited either cytochromes or hERG. Considering the biological profiling of the new sEH inhibitors, compounds **20** and **22** were selected as the candidates for the *in vivo* studies.

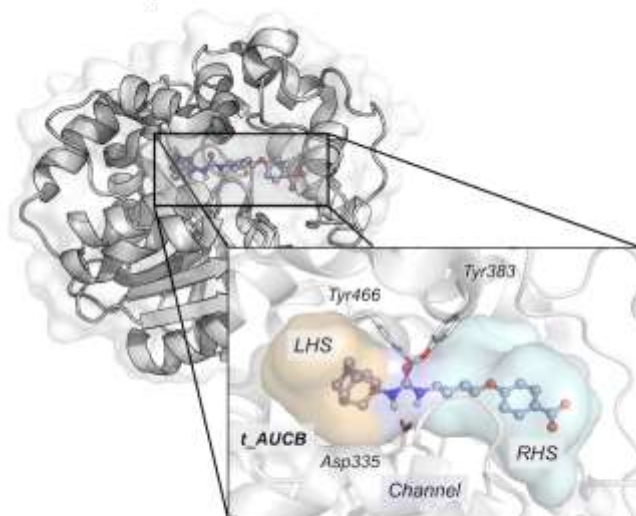
***In silico* study: Molecular basis of benzohomadamantane-derived soluble epoxide hydrolase inhibitors.** The incorporation of an aromatic ring into the adamantane scaffold can potentially impact the orientation and molecular interactions of benzohomodadamantane sEHI as compared to adamantane derivatives. To unravel how

bulky benzohomodamantene ureas are accommodated in the active site of sEH and to understand the molecular basis of their inhibitory mechanism, we performed molecular dynamics (MD) simulations for compounds *t*-AUCB, **20**, **22**, and **23**. The MD simulations revealed that the addition of an aromatic ring into the adamantane scaffold of *t*-AUCB triggers conformational rearrangements in the active site and adjacent regions to stabilize the aromatic ring of the benzohomodamantane scaffold. These interactions together with a network of hydrogen bonds and π -stacking interactions with the urea and benzoic acid moieties are key for retaining the inhibitors in the active site.

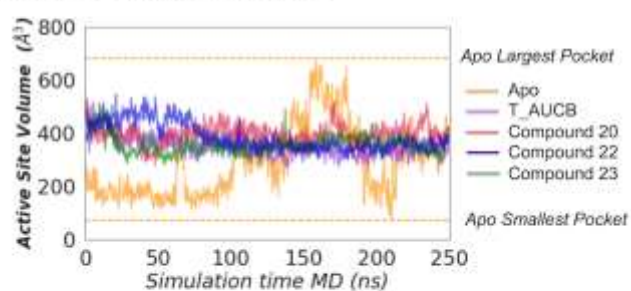
First, we explored the preferred binding mode of the selected sEHI and the flexibility of the active site of the sEH-inhibitor complex. The L-shaped active site pocket of sEH consists of three regions: the left-hand side (LHS) and the right-hand side (RHS) pockets, and a central narrow channel defined by catalytic residues Asp335, Tyr383, and Tyr466 that connects the LHS and RHS hydrophobic cavities (see Figure 5).²⁵ Previously, we showed that the active site of EHs present high plasticity.^{19,26} Available x-ray structures of sEH in complex with adamantyl ureas indicate that the adamantane scaffold can occupy both LHS and RHS pockets.²⁷ In the case of *t*-AUCB (PDB: 5AM3), the inhibitor is orientated with the benzoic acid group occupying the RHS, while adamantane sits in the LHS (see Figure 5). To corroborate that this is also the preferred orientation for benzohomodamantane derivatives, we carried out molecular docking calculations for compounds **20**, **22**, and **23**. All the binding poses featuring the urea moiety interacting with Asp335 oriented the benzohomodamantane scaffold in the LHS and the benzoic acid in the RHS, as observed in *t*-AUCB. The LHS pocket presents enough space to accommodate the bulky benzohomodamantane scaffold (see Figure 5). To evaluate the stability and molecular interactions of the inhibitor in the active site of sEH, we carried out three replicas of 250 ns of MD simulations for *t*-AUCB, **20**, **22**, and **23** starting from

this orientation, i.e. the benzohomadamantane occupying the LHS pocket. All inhibitors show considerable stability and no sign of unbinding or significant reorientations are observed along the MD simulation time. To evaluate the impact of the inhibitors on the active site conformational plasticity, we monitored the changes on the active site volume along the MD simulations (see Figure 5b) using the POcket Volume MEasurer (POVME).²⁸ As observed previously, in the *apo* state, the total volume encompassing LHS, RHS and central channel displays wide fluctuations from 70 to 700 Å³ (average volume 290 ± 133 Å³).¹⁹ When *t*-AUCB, **20**, **22**, and **23** compounds are bound in the active site, an expansion of the active site volume with respect to the average *apo* value is observed, which becomes stable at around 330-400 Å³ (see Figure 5b and 5c). The average volumes determined for the last 150 ns of each MD simulation are 335 ± 33 Å³, 396 ± 37 Å³, 351 ± 25 Å³, and 356 ± 32 Å³ for *t*-AUCB, **20**, **22**, and **23**, respectively. As expected, benzohomadamantane inhibitors show wider active sites than *t*-AUCB, being compound **20**, with a bulkier methyl group, the one with the larger volume. All inhibitors are able to restrict the conformational plasticity of the active site indicating that they are tightly bound.

a) sEH x-ray structure (PDB ID: 5AM3) in complex with *t*-AUCB and active site pocket



b) Active site volume fluctuations



c) Representative active site volume Compound 22

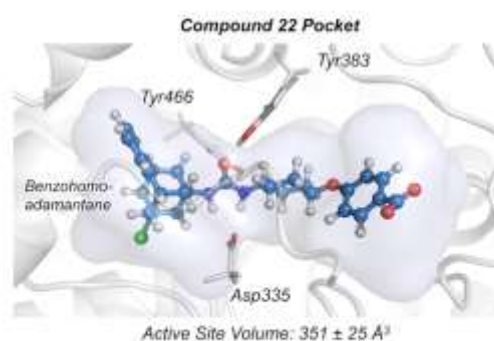


Figure 5. a) Representation of sEH structure (PDB: 5AM3), active site catalytic residues (nucleophilic Asp335, Tyr383, Tyr466), and *t*-AUCB inhibitor. Left-hand side (LHS) pocket is colored in orange, right-hand side (RHS) pocket is colored in cyan, and the central channel in purple. b) Plot of the fluctuations of the active site volume for the apo state (orange line, 290 ± 133 Å³), *t*-AUCB (purple line, 335 ± 33 Å³), compound **20** (red line, 396 ± 37 Å³), compound **22** (blue line, 351 ± 25 Å³), and compound **23** bound (green line, 356 ± 32 Å³) along a representative 250 ns MD simulation trajectory. The average volumes are calculated for the last 150 ns of the MD simulation. c) Representative sEH structure with the active site volume obtained from MD simulations of compound **22**.

To gain a deeper insight into the molecular basis of the inhibitory mechanism of benzohomoadamantane ureas, the non-covalent interactions between the selected inhibitors and the active site residues of sEH were analyzed with NCIPLOT on the most visited MD conformations (see Figures 6 and S1).²⁹ First, we analyzed the interactions established in the RHS pocket and the central channel where all inhibitors share a common scaffold. For *t*-AUCB, **20**, **22**, and **23** compounds, the carboxylate unit of the benzoic acid group is stabilized by two hydrogen bonds with Ser412 and Ser415 that are located at the entrance of the RHS pocket, being the interaction with Ser415 more stable along the MD simulations (see Figure 6b). The aromatic ring of the benzoic acid is further stabilized in the RHS pocket through π - π stacking interactions by the side chains of Trp525 and Phe497. The side chain of Phe497 moves from the solvent to the active site to form a network of stable π - π stacking interactions that includes the benzoic acid group and the aromatic side chains of residues Trp525, Phe497, and catalytic Tyr383. The urea moiety establishes hydrogen bonds with three catalytic residues: Asp335, Tyr383, and Tyr466 located in the central channel of the active site pocket. MD simulations show that the three hydrogen bonds remain significantly stable along the whole simulation time for all inhibitors with no significant differences (see Figure 6c). *t*-AUCB and **20** are able to retain a tighter hydrogen bond (below 3 Å) between the carbonyl of the urea and the OH of Tyr466 than halogenated compounds **22** and **23**. These results indicate that all inhibitors remain stable in the active site pocket forming similar interactions consistent with reported IC₅₀ values. Previously, we have shown that less potent inhibitors displayed fluctuations in the interactions between the urea motif and the catalytic residues shifting the ensemble towards longer distances.¹⁹ All inhibitors share a common scaffold on the RHS of the urea and MD simulations reported a similar behavior in terms of interactions and conformational dynamics in the RHS and central channel regions. The network of

hydrogen bonds and π - π stacking interactions is key to retain the inhibitor in the active site.

Significant differences were observed in the LHS pocket, where the benzohomoadamantane scaffold is placed. For *t*-AUCB, **20**, **22**, and **23** the adamantane unit is mostly stabilized by the side chain of Trp336 through stable CH... π interactions (see Figure 6d). In all cases, additional hydrophobic interactions with the side chains of Met339 and Val498 that wrap the adamantane in the LHS pocket are observed. The incorporation of an aromatic ring into the adamantane scaffold of *t*-AUCB induces a series of conformational rearrangements in the active site that further stabilize both the adamantane and aromatic groups. In particular, the benzohomoadamantane scaffold is reoriented in the beginning of the MD simulations to position the aromatic ring towards the amide group of the side chain of Gln384 for establishing NH... π interactions that retain the benzohomoadamantane group fixed in the LHS pocket (see Figure 6d). This interaction is observed in all MD simulations in the presence of **20**, **22**, and **23** inhibitors and, once formed, remains stable along the whole simulation time. In *t*-AUCB, the amide group of Gln384 forms a network of hydrogen bond interactions with the OH group of Tyr383 and the urea moiety that is partially disrupted in the presence of benzohomoadamantane. Additionally, Phe381 moves away from the LHS pocket to accommodate the aromatic ring of **20**, **22**, and **23** establishing frequent π -stacking interactions. Met468, that in the *t*-AUCB x-ray structure is pointing towards the solvent, moves towards the active site to establish hydrophobic interactions with benzohomoadamantane moiety. Finally, the symmetric adamantyl unit in *t*-AUCB freely rotates inside the LHS pocket, while the asymmetry introduced in the benzohomoadamantane scaffold limits its rotation by establishing strong permanent interactions (see Figure S2). The enthalpic gain of π -stacking and NH... π interactions is

compensated by entropic penalty of the reduced rotation. This limited flexibility can pose some impediments in the binding pathway of benzohomodamante derivatives.

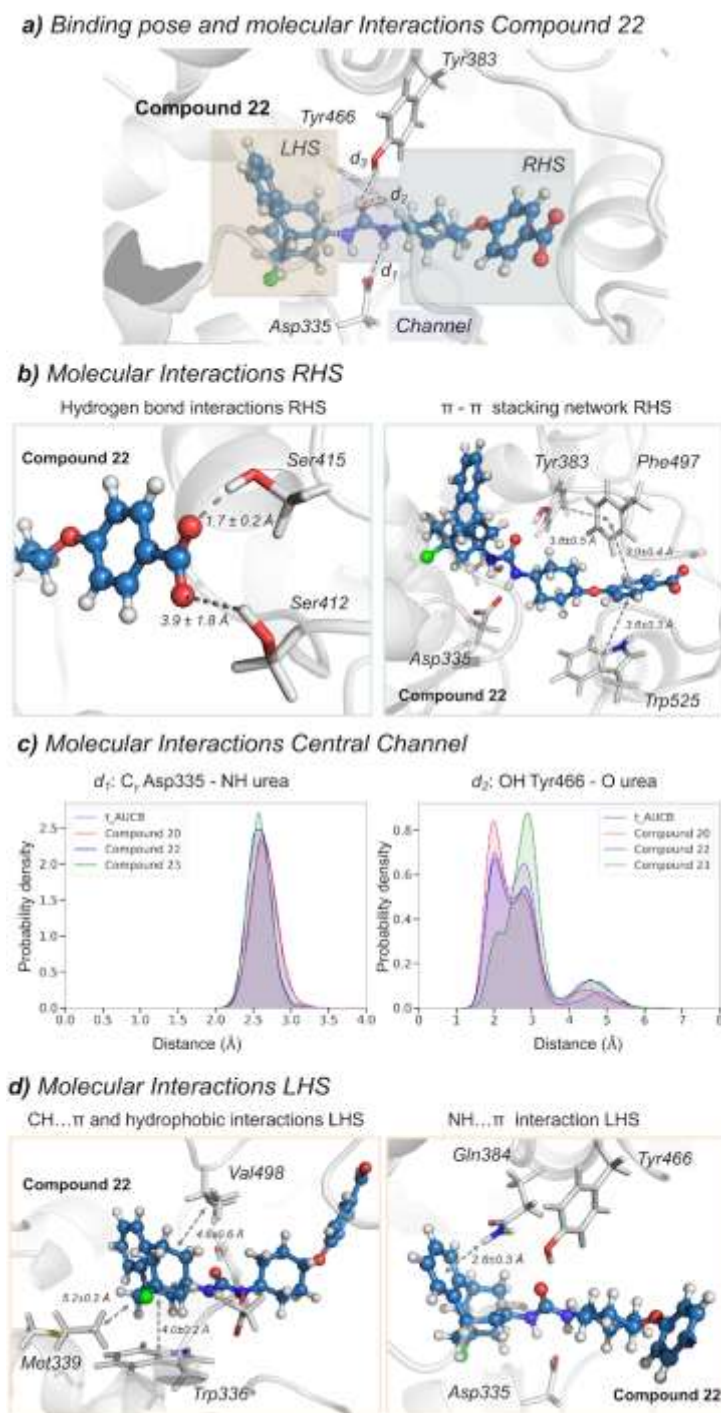


Figure 6. a) Representative structure of **22** bound in the active site of sEH obtained from the most visited conformations along the MD simulations. The benzohomoadamantane moiety occupies the LHS pocket while the benzoic acid group lays in the RHS pocket. The central urea unit establishes hydrogen bonds with Asp335 (d_1), Tyr466 (d_2), and Tyr383 (d_3). b) Most relevant molecular interactions in the RHS. Average distances (in

Å) obtained from the last 150 ns of MD simulations are represented. Hydrogen bonds between the oxygens of the carboxylate group of **22** and the hydrogen of the OH group of Ser412 and Ser415. The π - π stacking average distances are computed between the most proximal carbon atoms of each ring. c) Histogram plots of the distance between the carboxylic group of the catalytic Asp335 and the amide groups of the inhibitor ($d_1(\text{C}\gamma\text{Asp335-NHINH})$) and the distance between the carbonyl group of the urea inhibitor and the OH group of Tyr466 residue ($d_2(\text{OHTyr466-OINH})$) along the MD simulations of *t*-AUCB (purple), **20** (red), **22** (blue) and **23** (green). d) Most relevant molecular interactions in the LHS. Average distances (in Å) obtained from the last 150 ns of MD simulations are represented. CH... π interaction is calculated between the carbon of benzohomoadamantane unit and the most proximal carbon atom of Trp336. The NH... π interaction is monitored between the amide hydrogen of Gln384 and the center of the aromatic ring of the benzohomoadamantane scaffold.

A significant conformational rearrangement is observed when comparing the hydrocarbon-based compounds *t*-AUCB and **20** with the halogenated compounds **22** (see Figure 7) and **23**. The loop (493-500) containing Leu499 is significantly displaced from the reference x-ray structure in the case of **22** and **23**. This rearrangement includes the motion of the bulky Leu499 side chain that leaves the active site when halogenated compounds are present and the approximation of the carbonyl backbone of Val498 towards the benzohomoadamantane moiety (see Figure 7b and 7c). The hypothesis is that the dipole moment generated by halogens F and Cl on the benzohomoadamantane scaffold induces a displacement of the loop to favor stabilization with the carbonyl backbone of Val498. In the case of *t*-AUCB and **20**, Leu499 remains in the active site establishing hydrophobic interactions with the adamantane scaffold (Figure 7b). Similar conformational changes in loops located at the vicinity of the active site have been described in other EH as key for substrate binding.²⁶ The molecular insight gained from MD simulations paves the way towards the rational improvement of benzohomoadamantane scaffolds for enhanced inhibition.

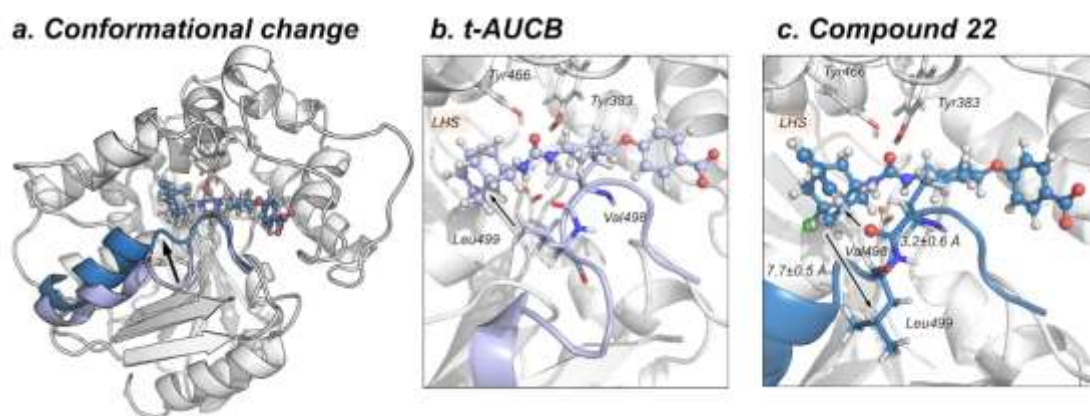


Figure 7. a) Overlay of two representative structures of *t*-AUCB (purple) and **22** (blue) bound in the active site of sEH. The image indicates the motion of the loop (493-500) containing Val498 and Leu499 with a black arrow. The loop is colored in purple for the *t*-AUCB conformation and in blue for the **22** conformation. b) Most visited active site conformation with *t*-AUCB bound, where Leu499 is pointing towards the adamantane moiety. c) Most visited active site conformation with **22** bound, where Leu499 is displaced from the active site and Val498 carbonyl points towards the benzohomodamantane moiety.

Pharmacokinetic studies of selected compounds 20 and 22. The pharmacokinetic characterization of **20** and **22** was performed in male C57BL/6 mice by intraperitoneal administration of 3 mg/kg of each compound. As shown in Table 4, both compounds demonstrated good absorption and elimination characteristics. Notwithstanding, compound **22** presented a better profile than **20** considering its larger half-life (5.2 h), higher C_{max} (3583 ng/mL) and AUC (23328.12 h*ng/mL) and lowest clearance (0.13 L/h/Kg). Considering its superior pharmacokinetic profile and its better potency and solubility (Tables 2 and 4), **22** was selected for conducting the *in vivo* efficacy study in the well-known murine model of cerulein-induced acute pancreatitis (AP).³⁰⁻³²

Cpd	Dose	HL (h)	Tmax (h)	Cmax (ng/mL)	AUClast (h*ng/mL)	AUCINF (h*ng/mL)	Vd (L/Kg)	Cl (L/h/Kg)
20	3 mg/Kg	1.17	0.50	1610	2260.38	2323.36	2.18	1.29
22	3 mg/Kg	5.2	2	3583.33	22543.28	23328.12	0.96	0.13

Table 4: Pharmacokinetic parameters in male C57BL/6 mouse for compounds **20** and **22** after 3 mg/kg IP administration. See experimental section and Tables S2 and S3 and Figures S3 and S4 in the supporting information.

***In vivo* efficacy study.** AP is a potentially life-threatening gastrointestinal disease, and its incidence has been increasing over the last few decades. The onset of the disease is thought to be triggered by intra-acinar cell activation of digestive enzymes that results in interstitial edema, inflammation and acinar cell death that often leads to systemic inflammation response.³⁰⁻³³ The efficacy of the new sEHI **22** at 0.1 and 0.3 mg/kg was assessed in the cerulein-induced AP murine model. The experimental procedure for the *in vivo* efficacy study was followed as described in already published protocols.³⁴ AP was induced by twelve intraperitoneal injections of cerulein (or vehicle in the Blank group) at 1 hour intervals. Fourteen hours after the first injection of cerulein, compound **22** was intraperitoneally administered in one injection and, after 24 h of the first injection of cerulein, mice were anesthetized and sacrificed by cervical dislocation and pancreas were analyzed.

First, the health status of the animals was analyzed by monitoring their body weight. Percentage of body weight change at the end of the study vs body weight at t = 0 h was calculated as a gross indicator of mice general status. After food replacement (with the last cerulein injection), control animals recovered weight, fact that, as expected, was not observed in the cerulein group. In contrast, treated animals with both doses (0.3 and 0.1 mg/kg) of **22** showed an increment in body weight, although only the group treated at 0.3 mg/Kg reached statistical significance ($p < 0.01$ vs Cerulein group) (Figure 8).

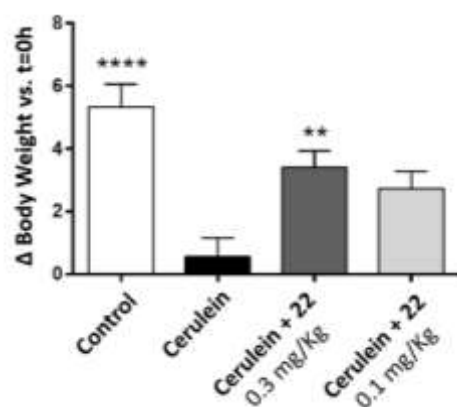


Figure 8. Percentage of body weight change at the end of the study vs $t = 0$ h. Effect of 12 consecutive administrations of cerulein (50 $\mu\text{g}/\text{kg}$, IP) and treatment with **22** (single dose, 0.3 mg/kg or 0.1 mg/kg, IP) on C57BL/6 male mice body weight. Results are expressed as mean \pm SEM ($n = 3-9$). * $p < 0.05$, ** $p < 0.01$, **** $p < 0.0001$ vs Cerulein group (ANOVA-one way).

In addition, we measured compound concentration in plasma and pancreatic tissue at 10 hours post-administration. Taking into account that **22** is a subnanomolar inhibitor of the murine enzyme, we confirmed that the administration of both doses produced enough plasma levels of compound **22** to inhibit the sEH (175 nM for the dosage of 0.3 mg/Kg and 14 nM for the dosage of 0.1 mg/Kg). Moreover, compound concentration in pancreas was also analyzed showing 29.9 ng/g for the dosage of 0.3 mg/kg, confirming that **22** was able to reach the pancreatic tissue. In contrast, no pancreatic levels were detected with the administration of 0.1 mg/kg of **22**.

Finally, histologic analysis of pancreas was assessed in order to determine the severity of the cerulein-induced pancreatitis and the effect produced by treatment with **22**. Pathologic changes were studied on H&E-stained pancreas sections from control, cerulein-treated and cerulein- and **22**-treated mice. As expected, histologic analysis of pancreas showed that cerulein control group presented pancreatic damage representative of AP, including edema, necrosis and infiltration of inflammatory cells. By contrast, treatment with both doses of **22** ameliorated cerulein-induced effects, being the higher dose of 0.3 mg/kg the

one that more efficiently reversed the pancreatic damage, edema and neutrophils infiltration (Figure 9 and Tables S4-S7 in the supporting information).

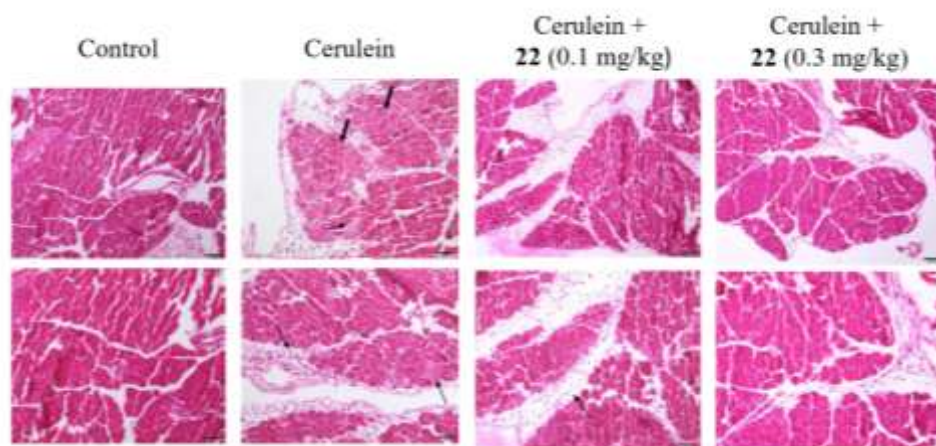


Figure 9. Representative H&E-stained sections of the pancreas from the *in vivo* efficacy study. Arrow indicates inflammatory cells and edema. Bold arrow indicates intracellular vacuole.

3. Conclusions

sEH has been identified as a suitable target for several inflammatory diseases. For this reason, many adamantane-based and aryl-based sEHI have been designed and two selected compounds, AR9281 and EC5026, have reached human clinical trials. In this work we have found that the aromatic and adamantane fragment can be merged leading to the very versatile benzohomoadamantane scaffold. Therefore, three series of compounds replacing the adamantane moiety of AR9281, **7** and *t*-AUCB by this new polycycle have been synthesized and biologically evaluated. The *in vitro* profiling of these sEHI (solubility, cytotoxicity, metabolic stability, CYP450s, *h*LOX-5, *h*COX-2 and *h*ERG inhibition) allowed to select a suitable candidate for an *in vivo* efficacy study in a murine model of AP, for which sEHI showed effectiveness at ameliorating this condition.^{19,34-35} The administration of **22** improved the general health status of cerulein-induced AP mice and significantly reduced pancreatic damage. Hence, the

benzohomoadamantane moiety emerges as a suitable hydrophobic scaffold for the design of novel sEHIs. The molecular insight provided by MD simulations indicated that sEH reshapes the active site pocket to stabilize the aromatic ring of the benzohomoadamantane scaffold. Due to the promising results obtained with compound **22**, more research around benzohomoadamantane-based sEHIs for the treatment of inflammatory and pain related diseases is currently ongoing.

EXPERIMENTAL SECTION

Chemical Synthesis. General methods. Commercially available reagents and solvents were used without further purification unless stated otherwise. Preparative normal phase chromatography was performed on a CombiFlash Rf 150 (Teledyne Isco) with pre-packed RediSep Rf silica gel cartridges. Thin-layer chromatography was performed with aluminum-backed sheets with silica gel 60 F254 (Merck, ref 1.05554), and spots were visualized with UV light and 1% aqueous solution of KMnO_4 . Melting points were determined in open capillary tubes with a MFB 595010M Gallenkamp. 400 MHz ^1H and 100.6 MHz ^{13}C NMR spectra were recorded on a Varian Mercury 400 or on a Bruker 400 Avance III spectrometers. 500 MHz ^1H and 125.7 ^{13}C NMR spectra were recorded on a Varian Inova 500 spectrometer. The chemical shifts are reported in ppm (δ scale) relative to internal tetramethylsilane, and coupling constants are reported in Hertz (Hz). Assignments given for the NMR spectra of selected new compounds have been carried out on the basis of DEPT, COSY $^1\text{H}/^1\text{H}$ (standard procedures), and COSY $^1\text{H}/^{13}\text{C}$ (gHSQC and gHMBC sequences) experiments. IR spectra were run on Perkin-Elmer Spectrum RX I, Perkin-Elmer Spectrum TWO or Nicolet Avatar 320 FT-IR spectrophotometers. Absorption values are expressed as wave-numbers (cm^{-1}); only significant absorption bands are given. High-resolution mass spectrometry (HRMS) analyses were performed with an LC/MSD TOF Agilent Technologies spectrometer. The

elemental analyses were carried out in a Flash 1112 series Thermofinnigan elemental microanalyzer (A5) to determine C, H, N and S. The structure of all new compounds was confirmed by elemental analysis and/or accurate mass measurement, IR, ¹H NMR and ¹³C NMR. The analytical samples of all the new compounds, which were subjected to pharmacological evaluation, possessed purity ≥95% as evidenced by their elemental analyses.

1-(9-methyl-5,6,8,9,10,11-hexahydro-7H-5,9:7,11-dimethanobenzo[9]annulen-7-yl)-3-(4-(trifluoromethyl)phenyl)thiourea, 9. To a solution of 9-methyl-5,6,8,9,10,11-hexahydro-7H-5,9:7,11-dimethanobenzo[9]annulen-7-amine hydrochloride (250 mg, 0.95 mmol) in DCM (2 mL), 1-isothiocyanato-4-(trifluoromethyl)benzene (193 mg, 0.95 mmol) and Et₃N (287 mg, 2.84 mmol) were added. The reaction mixture was stirred at room temperature overnight and then the solvent was evaporated under vacuum. The residue was dissolved in EtOAc (30 mL) and water (20 mL) and phases were separated. The aqueous phase was extracted with further EtOAc (2 x 30 mL). The combined organic phases were dried over anh. Na₂SO₄, filtered and concentrated under vacuum to obtain 369 mg of a yellow solid. The product was washed with Et₂O to obtain thiourea **9** (188 mg, 46% yield) as a white solid, mp 158-159 °C. IR (NaCl disk): 3283, 2911, 2834, 1615, 1532, 1493, 1454, 1422, 1324, 120, 1166, 1124, 1067, 1015, 948, 909, 837, 759, 732, 697, 665 cm⁻¹. ¹H-NMR (400 MHz, CDCl₃) δ: 0.95 (s, 3 H, C9-CH₃), 1.57 [d, *J* = 13.6 Hz, 2 H, 10(13)-H_{ax}], 1.67 (dd, *J* = 13.2 Hz, *J'* = 6.0 Hz, 2 H, 10(13)-H_{eq}), 2.00 (s, 2 H, 8-H), 2.31-2.40 [c.s., 4 H, 6(12)-H₂], 3.12 [broad s, 2 H, 5(11)-H], 6.11 (s, 1 H, C7-NH), 7.05 [m, 2 H, 1(4)-H], 7.09 [m, 2 H, 2(3)-H], 7.28 [d, *J* = 8.2 Hz, 2 H, 2'(6')-H], 7.64 [d, *J* = 8.2 Hz, 2 H, 3'(5')-H], 7.81 (s, 1 H, C1'-NH). ¹³C-NMR (100.5 MHz, CDCl₃) δ: 32.2 (CH₃, C9-CH₃), 33.9 (C, C9), 38.9 [CH₂, C6(12)], 40.9 [CH, C5(11)], 41.1 [CH₂, C10(13)], 47.5 (CH₂, C8), 57.7 (C, C7), 123.7 (q, ¹*J*_{C-F} = 272 Hz, C, CF₃), 123.8 [CH,

C2'(6'), 126.5 [CH, C2(3)], 127.2 [q, $^3J_{C-F} = 3.7$ Hz, CH, C3'(5')], 128.0 [CH, C1(4)], 128.1 (C, $^2J_{C-F} = 33.1$ Hz, CH, C4') 140.1 (C, C1'), 145.8 [C, C4a(11a)], 178.2 (C, CS).

***p*-Tolyl**

(9-methyl-5,6,8,9,10,11-hexahydro-7H-5,9:7,11-

dimethanobenzo[9]annulen-7-yl)carbamate, 11. To a solution of 9-methyl-

5,6,8,9,10,11-hexahydro-7H-5,9:7,11-dimethanobenzo[9]annulen-7-amine

hydrochloride (250 mg, 0.95 mmol) in DCM (2 mL), *p*-tolyl chloroformate (194 mg,

1.14 mmol) and Et₃N (287 mg, 2.84 mmol) were added. The reaction mixture was stirred

at room temperature overnight and then the solvent was evaporated under vacuum. The

residue was dissolved in EtOAc (30 mL) and water (20 mL) and phases were separated.

The aqueous phase was extracted with further EtOAc (2 x 30 mL). The combined organic

phases were dried over anh. Na₂SO₄, filtered and concentrated under vacuum to obtain

300 mg of a yellow gum. Column chromatography (SiO₂, Hexane/Ethyl Acetate

mixture) gave carbamate **11** (46 mg, 14% yield) as a white solid, mp 114-115 °C. IR

(NaCl disk): 3330, 3018, 2944, 2919, 2854, 1744, 1591, 1531, 1502, 1452, 1379, 1362,

1345, 1255, 1214, 1198, 1167, 1137, 1069, 1042, 1014, 987, 948, 900, 825, 757 cm⁻¹. ¹H-

NMR (400 MHz, CDCl₃) δ: 0.94 (s, 3 H, C9-CH₃), 1.56 [d, $J = 13.6$ Hz, 2 H, 10(13)-

H_{ax}], 1.66 [dd, $J = 13.6$ Hz, $J' = 6.0$ Hz, 2 H, 10(13)-H_{eq}], 1.85 (s, 2 H, 8-H), 2.01 [d, $J =$

13.2 Hz, 2 H, 6(12)-H_{ax}], 2.18 [dd, $J = 13.2$ Hz, $J' = 6.8$ Hz, 2 H, 6(12)-H_{eq}], 2.32 (s, 3

H, C4'-CH₃), 3.10 [t, $J = 5.6$ Hz, 2 H, 5(11)-H], 4.92 (s, 1 H, NH), 6.97-7.00 [dm, $J = 8.2$

Hz, 2 H, 2'(6')-H], 7.06 [cs, 2 H, 1(4)-H], 7.09 [c.s., 2 H, 2(3)-H], 7.12-7.14 [broad d, $J =$

8.2 Hz, 2 H, 3'(5')-H]. ¹³C-NMR (100.5 MHz, CDCl₃) δ: 20.8 (CH₃, Ar-CH₃), 32.2

(CH₃, C9-CH₃), 33.7 (C, C9), 39.3 [CH₂, C6(12)], 40.9 [CH, C5(11)], 41.1 [CH₂,

C10(13)], 47.1 (CH₂, C8), 53.8 (C, C7), 121.4 [CH, C2'(6')], 126.3 [CH, C2(3)], 128.0

[CH, C1(4)], 129.6 [CH, C3'(5')], 134.6 (C, C4'), 146.1 [C, C4a(11a)], 148.6 (C, C1'),

152.4 (C, CO).

1-(9-methyl-5,6,8,9,10,11-hexahydro-7H-5,9:7,11-dimethanobenzo[9]annulen-7-yl)-3-(2,3,4-trifluorophenyl)urea, 13. To a solution of 9-methyl-5,6,8,9,10,11-hexahydro-7H-5,9:7,11-dimethanobenzo[9]annulen-7-amine hydrochloride (193 mg, 0.73 mmol) in anh. DCM (6.5 mL) were added 2,3,4-trifluorophenyl isocyanate (105 mg, 0.61 mmol) and triethylamine (246 mg, 2.43 mmol) under nitrogen atmosphere. The reaction mixture was stirred at room temperature overnight and the solvent was evaporated under vacuum. Column chromatography (SiO₂, hexane/EtOAc mixture) of the crude and concentration under vacuum of the appropriate fractions gave urea **13** (38 mg, 13% yield) as a white solid, mp 206-207 °C. IR (ATR) ν : 3331, 2903, 2839, 1654, 1556, 1510, 1473, 1361, 1344, 1290, 1237, 1174, 1101, 1038, 1019, 1004, 800, 756, 690, 669, 625 cm⁻¹. ¹H-NMR (500 MHz, CD₃OD) δ : 0.94 (s, 3 H, C9-CH₃), 1.50 [d, J = 13.5 Hz, 2 H, 10(13)-H_{ax}], 1.69 [m, 2 H, 10(13)-H_{eq}], 1.77 (s, 2 H, 8-H), 2.10 [m, 2 H, 6(12)-H_{eq}], 2.15 [d, J = 13 Hz, 2 H, 6(12)-H_{ax}], 3.08 [tt, J = 6 Hz, J' = 1.5 Hz, 2 H, 5(11)-H], 6.98 (m, 1 H, 5'-H), 7.04 [broad s, 4 H, 1(4)-H and 2(3)-H], 7.66 (m, 1 H, 6'-H). ¹³C-NMR (125.7 MHz, CD₃OD) δ : 32.9 (CH₃, C9-CH₃), 34.6 (C, C9), 40.6 [CH₂, C6(12)], 42.5 [CH, C5(11)], 42.5 [CH₂, C10(13)], 49.0 (CH₂, C8), 54.5 (C, C7), 112.2 (CH, dd, ² J_{C-F} = 17.8 Hz, ³ J_{C-F} = 3.9 Hz, C5'), 116.6 (CH, C6'), 127.0 (C, dd, ² J_{C-F} = 8.0 Hz, ³ J_{C-F} = 2.4 Hz Ar-C1'), 127.4 [CH, C2(3)], 129.0 [CH, C1(4)], 141.0 (C, dt, ¹ J_{C-F} = 247.8 Hz, ² J_{C-F} = 14.9 Hz, Ar-C3'), 143.6 (C, dd, ¹ J_{C-F} = 245.7 Hz, ² J_{C-F} = 12.8 Hz, Ar-C4'), 147.3 (C, dd, ¹ J_{C-F} = 242.6 Hz, ² J_{C-F} = 10.3 Hz, Ar-C2'), 147.6 [C, C4a(C11a)], 156.1 (C, CO). MS (DIP), m/z (%); significant ions: 400 (M⁺, <1), 253 (19), 228 (14), 211 [(C₁₆H₁₉)⁺, 16], 172 (23), 155 (54), 149 (56), 148 (100), 147 (52), 143 (22), 141 (20), 129 (21), 128 (18), 115(16).

1-(5-methyl-1,5,6,7-hexahydro-1,5:3,7-dimethanobenzo[*e*]oxonin-3(2H)-yl)-3-(2,3,4-trifluorophenyl)urea, 14. To a solution of 5-methyl-1,5,6,7-tetrahydro-1,5:3,7-dimethanobenzo[*e*]oxonin-3(2H)-amine hydrochloride (250 mg, 0.94 mmol) in anh.

DCM (8.5 mL) were added 2,3,4-trifluorophenyl isocyanate (135 mg, 0.78 mmol) and triethylamine (316 mg, 3.13 mmol) under nitrogen atmosphere. The reaction mixture was stirred at room temperature overnight and the solvent was evaporated under vacuo to furnish pure urea **14** as a white solid (205 mg, 54% yield), mp 257-259 °C. IR (ATR) ν : 3295, 3241, 3118, 2916, 2173, 1693, 1620, 1564, 1510, 1493, 1468, 1462, 1356, 1345, 1320, 1302, 1286, 1273, 1254, 1229, 1210, 1181, 1167, 1111, 1091, 1074, 1049, 1035, 1008, 999, 958, 906, 820, 812, 763, 646 cm^{-1} . $^1\text{H-NMR}$ (400 MHz, DMSO- d_6) δ : 1.18 (s, 3 H, C5- CH_3), 1.56 [d, $J = 13.6$ Hz, 2 H, 6(13)- H_b], 1.84 [m, 2 H, 6(13)- H_a], 1.97 [d, $J = 13.2$ Hz, 2 H, 2(12)- H_b], 2.20 [m, 2 H, 2(12)- H_a], 3.16 [t, $J = 5.5$ Hz, 2 H, 1(7)-H], 4.06 (s, 1 H, C3-NH), 7.14 (complex signal, 5 H, 8(11)-H, 9(10)-H, 5'-H), 7.84 (m, 1 H, 6'-H), 8.52 (broad s, 1 H, C1'-NH). $^{13}\text{C-NMR}$ (100.6 MHz, DMSO- d_6) δ : 31.1 (CH_3 , C5- CH_3), 37.4 [CH_2 , C2(12)], 38.1 [CH_2 , C6(13)], 38.2 [CH , C1(7)], 73.4 (C, C5), 82.7 (C, C3), 111.6 (CH , dd, $^2J_{\text{C-F}} = 17.2$ Hz, $^3J_{\text{C-F}} = 3.5$ Hz, C5'), 114.3 (CH , broad s, C6'), 126.0 (C, dd, $^2J_{\text{C-F}} = 7.8$ Hz, $^3J_{\text{C-F}} = 3.0$ Hz, C1'), 126.5 [CH , C9(10)], 128.2 [CH , C8(11)], 139.0 (C, dd, $^1J_{\text{C-F}} = 246$ Hz, $^2J_{\text{C-F}} = 15$ Hz, C3'), 141.0 (C, dd, $^1J_{\text{C-F}} = 248$ Hz, $^2J_{\text{C-F}} = 12$ Hz, C4'), 144.7 (C, dd, $^1J_{\text{C-F}} = 241$ Hz, $^2J_{\text{C-F}} = 11$ Hz, C2'), 145.5 [C, C7a(C11a)], 152.3 (C, CO). MS (DIP), m/z (%); significant ions: 402 (M^+ , 48), 171 (13), 170 (34), 169 (21), 157 (20), 156 (18), 155 (53), 154 (14), 153 (11), 148 (18), 147 [$(\text{C}_6\text{H}_4\text{F}_3\text{N})^+$, 100], 146 (53), 145 (15), 143 (25), 142 (21), 141 (23), 131 (12), 130 (15), 129 (65), 128 (46), 127 (22), 116 (12), 115 (55), 91 (17), 84 (19), 83 (28), 71 (15), 70 (16), 69 (21). HRMS-ESI $^+$ m/z [$\text{M}+\text{H}$] $^+$ calcd for [$\text{C}_{22}\text{H}_{21}\text{F}_3\text{N}_2\text{O}_2+\text{H}$] $^+$: 403.1633, found: 403.1631.

1-(1-acetylpiperidin-4-yl)-3-(9-methyl-5,6,8,9,10,11-hexahydro-7H-5,9:7,11-dimethanobenzo[9]annulen-7-yl)urea, 16. To a solution of 9-methyl-5,6,8,9,10,11-hexahydro-7H-5,9:7,11-dimethanobenzo[9]annulen-7-amine hydrochloride (180 mg, 0.68 mmol) in DCM (3 mL) and saturated aqueous NaHCO_3 solution (2 mL), triphosgene

(102 mg, 0.34 mmol) was added. The biphasic mixture was stirred at room temperature for 30 minutes and then the two phases were separated, and the organic layer was washed with brine (5 mL), dried over anh. Na₂SO₄, filtered and evaporated under vacuum to obtain 1-2 mL of a solution of the isocyanate in DCM. To this solution were added 1-(4-aminopiperidin-1-yl)ethan-1-one hydrochloride (122 mg, 0.68 mmol) and Et₃N (138 mg, 1.36 mmol). The mixture was stirred overnight at room temperature, diluted with further DCM (10 mL) and washed with 2N NaOH solution (2 x 10 mL). Organics were dried over anh. Na₂SO₄, filtered and concentrated under vacuum to obtain a yellow oil (232 mg). Column chromatography (SiO₂, DCM/methanol mixtures) gave urea **16** as a white solid (143 mg, 53% yield). The analytical sample was obtained by crystallization from hot EtOAc (113 mg), mp 206-207 °C. IR (NaCl disk): 3359, 3065, 3016, 2938, 2906, 2860, 1644, 1620, 1555, 1493, 1452, 1360, 1344, 1319, 1267, 1228, 1212, 1136, 1090, 1049 cm⁻¹. ¹H-NMR (400 MHz, CDCl₃) δ: 0.90 (s, 3 H, C9-CH₃), 1.13 (dq, *J* = 12.0 Hz, *J*' = 4.0 Hz, 1 H, 3'-H_{ax} or 5'-H_{ax}), 1.20 (dq, *J* = 12.0 Hz, *J*' = 4.0 Hz, 1 H, 5'-H_{ax} or 3'-H_{ax}), 1.52 [d, *J* = 13.2 Hz, 2 H, 10(13)-H_{ax}], 1.62 [dd, *J* = 6 Hz, *J*' = 12.8 Hz, 2 H, 10(13)-H_{eq}], 1.80 (s, 2 H, 8-H), 1.85 (m, 1 H, 3'-H_{eq} or 5'-H_{eq}), 1.93 [d, *J* = 12.8 Hz, 2 H, 6(12)-H_{ax}], 2.01 (m, 1 H, 5'-H_{eq} or 3'-H_{eq}), 2.06 (s, 3 H, COCH₃), 2.12 [dd, *J* = 12.8 Hz, *J*' = 6.0 Hz, 2 H, 6(12)-H_{eq}], 2.70 (m, 1 H, 6'-H_{ax} or 2'-H_{ax}), 3.02-3.14 [complex signal, 3 H, 5(11)-H, 2'-H_{ax} or 6'-H_{ax}], 3.68-3.78 (complex signal, 2 H, 4'-H, 2'-H_{eq} or 6'-H_{eq}), 4.41 (dm, *J* = 13.6 Hz, 1 H, 6'-H_{eq} or 2'-H_{eq}), 4.62-4.68 (complex signal, 2 H, C7-NH and C4'-NH), 7.02 [m, 2 H, 1(4)-H], 7.06 [m, 2 H, 2(3)-H]. ¹³C-NMR (100.5 MHz, CDCl₃) δ: 21.4 (CH₃, COCH₃), 32.3 (CH₃, C9-CH₃), 32.4 (CH₂, C3' or C5'), 33.6 (CH₂, C5' or C3'), 33.7 (C, C9), 39.9 [CH₂, C6(12)], 40.7 (CH₂, C6' or C2'), 41.1 [CH, C5(11)], 41.2 [CH₂, C10(13)], 45.4 (CH₂, C2' or C6'), 46.7 (CH, C4'), 48.0 (CH₂, C8), 53.4 (C, C7),

126.2 [CH, C2(3)], 128.0 [CH, C1(4)], 146.3 [C, C4a(11a)], 156.4 (C, NHCONH), 169.0 (C, COCH₃).

1-(1-acetylpiperidin-4-yl)-3-(5-methyl-1,5,6,7-tetrahydro-1,5:3,7-

dimethanobenzo[e]oxonin-3(2H)-yl)urea, 17. To a solution of 5-methyl-1,5,6,7-tetrahydro-1,5:3,7-dimethanobenzo[e]oxonin-3(2H)-amine hydrochloride (180 mg, 0.68 mmol) in DCM (3 mL) and saturated aqueous NaHCO₃ solution (2 mL), triphosgene (102 mg, 0.34 mmol) was added. The biphasic mixture was stirred at room temperature for 30 minutes and then the two phases were separated and the organic one was washed with brine (5 mL), dried over anh. Na₂SO₄, filtered and evaporated under vacuum to obtain 1-2 mL of a solution of isocyanate in DCM. To this solution were added 1-(4-aminopiperidin-1-yl)ethan-1-one hydrochloride (122 mg, 0.68 mmol) and Et₃N (139 mg, 1.37 mmol). The mixture was stirred overnight at room temperature, diluted with further DCM (10 mL) and washed with 2N NaOH solution (2 x 10 mL). The organic layer was dried over anh. Na₂SO₄, filtered and concentrated under vacuum to obtain a yellow residue (206 mg). Column chromatography (SiO₂, DCM/methanol mixtures) furnished urea **17** as a white solid (135 mg, 49% yield). The analytical sample was obtained by crystallization from hot EtOAc (112 mg), mp 208-209 °C. IR (NaCl disk): 3357, 3054, 3012, 2969, 2926, 2853, 1646, 1611, 1546, 1492, 1450, 1358, 1324, 1268, 1222, 1156, 1101, 1088, 1035, 1212, 991, 947, 918, 900, 866, 829, 760, 733, 699 cm⁻¹. ¹H-NMR (400 MHz, CDCl₃) δ: 1.26 (s, 3H, C9-CH₃), 1.32-1.42 (complex signal, 2 H, 3'-H_{ax}, 5'-H_{ax}), 1.66-1.67 [complex signal, 4 H, 2-H_{ax}, 12-H_{ax}, 6(13)-H_{ax}], 1.85-1.91 [m, 2 H, 6(13)-H_{eq}], 1.97 (m, 1 H, 3'-H_{eq} or 5'-H_{eq}), 2.08 (m, 1 H, 5'-H_{eq} or 3'-H_{eq}), 2.10 (s, 3 H, COCH₃), 2.24-2.34 (complex signal, 2 H, 2-H_{eq}, 12-H_{eq}), 2.95 (ddd, *J* = 3.2 Hz, *J*' = 10.8 Hz, 1 H, 2'-H_{ax} or 6'-H_{ax}), 3.16-3.26 [complex signal, 3 H, 6'-H_{ax} or 2'-H_{ax}, 1(7)-H], 3.72 (m, 1 H, 2'-H_{eq} or 6'-H_{eq}), 3.89 (m, 1 H, 4'-H), 4.34 (m, 1 H, 2'-H_{eq} or 6'-H_{eq}), 4.78 (s, 1 H,

C3-NH), 6.34 (d, $J = 7.5$ Hz, 1 H, 4'-NH), 7.09-7.15 (complex signal, 4 H, 8-H, 9-H, 10-H, 11-H). ^{13}C -NMR (100.5 MHz, CDCl_3) δ : 21.4 (CH_3 , COCH_3), 31.5 (CH_3 , C5- $\underline{\text{C}}\text{H}_3$), 32.1 (CH_2 , C3' or 5'), 33.2 (CH_2 , C5' or C3'), 37.4 (CH_2 , C2 or C12), 37.6 (CH_2 , C12 or C2), 38.4 [CH_2 , C6 (13)], 38.8 [CH , C1(7)], 40.2 (CH_2 , C6' or C2'), 45.0 (CH_2 , C2' or C6'), 46.5 (CH , C4'), 74.6 (C, C5), 82.6 (C, C3), 126.94 (CH , C9 or C10), 126.96 (CH , C10 or C9), 128.38 (CH , C8 or C11), 128.43 (CH , C11 or C8), 144.70 (C, C7a or C11a), 144.75 (C, C11a or C7a), 156.6 (CO, NHCONH), 168.9 (C, $\underline{\text{C}}\text{OCH}_3$).

1-(1-acetylpiperidin-4-yl)-3-(1,5,6,7-tetrahydro-1,5:3,7-dimethanobenzo[e]oxonin-3(2H)-yl)urea, 18. To a solution of 1,5,6,7-tetrahydro-1,5:3,7-dimethanobenzo[e]oxonin-3(2H)-amine hydrochloride (300 mg, 1.19 mmol) in DCM (6.5 mL) and saturated aqueous NaHCO_3 solution (6.3 mL), triphosgene (131 mg, 0.44 mmol) was added. The biphasic mixture was stirred at room temperature for 30 minutes and then the two phases were separated and the organic one was washed with brine (5 mL), dried over anhydrous Na_2SO_4 , filtered and evaporated under vacuum to obtain 1-2 mL of a solution of isocyanate in DCM. To this solution was added 1-(4-aminopiperidin-1-yl)ethan-1-one (203 mg, 1.43 mmol). The mixture was stirred overnight at room temperature and the solvent was evaporated under vacuum. Column chromatography (SiO_2 , DCM/Methanol mixtures) gave urea **18** as a white solid (90 mg, 20% yield). The analytical sample was obtained by a crystallization from hot Ethyl Acetate/ mixture, mp 120-121 °C. IR (ATR): 3340, 2921, 1856, 1730, 1632, 1552, 1493, 1453, 1356, 1327, 1299, 1274, 1244, 1204, 1122, 1088, 1047, 1025, 993, 947, 970, 907, 801, 760, 729, 643 cm^{-1} . ^1H -NMR (400 MHz, CDCl_3) δ : 1.33-1.45 (complex signal, 2 H, 3'- H_{ax} , 5'- H_{ax}), 1.68-1.84 [complex signal, 4 H, 2(12)- H_{ax} , 6(13)- H_{ax}], 1.97 (m, 1 H, 3'- H_{eq} or 5'- H_{eq}), 2.05-2.13 (complex signal, 4 H, 5'- H_{eq} or 3'- H_{eq} , COCH_3), 2.21 [m, 2 H, 6(13)- H_{eq}], 2.40 [m, 2 H, 2(12)- H_{eq}], 2.87 (ddd, $J = 11.2$ Hz, $J' = 3.2$ Hz, 1 H, 2'- H_{ax} or 6' H_{ax}), 3.13-

3.25 [complex signal, 3 H, 6'-H_{ax} or 2'-H_{ax}, 1(7)-H], 3.74 (dm, $J = 13.6$ Hz, 1 H, 6'-H_{eq} or 2'-H_{eq}), 3.90 (m, 1 H, 4'-H), 4.40 (dm, $J = 13.2$ Hz, 2'-H_{eq} or 6'-H_{eq}), 4.52 (t, $J = 5.6$ Hz, 1 H, 5-H), 4.78 (s, 1 H, 3-NH), 6.14 (d, $J = 7.6$ Hz, 1 H, 4'-NH), 7.08-7.16 [complex signal, 4 H, 8-H, 9-H, 10-H, 11-H]. ¹³C-NMR (100.5 MHz, CDCl₃) δ : 21.4 (CH₃, COCH₃), 32.2 (CH₂, C3' or C5'), 32.5 [CH₂, C6(13)], 33.2 (CH₂, C5' or C3'), 38.0 (CH₂, C2 or C12), 38.3 (CH₂, C12 or C2), 38.65 (CH, C7 or C1), 38.69 (CH, C1 or C7), 40.4 (CH₂, C2' or C6'), 45.2 (CH₂, C6' or C2'), 46.7 (CH, C4'), 71.7 (CH, C5), 80.9 (C, C3), 126.91 (CH, C9 or C10), 126.93 (CH, C10 or C9), 128.47 (CH, C8 or C11), 128.52 (CH, C11 or C8), 145.0 (C, C7a or C11a), 145.1 (C11a or C7a), 156.5 (CO, NHCONH), 168.9 (CO, COCH₃). HRMS: Calcd for [C₂₅H₃₁ClFN₃O₂+H]⁺: 460.2162; Found: 460.2165.

4-(((1*r*,4*r*)-4-(3-(9-methyl-5,6,8,9,10,11-hexahydro-7*H*-5,9:7,11-

dimethanobenzo[9]annulen-7-yl)ureido)cyclohexyl)oxy]benzoic acid, 20. To a solution of 9-methyl-5,6,8,9,10,11-hexahydro-7*H*-5,9:7,11-dimethanobenzo[9]annulen-7-amine hydrochloride (200 mg, 0.76 mmol) in DCM (3.5 mL) and saturated aqueous NaHCO₃ solution (2.2 mL) was added triphosgene (113 mg, 0.38 mmol). The biphasic mixture was stirred at room temperature for 30 minutes and then the two phases were separated, and the organic layer was washed with brine (5 mL), dried over anh. Na₂SO₄, filtered and evaporated under vacuum to obtain 1-2 mL of a solution of isocyanate in DCM. To this solution were added 4-(((1*r*,4*r*)-4-aminocyclohexyl)oxy]benzoic acid hydrochloride (206 mg, 0.76 mg), Et₃N (153 mg, 1.51 mmol) and DMF (5 mL). The mixture was stirred overnight at room temperature. The resulting suspension was evaporated, and the residue was suspended in DCM (20 mL) and washed with 2N HCl solution (2 x 10 mL). The resulting organic suspension was filtered, and the filtrate was dried over anh. Na₂SO₄, filtered and concentrated under vacuum to give a white gum. Crystallization from hot EtOAc provided benzoic acid **20** as a white solid (55 mg, 16%

yield), mp 182-183°C. IR (NaCl disk): 3335, 2921, 2855, 1692, 1681, 1642, 1632, 1602, 1564, 1537, 1504, 1494, 1469, 1453, 1419, 1360, 1307, 1248, 1163, 1122, 1096, 1969 cm^{-1} . $^1\text{H-NMR}$ (400 MHz, MeOD) δ : 0.91 (s, 3 H, C9- CH_3), 1.31 [m, 2 H, 3'(5')- H_{ax}], 1.47 [broad d, $J = 13.2$ Hz, 2 H, 10''(13'')- H_{ax}], 1.53 [m, 2 H, 2'(6')- H_{ax}], 1.66 [dd, $J = 12.8$ Hz, $J' = 6.4$ Hz, 2 H, 10''(13'')- H_{eq}], 1.70 (s, 2 H, 8''-H), 1.96 [m, 2 H, 3'(5')- H_{eq}], 2.00-2.11 [complex signal, 6 H, 2'(6')- H_{eq} , 6''(12'')- H_2], 3.05 [t, $J = 5.6$ Hz, 2 H, 5''(11'')-H], 3.48 (m, 1 H, 4'-H), 4.38 (m, 1 H, 1'-H), 6.95 [m, 2 H, 3(5)-H], 7.02-7.03 [complex signal, 4 H, 1''(2'')-H, 3''(4'')-H], 7.93 [m, 2 H, 2(6)-H]. $^{13}\text{C-NMR}$ (100.5 MHz, MeOD) δ : 31.2 [CH_2 , C2'(6')], 31.7 [CH_2 , C3'(5')], 32.9 (CH_3 , C9''- CH_3), 34.5 (C, C9''), 41.0 [CH_2 , C6''(12'')], 42.6 [CH, C5''(11'')], 42.6 [CH_2 , C10''(13'') or CH, C5''(11'')], 48.7 (CH, C4'), 49.3 (CH_2 , C8''), 54.1 (C, C7''), 76.0 (CH, C1'), 116.1 [CH, C3(5)], 123.8 (C, C1), 127.3 [CH, C2''(3'')], 128.9 [CH, C1''(4'')], 132.9 [CH, C2(6)], 147.7 [C, C4a''(11a'')], 159.5 (C, NHCONH), 163.3 (C, C4), 169.8 (C, CO_2H).

4-(((1*r*,4*r*)-4-(3-(5-methyl-1,5,6,7-tetrahydro-1,5:3,7-dimethanobenzo[*e*]oxonin-3(2*H*)-yl)ureido)cyclohexyl)oxy]benzoic acid, 21. To a solution of 5-methyl-1,5,6,7-tetrahydro-1,5:3,7-dimethanobenzo[*e*]oxonin-3(2*H*)-amine hydrochloride (200 mg, 0.75 mmol) in DCM (3.5 mL) and saturated aqueous NaHCO_3 solution (2.2 mL) was added triphosgene (113 mg, 0.38 mmol). The biphasic mixture was stirred at room temperature for 30 minutes and then the two phases were separated, and the organic layer was washed with brine (5 mL), dried over anhydrous Na_2SO_4 , filtered and evaporated under vacuum to obtain 1-2 mL of a solution of isocyanate in DCM. To this solution were added 4-(((1*r*,4*r*)-4-aminocyclohexyl)oxy]benzoic acid hydrochloride (206 mg, 0.76 mg) and Et_3N (153 mg, 1.52 mmol) and DMF (5 mL). The mixture was stirred overnight at room temperature. The resulting suspension was evaporated to obtain a white solid, which was suspended in DCM (20 mL) and washed with 2N HCl solution (2 x 10 mL). The resulting

organic suspension was filtered to afford benzoic acid **21** as white solid (200 mg, 54% yield), mp 220-222 °C. IR (NaCl disk): 3352, 2626, 1678, 1601, 1558, 1506, 1454, 1373, 1343, 1312, 1288, 1247, 1221, 1161, 1104, 1029, 997, 953, 776 cm⁻¹. ¹H-NMR (400 MHz, DMSO) δ: 1.14 (s, 3 H, C5-CH₃), 1.30 [q, *J* = 11.6 Hz, 2 H, 3'(5')-H_{ax}], 1.41-1.54 (complex signal, 4 H, 2'(6')-H_{ax}, 6''(13'')-H_{ax}), 1.76-1.87 [complex signal, 6 H, 3'(5')-H_{eq}, 2''(12'')-H_{ax}, 6''(13'')-H_{eq}], 2.01 [d, *J* = 9.2 Hz, 2 H, 2'(6')-H_{eq}], 2.19 [dd, *J* = 6 Hz, *J'* = 12.8 Hz, 2 H, 2''(12'')-H_{eq}], 3.12 [t, *J* = 6.0 Hz, 1''(7'')-H], 3.41 (m, 1 H, 4'-H), 4.45 (m, 1 H, 1'-H), 5.97 (d, *J* = 7.6 Hz, 1 H, 4'-NH), 6.11 (s, 1 H, 3''-NH), 7.01 [d, *J* = 8.4 Hz, 2 H, 3(5)-H], 7.08-7.14 [complex signal, 4 H, 8''(11'')-H, 9''(10'')-H], 7.85 [d, *J* = 8.4 Hz, 2 H, 2(6)-H], 12.55 (broad s, 1 H, COOH). ¹³C-NMR (100.5 MHz, DMSO) δ: 29.5 [CH₂, C2'(6')], 30.1 [CH₂, C3'(5')], 31.2 (CH₃, C5-CH₃), 37.5 [CH₂, C2''(12'')], 38.3 [2 signals, CH₂, C6''(13''), and CH, C1''(7'')], 46.6 (CH, C4'), 73.0 (C, C5''), 74.2 (CH, C1'), 82.2 (C, C3''), 115.1 [CH, C3(5)], 122.6 (C, C1), 126.4 [CH, C9''(10'')], 128.1 [CH, C8''(11'')], 131.4 [CH, C2(6)], 145.6 (C, C7a''(11a'')), 155.8 (C, NHCONH), 161.1 (C, C4), 167.0 (C, CO₂H). HRMS calcd for [C₂₉H₃₅N₂O₅+H]⁺: 491.254 Found: 491.254.

4-(((1*r*,4*r*)-4-(3-(9-chloro-5,6,8,9,10,11-hexahydro-7*H*-5,9:7,11-

dimethanobenzo[9]annulen-7-yl)ureido)cyclohexyl)oxy]benzoic acid, 22. To a solution of 9-chloro-5,6,8,9,10,11-hexahydro-7*H*-5,9:7,11-dimethanobenzo[9]annulen-7-amine hydrochloride (180 mg, 0.63 mmol) in DCM (3 mL) and saturated aqueous NaHCO₃ solution (2 mL), triphosgene (69 mg, 0.23 mmol) was added. The biphasic mixture was stirred at room temperature for 30 minutes and then the two phases were separated and the organic one was washed with brine (3 mL), dried over anh. Na₂SO₄, filtered and evaporated under vacuum to obtain 1-2 mL of a solution of isocyanate in DCM. To this solution were added DMF (4 mL), 4-(((1*r*,4*r*)-4-

aminocyclohexyl)oxy)benzoic acid hydrochloride (171 mg, 0.63 mmol) and Et₃N (127 mg, 1.26 mmol). The mixture was stirred overnight at room temperature and the solvent was then evaporated. The residue was dissolved in DCM (5 mL) and washed with 2N HCl (3 mL). The organic phase was dried over anh. Na₂SO₄, filtered and evaporated under vacuum to obtain benzoic acid **22** (217 mg, 67% yield) as a yellow residue. The analytical sample was obtained by a crystallization from hot Ethyl Acetate/Pentane mixtures, mp 201-202 °C. IR (ATR): 3355, 3299, 2932, 2856, 1697, 1682, 1631, 1605, 1555, 1498, 1469, 1452, 1428, 1406, 1373, 1357, 1322, 1301, 1253, 1163, 1100, 1077, 1041, 1027, 1013, 977, 946, 905, 844, 804, 772, 753, 695, 643, 634, 608 cm⁻¹. ¹H-NMR (400 MHz, MeOD) δ: 1.32 [m, 2 H, 3'(5')-H_{ax}], 1.54 [m, 2 H, 2'(6')-H_{ax}], 1.93-2.02 [complex signal, 4 H, 3'(5')-H_{eq}, 6''(12'')-H_{ax}], 2.03-2.15 [complex signal, 4 H, 2'(6')-H_{eq}, 10''(13'')-H_{ax}], 2.15-2.24 [m, 2 H, 6''(12'')-H_{eq}], 2.35-2.41 [m, 2 H, 10''(13'')-H_{eq}], 2.43 (s, 2 H, 8''-H), 3.17 [t, *J* = 6.0 Hz, 2 H, 5''(11'')-H], 3.49 (m, 1 H, 4'-H), 4.37 (m, 1 H, 1'-H), 6.95 [d, *J* = 8.6 Hz, 2 H, 3(5)-H], 7.04-7.12 [complex signal, 4 H, 1''(4'')-H, 2''(3'')-H], 7.94 [d, *J* = 8.6 Hz, 2 H, 2(6)-H]. ¹³C-NMR (100.5 MHz, MeOD) δ: 31.1 [CH₂, C2'(6')], 31.6 [CH₂, C3'(5')], 40.0 [CH₂, C6''(12'')], 42.7 [CH, C5''(11'')], 46.0 [CH₂, C10''(13'')], 48.7 (CH, C4''), 52.1 (CH, C8''), 56.3 (C, C7''), 70.5 (C, C9''), 76.0 (CH, C1'), 116.1 [CH, C5(3)], 123.9 (C, C1), 127.9 [CH, C2''(3'')], 129.1 [CH, C1''(4'')], 132.9 [CH, C2(6)], 146.3 [C, C4a''(11a'')], 159.2 (C, NHCONH), 163.2 (C, C4), the signal from CO₂H was not observed. HRMS: Calcd for [C₂₉H₃₃ClN₂O₄-H]⁻: 507.2056; Found: 507.2057.

4-(((1*r*,4*r*)-4-(3-(9-fluoro-5,6,8,9,10,11-hexahydro-7*H*-5,9:7,11-dimethanobenzo[9]annulen-7-yl)ureido)cyclohexyl)oxy)benzoic acid, **23.** To a solution of 9-fluoro-5,6,8,9,10,11-hexahydro-7*H*-5,9:7,11-dimethanobenzo[9]annulen-7-amine hydrochloride (180 mg, 0.67 mmol) in DCM (3 mL) and saturated aqueous

NaHCO₃ solution (2 mL), triphosgene (74 mg, 0.25 mmol) was added. The biphasic mixture was stirred at room temperature for 30 minutes and then the two phases were separated and the organic one was washed with brine (3 mL), dried over anh. Na₂SO₄, filtered and evaporated under vacuum to obtain 1-2 mL of a solution of isocyanate in DCM. To this solution were added DMF (4 mL), 4-(((1*r*,4*r*)-4-aminocyclohexyl)oxy)benzoic acid hydrochloride (182 mg, 0.67 mmol) and Et₃N (136 mg, 1.34 mmol). The mixture was stirred overnight at room temperature and the solvent was then evaporated. The residue was dissolved in DCM (5 mL) and washed with 2N HCl (3 mL). The organic phase was dried over anh. Na₂SO₄, filtered and evaporated under vacuum to obtain benzoic acid **23** (240 mg, 72% yield) as a yellow residue. The analytical sample was obtained by a crystallization from hot Ethyl Acetate/Pentane mixtures, mp 253-254 °C. IR (ATR): 3325, 2929, 2859, 1682, 1629, 1606, 1558, 1511, 1424, 1359, 1317, 1282, 1251, 1221, 1165, 1104, 1090, 1003, 938, 851, 772, 697, 642 cm⁻¹. ¹H-NMR (400 MHz, MeOD) δ: 1.31 [dq, *J* = 3.2 Hz, *J'* = 13.2 Hz, 2 H, 3'(5')-H_{ax}], 1.54 [dq, *J* = 3.2 Hz, *J'* = 12.8 Hz, 2 H, 2'(6')-H_{ax}], 1.81 [d, *J* = 12 Hz, 2 H, 10''(13'')-H_{ax}], 1.93-2.02 [complex signal, 4 H, 3'(5')-H_{eq}, 6''(12'')-H_{ax}], 2.07-2.19 [complex signal, 8 H, 2'(6')-H_{eq}, 4-H, 6''(12'')-H_{eq}, 10''(13'')-H_{eq}], 3.23 [t, 2 H, *J* = 7.2 Hz, 5''(11'')-H], 3.49 (m, 1 H, 4'-H), 4.37 (m, 1 H, 1'-H), 6.95 [d, *J* = 8.8 Hz, 2 H, 3(5)-H], 7.09 [broad s, 4 H, 1''(4'')-H, 2''(3'')-H], 7.94 [d, *J* = 8.8 Hz, 2 H, 2(6)-H]. ¹³C-NMR (100.5 MHz, MeOD) δ: 31.1 [CH₂, C2'(6')], 31.6 [CH₂, C3'(5')], 40.4 [CH₂, d, ⁴*J*_{C-F} = 1.9 Hz, C6''(12'')], 41.1 [CH, d, ³*J*_{C-F} = 13.3 Hz, C5''(11'')], 41.4 [CH₂, d, ²*J*_{C-F} = 20 Hz, C10''(13'')], 47.9 (CH₂, d, ²*J*_{C-F} = 17.9 Hz, C8''), 48.7 (CH, C4'), 57.6 (C, d, ³*J*_{C-F} = 11.2 Hz, C7''), 76.0 (CH, C1'), 95.4 (C, d, ¹*J*_{C-F} = 177 Hz, C9''), 116.1 [CH, C3(5)], 123.9 (C, C1), 127.9 [CH, C2''(3'')], 129.1 [CH, C1''(C4'')], 132.8 [CH, C2(6)], 146.4 [C, C4a''(11a'')], 159.2 (C,

NHCONH), 163.2 (C, C4), 169.8 (C, CO₂H). HRMS: Calculate for [C₂₉H₃₃FN₂O₄-H]⁻: 491.2352; Found: 491.2334.

Determination of IC₅₀ sEH inhibitors in human, murine and rat purified sEH. IC₅₀ is the concentration of a compound that reduces the sEH activity by 50%. The IC₅₀ values reported herein were determined using a fluorescent based assay (CMNPC as substrate).¹⁶ The fluorescent assay was used with purified recombinant human, mouse or rat sEH proteins. The enzymes were incubated at 30 °C with the inhibitors ([I]_{final} = 0.4 – 100,000 nM) for 5 min in 100 mM sodium phosphate buffer (200 μL, pH 7.4) containing 0.1 mg/mL of BSA and 1% of DMSO. The substrate (CMNPC) was then added ([S]_{final} = 5 μM). Activity was assessed by measuring the appearance of the fluorescent 6-methoxynaphthaldehyde product ($\lambda_{\text{ex}} = 330 \text{ nm}$, $\lambda_{\text{em}} = 465 \text{ nm}$) every 30 seconds for 10 min at 30 °C on a SpectraMax M2 (Molecular Devices). Results were obtained by regression analysis from a linear region of the curve. All measurements were performed in triplicate and the mean is reported. *t*-TUCB, a classic sEHI, was run in parallel and the obtained IC₅₀s were corroborated with reported literature values,³⁶ to validate the experimental results.

***In silico* study. Molecular Dynamics Simulations Details.** The parameters for *t*-AUCB, **20**, **22** and **23**, for the MD simulations were generated within the ANTECHAMBER module of AMBER 18³⁷ using the general AMBER force field (GAFF),³⁸ with partial charges set to fit the electrostatic potential generated at the HF/6-31G(d) level by the RESP model.³⁹ The charges were calculated according to the Merz-Singh-Kollman scheme⁴⁰⁻⁴¹ using Gaussian 09.⁴²

MD simulations of sEH were carried out using PDB 5AM3 (crystallized with *t*-AUCB)²⁷ as a starting point. For the MD simulations in the *apo* state the *t*-AUCB was removed

from the active site. The benzohomodamanatane derivatives corresponding to **20**, **22**, and **23** were manually prepared using *t*-AUCB structure as starting point. Molecular docking calculations using the SwissDock software were carried out to assess the preferred orientation of **20**, **22**, and **23**.⁴³⁻⁴⁴ From these coordinates, conventional MD simulations were used to explore the conformational plasticity of sEH in the *apo* state and in the presence of *t*-AUCB, **20**, **22**, and **23** bound in the active site. Amino acid protonation states were predicted using the H++ server (<http://biophysics.cs.vt.edu/H++>). The MD simulations have been carried with the following protonation of histidine residues: HIE146, HIE239, HIP251, HID265, HIP334, HIE420, HIE506, HIE513, HIE518, and HIP524.

Each system was immersed in a pre-equilibrated truncated octahedral box of water molecules with an internal offset distance of 10 Å. All systems were neutralized with explicit counterions (Na⁺ or Cl⁻). A two-stage geometry optimization approach was performed. First, a short minimization of the positions of water molecules with positional restraints on solute by a harmonic potential with a force constant of 500 kcal mol⁻¹ Å⁻² was done. The second stage was an unrestrained minimization of all the atoms in the simulation cell. Then, the systems were gently heated in six 50 ps steps, increasing the temperature by 50 K each step (0-300 K) under constant-volume, periodic-boundary conditions and the particle-mesh Ewald approach⁴⁵ to introduce long-range electrostatic effects. For these steps, a 10 Å cut-off was applied to Lennard-Jones and electrostatic interactions. Bonds involving hydrogen were constrained with the SHAKE algorithm.⁴⁶ Harmonic restraints of 10 kcal mol⁻¹ were applied to the solute, and the Langevin equilibration scheme was used to control and equalize the temperature.⁴⁷ The time step was kept at 2 fs during the heating stages, allowing potential inhomogeneities to self-adjust. Each system was then equilibrated for 2 ns with a 2 fs timestep at a constant

pressure of 1 atm (NPT ensemble). Finally, conventional MD trajectories at constant volume and temperature (300 K) were collected. In total, three replicas of 250 ns MD simulations for sEH in the *apo* state and in the presence of *t*-AUCB, **20**, **22**, and **23**. Gathering a total of 3.75 μ s of MD simulation time. Each MD simulation was clusterized based on active site residues and the structures corresponding to the most populated clusters were used in the non-covalent interactions analysis.

Microsomal stability. The human, rat and mice recombinant microsomes employed were purchased from Tebu-Xenotech. The compound was incubated at 37 °C with the microsomes in a 50 mM phosphate buffer (pH = 7.4) containing 3 mM MgCl₂, 1 mM NADP, 10 mM glucose-6-phosphate and 1 U/mL glucose-6-phosphate-dehydrogenase. Samples (75 μ L) were taken from each well at 0, 10, 20, 40 and 60 min and transferred to a plate containing 4 °C 75 μ L acetonitrile and 30 μ L of 0.5% formic acid in water were added for improving the chromatographic conditions. The plate was centrifuged (46000 g, 30 min) and supernatants were taken and analyzed in a UPLC-MS/MS (Xevo-TQD, Waters) by employing a BEH C18 column and an isocratic gradient of 0.1% formic acid in water: 0.1% formic acid acetonitrile (60:40). The metabolic stability of the compounds was calculated from the logarithm of the remaining compounds at each of the time points studied.

Solubility. A 10 mM stock solution of the compound was serially diluted in 100% DMSO and 1 μ L of this solution was added to a 384-well UV-transparent plate (Greiner) containing 99 μ L of PBS. The plate was incubated at 37 °C for 2 h and the light scattering was measured in a Nephelostar Plus reader (BMG LABTECH). The data was fitted to a segmented linear regression for measuring the compound solubility.

Permeability. The Caco-2 cells were cultured to confluency, trypsinized and seeded onto a 96-filter transwell insert (Corning) at a density of ~10,000 cells/well in DMEM cell culture medium supplemented with 10% Foetal Bovine Serum, 2 mM L-Glutamine and 1% penicillin/streptomycin. Confluent Caco-2 cells were subcultured at passages 58-62 and grown in a humidified atmosphere of 5% CO₂ at 37°C. Following an overnight attachment period (24 h after seeding), the cell medium was replaced with fresh medium in both the apical and basolateral compartments every other day. The cell monolayers were used for transport studies 21 days post seeding. The monolayer integrity was checked by measuring the transepithelial electrical resistance (TEER) obtaining values $\geq 500 \Omega/\text{cm}^2$. On the day of the study, after the TEER measurement, the medium was removed and the cells were washed twice with pre-warmed (37 °C) Hank's Balanced Salt Solution (HBSS) buffer to remove traces of medium. Stock solutions were made in dimethyl sulfoxide (DMSO), and further diluted in HBSS (final DMSO concentration 1%). Each compound and reference compounds (Colchicine, E3S) were all tested at a final concentration of 10 μM . For A \rightarrow B directional transport, the donor working solution was added to the apical (A) compartment and the transport media as receiver working solution was added to the basolateral (B) compartment. For B \rightarrow A directional transport, the donor working was added to the basolateral (B) compartment and transport media as receiver working solution was added to the apical (A) compartment. The cells were incubated at 37 °C for 2 hours with gentle stirring.

At the end of the incubation, samples were taken from both donor and receiver compartments and transferred into 384-well plates and analyzed by UPLC-MS/MS. The detection was performed using an ACQUITY UPLC /Xevo TQD System. After the assay, Lucifer yellow was used to further validate the cell monolayer integrity, cells were

incubated with LY 10 μ M in HBSS for 1 hour at 37°C, obtaining permeability (Papp) values for LY of ≤ 10 nm/s confirming the well-established Caco-2 monolayer.

Cytotoxicity in SH-SY5Y cells. Cytotoxicity was evaluated in the human neuroblastoma SH-SY5Y cell line (ATCC Number: CRL-2266). Cells were cultured in Minimum Essential Medium / Ham's-F12 (1:1, v/v) medium, supplemented with non-essential amino acids, 10% fetal bovine serum, 1 mM glutamine and 50 μ g/ml gentamycin (all reagents from Gibco, Invitrogen). For experiments, cells were seeded at 3×10^5 cells/ml (100 μ l/well) in 96-well plates (Nunc). After 24 h, the testing compounds were added concentrate to triplicate wells to obtain the final different concentrations up to 100 μ M. Compounds were incubated for further 24 h. At termination, cytotoxicity was analysed by the propidium iodide (PI) fluorescence stain assay. All compounds were tested in three independent experiments using different cell passages. The PI assay measures cell death. PI enters into the cells with damaged membranes and greatly increases the fluorescence by binding to DNA. PI reagent (Molecular Probes) at the final concentration of 7.5 μ g/ml was added to the cells and incubated for 1 h. The resulting fluorescence was measured by a Gemini XPS Microplate reader (Millipore) at 530 nm excitation and 645 nm emission. Percentage of cell death induced by the treatments was calculated from to the fluorescence of treated cells (Ft) relative to that of control cells (Fmin) and cells incubated with Triton X100 (Fmax) as the 0% and 100% cell death, respectively [% = ((Ft-Fmin)/(Fmax-Fmin)) x 100].

Inhibition of human lipoxygenase-5 (hLOX-5). AA and 2',7'-dichlorodihydrofluorescein diacetate (H₂DCFDA) were obtained from Sigma. Human recombinant LOX-5 was purchased from Cayman Chemical. For the determination of hLOX-5 activity, the method described by Pufahl *et al.* was followed.⁴⁸ The assay solution consisted of 50 mM Tris (pH 7.5), 2 mM EDTA, 2 mM CaCl₂, 3 μ M AA, 10 μ M

ATP, 10 μ M H₂DCFDA and 100 mU/well *h*LOX-5. For the enzyme inhibition studies the compounds to be tested were added to the assay solution prior to AA and ATP and were preincubated for a period of 10 min at room temperature, after which AA and ATP were added. The enzymatic reaction was carried out for 20 min and terminated by the addition of 40 μ L of acetonitrile. The fluorescence measurement, 485 nm excitation and 520 nm emission, was performed on a FLUOstar OPTIMA (BMG LABTECH, Offenburg, Germany.). The IC₅₀ is defined as the concentration of compound that inhibits enzymatic activity by 50% over the untreated enzyme control.

Pharmacokinetic study. 24 male C57BL/6 mice (21 grams aprox.) were supplied by Envigo (Barcelona, Spain) (Ref. 15131). During the experimental procedure animals were identified with permanent marker (tail code numbers). Plasma samples were obtained at 0, 0.25, 0.5, 1, 2, 4, 6, and 24 hours post-dosing. Upon arrival, animals were housed in groups of 3 animals/cage in polycarbonate maintenance cages (type IIL; 365 x 207 x 140 mm, with a surface area of 530 cm²) with absorbent bedding (Lignocel, JRS). Animals were kept in an environmentally controlled room (ventilation 10-15 air changes per hour, temperature 22 \pm 3°C and humidity 35-70%) on a 12-h light/dark cycle. A period of at least 5 days of observation and acclimatization underwent between the date of arrival and the start of the procedure. During this period, the animals were observed to check their general health state. The maintenance diet was supplied by Harlan Interfauna Ibérica S.L. (2014 Harlan Teklad Global Diets) and was provided to the animals *ad libitum*. Diet was analyzed by the manufacturer to detect possible contaminants. Tap water was supplied by CASSA (Servei d'Aigües de Sabadell) and was provided to the animals by bottles *ad libitum*. The animals were maintained in accordance with European Directive for the Protection of Vertebrate Animals Used for Experimental and other Scientific Purposes (86/609/EU). Decree 214/1997 of 30th July. Ministry of Agriculture, Livestock

and Fishing of the autonomous government of Catalonia, Spain. Royal Decree 53/2013 of 1st February (Spain) Animal care including environmental and housing conditions conformed to the applicable Standard Operating Procedures regarding laboratory animals of Draconis Pharma S.L. All the experimental procedures were approved by the Animal Experimentation Ethical Committee of Universitat Autònoma de Barcelona (procedure number: 3718) and by the Animal Experimentation Commission of the Generalitat de Catalunya (Catalan Government) (DAAM:9590). Formulations were prepared the day of the study. Vehicle was 10% of 2-hydroxypropyl- β - cyclodextrin, (CAS 128446-35-5) Sigma-Aldrich (Ref.332607-25G). 21 mice were intraperitoneally administered with a single dose of 3 mg/kg of **22**. The volume of administration was 10 mL/kg. Animals were weighed before each administration to adjust the required volume. Blood samples were collected at different times post administration: 0, 0.25, 0.5, 1, 2, 4, 6 and 24 h. Three mice were not administered and referred as t = 0. Blood samples (0.5-0.8 mL) were collected from anesthetized animals with isoflurane by cava vein puncture in tubes containing K2-EDTA 5%. Blood samples were centrifuged at 10.000 rpm for 5 min to obtain plasma that were stored at -20 °C until analysis. Analytical measurements were performed by liquid chromatography-tandem mass spectrometry (LC-MS/MS). Pharmacokinetics parameters were calculated with Phoenix 64 (WinNonlin).

In vivo efficacy study. Forty-one male C57BL/6 mice (eight week-old; approximately 24 g) were supplied by Envigo (Barcelona, Spain) (Ref.16512). During the experimental procedure, animals were identified with permanent marker (tail code numbers). Upon arrival, animals were housed in groups of 8-9 animals/cage in polysulfone maintenance cages (480 x 265 x 210 mm, with a surface area of 940 cm²), with wire tops and wood chip bedding. Animals were kept in an environmentally controlled room (ventilation, temperature 22 \pm 2°C and humidity 35-65%) on a 12-h light/dark cycle. A period of 7

days of acclimatization underwent between the date of arrival and the start of the procedure. During this period, the animals were observed to check their general health state. The maintenance diet was supplied by Harlan Interfauna Ibérica S.L. (2018 Harlan Teklad Global Diets). Diet will be provided to the animals *ad libitum*, but they were fasted overnight before first cerulein injection, and food was replaced after last cerulein injection. Tap water was supplied by CASSA (Servei d'Aigües de Sabadell) *ad libitum*. The animals were maintained in accordance with European Directive for the Protection of Vertebrate Animals Used for Experimental and other Scientific Purposes (86/609/EU). Decree 214/1997 of 30th July. Ministry of agriculture, livestock and fishing of the Autonomous Government of Catalonia, Spain. Royal Decree 53/2013 of 1st February (Spain). All the experimental procedures were approved by the Ethical Committee on human and animal experimentation (CEEAH) of Universitat Autònoma de Barcelona (UAB) (procedure number: 4107) and by the Animal Experimentation Commission of the Generalitat de Catalunya (Catalan Government) (DAAM: 10146). The test item was dissolved in vehicle 10% 2-hydroxypropyl- β -cyclodextrin (CAS 128446-35-5) Sigma-Aldrich (Ref.332607). Vehicle was prepared the day before and kept at 4 °C. Pancreatitis induction: Mice (n=41) were weighed, identified by a distinct number at the base of the tail and fasted overnight. Cerulein (cerulein and cerulein + **22** groups) (50 μ g/kg, prepared in 0.9% NaCl) or vehicle (0.9% NaCl) (Control group) were intraperitoneally injected (V= 5 mL/kg) 12 consecutive times, at 1-hour intervals (h=0-11). Food was replaced after last injection. A satellite experiment was designed where animals (n=3) were distributed in control, cerulein and cerulein + **22**-treated groups. Pancreatitis was induced by 7 injections of cerulein (or vehicle in control group) at 1-hour intervals (h=0-6). Treatments: Test item was administered intraperitoneally in one injection to **22**_03 (0.3 mg/kg) and **22**_01 (0.1 mg/kg) groups at 14-hour after the first cerulein injection. Animals

from control and group received vehicle administration (10% 2- hydroxypropyl- β -cyclodextrin) (V= 10mL/kg). Extra groups were treated 2-hour after the first cerulein injection: **22** (0.3 mg/kg), control and cerulein group (10% 2-hydroxypropyl- β -cyclodextrin). Study end: 24 h after the first cerulein injection, animals were weighed and anesthetized with isoflurane. Blood was collected from vena cava in an eppendorf containing K2-EDTA and centrifuged at 10000 rpm for 5 minutes for plasma collection. Plasma was stored at -80°C until analysis. Mice were sacrificed by cervical dislocation and pancreas were dissected and weighed. Pancreas from 3 animals were frozen in liquid N₂ and stored at -80°C until analysis. Pancreas from 5 mice were sectioned and one part was placed in 10% formalin and sent to Anapath (Granada, Spain) for histology analysis and the other was immediately placed in RNase-free eppendorfs, frozen in N₂ and stored at -80 °C for gene expression assays.

Histologic analysis. Pancreatic samples were treated with increasing grade alcohols, two xylol baths and embedded in paraffin. They were subsequently cut using a microtome and processed for staining. For the deparaffinization of the samples, 2 xylene baths (10 minutes) and 3 alcohols were used in decreasing solutions (100%, 90% and 70%) (5 minutes) and subsequently stained with hematoxylin (5 minutes) and eosin (5 minutes). During the dehydration process after staining with eosin, alcohols in increasing solution (70%, 96% and 100%) and xylene were used again. Finally, the samples were mounted with DPX.

The assigned scores were the following: 0 (no changes): when no lesions were observed or the observed changes were within normality; 1 (minimal): when changes were few but exceeded those considered normal; 2 (light): lesions were identifiable but with moderate severity; 3 (moderate): important injuries but they can still increase in severity; 4 (very serious): the lesions are very serious and occupy most of the analyzed tissue. The lesions

were evaluated in the most affected lobes of all the pancreas. In the case of assessment of atrophy, it was determined based on the percentage of atrophied tissue as: 0 without atrophy; 1: 0-25% of atrophic parenchyma; 2: between 25-50%; 3: between 50-75% and 4: between 75 and 100%.

ASSOCIATED CONTENT

Supporting Information

¹H and ¹³C NMR spectra and elemental analysis data of the new compounds, non-covalent interactions between the inhibitors and the active site residues of sEH, plot of the dihedral angle that describes the rotation of the adamantane moiety in the left-hand-side pocket of the sEH active site along the MD simulations, pharmacokinetic data of compounds **20** and **22**, and histologic scoring of pancreatic tissues of mice treated with **22** (PDF). Molecular formula string and data (CSV). This material is available free of charge via the Internet at <http://pubs.acs.org>.

AUTHOR INFORMATION

Corresponding author

*E-mail: svazquez@ub.edu Phone: +34 934024533

ORCID

Santiago Vázquez: 0000-0002-9296-6026

Notes

S.C., E.V. and S.V. are inventors of the Universitat de Barcelona patent application on sEH inhibitors WO2019/243414. C.M. and B.D.H. are inventors of the University of California patents on sEH inhibitors licensed to EicOsis. None of the other authors has any disclosures to declare.

Contributions

S.V. conceived the idea. S.C. and E.V. synthesized and chemically characterized the compounds. J.P.-D. and M.V.-C. designed and carried out the *in vivo* experiments. C.M. and B.D.H. performed the determination of the IC₅₀ in human, murine and rat sEH. F.F., C.C.-T. and S.O. performed MD calculations. M.I.L. and J.M.B. carried out DMPK studies. R.C., C.G.-F., M.P. and C.S. performed cytotoxicity studies. C.P. and M.I.R.-F. performed the *h*LOX-5 studies. S.C., S.O., C.M., B.D.H., F.F., and S.V. analyzed the data. S.C., C.C.-T., F.F. and S.V. wrote the manuscript with feedback from all the authors. All authors have given approval to the final version of the manuscript.

ACKNOWLEDGEMENTS

This work was funded by the Spanish *Ministerio de Economía, Industria y Competitividad* (Grants SAF2017-82771-R to S.V., RTI2018-093999-B-100 to M. V.-C., RTI2018-093955-B-C21 to M.I.R.-F., SAF2016-77703-C2 to M.P. and C.S., PGC2018-102192-B-I00 to S.O. and RTI2018-101032-J-I00 to F.F.), the *CaixaImpulse 2015 Programme*, the *Spain EIT Health* (Proof of concept 2016), the European Regional Development Fund (ERDF), the *Xunta de Galicia* (ED431G 2019/02 and ED431C 2018/21), the *Fundació Bosch i Gimpera, Universitat de Barcelona* (F2I grant), the *Generalitat de Catalunya* (2017 SGR 106, 2017 SGR 124 and 2017 SGR 1707), the *European Research Council* (ERC-2015-StG-679001-NetMoDEzyme to S.O.), and the *European Community* (MSCA-IF-2014-EF-661160-MetAccembly to F.F.). S.C. and E.V. acknowledge PhD fellowships from the *Universitat de Barcelona* (APIF grant) and the *Institute of Biomedicine of the University of Barcelona* (IBUB), respectively. Partial support was provided by NIH-NIEHS River Award R35 ES03443, NIH-NIEHS Superfund Program P42 ES004699, NINDS R01 DK107767, and NIDDK R01

DK103616 to B.D.H. The content is solely the responsibility of the authors and does not necessarily represent the official views of the National Institutes of Health.

ABBREVIATIONS USED

AP, Acute Pancreatitis; ATR, Attenuated Total Reflectance; BEH, Ethylene Bridged Hybrid; BFC, Benzyloxytrifluoromethylcoumarin; CER, cerulein; COXs, cyclooxygenases; CYPs, Cytochrome P450s, DBF, Dibenzylfluorescein; DMPK, Drug metabolism pharmacokinetics; EETs, Epoxyeicosatrienoic Acids; EtOAc, Ethyl Acetate; H&E, Hematoxylin and Eosin; hsEH, human soluble epoxide hydrolase; LHS, left-hand side; LOXs, Lipoxygenases; ND, Not Determined; RHS, right-hand side; sEH, soluble Epoxide Hydrolase; sEHI, soluble epoxide hydrolase inhibitors.

REFERENCES

- 1- Merirer, K.; Steinhilber, D.; Proschak, E. Inhibitors of the arachidonic acid cascade: interfering with multiple pathways. *Basic Clin. Pharmacol. Toxicol.* **2014**, *114*, 83-91.
- 2- Kaspera, R.; Totah, R. A. Epoxyeicosatrienoic acids: formation, metabolism and potential role in tissue physiology and pathology. *Expert Opin. Drug Metab. Toxicol.* **2009**, *5*, 757-771.
- 3- Morisseau, C.; Hammock, B. D. Impact of soluble epoxide hydrolase and epoxyeicosanoids on human health. *Annu. Rev. Pharmacol. Toxicol.* **2013**, *53*, 37-58.
- 4- Harris T. R.; Hammock, B. D. Soluble epoxide hydrolase: gene structure, expression and deletion. *Gene* **2013**, *526*, 61-74.

- 5- Morisseau, C.; Hammock, B. D. Impact of soluble epoxide hydrolase and epoxyeicosanoids on human health. *Annu. Rev. Pharmacol. Toxicol.* **2013**, *53*, 37-58.
- 6- Shen, H. C.; Hammock, B. D. Discovery of inhibitors of soluble epoxide hydrolase: a target with multiple potential therapeutic indications. *J. Med. Chem.* **2012**, *55*, 1789-1808.
- 7- Amano, Y.; Yamaguchi, T.; Tanabe, E. Structural insights into binding of inhibitors to soluble epoxide hydrolase gained by fragment screening and X-ray crystallography. *Bioorg. Med. Chem.* **2014**, *22*, 2427-2434.
- 8- Chen, D.; Whitcomb, R.; MacIntyre, E.; Tran, V.; Do, Z. N.; Sabry, J.; Patel, D. V.; Anandan, S. K.; Gless, R.; Webb, H. K. Pharmacokinetics and Pharmacodynamics of AR9281, an inhibitor of soluble epoxide hydrolase, in single- and multiple-dose studies in healthy human subjects. *J. Clin. Pharmacol.* **2012**, *53*, 319-328.
- 9- Lazaar, A. L.; Yang, L.; Boardley, R. L.; Goyal, N. S.; Robertson, J.; Baldwin, S. J.; Newby, D. E.; Wilkinson, I. B.; Tal-Singer, R.; Mayer, R. J.; Cheriyan, J. Pharmacokinetics, pharmacodynamics and adverse event profile of GSK2256294, a novel soluble epoxide hydrolase inhibitor. *British J. Clin. Pharmacol.* **2016**, *81*, 971-979.
- 10- Safety, Tolerability, and Pharmacokinetics of Oral EC5026 in Healthy Human Subjects. (2019) U.S. National Library of Medicine. Clinicaltrials.gov. Identifier NCT04228302.
- 11- Codony, S.; Valverde, E.; Leiva, R.; Brea, J.; Loza, M. I.; Morisseau, C.; Hammock, B. D.; Vázquez, S. Exploring the size of the lipophilic unit of the soluble epoxide hydrolase inhibitors. *Bioorg. Med. Chem.* **2019**, *27*, 115078.

- 12- Duque, M. D.; Camps, P.; Torres, E.; Valverde, E.; Sureda, F. X.; López-Querol, M.; Camins, A.; Prathalingam, S. R.; Kelly, J. M.; Vázquez, S. New oxapolycyclic cage amines with NMDA receptor antagonist and trypanocidal activities. *Bioorg. Med. Chem.* **2010**, *18*, 46-57.
- 13- Torres, E.; Duque, M. D.; López-Querol, M.; Taylor, M. C.; Naesens, L.; Ma, C.; Pinto, L. H.; Sureda, F. X.; Kelly, J. M.; Vázquez, S. Synthesis of benzopolycyclic cage amines: NMDA receptor antagonist, trypanocidal and antiviral activities. *Bioorg. Med. Chem.* **2012**, *20*, 942-948.
- 14- Valverde, E.; Sureda, F. X.; Vázquez, S. Novel benzopolycyclic amines with NMDA receptor antagonist activity. *Bioorg. Med. Chem.* **2014**, *22*, 2678-2683.
- 15- Barniol-Xicota, M.; Escandell, A.; Valverde, E.; Julián, E.; Torrents, E.; Vázquez, S. Antibacterial activity of novel benzopolycyclic amines. *Bioorg. Med. Chem.* **2015**, *23*, 290-296.
- 16- Morisseau, C.; Hammock, B. D. Measurement of soluble epoxide hydrolase (sEH) activity. *Curr. Protoc. Toxicol.* **2007**, Chapter 4, Unit 4.23.
- 17- Burnistrov, V.; Morisseau, C.; Pitushkin, D.; Karlov, D.; Fayzullin, R. R.; Butov, G. M.; Hammock, B. D. Adamantyl thioureas as soluble epoxide hydrolase inhibitors. *Bioorg. Med. Chem. Lett.* **2018**, *28*, 2302-2313.
- 18- James, R.; Hammock, B. D. Potent urea and carbamate inhibitors of soluble epoxide hydrolase inhibitors. *Proc. Natl. Acad. Sci. U. S. A.* **1999**, *96*, 8849-8854.
- 19- Codony, S.; Pujol, E.; Pizarro, J.; Feixas, F.; Valverde, E.; Loza, M. I.; Brea, J. M.; Saez, E.; Oyarzabal, Y.; Pineda-Lucena, A.; Pérez, B.; Pérez, C.; Rodríguez-Franco, M. I.; Leiva, R.; Osuna, S.; Morisseau, C.; Hammock, B. D.; Vázquez-Carrera, M.; Vázquez, S. 2-Oxaadamant-1-yl ureas as soluble epoxide hydrolase

- inhibitors: *in vivo* evaluation in a murine model of acute pancreatitis. *J. Med. Chem.* **2020**, <https://pubs.acs.org/doi/abs/10.1021/acs.jmedchem.0c00310>
- 20- Hammock, B. D.; Hwang, S. H.; Weckler, A. T.; Morisseau, C. Sorafenib derivatives as soluble epoxide hydrolase inhibitors. WO 2012/112570 A1, Aug 23, 2012.
- 21- Liu, J.-Y.; Tsai, H.-J.; Morisseau, C.; Lango, J.; Hwang, S. H.; Watanabe, T.; Kim, I.-H.; Hammock, B. D. In vitro and in vivo metabolism of N-adamantyl substituted urea-based soluble epoxide hydrolase inhibitors. *Biochem Pharmacol.* **2015**, *98*, 718–731.
- 22- Hodek, P.; Janščak, P.; Anzenbacher, P.; Burkhard, J.; Janků, J.; Vodička L. Metabolism of diamantine by rat liver microsomal cytochromes P-450. *Xenobiotica* **1988**, *18*, 1109–1118
- 23- Burnistrov, V.; Morisseau, C.; Harris, T. R.; Butov, G.; Hammock, B. D. Effects of adamantine alterations on soluble epoxide hydrolase inhibition potency, physical properties and metabolic stability. *Bioorg. Chem.* **2018**, *76*, 510–527.
- 24- Hwang, S. H.; Tsai, H.-J.; Liu, J.-Y.; Morisseau, C.; Hammock, B. D. Orally bioavailable potent soluble epoxide hydrolase inhibitors. *J. Med. Chem.* **2007**, *50*, 3852–3840.
- 25- Evans, R.; Hovan, L.; Tribello, G. A.; Cossins, B. P.; Estarellas, C.; Gervasio, F. L. Combining machine learning and enhanced sampling techniques for efficient and accurate calculations of absolute binding free energies. *J. Chem. Theory Comput.* **2020**, *16*, 4641–4654.
- 26- Serrano-Hervás, E.; Casadevall, G.; Garcia-Borràs, M.; Feixas, F.; Osuna, S. Epoxide hydrolase conformational heterogeneity for the resolution of bulky

- pharmacologically relevant epoxide substrates. *Chem. Eur. J.* **2018**, *24*, 12254-12258.
- 27- Öster, L.; Tapani, S.; Xue, Y.; Käck, H. Successful generation of structural information for fragment-based drug discovery. *Drug Discovery Today* **2015**, *20*, 1104-1111.
- 28- Durrant, J. D.; Votapka, L.; Sorensen, J.; Amaro, R. E. POVME 2.0: An enhanced tool for determining pocket shape and volume characteristics. *J. Chem. Theory Comput.* **2014**, *10*, 5047-5056.
- 29- Contreras-García, J.; Johnson, E. R.; Keinan, S.; Chaudret, R.; Piquemal, J.-P.; Beratan, D. N.; Yang, W. NCIPLLOT: a program for plotting noncovalent interaction regions. *J. Chem. Theory Comput.* **2011**, *7*, 625-632.
- 30- Yadav, D.; Lowenfels, A. B. The epidemiology of pancreatitis and pancreatic cancer. *Gastroenterology* **2013**, *144*, 1252-1261.
- 31- Forsmark, C. E.; Vege, S. S.; Wilcox, C. M. Acute pancreatitis. *N. Engl. J. Med.* **2016**, *375*, 1972-1981.
- 32- Krishna, S. G.; Kamboj, A. K.; Hart, P. A.; Hinton, A. ; Conwell, D. L. The changing epidemiology of acute pancreatitis hospitalizations: a decade of trends and the impact of chronic pancreatitis. *Pancreas* **2017**, *46*, 482-488.
- 33- Afghani, E.; Pandol, S. J.; Shimosegawa, T.; Sutton, R.; Wu, B. U.; Vege, S. S.; Gorelick, F.; Hirota, M.; Windsor, J.; Lo, S. K.; Freeman, M. L.; Lerch, M. M.; Tsuji, Y.; Melmed, G. Y.; Wassef, W.; Mayerle, J. Acute pancreatitis-progress and challenges: a report on an international symposium. *Pancreas* **2015**, *44*, 1195–1210.

- 34- Bettaieb, A.; Chahed, S.; Bachaalany, S.; Griffey, S.; Hammock, B. D.; Haj, F. G. Soluble epoxide hydrolase pharmacological inhibition ameliorates experimental acute pancreatitis in mice. *Mol. Pharmacol.* **2015**, *88*, 281-90.
- 35- Bettaieb, A.; Chahed, S.; Tabet, G.; Yang, J.; Morisseau, C; Griffey, S.; Hammock, B. D.; Haj, F. G. Effects of soluble epoxide hydrolase deficiency on acute pancreatitis in mice. *PLoS One* **2014**, *9*, e113019.
- 36- Wagner, K.; Inceoglu, B.; Dong, H.; Yang, J.; Hwang, S. H.; Jones, P.; Morisseau, C.; Hammock, B. D. Comparative efficacy of 3 soluble epoxide hydrolase inhibitors in rat neuropathic and inflammatory pain models. *Eur. J. Pharmacol.* **2013**, *700*, 93-101.
- 37- Case, D. A.; Ben-Shalom, I. Y.; Brozell, S. R.; Cerutti, D. S.; Cheatham, T. E. I.; Cruzeiro, V. W. D.; Darden, T. A.; Duke, R. E.; Ghoreishi, D.; Gilson, M. K.; Gohlke, H.; Goetz, A. W.; Greene, D.; Harris, R.; Homeyer, N.; Izadi, S.; Kovalenko, A.; Kurtzman, T.; Lee, T. S.; LeGrand, S.; Li, P.; Lin, C.; Liu, J.; Luchko, T.; Luo, R.; Mermelstein, D. J.; Merz, K. M.; Miao, Y.; Monard, G.; Nguyen, C.; Nguyen, H.; Omelyan, I.; Onufriev, A.; Pan, F.; Qi, R.; Roe, D. R.; Roitberg, A.; Sagui, C.; Schott-Verdugo, S.; Shen, J.; Simmerling, C. L.; Smith, J.; Salomon-Ferrer, R.; Swails, J.; Walker, R. C.; Wang, J.; Wei, H.; Wolf, R. M.; Wu, X.; Xiao, L.; York, D. M.; Kollman, P. A. (2018), AMBER 2018, University of California, San Francisco.
- 38- Wang, J.; Wolf, R. M.; Caldwell, J. W.; Kollman, P. A.; Case, D. A. Development and testing of a general amber force field. *J. Comput. Chem.* **2004**, *25*, 1157-1174.

- 39- Bayly, C. I.; Cieplak, P.; Cornell, W.; Kollman, P. A. A well-behaved electrostatic potential based method using charge restraints for deriving atomic charges: the RESP model. *J. Phys. Chem.* **1993**, *97*, 10269-10280.
- 40- Besler, B. H.; Merz Jr., K. M.; Kollman, P. A. Atomic charges derived from semiempirical methods. *J. Comput. Chem.* **1990**, *11*, 431-439.
- 41- Singh, U. C.; Kollman, P. A. An approach to computing electrostatic charges for molecules. *J. Comput. Chem.* **1984**, *5*, 129-145.
- 42- Frisch, M. J.; Trucks, G. W.; Schlegel, H. B.; Scuseria, G. E.; Robb, M. A.; Cheeseman, J. R.; Scalmani, G.; Barone, V.; Mennucci, B.; Petersson, G. A.; Nakatsuji, H.; Caricato, M.; Li, X.; Hratchian, H. P.; Izmaylov, A. F.; Bloino, J.; Zheng, G.; Sonnenberg, J. L.; Hada, M.; Ehara, M.; Toyota, K.; Fukuda, R.; Hasegawa, J.; Ishida, M.; Nakajima, T.; Honda, Y.; Kitao, O.; Nakai, H.; Vreven, T.; Montgomery Jr., J. A.; Peralta, J. E.; Ogliaro, F.; Bearpark, M.; Heyd, J. J.; Brothers, E.; Kudin, K. N.; Staroverov, V. N.; Kobayashi, R.; Normand, J.; Raghavachari, K.; Rendell, A.; Burant, J. C.; Iyengar, S. S.; Tomasi, J.; Cossi, M.; Rega, N.; Millam, J. M.; Klene, M.; Knox, J. E.; Cross, J. B.; Bakken, V.; Adamo, C.; Jaramillo, J.; Gomperts, R.; Stratmann, R. E.; Yazyev, O.; Austin, A. J.; Cammi, R.; Pomelli, C.; Ochterski, J. W.; Martin, R. L.; Morokuma, K.; Zakrzewski, V. G.; Voth, G. A.; Salvador, P.; Dannenberg, J. J.; S. Dapprich; Daniels, A. D.; Farkas, Ö.; Foresman, J. B.; Ortiz, J. V.; Cioslowski, J.; Fox, D. J. *Gaussian 09*, Gaussian 09, Revision A.02; Gaussian, Inc.: Pittsburgh, PA, 2009).
- 43- Grosdidier, A.; Zoete, V.; Michielin, O. SwissDock, a protein-small molecule docking web service based on EADock DSS. *Nucleic Acids Res.* **2011**, *39*, W270–W277.

- 44- Grosdidier, A.; Zoete, V.; Michielin, O. Fast docking using the CHARMM force field with EADock DSS. *J. Comput. Chem.* **2011**, *32*, 2149-2159.
- 45- Sagui, C.; Darden, T. A. Molecular dynamics simulations of biomolecules: long-range electrostatic effects. *Annu. Rev. Biophys. Biomol. Struct.* **1999**, *28*, 155-179.
- 46- Ryckaert, J.-P.; Ciccotti, G.; Berendsen, H. J. C. Numerical integration of the cartesian equations of motion of a system with constraints: molecular dynamics of *n*-alkanes. *J. Comp. Phys.* **1977**, *23*, 327-341.
- 47- Wu, X.; Brooks, B. R. Self-guided Langevin dynamics simulation method. *Chem. Phys. Lett.* **2003**, *381*, 512-518.
- 48- Pufahl, R. A.; Kasten, T. P.; Hills, R.; Gierse, J. K.; Reitz, B. A.; Weinberg, R. A.; Masferrer, J. L. Development of a fluorescence-based enzyme assay of human 5-lipoxygenase. *Anal. Biochem.* **2007**, *364*, 204-212.

Supporting Information

From the design to the *in vivo* evaluation of 3.3.4 benzohomoadamantane-derived soluble epoxide hydrolase inhibitors for the treatment of acute pancreatitis

Sandra Codony¹, Carla Calvó-Tusell², Elena Valverde¹, Silvia Osuna^{2,3}, Christophe Morisseau⁴, M. Isabel Loza⁵, José Brea⁵, Concepción Pérez⁶, María Isabel Rodríguez-Franco⁶, Javier Pizarro-Delgado^{7,8,9}, Rubén Corpas^{10,11}, Christian Griñán-Ferré¹², Mercè Pallàs¹², Coral Sanfeliu^{10,11}, Manuel Vázquez-Carrera^{7,8,9}, Bruce D. Hammock⁴, Ferran Feixas², Santiago Vázquez^{1}*

¹Laboratori de Química Farmacèutica (Unitat Associada al CSIC), Departament de Farmacologia, Toxicologia i Química Terapèutica, Facultat de Farmàcia i Ciències de l'Alimentació, and Institute of Biomedicine (IBUB), Universitat de Barcelona, Av. Joan XXIII, 27-31, 08028 Barcelona, Spain.

²CompBioLab Group, Departament de Química and Institut de Química Computacional i Catàlisi (IQCC), Universitat de Girona, C/ Maria Aurèlia Capmany 69, 17003 Girona, Spain.

³Institució Catalana de Recerca i Estudis Avançats (ICREA), 08010 Barcelona, Spain.

⁴Department of Entomology and Nematology and Comprehensive Cancer Center, University of California, Davis, CA 95616, USA.

⁵Drug Screening Platform/Biofarma Research Group, CIMUS Research Center. Departamento de Farmacología, Farmacia e Tecnología Farmacéutica. University of Santiago de Compostela (USC), 15782 Santiago de Compostela, Spain.

⁶Institute of Medicinal Chemistry, Spanish National Research Council (CSIC), C/Juan de la Cierva 3, 28006 Madrid, Spain.

⁷Pharmacology Section. Department of Pharmacology, Toxicology and Medicinal Chemistry, Faculty of Pharmacy and Food Sciences, University of Barcelona, and Institute of Biomedicine of the University of Barcelona (IBUB), Av. Joan XXIII, 27-31, 08028 Barcelona, Spain.

⁸Spanish Biomedical Research Center in Diabetes and Associated Metabolic Diseases (CIBERDEM)-Instituto de Salud Carlos III, 28029 Madrid, Spain.

⁹Pediatric Research Institute-Hospital Sant Joan de Déu, 08950 Esplugues de Llobregat, Spain.

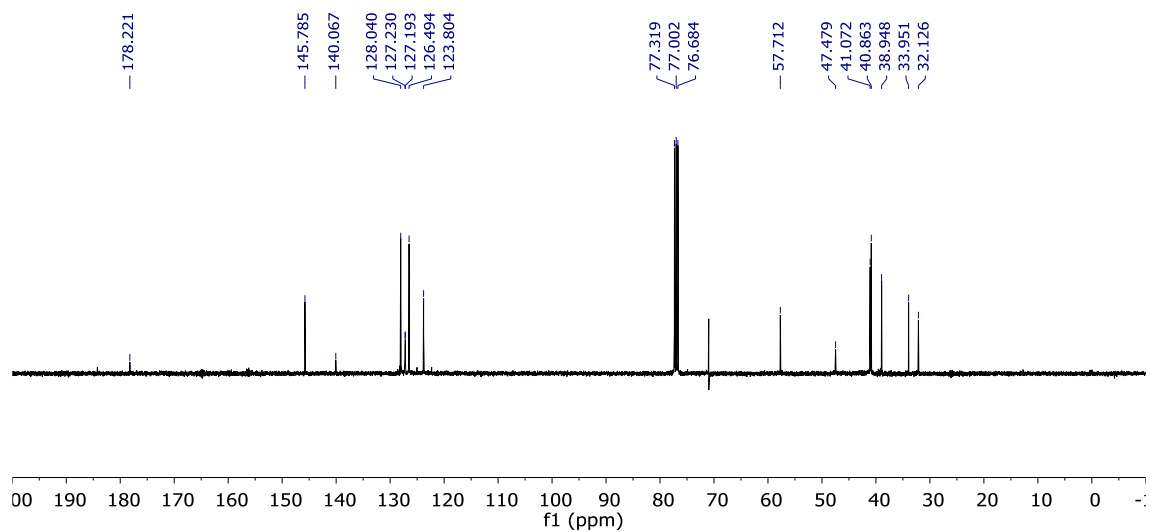
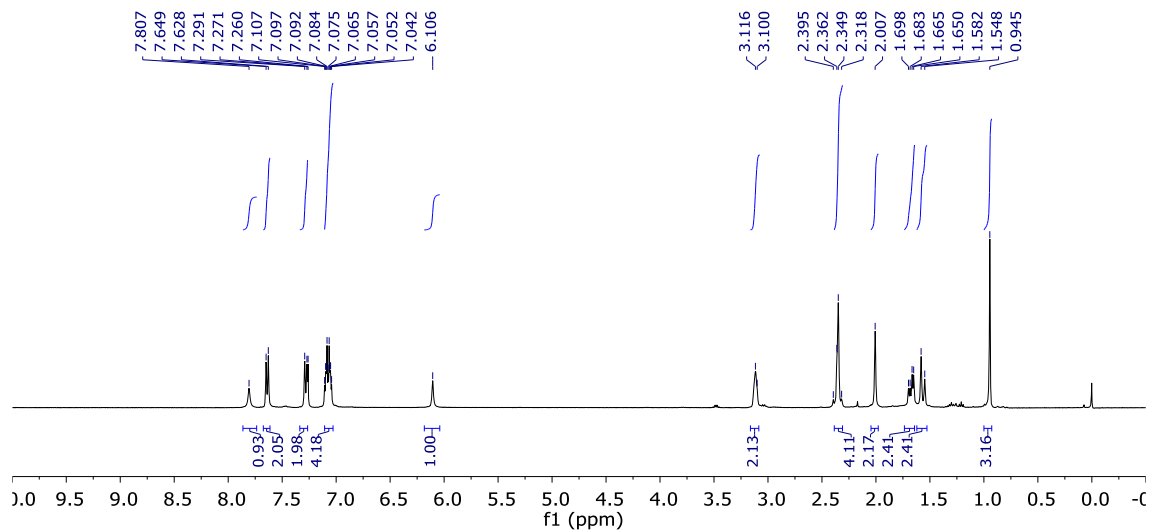
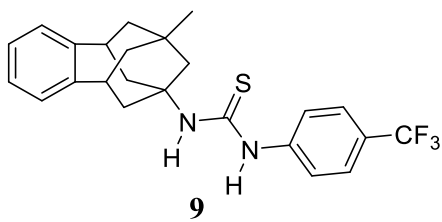
¹⁰Institute of Biomedical Research of Barcelona (IIBB), CSIC and IDIBAPS, 08036 Barcelona, Spain.

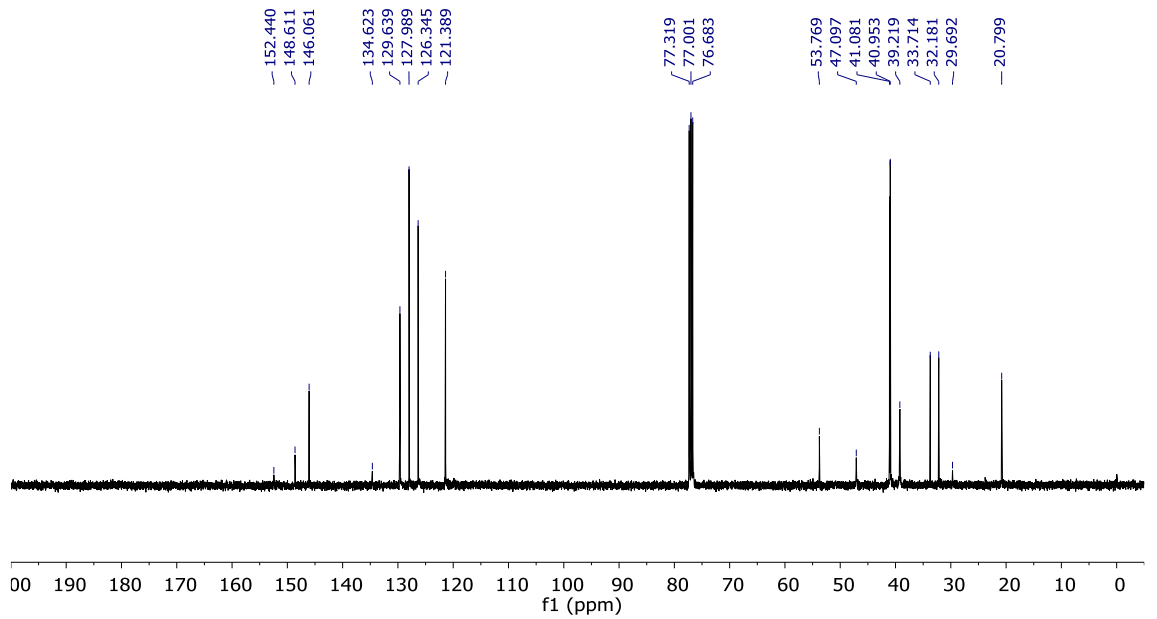
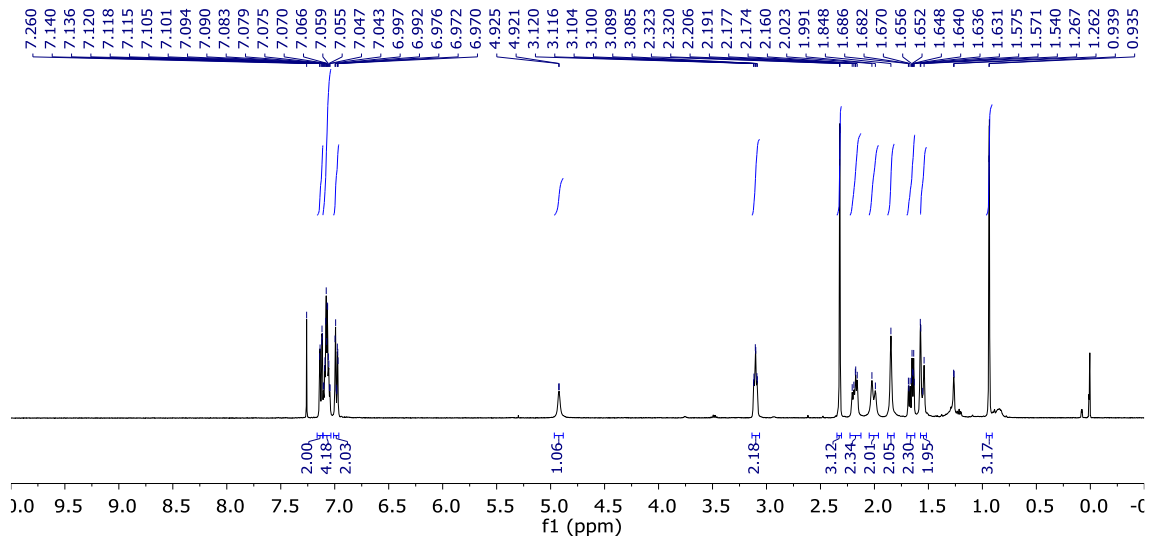
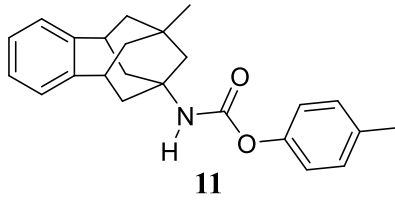
¹¹CIBER Epidemiology and Public Health (CIBERESP)-Instituto de Salud Carlos III, 28029, Madrid, Spain.

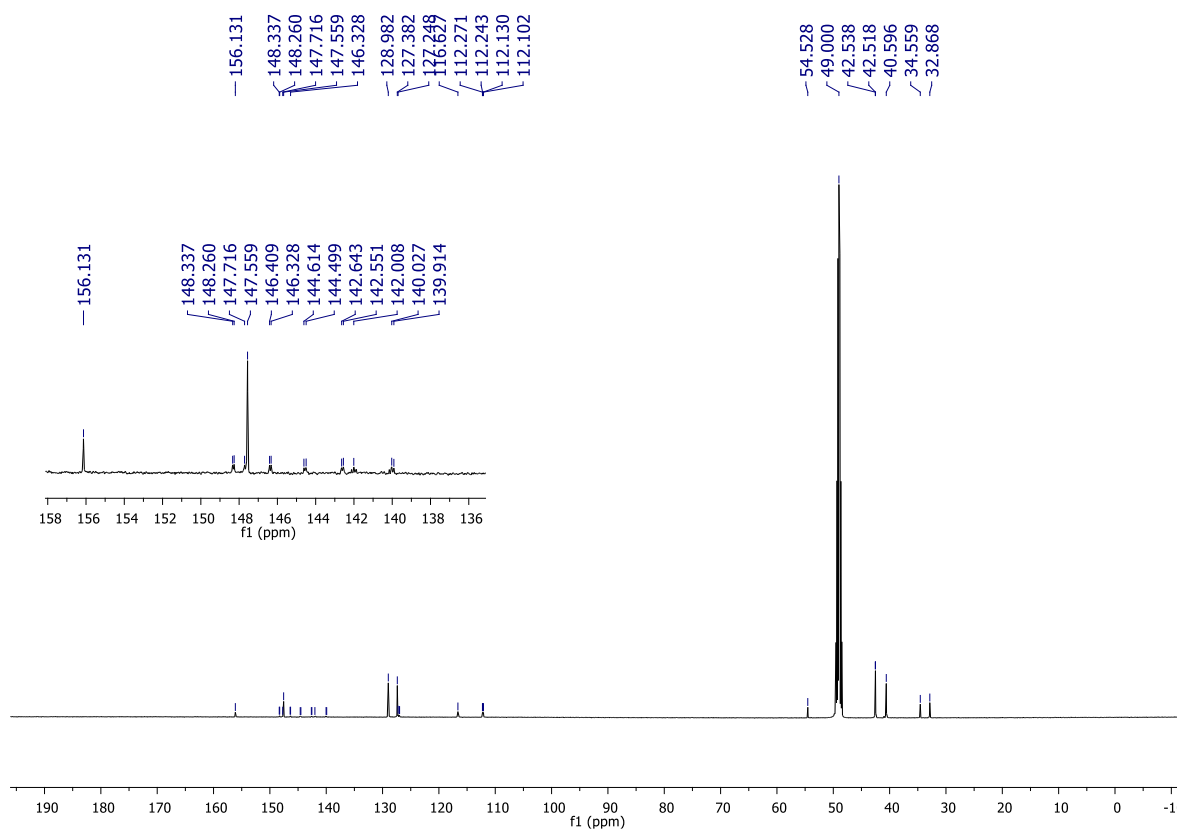
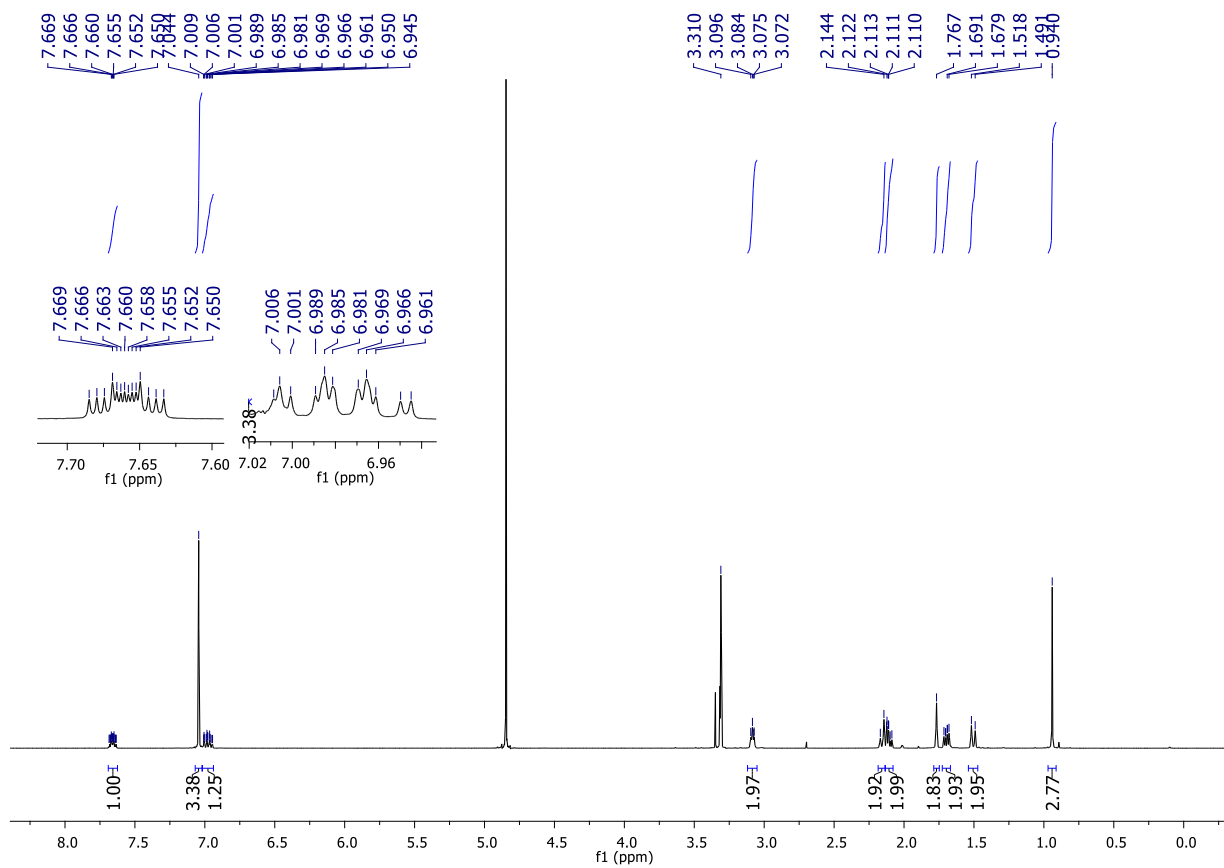
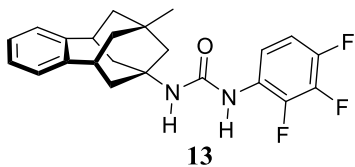
¹²Pharmacology Section. Department of Pharmacology, Toxicology and Medicinal Chemistry, Faculty of Pharmacy and Food Sciences, and Institut de Neurociències, University of Barcelona, Av. Joan XXIII, 27-31, 08028 Barcelona, Spain.

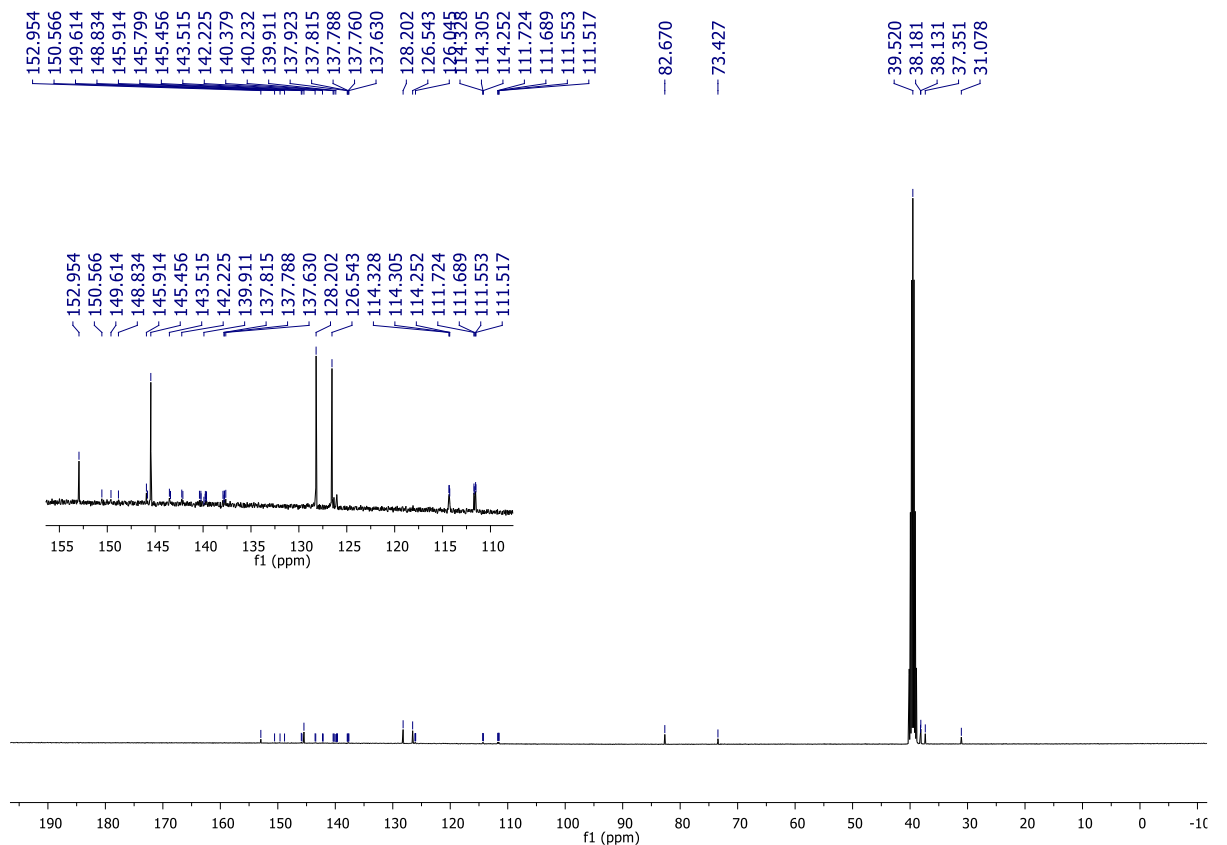
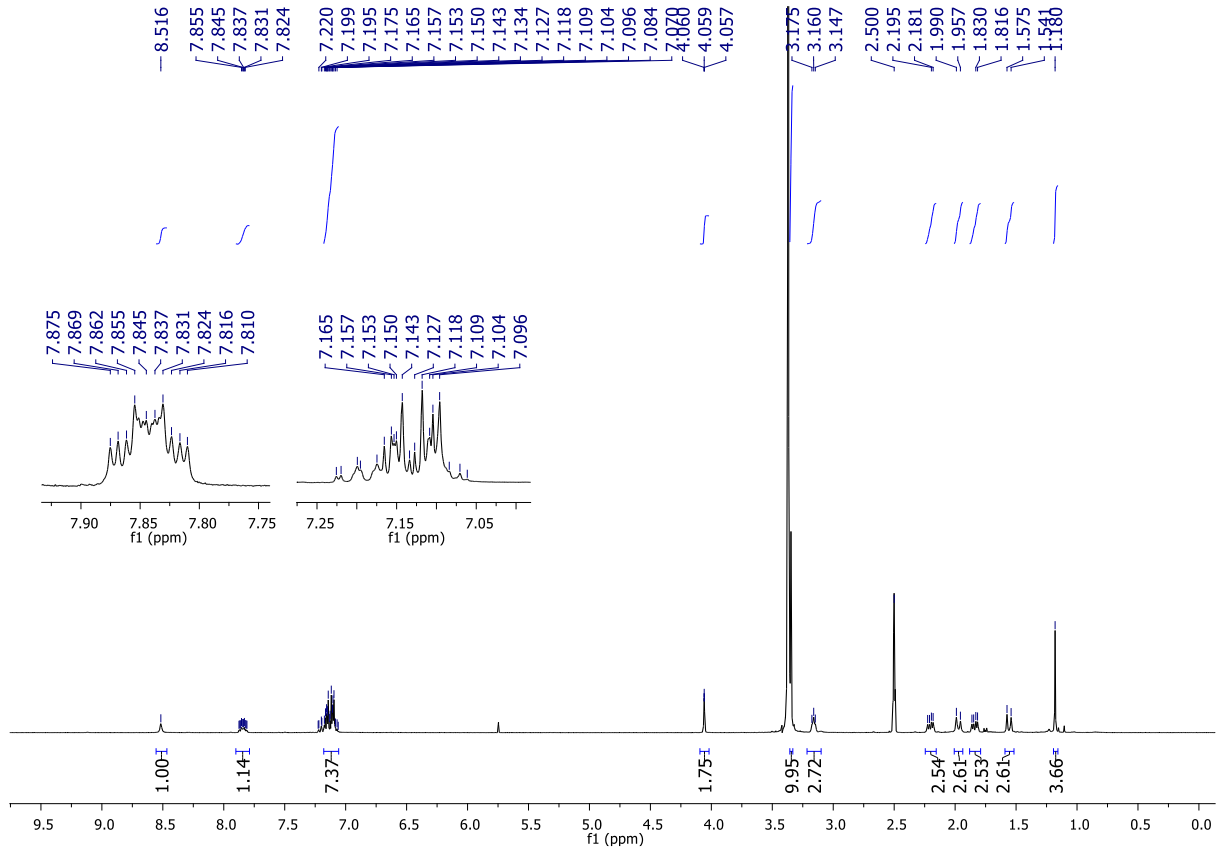
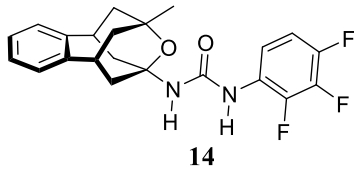
Table of contents

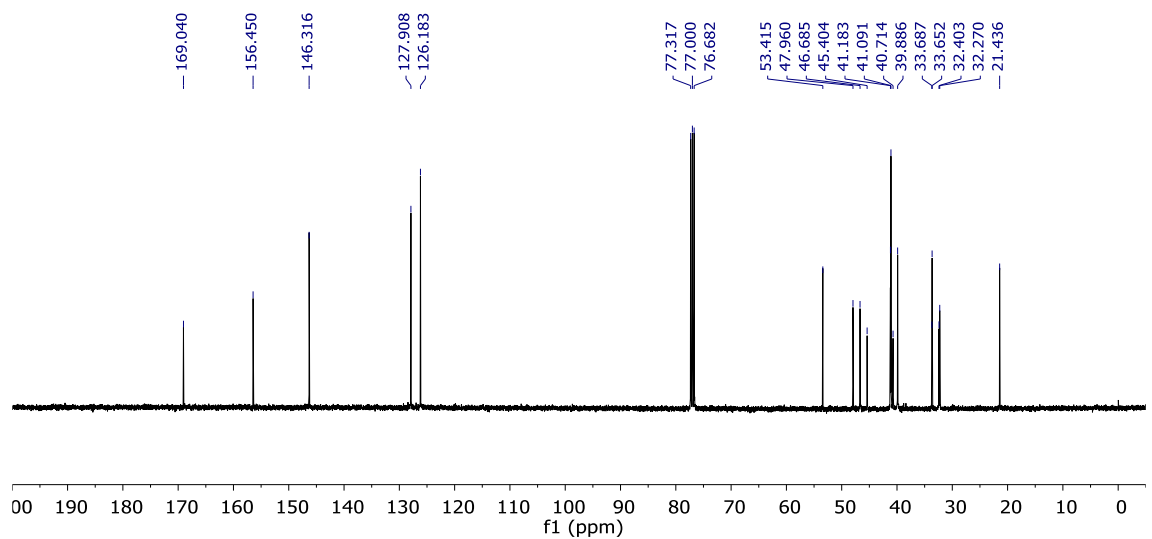
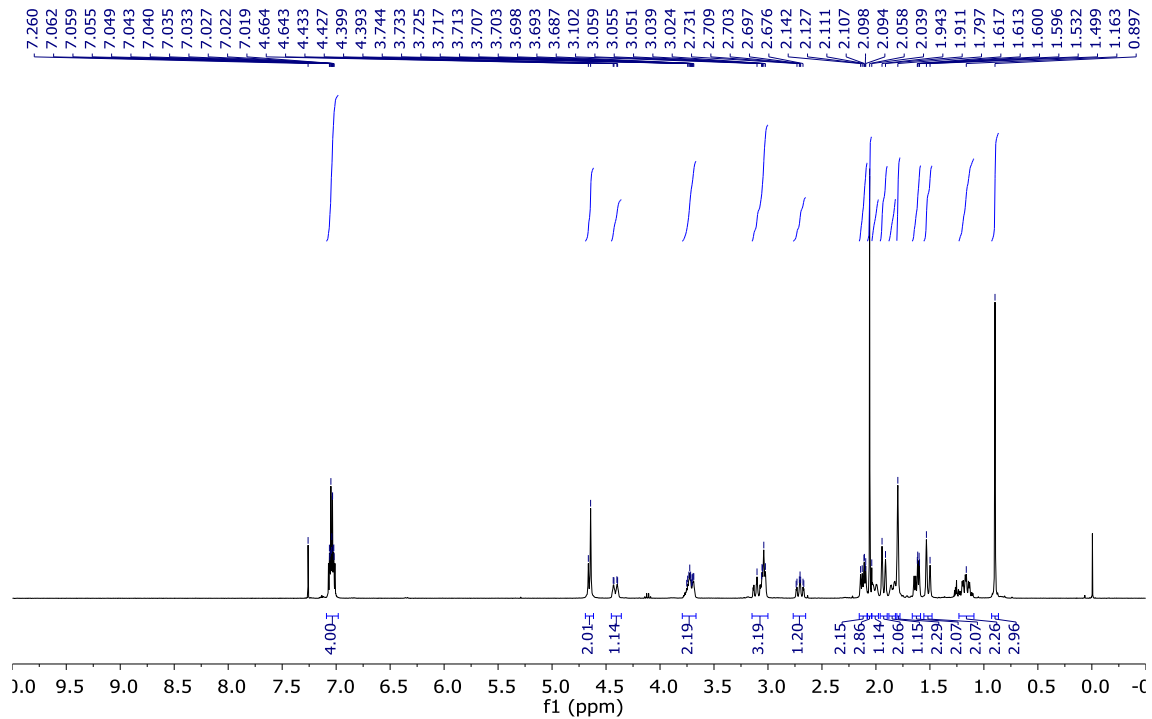
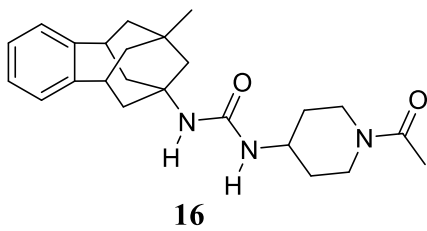
¹ H and ¹³ C NMR spectra of compound 9	Page S4
¹ H and ¹³ C NMR spectra of compound 11	Page S5
¹ H and ¹³ C NMR spectra of compound 13	Page S6
¹ H and ¹³ C NMR spectra of compound 14	Page S7
¹ H and ¹³ C NMR spectra of compound 16	Page S8
¹ H and ¹³ C NMR spectra of compound 17	Page S9
¹ H and ¹³ C NMR spectra of compound 18	Page S10
¹ H and ¹³ C NMR spectra of compound 20	Page S11
¹ H and ¹³ C NMR spectra of compound 21	Page S12
¹ H and ¹³ C NMR spectra of compound 22	Page S13
¹ H and ¹³ C NMR spectra of compound 23	Page S14
Table S1: Elemental analysis data	Page S15
Figure S1: Non-covalent interactions of <i>t</i> -AUCB, 20 , 22 , and 23	Page S16
Figure S2: Rotation of adamantane scaffold in the active site pocket	Page S17
Table S2: Mean of concentrations of 20 in mouse plasma	Page S18
Table S3: Mean of concentrations of 22 in mouse plasma.	Page S19
Figure S3: Concentrations of 20 in mouse plasma after ip administration	Page S20
Figure S4: Concentrations of 22 in mouse plasma after ip administration	Page S20
Table S4: Histologic scoring of pancreatic tissues of control group	Page S21
Table S5: Histologic scoring of pancreatic tissues of mice treated with cerulein	Page S21
Table S6: Histologic scoring of pancreatic tissues of mice treated with cerulein and 22 at 0.1 mg/kg.	Page S21
Table S7: Histologic scoring of pancreatic tissues of mice treated with cerulein and 22 at 0.3 mg/kg.	Page S21

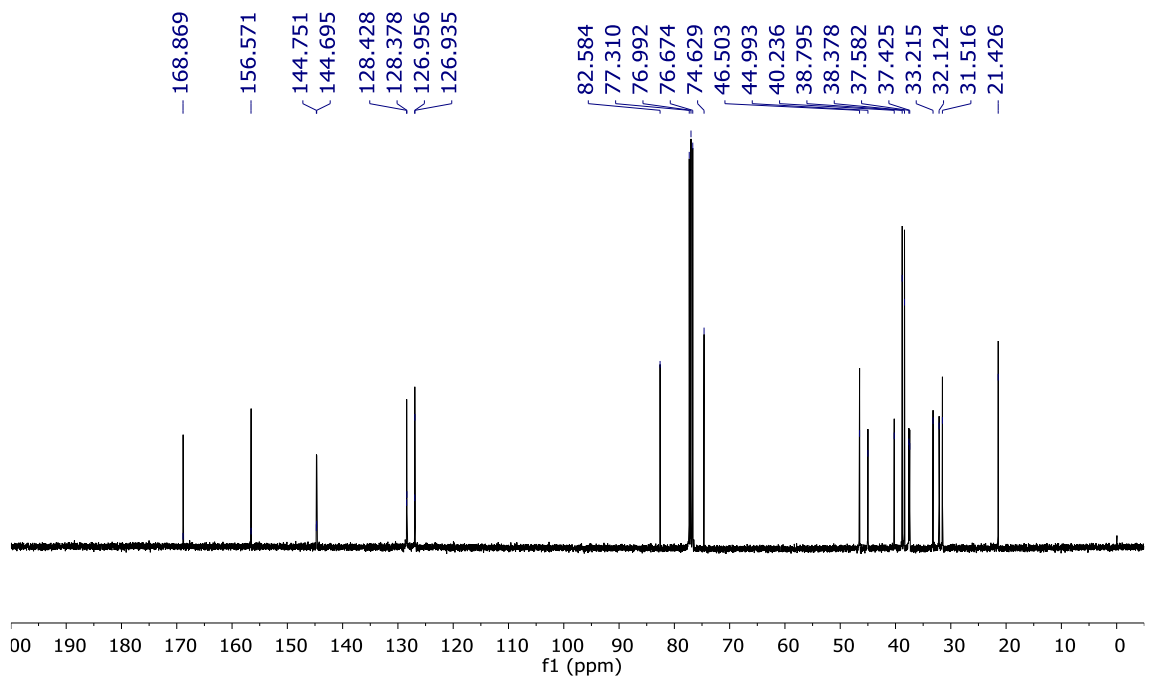
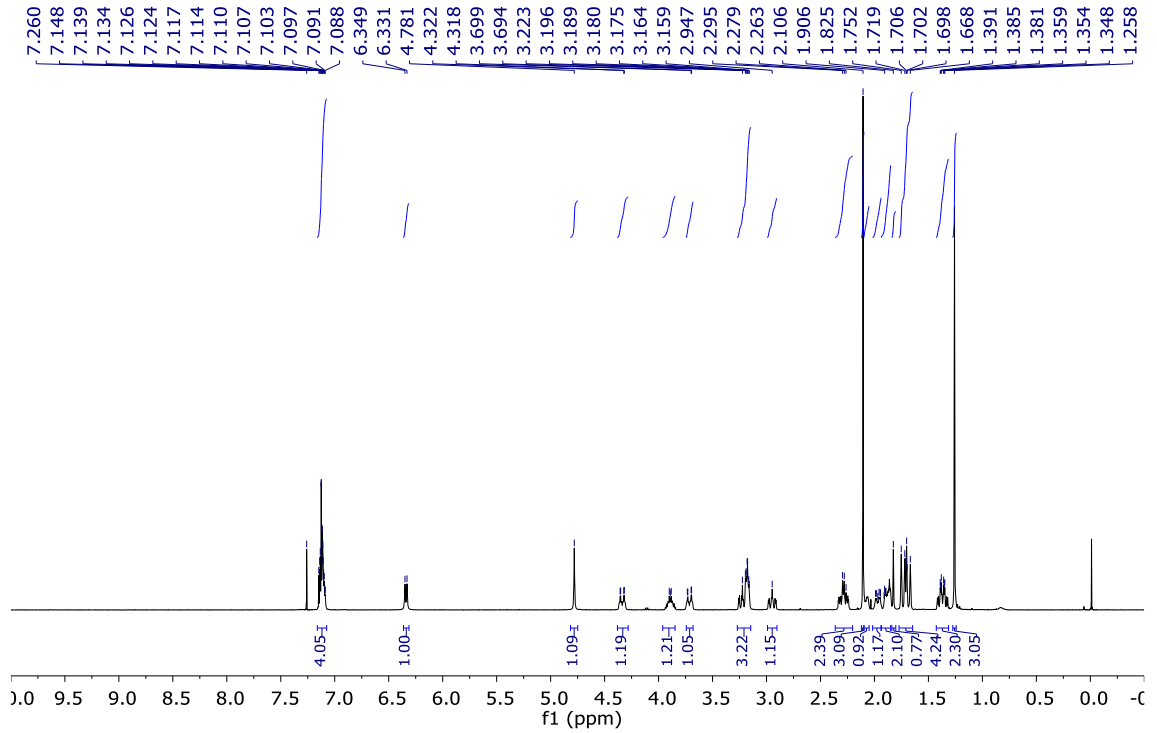
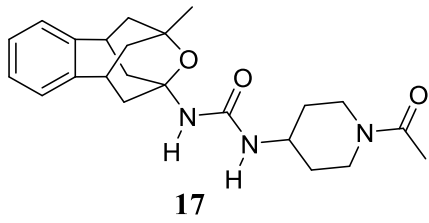


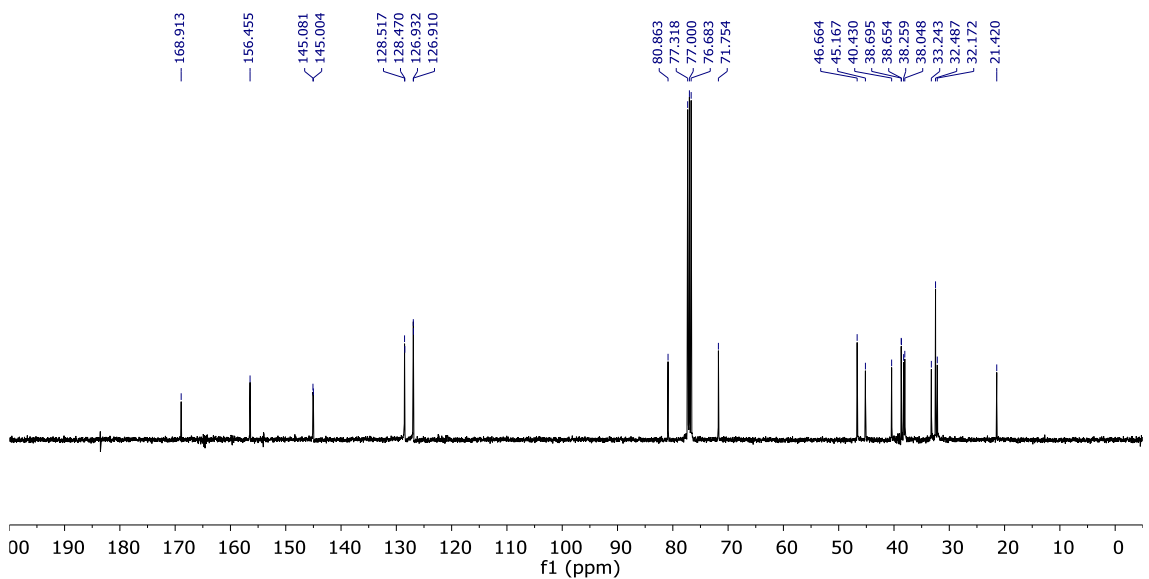
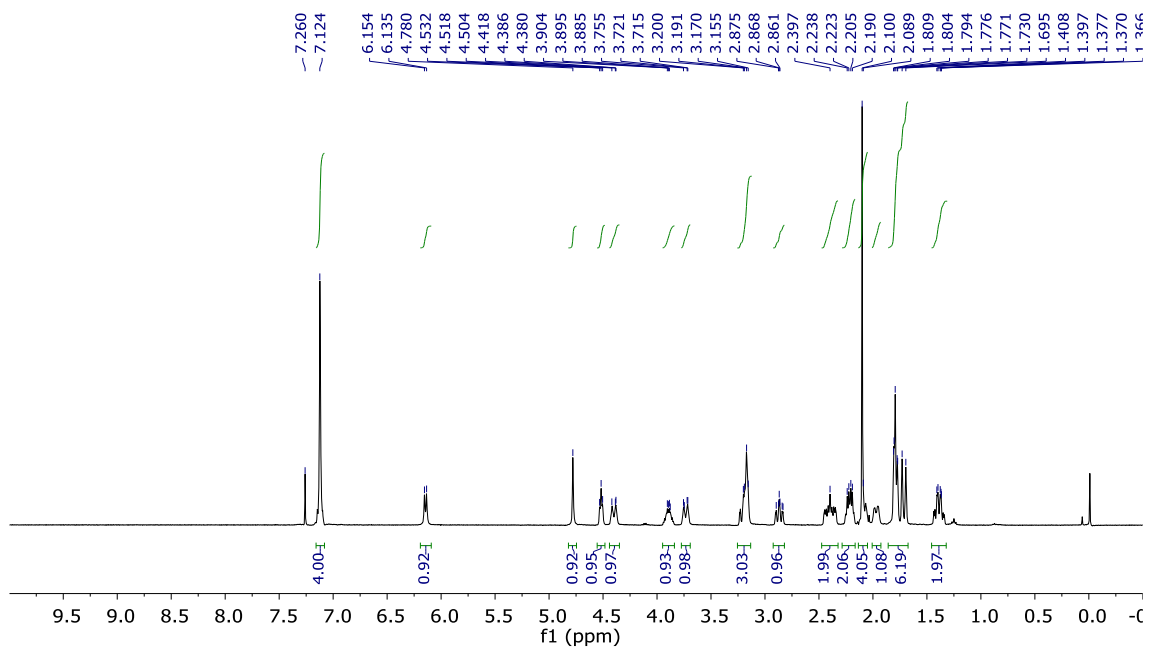
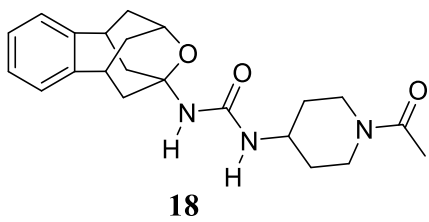


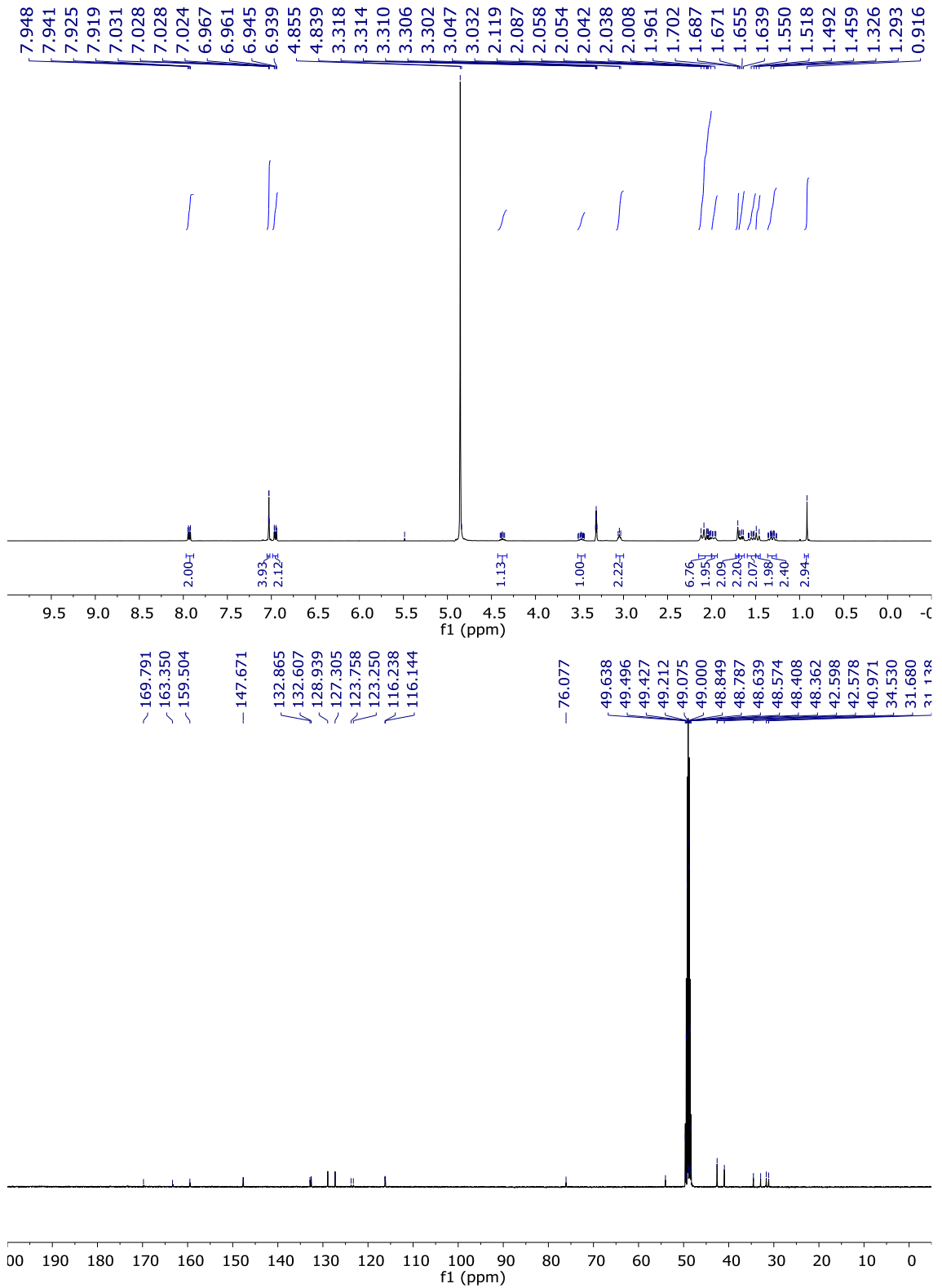
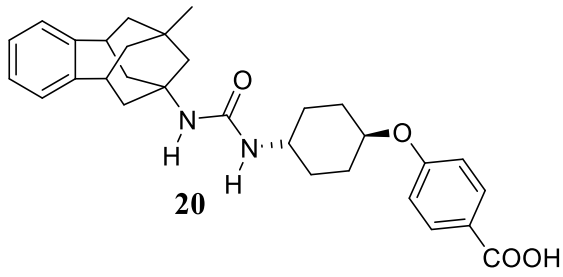


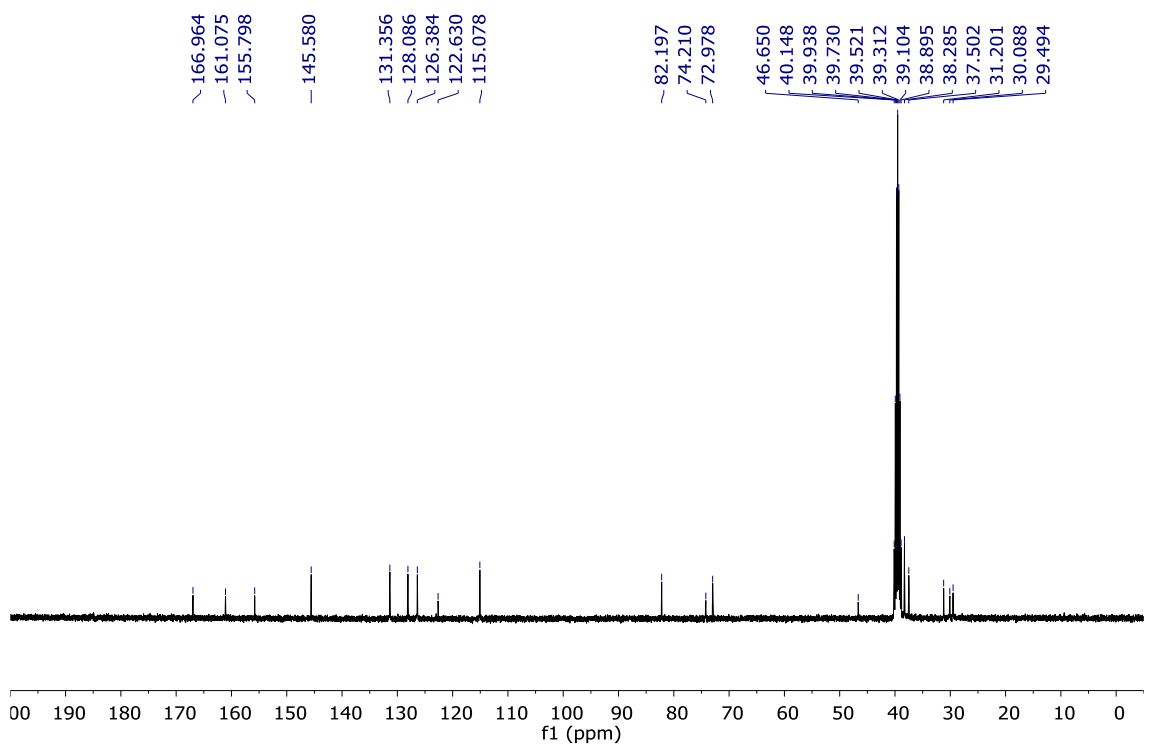
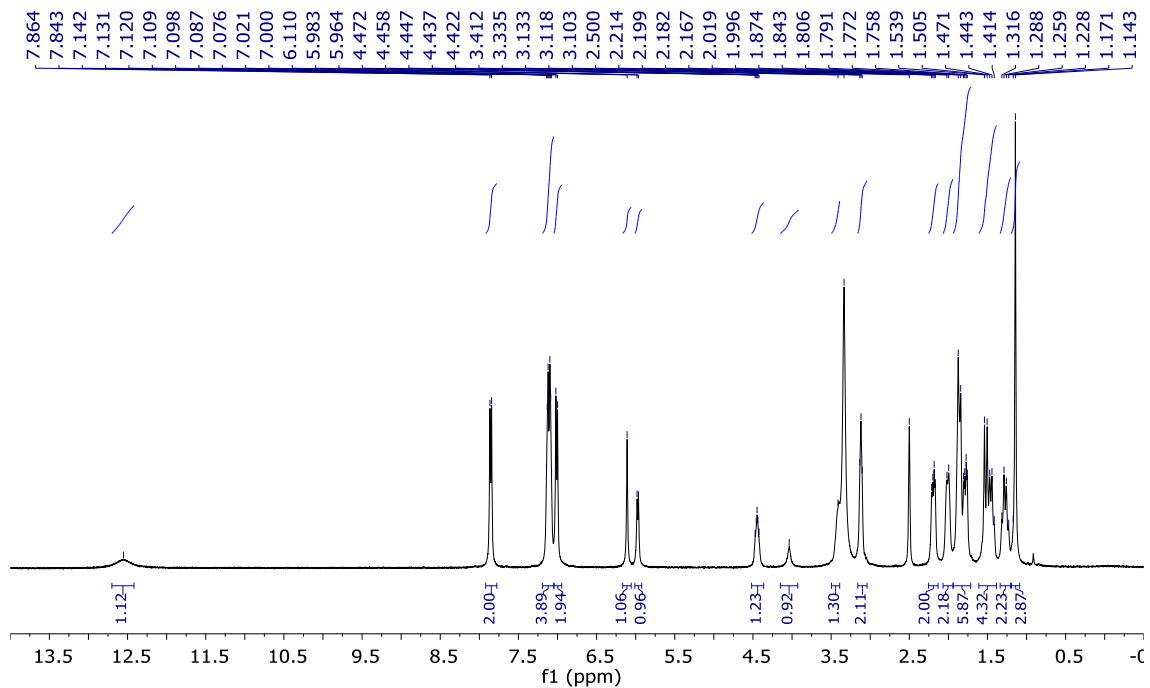
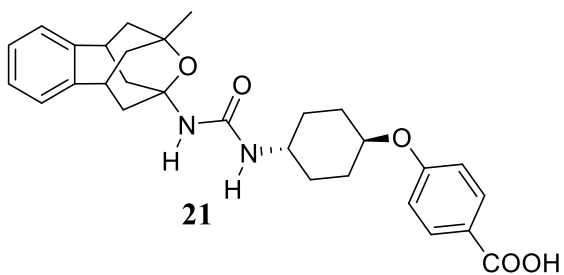


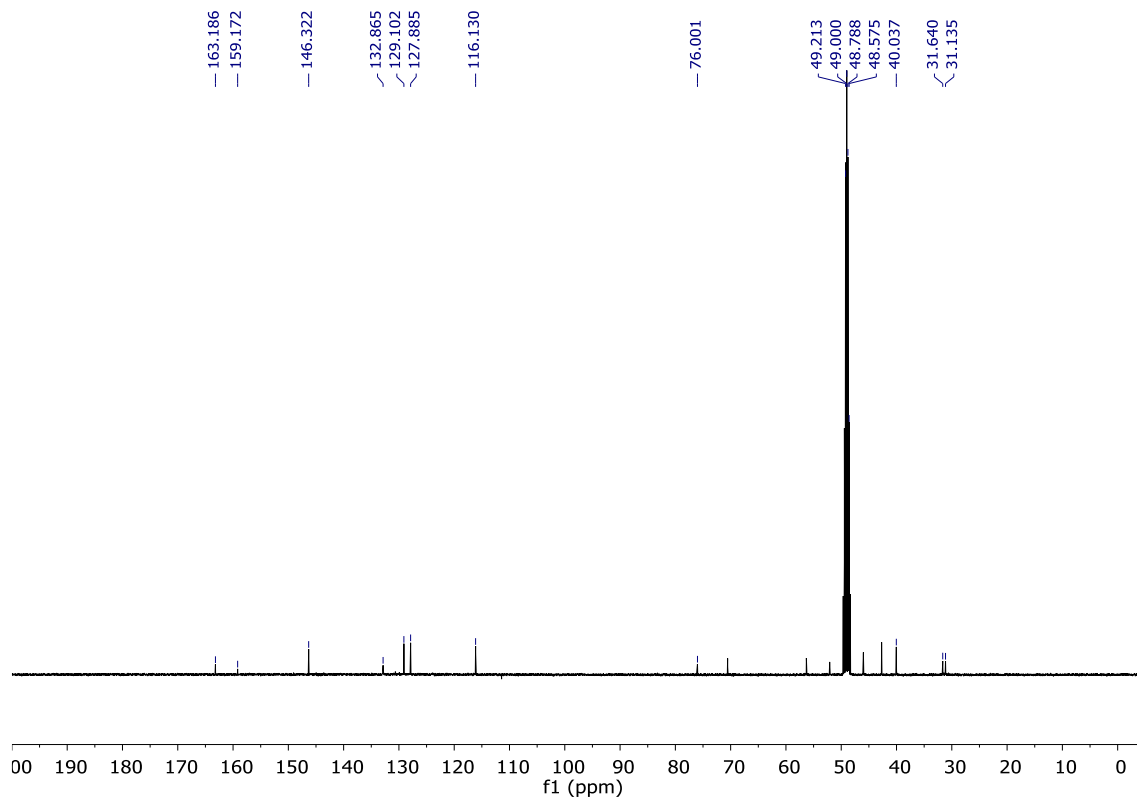
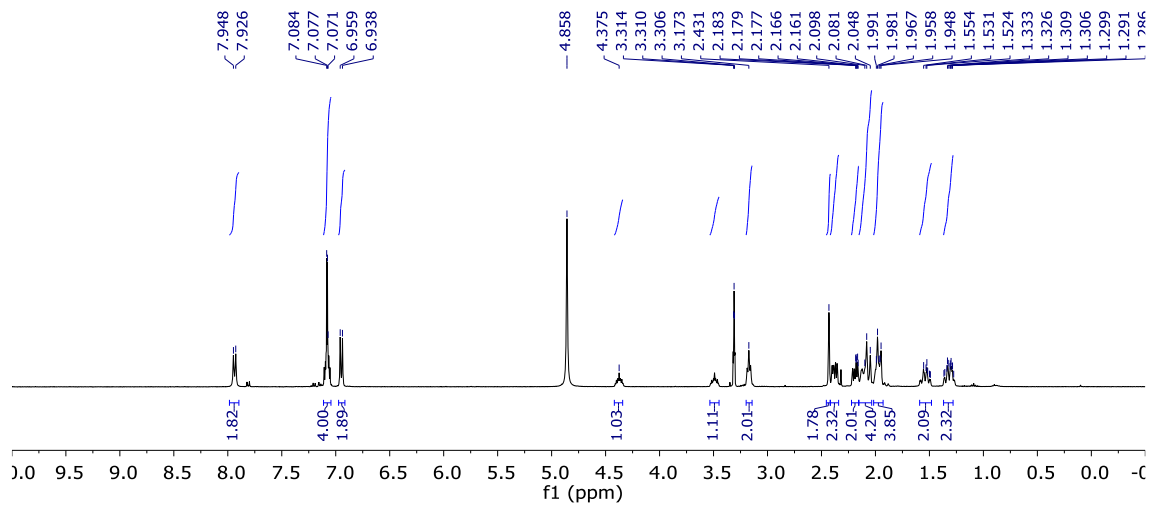
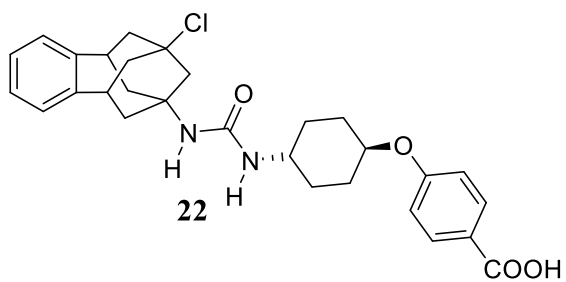


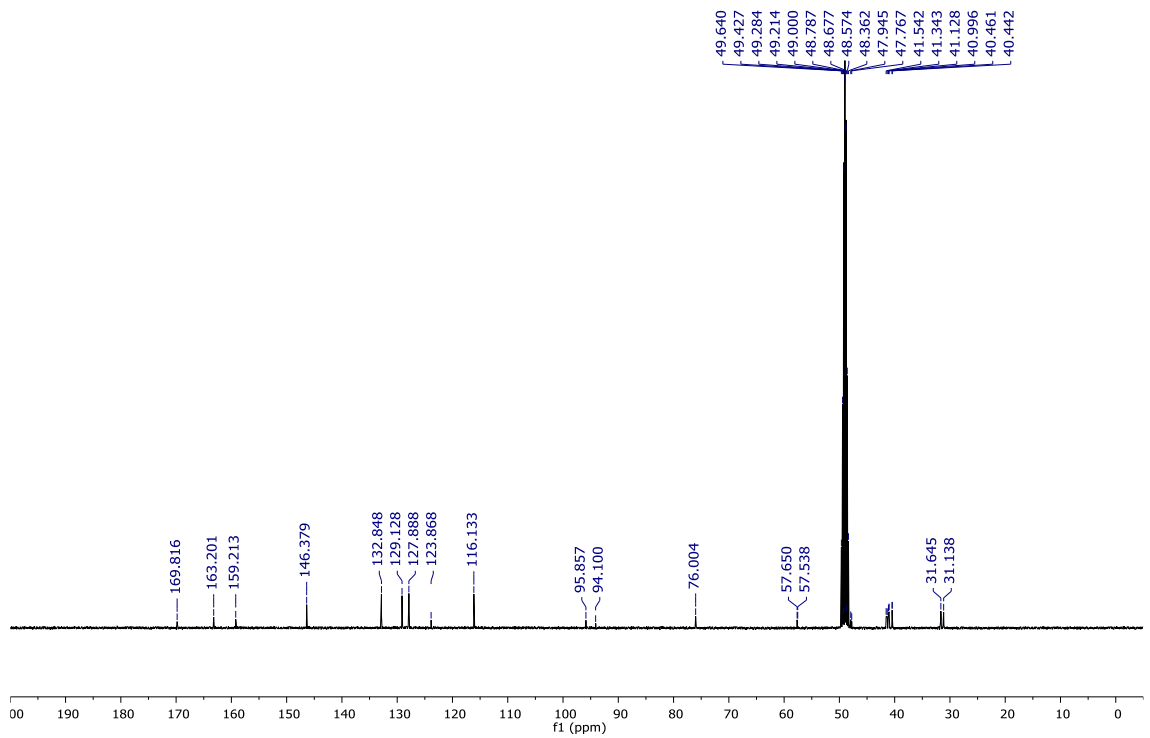
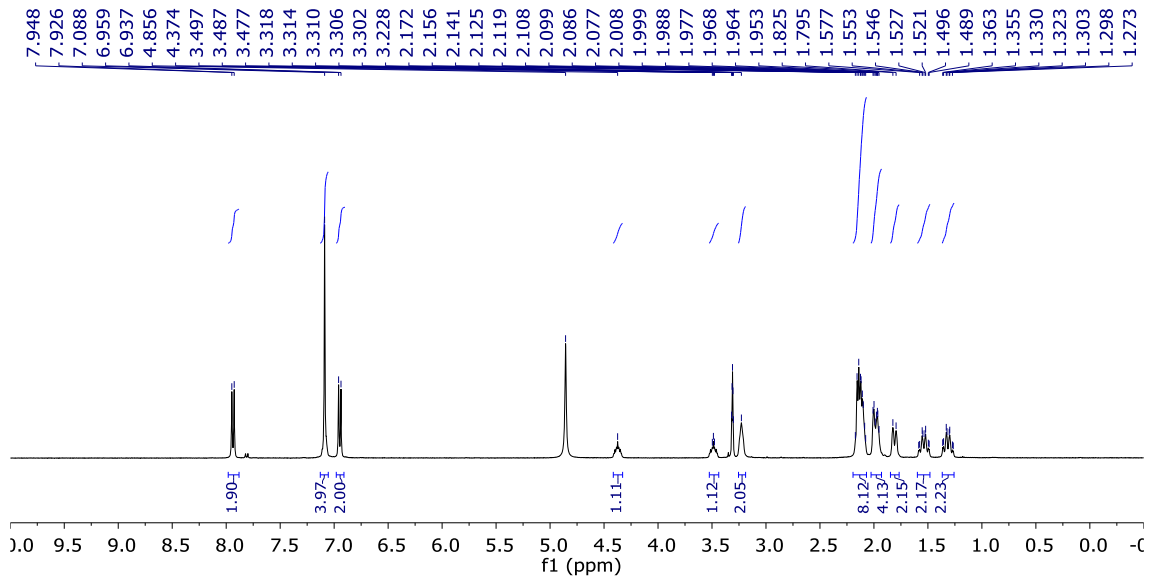
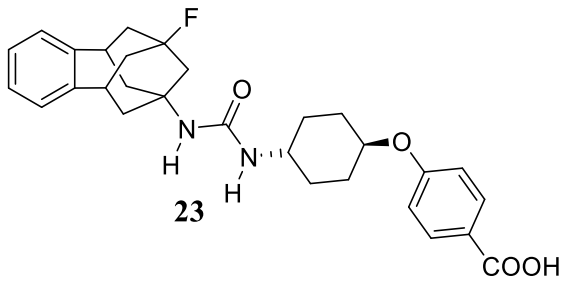












Compound	Molecular Formula	Calculated			Found		
		C	H	N	C	H	N
9	C ₂₄ H ₂₅ F ₃ N ₂ S	66.96	5.85	6.51	66.79	5.95	6.37
11	C ₂₄ H ₂₇ NO ₂ · 0.15 H ₂ O	79.15	7.56	3.85	79.34	7.92	3.48
13	C ₂₃ H ₂₃ F ₃ N ₂ O	68.99	5.79	7.00	68.94	5.92	6.71
14	C ₂₂ H ₂₁ F ₃ N ₂ O ₂ · 0.1 H ₂ O	65.37	5.29	6.93	65.18	5.31	6.73
16	C ₂₄ H ₃₃ N ₃ O ₂ · 0.25 EtOAc	71.91	8.45	10.06	71.73	8.43	10.27
17	C ₂₃ H ₃₁ N ₃ O ₃	69.49	7.86	10.57	69.47	7.92	10.38
18	C ₂₂ H ₂₉ N ₃ O ₃ · 0.95 H ₂ O	65.96	7.77	10.49	66.25	7.67	10.13
20	C ₃₀ H ₃₆ N ₂ O ₄ · 1.5 H ₂ O	69.88	7.62	5.43	69.53	7.37	5.10
21	C ₂₉ H ₃₄ N ₂ O ₅ · 0.5 CH ₂ Cl ₂	66.06	6.58	5.21	66.20	6.43	5.17
22	C ₂₉ H ₃₃ ClN ₂ O ₄ · 1 CH ₃ OH	66.59	6.89	5.18	66.85	6.62	4.91
23	C ₂₉ H ₃₃ FN ₂ O ₄ · 0.45 CH ₃ OH	69.77	6.92	5.53	69.68	6.79	5.57

Table S1: Elemental analysis data.

Non-covalent interactions between the inhibitors and the active site residues of sEH

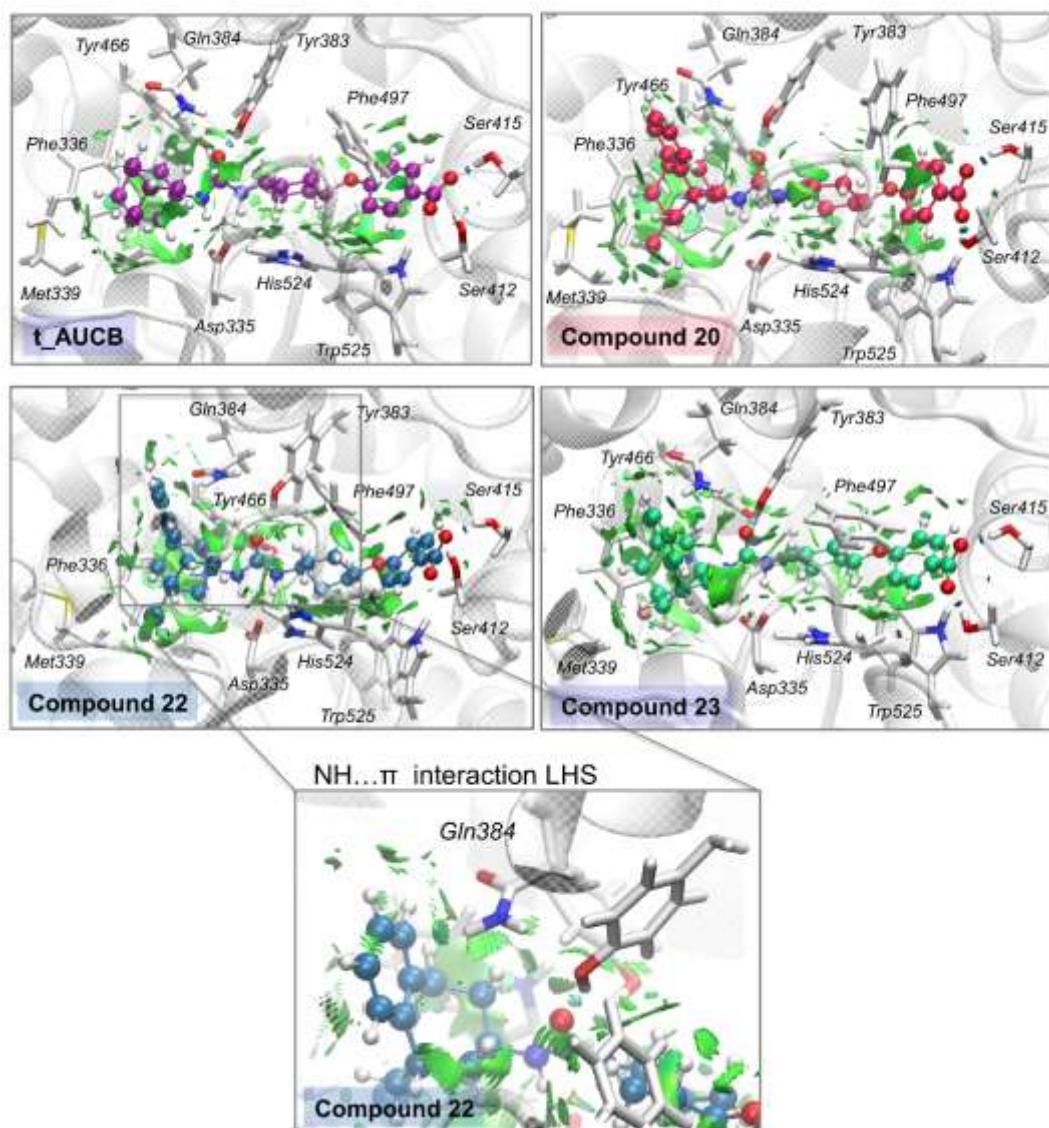


Figure S1: Representation of the noncovalent interactions (computed with NCIPLOT) at the active site of soluble epoxide hydrolase active site in the presence of compounds t-AUCB, **20**, **22**, and **23**. The weak interactions are shown as green surfaces, hydrogen-bonds are depicted in blue, and repulsive interactions in red. The interaction surface of the NH... π interaction between the side chain of Gln384 and the aromatic ring of the benzohomoadamantane scaffold of compound **22** is highlighted. The non-covalent interactions are calculated for the representative structures of the most populated cluster obtained from the MD simulations.

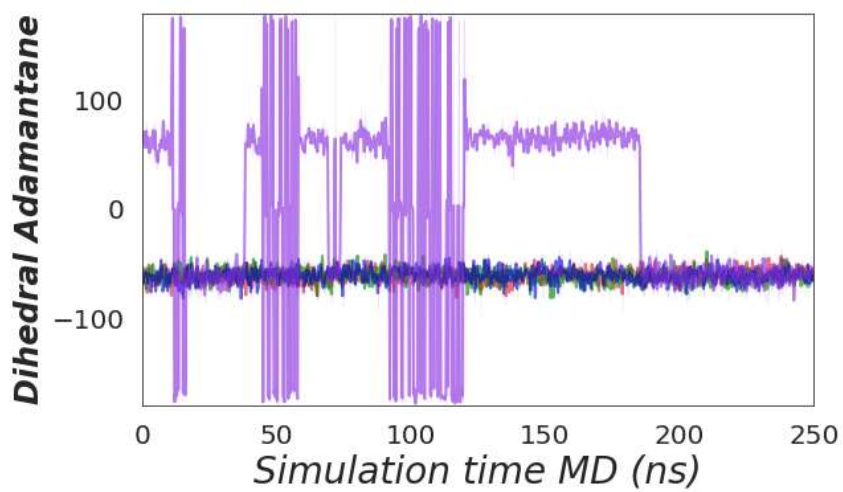


Figure S2: Plot of the dihedral angle that describes the rotation of the adamantane moiety in the LHS pocket of the sEH active site along the MD simulations. *t*-AUCB is shown in purple, compound **20** in red, compound **22** in blue, and compound **23** in green.

Time	ID	Total Concentration (ng/mL)	Mean (ng/mL)	SD (ng/mL)
0 h	Mouse 1	0	0	0
	Mouse2	0		
	Mouse3	0		
0.25 h	Mouse 1	787	767.5	27.6
	Mouse2	5400 ^a		
	Mouse3	748		
0.5 h	Mouse 1	1470	1610.0	475.7
	Mouse2	2140		
	Mouse3	1220		
1 h	Mouse 1	1000	970.3	345.5
	Mouse2	1300		
	Mouse3	611		
2 h	Mouse 1	475	397.3	112.8
	Mouse2	449		
	Mouse3	268		
4 h	Mouse 1	0	51.9	45.4
	Mouse2	71.3		
	Mouse3	84.3		
6 h	Mouse 1	21.7	37.3	14.3
	Mouse2	40.2		
	Mouse3	49.9		
24 h	Mouse 1	0	0	0
	Mouse2	0		
	Mouse3	0		

Table S2: Mean of concentrations of **20** in mouse plasma at different times after ip administration at 3 mg/Kg. ^aThis mouse was excluded for mean and SD calculations because it was considered as a significant outlier P<0.05.

Time	ID	Total Concentration (ng/mL)	Mean (ng/mL)	SD (ng/mL)
	Mouse 1	0		
0 h	Mouse2	0	0	0
	Mouse3	0		
	Mouse 1	151		
0.25 h	Mouse2	291	354.7	241.9
	Mouse3	622		
	Mouse 1	1350		
0.5 h	Mouse2	1520	1616.7	325.9
	Mouse3	1980		
	Mouse 1	600		
1 h	Mouse2	1100	1446.7	1063.3
	Mouse3	2640		
	Mouse 1	2440.0		
2 h	Mouse2	2640.0	3583.3	1089.9
	Mouse3	5670.0		
	Mouse 1	1240.0		
4 h	Mouse2	1960.0	1516.7	387.9
	Mouse3	1350.0		
	Mouse 1	1160		
6 h	Mouse2	734.0	1141.3	398.3
	Mouse3	1530		
	Mouse 1	181.0		
24 h	Mouse2	40.6	104.6	71.0
	Mouse3	92.3		

Table S3: Mean of concentrations of **22** in mouse plasma at different times after ip administration at 3 mg/Kg.

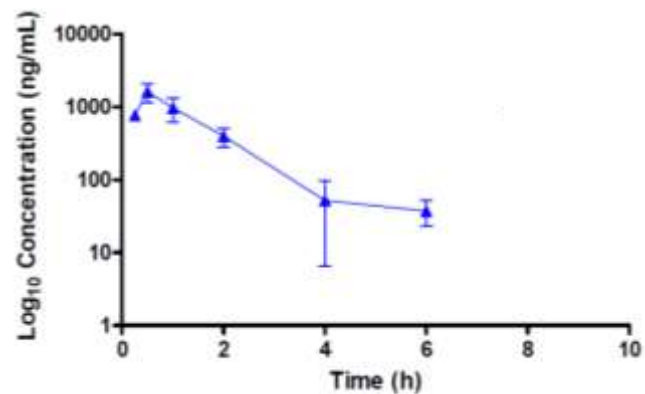


Figure S3: Plasma concentration (scale log 10) vs time for ip administration at 3 mg/Kg of compound **20**.

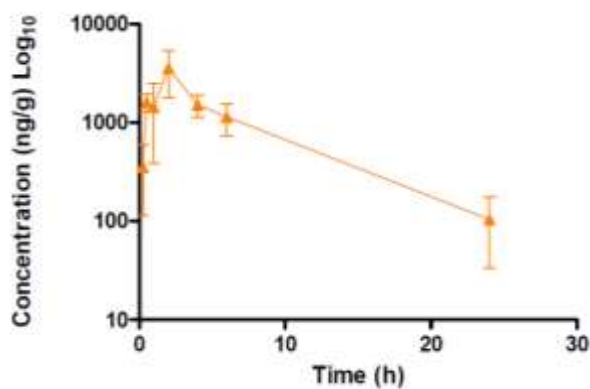


Figure S4: Plasma concentration (scale log 10) vs time for ip administration at 3 mg/Kg of compound **22**.

Control Group	Sample 1	Sample 2	Sample 3	Sample 4	Sample 5
<i>Parenchymal atrophy</i>	0	0	0	0	0
<i>Vacuolar degeneration of cells</i>	0	0	0	0	0
<i>Edema</i>	0	0	0	0	0
<i>Hemorrhage</i>	0	0	0	0	0
<i>Mononuclear inflammatory cells</i>	0	0	0	0	0
<i>Polimorfonuclear inflammatory cells</i>	0	0	0	0	0
<i>Necrosis</i>	0	0	0	0	0
<i>Total</i>	0	0	0	0	0

Table S4: Histologic scoring of pancreatic tissues of control group.

Cerulein Group	Sample 1	Sample 2	Sample 3	Sample 4	Sample 5
<i>Parenchymal atrophy</i>	2	2	3	1	2
<i>Vacuolar degeneration of cells</i>	1	2	2	1	2
<i>Edema</i>	2	1	2	2	2
<i>Hemorrhage</i>	0	0	0	0	0
<i>Mononuclear inflammatory cells</i>	1	1	2	1	1
<i>Polimorfonuclear inflammatory cells</i>	1	2	3	1	2
<i>Necrosis</i>	1	0	2	1	0
<i>Total</i>	8	8	14	7	9

Table S5: Histologic scoring of pancreatic tissues of mice treated with cerulein.

Cerulein + 22 (0.1 mg/Kg)	Sample 1	Sample 2	Sample 3	Sample 4	Sample 5
<i>Parenchymal atrophy</i>	3	1	0	1	3
<i>Vacuolar degeneration of cells</i>	1	0	0	0	2
<i>Edema</i>	2	3	0	1	2
<i>Hemorrhage</i>	0	0	0	0	0
<i>Mononuclear inflammatory cells</i>	1	0	0	0	0
<i>Polimorfonuclear inflammatory cells</i>	1	2	0	1	3
<i>Necrosis</i>	2	1	0	0	0
<i>Total</i>	10	7	0	3	11

Table S6: Histologic scoring of pancreatic tissues of mice treated with cerulein and 22 at 0.1 mg/kg.

Cerulein + 22 (0.3 mg/Kg)	Sample 1	Sample 2	Sample 3	Sample 4	Sample 5
<i>Parenchymal atrophy</i>	1	0	1	1	2
<i>Vacuolar degeneration of cells</i>	0	0	1	0	1
<i>Edema</i>	1	1	1	1	0
<i>Hemorrhage</i>	0	0	0	0	0
<i>Mononuclear inflammatory cells</i>	0	0	0	0	0
<i>Polimorfonuclear inflammatory cells</i>	1	0	1	1	1
<i>Necrosis</i>	0	0	0	0	0
<i>Total</i>	3	1	4	3	4

Table S7: Histologic scoring of pancreatic tissues of mice treated with cerulein and 22 at 0.3 mg/kg.

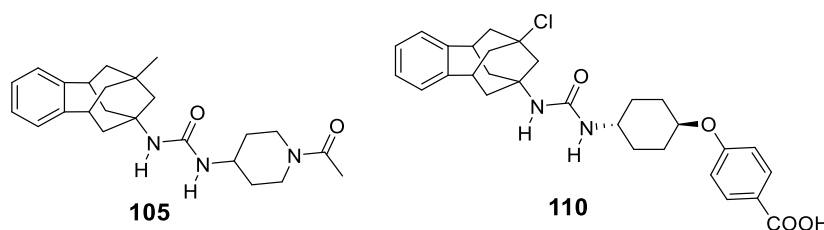
CHAPTER 4

BENZOHOMOADAMANTANE-BASED

sEHIs (II)

Introduction

As shown in the previous Chapter of the present Thesis, the replacement of the adamantane moiety or the aromatic ring of known sEHs by the benzohomoadamantane scaffold led to potent compounds endowed with favourable DMPK properties. Indeed, the *t*-AUCB analog **110** showed efficacy in an *in vivo* model of AP. Nevertheless, the substitution of the hydrophobic moiety of the clinical candidate AR9281 by the new polycyclic scaffold led to compound **105** endowed with excellent inhibitory potency against the human and murine sEH but with limited water solubility and very poor microsomal stability in human and mouse species (Table 4).



Cpd	sEH IC ₅₀ (nM) ^a		Microsomal Stability ^b (h/m)	Solubility ^c (μM)
	human	murine		
105	4	6.0	1/0.5	38
110	0.4	0.4	89/29	13

Table 4. Structure and properties of **105** and **110**. ^aReported IC₅₀ values are the average of three replicates. The fluorescent assay as performed here has a standard error between 10 and 20% suggesting that differences of two-fold or greater are significant. Because of the limitations of the assay it is difficult to distinguish among potencies < 0.5 nM.²⁰⁹ ^bPercentage of remaining compound after 60 min of incubation with human and mice microsomes obtained from Tebu-Xenotech in the presence of NADP at 37 °C. ^cSolubility in a 1% DMSO : 99% PBS buffer solution.

Taking into account that the clinical candidates AR9281 and EC5056 present similar structures featuring a piperidine moiety in their RHS, in this work we have synthesized a new family of benzohomoadamantane-based piperidine derivatives exploring urea and amide groups as the main pharmacophores, the position R of the scaffold and the substituent of the piperidine (R'), replacing the acetyl group of **105** by other fragments selected from previous series of known sEHs.^{113,114}

With these explorations, we expected the new compounds to improve the solubility and, more important, the microsomal stability values of **105** while keeping its excellent inhibitory activity (Figure 36).

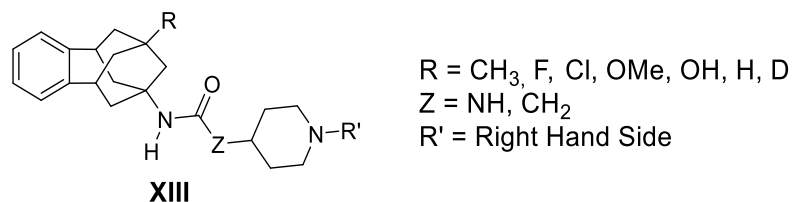


Figure 36. General structure **XIII** of the new family of sEHIs.

Discussion

3.4.2

The synthesis of the new compounds was performed in a similar way than that used for the obtention of **105**. Therefore, the synthesis of the corresponding benzohomoadamantane amines was first required. Apart from the polycyclic amines **82**, **83** and **84** featuring a methyl, chlorine and fluorine atoms in the R position, whose synthesis has been shown in the previous Chapter of the present Thesis (See Scheme 18, Chapter 3), amines **112-115** were also synthesized in order to further explore the R position of the polycyclic scaffold (Figure 37).

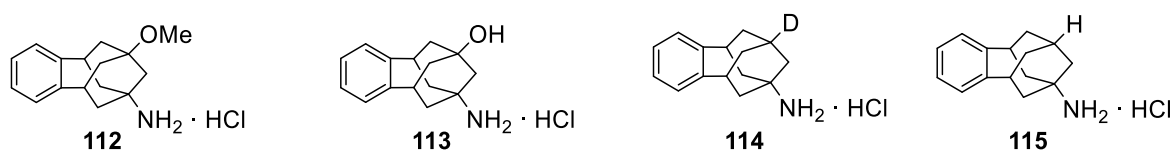
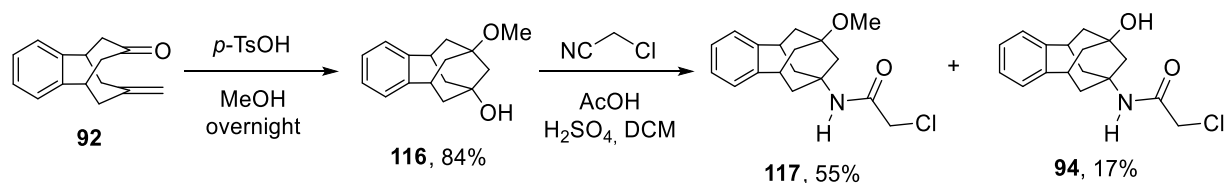


Figure 37. New benzohomoadamantane amines **112-115**.

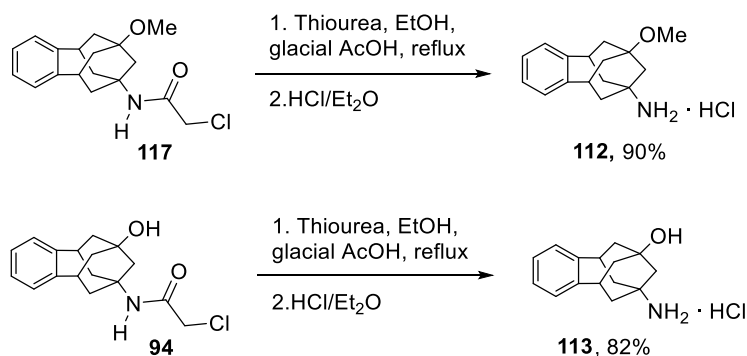
For the obtention of **112**, enone **92** was treated with *p*-toluenesulfonic acid and methanol providing alcohol **116**, which was subjected to a Ritter reaction affording the corresponding chloroacetamide **117** in moderate yield. In this reaction, the mechanism involved the protonation of the hydroxyl group and the formation of a tertiary carbocation. Then, the reaction continued with the addition of the nitrogen atom of the nitrile group to the carbocation, as shown in Scheme 13 (Chapter 3). Of note, after the work-up and the purification of the reaction mixture by column chromatography, in addition to the expected chloroacetamide **117** isolated in 55% yield, we were able to

isolate and fully characterized a significant side product, the chloroacetamide **94**, isolated in 17% yield. Very likely this impurity results from the protonation of the methoxy group, followed by elimination of methanol, trapping of the carbocation by acetate and hydrolysis during the work-up (Scheme 21).



Scheme 21. Synthesis of acetamide **117**.

Amines **112** and **113** were then obtained by deprotection of the acetamides **117** and **94** using thiourea and glacial acetic acid in absolute ethanol at reflux. Once deprotected, **112** and **113** were treated with an excess of hydrogen chloride in diethyl ether to obtain the corresponding hydrochlorides in excellent yields (Scheme 22).

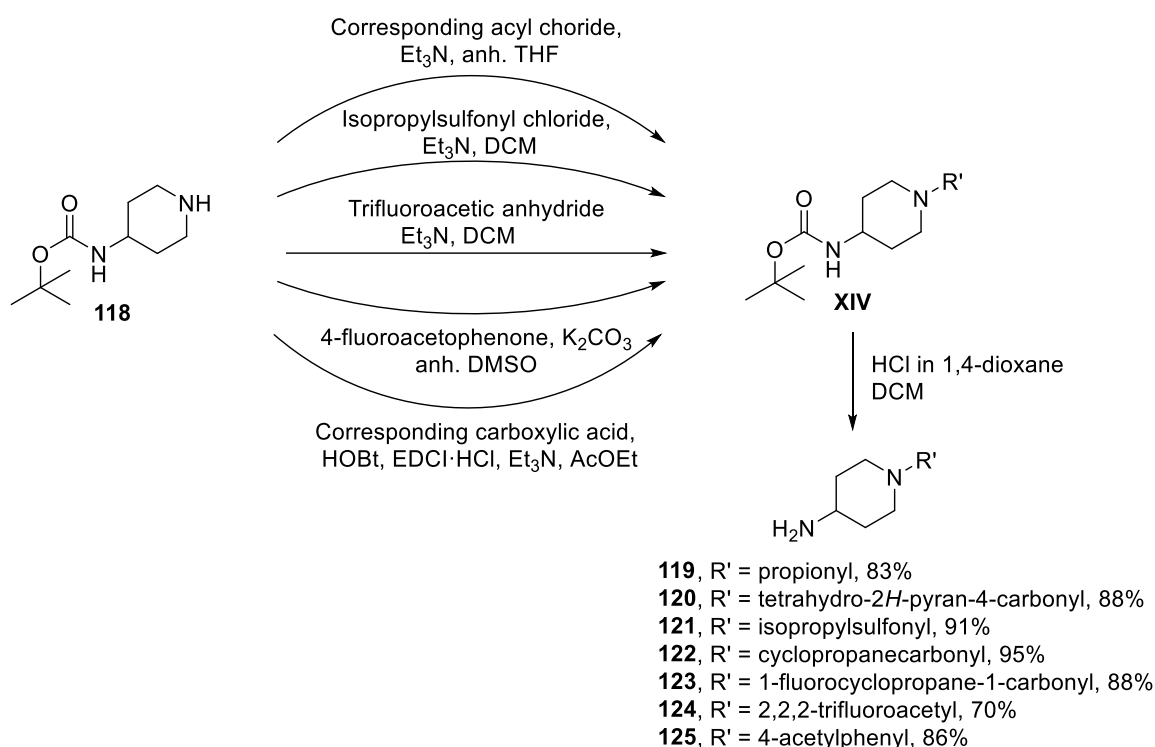


Scheme 22. Deprotection of acetamides **117** and **94**.

It should be noted that while the present Thesis was ongoing, a colleague within our group, Andreea L. Turcu, was also working on her PhD Thesis, partially focused on the synthesis of new benzohomoadamantane amines as blockers of the NMDA channel of the glutamate.²¹⁸ Hence, she was the responsible for the synthesis of the new polycyclic amines **114** and **115**, which were used in this work as starting materials for the synthesis of some of the new sEHIs (Figure 37).

²¹⁸ Turcu, A. L. Ph.D. Dissertation, University of Barcelona, in progress.

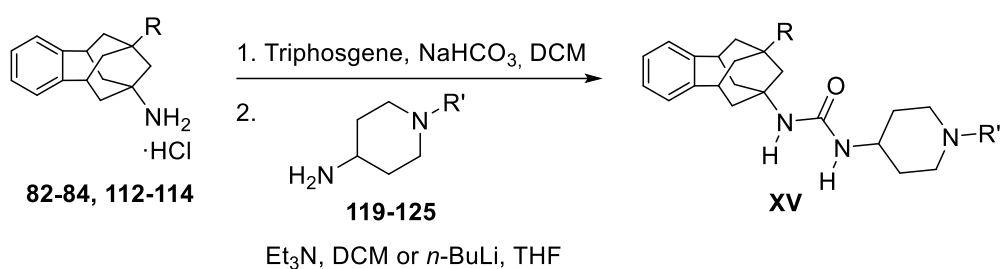
Once the polycyclic amines (LHS) of the new sEHIs were obtained, the next step was the obtention of the RHS, that is, the substituted piperidines. Unlike the 1-acetyl-4-aminopiperidine that was commercially available, the other substituted piperidines were prepared starting from the commercially available boc-protected aminopiperidine **118** following standard procedures (Scheme 23). Therefore, the reaction of **118** with selected acyl and sulfonyl chlorides led to several substituted piperidines of general structure **XIV**. Alternatively, the reaction of amine **118** with carboxylic acids in the presence of coupling agents furnished the corresponding amides. Finally, and following a disclosed procedure,²¹⁹ the reaction of **118** with 4-fluoroacetophenone in the presence of potassium carbonate in anhydrous DMSO afforded the 4-acetylphenyl-boc-protected aminopiperidine through a nucleophilic aromatic substitution. Subsequently, the protecting group of the piperidines of general structure **XIV** was removed by the treatment with hydrogen chloride in 1,4-dioxane in DCM, giving the desired substituted piperidines **119-125** in good to excellent overall yields (Scheme 23).



Scheme 23. Synthesis of the substituted piperidines **119-125**.

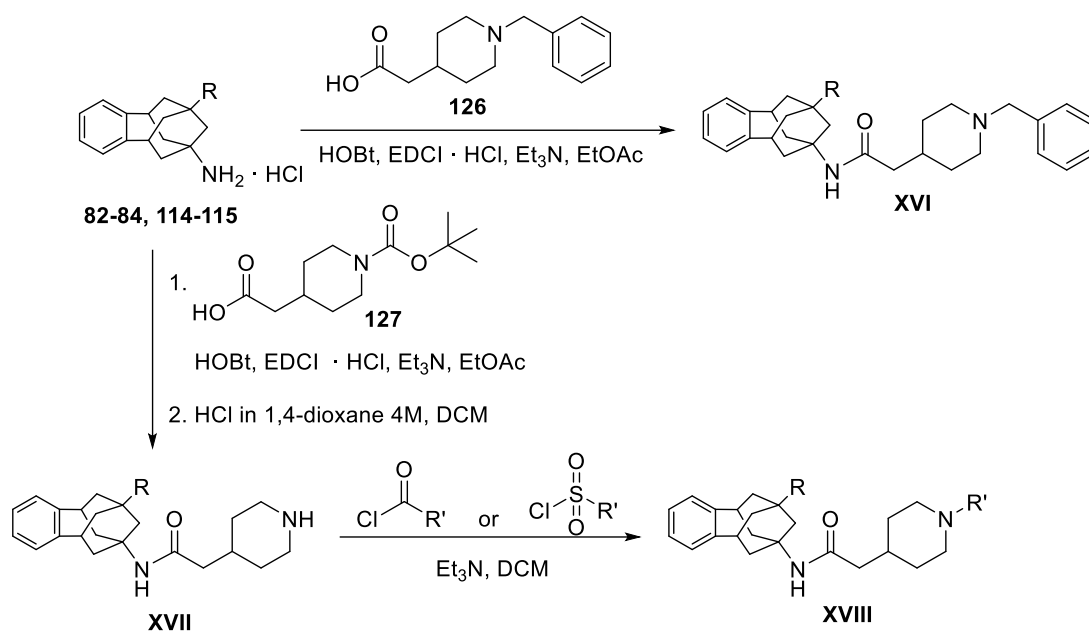
²¹⁹ Xie, L.; Ochterski, J. W.; Gao, Y.; Han, B.; Caldwell, T. M.; Xu, Y.; Peterson, J. M.; Ge, P.; Ohliger, R. (Neurogen). WO2007/016496 A2, August 2, 2005.

Finally, the new ureas were obtained following the procedure previously applied in the present Thesis. Thus, the reaction of the corresponding benzohomoadamantane amines **82-84** and **112-114** with triphosgene in an aqueous solution of sodium hydrogen carbonate and dichloromethane afforded the isocyanates. Then, the addition of the corresponding substituted aminopiperidines **119-125** in dichloromethane provided the desired ureas of general structure **XV**. Of note, for the obtention of ureas **133** and **145**, derived from **121**, the use of a strong base such as *n*-butyllithium was required for increasing the nucleophilic character of the 1-(isopropylsulfonyl)piperidin-4-amine (Scheme 24).



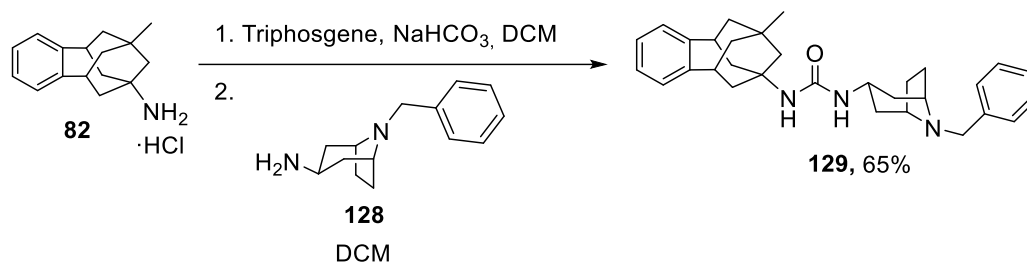
Scheme 24. General synthetic pathway for the obtention of the new urea-based sEHI.

Additionally, amide-based sEHIs were also synthesized in order to further explore the main pharmacophore of this new family. With this purpose, the corresponding polycyclic amine **82** was reacted with 2-(1-benzylpiperidin-4-yl)acetic acid in the presence of coupling agents in ethyl acetate affording amides with general structure **XVI** in good yields. On the other hand, the synthesis of amides of general structure **XVIII** involved the reaction of the polycyclic amines **82-84**, **114** and **115** with 2-[1-(*tert*-butoxycarbonyl)piperidin-4-yl]acetic acid in the presence of coupling agents in ethyl acetate to obtain the corresponding boc-protected amides, followed by removal of the boc group in acidic media to obtain amides with general structure **XVII**. Then, the addition of the corresponding acyl chlorides or sulfonyl chlorides furnished the desired amides of general structure **XVIII** in moderate yields (Scheme 25).



Scheme 25. General synthetic pathway for the obtention of the new amide-based sEHIs.

To close this new family, and in order to explore the impact of having a bridge in the piperidine moiety, compound **129** was synthesized in good yield by the reaction of the isocyanate derived from amine **82** with the commercially available 8-benzyl-8-azabicyclo[3.2.1]octan-3-*exo*-amine **128** in dichloromethane (Scheme 26).



Scheme 26. Synthesis of urea **129**.

The structures of all the benzohomoadamantane-based piperidine derivatives with general structure **XIII** synthesized in the present Thesis are collected in Figure 38. It is noteworthy that some compounds of this project, which are coloured in grey, have been

synthesized during the writing of the present Thesis, in the context of the PhD Theses of Beatrice Jora²²⁰ and Juan Martín PhD Theses,²²¹ currently ongoing.

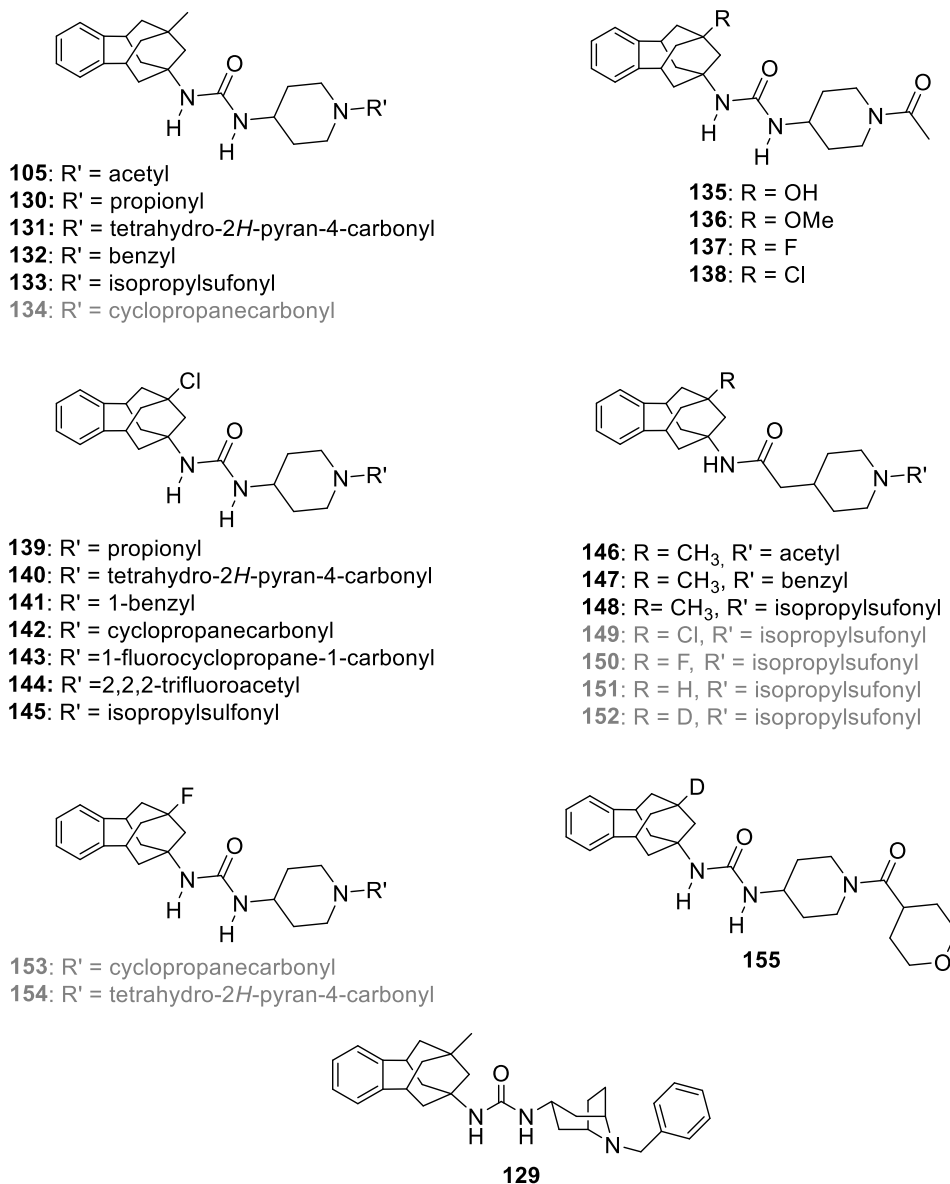


Figure 38. Structure of the new sEHI with general structure **XIII** synthesized in this work.

Then, this new family of compounds was subjected to a screening cascade in order to select a candidate for *in vivo* studies: potency as human and murine sEHIs, tested by Dr. Christophe Morisseau, from the group of Bruce D. Hammock at the UCD; microsomal

²²⁰ Jora, B. E. PhD Dissertation, University of Barcelona, in progress.

²²¹ Martín López, J. PhD Dissertation, University of Barcelona, in progress.

stability (human, mouse and rat species), hERG inhibition, CYP inhibition, solubility and permeability through Caco-2 cells, performed by the group of Prof. M. Isabel Loza and Prof. José M. Brea of the Drug Screening Platform/Biofarma Research Group of the University of Santiago de Compostela (Spain); PAMPA-BBB performed by Prof. Belén Pérez of the Autonomous University of Barcelona (Spain); cytotoxicity in SH-SY5Y cells evaluated by Drs Coral Sanfeliu and Rubén Corpas of the Institute of Biomedical Research of Barcelona (CSIC); and finally, selectivity over *h*LOX-5, measured by the group of Dr Maria I. Rodríguez Franco, from the Institute of Medicinal Chemistry (CSIC, Madrid); and *h*COX-2, assessed by the company Eurofins.

Taking into account that compound **105** presented high inhibitory activities against the human and murine enzymes but unacceptable stability against human and murine microsomes, we first decided to evaluate the potency and microsomal stability of some analogs of **105**, exploring the substituent R' of the piperidine ring. As reported in the draft manuscript, regardless of the substituent of the piperidine ring, all the compounds showed potency in the low nanomolar or subnanomolar range in both human and murine enzymes. However, the microsomal stability of the new ureas were similar than that of the compound **105**. Given that the microsomal stability was not improved with the exploration of the substitution of the piperidine moiety, we moved to another strategy.

Then, the next step was the change of the pharmacophore from urea to amide. Amides **146-148** showed to be less potent than their urea-counterparts **105**, **132** and **133**, respectively. Given that amide **148** presented human IC₅₀ in the low nanomolar range, its microsomal stability was evaluated. Regrettably, no compound was detected after being incubated for 1h with human and murine microsomes.

Therefore, the next strategy for improving the stability of the compounds was the exploration of the R position of the polycyclic scaffold. As expected, those compounds bearing a polar group in R position, **135** and **136**, presented higher IC₅₀ values than **105**. In contrast, when the methyl group of the previous benzohomoadamantane-based sEHIs was replaced by halogen atoms, the compounds presented inhibitory activities in the low nanomolar or subnanomolar range. Additionally, and more important, all the compounds featuring halogen atoms in the R position exhibited highly improved stabilities in human, mice and rat microsomes than their methyl analogs.

Given these good results, some analogs of the most potent amide **148** exploring its R position were then synthesized and evaluated, replacing its methyl group by chlorine,

fluorine, hydrogen and deuterium atoms with the aim to improve the poor microsomal stability of the previously synthesized amide derivatives. Of note, the new amides exhibited better inhibitory potencies than their methylated analog **148**, but the microsomal stabilities were not enhanced. For this reason, no further amides were synthesized.

Taking into account the potency and the microsomal stability of the new sEHIs, ureas **139**, **140**, **142**, **143**, **144**, **145**, **153** and **154** were selected and further evaluated in terms of solubility, BBB predicted permeation, cytochrome inhibition and cytotoxicity. Finally, we selected compound **140**, endowed with excellent inhibitory activity, good solubility and microsomal stability values and significant selectivity over cytochromes, *h*LOX-5 and *h*COX-2, for *in vivo* studies in a predictive murine model of NP. The biological profile of the selected compound is collected in Table 5.

Before conducting the *in vivo* efficacy study, we performed a PK assay which proved that the intraperitoneal administration of **140** led to good bioavailability and elimination characteristics.

As a final point, the *in vivo* efficacy study was performed. Certainly, murine models of NP are somehow difficult as they involve, for example, surgery²²² (e.g., peripheral nerve ligation model) or pre-treatments with metabolic (e.g., diabetic NP) or toxic agents²²³ (e.g., chemotherapy-induced NP models).^{224,225} For this reason, a very predictive model used for testing putative efficacy in NP is the capsaicin murine model of allodynia.²²⁶ Although it is not strictly a NP model, typically active compounds in the capsaicin model show analgesia in NP models.

The study in the capsaicin murine model was carried out by Dr. José Manuel Entrena and Dr. Enrique J. Cobos, from the Universidad de Granada. This study demonstrated that **140** reduced mechanical allodynia in a dose-dependent manner and outperformed other sEHI tested, such as TPPU and AS2586114. Taking into account these promising results, further studies with **140** in NP models are ongoing. The results of this work are disclosed in a draft article included in the following pages of this Thesis.

²²² Challa, S. R. *Int J Neurosci.* **2015**, *125*, 170-174.

²²³ Hama, A.; Takamatsu, H. *CNS Neurol Disord Drug Targets* **2016**, *15*, 7-19.

²²⁴ Colleoni, M.; Sacerdote, P. *Biochim. Biophys. Acta* **2010**, *1802*, 924-933.

²²⁵ Gao, F.; Zheng, Z. M. *Exp Clin Endocrinol Diabetes* **2014**, *122*, 100-106.

²²⁶ Baron, R. *Lancet* **2000**, *356*, 785-786.

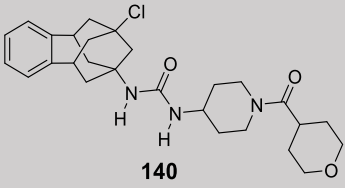
Compound		
sEH IC ₅₀ (nM)		Human: 0.4 Mice: 0.1 Rat: 0.4
PAMPA-BBB		CNS+
Solubility in 1% DMSO:99% PBS buffer (μM)		57
Liver microsomal stability (% parent at 60 min)		Human: 47 Mice: 64 Rat: 46
Selectivity over CYP2C19 (% inh. at 10 μM)		38 ± 4
hERG (% inh. at 10 μM)		1 ± 2
hCOX-2 IC ₅₀ (μM)		<i>pending</i>
hLOX-5		>100
Cytotoxicity – LD ₅₀ (μM) (SH-SY5Y cells)		Propidium iodide >100 MTT >100
Permeability (Caco-2 cells)	-Papp (nm/s) A→B	5.56
	B→A	17.6
	-Efflux Ratio	3.1

Table 5. Biological profiling of the selected compound **140**.

As mentioned, some compounds of this project were synthesized and evaluated during the writing of the present Thesis, such as compounds **153** and **154**, that presented enhanced biological profiles than **140**. Hence, new *in vivo* studies with these two compounds are envisaged, starting with PK assays and, depending on these results, a new efficacy study in the capsaicin murine model of allodynia.

Noteworthy, the new sEHIs described herein bearing the benzohomoadamantane scaffold as well as the ones described in Chapters 3 and 5 of the present Thesis have been protected by a patent application,²¹⁷ which is currently under exam. The mentioned document is attached at the end of the Chapter 5.

^{3.4.3}
Synthesis, *in vitro* profiling and *in vivo*
evaluation of benzohomoadamantane-based
soluble epoxide hydrolase inhibitors for
neuropathic pain

*Sandra Codony¹, José Entrena², Carla Calvó-Tusell³, Juan Martín¹, Beatrice Jora¹,
Ferran Feixas³, Rubén Corpas⁴, Christophe Morisseau⁵, Andreea L. Turcu¹, Belén
Pérez⁶, Concepción Pérez⁷, María Isabel Rodríguez-Franco⁷, José M. Brea⁸, Coral
Sanfeliu⁴, Silvia Osuna^{3,9}, Bruce D. Hammock⁵, Enrique J. Cobos², M. Isabel Loza⁸,
Santiago Vázquez^{1*}*

¹Laboratori de Química Farmacèutica (Unitat Associada al CSIC), Facultat de Farmàcia i Ciències de l'Alimentació, and Institute of Biomedicine (IBUB), Universitat de Barcelona, Av. Joan XXIII, 27-31, 08028 Barcelona, Spain.

² Department of Pharmacology, School of Medicine, University of Granada, Avenida de la Investigación 11, 18016, Granada, Spain.

³CompBioLab Group, Departament de Química and Institut de Química Computacional i Catàlisi (IQCC), Universitat de Girona, C/ Maria Aurèlia Capmany 69, 17003 Girona, Spain.

⁴Institute of Biomedical Research of Barcelona (IBB), CSIC and IDIBAPS, Barcelona, Spain, and CIBER Epidemiology and Public Health (CIBERESP), Madrid, Spain.

⁵Department of Entomology and Nematology and Comprehensive Cancer Center, University of California, Davis, CA 95616, USA.

⁶Department of Pharmacology, Therapeutics and Toxicology, Institute of Neurosciences, Autonomous University of Barcelona, 08193 Bellaterra, Barcelona, Spain.

⁷Institute of Medicinal Chemistry, Spanish National Research Council (CSIC), C/Juan de la Cierva 3, 28006 Madrid, Spain.

⁸Drug Screening Platform/Biofarma Research Group, CIMUS Research Center. University of Santiago de Compostela (USC), Santiago de Compostela, Spain.

⁹Institució Catalana de Recerca i Estudis Avançats (ICREA), Barcelona, Spain.

KEYWORDS: benzohomoadamantane, neuropathic pain, soluble epoxide hydrolase, urea.

ABSTRACT

The soluble epoxide hydrolase (sEH) has been suggested as a pharmacological target for the treatment of several diseases including pain-related disorders. Taking into account that both adamantane and aromatic ring moieties fit very well in the hydrophobic pocket of the sEH and that the replacement of the adamantane nucleus of known sEH inhibitors (sEHI) by larger polycyclic rings is a good strategy to obtain very potent sEHI, we recently found that the substitution of the adamantane moiety of the clinical candidate AR9281 by the larger benzohomoadamantane scaffold led to very potent sEHI, but endowed with moderate experimental solubility and very poor stability in human and mouse microsomes. Herein, we report further medicinal chemistry around new benzohomoadamantane-based piperidines in order to improve the solubility and microsomal stability values of the previous hit. After a screening cascade (solubility, cytotoxicity, metabolic stability, CYP450s, hLOX-5, hCOX-2 and hERG inhibition), we selected a candidate with improved DMPK properties that was subsequently studied in a predictive *in vivo* model of NP. Our candidate reduced pain in the capsaicine-induced model of allodynia in a dose-dependent manner and outperformed other sEHI tested.

INTRODUCTION

Arachidonic acid (AA) is an essential ω -6, 20-carbon polyunsaturated fatty acid that is abundant in the phospholipids of cellular membrane. In response to a stimulus, phospholipase A2 promotes its cleavage from the membrane being released to the cytosol, where it can be metabolized leading to different classes of eicosanoids via three pathways.^{1,2} The cyclooxygenase (COX) pathway catalyses the production of prostaglandins (PGs), prostacyclins (PGIs) and thromboxanes (TXs), endowed with inflammatory properties. The lipoxygenase (LOX) pathway generates leukotrienes (LTs) which play a significant part in the cause of asthma, arthritis, allergy and inflammation.³ Both pathways have been extensively studied and pharmaceutically targeted.⁴⁻⁶ More recently, increasing attention is being paid to the third branch of the AA cascade, the cytochrome P450 (CYP) pathway that can convert AA to epoxyeicosatrienoic acids (EETs).⁷ EETs are reported to exhibit anti-inflammatory and anti-nociceptive properties,⁸ but they are rapidly degraded by the sEH enzyme (sEH, EPHX2, E.C. 3.3.2.3) to the less active or inactive corresponding dihydroxyeicosatrienoic acids (DHET). Therefore, sEH inhibition may lead to elevated EET levels thereby maintaining their beneficial properties.⁹⁻¹⁰ The use of selective sEH inhibitors (sEHI) in *in vivo* assays resulted in an increase of EET levels and the reduction of blood pressure and inflammatory and pain states. Thus, sEH has been suggested as a pharmacological target for the treatment of several diseases including pain-related disorders.¹¹⁻¹⁶

Given that sEH presents a hydrophobic pocket, several potent sEHI developed in the last years feature an adamantane moiety or an aromatic ring in their structure, such as AR9281, **1**, and EC5026, **3**, two of the sEHI that have reached clinical trials.¹⁷⁻¹⁸ The first to enter was the adamantane-based AR9281 by Arete Therapeutics for the treatment of

hypertension in diabetic patients, but failed largely because of its poor pharmacokinetic properties. Very recently, EicOsis has replaced the adamantane moiety of AR9281 by an aromatic ring for its drug candidate EC5026, currently in Phase 1 clinical trials for the treatment of neuropathic pain (NP). Interestingly, both clinical candidates present similar structures: a left hand side hydrophobic moiety (black), a urea group (green), a piperidine residue (blue) and a right hand side (RHS) acyl group (red) (Figure 1). Also, from the adamantane-based inhibitor **2**, Eicosis is currently advancing the analog **4** for veterinary clinical trials (Figure 1).

Taking into account that both adamantane and aromatic ring moieties fit very well in the hydrophobic pocket of the sEH and that the replacement of the adamantane nucleus of known sEHI by larger polycyclic rings is a good strategy to obtain very potent sEHI,¹⁹ we recently found that the substitution of the adamantane moieties of AR9281 and *t*-AUCB by the larger benzohomoadamantane scaffold led to the potent sEHI **5** and **6**, respectively (Figure 1). Further *in vitro* studies with these compounds demonstrated that while **5** had moderate experimental solubility and very poor stability in human and mouse microsomes, compound **6** was endowed with favorable DMPK properties and showed effectivity in *in vivo* models of acute pancreatitis.²⁰

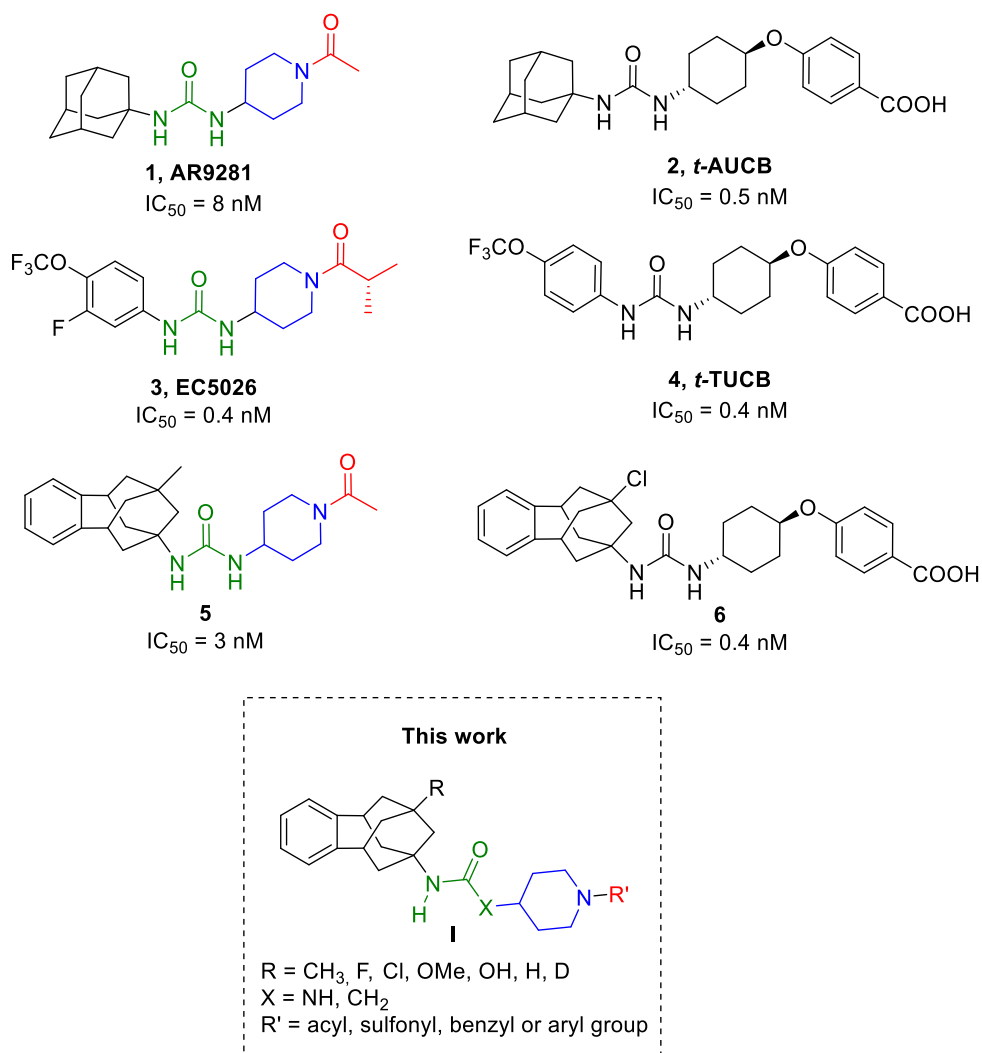


Figure 1. Structures and IC_{50} values in the human sEH of AR9281, **1**, *t*-AUCB, **2**, EC5026, **3**, *t*-TUCB, **4**, **5** and **6**, and general structure **I** of the new benzohomoadamantane-based piperidine derivatives reported on this work.

Herein, we report further medicinal chemistry around inhibitor **5**. New benzohomoadamantane-based piperidine derivatives featuring urea and amide groups as the main pharmacophores, different substituents in the position R of the polycyclic scaffold and a broad selection of substituents at the nitrogen atom of the piperidine (R') were synthesized in order to improve the solubility and microsomal stability values of the previous hit **5**. After a screening cascade, a selected candidate with improved DMPK properties was subsequently studied in a predictive *in vivo* model of NP and in a murine model of visceral pain.

RESULTS AND DISCUSSION

Synthesis of new sEHI. For the preparation of the new sEHI, amines **7a-7g**, previously described by our group, were used as starting materials (Figure 2).²¹⁻²⁴

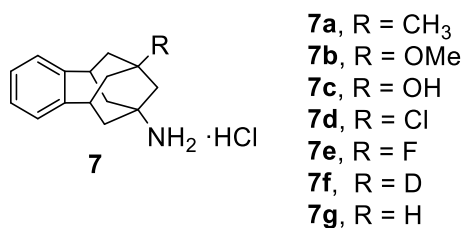
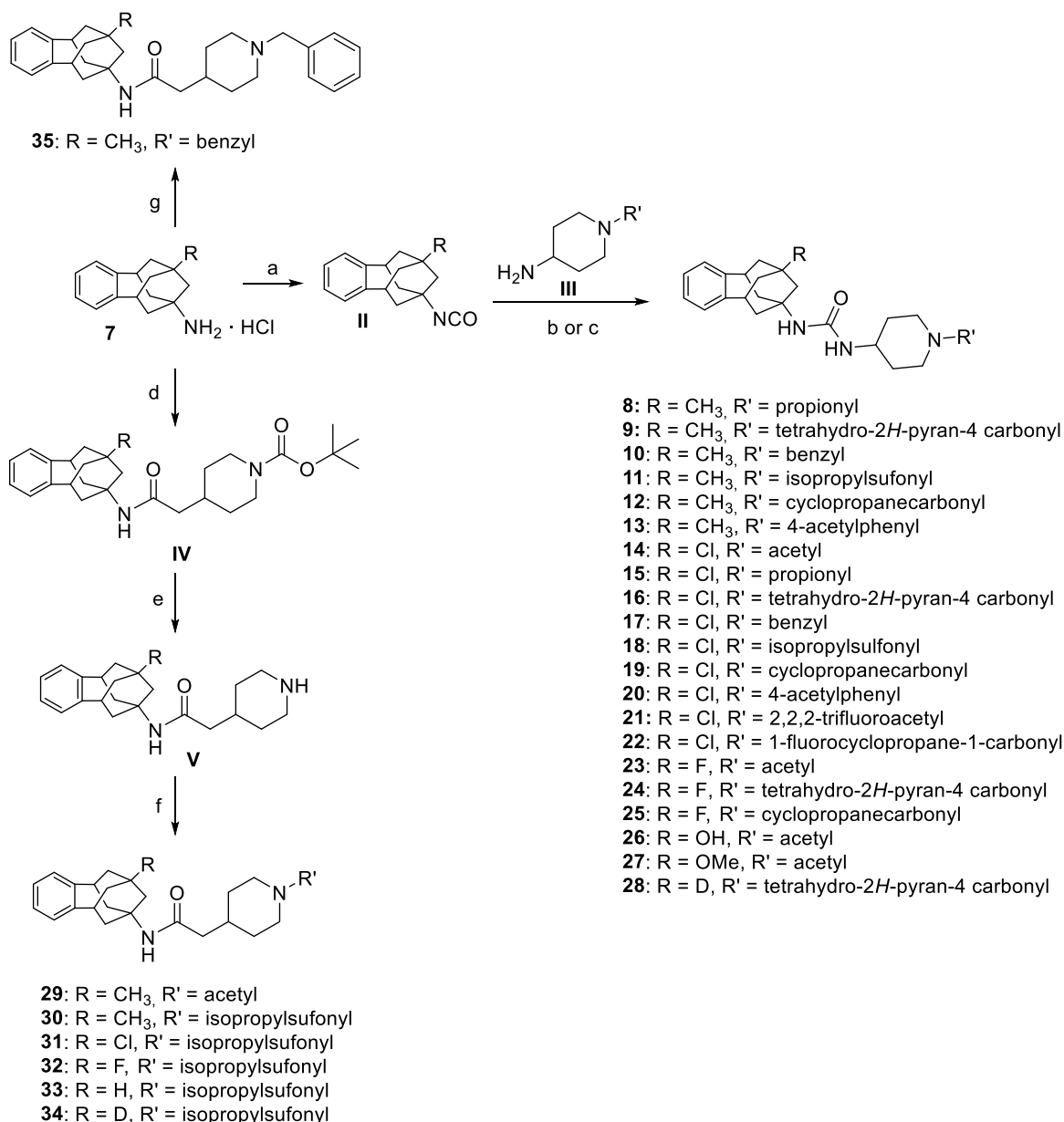


Figure 2. Benzohomoadamantane amines **7a-7g** used in this work.

The synthesis of the novel urea-based sEHI was straightforward and involved the reaction of the benzohomoadamantane amines **7a-g** with triphosgene to obtain the corresponding isocyanates, followed by the addition of the required substituted aminopiperidine of general structure **III** to form the final ureas **8-28** (Scheme 1).

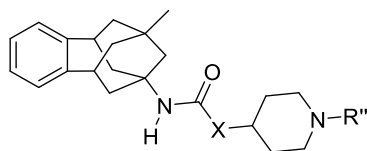
Given that amides were shown to also bind strongly to the catalytic side of the enzyme and that amides typically present improved water solubility over ureas,²⁵ we additionally synthesized some amides bearing the benzohomoadamantane scaffold. Amide **35** was obtained from amine **7a** and commercially available 2-(1-benzylpiperidin-4-yl)acetic acid in the presence of HOBt and EDCI. On the other hand, the synthesis of amides **29-34** involved the reaction of amines **7a** and **7d-g** with 2-(1-(*tert*-butoxycarbonyl)piperidin-4-yl)acetic acid in the presence of HOBt and EDCI to obtain the *N*-*boc*-protected piperidine amide of general structure **IV**. The removal of the *boc* group in acidic media followed by the addition of the corresponding acyl chloride or sulfonyl chloride furnished the desired amides **29-34** (Scheme 1).



Scheme 1. Synthesis of the new sEHI. a) Triphosgene, NaHCO₃, DCM, 30 min. b) DCM, overnight. c) *n*-BuLi, anh. THF, anh. DCM, overnight. d) 2-(1-(*tert*-butoxycarbonyl)piperidin-4-yl)acetic acid, HOBt, EDCI · HCl, Et₃N, EtOAc, 24 h. e) HCl / Dioxane 4 M, DCM, overnight. f) Corresponding acyl chloride or corresponding sulfonyl chloride, Et₃N, DCM. g) 2-(1-benzylpiperidin-4-yl)acetic acid, HOBt, EDCI · HCl, Et₃N, EtOAc, 24h. See experimental and supporting information for further details.

All the new compounds were fully characterized through their spectroscopic data and elemental analyses (see experimental and supporting information for further details).

sEH inhibition and microsomal stability. Compound **5** presented high inhibitory activities against the human and murine enzymes and moderate experimental aqueous solubility (38 μM), but unacceptable stability in human and murine microsomes (Table 1).²⁰ As it is known that the acyl chain of piperidine-based sEHI is a suitable position for metabolism,²⁶ we first decided to explore new piperidine derivatives replacing the acetyl group of **5** by other fragments selected from previous series of known sEHI.²⁷⁻²⁸ With this modification, we expected to maintain the excellent potency of **5** and to improve the microsomal stability. Compounds **8-13** were synthesized maintaining the methyl group in the position R of the benzohomoadamantane scaffold and replacing the acetyl group of **5** by propionyl, tetrahydro-2*H*-pyran-4 carbonyl, cyclopropanecarbonyl, isopropylsulfonyl, benzyl and 4-acetylphenyl groups, respectively (Scheme 1). The inhibitory activity against the human and murine enzymes of the new ureas was evaluated, as well as their stabilities in human, mice and rat microsomes (Table 1).



Compound	X	R'	sEH		Microsomal Stability ^b (h/m/r)
			IC ₅₀ (nM) ^a		
			Human	Murine	
5	NH		4	6	1/0.5/ND ^c
8	NH		1	10	0.8/0.2/0.0
9	NH		1	2.5	0.1/0.2/0.0

10	NH		0.4	0.4	30/66/0.2
11	NH		0.4	6.3	0.7/1.1/0.2
12	NH		1.5	18	0.1/0.6/ND
13	NH		2.9	21.8	0.7/1.1/0.2
29	CH ₂		115	0.4	ND
30	CH ₂		30	0.4	0.0/0.0/ND
35	CH ₂		413	21	ND

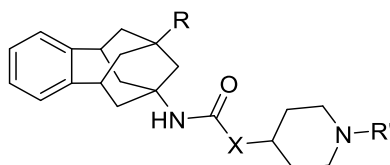
Table 1. Inhibition of human and murine sEH and microsomal stability values of known **5** and the new sEHI **8-13** and **29, 30** and **35**. ^aThe average of three replicates has been calculated to obtain the IC₅₀ values. This fluorescent assay has a standard error between 10 and 20% suggesting that differences of two-fold or greater are significant. The limitations of the assay show that it is difficult to distinguish among potencies < 0.5 nM.²⁹ ^bPercentage of remaining compound after 60 min of incubation with human, mice and rat microsomes obtained from Tebu-Xenotech in the presence of NADP at 37 °C. ^cND: not determined.

Gratifyingly, regardless of the substituent of the piperidine ring, all the compounds showed potency in the low nanomolar or even subnanomolar ranges in both the human and murine enzymes (Table 1). Interestingly, the most potent compound, **10**, presented inhibitory activities in the subnanomolar range for both enzymes. However, except for compound **10**, the microsomal stability of these new ureas was very poor, similar to that of the compound **5** (Table 1). Consequently, we moved to another strategy for improving the microsomal stability of the compounds. In this sense, we wondered if the replacement of the urea as a pharmacophore by an amide group may increase the microsomal stability.

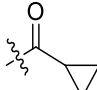
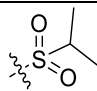
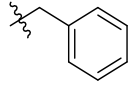
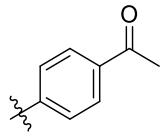
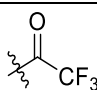
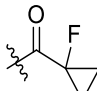
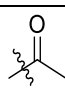
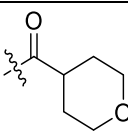
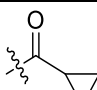
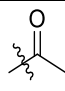
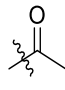
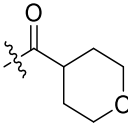
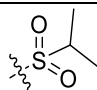
Additionally, it has been reported that amides typically present improved water solubility over ureas.²⁵ Considering this, amides **29**, **30** and **35** were synthesized and evaluated.

As shown in Table 1, for the human enzyme, the new amides **29**, **30** and **35** were less potent than their urea-counterparts **5**, **11** and **12**, respectively. Surprisingly, all the amides were potent inhibitors of the murine sEH. Overall, the best amide, **30**, presented human IC₅₀ in the low nanomolar range and its microsomal stability was evaluated. Unfortunately, no compound was detected after being incubated for 1 h with human and murine microsomes.

Therefore, the next step for improving the stability of the compounds was the exploration of the R position of the benzohomoadamantane scaffold, replacing the methyl group of the new urea-based inhibitors endowed with low nanomolar IC₅₀ values by other substituents such as halogen atoms or polar groups, in order to explore if the inhibitory activity was maintained while improving the microsomal stability.



Cpd	R	X	R'	sEH ^a		Microsomal Stability ^b (h/m/r)
				IC ₅₀ (nM) ^a		
				Human	Murine	
14	Cl	NH		1.6	0.8	50/8/0.1
15	Cl	NH		0.6	1.0	78/52/14
16	Cl	NH		0.4	1.0	47/64/46

17	Cl	NH		0.4	0.4	63/73/91
18	Cl	NH		0.6	1.1	97/96/95
19	Cl	NH		0.6	2.4	36/68/16
20	Cl	NH		0.9	2.3	31/1.8/1.2
21	Cl	NH		0.4	0.4	98/77/89
22	Cl	NH		0.6	0.8	99/68/97
23	F	NH		9	23	40/30/8
24	F	NH		0.4	0.5	66/84/58
25	F	NH		0.4	0.4	58/60/30
26	OH	NH		207	248	ND ^c
27	OMe	NH		48	1.0	ND
28	D	NH		0.4	0.4	49/89/48
31	Cl	CH ₂		1.0	0.4	7/1.4/0.0

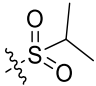
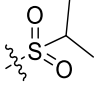
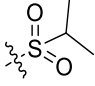
32	F	CH ₂		1.6	0.4	5.5/5.1/0.0
33	H	CH ₂		2.8	0.5	0.6/0.2/0.0
34	D	CH ₂		2.4	0.4	1.3/0.5/0.0

Table 2. Inhibition of human and murine sEH and microsomal stability of new sEHI **14-28** and **31-34**. ^aThe average of three replicates has been calculated to obtain the IC₅₀ values. This fluorescent assay has a standard error between 10 and 20% suggesting that differences of two-fold or greater are significant. The limitations of the assay show that it is difficult to distinguish among potencies < 0.5 nM.²⁹ ^bPercentage of remaining compound after 60 min of incubation with human, mice and rat microsomes obtained from Tebu-Xenotech in the presence of NADP at 37 °C. °ND: not determined.

The potency of these compounds was measured in the human and murine enzymes. As expected, taking into account that sEH presents a hydrophobic pocket, those compounds bearing a polar group in R position, **26** and **27**, presented higher IC₅₀ values than **5**. Of note, the most important drop in the inhibitory activity was produced by the replacement of the methyl group of **5** by the hydroxyl group leading to compound **26** (Table 2). In contrast, when the methyl group was replaced by chlorine or fluorine atoms, the inhibitory activities against the human and murine enzymes were maintained or even improved, as most of them presented IC₅₀ values in the low nanomolar or even the subnanomolar range (Table 2).

Then, the microsomal stability of the most potent compounds was evaluated. Gratifyingly, all the compounds featuring halogen atoms in the R position of the benzohomoadamantane scaffold presented improved stabilities in human, mice and rat microsomes than their methyl-analogs (Table 2). Satisfyingly, the chlorinated compounds **18**, **21** and **22** exhibited excellent microsomal stabilities in the three species.

Given that the substitution of the methyl group by other radicals seemed to be a promising strategy for increasing the microsomal stability of the compounds while maintaining or even improving the inhibitory activity, some analogs of amide **30** were then synthesized and evaluated (**31-34**). In this series, the methyl group of **30** was replaced by chlorine, fluorine, hydrogen and deuterium atoms. Once again, the new amides presented inhibitory activities in the low or subnanomolar range in both human and murine sEH, exhibiting all of them higher inhibitory potencies than their methyl analog **30**. Regrettably, the microsomal stabilities were not enhanced, detecting in all cases less than 10% of the compound after being incubated for 1 h with human, murine and rat microsomes. Therefore, the replacement of the methyl group by other radicals in the amide series did not improve their microsomal stabilities, and amides were not further explored.

Further profiling of the selected inhibitors. Taking into account the potency and the microsomal stability of the halogen-substituted sEHI, eight compounds were selected for further evaluation. Therefore, the compounds that exhibited excellent inhibitory activities and that remained unaltered more than 50% after the incubation with human and murine microsomes, moved forward in the screening cascade. Next, solubility, permeability through the blood-brain barrier (BBB), cytotoxicity and cytochrome inhibition of the selected compounds **15**, **16**, **17**, **18**, **21**, **22**, **24** and **25** were experimentally measured.

While compounds **15**, **17**, **18**, **21** and **22** exhibited limited solubility values lower than 20 μM , compounds **16**, **24** and **25** displayed good to excellent solubility values. Additionally, the selected compounds were further tested for predicted brain permeation in the widely used *in vitro* parallel artificial membrane permeability assay-blood brain barrier (PAMPA-BBB) model.³⁰ Compounds **15**, **16** and **25** showed CNS+ proving their potential capacity to reach CNS, whereas the other compounds presented uncertain BBB permeation (CNS+/-). Next, the cytotoxicity of the new sEHI was tested using the

propidium iodide (PI) and MTT assays in SH-SY5Y cells. Interestingly, none of the selected compounds showed to be cytotoxic at the highest concentration tested (100 μ M) (Table 4).

Compound	Solubility ^a (μ M)	PAMPA-BBB	Toxicity LD ₅₀ (μ M)		Cytochrome inhibition ^d	
			PI ^b	MTT ^c	CYP 2C9	CYP 2C19
15	18	CNS +	>100	>100	30 \pm 4	46 \pm 3
16	57	CNS +	>100	>100	34 \pm 1	38 \pm 4
17	19	CNS +/-	>100	>100	34 \pm 2	1.5 μ M
18	19	CNS +/-	>100	>100	38 \pm 1	1.48 μ M
21	16	CNS +/-	>100	>100	54 \pm 1	0.63 μ M
22	17	CNS +/-	>100	>100	43 \pm 3	0.78 μ M
24	95	CNS +/-	>100	>100	30 \pm 3	32 \pm 4
25	92	CNS +	>100	>100	17 \pm 2	26 \pm 5

Table 4. Solubility values, PAMPA-BBB, toxicity and cytochrome inhibition of selected sEHI. ^aSolubility measured in a 1% DMSO: 99% PBS buffer solution. ^bsEHI cytotoxicity tested by propidium iodide (PI) staining after 24h incubation in SH-SY5Y cells. ^csEHI cytotoxicity tested by 3-[4,5-dimethylthiazole-2-yl]-2,5-diphenyltetrazolium bromide (MTT) assay after 24h incubation in SH-SY5Y cells. ^dThe cytochrome inhibition was tested at 10 μ M. IC₅₀ was calculated for those compounds that presented >50% of inhibition. See the experimental section for further details.

Finally, cytochromes inhibition was measured, taking special attention to CYPs 2C19 and 2C9, as these isoforms are two of the main producers of EETs, the substrates of the sEH. Unfortunately, compounds **17**, **18**, **21** and **22** inhibited CYP 2C19 in the low micromolar range. In contrast, compounds **15**, **16**, **24** and **25** did not inhibit significantly these subfamilies of cytochromes (Table 3). Additionally, CYPs 2D6, 1A2 and 3A4 were also evaluated, showing IC₅₀ values higher than 10 μ M for all the selected compounds (see Table S1 in the Supporting Information).

After performing the screening cascade, we selected compounds **16**, **24** and **25** for the *in vivo* studies in a predictive murine model of NP. These compounds exhibited excellent inhibitory activities against the human and murine enzymes, moderate metabolic stability, good solubility and did not inhibit significantly cytochromes. Notwithstanding, hERG inhibition and Caco-2 assays were also performed in order to additionally characterize the selected compounds. Nicely, any of the compounds inhibited significantly hERG at 10 μ M and displayed moderate permeability in Caco-2 cells (see Table S2 in Supporting Information). Finally, they were tested for selectivity against *hCOX-2* and *hLOX-5*, two enzymes involved in the AA cascade. Gratifyingly, they did not present significant inhibition of these enzymes (see Table S2 in Supporting Information).

Pharmacokinetic study of 16. A study was conducted in order to determine the pharmacokinetic profile in plasma of compound **16** when administered by intraperitoneal route at a single dose of 1 mg/kg (Table S3 and Figures S1 and S2 in Supporting information).

Compound	Dose	HL (h)	Tmax (h)	Cmax (ng/mL)	AUClast (h*ng/mL)	AUCINF (h*ng/mL)	Vd (L/Kg)	Cl (L/h/Kg)
16	1 mg/Kg	0.26	0.25	2453.33	1225.62	1232.66	0.30	0.81

Table 6: Pharmacokinetic parameters in male C57/BI6 mouse for compound **16** after 1 mg/kg IP administration.

As shown in Table 6, compound **16** demonstrated good bioavailability and elimination characteristics according to their pharmacokinetic parameters. Thus, this compound was then evaluated in pain-related *in vivo* efficacy studies.

***In vivo* efficacy studies.** A first *in vivo* efficacy study was performed in the very predictive capsaicin murine model of allodynia, used for testing putative efficacy in NP.

Although it is not strictly a NP model, typically, active compounds in the capsaicin model show analgesia in NP models. This study demonstrated that **16** reduced allodynia in a dose-dependent manner and outperformed other sEHI tested, such as TPPU and AS2586114 (Figure 3).

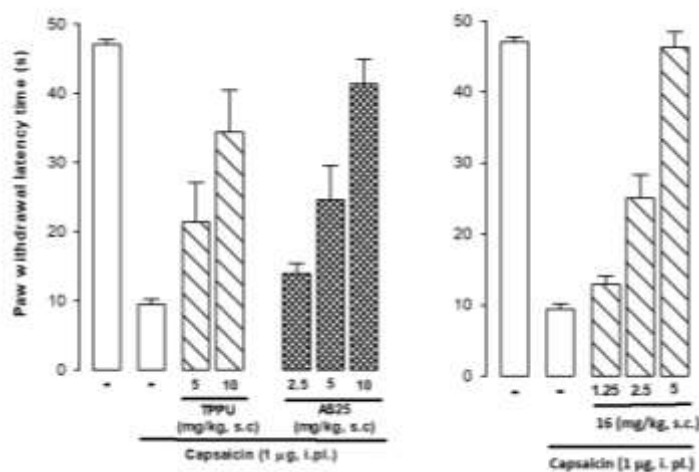


Figure 3. Results of the *in vivo* efficacy study of allodynia produced by capsaicine for TPPU, AS2586114 and compound **16**.

Given that compound **16** showed excellent efficacy in abolishing allodynia in the predictive model of NP, we have scheduled an *in vivo* assay for **16** in a very well-known model chemotherapy-induced NP.

CONCLUSIONS

sEH has been identified as a suitable target for several inflammatory and pain-related diseases. In this work we report further medicinal chemistry around new benzohomoadamantane-based piperidine derivatives, analogs of the clinical candidates AR9281 and EC5026, in order to improve the solubility and microsomal stability values of the previous hit. In this work we have found that the introduction of a halogen atom in the position 9 of the benzohomoadamantane scaffold led to very potent compounds with

improved DMPK properties. The in vitro profiling of these new sEHIs (solubility, cytotoxicity, metabolic stability, CYP450s, hLOX-5, hCOX-2 and hERG inhibition) allowed to select a suitable candidate for an in vivo efficacy study in a predictive murine model of NP. The administration of compound **16** reduced pain in the capsaicin murine model of allodynia in a dose-dependent manner and outperformed other sEHIs tested.. Hence, this study opens a whole range of applications of the benzohomoadamantane-based sEHIs in the pain field.

EXPERIMENTAL SECTION

Chemical synthesis. General methods. Commercially available reagents and solvents were used without further purification unless stated otherwise. Preparative normal phase chromatography was performed on a CombiFlash Rf 150 (Teledyne Isco) with pre-packed RediSep Rf silica gel cartridges. Thin-layer chromatography was performed with aluminum-backed sheets with silica gel 60 F254 (Merck, ref 1.05554), and spots were visualized with UV light and 1% aqueous solution of KMnO₄. Melting points were determined in open capillary tubes with a MFB 595010M Gallenkamp. 400 MHz ¹H and 100.6 MHz ¹³C NMR spectra were recorded on a Varian Mercury 400 or on a Bruker 400 Avance III spectrometers. 500 MHz ¹H NMR spectra were recorded on a Varian Inova 500 spectrometer. The chemical shifts are reported in ppm (δ scale) relative to internal tetramethylsilane, and coupling constants are reported in Hertz (Hz). Assignments given for the NMR spectra of selected new compounds have been carried out on the basis of DEPT, COSY 1H/1H (standard procedures), and COSY ¹H/¹³C (gHSQC and gHMBC sequences) experiments. IR spectra were run on Perkin-Elmer Spectrum RX I, Perkin-Elmer Spectrum TWO or Nicolet Avatar 320 FT-IR spectrophotometers. Absorption values are expressed as wave-numbers (cm⁻¹); only significant absorption bands are given. High-resolution mass spectrometry (HRMS) analyses were performed with an

LC/MSD TOF Agilent Technologies spectrometer. The elemental analyses were carried out in a Flash 1112 series Thermofinnigan elemental microanalyzer (A5) to determine C, H, N and S. The structure of all new compounds was confirmed by elemental analysis and/or accurate mass measurement, IR, ¹H NMR and ¹³C NMR. The analytical samples of all the new compounds, which were subjected to pharmacological evaluation, possessed purity ≥95% as evidenced by their elemental analyses.

1-(9-methyl-5,6,8,9,10,11-hexahydro-7H-5,9:7,11-dimethanobenzo[9]annulen-7-yl)-3-(1-propionylpiperidin-4-yl)urea, 8. To a solution of 9-methyl-5,6,8,9,10,11-hexahydro-7H-5,9:7,11-dimethanobenzo[9]annulen-7-amine hydrochloride (464 mg, 1.76 mmol) in DCM (10 mL) saturated aqueous NaHCO₃ solution (10 mL) and triphosgene (193 mg, 0.65 mmol) were added. The biphasic mixture was stirred at room temperature for 30 minutes and then the two phases were separated and the organic layer was washed with brine (5 mL), dried over anh. Na₂SO₄, filtered and evaporated under vacuum to obtain 1-2 mL of a solution of the isocyanate in DCM. To this solution was added 1-(4-aminopiperidin-1-yl)propan-1-one (350 mg, 2.24 mmol). The reaction mixture was stirred at room temperature overnight and the solvent was evaporated under vacuum to obtain a white solid (741 mg). Column chromatography (SiO₂, DCM/methanol mixtures) gave urea **8** (597 mg, 83% yield) as a white solid. The analytical sample was obtained by crystallization from hot EtOAc and DCM (300 mg), mp 207-208 °C. IR (NaCl disk): 3357, 2917, 2859, 1644, 1620, 1556, 1493, 1450, 1361, 1344, 1319, 1264, 1221, 1132, 1068, 1024, 971, 949, 758 cm⁻¹. ¹H-NMR (400 MHz, CDCl₃) δ: 0.90 (s, 3 H, C9-CH₃), 1.11 (t, *J* = 7.2 Hz, 3 H, COCH₂CH₃), 1.14 [m, 2 H, COCH₂CH₃, 5'(3')-H_{ax}], 1.52 [d, *J* = 13.4 Hz, 2 H, 10(13)-H_{ax}], 1.62 [dd, *J* = 13.4 Hz, *J'* = 6.0 Hz, 2 H, 10(13)-H_{eq}], 1.77-1.86 (complex signal, 3 H, 8-H₂, 5'-H_{eq} or 3'-H_{eq}), 1.93 [d, *J* = 12.8 Hz, 2 H, 6(12)-H_{ax}], 2.02 (d, *J* = 12.0 Hz, 1 H, 3'-H_{eq} or 5'-H_{eq}), 2.12 [dd, *J* = 12.8 Hz, *J'* = 6.0

Hz, 2 H, 6(12)-H_{eq}], 2.32 (m, 2 H, COCH₂CH₃), 2.70 (m, 1 H, 2'-H_{ax} or 6'-H_{ax}), 3.00-3.12 [complex signal, 3 H, 5(11)-H, 6'-H_{ax} or 2'-H_{ax}], 3.70-3.77 (complex signal, 2 H, 4'-H, 6'-H_{eq} or 2'-H_{eq}), 4.47 (d, *J* = 13.6 Hz, 1 H, 2'-H_{eq} or 6'-H_{eq}), 4.64-4.72 (complex signal, 2 H, C7-NH, C4'-NH), 7.02 [m, 2 H, 1(4)-H], 7.05 [m, 2 H, 2(3)-H]. ¹³C-NMR (100.6 MHz, CDCl₃) δ: 9.7 (CH₃, COCH₂CH₃), 26.6 (CH₂, COCH₂CH₃), 32.3 (CH₃, C9-CH₃), 32.4 (CH₂, C3' or C5'), 33.6 (C, C9), 33.9 (CH₂, C5' or C3'), 39.9 [CH₂, C6(12)], 40.9 (CH₂, C6' or C2'), 41.1 [CH, C5(11)], 41.2 [CH₂, C10(13)], 44.5 (CH₂, C2' or C6'), 46.7 (CH, C4'), 48.0 (CH₂, C8), 53.4 (C, C7), 126.2 [CH, C2(3)], 127.9 [CH, C1(4)], 146.3 [C, C4a(11a)], 156.5 (C, NHCONH), 172.4 (NCOCH₂CH₃). Anal. Calcd for C₂₅H₃₅N₃O₂·0.25 H₂O: C 72.52, H 8.64, N 10.15. Found: C 72.65, H 8.49, N 9.82. HRMS: Calcd for [C₂₅H₃₅N₃O₂+H]⁺: 410.2802; Found: 410.2801.

1-(9-methyl-5,6,8,9,10,11-hexahydro-7H-5,9:7,11-dimethanobenzo[9]annulen-7-yl)-3-(1-(tetrahydro-2H-pyran-4-carbonyl)piperidin-4-yl)urea, 9. To a solution of 9-methyl-5,6,8,9,10,11-hexahydro-7H-5,9:7,11-dimethanobenzo[9]annulen-7-amine hydrochloride (258 mg, 0.98 mmol) in DCM (4 mL) saturated aqueous NaHCO₃ solution (4 mL) and triphosgene (107 mg, 0.36 mmol) were added. The biphasic mixture was stirred at room temperature for 30 minutes and then the two phases were separated and the organic layer was washed with brine (2 mL), dried over anh. Na₂SO₄, filtered and evaporated under vacuum to obtain 1-2 mL of a solution of the isocyanate in DCM. To this solution was added (4-aminopiperidin-1-yl)(tetrahydro-2H-pyran-4-yl)methanone (215 mg, 1.01 mmol). The reaction mixture was stirred at room temperature overnight and the solvent was evaporated under vacuum to obtain a yellow residue (534 mg). Column chromatography (SiO₂, DCM/Methanol mixtures) gave urea **9** (207 mg, 45% yield) as a white solid, mp 224-225 °C. IR (NaCl disk): 3357, 3064, 3017, 2945, 2919, 2850, 1640, 1614, 1553, 1493, 1446, 1361, 1344, 1320, 1278, 1261, 1238, 1211, 1126,

1089, 1068, 1018, 984, 941, 874, 818, 759, 733 cm^{-1} . $^1\text{H-NMR}$ (400 MHz, CDCl_3) δ : 0.90 (s, 3 H, C9-CH_3), 1.17 [m, 2 H, $3'(5')\text{-H}_{\text{ax}}$], 1.50-1.65 [complex signal, 6 H, $3''(5'')\text{-H}_{\text{ax}}$, $10(13)\text{-H}_2$], 1.79 (s, 2 H, 8-H), 1.82-1.90 [complex signal, 3 H, $5'\text{-H}_{\text{eq}}$ or $3'\text{-H}_{\text{eq}}$, $3''(5'')\text{-H}_{\text{eq}}$], 1.94 [d, $J = 12.8$ Hz, 2 H, $6(12)\text{-H}_{\text{ax}}$], 2.03-2.16 [complex signal, 3 H, $6(12)\text{-H}_{\text{eq}}$, $3'\text{-H}_{\text{eq}}$ or $5'\text{-H}_{\text{eq}}$], 2.65-2.79 (complex signal, 2 H, $2'\text{-H}_{\text{ax}}$ or $6'\text{-H}_{\text{ax}}$, $4''\text{-H}$), 3.00-3.17 [complex signal, 3 H, $6'\text{-H}_{\text{ax}}$ or $2'\text{-H}_{\text{ax}}$, $5(11)\text{-H}$], 3.43 [m, 2 H, $2''(6'')\text{-H}_{\text{ax}}$], 3.69-3.88 (complex signal, 2 H, $4'\text{-H}$, $2'\text{-H}_{\text{eq}}$ or $6'\text{-H}_{\text{eq}}$), 3.99 [m, 2 H, $2''(6'')\text{-H}_{\text{eq}}$], 4.48 (m, 2 H, $2'\text{-H}_{\text{eq}}$ or $6'\text{-H}_{\text{eq}}$), 7.02 [m, 2 H, $1(4)\text{-H}$], 7.06 [m, 2 H, $2(3)\text{-H}$]. $^{13}\text{C-NMR}$ (100.6 MHz, CDCl_3) δ : 29.1 [CH_2 , $\text{C}3''(5'')$], 32.3 (CH_3 , C9-CH_3), 32.4 (CH_2 , $\text{C}5'$ or $\text{C}3'$), 33.7 (C, C9), 34.1 (CH_2 , $\text{C}3'$ or $\text{C}5'$), 37.6 (CH, $\text{C}4''$), 39.9 [CH_2 , $\text{C}6(12)$], 41.1 [CH, $\text{C}5(11)$], 41.2 [CH_2 , $\text{C}10(13)$], 44.3 [CH_2 , $\text{C}2'(6')$], 47.0 (CH, $\text{C}4'$), 48.0 (CH_2 , C8), 53.5 (C, C7), 67.1 [CH_2 , $\text{C}2''(6'')$], 126.2 [CH, $\text{C}2(3)$], 127.9 [CH, $\text{C}1(4)$], 146.3 [C, $\text{C}4\text{a}(11\text{a})$], 156.3 (C, NHCONH), 172.8 (C, NCOR). Anal. Calcd for $\text{C}_{28}\text{H}_{39}\text{N}_3\text{O}_3$: C 72.23, H 8.44, N 9.02. Found: C 72.33, H 8.40, N 8.83. HRMS: Calcd for $[\text{C}_{28}\text{H}_{39}\text{N}_3\text{O}_3+\text{H}]^+$: 466.3064; Found: 466.3065.

1-(1-benzylpiperidin-4-yl)-3-(9-methyl-5,6,8,9,10,11-hexahydro-7H-5,9:7,11-dimethanobenzo[9]annulen-7-yl)urea, 10. To a solution of 9-methyl-5,6,8,9,10,11-hexahydro-7H-5,9:7,11-dimethanobenzo[9]annulen-7-amine hydrochloride (250 mg, 0.95 mmol) in DCM (4.5 mL) and saturated aqueous NaHCO_3 solution (3 mL) was added triphosgene (140 mg, 0.47 mmol). The biphasic mixture was stirred at room temperature for 30 minutes and then the two phases were separated and the organic layer was washed with brine (5 mL), dried over anhydrous Na_2SO_4 , filtered and evaporated under vacuum to obtain 1-2 mL of a solution of the isocyanate in DCM. To this solution was added 1-benzylpiperidin-4-amine (216 mg, 1.13 mmol). The reaction mixture was stirred at room temperature for 24 h and the solvent was evaporated under vacuum to obtain a yellow

gum. Column chromatography (SiO₂, DCM/methanol mixtures) gave urea **10** as a white solid (159 mg, 38% yield), mp 106-107 °C. IR (NaCl disk): 3318, 3058, 3025, 2945, 2918, 2838, 2792, 2761, 1632, 1559, 1493, 1453, 1361, 1343, 1321, 1302, 1281, 1234, 1209, 1136, 1120, 1066, 1028, 909, 757, 733, 698 cm⁻¹. ¹H-NMR (400 MHz, CDCl₃) δ: 0.90 (s, 3 H, C9-CH₃), 1.43 [dq, *J* = 10.8 Hz, *J'* = 4.0 Hz, 2 H, 3'(5')-H_{ax}], 1.52 [d, *J* = 14.0 Hz, 10(13)-H_{ax}], 1.62 [dd, *J* = 13.0 Hz, *J'* = 5.6 Hz, 10(13)-H_{eq}], 1.80 (s, 2 H, 8-H), 1.88 [m, 2 H, 3'(5')-H_{eq}], 1.94 [d, *J* = 13.2 Hz, 2 H, 6(12)-H_{ax}], 2.09-2.15 [complex signal, 4 H, 6(12)-H_{eq} 2'(6')-H_{ax}], 2.83 [dm, *J* = 11.6 Hz, 2 H, 2'(6')-H_{eq}], 3.04 [t, *J* = 6.0 Hz, 2 H, 5(11)-H], 3.52 (complex signal, 3 H, 4'-H, CH₂-C₆H₅), 4.24-4.33 (complex signal, 2 H, C7-NH, C4'-NH), 7.02 [m, 2 H, 1(4)-H], 7.05 [m, 2 H, 2(3)-H], 7.26 (m, 1 H, Ar-H_{para}), 7.29-7.33 (complex signal, 4 H, Ar-H_{ortho}, Ar-H_{meta}). ¹³C-NMR (100.6 MHz, CDCl₃) δ: 32.3 (CH₃, C5-CH₃), 32.7 [CH₂, C3'(5')], 33.7 (C, C9), 39.0 [CH₂, C6(12)], 41.1 [CH, C5(11)], 41.2 [CH₂, C10(13)], 47.0 (CH, C4'), 48.0 (CH₂, C8), 52.4 [CH₂, C2'(6')], 53.5 (C, C7), 62.9 (CH₂, CH₂-C₆H₅), 126.2 [CH, C2(3)], 127.3 (CH, Ar-CH_{para}), 127.9 [CH, C1(4)], 128.3 [CH, Ar-CH_{meta}], 129.3 [CH, Ar-CH_{ortho}], 137.5 (C, Ar-C_{ipso}), 146.3 [C, C4a(11a)], 156.4 (C, NHCONH). Anal. Calcd for C₂₉H₃₇N₃O·0.5 H₂O: C 76.95, H 8.46, N 9.28. Found: C 76.99, H 8.26, N 8.98. HRMS: Calcd for [C₂₉H₃₇N₃O+H]⁺: 444.3009; Found: 444.3002.

1-[1-(isopropylsulfonyl)piperidin-4-yl]-3-(9-methyl-5,6,8,9,10,11-hexahydro-7H-5,9:7,11-dimethanobenzo[9]annulen-7-yl)urea, 11. To a solution of 9-methyl-5,6,8,9,10,11-hexahydro-7H-5,9:7,11-dimethanobenzo[9]annulen-7-amine hydrochloride (300 mg, 1.14 mmol) in DCM (6 mL) and saturated aqueous NaHCO₃ solution (4 mL) was added triphosgene (169 mg, 0.57 mmol). The biphasic mixture was stirred at room temperature for 30 minutes and then the two phases were separated and

the organic layer was washed with brine (5 mL), dried over anh. Na₂SO₄, filtered and evaporated under vacuum to obtain 1-2 mL of a solution of the isocyanate in DCM.

To a solution of 1-(isopropylsulfonyl)piperidin-4-amine (233 mg, 1.13 mmol) in anh. THF (5 mL) under argon atmosphere at -78°C, was added dropwise a solution of *n*-butyllithium (2.5 M in hexanes, 0.59 mL, 1.47 mmol) during 20 minutes. After the addition, the mixture was tempered to 0°C using an ice bath. This solution was added carefully to the solution of the isocyanate from the previous step cooled to 0°C, under argon atmosphere. The reaction mixture was stirred at room temperature overnight. Methanol (2 mL) was then added to quench any unreacted *n*-butyllithium. The solvents were evaporated under vacuum to give an orange gum (506 mg). This residue was dissolved in EtOAc (10 mL) and washed with 2N HCl solution (2 x 5 mL) and the organic layer was dried over anh. Na₂SO₄, filtered and concentrated in vacuum to obtain a white gum (241 mg). Column chromatography (SiO₂, DCM/methanol mixtures) gave a white solid. Crystallization from hot DCM:pentane provided urea **11** (66 mg, 13% yield) as a white solid, mp 218-219°C. IR (NaCl disk): 3364, 3062, 3013, 2946, 2920, 2854, 1710, 1638, 1553, 1494, 1453, 1361, 1320, 1305, 1266, 1249, 1232, 1168, 1134, 1091, 1045, 943, 881, 841, 759, 732, 666, 593, 555 cm⁻¹. ¹H-NMR (400 MHz, CDCl₃) δ: 0.90 (s, 3 H, C9-CH₃), 1.31 [d, *J* = 6.8 Hz, 6 H, CH(CH₃)₂], 1.36 [dq, *J* = 12.0 Hz, *J*' = 4.0 Hz, 3'(5')-H_{ax}], 1.52 [d, *J* = 13.2 Hz, 2 H, 10(13)-H_{ax}], 1.61 [m, 2 H, 10(13)-H_{eq}], 1.79 (s, 2 H, 8-H), 1.92-1.97 [complex signal, 4 H, 3'(5')-H_{eq}, 6(12)-H_{ax}], 2.12 [dd, *J* = 12.8 Hz, *J*' = 6.4 Hz, 2 H, 6(12)-H_{eq}], 2.92 [m, 2 H, 2'(6')-H_{ax}], 3.04 [t, *J* = 6.4 Hz, 2 H, 5(11)-H], 3.15 (sept, *J* = 6.8 Hz, 1 H, CH(CH₃)₂), 3.67 (m, 1 H, 4'-H), 3.78 [dm, *J* = 13.2 Hz, 2 H, 2'(6')-H_{eq}], 4.35 (s, 1 H, C7-NH), 4.41 (d, *J* = 8.0 Hz, C4'-NH), 7.03 [m, 2 H, 1(4)-H], 7.06 [m, 2 H, 2(3)-H]. ¹³C-NMR (100.6 MHz, CDCl₃) δ: 16.7 [CH₃, CH(CH₃)₂], 32.3 (CH₃, C9-CH₃), 33.4 [CH₂, C3'(5')], 33.7 (C, C9), 39.8 [CH₂, C6(12)], 41.1 [CH, C5(11)], 41.2

[CH₂, C10(13)], 45.7 [CH₂, C2'(6')], 46.6 (CH, C4'), 48.0 (CH₂, C8), 53.4 [CH, C̄H(CH₃)₂], 53.5 (C, C7), 126.2 (CH, C2(3)), 127.9 [CH, C1(4)], 146.3 [C, C4a(11a)], 156.2 (C, NHCONH). Anal. Calcd for C₂₅H₃₇N₃O₃S: C 65.33, H 8.11, N 9.14. Found: C 65.41, H 8.31, N 8.93. HRMS: Calcd for [C₂₅H₃₇N₃O₃S+H]⁺: 460.2628; Found: 460.2623.

1-(9-methyl-5,6,8,9,10,11-hexahydro-7H-5,9:7,11-dimethanobenzo[9]annulen-7-yl)-3-(1-(cyclopropanecarbonyl)piperidin-4-yl)urea, 12. To a solution of 9-methyl-5,6,8,9,10,11-hexahydro-7H-5,9:7,11-dimethanobenzo[9]annulen-7-amine hydrochloride (112.5 mg, 0.43 mmol) in DCM (6 mL) saturated aqueous NaHCO₃ solution (5 mL) and triphosgene (93.8 mg, 0.16 mmol) were added. The biphasic mixture was stirred at room temperature for 30 minutes and then the two phases were separated and the organic layer was washed with brine (5 mL), dried over anhydrous Na₂SO₄, filtered and evaporated under vacuum to obtain 2-3 mL of a solution of the isocyanate in DCM. To this solution was added (4-aminopiperidin-1-yl)(tetrahydro-2H-pyran-4-yl)methanone (72 mg, 0.43 mmol). The mixture was stirred overnight at room temperature and the solvent was then evaporated. Column chromatography (SiO₂, DCM/Methanol mixtures) provided urea **12** as a white solid (60 mg, 33% yield), mp 115-120 °C. IR (ATR): 3341, 2899, 1633, 1607, 1549, 1448, 1311, 1222, 1128, 1064, 1027, 979, 756. ¹H-NMR (400 MHz, CDCl₃) δ: 0.72 [dd, 2 H, *J* = 6.0 Hz, *J'* = 2.0 Hz, 8'(9')-H_{ax}], 0.90 (s, 3 H, 9'-H), 0.93 [m, 2 H, 8'(9')-H_{eq}], 1.20 [m, 2 H, 3'(5')-H_{eq}], 1.52 [d, 2 H, *J* = 13.2 Hz, 10(13)-H_{ax}], 1.63 [dd, 2 H, *J* = 13.2 Hz, *J'* = 5.6 Hz, 10(13)-H_{eq}], 1.73 (m, 2 H, 7'-H), 1.80 [m, 3 H, 8-H, 3' or 5'-H_{eq}], 1.95 [d, 2 H, *J* = 12.8 Hz, 6(12)-H_{ax}], 2.04 [d, 1 H, *J* = 12.0 Hz, 3' or 5'-H_{eq}], 2.13 [dd, 2 H, *J* = 12.0 Hz, *J'* = 6.4 Hz, 6(12)-H_{eq}], 2.73 [t, 1 H, *J* = 11.6 Hz, 2' or 6'-H_{ax}], 3.04 [t, 2 H, *J* = 12.0 Hz, 5(11)-H], 3.20 [t, 1 H, *J* = 12 Hz, 2' or 6'-H_{ax}], 3.75 (m, 1 H, 4'-H), 4.1 [d, 1 H, *J* = 10.8 Hz, 2' or 6'-H_{eq}], 4.4 [d, 1 H, *J* = 10 Hz,

2' or 6'-H_{eq}], 4.5 [d, 1 H, $J = 10.8$ Hz, NHCONH], 4.6 (s, 1 H, NHCONH), 7.03 [m, 2 H, 1(4)-H], 7.05 [m, 2 H, 2(3)-H]. ¹³C-NMR (100.5 MHz, CDCl₃) δ : 7.49 [CH₂, C8'(9')], 11.14 (CH, C7'), 32.43 (CH₃, C9'), 32.53 (CH₂, C3' or 5'), 33.82 (CH₂, C3' or 5'), 40.03 [CH₂, C6(12)], 41.26 [CH, C5(11)], 41.35 [CH₂, C10(13)], 41.66 [CH₂, C2' or 6'], 44.71 [CH₂, C2' or 6'], 47.04 (CH, C4'), 48.13 (CH₂, C8), 53.58 (C, C7), 126.33 [CH, C(1)4], 128.07 [CH, C2(3)], 146.49 {C, C4_a(11_a)}, 156.57 (C, NHCONH), 172.22 (C, NCOR). Anal. Calcd for C₂₆H₃₅N₃O₂ · 0.1 CH₂Cl₂: C 72.89 H 8.25, N 9.77. Found: C 73.08, H 8.23, N 9.53. HRMS: Calcd for [C₂₆H₃₅N₃O₂+H]⁺: 422.2802, found: 422.2808.

1-(1-(4-acetylphenyl)piperidin-4-yl)-3-(9-methyl-5,6,8,9,10,11-hexahydro-7H-

5,9:7,11-dimethanobenzo[9]annulen-7-yl)urea, 13. To a solution of 9-methyl-5,6,8,9,10,11-hexahydro-7H-5,9:7,11-dimethanobenzo[9]annulen-7-amine hydrochloride (241 mg, 0.91 mmol) in DCM (5 mL) saturated aqueous NaHCO₃ solution (5 mL) and triphosgene (104 mg, 0.35 mmol) were added. The biphasic mixture was stirred at room temperature for 30 minutes and then the two phases were separated and the organic layer was washed with brine (5 mL), dried over anhydrous Na₂SO₄, filtered and evaporated under vacuum to obtain 1-2 mL of a solution of the isocyanate in DCM. To this solution was added 1-(4-(4-aminopiperidin-1-yl)phenyl)ethan-1-one (250 mg, 1.14 mmol). The reaction mixture was stirred at room temperature overnight and the solvent was evaporated under vacuum to obtain an orange solid (475 mg). Column chromatography (SiO₂, Hexane/EtOAc mixtures) gave urea **13** (120 mg, 28% yield) as a yellowish solid, mp 211-212 °C. IR (NaCl disk): 3358, 2919, 2844, 1666, 1633, 1597, 1552, 1519, 1493, 1452, 1427, 1390, 1360, 1307, 1281, 1225, 1193, 1129, 1068, 956, 915, 826, 758 cm⁻¹. ¹H-NMR (400 MHz, CDCl₃) δ : 0.90 (s, 3 H, C9-CH₃), 1.39 [dq, $J = 11.2$ Hz, $J' = 4.4$ Hz, 2 H, 5'(3')-H_{ax}], 1.55 [d, $J = 13.0$ Hz, 2 H, 10(13)-H_{ax}], 1.63 [dd, $J = 13.0$ Hz, $J' = 5.2$ Hz, 2 H, 10(13)-H_{eq}], 1.80 (s, 2 H, 8-H₂), 1.91-2.03 [complex signal,

4 H, 6(12)-H_{ax}, 3'-H_{eq} or 5'-H_{eq}], 2.13 [dd, $J = 12.0$ Hz, $J' = 6.0$ Hz, 6(12)-H_{eq}], 2.50 (s, 3 H, COCH₃), 2.97 (m, 2 H, 2'(6')-H_{ax}), 3.04 [t, $J = 6.4$ Hz, 2 H, 5(11)-H], 3.69-3.82 [complex signal, 3 H, 4'-H, 2'(6')-H_{eq}], 4.36-4.41 (complex signal, 2 H, 7-NH, 4'-NH), 6.81 [d, $J = 9.0$ Hz, 2''(6'')-H], 7.02 [m, 2 H, 1(4)-H], 7.06 [m, 2 H, 2(3)-H], 7.82 [d, $J = 9.0$ Hz, 2 H, 3''(5'')-H]. ¹³C-NMR (100.6 MHz, CDCl₃) δ : 26.1 (CH₃, COCH₃), 32.2 [CH₂, C3'(5')], 32.3 (CH₃, C9-CH₃), 33.7 (C, C9), 39.9 [CH₂, C6(12)], 41.1 [CH, C5(11)], 41.2 [CH₂, C10(13)], 46.7 [CH₂, C2'(6')], 46.9 (CH, C4'), 48.0 (CH₂, C8), 53.5 (C, C7), 113.4 [CH, C2''(6'')], 126.2 [CH, C2(C3)], 127.0 (C, C4''), 127.9 [CH, C1(4)], 130.5 [CH, C3''(5'')], 146.3 [C, C4a(11a)], 153.8 (C, C1''), 156.3 (C, NHCONH), 196.6 (C, COCH₃). HRMS: Calcd for [C₃₀H₃₇N₃O₂+H]⁺: 472.2959; Found: 472.2962. Anal. Calcd for C₃₀H₃₇N₃O₂ · 0.2 Ethyl Acetate: C 75.61, H 7.95, N 8.59. Found: C 75.81, H 7.86, N 8.29.

1-(1-acetylpiperidin-4-yl)-3-(9-chloro-5,6,8,9,10,11-hexahydro-7H-5,9:7,11-

dimethanobenzo[9]annulen-7-yl)urea, 14. To a solution of 9-chloro-5,6,8,9,10,11-hexahydro-7H-5,9:7,11-dimethanobenzo[9]annulen-7-amine hydrochloride (150 mg, 0.53 mmol) in DCM (3 mL) saturated aqueous NaHCO₃ solution (3 mL) and triphosgene (58 mg, 0.20 mmol) were added. The biphasic mixture was stirred at room temperature for 30 minutes and then the two phases were separated and the organic layer was washed with brine (3 mL), dried over anhydrous Na₂SO₄, filtered and evaporated under vacuum to obtain 1-2 mL of a solution of the isocyanate in DCM. To this solution was added 1-(4-aminopiperidin-1-yl)ethan-1-one (90 mg, 0.63 mmol). The reaction mixture was stirred at room temperature overnight and the solvent was evaporated under vacuum to obtain a white solid (204 mg). Column chromatography (SiO₂, DCM/Methanol mixtures) gave urea **14** (115 mg, 52% yield) as a white solid, mp 209-210°C. IR (NaCl disk): 3358, 3019, 2926, 2855, 1644, 1619, 1556, 1494, 1452, 1358, 1319, 1301, 1268, 1228, 1206, 1135,

1090, 1050, 991, 969, 947, 802, 761, 735 cm^{-1} . $^1\text{H-NMR}$ (400 MHz, CDCl_3) δ : 1.15 (m, 1 H, 5'- H_{ax} or 3'- H_{ax}), 1.18 [m, 1 H, 3'- H_{ax} or 5'- H_{ax}], 1.85 (d, $J = 13.6$ Hz, 1 H, 5'- H_{eq} or 3'- H_{eq}), 1.93 [d, $J = 13.2$ Hz, 2 H, 6(12)- H_{ax}], 2.02 (m, 1 H, 3'- H_{eq} or 5'- H_{eq}), 2.06 (s, 3 H, COCH_3), 2.15 [d, $J = 13.6$ Hz, 2 H, 10(13)- H_{ax}], 2.21 [m, 2 H, 6(12)- H_{eq}], 2.35 [dd, $J = 12.8$ Hz, $J' = 6.0$ Hz, 2 H, 10(13)- H_{eq}], 2.45 (m, 1 H, 8- H_a), 2.48 (m, 1 H, 8- H_b), 2.72 (m, 1 H, 2'- H_{ax} or 6'- H_{ax}), 3.05-3.19 (complex signal, 3 H, 5(11)-H, 6'- H_{ax} or 2'- H_{ax}), 3.67-3.80 (complex signal, 2 H, 4'-H, 6'- H_{eq} or 2'- H_{eq}), 4.41 (dm, $J = 13.6$ Hz, 1 H, 2'- H_{eq} or 6'- H_{eq}), 4.78 (d, $J = 7.6$ Hz, 1 H, C4'-NH), 4.85 (s, 1 H, C7-NH), 7.04 [m, 2 H, 1(4)-H], 7.09 [m, 2 H, 2(3)-H]. $^{13}\text{C-NMR}$ (100.6 MHz, CDCl_3) δ : 21.5 (CH_3 , COCH_3), 32.4 (CH_2 , C5' or C3'), 33.7 (CH_2 , C3' or C5'), 38.89 (CH_2 , C6 or C12), 38.96 (CH_2 , C12 or C6), 40.7 (CH_2 , C2' or C6'), 41.2 [CH, C5(11)], 44.47 (CH_2 , C10 or C13), 44.50 (CH_2 , C13 or C10), 45.4 (CH_2 , C6' or C2'), 46.6 (CH, C4'), 50.8 (CH_2 , C8), 55.5 (C, C7), 69.5 (C, C9), 126.8 [CH, C2(3)], 128.1 [CH, C1(4)], 144.7 (CH, C4a or C11a), 144.8 (CH, C11a or C4a), 156.2 (C, NHCONH), 169.17 (C, COCH_3). Anal. Calcd for $\text{C}_{23}\text{H}_{30}\text{ClN}_3\text{O}_2 \cdot 0.75$ Ethyl Acetate: C 64.78, H 7.53, N 8.72. Found: C 64.73, H 7.56, N 8.89. HRMS: Calcd for $[\text{C}_{23}\text{H}_{30}\text{ClN}_3\text{O}_2 + \text{H}]^+$: 416.2099; Found: 416.2100.

1-(9-chloro-5,6,8,9,10,11-hexahydro-7H-5,9:7,11-dimethanobenzo[9]annulen-7-yl)-3-(1-propionylpiperidin-4-yl)urea, 15. To a solution of 9-chloro-5,6,8,9,10,11-hexahydro-7H-5,9:7,11-dimethanobenzo[9]annulen-7-amine hydrochloride (150 mg, 0.53 mmol) in DCM (4 mL) and saturated aqueous NaHCO_3 solution (3 mL), triphosgene (56 mg, 0.19 mmol) was added. The biphasic mixture was stirred at room temperature for 30 minutes and then the two phases were separated and the organic one was washed with brine (3 mL), dried over anhydrous Na_2SO_4 , filtered and evaporated under vacuum to obtain 1-2 mL of a solution of isocyanate in DCM. To this solution was added 1-(4-aminopiperidin-1-yl)propan-1-one (83 mg, 0.53 mmol). The mixture was stirred

overnight at room temperature and the solvent was then evaporated. Column chromatography (SiO₂, DCM/Methanol mixtures) provided an orange solid. The analytical sample was obtained by a crystallization from hot Ethyl Acetate/Pentane mixtures to obtain a urea **15** as a yellowish solid (79 mg, 35% yield), mp 155-156 °C. IR (ATR): 3359, 2924, 2852, 1681, 1652, 1637, 1612, 1565, 1447, 1373, 1356, 1322, 1297, 1263, 1221, 1134, 1075, 1045, 1022, 967, 946, 908, 804, 755, 618, 559 cm⁻¹. ¹H-NMR (400 MHz, CDCl₃) δ: 1.11 (t, *J* = 7.2 Hz, 3 H, COCH₂CH₃), 1.13 [m, 2 H, 5'(3')-H_{ax}], 1.84 (d, *J* = 12.8 Hz, 1 H, 5'-H_{eq} or 3'-H_{eq}), 1.94 [d, *J* = 12.8 Hz, 2 H, 6(12)-H_{ax}], 2.00 (d, *J* = 12.4 Hz, 3'-H_{eq} or 5'-H_{eq}), 2.14 [d, *J* = 13.2 Hz, 2 H, 10(13)-H_{ax}], 2.21 [m, 2 H, 6(12)-H_{eq}], 2.29-2.40 [complex signal, 4 H, 10(13)-H_{eq}, COCH₂CH₃], 2.48 (m, 2 H, 8-H), 2.70 (m, 1 H, 2'-H_{ax} or 6'-H_{ax}), 3.08 (m, 1 H, 6'-H_{ax} or 2'-H_{ax}), 3.14 [t, *J* = 6.4 Hz, 2 H, 5(11)-H], 3.68-3.82 (complex signal, 2 H, 6'-H_{eq} or 2'-H_{eq}, 4'-H), 4.45 (dm, *J* = 13.6 Hz, 1 H, 2'-H_{eq} or 6'-H_{eq}), 4.68 (d, *J* = 8.0 Hz, 1 H, C4'-NH), 4.75 (s, 1 H, C7-NH), 7.05 [m, 2 H, 1(4)-H], 7.10 [m, 2 H, 2(3)-H]. ¹³C-NMR (100.6 MHz, CDCl₃) δ: 9.7 (CH₃, COCH₂CH₃), 26.6 (CH₂, COCH₂CH₃), 32.4 (CH₂, C5' or C3'), 33.9 (CH₂, C3' or C5'), 38.9 [CH₂, C6(12)], 40.9 (CH₂, C2' or C6'), 41.2 [CH, C5(11)], 44.5 [2 CH₂, C10(13), C6' or C2'], 46.7 (CH, C4'), 50.8 (CH₂, C8), 55.5 (C, C7), 69.5 (C, C9), 126.8 [CH, C2(3)], 128.1 [CH, C1(4)], 144.8 [C4a(11a)], 156.1 (NHCONH), 172.5 (NCOR). HRMS: Calcd for [C₂₄H₃₂ClN₃O₂+H]⁺: 430.2256; Found: 430.2253. Anal. Calcd for C₂₄H₃₂ClN₃O₂·0.75 H₂O: C 65.00, H 7.61, N 9.47. Found: C 65.27, H 7.51, N 9.15.

1-(9-chloro-5,6,8,9,10,11-hexahydro-7H-5,9:7,11-dimethanobenzo[9]annulen-7-yl)-3-(1-(tetrahydro-2H-pyran-4-carbonyl)piperidin-4-yl)urea, 16. To a solution of 9-chloro-5,6,8,9,10,11-hexahydro-7H-5,9:7,11-dimethanobenzo[9]annulen-7-amine hydrochloride (130 mg, 0.46 mmol) in DCM (4 mL) and saturated aqueous NaHCO₃ solution (3 mL), triphosgene (50 mg, 0.17 mmol) was added. The biphasic mixture was

stirred at room temperature for 30 minutes and then the two phases were separated and the organic one was washed with brine (3 mL), dried over anhydrous Na_2SO_4 , filtered and evaporated under vacuum to obtain 1-2 mL of a solution of isocyanate in DCM. To this solution was added (4-aminopiperidin-1-yl)(tetrahydro-2H-pyran-4-yl)methanone (97 mg, 0.46 mmol). The mixture was stirred overnight at room temperature and the solvent was then evaporated. Column chromatography (SiO_2 , DCM/Methanol mixtures) provided urea **16** as a yellowish solid (90 mg, 41% yield). The analytical sample was obtained by washing the product with ethyl acetate to obtain a white solid, mp 214-215 °C. IR (ATR): 2924, 2851, 1675, 1610, 1546, 1493, 1451, 1361, 1319, 1296, 1282, 1246, 1225, 1208, 1120, 1084, 1017, 991, 946, 908, 874, 810, 755, 730, 696, 644, 619, 564 cm^{-1} . $^1\text{H-NMR}$ (400 MHz, CDCl_3) δ : 1.18 [dq, $J = 12.0$ Hz, $J' = 4.0$ Hz, 2 H, 3'(5')- H_{ax}], 1.56 [m, 2 H, 3''(5'')- H_{ax}], 1.80-1.91 [complex signal, 3 H, 3''(5'')- H_{eq} , 3'- H_{eq} or 5'- H_{eq}], 1.94 [d, $J = 13.2$ Hz, 2 H, 6(12)- H_{ax}], 2.08 (d, $J = 12.8$ Hz, 1 H, 5'- H_{eq} or 3'- H_{eq}), 2.16 [d, 2 H, 10(13)- H_{ax}], 2.20 [m, 2 H, 6(12)- H_{eq}], 2.36 [dd, $J = 13.2$ Hz, $J' = 6.4$ Hz, 2 H, 10(13)- H_{eq}], 2.48 (s, 2 H, 8-H), 2.66-2.78 (complex signal, 2 H, 4''-H, 6'- H_{ax} or 2'- H_{ax}), 3.11 (m, 1 H, 2'- H_{ax} or 6'- H_{ax}), 3.15 [t, $J = 6.0$ Hz, 2 H, 5(11)-H], 3.43 [t, $J = 11.6$ Hz, 2 H, 2''(6'')- H_{ax}], 3.75 (m, 1 H, 4'-H), 3.83 (d, $J = 13.2$ Hz, 1 H, 2'- H_{eq} or 6'- H_{eq}), 3.99 [dm, $J = 11.6$ Hz, 2''(6'')- H_{eq}], 4.46 (m, 1 H, 6'- H_{eq} or 2'- H_{eq}), 4.51 (d, $J = 7.6$ Hz, 1 H, C4'-NH), 4.57 (s, 1 H, C7-NH), 7.06 [m, 2 H, 1(4)-H], 7.09 [m, 2 H, 2(3)-H]. $^{13}\text{C-NMR}$ (100.6 MHz, CDCl_3) δ : 29.1 [CH_2 , C3''(5'')], 32.4 (CH_2 , C5' or C3'), 34.2 (CH_2 , C3' or C5'), 37.6 (CH, C4''), 38.9 [CH_2 , C6(12)], 41.1 (CH_2 , C6' or C2'), 41.2 [CH, C5(11)], 44.3 (CH_2 , C2' or C6'), 44.5 [CH_2 , C10(13)], 47.0 (CH, C4'), 50.8 (CH_2 , C8), 55.6 (C, C7), 67.2 [CH_2 , C2''(6'')], 69.5 (C, C9), 126.8 [CH, 2(3)], 128.1 [CH, 1(4)], 144.7 [C, C5a(11a)], 156.0 (NHCONH), 172.9 (NCOR). HRMS: Calcd for $[\text{C}_{27}\text{H}_{36}\text{ClN}_3\text{O}_3+\text{H}]^+$: 486.2518;

Found: 486.2522. Anal. Calcd for C₂₇H₃₆ClN₃O₃: C 66.72, H 7.47, N 8.65. Found: C 66.92, H 7.40, N 8.43.

1-(1-benzylpiperidin-4-yl)-3-(9-chloro-5,6,8,9,10,11-hexahydro-7H-5,9:7,11-dimethanobenzo[9]annulen-7-yl)urea, 17. To a solution of 9-chloro-5,6,8,9,10,11-hexahydro-7H-5,9:7,11-dimethanobenzo[9]annulen-7-amine hydrochloride (130 mg, 0.46 mmol) in DCM (4 mL) and saturated aqueous NaHCO₃ solution (3 mL), triphosgene (50 mg, 0.17 mmol) was added. The biphasic mixture was stirred at room temperature for 30 minutes and then the two phases were separated and the organic one was washed with brine (4 mL), dried over anh. Na₂SO₄, filtered and evaporated under vacuum to obtain 1-2 mL of a solution of isocyanate in DCM. To this solution was added 1-benzylpiperidin-4-amine (87 mg, 0.46 mmol). The mixture was stirred overnight at room temperature and the solvent was then evaporated. Column chromatography (SiO₂, DCM/Methanol mixtures) provided urea **17** as a yellowish solid (74 mg, 35% yield), mp 104-105 °C. IR (ATR): 3322, 2928, 2854, 1763, 1635, 1598, 1555, 1494, 1451, 1356, 1319, 1282, 1231, 1079, 1048, 990, 908, 803, 758, 739, 698, 633, 598, 563 cm⁻¹. ¹H-NMR (400 MHz, CDCl₃) δ: 1.42 [dq, *J* = 11.2 Hz, *J* = 4 Hz, 2 H, 3'(5')-H_{ax}], 1.87 [dm, *J* = 11.6 Hz, 2 H, 3'(5')-H_{eq}], 1.93 [d, *J* = 12.8 Hz, 2 H, 6(12)-H_{ax}], 2.06-2.17 [complex signal, 4 H, 10(13)-H_{ax}, 2'(6')-H_{ax}], 2.20 [dd, *J* = 12.8 Hz, *J'* = 6.4 Hz, 2 H, 6(12)-H_{eq}], 2.35 [dd, *J* = 12.8 Hz, *J* = 6.0 Hz, 2 H, 10(13)-H_{eq}], 2.48 (s, 2 H, 8-H), 2.82 (d, *J* = 11.6 Hz, 2 H, 2'(6')-H_{eq}], 3.14 [t, *J* = 6.8 Hz, 2 H, 5(11)-H], 3.44-3.56 [complex signal, 3 H, 4'-H, CH₂-C₆H₅], 4.34 (d, *J* = 7.6 Hz, 1 H, C4'-NH), 4.40 (s, 1 H, C7-NH), 7.04 [m, 2 H, 1(4)-H], 7.09 [m, 2 H, 2(3)-H], 7.25 (m, 1 H, Ar-H_{para}), 17.28-7.33 [complex signal, 4 H, Ar-H_{ortho}, Ar-H_{meta}]. ¹³C-NMR (100.6 MHz, CDCl₃) δ: 32.7 [CH₂, C3'(5')], 38.9 [CH₂, C6(12)], 41.2 [CH, C5(11)], 44.5 [CH₂, C10(13)], 47.1 (CH, C4'), 50.8 (CH₂, C8), 52.4 [CH₂, C2'(6')], 55.6 (C, C7), 62.9 (CH₂, CH₂-C₆H₅), 69.5 (C, C9), 126.8 [CH, C2(3)], 127.2 (CH, Ar-

CH_{para}), 128.1 [CH, C1(4)], 128.3 (CH, Ar-CH_{meta}), 129.2 (CH, Ar-CH_{ortho}), 137.7 (C, Ar-C_{ipso}), 144.8 [C, C4a(11a)], 156.1 (C, NHCONH). HRMS: Calcd for [C₂₈H₃₄ClN₃O+H]⁺: 464.2463; Found: 464.2461. Anal. Calcd for C₂₈H₃₄ClN₃O·0.4 H₂O: C 71.36, H 7.44, N 8.92. Found: C 71.62, H 7.36, N 8.53.

1-(9-chloro-5,6,8,9,10,11-hexahydro-7H-5,9:7,11-dimethanobenzo[9]annulen-7-yl)-3-(1-(isopropylsulfonyl)piperidin-4-yl)urea, 18. To a solution of 9-chloro-5,6,8,9,10,11-hexahydro-7H-5,9:7,11-dimethanobenzo[9]annulen-7-amine hydrochloride (268 mg, 0.94 mmol) in DCM (8 mL) and saturated aqueous NaHCO₃ solution (5 mL) was added triphosgene (103 mg, 0.35 mmol). The biphasic mixture was stirred at room temperature for 30 minutes and then the two phases were separated and the organic layer was washed with brine (5 mL), dried over anh. Na₂SO₄, filtered and evaporated under vacuum to obtain 1-2 mL of a solution of the isocyanate in DCM.

To a solution of 1-(isopropylsulfonyl)piperidin-4-amine (194 mg, 0.94 mmol) in anh. THF (8 mL) under argon atmosphere at -78°C, was added dropwise a solution of *n*-butyllithium (2.5 M in hexanes, 0.49 mL, 1.22 mmol) during 20 minutes. After the addition, the mixture was tempered to 0°C using an ice bath. This solution was added carefully to the solution of the isocyanate from the previous step cooled to 0°C, under argon atmosphere. The reaction mixture was stirred at room temperature overnight. Methanol (2 mL) was then added to quench any unreacted *n*-butyllithium. The solvents were evaporated under vacuum to give a yellow residue (690 mg). Column chromatography (SiO₂, DCM/Methanol mixtures) gave a white solid. Crystallization from hot DCM:pentane provided urea **18** as a yellowish solid (75 mg, 17% yield). The analytical sample was obtained by crystallization from hot Ethyl Acetate/Pentane mixtures, mp 223-224 °C. IR (NaCl disk): 3407, 3370, 2926, 2856, 1672, 1538, 1494, 1451, 1353, 1304, 1296, 1223, 1209, 1177, 1130, 1090, 1045, 972, 949, 903, 885, 841,

805, 767, 735, 668, 623 cm^{-1} . $^1\text{H-NMR}$ (400 MHz, CDCl_3) δ : 1.31 [d, $J = 6.8$ Hz, 6 H, $\text{CH}(\underline{\text{CH}_3})_2$], 1.37 [dq, $J = 12.4$ Hz, $J' = 4.0$ Hz, 2 H, 3'(5')- H_{ax}], 1.91-1.99 [complex signal, 4 H, 6(12)- H_{ax} , 3'(5')- H_{eq}], 2.15 [d, $J = 13.2$ Hz, 2 H, 10(13)- H_{ax}], 2.20 [dd, $J = 13.6$ Hz, $J' = 5.6$ Hz, 6(12)- H_{eq}], 2.35 [dd, $J = 13.6$ Hz, $J' = 5.6$ Hz, 10(13)- H_{eq}], 2.47 (s, 2 H, 8-H), 2.93 [dt, $J = 13.2$ Hz, $J' = 2.6$ Hz, 2 H, 2'(6')- H_{ax}], 3.11-3.22 [complex signal, 3 H, $\underline{\text{CH}}(\text{CH}_3)_2$, 5(11)-H], 3.67 (m, 1 H, 4'-H), 3.79 [dm, $J = 13.2$ Hz, 2 H, 2'(6')- H_{eq}], 4.50 (s, 1 H, C7-NH), 4.54 (d, $J = 7.6$ Hz, C4'-NH), 7.04 [m, 2 H, 1(4)-H], 7.10 [m, 2 H, 2(3)-H]. $^{13}\text{C-NMR}$ (100.6 MHz, CDCl_3) δ : 16.7 [CH_3 , $\text{CH}(\underline{\text{CH}_3})_2$], 33.4 [CH_2 , C3'(5')], 38.9 [CH_2 , C6(12)], 41.2 [CH, C5(11)], 44.5 [CH_2 , C10(13)], 45.7 [CH_2 , C2'(6')], 46.6 (CH, C4'), 50.8 (CH_2 , C8), 53.4 [CH, $\underline{\text{CH}}(\text{CH}_3)_2$], 55.6 (C, C7), 69.5 (C, C9), 126.8 [CH, C2(3)], 128.1 [CH, C1(4)], 144.8 [C, C4a(11a)], 156.0 (C, NHCONH). HRMS: Calcd for $[\text{C}_{24}\text{H}_{34}\text{ClN}_3\text{O}_3\text{S}+\text{H}]^+$: 480.2082; Found: 480.2084. Anal. Calcd for $\text{C}_{24}\text{H}_{34}\text{ClN}_3\text{O}_3\text{S}\cdot 0.05$ Ethyl Acetate: C 60.00, H 7.16, N 8.67. Found: C 60.38, H 7.08, N 8.27.

1-(9-chloro-5,6,8,9,10,11-hexahydro-7H-5,9:7,11-dimethanobenzo[9]annulen-7-yl)-3-(1-(cyclopropanecarbonyl)piperidin-4-yl)urea, 19. To a solution of 9-chloro-5,6,8,9,10,11-hexahydro-7H-5,9:7,11-dimethanobenzo[9]annulen-7-amine hydrochloride (130 mg, 0.46 mmol) in DCM (4 mL) and saturated aqueous NaHCO_3 solution (3 mL), triphosgene (50 mg, 0.17 mmol) was added. The biphasic mixture was stirred at room temperature for 30 minutes and then the two phases were separated and the organic one was washed with brine (3 mL), dried over anhydrous Na_2SO_4 , filtered and evaporated under vacuum to obtain 1-2 mL of a solution of isocyanate in DCM. To this solution was added (4-aminopiperidin-1-yl)(cyclopropyl)methanone (77 mg, 0.46 mmol). The mixture was stirred overnight at room temperature and the solvent was then evaporated. Column chromatography (SiO_2 , DCM/Methanol mixtures) provided urea **19** as a white solid (70 mg, 35% yield), mp 119-120 $^\circ\text{C}$. IR (ATR): 3367, 3330, 2926, 2853,

1682, 1654, 1605, 1565, 1550, 1481, 1452, 1374, 1357, 1319, 1299, 1264, 1224, 1128, 1088, 1036, 1013, 993, 967, 948, 925, 911, 870, 799, 755, 735, 700, 632, 604, 564 cm⁻¹. ¹H-NMR (400 MHz, CDCl₃) δ: 0.75 (m, 2 H, 2''(3'')-H_{ax}), 0.94 [m, 2 H, 2''(3'')-H_{eq}], 1.23 [m, 2 H, 3'(5')-H_{ax}], 1.74 (m, 1 H, 1''-H), 1.88 (m, 1 H, 5'-H_{eq} or 3'-H_{eq}), 1.95 [d, *J* = 13.2 Hz, 2 H, 6(12)-H_{ax}], 2.08 (m, 1 H, 3'-H_{eq} or 5'-H_{eq}), 2.16 [d, *J* = 13.2 Hz, 2 H, 10(13)-H_{ax}], 2.23 [m, 2 H, 6(12)-H_{eq}], 2.37 [dd, *J* = 12.0 Hz, *J*' = 6.4 Hz, 2 H, 10(13)-H_{ax}], 2.50 (s, 2 H, 8-H), 2.73 (broad t, *J* = 12.0 Hz, 1 H, 2'-H_{ax} or 6'-H_{ax}), 3.16 [t, *J* = 6.4 Hz, 2 H, 5(11)-H], 3.21 (m, 1 H, 6'-H_{ax} or 2'-H_{ax}), 3.77 (m, 1 H, 4'-H), 4.14 (m, 1 H, 6'-H_{eq} or 2'-H_{eq}), 4.23 (d, *J* = 8.0 Hz, 1 H, C4'-NH), 4.30 (s, 1 H, C7-NH), 4.48 (dm, *J* = 12.0 Hz, 1 H, 3'-H_{eq} or 5'-H_{eq}), 7.05 [m, 2 H, 1(4)-H], 7.11 [m, 2 H, 2(3)-H]. ¹³C-NMR (100.6 MHz, CDCl₃) δ: 7.4 [CH₂, C2''(3'')], 11.0 (CH, C1''), 32.3 (CH₂, C5' or C3'), 34.1 (CH₂, C3' or C5'), 38.9 [CH₂, C6(12)], 41.3 [CH, C5(11)], 41.6 (CH₂, C2' or C6'), 44.5 [CH₂, C10(13)], 44.6 (CH₂, C6' or C2'), 46.7 (CH, C4'), 50.8 (CH₂, C8), 55.5 (C, C7), 69.6 (C, C9), 126.8 [CH, C2(3)], 128.1 [CH, C1(4)], 144.8 (C, C4a(11a)), 156.3 (C, NHCONH), 172.2 (C, NCOR). HRMS: Calcd for [C₂₅H₃₂ClN₃O₂+H]⁺: 442.2256; Found: 442.2262. Anal. Calcd for C₂₅H₃₂ClN₃O₂·0.75 H₂O: C 66.05, H 7.41, N 9.24. Found: C 66.21, H 7.31, N 9.00.

1-(1-(4-acetylphenyl)piperidin-4-yl)-3-(9-chloro-5,6,8,9,10,11-hexahydro-7H-

5,9:7,11-dimethanobenzo[9]annulen-7-yl)urea, 20. To a solution of 9-chloro-5,6,8,9,10,11-hexahydro-7H-5,9:7,11-dimethanobenzo[9]annulen-7-amine

hydrochloride (100 mg, 0.35 mmol) in DCM (3 mL) and saturated aqueous NaHCO₃ solution (2 mL), triphosgene (38 mg, 0.13 mmol) was added. The biphasic mixture was stirred at room temperature for 30 minutes and then the two phases were separated and the organic one was washed with brine (3 mL), dried over anh. Na₂SO₄, filtered and evaporated under vacuum to obtain 1-2 mL of a solution of isocyanate in DCM. To this

solution was added 1-(4-(4-aminopiperidin-1-yl)phenyl)ethan-1-one (76 mg, 0.35 mmol). The mixture was stirred overnight at room temperature and the solvent was then evaporated. Column chromatography (SiO₂, Hexane/Ethyl Acetate mixtures) provided urea **20** as a white solid (35 mg, 20% yield), mp 109-110 °C. IR (ATR): 3310, 2919, 2854, 1670, 1640, 1597, 1556, 1516, 1451, 1429, 1384, 1356, 1283, 1221, 1191, 1122, 1082, 1045, 1000, 957, 945, 923, 917, 814, 754, 592 cm⁻¹. ¹H-NMR (400 MHz, CDCl₃) δ: 1.39 [dq, *J* = 11.2 Hz, *J'* = 4.0 Hz, 2 H, 3'(5')-H_{ax}], 1.95 [d, *J* = 12.8 Hz, 2 H, 6(12)-H_{ax}], 1.99 [m, 2 H, 3'(5')-H_{eq}], 2.15 [d, *J* = 12.8 Hz, 2 H, 10(13)-H_{ax}], 2.22 [dd, *J* = 12.8 Hz, *J'* = 6.0 Hz, 6(12)-H_{eq}], 2.36 [dd, *J* = 12.8 Hz, *J'* = 6.0 Hz, 10(13)-H_{eq}], 2.48-2.51 (complex signal, 5 H, COCH₃, 8-H₂), 2.98 [m, 2 H, 2'(6')-H_{ax}], 3.15 [t, *J* = 6.4 Hz, 2 H, 5(11)-H], 3.71-3.83 [complex signal, 3 H, 4'-H, 2'(6')-H_{eq}], 4.48 (d, *J* = 7.6 Hz, 4'-NH), 4.54 (s, 1 H, 7-NH), 6.81 [d, *J* = 8.8 Hz, 2 H, 2''(6'')-H], 7.04 [m, 2 H, 1(4)-H], 7.10 [m, 2 H, 2(3)-H], 7.82 [d, *J* = 8.8 Hz, 2 H, 3''(5'')-H]. ¹³C-NMR (100.6 MHz, CDCl₃) δ: 26.1 (CH₃, COCH₃), 32.1 [CH₂, C3'(5')], 38.9 [CH₂, C6(12)], 41.2 [CH, C5(11)], 44.5 [CH₂, C10(13)], 47.0 [CH₂, C2'(6')], 46.9 (CH, C4'), 50.8 (CH₂, C8), 55.7 (C, C7), 69.5 (C, C9), 113.4 [CH, C2''(6'')], 126.8 [CH, C2(3)], 126.9 (C, C4''), 128.1 [CH₂, C1(4)], 130.5 [CH, C3''(5'')], 144.7 [C, C4a(11a)], 153.8 (C, C1''), 156.0 (C, NHCONH), 196.8 (C, COCH₃). HRMS: Calcd for [C₂₉H₃₄ClN₃O₂+H]⁺: 492.2412; Found: 492.2415. Anal. Calcd for C₂₉H₃₄ClN₃O₂·0.2 Ethyl Acetate · 0.2 Hexane: C 70.66, H 7.35, N 7.97. Found: C 70.86, H 7.17, N 7.77.

1-(9-chloro-5,6,8,9,10,11-hexahydro-7H-5,9:7,11-dimethanobenzo[9]annulen-7-yl)-3-(1-(2,2,2-trifluoroacetyl)piperidin-4-yl)urea, 21. To a solution of 9-chloro-5,6,8,9,10,11-hexahydro-7H-5,9:7,11-dimethanobenzo[9]annulen-7-amine hydrochloride (130 mg, 0.46 mmol) in DCM (4 mL) and saturated aqueous NaHCO₃ solution (3 mL), triphosgene (50 mg, 0.17 mmol) was added. The biphasic mixture was

stirred at room temperature for 30 minutes and then the two phases were separated and the organic one was washed with brine (3 mL), dried over anh. Na₂SO₄, filtered and evaporated under vacuum to obtain 1-2 mL of a solution of isocyanate in DCM. To this solution was added 1-(4-aminopiperidin-1-yl)-2,2,2-trifluoroethan-1-one hydrochloride (106 mg, 0.46 mmol) and Et₃N (92 mg, 0.91 mmol). The mixture was stirred overnight at room temperature and the mixture was washed with water (15 mL). The organic phase was dried over anh. Na₂SO₄, filtered and evaporated under vacuum to obtain an orange gum (196 mg). Column chromatography (SiO₂, DCM/Methanol mixtures) provided urea **21** as a yellowish solid (55 mg, 26% yield). The analytical sample was obtained by a crystallization from hot Ethyl Acetate/Pentane mixtures, mp 188-189 °C. IR (ATR): 3348, 2926, 2859, 1689, 1634, 1556, 1495, 1466, 1454, 1357, 1298, 1266, 1203, 1179, 1137, 1091, 1044, 1009, 992, 971, 946, 897, 802, 757, 698, 660, 623, 599, 556 cm⁻¹. ¹H-NMR (400 MHz, CDCl₃) δ: 1.30 [m, 2 H, 5'(3')-H_{ax}], 1.94 [d, *J* = 12.8 Hz, 2 H, 6(12)-H_{ax}], 2.03 [m, 2 H, 5'(3')-H_{eq}], 2.16 [d, *J* = 13.6 Hz, 2 H, 10(13)-H_{ax}], 2.20 [m, 2 H, 6(12)-H_{eq}], 2.36 [dd, *J* = 13.6 Hz, *J'* = 13.6 Hz, 2 H, 10(13)-H_{eq}], 2.47 (s, 2 H, 8-H), 2.89 (t, *J* = 12.0 Hz, 1 H, 2'-H_{ax} or 6'-H_{ax}), 3.13-3.25 [complex signal, 3 H, 5(11)-H, 6'-H_{ax} or 2'-H_{ax}], 3.80 (m, 1 H, 4'-H), 3.95 (d, *J* = 14.0 Hz, 1 H, 6'-H_{eq} or 2'-H_{eq}), 4.28 (d, *J* = 7.6 Hz, 1 H, C4'-NH), 4.32 (s, 1 H, C7-NH), 4.42 (dm, *J* = 14.0 Hz, 2'-H_{eq} or 6'-H_{eq}), 7.05 [m, 2 H, 1(4)-H], 7.09 [m, 2 H, 2(3)-H]. ¹³C-NMR (100.6 MHz, CDCl₃) δ: 32.2 (CH₂, C5' or C3'), 33.3 (CH₂, C3' or C5'), 38.91 (CH₂, C6 or C12), 38.92 (CH₂, C12 or C6), 41.2 [CH, C5(11)], 42.8 (CH₂, C2' or C6'), 44.4 [CH₂, C10(13)], 44.7 (q, ⁴*J*_{C-F} = 3.5 Hz, CH₂, C6' or C2'), 46.7 (CH, C4'), 50.8 (CH₂, C8), 55.8 (C, C7), 69.3 (C, C9), 116.5 (q, ¹*J*_{C-F} = 287.7 Hz, C, CF₃), 126.8 [CH, C2(3)], 128.1 [CH, C1(4)], 144.7 [C, C4a(11a)], 155.3 (C, NCOR), 155.6 (C, NHCONH). HRMS: Calcd for [C₂₃H₂₇ClF₃N₃O₂-H]⁻: 468.1671;

Found: 468.1671. Anal. Calcd for $C_{23}H_{27}ClF_3N_3O_2 \cdot 0.75 CH_3OH$: C 57.75, H 6.12, N 8.51. Found: C 58.04, H 5.82, N 8.20.

1-(9-chloro-5,6,8,9,10,11-hexahydro-7H-5,9:7,11-dimethanobenzo[9]annulen-7-yl)-3-(1-(1-fluorocyclopropane-1-carbonyl)piperidin-4-yl)urea, 22. To a solution of 9-chloro-5,6,8,9,10,11-hexahydro-7H-5,9:7,11-dimethanobenzo[9]annulen-7-amine hydrochloride (130 mg, 0.46 mmol) in DCM (4 mL) and saturated aqueous $NaHCO_3$ solution (3 mL), triphosgene (50 mg, 0.17 mmol) was added. The biphasic mixture was stirred at room temperature for 30 minutes and then the two phases were separated and the organic one was washed with brine (3 mL), dried over anh. Na_2SO_4 , filtered and evaporated under vacuum to obtain 1-2 mL of a solution of isocyanate in DCM. To this solution were added (4-aminopiperidin-1-yl)(1-fluorocyclopropyl)methanone hydrochloride (101 mg, 0.46 mmol) and Et_3N (92 mg, .91 mmol). The mixture was stirred overnight at room temperature and the mixture was washed with water (10 mL). The organic phase was dried over anh. Na_2SO_4 , filtered and evaporated under vacuum to obtain an orange gum (140 mg). Column chromatography (SiO_2 , DCM/Methanol mixtures) provided urea **22** as a yellowish solid (20 mg, 10% yield). The analytical sample was obtained by a crystallization from hot Ethyl Acetate/Pentane mixtures, mp 120-121 °C. IR (ATR): 3340, 2921, 2856, 1730, 1632, 1553, 1493, 1453, 1439, 1356, 1327, 1299, 1274, 1244, 1204, 1122, 1088, 1047, 1025, 993, 970, 947, 907, 801, 760, 729, 697, 680, 643 cm^{-1} . 1H -NMR (400 MHz, $CDCl_3$) δ : 1.14 -1.38 [complex signal, 6 H, 2''(3'')- H_2 , 5'(3')- H_{ax}], 1.95 [d, $J = 13.2$ Hz, 2 H, 6(12)- H_{ax}], 2.00 [m, 2 H, 5'(3')- H_{eq}], 2.16 [d, $J = 13.2$ Hz, 2 H, 10(13)- H_{ax}], 2.22 [dd, $J = 12.4$ Hz, $J' = 5.6$ Hz, 2 H, 6(12)- H_{eq}], 2.36 [dd, $J = 12.4$ Hz, $J' = 6$ Hz, 10(13)- H_{eq}], 2.49 (s, 2 H, 8-H), 2.83 (m, 1 H, 2'- H_{ax} or 6'- H_{ax}), 3.15 (broad signal, 1 H, 6'- H_{ax} or 2'- H_{ax}), 3.16 [t, $J = 6.4$ Hz, 2 H, 5(11)-H], 3.79 (m, 1 H, 4'-H), 4.21 (d, $J = 8.0$ Hz, 1 H, C4'-NH), 4.27 (s, 1 H, C7-NH), 4.18-4.22 (m, 2 H, 2'-

H_{eq}, 6'-H_{eq}), 7.06 [m, 2 H, 2(3)-H], 7.10 [m, 2 H, 1(4)-H]. ¹³C-NMR (100.6 MHz, CDCl₃) δ: 11.8 [CH₂, 2''(3'')-H], 33.6 [CH₂, C3'(5')], 38.9 [CH₂, C6(12)], 41.2 [CH, C5(11)], 44.5 [2 CH₂, C10(13), C2'(6')], 47.2 (CH, C4'), 50.8 (CH₂, C8), 55.7 (C, C7), 69.4 (C, C9), 79.2 (C, C1''), 126.8 [CH, C2(3)], 128.1 [CH, C1(4)], 144.7 [C, C4a(11a)], 155.7 (C, NHCONH), 166.5 (C, NCOR). HRMS: Calcd for [C₂₅H₃₁ClFN₃O₂+H]⁺: 460.2162; Found: 460.2165. HPLC/MS (m/z) (M+H) = 460.9, t_r = 3.6 (λ = 220 nm, 90.6% purity).

1-(1-acetylpiperidin-4-yl)-3-(9-fluoro-5,6,8,9,10,11-hexahydro-7H-5,9:7,11-dimethanobenzo[9]annulen-7-yl)urea, 23. To a solution of 9-fluoro-5,6,8,9,10,11-hexahydro-7H-5,9:7,11-dimethanobenzo[9]annulen-7-amine hydrochloride (143 mg, 0.53 mmol) in DCM (4 mL) and saturated aqueous NaHCO₃ solution (2 mL) was added triphosgene (78 mg, 0.26 mmol). The biphasic mixture was stirred at room temperature for 30 minutes and then the two phases were separated and the organic layer was washed with brine (5 mL), dried over anh. Na₂SO₄, filtered and evaporated under vacuum to obtain 1-2 mL of a solution of the isocyanate in DCM. To this solution was added 1-(4-aminopiperidin-1-yl)ethan-1-one (90 mg, 0.63 mmol). The reaction mixture was stirred at room temperature overnight and the solvent was evaporated under vacuum to obtain a yellow gum (259 mg). Column chromatography (SiO₂, DCM/methanol mixtures) gave urea **23** (180 mg, 85% yield). The analytical sample was obtained by crystallization from hot DCM (57 mg), mp 228-229°C. IR (NaCl disk): 3357, 3063, 3018, 2928, 2857, 1684, 1643, 1618, 1553, 1494, 1451, 1359, 1341, 1317, 1267, 1227, 1207, 1135, 1097, 1042, 1004 cm⁻¹. ¹H-NMR (400 MHz, CDCl₃) δ: 1.15 [dq, *J* = 12.0 Hz, *J*' = 4.0 Hz, 1 H, 5'-H_{ax} or 3'-H_{ax}], 1.16 (dq, *J* = 12.0 Hz, *J*' = 4.0 Hz, 2 H, 3'-H_{ax} or 5'-H_{ax}), 1.83-2.04 [complex signal, 6 H, 10(13)-H_{ax}, 6-H_{ax}, 12-H_{ax}, 5'-H_{eq} or 3'-H_{eq}], 2.06 (s, 3 H, COCH₃), 2.09-2.26 [complex signal, 6 H, 8-H₂, 10(13)-H_{eq}, 6-H_{eq}, 12-H_{eq}], 2.71 (m, 1 H, 6'-H_{ax} or 2'-H_{ax}), 3.12 (m, 1 H, 2'-H_{ax} or 6'-H_{ax}), 3.21 [t, *J* = 7.2 Hz, 2 H, 5(11)-H], 3.69-3.77

(complex signal, 2 H, 4'-H, 6'-H_{eq} or 2'-H_{eq}), 4.42 (dm, $J = 13.6$ Hz, 1 H, 2'-H_{eq} or 6'-H_{eq}), 4.71 (d, $J = 7.6$ Hz, 1 H, C4'-NH), 4.82 (s, 1 H, C7-NH), 7.06 [m, 2 H, 1(4)-H], 7.10 [m, 2 H, 2(3)-H]. ¹³C-NMR (100.6 MHz, CDCl₃) δ : 21.4 (CH₃, COCH₃), 32.3 (CH₂, C5' or C3'), 33.7 (C3' or C5'), 39.3 (CH₂, d, $^4J_{C-F} = 2.2$ Hz, C6 or C12), 39.3 (CH₂, d, $^4J_{C-F} = 2.2$ Hz, C12 or C6), 39.6 [CH, d, $^3J_{C-F} = 13.3$ Hz, C5(11)], 40.1 [CH₂, d, $^2J_{C-F} = 20.1$ Hz, C10(13)], 40.7 (CH₂, C6' or C2'), 45.4 (CH₂, C2' or C6'), 46.6 (CH, C4'), 46.8 (CH₂, C8), 56.8 (C, d, $^3J_{C-F} = 11.4$ Hz, C7), 94.4 (C, d, $^1J_{C-F} = 176.9$, C9), 126.8 [CH, C2(3)], 128.1 [CH, C1(4)], 144.8 [C, d, $^4J_{C-F} = 2.0$ Hz, C4a(11a)], 156.2 (C, NHCONH), 169.1 (C, COCH₃). Anal. Calcd for C₂₃H₃₀FN₃O₂·0.5 H₂O: C 67.62, H 7.65, N 10.29. Found: C 67.61, H 7.93, N 9.94. HRMS: Calcd for [C₂₃H₃₀FN₃O₂+H]⁺: 400.2395; Found: 400.2395.

1-(9-fluoro-5,6,8,9,10,11-hexahydro-7H-5,9:7,11-dimethanobenzo[9]annulen-7-yl)-3-(1-(tetrahydro-2H-pyran-4-carbonyl)piperidin-4-yl)urea, 24. To a solution of 9-fluoro-5,6,8,9,10,11-hexahydro-7H-5,9:7,11-dimethanobenzo[9]annulen-7-amine hydrochloride (150 mg, 0.56 mmol) in DCM (4.5 mL) saturated aqueous NaHCO₃ solution (3.5 mL) and triphosgene (61.5 mg, 0.21 mmol) were added. The biphasic mixture was stirred at room temperature for 30 minutes and then the two phases were separated and the organic layer was washed with brine (3.5 mL), dried over anh. Na₂SO₄, filtered and evaporated under vacuum to obtain 1-2 mL of a solution of the isocyanate in DCM. To this solution was added (4-aminopiperidin-1-yl)(tetrahydro-2H-pyran-4-yl)methanone (119 mg, 0.56 mmol). The mixture was stirred overnight at room temperature and the solvent was then evaporated. Column chromatography (SiO₂, DCM/Methanol mixtures) provided urea **24** as a yellowish solid (75 mg, 28% yield), mp 210-213 °C. IR (ATR): 3351, 2926, 2850, 1609, 1549, 1444, 1358, 1306, 1210, 1125, 1089, 1005, 983, 867, 760 cm⁻¹. ¹H-NMR (400 MHz, CDCl₃) δ : 1.17 [dq, 2 H, $J = 12.0$

Hz, $J' = 4.0$ Hz, 3'(5')-H_{ax}], 1.56 [t, 2 H, $J = 10.8$ Hz, 3''(5'')-H_{ax}], 1.76-2.00 [complex signal, 7 H, 10(13)-H_{ax}, 6(12)-H_{ax}, 3''(5'')-H_{eq}, 3'-H_{eq} or 5'-H_{eq}], 2.02-2.20 [complex signal, 5 H, 10(13)-H_{eq}, 6(12)-H_{eq}, 5'-H_{eq} or 3'-H_{eq}], 2.21 (d, 2 H, $J = 6.0$ Hz, 8-H₂), 2.65-2.80 (complex signal, 2 H, 4''-H, 2'-H_{ax} or 6'-H_{ax}), 3.11 (t, 1H, $J = 12.4$ Hz, 6'-H_{ax} or 2'-H_{ax}), 3.21 [broad signal, s, 2 H, 5(11)-H], 3.43 [t, 2 H, $J = 11.2$ Hz, 2''(6'')-H_{ax}], 3.75 (m, 1 H, 4'-H), 3.83 (d, 1 H, $J = 13.2$ Hz, 2'-H_{eq} or 6'-H_{eq}), 3.99 [dd, 2 H, $J = 11.6$ Hz, $J' = 2.0$ Hz, 2''(6'')-H_{eq}], 4.47 (d, 1 H, $J = 14.0$ Hz, 6'-H_{eq} or 2'-H_{eq}), 4.55 (d, 1 H, $J = 7.6$ Hz, C4'-NH), 4.64 (s, 1 H, C7-NH), 7.06 [m, 2 H, 1(4)-H], 7.11 [m, 2 H, 2(3)-H]. ¹³C-NMR (100.6 MHz, CDCl₃) δ : 29.1 [CH₂, C3''(5'')], 32.4 (CH₂, C3' or 5'), 34.2 (CH₂, C5' or 3'), 37.6 (CH, C4''), 39.3 [CH₂, C6(12)], 39.5 [CH, $^3J_{C-F} = 13.4$ Hz, C5(11)], 40.1 [CH₂, d, $^2J_{C-F} = 20.1$ Hz, C10(13)], 41.1 (CH₂, C2' or 6'), 44.3 (CH₂, C2' or 6'), 46.7 (CH₂, d, $^2J_{C-F} = 17.9$ Hz, C8), 46.9 (CH, C4'), 56.9 (C, d, $^3J_{C-F} = 11.5$ Hz, C7), 67.1 (CH₂, C2''(6'')), 94.4 [C, d, $^1J_{C-F} = 177.2$ Hz, C9), 126.8 [CH, C1(4)], 128.1 [CH, C2(3)], 144.8 [C, C1'(4')], 156.0 (C, NHCONH), 172.9 (C, NCOR). Anal. Calcd for C₂₇H₃₆FN₃O₃ · 0.2 CH₂Cl₂: C 67.14, H 7.54, N 8.64. Found: C 67.47, H 7.57, N 8.29. HRMS: Calcd for [C₂₇H₃₆FN₃O₃+H]: 470.2813, found: 470.2815.

1-(9-fluoro-5,6,8,9,10,11-hexahydro-7H-5,9:7,11-dimethanobenzo[9]annulen-7-yl)-3-(1-(cyclopropanecarbonyl)piperidin-4-yl)urea, 25. To a solution of 9-fluoro-5,6,8,9,10,11-hexahydro-7H-5,9:7,11-dimethanobenzo[9]annulen-7-amine hydrochloride (150 mg, 0.56 mmol) in DCM (4.5 mL) saturated aqueous NaHCO₃ solution (3.5 mL) and triphosgene (61.5 mg, 0.21 mmol) were added. The biphasic mixture was stirred at room temperature for 30 minutes and then the two phases were separated and the organic layer was washed with brine (3.5 mL), dried over anh. Na₂SO₄, filtered and evaporated under vacuum to obtain 1-2 mL of a solution of the isocyanate in DCM. To this solution was added (4-aminopiperidin-1-yl)(tetrahydro-2H-pyran-4-

yl)methanone (94.2 mg, 0.56 mmol). The mixture was stirred overnight at room temperature and the solvent was then evaporated. Column chromatography (SiO₂, DCM/Methanol mixtures) provided urea **25** as a white solid (60 mg, 25% yield), mp 187–191 °C. IR (ATR): 3320, 2934, 1630, 1568, 1450, 1358, 1317, 1221, 1125, 865, 767, 734, 569. ¹H-NMR (400 MHz, CDCl₃) δ: 0.75 [dd, 2 H, *J* = 8.0 Hz, *J*' = 3.2 Hz, 8'(9')-H_{ax}], 0.93 [dd, 2 H, *J* = 9.6 Hz, *J*' = 4.8 Hz, 8'(9')-H_{eq}], 1.20 [complex signal, 2 H, 3'(5')-H_{ax}], 1.74 (tt, 1 H, *J* = 8.0 Hz, *J*' = 4.8 Hz, 7'-H), 1.95 – 1.85 [d, 4 H, *J* = 12.8 Hz, 10(13)-H_{ax}, 6(12)-H_{ax}; d, 1 H, *J* = 12.4 Hz, 3' or 5'-H_{eq}], 2.2 – 2.1 [complex signal, 5 H, 10(13)-H_{eq}, 6(12)-H_{eq}, 3' or 5'-H_{eq}], 2.25 (d, 2 H, *J* = 5.2 Hz, 8-H), 2.75 (t, 2 H, *J* = 12 Hz, 2' or 6'-H_{ax}), 3.20 [m, 3 H, 5(11)-H, 2' or 6'-H_{ax}], 3.75 (m, 1 H, 4'-H), 4.10 (broad signal, d, 1 H, *J* = 14 Hz, 2' or 6'-H_{eq}), 4.37 (d, 1 H, *J* = 7.6 Hz, HNCONH), 4.50 – 4.45 (s, 1 H, HNCONH; s, 1 H, 2' or 6'-H_{eq}), 7.07 [broad signal, 2 H, 2(3)-H], 7.11 [broad signal, 2 H, 1(4)-H]. ¹³C-NMR (100.5 MHz, CDCl₃) δ: 7.51 [CH₂, C8'(9')], 11.15 (CH, C7'), 32.54 (CH₂, C5' or 3'), 34.41 (CH₂, C5' or 3'), 39.47 [CH, C5(11)], 39.80 [CH₂, d, ⁴*J*_{C-F} = 14.07 Hz, C6(12)], 40.34 [CH₂, d, ²*J*_{C-F} = 20.1 Hz, C10(13)], 41.66 (CH₂, C2' or 6'), 44.71 (CH₂, C2' or 6'), 46.94 (CH₂, d, ²*J*_{C-F} = 18.09 Hz, C8), 47.22 (CH, C4'), 57.19 (C, C7), 94.53 (C, d, ¹*J*_{C-F} = 176.88 Hz, C9), 126.99 [CH, C1(4)], 128.27 [CH, C2(3)], 144.97 [CH, C1'(4')], 156.09 (C, HNCONH), 172.26 (C, CO). Anal. Calcd for C₂₅H₃₂FN₃O₂ · 0.1 CH₂Cl₂: C 69.46 H 7.48, N 9.68. Found: C 69.64, H 7.52, N 9.45. Accurate mass: Calculate for [C₂₅H₃₂FN₃O₂+H]⁺: 426.2551, found: 426.2556.

1-(1-(isopropylsulfonyl)piperidin-4-yl)-3-(9-methyl-5,6,8,9,10,11-hexahydro-7H-5,9:7,11-dimethanobenzo[9]annulen-7-yl)urea, 26. To a solution of 1-(4-aminopiperidin-1-yl)ethan-1-one (192 mg, 1.35 mmol) in DCM (4 mL) and saturated aqueous NaHCO₃ solution (3 mL) triphosgene (200 mg, 0.67 mmol) was added. The biphasic mixture was stirred at room temperature for 30 minutes and then the two phases

were separated and the organic one was washed with brine (5 mL), dried over anhydrous Na_2SO_4 , filtered and evaporated under vacuum to obtain 1-2 mL of a solution of the isocyanate in DCM. To this solution was added 9-amino-5,6,8,9,10,11-hexahydro-7*H*-5,9:7,11-dimethanobenzo[9]annulen-7-ol hydrochloride (300 mg, 1.13 mmol) followed by Et_3N (228 mg, 2.25 mmol). The reaction mixture was stirred at room temperature overnight and the solvent was evaporated under vacuum. Column chromatography (SiO_2 , DCM/methanol mixtures) gave urea **26** (19 mg, 4.2% yield) as a grey solid, mp 222-223°C. IR (NaCl disk): 3313, 2922, 2852, 1733, 1716, 1699, 1646, 1622, 1558, 1542, 1507, 1491, 1472, 1456, 1358, 1337, 1319, 1301, 1265, 1231, 1204, 1134, 1104, 1053 cm^{-1} . $^1\text{H-NMR}$ (400 MHz, CDCl_3) δ : 1.20 [m, 2 H, 3'(5')- H_{ax}], 1.76 [d, $J = 12.8$ Hz, 2 H, 6(12)- H_{ax}], 1.86-2.02 [complex signal, 6 H, 3'(5')- H_{eq} , 10(13)- H_{ax} , 6(12)- H_{eq}], 2.04 (s, 2 H, 8-H), 2.07 (s, 3 H, COCH_3), 2.14 [m, 2 H, 10(12)- H_{eq}], 2.70 (m, 1 H, 6'- H_{ax} or 2'- H_{ax}), 3.12 (ddd, $J = 14.4$ Hz, $J' = 12.0$ Hz, $J'' = 2.4$ Hz, 1 H, 2'- H_{ax} or 6'- H_{ax}), 3.17 [t, $J = 6.0$ Hz, 2 H, 5(11)-H], 3.67-3.78 [complex signal, 2 H, 4'-H, 2'- H_{eq} or 6'- H_{eq}], 4.24 (d, $J = 7.6$ Hz, 1 H, C4'-NH), 4.34 (s, 1 H, C7-NH), 4.47 [dm, $J = 14.0$ Hz, 1 H, 6'- H_{eq} or 2'- H_{eq}], 7.06 [m, 2 H, 1(4)-H], 7.09 [m, 2 H, 2(3)-H]. $^{13}\text{C-NMR}$ (100.6 MHz, CDCl_3) δ : 21.4 (CH_3 , COCH_3), 32.4 (CH_2 , C5' or C3'), 33.6 (CH_2 , C3' or C5'), 39.4 [CH_2 , C10(13)], 40.1 [CH, C5(11)], 40.7 (CH_2 , C6' or C2'), 42.5 [CH_2 , C6(12)], 45.4 (CH_2 , C2' or C6'), 47.1 (CH, C4'), 49.1 (CH_2 , C8), 56.3 (C, C7), 71.0 (C, C9), 126.6 [CH, C2(3)], 128.1 [CH, C1(4)], 145.2 [C, C4a(11a)], 155.9 (C, NHCONH), 169.0 (C, COCH_3). Anal. Calcd for $\text{C}_{23}\text{H}_{31}\text{N}_3\text{O}_3 \cdot \text{CH}_3\text{OH}$: C 67.11, H 8.21, N 9.78. Found: C 67.25, H 8.15, N 9.72. HRMS: Calcd for $[\text{C}_{23}\text{H}_{31}\text{N}_3\text{O}_3 + \text{H}]^+$: 398.2438; Found: 398.2440.

1-(1-acetylpiperidin-4-yl)-3-(9-methoxy-5,6,8,9,10,11-hexahydro-7*H*-5,9:7,11-dimethanobenzo[9]annulen-7-yl)urea, 27. To a solution of 9-methoxy-5,6,8,9,10,11-hexahydro-7*H*-5,9:7,11-dimethanobenzo[9]annulen-7-amine (300 mg, 1.23 mmol) in

DCM (4.5 mL) and saturated aqueous NaHCO₃ solution (3 mL) triphosgene (183 mg, 0.62 mmol) was added. The biphasic mixture was stirred at room temperature for 30 minutes and then the two phases were separated and organics were washed with brine (5 mL), dried over anh. Na₂SO₄, filtered and evaporated under vacuum to obtain 1-2 mL of a solution of the isocyanate in DCM. To this solution was added 1-(4-aminopiperidin-1-yl)ethan-1-one (210 mg, 1.47 mmol). The reaction mixture was stirred at room temperature overnight and the solvent was evaporated under vacuum to obtain a white gum (521 mg). Column chromatography (SiO₂, DCM/methanol mixtures) gave urea **27** (148 mg, 30% yield) as a white solid. The analytical sample was obtained by crystallization from hot EtOAc, mp 212-213°C. IR (NaCl disk): 3358, 3044, 3019, 2931, 2847, 2823, 1646, 1618, 1555, 1495, 1452, 1356, 1319, 1266, 1229, 1135, 1095, 1076, 972, 849, 756, 735 cm⁻¹. ¹H-NMR (400 MHz, CDCl₃) δ: 1.12 (dq, *J* = 11.6 Hz, *J*' = 4.0 Hz, 1 H, 3'-H_{ax} or 5'-H_{ax}), 1.19 (dq, *J* = 11.6 Hz, *J*' = 4.0 Hz, 1 H, 5'-H_{ax} or 3'-H_{ax}), 1.79-1.86 [complex signal, 3 H, 6(12)-H_{ax}, 5'-H_{eq} or 3'-H_{eq}], 1.92 [dm, *J* = 12.4 Hz, 6(12)-H_{eq}], 1.98-2.02 [complex signal, 5 H, 10(13)-H_{ax}, 8-H₂, 5'-H_{eq} or 3'-H_{eq}], 2.06 (s, 3 H, COCH₃), 2.10 [m, 2 H, 10(13)-H_{eq}], 2.70 (m, 1 H, 6'-H_{ax} or 2'-H_{ax}), 3.10 (ddd, *J* = 14.4 Hz, *J*' = 12.4 Hz, *J*'' = 2.4 Hz, 1 H, 2'-H_{ax} or 6'-H_{ax}), 3.17 [t, *J* = 6.0 Hz, 2 H, 5(11)-H], 3.22 (s, 3 H, OCH₃), 3.68-3.77 (complex signal, 2 H, 4'-H, 6'-H_{eq} or 2'-H_{eq}), 4.41 (dm, *J* = 13.6 Hz, 1 H, 2'-H_{eq} or 6'-H_{eq}), 4.73 (d, *J* = 8.0 Hz, 1 H, C4'-NH), 4.76 (s, 1 H, C7-NH), 7.05 [m, 2 H, 1(4)-H], 7.08 (m, 2 H, 2(3)-H]. ¹³C-NMR (100.6 MHz, CDCl₃) δ: 21.4 (CH₃, COCH₃), 32.4 (CH₂, C5' or C3'), 33.7 (CH₂, C3' or C5'), 38.2 [CH₂, C6(12)], 39.71 (CH₂, C10 or C13), 39.73 (CH₂, C13 or C10), 39.8 [CH, C5(11)], 40.7 (CH₂, C6' or C2'), 45.4 (CH₂, C2' or C6'), 45.6 (CH₂, C8), 46.6 (CH, C4'), 48.2 (CH₃, OCH₃), 55.8 (C, C7), 74.8 (C, C9), 126.6 CH, C2(3)], 128.0 [CH, C1(4)], 145.4 [C, C4a(11a)], 156.3 (C, NHCONH), 169.1 (C, COCH₃). Anal. Calcd for C₂₄H₃₃N₃O₃: C 70.04, H 8.08, N

10.21. Found: C 69.63, H 8.28, N 9.86. HRMS: Calcd for $[C_{24}H_{33}N_3O_3+H]^+$: 412.2595; Found: 412.2595.

1-(5,6,8,9,10,11-hexahydro-7H-5,9:7,11-dimethanobenzo[9]annulen-7-yl-9-d)-3-(1-(tetrahydro-2H-pyran-4-carbonyl)piperidin-4-yl)urea, 28. To a solution of 5,6,8,9,10,11-hexahydro-7H-5,9:7,11-dimethanobenzo[9]annulen-9-d-7-amine hydrochloride (82 mg, 0.32 mmol) in DCM (2 mL) and saturated aqueous $NaHCO_3$ solution (2 mL), triphosgene (36 mg, 0.12 mmol) was added. The biphasic mixture was stirred at room temperature for 30 minutes and then the two phases were separated and the organic one was washed with brine (3 mL), dried over anhydrous Na_2SO_4 , filtered and evaporated under vacuum to obtain 1-2 mL of a solution of isocyanate in DCM. To this solution was added (4-aminopiperidin-1-yl)(tetrahydro-2H-pyran-4-yl)methanone (68 mg, 0.32 mmol). The mixture was stirred overnight at room temperature and the solvent was then evaporated. Column chromatography (SiO_2 , DCM/Methanol mixtures) provided urea **28** as a white solid (83 mg, 56% yield). The analytical sample was obtained by crystallization from hot EtOAc, mp 125-126 °C. IR (ATR): 3318, 2902, 2849, 1630, 1557, 1491, 1445, 1361, 1318, 1300, 1274, 1238, 1213, 1123, 1108, 1090, 1040, 1016, 987, 972, 872, 823, 750 cm^{-1} . 1H -NMR (400 MHz, $CDCl_3$) δ : 1.17 [dt, $J = 12.0$ Hz, $J' = 4.0$ Hz, 2 H, 3'- H_{ax} or 5'- H_{ax}], 1.20 [dt, $J = 12.0$ Hz, $J' = 4.0$ Hz, 2 H, 5'- H_{ax} or 3'- H_{ax}], 1.56 [m, 2 H, 3''(5'')- H_{ax}], 1.73 [d, $J = 13.2$ Hz, 2 H, 10(13)- H_{ax}], 1.80-1.90 [complex signal, 3 H, 3''(5'')- H_{eq} , 5'- H_{eq} or 3'- H_{eq}], 1.92 [dd, $J = 13.2$ Hz, $J' = 6.0$ Hz, 2 H, 10(13)- H_{eq}], 1.98-2.10 [complex signal, 5 H, 6(12)- H_{ax} , 8- H_2 , 3'- H_{eq} or 5'- H_{eq}], 2.18 [m, 2 H, 6(12)- H_{eq}], 2.65-2.76 [complex signal, 2 H, 4''-H, 2'- H_{ax} or 6'- H_{ax}], 3.03 [t, $J = 6.0$ Hz, 2 H, 5(11)-H], 3.10 (m, 1 H, 6'- H_{ax} or 2'- H_{ax}), 3.43 [m, 2 H, 2''(6'')- H_{ax}], 3.75 (m, 1 H, 4'-H), 3.82 (d, $J = 13.0$ Hz, 1 H, 6'- H_{eq} or 2'- H_{eq}), 3.99 [dm, $J = 11.4$ Hz, 2 H, 2''(6'')- H_{eq}], 4.27-4.34 [complex signal, 2 H, C7-NH, C4'-NH], 4.48 (d, $J = 13.0$ Hz, 1 H, 2'- H_{eq}

or 6'-H_{eq}], 7.03 [m, 2 H, 1(4)-H], 7.05 [m, 2 H, 2(3)-H]. ¹³C-NMR (100.6 MHz, CDCl₃) δ: 29.2 [CH₂, C3''(5'')], 30.7 (CD, t, ¹J_{C-D} = 19.8 Hz, C9), 32.4 (CH₂, C5' or C3'), 34.1 (CH₂, C3' or C5'), 34.3 [CH₂, C10(13)], 37.6 (CH, C4''), 40.5 [CH₂, C6(12)], 41.1 [CH₂, C2' or C6'), 41.2 [CH, C5(11) and CH₂, C8], 44.3 (CH₂, C6' or C2'), 47.1 (CH, C4'), 51.9 (C, C7), 67.2 [CH₂, C2''(6'')], 126.2 [CH, C2(3)], 128.0 [CH, C1(4)], 146.6 [C, C4a(11a)], 156.1 (C, NHCONH), 172.8 (C, NCOR). HRMS: Calcd for [C₂₇H₃₆DN₃O₃+H]⁺: 453.297; Found: 453.2974. Anal. Calcd for C₂₇H₃₆DN₃O₃·1 H₂O: C 68.91, H 8.14, N 8.93. Found: C 69.28, H 7.94, N 8.69

***tert*-butyl 4-(2-((9-methyl-5,6,8,9,10,11-hexahydro-7*H*-5,9:7,11-dimethanobenzo[9]annulen-7-yl)amino)-2-oxoethyl)piperidine-1-carboxylate.** To a suspension of 9-methyl-5,6,8,9,10,11-hexahydro-7*H*-5,9:7,11-dimethanobenzo[9]annulen-7-amine hydrochloride (500 mg, 1.89 mmol) in EtOAc (5 mL), 2-(1-(*tert*-butoxycarbonyl)piperidin-4-yl)acetic acid (461 mg, 1.89 mmol), HOBT (384 mg, 2.84 mmol), EDC·HCl (440 mg, 2.84 mmol) and Et₃N (767 mg, 7.58 mmol) were added. The mixture was stirred at room temperature for 24 h. Water (10 mL) and DCM (20 mL) were added to the resulting suspension and the 2 phases were separated. The organic phase was washed with sat. NaHCO₃ aqueous solution (10 mL), brine (10 ml), 2N HCl solution (10 mL) and 2N NaOH (10 mL), dried over anhydrous Na₂SO₄, filtered and concentrated under vacuum to give a yellow solid (515 mg, 60% yield). ¹H-NMR (400 MHz, CDCl₃) δ: 0.92 (s, 3H), 1.11 (dq, *J* = 4.4 Hz, *J*' = 11.6 Hz, 2 H), 1.4 (s, 9 H), 1.54 (d, *J* = 13.6 Hz, 2 H), 1.63-1.68 (complex signal, 4 H), 1.84 (s, 2 H), 1.91 (m, 1 H), 1.97 (s, 2 H), 2.0 (d, *J* = 12.8 Hz, 2 H), 2.14-2.18 (complex signal, 2 H), 2.69 (t, *J* = 13.2 Hz, 2 H), 3.06 (t, *J* = 6.0 Hz, 2 H), 4.06 (broad signal, 2 H), 5.14 (s, 1 H), 7.02-7.08 (complex signal, 4 H).

***N*-(9-methyl-5,6,8,9,10,11-hexahydro-7*H*-5,9:7,11-dimethanobenzo[9]annulen-7-yl)-2-(piperidin-4-yl)acetamide.** To a solution of *tert*-butyl 4-(2-((9-methyl-5,6,8,9,10,11-hexahydro-7*H*-5,9:7,11-dimethanobenzo[9]annulen-7-yl)amino)-2-oxoethyl)piperidine-1-carboxylate (250 mg, 0.55 mmol) in DCM (4 mL) was added 4M HCl in 1,4-dioxane (0.5 ml). The reaction mixture was stirred at room temperature for 3 days. Then, the solvent was evaporated under vacuum and the residue was dissolved in DCM (10 mL) and washed with 5N NaOH solution, dried over anh. Na₂SO₄, filtered and concentrated under vacuum to give a yellow solid (189 mg, 97% yield). ¹H-NMR (400 MHz, CDCl₃) δ: 0.91 (s, 3H), 1.12 (dq, *J* = 4 Hz, *J*' = 12.0 Hz, 2 H), 1.53 (d, *J* = 13.2 Hz, 2 H), 1.62-1.71 (complex signal, 4 H), 1.84 (s, 2 H), 1.88 (m, 1 H), 1.95-2.01 (complex signal, 4 H), 2.14-2.19 (complex signal, 2 H), 2.6 (dt, *J* = 2.8 Hz, *J*' = 12.0 Hz, 2 H), 3.00-3.07 (complex signal, 4 H), 5.15 (s, 1 H), 7.02-7.09 (complex signal, 4 H).

2-(1-acetylpiperidin-4-yl)-*N*-(9-methyl-5,6,8,9,10,11-hexahydro-7*H*-5,9:7,11-dimethanobenzo[9]annulen-7-yl)acetamide, **24.** To a solution of *N*-(9-methyl-5,6,8,9,10,11-hexahydro-7*H*-5,9:7,11-dimethanobenzo[9]annulen-7-yl)-2-(piperidin-4-yl)acetamide (200 mg, 0.57 mmol) in anh. DCM (5 mL) under argon atmosphere was added anh. Et₃N (69 mg, 0.68 mmol). The mixture was cooled down to 0°C and acetyl chloride (45 mg, 0.57 mmol) was added dropwise. Then, the reaction mixture was stirred at room temperature overnight and quenched by addition of 2N HCl solution (3 mL). The two phases were separated and the aqueous layer was extracted with EtOAc (2 x 20 mL). The combined organic phases were washed with 2N NaOH solution, dried over anh. Na₂SO₄, filtered and concentrated under vacuum. Column chromatography (SiO₂, Hexane/EtOAc mixtures) gave acetamide **24** as a white solid (134 mg, 60% yield), mp 85-86 °C. IR (NaCl disk): 3315, 3060, 3017, 2916, 2860, 1631, 1544, 1493, 1450, 1361, 1304, 1273, 1241, 1197, 1165, 1138, 1096, 1048 cm⁻¹. ¹H-NMR (400 MHz, CDCl₃) δ:

0.91 (s, 3 H, C9''-CH₃), 1.10 [m, 2 H, 3'(5')-H_{ax}], 1.53 [d, *J* = 13.6 Hz, 2 H, 10''(13'')-H_{ax}], 1.65 [dm, *J* = 12.8 Hz, 10''(13'')-H_{eq}], 1.71 (d, *J* = 12.8 Hz, 1 H, 5'-H_{eq} or 3'-H_{eq}), 1.76 (d, *J* = 12.4 Hz, 1 H, 3'-H_{eq} or 5'-H_{eq}), 1.83 (s, 2 H, 8''-H), 1.96-2.04 [complex signal, 5 H, 2-H₂, 4'-H, 6''(12'')-H_{ax}], 2.06 (s, 3 H, COCH₃), 2.15 [m, 2 H, 6''(12'')-H_{eq}], 2.53 (t, *J* = 12.4 Hz, 1 H, 2'-H_{ax} or 6'-H_{ax}), 3.03 (m, 1 H, 6'-H_{ax} or 2'-H_{ax}), 3.08 [broad t, *J* = 6.0 Hz, 2 H, 5''(11'')-H], 3.76 (d, *J* = 13.6 Hz, 1 H, 6'-H_{eq} or 2'-H_{eq}), 4.58 (d, *J* = 13.2 Hz, 1 H, 2'-H_{eq} or 6'-H_{eq}), 5.25 (s, 1H, NH), 7.03 [m, 2 H, 1''(4'')-H], 7.06 [m, 2 H, 2''(3'')-H]. ¹³C-NMR (100.6 MHz, CDCl₃) δ: 21.5 (CH₃, COCH₃), 31.6 (CH₂, C5' or C3'), 32.2 (CH₃, C9-CH₃), 32.4 (CH₂, C3' or C5'), 33.56 (C or CH, C9'' or C4'), 33.57 (CH or C, C4' or C9''), 39.0 (CH₂, C6'' or C12''), 39.1 (CH₂, C12'' or C6''), 40.9 [CH, C5''(11'')], 41.1 [CH₂, C10''(13'')], 41.7 (CH₂, C2' or C6'), 44.4 (CH₂, C2), 46.5 (CH₂, C6' or C2'), 47.2 (CH₂, C8''), 54.7 (C, C7''), 126.3 [CH, C2''(3'')], 128.0 [CH, C1''(4'')], 146.1 [C, C4a''(11a'')], 168.7 (C, COCH₃), 170.4 (C, NHCO). Anal. Calcd for C₂₅H₃₄N₂O₂·0.5 H₂O: C 74.41, H 8.74, N 6.94. Found: C 74.36, H 8.79, N 6.74. HRMS: Calcd for [C₂₅H₃₄N₂O₂+H]⁺: 395.2693; Found: 395.2691.

2-[1-(isopropylsulfonyl)piperidin-4-yl]-N-(9-methyl-5,6,8,9,10,11-hexahydro-7H-5,9:7,11-dimethanobenzo[9]annulen-7-yl)acetamide, 25. To a solution of *N*-(9-methyl-5,6,8,9,10,11-hexahydro-7H-5,9:7,11-dimethanobenzo[9]annulen-7-yl)-2-(piperidin-4-yl)acetamide (185 mg, 0.52 mmol) in DCM (5 mL) was added Et₃N (63 mg, 0.63 mmol). The mixture was cooled down to 0 °C and propane-2-sulfonyl chloride (74 mg, 0.52 mmol) was added dropwise. Then, the reaction mixture was stirred at room temperature overnight and quenched by addition of 2N HCl solution (3 mL). The two phases were separated and the aqueous phase was extracted with EtOAc (2 x 20 mL). The combined organic phases were washed with 5N NaOH solution, dried over anh. Na₂SO₄, filtered and concentrated under vacuum to give a yellow solid. Column chromatography

(SiO₂, Hexane/EtOAc mixtures) gave acetamide **25** as a white solid (145 mg, 60% yield). The analytical sample was obtained by crystallization from hot EtOAc, mp 172 -173 °C. IR (NaCl disk): 3365, 3319, 3059, 3018, 2916, 2852, 1648, 1536, 1493, 1452, 1361, 1323, 1309, 1265, 1190, 1167, 1138, 1091, 1044, 1011, 993, 945, 905, 881, 801, 759, 732, 702, 665 cm⁻¹. ¹H-NMR (400 MHz, CDCl₃) δ: 0.91 (s, 3 H, C9''-CH₃), 1.25 [dq, *J* = 12.0 Hz, *J*' = 4.0 Hz, 2 H, 3'(5')-H_{ax}], 1.31 [d, *J* = 6.8 Hz, 6 H, CH(CH₃)₂], 1.53 [d, *J* = 13.6 Hz, 2 H, 10''(13'')-H_{ax}], 1.65 [dm, *J* = 13.6 Hz, 2 H, 10''(13'')-H_{eq}], 1.74 [dm, *J* = 12.0 Hz, 2 H, 3'(5')-H_{eq}], 1.82 (s, 2 H, 8''-H₂), 1.93 (m, 1 H, 4'-H), 1.97-2.04 [complex signal, 4 H, 2-H₂, 6''(12'')-H_{ax}], 2.15 [dd, *J* = 11.6 Hz, *J*' = 6.0 Hz, 6''(12'')-H_{eq}], 2.85 [dt, *J* = 12.4 Hz, *J*' = 2.4 Hz, 2 H, 2'(6')-H_{ax}], 3.06 [t, *J* = 6.0 Hz, 2 H, 5''(11'')-H], 3.15 [sept, *J* = 6.8 Hz, 1 H, CH(CH₃)₂], 3.80 [dt, *J* = 12.8 Hz, *J*' = 2.0 Hz, 2 H, 2'(6')-H_{eq}], 5.22 (s, 1 H, NH), 7.03 [m, 2 H, 1''(4'')-H], 7.07 [m, 2 H, 2''(3'')-H]. ¹³C-NMR (100.6 MHz, CDCl₃) δ: 16.8 [CH₃, CH(CH₃)₂], 32.2 (CH₃, C9-CH₃), 32.3 [CH₂, C3'(5')], 33.1 (CH, C4'), 33.6 (C, C9''), 39.1 [CH₂, C6''(12'')], 41.0 [CH, C5''(11'')], 41.1 [CH₂, C10''(13'')], 44.4 (CH₂, C2), 46.5 [CH₂, C2'(6')], 47.2 (CH₂, C8''), 53.2 [CH, CH(CH₃)₂], 54.7 (C, C7''), 126.3 [CH, C2''(3'')], 128.0 [CH, C1''(4'')], 146.1 [C, C4a''(11a'')], 170.3 (C, CO). Anal. Calcd for C₂₆H₃₈N₂O₃S: C 68.09, H 8.35, N 6.11. Found: C 67.75 H 8.62, N 5.74. HRMS: Calcd for [C₂₆H₃₈N₂O₃S+H]⁺: 459.2676; Found: 459.2675.

2-(1-benzylpiperidin-4-yl)-N-(9-methyl-5,6,8,9,10,11-hexahydro-7H-5,9:7,11-dimethanobenzo[9]annulen-7-yl)acetamide, 30. To a suspension of 9-methyl-5,6,8,9,10,11-hexahydro-7H-5,9:7,11-dimethanobenzo[9]annulen-7-amine hydrochloride (250 mg, 0.95 mmol) in EtOAc (5 mL), 2-(1-benzylpiperidin-4-yl)acetic acid hydrochloride (255 mg, 0.95 mmol), HOBt (192 mg, 1.42 mmol), EDC·HCl (220 mg, 1.42 mmol) and Et₃N (480 mg, 4.74 mmol) were added. The mixture was stirred at

room temperature for 24 h. Water (10 mL) and DCM (10 mL) were added to the resulting suspension and the 2 phases were separated. The organic phase was washed with sat. NaHCO₃ aqueous solution (10 mL), brine (10 ml), dried over anh. Na₂SO₄, filtered and concentrated under vacuum to give a yellow gum (479 mg). Column chromatography (SiO₂, DCM/Methanol mixtures) gave acetamide **30** as a white solid (280 mg, 67% yield). The analytical sample was obtained by crystallization from hot EtOAc and Et₂O, mp 145-146 °C. IR (NaCl disk): 3302, 3060, 3025, 2917, 2842, 2799, 2756, 1641, 1545, 1493, 1452, 1361, 1343, 1309, 1279, 1211, 1185, 1144, 1078, 1009, 974, 944, 917, 794, 757, 737, 698 cm⁻¹. ¹H-NMR (400 MHz, CDCl₃) δ: 0.91 (s, 3 H, C9''-CH₃), 1.27 [dq, *J* = 12.4 Hz, *J'* = 3.6 Hz, 2 H, 3'(5')-H_{ax}], 1.53 [d, *J* = 13.2 Hz, 2 H, 10''(13'')-H_{ax}], 1.62-1.70 [complex signal, 4 H, 3'(5')-H_{eq}, 10''(13'')-H_{eq}], 1.77 (m, 1 H, 4'-H), 1.84 (s, 2 H, 8''-H), 1.94-2.02 (complex signal, 6 H, 6''(12'')-H_{ax}, 2-H, 6'(2')-H_{ax}), 2.16 [dd, *J* = 12 Hz, *J'* = 6 Hz, 6''(12'')-H_{eq}], 2.86 [dt, *J* = 11.6 Hz, *J'* = 2.8 Hz, 2 H, 2'(6')-H_{eq}], 3.06 [t, *J* = 6 Hz, 2 H, 5''(11'')-H], 3.48 (s, 2 H, CH₂-C₆H₅), 5.20 (s, 1 H, NH), 7.03 [m, 2 H, 1''(4'')-H], 7.06 [m, 2 H, 2''(3'')-H], 7.23 (m, 1 H, Ar-H_{para}), 7.27-7.32 (complex signal, 4 H, Ar-H_{ortho}, Ar-H_{meta}). ¹³C-NMR (100.6 MHz, CDCl₃) δ: 32.0 [CH₂, C3'(5')], 32.2 (CH₃, C9''-CH₃), 33.4 (C, C9''), 33.5 (CH, C4'), 39.1 [CH₂, C6''(12'')], 40.9 [CH, C5''(11'')], 41.1 [CH₂, C10''(13'')], 44.9 (CH₂, C2), 47.1 (CH₂, C8''), 53.5 (CH₂, C2'(6')), 54.4 (C, C7''), 63.3 (CH₂, CH₂-C₆H₅), 126.2 [CH, C2''(3'')], 126.9 (CH, Ar-CH_{para}), 127.9 [CH, C1''(4'')], 128.1 [CH, Ar-CH_{meta}], 129.2 [CH, Ar-CH_{ortho}], 138.3 (C, Ar-C_{ipso}), 146.1 [C, C4a''(11a'')], 171.0 (C, NHCO). HRMS: Calcd for [C₃₀H₃₈N₂O+H]⁺: 443.3057; Found: 443.3061.

***N*-(9-chloro-5,6, 8,9,10,11-hexahydro-7*H*-5,9:7,11-dimethanobenzo[9]annulen-7-yl)-2-(1-(isopropylsulfonyl)piperidin-4-yl)acetamide, 31.** To a solution of *N*-(9-chloro-5,6,8,9,10,11-hexahydro-7*H*-5,9:7,11-dimethanobenzo[9]annulen-7-yl)-2-(piperidin-4-

yl)acetamide hydrochloride (75 mg, 0.18 mmol) and triethylamine (100 μ L, 73 mg, 0.72 mmol) in anh. DCM (1 mL) was added 2-propanesulfonyl chloride (31 μ L, 32.8 mg, 0.27 mmol). Then, the mixture was stirred at RT overnight. NaHCO₃ sat. (15 mL) was added followed by EtOAc (10 mL) and the mixture was partitioned. The aqueous layer was extracted again with EtOAc (10 mL). Both organic layers were joined, dried over Na₂SO₄ anh., filtered and solvents were concentrated *in vacuo*. The resulting crude was purified by column chromatography in silica gel (using as eluent mixtures of EtOAc in hexane from 0% to 70%). Fractions containing the desired product were collected and concentrated *in vacuo* to afford acetamide **31** (37 mg, 40% yield) as a reddish solid, mp: 163-164 °C. IR (ATR): 3305, 2922, 2906, 2858, 1643, 1548, 1356, 1321, 1276, 1196, 1138, 1058, 1047, 952, 935, 799, 764, 738, 658 cm⁻¹. ¹H NMR (400 MHz, CD₃OD) δ : 1.22 [m, 2 H, 3''(5'')-H_{ax}], 1.29 [d, J = 6.8 Hz, 6 H, CH(CH₃)₂], 1.72 [m, 2 H, 3''(5'')-H_{eq}], 1.88 (m, 1 H, 4-H''), 2.02-2.12 [complex signal, 6 H, 2-H, 6'(12')-H_{ax}, 10'(13')-H_{ax}], 2.22 [m, 2 H, 6'(12')-H_{eq}], 2.40 [m, 2 H, 10'(13')-H_{eq}], 2.48 (s, 2 H, 8'-H), 2.90 [m, 2 H, 2''(6'')-H_{ax}], 3.19 [m, 2 H, 5'(11')-H], 3.28 [sept, J = 6.8 Hz, 1 H, CH(CH₃)₂], 3.76 m, [2 H, 2''(6'')-H_{eq}], 7.05-7.14 [complex signal, 4 H, 1'(4')2'(3')-H]. ¹³C NMR (100.6 MHz, CD₃OD) δ : 17.0 [CH₃, CH(CH₃)₂], 33.3 [CH₂, C3''(5'')], 34.6 (CH, C4''), 38.9 [CH₂, C6'(12')], 42.6 [CH, C5'(11')], 44.4 (CH₂, C2), 45.9 [CH₂, C10'(13')], 47.4 [CH₂, C2''(6'')], 51.0 (CH₂, C8'), 54.0 [CH, CH(CH₃)₂], 57.6 (C, C7'), 70.3 (C, C9'), 128.0 [CH, C2'(3')], 129.1 [CH, C1'(4')], 146.2 [C, C4a(11a)], 173.8 (C, CO). Anal. calcd for C₂₅H₃₅ClN₂O₃S: C 62.68, H 7.36, N 5.85. Found: C 62.63, H 7.31, N 5.68. HRMS: Calcd for [C₂₅H₃₅ClN₂O₃S+H]⁺: 479.2130, found: 479.2143.

***N*-(9-fluoro-5,6,8,9,10,11-hexahydro-7*H*-5,9:7,11-dimethanobenzo[9]annulen-7-yl)-2-(1-(isopropylsulfonyl)piperidin-4-yl)acetamide, 32.** To a solution of *N*-(9-fluoro-5,6,8,9,10,11-hexahydro-7*H*-5,9:7,11-dimethanobenzo[9]annulen-7-yl)-2-(piperidin-4-

yl)acetamide (186 mg, 0.52 mmol) and triethylamine (87 μ L, 63 mg, 0.63 mmol) in DCM (2 mL) was added 2-propanesulfonyl chloride (70 μ L, 89 mg, 0.63 mmol) under ice-bath. Then, the mixture was allowed to warm up to RT and stirred overnight. NaHCO₃ sat. (15 mL) was added followed by EtOAc (15 mL) and the mixture was partitioned. The aqueous layer was extracted with EtOAc/MeOH 9/1 (2 x 15 mL). All organic layers were joined, dried over Na₂SO₄ anh., filtered and solvents were concentrated *in vacuo*. The resulting crude was purified by column chromatography in silica gel (using as eluent mixtures of EtOAc in hexane from 0% to 70%). Fractions containing the desired product were collected and concentrated *in vacuo* to afford acetamide **32** (123 mg, 51% yield) as a white solid, mp 192-193 °C. IR (ATR): 3342, 2914, 2855, 1663, 1536, 1449, 1316, 1138, 1045, 1017, 998, 953, 940, 865, 761, 753, 732, 652 cm⁻¹. ¹H NMR (400 MHz, CDCl₃) δ : 1.24 [m, 2 H, 3''(5'')-H_{ax}], 1.31 [d, J = 6.8 Hz, 6 H, CH(CH₃)₂], 1.73 [m, 2 H, 3''(5'')-H_{eq}], 1.88-2.04 [complex signal, 7 H, 2-H, 6'(12')-H_{ax}, 10'(13')-H_{ax}, 4''-H], 2.10-2.23 [complex signal, 4 H, 6'(12')-H_{eq}, 10'(13')-H_{eq}], 2.26 (d, J = 6.3 Hz, 2 H, 8'-H), 2.85 [m, 2 H, 2''(6'')-H_{ax}], 3.14 [sept, J = 7.0 Hz, 1 H, CH(CH₃)₂], 3.23 [m, 2 H, 5'(11')-H], 3.80 [m, 2 H, 2''(6'')-H_{eq}], 5.42 (broad s, 1 H, NH), 7.07 [m, 2 H, 1'(4')-H], 7.13 [m, 2 H, 2'(3')-H]. ¹³C NMR (100.6 MHz, CDCl₃) δ : 16.9 [CH₃, CH(CH₃)₂], 32.4 [CH₂, C3''(5'')], 33.2 (CH, C4''), 38.7 [CH₂, C6'(12')], 39.6 [d, ³ J_{CF} = 13.3 Hz, CH, C5'(11')], 40.2 [d, ² J_{CF} = 20.2 Hz, CH₂, C10'(13')], 44.3 (CH₂, C2), 46.1 (d, ² J_{CF} = 18.5 Hz, CH₂, C8'), 46.7 [CH₂, C2''(6'')], 53.4 [CH, CH(CH₃)₂], 58.0 (d, ³ J_{CF} = 11.4 Hz, C, C7'), 94.2 (d, ¹ J_{CF} = 177.6 Hz, C, C9'), 127.1 [CH, C2'(3')], 128.3 [CH, C1'(4')], 144.8 [C, C4a(11a)], 170.6 (C, CO). Anal. calcd for C₂₅H₃₅FN₂O₃S: C 64.91, H 7.63, N 6.06. Found: C 65.08, H 7.97, N 5.74. HRMS: Calcd for [C₂₅H₃₅FN₂O₃S+H]⁺: 463.2425, found: 463.2425.

***N*-(5,6,8,9,10,11-hexahydro-7*H*-5,9:7,11-dimethanobenzo[9]annulen-7-yl)-2-(1-(isopropylsulfonyl)piperidin-4-yl)acetamide, 33.** To a solution of *N*-(5,6,8,9,10,11-hexahydro-7*H*-5,9:7,11-dimethanobenzo[9]annulen-7-yl)-2-(piperidin-4-yl)acetamide (90 mg, 0.27 mmol) and triethylamine (150 μ L, 109 mg, 1.08 mmol) in anh. MeCN (1 mL) was added 2-propanesulfonyl chloride (60 μ L, 39.4 mg, 0.53 mmol). Then, the mixture was stirred at RT overnight. NaHCO₃ sat. was added followed by EtOAc and the mixture was partitioned. The aqueous layer was extracted again with EtOAc. Both organic layers were joined, dried over Na₂SO₄ anh., filtered and solvents were concentrated *in vacuo*. The resulting crude was purified by column chromatography in silica gel (using as eluent mixtures of EtOAc in hexane from 0% to 70%). Fractions containing the desired product were collected and concentrated *in vacuo* to afford acetamide **33** (68 mg, 55% yield) as a white solid, mp: 136-137 °C. IR (ATR): 3301, 2922, 2858, 1642, 1548, 1355, 1320, 1276, 1195, 1137, 1047, 951, 935, 799, 764, 738, 684, 657, 618 cm⁻¹. ¹H NMR (400 MHz, CD₃OD) δ : 1.24 [m, 2 H, 3''(5'')-H_{ax}], 1.29 [d, $J = 6.8$ Hz, 6 H, CH(CH₃)₂], 1.68-1.77 [complex signal, 4 H, 10'(13')-H_{ax}, 3''(5'')-H_{eq}], 1.86 (m, 1 H, 4''-H), 2.00 [m, 2 H, 10'(13')-H_{eq}], 2.02-2.09 (complex signal, 4 H, 2-H, 8'-H), 2.16 [m, 2 H, 6'(12')-H_{ax}], 2.23 [m, 2 H, 6'(12')-H_{eq}], 2.32 (m, 1 H, 9'-H), 2.90 [m, 2 H, 2''(6'')-H_{ax}], 3.04 [broad t, $J = 6.0$ Hz, 2 H, 5'(11')-H], 3.26 [sept, $J = 6.8$ Hz, 1 H, CH(CH₃)₂], 3.76 [dm, $J = 12.8$ Hz, 2 H, 2''(6'')-H_{eq}], 7.03 [s, 4 H, 1'(4')-H, 2'(3')-H]. ¹³C NMR (100.6 MHz, CD₃OD) δ : 17.0 [CH₃, CH(CH₃)₂], 32.6 (CH, C9'), 33.3 [CH₂, C3''(5'')], 34.6 (CH, C4''), 35.7 [CH₂, C10'(13')], 40.4 [CH₂, C6'(12')], 41.4 (CH₂, C2), 42.6 [CH, C5'(11')], 44.5 (CH₂, C8'), 47.4 [CH₂, 2''(6'')], 53.9 (CH, CH(CH₃)₂), 54.0 (C, C7'), 127.3 [CH, C2'(3')], 129.0 [CH, C1'(4')], 148.0 [C, C4a'(11a')], 173.6 (C, CO). Anal. calcd for C₂₅H₃₆N₂O₃S: C 67.53, H 8.16, N 6.30. Calcd for C₂₅H₃₆N₂O₃S·0.2 H₂O:

C 66.99, H 8.19, N 6.25. Found: C 67.04, H 8.12, N 6.09. HRMS: Calcd for $[C_{25}H_{36}N_2O_3S+H]^+$: 445.2519, found: 445.2528.

***N*-(5,6,8,9,10,11-hexahydro-7*H*-5,9:7,11-dimethanobenzo[9]annulen-7-yl-9-*d*)-2-(1-(isopropylsulfonyl)piperidin-4-yl)acetamide, 34.** To a solution of *N*-(5,6,8,9,10,11-hexahydro-7*H*-5,9:7,11-dimethanobenzo[9]annulen-7-yl-9-*d*)-2-(piperidin-4-yl)acetamide (111 mg, 0.33 mmol) and triethylamine (184 μ L, 133 mg, 1.32 mmol) in anh. MeCN (1 mL) was added 2-propanesulfonyl chloride (73 μ L, 53 mg, 0.65 mmol). Then, the mixture was stirred at RT overnight. NaHCO₃ sat. (20 mL) was added followed by EtOAc (15 mL) and the mixture was partitioned. The aqueous layer was extracted again with EtOAc (15 mL). Both organic layers were joined, dried over Na₂SO₄ anh., filtered and solvents were concentrated *in vacuo*. The resulting crude was purified by Biotage purification system in silica gel (using as eluent mixtures of EtOAc in hexane from 0% to 70%). Fractions containing the desired product were collected and concentrated *in vacuo* to afford acetamide **34** (97 mg, 66% yield) as a white solid, mp: 138-139 °C. IR (ATR) ν : 3299, 2922, 2857, 1643, 1549, 1321, 1276, 1138, 1047, 952, 934, 764, 738, 656 cm^{-1} . ¹H NMR (400 MHz, CD₃OD) δ : 1.22 [m, 2 H, 3''(5'')-H_{ax}], 1.29 [d, $J = 6.9$ Hz, 6 H, CH(CH₃)₂], 1.68-1.76 [complex signal, 4 H, 10'(13')-H_{ax}, 3''(5'')-H_{eq}], 1.86 (m, 1H, 4''-H), 1.99 [m, 2 H, 10'(13')-H_{eq}], 2.03-2.08 (complex signal, 4 H, 2-H, 8'-H), 2.16 [m, 2 H, 6'(12')-H_{ax}], 2.23 [m, 2 H, 6'(12')-H_{eq}], 2.89 [m, 2 H, 2''(6'')-H_{ax}], 3.03 [m, 2 H, 5'(11')-H], 3.25 [sept, $J = 6.8$ Hz, 1 H, CH(CH₃)₂], 3.76 [dm, $J = 12.4$ Hz, 2 H, 2''(6'')-H_{eq}], 7.03 [s, 4 H, 1'(4')-H, 2'(3')-H]. ¹³C NMR (100.6 MHz, CD₃OD) δ : 17.0 [CH₃, CH(CH₃)₂], 32.1 (CD, t, ¹ $J_{C-D} = 19.5$ Hz, C9'), 33.3 [CH₂, C3''(5'')], 34.6 (CH, C4''), 35.6 [CH₂, C10'(13')], 40.4 [CH₂, C6'(12')], 41.3 (CH₂, C2), 42.6 [CH, C5'(11')], 44.5 (CH₂, C8'), 47.4 [CH₂, 2''(6'')], 53.9 [CH, CH(CH₃)₂], 54.0 (C, C7'), 127.3 [CH, C2'(3')], 129.0 [CH, C1'(4')], 148.0 [C, C4a'(11a')], 173.6 (C, CO).

Anal. calcd for $C_{25}H_{35}DN_2O_3S$: C 67.38, H 8.37, N 6.29. Calcd for $C_{25}H_{35}DN_2O_3S \cdot 0.3 H_2O$: C 66.58, H 7.96, N 6.21. Found: C 66.68, H 8.05, N 6.10. HRMS: Calcd for $[C_{25}H_{35}DN_2O_3S+H]^+$: 446.2582, found: 446.2589.

Enzymatic sEH activity assay. The assay was performed as previously described.²⁹ All hsEH, msEH and rsEH IC_{50} values were determined by a fluorescence-based assay system in a 96-well format. Nonfluorescent MNPC cyano(6-methoxy-naphthalen-2-yl)methyl trans-[(3-phenyloxiran-2-yl)methyl] carbonate was used as the assay substrate at a concentration of 5 μ M. This substrate is hydrolyzed by the sEH to the fluorescent 6-methoxynaphthaldehyde. The formation of the product was measured ($\lambda_{em} = 330$ nm, $\lambda_{ex} = 465$ nm) by a Molecular Device M-2 plate reader. All measurements were performed in triplicate.

Microsomal stability. The human, rat and mice recombinant microsomes employed were purchased from Tebu-Xenotech. The compound was incubated at 37 °C with the microsomes in a 50 mM phosphate buffer (pH = 7.4) containing 3 mM $MgCl_2$, 1 mM NADP, 10 mM glucose-6-phosphate and 1 U/mL glucose-6-phosphate-dehydrogenase. Samples (75 μ L) were taken from each well at 0, 10, 20, 40 and 60 min and transferred to a plate containing 4 °C 75 μ L acetonitrile and 30 μ L of 0.5% formic acid in water were added for improving the chromatographic conditions. The plate was centrifuged (46000 g, 30 min) and supernatants were taken and analyzed in a UPLC-MS/MS (Xevo-TQD, Waters) by employing a BEH C18 column and an isocratic gradient of 0.1% formic acid in water: 0.1% formic acid acetonitrile (60:40). The metabolic stability of the compounds was calculated from the logarithm of the remaining compounds at each of the time points studied.

Solubility. A 10 mM stock solution of the compound was serially diluted in 100% DMSO and 1 μ L of this solution was added to a 384-well UV-transparent plate (Greiner) containing 99 μ L of PBS. The plate was incubated at 37 °C for 2 h and the light scattering was measured in a Nephelostar Plus reader (BMG LABTECH). The data was fitted to a segmented linear regression for measuring the compound solubility.

Parallel Artificial Membrane Permeation Assays - Blood-Brain Barrier (PAMPA-BBB). To evaluate the brain penetration of the different compounds, a parallel artificial membrane permeation assay for blood-brain barrier was used, following the method described by Di *et al.*³⁰ The *in vitro* permeability (Pe) of fourteen commercial drugs through lipid extract of porcine brain membrane together with the test compounds were determined. Commercial drugs and assayed compounds were tested using a mixture of PBS:EtOH (70:30). Assay validation was made by comparing the experimental permeability with the reported values of the commercial drugs by bibliography and lineal correlation between experimental and reported permeability of the fourteen commercial drugs using the parallel artificial membrane permeation assay was evaluated ($y = 1.5219x - 0.9129$; $R^2 = 0.9387$). From this equation, and taking into account the limits established by Di *et al.*³⁸ for BBB permeation, we established the ranges of permeability as compounds of high BBB permeation (CNS+): $Pe (10^{-6} \text{ cm}^{\text{s}^{-1}}) > 5.149$; compounds of low BBB permeation (CNS-): $Pe (10^{-6} \text{ cm}^{\text{s}^{-1}}) < 2.131$ and compounds of uncertain BBB permeation (CNS+/-): $5.149 > Pe (10^{-6} \text{ cm}^{\text{s}^{-1}}) > 2.131$.

Cytotoxicity in SH-SY5Y cells. Cytotoxicity was evaluated in the human neuroblastoma SH-SY5Y cell line (ATCC Number: CRL-2266). Cells were cultured in Minimum Essential Medium / Ham's-F12 (1:1, v/v) medium, supplemented with non-essential amino acids, 10% fetal bovine serum, 1 mM glutamine and 50 μ g/ml gentamycin (all reagents from Gibco, Invitrogen). For experiments, cells were seeded at 3×10^5 cells/ml

(100 µl/well) in 96-well plates (Nunc). After 24 h, the testing compounds were added concentrate to triplicate wells to obtain the final different concentrations up to 100 µM. Compounds were incubated for further 24 h. At termination, cytotoxicity was analysed by the propidium iodide (PI) fluorescence stain assay and the 3-(4,5-dimethylthiazol-2-yl)-2,5-diphenyl tetrazolium bromide (MTT) colorimetric assay. All compounds were tested in three independent experiments using different cell passages.

The PI assay measures cell death. PI enters into the cells with damaged membranes and greatly increases the fluorescence by binding to DNA. PI reagent (Molecular Probes) at the final concentration of 7.5 µg/ml was added to the cells and incubated for 1 h. The resulting fluorescence was measured by a Gemini XPS Microplate reader (Millipore) at 530 nm excitation and 645 nm emission. Percentage of cell death induced by the treatments was calculated from to the fluorescence of treated cells (Ft) relative to that of control cells (Fmin) and cells incubated with Triton X100 (Fmax) as the 0% and 100% cell death, respectively [% = ((Ft-Fmin)/(Fmax-Fmin)) x 100].

The MTT assay quantifies cellular metabolic activity as an indicator of cell viability and proliferation. MTT is a tetrazolium salt that when oxidised by metabolically active cells gives blue formazan crystals, that may be solubilized by a combination of a detergent (SDS) and an organic solvent (dimethylformamide) (all Sigma reagents). MTT was added to cultured cells at the final concentration of 0.5 mg/ml and incubated for 2 h. Then the solubilizing buffer was added to the wells and the culture plates were wrapped with Parafilm to avoid evaporation and maintained at 37°C overnight. The resulting colorimetric reaction was measured by a Multiskan Spectrum Spectrophotometer (Thermo) at 570 nm and a reference 630 nm wavelength. Results were given as a percentage of control cells values.

Cytochrome P450 inhibition assay. The objective of this study was to screen the inhibition potential of the compounds using recombinant human cytochrome P450 enzymes CYP3A4 (BFC and DBF substrates) and probe substrates with fluorescent detection. Incubations were conducted in a 200 μ L volume in 96-well microtiter plates (COSTAR 3915). The addition of the mixture buffer-cofactor (KH_2PO_4 buffer, 1.3 mM NADP, 3.3 mM MgCl_2 , 0.4 U/mL glucose- 6-phosphate dehydrogenase), control supersomes, the Standard inhibitor Ketoconazole (Sigma K1003), and previously diluted compounds to plates was carried out by a liquid handling station (Zephyr Caliper). The plate was then preincubated at 37 $^\circ\text{C}$ for 5 min in 100 μ L volume, and reaction was initiated by the addition of prewarmed enzyme/substrate (E/S) mix. The E/S mix contained buffer (KH_2PO_4), enzyme (CYP), substrate 7-benzyloxytrifluoromethyl coumarin (7-BFC), and Dibenzylfluorescein (DBF) in a reaction volume of 200 μ L. Reactions were terminated after various times depending on the substrate by addition of STOP solution (ACN/TrisHCl 0.5 M 80:20 (BFC) or 2 N NaOH for CYP3A4 (DBF). Fluorescence per well was measured using a fluorescence plate reader (Tecan M1000 pro) and percentage of inhibition was calculated.

Permeability. The Caco-2 cells were cultured to confluency, trypsinized and seeded onto a filter transwell inserted at a density of $\sim 10,000$ cells/well in DMEM cell culture medium. Confluent Caco-2 cells were subcultured at passages 58-62 and grown in a humidified atmosphere of 5% CO_2 at 37 $^\circ\text{C}$. Following an overnight attachment period (24 h after seeding), the cell medium was replaced with fresh medium in both the apical and basolateral compartments every other day. The cell monolayers were used for transport studies 21 days post seeding. The monolayer integrity was checked by measuring the transepithelial electrical resistance (TEER) obtaining values $\geq 500 \Omega/\text{cm}^2$. On the day of the study, after the TEER measurement, the medium was removed and the

cells were washed twice with pre-warmed (37°C) Hank's Balanced Salt Solution (HBSS) buffer to remove traces of medium. Stock solutions were made in dimethyl sulfoxide (DMSO), and further diluted in HBSS (final DMSO concentration 1%). Each compound and reference compounds (Colchicine, E3S) were all tested at a final concentration of 10 μ M. For A \rightarrow B directional transport, the donor working solution was added to the apical (A) compartment and the transport media as receiver working solution was added to the basolateral (B) compartment. For B \rightarrow A directional transport, the donor working was added to the basolateral (B) compartment and transport media as receiver working solution was added to the apical (A) compartment. The cells were incubated at 37°C for 2 hours with gentle stirring.

At the end of the incubation, samples were taken from both donor and receiver compartments and transferred into 384-well plates and analyzed by UPLC-MS/MS. The detection was performed using an ACQUITY UPLC /Xevo TQD System. After the assay, Lucifer yellow was used to further validate the cell monolayer integrity, cells were incubated with LY 10 μ M in HBSS for 1hour at 37°C, obtaining permeability (P_{app}) values for LY of ≤ 10 nm/s confirming the well-established Caco-2 monolayer.

Inhibition of human lipoxygenase-5 (hLOX-5). AA and 2',7'-dichlorodihydrofluorescein diacetate (H₂DCFDA) were obtained from Sigma. Human recombinant LOX-5 was purchased from Cayman Chemical. For the determination of *h*LOX-5 activity, the method described by Pufahl et al. was followed.³¹ The assay solution consisted of 50 mM Tris (pH 7.5), 2 mM EDTA, 2 mM CaCl₂, 3 μ M AA, 10 μ M ATP, 10 μ M H₂DCFDA and 100 mU/well *h*LOX-5. For the enzyme inhibition studies the compounds to be tested were added to the assay solution prior to AA and ATP and were preincubated for a period of 10 min at room temperature, after which AA and ATP were added. The enzymatic reaction was carried out for 20 min and terminated by the addition

of 40 µL of acetonitrile. The fluorescence measurement, 485 nm excitation and 520 nm emission, was performed on a FLUOstar OPTIMA (BMG LABTECH, Offenburg, Germany.). The IC₅₀ is defined as the concentration of compound that inhibits enzymatic activity by 50% over the untreated enzyme control.

Pharmacokinetic study. 24 male C57BL/6 mice (21 grams aprox.) were supplied by ENVIGO (#16338). During the experimental procedure animals were identified with permanent marker (tail code numbers). Plasma samples were obtained at 0, 0.25, 0.5, 1, 2, 4, 6, 8 and 24 hours post-dosing. Upon arrival, animals were housed in groups of 3 animals/cage in polycarbonate maintenance cages (type IIL; 365 x 207 x 140 mm, with a surface area of 530 cm²) with absorbent bedding (Lignocel, JRS). Animals were kept in an environmentally controlled room (ventilation 10-15 air changes per hour, temperature 22±3°C and humidity 35-70%) on a 12-h light/dark cycle. A period of at least 5 days of observation and acclimatisation underwent between the date of arrival and the start of the procedure. During this period, the animals were observed to check their general health state. The maintenance diet was supplied by Harlan Interfauna Ibérica S.L. (2014 Harlan Teklad Global Diets) and was provided to the animals *ad libitum*. Diet was analysed by the manufacturer to detect possible contaminants. Tap water was supplied by CASSA (Servei d'Aigües de Sabadell) and was provided to the animals by bottles *ad libitum*. The animals were maintained in accordance with European Directive for the Protection of Vertebrate Animals Used for Experimental and other Scientific Purposes (86/609/EU). Decree 214/1997 of 30th July. Ministry of Agriculture, Livestock and Fishing of the autonomous government of Catalonia, Spain. Royal Decree 53/2013 of 1st February (Spain) Animal care including environmental and housing conditions conformed to the applicable Standard Operating Procedures regarding laboratory animals of Draconis Pharma S.L. All the experimental procedures were approved by the Animal

Experimentation Ethical Committee of Universitat Autònoma de Barcelona (procedure number: 3718) and by the Animal Experimentation Commission of the Generalitat de Catalunya (Catalan Government) (DAAM:9590). Formulations were prepared the day of the study. Vehicle was 10% of 2-hydroxypropyl- β - cyclodextrin, (CAS 128446-35-5) Sigma-Aldrich (Ref.332607-25G). 21 mice were intraperitoneally administered with a single dose of 3 mg/kg of **25**. The volume of administration was 10 mL/kg. Animals were weighed before each administration to adjust the required volume. Blood samples were collected at different times post administration: 0, 0.25, 0.5, 1, 2, 4, 6, 8 and 24 h. 3 mice were not administered and referred as t=0. Blood samples (0.5-0.8 mL) were collected from anesthetised animals with isoflurane by cava vein puncture in tubes containing K2-EDTA 5%. Blood samples were centrifuged at 10.000 rpm for 5 min to obtain plasma that were stored at -20°C until analysis. Analytical measurements were performed by liquid chromatography-tandem mass spectrometry (LC-MS/MS). Pharmacokinetics parameters were calculated with Phoenix 64 (WinNonlin).

Evaluation of capsaicin-induced mechanical hypersensitivity. Animals were placed in the experimental room (under low illumination) to allow them to acclimatize to the study room for 1 h before the experiments were begun. After that time, the animals were placed into individual test compartments for 2 h before the test to habituate them to the test conditions. The test compartments had black walls and were situated on an elevated mesh-bottomed platform with a 0.5 cm² grid to provide access to the ventral surface of the hind paws. In all experiments, punctate mechanical stimulation was applied with a Dynamic Plantar Aesthesiometer (Ugo Basile, Varese, Italy) at 15 min after the administration of capsaicin (1 μ g, time to maximum effect, data not shown) or its solvent. Briefly, a nonflexible filament (0.5 mm diameter) was electronically driven into the ventral side of the paw previously injected with capsaicin or solvent (i.e., the right hind paw), at least 5

mm away from the site of the injection towards the fingers. When a paw withdrawal response occurred, the stimulus was automatically terminated, and the response latency time was automatically recorded. A cut-off time of 50 s was used. In all experiments, the filament was applied to the right hind paw of each mouse three times, separated by intervals of 0.5 min, and the mean value of the three trials was considered the withdrawal latency time of the animal. Compound **16** was administered s.c. 30 min before the i.pl. administration of capsaicin or DMSO 1% (i.e., 45 min before we evaluated the response to the mechanical punctate stimulus). The antiallodynic effects of **16** were evaluated in capsaicin-sensitized mice using a mechanical stimulation of 0.5 g force. This intensity of the mechanical stimulus did not induce paw withdrawal in DMSO-treated mice, but markedly reduced paw withdrawal latency time in capsaicin-sensitized mice.

REFERENCES

1. Harizi, H.; Corcuff, J. B.; Gualde, N. Arachidonic-acid-derived eicosanoids: roles in biology and immunopathology. *Trends Mol. Med.* **2008**, *14*, 461-469.
2. Hanna, V. S.; Hafez, E. A. A. Synopsis of Arachidonic acid metabolism: a review. *J. Adv.Res.* **2018**, *11*, 23-32.
3. Funk, C. D. Prostaglandins and leukotrienes: Advances in Eicosanoid Biology. *Science* **2001**, *294*, 1871-1875.
4. Meirer, K.; Steinhilber, D.; Proschak, E. Inhibitors of the Arachidonic AcidCascade: Interfering with Multiple Pathways. *Basic Clin. Pharmacol. Toxicol.* **2014**, *114*, 83–91.
5. Rubin, P.; Mollison, K. W. Pharmacotherapy of diseases mediated by 5-lipoxygenase pathway eicosanoids. *Prostaglandins Other Lipid Mediat.* **2007**, *83*, 188-197.

6. Sinha, S.; Doble, M.; Manju, S. L. 5-Lipoxygenase as a drug target: A review on trends in inhibitors structural design, SAR and mechanism based approach. *Bioorg. Med. Chem.* **2019**, *27*, 3745-3759.
7. Spector, A. A.; Norris, A. W. Action of epoxyeicosatrienoic acids on cellular function. *Am. J. Physiol. Cell. Physiol.* **2007**, *292*, C996-C1012.
8. Kaspera, R.; Totah, R. A. Epoxyeicosatrienoic acids: formation, metabolism and potential role in tissue physiology and pathophysiology. *Expert Opin. Drug Metab. Toxicol.* **2009**, *5*, 757-771.
9. Harris, T. R.; Hammock, B. D. Soluble epoxide hydrolase: Gene structure, expression and deletion. *Gene.* **2013**, *526*, 61-74.
10. Morisseau, C.; Hammock, B. D. Epoxide hydrolases: mechanisms, inhibitor designs and biological roles. *Annu. Rev. Pharmacol. Toxicol.* **2005**, *45*, 311-333.
11. Imig, J. D.; Hammock, B. D. Soluble epoxide hydrolase as a therapeutic target for cardiovascular diseases. *Nat. Rev. Drug. Discov.* **2009**, *8*, 794-805.
12. Wang, Z. H.; Davis, B. B.; Jiang, D. Q.; Zhao, T. T.; Xu, D. Y. Soluble Epoxide Hydrolase Inhibitors and Cardiovascular Diseases. *Curr. Vasc. Pharmacol.* **2013**, *11*, 105-111.
13. Kodani, S. D.; Hammock, B. D. Epoxide Hydrolases: Drug Metabolism to Therapeutics for Chronic Pain. *Drug Metab. Dispos.* **2015**, *43*, 788-802.
14. Pillarisetti, S.; Khanna, I. A multimodal disease modifying approach to treat neuropathic pain- inhibition of soluble epoxide hydrolase (sEH). *Drug Discov. Today.* **2015**, *20*, 1382-1390.

15. Wagner, K. M.; McReynolds, C. B.; Schmidt, W. K.; Hammock, B. D. Soluble epoxide hydrolase as therapeutic target for pain, inflammatory and neurodegenerative diseases. *Pharmacol Ther.* **2017**, *180*, 62-76.
16. Wagner, K.; Inceoglu, B.; Dong, H.; Yang, J.; Hwang, S. H.; Jones, P.; Morisseau, C.; Hammock, B. D. Comparative efficacy of 3 soluble epoxide hydrolase inhibitors in rat neuropathic and inflammatory pain models. *Eur. J. Pharmacol.* **2013**, *700*, 93-101.
17. Chen, D.; Whitcomb, R.; MacIntyre, E.; Tran, V.; Do, Z. N.; Sabry, J.; Patel, D. V.; Anandan, S. K.; Gless, R.; Webb, H. K. Pharmacokinetics and Pharmacodynamics of AR9281, an inhibitor of soluble epoxide hydrolase, in single- and multiple-dose studies in healthy human subjects. *J. Clin. Pharmacol.* **2012**, *53*, 319-328.
18. Safety, Tolerability, and Pharmacokinetics of Oral EC5026 in Health Human Subjects. (2019) U.S. National Library of Medicine. Clinicaltrials.gov. Identifier NCT04228302.
19. Codony, S.; Valverde, E.; Leiva, R.; Brea, J.; Loza, M. I.; Morisseau, C.; Hammock, B. D.; Vázquez, S. Exploring the size limit of the lipophilic unit of the soluble epoxide hydrolase inhibitors. *Bioorg. Med. Chem.* **2019**, *27*, 1115078.
20. Codony, S.; Calvó-Tusell, C.; Valverde, E.; Osuna, S.; Morisseau, C.; Loza, M. I.; Brea, J.; Pérez, C.; Rodríguez-Franco, M. I.; Pizarro-Delgado, J.; Corpas, R.; Griñán-Ferré, C.; Pallàs, M.; Sanfeliu, C.; Vázquez-Carrera, M.; Hammock, B. D.; Feixas, F.; Vázquez, S. From the design to the *in vivo* evaluation of benzohomoadamantane-derived soluble epoxide hydrolase inhibitors for the treatment of acute pancreatitis, submitted to *J. Med. Chem.*

21. Torres, E.; Duque, M. D.; López-Querol, M.; Taylor, M. C.; Naesens, L.; Ma, C.; Pinto, L. H.; Sureda, F. X.; Kelly, J. M.; Vázquez, S. Synthesis of benzopolycyclic cage amines: NMDA receptor antagonist, trypanocidal and antiviral activities. *Bioorg. Med. Chem.* **2012**, *20*, 942-948.
22. Valverde, E.; Sureda, F. X.; Vázquez, S. Novel benzopolycyclic amines with NMDA receptor antagonist activity. *Bioorg. Med. Chem.* **2014**, *22*, 2678-2683.
23. Barniol-Xicotà, M.; Escandell, A.; Valverde, E.; Julián, E.; Torrents, E.; Vázquez, S. Antibacterial activity of novel benzopolycyclic amines. *Bioorg. Med. Chem.* **2015**, *23*, 290-296.
24. Turcu, A. L. Ph.D. Dissertation, University of Barcelona, in progress.
25. Kim, I. H.; Heirtzler, F. R.; Morisseau, C.; Nishi, K.; Tsai, H.-J.; Hammock, B. D. Optimization of Amide-Based Inhibitors of Soluble Epoxide Hydrolase with Improved Water Solubility. *J. Med. Chem.* **2005**, *48*, 3621-3629.
26. Wan, D.; Yang, J.; McReynolds, C. B.; Barnych, B.; Wagner, K. M.; Morisseau, C.; Hwang, S. H.; Sun, J.; Blöcher, R.; Hammock, B. D. *In vitro* and *in vivo* Metabolism of a Potent Inhibitor of Soluble Epoxide Hydrolase, 1-(1-Propionylpiperidin-4-yl)-3-(4-(trifluoromethoxy)phenyl)urea. *Front. Pharmacol.* **2019**, *10*, 464.
27. Jones, P. D.; Tsai, H.-J.; Do, Z. N.; Morisseau, C.; Hammock, B. D. Synthesis and SAR of conformationally restricted inhibitors of soluble epoxide hydrolase. *Bioorg. Med. Chem. Lett.* **2006**, *16*, 5212-5216.
28. Rose, T. E.; Morisseau, C.; Liu, J.-Y.; Inceoglu, B.; Jones, P. D.; Sanborn, J. R.; Hammock, B. D. 1-Aryl-3(1-acylpiperidin-4-yl)urea inhibitors of human and murine soluble epoxide hydrolase: structure – activity relationships, pharmacokinetics, and reduction of inflammatory pain. *J. Med. Chem.* **2010**, *53*,

7067-7075

29. Jones, P. D.; Wolf, N. M.; Morisseau, C.; Whetstone, P.; Hock, B.; Hammock, B. D. Fluorescent substrates for soluble epoxide hydrolase and application to inhibition studies. *Anal. Biochem.* **2005**, *343*, 66–75.
30. Di, L.; Kerns, E. H.; Fan, K.; McConnell, O. J.; Carter, G. T. High throughput artificial membrane permeability assay for blood-brain barrier. *Eur. J. Med. Chem.* **2003**, *38*, 223-232.
31. Pufahl, R. A.; Kasten, T. P.; Hills, R.; Gierse, J. K.; Reitz, B. A.; Weinberg, R. A.; Masferrer, J. L. Development of a fluorescence-based enzyme assay of human 5-lipoxygenase. *Anal. Biochem.* **2007**, *364*, 204-212.

Supplementary material

Synthesis, *in vitro* profiling and *in vivo* evaluation of benzohomoadamantane-based soluble epoxide hydrolase inhibitors for neuropathic pain

Sandra Codony¹, José Entrena², Carla Calvó-Tusell³, Juan Martín¹, Beatrice Jora¹, Ferran Feixas³, Rubén Corpas⁴, Christophe Morisseau⁵, Andreea L. Turcu¹, Belén Pérez⁶, Concepción Pérez⁷, María Isabel Rodríguez-Franco⁷, José M. Brea⁸, Coral Sanfeliu⁴, Sílvia Osuna^{3,9}, Bruce D. Hammock⁵, Enrique J. Cobos², M. Isabel Loza⁸, Santiago Vázquez^{1}*

¹Laboratori de Química Farmacèutica (Unitat Associada al CSIC), Facultat de Farmàcia i Ciències de l'Alimentació, and Institute of Biomedicine (IBUB), Universitat de Barcelona, Av. Joan XXIII, 27-31, 08028 Barcelona, Spain.

² Department of Pharmacology, School of Medicine, University of Granada, Avenida de la Investigación 11, 18016, Granada, Spain.

³CompBioLab Group, Departament de Química and Institut de Química Computacional i Catàlisi (IQCC), Universitat de Girona, C/ Maria Aurèlia Capmany 69, 17003 Girona, Spain.

⁴Institute of Biomedical Research of Barcelona (IBB), CSIC and IDIBAPS, Barcelona, Spain, and CIBER Epidemiology and Public Health (CIBERESP), Madrid, Spain.

⁵Department of Entomology and Nematology and Comprehensive Cancer Center, University of California, Davis, CA 95616, USA.

⁶Department of Pharmacology, Therapeutics and Toxicology, Institute of Neurosciences, Autonomous University of Barcelona, 08193 Bellaterra, Barcelona, Spain.

⁷Institute of Medicinal Chemistry, Spanish National Research Council (CSIC), C/Juan de la Cierva 3, 28006 Madrid, Spain.

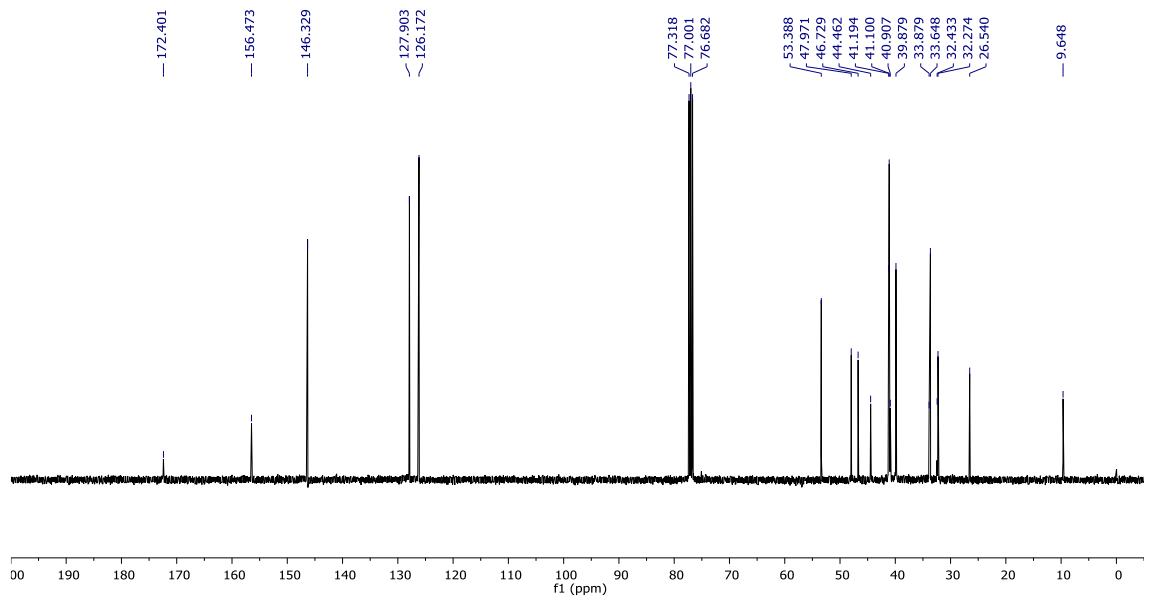
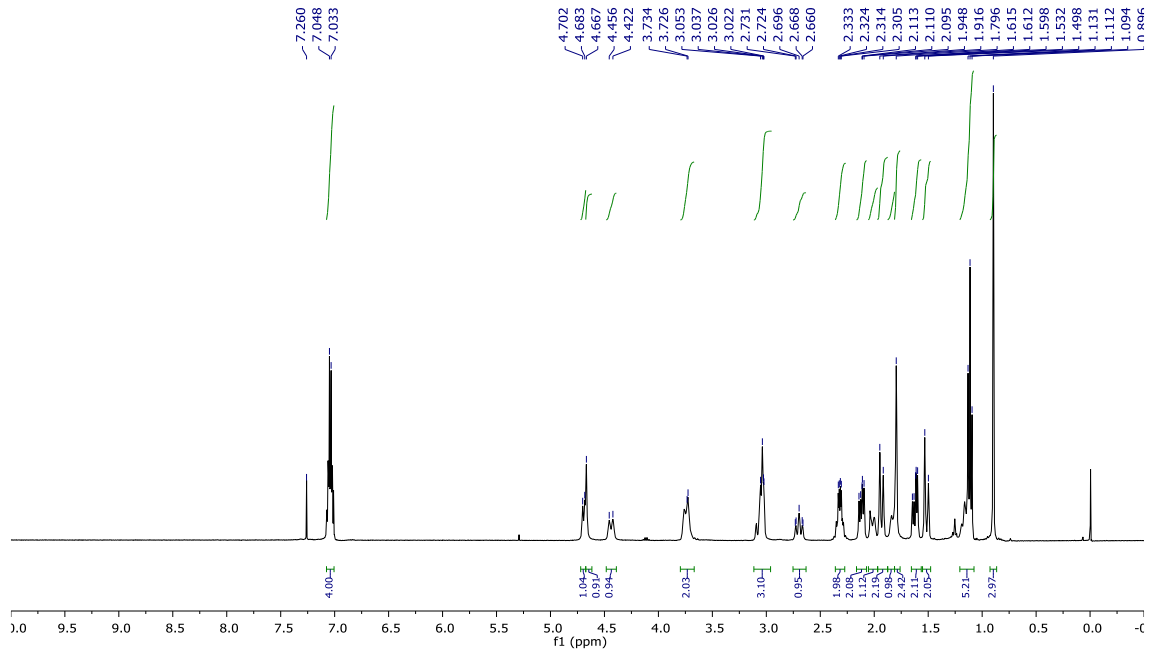
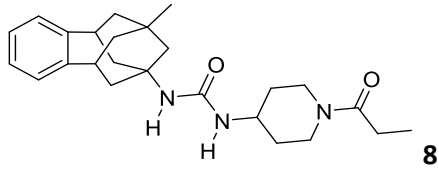
⁸Drug Screening Platform/Biofarma Research Group, CIMUS Research Center. University of Santiago de Compostela (USC), Santiago de Compostela, Spain.

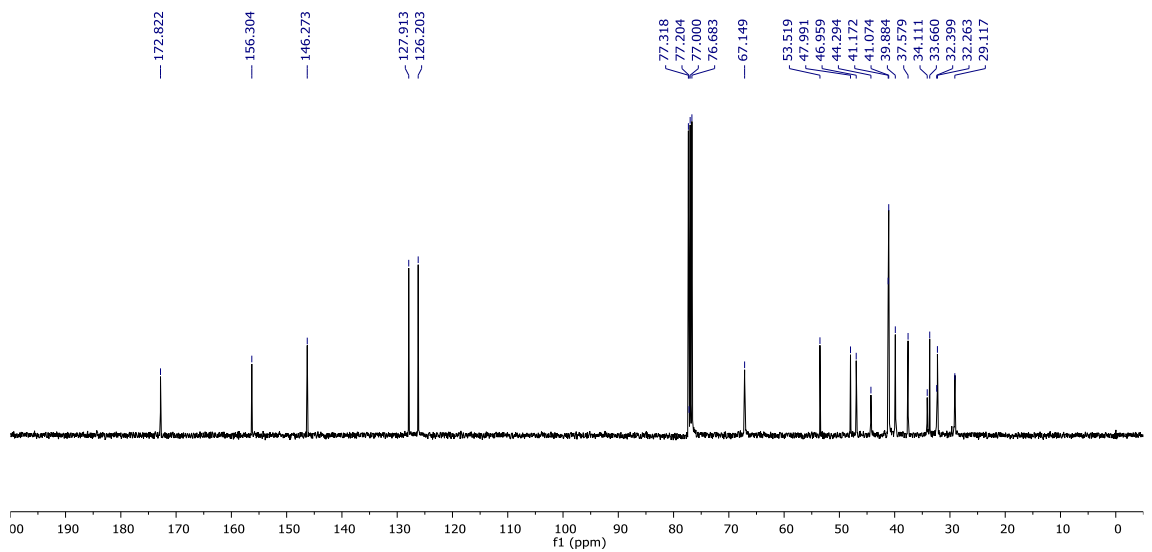
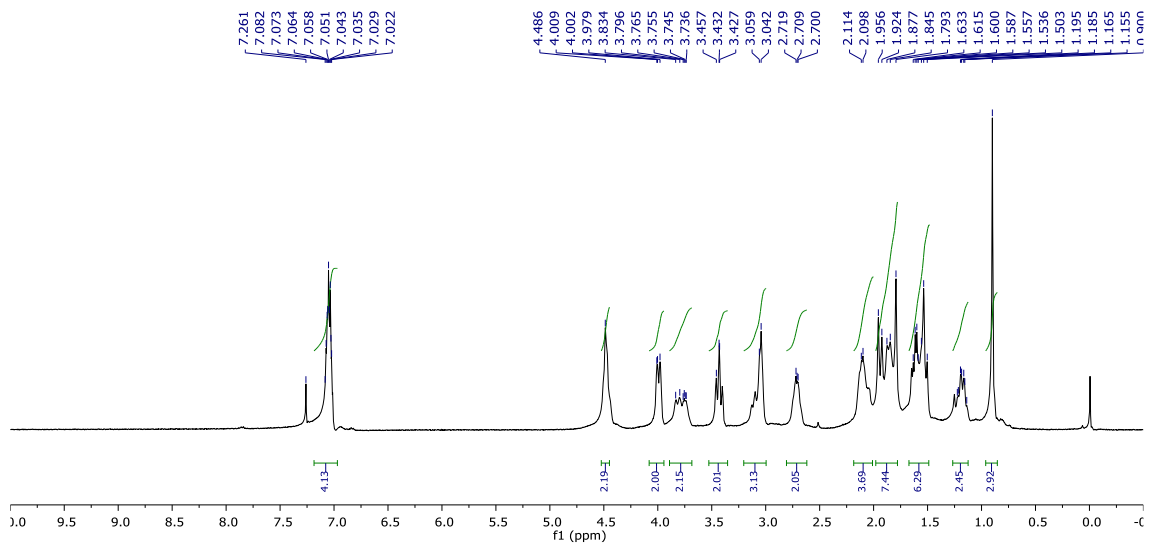
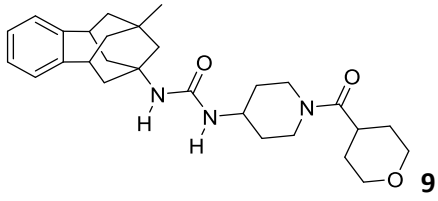
⁹Institució Catalana de Recerca i Estudis Avançats (ICREA), Barcelona, Spain.

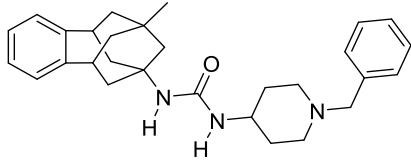
Table of contents

^1H and ^{13}C NMR spectra of compound 8	Page S5
^1H and ^{13}C NMR spectra of compound 9	Page S6
^1H and ^{13}C NMR spectra of compound 10	Page S7
^1H and ^{13}C NMR spectra of compound 11	Page S8
^1H and ^{13}C NMR spectra of compound 12	Page S9
^1H and ^{13}C NMR spectra of compound 13	Page S10
^1H and ^{13}C NMR spectra of compound 14	Page S11
^1H and ^{13}C NMR spectra of compound 15	Page S12
^1H and ^{13}C NMR spectra of compound 16	Page S13
^1H and ^{13}C NMR spectra of compound 17	Page S14
^1H and ^{13}C NMR spectra of compound 18	Page S15
^1H and ^{13}C NMR spectra of compound 19	Page S16
^1H and ^{13}C NMR spectra of compound 20	Page S17
^1H and ^{13}C NMR spectra of compound 21	Page S18
^1H and ^{13}C NMR spectra of compound 22	Page S19
^1H and ^{13}C NMR spectra of compound 23	Page S20
^1H and ^{13}C NMR spectra of compound 24	Page S21
^1H and ^{13}C NMR spectra of compound 25	Page S22
^1H and ^{13}C NMR spectra of compound 26	Page S23
^1H and ^{13}C NMR spectra of compound 27	Page S24
^1H and ^{13}C NMR spectra of compound 28	Page S25
^1H and ^{13}C NMR spectra of compound 29	Page S26
^1H and ^{13}C NMR spectra of compound 30	Page S27
^1H and ^{13}C NMR spectra of compound 31	Page S28
^1H and ^{13}C NMR spectra of compound 32	Page S29
^1H and ^{13}C NMR spectra of compound 33	Page S30
^1H and ^{13}C NMR spectra of compound 34	Page S31
^1H and ^{13}C NMR spectra of compound 35	Page S32
Table S1	Page S33

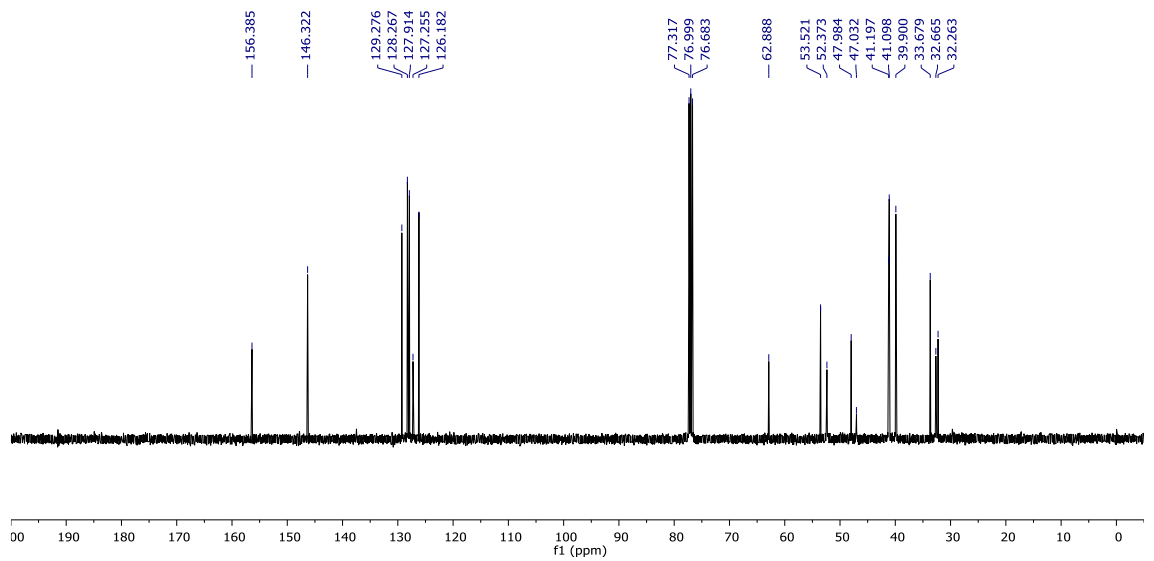
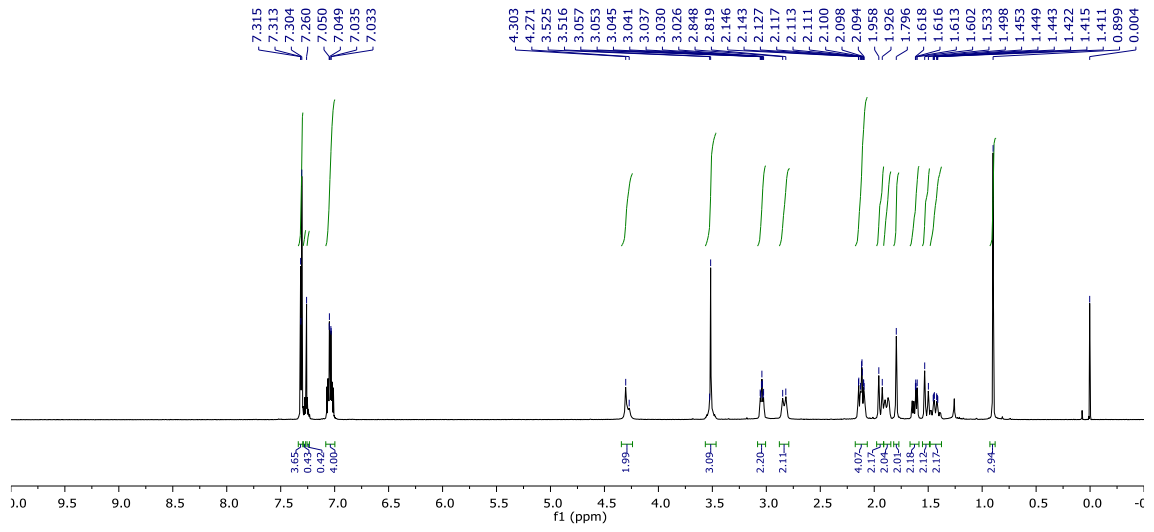
Table S2	Page S33
Table S3	Page S34
Figure S1	Page S35
Figure S2	Page S35

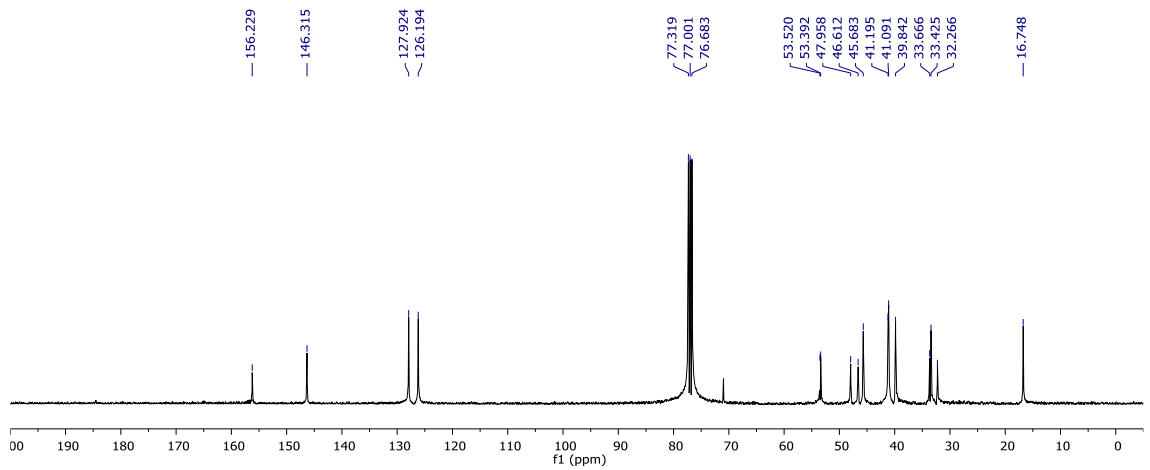
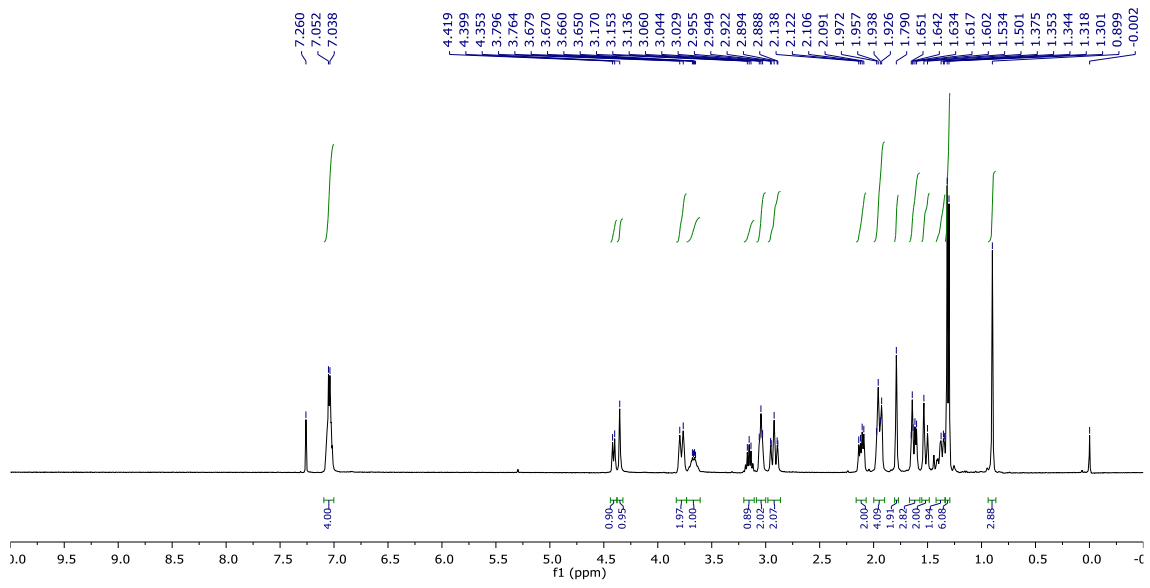
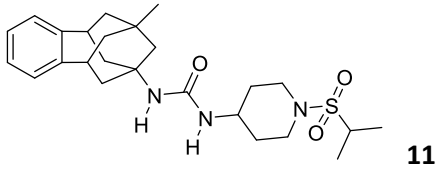


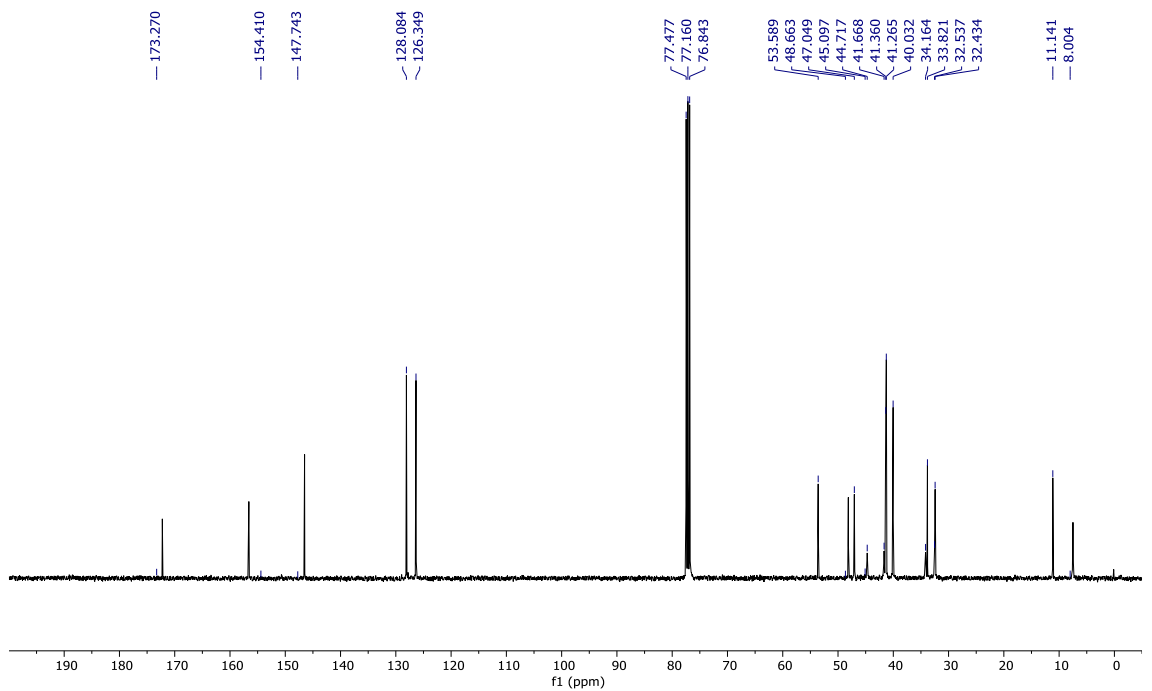
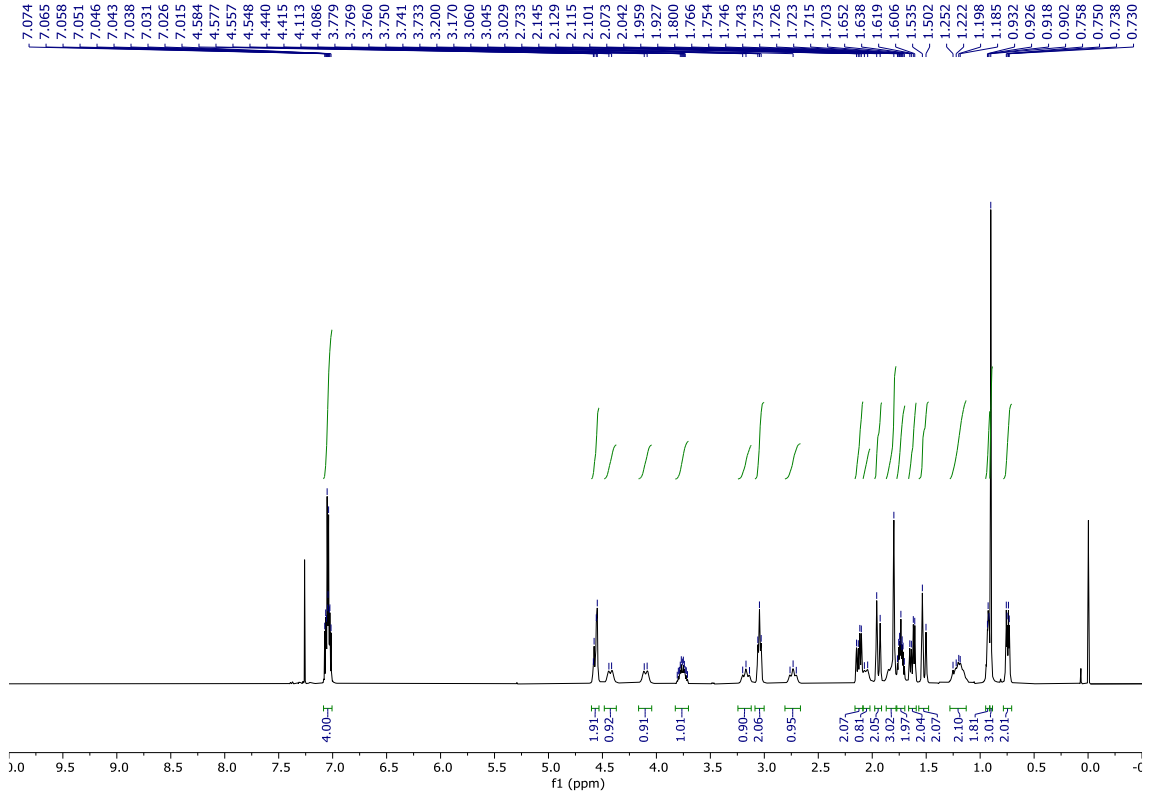
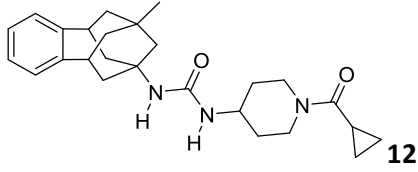


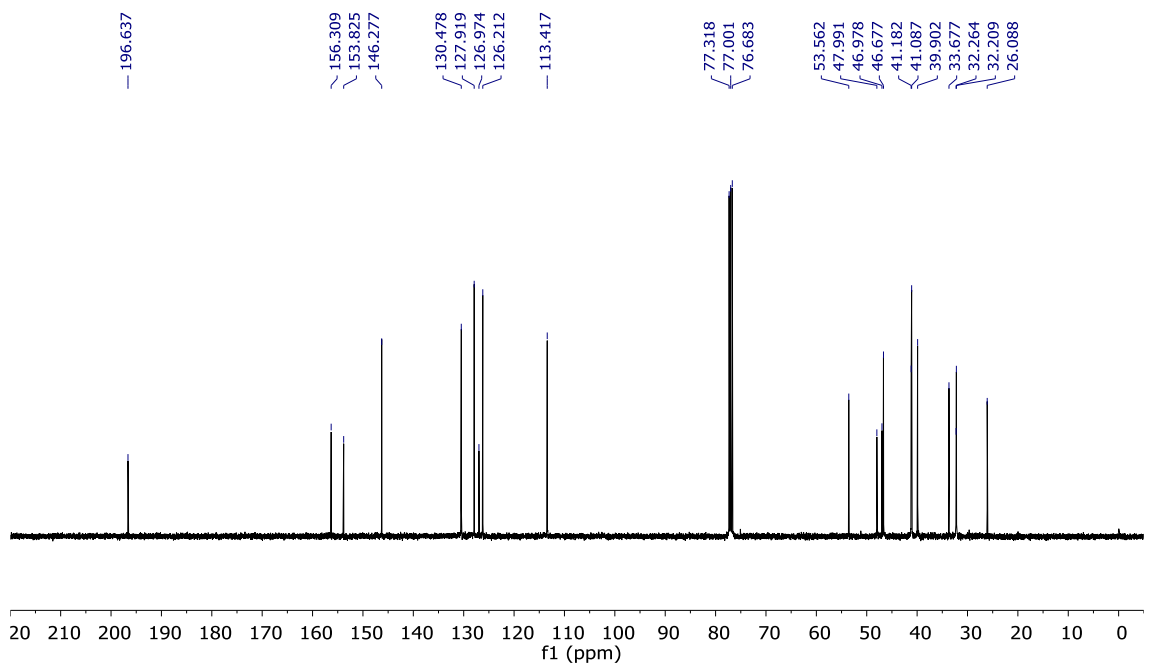
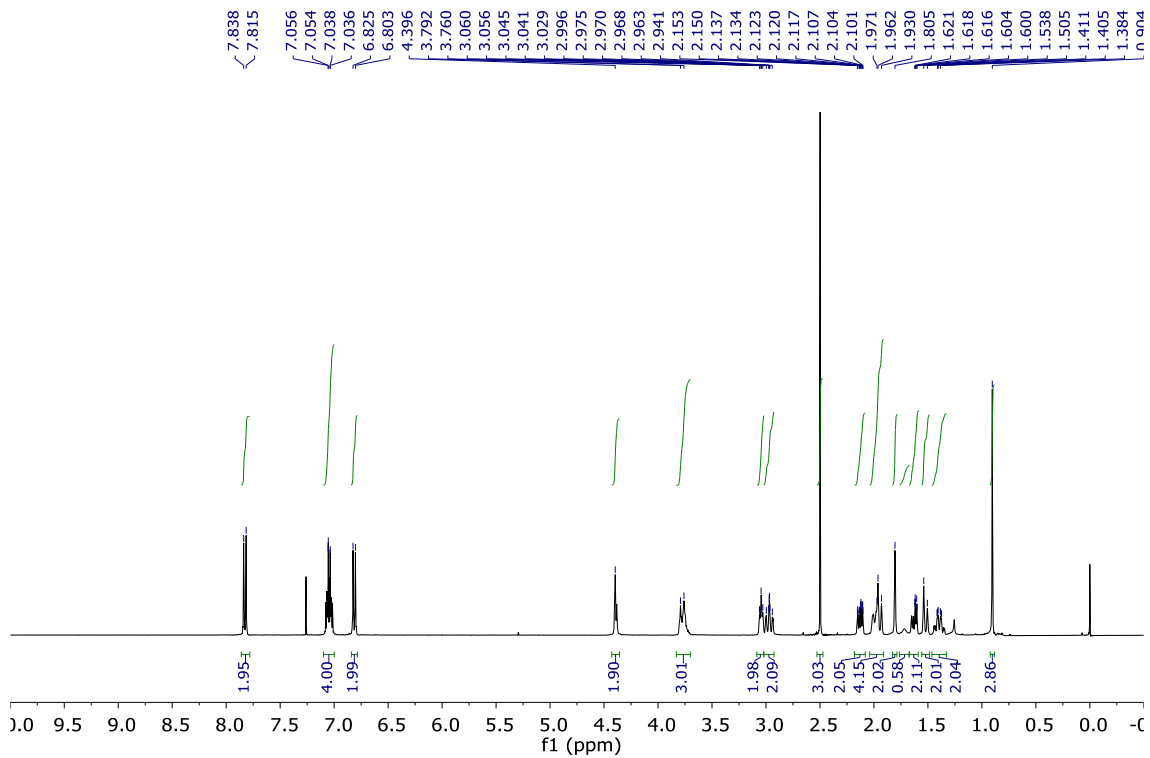
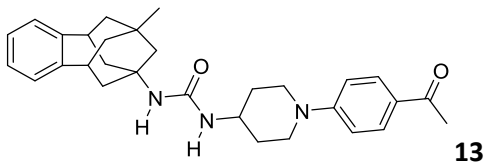


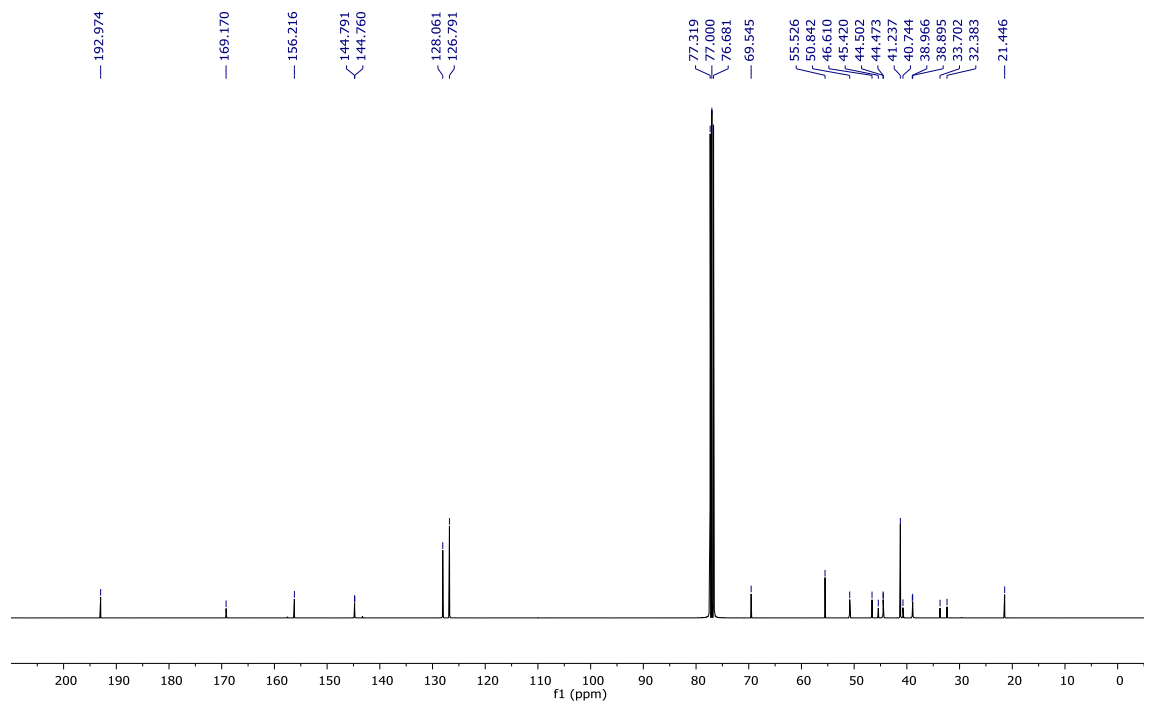
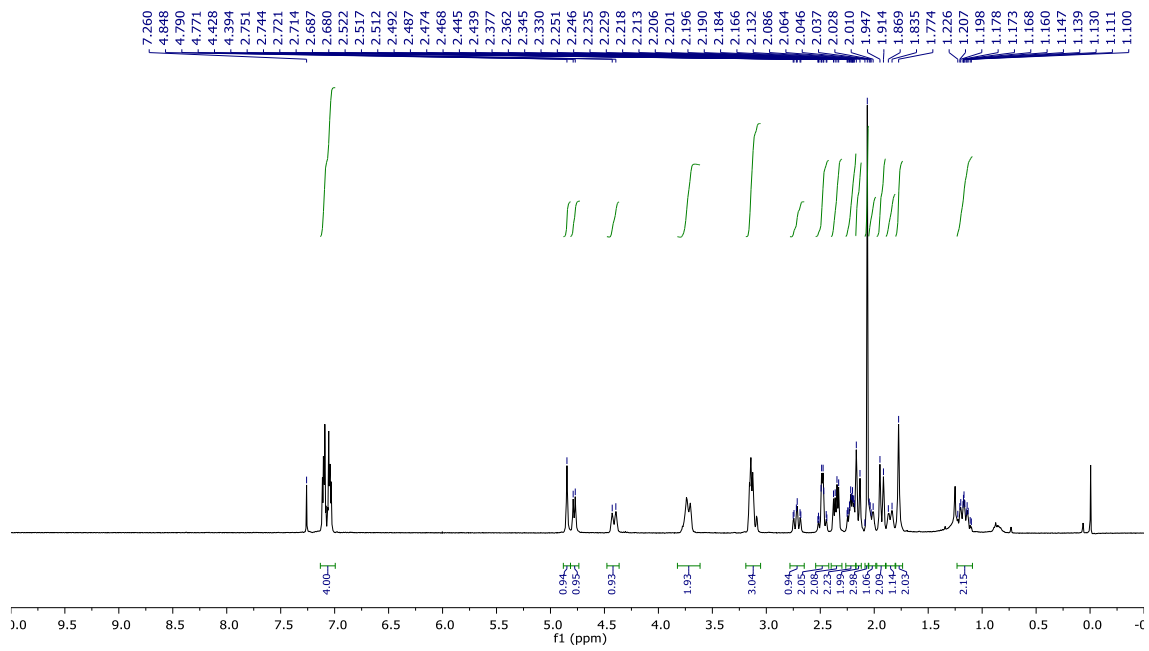
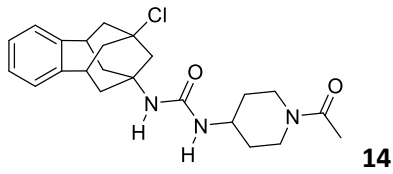
10

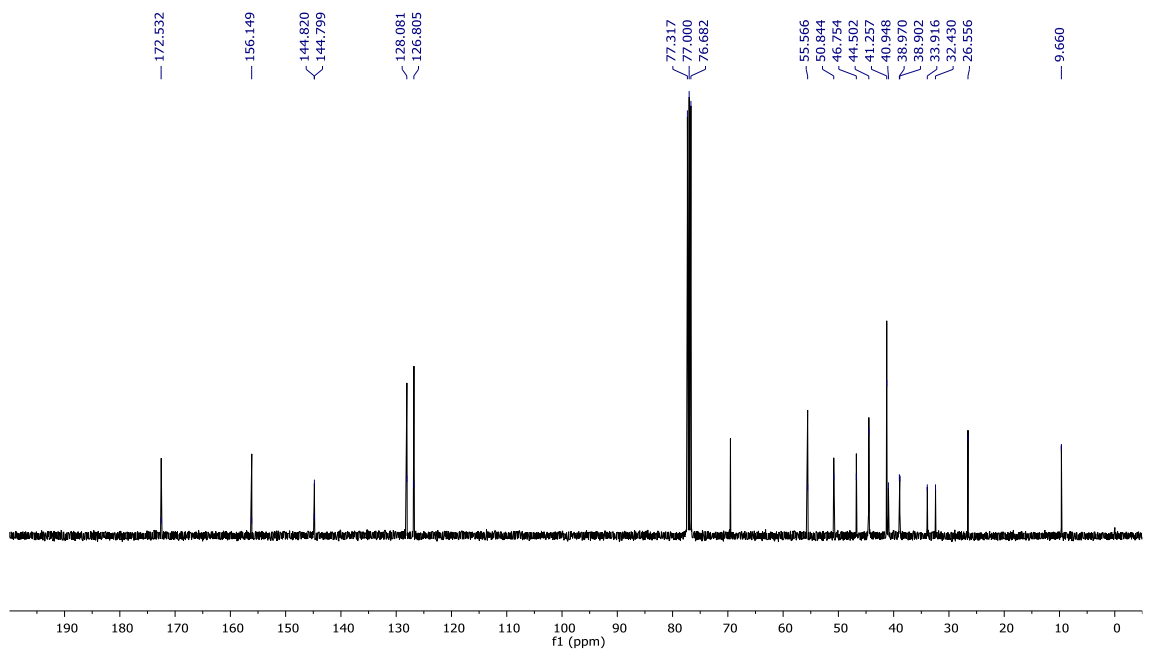
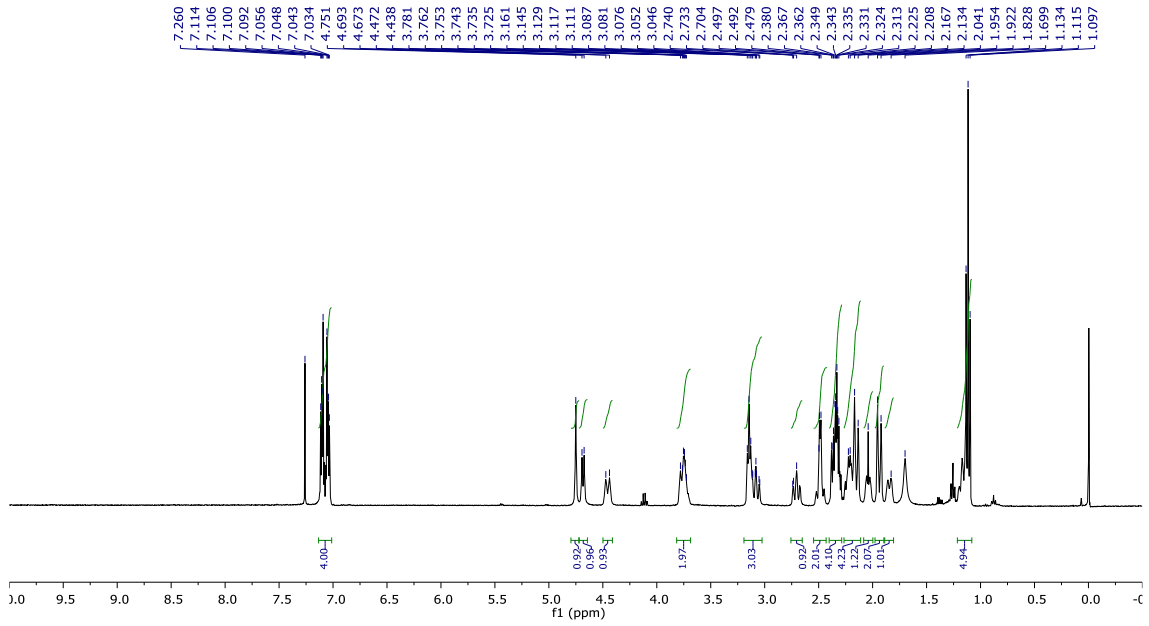
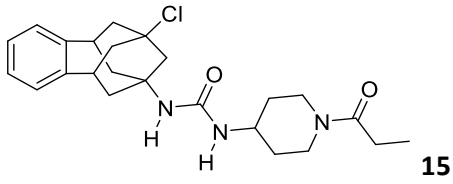


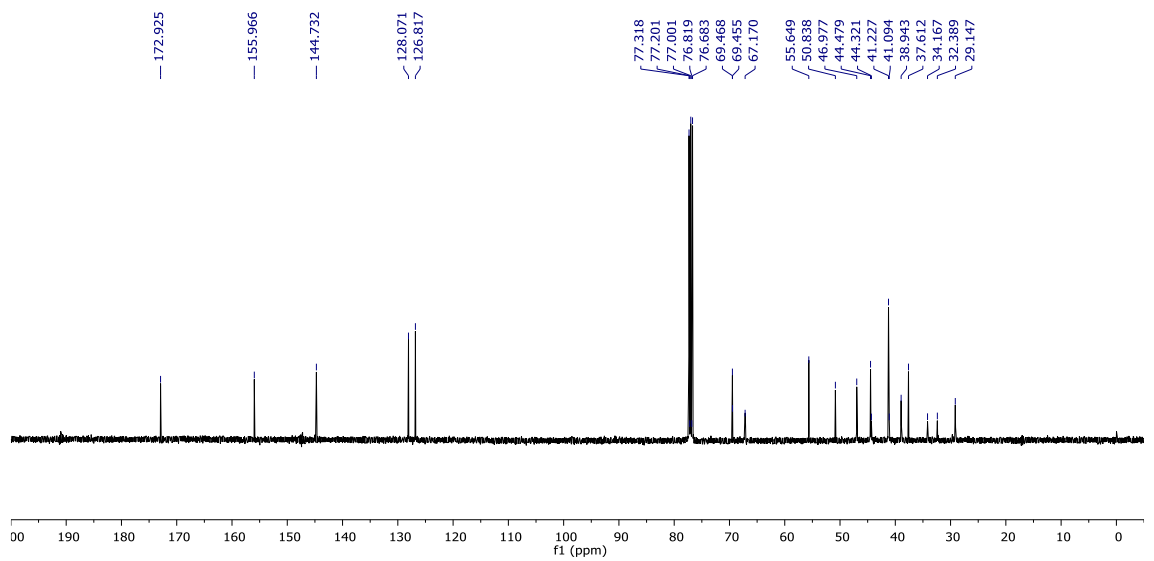
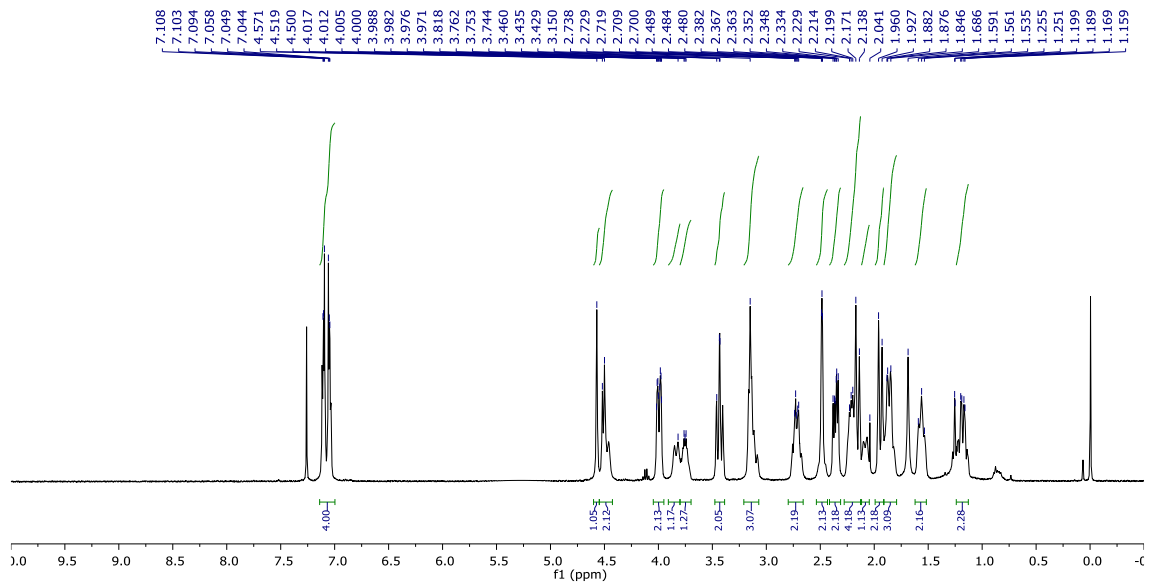
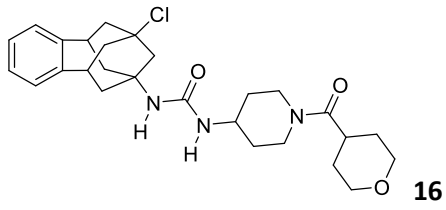


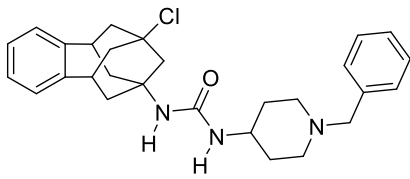




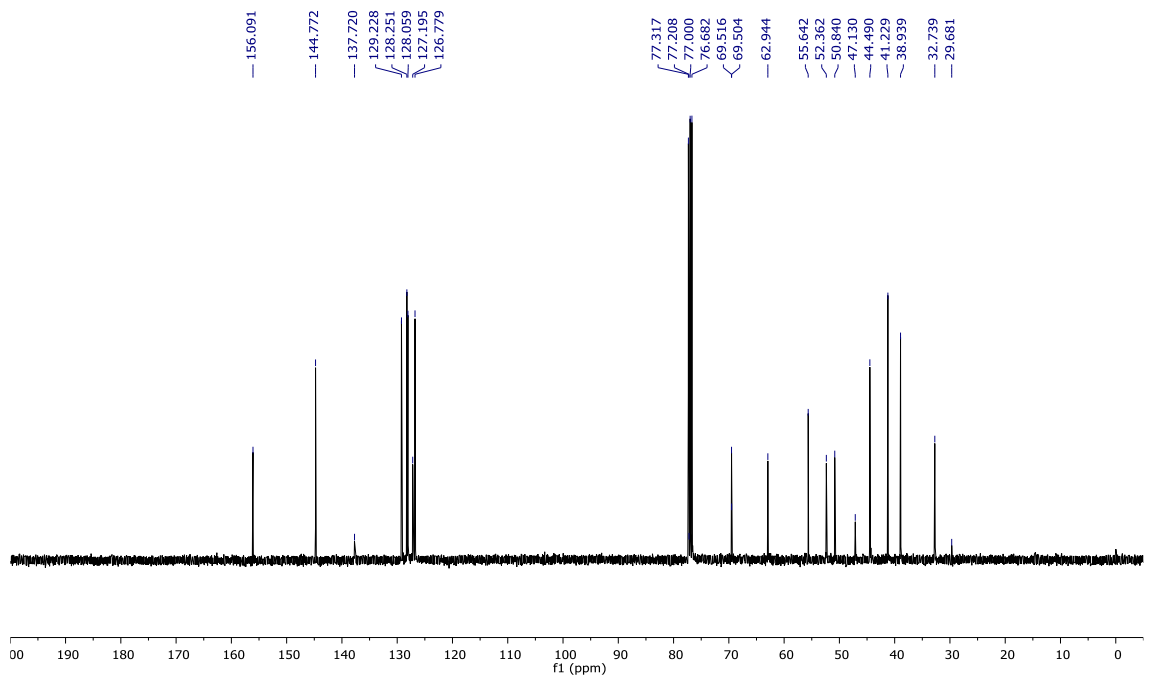
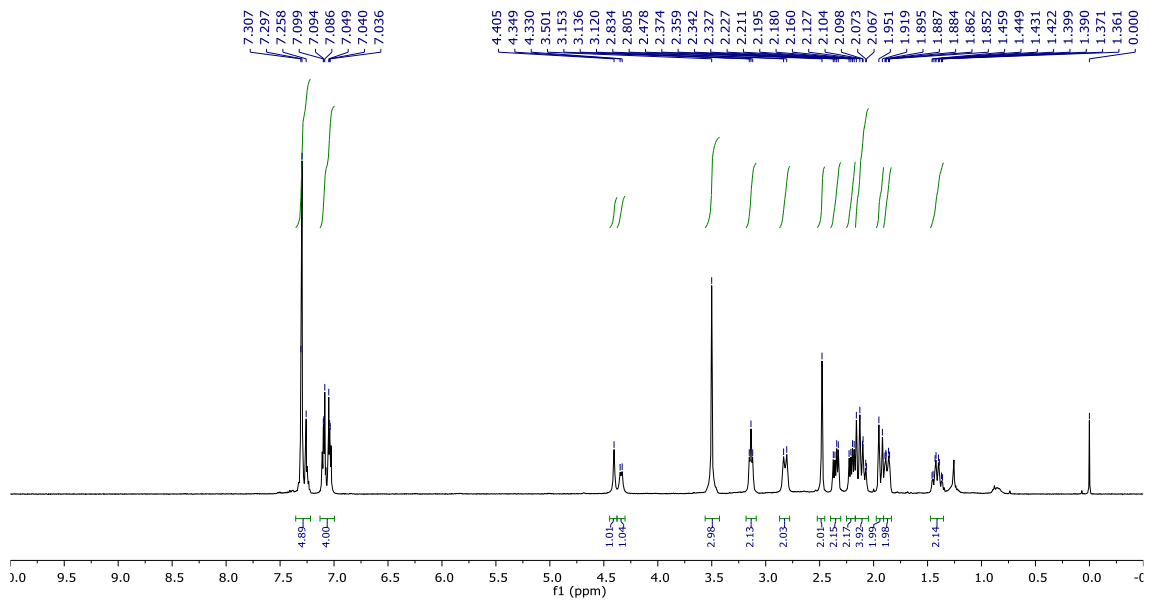


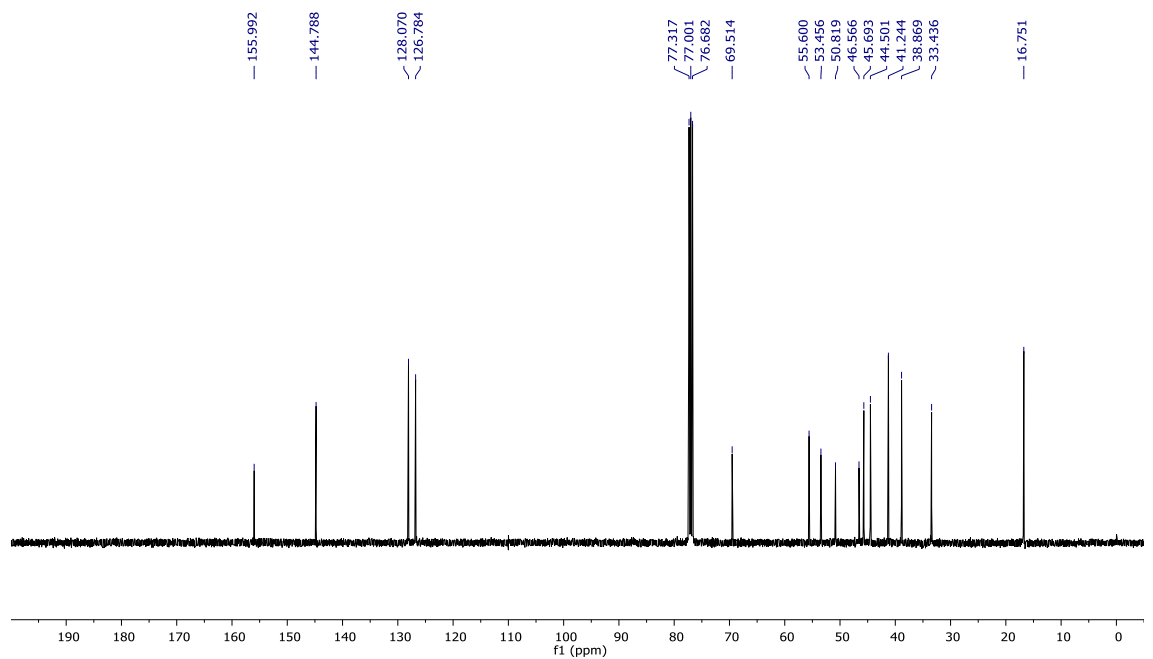
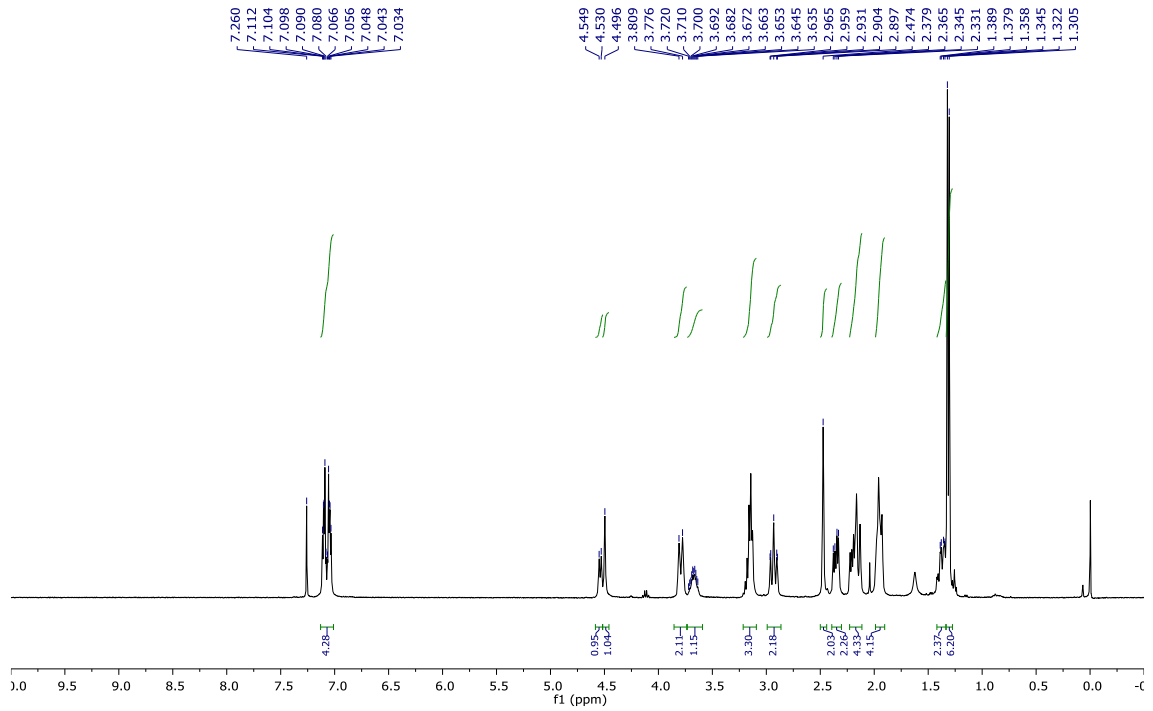
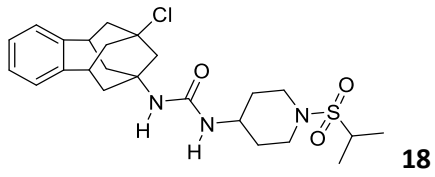


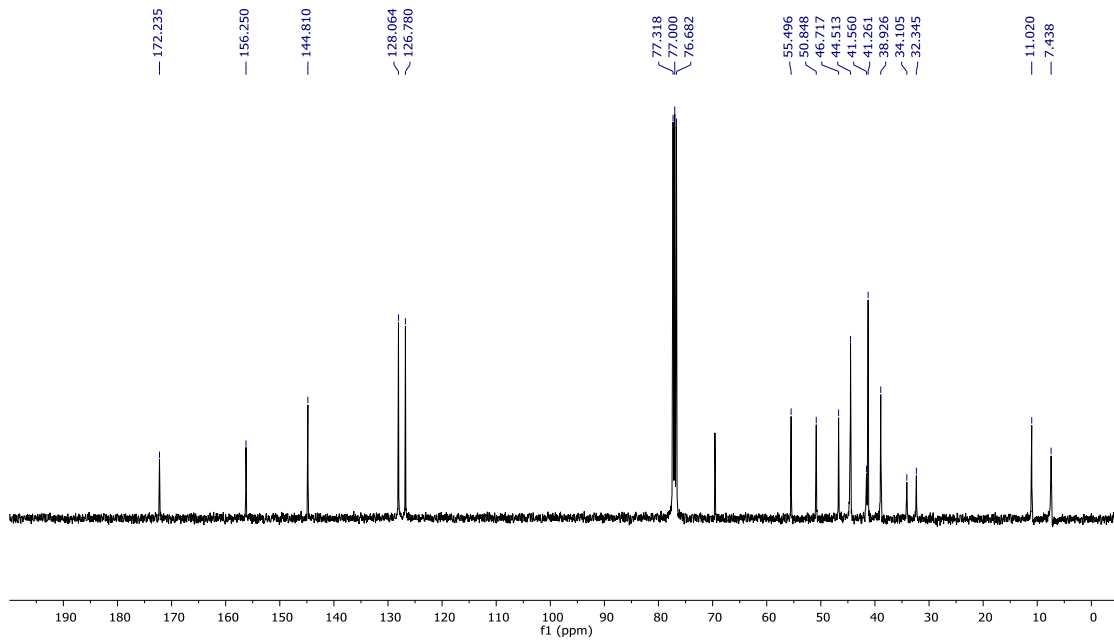
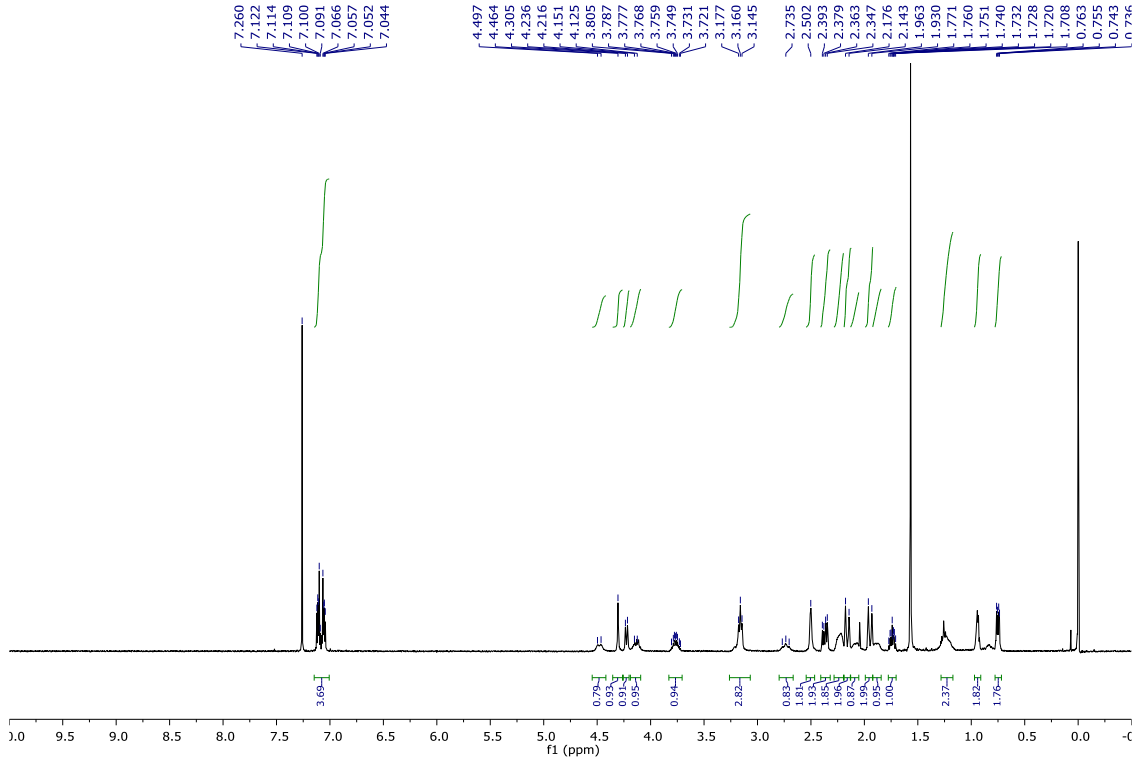
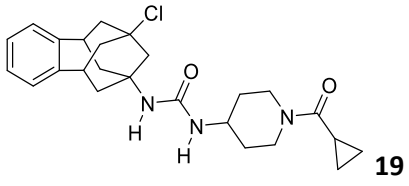


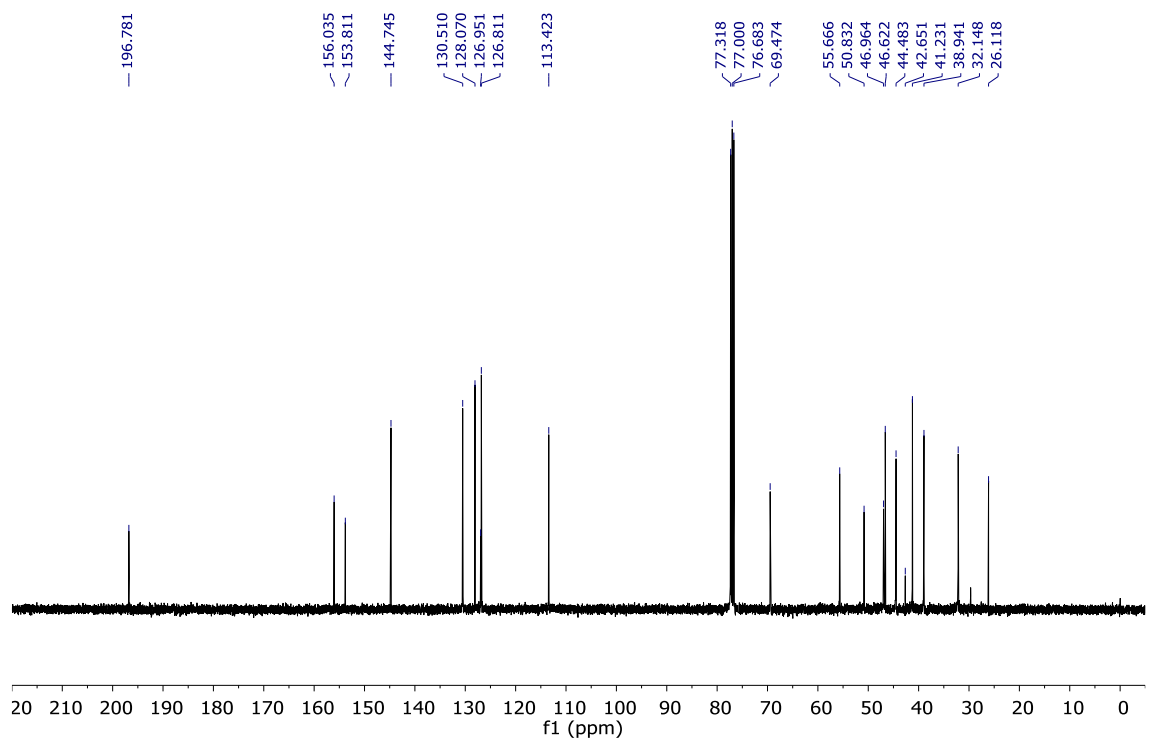
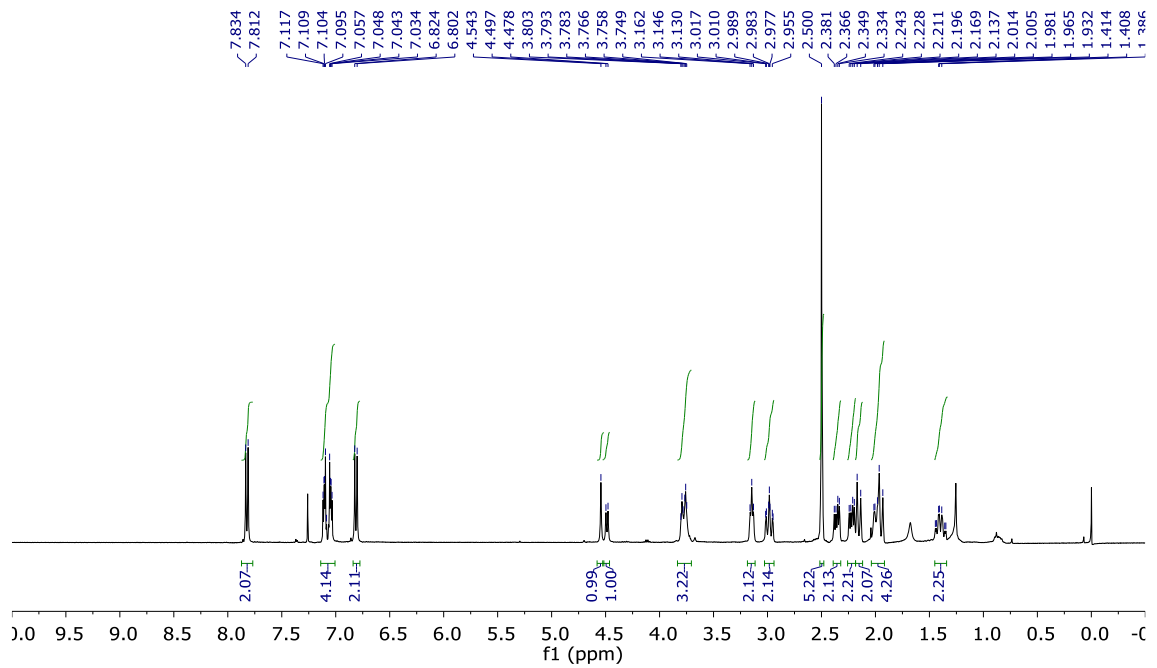
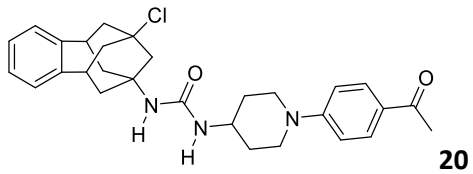


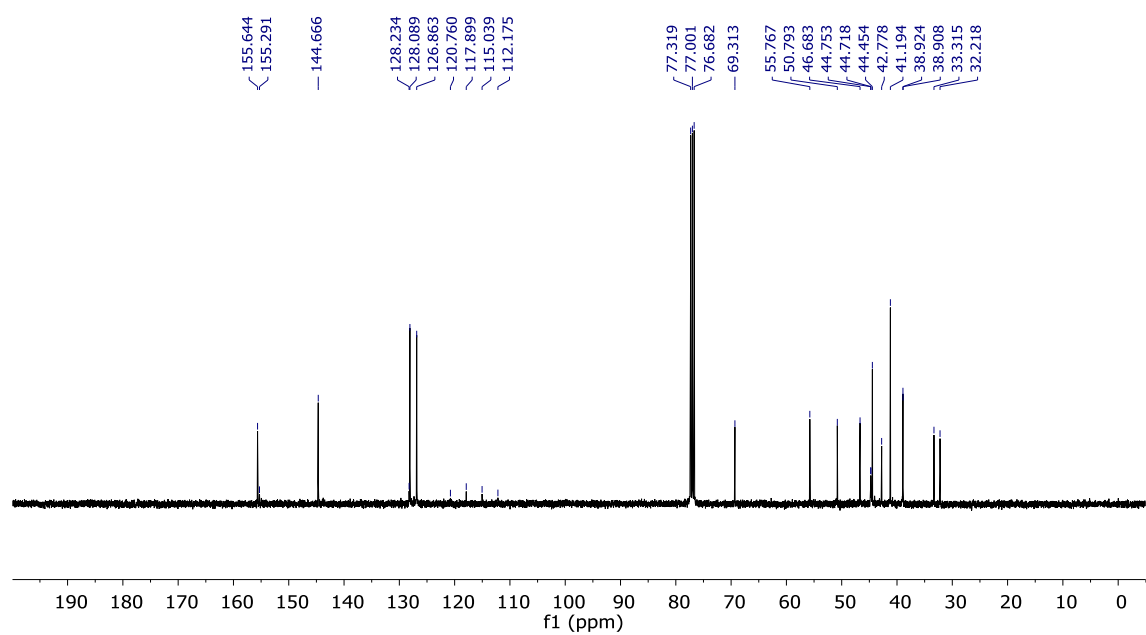
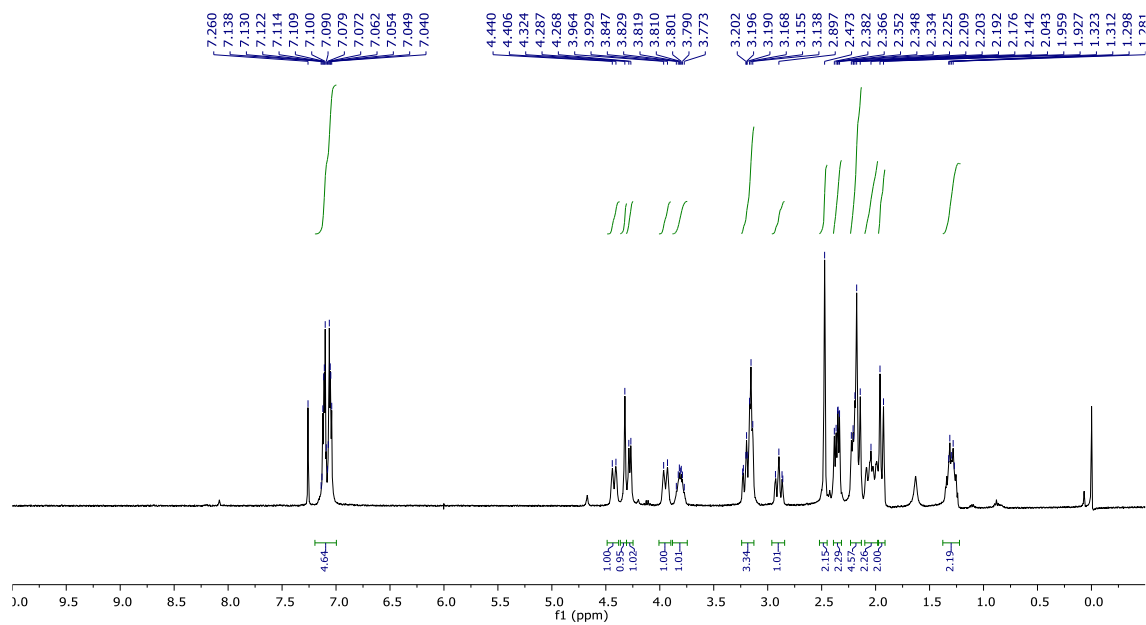
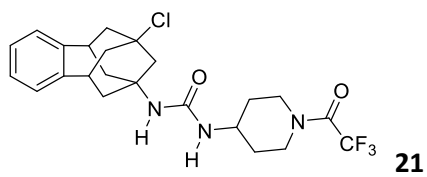
17

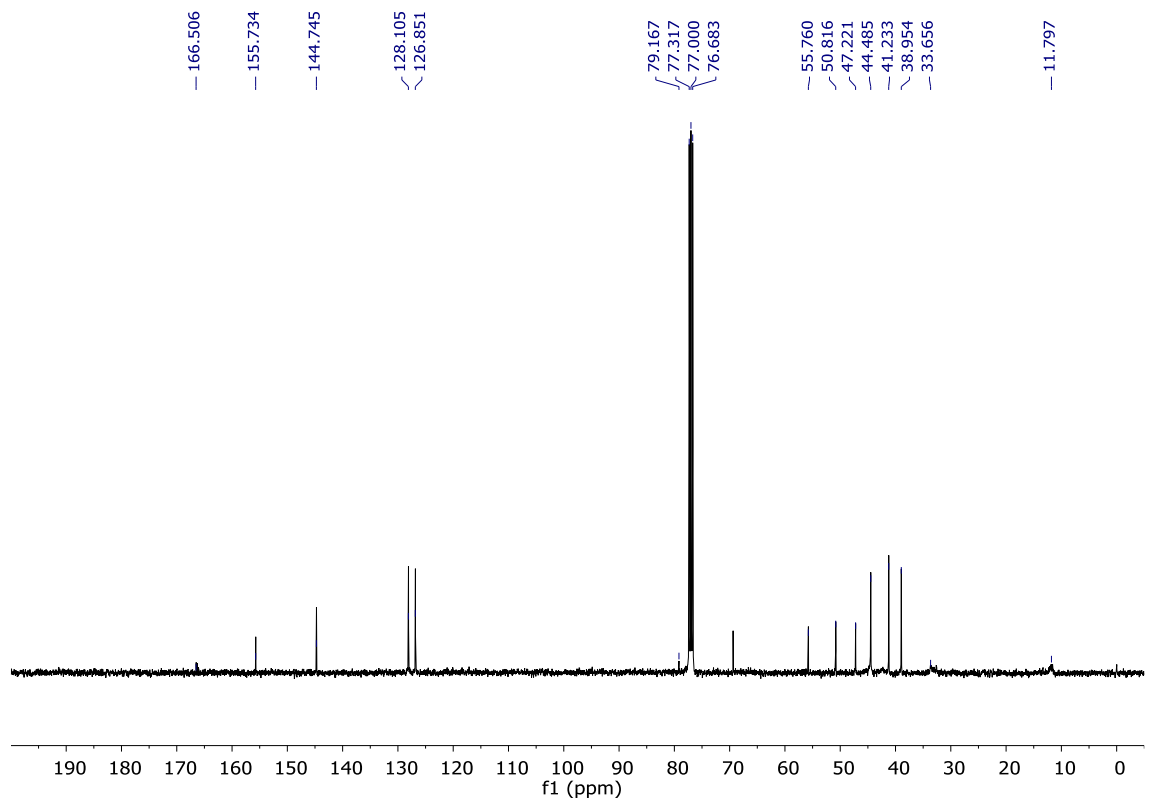
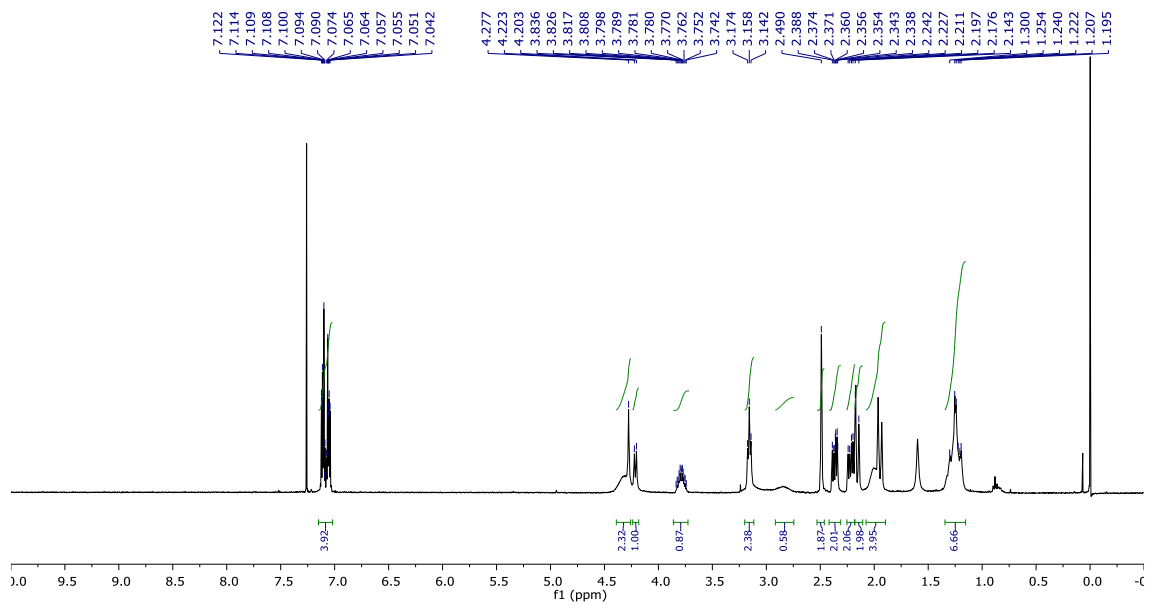
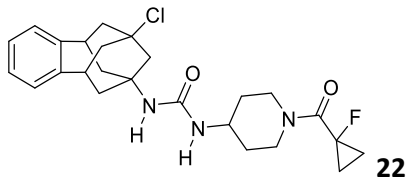


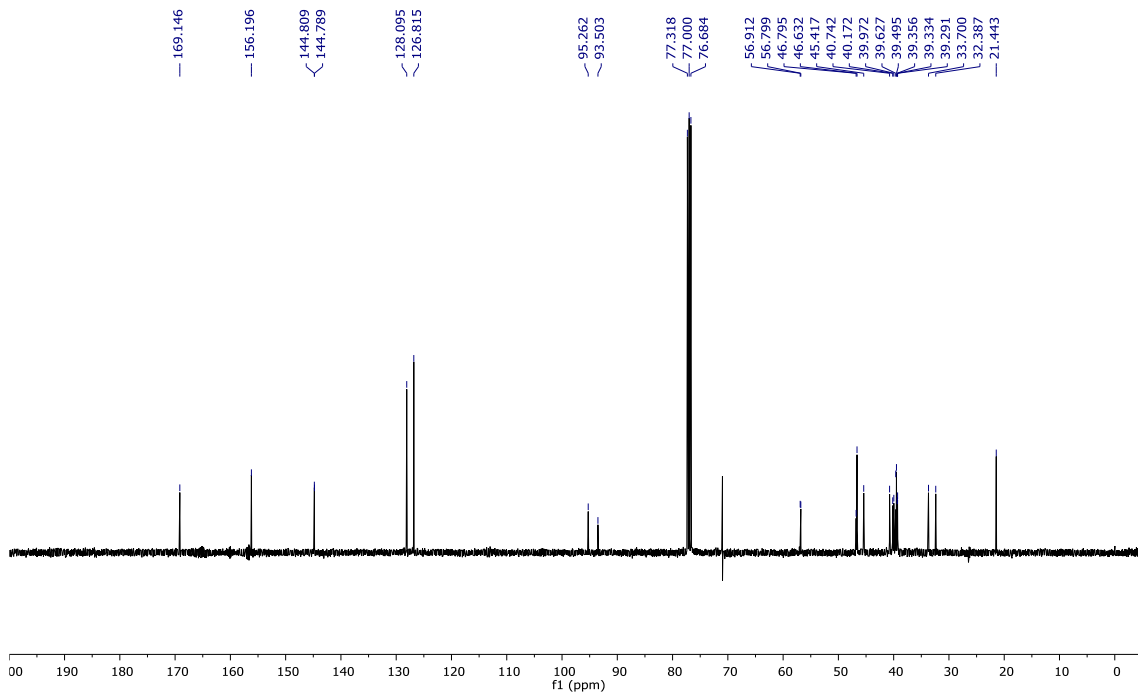
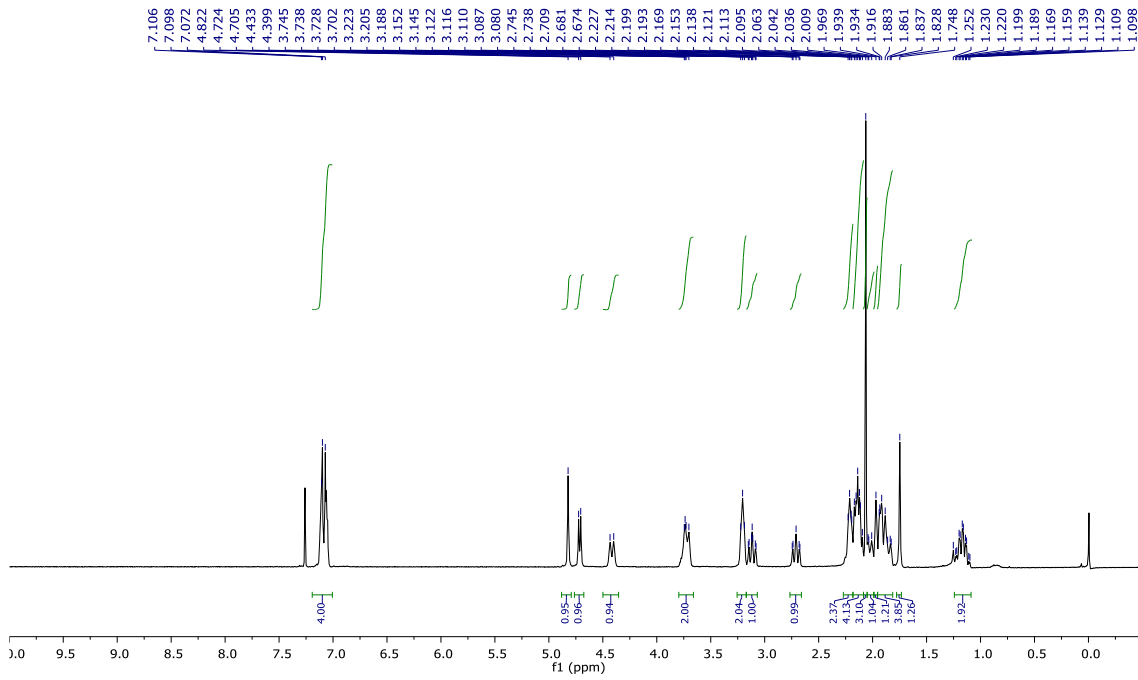
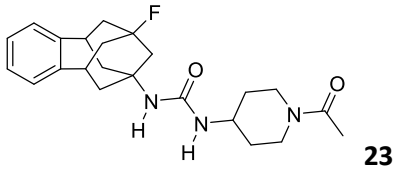


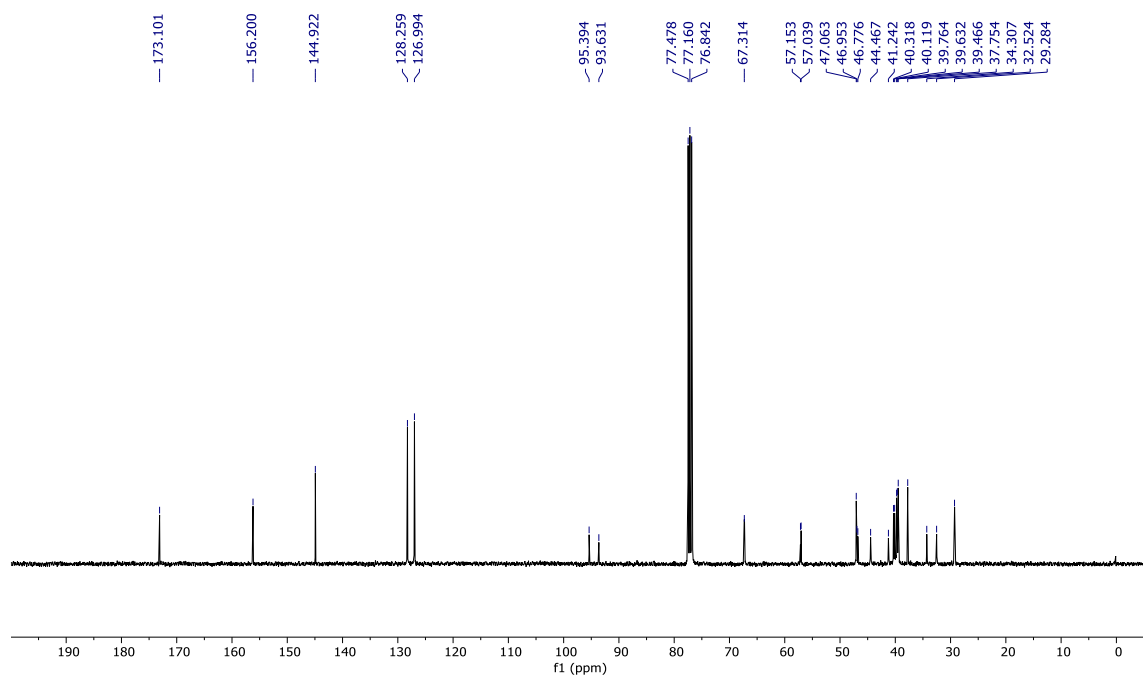
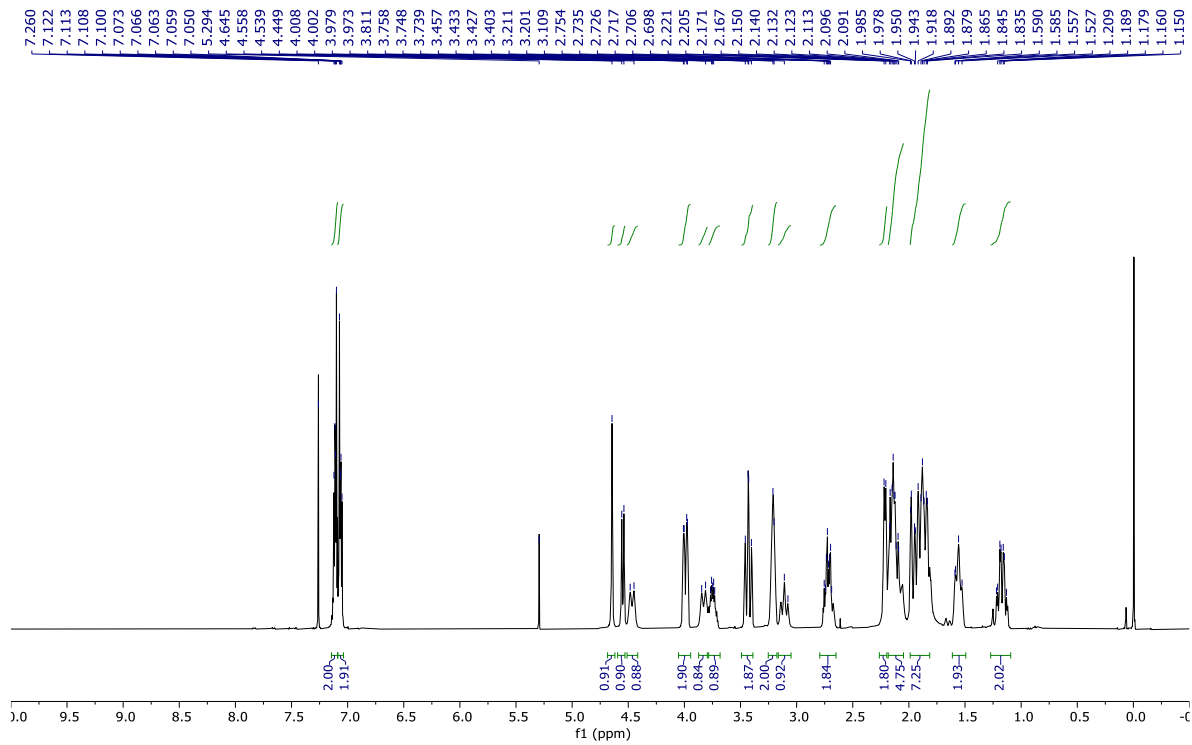
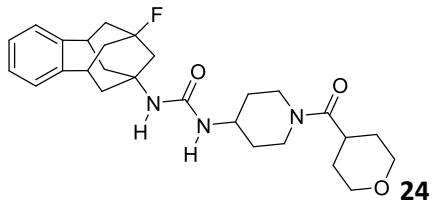


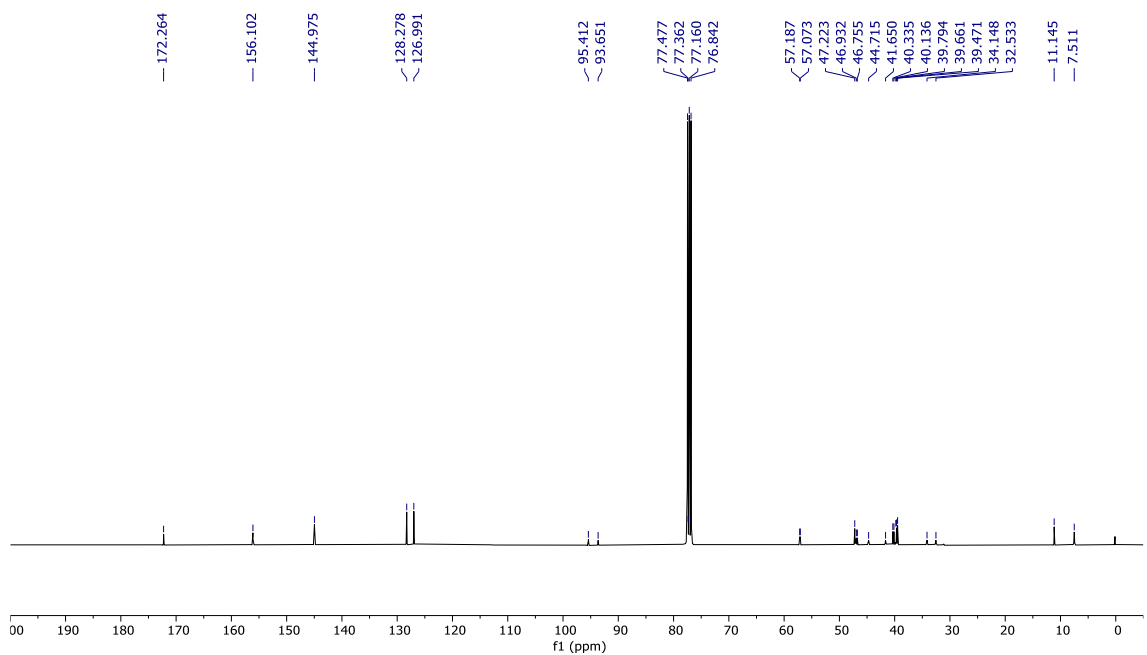
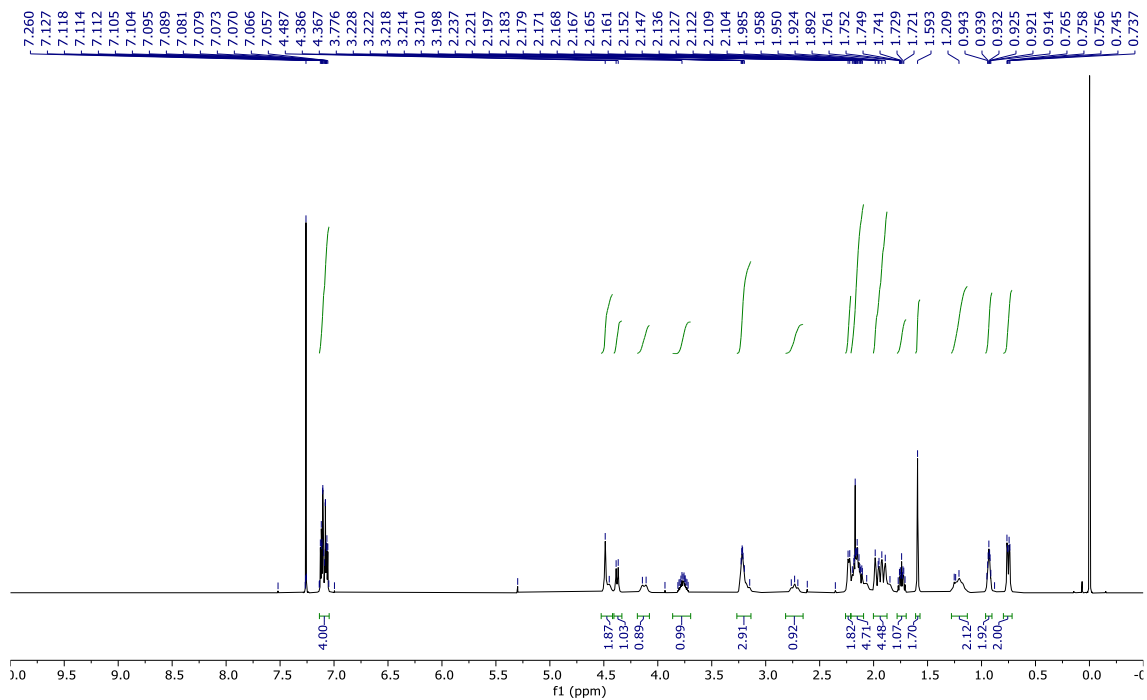
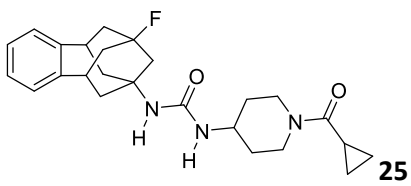


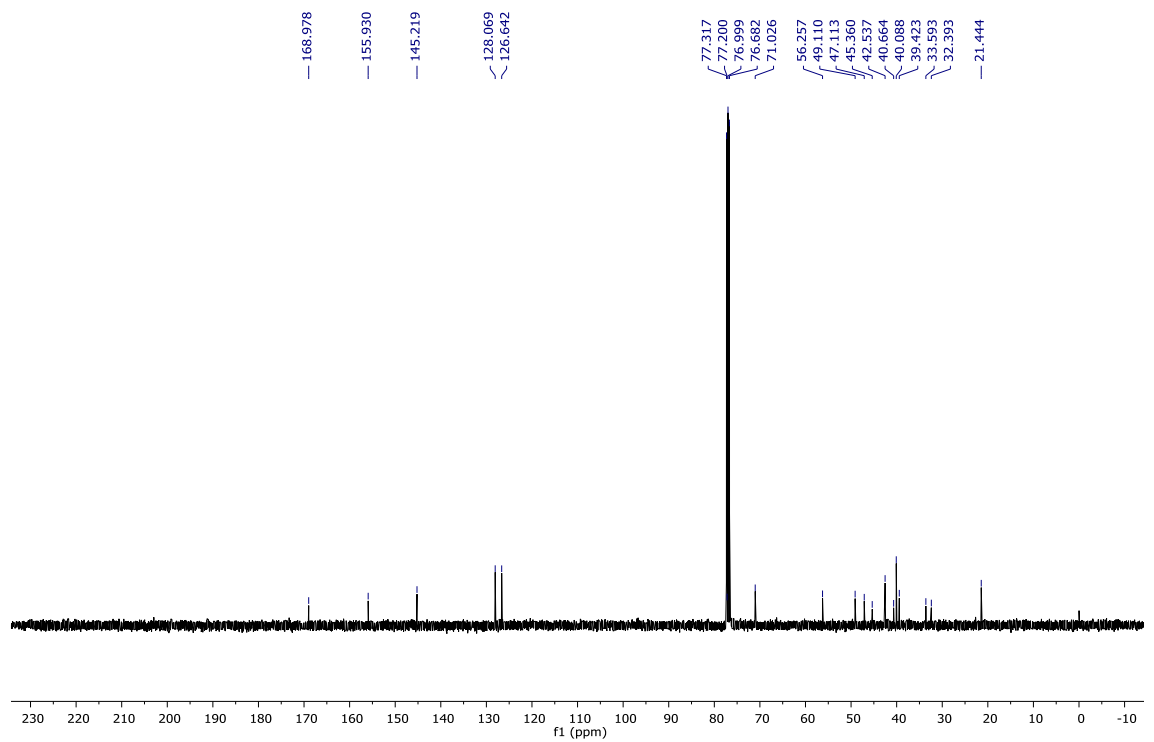
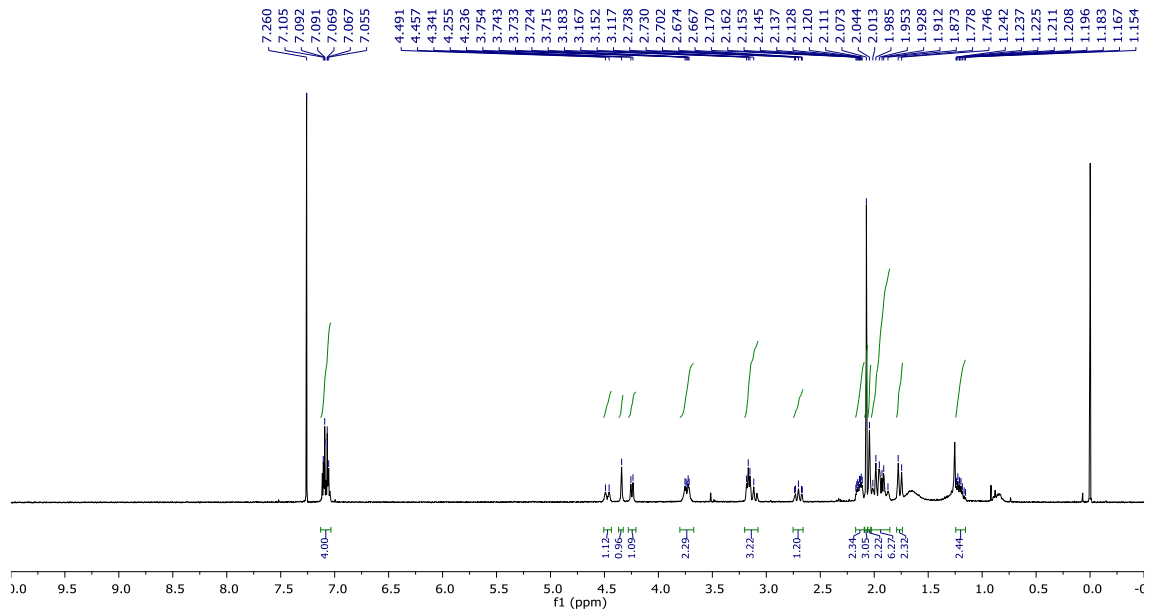
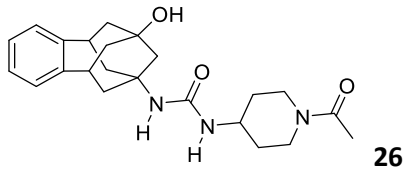


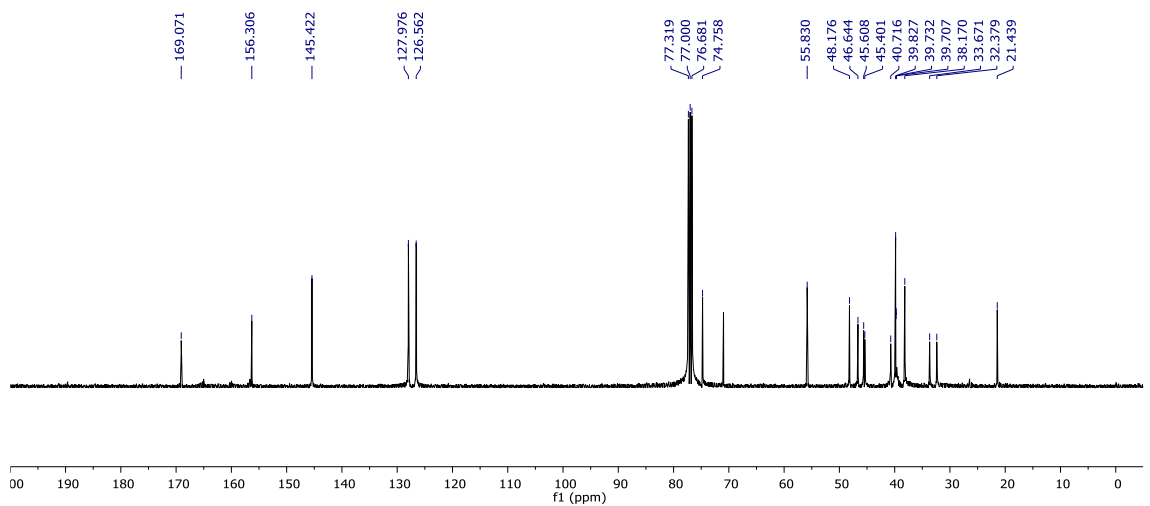
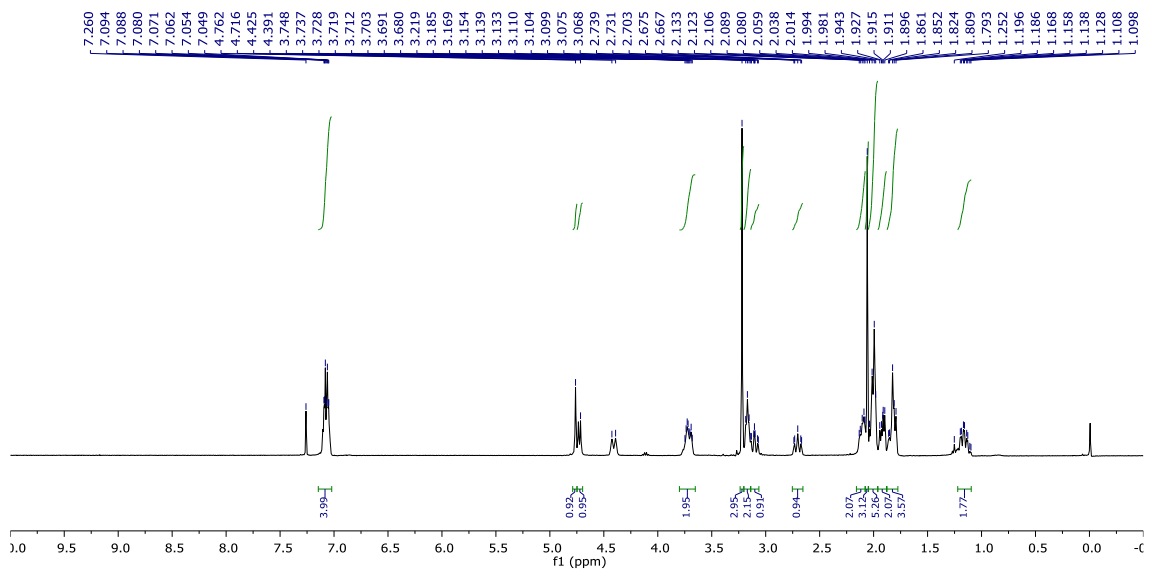
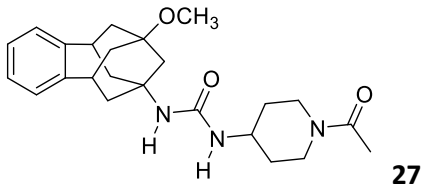


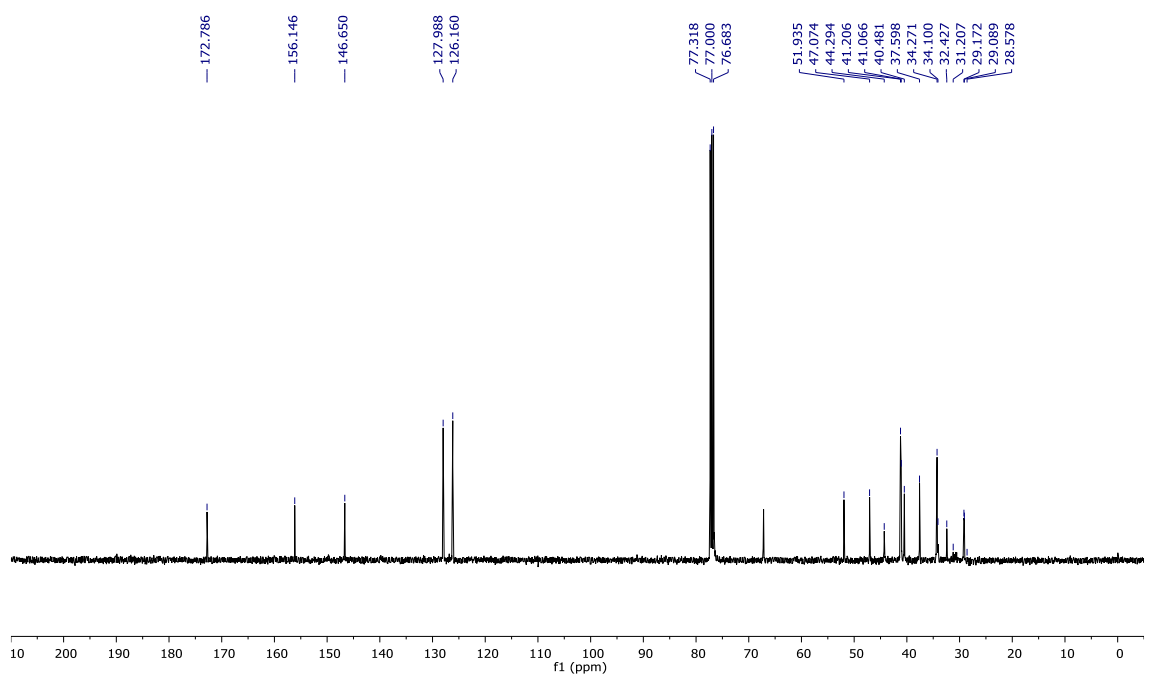
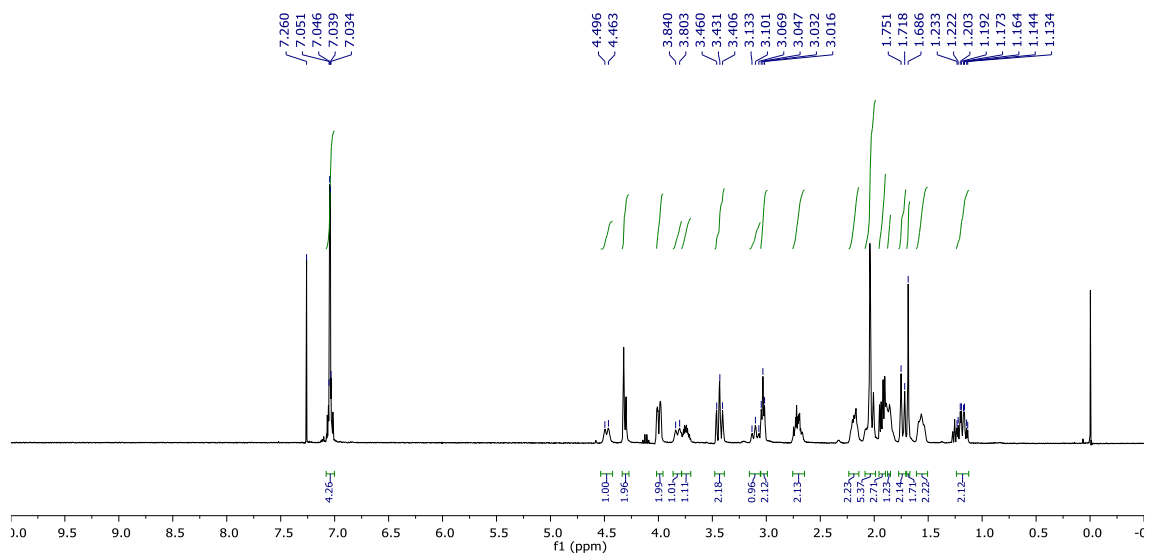
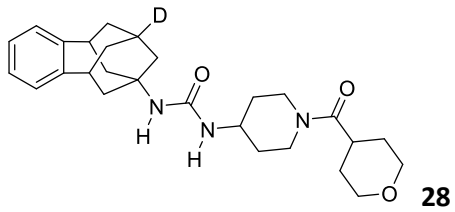


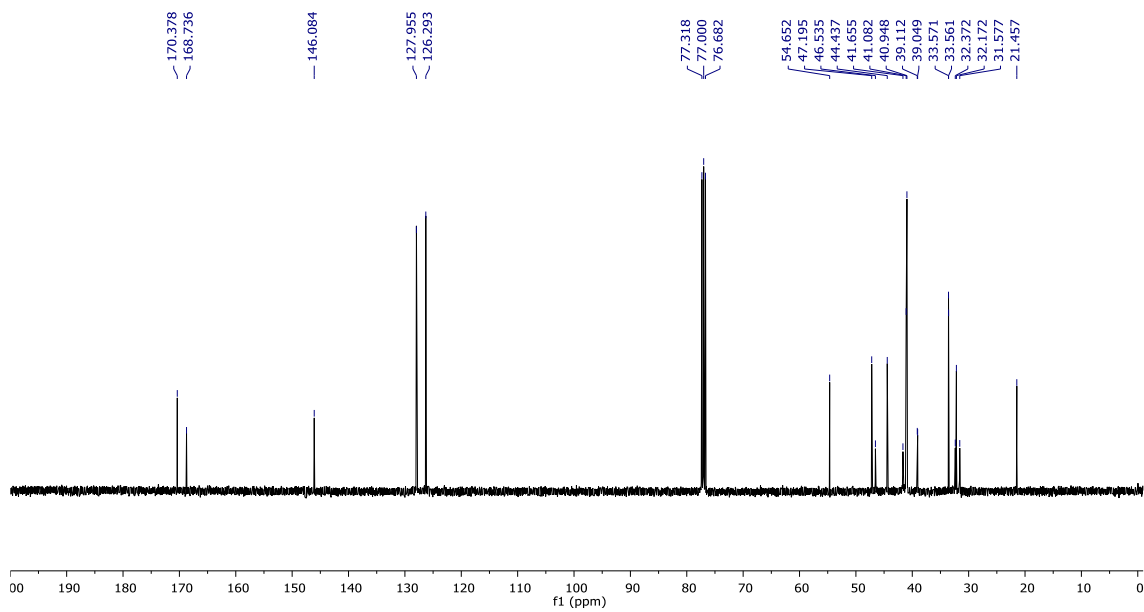
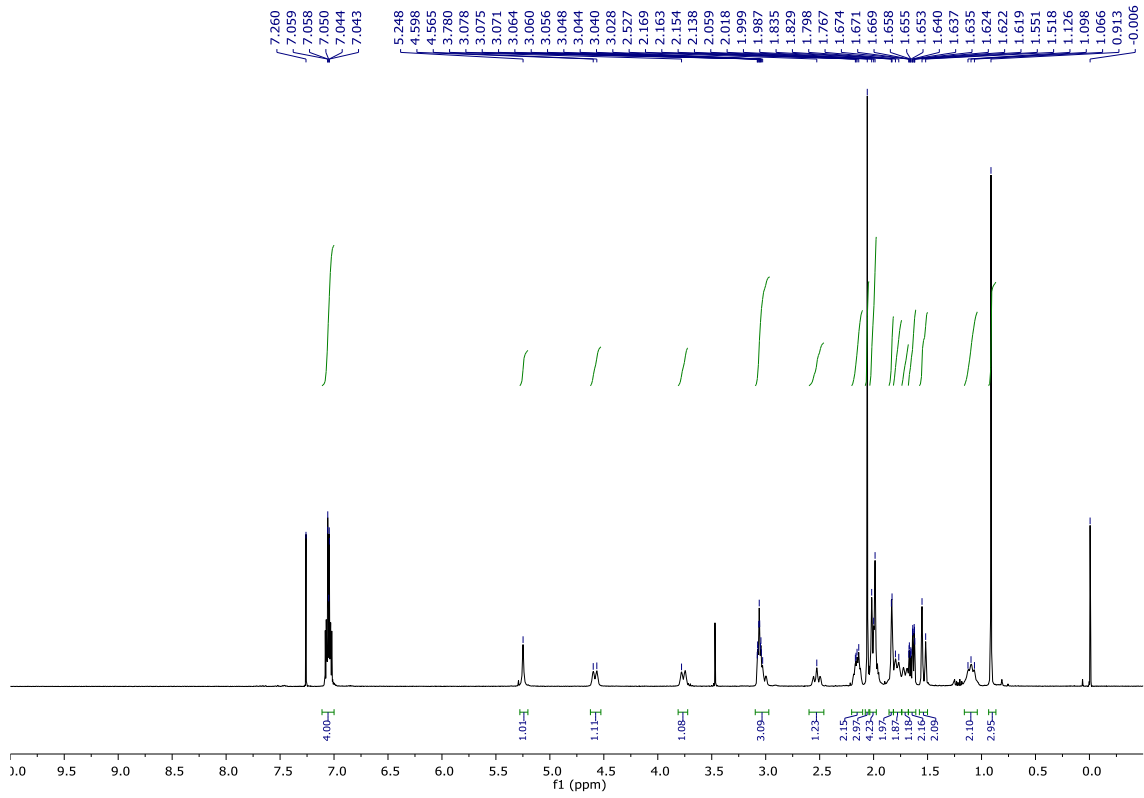
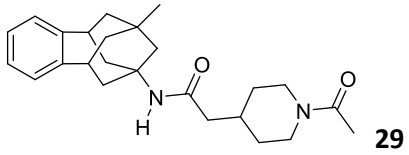


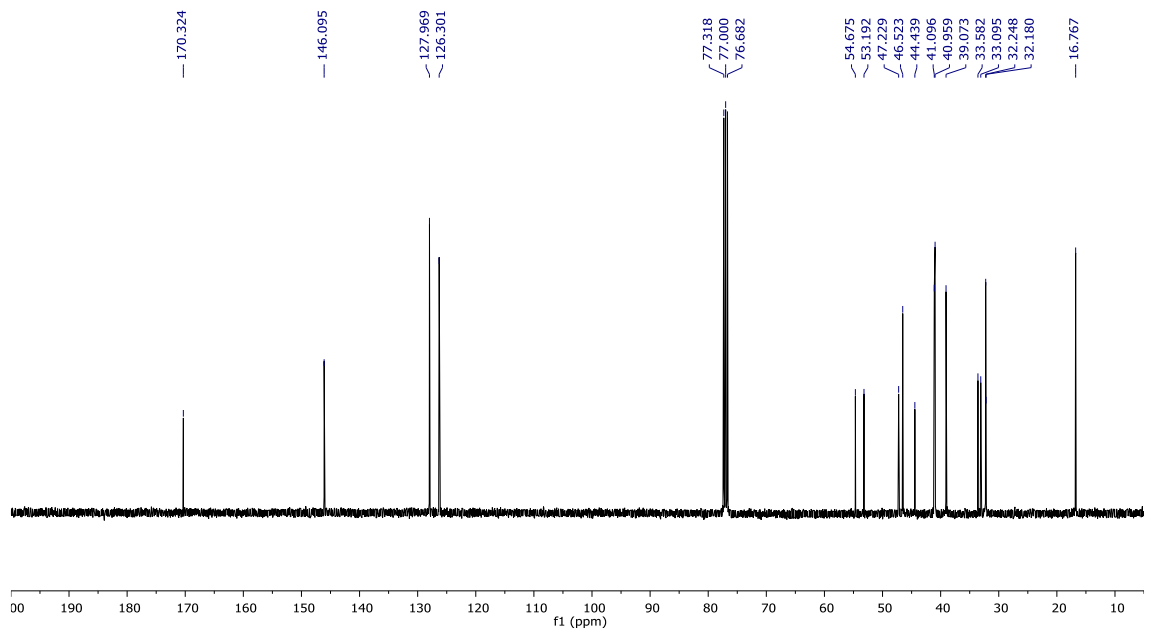
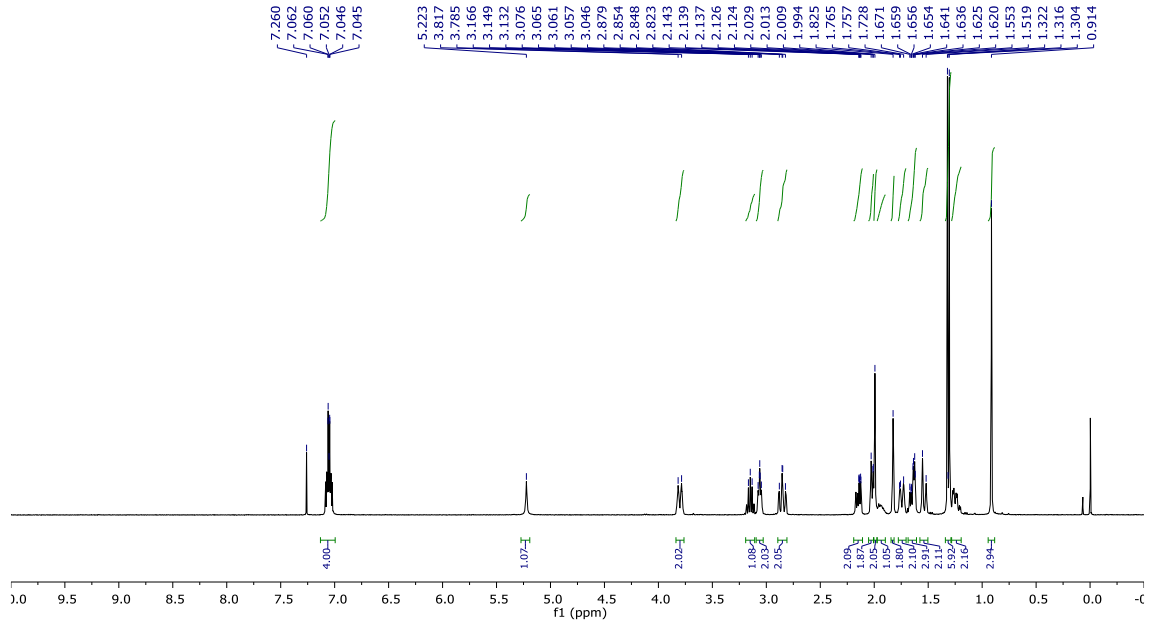
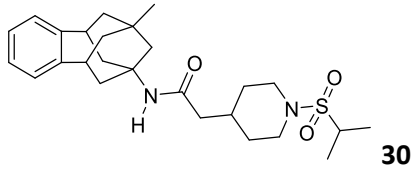


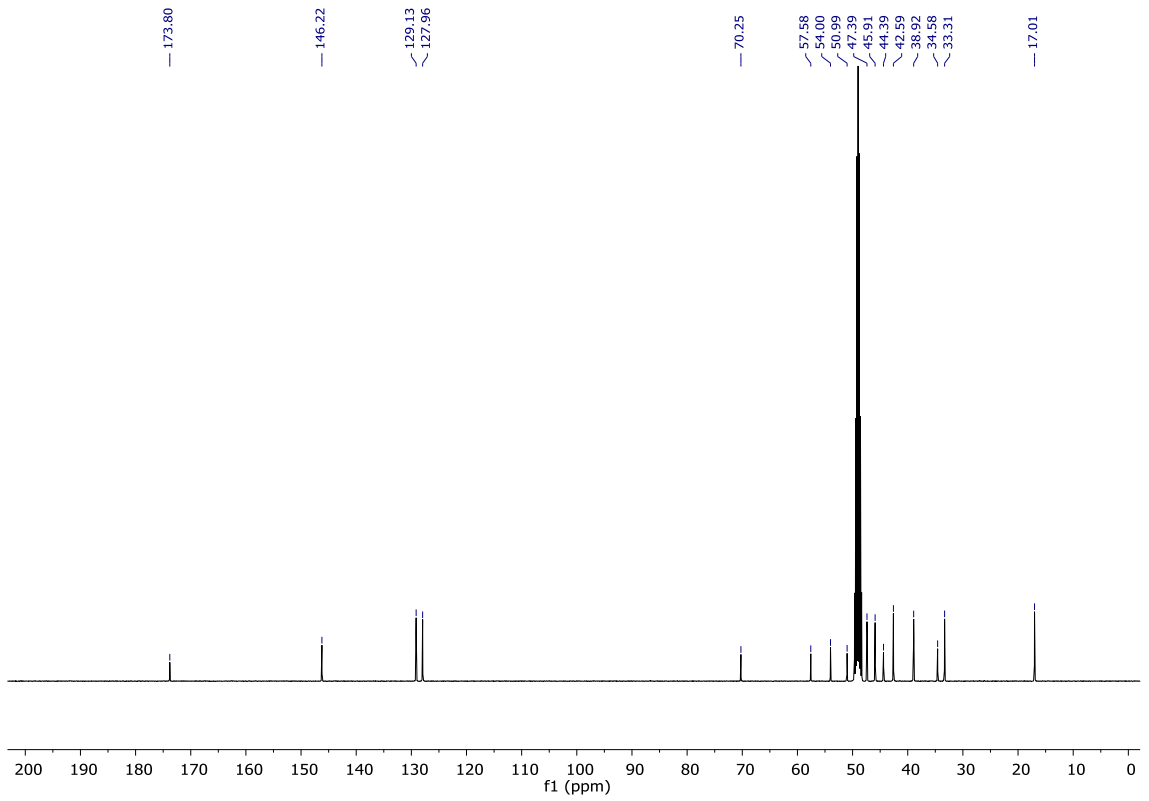
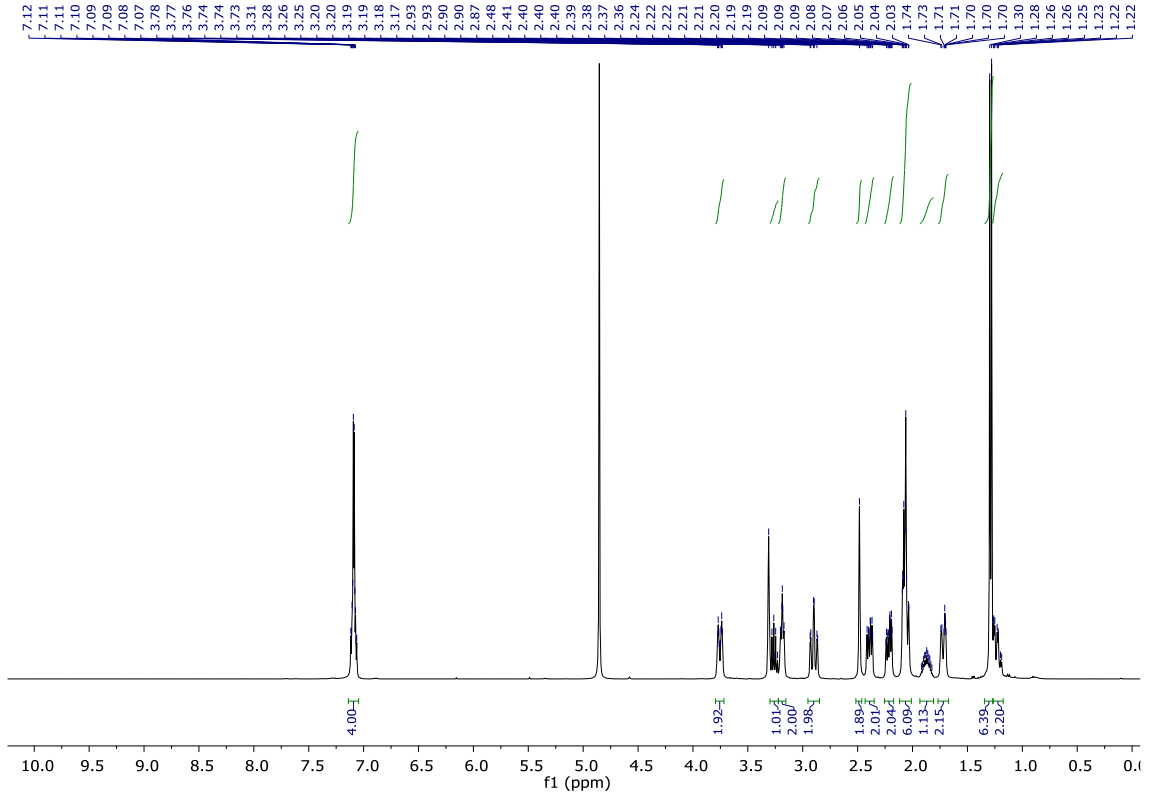
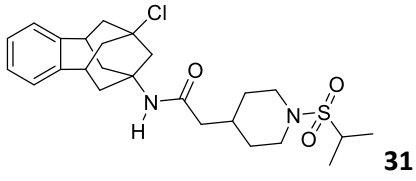


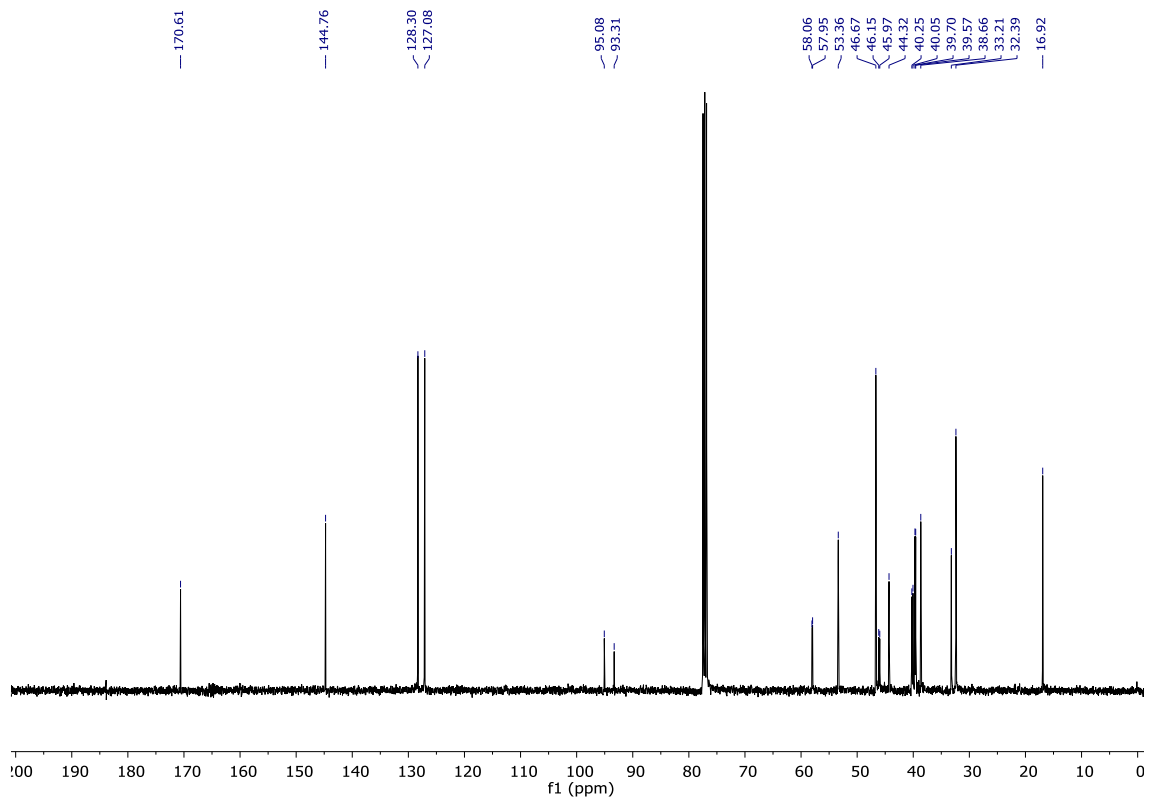
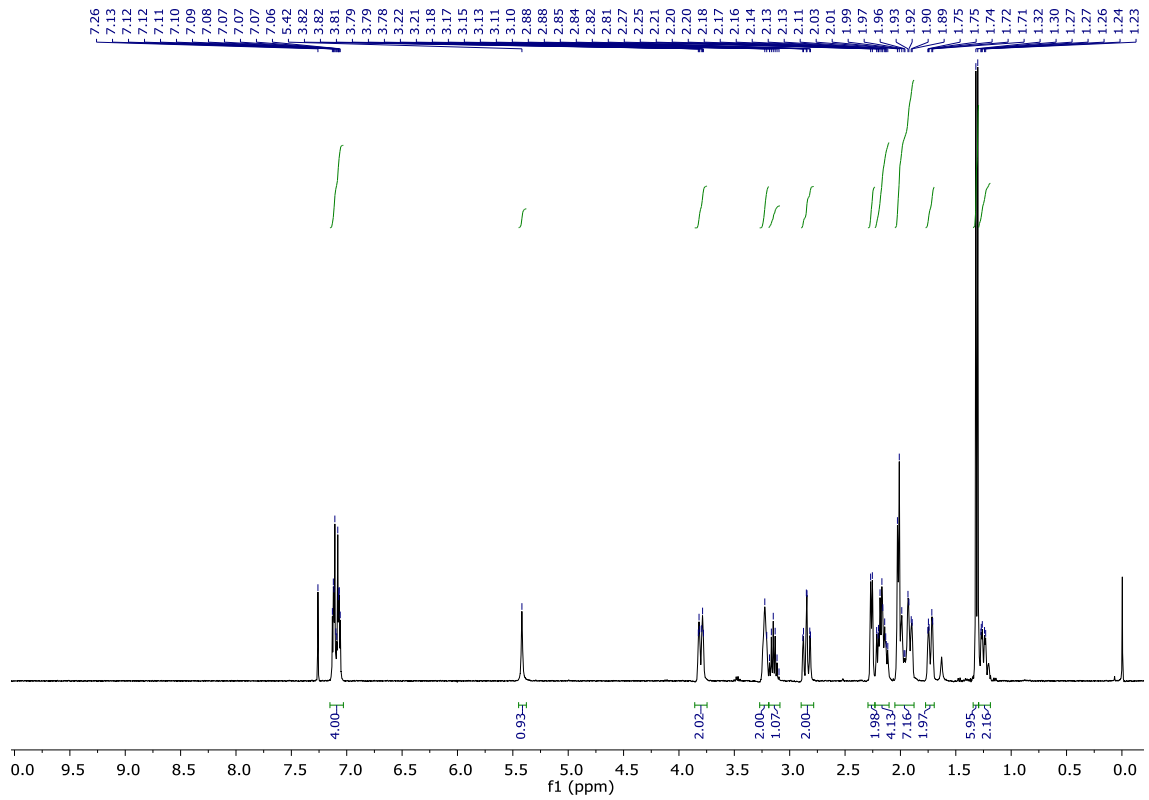
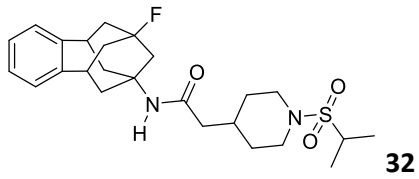


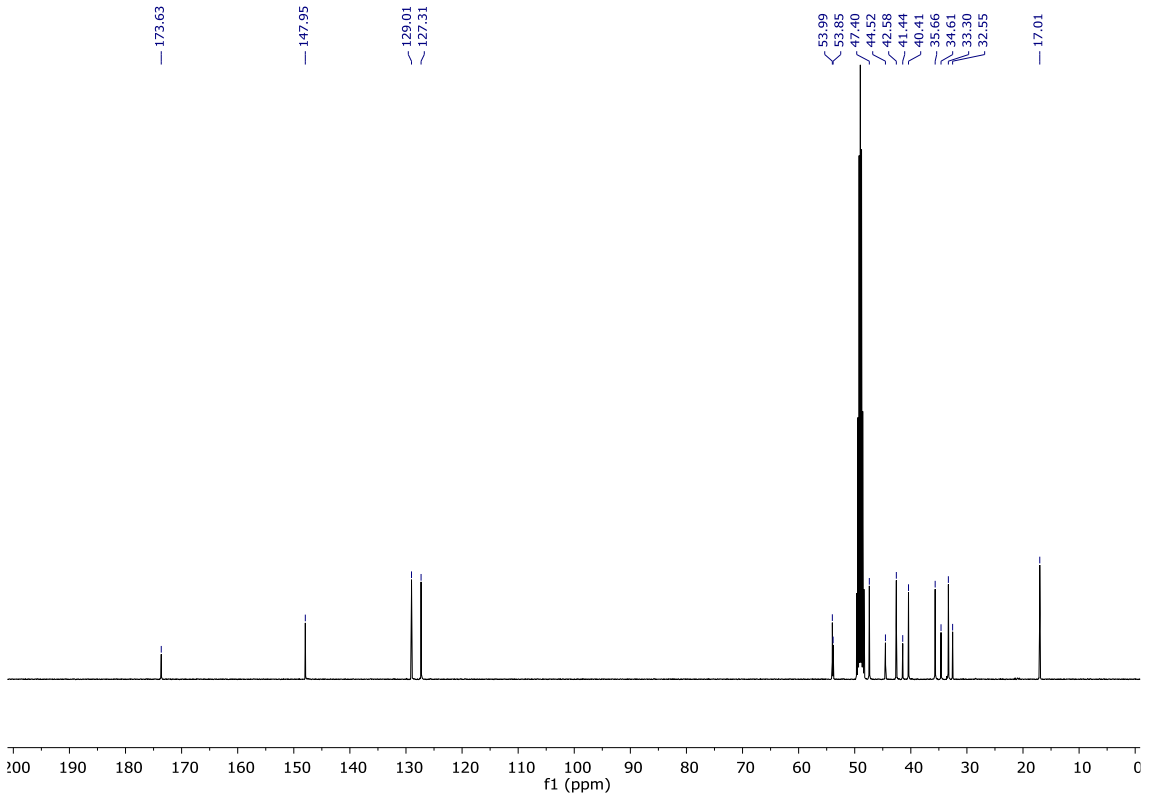
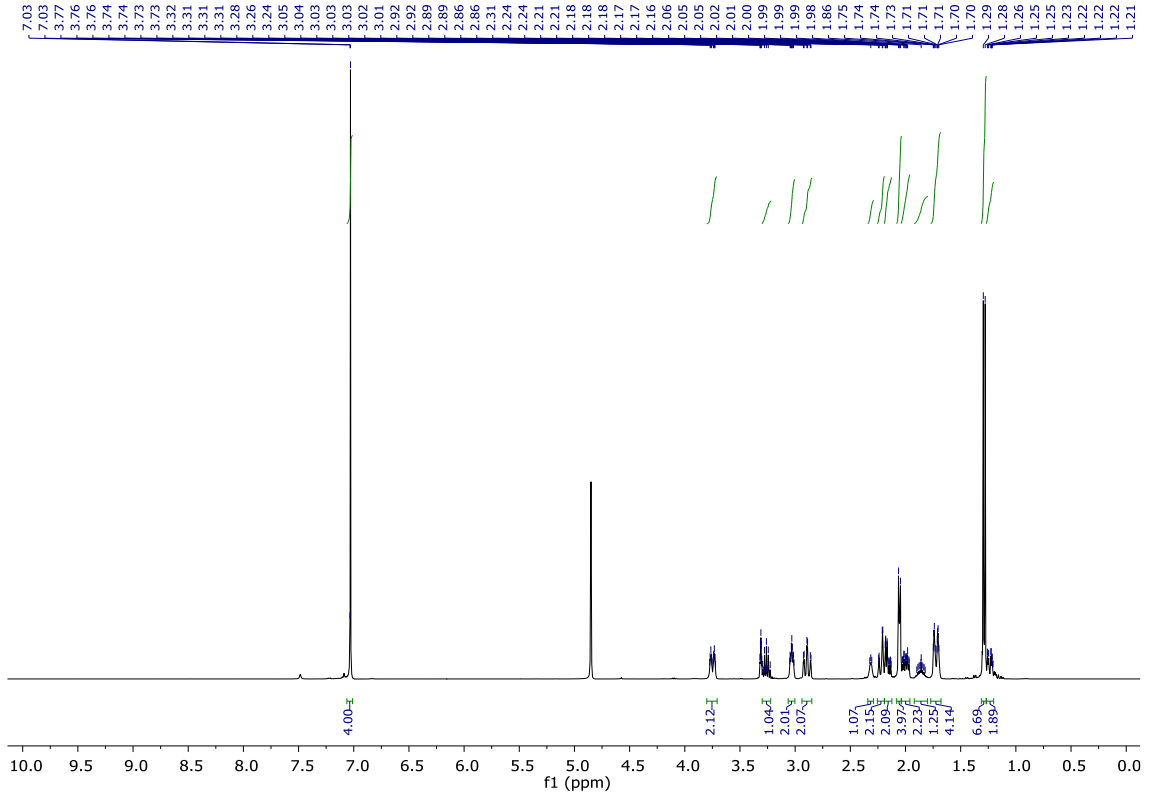
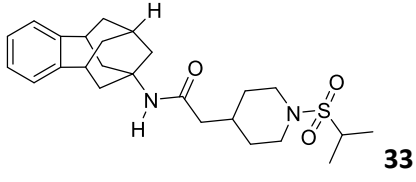


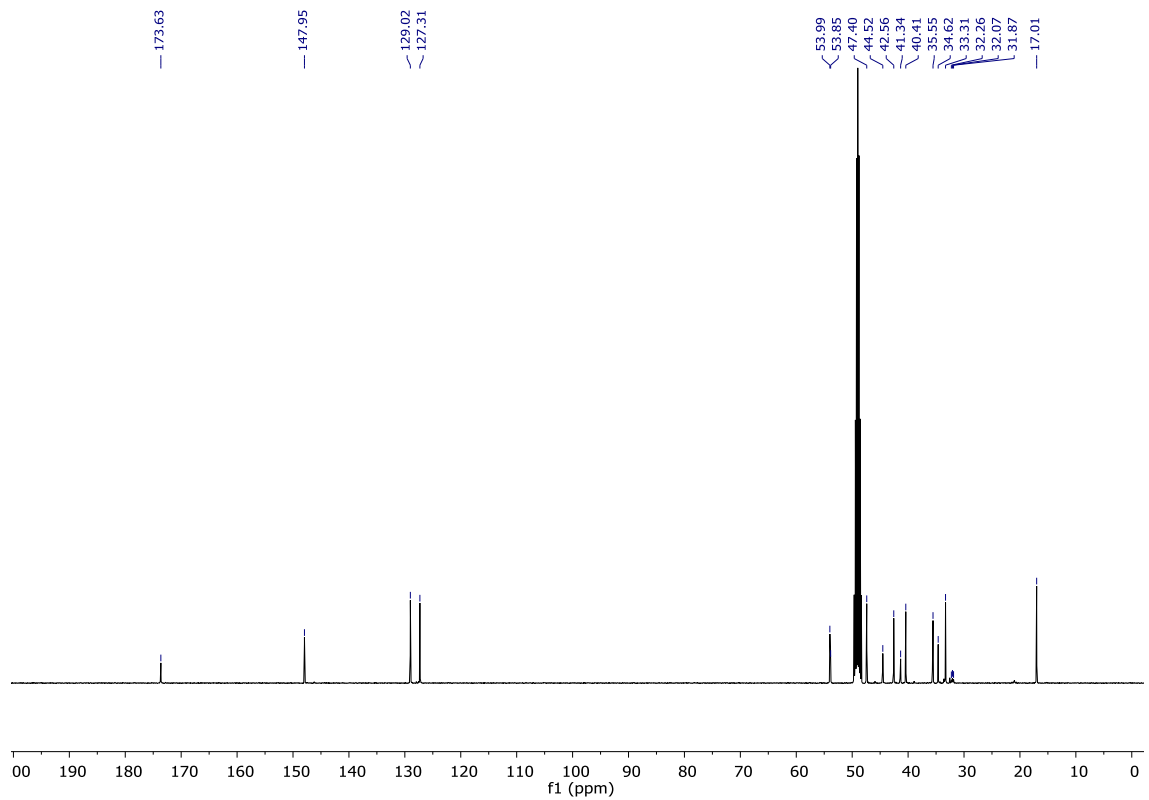
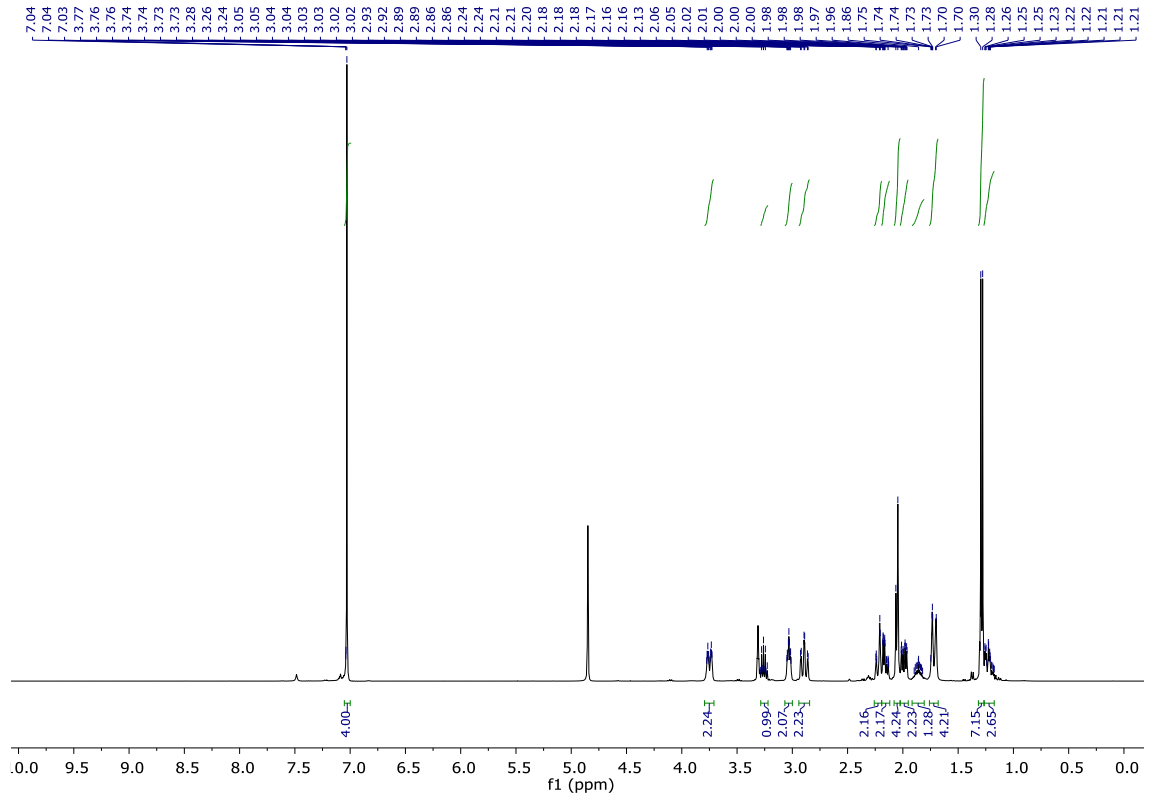
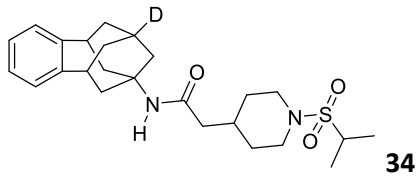


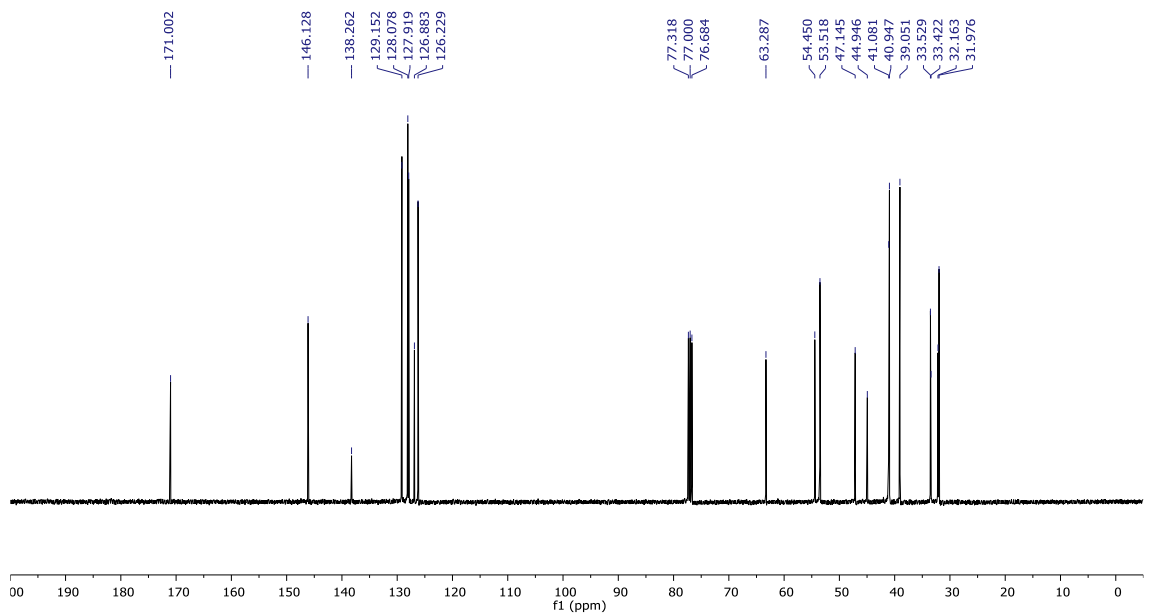
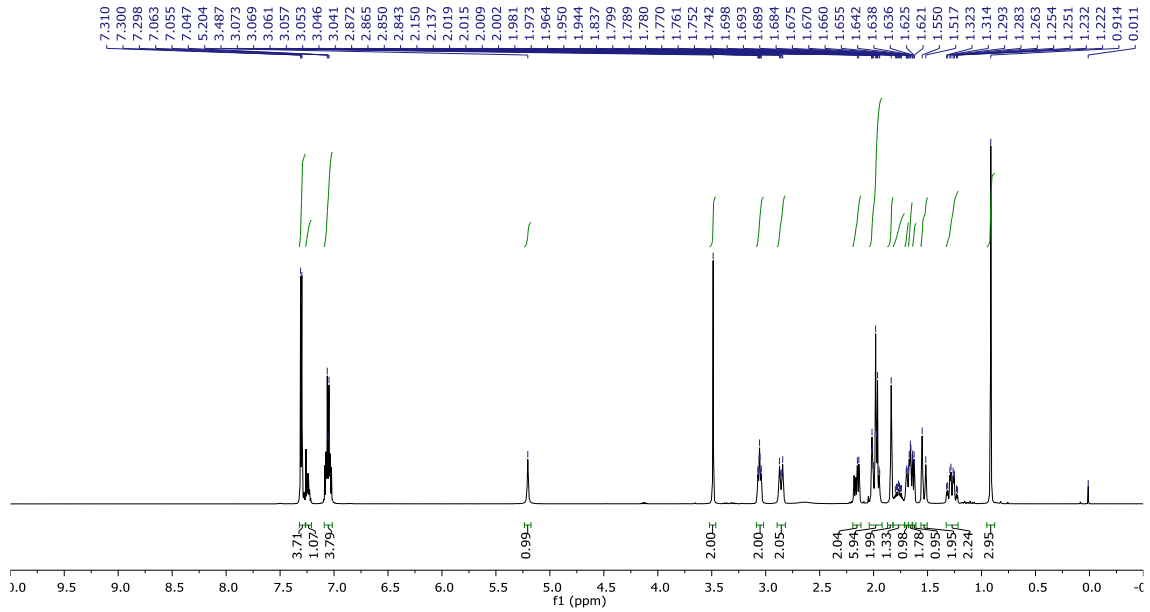
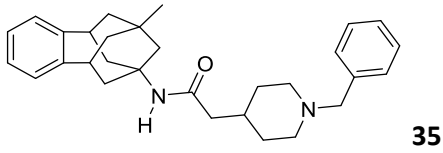












Compound	Cytochrome inhibition ^a			
	CYP	CYP	CYP 3A4 ^b	
	1A2	2D6	(BFC)	(DBF)
16	18 ± 1	43 ± 2	1 ± 1	25 ± 3
24	24 ± 1	37 ± 3	2 ± 2	8 ± 3
25	24 ± 2	13 ± 5	1 ± 1	2 ± 1

Table S1. Inhibition (expressed as % of inhibition at 10 μ M or IC₅₀) of recombinant human cytochromes P450 enzymes ^aThe cytochrome inhibition was tested at 10 μ M. IC₅₀ was calculated for those compounds that presented >50% of inhibition. ^bFor the study of CYP3A4, two different substrates were used: benzyloxytrifluoromethylcoumarin (BFC) and dibenzylfluorescein (DBF).

Compound	IC ₅₀ hLOX-5	hCOX-2 (10 μ M)	hERG	Permeability (Caco-2)		ER ^d
			% Inhibition (10 μ M)	Papp (nm/s) A→B	B→A	
16	>100	>100	>100	5.56	17.16	3.1
24	>100	>100	>100	32.9	301.7	9.2
25	>100	>100	>100	26.9	235.4	8.8

Table S2. IC₅₀ in human LOX-5 (hLOX-5), inhibition (expressed as % of inhibition) of human COX-2 (*h*COX-2) at 10 μ M, hERG inhibition and permeability assay in Caco-2 cells for compounds **16**, **24** and **25**. Inhibition of *h*COX-2 was performed at Eurofins (catalogue reference 4186).

Time	ID	Total Concentration (ng/mL)	Mean (ng/mL)	SD (ng/mL)
	Mouse 1	0		
0 h	Mouse2	0	0	0
	Mouse3	0		
	Mouse 1	2790		
0.25 h	Mouse2	2410	2453.3	317.2
	Mouse3	2160		
	Mouse 1	1390		
0.5 h	Mouse2	1690	1350	361.7
	Mouse3	970		
	Mouse 1	156		
1 h	Mouse2	167	128.7	57.1
	Mouse3	63		
	Mouse 1	34.9		
2 h	Mouse2	6.4	19.1	14.5
	Mouse3	15.9		
	Mouse 1	0		
4 h	Mouse2	0	0	0
	Mouse3	0		
	Mouse 1	0		
6 h	Mouse2	0	0	0
	Mouse3	0		
	Mouse 1	0		
24 h	Mouse2	0	0	0
	Mouse3	0		

Table S3. Mean of concentrations of compound **16** in mouse plasma at different times after intraperitoneal administration at 1 mg/Kg.

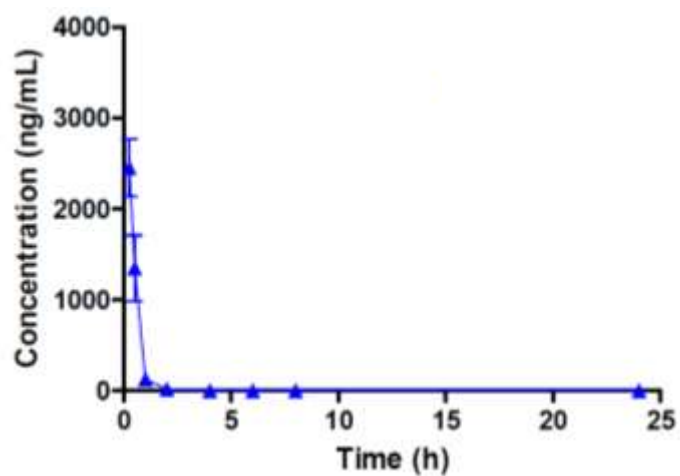


Figure S1. Plasma concentration vs time for compound **16** (1 mg/Kg, IP) in mouse.

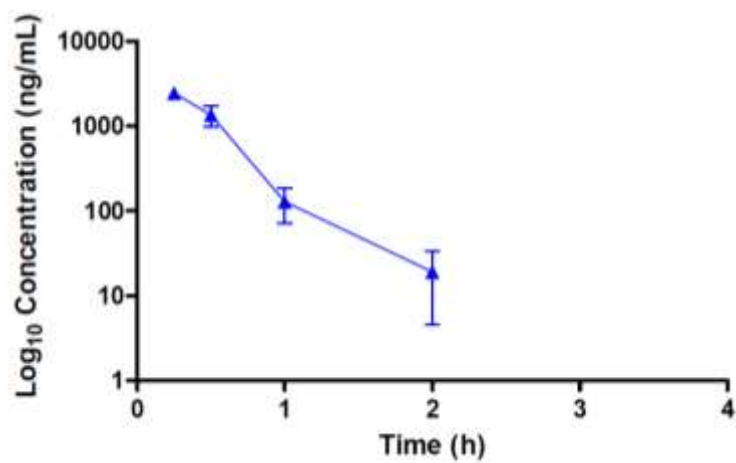


Figure S2. Plasma concentration (in log₁₀ scale) vs time for compound **16** (1 mg/Kg, IP) in mouse.

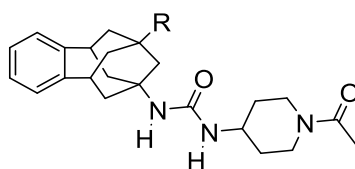
CHAPTER 5

BENZOHOMOADAMANTANE-BASED

sEHIs (III)

Introduction

As we have previously discussed in Chapters 3 and 4, we found that the replacement of the adamantane nucleus or the aromatic ring of known sEHIs by the benzohomoadamantane moiety led to very potent compounds endowed with good DMPK properties, but they presented some limitations in terms of microsomal stability, especially the compounds featuring a substituted piperidine in the RHS of the molecule. Indeed, in Chapter 4, we described that the substitution of the methyl group of **104** by halogen atoms produced an improvement of the stability in human, mice and rat microsomes, as well as better solubility values (Table 6).



Cpd	R	sEH IC ₅₀ (nM) ^a		Microsomal Stability ^b (h/m/r)	Solubility ^c (μM)
		human	murine		
105	CH ₃	4.0	6.0	1/0.5/ND	38
137	F	2.0	23	40/30/8	45
138	Cl	1.5	0.8	50/8/0.1	94

Table 6. Potency, microsomal stability and solubility of **105**, **137** and **138**. ^aReported IC₅₀ values are the average of three replicates. The fluorescent assay as performed here has a standard error between 10 and 20% suggesting that differences of two-fold or greater are significant. Because of the limitations of the assay it is difficult to distinguish among potencies < 0.5 nM.²⁰⁹ ^bPercentage of remaining compound after 60 min of incubation with human, mice and rat microsomes obtained from Tebu-Xenotech in the presence of NADP at 37 °C. ^cSolubility in a 1% DMSO : 99% PBS buffer solution.

Notwithstanding, apart from exploring the R position of the benzohomoadamantane scaffold, this polycycle can be further explored by replacing hydrogen atoms of the aromatic ring by different groups. In this work, several electron donating and electron withdrawing groups were introduced in the aromatic ring in order to evaluate the potency of these new compounds of general structure **XIX** and, more interestingly, to explore the impact of that substitution in terms of microsomal stability and other DMPK properties (Figure 39).

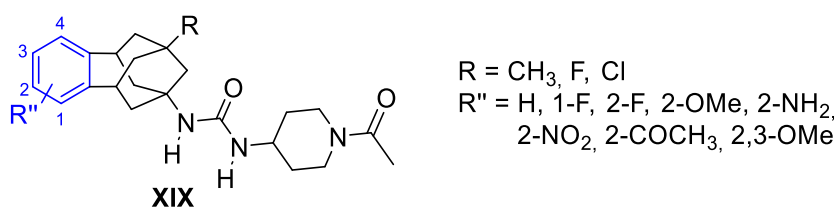


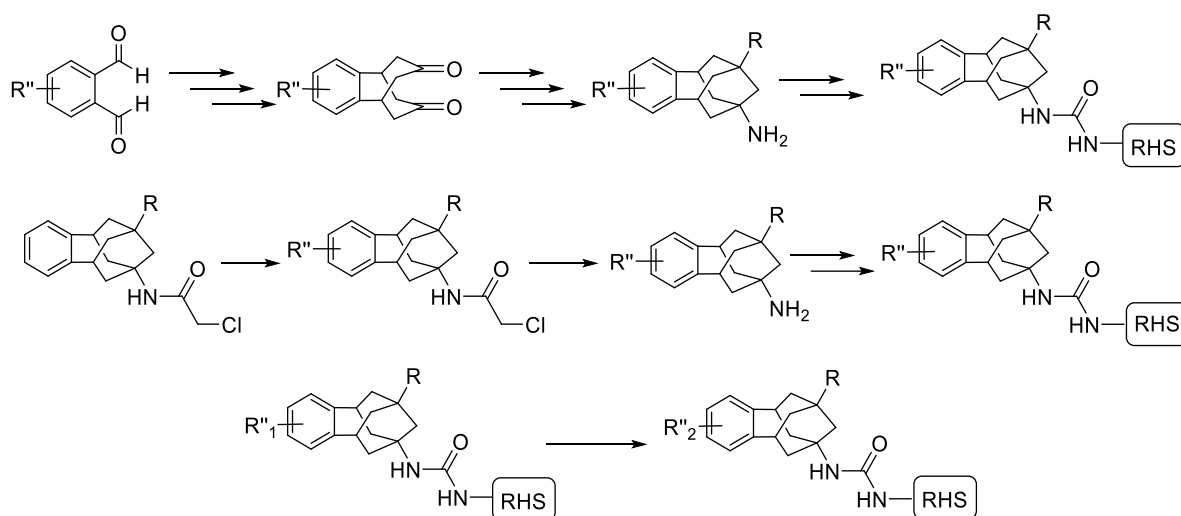
Figure 39. General structure **XIX** of the new compounds, exploring the substitution of the aromatic ring.

Discussion and results

In ~~3.5.1~~ this work, the hydrogen atoms of the aromatic ring of the benzohomoadamantane scaffold were replaced by 1-fluorine or 2-fluorine atoms, 2-methoxy, 2-amino, 2-nitro, 2-acetyl and, additionally, positions 2 and 3 were simultaneously replaced by two methoxy groups, in order to obtain new ureas of general structure **XIX** as new sEHIs. It is worth mentioning that all the compounds studied in the previous chapters are non-chiral, because the positions 2 and 3 of the unsubstituted aromatic ring are equivalent and the same is true for the positions 1 and 4. However, the introduction of a single substituent in the aromatic ring turns the molecule chiral, and all the compounds that we will present in this chapter have been synthesized and evaluated as racemic mixtures.

A key point for the synthesis of these compounds was the introduction of the radical in the aromatic ring. This introduction was made following 3 different procedures (Scheme 27).

In the first approach, the synthetic pathway was the same as the one followed for the obtention of the compounds bearing a non-substituted aromatic ring, but starting from a suitably substituted *o*-phthalaldehyde, instead of using *o*-phthalaldehyde **85** (see Scheme 18, Chapter 3). In some cases, the substituted *o*-phthalaldehydes were not commercially available and their synthesis was required.



Scheme 27. Simplified synthetic routes followed for the obtention of the new sEHIs with general structure **XIX**.

As mentioned in Chapter 4, the PhD Tesis of Andreea L. Turcu was partially focused on the synthesis of new benzohomoadamantane amines.²¹⁸ Hence, she was the main responsible for the synthesis of these new polycyclic amines, which were used in this work as starting materials for the synthesis of the desired ureas (Figure 40). Of note, amine **161** was synthesized by Beatrice Jora in the context of her PhD Tesis.²²⁰

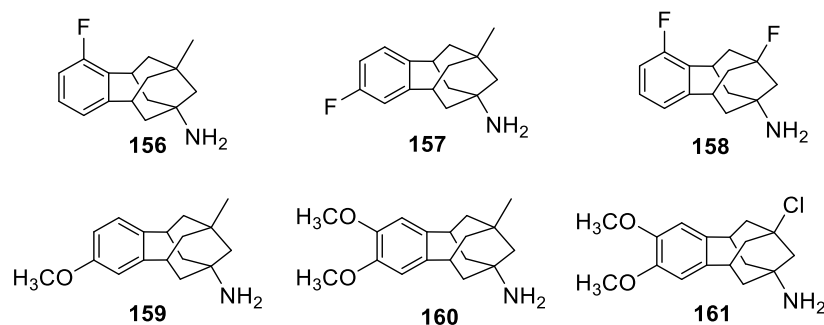
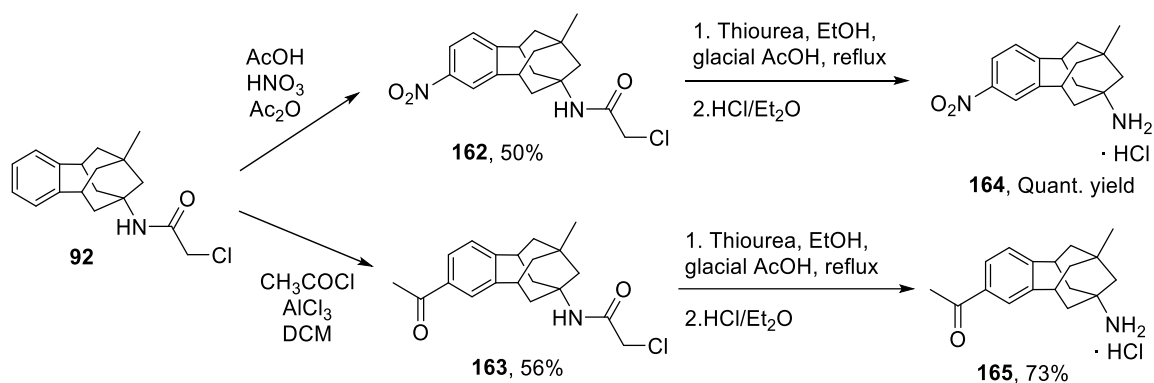


Figure 40. Structure of the substituted amines used as starting materials for the preparation of the new ureas.

The second synthetic pathway revolved around the substitution of the aromatic ring using electrophilic aromatic substitution (S_{EAr}) reactions on the corresponding unsubstituted polycyclic chloroacetamide. Thus, chloroacetamide **92** was treated with acetic anhydride, glacial acetic acid and fuming nitric acid to provide the 2-nitro-substituted chloroacetamide **162** in moderate yield. Additionally, the Friedel-Craft reaction of **92** with acetyl chloride and aluminium chloride in dichloromethane led to

the 2-acetyl-substituted chloroacetamide **163** in moderate yield. Deprotection of **162** and **163** using thiourea and acetic acid in ethanol under reflux furnished the amines **164** and **165**, which were treated with an excess of HCl in diethyl ether to obtain the corresponding hydrochlorides in medium to excellent yields (Scheme 28).



Scheme 28. Synthesis of chloroacetamides **162** and **163** and their deprotection, providing the amines **164** and **165**.

Once the polycyclic amines **156-161**, **164** and **165** were obtained, the isocyanates of the corresponding benzohomoadamantane amines were then prepared by treating them with triphosgene in a solution of aqueous sodium hydrogen carbonate and dichloromethane. Then, the addition of the corresponding substituted aminopiperidines in dichloromethane provided the desired ureas **166-173** (Figure 41).

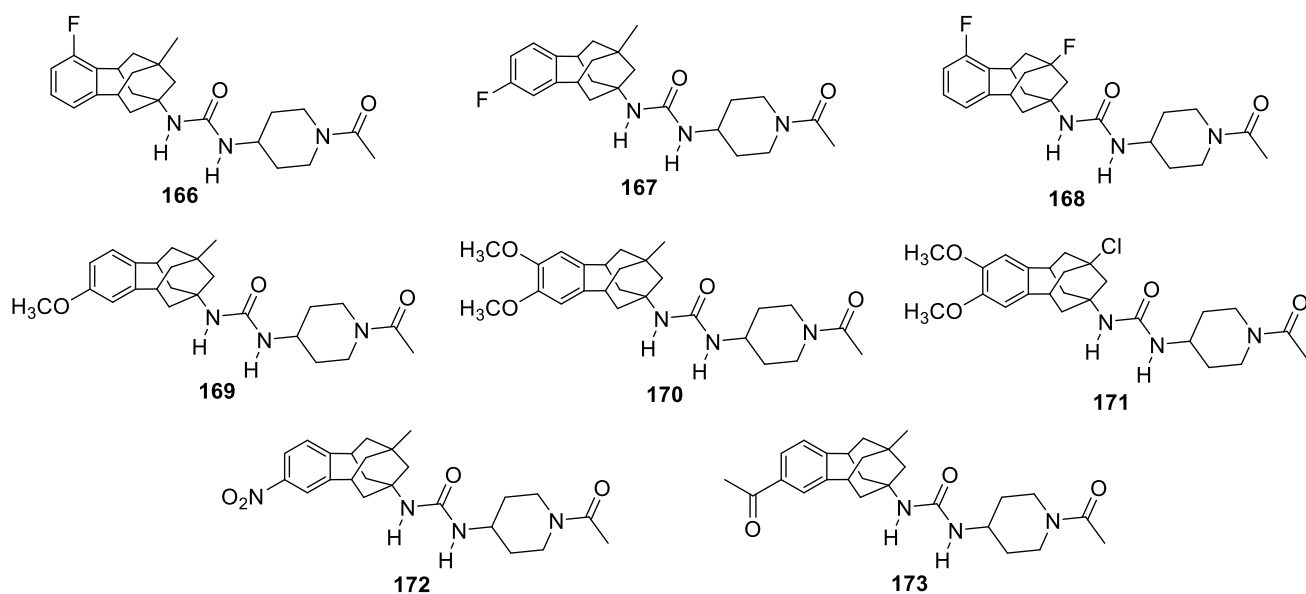
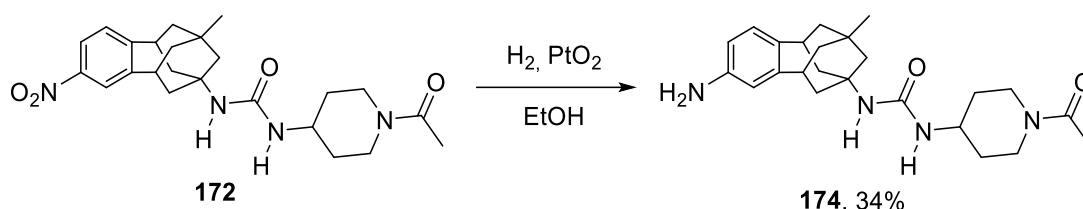


Figure 41. Ureas **166-173** synthesized in this work.

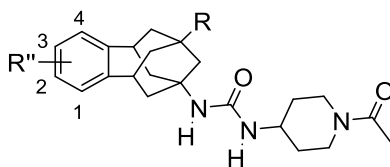
The third procedure involved the modification of the substituent of the aromatic ring R'' of the final urea. Therefore, the nitro group of urea **172** was easily converted to an amino group by catalytic hydrogenation at atmospheric pressure in ethanol using palladium over carbon as catalyst, affording the desired urea **174** in moderate yield (Scheme 29).



Scheme 29. Catalytic hydrogenation of urea **172** to afford urea **174**.

In order to explore the impact of the substitution in the aromatic ring of the benzohomoadamantane scaffold, the potency of the new ureas as sEHIs was evaluated by Dr Christophe Morisseau, from the group of Prof. Bruce D. Hammock at UCD. Moreover, the microsomal stability, solubility and cytochrome inhibition assays were performed by the group of Prof. M. Isabel Loza and Prof. José M. Brea of the Drug Screening Platform/Biofarma Research Group of the University of Santiago de Compostela. Additionally, predicted PAMPA-BBB was evaluated by Dr. Belén Pérez of the Autonomous University of Barcelona.

First, the potency of the new compounds as sEHIs was evaluated. Gratifyingly, the introduction of a plethora of different substituents in the benzohomoadamantane scaffold was not deleterious for the activity. Indeed, some derivatives were more potent than the unsubstituted urea **105** with several compounds in the low nanomolar or even in the subnanomolar range (Table 7). Even the less potent compound, aniline **174**, which exhibited IC₅₀ values of 25 nM and 17.1 nM in the human and murine enzymes respectively, was an acceptable inhibitor. Taking into account that the sEH present a hydrophobic pocket, it was reasonable that the addition of the polar amino group in the aromatic ring produced a drop in terms of potency. Taking this into account and our concerns regarding the potential toxicity related with the aniline group, this compound was not further evaluated.



Cpd	R	R''	sEH IC ₅₀ (nM) ^a		Microsomal Stability ^b (h/m/r)	Solubility ^c (μM)	PAMPA-BBB	Cytochrome inhibition (10 μM, 2C19)
			human	murine				
105	CH ₃	H	4.0	6.0	1/0.5/ND	38	CNS +	19%
166	CH ₃	1-F	0.9	0.8	16/1/0.1	45	CNS +	<26 %
167	CH ₃	2-F	0.9	0.6	22/4/0.1	28	CNS +	<40 %
168	F	1-F	2.1	1.4	69/41/82	98	CNS +/-	37 %
169	CH ₃	2-OCH ₃	1.2	1.7	33/32/8	89	CNS +/-	<48 %
170	CH ₃	2,3-OCH ₃	1.3	2.2	100/70/42	90	CNS -	25 %
171	Cl	2,3-OCH ₃	0.9	2.5	69/17/58	76	CNS-	37%
172	CH ₃	2-NO ₂	4.5	4.5	100/27/45	35	CNS +/-	<36 %
173	CH ₃	2-COCH ₃	4.1	6.7	92/70/41	86	CNS -	<29 %
174	CH ₃	2-NH ₂	25	17.1	ND	ND	ND	ND

Table 7. Potency in human and murine enzymes, microsomal stability and solubility values of **105**, **166-174**. ^aReported IC₅₀ values are the average of three replicates. The fluorescent assay as performed here has a standard error between 10 and 20% suggesting that differences of two-fold or greater are significant. Because of the limitations of the assay it is difficult to distinguish among potencies < 0.5 nM.²⁰⁹ ^bPercentage of remaining compound after 60 min of incubation with human, mice and rat microsomes obtained from Tebu-Xenotech in the presence of NADP at 37 °C. ^cSolubility in a 1% DMSO : 99% PBS buffer solution.

Next, the experimental solubility was measured. Apart from compounds **167** and **172** that presented moderate solubility values, most of them showed improved solubility than **105** (Table 7). The most soluble compounds were **168**, **169**, **170** and **173**, with experimental solubility values between 86 μM and 98 μM.

Regarding the microsomal stability, most of the new substituted compounds presented higher stability against human, murine and rat microsomes than **105** (Table 7). In particular, compounds bearing either a nitro or a ketone group in the position 2 of

the aromatic ring, **172** and **173**, respectively, and the di-substituted **170** presented much higher stability against the microsomes than the unsubstituted **105**.

On the other hand, the PAMPA-BBB assay was performed. While the predicted brain permeability of compounds **105**, **166** and **167** showed CNS+ proving their potential capacity to reach CNS, compounds **168**, **169** and **172** presented uncertain BBB permeation (CNS+/-). In contrast, the more polar compounds **170**, **171**, **173** presented CNS-, showing predicted low BBB permeation (Table 7). Interestingly, non-BBB penetrant candidates are attractive for the treatment of peripheral diseases, in order to avoid possible central side effects.

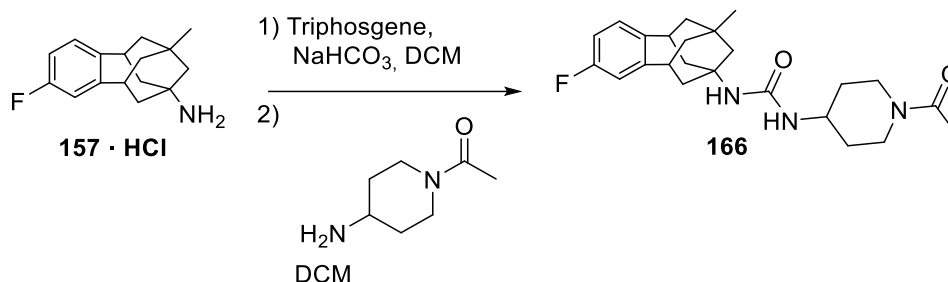
Finally, the cytochromes inhibition was measured, paying special attention to CYP 2C19, as it is one of the subfamilies in charge of producing EETs, the substrate of the sEH. Gratifyingly, all of the compounds inhibited CYPs less than 50 % at 10 μ M (Table 7).

With all these results in hand, we can conclude that the substitution of the aromatic ring is a good strategy in order to obtain extremely potent sEHIs with improved microsomal stability and solubility values, two critical parameters for drug discovery. For these reasons, additional work around the substitution of the aromatic ring is still ongoing by other members of the research group, in order to further explore the substitution of the polycyclic scaffold and to obtain new sEHIs with excellent inhibitory activities and DMPK properties (See section 4 of the present Thesis: Perspectives).

Given that more research around the aromatic ring of the benzohomoadamantane scaffold is currently being conducted, the results presented in this Chapter have not been published as a scientific article yet. Nevertheless, all the compounds bearing the benzohomoadamantane scaffold described in Chapters 3, 4 and 5 of the present Thesis have been disclosed in a patent application,²¹⁷ which is currently under exam. The mentioned document is attached at the end of this Chapter.

Experimental section

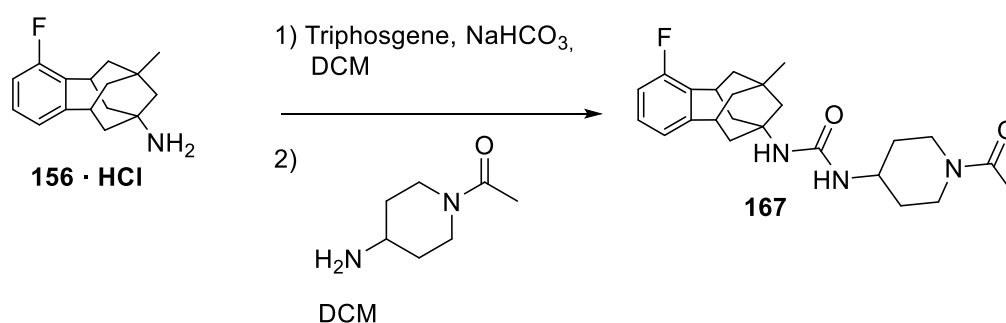
Preparation of 1-(1-acetylpiperidin-4-yl)-3-(2-fluoro-9-methyl-5,6,8,9,10,11-hexahydro-7H-5,9:7,11-dimethanobenzo[9]annulen-7-yl)urea



To a solution of 2-fluoro-9-methyl-5,6,8,9,10,11-hexahydro-7H-5,9:7,11-dimethanobenzo[9]annulen-7-amine hydrochloride (150 mg, 0.53 mmol) in DCM (3 mL) saturated aqueous NaHCO₃ solution (3 mL) and triphosgene (59 mg, 0.20 mmol) were added. The biphasic mixture was stirred at room temperature for 30 minutes and then the two phases were separated and the organic layer was washed with brine (3 mL), dried over anh. Na₂SO₄, filtered and evaporated under vacuum to obtain 1-2 mL of a solution of the isocyanate in DCM. To this solution was added 1-(4-aminopiperidin-1-yl)ethan-1-one (91 mg, 0.64 mmol). The reaction mixture was stirred at room temperature overnight and the solvent was evaporated under vacuum to obtain a yellowish oil (165 mg). Column chromatography (SiO₂, DCM/Methanol mixtures) gave 1-(1-acetylpiperidin-4-yl)-3-(2-fluoro-9-methyl-5,6,8,9,10,11-hexahydro-7H-5,9:7,11-dimethanobenzo[9]annulen-7-yl)urea (103 mg, 49 % yield) as a white solid, mp 269-270 °C. IR (NaCl disk): 3357, 2919, 2856, 1644, 1620, 1555, 1499, 1453, 1361, 1342, 1320, 1228, 1153, 1138, 1064, 967, 863, 818 cm⁻¹. ¹H-NMR (400 MHz, CDCl₃) δ: 0.90 (s, 3 H, C9-CH₃), 1.17 [dq, *J* = 11.6 Hz, *J*' = 4.0 Hz, 2 H, 3'(5')-H_{ax}], 1.49 (m, 2 H, 10-H_{ax}, 13-H_{ax}), 1.57-1.64 (complex signal, 2 H, 10-H_{eq}, 13-H_{eq}), 1.76 (s, 2 H, 8-H), 1.85 (m, 1 H, 5'-H_{eq} or 3'-H_{eq}), 1.91-2.13 (complex signal, 8 H, COCH₃, 6-H, 12-H, 2'-H_{eq} or 6'-H_{eq}), 2.70 (m, 1 H, 2'-H_{ax} or 6'-H_{ax}), 2.98 (t, *J* = 6.0 Hz, 1 H, 11-H or 5-H), 3.04 (t, *J* = 6.0 Hz, 1 H, 5-H or 11-H), 3.11 (m, 1 H, 6'-H_{ax} or 2'-H_{ax}), 3.69-3.78 (complex signal, 2 H, 4'-H, 6'-H_{eq} or 2'-H_{eq}), 4.42 (d, *J* = 13.6 Hz, 1 H, 2'-H_{eq} or 6'-H_{eq}), 4.58-4.65 (complex signal, 2 H, C7-NH, C4'-NH), 6.69-6.75 (complex signal, 2 H, 3-H, 1-H), 6.97 (dd, *J* = 8.0 Hz, *J*' = 5.6 Hz, 1 H, 4-H). ¹³C-NMR (100.5 MHz, CDCl₃) δ: 21.4 (CH₃, COCH₃), 32.2 (CH₃, C9-CH₃), 32.4 (CH₂, C5' or

C3'), 33.6 (C, C9), 33.7 (CH₂, C3' or C5'), 39.6 (CH₂, C6 or C12), 39.9 (CH₂, C12 or C6), 40.3 (CH, C5 or C11), 40.7 (CH₂, C2' or C6'), 40.9 (CH, C11 or C5), 41.2 (CH₂, C10, C13), 45.4 (CH₂, C6' or C2'), 46.7 (CH, C4'), 47.9 (CH₂, C8), 53.2 (C, C7), 112.1 (d, ²J_{C-F} = 20.32 Hz, CH, C1), 114.6 (d, ²J_{C-F} = 20.72 Hz, CH, C3), 129.3 (d, ³J_{CF} = 7.94 Hz, CH, C4), 142.5 (d, ⁴J_{CF} = 3.11 Hz, C, C4a), 148.4 (d, ³J_{CF} = 6.63 Hz, C, C11a), 156.4 (C, NH₂CONH), 161.1 (d, ¹J_{CF} = 243.45, C, C2-F), 169.1 (C, COCH₃). Accurate mass: Calculate for [C₂₄H₃₂FN₃O₂+H]⁺: 414.2551; Found: 414.2553. Anal. Calcd for C₂₄H₃₂FN₃O₂ · 0.25 DCM: C 66.99, H 7.53, N 9.66. Found: C 67.22, H 7.84, N 9.32.

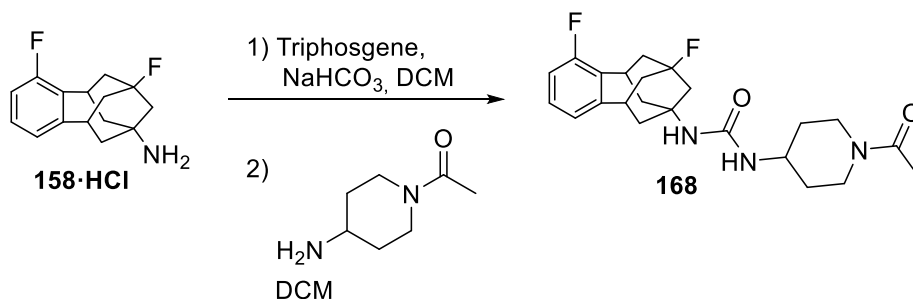
Preparation of 1-(1-acetylpiperidin-4-yl)-3-(1-fluoro-9-methyl-5,6,8,9,10,11-hexahydro-7H-5,9,7,11-dimethanobenzo[9]annulen-7-yl)urea



To a solution of 1-fluoro-9-methyl-5,6,8,9,10,11-hexahydro-7H-5,9,7,11-dimethanobenzo[9]annulen-7-amine hydrochloride (150 mg, 0.53 mmol) in DCM (3 mL) saturated aqueous NaHCO₃ solution (3 mL) and triphosgene (58 mg, 0.20 mmol) were added. The biphasic mixture was stirred at room temperature for 30 minutes and then the two phases were separated and the organic layer was washed with brine (3 mL), dried over anh. Na₂SO₄, filtered and evaporated under vacuum to obtain 1-2 mL of a solution of the isocyanate in DCM. To this solution was added 1-(4-aminopiperidin-1-yl)ethan-1-one (91 mg, 0.64 mmol). The reaction mixture was stirred at room temperature overnight and the solvent was evaporated under vacuum to obtain a yellow oil (320 mg). Column chromatography (SiO₂, DCM/Methanol mixtures) gave 1-(1-acetylpiperidin-4-yl)-3-(1-fluoro-9-methyl-5,6,8,9,10,11-hexahydro-7H-5,9,7,11-dimethanobenzo[9]annulen-7-yl)urea (160 mg, 73 % yield) as a white solid, mp 122-123 °C. IR (NaCl disk): 3351, 2944, 2918, 2861, 1642, 1618, 1555, 1462, 1362, 1321, 1238, 1137, 1066, 976, 885, 798, 749. cm⁻¹. ¹H-NMR (400 MHz, CDCl₃) δ: 0.90 (s, 3 H, C9-CH₃), 1.18 [dq, J = 12.0 Hz, J' = 4.0 Hz, 2 H, 3'(5')-H_{ax}], 1.42-1.54 (complex signal, 2 H, 10-H_{ax}, 13-H_{ax}), 1.59-1.67 (complex signal, 10-H_{eq}, 13-H_{eq}), 1.71 (d, J = 11.6 Hz, 1 H, 8-H_a), 1.77-1.89 (complex signal, 2 H, 3'-H_{eq} or 5'-H_{eq}, 8-H_b), 1.89-2.05 (complex signal, 4 H, 3'-H_{eq}

or 5'-H_{eq}, 6-H_{ax}, 12-H_{ax}, 6-H_{eq} or 12-H_{eq}), 2.06 (s, 3 H, COCH₃), 2.14 (m, 1 H, 12-H_{eq} or 6-H_{eq}), 2.72 (m, 1 H, 2'-H_{ax} or 6'-H_{ax}), 3.05-3.16 (complex signal, 2 H, 6'-H_{ax} or 2'-H_{ax}, 11-H), 3.64-3.78 (complex signal, 3 H, 4'-H, 6'-H_{eq} or 2'-H_{eq}, 5-H), 4.41 (dm, *J* = 12.8 Hz, 1 H, 2'-H_{eq} or 6'-H_{eq}), 4.66-4.71 (complex signal, 2 H, C4'-NH, C7-NH), 6.79-6.86 (complex signal, 2 H, 2-H, 4-H), 6.98 (td, *J* = 8.0 Hz, *J'* = 5.6 Hz, 1 H, 3-H). ¹³C-NMR (100.5 MHz, CDCl₃) δ: 21.4 (CH₃, COCH₃), 28.5 (C, C9), 28.6 (CH, C5), 32.2 (CH₃, C9-CH₃), 32.4 (CH₂, C5' or C3'), 33.6 (CH₂, C3' or C5'), 39.3 (CH₂, C6 or C12), 39.5 (CH₂, C12 or C6), 40.6 (CH₂, C10 or C13), 40.7 (CH₂, C2' or C6'), 40.9 (CH₂, C13 or C10), 41.0 (d, ³*J*_{C-F} = 2.21 Hz, CH, C11), 45.4 (CH₂, C6' or C2'), 46.7 (CH, C4'), 47.9 (CH₃, C8), 53.3 (C, C7), 113.1 (²*J*_{C-F} = 24.85 Hz, CH, C2), 123.3 (⁴*J*_{C-F} = 3.02 Hz, CH, C4), 126.8 (³*J*_{C-F} = 9.35 Hz, CH, C3), 128.7 (²*J*_{C-F} = 28.84 Hz, C, C11a), 132.6 (³*J*_{C-F} = 13.36 Hz, C, C4a), 154.4 (C, NHCONH), 159.1 (¹*J*_{C-F} = 242.75 Hz, C, C1-F), 169.1 (C, COCH₃). Accurate mass: Calculate for [C₂₄H₃₂FN₃O₂+H]⁺: 414.2551; Found: 414.2554. Anal. Calcd for C₂₄H₃₂FN₃O₂ · 0.3 H₂O: C 66.24, H 7.97, N 9.66. Found: C 67.47, H 7.86, N 9.36.

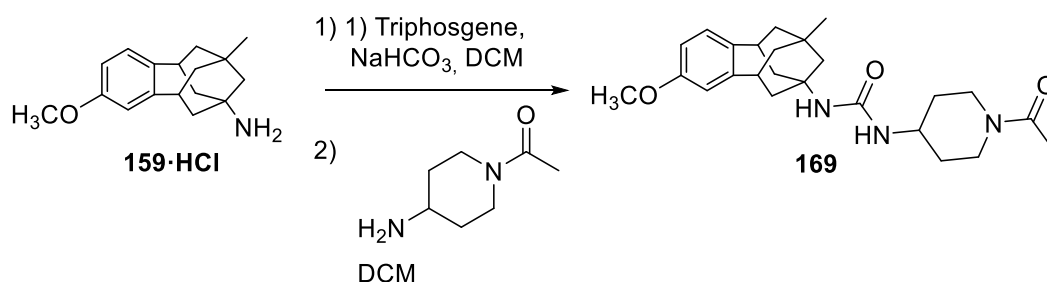
Preparation of 1-(1-acetylpiperidin-4-yl)-3-(1,9-difluoro-5,6,8,9,10,11-hexahydro-7H-5,9:7,11-dimethanobenzo[9]annulen-7-yl)urea



To a solution of 1,9-difluoro-5,6,8,9,10,11-hexahydro-7H-5,9:7,11-dimethanobenzo[9]annulen-7-amine hydrochloride (120 mg, 0.42 mmol) in DCM (3 mL) and saturated aqueous NaHCO₃ solution (3 mL), triphosgene (46 mg, 0.16 mmol) was added. The biphasic mixture was stirred at room temperature for 30 minutes and then the two phases were separated and the organic one was washed with brine (3 mL), dried over anhydrous Na₂SO₄, filtered and evaporated under vacuum to obtain 1-2 mL of a solution of isocyanate in DCM. To this solution was added 1-(4-aminopiperidin-1-yl)ethan-1-one (72 mg, 0.50 mmol). The mixture was stirred overnight at room temperature and the solvent was then evaporated. Column chromatography (SiO₂, DCM/Methanol mixtures) provided 1-(1-acetylpiperidin-4-yl)-3-(1,9-difluoro-5,6,8,9,10,11-hexahydro-7H-5,9:7,11-dimethanobenzo[9]annulen-7-yl)urea as a yellowish solid (84 mg, 48% yield).

Analytical sample was obtained by crystallization from hot Ethyl Acetate/Pentane, mp 248-249 °C. IR (ATR): 3382, 3266, 2923, 2164, 1645, 1622, 1562, 1503, 1464, 1454, 1425, 1362, 1341, 1325, 1318, 1304, 1244, 1232, 1185, 1135, 1099, 1059, 1036, 1015, 995, 978, 952, 929, 891, 868, 795, 746, 717, 695, 645, 625, 605, 590 cm^{-1} . $^1\text{H-NMR}$ (400 MHz, CDCl_3) δ : 1.19 [m, 2 H, 3'(5')- H_{ax}], 1.79-1.93 (complex signal, 3 H, 5'- H_{eq} or 3'- H_{eq} , 10- H_{ax} , 13- H_{ax}), 1.96-2.06 (complex signal, 2 H, 6- H_{ax} , 12- H_{ax}), 2.07 (s, 3 H, COCH_3), 2.08-2.27 (complex signal, 7 H, 8-H, 3'- H_{eq} or 5'- H_{eq} , 6- H_{eq} , 12- H_{eq} , 10- H_{eq} , 13- H_{eq}), 2.70 (m, 1 H, 2'- H_{ax} or 6'- H_{ax}), 3.12 (m, 1 H, 6'- H_{ax} or 2'- H_{ax}), 3.26 (t, $J = 7.2$ Hz, 1 H, 11-H), 3.69-3.80 (complex signal, 2 H, 4'-H, 6'- H_{eq} or 2'- H_{eq}), 3.86 (t, $J = 7.2$ Hz, 1 H, 5-H), 4.39 (d, $J = 7.6$ Hz, 1 H, C4'-NH), 4.47 (dm, $J = 13.6$ Hz, 1 H, 2'- H_{eq} or 6'- H_{eq}), 4.53 (s, 1 H, C7-NH), 6.84-6.93 (complex signal, 2 H, 2-H, 4-H), 7.04 (td, $J = 8.0$ Hz, $J' = 5.6$ Hz, 1 H, 3-H). $^{13}\text{C-NMR}$ (100.5 MHz, CDCl_3) δ : 21.4 (CH_3 , COCH_3), 27.3 (CH, C5), 32.4 (CH_2 , C3' or C5'), 33.7 (CH_2 , C5' or C3'), 38.8 (CH_2 , C6 or C12), 38.9 (CH_2 , C12 or C6), 39.4 (CH, C11), 39.6 (CH_2 , C10 or C13), 39.7 (CH_2 , C13 or C10), 40.7 (CH_2 , C2' or C6'), 45.4 (CH_2 , C6' or C2'), 46.7 (CH_2 , C8), 46.9 (CH, C4'), 56.9 (d, $^3J_{\text{C-F}} = 11.45$ Hz, C, C7), 94.1 (d, $^1J_{\text{C-F}} = 177.18$, C, C9), 113.7 (d, $^2J_{\text{C-F}} = 24.54$ Hz, CH, C2), 123.5 (d, $^4J_{\text{C-F}} = 3.2$ Hz, CH, C4), 127.5 ($^3J_{\text{C-F}} = 9.25$ Hz, CH, C3), 143.3 (C, C11a), 155.9 (C, C4a), 157.6 (C, NHCONH), 159.0 (d, $^1J_{\text{C-F}} = 243.45$ Hz, C, C9-F), 169.1 (C, COCH_3). Accurate mass: Calculate for $[\text{C}_{23}\text{H}_{29}\text{F}_2\text{N}_3\text{O}_2+\text{H}]^+$: 418.2301; Found: 418.2300.

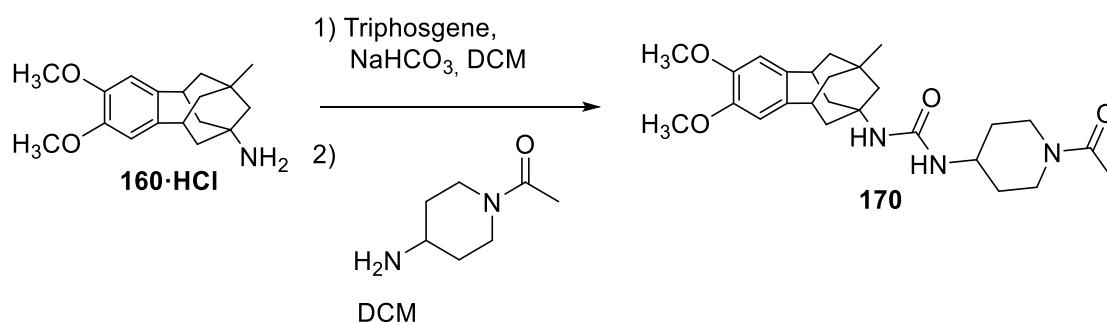
Preparation of 1-(1-acetylpiperidin-4-yl)-3-(2-methoxy-9-methyl-5,6,8,9,10,11-hexahydro-7H-5,9:7,11-dimethanobenzo[9]annulen-7-yl)urea



To a solution of 2-methoxy-9-methyl-5,6,8,9,10,11-hexahydro-7H-5,9:7,11-dimethanobenzo[9]annulen-7-amine hydrochloride (150 mg, 0.51 mmol) in DCM (3 mL) saturated aqueous NaHCO_3 solution (3 mL) and triphosgene (56 mg, 0.19 mmol) were added. The biphasic mixture was stirred at room temperature for 30 minutes and then the two phases were separated and the organic layer was washed with brine (3 mL), dried over anhydrous Na_2SO_4 , filtered and evaporated under vacuum to obtain 1-2 mL of a

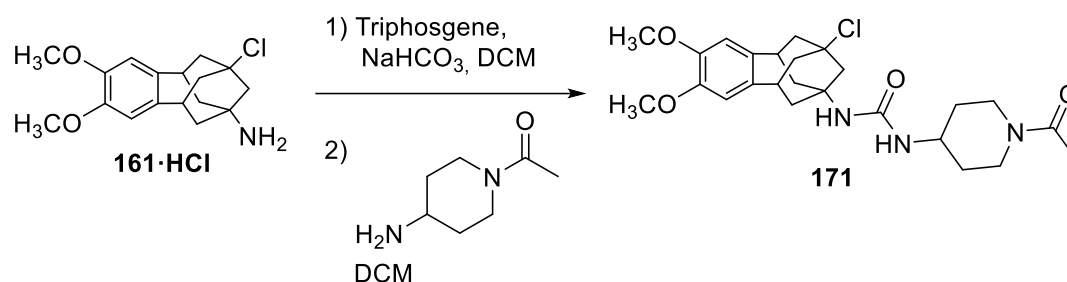
solution of the isocyanate in DCM. To this solution was added 1-(4-aminopiperidin-1-yl)ethan-1-one (87 mg, 0.61 mmol). The reaction mixture was stirred at room temperature overnight and the solvent was evaporated under vacuum to obtain a brown oil (256 mg). Column chromatography (SiO₂, DCM/Methanol mixtures) gave 1-(1-acetylpiperidin-4-yl)-3-(2-methoxy-9-methyl-5,6,8,9,10,11-hexahydro-7H-5,9:7,11-dimethanobenzo[9]annulen-7-yl)urea (121 mg, 56 % yield) as a white solid, mp 116-117 °C. IR (NaCl disk): 3359, 2905, 2861, 1644, 1619, 1551, 1501, 1452, 1360, 1343, 1319, 1267, 1227, 1153, 1136, 1042, 973, 807, 736 cm⁻¹. ¹H-NMR (400 MHz, CDCl₃) δ: 0.89 (s, 3 H, C9-CH₃), 1.16 [m, 2 H, 5'(3')-H_{ax}], 1.44-1.55 (complex signal, 2 H, 10-H_{ax}, 13-H_{ax}), 1.57-1.65 (complex signal, 2 H, 10-H_{eq}, 13-H_{eq}), 1.75-1.93 (complex signal, 5 H, 8-H, 6-H_{ax}, 12-H_{ax}, 5'-H_{eq} or 3'-H_{eq}), 2.01 (dm, *J* = 12.0 Hz, 1 H, 3'-H_{eq} or 5'-H_{eq}), 2.06 (s, 3 H, COCH₃), 2.12 (m, 2 H, 6-H_{eq}, 12-H_{eq}), 2.70 (m, 1 H, 2'-H_{ax} or 6'-H_{ax}), 2.95-3.04 (complex signal, 2 H, 5-H, 11-H), 3.10 (m, 1 H, 6'-H_{ax} or 2'-H_{ax}), 3.67-3.77 (complex signal, 5 H, C2-OCH₃, 4'-H, 6'-H_{eq} or 2'-H_{eq}), 4.42 (dm, *J* = 13.6 Hz, 1 H, 2'-H_{eq} or 6'-H_{eq}), 4.54-4.63 (complex signal, 2 H, C7-NH, C4'-NH), 6.56-6.63 (complex signal, 2 H, 1-H, 3-H), 6.95 (d, *J* = 8.0 Hz, 4-H). ¹³C-NMR (100.5 MHz, CDCl₃) δ: 21.4 (CH₃, COCH₃), 32.3 (CH₃, C9-CH₃), 32.4 (CH₂, C5' or C3'), 33.5 (C, C9), 33.6 (CH₂, C3' or C5'), 39.8 (CH₂, C12 or C6), 40.2 (CH, C5 or C11), 40.3 (CH₂, C6 or C12), 40.7 (CH₂, C2' or C6'), 41.3 (CH, C11 or C5), 41.6 (CH₂, C10 or C13), 45.4 (CH₂, C6' or C2'), 46.7 (CH, C4'), 47.9 (CH₂, C8), 53.4 (C, C7), 55.2 (CH₃, C2-OCH₃), 110.3 (CH, C1), 114.0 (CH, C3), 128.9 (CH, C4), 138.8 (CH, C4a), 147.7 (C, C11a), 156.4 (C, NHCONH), 157.8 (C, C2), 169.0 (C, COCH₃). Accurate mass: Calculate for [C₂₅H₃₅N₃O₃+H]⁺: 426.2571; Found: 426.2760. Anal. Calcd for C₂₅H₃₅N₃O₃ · 0.15 DCM: C 68.92, H 8.12, N 9.59. Found: C 68.96, H 8.12, N 9.39.

Preparation of 1-(1-acetylpiperidin-4-yl)-3-(2,3-dimethoxy-9-methyl-5,6,8,9,10,11-hexahydro-7H-5,9:7,11-dimethanobenzo[9]annulen-7-yl)urea



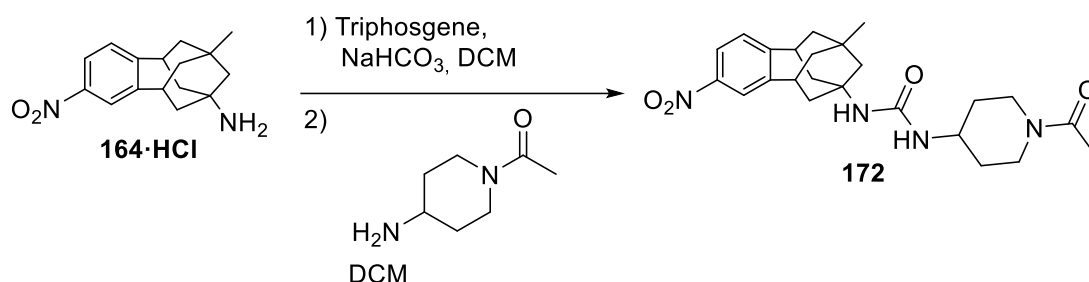
To a solution of 2,3-dimethoxy-9-methyl-5,6,8,9,10,11-hexahydro-7*H*-5,9:7,11-dimethanobenzo[9]annulen-7-amine hydrochloride (150 mg, 0.46 mmol) in DCM (3 mL) saturated aqueous NaHCO₃ solution (3 mL) and triphosgene (51 mg, 0.17 mmol) were added. The biphasic mixture was stirred at room temperature for 30 minutes and then the two phases were separated and the organic layer was washed with brine (3 mL), dried over anhydrous Na₂SO₄, filtered and evaporated under vacuum to obtain 1-2 mL of a solution of the isocyanate in DCM. To this solution was added 1-(4-aminopiperidin-1-yl)ethan-1-one (79 mg, 0.55 mmol). The reaction mixture was stirred at room temperature overnight and the solvent was evaporated under vacuum to obtain a yellow oil (334 mg). Column chromatography (SiO₂, DCM/Methanol mixtures) gave 1-(1-acetylpiperidin-4-yl)-3-(2,3-dimethoxy-9-methyl-5,6,8,9,10,11-hexahydro-7*H*-5,9:7,11-dimethanobenzo[9]annulen-7-yl)urea (168 mg, 80 % yield) as a white solid, mp 127-128 °C. IR (NaCl disk): 3365, 3052, 2913, 2862, 2834, 1643, 1616, 1553, 1516, 1452, 1360, 1343, 1320, 1293, 1252, 1232, 1168, 1137, 1092, 1019, 974, 863, 801, 734 cm⁻¹. ¹H-NMR (400 MHz, CDCl₃) δ: 0.90 (s, 3 H, C9-CH₃), 1.16 [m, 2 H, 3'(5')-H_{ax}], 1.51 [d, *J* = 13.2 Hz, 2 H, 10(13)-H_{ax}], 1.61 [dd, *J* = 13.6 Hz, *J'* = 6.4 Hz, 2 H, 10(13)-H_{eq}], 1.80 (s, 2 H, 8-H), 1.82-1.93 [complex signal, 3 H, 6(12)-H_{ax}, 3'-H_{eq} or 5'-H_{eq}], 1.99-2.05 (dm, *J* = 12.4 Hz, 1 H, 5'-H_{eq} or 3'-H_{eq}), 2.06 (s, 3 H, COCH₃), 2.12 [dd, *J* = 12.8, *J'* = 6.4 Hz, 2 H, 6(12)-H_{eq}], 2.69 (m, 1 H, 2'-H_{ax} or 6'-H_{ax}), 2.96 [t, *J* = 6.0 Hz, 2 H, 5(11)-H], 3.10 (m, 1 H, 6'-H_{ax} or 2'-H_{ax}), 3.67-3.77 (complex signal, 2 H, 4'-H, 6'-H_{eq} or 2'-H_{eq}), 3.82 [s, 6 H, C2(3)-OCH₃], 4.38 (d, *J* = 7.6 Hz, 1 H, 4'-NH), 4.44 (dm, *J* = 13.2 Hz, 1 H, 2'-H_{eq} or 6'-H_{eq}), 4.50 (s, 1 H, 7-NH), 6.59 [s, 2 H, 1(4)-H]. ¹³C-NMR (100.5 MHz, CDCl₃) δ: 21.4 (CH₃, COCH₃), 32.3 (CH₃, C9-CH₃), 32.4 (CH₂, C3' or C5'), 33.6 (C, C9), 33.6 (CH₂, C5' or C3'), 40.1 [CH₂, C6(12)], 40.7 [CH, C5(11), CH₂, C2' or C6'], 41.4 [CH₂, C10(13)], 45.4 (CH₂, C6' or C2'), 46.9 (CH, C4'), 47.9 (CH₂, C8), 53.5 (C, C7), 56.0 [CH₃, C2(3)-OCH₃], 112.2 [CH, C1(4)], 138.7 [C, C4a(11a)], 146.7 [C, C2(3)], 156.3 (C, NHCONH), 169.0 (C, COCH₃). Accurate mass: Calculate for [C₂₆H₃₇N₃O₄+H]⁺: 456.2857; Found: 456.2859. Anal. Calcd for C₂₆H₃₇N₃O₄ · 0.85 H₂O: C 66.32, H 8.28, N 8.92. Found: C 66.52, H 8.05, N 8.70.

Obtention of 1-(1-acetylpiperidin-4-yl)-3-(9-chloro-2,3-dimethoxy-5,6,8,9,10,11-hexahydro-7*H*-5,9:7,11-dimethanobenzo[9]annulen-7-yl)urea



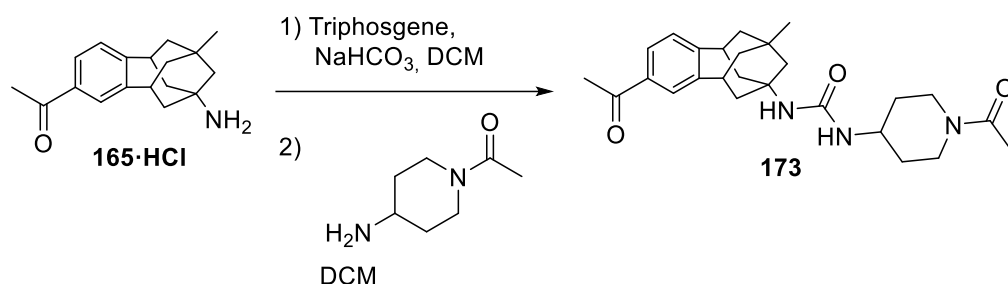
To a solution of 1 9-chloro-2,3-dimethoxy-5,6,8,9,10,11-hexahydro-7*H*-5,9:7,11-dimethanobenzo[9]annulen-7-amine hydrochloride (104 mg, 0.3 mmol) in DCM (3 mL) and saturated aqueous NaHCO₃ solution (2 mL), triphosgene (33 mg, 0.11 mmol) was added. The biphasic mixture was stirred at room temperature for 30 minutes and then the two phases were separated and the organic one was washed with brine (3 mL), dried over anhydrous Na₂SO₄, filtered and evaporated under vacuum to obtain 1-2 mL of a solution of isocyanate in DCM. To this solution was added 1-(4-aminopiperidin-1-yl)ethan-1-one (43 mg, 0.3 mmol). The mixture was stirred overnight at room temperature and the solvent was then evaporated. Column chromatography (SiO₂, DCM/Methanol mixtures) provided 1-(1-acetylpiperidin-4-yl)-3-(9-chloro-2,3-dimethoxy-5,6,8,9,10,11-hexahydro-7*H*-5,9:7,11-dimethanobenzo[9]annulen-7-yl)urea as a yellowish solid (79 mg, 55% yield), mp 148-149 °C. IR (ATR): 3355, 2923, 2851, 1615, 1550, 1517, 1450, 1376, 1359, 1346, 1335, 1318, 1303, 1287, 1249, 1226, 1163, 1089, 1023, 984, 945, 863, 815 cm⁻¹. ¹H-NMR (400 MHz, CDCl₃) δ: 1.14 [m, 2 H, 3'(5')-H_{ax}], 1.86-1.92 [complex signal, 3 H, 6(12)-H_{ax}, 5'-H_{eq} or 3'-H_{eq}], 2.00 (m, 1 H, 3'-H_{eq} or 5'-H_{eq}), 2.06 (s, 3 H, COCH₃), 2.10-2.24 [complex signal, 4 H, 10(13)-H_{ax}, 6(12)-H_{eq}], 2.34 [dd, *J* = 12.8 Hz, *J'* = 6.4 Hz, 2 H, 10(13)-H_{eq}], 2.48 (m, 2 H, 8-H), 2.71 (m, 1 H, 2'-H_{ax} or 6'-H_{ax}), 3.05 [t, *J* = 6.4 Hz, 2 H, 5(11)-H], 3.12 (m, 1 H, 6'-H_{ax} or 2'-H_{ax}), 3.68-3.78 (complex signal, 2 H, 4'-H, 2'-H_{eq} or 6'-H_{eq}), 3.83 [s, 6 H, 2(3)-OCH₃], 4.41 (dm, *J* = 14.0 Hz, 1 H, 2'-H_{eq} or 6'-H_{eq}), 4.71 (d, *J* = 8.0 Hz, 1 H, 4'-NH), 4.83 (s, 1 H, 7-NH), 6.59 [s, 2 H, 1(4)-H]. ¹³C-NMR (100.5 MHz, CDCl₃) δ: 21.4 (CH₃, COCH₃), 32.3 (CH₂, C5' or C3'), 33.7 (CH₂, C3' or C5'), 39.1 [CH₂, C6(12)], 40.7 (CH₂, C2' or C6'), 40.8 [CH, C5(11)], 44.7 [CH₂, C10(13)], 45.4 (CH₂, C6' or C2'), 46.6 (CH, C4'), 50.8 (CH₂, C8), 55.5 [CH₃, C2(3)-OCH₃], 56.0 (C, C7), 69.6 (C, C9), 112.1 [CH, C1(4)], 137.2 [C, C2(3)], 146.9 [C, C4a(11a)], 156.2 (C, NHCONH), 169.12 (C, COCH₃). Accurate mass: Calculate for [C₂₅H₃₄ClN₃O₄+H]⁺: 476.2311; Found: 476.2313. Anal. Calcd for C₂₅H₃₄ClN₃O₄ · 1.05 MeOH: C 61.39, H 7.55, N 8.24. Found: C 61.55, H 7.16, N 7.86.

Preparation of 1-(1-acetylpiperidin-4-yl)-3-(9-methyl-2-nitro-5,6,8,9,10,11-hexahydro-7*H*-5,9:7,11-dimethanobenzo[9]annulen-7-yl)urea



To a solution of 9-methyl-2-nitro-5,6,8,9,10,11-hexahydro-7*H*-5,9:7,11-dimethanobenzo[9]annulen-7-amine hydrochloride (600 mg, 1.94 mmol) in DCM (10 mL) saturated aqueous NaHCO₃ solution (10 mL) and triphosgene (213 mg, 0.718 mmol) were added. The biphasic mixture was stirred at room temperature for 30 minutes and then the two phases were separated and the organic layer was washed with brine (5 mL), dried over anhydrous Na₂SO₄, filtered and evaporated under vacuum to obtain 1-2 mL of a solution of the isocyanate in DCM. To this solution was added 1-(4-aminopiperidin-1-yl)ethan-1-one (331 mg, 2.33 mmol). The reaction mixture was stirred at room temperature overnight and the solvent was evaporated under vacuum to obtain a brown solid (840 mg). Column chromatography (SiO₂, DCM/methanol mixtures) gave 1-(1-acetylpiperidin-4-yl)-3-(9-methyl-2-nitro-5,6,8,9,10,11-hexahydro-7*H*-5,9:7,11-dimethanobenzo[9]annulen-7-yl)urea (640 mg, 75% yield) as a yellowish solid, mp 155-156 °C. IR (NaCl disk): 3360, 2918, 2237, 1619, 1552, 1522, 1454, 1345, 1322, 1266, 1230, 1164, 1137, 1081, 974, 949, 911, 865, 838, 798, 761, 731, 644 cm⁻¹. ¹H-NMR (400 MHz, CDCl₃) δ: 0.93 (s, 3 H, C9-CH₃), 1.17 [dq, *J* = 11.2 Hz, *J*' = 3.6 Hz, 2 H, 3'(5')-H_{ax}], 1.51 (complex signal, 2 H, 10-H_{ax}, 13-H_{ax}), 1.65-1.88 (complex signal, 5 H, 10-H_{eq}, 13-H_{eq}, 8-H, 5'-H_{eq} or 3'-H_{eq}), 2.02-2.11 (complex signal, 8 H, COCH₃, 6-H, 12-H, 3'-H_{eq} or 5'-H_{eq}), 2.70 (m, 1 H, 2'-H_{ax} or 6'-H_{ax}), 3.12 (m, 1 H, 6'-H_{ax} or 2'-H_{ax}), 3.18 (complex signal, 2 H, 5-H, 11-H), 3.73 (complex signal, 2 H, 4'-H, 6'-H_{eq} or 2'-H_{eq}), 4.55 (d, *J* = 7.6 Hz, 1 H, C4'-NH), 4.62 (s, 1 H, C7-NH), 7.18 (m, 1 H, 1-H). ¹³C-NMR (100.5 MHz, CDCl₃) δ: 21.4 (CH₃, COCH₃), 32.1 (CH₃, C9-CH₃), 32.4 (CH₂, C5' or C3'), 33.6 (C, C9), 33.7 (CH₂, C3' or C5'), 39.0 (CH₂, C6 or C12), 39.4 (CH₂, C12 or C6), 40.5 (CH₂, C10 or C13), 40.7 (CH₂, C2' or C6'), 41.0 (CH, C5, C11), 45.4 (CH₂, C6' or C2'), 46.8 (CH, C4'), 47.7 (CH₂, C8), 121.6 (CH C1), 122.8 (CH, C3), 128.9 (CH, C4), 146.2 (C, C4a or C11a), 147.8 (C, C11a or C4a), 154.16 (C, C2), 156.3 (C, NHCONH), 169.1 (C, COCH₃). Anal. Calcd for C₂₄H₃₂N₄O₄: C 65.43, H 7.32, N 12.72. Found: C 65.22, H 7.45, N 12.56. Accurate mass: Calculate for [C₂₄H₃₂N₄O₄+H]⁺: 441.2496; Found: 441.2495.

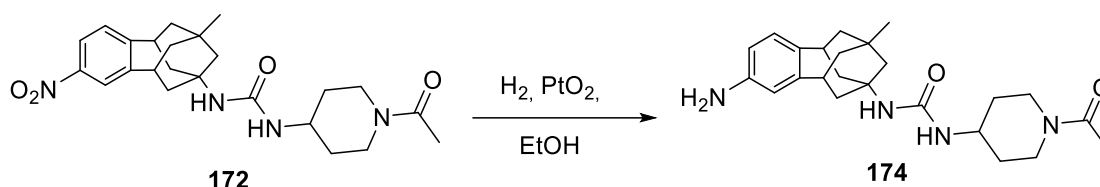
Preparation of 1-(2-acetyl-9-methyl-5,6,8,9,10,11-hexahydro-7*H*-5,9:7,11-dimethanobenzo[9]annulen-7-yl)-3-(1-acetylpiperidin-4-yl)urea



To a solution of 1-(7-amino-9-methyl-6,7,8,9,10,11-hexahydro-5*H*-5,9:7,11-dimethanobenzo[9]annulen-2-yl)ethan-1-one hydrochloride (300 mg, 0.98 mmol) in DCM (5 mL) and saturated aqueous NaHCO₃ solution (3.52 mL) was added triphosgene (145 mg, 0.49 mmol). The biphasic mixture was stirred at room temperature for 30 minutes and then the two phases were separated and the organic layer was washed with brine (5 mL), dried over anh. Na₂SO₄, filtered and evaporated under vacuum to obtain 1-2 mL of a solution of the isocyanate in DCM. To this solution was added 1-(4-aminopiperidin-1-yl)ethan-1-one (167 mg, 1.17 mmol). The reaction mixture was stirred at room temperature overnight and the solvent was evaporated under vacuum to obtain a yellow gum (483 mg). Column chromatography (SiO₂, DCM/methanol mixtures) gave 1-(2-acetyl-9-methyl-5,6,8,9,10,11-hexahydro-7*H*-5,9:7,11-dimethanobenzo[9]annulen-7-yl)-3-(1-acetyl-piperidin-4-yl)urea (324 mg, 76% yield), mp 144-145°C. IR (NaCl disk): 3363, 3005, 2918, 2861, 2239, 1679, 1619, 1552, 1453, 1426, 1361, 1320, 1272, 1229, 1203, 1137, 1106, 1057, 973, 950, 917, 830, 731, 645 cm⁻¹. ¹H-NMR (400 MHz, CDCl₃) δ: 0.91 (s, 3 H, C9-CH₃), 1.09-1.20 [complex signal, 2 H, 5'(3')-H_{ax}], 1.49 (d, *J* = 13.6 Hz, 2 H, 10-H_{ax}, 13-H_{ax}), 1.65 (dd, *J* = 13.2 Hz, *J'* = 6.0 Hz, 2 H, 10-H_{eq}, 13-H_{eq}), 1.75 (dm, *J* = 11.6 Hz, 1 H, 8-H_a), 1.79-1.97 (complex signal, 4 H, 8-H_b, 5'-H_{eq} or 3'-H_{eq}, 6-H_{ax}, 12-H_{ax}), 2.01 (m, 1 H, 2'-H_{eq} or 6'-H_{eq}), 2.05 (s, 3 H, NCOCH₃), 2.09 (m, 1 H, 6-H_{eq} or 12-H_{eq}), 2.21 (m, 1 H, 12-H_{eq} or 6-H_{eq}), 2.55 (s, 3 H, C2-COCH₃), 2.65-2.75 (complex signal, 1 H, 2'-H_{ax} or 6'-H_{ax}), 3.07-3.17 (complex signal, 3 H, 5-H, 11-H, 6'-H_{ax} or 2'-H_{ax}), 3.66-3.77 (complex signal, 2 H, 4'-H, 6'-H_{eq} or 2'-H_{eq}), 4.42 (d, *J* = 13.6 Hz, 1H, 2'-H_{eq} or 6'-H_{eq}), 4.71 (d, *J* = 6.8 Hz, 1 H, C4'-NH), 4.76 (s, 1 H, C7-NH), 7.12 (d, *J* = 7.6 Hz, 1 H, 1-H), 7.62-7.67 (complex signal, 2 H, 3-H, 4-H). ¹³C-NMR (100.5 MHz, CDCl₃) δ: 21.4 (CH₃, NCOCH₃), 26.6 (CH₃, C2-COCH₃), 31.5 (C, C9), 32.2 (CH₃, C9-CH₃), 32.4 (CH₂, C5' or C3'), 33.6 (CH₂, C3' or C5'), 39.3 (CH₂, C12 or C6), 39.8 (CH₂, C6 or C12), 40.7 (CH₂, C2' or C6'), 41.0 (CH₂, C10, C13), 41.07 (CH, C5 or C11), 41.1 (CH, C11 or C5), 45.4 (CH₂, C6' or C2'), 46.7 (CH, C4'), 47.7 (CH₂, C8), 53.2 (C, C7), 126.8 (CH, C3), 127.6 (CH, C4), 128.3 (CH, C1), 135.3 (C, C2), 146.7 (C, C11a), 152.4 (C, C4a), 156.4 (C, NHCONH), 169.0 (C, NCOCH₃), 198.3 (C, C2-COCH₃). Anal. Calcd for C₂₆H₃₅N₃O₃ · 0.45 MeOH: C 70.29, H 8.21, N 9.30.

Found: C 70.64, H 8.56, N 8.88. Accurate mass: Calculate for $[C_{26}H_{35}N_3O_3+H]^+$: 438.2751;
Found: 438.2746.

Preparation of 1-(1-acetylpiperidin-4-yl)-3-(2-amino-9-methyl-5,6,8,9,10,11-hexahydro-7H-5,9:7,11-dimethanobenzo[9]annulen-7-yl)urea



To a solution of 1-(1-acetylpiperidin-4-yl)-3-(9-methyl-2-nitro-5,6,8,9,10,11-hexahydro-7H-5,9:7,11-dimethanobenzo[9]annulen-7-yl)urea (260 mg, 0.59 mmol) in EtOH (17 ml) was added PtO₂ (20 mg). The mixture was hydrogenated at room temperature and atmospheric pressure for 8 days. The resulting suspension was filtered and the filtrate was evaporated under vacuum to obtain a dark brown solid (223 mg), which was dissolved in DCM (10 mL) and washed with Et₂O obtaining a white solid (140 mg). Column chromatography (SiO₂, DCM/Methanol mixtures) gave a white solid (82 mg, 34% yield), mp 150-151 °C. IR (NaCl disk): 3344, 3006, 2905, 2853, 1614, 1556, 1505, 1454, 1360, 1344, 1320, 1303, 1266, 1229, 1194, 1162, 1136, 1060, 974, 868, 820, 734 cm⁻¹. ¹H-NMR (400 MHz, CDCl₃) δ: 0.88 (s, 3 H, C9-CH₃), 1.15 [m, 2 H, 5'(3')-H_{ax}], 1.43-1.53 (complex signal, 2 H, 10-H_{ax}, 13-H_{ax}), 1.56-1.62 (complex signal, 2 H, 10-H_{eq}, 13-H_{eq}), 1.75-1.86 (complex signal, 5 H, 8-H, 5'-H_{eq} or 3'-H_{eq}, 6-H_{ax}, 12-H_{ax}), 1.99 (dm, *J* = 12.0 Hz, 1 H, 3'-H_{eq} or 5'-H_{eq}), 2.04-2.10 (complex signal, 4 H, COCH₃, 6-H_{eq} or 12-H_{eq}), 2.15 (m, 1 H, 12-H_{eq} or 6-H_{eq}), 2.69 (m, 1 H, 2'-H_{ax} or 6'-H_{ax}), 2.85 (t, *J* = 6.0 Hz, 1 H, 11-H or 5-H), 2.94 (t, *J* = 6.0 Hz, 1 H, 5-H or 11-H), 3.09 (m, 1 H, 6'-H_{ax} or 2'-H_{ax}), 3.67-3.76 (complex signal, 2 H, 4'-H, 6'-H_{eq} or 2'-H_{eq}), 4.41 (dm, *J* = 13.6 Hz, 1 H, 2'-H_{eq} or 6'-H_{eq}), 4.62 (d, *J* = 8.0 Hz, 1 H, C4'-NH), 4.66 (s, 1 H, C7-NH), 6.37-6.41 (complex signal, 2 H, 1-H, 3-H), 6.82 (d, *J* = 7.6 Hz, 1 H, 4-H). ¹³C-NMR (100.5 MHz, CDCl₃) δ: 21.4 (CH₃, COCH₃), 32.29 (CH₃, C9-CH₃), 32.36 (CH₂, C5' or C3'), 33.5 (C, C9), 33.6 (CH₂, C3' or C5'), 39.8 (CH₂, C12 or C6), 40.2 (CH, C5 or C11), 40.6 (CH₂, C6 or C12), 40.7 (CH₂, C2' or C6'), 41.2 (CH, C11 or C5), 41.7 (CH₂, C10, C13), 45.4 (CH₂, C6' or C2'), 46.7 (CH₂, C8), 53.4 (C, C7), 112.4 (CH, C1), 115.2 (CH, C3), 128.9 (CH, C4), 136.9 (C, C2), 144.3 (C, C4a), 147.4 (C, C11a), 156.5 (C, NHCONH), 169.0 (C, COCH₃). Accurate mass: Calculate for $[C_{24}H_{35}N_4O_2+H]^+$: 411.2755; Found: 411.2756.

Patent application

(12) INTERNATIONAL APPLICATION PUBLISHED UNDER THE PATENT COOPERATION TREATY (PCT)

(19) World Intellectual Property
Organization
International Bureau



(10) International Publication Number
WO 2019/243414 A1

(43) International Publication Date
26 December 2019 (26.12.2019)

(51) International Patent Classification:

C07C 271/56 (2006.01) C07D 451/04 (2006.01)
C07C 275/26 (2006.01) C07D 493/08 (2006.01)
C07C 335/16 (2006.01) A61K 31/27 (2006.01)
C07D 211/34 (2006.01) A61K 31/17 (2006.01)
C07D 211/58 (2006.01) A61P 9/00 (2006.01)
C07D 211/96 (2006.01) A61P 29/00 (2006.01)
C07D 277/82 (2006.01) A61P 25/00 (2006.01)

SC, SD, SE, SG, SK, SL, SM, ST, SV, SY, TH, TJ, TM, TN,
TR, TT, TZ, UA, UG, US, UZ, VC, VN, ZA, ZM, ZW.

(84) Designated States (unless otherwise indicated, for every kind of regional protection available): ARIPO (BW, GH, GM, KE, LR, LS, MW, MZ, NA, RW, SD, SL, ST, SZ, TZ, UG, ZM, ZW), Eurasian (AM, AZ, BY, KG, KZ, RU, TJ, TM), European (AL, AT, BE, BG, CH, CY, CZ, DE, DK, EE, ES, FI, FR, GB, GR, HR, HU, IE, IS, IT, LT, LU, LV, MC, MK, MT, NL, NO, PL, PT, RO, RS, SE, SI, SK, SM, TR), OAPI (BF, BJ, CF, CG, CI, CM, GA, GN, GQ, GW, KM, ML, MR, NE, SN, TD, TG).

(21) International Application Number:

PCT/EP2019/066181

(22) International Filing Date:

19 June 2019 (19.06.2019)

(25) Filing Language:

English

(26) Publication Language:

English

(30) Priority Data:

18382445.7 20 June 2018 (20.06.2018) EP

(71) Applicant: UNIVERSITAT DE BARCELONA [ES/ES];
Centro de Patentes UB, E-08028 Barcelona (ES).

(72) Inventors: CODONY I GISBERT, Sandra; Sant
Hermenegild, 20-22, 1^o, 1^o, E-08006 Barcelona (ES).
GALDEANO CANTADOR, Carlos; Espigol, 4, E-08328
Alella, Barcelona (ES). LEIVA MARTÍNEZ, Rosana;
Avenida Madrid, 51-53, 1^o 5a, E-08028 Barcelona
(ES). LARISA TURCU, Andreea; Amadeu I. 3 Spain,
E-08812 Sant Pere de Ribes, Barcelona (ES). VALVERDE
MURILLO, Elena; Abat Escarré, 12, E-43711 Banyeres
del Penedès, Tarragona (ES). VÁZQUEZ CRUZ, Santia-
go; Avenida Can Corts, 15, 3-2, E-08940 Cornellà del Llo-
bregat, Barcelona (ES).

(74) Agent: ABG INTELLECTUAL PROPERTY LAW,
S.L.; Avda. de Burgos, 16D, Edificio EUROMOR, 28036
Madrid (ES).

(81) Designated States (unless otherwise indicated, for every kind of national protection available): AE, AG, AL, AM, AO, AT, AU, AZ, BA, BB, BG, BH, BN, BR, BW, BY, BZ, CA, CH, CL, CN, CO, CR, CU, CZ, DE, DJ, DK, DM, DO, DZ, EC, EE, EG, ES, FI, GB, GD, GE, GH, GM, GT, HN, HR, HU, ID, IL, IN, IR, IS, JO, JP, KE, KG, KH, KN, KP, KR, KW, KZ, LA, LC, LK, LR, LS, LU, LY, MA, MD, ME, MG, MK, MN, MW, MX, MY, MZ, NA, NG, NI, NO, NZ, OM, PA, PE, PG, PH, PL, PT, QA, RO, RS, RU, RW, SA,

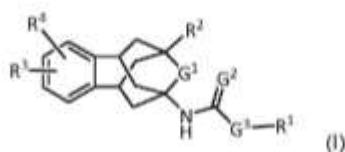
Published:

— with international search report (Art. 21(3))



WO 2019/243414 A1

(54) Title: POLYCYCLIC COMPOUNDS AS SOLUBLE EPOXIDE HYDROLASE INHIBITORS



(57) Abstract: The present invention relates to soluble epoxide hydrolase (sEH) inhibitors of formula (I) to processes for their obtention and to their therapeutic indications.

POLYCYCLIC COMPOUNDS AS SOLUBLE EPOXIDE HYDROLASE INHIBITORS

The present invention relates to the field of pharmaceutical products for human and veterinary medicine, particularly to soluble epoxide hydrolase (sEH) inhibitors and their
5 therapeutic indications.

BACKGROUND ART

A total of more than 100 patent publications have described multiple classes of sEH
10 inhibitors, based on different chemical structures, such as amides, thioamides, ureas, thioureas, carbamates, acyl hydrazones and chalcone oxides (cf. e.g. H.C. Shen, "Soluble epoxide hydrolase inhibitors: a patent review", *Expert Opin Ther Patents* 2010, vol. 20, pp. 941-956, a review with 149 references).

sEH inhibition has been associated to various beneficial biological effects, that may be translated into various therapeutic treatments (cf. e.g. H.C. Shen and B.D. Hammock, "Discovery of inhibitors of soluble epoxide hydrolase: A target with multiple potential therapeutic indications", *J Med Chem.* 2012, vol. 55, pp. 1789-1808, a review with 117 references; K.M. Wagner et al. "Soluble epoxide hydrolase as a therapeutic target for
20 pain, inflammatory and neurodegenerative diseases", *Pharmacol Ther.* 2017, vol 180, pp 62-76, a review with 186 references).

More specifically the documents cited below have described the usefulness of sEH inhibition in the treatment of the following diseases: hypertension (*Recent Pat
25 Cardiovasc Drug Discov.* 2006 Jan;1(1):67-72), atherosclerosis (*J Cardiovasc Pharmacol.* 2008 Oct;52(4):314-23), pulmonary diseases such as chronic obstructive pulmonary disorder, asthma, sarcoidosis, and cystic fibrosis, (*Am J Respir Cell Mol Biol.* 2012 May;46(5):614-22 / *Am J Respir Crit Care Med.* 2014 Oct 15;190(8):848-50 / *Resp. Res.*, 2018, 19:236 / *Free Rad. Biol. Med.*, 2012, 53, 160), kidney diseases such
30 as acute kidney injury, diabetic nephrology, chronic kidney diseases, hypertension-mediated kidney disorders and high fat diet-mediated renal injury (*Bioorg Med Chem Lett.* 2014 Jan 15;24(2):565-70 / *Am J Physiol Renal Physiol.* 2013 Jan 15;304(2):F168-76 / *Am J Physiol Renal Physiol.* 2014 Oct 15;307(8):F971-80 / *Frontiers Pharmacol.* 2019, 9:1551 / *Proc Natl Acad Sci USA.* 2019, 116:5154-5159),
35 stroke (*J Biol Chem.* 2014 Dec 26;289(52):35826-38 / *PLoS One.* 2014 May 13;9(5):e97529), pain (*J Agric Food Chem.* 2011 Apr 13;59(7):2816-24 / *Inflamm Allergy Drug Targets.* 2012 Apr;11(2):143-58), neuropathic pain (*J Agric Food Chem.*

2011 Apr 13;59(7):2816-24 / *Drug Discov Today* 2015 Nov;20(11):1382-90 / *Proc Natl Acad Sci U S A.* 2015 Jul 21;112(29):9082-7), inflammation (*Inflamm Allergy Drug Targets.* 2012 Apr;11(2):143-58 / *Proc Natl Acad Sci U S A.* 2005 Jul 12;102(28):9772-7), pancreatitis in particular acute pancreatitis (*Mol Pharmacol.* 2015 Aug;88(2):281-90), immunological disorders (WO 00/23060 A2), neurodevelopmental disorders such as schizophrenia and autism spectrum disorder (*Proc Natl Acad Sci USA,* 2019, 116:7083-7088), eye diseases (WO 2007/009001 A1 / *Frontiers Pharmacol.* 2019, 10:95) in particular diabetic keratopathy (*Diabetes.* 2018 Jun;67(6):1162-1172), wet age-related macular degeneration (*ACS Chem Biol.* 2018 Jan 19; 13:45-52) and retinopathy (*Nature.* 2017 Dec 14;552(7684):248-252) such as premature retinopathy and diabetic retinopathy, cancer (*Prog Lipid Res.* 2014 Jan;53:108-23), obesity (*Nutr Metab Cardiovasc Dis.* 2012 Jul;22(7):598-604), including obesity-induced colonic inflammation (*Proc Natl Acad Sci U S A.* 2018 May 15;115(20):5283-5288), diabetes (*Proc Natl Acad Sci U S A.* 2011 May 31;108(22):9038-43), metabolic syndrome (*Exp Diabetes Res.* 2012;2012:758614), preeclampsia (*Med. Hypotheses,* 2017 Oct;108:81-5), anorexia nervosa ("Pharmacokinetic optimization of six soluble epoxide hydrolase inhibitors for the therapeutic use in a murine model of anorexia" Abstracts of Papers, 241st ACS National Meeting & Exposition, Anaheim, CA, United States, March 27-31, 2011 (2011), MEDI-92), depression (*J Neurosci Res.* 2017 Dec;95(12):2483-2492), male sexual dysfunction (*Biomed. & Pharmacother.* 2019, 115: 108897) such as erectile dysfunction (*Phytother Res.* 2016 Jul;30(7):1119-27), wound healing (*J Surg Res.* 2013 Jun 15;182(2):362-7 / *BioRxiv.* 2019 March 8, doi:10.1101/571984), NSAID-induced ulcers (*J Pharmacol Exp Ther.* 2016 Jun;357(3):529-36), emphysema (*Am J Respir Cell Mol Biol.* 2012 May;46(5):614-22), scrapie (*Life Sci.* 2013 Jun 21;92(23):1145-50), Parkinson's disease (*Mol Neurobiol.* 2015 Aug;52(1):187-95 / *Proc Natl Acad Sci. USA,* 2018, 115:E5815-E5823), arthritis (*Drug Metab Dispos.* 2015 May;43(5):788-802), arrhythmia (*Cardiovasc Ther.* 2011 Apr;29(2):99-111), cardiac fibrosis (*Alcoholism.* 2018, 42, 1970), Alzheimer's disease (*Pharmacol Ther.* 2017 Dec;180:62-76 / *BioRxiv.* 2019 Apr 10, doi:10.1101/605055), Raynaud's syndrome (WO 2003/002555 A1), Niemann-Pick-type C disease (*Experimental Molecular Medicine.* 2018, 50:149), cardiomyopathy (*Int J Cardiol.* 2012 Mar 8;155(2):181-7), vascular cognitive impairment (*Prostaglandins Other Lipid Mediat.* 2014 Oct;113-115:30-7), mild cognitive impairment (*Pharmacol Ther.* 2017 Dec;180:62-76), inflammatory bowel diseases (*Dig Dis Sci.* 2012 Oct;57(10):2580-91 / *PLoS One.* 2019 Apr 19, 14(4):e0215033), cirrhosis (*Toxicol Appl Pharmacol.* 2015 Jul 15;286(2):102-11), non-alcoholic fatty liver disease (*PLoS One.* 2014 Oct 13, 9(10):e110162), non-alcoholic steatohepatitis (*Am J Physiol Gastrointest Liver Physiol.* 2019, 316, G527-

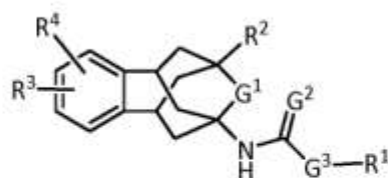
G538), liver fibrosis (*Clinics Res Hepatol Gastroenterol* 2018, 42, 118-125), osteoporosis (*FASEB J.* 2015 Mar;29(3):1092-101), chronic periodontitis (*J Pharmacol Exp Ther.* 2017 Jun;361(3):408-416), sepsis (*FASEB J.* March 2008 22 (Meeting Abstract Supplement) 479.17), seizure disorders such as epilepsy (*PLoS One.* 2013 Dec 11;8(12):e80922), dementia (*Prostaglandins Other Lipid Mediat.* 2014 Oct;113-115:30-7), edema such as cerebral edema (*Stroke.* 2015 Jul;46(7):1916-22.), attention-deficit hyperactivity disorder (WO 2017/120012 A1), schizophrenia (*Proc Natl Acad Sci U S A.* 2016 Mar 29;113(13):E1944-52), drug dependency (WO 2017/120012 A1), social anxiety (WO 2017/120012 A1), colitis (*Anticancer Res.* 2013 Dec;33(12):5261-5271), amyotrophic lateral sclerosis (WO 2016/133788 A1), chemotherapy induced side effects (*Toxicology.* 2017 Aug 15;389:31-41), laminitis (*Equine Vet J.* 2017 May;49(3):345-351), inflammatory joint pain and synovitis (*J Vet Pharmacol Ther.* 2018 Apr;41(2):230-238), endothelial dysfunction (*Prostaglandins Other Lipid Mediat.* 2017 Jul;131:67-74), subarachnoid hemorrhage (*Stroke.* 2015 Jul;46(7):1916-22), including aneurysmal subarachnoid hemorrhage (*J Neurosurg Anesthesiol.* 2015 Jul; 27(3):222-240), traumatic brain injury (*Oncotarget.* 2017 Sep 21;8(61):103236-60), cerebral ischemia (*Scientific Reports.* 2018, 8:5279), and diabetes-induced learning and memory impairment (*Prostaglandins Other Lipid Mediat.* 2018 May;136:84-89).

Despite the high inhibitory activity of many of the reported sEH inhibitory compounds, until now no sEH inhibitor has reached the market. Thus, there is a need to develop new sEH inhibitors.

The inventors have now found a new family of polycyclic compounds having high inhibitory activity for soluble epoxide hydrolase.

SUMMARY OF INVENTION

An aspect of the present invention relates to the provision of compounds of formula (I)



30

(I)

or a stereoisomer or a pharmaceutically acceptable salt thereof, wherein:

G^1 represents an oxygen atom or a methylene group or a single bond;

G^2 represents an oxygen atom or a sulphur atom;

G^3 represents a radical selected from the group consisting of $-NH-(CH_2)_m-$, $-O-(CH_2)_m-$ and $-(CH_2)_n-$;

5 m is an integer from 0 to 6;

n is an integer from 1 to 7;

R^1 is a radical selected from the group consisting of:

- 10 a) C_6-C_{10} aryl which may be optionally substituted by 1 to 4 substituents selected from the group consisting of halogen atoms, C_1-C_6 acyl, nitro (NO_2), cyano ($C\equiv N$), trifluoromethyl (CF_3), trifluoromethoxy (OCF_3), pentafluorosulfanyl (SF_5), sulfonyl (SO_3H), fluorosulfonyl (SO_2F), carboxylic group ($COOH$), amino (NH_2), mono- C_1-C_6 alkylamino, di- C_1-C_6 alkylamino, C_1-C_6 alkoxy, C_1-C_6 alkyl, C_1-C_6 alkoxy carbonylmethyl and methylaminocarbonylpyridyloxy;
- 15 b) heteroaryl having from 2 to 11 carbon atoms and 1, 2 or 3 heteroatoms selected from the group consisting of N, O and S and which may be optionally substituted by 1 to 4 substituents selected from the group consisting of halogen atoms, C_1-C_6 acyl, nitro (NO_2), cyano ($C\equiv N$), trifluoromethyl (CF_3), trifluoromethoxy (OCF_3), pentafluorosulfanyl (SF_5), sulfonyl (SO_3H), fluorosulfonyl (SO_2F), carboxylic group ($COOH$), amino (NH_2), mono- C_1-C_6 alkylamino, di- C_1-C_6 alkylamino, C_1-C_6 alkoxy, C_1-C_6 alkyl and C_1-C_6 alkoxy carbonylmethyl;
- 20 c) saturated or partially unsaturated, monocyclic or bicyclic heterocyclyl having from 5 to 11 carbon atoms and 1, 2 or 3 heteroatoms selected from the group consisting of N, O and S and which may be optionally substituted by 1 to 4 substituents selected from the group consisting of halogen atoms, C_1-C_6 acyl, C_3-C_6 cycloalkyl- $C(=O)$, nitro (NO_2), cyano ($C\equiv N$), trifluoromethyl (CF_3), trifluoromethylcarbonyl (CF_3CO), pentafluorosulfanyl (SF_5), sulfonyl (SO_3H), carboxylic group ($COOH$), amino (NH_2), mono- C_1-C_6 alkylamino, di- C_1-C_6 alkylamino, C_1-C_6 alkoxy, C_1-C_6 alkyl, C_1-C_6 alkoxy carbonylmethyl, C_1-C_6 alkylsulfonyl, C_3-C_6 cycloalkylsulfonyl, benzyl, heteroarylmethyl, pyridincarbonyl, phenylcarbonyl, tetrahydropyrancarboxyl, C_6-C_{10} arylsulfonyl which may be optionally substituted by 1 to 2 substituents selected from the group consisting of halogen atoms, nitro (NO_2), cyano ($C\equiv N$), trifluoromethyl (CF_3), trifluoromethoxy (OCF_3), pentafluorosulfanyl (SF_5), sulfonyl (SO_3H), carboxylic group ($COOH$), amino (NH_2), mono- C_1-C_6 alkylamino, di- C_1-C_6 alkylamino, C_1-C_6 alkoxy, C_1-C_6 alkyl, C_1-C_6 alkoxy carbonylmethyl and phenyl which may be optionally substituted by 1 to 4 substituents selected from the group consisting
- 25
- 30
- 35

of halogen atoms, C₁-C₆ acyl, nitro (NO₂), cyano (C≡N), trifluoromethyl (CF₃), trifluoromethoxy (OCF₃), pentafluorosulfanyl (SF₅), sulfonyl (SO₃H), fluorosulfonyl (SO₂F), carboxylic group (COOH), amino (NH₂), mono-C₁-C₆ alkylamino, di-C₁-C₆ alkylamino, C₁-C₆ alkoxy, C₁-C₆ alkyl, C₃-C₆ cycloalkyl and C₁-C₆ alkoxy carbonylmethyl;

5 d) C₆-C₁₀ cycloalkyl which may be optionally substituted by 1 to 4 substituents selected from the group consisting of halogen atoms, C₁-C₆ acyl, nitro (NO₂), cyano (C≡N), trifluoromethyl (CF₃), trifluoromethoxy (OCF₃), pentafluorosulfanyl (SF₅), sulfonyl (SO₃H), carboxylic group (COOH), amino (NH₂), mono-C₁-C₆ alkylamino, di-C₁-C₆ alkylamino, C₁-C₆ alkoxy, C₁-C₆ alkyl, C₁-C₆ alkoxy carbonylmethyl, pyridinyloxy which may be unsubstituted or substituted by a group selected from COOH and CONHCH₃, and phenoxy which may be unsubstituted or substituted by COOH, COOR⁵, CONH₂, CN or OH;

R² is a radical selected from the group consisting of hydrogen or deuterium atoms, halogen atoms, methyl, hydroxy and C₁-C₆ alkoxy;

R³ and R⁴ are radicals which may be identical or different and which are independently selected from the group consisting of hydrogen atoms, halogen atoms, C₁-C₆ acyl, nitro (NO₂), cyano (C≡N), carboxylic group (COOH), hydroxy (OH), trifluoromethyl (CF₃), trifluoromethoxy (OCF₃), pentafluorosulfanyl (SF₅), sulfonyl (SO₃H), fluorosulfonyl (SO₂F), amino (NH₂), mono-C₁-C₆ alkylamino, di-C₁-C₆ alkylamino, C₁-C₆ alkoxy, C₁-C₆ alkyl and C₁-C₆ alkoxy carbonylmethyl;

or R³ and R⁴ may form together a radical -O-(CH₂)_p-O-, wherein p is an integer from 1 to 3;

R⁵ is a radical selected from C₁-C₆ alkyl and C₃-C₆ cycloalkyl.

25 In a particular embodiment G¹ represents a methylene group.

In a particular embodiment G¹ represents an oxygen atom.

30 In a particular embodiment G¹ represents a single bond.

In a particular embodiment G² represents an oxygen atom.

In a particular embodiment G³ represents a radical selected from the group consisting of -NH-(CH₂)_m- wherein m is an integer from 0 to 6 and -(CH₂)_n- wherein n is an integer from 1 to 7, more particularly G³ represents a radical -NH-(CH₂)_m- wherein m is an integer from 0 to 6.

In a particular embodiment when G^3 is selected from the group consisting of $-NH-(CH_2)_m-$ and $-O-(CH_2)_m-$ wherein m has a value of 0.

- 5 In a particular embodiment when G^3 is $-(CH_2)_n-$ wherein n has a value of 1.

In a particular embodiment R^1 is selected from the group consisting of substituted or unsubstituted phenyl, substituted or unsubstituted cyclohexyl and substituted or unsubstituted piperidiny. In a more specific embodiment the substituents are selected
 10 from the group consisting of methyl, trifluoromethyl, acetyl, 4-carboxy-phenoxy, isopropyl-sulfonyl, benzyl, tert-butoxycarbonyl, trifluorophenyl, propionyl, tetrahydropyran-4-carbonyl, 2-fluorobenzoyl, acetylphenyl, and 8-benzyl.

In a particular embodiment R^2 is selected from the group consisting of hydrogen atoms,
 15 fluorine atoms, chlorine atoms, methyl, hydroxyl and C_1-C_3 alkoxy. When G^1 represents an oxygen atom R^2 is preferably selected from the group consisting of hydrogen and deuterium atoms and methyl.

In another particular embodiment R^2 is preferably selected from the group consisting of
 20 hydrogen, methyl, hydroxyl, methoxy, fluorine and chlorine, more specifically methyl.

In a particular embodiment R^3 and R^4 are radicals which may be identical or different and which are independently selected from the group consisting of hydrogen atoms, halogen atoms, C_1-C_6 acyl, trifluoromethyl (CF_3), trifluoromethoxy (OCF_3), nitro (NO_2), amino (NH_2) and C_1-C_6 alkoxy. In a particular embodiment R^3 and R^4 may be selected
 25 from the group consisting of hydrogen, fluorine, acetyl, nitro, amino and methoxy.

In a particular embodiment R^3 is hydrogen and R^4 is a radical selected from the group consisting of hydrogen atoms, halogen atoms, C_1-C_6 acyl, trifluoromethyl (CF_3), trifluoromethoxy (OCF_3), nitro (NO_2), amino (NH_2) and C_1-C_6 alkoxy.

- 30 In a particular embodiment the compound is selected from the group consisting of:

- i. *p*-tolyl (9-methyl-5,6,8,9,10,11-hexahydro-7*H*-5,9:7,11-dimethanobenzo[9]annulen-7-yl)carbamate
 - ii. 1-(9-methyl-5,6,8,9,10,11-hexahydro-7*H*-5,9:7,11-dimethanobenzo[9]annulen-7-yl)-3-(4-(trifluoromethyl)phenyl)thiourea
- 35

- iii. 1-(1-acetylpiperidin-4-yl)-3-(5-methyl-1,5,6,7-tetrahydro-1,5:3,7-dimethanobenzo[e]oxonin-3(2*H*)-yl)urea
- iv. 1-(1-acetylpiperidin-4-yl)-3-(1,5,6,7-tetrahydro-1,5:3,7-dimethanobenzo[e]oxonin-3(2*H*)-yl)urea
- 5 v. 1-(1-acetylpiperidin-4-yl)-3-(9-methyl-5,6,8,9,10,11-hexahydro-7*H*-5,9:7,11-dimethanobenzo[9]annulen-7-yl)urea
- vi. 1-(1-acetylpiperidin-4-yl)-3-(9-hydroxy-5,6,8,9,10,11-hexahydro-7*H*-5,9:7,11-dimethanobenzo[9]annulen-7-yl)urea
- vii. 1-(1-acetylpiperidin-4-yl)-3-(9-methoxy-5,6,8,9,10,11-hexahydro-7*H*-5,9:7,11-dimethanobenzo[9]annulen-7-yl)urea
- 10 viii. 1-(1-acetylpiperidin-4-yl)-3-(9-fluoro-5,6,8,9,10,11-hexahydro-7*H*-5,9:7,11-dimethanobenzo[9]annulen-7-yl)urea
- ix. 1-(1-acetylpiperidin-4-yl)-3-(9-chloro-5,6,8,9,10,11-hexahydro-7*H*-5,9:7,11-dimethanobenzo[9]annulen-7-yl)urea
- 15 x. 4-(((1*r*,4*r*)-4-(3-(5-methyl-1,5,6,7-tetrahydro-1,5:3,7-dimethanobenzo[e]oxonin-3(2*H*)-yl)ureido)cyclohexyl)oxy)benzoic acid
- xi. 4-(((1*r*,4*r*)-4-(3-(9-methyl-5,6,8,9,10,11-hexahydro-7*H*-5,9:7,11-dimethanobenzo[9]annulen-7-yl)ureido)cyclohexyl)oxy)benzoic acid
- xii. 1-[1-(isopropylsulfonyl)piperidin-4-yl]-3-(9-methyl-5,6,8,9,10,11-hexahydro-7*H*-5,9:7,11-dimethanobenzo[9]annulen-7-yl)urea
- 20 xiii. 1-(1-benzylpiperidin-4-yl)-3-(9-methyl-5,6,8,9,10,11-hexahydro-7*H*-5,9:7,11-dimethanobenzo[9]annulen-7-yl)urea
- xiv. 1-(2-acetyl-9-methyl-5,6,8,9,10,11-hexahydro-7*H*-5,9:7,11-dimethanobenzo[9]annulen-7-yl)-3-(1-acetylpiperidin-4-yl)urea
- 25 xv. 1-(1-acetylpiperidin-4-yl)-3-(9-methyl-2-nitro-5,6,8,9,10,11-hexahydro-7*H*-5,9:7,11-dimethanobenzo[9]annulen-7-yl)urea
- xvi. 1-(1-acetylpiperidin-4-yl)-3-(2-amino-9-methyl-5,6,8,9,10,11-hexahydro-7*H*-5,9:7,11-dimethanobenzo[9]annulen-7-yl)urea
- xvii. *tert*-butyl 4-(2-((9-methyl-5,6,8,9,10,11-hexahydro-7*H*-5,9:7,11-dimethanobenzo[9]annulen-7-yl)amino)-2-oxoethyl)piperidine-1-carboxylate
- 30 xviii. *N*-(9-methyl-5,6,8,9,10,11-hexahydro-7*H*-5,9:7,11-dimethanobenzo[9]annulen-7-yl)-2-(piperidin-4-yl)acetamide
- xix. 2-[1-(isopropylsulfonyl)piperidin-4-yl]-*N*-(9-methyl-5,6,8,9,10,11-hexahydro-7*H*-5,9:7,11-dimethanobenzo[9]annulen-7-yl)acetamide
- 35 xx. 2-(1-acetylpiperidin-4-yl)-*N*-(9-methyl-5,6,8,9,10,11-hexahydro-7*H*-5,9:7,11-dimethanobenzo[9]annulen-7-yl)acetamide

- xxi. 1-(9-methyl-6,7,8,9,10,11-hexahydro-5*H*-5,9:7,11-dimethanobenzo[9]annulen-7-yl)-3-(2,3,4-trifluorophenyl)urea
- xxii. 1-(5-methyl-1,5,6,7-tetrahydro-1,5:3,7-dimethanobenzo[*e*]oxonin-3(2*H*)-yl)-3-(2,3,4-trifluorophenyl)urea
- 5 xxiii. 2-(1-benzylpiperidin-4-yl)-*N*-(9-methyl-5,6,8,9,10,11-hexahydro-7*H*-5,9:7,11-dimethanobenzo[9]annulen-7-yl)acetamide
- xxiv. 1-(9-methyl-5,6,8,9,10,11-hexahydro-7*H*-5,9:7,11-dimethanobenzo[9]annulen-7-yl)-3-(1-propionylpiperidin-4-yl)urea
- xxv. 1-(1-(4-acetylphenyl)piperidin-4-yl)-3-(9-methyl-5,6,8,9,10,11-hexahydro-7*H*-5,9:7,11-dimethanobenzo[9]annulen-7-yl)urea
- 10 xxvi. 1-(9-methyl-5,6,8,9,10,11-hexahydro-7*H*-5,9:7,11-dimethanobenzo[9]annulen-7-yl)-3-(1-(tetrahydro-2*H*-pyran-4-carbonyl)piperidin-4-yl)urea
- xxvii. 1-(1-(2-fluorobenzoyl)piperidin-4-yl)-3-(9-methyl-5,6,8,9,10,11-hexahydro-7*H*-5,9:7,11-dimethanobenzo[9]annulen-7-yl)urea
- 15 xxviii. 1-((1*R*,3*s*,5*S*)-8-benzyl-8-azabicyclo[3.2.1]octan-3-yl)-3-(9-methyl-5,6,8,9,10,11-hexahydro-7*H*-5,9:7,11-dimethanobenzo[9]annulen-7-yl)urea
- xxix. 1-(1-acetylpiperidin-4-yl)-3-(2-fluoro-9-methyl-5,6,8,9,10,11-hexahydro-7*H*-5,9:7,11-dimethanobenzo[9]annulen-7-yl)urea
- xxx. 1-(1-acetylpiperidin-4-yl)-3-(2-methoxy-9-methyl-5,6,8,9,10,11-hexahydro-7*H*-5,9:7,11-dimethanobenzo[9]annulen-7-yl)urea
- 20 xxxi. 1-(1-acetylpiperidin-4-yl)-3-(1-fluoro-9-methyl-5,6,8,9,10,11-hexahydro-7*H*-5,9:7,11-dimethanobenzo[9]annulen-7-yl)urea
- xxxii. 1-(1-acetylpiperidin-4-yl)-3-(2,3-dimethoxy-9-methyl-5,6,8,9,10,11-hexahydro-7*H*-5,9:7,11-dimethanobenzo[9]annulen-7-yl)urea
- 25 xxxiii. 1-(1-acetylpiperidin-4-yl)-3-(5,8,9,10-tetrahydro-5,8:7,10-dimethanobenzo[8]annulen-7(6*H*)-yl)urea
- xxxiv. 1-(benzo[*d*]thiazol-2-yl)-3-(9-methoxy-5,6,8,9,10,11-hexahydro-7*H*-5,9:7,11-dimethanobenzo[9]annulen-7-yl)urea
- xxxv. 1-(1-acetylpiperidin-4-yl)-3-(1,9-difluoro-5,6,8,9,10,11-hexahydro-7*H*-5,9:7,11-dimethanobenzo[9]annulen-7-yl)urea
- 30 xxxvi. 1-(1-acetylpiperidin-4-yl)-3-(1,5,6,7-tetrahydro-1,5:3,7-dimethanobenzo[*e*]oxonin-3(2*H*)-yl-5-*d*)urea

Another aspect of the present invention relates to pharmaceutical or veterinary compositions comprising therapeutically effective amounts of compounds of formula (I), or stereoisomers or pharmaceutically acceptable salts thereof, and preferably adequate amounts of pharmaceutically acceptable excipients. Pharmacy in the context of the

present invention relates both to human medicine and veterinary medicine.

Another aspect of the present invention relates to compounds of formula (I), or stereoisomers or pharmaceutically acceptable salts thereof, and to compositions
5 comprising therapeutically effective amounts of compounds of formula (I), or stereoisomers or pharmaceutically acceptable salts thereof, for use as a medicament.

In a particular embodiment the present invention relates to compounds of formula (I), or stereoisomers or pharmaceutically acceptable salts thereof, and to compositions
10 comprising therapeutically effective amounts of compounds of formula (I), or stereoisomers or pharmaceutically acceptable salts thereof for use in the treatment or prevention in an animal, including a human, of a disease or disorder susceptible of improvement by inhibition of soluble epoxide hydrolase.

15 Another aspect of the present invention relates to the use of compounds of formula (I), or stereoisomers or pharmaceutically acceptable salts thereof, or compositions comprising therapeutically effective amounts of compounds of formula (I), or stereoisomers or pharmaceutically acceptable salts thereof, in the manufacture of a
20 medicament.

In a particular embodiment the present invention relates to the use of compounds of formula (I), or stereoisomers or pharmaceutically acceptable salts thereof, or compositions comprising therapeutically effective amounts of compounds of formula (I), or stereoisomers or pharmaceutically acceptable salts thereof, in the manufacture of a
25 medicament for the treatment or prevention in an animal, including a human, of a disease or disorder susceptible of improvement by inhibition of soluble epoxide hydrolase.

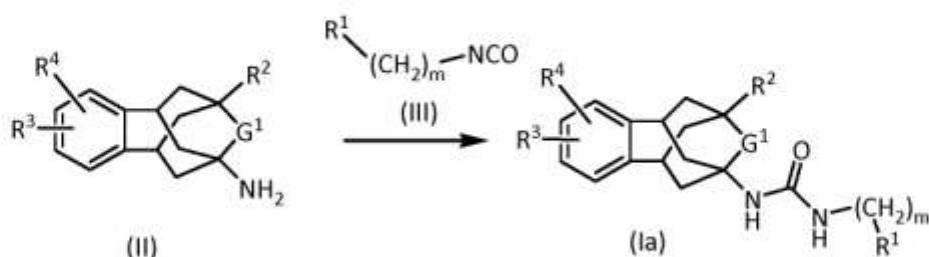
In particular embodiments the disease or disorder susceptible of improvement by
30 inhibition of soluble epoxide hydrolase are selected from the group consisting of hypertension, atherosclerosis, pulmonary diseases such as chronic obstructive pulmonary disorder, asthma, sarcoidosis and cystic fibrosis, kidney diseases such as acute kidney injury, diabetic nephrology, chronic kidney diseases, hypertension-mediated kidney disorders and high fat diet-mediated renal injury, stroke, pain,
35 neuropathic pain, inflammation, pancreatitis in particular acute pancreatitis, immunological disorders, neurodevelopmental disorders such as schizophrenia and autism spectrum disorder, eye diseases in particular diabetic keratopathy, wet age-

related macular degeneration and retinopathy such as premature retinopathy and diabetic retinopathy, cancer, obesity, including obesity-induced colonic inflammation, diabetes, metabolic syndrome, preeclampsia, anorexia nervosa, depression, male sexual dysfunction such as erectile dysfunction, wound healing, NSAID-induced ulcers, 5 emphysema, scrapie, Parkinson's disease, arthritis, arrhythmia, cardiac fibrosis, Alzheimer's disease, Raynaud's syndrome, Niemann-Pick-type C disease, cardiomyopathy, vascular cognitive impairment, mild cognitive impairment, inflammatory bowel diseases, cirrhosis, non-alcoholic fatty liver disease, non-alcoholic steatohepatitis, liver fibrosis, osteoporosis, chronic periodontitis, sepsis, seizure 10 disorders such as epilepsy, dementia, edema such as cerebral edema, attention-deficit hyperactivity disorder, schizophrenia, drug dependency, social anxiety, colitis, amyotrophic lateral sclerosis, chemotherapy induced side effects, laminitis, inflammatory joint pain and synovitis, endothelial dysfunction, subarachnoid hemorrhage, including aneurysmal subarachnoid hemorrhage, traumatic brain injury, 15 cerebral ischemia and diabetes-induced learning and memory impairment.

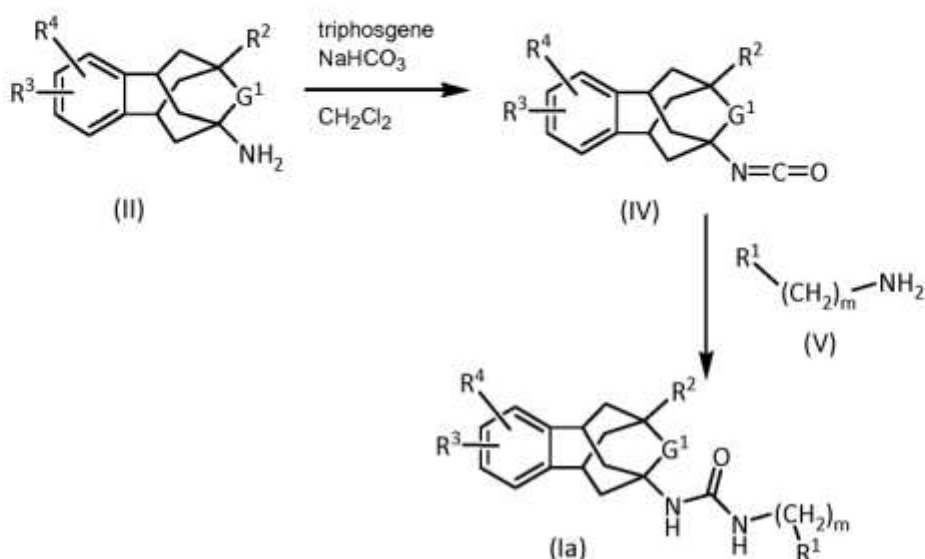
In another aspect, the present invention relates to methods of treatment or prevention in an animal, including a human, of a disease or disorder susceptible of improvement by inhibition of soluble epoxide hydrolase, by administration of pharmaceutical or 20 veterinary compositions comprising compounds of formula (I). Methods for treatment of the aforementioned particular diseases and disorders are particular embodiments of the present invention.

According to another aspect of the present invention, the compounds of formula (Ia) 25 wherein G^2 is oxygen, G^3 is $-NH-(CH_2)_m-$ may be prepared by reacting the amine of formula (II), preferably in the form of a salt such as the hydrochloride with isocyanate of formula (III), in an inert solvent such as dichloromethane (DCM), and in the presence of a base such as triethylamine.

11



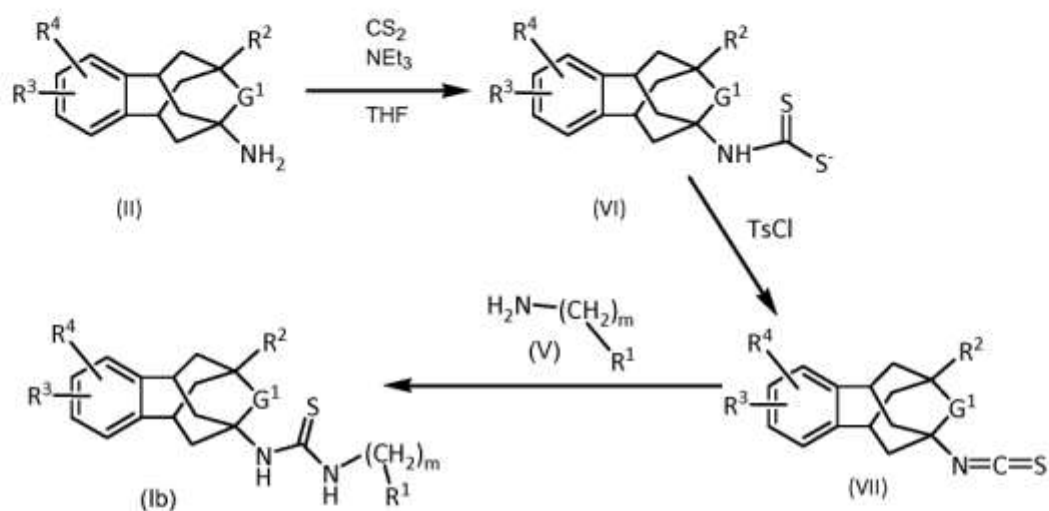
- According to another aspect of the present invention, the compounds of formula (Ia), wherein G² is oxygen, G³ is $-NH-(CH_2)_m-$, may also be prepared by converting in a first step the amine of formula (II), preferably in the form of a salt, into isocyanate of formula (IV) by reaction with an (NH₂→NCO)-converting reagent, such as triphosgene, in an inert solvent, such as DCM. In a second step, the amine of formula (V) is reacted with the isocyanate of formula (IV) to yield compound of formula (Ia). The coupling reaction may be carried out without catalyst and the reaction conveniently takes place at room temperature in the presence of an organic solvent, typically DCM, tetrahydrofuran (THF) or *N,N*-dimethylformamide (DMF).



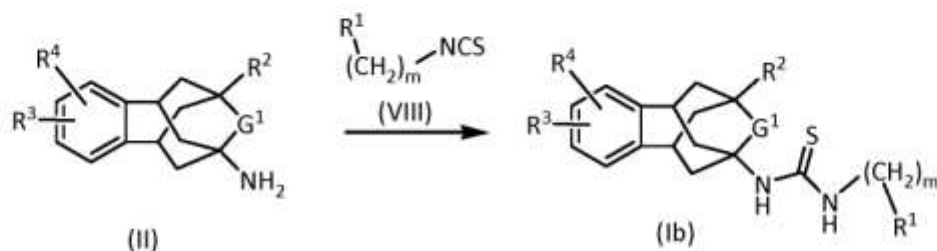
10

- According to another aspect of the present invention, the compounds of formula (Ib), wherein G² is sulfur, G³ is $-NH-(CH_2)_m-$, may be prepared by converting in a first step the amine of formula (II) preferably in the form of a salt, into a dithiocarbamate salt of formula (VI) by reaction with carbon disulfide in an inert solvent, such as THF, in the presence of a base, such as triethylamine. In a second step, the dithiocarbamate salt is decomposed in the presence of tosyl chloride to yield the isothiocyanate of formula (VII) which is subsequently reacted with an amine of formula $R^1-(CH_2)_m-NH_2$ of formula (V) to yield compound of formula (Ib).

12

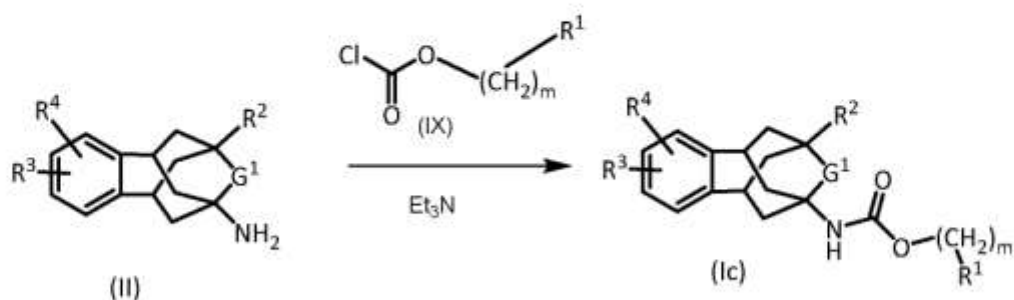


- According to another aspect of the present invention, the compounds of formula (Ib) wherein G² is sulphur and G³ is -NH-(CH₂)_m- may also be prepared by reacting the amine of formula (II), preferably in the form of a salt such as the hydrochloride with thioisocyanate of formula SCN-(CH₂)_m-R¹ (VIII), in an inert solvent, such as DCM, and in the presence of a base such as triethylamine.

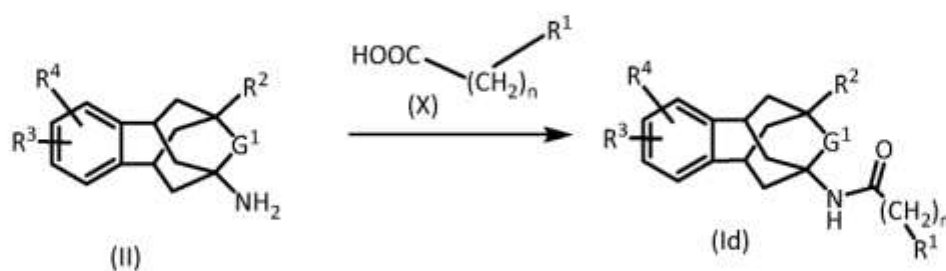


- According to another aspect of the present invention, the compounds of formula (Ic), wherein G² and G³ are both oxygen, may be prepared by reacting the amine of formula (II) with the chloroformate of formula (IX) in the presence of a base such as triethylamine.

13



- According to another aspect of the present invention, the compounds of formula (Id), wherein G² is oxygen and G³ is -(CH₂)_n-, may be prepared by reacting the amine of formula (II), preferably in the form of a salt such as the hydrochloride, with a carboxylic acid of formula (X) in the presence of a coupling agent such as EDCI or HOBt or using an acyl chloride in the presence of a base, such as triethylamine, in an organic solvent such as ethyl acetate.

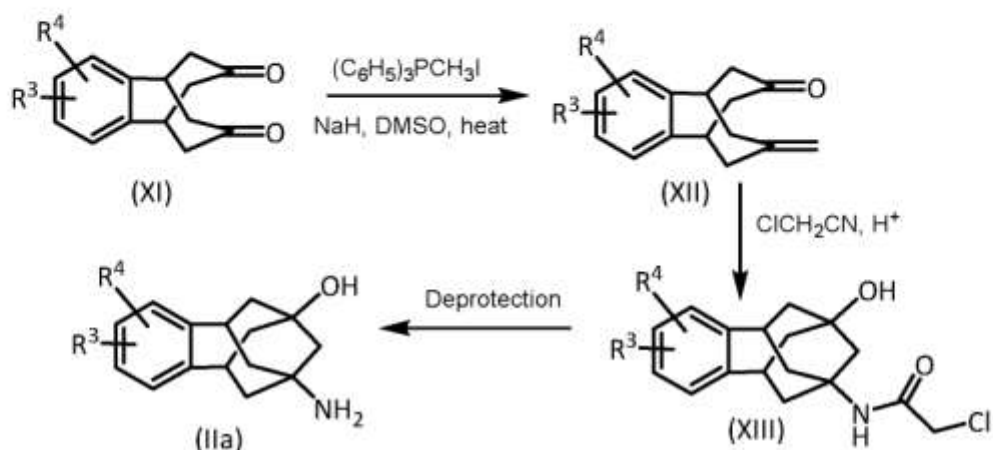


- 10 The amines of formula (II) may be obtained using a range of different reactions depending on the nature of the substituents G¹, R², R³ and R⁴ and some amines of formula (II) are disclosed in the art (see for example *Bioorg Med Chem.* 2010, 18, 46; *Bioorg Med Chem.* 2012, 20, 942; *Bioorg Med Chem.* 2014, 22, 2678; *Bioorg Med Chem.* 2015, 23, 290).

15

When G¹ is CH₂ and R² is OH the amines of formula (IIa) may be prepared according to the reaction scheme shown below:

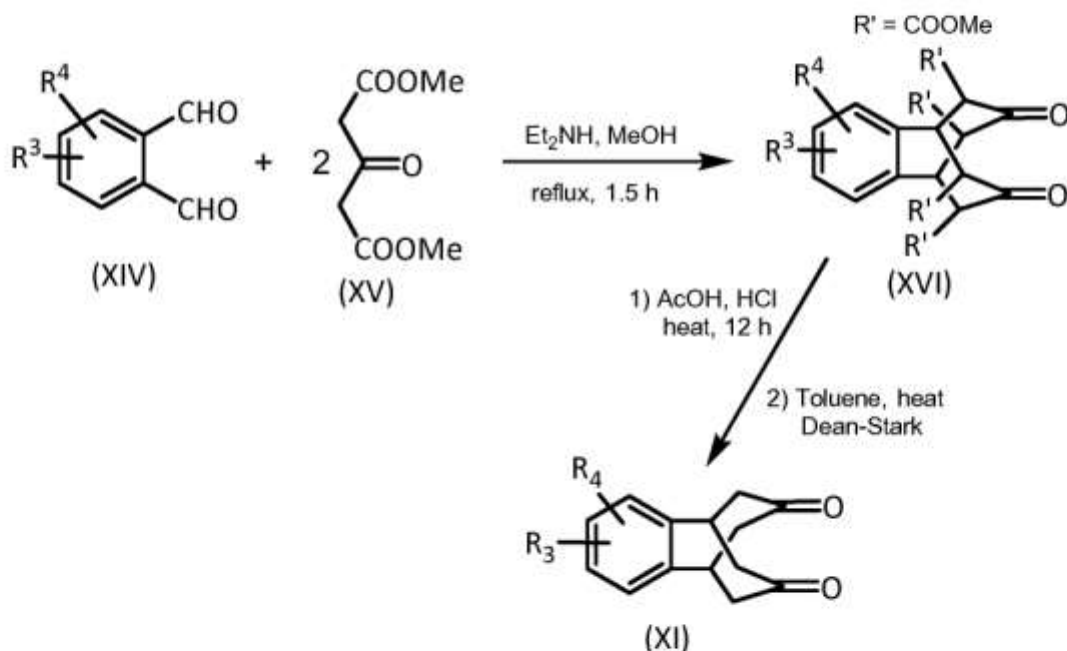
20



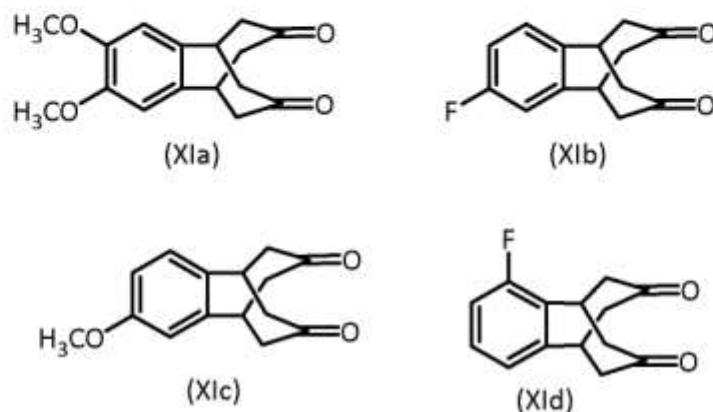
The deprotection step of the chloroacetamide to yield the final amine (IIa) may be carried out by refluxing overnight the compound (XIII) in the presence of thiourea and acetic acid in ethanol.

5

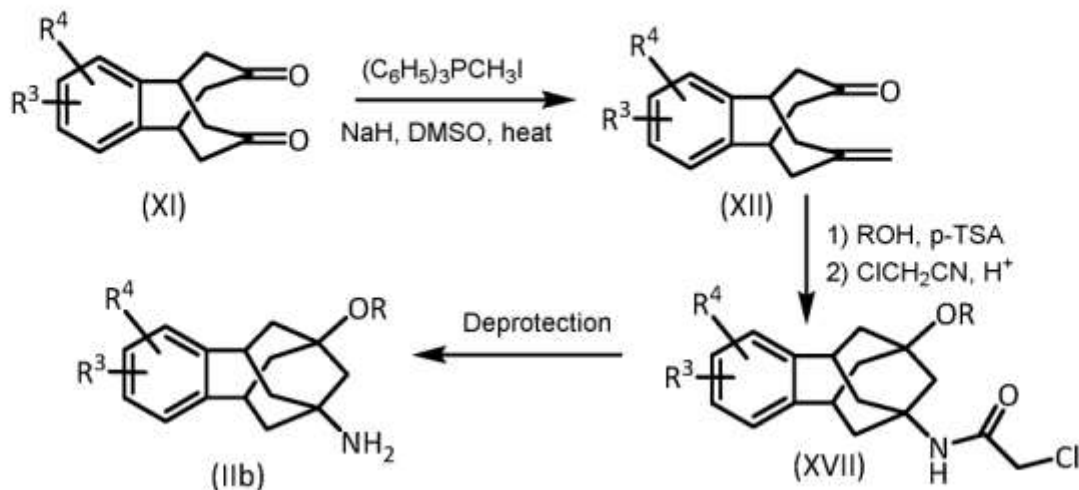
Diketone (XI) is a known compound when $R^3 = R^4 = H$ (*Liebigs Ann Chem.* 1973; 1839-1850). In general, substituted diketones of formula (XI) may be prepared from substituted *o*-phthalaldehydes (XIV) according to the reaction scheme shown below.

10 Starting from suitably substituted *o*-phthalaldehyde derivatives of formula (XIV) and

following the reaction scheme shown above, it is also possible to prepare diketones (XI) with different substituents such as those shown below:



When G^1 is CH_2 and R^2 is $\text{C}_1\text{-C}_6$ alkoxy the amines of formula (IIb) may be prepared according to the reaction scheme shown below:



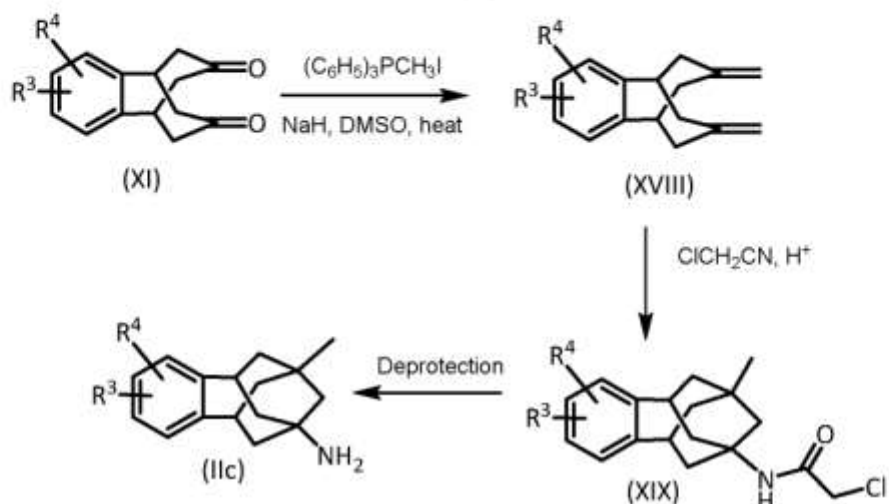
wherein R is C_{1-6} alkyl

5

The deprotection step of the chloroacetamide to yield the final amine (IIb) may be carried out by refluxing overnight the compound (XVII) in the presence of thiourea and acetic acid in ethanol.

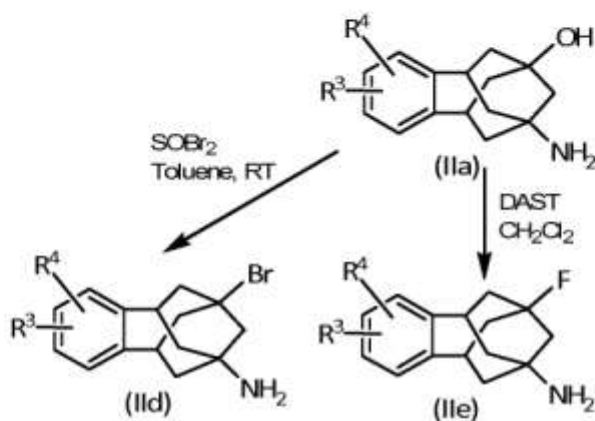
10 When G^1 is CH_2 and R^2 is methyl the amines of formula (IIc) may be prepared according to the reaction scheme shown below:

16

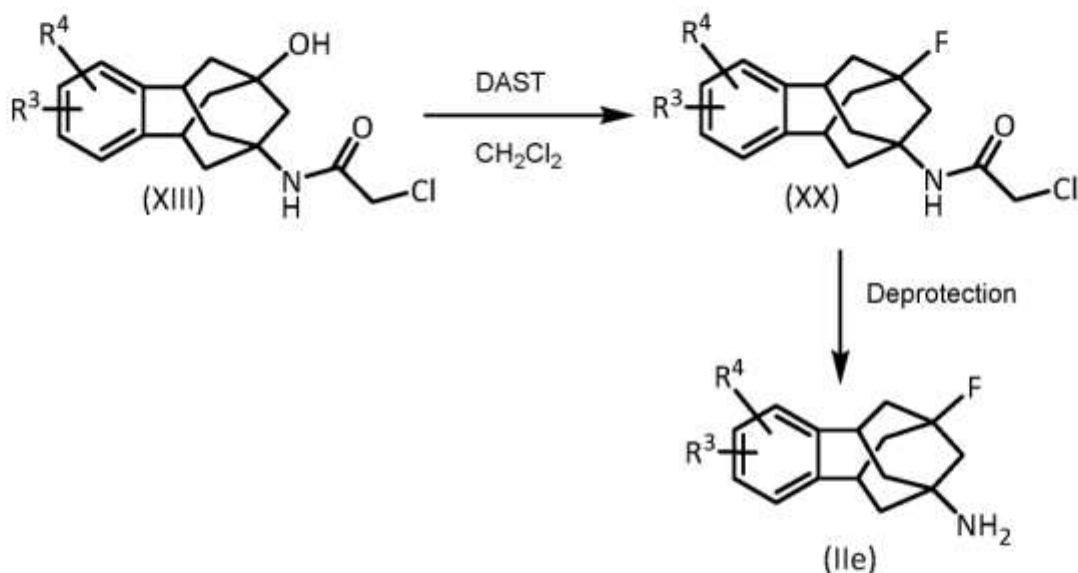


The deprotection step of the chloroacetamide to yield the final amine (IIc) may be carried out by refluxing overnight the compound (XIX) in the presence of thiourea and acetic acid in ethanol.

- 5 When G¹ is CH₂ and R² is bromine or fluorine the amines of formula (II d) and (II e) may be prepared according to the reaction scheme shown below:

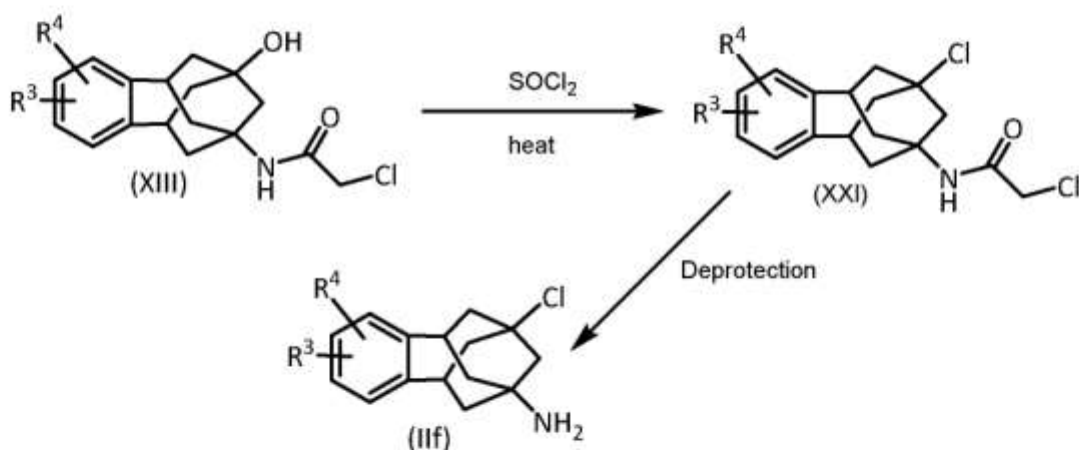


Alternatively, the amine (Ile) may be obtained starting from compound (XIII) according to the scheme below:



- The deprotection step of the chloroacetamide to yield the final amine (Ile) may be carried out by refluxing overnight the compound (XX) in the presence of thiourea and acetic acid in ethanol.
- 5

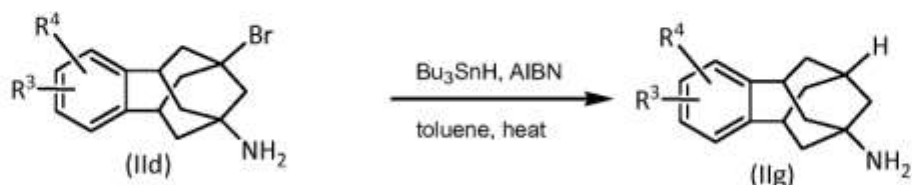
When G^1 is CH_2 and R^2 is chlorine the amines of formula (IIf) may be prepared according to the reaction scheme shown below:



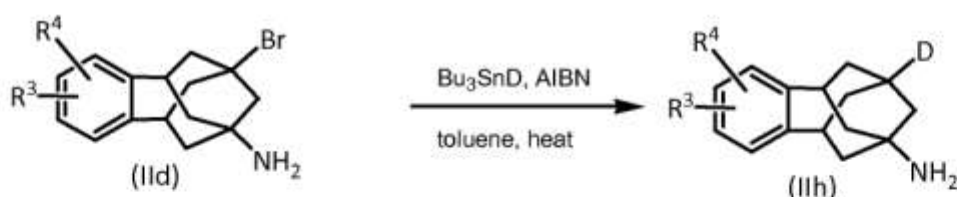
- 10 The deprotection step of the chloroacetamide to yield the final amine (IIf) may be carried out by refluxing overnight the compound (XXI) in the presence of thiourea and acetic acid in ethanol.

When G^1 is CH_2 and R^2 is hydrogen the amines of formula (IIg) may be prepared

according to the reaction scheme shown below:

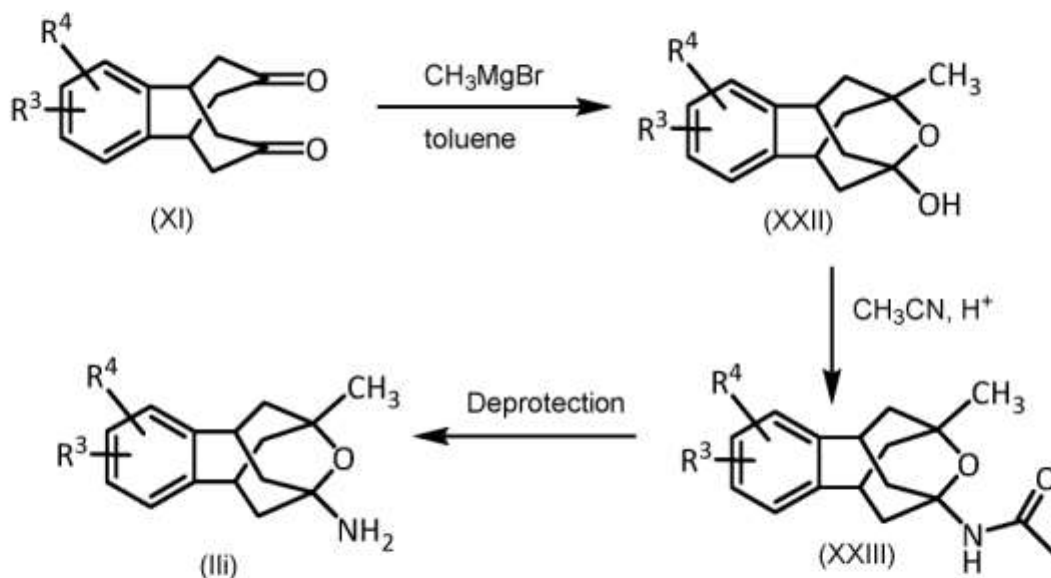


- 5 When G¹ is CH₂ and R² is deuterium the amines of formula (IIh) may be prepared according to the reaction scheme shown below:



When G¹ is O and R² is methyl the amines of formula (III) may be prepared according to the reaction scheme shown below:

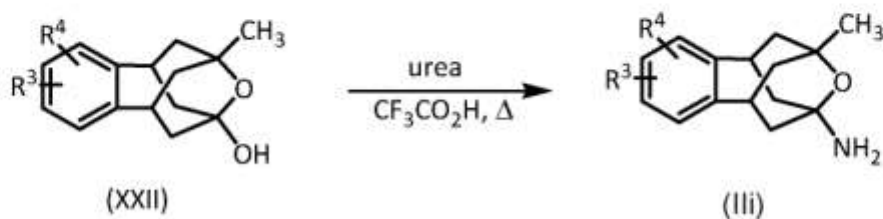
10



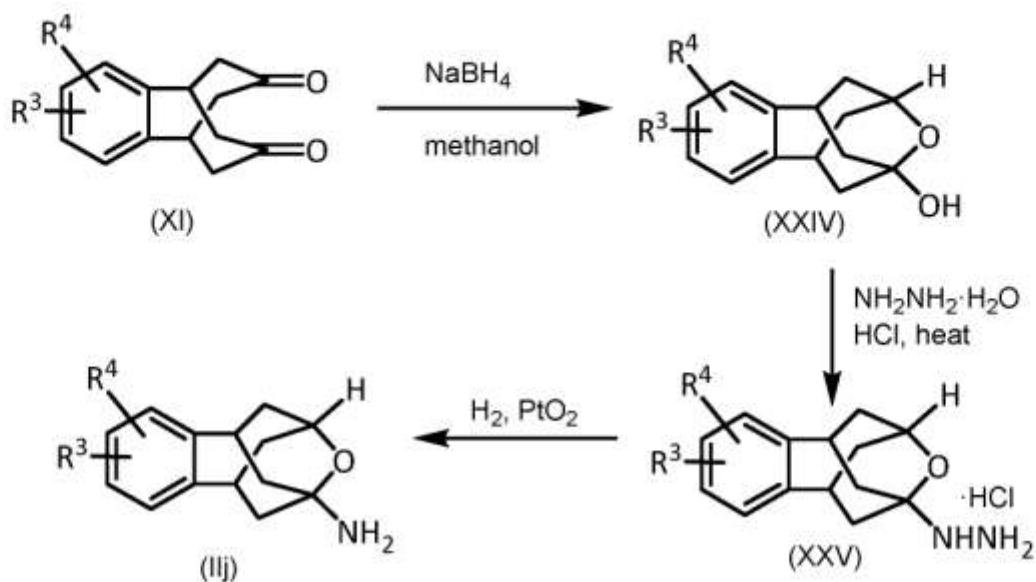
The deprotection step of the acetamide to yield the final amine (III) may be carried out by refluxing overnight the compound (XXIII) in the presence of conc. HCl as reported for R³ = R⁴ = H in *Bioorg Med Chem* 2010, 18, 46-57.

15

Alternatively, when G^1 is O and R^2 is methyl the amines of formula (Iii) may be prepared according to the reaction scheme shown below:

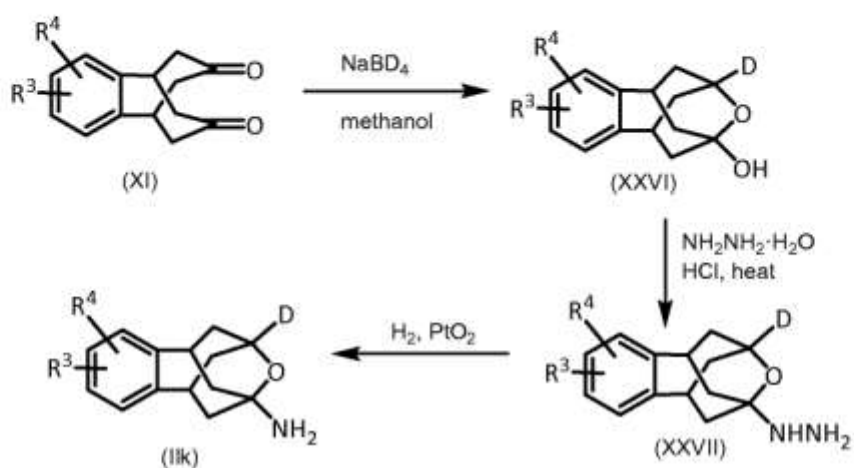


- 5 When G^1 is O and R^2 is hydrogen the amines of formula (Iij) may be prepared according to the reaction scheme shown below:



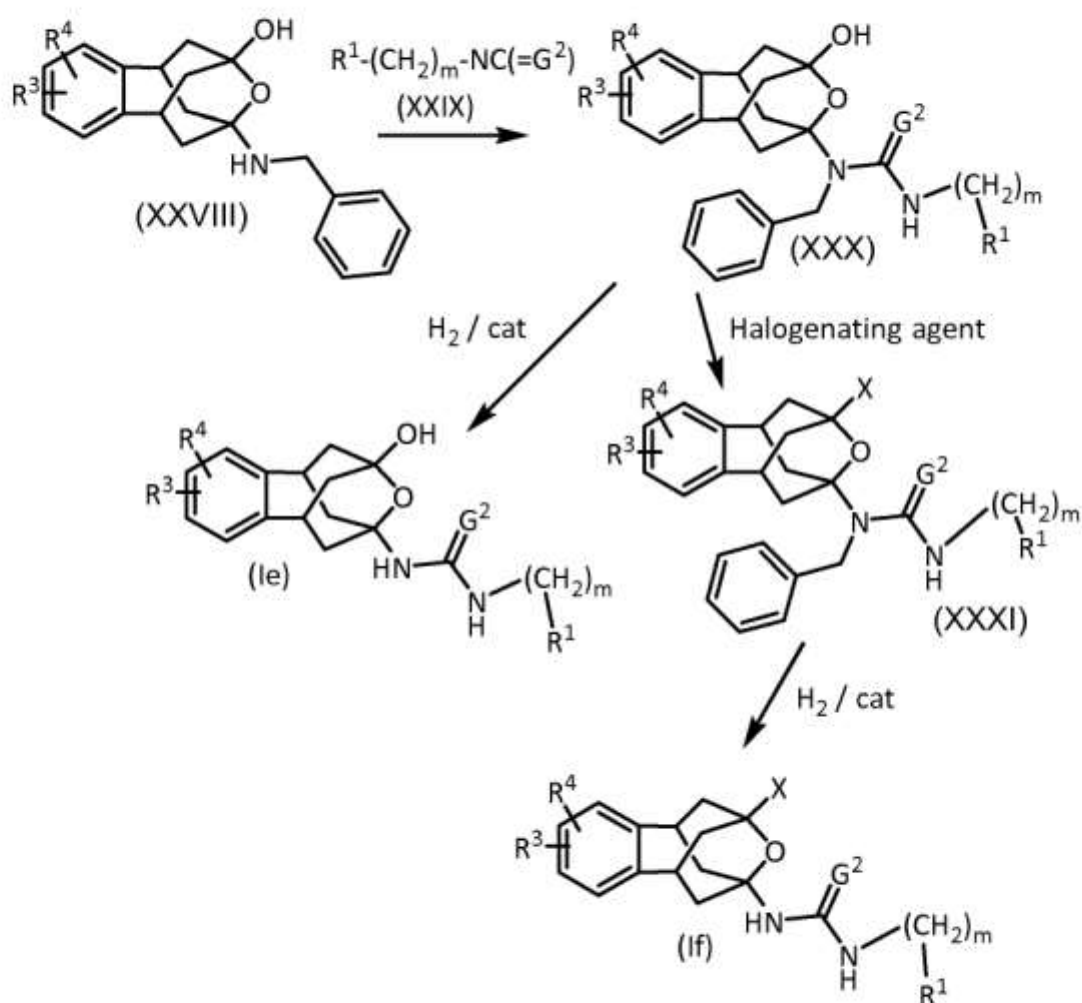
- 10 When G^1 is O and R^2 is deuterium the amines of formula (Iik) may be prepared according to the reaction scheme shown below:

20



When G^1 is O and R^2 is a halogen or a hydroxyl group the compounds of formula (Ie) and (If) may be prepared according to the reaction scheme shown below:

5



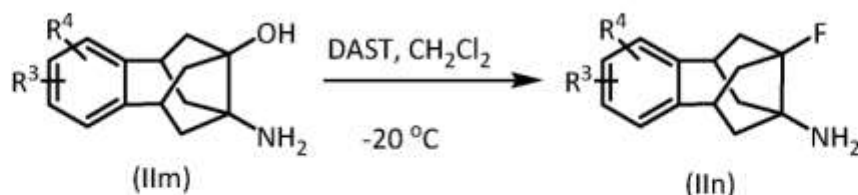
When X is fluorine in the second step compound (XXX) is converted to compound (XXXI) using (diethylamino)sulfur trifluoride (DAST) as halogenating agent, when X is chlorine the halogenating agent is SOCl_2 and when X is bromine the halogenating agent is SOBr_2 .

5

The preparation of compound (XXVIII) is described from compound (XI) (for $\text{R}^3=\text{R}^4=\text{H}$) in patent application DE 2 210 799 A1. The synthetic process described therein may be also used for the preparation of compounds where R^3 and/or R^4 are different from hydrogen.

10

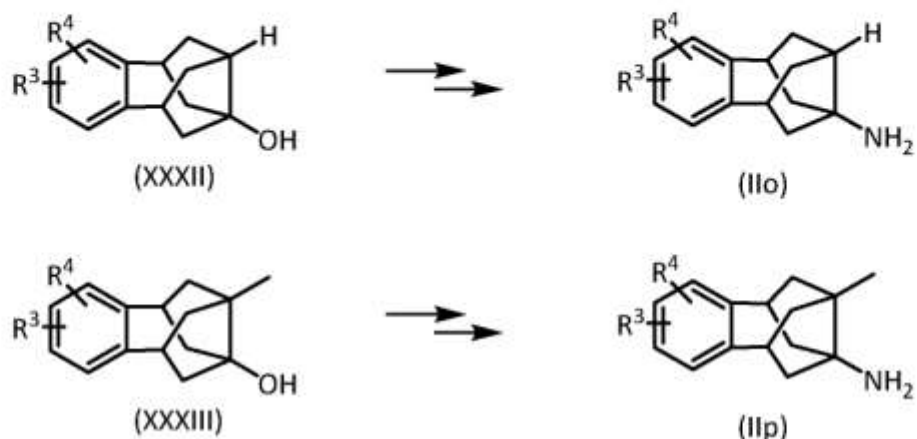
When G^1 is a bond and R^2 is a fluorine the compounds of formula (II n) may be prepared according to the reaction scheme shown below:



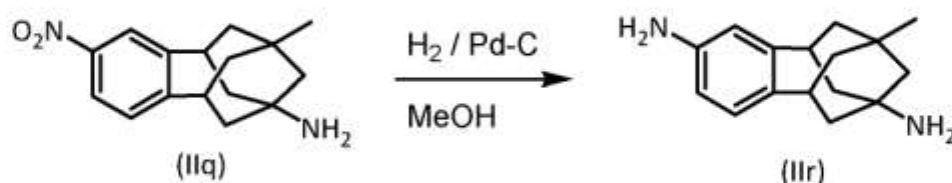
The preparation of compound (II m) is described (for $\text{R}^3=\text{R}^4=\text{H}$) in *Liebigs Ann.* 1995, 523-535. The synthetic process described therein may be also used for the preparation of compounds where R^3 and/or R^4 are different from hydrogen.

Compounds of formula (II o) and (II p) may be prepared, respectively, from compounds (XXXII) and (XXXIII) through one or more well-known reactions. Compounds (XXXII) and (XXXIII) are synthesized from compounds of formula (XI) according to methods reported in the literature for $\text{R}^3=\text{R}^4=\text{H}$ (*Liebigs Ann Chem.* 1973; 1839-1850 and *Aust J Chem.* 1983, 36, 2465-2472) which methods may also be used for the preparation of compounds where R^3 and/or R^4 are different from hydrogen.

22



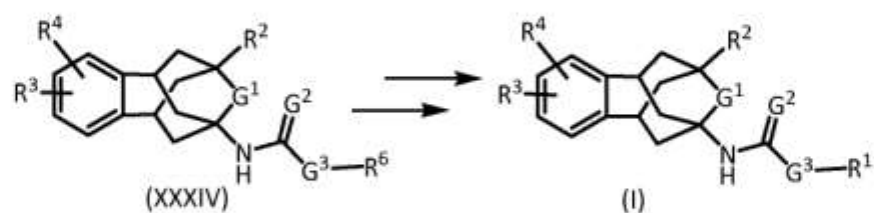
It is also possible to convert some compounds of formula (II) to other compounds of formula (II) by modifying the nature of the groups R³ and R⁴ by conventional methods known to the person skilled in the art. As an example, compound of formula (IIq) may be converted to compound of formula (IIr) by catalytic hydrogenation.



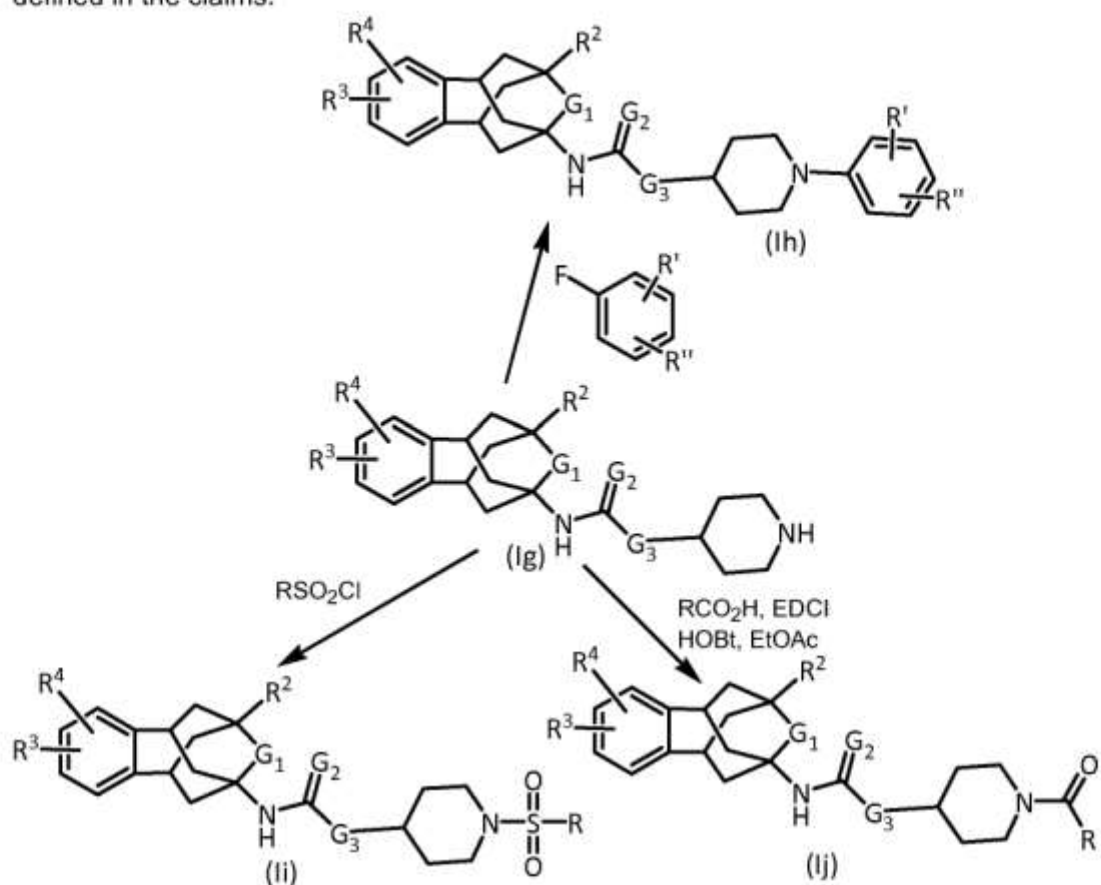
It is worth mentioning that it is possible to convert some compounds of formula (I) of the invention to other compounds of formula (I) by modifying the nature of the groups R³ and R⁴ by conventional methods known to the person skilled in the art. As an example, compounds of formula (I) wherein R³ and R⁴ are hydrogen atoms may be converted to compounds where one R³ and R⁴ is hydrogen and the other one is a C₁₋₆ acyl group through a Friedel-Craft reaction. As another example compounds of formula (I) wherein R³ and/or R⁴ are a nitro group may be converted to compounds where said R³ and/or R⁴ is an amino group by catalytic hydrogenation.

Finally, it is worth mentioning that the compounds of the invention may also be prepared following the methods explained above from precursors of formula (XXXIV) wherein the rest R⁶ is a precursor of the rest R¹ which is converted into said rest R¹ through one or more well-known reactions. It is also possible that the rest R⁶ is already a group R¹ which is converted into another group R¹ through one or more well-known reactions.

23



Examples of said synthetic strategy are provided below wherein the group R^6 is an unsubstituted piperidinyl rest and R^1 is a piperidinyl rest carrying substituents as defined in the claims:



5

The reaction of compound (I) to yield compound (Ih) is carried out using K_2CO_3 and anhydrous DMSO applying heat. The reaction of compound (I) to yield compound (Ij) is carried out either as shown (RCO_2H , EDCl, HOBt, EtOAc) or using RCOCl and Et_3N in DCM.

10

In addition to the three kind of derivatives shown in the scheme above, it is also possible to go from the unsubstituted piperidine in (I) to benzyl piperidines. The procedure involves the reaction of the piperidine (I) with benzaldehydes and sodium

cyanoborohydride in acetic acid / methanol.

As used herein, the term methylene designates the radical $-(CH_2)-$.

- 5 As used herein the term aryl designates an aromatic carbocyclic ring which may be unsubstituted or substituted. Non-limiting examples of unsubstituted aryl groups are phenyl and anthranyl.

- As used herein the term halogen atoms designates atoms selected from the group consisting of chlorine, fluorine, bromine and iodine atoms, preferably fluorine, chlorine or bromine atoms. The term halo when used as a prefix has the same meaning.
- 10

- As used herein the term C_p acyl designates a group alkyl having $p-1$ carbon atoms which is linked to a carbonyl group ($CH_3-(CH_2)_{p-2}-CO-$). Non limiting examples of acyl groups are acetyl, propionyl, butyryl, valeryl and caproyl.
- 15

- As used herein the term C_q alkyl designates linear or branched hydrocarbon radicals ($C_qH_{2q+1}-$). Non-limiting examples of alkyl groups are methyl, ethyl, *n*-propyl *i*-propyl, *n*-butyl, *i*-butyl, *sec*-butyl, *tert*-butyl, *n*-pentyl, *i*-pentyl and *n*-hexyl.
- 20

- As used herein the term mono- C_r -alkylamino designates a C_r -alkyl linked to a group NH (C_r -alkyl-NH-). Non-limiting examples of monoalkylamino groups are methylamino (CH_3-NH-), ethylamino (CH_3-CH_2-NH-) and *n*-propylamino ($CH_3-CH_2-CH_2-NH-$).

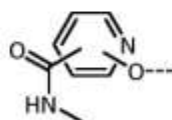
- 25 As used herein the term di- C_s -alkylamino designates two alkyl rest linked to a group N ($(C_s$ -alkyl) $_2$ -N-) wherein the two alkyl rests may have the same or different number of carbon atoms. Non-limiting examples of dialkylamino groups are dimethylamino ($(CH_3)_2NH-$), diethylamino ($(CH_3-CH_2)_2N-$), ethylmethylamino ($(CH_3)(CH_3-CH_2)N-$) and di-*n*-propylamino ($(CH_3-CH_2-CH_2)_2N-$).

- 30 As used herein the term C_l alkoxy designates a linear or branched alkyl group linked to an oxygen atom ($CH_3-(CH_2)_{l-1}-O-$). Non-limiting examples of alkoxy groups are methoxy, ethoxy, *n*-propoxy, *i*-propoxy, *n*-butoxy, *i*-butoxy, *sec*-butoxy, *tert*-butoxy, *n*-pentoxy, *i*-pentoxy and *n*-hexoxy.

- 35 As used herein the term C_u alkoxy carbonylmethyl designates a C_u alkoxy rest linked to a group $-CO-CH_2-$ ($(CH_3-(CH_2)_{u-1})-O-CO-CH_2-$). Non-limiting examples of

alkoxycarbonylmethyl groups are methoxycarbonylmethyl and ethoxycarbonylmethyl.

As used herein the term methylaminocarbonylpyridyloxy is used to designate the group:



5

As used herein the term heteroaryl designates an heteroaromatic ring containing carbon, hydrogen and one or more heteroatoms selected from N, O and S as part of the ring. Said radicals may be unsubstituted or substituted by one or more substituents. Non-limiting examples of heteroaryl groups are pyridyl, pyrimidinyl, furyl, thienyl, pyrazolyl, oxazolyl and thiazolyl.

10

As used herein the term saturated or partially unsaturated heterocyclyl is used to designate a non-aromatic ring containing carbon, hydrogen and one or more heteroatoms selected from N, O and S as part of the ring. In particular, an heterocyclyl group may be monocyclic or bicyclic. Non-limiting examples of saturated heterocyclyl groups are piperidinyl, morpholinyl, tetrahydropyranyl and piperazinyl.

15

As used herein the term cycloalkyl designates hydrocarbon cyclic groups. Said cycloalkyl groups may have a single cyclic ring or a polycyclic ring. Non-limiting examples of cycloalkyl groups are cyclopropyl, cyclobutyl, cyclopentyl and cyclohexyl.

20

As used herein the term alkylsulfonyl designates a linear or branched alkyl group linked to a sulfonyl group ($\text{CH}_3\text{-(CH}_2\text{)}_{n-1}\text{-SO}_2\text{-}$). Non-limiting examples of alkylsulfonyl groups are methylsulfonyl ($\text{CH}_3\text{-SO}_2\text{-}$), ethylsulfonyl ($\text{CH}_3\text{-CH}_2\text{-SO}_2\text{-}$) and *n*-propylsulfonyl ($\text{CH}_3\text{-CH}_2\text{-CH}_2\text{-SO}_2\text{-}$).

25

As used herein the term cycloalkylsulfonyl designates a cycloalkyl group linked to a sulfonyl group. Non-limiting examples of cycloalkylsulfonyl groups are cyclopropylsulfonyl, cyclobutylsulfonyl, cyclopentylsulfonyl and cyclohexylsulfonyl.

30

As used herein the term arylsulfonyl designates an aryl group linked to a sulfonyl group. Non-limiting examples of arylsulfonyl groups are phenylsulfonyl and naphthalenesulfonyl.

As used herein the term pyridincarbonyl designates a pyridyl group linked to a carbonyl group (C₅H₄N-CO-).

- 5 As used herein the term phenylcarbonyl designates a phenyl group linked to a carbonyl group (C₆H₅-CO-).

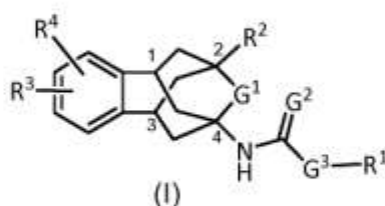
As used herein the term tetrahydropyrancarboxyl designates a tetrahydropyranyl group linked to a carbonyl group (C₅H₉O-CO-).

10

- As used herein the term pharmaceutically acceptable salt designates any salt which, upon administration to the patient is capable of providing (directly or indirectly) a compound as described herein. For instance, pharmaceutically acceptable salts of compounds provided herein are synthesized from the parent compound, which
- 15 contains a basic or acidic moiety, by conventional chemical methods. Generally, such salts are, for example, prepared by reacting the free acid or base forms of these compounds with a stoichiometric amount of the appropriate base or acid in water or in an organic solvent or in a mixture of both. Generally, non-aqueous media like ether, ethyl acetate, ethanol, 2-propanol or acetonitrile are preferred. Examples of the acid
- 20 addition salts include mineral acid addition salts such as, for example, hydrochloride, hydrobromide, hydroiodide, sulfate, nitrate, phosphate, and organic acid addition salts such as, for example, acetate, trifluoroacetate, maleate, fumarate, citrate, oxalate, succinate, tartrate, malate, mandelate, methanesulfonate and *p*-toluenesulfonate. Examples of the alkali addition salts include inorganic salts such as, for example,
- 25 sodium, potassium, calcium and ammonium salts, and organic alkali salts such as, for example, ethylenediamine, ethanolamine, *N,N*-dialkyl ethanolamine, triethanolamine and basic aminoacids salts.

- As used herein the term stereoisomers designates molecules that have the same
- 30 molecular formula and sequence of bonded atoms (constitution), but differ in the three-dimensional orientations of their atoms in space. The compounds of formula (I) have at least two chiral carbon atoms (marked as 1 and 3 in the formula depicted below) and, thus, several stereoisomers of said compounds may exist. Said stereoisomers are encompassed by formula (I).

27



Throughout the description and claims the word "comprise" and variations of the word, are not intended to exclude other technical features, additives, components, or steps. Furthermore, the word "comprise" encompasses the case of "consisting of". Additional objects, advantages and features of the invention will become apparent to those skilled in the art upon examination of the description or may be learned by practice of the invention. The following examples are provided by way of illustration, and they are not intended to be limiting of the present invention. Furthermore, the present invention covers all possible combinations of particular and preferred embodiments described herein.

5

10

ABREVIATIONS:

The following abbreviations have been used along the present application:

15	anh.:	anhydrous
	AcOH:	acetic acid
	AcCl:	acetyl chloride
	AIBN:	azobisisobutyronitrile
	Bis/Tris:	2-Bis(2-hydroxyethyl)amino-2-(hydroxymethyl)-1,3-propanediol
20	BSA:	bovine serum albumin
	Bu ₃ SnD:	tributyl(deuterio)stannane
	Calcd:	calculated
	d:	doublet
	DAST:	diethylaminosulfur trifluoride
25	Dec:	decomposes
	DCM:	dichloromethane
	DMF:	<i>N,N</i> -dimethylformamide
	DMSO:	dimethylsulfoxide
	dq	doublet of quartets
30	dt	doublet of triplets
	EDCI:	1-ethyl-3-(3-dimethylaminopropyl)carbodiimide
	ESI:	electrospray ionization
	Et ₂ O:	diethylether

	Et ₃ N:	triethylamine
	EtOAc:	ethyl acetate
	EtOH:	ethanol
	HOBt:	hydroxybenzotriazole
5	h:	hours
	Hz	Hertz
	HRMS:	high resolution mass spectroscopy
	IR:	infrared
	m:	multiplet
10	MeOH:	methanol
	mp:	melting point
	<i>n</i> -Bu:	<i>n</i> -butyl
	NMR:	nuclear magnetic resonance
	NSAID:	non steroidal anti-inflammatory drug
15	<i>p</i> -TSA:	<i>p</i> -toluenesulfonic acid
	PHOME:	cyano(6-methoxynaphthalen-2-yl)methyl 2-(3-phenyloxiran-2-yl)acetate
	s:	singlet
	sEH:	soluble epoxide hydrolase
	t:	triplet
20	THF:	tetrahydrofuran
	TPPU:	<i>N</i> -[1-(1-Oxopropyl)-4-piperidiny]- <i>N'</i> -[4-(trifluoromethoxy)phenyl]urea
	UV:	ultraviolet

EXAMPLES

25

Analytical methods

- Melting points were determined in open capillary tubes with a MFB 595010 M Gallenkamp melting point apparatus.
- Infrared (IR) spectra were run either on a Perkin-Elmer Spectrum RX I
30 spectrophotometer (using the attenuated total reflectance technique) or on a spectrophotometer Nicolet Avatar 320 FT-IR. Absorption values are expressed as wavenumbers (cm⁻¹); only significant absorption bands are given.
- Elemental analyses were carried out at the Microanalysis Service of the IIQAB (CSIC, Barcelona, Spain) with a Carlo Erba model 1106 analyzer.
- 35 - Preparative normal phase chromatography was performed on a CombiFlash Rf 150 (Teledyne Isco) with pre-packed RediSep Rf silica gel cartridges. Thin-layer chromatography was performed with aluminum-backed sheets with silica gel 60 F254

(Merck, ref 1.05554 or Sigma-Aldrich, ref 60805), and spots were visualized with UV light, 1% aqueous solution of KMnO_4 and/or iodine.

- High-resolution mass spectrometry (HRMS) analyses were performed with an LC/MSD TOF Agilent Technologies spectrometer.

5 - Analytical grade solvents were used for crystallization, while pure for synthesis solvents were used in the reactions, extractions and column chromatography.

- The analytical samples of all of the new compounds which were subjected to pharmacological evaluation possess a purity $\geq 95\%$ as evidenced by their elemental analysis.

10

Reference example 1: 2-fluoro-5,6,8,9-tetrahydro-7H-5,9-propanobenzo[7]annulene-7,11-dione.

In a round-bottomed flask equipped with a condenser and magnetic stirring a solution of 4-fluorophthalaldehyde (3.08 g, 20 mmol) and dimethyl 3-oxopentanedioate (6.98 g, 40 mmol) in MeOH (60 mL) was prepared. Four drops of diethylamine were added and the reaction was heated at reflux for 1.5 h, the reaction was cooled down and 7 drops more of diethylamine were added and the reaction was stored at 4°C overnight. The precipitate was filtered off under vacuum and was washed with cold MeOH (4 mL), obtaining tetramethyl 2-fluoro-7,11-dioxo-6,7,8,9-tetrahydro-5H-5,9-propanobenzo[7]annulene-6,8,10,12-tetracarboxylate as white needles (3.05 g). A solution of this solid in glacial acetic acid (18 mL) and conc. HCl (5 mL) was heated at reflux for 12 h. The solvent was removed under vacuum to give a solid. A solution of this solid in toluene (50 mL) was heated a reflux for 16 h in a Dean-Stark apparatus. The toluene was removed under vacuum to give pure 2-fluoro-5,6,8,9-tetrahydro-7H-5,9-propanobenzo[7]annulene-7,11-dione (1.53 g, 33% overall yield) as a light brown solid. mp 105-107 °C. IR (NaCl disk): 2923, 2848, 1710, 1607, 1593, 1490, 1428, 1380, 1346, 1253, 1208, 1119, 1074, 985, 944, 865, 806 cm^{-1} . HRMS-ESI+ m/z $[\text{M}+\text{H}]^+$ calcd for $[\text{C}_{14}\text{H}_{13}\text{FO}_2+\text{H}]^+$: 233.0972, found: 233.0967.

30 **Reference example 2: 2-methoxy-5,6,8,9-tetrahydro-7H-5,9-propanobenzo[7]annulene-7,11-dione:**

From 4-methoxyphthalaldehyde (10.2 g, 61.9 mmol), dimethyl 3-oxopentanedioate (21.5 g, 124 mmol) and diethylamine (28 drops) in MeOH (380 mL) and following the procedure described in reference example 1, tetramethyl 2-methoxy-7,11-dioxo-6,7,8,9-tetrahydro-5H-5,9-propanobenzo[7]annulene-6,8,10,12-tetracarboxylate was obtained (19.4 g, 66% yield). From the aforementioned tetracarboxylate (250 mg, 0.5 mmol), conc. HCl (0.4 mL) and glacial acetic acid (1.4 mL) and following the procedure

described in reference example 1, 2-methoxy-5,6,8,9-tetrahydro-7*H*-5,9-propanobenzo[7]annulene-7,11-dione (125 mg, 98% yield) was obtained.
mp 157-158 °C. IR (NaCl disk): 2941, 2910, 2837, 1701, 1610, 1585, 1504, 1431, 1414, 1370, 1321, 1300, 1266, 1166, 1094, 1033, 989 cm⁻¹. HRMS-ESI+ m/z [M+H]⁺
5 calcd for [C₁₅H₁₆O₃+H]⁺: 245.1172, found: 245.1180.

Reference example 3: 2,3-dimethoxy-5,6,8,9-tetrahydro-7*H*-5,9-propanobenzo[7]annulene-7,11-dione:

From 4,5-dimethoxyphthalaldehyde (6.54 g, 33.7 mmol), dimethyl 3-oxopentanedioate
10 (11.7 g, 67.4 mmol) and diethylamine (19 drops) in MeOH (130 mL) and following the procedure described in reference example 1, tetramethyl 2,3-dimethoxy-7,11-dioxo-6,7,8,9-tetrahydro-5*H*-5,9-propanobenzo[7]annulene-6,8,10,12-tetracarboxylate was obtained (6.84 g, 40% yield). From the aforementioned tetracarboxylate (6.84 g, 13.5 mmol), conc. HCl (10 mL) and glacial acetic acid (35 mL), and following the procedure
15 described in reference example 1, 2,3-dimethoxy-5,6,8,9-tetrahydro-7*H*-5,9-propanobenzo[7]annulene-7,11-dione (2.8 g, 76% yield) was obtained.
mp 236-237 °C. IR (NaCl disk): 2952, 2840, 1698, 1605, 1516, 1467, 1451, 1416, 1355, 1336, 1254, 1221, 1192, 1162, 1025, 1002, 880, 811 cm⁻¹. HRMS-ESI+ m/z [M+H]⁺ calcd for [C₁₆H₁₈O₄+H]⁺: 275.1278, found: 275.1279.

20

Reference example 4: 1-fluoro-5,6,8,9-tetrahydro-7*H*-5,9-propanobenzo[7]annulene-7,11-dione.

From 3-fluorophthalaldehyde (11.2 g, 73.6 mmol), dimethyl 3-oxopentanedioate (25.6 g, 147 mmol) and diethylamine (33 drops) in MeOH (220 mL) and following the
25 procedure described in reference example 1, tetramethyl 1-fluoro-7,11-dioxo-6,7,8,9-tetrahydro-5*H*-5,9-propanobenzo[7]annulene-6,8,10,12-tetracarboxylate was obtained (18.5 g, 54% yield). The aforementioned tetracarboxylate (18.5 g, 39.9 mmol), conc. HCl (31 mL) and glacial acetic acid (103 mL), and following the procedure described in reference example 1, 1-fluoro-5,6,8,9-tetrahydro-7*H*-5,9-propanobenzo[7]annulene-
30 7,11-dione was obtained (8.73 g, 94% yield).
mp > 150 °C (dec.). IR (NaCl disk): 2940, 2908, 1701, 1619, 1585, 1468, 1421, 1370, 1303, 1245, 1222, 1203, 1072, 1052, 988, 931, 897, 789, 746 cm⁻¹. HRMS-ESI+ m/z [M+H]⁺ calcd for [C₁₄H₁₃FO₂+H]⁺: 233.0972, found: 233.0976.

35 **Reference example 5: 2-fluoro-7,11-dimethylene-6,7,8,9-tetrahydro-5*H*-5,9-propanobenzo[7]annulene.**

In a 3-necked round-bottomed flask equipped with magnetic stirring and argon atmosphere, a suspension of NaH (1.08 g, 60 % purity, 27.0 mmol) in anhydrous DMSO (13.3 mL) was heated at 75 °C over 45 min. The green suspension was cooled down to room temperature and methyltriphenylphosphonium iodide (10.92 g, 27.0 mmol) diluted in anhydrous DMSO (22 mL) and 2-fluoro-5,6,8,9-tetrahydro-7*H*-5,9-propanobenzo[7]annulene-7,11-dione (1.53 g, 6.59 mmol) diluted in anhydrous DMSO (50 mL) were sequentially added. The resulting mixture was heated at 90 °C overnight. The reaction was cooled down and poured into water (80 mL). The aqueous layer was extracted with hexane (4 x 80 mL). The combined organic extracts were dried over anh. Na₂SO₄, filtered and concentrated under vacuum. Column chromatography (SiO₂, Hexane/Ethyl Acetate mixtures) gave 2-fluoro-7,11-dimethylene-6,7,8,9-tetrahydro-5*H*-5,9-propanobenzo[7]annulene as a colorless wax (1.09, 73% yield).
mp 108-109 °C. IR (NaCl disk): 3072, 2985, 2921, 2844, 1639, 1612, 1592, 1494, 1451, 1444, 1363, 1246, 1162, 1135, 1095, 1048, 974, 951, 930, 887, 820, 716, 658, 638, 598, 528 cm⁻¹.

Reference example 6: 2-methoxy-7,11-dimethylene-6,7,8,9-tetrahydro-5*H*-5,9-propanobenzo[7]annulene.

From 2-methoxy-5,6,8,9-tetrahydro-7*H*-5,9-propanobenzo[7]annulene-7,11-dione (4 g, 16.4 mmol) and following the procedure described in reference example 5, 2-methoxy-7,11-dimethylene-6,7,8,9-tetrahydro-5*H*-5,9-propanobenzo[7]annulene was obtained (1.5 g, 38 % yield).
mp 68-69°C. IR (NaCl disk): 3068, 2979, 2911, 2833, 1639, 1609, 1580, 1501, 1464, 1449, 1431, 1363, 1313, 1260, 1203, 1172, 1152, 1109, 1034, 955, 929, 889, 851, 809, 661, 613 cm⁻¹. HRMS-ESI+ m/z [M+H]⁺ calcd for [C₁₇H₂₀O+H]⁺: 241.1587, found: 241.1588.

Reference example 7: 2,3-dimethoxy-7,11-dimethylene-6,7,8,9-tetrahydro-5*H*-5,9-propanobenzo[7]annulene.

From 2,3-dimethoxy-5,6,8,9-tetrahydro-7*H*-5,9-propanobenzo[7]annulene-7,11-dione (2.8 g, 10.2 mmol) and following the procedure described in reference example 5, 2,3-dimethoxy-7,11-dimethylene-6,7,8,9-tetrahydro-5*H*-5,9-propanobenzo[7]annulene was obtained (633 mg, 23% yield).
mp 74-75 °C. IR (NaCl disk): 3068, 2977, 2913, 2832, 1639, 1606, 1515, 1464, 1450, 1429, 1414, 1358, 1342, 1293, 1261, 1240, 1225, 1191, 1173, 1103, 1023, 956, 931,

889, 804, 634 cm^{-1} . HRMS-ESI+ m/z $[M+H]^+$ calcd for $[\text{C}_{18}\text{H}_{22}\text{O}_2+\text{H}]^+$: 271.1693, found: 271.1688.

Reference example 8: 1-fluoro-7,11-dimethylene-6,7,8,9-tetrahydro-5H-5,9-propanobenzo[7]annulene.

- 5 From 1-fluoro-5,6,8,9-tetrahydro-7H-5,9-propanobenzo[7]annulene-7,11-dione (4 g, 17.2 mmol) and following the procedure described in reference example 5, 1-fluoro-7,11-dimethylene-6,7,8,9-tetrahydro-5H-5,9-propanobenzo[7]annulene was obtained as a colourless oil (2.69 g, 69% yield).
- 10 IR (NaCl disk): 3071, 2981, 2921, 2838, 1639, 1614, 1583, 1464, 1446, 1429, 1365, 1248, 1046, 991, 935, 919, 895 cm^{-1} . HRMS-ESI+ m/z $[M+H]^+$ calcd for $[\text{C}_{16}\text{H}_{17}\text{F}+\text{H}]^+$: 229.1387, found: 229.1392.

Reference example 9: 1-fluoro-7-methylene-6,7,8,9-tetrahydro-5H-5,9-propanobenzo[7]annulen-11-one

- 15 In a 3-necked round-bottomed flask equipped with magnetic stirring and argon atmosphere, a suspension of NaH (1.01 g, 60 % purity, 25.2 mmol) in anhydrous DMSO (50 mL) was heated at 75 °C over 45 min. The green suspension was cooled down to room temperature and methyltriphenylphosphonium iodide
- 20 (10.61 g, 25.33 mmol) diluted in anhydrous DMSO (58 mL) and 1-fluoro-5,6,8,9-tetrahydro-7H-5,9-propanobenzo[7]annulene-7,11-dione (4.72 g, 20.3 mmol, from reference example 4) diluted in anhydrous DMSO (50 mL) were sequentially added. The resulting mixture was heated at 90 °C overnight. The reaction was cooled down and poured into water (80 mL). The aqueous layer was extracted with hexane (5 x 80
- 25 mL). The combined organic extracts were dried over anh. Na_2SO_4 , filtered and concentrated under vacuum. Column chromatography (SiO_2 , Hexane/Ethyl Acetate mixtures) afforded 1-fluoro-7-methylene-6,7,8,9-tetrahydro-5H-5,9-propanobenzo[7]annulen-11-one (2.16, 55% yield).
- mp 96 °C. IR (ATR): 2927, 2913, 2895, 1688, 1613, 1583, 1432, 1406, 1366, 1247, 30 1196, 1104, 1049, 1034, 1002, 970, 921, 911, 883, 819, 789, 749, 715, 657 cm^{-1} . HRMS-ESI+ m/z $[M+H]^+$ calcd for $[\text{C}_{15}\text{H}_{15}\text{FO}+\text{H}]^+$: 231.1180, found: 231.1180.

Reference example 10: 2-chloro-N-(2-fluoro-9-methyl-5,6,8,9,10,11-hexahydro-7H-5,9:7,11-dimethanobenzo[9]annulen-7-yl)acetamide.

- 35 A suspension of 2-fluoro-7,11-dimethylene-6,7,8,9-tetrahydro-5H-5,9-propanobenzo[7]annulene (1.09 g, 4.77 mmol), chloroacetonitrile (1.2 mL, 19.1 mmol) and acetic acid (3.5 mL) was cooled to 0 °C and concentrated H_2SO_4 (1.53 mL, 28.6

- mmol) was added dropwise ($T < 10\text{ }^{\circ}\text{C}$). The mixture was allowed to reach room temperature and was stirred overnight. The suspension was added to ice (20 g) and after 10 min stirring, the suspension was extracted with DCM (3 x 15 mL). The combined organic layers were washed with NaOH 10 N (1 x 25 mL) and dried with anh.
- 5 Na_2SO_4 , filtered and concentrated under vacuum to obtain 2-chloro-*N*-(2-fluoro-9-methyl-5,6,8,9,10,11-hexahydro-7*H*-5,9:7,11-dimethanobenzo[9]annulen-7-yl)acetamide as a white solid (1.2 g, 78% yield).
mp 141-144 $^{\circ}\text{C}$. IR (NaCl disk): 3399, 3313, 3067, 2944, 2920, 2851, 1657, 1607, 1591, 1518, 1498, 1451, 1361, 1345, 1252, 1179, 1145, 966, 963, 863, 820 cm^{-1} .
- 10 HRMS-ESI+ m/z $[\text{M}+\text{H}]^+$ calcd for $[\text{C}_{18}\text{H}_{21}\text{ClFNO}+\text{H}]^+$: 322.1368, found: 322.1370.

Reference example 11: 2-chloro-*N*-(2-methoxy-9-methyl-5,6,8,9,10,11-hexahydro-7*H*-5,9:7,11-dimethanobenzo[9]annulen-7-yl)acetamide.

- From 2-methoxy-7,11-dimethylene-6,7,8,9-tetrahydro-5*H*-5,9-propanobenzo[7]
- 15 annulene (1.5 g, 6.24 mmol), and following the procedure described in reference example 10, 2-chloro-*N*-(2-methoxy-9-methyl-5,6,8,9,10,11-hexahydro-7*H*-5,9:7,11-dimethanobenzo[9]annulen-7-yl)acetamide was obtained (1.18 g, 57% yield).
mp 144-145 $^{\circ}\text{C}$. IR (NaCl disk): 3403, 3304, 3062, 2997, 2945, 2905, 2860, 2838, 1662, 1609, 1582, 1528, 1499, 1454, 1382, 1361, 1311, 1267, 1242, 1198, 1180, 1154,
- 20 1043, 1013, 955, 873 cm^{-1} . HRMS-ESI+ m/z $[\text{M}+\text{H}]^+$ calcd for $[\text{C}_{19}\text{H}_{24}\text{ClNO}_2+\text{H}]^+$: 334.1568, found: 334.1569.

Reference example 12: 2-chloro-*N*-(2,3-dimethoxy-9-methyl-5,6,8,9,10,11-hexahydro-7*H*-5,9:7,11-dimethanobenzo[9]annulen-7-yl)acetamide.

- 25 From 2,3-dimethoxy-7,11-dimethylene-6,7,8,9-tetrahydro-5*H*-5,9-propanobenzo[7]annulene (498 mg, 1.84 mmol), and following the procedure described in reference example 10, 2-chloro-*N*-(2,3-dimethoxy-9-methyl-5,6,8,9,10,11-hexahydro-7*H*-5,9:7,11-dimethanobenzo[9]annulen-7-yl)acetamide was obtained (501 mg, 75% yield).
mp 204-205 $^{\circ}\text{C}$. IR (NaCl disk): 3306, 2941, 2907, 2861, 2838, 1666, 1605, 1516,
- 30 1467, 1452, 1415, 1381, 1361, 1345, 1293, 1252, 1231, 1191, 1168, 1092, 1021, 948, 861, 802 cm^{-1} . HRMS-ESI+ m/z $[\text{M}+\text{H}]^+$ calcd for $[\text{C}_{20}\text{H}_{26}\text{ClNO}_3+\text{H}]^+$: 364.1674, found: 364.1674.

Reference example 13: 2-chloro-*N*-(1-fluoro-9-hydroxy-5,6,8,9,10,11-hexahydro-7*H*-5,9:7,11-dimethanobenzo[9]annulen-7-yl)acetamide.

- 35 A solution of 1-fluoro-7-methylene-6,7,8,9-tetrahydro-5*H*-5,9-propanobenzo[7]annulen-11-one (2.06 g, 8.94 mmol), chloroacetonitrile (0.6 mL, 9.83 mmol) in DCM (21 mL)

was cooled to 0 °C and concentrated H₂SO₄ (0.75 mL) was added dropwise (T < 10 °C). The mixture was allowed to reach room temperature and was stirred overnight. The suspension was added to ice (20 g) and after 10 min stirring, the suspension was extracted with DCM (3 x 15 mL). The combined organic layers were washed with
5 NaOH 10 N (1 x 25 mL) and dried with anh. Na₂SO₄, filtered and concentrated under vacuum. Column chromatography (SiO₂, Hexane/Ethyl Acetate mixtures) gave 2-chloro-*N*-(1-fluoro-9-hydroxy-5,6,8,9,10,11-hexahydro-7*H*-5,9:7,11-dimethanobenzo[9]annulen-7-yl)acetamide as a white solid (921 mg, 32% yield).
mp 150 °C. IR (ATR): 3406, 3272, 3075, 2926, 2905, 2850, 1661, 1561, 1466, 1443,
10 1409, 1362, 1341, 1311, 1298, 1243, 1218, 1158, 1105, 1037, 991, 974, 891, 884, 791, 734, 679, 625 cm⁻¹. HRMS-ESI+ *m/z* [M+H]⁺ calcd for [C₁₇H₁₉ClFNO₂+H]⁺: 324.1161, found: 324.1162.

Reference example 14: 2-chloro-*N*-(1-fluoro-9-methyl-5,6,8,9,10,11-hexahydro-7*H*-5,9:7,11-dimethanobenzo[9]annulen-7-yl)acetamide.

15 From 1-fluoro-7,11-dimethylene-6,7,8,9-tetrahydro-5*H*-5,9-propanobenzo[7]annulene (2.36 g, 10.36 mmol), and following the procedure described in reference example 10, 2-chloro-*N*-(1-fluoro-9-methyl-5,6,8,9,10,11-hexahydro-7*H*-5,9:7,11-dimethanobenzo[9]annulen-7-yl)acetamide was obtained (2.28 g, 68% yield). The
20 analytical sample was obtained by crystallization from DCM.
mp 154-155 °C. IR (NaCl disk): 3402, 3308, 3073, 2947, 2911, 2863, 2840, 1660, 1613, 1583, 1529, 1463, 1363, 1348, 1312, 1242, 1186, 1155, 979, 798, 748 cm⁻¹. HRMS-ESI+ *m/z* [M+H]⁺ calcd for [C₁₈H₂₁ClFNO+H]⁺: 322.1368, found: 322.1374.

Reference example 15: 2-chloro-*N*-(1,9-difluoro-5,6,8,9,10,11-hexahydro-7*H*-5,9:7,11-dimethanobenzo[9]annulen-7-yl)acetamide.

A solution of 2-chloro-*N*-(1-fluoro-9-hydroxy-5,6,8,9,10,11-hexahydro-7*H*-5,9:7,11-dimethanobenzo[9]annulen-7-yl)acetamide (611 mg, 1.89 mmol) in DCM (10 mL) was cooled to -30 °C with a dry ice in an acetone bath. Then DAST (2.8 mL, 1 M in DCM,
30 2.8 mmol) was added and the reaction mixture was stirred with the dry ice in an acetone bath overnight. To the resulting solution water (10 mL) was added and the pH adjusted to ~12 with NaOH 1 N. The two layers were separated, the aqueous phase was extracted further with DCM (2 x 8 mL), and the combined organic phases were dried over anh. Na₂SO₄, filtered and concentrated under vacuum. Crystallization from
35 DCM/Pentane afforded 2-chloro-*N*-(1,9-difluoro-5,6,8,9,10,11-hexahydro-7*H*-5,9:7,11-dimethanobenzo[9]annulen-7-yl)acetamide (420 mg, 68% yield).

mp 180 °C. IR (ATR): 3276, 3075, 2964, 2940, 2901, 2858, 1671, 1650, 1552, 1463, 1442, 1360, 1317, 1282, 1242, 1175, 1143, 1104, 1066, 1018, 1004, 979, 929, 901, 887, 865, 799, 746, 737, 696, 662 cm⁻¹. HRMS-ESI⁺ *m/z* [M+H]⁺ calcd for [C₁₇H₁₈ClF₂NO+H]⁺: 326.1118, found: 326.1116.

5

Reference example 16: 2-fluoro-9-methyl-5,6,8,9,10,11-hexahydro-7H-5,9:7,11-dimethanobenzo[9]annulen-7-amine hydrochloride.

Thiourea (25 mg, 0.32 mmol) and glacial acetic acid (200 µL) were added to a solution of 2-chloro-*N*-(2-fluoro-9-methyl-5,6,8,9,10,11-hexahydro-7H-5,9:7,11-dimethanobenzo
10 [9]annulen-7-yl)acetamide (87 mg, 0.27 mmol) in absolute ethanol (5 mL) and the mixture was heated at reflux overnight. The resulting suspension was then tempered to room temperature, water (5 mL) was added and the pH adjusted to 12 with 5 N NaOH solution. EtOAc (5 mL) was added, the phases were separated and the aqueous phase was extracted with further EtOAc (2 x 5 mL). The combined organic layers were dried
15 over anh. Na₂SO₄, filtered and concentrated under vacuum to give a light brown oil. Its hydrochloride was obtained by adding an excess of Et₂O/HCl to a solution of the amine in ethyl acetate, followed by filtration of the resulting beige precipitate affording 2-fluoro-9-methyl-5,6,8,9,10,11-hexahydro-7H-5,9:7,11 dimethanobenzo[9]annulen-7-amine hydrochloride (18 mg, 24% yield).

20 mp >300 °C (dec.). IR (KBr disk): 3200-2500 (2983, 2945, 2917, 2867), 2059, 1612, 1595, 1501, 1456, 1444, 1431, 1379, 1364, 1302, 1283, 1256, 1246, 1186, 1157, 1143, 1132, 1030, 1004, 962, 863, 814 cm⁻¹. Anal. Calcd for C₁₆H₂₀FN· 2.6 HCl: C 56.50, H 6.70, N 4.12. Found: C 56.18, H 6.40, N 4.01.

25 **Reference example 17: 2-methoxy-9-methyl-5,6,8,9,10,11-hexahydro-7H-5,9:7,11-dimethanobenzo[9]annulen-7-amine hydrochloride.**

From 2-chloro-*N*-(2-methoxy-9-methyl-5,6,8,9,10,11-hexahydro-7H-5,9:7,11-dimethanobenzo[9]annulen-7-yl)acetamide (1.10 g, 3.95 mmol), and following the procedure described in reference example 16, 2-methoxy-9-methyl-5,6,8,9,10,11-
30 hexahydro-7H-5,9:7,11-dimethanobenzo[9]annulen-7-amine hydrochloride was obtained. The analytical sample was obtained by crystallization from DCM/Pentane (779 mg, 81 % yield).

mp >250 °C (dec.). IR (KBr disk): 3200-2500 (2985, 2942, 2908), 2056, 1735, 1609, 1582, 1499, 1449, 1379, 1364, 1334, 1305, 1268, 1252, 1205, 1170, 1132, 1103, 1040,
35 1001, 954, 869, 849, 815, 756, 692 cm⁻¹. HRMS-ESI⁺ *m/z* [M+H]⁺ calcd for [C₁₇H₂₃NO+H]⁺: 258.1852, found: 258.1862.

Reference example 18: 2,3-dimethoxy-9-methyl-5,6,8,9,10,11-hexahydro-7H-5,9:7,11-dimethanobenzo[9]annulen-7-amine hydrochloride.

From 2-chloro-*N*-(2,3-dimethoxy-9-methyl-5,6,8,9,10,11-hexahydro-7H-5,9:7,11-dimethanobenzo[9]annulen-7-yl)acetamide (436 mg, 1.2 mmol), and following the
5 procedure described in reference example 16, 2,3-dimethoxy-9-methyl-5,6,8,9,10,11-hexahydro-7H-5,9:7,11-dimethanobenzo[9]annulen-7-amine hydrochloride was obtained (285 mg, 73% yield).

mp >200 °C (dec.). IR (KBr disk): 3200-2500 (2993, 2918, 2831), 2047, 1701, 1606, 1517, 1451, 1416, 1386, 1365, 1327, 1310, 1291, 1252, 1237, 1192, 1174, 1131, 1098,
10 1031, 973, 950, 863, 798, 586, 543 cm⁻¹. HRMS-ESI+ m/z [M+H]⁺ calcd for [C₁₈H₂₅NO₂+H]⁺: 288.1958, found: 288.1954.

Reference example 19: 1-fluoro-9-methyl-5,6,8,9,10,11-hexahydro-7H-5,9:7,11-dimethanobenzo[9]annulen-7-amine hydrochloride.

15 From 2-chloro-*N*-(1-fluoro-9-methyl-5,6,8,9,10,11-hexahydro-7H-5,9:7,11-dimethanobenzo[9]annulen-7-yl)acetamide (1 g, 3.11 mmol), and following the procedure described in reference example 16, 1-fluoro-9-methyl-5,6,8,9,10,11-hexahydro-7H-5,9:7,11-dimethanobenzo[9]annulen-7-amine hydrochloride was obtained. The analytical sample was obtained by crystallization from Methanol (521
20 mg, 59 % yield).

mp >200 °C (dec.). IR (KBr disk): 3200-2500 (2945, 2717), 2060, 1677, 1608, 1584, 1511, 1464, 1390, 1380, 1366, 1317, 1303, 1248, 1214, 1199, 1165, 1132, 1071, 1052, 1032, 1000, 977, 946, 885, 877, 854, 798, 747, 623 cm⁻¹. HRMS-ESI+ m/z [M+H]⁺ calcd for [C₁₆H₂₀FN+H]⁺: 246.1653, found: 246.1649.

25

Reference example 20: 2-chloro-*N*-(9-methyl-2-nitro-5,6,8,9,10,11-hexahydro-7H-5,9:7,11-dimethanobenzo[9]annulen-7-yl)acetamide.

To a cold (0°C) solution of known 2-chloro-*N*-(9-methyl-5,6,8,9,10,11-hexahydro-7H-5,9:7,11-dimethanobenzo[9]annulen-7-yl)acetamide (*Bioorg Med Chem.* 2012, 20, 942)
30 (3 g, 9.87 mmol) in acetic anhydride (10.5 mL) were carefully added glacial acetic acid (1.6 mL) and fuming nitric acid (1.85 mL). The mixture was allowed to reach room temperature and left stirring overnight. The obtained yellow solution was then poured to ice-water (20 mL), and extracted with DCM (3 x 40 mL). The combined organic extracts were washed with aqueous 2 N NaOH (1 x 40 mL), water (1 x 40 mL) and
35 brine (1 x 40 mL). The organic layer was dried over anh. Na₂SO₄, filtered and concentrated under vacuum to give a yellow residue. Purification by column chromatography (SiO₂, Hexane/Ethyl Acetate mixtures) gave 2-chloro-*N*-(9-methyl-2-

nitro-5,6,8,9,10,11-hexahydro-7*H*-5,9:7,11-dimethanobenzo[9]annulen-7-yl)acetamide (2.92 g, 85% yield) as a white solid.

mp 174 °C. IR (KBr disk): 3403, 3288, 3077, 2946, 2922, 2847, 1667, 1607, 1588, 1520, 1456, 1409, 1348, 1229, 1166, 1136, 1082, 1051, 1009, 972, 945, 896, 865, 841, 5 797, 740, 764, 704, 666 cm⁻¹. HRMS-ESI+ m/z [M+H]⁺ calcd for [C₁₈H₂₁ClN₂O₃+H]⁺: 349.1313, found: 349.1313.

Reference example 21: 9-methyl-2-nitro-5,6,8,9,10,11-hexahydro-7*H*-5,9:7,11-dimethanobenzo[9]annulen-7-amine hydrochloride.

10 From 2-chloro-*N*-(9-methyl-2-nitro-5,6,8,9,10,11-hexahydro-7*H*-5,9:7,11-dimethanobenzo[9]annulen-7-yl)acetamide (677 mg, 1.94 mmol) and following the procedure described in reference example 16, 9-methyl-2-nitro-5,6,8,9,10,11-hexahydro-7*H*-5,9:7,11-dimethanobenzo[9]annulen-7-amine hydrochloride was obtained (443 mg, 74% yield).

15 mp >225 °C (dec.). IR (KBr disk): 3200-2500 (2928, 2641, 2603, 2535), 2066, 1648, 1612, 1591, 1522, 1487, 1458, 1352, 1304, 1286, 1256, 1221, 1181, 1134, 1088, 1031, 955, 946, 895, 884, 865, 836, 799, 766 cm⁻¹. HRMS-ESI+ m/z [M+H]⁺ calcd for [C₁₆H₂₀N₂O₂+H]⁺: 273.1598, found: 273.1604.

20 **Reference example 22: 1,9-difluoro-5,6,8,9,10,11-hexahydro-7*H*-5,9:7,11-dimethanobenzo[9]annulen-7-amine hydrochloride.**

From 2-chloro-*N*-(1,9-difluoro-5,6,8,9,10,11-hexahydro-7*H*-5,9:7,11-dimethanobenzo[9]annulen-7-yl)acetamide (382 mg, 1.17 mmol), and following the procedure described in reference example 16, 1,9-difluoro-5,6,8,9,10,11-hexahydro-25 7*H*-5,9:7,11-dimethanobenzo[9]annulen-7-amine hydrochloride was obtained (218 mg, 65 % yield). The analytical sample was obtained by crystallization from methanol.

mp >200 °C (dec.). IR (ATR): 2980-2831 (2950, 2911, 2867), 2703, 2676, 2559, 2063, 1611, 1588, 1509, 1465, 1445, 1363, 1321, 1246, 1194, 1105, 1095, 1008, 1002, 988, 967, 903, 888, 860, 801, 743, 673 cm⁻¹. HRMS-ESI+ m/z [M+H]⁺ calcd for 30 [C₁₅H₁₇F₂N+H]⁺: 250.1402, found: 250.1401.

Reference example 23: 9-methyl-5,6,8,9,10,11-hexahydro-7*H*-5,9:7,11-dimethanobenzo[9]annulene-2,7-diamine dihydrochloride.

To a solution of amine 9-methyl-2-nitro-5,6,8,9,10,11-hexahydro-7*H*-5,9:7,11-dimethanobenzo[9]annulen-7-amine (201 mg, 0.738 mmol) in methanol (25 mL), Pd on 35 charcoal (68.6 mg, cat. 10% Pd) was added and the resulting suspension was hydrogenated at 1 atm of H₂ at room temperature for 48 h. The black suspension was

filtered and the solvent removed by concentration under vacuum to give 9-methyl-5,6,8,9,10,11-hexahydro-7*H*-5,9:7,11-dimethanobenzo[9]annulene-2,7-diamine as a brown solid (130 mg, 89% yield). Its dihydrochloride was obtained by addition of an excess of Et₂O/HCl to a solution of the diamine in methanol followed by filtration of the
5 resulting brown precipitate.
mp 294-295 °C. IR (KBr disk): 3200-2500 (3024, 2912, 2847, 2588), 1994, 1598, 1502, 1454, 1381, 1365, 1303, 1261, 1173, 1131, 1021, 957, 877, 827, 576, 473 cm⁻¹. Anal. Calcd. for C₁₆H₂₂N₂·3.4 HCl: C 52.46, H 6.99, N 7.65. Found C 52.64, H 7.18, N 7.43.

10 **Reference example 24: 2-chloro-*N*-(2-hydroxy-9-methyl-5,6,8,9,10,11-hexahydro-7*H*-5,9:7,11-dimethanobenzo[9]annulen-7-yl)acetamide.**

To a solution of *N*-(2-amino-9-methyl-5,6,8,9,10,11-hexahydro-7*H*-5,9:7,11-dimethanobenzo[9]annulen-7-yl)-2-chloroacetamide (999 mg, 3.10 mmol) in H₂O (5 mL) and conc. HCl (5 mL), at 0 °C, was added dropwise a solution of sodium nitrite
15 (427 mg, 6.21 mmol) in H₂O (2 mL). To the resulting solution was added CuCl (652 mg, 6.56 mmol) in conc. HCl (3 mL) and over 10 min gas evolution was observed. The resulting solution was warmed to 60 °C for 90 minutes, then was cooled to room temperature, diluted in H₂O (60 mL) and extracted with DCM (4 x 90 mL). The combined organic extracts were washed with sat. NaHCO₃ and brine, were dried over
20 anhyd. Na₂SO₄, filtered and concentrated under vacuum to give a dark green solid. Purification by column chromatography (SiO₂, Hexane/Ethyl Acetate mixture) gave the 2-chloro-*N*-(2-hydroxy-9-methyl-5,6,8,9,10,11-hexahydro-7*H*-5,9:7,11-dimethanobenzo[9]annulen-7-yl)acetamide (78 mg, 9% yield) as a white solid.
mp 98-100 °C. IR (NaCl disk): 3300-2700 (3266, 3186, 3118, 2966, 2942, 2916, 2861),
25 2175, 1590, 1568, 1504, 1451, 1426, 1376, 1356, 1309, 1267, 1161, 1130, 1081, 1058, 827, 804 cm⁻¹. HRMS-ESI- m/z [M-H]⁻ calcd for [C₁₈H₂₂ClNO₂-H]⁻: 318.1266, found: 318.1272.

30 **Reference example 25: 2-hydroxy-9-methyl-5,6,8,9,10,11-hexahydro-7*H*-5,9:7,11-dimethanobenzo[9]annulen-7-amine hydrochloride.**

From 2-chloro-*N*-(2-hydroxy-9-methyl-5,6,8,9,10,11-hexahydro-7*H*-5,9:7,11-dimethanobenzo[9]annulen-7-yl)acetamide (72 mg, 0.23 mmol), and following the procedure described in reference example 16, 2-hydroxy-9-methyl-5,6,8,9,10,11-hexahydro-7*H*-5,9:7,11-dimethanobenzo[9]annulen-7-amine hydrochloride was
35 obtained (42 mg, 67% yield). The analytical sample was obtained by crystallization from Methanol/Diethyl ether.

mp 183-185 °C. Anal. Calcd for $C_{16}H_{21}NO \cdot 1.7HCl \cdot 1H_2O$: C 59.43, H 7.70, N 4.33. Found C 59.63, H 7.44, N 4.77.

Reference example 26: N-(9-methyl-2-nitro-5,6,8,9,10,11-hexahydro-7H-5,9:7,11-dimethanobenzo[9]annulen-7-yl)acetamide.

To a cold (0 °C) solution of known (*Tetrahedron Lett.* 1987, 28, 1585-1588) *N*-(9-methyl-5,6,8,9,10,11-hexahydro-7H-5,9:7,11-dimethanobenzo[9]annulen-7-yl)acetamide (2.68 g, 9.93 mmol) in acetic anhydride (10.6 mL) were carefully added glacial acetic acid (1.6 mL) and fuming nitric acid (1.86 mL). The mixture was allowed to reach room temperature and left stirring overnight. The obtained yellow solution was then poured to ice-water (20 mL), and extracted with DCM (3 x 40 mL). The combined organic extracts were washed with aqueous 2 N NaOH (1 x 40 mL), water (1 x 40 mL) and brine (1 x 40 mL). The organic layer was dried over anhydrous Na_2SO_4 , filtered and concentrated under vacuum to give a yellow residue. Purification by column chromatography (SiO_2 , Hexane/Ethyl Acetate mixtures) gave *N*-(9-methyl-2-nitro-5,6,8,9,10,11-hexahydro-7H-5,9:7,11-dimethanobenzo[9]annulen-7-yl)acetamide (1.88 g, 60% yield) as a white solid.

mp 174-176 °C. IR (NaCl disk): 3398, 3301, 3201, 3063, 2943, 2917, 2863, 1653, 1588, 1523, 1455, 1346, 1322, 1304, 1268, 1245, 1217, 1166, 1141, 1124, 1081, 1037, 1010, 945, 893, 865, 838, 798, 763, 740, 701 cm^{-1} . HRMS-ESI+ m/z $[M+H]^+$ calcd for $[C_{18}H_{22}N_2O_3+H]^+$: 315.1703, found: 315.1714.

Reference example 27: N-(2-amino-9-methyl-5,6,8,9,10,11-hexahydro-7H-5,9:7,11-dimethanobenzo[9]annulen-7-yl)acetamide.

From *N*-(9-methyl-2-nitro-5,6,8,9,10,11-hexahydro-7H-5,9:7,11-dimethanobenzo[9]annulen-7-yl)acetamide (2.64 g, 8.41 mmol), PtO_2 (258 mg) in absolute EtOH and following the procedure described in the reference example 23, *N*-(2-amino-9-methyl-5,6,8,9,10,11-hexahydro-7H-5,9:7,11-dimethanobenzo[9]annulen-7-yl)acetamide (1.9 g, 80% yield) was obtained after purification by column chromatography (SiO_2 , Hexane/Ethyl Acetate mixtures).

mp 112-113 °C. IR (NaCl disk): 3432, 3324, 3224, 3056, 3004, 2938, 2903, 2856, 2835, 1651, 1618, 1546, 1507, 1447, 1362, 1344, 1300, 1262, 1194, 1164, 1136, 1065, 862, 735, 701 cm^{-1} . HRMS-ESI+ m/z $[M+H]^+$ calcd for $[C_{18}H_{24}N_2O+H]^+$: 285.1961, found: 285.1972.

Reference example 28: N-(2-chloro-9-methyl-5,6,8,9,10,11-hexahydro-7H-5,9:7,11-dimethanobenzo[9]annulen-7-yl)acetamide.

From *N*-(2-amino-9-methyl-5,6,8,9,10,11-hexahydro-7*H*-5,9:7,11-dimethanobenzo[9]annulen-7-yl)acetamide hydrochloride (1.04 g, 3.25 mmol) in H₂O (6 mL) and conc. HCl (6 mL), sodium nitrite (448 mg, 6.5 mmol) in H₂O (2 mL), CuCl (691 mg, 6.99 mmol) dissolved in conc. HCl solution (3 mL), and following the procedure described in reference example 24, *N*-(2-chloro-9-methyl-5,6,8,9,10,11-hexahydro-7*H*-5,9:7,11-dimethanobenzo[9]annulen-7-yl)acetamide was obtained (210 mg, 21% yield).
mp 190-191 °C. IR (NaCl disk): 3301, 3196, 3071, 2921, 2855, 1651, 1594, 1549, 1487, 1454, 1414, 1364, 1343, 1308, 1281, 1263, 1211, 1139, 1109, 1012, 950, 875, 820 cm⁻¹. HRMS-ESI+ *m/z* [M+H]⁺ calcd for [C₁₈H₂₂ClNO+H]⁺: 304.1463, found: 304.1460.

Reference example 29: 2-chloro-9-methyl-5,6,8,9,10,11-hexahydro-7*H*-5,9:7,11-dimethanobenzo[9]annulen-7-amine hydrochloride.

A mixture of *N*-(2-chloro-9-methyl-5,6,8,9,10,11-hexahydro-7*H*-5,9:7,11-dimethanobenzo[9]annulen-7-yl)acetamide (190 mg, 0.63 mmol), conc. HCl (4 mL), H₂O (8 mL) and isopropanol (6 mL) was stirred under reflux for 4 days. The solution was cooled down and isopropanol was concentrated under vacuum. The aqueous phase was extracted with EtOAc (3 x 8 mL) and then was basified with a solution of 5 N NaOH. The base aqueous solution was extracted with further EtOAc (3 x 10 mL), dried over anh. Na₂SO₄, filtered and concentrated under vacuum to give a yellow oil. Purification by column chromatography (SiO₂, Hexane/Ethyl Acetate mixtures) gave 2-chloro-9-methyl-5,6,8,9,10,11-hexahydro-7*H*-5,9:7,11-dimethanobenzo[9]annulen-7-amine. Its hydrochloride was obtained by adding an excess of Et₂O/HCl to a solution of the amine in EtOAc (10 mg, 5.5% yield).
mp > 250 °C. IR (KBr disk): 3200-2500 (2990, 2950, 2916, 2861), 2058, 1597, 1570, 1509, 1488, 1454, 1416, 1380, 1365, 1302, 1217, 1155, 1133, 1093, 1032, 1000, 948, 875, 820, 771, 673 cm⁻¹. Anal. Calcd for C₁₆H₂₀ClN·1.35 HCl: C 61.79, H 6.95, N 4.50. Found C 61.70, H 6.78, N 4.93.

Reference example 30: 5,8,9,10-tetrahydro-5,8:7,10-dimethanobenzo[8]annulen-7(6*H*)-yl methanesulfonate.

To a solution of 5,8,9,10-tetrahydro-5,8:7,10-dimethanobenzo[8]annulen-7(6*H*)-ol (1.19 g, 5.97 mmol) in pyridine (9 mL), (prepared as reported in *Liebigs Ann Chem.* 1973; 1839-1850), mesyl chloride (2.32 mL, 29.28 mmol) was added slowly with stirring at room temperature. The mixture was then heated at 120 °C for 5 h. After cooling, crushed ice (100 g) was added and the mixture was extracted with DCM (5 x 40 mL). The combined organic phase was washed with 2 N HCl (2 x 40 mL), H₂O (2 x 40 mL),

saturated aqueous NaHCO₃ (2 x 40 mL), and dried over anh. Na₂SO₄. After filtration and removal of the solvent under reduced pressure, 5,8,9,10-tetrahydro-5,8:7,10-dimethanobenzo[8]annulen-7(6*H*)-yl methanesulfonate (1.32 g, 80% yield) was isolated as a dark oil that was used in the next step without further purification.

- 5 IR (NaCl disk): 3060, 3010, 2934, 2857, 1488, 1451, 1341, 1232, 1175, 1145, 1102, 1046, 1012, 992, 966, 923, 853, 800, 753 cm⁻¹. HRMS-ESI+ m/z [M+H]⁺ calcd for [C₁₅H₁₈O₃S+NH₄]⁺: 296.1315, found: 296.1318.

Reference example 31: 7-iodo-5,6,7,8,9,10-hexahydro-5,8:7,10-dimethanobenzo[8]annulene.

- 10 A mixture of H₃PO₄ (99%, 135 g), 5,8,9,10-tetrahydro-5,8:7,10-dimethanobenzo[8]annulen-7(6*H*)-yl methanesulfonate (1.32 g, 4.75 mmol) and NaI (63 g, 420 mmol) were stirred at 150 °C for 6 h. After cooling, H₂O (150 mL) was added slowly to the mixture. The resulting purple solution was extracted with DCM (4 x 80 mL) and the combined organic phase was washed with 10% aqueous sodium thiosulfate (1
- 15 x 100 mL), dried over anh. Na₂SO₄ and the solvent was removed under vacuum to obtain 7-iodo-5,6,7,8,9,10-hexahydro-5,8:7,10-dimethanobenzo[8]annulene as a white solid (1.39 g, 95 %).

- mp 132-133 °C. IR (NaCl disk) 3052, 3013, 2950, 2892, 2852, 1490, 1447, 1304, 1278, 1232, 1215, 1095, 1046, 1032, 967, 830, 778, 755 cm⁻¹. GC-MS (EI): 310 [(M)⁺, 2], 183 [(M-I)⁺, 100], 141 (73), 129 (23), 128 (15).

Reference example 32: 5,8,9,10-tetrahydro-5,8:7,10-dimethanobenzo[8]annulene-7(6*H*)-carboxylic acid.

- 25 To a solution of 7-iodo-5,8,9,10-tetrahydro-5,8:7,10-dimethanobenzo[8]annulene (2.03 g, 6.5 mmol) in dry and degassed toluene (20 mL) was added methyl oxalyl chloride (2.39 g, 19.5 mmol) and bis(tributyltin) (4.5 g, 7.8 mmol). The mixture was irradiated in a quartz reactor under argon atmosphere with a 125 W Hg lamp for 20 h. Then, DCM (15 mL), methanol (0.6 mL) and triethylamine (1.2 mL) were successively added to the
- 30 reaction mixture at 0° C and was concentrated under vacuum to give a dark oil (3.99 g). A solution of this oil in a 40% methanol solution of KOH (50 mL) was heated to reflux for 2 h. Water (50 mL) was added and the reaction was refluxed for 3 h. The reaction mixture was allowed to cool down to room temperature and the methanol was removed under vacuum. Water (40 mL) was added to the residue and the aqueous
- 35 layer was washed with DCM (4 x 50 mL). After that, the aqueous phase was acidified with conc. HCl until pH=1 and extracted with DCM (4 x 50 mL). The organic extracts were dried over anh. Na₂SO₄, filtered and concentrated under reduced pressure to give

5,8,9,10-tetrahydro-5,8:7,10-dimethanobenzo[8]annulene-7(6*H*)-carboxylic acid as a brown solid (555 mg, 37% overall yield). An analytical sample of the acid was obtained by crystallization from DCM/Pentane.

mp 188-189 °C. IR (NaCl disk): 3300-2800 (3065, 3011, 2946, 2858), 1690, 1488,
5 1450, 1410, 1318, 1290, 1231, 1218, 1092, 1052, 1038, 941 cm⁻¹. HRMS-ESI- m/z [M-H]⁻ calcd for [C₁₅H₁₆O₂-H]: 227.1078, found: 227.1078.

Reference example 33: 5,8,9,10-tetrahydro-5,8:7,10-dimethanobenzo[8]annulene-7(6*H*)-amine hydrochloride.

10 To a solution of 5,8,9,10-tetrahydro-5,8:7,10-dimethanobenzo[8]annulene-7(6*H*)-carboxylic acid (90 mg, 0.39 mmol) in toluene (1.2 mL), Et₃N (73 μL, 0.53 mmol) and diphenylphosphoryl azide (159 mg, 0.58 mmol) were added and heated at reflux for 3 h. The mixture was cooled down and washed with 1 N HCl (10 X 2 mL). Thereafter, to the organic layer was added 6 N HCl (1.6 mL) and the suspension was heated at reflux
15 for 24 h. The reaction mixture was then cooled to room temperature and the two phases were separated. The aqueous phase was extracted with ethyl acetate (3 x 3 mL). The combined organic phases were washed with 5 N NaOH (3 x 10 mL), dried over anh. Na₂SO₄, filtered and concentrated under vacuum to give 5,8,9,10-tetrahydro-5,8:7,10-dimethanobenzo[8]annulene-7(6*H*)-amine. Its hydrochloride was obtained by
20 adding an excess of HCl in methanol to a solution of the amine in methanol. The methanol was removed under reduced pressure to give 5,8,9,10-tetrahydro-5,8:7,10-dimethanobenzo[8]annulene-7(6*H*)-amine hydrochloride as a brown solid (35 mg, 45% yield). An analytical sample was obtained by crystallization from Methanol/Diethyl ether.
25 mp > 250 °C (dec). IR (KBr disk): 3100-2500 (2943, 2881), 2043, 1622, 1598, 1501, 1448, 1336, 1246, 1089, 1057, 1028, 952, 769, 749, 614 cm⁻¹. HRMS-ESI+ m/z [M+H]⁺ calcd for [C₁₄H₁₇N+H]⁺: 200.1434, found: 200.1432.

Example 34: *p*-tolyl (9-methyl-5,6,8,9,10,11-hexahydro-7*H*-5,9:7,11-dimethanobenzo[9]annulene-7-yl)carbamate.

30 To a solution of 9-methyl-5,6,8,9,10,11-hexahydro-7*H*-5,9:7,11-dimethanobenzo[9]annulene-7-amine hydrochloride (250 mg, 0.95 mmol) in DCM (2 mL), *p*-tolyl chloroformate (194 mg, 1.14 mmol) and Et₃N (287 mg, 2.84 mmol) were added. The reaction mixture was stirred at room temperature overnight and then the solvent was
35 evaporated under vacuum. The residue was dissolved in EtOAc (30 mL) and water (20 mL) and phases were separated. The aqueous phase was extracted with further EtOAc (2 x 30 mL). The combined organic phases were dried over anh. Na₂SO₄, filtered and

concentrated under vacuum to obtain 300 mg of a yellow gum. Column chromatography (SiO₂, Hexane/Ethyl Acetate mixtures) gave *p*-tolyl (9-methyl-5,6,8,9,10,11-hexahydro-7*H*-5,9:7,11-dimethanobenzo[9]annulen-7-yl)carbamate (46 mg, 14% yield) as a white solid.

- 5 mp 114-115 °C. IR (NaCl disk): 3330, 3018, 2944, 2919, 2854, 1744, 1591, 1531, 1502, 1452, 1379, 1362, 1345, 1255, 1214, 1198, 1167, 1137, 1069, 1042, 1014, 987, 948, 900, 825, 757 cm⁻¹. Anal. Calcd for C₂₄H₂₇NO₂ · 0.3 C₅H₁₂ · 0.05 CH₂Cl₂: C 79.22, H 7.99, N 3.62. Found: C 79.23, H 7.88, N 3.45.

10 **Example 35: 1-(9-methyl-5,6,8,9,10,11-hexahydro-7*H*-5,9:7,11-dimethanobenzo[9]annulen-7-yl)-3-(4-(trifluoromethyl)phenyl)thiourea.**

To a solution of 9-methyl-5,6,8,9,10,11-hexahydro-7*H*-5,9:7,11-dimethanobenzo[9]annulen-7-amine hydrochloride (250 mg, 0.95 mmol) in DCM (2 mL), 1-isothiocyanato-4-(trifluoromethyl)benzene (193 mg, 0.95 mmol) and Et₃N (287 mg, 2.84 mmol) were added. The reaction mixture was stirred at room temperature overnight and then the solvent was evaporated under vacuum. The residue was dissolved in EtOAc (30 mL) and water (20 mL) and phases were separated. The aqueous phase was extracted with further EtOAc (2 x 30 mL). The combined organic phases were dried over anh. Na₂SO₄, filtered and concentrated under vacuum to obtain

15 369 mg of a yellow solid. The product was washed with Et₂O to obtain 1-(9-methyl-5,6,8,9,10,11-hexahydro-7*H*-5,9:7,11-dimethanobenzo[9]annulen-7-yl)-3-(4-(trifluoromethyl)phenyl)thiourea (188 mg, 46% yield) as a white solid.

- 20 mp 158-159°C. IR (NaCl disk): 3283, 2911, 2834, 1615, 1532, 1493, 1454, 1422, 1324, 120, 1166, 1124, 1067, 1015, 948, 909, 837, 759, 732, 697, 665 cm⁻¹. Anal. Calcd for C₂₄H₂₅F₃N₂S: C 66.96, H 5.85, N 6.51. Found: C 66.79, H 5.95, N 6.37.

Example 36: 1-(1-acetylpiperidin-4-yl)-3-(5-methyl-1,5,6,7-tetrahydro-1,5:3,7-dimethanobenzo[*e*]oxonin-3(2*H*)-yl)urea.

To a solution of 5-methyl-1,5,6,7-tetrahydro-1,5:3,7-dimethanobenzo[*e*]oxonin-3(2*H*)-amine hydrochloride (180 mg, 0.69 mmol) in DCM (3 mL) and saturated aqueous NaHCO₃ solution (2 mL), triphosgene (102 mg, 0.34 mmol) was added. The biphasic mixture was stirred at room temperature for 30 minutes and then the two phases were separated and the organic one was washed with brine (5 mL), dried over anh. Na₂SO₄, filtered and evaporated under vacuum to obtain 1-2 mL of a solution of isocyanate in

30 DCM. To this solution were added 1-(4-aminopiperidin-1-yl)ethan-1-one hydrochloride (122 mg, 0.68 mmol) and Et₃N (139 mg, 1.37 mmol). The mixture was stirred overnight at room temperature, diluted with further DCM (10 mL) and washed with 2N NaOH

35

solution (2 x 10 mL). The organic layer was dried over anh. Na₂SO₄, filtered and concentrated under vacuum to obtain a yellow residue (206 mg). Column chromatography (SiO₂, DCM/Methanol mixtures) gave 1-(1-acetylpiperidin-4-yl)-3-(5-methyl-1,5,6,7-tetrahydro-1,5:3,7-dimethanobenzo[e]oxonin-3(2*H*)-yl)urea as a white solid (135 mg, 49% yield). The analytical sample was obtained by crystallization from hot EtOAc (112 mg).

mp 208-209 °C. IR (NaCl disk): 3357, 3054, 3012, 2969, 2926, 2853, 1646, 1611, 1546, 1492, 1450, 1358, 1324, 1268, 1222, 1156, 1101, 1088, 1035, 1212, 991, 947, 918, 900, 866, 829, 760, 733, 699 cm⁻¹. Anal. Calcd for C₂₃H₃₁N₃O₃: C 69.49, H 7.86, N 10.57. Found: C 69.47, H 7.92, N 10.38.

Example 37: 1-(1-acetylpiperidin-4-yl)-3-(1,5,6,7-tetrahydro-1,5:3,7-dimethanobenzo[e]oxonin-3(2*H*)-yl)urea.

To a solution of 1,5,6,7-tetrahydro-1,5:3,7-dimethanobenzo[e]oxonin-3(2*H*)-amine hydrochloride (300 mg, 1.19 mmol) in DCM (7 mL) and saturated aqueous NaHCO₃ solution (7 mL), triphosgene (130 mg, 0.44 mmol) was added. The biphasic mixture was stirred at room temperature for 30 minutes and then the two phases were separated and the organic one was washed with brine (10 mL), dried over anh. Na₂SO₄, filtered and evaporated under vacuum to obtain 1-2 mL of a solution of isocyanate in DCM. To this solution were added 1-(4-aminopiperidin-1-yl)ethan-1-one hydrochloride (203 mg, 1.43 mmol) and Et₃N (292 mg, 2.88 mmol). The mixture was stirred overnight at room temperature, diluted with further DCM (10 mL) and washed with 2N NaOH solution (2 x 10 mL). The organic layer was dried over anh. Na₂SO₄, filtered and concentrated under vacuum to obtain a yellow residue (400 mg). Column chromatography (SiO₂, DCM/Methanol mixtures) gave 1-(1-acetylpiperidin-4-yl)-3-(1,5,6,7-tetrahydro-1,5:3,7-dimethanobenzo[e]oxonin-3(2*H*)-yl)urea as a white solid (50 mg, 49% yield).

mp 200-202 °C. IR (NaCl disk): 3347, 3065, 3016, 2922, 1645, 1624, 1548, 1492, 1451, 1436, 1362, 1323, 1268, 1230, 1211, 1196, 1109, 1073, 1022, 980, 967 cm⁻¹. HRMS-ESI+ m/z [M+H]⁺ calcd for [C₂₂H₂₉N₃O₃+H]⁺: 384.2282, found: 384.2285.

Example 38: 1-(1-acetylpiperidin-4-yl)-3-(9-methyl-5,6,8,9,10,11-hexahydro-7*H*-5,9:7,11-dimethanobenzo[9]annulen-7-yl)urea.

To a solution of 5-methyl-1,5,6,7-tetrahydro-1,5:3,7-dimethanobenzo[e]oxonin-3(2*H*)-amine hydrochloride (180 mg, 0.69 mmol) in DCM (3 mL) and saturated aqueous NaHCO₃ solution (2 mL), triphosgene (102 mg, 0.34 mmol) was added. The biphasic mixture was stirred at room temperature for 30 minutes and then the two phases were

separated and the organic layer was washed with brine (5 mL), dried over anh. Na₂SO₄, filtered and evaporated under vacuum to obtain 1-2 mL of a solution of the isocyanate in DCM. To this solution were added 1-(4-aminopiperidin-1-yl)ethan-1-one hydrochloride (122 mg, 0.68 mmol) and Et₃N (138 mg, 1.36 mmol). The mixture was stirred overnight at room temperature, diluted with further DCM (10 mL) and washed with 2N NaOH solution (2 x 10 mL). Organics were dried over anh. Na₂SO₄, filtered and concentrated under vacuum to obtain a yellow oil (232 mg). Column chromatography (SiO₂, DCM/Methanol mixtures) gave 1-(1-acetylpiperidin-4-yl)-3-(9-methyl-5,6,8,9,10,11-hexahydro-7H-5,9:7,11-dimethanobenzo[9]annulen-7-yl)urea as a white solid (143 mg, 53% yield). The analytical sample was obtained by crystallization from hot EtOAc (113 mg).
mp 206-207 °C. IR (NaCl disk): 3359, 3065, 3016, 2938, 2906, 2860, 1644, 1620, 1555, 1493, 1452, 1360, 1344, 1319, 1267, 1228, 1212, 1136, 1090, 1049 cm⁻¹. Anal. Calcd for C₂₄H₃₃N₃O₂·0.21 Ethyl Acetate: C 71.91, H 8.45, N 10.06. Found: C 71.73, H 8.43, N 10.27.

Example 39: 1-(1-acetylpiperidin-4-yl)-3-(9-hydroxy-5,6,8,9,10,11-hexahydro-7H-5,9:7,11-dimethanobenzo[9]annulen-7-yl)urea.

To a solution of 1-(4-aminopiperidin-1-yl)ethan-1-one (192 mg, 1.35 mmol) in DCM (4 mL) and saturated aqueous NaHCO₃ solution (3 mL) triphosgene (200 mg, 0.68 mmol) was added. The biphasic mixture was stirred at room temperature for 30 minutes and then the two phases were separated and the organic one was washed with brine (5 mL), dried over anh. Na₂SO₄, filtered and evaporated under vacuum to obtain 1-2 mL of a solution of the isocyanate in DCM. To this solution was added 9-amino-5,6,8,9,10,11-hexahydro-7H-5,9:7,11-dimethanobenzo[9]annulen-7-ol hydrochloride (300 mg, 1.14 mmol) followed by Et₃N (228 mg, 2.25 mmol). The reaction mixture was stirred at room temperature overnight and the solvent was evaporated under vacuum. Column chromatography (SiO₂, DCM/Methanol mixtures) gave 1-(1-(isopropylsulfonyl)piperidin-4-yl)-3-(9-methyl-5,6,8,9,10,11-hexahydro-7H-5,9:7,11-dimethanobenzo[9]annulen-7-yl)urea (19 mg, 4.2% yield) as a grey solid.
mp 222-223 °C. IR (NaCl disk): 3313, 2921, 2852, 1733, 1716, 1646, 1621, 1557, 1542, 1506, 1490, 1472, 1455, 1358, 1336, 1318, 1300, 1265, 1231, 1204, 1134, 1104, 1053 cm⁻¹. Anal. Calcd for C₂₃H₃₁N₃O₃·0.2 C₅H₁₂ · 0.9 H₂O: C 67.33, H 8.29, N 9.81. Found: C 67.25, H 8.15, N 9.72

Example 40: 1-(1-acetylpiperidin-4-yl)-3-(9-methoxy-5,6,8,9,10,11-hexahydro-7H-5,9:7,11-dimethanobenzo[9]annulen-7-yl)urea.

To a solution of 9-methoxy-5,6,8,9,10,11-hexahydro-7H-5,9:7,11-dimethanobenzo[9]annulen-7-amine (300 mg, 1.23 mmol) in DCM (4.5 mL) and saturated aqueous NaHCO₃ solution (3 mL) triphosgene (183 mg, 0.61 mmol) was added. The biphasic mixture was stirred at room temperature for 30 minutes and then the two phases were separated and organics were washed with brine (5 mL), dried over anh. Na₂SO₄, filtered and evaporated under vacuum to obtain 1-2 mL of a solution of the isocyanate in DCM. To this solution was added 1-(4-aminopiperidin-1-yl)ethan-1-one (210 mg, 1.47 mmol). The reaction mixture was stirred at room temperature overnight and the solvent was evaporated under vacuum to obtain a white gum (521 mg). Column chromatography (SiO₂, DCM/Methanol mixtures) gave 1-(1-acetylpiperidin-4-yl)-3-(9-methoxy-5,6,8,9,10,11-hexahydro-7H-5,9:7,11-dimethanobenzo[9]annulen-7-yl)urea (148 mg, 30% yield) as a white solid. The analytical sample was obtained by crystallization from hot EtOAc (119 mg). mp 212-213 °C. IR (NaCl disk): 3358, 2930, 2847, 1646, 1617, 1555, 1495, 1451, 1356, 1319, 1266, 1228, 1094, 1075, 972, 849, 755, 735 cm⁻¹. Anal. Calcd for C₂₄H₃₃N₃O₃·0.15 EtOAc: C 69.56, H 8.12, N 9.89. Found: C 69.63, H 8.28, N 8.86

Example 41: 1-(1-acetylpiperidin-4-yl)-3-(9-fluoro-5,6,8,9,10,11-hexahydro-7H-5,9:7,11-dimethanobenzo[9]annulen-7-yl)urea.

To a solution of 9-fluoro-5,6,8,9,10,11-hexahydro-7H-5,9:7,11-dimethanobenzo[9]annulen-7-amine (143 mg, 0.53 mmol) in DCM (4 mL) and saturated aqueous NaHCO₃ solution (2 mL) was added triphosgene (78 mg, 0.26 mmol). The biphasic mixture was stirred at room temperature for 30 minutes and then the two phases were separated and the organic layer was washed with brine (5 mL), dried over anh. Na₂SO₄, filtered and evaporated under vacuum to obtain 1-2 mL of a solution of the isocyanate in DCM. To this solution was added 1-(4-aminopiperidin-1-yl)ethan-1-one (90 mg, 0.63 mmol). The reaction mixture was stirred at room temperature overnight and the solvent was evaporated under vacuum to obtain a yellow gum (259 mg). Column chromatography (SiO₂, DCM/Methanol mixtures) gave 1-(1-acetylpiperidin-4-yl)-3-(9-fluoro-5,6,8,9,10,11-hexahydro-7H-5,9:7,11-dimethanobenzo[9]annulen-7-yl)urea (180 mg, 85% yield). The analytical sample was obtained by crystallization from hot DCM (57 mg). mp 228-229 °C. IR (NaCl disk): 3357, 2927, 2856, 1643, 1618, 1553, 1494, 1451, 1358, 1340, 1316, 1267, 1227, 1207, 1134, 1097, 1042, 1004 cm⁻¹. Anal. Calcd for C₂₃H₃₀FN₃O₂·0.15 C₅H₁₂·0.62 H₂O: C 67.59, H 7.91, N 9.96. Found: C 67.61, H 7.93, N 8.94.

Example 42: 1-(1-acetylpiperidin-4-yl)-3-(9-chloro-5,6,8,9,10,11-hexahydro-7H-5,9:7,11-dimethanobenzo[9]annulen-7-yl)urea.

To a solution of 9-chloro-5,6,8,9,10,11-hexahydro-7H-5,9:7,11-dimethanobenzo[9]annulen-7-amine hydrochloride (150 mg, 0.53 mmol) in DCM (3 mL) saturated aqueous NaHCO₃ solution (3 mL) and triphosgene (58 mg, 0.20 mmol) were added. The biphasic mixture was stirred at room temperature for 30 minutes and then the two phases were separated and the organic layer was washed with brine (3 mL), dried over anh. Na₂SO₄, filtered and concentrated under vacuum to obtain 1-2 mL of a solution of the isocyanate in DCM. To this solution was added 1-(4-aminopiperidin-1-yl)ethan-1-one (90 mg, 0.63 mmol). The reaction mixture was stirred at room temperature overnight and the solvent was evaporated under vacuum to obtain a white solid (204 mg). Column chromatography (SiO₂, DCM/Methanol mixtures) gave 1-(1-acetylpiperidin-4-yl)-3-(9-chloro-5,6,8,9,10,11-hexahydro-7H-5,9:7,11-dimethanobenzo[9]annulen-7-yl)urea (115 mg, 55% yield) as a white solid. mp 209-210 °C. IR (NaCl disk): 3358, 3019, 2926, 2855, 1644, 1619, 1556, 1494, 1452, 1358, 1319, 1301, 1268, 1228, 1206, 1135, 1090, 1050, 991, 969, 947, 802, 761, 735 cm⁻¹. HRMS-ESI+ m/z [M+H]⁺ calcd for [C₂₃H₃₀ClN₃O₂+H]⁺: 416.2099, found: 416.2100.

Example 43: 4-(((1r,4r)-4-(3-(5-methyl-1,5,6,7-tetrahydro-1,5:3,7-dimethanobenzo[e]oxonin-3(2H)-yl)ureido)cyclohexyl)oxy)benzoic acid.

To a solution of 5-methyl-1,5,6,7-tetrahydro-1,5:3,7-dimethanobenzo[e]oxonin-3(2H)-amine hydrochloride (200 mg, 0.76 mmol) in DCM (3.5 mL) and saturated aqueous NaHCO₃ solution (2.2 mL) was added triphosgene (113 mg, 0.38 mmol). The biphasic mixture was stirred at room temperature for 30 minutes and then the two phases were separated and the organic layer was washed with brine (5 mL), dried over anh. Na₂SO₄, filtered and evaporated under vacuum to obtain 1-2 mL of a solution of isocyanate in DCM. To this solution were added 4-(((1r,4r)-4-aminocyclohexyl)oxy)benzoic acid hydrochloride (206 mg, 0.76 mmol) and Et₃N (153 mg, 1.52 mmol). The mixture was stirred overnight at room temperature. The resulting suspension was evaporated to obtain a white solid, which was suspended in DCM (20 mL) and washed with 2N HCl solution (2 x 10 mL). The resulting organic suspension was filtered to afford a white solid (200 mg, 54% yield). mp: 220-222 °C. IR (NaCl disk): 3352, 2626, 1678, 1601, 1558, 1506, 1454, 1373, 1343, 1312, 1288, 1247, 1221, 1161, 1104, 1029, 997, 953, 776 cm⁻¹. HRMS-ESI+ m/z [M+H]⁺ calcd for [C₂₉H₃₄N₂O₅+H]⁺: 491.254, found: 491.254.

Example 44: 4-(((1r,4r)-4-(3-(9-methyl-5,6,8,9,10,11-hexahydro-7H-5,9:7,11-dimethanobenzo[9]annulen-7-yl)ureido)cyclohexyl)oxy)benzoic acid.

To a solution of 5-methyl-1,5,6,7-tetrahydro-1,5:3,7-dimethanobenzo[e]oxonin-3(2H)-amine hydrochloride (180 mg, 0.69 mmol) in DCM (3 mL) and saturated aqueous NaHCO₃ solution (2 mL) was added triphosgene (102 mg, 0.34 mmol). The biphasic mixture was stirred at room temperature for 30 minutes and then the two phases were separated and the organic layer was washed with brine (5 mL), dried over anh. Na₂SO₄, filtered and evaporated under vacuum to obtain 1-2 mL of a solution of isocyanate in DCM. To this solution were added 4-(((1r,4r)-4-aminocyclohexyl)oxy)benzoic acid hydrochloride (206 mg, 0.76 mmol) and Et₃N (153 mg, 1.52 mmol). The mixture was stirred overnight at room temperature. The resulting suspension was evaporated and the residue was suspended in DCM (20 mL) and washed with 2N HCl solution (2 x 10 mL). The resulting organic suspension was filtered and the filtrate was dried over anh. Na₂SO₄, filtered and concentrated under vacuum to give a white gum. Crystallization from hot EtOAc provided 4-(((1r,4r)-4-(3-(9-methyl-5,6,8,9,10,11-hexahydro-7H-5,9:7,11-dimethanobenzo[9]annulen-7-yl)ureido)cyclohexyl)oxy)benzoic acid as a white solid (55 mg, 16% yield). mp 182-183 °C. IR (NaCl disk): 3335, 2921, 2855, 1692, 1681, 1642, 1632, 1602, 1564, 1537, 1504, 1494, 1469, 1453, 1419, 1360, 1307, 1248, 1163, 1122, 1096, 1969 cm⁻¹. Anal. Calcd for C₃₀H₃₆N₂O₄·1,5 H₂O: C 69.88, H 7.62, N 5.43. Found: C 69.53, H 7.37, N 5.10.

Reference example 45: tert-butyl [1-(isopropylsulfonyl)piperidin-4-yl] carbamate.

To a solution of *tert*-butyl (piperidin-4-yl)carbamate (850 mg, 4.24 mmol) in DCM (7 mL) was added Et₃N (858 mg, 8.48 mmol). The mixture was cooled down to 0 °C with an ice bath and then propane-2-sulfonyl chloride (725 mg, 5.09 mmol) was added dropwise. The reaction mixture was stirred at room temperature overnight. The suspension was washed with 2N NaOH solution (2 x 5 mL) and the organic phase was dried over anh. Na₂SO₄, filtered and concentrated under vacuum to obtain *tert*-butyl [1-(isopropylsulfonyl)piperidin-4-yl] carbamate (1.15 g, 89% yield).

Reference example 46: 1-(isopropylsulfonyl)piperidin-4-amine.

To a solution of *tert*-butyl (1-(isopropylsulfonyl)piperidin-4-yl)carbamate (1.15 g, 3.75 mmol) in dissolved in DCM (5 mL) and 4 M HCl in 1,4-dioxane (2 mL) was added. The mixture was stirred at room temperature for 2 days and the solvents were evaporated under vacuum. The residue was then dissolved in DCM (5 mL) and washed with 5N NaOH solution (5 mL). The organic layer was dried over anh. Na₂SO₄, filtered and

concentrated under vacuum to give 1-(isopropylsulfonyl)piperidin-4-amine (704 mg, 91% yield) as a yellow oil.

Example 47: 1-[1-(isopropylsulfonyl)piperidin-4-yl]-3-(9-methyl-5,6,8,9,10,11-hexahydro-7H-5,9:7,11-dimethanobenzo[9]annulen-7-yl)urea.

To a solution of 5-methyl-1,5,6,7-tetrahydro-1,5:3,7-dimethanobenzo[e]oxonin-3(2H)-amine hydrochloride (300 mg, 1.13 mmol) in DCM (6 mL) and saturated aqueous NaHCO₃ solution (4 mL) was added triphosgene (169 mg, 0.57 mmol). The biphasic mixture was stirred at room temperature for 30 minutes and then the two phases were separated and the organic layer was washed with brine (5 mL), dried over anh. Na₂SO₄, filtered and evaporated under vacuum to obtain 1-2 mL of a solution of the isocyanate in DCM.

To a solution of 1-(isopropylsulfonyl)piperidin-4-amine (233 mg, 1.13 mmol) in anh. THF (5 mL) under argon atmosphere at -78 °C, was added dropwise a solution of *n*-butyllithium (2.5 M in hexanes, 0.59 mL, 1.47 mmol) during 20 minutes. After the addition, the mixture was tempered to 0 °C using an ice bath. This solution was added carefully to the solution of the isocyanate from the previous step cooled to 0 °C, under argon atmosphere. The reaction mixture was stirred at room temperature overnight. Methanol (2 mL) was then added to quench any unreacted *n*-butyllithium. The solvents were evaporated under vacuum to give an orange gum (506 mg). This residue was dissolved in EtOAc (10 mL) and washed with 2N HCl solution (2 x 5 mL) and the organic layer was dried over anh. Na₂SO₄, filtered and concentrated under vacuum to obtain a white gum (241 mg). Column chromatography (SiO₂, DCM/Methanol mixtures) gave a white solid. Crystallization from hot DCM/Pentane provided pure 1-(1-(isopropylsulfonyl)piperidin-4-yl)-3-(9-methyl-5,6,8,9,10,11-hexahydro-7H-5,9:7,11-dimethanobenzo[9]annulen-7-yl)urea (66 mg, 13% yield) as a white solid.

mp 218-219 °C. IR (NaCl disk): 3364, 3061, 3012, 2945, 2919, 2853, 1709, 1638, 1553, 1493, 1453, 1360, 1319, 1305, 1265, 1248, 1232, 1133, 1091, 1045, 943, 880, 841, 759, 732, 665, 592, 555 cm⁻¹. Anal. Calcd for C₂₅H₃₇N₃O₃S: C 65.33, H 8.11, N 9.14. Found: C 65.41, H 8.31, N 8.93

Example 48: 1-(1-benzylpiperidin-4-yl)-3-(9-methyl-5,6,8,9,10,11-hexahydro-7H-5,9:7,11-dimethanobenzo[9]annulen-7-yl)urea.

To a solution of 5-methyl-1,5,6,7-tetrahydro-1,5:3,7-dimethanobenzo[e]oxonin-3(2H)-amine hydrochloride (250 mg, 0.95 mmol) in DCM (4.5 mL) and saturated aqueous NaHCO₃ solution (3 mL) was added triphosgene (140 mg, 0.47 mmol). The biphasic mixture was stirred at room temperature for 30 minutes and then the two phases were

separated and the organic layer was washed with brine (5 mL), dried over anh. Na₂SO₄, filtered and evaporated under vacuum to obtain 1-2 mL of a solution of the isocyanate in DCM. To this solution was added 1-(4-aminopiperidin-1-yl)ethan-1-one (216 mg, 1.13 mmol). The reaction mixture was stirred at room temperature for 24 h and the solvent was evaporated under vacuum to obtain a yellow gum. Column chromatography (SiO₂, DCM/Methanol mixtures) gave the title compound as a white solid (159 mg, 36% yield).

mp 106-107 °C. IR (NaCl disk): 3318, 3058, 3025, 2945, 2918, 2838, 2792, 2761, 1632, 1559, 1493, 1453, 1361, 1343, 1321, 1302, 1281, 1234, 1209, 1136, 1120, 1066, 1028, 909, 757, 733, 698 cm⁻¹. Anal. Calcd for C₂₉H₃₇N₃O·0.5 Methanol: C 77.09, H 8.55, N 9.14. Found: C 77.19, H 8.36, N 8.98.

Reference example 49: N-(2-acetyl-9-methyl-5,6,8,9,10,11-hexahydro-7H-5,9:7,11-dimethanobenzo[9]annulen-7-yl)-2-chloroacetamide.

To a solution of 2-chloro-N-(9-methyl-5,6,8,9,10,11-hexahydro-7H-5,9:7,11-dimethanobenzo[9]annulen-7-yl)acetamide (2.0 g, 6.58 mmol) in DCM (50 mL) was added acetyl chloride (5.16 g, 65.8 mmol). Then, the mixture was treated with AlCl₃ (4.38 g, 32.9 mmol) and the resulting orange mixture was stirred for 1 h at room temperature. The solution was poured over ice (50 g) and saturated aqueous NaHCO₃ solution (40 mL) was added. After stirring 20 min, the mixture was extracted with DCM (3 x 50 mL) and the combined organic phases were dried over anh. Na₂SO₄, filtered and concentrated under vacuum to obtain a green gum (1.85 g). Column chromatography (SiO₂, Hexane/Ethyl Acetate mixtures) gave N-(2-acetyl-9-methyl-5,6,8,9,10,11-hexahydro-7H-5,9:7,11-dimethanobenzo[9]annulen-7-yl)-2-chloroacetamide (1.27 g, 56% yield) as a yellowish solid.

Reference example 50: 1-(7-amino-9-methyl-6,7,8,9,10,11-hexahydro-5H-5,9:7,11-dimethanobenzo[9]annulen-2-yl)ethan-1-one hydrochloride.

A mixture of N-(2-acetyl-9-methyl-5,6,8,9,10,11-hexahydro-7H-5,9:7,11-dimethanobenzo[9]annulen-7-yl)-2-chloroacetamide (1.18 g, 3.43 mmol), thiourea (313 mg, 4.12 mmol), acetic acid (1.3 mL) and ethanol (6 mL) was stirred at reflux overnight. The mixture was tempered to room temperature and water (40 mL) and 10N NaOH solution (14 mL) were added. The mixture was extracted with EtOAc (3 x 50 mL) and the combined organic extracts were dried over anh. Na₂SO₄, filtered and concentrated under vacuum to obtain a yellow residue (980 mg) which was dissolved in EtOAc (5 mL) and an excess of HCl/Et₂O was added. The resulting suspension was filtrated obtaining a beige solid. This product was dissolved in DCM (50 mL) and washed with

5N NaOH solution (40 mL). The organic layer was dried over anh. Na₂SO₄, filtered and concentrated under vacuum to obtain a yellow residue which was dissolved in EtOAc (5 mL) and an excess of HCl/Et₂O was added. The resulting suspension was filtered obtaining
1-(7-amino-9-methyl-6,7,8,9,10,11-hexahydro-5*H*-5,9:7,11-dimethanobenzo[9]annulen-2-yl)ethan-1-one as its hydrochloride (758 mg, 73% yield)
5 as a beige solid.

Example 51: 1-(2-acetyl-9-methyl-5,6,8,9,10,11-hexahydro-7*H*-5,9:7,11-dimethanobenzo[9]annulen-7-yl)-3-(1-acetylpiperidin-4-yl)urea.

10 To a solution of 1-(7-amino-9-methyl-6,7,8,9,10,11-hexahydro-5*H*-5,9:7,11-dimethanobenzo[9]annulen-2-yl)ethan-1-one hydrochloride (300 mg, 0.98 mmol) in DCM (5 mL) and saturated aqueous NaHCO₃ solution (3.52 mL) was added triphosgene (145 mg, 0.49 mmol). The biphasic mixture was stirred at room temperature for 30 minutes and then the two phases were separated and the organic layer was washed with brine
15 (5 mL), dried over anh. Na₂SO₄, filtered and evaporated under vacuum to obtain 1-2 mL of a solution of the isocyanate in DCM. To this solution was added 1-(4-aminopiperidin-1-yl)ethan-1-one (167 mg, 1.17 mmol). The reaction mixture was stirred at room temperature overnight and the solvent was evaporated under vacuum to obtain a yellow gum (483 mg). Column chromatography (SiO₂, DCM/Methanol mixtures) gave
20 1-(2-acetyl-9-methyl-5,6,8,9,10,11-hexahydro-7*H*-5,9:7,11-dimethanobenzo[9]annulen-7-yl)-3-(1-acetylpiperidin-4-yl)urea (324 mg, 76% yield).
mp 144-145 °C. IR (NaCl disk): 3363, 3005, 2918, 2861, 2239, 1679, 1619, 1552, 1453, 1426, 1361, 1320, 1272, 1229, 1203, 1137, 1106, 1057, 973, 950, 917, 830, 731, 645 cm⁻¹. Anal. Calcd for C₂₆H₃₅N₃O₃·0.15 C₅H₁₂·0.6 C₃H₆O: C 70.96, H 8.43, N 8.70.
25 Found: C 70.83, H 8.60, N 8.88

Example 52: 1-(1-acetylpiperidin-4-yl)-3-(9-methyl-2-nitro-5,6,8,9,10,11-hexahydro-7*H*-5,9:7,11-dimethanobenzo[9]annulen-7-yl)urea.

To a solution of 9-methyl-2-nitro-5,6,8,9,10,11-hexahydro-7*H*-5,9:7,11-dimethanobenzo[9]annulen-7-amine hydrochloride (600 mg, 1.94 mmol) in DCM (10 mL) saturated aqueous NaHCO₃ solution (10 mL) and triphosgene (213 mg, 0.718 mmol) were added. The biphasic mixture was stirred at room temperature for 30 minutes and then the two phases were separated and the organic layer was washed with brine (5 mL), dried over anh. Na₂SO₄, filtered and evaporated under vacuum to obtain 1-2 mL
30 of a solution of the isocyanate in DCM. To this solution was added 1-(4-aminopiperidin-1-yl)ethan-1-one (331 mg, 2.33 mmol). The reaction mixture was stirred at room temperature overnight and the solvent was evaporated under vacuum to obtain a

brown solid (840 mg). Column chromatography (SiO₂, DCM/Methanol mixtures) gave 1-(1-acetylpiperidin-4-yl)-3-(9-methyl-2-nitro-5,6,8,9,10,11-hexahydro-7H-5,9:7,11-dimethanobenzo[9]annulen-7-yl)urea (640 mg, 75% yield) as a yellowish solid.
mp 155-156 °C. IR (NaCl disk): 3360, 2918, 2237, 1619, 1552, 1522, 1454, 1345,
5 1322, 1266, 1230, 1164, 1137, 1081, 974, 949, 911, 865, 838, 798, 761, 731, 644 cm⁻¹.
Anal. Calcd for C₂₄H₃₂N₄O₄: C 65.43, H 7.32, N 12.72. Found: C 65.22, H 7.45, N 12.56.

Example 53: 1-(1-acetylpiperidin-4-yl)-3-(2-amino-9-methyl-5,6,8,9,10,11-hexahydro-7H-5,9:7,11-dimethanobenzo[9]annulen-7-yl)urea.

To a solution of 1-(1-acetylpiperidin-4-yl)-3-(9-methyl-2-nitro-5,6,8,9,10,11-hexahydro-7H-5,9:7,11-dimethanobenzo[9]annulen-7-yl)urea (260 mg, 0.59 mmol) in EtOH (17 ml) was added PtO₂ (20 mg). The mixture was hydrogenated at room temperature and atmospheric pressure for 8 days. The resulting suspension was filtered and the filtrate
15 was evaporated under vacuum to obtain a dark brown solid (223 mg), which was dissolved in DCM (10 mL). To this solution, Et₂O was added and a white solid precipitated (140 mg). Column chromatography (SiO₂, DCM/Methanol mixtures) gave a white solid (82 mg, 34% yield).

mp 150-151 °C. IR (NaCl disk): 3344, 3006, 2905, 2853, 1614, 1556, 1505, 1454,
20 1360, 1344, 1320, 1303, 1266, 1229, 1194, 1162, 1136, 1060, 974, 868, 820, 734 cm⁻¹.
HRMS-ESI+ m/z [M+H]⁺ calcd for [C₂₄H₃₄N₄O₂+H]⁺: 411.2755, found: 411.2756.

Example 54: tert-butyl 4-(2-((9-methyl-5,6,8,9,10,11-hexahydro-7H-5,9:7,11-dimethanobenzo[9]annulen-7-yl)amino)-2-oxoethyl)piperidine-1-carboxylate.

To a suspension of 9-methyl-5,6,8,9,10,11-hexahydro-7H-5,9:7,11-dimethanobenzo[9]annulen-7-amine hydrochloride (500 mg, 1.89 mmol) in EtOAc (5 mL), 2-(1-(tert-butoxycarbonyl)piperidin-4-yl)acetic acid (461 mg, 1.89 mmol), HOBt (384 mg, 2.84 mmol), EDC·HCl (440 mg, 2.84 mmol) and Et₃N (767 mg, 7.58 mmol) were added. The mixture was stirred at room temperature for 24 h. Water (10 mL) and DCM
30 (20 mL) were added to the resulting suspension and the 2 phases were separated. The organic phase was washed with saturated aqueous NaHCO₃ solution (1x10 mL), brine (1x10 mL), 2N HCl solution (1x10 mL) and 2N NaOH (1x10 mL), dried over anh. Na₂SO₄, filtered and concentrated under vacuum to give a yellow solid (515 mg, 60% yield).

35 ¹H-NMR (400 MHz, CDCl₃) δ: 0.92 (s, 3H), 1.11 (dq, J = 4.4 Hz, J' = 11.6 Hz, 2H), 1.4 (s, 9H), 1.54 (d, J = 13.6 Hz, 2H), 1.63-1.68 (complex signal, 4H), 1.84 (s, 2H), 1.91 (m, 1H), 1.97 (s, 2H), 2.0 (d, J = 12.8 Hz, 2H), 2.14-2.18 (complex signal, 2H), 2.69 (t, J =

13.2 Hz, 2H), 3.06 (t, $J = 6$ Hz, 2H), 4.06 (broad signal, 2H), 5.14 (s, 1H), 7.02-7.08 (complex signal, 4H).

Example 55: N-(9-methyl-5,6,8,9,10,11-hexahydro-7H-5,9:7,11-dimethanobenzo[9]annulen-7-yl)-2-(piperidin-4-yl)acetamide.

To a solution of *tert*-butyl 4-(2-((9-methyl-5,6,8,9,10,11-hexahydro-7H-5,9:7,11-dimethanobenzo[9]annulen-7-yl)amino)-2-oxoethyl)piperidine-1-carboxylate (250 mg, 0.55 mmol) in DCM (4 mL) was added 4M HCl in 1,4-dioxane (0.5 ml). The reaction mixture was stirred at room temperature for 3 days. Then, the solvent was evaporated under vacuum and the residue was dissolved in DCM (10 mL) and washed with 5N NaOH solution, dried over anh. Na₂SO₄, filtered and concentrated under vacuum to give a yellow solid (189 mg, 97% yield).

¹H-NMR (400 MHz, CDCl₃) δ : 0.91 (s, 3H), 1.12 (dq, $J = 4$ Hz, $J' = 12.0$ Hz, 2H), 1.53 (d, $J = 13.2$ Hz, 2H), 1.62-1.71 (complex signal, 4H), 1.84 (s, 2H), 1.88 (m, 1H), 1.95-2.01 (complex signal, 4H), 2.14-2.19 (complex signal, 2H), 2.6 (dt, $J = 2.8$ Hz, $J' = 12.0$ Hz, 2H), 3.00-3.07 (complex signal, 4H), 5.15 (s, 1H), 7.02-7.09 (complex signal, 4H).

Example 56: 2-[1-(isopropylsulfonyl)piperidin-4-yl]-N-(9-methyl-5,6,8,9,10,11-hexahydro-7H-5,9:7,11-dimethanobenzo[9]annulen-7-yl)acetamide.

To a solution of *N*-(9-methyl-5,6,8,9,10,11-hexahydro-7H-5,9:7,11-dimethanobenzo[9]annulen-7-yl)-2-(piperidin-4-yl)acetamide (185 mg, 0.52 mmol) in DCM (5 mL) was added Et₃N (63 mg, 0.63 mmol). The mixture was cooled down to 0 °C and propane-2-sulfonyl chloride (74 mg, 0.52 mmol) was added dropwise. Then, the reaction mixture was stirred at room temperature overnight and quenched by addition of 2N HCl solution (3 mL). The two phases were separated and the aqueous phase was extracted with EtOAc (2 x 20 mL). The combined organic phases were washed with 5N NaOH solution, dried over anh. Na₂SO₄, filtered and concentrated under vacuum to give a yellow solid. Column chromatography (SiO₂, Hexane/Ethyl Acetate mixtures) gave a white solid (145 mg, 60% yield). The analytical sample was obtained by crystallization from hot EtOAc (76 mg).

mp 172 -173 °C. IR (NaCl disk): 3365, 3319, 3058, 3017, 2916, 2852, 1648, 1536, 1493, 1451, 1361, 1322, 1308, 1264, 1167, 1137, 1044, 1011, 993, 944, 904, 880, 800, 758, 731, 701, 665 cm⁻¹. Anal. Calcd for C₂₆H₃₈N₂O₃S·0.25 Methanol: C 67.56, H 8.42, N 6.00. Found: C 67.75 H 8.62, N 5.74.

Example 57: 2-(1-acetyl)piperidin-4-yl)-N-(9-methyl-5,6,8,9,10,11-hexahydro-7H-5,9:7,11-dimethanobenzo[9]annulen-7-yl)acetamide.

To a solution of *N*-(9-methyl-5,6,8,9,10,11-hexahydro-7*H*-5,9:7,11-dimethanobenzo[9]annulen-7-yl)-2-(piperidin-4-yl)acetamide (200 mg, 0.57 mmol) in anh. DCM (5 mL) under argon atmosphere was added anh. Et₃N (69 mg, 0.68 mmol). The mixture was cooled down to 0°C and acetyl chloride (45 mg, 0.57 mmol) was added dropwise.

5 Then, the reaction mixture was stirred at room temperature overnight and quenched by addition of 2N HCl solution (3 mL). The two phases were separated and the aqueous layer was extracted with EtOAc (2 x 20 mL). The combined organic phases were washed with 2N NaOH solution, dried over anh. Na₂SO₄, filtered and concentrated under vacuum. Column chromatography (SiO₂, Hexane/Ethyl Acetate mixtures) gave a

10 white solid (134 mg, 48% yield).
mp 85-86 °C. IR (NaCl disk): 3314, 3060, 3016, 2915, 2859, 2239, 1630, 1544, 1492, 1450, 1361, 1303, 1273, 1196, 1164, 1137, 1096, 1048 cm⁻¹. Anal. Calcd for C₂₅H₃₄N₂O₂·0.15 DCM: C 74.17, H 8.49, N 6.88. Found: C 74.31, H 8.73, N 6.72.

15 **Example 58: 1-(9-methyl-6,7,8,9,10,11-hexahydro-5*H*-5,9:7,11-dimethanobenzo[9]annulen-7-yl)-3-(2,3,4-trifluorophenyl)urea.**

To a solution of 5-methyl-1,5,6,7-tetrahydro-1,5:3,7-dimethanobenzo[*e*]oxonin-3(2*H*)-amine (273 mg, 1.2 mmol) in anhydrous DCM (10 mL), 2,3,4-trifluorophenylisocyanate (147 mg, 1.0 mmol) and triethylamine (0.55 mg, 4 mmol) were added. The reaction

20 mixture was stirred at room temperature overnight. Then the solvent was removed under vacuum. Column chromatography (SiO₂, Hexane/Ethyl Acetate mixture) of the crude and concentration under vacuum of the appropriate fractions gave the urea (38 mg, 13% yield) as a white solid.

mp 206-207 °C. IR (ATR): 3331, 2903, 2839, 1654, 1556, 1510, 1473, 1361, 1344,

25 1290, 1237, 1174, 1101, 1038, 1019, 1004, 800, 756, 690, 669, 625 cm⁻¹. Anal. Calcd for C₂₃H₂₃F₃N₂O: C 68.99, H 5.79, N 7.00. Found: C 68.94, H 5.92, N 6.71.

Example 59: 1-(5-methyl-1,5,6,7-tetrahydro-1,5:3,7-dimethanobenzo[*e*]oxonin-3(2*H*)-yl)-3-(2,3,4-trifluorophenyl)urea.

To a solution of 5-methyl-1,5,6,7-tetrahydro-1,5:3,7-dimethanobenzo[*e*]oxonin-3(2*H*)-

30 amine (275 mg, 1.2 mmol) in anhydrous DCM (10 mL), 2,3,4-trifluorophenylisocyanate (147 mg, 1.0 mmol) and triethylamine (0.55 mg, 4 mmol) were added. The reaction mixture was stirred at room temperature overnight. Then the solvent was removed under vacuum. The desired urea was obtained as a white solid (205 mg, 54% yield).

mp 257-259 °C. IR (ATR): 3295, 3241, 3118, 2916, 2173, 1693, 1620, 1564, 1510, 1493, 1468, 1462, 1356, 1345, 1320, 1302, 1286, 1273, 1254, 1229, 1210, 1181, 1167, 1111, 1091, 1074, 1049, 1035, 1008, 999, 958, 906, 820, 812, 763, 646 cm⁻¹. Anal. Calcd for C₂₂H₂₁F₃N₂O₂·0.1H₂O: C 65.37, H 5.29, N 6.93. Found: C 65.18, H 5.31, N 6.73. HRMS-ESI+ m/z [M+H]⁺ calcd for [C₂₂H₂₁F₃N₂O₂+H]⁺: 403.1633, found: 403.1631.

Example 60: 2-(1-benzylpiperidin-4-yl)-N-(9-methyl-5,6,8,9,10,11-hexahydro-7H-5,9:7,11-dimethanobenzo[9]annulen-7-yl)acetamide.

To a suspension of 9-methyl-5,6,8,9,10,11-hexahydro-7H-5,9:7,11-dimethanobenzo[9]annulen-7-amine hydrochloride (250 mg, 0.95 mmol) in EtOAc (5 mL), 2-(1-benzylpiperidin-4-yl)acetic acid hydrochloride (255 mg, 0.95 mmol), HOBT (192 mg, 1.42 mmol), EDC-HCl (220 mg, 1.42 mmol) and Et₃N (480 mg, 4.74 mmol) were added. The mixture was stirred at room temperature for 24 h. Water (10 mL) and DCM (10 mL) were added to the resulting suspension and the 2 phases were separated. The organic phase was washed with saturated aqueous NaHCO₃ solution (1x10 mL), brine (1x10 ml), dried over anh. Na₂SO₄, filtered and concentrated under vacuum to give a yellow gum (479 mg). Column chromatography (SiO₂, DCM/Methanol mixtures) gave a white solid (280 mg, 67% yield). The analytical sample was obtained by crystallization from hot EtOAc and Et₂O (124 mg).

mp 145-146 °C. IR (NaCl disk): 3302, 3060, 3024, 2917, 2841, 2798, 2755, 1641, 1544, 1493, 1452, 1361, 1342, 1309, 1279, 1211, 1184, 1143, 1077, 1008, 974, 943, 916, 794, 756, 737, 697 cm⁻¹. HRMS-ESI+ m/z [M+H]⁺ calcd for [C₃₀H₃₈N₂O+H]⁺: 443.3057, found: 443.3061.

Reference example 61: tert-butyl (1-propionylpiperidin-4-yl)carbamate.

To a solution of *tert*-butyl piperidin-4-ylcarbamate (500 mg, 2.49 mmol) in anh. THF (5 mL) was added Et₃N (252 mg, 2.49 mmol). The mixture was cooled down to 0 °C with an ice bath and then propionyl chloride (230 mg, 2.49 mmol) was added dropwise. The reaction mixture was stirred at room temperature for 2h. The suspension was filtrated and the filtered was evaporated to obtain the carbamate as a yellowish solid (661 mg, quantitative yield).

Reference example 62: 1-(4-aminopiperidin-1-yl)propan-1-one.

To a solution of *tert*-butyl (1-propionylpiperidin-4-yl)carbamate (660 g, 2.57 mmol) in DCM (3 mL) 4 M HCl in 1,4-dioxane (2 mL) was added. The mixture was stirred at room temperature overnight and the solvents were evaporated under vacuum. The residue was then dissolved in DCM (5 mL) and washed with 5N NaOH solution (5 mL).

The organic layer was dried over anhydrous Na_2SO_4 , filtered and concentrated under vacuum to give 1-(4-aminopiperidin-1-yl)propan-1-one (335 mg, 83% yield) as a yellow oil.

Example 63: 1-(9-methyl-5,6,8,9,10,11-hexahydro-7H-5,9:7,11-dimethanobenzo[9]annulen-7-yl)-3-(1-propionylpiperidin-4-yl)urea.

To a solution of 9-methyl-5,6,8,9,10,11-hexahydro-7H-5,9:7,11-dimethanobenzo[9]annulen-7-amine hydrochloride (464 mg, 1.76 mmol) in DCM (10 mL) saturated aqueous NaHCO_3 solution (10 mL) and triphosgene (193 mg, 0.65 mmol) were added. The biphasic mixture was stirred at room temperature for 30 minutes and then the two phases were separated and the organic layer was washed with brine (5 mL), dried over anhydrous Na_2SO_4 , filtered and evaporated under vacuum to obtain 1-2 mL of a solution of the isocyanate in DCM. To this solution was added 1-(4-aminopiperidin-1-yl)propan-1-one (350 mg, 2.11 mmol). The reaction mixture was stirred at room temperature overnight and the solvent was evaporated under vacuum to obtain a white solid (741 mg). Column chromatography (SiO_2 , DCM/Methanol mixtures) gave 1-(9-methyl-5,6,8,9,10,11-hexahydro-7H-5,9:7,11-dimethanobenzo[9]annulen-7-yl)-3-(1-propionylpiperidin-4-yl)urea (597 mg, 83% yield) as a white solid. The analytical sample was obtained by crystallization from hot EtOAc and DCM (300 mg). mp 207-208 °C. IR (NaCl disk): 3357, 2917, 2858, 1644, 1620, 1555, 1493, 1449, 1360, 1344, 1318, 1263, 1221, 1131, 1067, 1023, 971, 948, 758 cm^{-1} . Anal. Calcd for $\text{C}_{25}\text{H}_{35}\text{N}_3\text{O}_2 \cdot 0.15 \text{ EtOAc}$: C 72.73, H 8.63, N 9.94. Found: C 72.65, H 8.49, N 9.82.

Example 64: 1-(1-(4-acetylphenyl)piperidin-4-yl)-3-(9-methyl-5,6,8,9,10,11-hexahydro-7H-5,9:7,11-dimethanobenzo[9]annulen-7-yl)urea.

To a solution of 9-methyl-5,6,8,9,10,11-hexahydro-7H-5,9:7,11-dimethanobenzo[9]annulen-7-amine hydrochloride (241 mg, 0.95 mmol) in DCM (5 mL) saturated aqueous NaHCO_3 solution (5 mL) and triphosgene (104 mg, 0.35 mmol) were added. The biphasic mixture was stirred at room temperature for 30 minutes and then the two phases were separated and the organic layer was washed with brine (5 mL), dried over anhydrous Na_2SO_4 , filtered and evaporated under vacuum to obtain 1-2 mL of a solution of the isocyanate in DCM. To this solution was added 1-(4-(4-aminopiperidin-1-yl)phenyl)ethan-1-one (250 mg, 1.15 mmol, prepared following the procedure reported in WO2007016496). The reaction mixture was stirred at room temperature overnight and the solvent was evaporated under vacuum to obtain an orange solid (475 mg). Column chromatography (SiO_2 , Hexane/Ethyl Acetate mixtures) gave 1-(1-(4-acetylphenyl)piperidin-4-yl)-3-(9-methyl-5,6,8,9,10,11-hexahydro-7H-5,9:7,11-dimethanobenzo[9]annulen-7-yl)urea (120 mg, 27% yield) as a yellowish solid.

mp 211-212 °C. IR (NaCl disk): 3357, 2919, 2844, 1666, 1633, 1596, 1552, 1518, 1493, 1452, 1427, 1389, 1359, 1306, 1281, 1224, 1193, 1128, 1068, 956, 915, 825, 758 cm⁻¹. HRMS-ESI+ m/z [M+H]⁺ calcd for [C₃₀H₃₇N₃O₂+H]⁺: 472.2959, found: 472.2962.

5

Example 65: 1-(9-methyl-5,6,8,9,10,11-hexahydro-7H-5,9:7,11-dimethanobenzo[9]annulen-7-yl)-3-(1-(tetrahydro-2H-pyran-4-carbonyl)piperidin-4-yl)urea.

To a solution of 9-methyl-5,6,8,9,10,11-hexahydro-7H-5,9:7,11-dimethanobenzo[9]annulen-7-amine hydrochloride (258 mg, 0.98 mmol) in DCM (4 mL) saturated aqueous
10 NaHCO₃ solution (4 mL) and triphosgene (107 mg, 0.36 mmol) were added. The biphasic mixture was stirred at room temperature for 30 minutes and then the two phases were separated and the organic layer was washed with brine (2 mL), dried over anhydrous Na₂SO₄, filtered and evaporated under vacuum to obtain 1-2 mL of a solution of the isocyanate in DCM. To this solution was added (4-aminopiperidin-1-yl)(tetrahydro-
15 2H-pyran-4-yl)methanone (215 mg, 1.10 mmol). The reaction mixture was stirred at room temperature overnight and the solvent was evaporated under vacuum to obtain a yellow residue (534 mg). Column chromatography (SiO₂, DCM/Methanol mixtures) gave 1-(9-methyl-5,6,8,9,10,11-hexahydro-7H-5,9:7,11-dimethanobenzo[9]annulen-7-yl)-3-(1-(tetrahydro-2H-pyran-4-carbonyl)piperidin-4-yl)urea (207 mg, 45% yield) as a
20 white solid.

mp 224-225 °C. IR (NaCl disk): 3356, 3064, 2945, 2919, 2850, 1639, 1613, 1552, 1493, 1446, 1360, 1344, 1320, 1278, 1261, 1238, 1211, 1126, 1089, 1068, 1018, 983, 941, 874, 818, 758, 733 cm⁻¹. HRMS-ESI+ m/z [M+H]⁺ calcd for [C₂₈H₃₉N₃O₃+H]⁺: 466.3064, found: 466.3065.

25

Example 66: 1-(1-(2-fluorobenzoyl)piperidin-4-yl)-3-(9-methyl-5,6,8,9,10,11-hexahydro-7H-5,9:7,11-dimethanobenzo[9]annulen-7-yl)urea.

To a solution of 9-methyl-5,6,8,9,10,11-hexahydro-7H-5,9:7,11-dimethanobenzo[9]annulen-7-amine hydrochloride (247 mg, 0.93 mmol) in DCM (4 mL)
30 saturated aqueous NaHCO₃ solution (4 mL) and triphosgene (103 mg, 0.36 mmol) were added. The biphasic mixture was stirred at room temperature for 30 minutes and then the two phases were separated and the organic layer was washed with brine (3 mL), dried over anhydrous Na₂SO₄, filtered and evaporated under vacuum to obtain 1-2 mL of a solution of the isocyanate in DCM. To this solution was added (4-aminopiperidin-1-yl)(2-fluorophenyl)methanone (250 mg, 1.12 mmol). The reaction mixture was stirred at
35 room temperature overnight and the solvent was evaporated under vacuum to obtain a white solid (486 mg). Column chromatography (SiO₂, DCM/Methanol mixtures) gave 1-

(1-(2-fluorobenzoyl)piperidin-4-yl)-3-(9-methyl-5,6,8,9,10,11-hexahydro-7*H*-5,9:7,11-dimethanobenzo[9]annulen-7-yl)urea (285 mg, 45% yield) as a white solid.
mp 265-266 °C. IR (NaCl disk): 3368, 2920, 2854, 1614, 1549, 1492, 1452, 1364, 1318, 1282, 1222, 1122, 1089, 1029, 974, 948, 817, 755 cm⁻¹. HRMS-ESI+ m/z [M+H]⁺
5 calcd for [C₂₉H₃₄FN₃O₂+H]⁺: 476.2708, found: 476.2711.

Example 67: 1-((1*R*,3*s*,5*S*)-8-benzyl-8-azabicyclo[3.2.1]octan-3-yl)-3-(9-methyl-5,6,8,9,10,11-hexahydro-7*H*-5,9:7,11-dimethanobenzo[9]annulen-7-yl)urea.

To a solution of 9-methyl-5,6,8,9,10,11-hexahydro-7*H*-5,9:7,11-dimethanobenzo[9]annulen-7-amine hydrochloride (253 mg, 0.96 mmol) in DCM (4 mL) saturated aqueous NaHCO₃ solution (4 mL) and triphosgene (105 mg, 0.35 mmol) were added. The biphasic mixture was stirred at room temperature for 30 minutes and then the two phases were separated and the organic layer was washed with brine (3 mL), dried over anhydrous Na₂SO₄, filtered and evaporated under vacuum to obtain 1-2 mL of a solution of the isocyanate in DCM. To this solution was added (1*R*,3*s*,5*S*)-8-benzyl-8-azabicyclo[3.2.1]octan-3-amine (250 mg, 1.15 mmol). The reaction mixture was stirred at room temperature overnight and the solvent was evaporated under vacuum to obtain a yellow gum (498 mg). Column chromatography (SiO₂, DCM/Methanol mixtures) gave 1-((1*R*,3*s*,5*S*)-8-benzyl-8-azabicyclo[3.2.1]octan-3-yl)-3-(9-methyl-5,6,8,9,10,11-hexahydro-7*H*-5,9:7,11-dimethanobenzo[9]annulen-7-yl)urea (293 mg, 65% yield) as a white solid. The analytical sample was obtained by crystallization from hot mixture EtOAc:Et₂O (187 mg).
mp 100-101 °C. IR (NaCl disk): 3319, 3022, 2944, 2919, 2843, 1632, 1557, 1493, 1452, 1344, 1321, 1304, 1279, 1263, 1235, 1164, 1122, 1056, 1027, 756, 729, 696
25 cm⁻¹. HRMS-ESI+ m/z [M+H]⁺ calcd for [C₃₁H₃₉N₃O+H]⁺: 470.3166, found: 470.3168.

Example 68: 1-(1-acetylpiperidin-4-yl)-3-(2-fluoro-9-methyl-5,6,8,9,10,11-hexahydro-7*H*-5,9:7,11-dimethanobenzo[9]annulen-7-yl)urea.

To a solution of 2-fluoro-9-methyl-5,6,8,9,10,11-hexahydro-7*H*-5,9:7,11-dimethanobenzo[9]annulen-7-amine hydrochloride (150 mg, 0.53 mmol) in DCM (3 mL) saturated aqueous NaHCO₃ solution (3 mL) and triphosgene (59 mg, 0.20 mmol) were added. The biphasic mixture was stirred at room temperature for 30 minutes and then the two phases were separated and the organic layer was washed with brine (3 mL), dried over anhydrous Na₂SO₄, filtered and evaporated under vacuum to obtain 1-2 mL of a solution of the isocyanate in DCM. To this solution was added 1-(4-aminopiperidin-1-yl)ethan-1-one (91 mg, 0.64 mmol). The reaction mixture was stirred at room temperature overnight and the solvent was evaporated under vacuum to obtain a yellowish oil (165
35

mg). Column chromatography (SiO₂, DCM/Methanol mixtures) gave 1-(1-acetylpiperidin-4-yl)-3-(2-fluoro-9-methyl-5,6,8,9,10,11-hexahydro-7H-5,9:7,11-dimethanobenzo[9]annulen-7-yl)urea (103 mg, 49% yield) as a white solid.
mp 269-270 °C. IR (NaCl disk): 3357, 2919, 2856, 1644, 1620, 1555, 1499, 1453,
5 1361, 1342, 1320, 1228, 1153, 1138, 1064, 967, 863, 818 cm⁻¹. HRMS-ESI+ m/z [M+H]⁺ calcd for [C₂₄H₃₂FN₃O₂+H]⁺: 414.2551, found: 414.2553.

Example 69: 1-(1-acetylpiperidin-4-yl)-3-(2-methoxy-9-methyl-5,6,8,9,10,11-hexahydro-7H-5,9:7,11-dimethanobenzo[9]annulen-7-yl)urea.

10 To a solution of 2-methoxy-9-methyl-5,6,8,9,10,11-hexahydro-7H-5,9:7,11-dimethanobenzo[9]annulen-7-aminehydrochloride (150 mg, 0.51 mmol) in DCM (3 mL) saturated aqueous NaHCO₃ solution (3 mL) and triphosgene (56 mg, 0.19 mmol) were added. The biphasic mixture was stirred at room temperature for 30 minutes and then the two phases were separated and the organic layer was washed with brine (3 mL), dried over
15 anh. Na₂SO₄, filtered and evaporated under vacuum to obtain 1-2 mL of a solution of the isocyanate in DCM. To this solution was added 1-(4-aminopiperidin-1-yl)ethan-1-one (87 mg, 0.61 mmol). The reaction mixture was stirred at room temperature overnight and the solvent was evaporated under vacuum to obtain a brown oil (256 mg). Column chromatography (SiO₂, DCM/Methanol mixtures) gave 1-(1-
20 acetylpiperidin-4-yl)-3-(2-methoxy-9-methyl-5,6,8,9,10,11-hexahydro-7H-5,9:7,11-dimethanobenzo[9]annulen-7-yl)urea (121 mg, 56 % yield) as a white solid.
mp 116-117 °C. IR (NaCl disk): 3359, 2905, 2861, 1644, 1619, 1551, 1501, 1452, 1360, 1343, 1319, 1267, 1227, 1153, 1136, 1042, 973, 807, 736 cm⁻¹. HRMS-ESI+ m/z [M+H]⁺ calcd for [C₂₅H₃₅N₃O₃+H]⁺: 426.2571, found: 4426.2760.

25

Example 70: 1-(1-acetylpiperidin-4-yl)-3-(1-fluoro-9-methyl-5,6,8,9,10,11-hexahydro-7H-5,9:7,11-dimethanobenzo[9]annulen-7-yl)urea.

To a solution of 1-fluoro-9-methyl-5,6,8,9,10,11-hexahydro-7H-5,9:7,11-dimethanobenzo[9]annulen-7-amine hydrochloride (150 mg, 0.53 mmol) in DCM (3 mL) saturated
30 aqueous NaHCO₃ solution (3 mL) and triphosgene (58 mg, 0.20 mmol) were added. The biphasic mixture was stirred at room temperature for 30 minutes and then the two phases were separated and the organic layer was washed with brine (3 mL), dried over anh. Na₂SO₄, filtered and evaporated under vacuum to obtain 1-2 mL of a solution of the isocyanate in DCM. To this solution was added 1-(4-aminopiperidin-1-yl)ethan-1-
35 one (91 mg, 0.64 mmol). The reaction mixture was stirred at room temperature overnight and the solvent was evaporated under vacuum to obtain a yellow oil (320 mg). Column chromatography (SiO₂, DCM/Methanol mixtures) gave 1-(1-

acetylpiperidin-4-yl)-3-(1-fluoro-9-methyl-5,6,8,9,10,11-hexahydro-7*H*-5,9:7,11-dimethanobenzo[9]annulen-7-yl)urea (160 mg, 73% yield) as a white solid.
mp 122-123 °C. IR (NaCl disk): 3351, 2944, 2918, 2861, 1642, 1618, 1555, 1462, 1362, 1321, 1238, 1137, 1066, 976, 885, 798, 749 cm⁻¹. HRMS-ESI+ m/z [M+H]⁺ calcd for [C₂₄H₃₂FN₃O₂+H]⁺: 414.2551, found: 414.2554.

Example 71: 1-(1-acetylpiperidin-4-yl)-3-(2,3-dimethoxy-9-methyl-5,6,8,9,10,11-hexahydro-7*H*-5,9:7,11-dimethanobenzo[9]annulen-7-yl)urea.

To a solution of 2,3-dimethoxy-9-methyl-5,6,8,9,10,11-hexahydro-7*H*-5,9:7,11-dimethanobenzo[9]annulen-7-amine hydrochloride (150 mg, 0.46 mmol) in DCM (3 mL) saturated aqueous NaHCO₃ solution (3 mL) and triphosgene (51 mg, 0.17 mmol) were added. The biphasic mixture was stirred at room temperature for 30 minutes and then the two phases were separated and the organic layer was washed with brine (3 mL), dried over anh. Na₂SO₄, filtered and evaporated under vacuum to obtain 1-2 mL of a solution of the isocyanate in DCM. To this solution was added 1-(4-aminopiperidin-1-yl)ethan-1-one (79 mg, 0.55 mmol). The reaction mixture was stirred at room temperature overnight and the solvent was evaporated under vacuum to obtain a yellow oil (334 mg). Column chromatography (SiO₂, DCM/Methanol mixtures) gave 1-(1-acetylpiperidin-4-yl)-3-(2,3-dimethoxy-9-methyl-5,6,8,9,10,11-hexahydro-7*H*-5,9:7,11-dimethanobenzo[9]annulen-7-yl)urea (168 mg, 80 % yield) as a white solid.
mp 127-128 °C. IR (NaCl disk): 3365, 3052, 2913, 2862, 2834, 1643, 1616, 1553, 1516, 1452, 1360, 1343, 1320, 1293, 1252, 1232, 1168, 1137, 1092, 1019, 974, 863, 801, 734 cm⁻¹. HRMS-ESI+ m/z [M+H]⁺ calcd for [C₂₆H₃₇N₃O₄+H]⁺: 456.2857, found: 456.2859.

Example 72: 1-(1-acetylpiperidin-4-yl)-3-(5,8,9,10-tetrahydro-5,8:7,10-dimethanobenzo[8]annulen-7(6*H*)-yl)urea.

To a solution of 5,8,9,10-tetrahydro-5,8:7,10-dimethanobenzo[8]annulen-7(6*H*)-amine hydrochloride (57 mg, 0.24 mmol) in DCM (1 mL) saturated aqueous NaHCO₃ solution (1 mL) and triphosgene (27 mg, 0.09 mmol) were added. The biphasic mixture was stirred at room temperature for 30 minutes and then the two phases were separated and the organic layer was washed with brine (1 mL), dried over anh. Na₂SO₄, filtered and evaporated under vacuum to obtain 1-2 mL of a solution of the isocyanate in DCM. To this solution was added 1-(4-aminopiperidin-1-yl)ethan-1-one (41 mg, 0.29 mmol). The reaction mixture was stirred at room temperature overnight and the solvent was evaporated under vacuum to obtain a brown gum (93 mg). Column chromatography

(SiO₂, DCM/Methanol mixtures) gave 1-(1-acetylpiperidin-4-yl)-3-(5,8,9,10-tetrahydro-5,8:7,10-dimethanobenzo[8]annulen-7(6*H*)-yl)urea (47 mg, 53 % yield) as a white solid. mp 98-99 °C. IR (NaCl disk): 3359, 3013, 2927, 2856, 2239, 1621, 1556, 1449, 1372, 1334, 1318, 1268, 1238, 1225, 1192, 1153, 1107, 1081, 1048, 1041, 972, 920, 756, 730 cm⁻¹. HRMS-ESI+ m/z [M+H]⁺ calcd for [C₂₂H₂₉N₃O₂+H]⁺: 4368.2333, found: 368.2331.

Example 73: 1-(benzo[d]thiazol-2-yl)-3-(9-methoxy-5,6,8,9,10,11-hexahydro-7*H*-5,9:7,11-dimethanobenzo[9]annulen-7-yl)urea.

To a solution of 9-methoxy-5,6,8,9,10,11-hexahydro-7*H*-5,9:7,11-dimethanobenzo[9]annulen-7-amine (250 mg, 1.03 mmol) in DCM (3 mL) saturated aqueous NaHCO₃ solution (3 mL) and triphosgene (113 mg, 0.38 mmol) were added. The biphasic mixture was stirred at room temperature for 30 minutes and then the two phases were separated and the organic layer was washed with brine (3 mL), dried over anhydrous Na₂SO₄, filtered and evaporated under vacuum to obtain 1-2 mL of a solution of the isocyanate in DCM.

To a solution of benzo[d]thiazol-2-amine (141 mg, 0.94 mmol) in anhydrous THF (8 mL) under argon atmosphere at -78 °C, was added dropwise a solution of *n*-butyllithium (2.5 M in hexanes, 0.38 mL, 0.94 mmol) during 20 minutes. After the addition, the mixture was tempered to 0 °C using an ice bath. This solution was added carefully to the solution of the isocyanate from the previous step cooled to 0 °C, under argon atmosphere. The reaction mixture was stirred at room temperature overnight. Methanol (3 mL) was then added to quench any unreacted *n*-butyllithium. The solvents were evaporated under vacuum to give a yellow solid (531 mg). Column chromatography (SiO₂, Hexane/Ethyl Acetate mixtures) gave a 1-(benzo[d]thiazol-2-yl)-3-(9-methoxy-5,6,8,9,10,11-hexahydro-7*H*-5,9:7,11-dimethanobenzo[9]annulen-7-yl)urea (65 mg, 15% yield) as a white solid.

mp 247-248 °C. IR (NaCl disk): 2926, 2851, 1712, 1675, 1593, 1537, 1445, 1358, 1268, 1217, 1556, 1116, 1080, 1044, 1015, 910, 845 cm⁻¹. HRMS-ESI+ m/z [M+H]⁺ calcd for [C₂₄H₂₅N₃O₂S+H]⁺: 420.1740, found: 368.2331.

Example 74: 1-(1-acetylpiperidin-4-yl)-3-(1,9-difluoro-5,6,8,9,10,11-hexahydro-7*H*-5,9:7,11-dimethanobenzo[9]annulen-7-yl)urea.

To a solution of 1,9-difluoro-5,6,8,9,10,11-hexahydro-7*H*-5,9:7,11-dimethanobenzo[9]annulen-7-amine hydrochloride (120 mg, 0.42 mmol) in DCM (3 mL) and saturated aqueous NaHCO₃ solution (3 mL), triphosgene (46 mg, 0.16 mmol) was added. The biphasic mixture was stirred at room temperature for 30 minutes and then the two phases were separated and the organic one was washed with brine (3 mL),

dried over anhydrous Na_2SO_4 , filtered and evaporated under vacuum to obtain 1-2 mL of a solution of isocyanate in DCM. To this solution was added 1-(4-aminopiperidin-1-yl)ethan-1-one (72 mg, 0.51 mmol). The mixture was stirred overnight at room temperature and the solvent was then evaporated. Column chromatography (SiO_2 , DCM/Methanol mixtures) afforded the urea (84 mg, 48% yield) as a yellowish solid. The analytical sample was obtained by crystallization from hot EtOAc/Pentane.

mp 248-249 °C. IR (ATR): 3382, 3266, 2923, 2164, 1645, 1622, 1562, 1503, 1464, 1454, 1425, 1362, 1341, 1325, 1318, 1304, 1244, 1232, 1185, 1135, 1099, 1059, 1036, 1015, 995, 978, 952, 929, 891, 868, 795, 746, 717, 695, 645, 625, 605, 590 cm^{-1} .

HRMS-ESI+ m/z $[\text{M}+\text{H}]^+$ calcd for $[\text{C}_{23}\text{H}_{29}\text{F}_2\text{N}_3\text{O}_2+\text{H}]^+$: 418.2301; Found: 418.2300.

Reference example 75: 1,5,6,7-tetrahydro-1,5:3,7-dimethanobenzo[e]oxonin-5-d-3(2H)-ol.

To a solution of 5,6,7,8-tetrahydro-7H-5,9-propanobenzo[7]annulene-7,11-dione (3.13 g, 14.6 mmol) in MeOH (88 mL), NaBD_4 (1 g, 23.9 mmol) was added portion-wise and the suspension was stirred under reflux for 6 h. The solution was cooled down and the solvent was removed under vacuum. To the obtained white solid, NaOH 2 N (100 mL) was added and the suspension was refluxed for 30 min. After that, the suspension was filtered and washed with H_2O (50 mL) to afford the 1,5,6,7-tetrahydro-1,5:3,7-dimethanobenzo[e]oxonin-5-d-3(2H)-ol (2.88 g, 91 % yield) as a white solid.

mp 200 °C. IR (ATR): 3304, 2957, 2941, 2927, 2913, 1492, 1461, 1451, 1431, 1383, 1356, 1339, 1328, 1278, 1253, 1234, 1219, 1189, 1157, 1141, 1127, 1082, 1047, 1017, 1002, 958, 935, 863, 844, 773, 755, 718, 673 cm^{-1} . HRMS-ESI+ m/z $[\text{M}+\text{H}]^+$ calcd for $[\text{C}_{14}\text{H}_{15}\text{DO}_2+\text{H}]^+$: 218.1286, found: 218.1297.

Reference example 76: (1,5,6,7-tetrahydro-1,5:3,7-dimethanobenzo[e]oxonin-3(2H)-yl-5-d)hydrazine hydrochloride.

A solution of 1,5,6,7-tetrahydro-1,5:3,7-dimethanobenzo[e]oxonin-5-d-3(2H)-ol (1.2 g, 5.52 mmol) in hydrazine hydrate (9 mL, aq. sol. 64%, 183.98 mmol) and HCl conc. (0.2 mL) was heated at reflux overnight. The solution was cooled down and the suspension was filtered. The obtained solid was dissolved in methanol and HCl/MeOH was added to afford (1,5,6,7-tetrahydro-1,5:3,7-dimethanobenzo[e]oxonin-3(2H)-yl-5-d)hydrazine hydrochloride (1.26 g, 85% yield).

mp 232-235 °C. IR (ATR): 3303, 3226, 2911, 2845, 2650, 1589, 1525, 1490, 1451, 1435, 1356, 1328, 1278, 1253, 1219, 1157, 1145, 1129, 1084, 1050, 1024, 1002, 958,

936, 892, 865, 830, 812, 771, 750, 721 cm^{-1} . HRMS-ESI+ m/z $[M+H]^+$ calcd for $[\text{C}_{14}\text{H}_{17}\text{DN}_2\text{O}+H]^+$: 232.1555, found: 232.1554.

Reference example 77: 1,5,6,7-tetrahydro-1,5:3,7-dimethanobenzo[e]oxonin-5-d-3(2H)-amine hydrochloride.

- 5 A solution of 1,5,6,7-tetrahydro-1,5:3,7-dimethanobenzo[e]oxonin-3(2H)-yl-5-d)hydrazine hydrochloride (1 g, 3.7 mmol) and PtO_2 (100 mg) in ethanol (100 mL) was hydrogenated at room temperature, at a pressure of 1 atm for 5 days. The resulting suspension was filtered and the residue washed with methanol. The solvent was removed under vacuum affording a white solid. The solid was dissolved in MeOH and an excess of HCl/MeOH was added. The solvent was evaporated to afford 1,5,6,7-tetrahydro-1,5:3,7-dimethanobenzo[e]oxonin-5-d-3(2H)-amine hydrochloride (791 mg, 85% yield) as a white solid. The analytical sample was obtained by crystallization from Methanol/ Et_2O .
- 10
- 15 mp 195 °C. IR (ATR): 3304, 3010, 2940, 2913, 2847, 1510, 1490, 1451, 1435, 1379, 1356, 1328, 1280, 1251, 1235, 1221, 1157, 1126, 1082, 1041, 1000, 957, 937, 866, 844, 773, 762, 755, 720, 670 cm^{-1} . HRMS-ESI+ m/z $[M+H]^+$ calcd for $[\text{C}_{14}\text{H}_{16}\text{DNO}+H]^+$: 217.1446, found: 217.1449.

20 **Example 78: 1-(1-acetylpiperidin-4-yl)-3-(1,5,6,7-tetrahydro-1,5:3,7-dimethanobenzo[e]oxonin-3(2H)-yl-5-d)urea.**

- From 1,5,6,7-tetrahydro-1,5:3,7-dimethanobenzo[e]oxonin-5-d-3(2H)-amine hydrochloride and following the procedure of example 37, 1-(1-acetylpiperidin-4-yl)-3-(1,5,6,7-tetrahydro-1,5:3,7-dimethano-benzo[e]oxonin-3(2H)-yl-5-d)urea was obtained
- 25

Example 79: *In vitro* determination of sEH inhibition activity

The following fluorescent assay was used for determination of the sEH inhibition activity (IC_{50}), with the substrate and comparative control compound (TPPU) indicated below.

- 30 **Substrate:** cyano(6-methoxynaphthalen-2-yl)methyl 2-(3-phenyloxiran-2-yl)acetate (PHOME; from Cayman Chemical, item number 10009134; CAS 1028430-42-3); cf. N.M. Wolf et al., *Anal. Biochem.* 2006, vol. 355, pp. 71-80.

TPPU: *N*-[1-(1-Oxopropyl)-4-piperidiny]-*N'*-[4-(trifluoromethoxy)phenyl]urea.

Solutions:

- 35 - Assay buffer: Bis/Tris HCl 25 mM pH 7.0 containing 0.1 mg/mL of bovine serum albumin (BSA).

- PHOME at 200 μ M in DMSO.
 - Solution of recombinant human sEH (hsEH) (Cayman Chemical, item number 10011669), diluted with assay buffer.
 - Inhibitors dissolved in DMSO at appropriated concentrations.
- 5 **Protocol:** In a black 96-well plate (Greiner Bio-One, item number 655900), fill the background wells with 90 μ L and the positive control and inhibitor wells with 85 μ L of assay buffer. Add 5 μ L of DMSO to background and positive control wells, and then add 5 μ L of inhibitor solution in inhibitor wells. Add 5 μ L of the solution of hsEH to the positive control and inhibitor wells and stir the mixture. Prepare a 1/21 dilution of the
- 10 solution of PHOME with assay buffer according to final volume required, and then add 105 μ L of each well. Shake carefully the plate for 10 seconds and incubate for 5 minutes at room temperature. Read the appearance of fluorescence with excitation wavelength: 337 nm, and emission wavelength: 460 nm (FLUOStar OPTIMA microplate reader, BMG). The intensity of fluorescence was used to analyze and
- 15 calculate the IC₅₀ values. Results were obtained by regression analysis from at least three data points in a linear region of the curve. IC₅₀ values are average of minimum three independent replicates.

20 **Tables 1 and 2: human sEH inhibition activity (IC₅₀, nM) of selected compounds (I)^a**

Ex.	TTPU	35	36	38	39	40	41	42	43	44	47	48	51	52	53	56
IC ₅₀	A	D	D	A	D	B	A	A	B	A	A	A	A	A	B	B

Ex.	57	58	59	60	63	64	65	66	67	68	69	70	71	72	73	74
IC ₅₀	D	A	B	D	A	A	A	A	A	A	A	A	A	B	D	A

- 25 ^a A means that IC₅₀ is lower than 10 nM, B means that IC₅₀ is at least 10 nM but less than 50 nM, C means that IC₅₀ is at least 50 nM but less than 100 nM and D means that IC₅₀ is at least 100 nM but less than 1000nM.

LIST OF REFERENCES

30 **Non-patent literature cited in the description**

1. Abstracts of Papers, 241st ACS National Meeting & Exposition, Anaheim, CA, United States, March 27-31, 2011 (2011), MEDI-92
2. ACS Chem Biol. 2018 Jan 19; 13:45-52

3. Alcoholism. 2018, 42, 1970
4. Am J Physiol Renal Physiol. 2013 Jan 15;304(2):F168-76
5. Am J Physiol Renal Physiol. 2014 Oct 15;307(8):F971-80
6. Am J Physiol Gastrointest Liver Physiol. 2019, 316, G527-G538
- 5 7. Am J Respir Cell Mol Biol. 2012 May;46(5):614-22
8. Am J Respir Crit Care Med. 2014 Oct 15;190(8):848-50
9. Anal Biochem. 2006;355:71-80
10. Anticancer Res. 2013 Dec;33(12):5261-5271
11. Aust J Chem. 1983; 36:2465-2472
- 10 12. Bioorg Med Chem. 2010, 18, 46
13. Bioorg Med Chem. 2012, 20, 942
14. Bioorg Med Chem. 2014, 22, 2678
15. Bioorg Med Chem. 2015, 23, 290
16. Bioorg Med Chem Lett. 2014 Jan 15;24(2):565-70
- 15 17. BioRxiv. 2019 March 8, doi: 10.1101/571984
18. BioRxiv. 2019 Apr 10, doi:10.1101/605055
19. Cardiovasc Ther. 2011 Apr;29(2):99-111
20. Clinics Res Hepatol Gastroenterol. 2018, 42, 118-125
21. Dig Dis Sci. 2012 Oct;57(10):2580-91
- 20 22. Drug Discov Today. 2015 Nov;20(11):1382-90
23. Drug Metab Dispos. 2015 May;43(5):788-802
24. Equine Vet J. 2017 May;49(3):345-351
25. Exp Diabetes Res. 2012:758614
26. Expert Opin Ther Patents. 2010, vol. 20, pp. 941-956
- 25 27. Experimental Molecular Medicine. 2018, 50:149
28. FASEB J. 2015 Mar;29(3):1092-101
29. FASEB J. March 2008 22 (Meeting Abstract Supplement) 479.17
30. *Free Rad Biol Med.*, 2012, 53, 160
31. Frontiers Pharmacol. 2019, 9:1551
- 30 32. Frontiers Pharmacol. 2019, 10:95
33. Biomed. & Pharmacother. 2019, 115: 108897
34. Inflamm Allergy Drug Targets. 2012 Apr;11(2):143-58
35. Int J Cardiol. 2012 Mar 8;155(2):181-7
36. J Agric Food Chem. 2011 Apr 13;59(7):2816-24
- 35 37. J Biol Chem. 2014 Dec 26;289(52):35826-38
38. J Cardiovasc Pharmacol. 2008 Oct;52(4):314-23
39. J Neurosci Res. 2017 Dec;95(12):2483-2492

40. J Pharmacol Exp Ther. 2016 Jun;357(3):529-36
41. J Pharmacol Exp Ther. 2017 Jun;361(3):408-416
42. J Surg Res. 2013 Jun 15;182(2):362-7
43. J Vet Pharmacol Ther. 2018 Apr;41(2):230-238
- 5 44. J Med Chem. 2012, vol. 55, pp. 1789-1808
45. J Neurosurg Anesthesiol. 2015 Jul; 27(3):222-240
46. Liebigs Ann Chem. 1973; 1839-1850
47. Liebigs Ann. 1995;523-535.
48. Life Sci. 2013 Jun 21;92(23):1145-50
- 10 49. Med Hypotheses, 2017 Oct;108:81-5
50. Mol Neurobiol. 2015 Aug;52(1):187-95
51. Mol Pharmacol. 2015 Aug;88(2):281-90
52. Nature. 2017 Dec 14;552(7684):248-252
53. Nutr Metab Cardiovasc Dis. 2012 Jul;22(7):598-604
- 15 54. Oncotarget. 2017 Sep 21;8(61):103236-60
55. Pharmacol Ther. 2017 Dec;180:62-76
56. Pharmacol Ther. 2017, vol 180, pp 62-76
57. Phytother Res. 2016 Jul;30(7):1119-27
58. PLoS One. 2013 Dec 11;8(12):e80922
- 20 59. PLoS One. 2014 May 13;9(5):e97529
60. PLoS One. 2014 Oct 13, 9(10):e110162
61. PLoS One. 2019 Apr 19, 14(4):e0215033
62. Proc Natl Acad Sci U S A. 2005 Jul 12;102(28):9772-7
63. Proc Natl Acad Sci U S A. 2011 May 31;108(22):9038-43
- 25 64. Proc Natl Acad Sci U S A. 2015 Jul 21;112(29):9082-7
65. Proc Natl Acad Sci U S A. 2016 Mar 29;113(13):E1944-52
66. Proc Natl Acad Sci U S A. 2018 May 15;115(20):5283-5288
67. Proc Natl Acad Sci U S A. 2018, 115:E5815-E5823
68. Proc Natl Acad Sci U S A. 2019, 116:5154-5159
- 30 69. Proc Natl Acad Sci U S A. 2019, 116:7083-7088
70. Prog Lipid Res. 2014 Jan;53:108-23
71. Prostaglandins Other Lipid Mediat. 2014 Oct;113-115:30-7
72. Prostaglandins Other Lipid Mediat. 2017 Jul;131:67-74
73. Prostaglandins Other Lipid Mediat. 2018 May;136:84-89
- 35 74. Recent Pat Cardiovasc Drug Discov. 2006 Jan;1(1):67-72.
75. *Resp Res.*, 2018, 19:236
76. Scientific Reports. 2018, 8:5279

77. Stroke. 2015 Jul;46(7):1916-22
78. Tetrahedron Lett. 1987, 28, 1585-1588.
79. Toxicol Appl Pharmacol. 2015 Jul 15;286(2):102-11
80. Toxicology. 2017 Aug 15;389:31-41

5

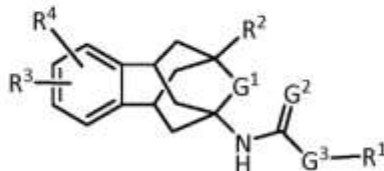
Patent documents cited in the description

81. WO 00/23060 A2
82. WO 2007/009001 A1
83. WO 2003/002555 A1
- 10 84. WO 2017/120012 A1
85. WO 2016/133788 A1
86. DE 2210799
87. WO 2007/016496 A2

15

CLAIMS

1. A compound of formula (I)



5

(I)

or a stereoisomer or a pharmaceutically acceptable salt thereof, wherein:

G¹ represents an oxygen atom or a methylene group or a single bond;

G² represents an oxygen atom or a sulphur atom;

G³ represents a radical selected from the group consisting of -NH-(CH₂)_m-, -O-
10 (CH₂)_m- and -(CH₂)_n-;

m is an integer from 0 to 6;

n is an integer from 1 to 7

R¹ is a radical selected from the group consisting of:

15 a) C₆-C₁₀ aryl which may be optionally substituted by 1 to 4 substituents selected from the group consisting of halogen atoms, C₁-C₆ acyl, nitro (NO₂), cyano (C≡N), trifluoromethyl (CF₃), trifluoromethoxy (OCF₃), pentafluorosulfanyl (SF₅), sulfonyl (SO₃H), fluorosulfonyl (SO₂F), carboxylic group (COOH), amino (NH₂), mono-C₁-C₆ alkylamino, di-C₁-C₆ alkylamino, C₁-C₆ alkoxy, C₁-C₆ alkyl, C₁-C₆ alkoxy carbonylmethyl and methylaminocarbonylpyridyloxy;

20 b) heteroaryl having from 2 to 11 carbon atoms and 1, 2 or 3 heteroatoms selected from the group consisting of N, O and S and which may be optionally substituted by 1 to 4 substituents selected from the group consisting of halogen atoms, C₁-C₆ acyl, nitro (NO₂), cyano (C≡N), trifluoromethyl (CF₃), trifluoromethoxy (OCF₃), pentafluorosulfanyl (SF₅), sulfonyl (SO₃H), fluorosulfonyl (SO₂F), carboxylic group (COOH), amino (NH₂), mono-C₁-C₆ alkylamino, di-C₁-C₆ alkylamino, C₁-C₆ alkoxy, C₁-C₆ alkyl and C₁-C₆ alkoxy carbonylmethyl;

25 c) saturated or partially unsaturated, monocyclic or bicyclic heterocyclyl having from 5 to 11 carbon atoms and 1, 2 or 3 heteroatoms selected from the group consisting of N, O and S and which may be optionally substituted by 1 to 4 substituents selected from the group consisting of halogen atoms, C₁-C₆ acyl, C₃-C₆ cycloalkyl-C(=O), nitro (NO₂), cyano (C≡N), trifluoromethyl (CF₃), trifluoromethylcarbonyl (CF₃CO), pentafluorosulfanyl (SF₅), sulfonyl (SO₃H),
30

5 carboxylic group (COOH), amino (NH₂), mono-C₁-C₆ alkylamino, di-C₁-C₆ alkylamino, C₁-C₆ alkoxy, C₁-C₆ alkyl, C₁-C₆ alkoxy carbonylmethyl, C₁-C₆ alkylsulfonyl, C₃-C₆ cycloalkylsulfonyl, benzyl, heteroarylmethyl, pyridincarbonyl, phenylcarbonyl, tetrahydropyran carbonyl, C₆-C₁₀ arylsulfonyl which may be optionally substituted by 1 to 2 substituents selected from the group consisting of halogen atoms, nitro (NO₂), cyano (C≡N), trifluoromethyl (CF₃), trifluoromethoxy (OCF₃), pentafluorosulfanyl (SF₅), sulfonyl (SO₃H), carboxylic group (COOH), amino (NH₂), mono-C₁-C₆ alkylamino, di-C₁-C₆ alkylamino, C₁-C₆ alkoxy, C₁-C₆ alkyl, C₁-C₆ alkoxy carbonylmethyl and phenyl which may be optionally substituted by 1 to 4 substituents selected from the group consisting of halogen atoms, C₁-C₆ acyl, nitro (NO₂), cyano (C≡N), trifluoromethyl (CF₃), trifluoromethoxy (OCF₃), pentafluorosulfanyl (SF₅), sulfonyl (SO₃H), fluorosulfonyl (SO₂F), carboxylic group (COOH), amino (NH₂), mono-C₁-C₆ alkylamino, di-C₁-C₆ alkylamino, C₁-C₆ alkoxy, C₁-C₆ alkyl, C₃-C₆ cycloalkyl and C₁-C₆ alkoxy carbonylmethyl;

10 d) C₆-C₁₀ cycloalkyl which may be optionally substituted by 1 to 4 substituents selected from the group consisting of halogen atoms, C₁-C₆ acyl, nitro (NO₂), cyano (C≡N), trifluoromethyl (CF₃), trifluoromethoxy (OCF₃), pentafluorosulfanyl (SF₅), sulfonyl (SO₃H), carboxylic group (COOH), amino (NH₂), mono-C₁-C₆ alkylamino, di-C₁-C₆ alkylamino, C₁-C₆ alkoxy, C₁-C₆ alkyl, C₁-C₆ alkoxy carbonylmethyl, pyridinyloxy which may be unsubstituted or substituted by a group selected from COOH and CONHCH₃, and phenoxy which may be unsubstituted or substituted by COOH, COOR⁵, CONH₂, CN or OH;

15 R² is a radical selected from the group consisting of hydrogen or deuterium atoms, halogen atoms, methyl, hydroxy and C₁-C₆ alkoxy;

20 R³ and R⁴ are radicals which may be identical or different and which are independently selected from the group consisting of hydrogen atoms, halogen atoms, C₁-C₆ acyl, nitro (NO₂), cyano (C≡N), carboxylic group (COOH), hydroxy (OH), trifluoromethyl (CF₃), trifluoromethoxy (OCF₃), pentafluorosulfanyl (SF₅), sulfonyl (SO₃H), fluorosulfonyl (SO₂F), amino (NH₂), mono-C₁-C₆ alkylamino, di-C₁-C₆ alkylamino, C₁-C₆ alkoxy, C₁-C₆ alkyl and C₁-C₆ alkoxy carbonylmethyl;

30 or R³ and R⁴ may form together a radical -O-(CH₂)_p-O-, wherein p is an integer from 1 to 3;

35 R⁵ is a radical selected from C₁-C₆ alkyl and C₃-C₆ cycloalkyl.

2. A compound according to claim 1 wherein G¹ represents a methylene group.

3. A compound according to any one of claims 1 to 2 wherein G^2 represents an oxygen atom.
4. A compound according to any one of claims 1 to 3 wherein G^3 represents a radical
5 selected from the group consisting of $-NH-(CH_2)_m-$ and $-(CH_2)_n-$, m is an integer from 0 to 6 and n is an integer from 1 to 7.
5. A compound according to claim 4 wherein G^3 represents a radical $-NH-(CH_2)_m-$ and
10 m is an integer from 0 to 6.
6. A compound according to any one of claims 1 to 5 wherein, when G^3 is selected from the group consisting of $-NH-(CH_2)_m-$ and $-O-(CH_2)_m-$, m has a value of 0 and wherein G^3 is $-(CH_2)_n-$ n has a value of 1.
- 15 7. A compound according to any one of claims 1 to 6 wherein R^1 is selected from the group consisting of substituted or unsubstituted phenyl, substituted or unsubstituted cyclohexyl and substituted or unsubstituted piperidinyl.
8. A compound according to any one of claims 1 to 7 wherein R^2 is selected from the
20 group consisting of hydrogen atoms, fluorine atoms, chlorine atoms, methyl, hydroxyl and C_1-C_3 alkoxy.
9. A compound according to any one of claims 1 to 8 wherein R^3 and R^4 are radicals which may be identical or different and which are independently selected from the
25 group consisting of hydrogen atoms, halogen atoms, C_1-C_6 acyl, trifluoromethyl (CF_3), trifluoromethoxy (OCF_3), nitro (NO_2), amino (NH_2) and C_1-C_6 alkoxy.
10. A compound according to any one of claims 1 to 9 wherein R^3 is hydrogen and R^4 is a radical selected from the group consisting of hydrogen atoms, halogen atoms,
30 C_1-C_6 acyl, trifluoromethyl (CF_3), trifluoromethoxy (OCF_3), nitro (NO_2), amino (NH_2) and C_1-C_6 alkoxy.
11. The compound according to any one of the claims 1 to 10, which is selected from the group consisting of:

- i. *p*-tolyl (9-methyl-5,6,8,9,10,11-hexahydro-7*H*-5,9:7,11-dimethanobenzo[9]annulen-7-yl)carbamate
- 5 ii. 1-(9-methyl-5,6,8,9,10,11-hexahydro-7*H*-5,9:7,11-dimethanobenzo[9]annulen-7-yl)-3-(4-(trifluoromethyl)phenyl)thiourea
- iii. 1-(1-acetylpiperidin-4-yl)-3-(5-methyl-1,5,6,7-tetrahydro-1,5:3,7-dimethanobenzo[*e*]oxonin-3(2*H*)-yl)urea
- 10 iv. 1-(1-acetylpiperidin-4-yl)-3-(1,5,6,7-tetrahydro-1,5:3,7-dimethanobenzo[*e*]oxonin-3(2*H*)-yl)urea
- v. 1-(1-acetylpiperidin-4-yl)-3-(9-methyl-5,6,8,9,10,11-hexahydro-7*H*-5,9:7,11-dimethanobenzo[9]annulen-7-yl)urea
- vi. 1-(1-acetylpiperidin-4-yl)-3-(9-hydroxy-5,6,8,9,10,11-hexahydro-7*H*-5,9:7,11-dimethanobenzo[9]annulen-7-yl)urea
- 15 vii. 1-(1-acetylpiperidin-4-yl)-3-(9-methoxy-5,6,8,9,10,11-hexahydro-7*H*-5,9:7,11-dimethanobenzo[9]annulen-7-yl)urea
- viii. 1-(1-acetylpiperidin-4-yl)-3-(9-fluoro-5,6,8,9,10,11-hexahydro-7*H*-5,9:7,11-dimethanobenzo[9]annulen-7-yl)urea
- ix. 1-(1-acetylpiperidin-4-yl)-3-(9-chloro-5,6,8,9,10,11-hexahydro-7*H*-5,9:7,11-dimethanobenzo[9]annulen-7-yl)urea
- 20 x. 4-(((1*r*,4*r*)-4-(3-(5-methyl-1,5,6,7-tetrahydro-1,5:3,7-dimethanobenzo[*e*]oxonin-3(2*H*)-yl)ureido)cyclohexyl)oxy)benzoic acid
- xi. 4-(((1*r*,4*r*)-4-(3-(9-methyl-5,6,8,9,10,11-hexahydro-7*H*-5,9:7,11-dimethanobenzo[9]annulen-7-yl)ureido)cyclohexyl)oxy)benzoic acid
- xii. 1-[1-(isopropylsulfonyl)piperidin-4-yl]-3-(9-methyl-5,6,8,9,10,11-hexahydro-7*H*-5,9:7,11-dimethanobenzo[9]annulen-7-yl)urea
- 25 xiii. 1-(1-benzylpiperidin-4-yl)-3-(9-methyl-5,6,8,9,10,11-hexahydro-7*H*-5,9:7,11-dimethanobenzo[9]annulen-7-yl)urea
- xiv. 1-(2-acetyl-9-methyl-5,6,8,9,10,11-hexahydro-7*H*-5,9:7,11-dimethanobenzo[9]annulen-7-yl)-3-(1-acetylpiperidin-4-yl)urea
- 30 xv. 1-(1-acetylpiperidin-4-yl)-3-(9-methyl-2-nitro-5,6,8,9,10,11-hexahydro-7*H*-5,9:7,11-dimethanobenzo[9]annulen-7-yl)urea
- xvi. 1-(1-acetylpiperidin-4-yl)-3-(2-amino-9-methyl-5,6,8,9,10,11-hexahydro-7*H*-5,9:7,11-dimethanobenzo[9]annulen-7-yl)urea
- xvii. *tert*-butyl 4-(2-((9-methyl-5,6,8,9,10,11-hexahydro-7*H*-5,9:7,11-dimethanobenzo[9]annulen-7-yl)amino)-2-oxoethyl)piperidine-1-carboxylate
- 35 xviii. *N*-(9-methyl-5,6,8,9,10,11-hexahydro-7*H*-5,9:7,11-dimethanobenzo[9]annulen-7-yl)-2-(piperidin-4-yl)acetamide

- xix. 2-[1-(isopropylsulfonyl)piperidin-4-yl]-*N*-(9-methyl-5,6,8,9,10,11-hexahydro-7*H*-5,9:7,11-dimethanobenzo[9]annulen-7-yl)acetamide
- xx. 2-(1-acetylpiperidin-4-yl)-*N*-(9-methyl-5,6,8,9,10,11-hexahydro-7*H*-5,9:7,11-dimethanobenzo[9]annulen-7-yl)acetamide
- 5 xxi. 1-(9-methyl-6,7,8,9,10,11-hexahydro-5*H*-5,9:7,11-dimethanobenzo[9]annulen-7-yl)-3-(2,3,4-trifluorophenyl)urea
- xxii. 1-(5-methyl-1,5,6,7-tetrahydro-1,5:3,7-dimethanobenzo[*e*]oxonin-3(2*H*)-yl)-3-(2,3,4-trifluorophenyl)urea
- xxiii. 2-(1-benzylpiperidin-4-yl)-*N*-(9-methyl-5,6,8,9,10,11-hexahydro-7*H*-5,9:7,11-dimethanobenzo[9]annulen-7-yl)acetamide
- 10 xxiv. 1-(9-methyl-5,6,8,9,10,11-hexahydro-7*H*-5,9:7,11-dimethanobenzo[9]annulen-7-yl)-3-(1-propionylpiperidin-4-yl)urea
- xxv. 1-(1-(4-acetylphenyl)piperidin-4-yl)-3-(9-methyl-5,6,8,9,10,11-hexahydro-7*H*-5,9:7,11-dimethanobenzo[9]annulen-7-yl)urea
- 15 xxvi. 1-(9-methyl-5,6,8,9,10,11-hexahydro-7*H*-5,9:7,11-dimethanobenzo[9]annulen-7-yl)-3-(1-(tetrahydro-2*H*-pyran-4-carbonyl)piperidin-4-yl)urea
- xxvii. 1-(1-(2-fluorobenzoyl)piperidin-4-yl)-3-(9-methyl-5,6,8,9,10,11-hexahydro-7*H*-5,9:7,11-dimethanobenzo[9]annulen-7-yl)urea
- xxviii. 1-((1*R*,3*s*,5*S*)-8-benzyl-8-azabicyclo[3.2.1]octan-3-yl)-3-(9-methyl-5,6,8,9,10,11-hexahydro-7*H*-5,9:7,11-dimethanobenzo[9]annulen-7-yl)urea
- 20 xxix. 1-(1-acetylpiperidin-4-yl)-3-(2-fluoro-9-methyl-5,6,8,9,10,11-hexahydro-7*H*-5,9:7,11-dimethanobenzo[9]annulen-7-yl)urea
- xxx. 1-(1-acetylpiperidin-4-yl)-3-(2-methoxy-9-methyl-5,6,8,9,10,11-hexahydro-7*H*-5,9:7,11-dimethanobenzo[9]annulen-7-yl)urea
- 25 xxxi. 1-(1-acetylpiperidin-4-yl)-3-(1-fluoro-9-methyl-5,6,8,9,10,11-hexahydro-7*H*-5,9:7,11-dimethanobenzo[9]annulen-7-yl)urea
- xxxii. 1-(1-acetylpiperidin-4-yl)-3-(2,3-dimethoxy-9-methyl-5,6,8,9,10,11-hexahydro-7*H*-5,9:7,11-dimethanobenzo[9]annulen-7-yl)urea
- xxxiii. 1-(1-acetylpiperidin-4-yl)-3-(5,8,9,10-tetrahydro-5,8:7,10-dimethanobenzo[8]annulen-7(6*H*)-yl)urea
- 30 xxxiv. 1-(benzo[*d*]thiazol-2-yl)-3-(9-methoxy-5,6,8,9,10,11-hexahydro-7*H*-5,9:7,11-dimethanobenzo[9]annulen-7-yl)urea
- xxxv. 1-(1-acetylpiperidin-4-yl)-3-(1,9-difluoro-5,6,8,9,10,11-hexahydro-7*H*-5,9:7,11-dimethanobenzo[9]annulen-7-yl)urea
- 35 xxxvi. 1-(1-acetylpiperidin-4-yl)-3-(1,5,6,7-tetrahydro-1,5:3,7-dimethanobenzo[*e*]oxonin-3(2*H*)-yl-5-*d*)urea

12. A pharmaceutical or veterinary composition comprising a therapeutically effective amount of a compound as defined in any one of the claims 1 to 11.
13. A compound as defined in any one of the claims 1 to 11 or a composition
5 according to claim 12 for use as a medicament.
14. A compound as defined in any one of the claims 1 to 11 or a composition according to claim 12 for use in the treatment or prevention in an animal, including a human, of a disease or disorder susceptible of improvement by inhibition of soluble
10 epoxide hydrolase.
15. The compound or composition for use according to claim 14, wherein the disease or disorder is selected from the group consisting of hypertension, atherosclerosis, pulmonary diseases such as chronic obstructive pulmonary disorder, asthma,
15 sarcoidosis and cystic fibrosis, kidney diseases such as acute kidney injury, diabetic nephrology, chronic kidney diseases, hypertension-mediated kidney disorders and high fat diet-mediated renal injury, stroke, pain, neuropathic pain, inflammation, pancreatitis in particular acute pancreatitis, immunological disorders, neurodevelopmental disorders such as schizophrenia and autism spectrum disorder, eye diseases in particular
20 diabetic keratopathy, wet age-related macular degeneration and retinopathy such as premature retinopathy and diabetic retinopathy, cancer, obesity, including obesity-induced colonic inflammation, diabetes, metabolic syndrome, preeclampsia, anorexia nervosa, depression, male sexual dysfunction such as erectile dysfunction, wound healing, NSAID-induced ulcers, emphysema, scrapie, Parkinson's disease, arthritis,
25 arrhythmia, cardiac fibrosis, Alzheimer's disease, Raynaud's syndrome, Niemann-Pick-type C disease, cardiomyopathy, vascular cognitive impairment, mild cognitive impairment, inflammatory bowel diseases, cirrhosis, non-alcoholic fatty liver disease, non-alcoholic steatohepatitis, liver fibrosis, osteoporosis, chronic periodontitis, sepsis, seizure disorders such as epilepsy, dementia, edema such as cerebral edema,
30 attention-deficit hyperactivity disorder, schizophrenia, drug dependency, social anxiety, colitis, amyotrophic lateral sclerosis, chemotherapy induced side effects, laminitis, inflammatory joint pain and synovitis, endothelial dysfunction, subarachnoid hemorrhage, including aneurysmal subarachnoid hemorrhage, traumatic brain injury, cerebral ischemia and diabetes-induced learning and memory impairment.
- 35 16. Use of a compound as defined in any one of claims 1 to 11 or a composition according to claim 12 in the manufacture of a medicament.

17. Use of a compound according to any of claims 1 to 11 or a composition according to claim 12 in the manufacture of a medicament for the treatment or prevention in an animal, including a human, of a disease or disorder susceptible of improvement by inhibition of soluble epoxide hydrolase.
- 5 18. Use according to claim 17, wherein the disease or disorder is selected from the group consisting of hypertension, atherosclerosis, pulmonary diseases such as chronic obstructive pulmonary disorder, asthma, sarcoidosis and cystic fibrosis, kidney diseases such as acute kidney injury, diabetic nephrology, chronic kidney diseases, hypertension-mediated kidney disorders and high fat diet-mediated renal injury, stroke,
10 pain, neuropathic pain, inflammation, pancreatitis in particular acute pancreatitis, immunological disorders, neurodevelopmental disorders such as schizophrenia and autism spectrum disorder, eye diseases in particular diabetic keratopathy, wet age-related macular degeneration and retinopathy such as premature retinopathy and diabetic retinopathy, cancer, obesity, including obesity-induced colonic inflammation,
15 diabetes, metabolic syndrome, preeclampsia, anorexia nervosa, depression, male sexual dysfunction such as erectile dysfunction, wound healing, NSAID-induced ulcers, emphysema, scrapie, Parkinson's disease, arthritis, arrhythmia, cardiac fibrosis, Alzheimer's disease, Raynaud's syndrome, Niemann-Pick-type C disease, cardiomyopathy, vascular cognitive impairment, mild cognitive impairment,
20 inflammatory bowel diseases, cirrhosis, non-alcoholic fatty liver disease, non-alcoholic steatohepatitis, liver fibrosis, osteoporosis, chronic periodontitis, sepsis, seizure disorders such as epilepsy, dementia, edema such as cerebral edema, attention-deficit hyperactivity disorder, schizophrenia, drug dependency, social anxiety, colitis, amyotrophic lateral sclerosis, chemotherapy induced side effects, laminitis,
25 inflammatory joint pain and synovitis, endothelial dysfunction, subarachnoid hemorrhage, including aneurysmal subarachnoid hemorrhage, traumatic brain injury, cerebral ischemia and diabetes-induced learning and memory impairment.
19. Method for the treatment or prevention of a disease or disorder susceptible of improvement by inhibition of soluble epoxide hydrolase comprising administering to an
30 animal, including a human, in need thereof an effective amount of a compound according to claim 1 or of a composition according to claim 12.
20. Method for the treatment according to claim 19, wherein the disease or disorder susceptible of improvement by inhibition of soluble epoxide hydrolase is selected from the group consisting of hypertension, atherosclerosis, pulmonary diseases such as
35 chronic obstructive pulmonary disorder, asthma, sarcoidosis and cystic fibrosis, kidney

diseases such as acute kidney injury, diabetic nephrology, chronic kidney diseases, hypertension-mediated kidney disorders and high fat diet-mediated renal injury, stroke, pain, neuropathic pain, inflammation, pancreatitis in particular acute pancreatitis, immunological disorders, neurodevelopmental disorders such as schizophrenia and
5 autism spectrum disorder, eye diseases in particular diabetic keratopathy, wet age-related macular degeneration and retinopathy such as premature retinopathy and diabetic retinopathy, cancer, obesity, including obesity-induced colonic inflammation, diabetes, metabolic syndrome, preeclampsia, anorexia nervosa, depression, male sexual dysfunction such as erectile dysfunction, wound healing, NSAID-induced ulcers,
10 emphysema, scrapie, Parkinson's disease, arthritis, arrhythmia, cardiac fibrosis, Alzheimer's disease, Raynaud's syndrome, Niemann-Pick-type C disease, cardiomyopathy, vascular cognitive impairment, mild cognitive impairment, inflammatory bowel diseases, cirrhosis, non-alcoholic fatty liver disease, non-alcoholic steatohepatitis, liver fibrosis, osteoporosis, chronic periodontitis, sepsis, seizure
15 disorders such as epilepsy, dementia, edema such as cerebral edema, attention-deficit hyperactivity disorder, schizophrenia, drug dependency, social anxiety, colitis, amyotrophic lateral sclerosis, chemotherapy induced side effects, laminitis, inflammatory joint pain and synovitis, endothelial dysfunction, subarachnoid hemorrhage, including aneurysmal subarachnoid hemorrhage, traumatic brain injury,
20 cerebral ischemia and diabetes-induced learning and memory impairment.

INTERNATIONAL SEARCH REPORT

International application No
PCT/EP2019/066181

<p>A. CLASSIFICATION OF SUBJECT MATTER</p> <p>INV. C07C271/56 C07C275/26 C07C335/16 C07D211/34 C07D211/58 C07D211/96 C07D277/82 C07D451/04 C07D493/08 A61K31/27 A61K31/17 A61P9/00 A61P29/00 A61P25/00</p> <p>According to International Patent Classification (IPC) or to both national classification and IPC</p>								
<p>B. FIELDS SEARCHED</p> <p>Minimum documentation searched (classification system followed by classification symbols) C07C C07D</p> <p>Documentation searched other than minimum documentation to the extent that such documents are included in the fields searched</p> <p>Electronic data base consulted during the international search (name of data base and, where practicable, search terms used) EPO-Internal, CHEM ABS Data, WPI Data</p>								
<p>C. DOCUMENTS CONSIDERED TO BE RELEVANT</p> <table border="1"> <thead> <tr> <th>Category*</th> <th>Citation of document, with indication, where appropriate, of the relevant passages</th> <th>Relevant to claim No.</th> </tr> </thead> <tbody> <tr> <td>A</td> <td> <p>HONG C. SHEN: "Soluble epoxide hydrolase inhibitors: a patent review", EXPERT OPINION ON THERAPEUTIC PATENTS, vol. 20, no. 7, 2010, pages 941-956, XP055182103, ISSN: 1354-3776, DOI: 10.1517/13543776.2010.484804 cited in the application the whole document figures pages 944, 946, 947, compounds 8, 11, 25, 34, 39</p> <p style="text-align: center;">----- -/--</p> </td> <td>1-20</td> </tr> </tbody> </table>			Category*	Citation of document, with indication, where appropriate, of the relevant passages	Relevant to claim No.	A	<p>HONG C. SHEN: "Soluble epoxide hydrolase inhibitors: a patent review", EXPERT OPINION ON THERAPEUTIC PATENTS, vol. 20, no. 7, 2010, pages 941-956, XP055182103, ISSN: 1354-3776, DOI: 10.1517/13543776.2010.484804 cited in the application the whole document figures pages 944, 946, 947, compounds 8, 11, 25, 34, 39</p> <p style="text-align: center;">----- -/--</p>	1-20
Category*	Citation of document, with indication, where appropriate, of the relevant passages	Relevant to claim No.						
A	<p>HONG C. SHEN: "Soluble epoxide hydrolase inhibitors: a patent review", EXPERT OPINION ON THERAPEUTIC PATENTS, vol. 20, no. 7, 2010, pages 941-956, XP055182103, ISSN: 1354-3776, DOI: 10.1517/13543776.2010.484804 cited in the application the whole document figures pages 944, 946, 947, compounds 8, 11, 25, 34, 39</p> <p style="text-align: center;">----- -/--</p>	1-20						
<p><input checked="" type="checkbox"/> Further documents are listed in the continuation of Box C. <input checked="" type="checkbox"/> See patent family annex.</p>								
<p>* Special categories of cited documents :</p> <p>"A" document defining the general state of the art which is not considered to be of particular relevance</p> <p>"E" earlier application or patent but published on or after the international filing date</p> <p>"L" document which may throw doubts on priority claim(s) or which is cited to establish the publication date of another citation or other special reason (as specified)</p> <p>"O" document referring to an oral disclosure, use, exhibition or other means</p> <p>"P" document published prior to the international filing date but later than the priority date claimed</p> <p>"T" later document published after the international filing date or priority date and not in conflict with the application but cited to understand the principle or theory underlying the invention</p> <p>"X" document of particular relevance; the claimed invention cannot be considered novel or cannot be considered to involve an inventive step when the document is taken alone</p> <p>"Y" document of particular relevance; the claimed invention cannot be considered to involve an inventive step when the document is combined with one or more other such documents, such combination being obvious to a person skilled in the art</p> <p>"&" document member of the same patent family</p>								
<p>Date of the actual completion of the international search</p> <p>25 July 2019</p>		<p>Date of mailing of the international search report</p> <p>08/08/2019</p>						
<p>Name and mailing address of the ISA/ European Patent Office, P.B. 5818 Patentlaan 2 NL - 2280 HV Rijswijk Tel. (+31-70) 340-2040, Fax: (+31-70) 340-3016</p>		<p>Authorized officer</p> <p>Ladenburger, Claude</p>						

INTERNATIONAL SEARCH REPORT

International application No
PCT/EP2019/066181

C(Continuation). DOCUMENTS CONSIDERED TO BE RELEVANT		
Category*	Citation of document, with indication, where appropriate, of the relevant passages	Relevant to claim No.
A	<p>HONG C. SHEN ET AL: "Discovery of inhibitors of soluble epoxide hydrolase: a target with multiple potential therapeutic indications", JOURNAL OF MEDICINAL CHEMISTRY, vol. 55, no. 5, 2012, pages 1789-1808, XP055190495, ISSN: 0022-2623, DOI: 10.1021/jm201468j cited in the application the whole document figures 5-7, 9, compounds 9, 11-13, 16, 17, 19-21, 27, 28 -----</p>	1-20
A	<p>ELENA VALVERDE ET AL: "Searching for novel applications of the benzohomoadamantane scaffold in medicinal chemistry: Synthesis of novel 11[beta]-HSD1 inhibitors", BIOORGANIC & MEDICINAL CHEMISTRY, vol. 23, no. 24, 2015, pages 7607-7617, XP029342467, ISSN: 0968-0896, DOI: 10.1016/J.BMC.2015.11.004 the whole document figures 3-5; schemes 1-3; table 1 -----</p>	1-20
A	<p>DE 22 61 637 A1 (BASF AG) 20 June 1974 (1974-06-20) page 6, paragraph 3; claims 1,12; examples 14-16 -----</p>	1-20

1

INTERNATIONAL SEARCH REPORT

Information on patent family members

International application No
PCT/EP2019/066181

Patent document cited in search report	Publication date	Patent family member(s)	Publication date
DE 2261637	A1	20-06-1974	NONE

4. CONCLUSIONS

In line with the objectives of this Thesis, several compounds presenting inhibitory activities against the sEH enzyme bearing different polycyclic scaffolds have been successfully designed, synthesized and biologically evaluated in both *in vitro* and *in vivo* assays. The main conclusions derived from each Chapter are summarized below.

4.1. 2-Oxaadamantane-based sEHIs

In Chapter 1, eleven compounds bearing the 2-oxaadamantane scaffold were synthesized, ten of them presenting a piperidine moiety in the RHS and one of them featuring an aromatic ring. Additionally, several aromatic derivatives were synthesized in the context of Eugènia Pujol's experimental postgraduate Master. Figure 42 summarizes the main features of the structure-activity relationships (SAR) of these new family of compounds.

The replacement of the methylene unit by an oxygen atom increases aqueous solubility although leads to less potent nanomolar inhibitors.
The drop in potency has been rationalized by molecular dynamics simulations

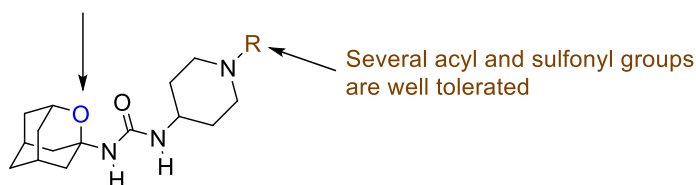


Figure 42. SAR of the 2-oxaadamantane-based sEHI.

- After a screening cascade, compound **42** was selected. The PK study of **42** allowed us to select the intraperitoneal route in the following *in vivo* studies, and the MTD assay showed that **42** was well tolerated.
- In both pre-induction and post-induction *in vivo* studies of cerulein-induced AP, **42** (30 mg/kg) diminished the overexpression of inflammatory and ER stress markers and reduced the pancreatic damage.

Overall, these positive results reinforce the hypothesis that sEHIs may be of clinical interest for treating and/or preventing AP.

4.2. Exploring the size of the lipophilic unit of sEHs

The objective of Chapter 2 was to assess if alterations in the size of the lipophilic unit attached to the urea significantly impacted its potency against the sEH as well as influencing solubility, permeability and metabolic stability. Therefore, three ring-contracted (**73**, **75** and **77**, derived from noradamantane) and four ring-expanded analogs (**74**, **76**, **78** and **79**, derived from diamantane) of the adamantane-based **AR9281**, **t-AUCB** and **10** were synthesized in the context of the present Thesis. The main conclusions of the biological evaluation of the new sEHs are collected in Figure 43.

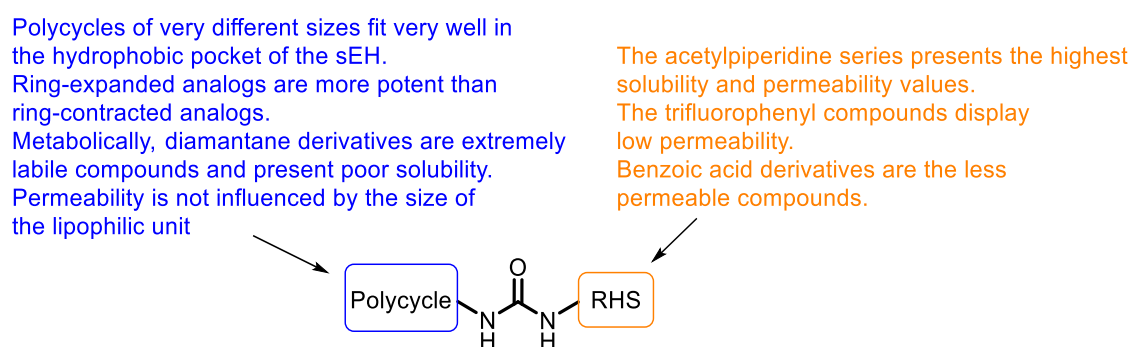


Figure 43. Results of the exploration of the size of the lipophilic unit of sEHs.

Altogether, we conclude that the catalytic center of the sEH enzyme can accommodate polycycles of very different sizes. Moreover, the replacement of the adamantane nucleus by the very large diamantane group leads to more potent compounds than the replacement by smaller ones.

4.3. Benzohomadamantane-based sEHs (I)

In Chapter 3 it was envisaged the synthesis of new sEHs bearing the very versatile benzohomadamantane scaffold as the hydrophobic moiety. Therefore, eleven compounds featuring this polycycle were synthesized and biologically evaluated. The main characteristics of these new compounds are collected in Figure 44.

In the AR9281 analogs, the substitution of the methyl group by an hydrogen atom is detrimental for the inhibitory activity

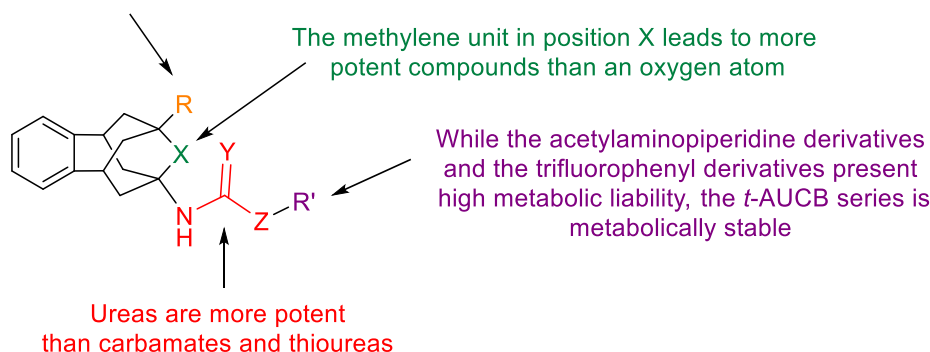


Figure 44. SAR of the first family of benzohomoadamantane-based sEHs.

- A screening cascade allowed us to select compounds **108** and **110**, and PK studies revealed that compound **110** exhibits better profile than **108**.
- In the cerulein-induced mouse model of AP, treatment with **110** (0.3 mg/Kg) resulted in an improved health status and less pancreatic damage, edema and neutrophils infiltration.

Therefore, we conclude that the benzohomoadamantane moiety is a suitable scaffold for the design and synthesis of novel sEHs with efficacy in *in vivo* studies.

4.4. Benzohomoadamantane-based sEHs (II and III)

The purpose of Chapters 4 and 5 was the synthesis of a new family of benzohomoadamantane-based piperidine derivatives in order to improve solubility and, more importantly, the microsomal stability of compound **105**. Therefore, thirty compounds were synthesized in the context of the present Thesis and all of them were biologically evaluated. The main characteristics of these new compounds are collected in Figure 45.

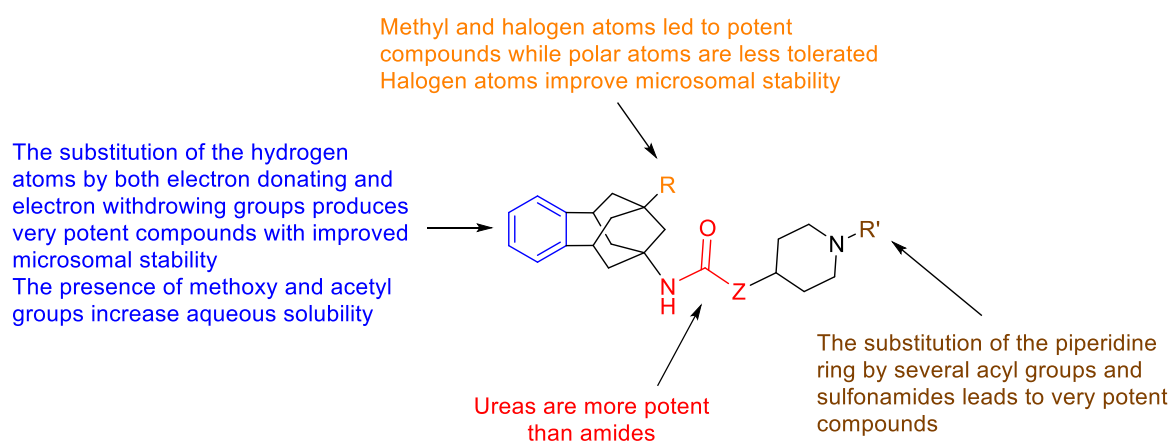


Figure 45. SAR of the second and third families of benzohomoadamantane-based sEHs.

- After performing a screening cascade, compound **140** was selected for *in vivo* studies in a murine model. Pharmacokinetics studies showed good bioavailability and elimination characteristics for **140**.
- The *in vivo* efficacy study in the predictive murine model of NP demonstrated that **140** reduced mechanical allodynia in a dose-dependent manner and outperformed other sEHs tested.

With these results, we conclude that the addition of a halogen atom in the R position of the benzohomoadamantane scaffold and the substitution of the aromatic ring are good approaches in order to improve the microsomal stability of benzohomoadamantane-based piperidine derivatives while keeping excellent inhibitory activities. In addition, the administration of a selected compound is effective in a predictive model of NP. For this reason, further studies with **140** in NP models are ongoing and additional work around the substitution of the aromatic ring is required in order to further explore the substitution of the polycyclic scaffold.

5. PERSPECTIVES

The promising results derived from the research conducted in the present Thesis encourages the group to further investigate the design, synthesis and evaluation of new sEHs. Some of the possible lines of research that can be developed in the near future are described below.

5.1. 3-Alkyl 2-oxadamantane derivatives

Interestingly, we have recently found that the introduction of several alkyl chains in the position 3 of the 2-oxadamantane nucleus increases the inhibitory potency against the human sEH. As shown in Figure 46, the replacement of the hydrogen atom of the position 3 of **16** (described in Chapter 1) by a methyl group (**175**) or ethyl group (**176**) led to more potent compounds, with IC_{50} values in the low nanomolar range.

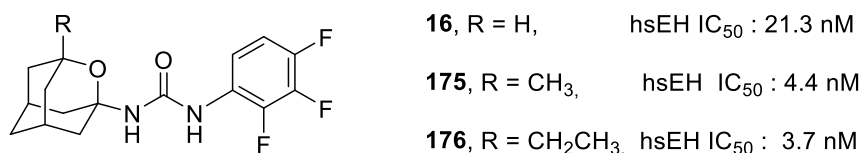


Figure 46. New ureas bearing the 2-oxadamantane scaffold alkylated in the position 3.

The next step is to evaluate the solubility of these new ureas. In the case that the solubility of **175** and **176** is not reduced due to the introduction of the alkyl chain, the group envisages to further explore the 2-oxadamante-based ureas as sEHs, especially those derivatives alkylated in the position 3 of the polycyclic system, introducing different groups such as methyl, ethyl, propyl or cyclopropyl, among others. As an example, it would be interesting to consider the synthesis of analogues of AR9281, *t*-AUCB or **42** alkylated at the position 3 of the 2-oxadamantane (Figure 47).

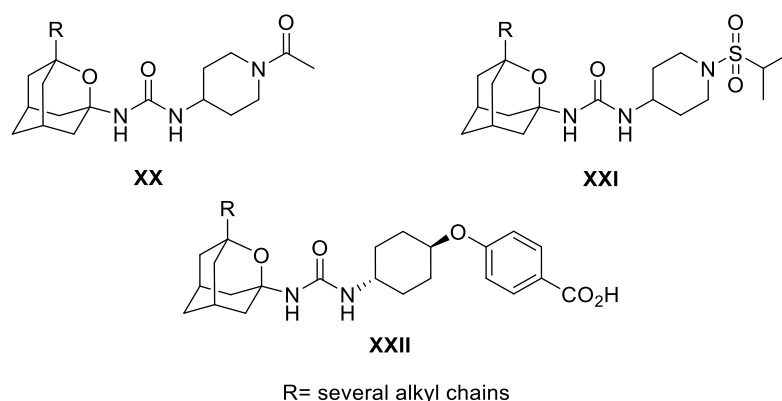


Figure 47. Analogs of AR9281, **42** and *t*-AUCB alkylated in the position 3 of the 2-oxadamantane moiety.

5.2. New benzohomadamantane-based sEHIs

Throughout the research conducted along the present Thesis, particularly in Chapters 3, 4 and 5, it has been demonstrated that the benzohomadamantane moiety is a suitable hydrophobic scaffold for the design and synthesis of new sEHIs. Therefore, it still remains a lot of work to do in order to expand the family of compounds derived from this versatile polycycle (Figure 48).

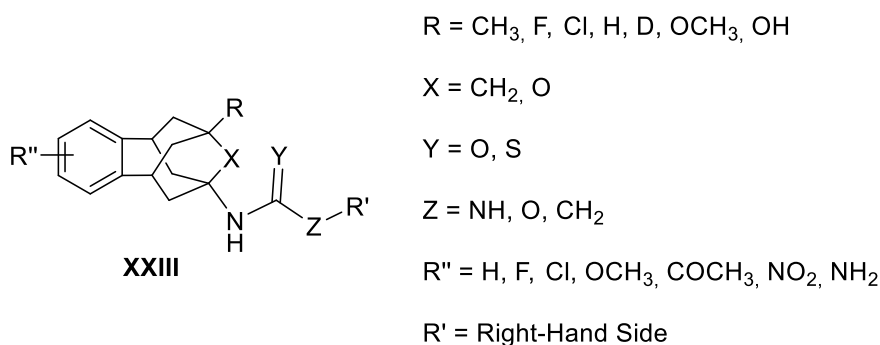


Figure 48. General structure **XXIII** presenting all the combinations of substituents to obtain new sEHIs bearing the benzohomadamantane scaffold.

New amides as sEHIs

Theoretically, amides might present better DMPK properties than ureas, such as better solubility values and higher stability against microsomes.¹¹⁶ However, in the case of sEHIs and specially those bearing the benzohomoadamantane scaffold, amides were less potent than ureas, as in the case of urea **105** and amide **146**.^{5.2.1.} Notwithstanding that, we have also observed that in the amide series, the substitution of the acyl group of the piperidine by a sulfonyl group increased the potency, as it happens in amide **148**, a good inhibitor of the human enzyme and endowed with excellent inhibitory activities of the murine and rat enzymes (Figure 49).

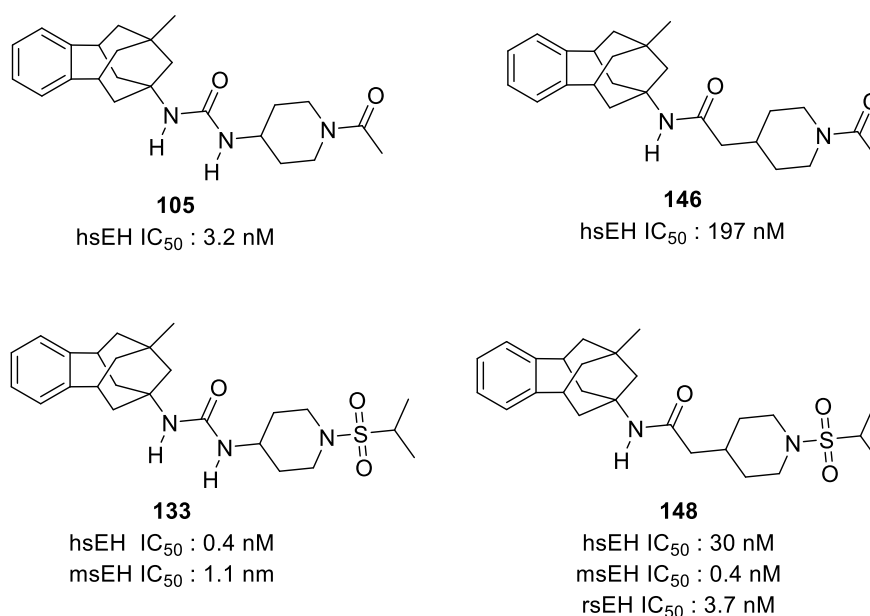


Figure 49. Structure and potency of ureas **105** and **133** and their respective amides **146** and **148**.

Consequently, these results encourage us to further explore the benzohomoadamantane-based amides and the preparation of new compounds with general formula **XXIV** is planned (Figure 50).

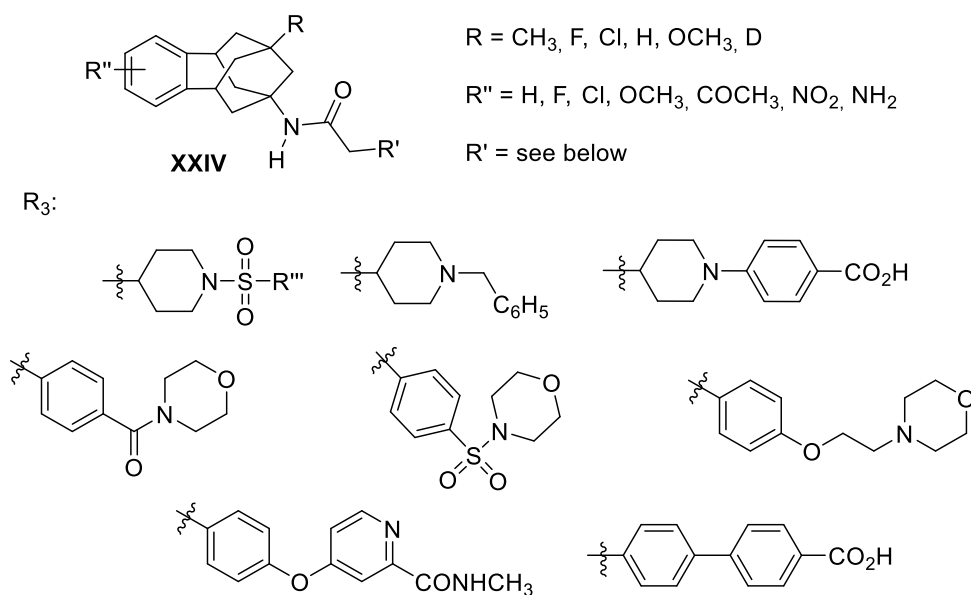


Figure 50. General structure **XXIV** of the new amides planned to be synthesized.

Further exploration of the aromatic ring

5.2.2.

In Chapter 5 of the present Thesis we observed that the introduction of different substituents in the aromatic ring of the benzohomoadamantane scaffold was a good strategy in order to obtain extremely potent sEHIs with improved microsomal stability and solubility values, two critical parameters in the drug discovery field and, in particular, in the discovery of new sEHIs. Thus, further exploration of the aromatic ring is required and the synthesis of new benzohomoadamantane-amines as starting materials for the obtention of new sEHIs is envisaged. For example, a myriad of combinations can be created between the substituent of the aromatic ring and the radical of the C9 position (R) of the polycyclic scaffold (Figure 51).

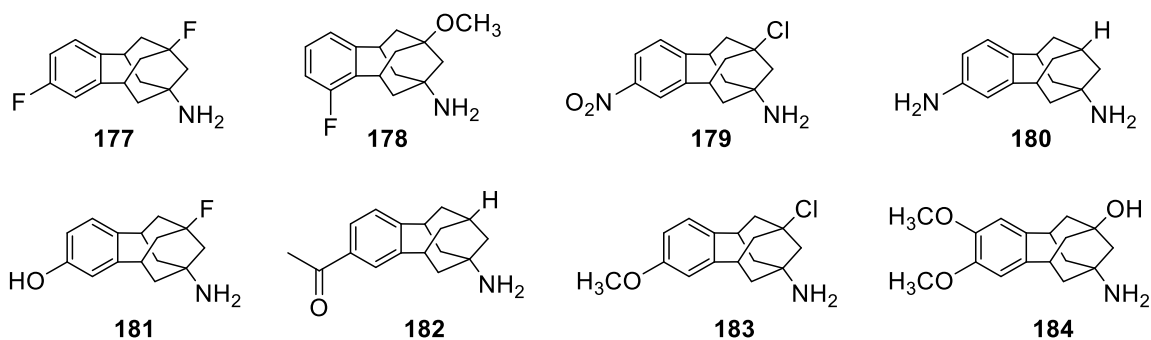


Figure 51. Examples of new polycyclic amines as starting materials for the synthesis of new sEHIs.

Additionally, new substitutions in the aromatic ring are also foreseen, such as the ones depicted in Figure 52.

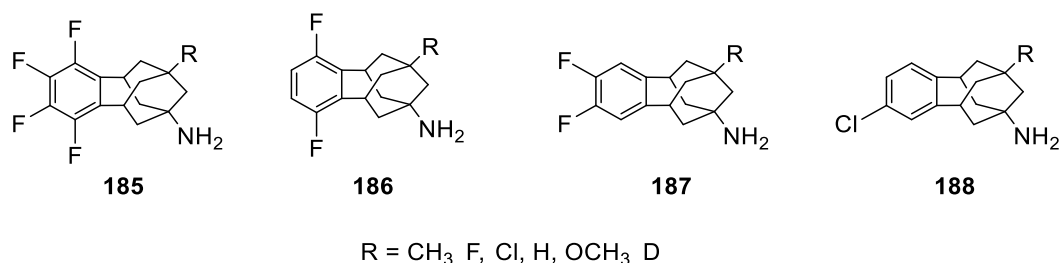


Figure 52. Examples of new possible substitutions of the aromatic ring.

Further exploration of the RHS

5.2.3. 5.2.3.1. Bicyclic compounds:

As mentioned in Chapter 4, we found that the piperidine ring can be replaced by a tropane ring, in particular in the *N*-benzylated derivatives, leading to the potent sEH **129**. This promising result opened the doors to the design and synthesis of new derivatives bearing different bicyclic systems instead of the piperidine moiety. Possible examples of the new compounds **189** and **190** are collected in Figure 53.

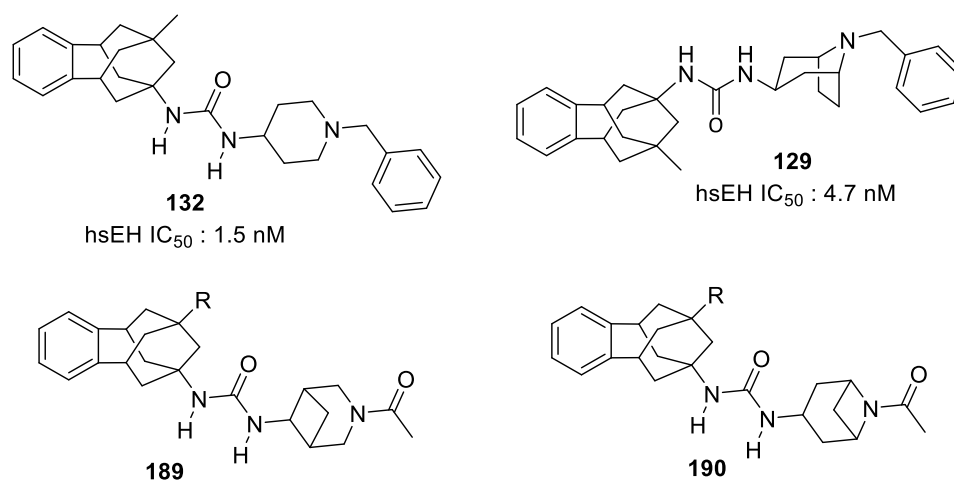


Figure 53. Structure and activity of **132** and **129** and possible new derivatives **189** and **190**.

5.2.3.2. Spirocycles:

As pointed out above, one of the main limitations in the discovery of new sEHIs is their limited aqueous solubility. A known strategy in Medicinal Chemistry to increase the solubility of the compounds is to increase the carbon bond saturation or the sp^3 fraction.²²⁷ In fact, polar spirocyclic scaffolds dramatically increase F_{sp^3} and have been successfully employed for the design of sEHIs.^{128,228,229,230,}

Moreover, unsubstituted 2-azaspiro[3.3]heptane has been suggested as an analogue of the piperidine moiety with an improved water solubility.²³¹ Therefore, the trifluorophenyl group of the potent sEHI **191** can be replaced by the benzohomoadamantane scaffold, or the piperidine moiety of the benzohomoadamantane-based **105** might be replaced by different spirocycles leading to, for example, ureas **192**, **193** and **194** (Figure 54).

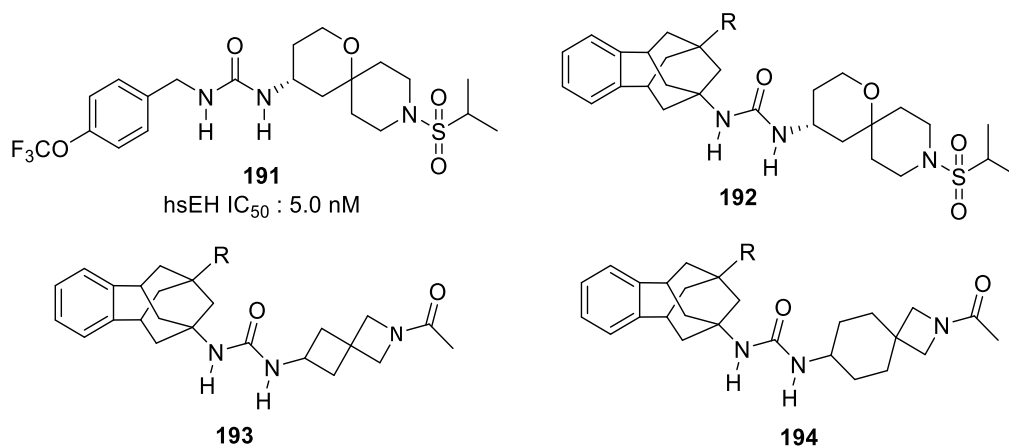


Figure 54. Structure of **191** and examples of new sEHIs bearing spirocycles in their structure.

²²⁷ Lovering, F.; Bikker, J.; Humblet, C. *J. Med. Chem.* **2009**, *21*, 6752-6756.

²²⁸ Ceccarelli, S. M.; Guerot, C.; Knust, H. (F. Hoffmann-La Roche). WO 2013/064467 A1, November 01, 2011.

²²⁹ Lukin, A.; Kramer, J.; Hartmann, M.; Weizel, L.; Hernandez-Olmos, V.; Falahati, K.; Burghardt, I.; Kalinchenkova, N.; Bagnyukova, D.; Zhurillo, N.; Rautio, J.; Forsberg, M.; Ihalainen, J.; Auriola, S.; Leppänen, J.; Konstantinov, I.; Pogoryelov, D.; Proschak, E.; Dar'in, D.; Krasavin, M. *Bioorg. Chem.* **2018**, *80*, 655-667.

²³⁰ Kato, Y.; Fuchi, N.; Saburi, H.; Nishimura, Y.; Watanabe, A.; Yagi, M.; Nakadera, Y.; Higashi, E.; Yamada, M.; Aoki, T. *Bioorg. Med. Chem. Lett.* **2013**, *23*, 5975-5979.

²³¹ Kirichok, A. A.; Shton, I.; Kliachyna, M.; Pishel, I.; Mykhailiuk, P. K. *Angew. Chem. Int. Ed.* **2017**, *56*, 8865-8869.

5.2.3.3. 3,3-disubstituted ureas:

It has been mentioned that at least one free NH of the urea group is needed in order to establish a hydrogen bond with the C-terminal domain of the sEH. Hence, several compounds presenting 3,3-disubstituted ureas have been published.^{232,233,234} Some of them presenting excellent inhibitory activities towards the sEH are shown in Figure 55. Taking this into account, we might consider replacing the trifluorophenyl group of some of these compounds by the benzohomoadamantane scaffold leading to structures **197**, **198** and **199**, among others (Figure 55).

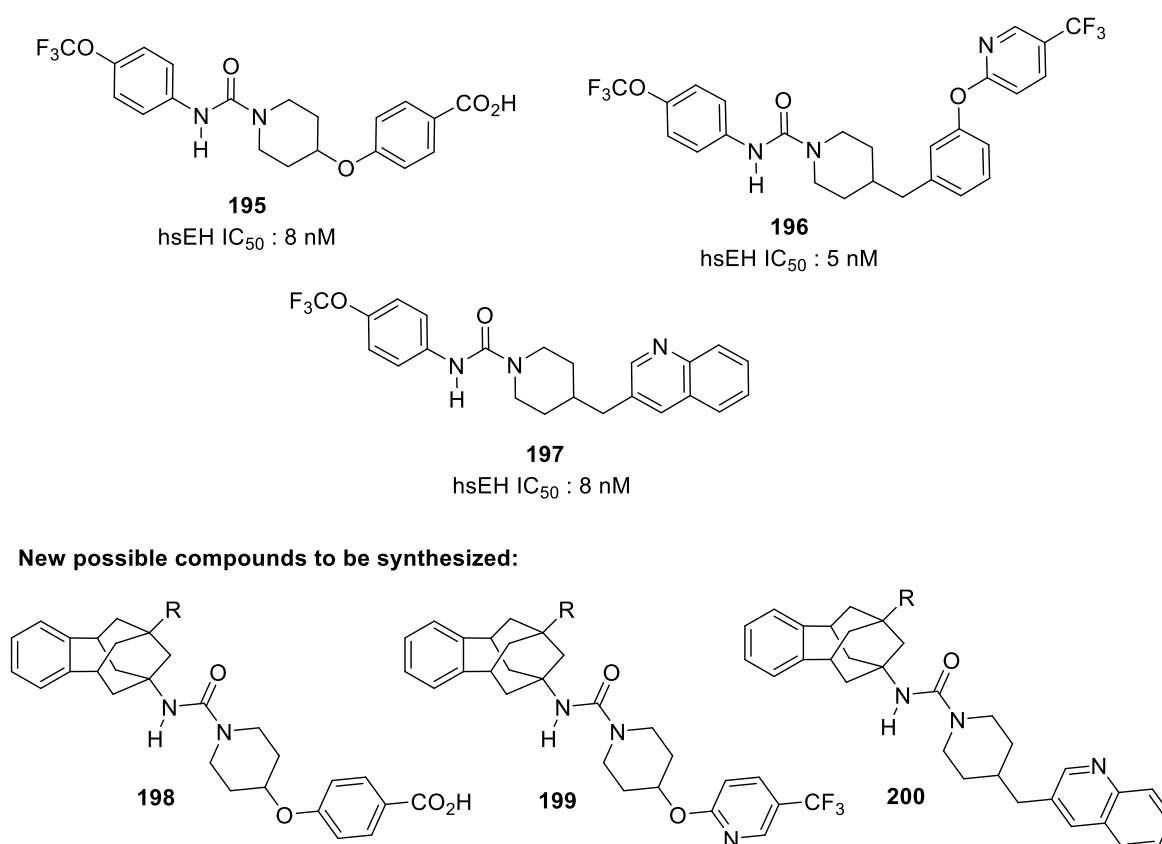


Figure 55. Structure and potency of **195**, **196** and **197**, and their possible benzohomoadamantane analogs **198**, **199** and **200**.

²³² Kodani, S. D.; Wan, D.; Wagner, K. M.; Hwang, S. H.; Morisseau, C; Hammock, B. D. *ACS Omega* **2018**, *3*, 14076-14086.

²³³ Hammock, B.; Kodani, S. (University of California). WO 2017/160861 A1, March 15, 2016.

²³⁴ Delombaert, S.; Eldrup, A. B.; Kowalski, J. A.; Mugge, I. A.; Soleymanzadeh, F.; Swinamer, A. D.; Taylor, S. J. (Boehringer Ingelheim). WO 2007/106705 A1, March 10, 2006.

5.2.3.4. Aromatic derivatives:

Several sEHIs described in the literature feature a substituted aromatic ring directly attached to the urea and some representative examples are shown in Figure 56.^{196,235,236,237,238,239}

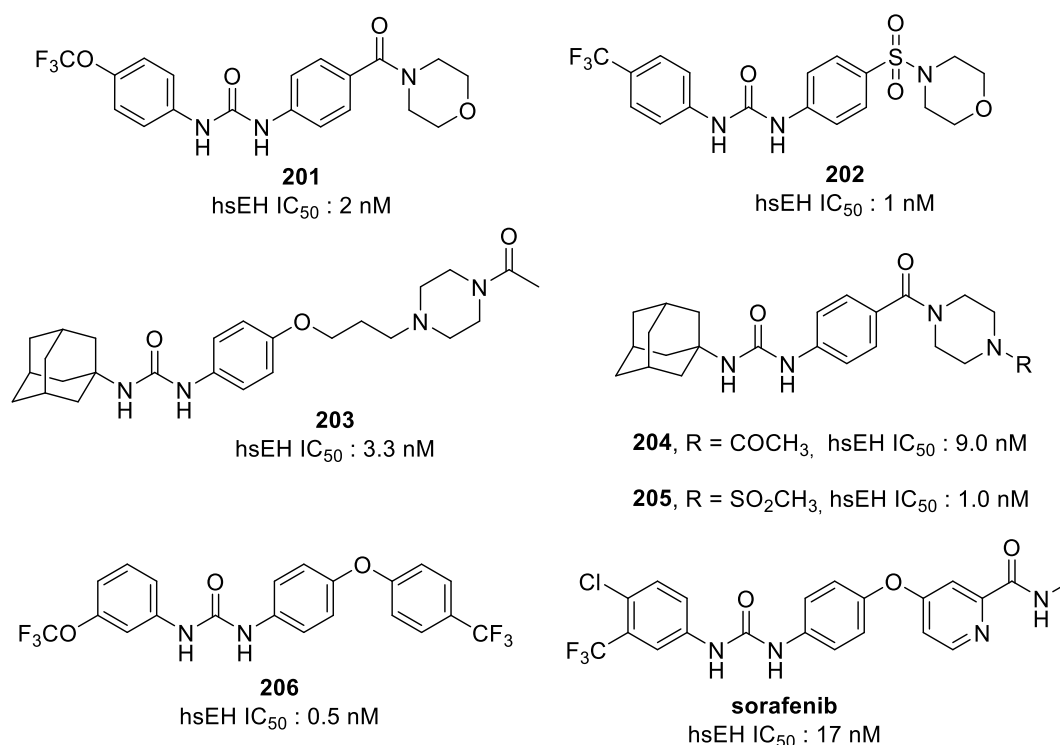


Figure 56. Structure and potency of **201-206** and sorafenib.

In this sense, it might be a good strategy to synthesize analogs of these compounds replacing the LHS by the benzohomoadamantane scaffold (Figure 57). Indeed, during

²³⁵ Anandan, S.-K.; Gless, R. D. *Bioorg. Med. Chem. Lett.* **2010**, *20*, 2740-2744.

²³⁶ Huang, S.-X.; Li, H.-Y.; Liu, J.-Y.; Morisseau, C.; Hammock, B. D.; Long, Y.-Q. *J. Med. Chem.* **2010**, *53*, 8376-8386.

²³⁷ Waltenberger, B.; Garsha, U.; Temml, V.; Liers, J.; Werz, O.; Schuster, D.; Stuppner, H. *J. Chem. Inf. Model.* **2016**, *56*, 747-762.

²³⁸ Vieder, L.; Romp, E.; Temml, V.; Fisher, J.; Kretzer, C.; Schoenthaler, M.; Taha, A.; Hernández-Olmos, V.; Sturm, S.; Schuster, D.; Werz, O.; Garsha, U.; Matuszczak. *ACS Med. Chem. Lett.* **2019**, *10*, 62-66.

²³⁹ Yefidoff-Freedman, R.; Fan, J.; Yan, L.; Zhang, Q.; Reis dos Santos, G. R.; Rana, S.; Contreras J. I.; Sahoo, R.; Wan, D.; Young, J.; Dias Teixeira, K. L.; Morisseau, C.; Halperin, J.; Hammock, B.; Natarajan, A.; Wang, P.; Chorev, M.; Aktas, B. H. *J. Med. Chem.* **2017**, *60*, 5392.

the writing of this PhD Thesis, another member of our laboratory, Andrea Bagán, has synthesized some of these compounds (e.g., **207** with R = methyl, F and Cl) and they showed to be subnanomolar inhibitors of the human and murine sEH.²⁴⁰

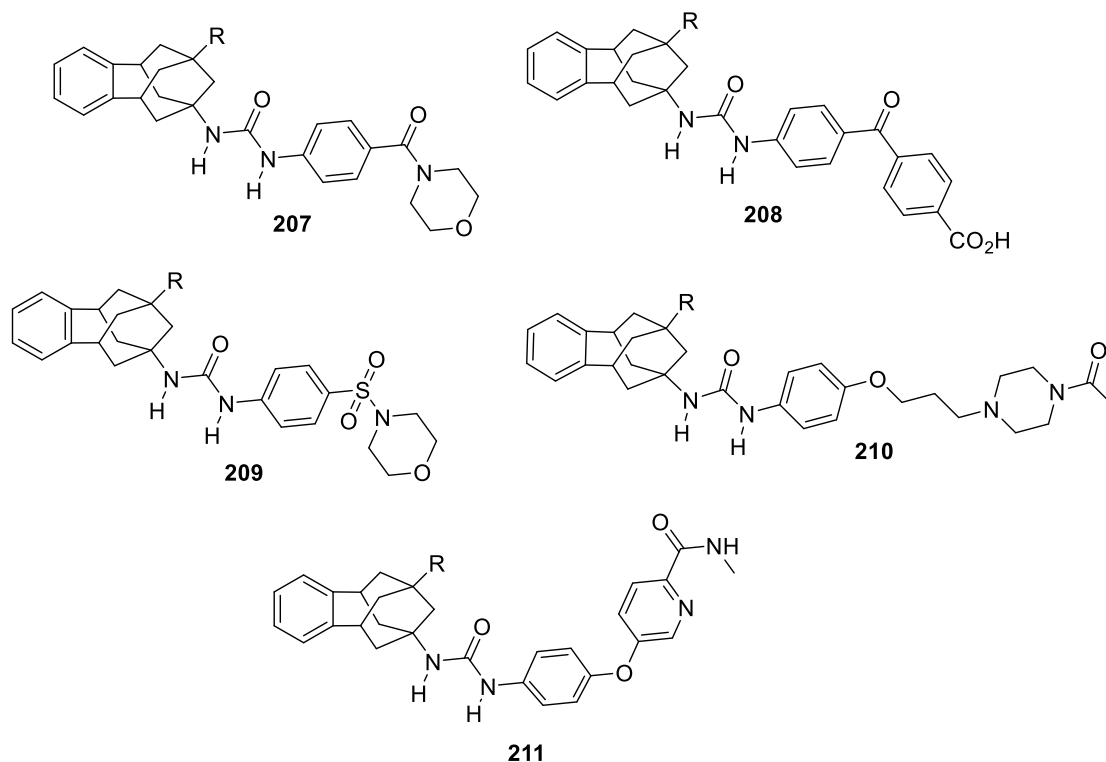


Figure 57. Possible new benzohomoadamantane-based ureas **207-211**.

Overall, it can be easily seen that the field of benzohomoadamantane-based sEHs is just starting to flourish and a lot of research that can be done revolving this new promising scaffold.

²⁴⁰ Bagán Polonio, A. Ph.D. Dissertation, University of Barcelona, in progress.

Results Dissemination

PUBLICATIONS RELATED TO SEHIS

1. *Synthesis, in vitro profiling and in vivo evaluation of benzohomoadamantane-based soluble epoxide hydrolase inhibitors for neuropathic pain.* Codony S.; Martín, J.; Jora, B.; Entrena J.; Feixas, F.; Corpas, R.; Morisseau, C.; Turcu, A. L.; Pérez B.; Pérez, C.; Rodríguez-Franco, M. I.; Brea, J. M.; Sanfeliu, C.; Osuna S.; Hammock, B. D.; Cobos, E. J.; Loza M. I.; Vázquez, S. *Scientific paper, writting in progress.*
2. *From the design to the in vivo evaluation of benzohomoadamantane-based soluble epoxide hydrolase inhibitors for the treatment of acute pancreatitis.* Codony, S.; Feixas, F.; Morisseau C.; Valverde, E.; Loza, M. I.; Brea, J. M.; Pérez, C.; Rodríguez-Franco, M. I.; Pizarro, J.; Vázquez-Carrera, M.; Corpas, R.; Sanfeliu, C.; Hammock B. D.; Osuna, S.; Vázquez, S. *Scientific paper, writting in progress.*
3. *2-Oxadamant-1-yl ureas as soluble epoxide hydrolase inhibitors: in vivo evaluation in a murine model of acute pancreatitis.* Codony, S.; Pujol, E.; Pizarro, J.; Feixas, F.; Valverde, E.; Loza, M. I.; Brea, J. M.; Saez, E.; Oyarzabal, J.; Pineda-Lucena, A.; Pérez, B.; Pérez, C.; Rodríguez-Franco, M. I.; Leiva, R.; Osuna, S.; Morisseau, C.; Hammock, B. D.; Vázquez-Carrera, M.; Vázquez, S. *J. Med. Chem.*, **2020**, 63, 9237-9257.
4. *Pharmacological inhibition of soluble epoxide hydrolase as a new therapy for Alzheimer's Disease.* Griñán-Ferré, C.; Codony, S.; Pujol, E.; Yang, J.; Leiva, R.; Escolano, C.; Puigoriol-Illamola, D.; Companys-Alemany, J.; Corpas, R.; Sanfeliu, C.; Loza, M. I.; Brea, J.; Morisseau, C.; Hammock, B. D.; Vázquez, S.; Pallàs M.; Galdeano, C. *Neurotherapeutics*, **2020**, <https://doi.org/10.1007/s13311-020-00854-1>.
5. *Exploring the size of the lipophilic unit of the soluble epoxide hydrolase inhibitors.* Codony, S.; Valverde, E.; Leiva, R.; Brea, J.; Loza, M. I.; Morisseau, C.; Hammock, B. D.; Vázquez, S. *Bioorg. Med. Chem.* **2019**, 27, 115078.

OTHER PUBLICATIONS

1. *Aniline-Based Inhibitors of Influenza H1N1 Virus Acting on Hemagglutinin-Mediated Fusion*. Leiva, R.; Barniol-Xicotá, M.; Codony, S.; Ginex, T.; Vanderlinden, E.; Montes, M.; Caffrey, M.; Luque, F. J.; Naesens, L.; Vázquez, S. *J. Med. Chem.* **2018**, *61*, 98-118.
2. *Palladium-catalyzed cocyclotrimerization of arynes with a pyramidalized alkene*. Alonso, J. M.; Quiroga, S.; Codony, S.; Turcu, A. L.; Barniol-Xicotá, M.; Pérez, D.; Guitián, E.; Vázquez, S.; Peña, D. *Chem. Comm.* **2018**, *54*, 5996-5999.
3. *Direct reductive alkylation of amine hydrochlorides with aldehyde bisulfite adducts*. Barniol-Xicotá, M.; Turcu, A. L.; Codony, S.; Escolano, C.; Vázquez, S. *Tetrahedron Lett.* **2014**, *55*, 2548-2550.

PATENT APPLICATIONS

1. *Multitarget compounds for the treatment of Alzheimer's disease*. Sandra Codony Gisbert, Caterina Pont Masanet, Santiago Vázquez Cruz, Diego Muñoz-Torreo López-Ibarra. EP19382219.4 (Universitat de Barcelona); priority date, March 28, 2019.
2. *Polycyclic compounds soluble epoxide hydrolase inhibitors*. Sandra Codony Gisbert, Carlos Galdeano Cantador, Rosana Leiva Martínez, Andreea Larisa Turcu, Elena Valverde Murillo, Santiago Vázquez Cruz. WO 2019/243414 A1 (Universitat de Barcelona); priority date, June 20, 2018.
3. *Phenoxyhexylurea derivatives for use in reducing accumulation of amyloid plaques and/or hyperphosphorylation of tau protein*. Sandra Codony Gisbert, Cristian Gaspar Griñan Ferré, Rosana Leiva Martínez, Mercè Pallàs Lliberia, Santiago Vázquez Cruz. EP18382267.5 (Universitat de Barcelona); priority date, April 20, 2018.
4. *Analogs of adamantylureas as soluble epoxide hydrolase inhibitors*. Santiago Vázquez Cruz, Elena Valverde Murillo, Rosana Leiva Martínez, Manuel Vázquez Carrera, Sandra Codony Gisbert. WO 2017/017048 A1 (Universitat de Barcelona); priority date, July 28, 2015.

SYMPOSIUM COMMUNICATIONS

1. Codony, S., Griñan-Ferré, C.; Pujol, E.; Yang, J.; Leiva, R.; Escolano, C.; Puigoriol-Illamola, D.; Companys-Alemany, J.; Corpas, R.; Sanfeliu, C.; Morisseau, C.; Hammock, B. D.; Galdeano, C.; Pallàs, M.; Vázquez, S. *UB-EV-52, a new chemical probe to establish soluble epoxide hydrolase as a target for the treatment of alzheimer's disease*. 11th Joint Meeting on Medicinal Chemistry, Prague (Czech Republic), Poster, **June 2019**.
2. Vázquez, S.; Codony, S.; Pizarro, J.; Loza, M. I.; Brea, J. M.; Morisseau, C.; Hammock, B. D.; Vázquez-Carrera, M. *Synthesis of a new family of soluble epoxide hydrolase inhibitors, in vitro profiling and in vivo evaluation in a murine model of acute pancreatitis*. 11th Joint Meeting on Medicinal Chemistry, Prague (Czech Republic), Poster, **June 2019**
3. Codony, S.; Pizarro, J.; Valverde, E.; Pujol, E.; Loza, M. I.; Brea, J. M.; Saez, E.; Oyarzábal, J.; Pérez, B.; Leiva, R.; Vázquez-Carrera, M.; Vázquez, S. *Novel Soluble Epoxide Hydrolase Inhibitors Featuring a 2-Oxadamantane Moiety: Synthesis, in vitro Profiling and in vivo Evaluation in Murine Models of Acute Pancreatitis*. ASPET Annual Meeting at Experimental Biology 2019, Orlando (Florida, EEUU), Poster, **April 2019**.
4. Galdeano, C.; Griñan-Ferré, C.; Codony, S.; Pujol, E.; Yang, J.; Leiva, R.; Escolano, C.; Puigoriol-Illamola, D.; Companys-Alemany, J.; Corpas, R.; Sanfeliu, C.; Morisseau, C.; Hammock, B. D.; Vázquez, S.; Pallàs, M. *Soluble Epoxide Hydrolase Inhibition as a New Therapeutic Strategy for the Treatment of Alzheimer's Disease*. EFMC-ISMIC 2018 XXV EFMC International Symposium on Medicinal Chemistry, Ljubljana (Slovenia), Poster, **September 2018**.
5. Codony, S.; Pizarro, J.; Valverde, E.; Pujol, E.; Loza, M. I.; Brea, J. M.; Saez, E.; Oyarzábal, J.; Pérez, B.; Leiva, R.; Vázquez-Carrera, M.; Vázquez, S. *Novel sEH inhibitors featuring a 2-oxadamantane moiety: from the design to in vivo evaluation in murine models of Acute Pancreatitis*. Italian-Spanish-Portuguese Joint Meeting on Medicinal Chemistry, Palermo (Italy), Oral Communication, **July 2018**.

6. Codony, S.; Pizarro, J.; Valverde, E.; Pujol, E.; Loza, M. I.; Brea, J. M.; Saez, E.; Oyarzábal, J.; Pérez, B.; Leiva, R.; Vázquez-Carrera, M.; Vázquez, S. *Novel Soluble Epoxide Hydrolase Inhibitors Featuring a 2-Oxaadamantane Moiety: From de Design to In Vivo Evaluation In Murine Models of Acute Pancreatitis*. V Simposium of Medicinal Chemistry Young Researchers (SEQT), Madrid (Spain), Poster, **June 2018**.
7. Codony, S.; Pizarro, J.; Valverde, E.; Pujol, E.; Loza, M. I.; Brea, J. M.; Saez, E.; Oyarzábal, J.; Pérez, B.; Leiva, R.; Vázquez-Carrera, M.; Vázquez, S. *Novel Soluble Epoxide Hydrolase Inhibitors Featuring a 2-Oxaadamantane Moiety: From de Design to In vivo Evaluation In Murine Models of Acute Pancreatitis*. VI SEQT Summer School: Medicinal Chemistry in Drug Discovery: The Pharma Perspective”, Toledo (Spain), Flash poster presentation, **June 2018**.
8. Codony, S.; Pizarro, J.; Valverde, E.; Pujol, E.; Loza, M. I.; Brea, J. M.; Saez, E.; Oyarzábal, J.; Pérez, B.; Leiva, R.; Vázquez-Carrera, M.; Vázquez, S. *Novel Soluble Epoxide Hydrolase Inhibitors Featuring a 2-Oxaadamantane Moiety: Synthesis, in vitro Profiling and in vivo Evaluation in Murine Models of Acute Pancreatitis*. ASPET Annual Meeting at Experimental Biology 2018, San Diego (California, EEUU), Poster, **April 2018**.
9. Codony, S.; Pizarro, J.; Valverde, E.; Pujol, E.; Loza, M. I.; Brea, J. M.; Saez, E.; Oyarzábal, J.; Pérez, B.; Leiva, R.; Vázquez-Carrera, M.; Vázquez, S. *Novel soluble epoxide hydrolase inhibitors featuring a 2-oxaadamantane moiety I: piperidine derivatives*. Hybrid Molecules and Polypharmacology in Drug Discovery, Würzburg (Germany), Poster, **November 2017**.
10. Pujol, E.; Pizarro, J.; Valverde, E.; Codony, S.; Loza, M. I.; Brea, J. M.; Saez, E.; Oyarzábal, J.; Pérez, B.; Leiva, R.; Vázquez-Carrera, M.; Vázquez, S. *Novel soluble epoxide hydrolase inhibitors featuring a 2-oxaadamantane moiety II: aromatic derivatives*. Hybrid Molecules and Polypharmacology in Drug Discovery, Würzburg (Germany), Poster, **November 2017**.

11. Codony, S.; Pizarro, J.; Valverde, E.; Pujol, E.; Loza, M. I.; Brea, J. M.; Saez, E.; Oyarzábal, J.; Pérez, B.; Leiva, R.; Vázquez-Carrera, M.; Vázquez, S. *Novel soluble epoxide hydrolase inhibitors featuring a 2-oxadamantane moiety I: piperidine derivatives*. 10th Joint Meeting on Medicinal Chemistry, Srebreno (Dubrovnik, Croatia), Poster, **June 2017**.

12. Pujol, E.; Pizarro, J.; Valverde, E.; Codony, S.; Loza, M. I.; Brea, J. M.; Saez, E.; Oyarzábal, J.; Pérez, B.; Leiva, R.; Vázquez-Carrera, M.; Vázquez, S. *Novel soluble epoxide hydrolase inhibitors featuring a 2-oxadamantane moiety II: aromatic derivatives*. 10th Joint Meeting on Medicinal Chemistry, Srebreno (Dubrovnik, Croatia), Poster, **June 2017**.

13. Codony, S.; Pizarro, J.; Valverde, E.; Pujol, E.; Loza, M. I.; Brea, J. M.; Saez, E.; Oyarzábal, J.; Pérez, B.; Leiva, R.; Vázquez-Carrera, M.; Vázquez, S. *Exploring 2-oxadamantylureas as novel soluble epoxide hydrolase inhibitors I: piperidine derivatives*. XIII Simposio de Investigadores Jóvenes – RSEQ – Sigma Aldrich, Logroño (Spain), Poster, **November 2016**.

14. Pujol, E.; Pizarro, J.; Valverde, E.; Codony, S.; Loza, M. I.; Brea, J. M.; Saez, E.; Oyarzábal, J.; Pérez, B.; Leiva, R.; Vázquez-Carrera, M.; Vázquez, S. *Exploring 2-oxadamantylureas as novel soluble epoxide hydrolase inhibitors II: aromatic derivatives*. XIII Simposio de Investigadores Jóvenes – RSEQ – Sigma Aldrich, Logroño (Spain), Poster, **November 2016**.

15. Codony, S.; Valverde, E.; Leiva, R.; Ginex, T.; Luque, F. J.; Hammock, B. D.; Morisseau, C.; Vázquez, S. *Exploring the size limit of the hydrophobic unit of Soluble Epoxide Hydrolase Inhibitors*. III Symposium of Medicinal Chemistry Young Researchers (SEQT), Barcelona (Spain), Poster, **June 2016**.

RESEARCH STAYS

1. **The Institute of Cancer Research (ICR)**, Sutton, London.

Supervisor: Dr. Swen Hoelder.

Research topic: Design, synthesis and biological evaluation of new IDH1 inhibitors (April 2019 - June 2019).

AWARDS

1. Outstanding Open Innovation Drug Discovery (OIDD) Collaborator by Eli Lilly & Co. (2017)